

Donald A. Nield  
Adrian Bejan

# Convection in Porous Media

*4th Edition*



# Convection in Porous Media



Donald A. Nield • Adrian Bejan

# Convection in Porous Media

Fourth Edition



Springer

Donald A. Nield  
Department of Engineering Science  
University of Auckland  
Auckland, 1142, New Zealand  
[d.nield@auckland.ac.nz](mailto:d.nield@auckland.ac.nz)

Adrian Bejan  
Department of Mechanical Engineering  
and Materials Science  
Duke University  
Durham, NC 27708, USA  
[abejan@duke.edu](mailto:abejan@duke.edu)

ISBN 978-1-4614-5540-0

ISBN 978-1-4614-5541-7 (eBook)

DOI 10.1007/978-1-4614-5541-7

Springer New York Heidelberg Dordrecht London

Library of Congress Control Number: 2012951652

© Springer Science+Business Media New York 2013

This work is subject to copyright. All rights are reserved by the Publisher, whether the whole or part of the material is concerned, specifically the rights of translation, reprinting, reuse of illustrations, recitation, broadcasting, reproduction on microfilms or in any other physical way, and transmission or information storage and retrieval, electronic adaptation, computer software, or by similar or dissimilar methodology now known or hereafter developed. Exempted from this legal reservation are brief excerpts in connection with reviews or scholarly analysis or material supplied specifically for the purpose of being entered and executed on a computer system, for exclusive use by the purchaser of the work. Duplication of this publication or parts thereof is permitted only under the provisions of the Copyright Law of the Publisher's location, in its current version, and permission for use must always be obtained from Springer. Permissions for use may be obtained through RightsLink at the Copyright Clearance Center. Violations are liable to prosecution under the respective Copyright Law.

The use of general descriptive names, registered names, trademarks, service marks, etc. in this publication does not imply, even in the absence of a specific statement, that such names are exempt from the relevant protective laws and regulations and therefore free for general use.

While the advice and information in this book are believed to be true and accurate at the date of publication, neither the authors nor the editors nor the publisher can accept any legal responsibility for any errors or omissions that may be made. The publisher makes no warranty, express or implied, with respect to the material contained herein.

Printed on acid-free paper

Springer is part of Springer Science+Business Media ([www.springer.com](http://www.springer.com))

*To our wives*

*Rachel Nield and Mary Bejan*

*Our children*

*Cherry, Alexandra, and Peter Nield*

*Cristina, Teresa, and William Bejan*

*Our grandchildren*

*Michael and Rachel van der Mark*

*Charlotte and Susan Nield*

*Elizabeth and John Hayman*



# Preface to the Fourth Edition

Papers on convection in porous media continue to be published at a rate that is now over 250 per year. This indication of the continued importance of the subject, together with the wide acceptance of the first, second, and third editions of the book, has encouraged us to prepare an expanded fourth edition. We have retained the basic structure and most of the text of the third edition. We have not attempted to be exhaustive in our choice of references, but nevertheless there are approximately 1,750 new citations to the literature! Again, we have made an effort to highlight new conceptual developments and engineering applications.

We found that it was possible to fit most of the new material under the existing section headings. However, we now have new sections on nanofluids, carbon dioxide sequestration, and the reaction scenarios that arise in a geological context.

Once again we decided that, except for a brief mention, convection in unsaturated media was beyond the scope of this book. Also, we are aware that there are some topics in the area of hydrology that could be regarded as coming under the umbrella of the title of our book but are not treated here.

We are grateful to a large number of people for their comments on the material in previous editions. Other colleagues have continued to improve our understanding of the subject of this book in ways too numerous to mention here.

We wish to thank our employers, the University of Auckland and Duke University, for their ongoing support.

Once again we relied on the expertise and hard work of Deborah Fraze for the preparation of our manuscript.

Auckland, New Zealand  
Durham, USA

Donald A. Nield  
Adrian Bejan



# Preface to the Third Edition

Papers on convection in porous media continue to be published at the rate what is now over 200 per year. The indication of the continued importance of the subject, together with the wide acceptance of the first and second editions of this volume, has encouraged us to prepare an expanded third edition. We have retained the basic structure and most of the text of the second edition. We have been somewhat selective in our choice of references, but nevertheless there are over 1,400 new references. Again, we have made an effort to highlight new conceptual developments and engineering applications.

We found that it was possible to fit a lot of the new material under the existing section headings. However, we now have new sections on bidisperse porous media, local thermal nonequilibrium, electrodiffusion, transverse heterogeneity in channels, thermal development of forced convection, effects of temperature-dependent viscosity, constructal multiscale flow structures, optimal spacings for plates separated by porous structures, control of convection using vertical vibration, and bioconvection.

Once again we decided that, except for a brief mention, convection in unsaturated media had to be beyond the scope of this book. Also, we are aware that there are some topics in the area of hydrology that could be regarded as coming under the umbrella of the title of our book but are not treated here.

We are grateful to a large number of people who provided us, prior to publication, with copies of their chapters of books that survey research on various topics. Other colleagues have continued to improve our understanding of the subject of this book in ways too numerous to mention here.

We wish to thank our employers, the University of Auckland and Duke University, for their ongoing support.

Once again we relied on the expertise and hard work of Linda Hayes and Deborah Fraze for the preparation of the electronic version of our manuscript.

Auckland, New Zealand  
Durham, USA

Donald A. Nield  
Adrian Bejan



# Preface to the Second Edition

Papers on convection in porous media continue to be published at the rate of over 100 per year. This indication of the continued importance of the subject, together with the wide acceptance of the first edition, has encouraged us to prepare an expanded second edition. We have retained the basic structure and most of the text of the first edition. With space considerations in mind, we have been selective in our choice of references, but nevertheless there are over 600 new references. We also made an effort to highlight new conceptual developments and engineering applications.

In the introductory material, we judged that Chaps. 2 and 3 needed little alteration (though there is a new Sect. 2.6 on other approaches to the topic), but our improved understanding of the basic modeling of flow through a porous medium has led to a number of changes in Chap. 1, both within the old sections and by the addition of a section on turbulence in porous media and a section on fractured media, deformable media, and complex porous structures.

In Chap. 4, on forced convection, we have added major new sections on compact heat exchangers, on heatlines for visualizing convection, and on constructal tree networks for the geometric minimization of the resistance to volume-to-point flows in heterogeneous porous media.

In Chap. 5 (external natural convection) there is a substantial amount of new material inserted in the existing sections. In Chaps. 6 and 7, on internal natural convection, we now have included descriptions of the effects of a magnetic field and rotation, and there are new sections on periodic heating and on sources in confined or partly confined regions; the latter is a reflection of the current interest in the problem of nuclear waste disposal. In Chap. 8, on mixed convection, there are no new sections, but in a new subsection we have given some prominence to the unified theory that has been developed for boundary layer situations. In Chap. 9, on double-diffusive convection (heat and mass transfer) there is a new section on convection produced by inclined gradients, a topic that has also been given wider coverage in the related section in Chap. 7.

In Chap. 10, which deals with convection with change of phase, we have a new subsection on the solidification of binary alloys, a research area that has blossomed

in the last decade. We also have a new section on spaces filled with fluid and fibers coated with a phase-change material. In the first edition we had little to say about two-phase flow, despite its importance in geothermal and other contexts. We now have included a substantial discussion on this topic, which we have placed at the end of Chap. 11 (geophysical aspects). Once again we decided that, except for a brief mention, convection in unsaturated media had to be beyond the scope of this book.

D.A.N. again enjoyed the hospitality of the Department of Mechanical Engineering and Materials Science at Duke University while on Research and Study Leave from the University of Auckland, and both of those institutions again provided financial support.

We are grateful for comments from Graham Weir and Roger Young on a draft of Sect. 11.9, a topic on which we had much to learn. We also are grateful to a large number of people who provided us with preprints of their papers prior to publication. Other colleagues have improved our understanding of the subject of this book in ways too numerous to mention here.

Once again we relied on the expertise and hard work of Linda Hayes for the preparation of the electronic version of our manuscript, and again the staff at the Engineering Library of Duke University made our search of the literature an enjoyable experience.

Auckland, New Zealand  
Durham, USA

Donald A. Nield  
Adrian Bejan

# Preface to the First Edition

In this book we have tried to provide a user-friendly introduction to the topic of convection in porous media. We have assumed that the reader is conversant with the basic elements of fluid mechanics and heat transfer, but otherwise the book is self-contained. Only routine classic mathematics is employed. We hope that the book will be useful both as a review (for reference) and as a tutorial work (suitable as a textbook in a graduate course or seminar).

This book brings into perspective the voluminous research that has been performed during the last two decades. The field recently has exploded because of worldwide concern with issues such as energy self-sufficiency and pollution of the environment. Areas of application include the insulation of buildings and equipment, energy storage and recovery, geothermal reservoirs, nuclear waste disposal, chemical reactor engineering, and the storage of heat-generating materials such as grain and coal. Geophysical applications range from the flow of groundwater around hot intrusions to the stability of snow against avalanches.

We believe that this book is timely because the subject is now mature in the sense that there is a corpus of material that is unlikely to require major revision in the future. As the reader will find, the relations for heat transfer coefficients and flow parameters for the case of saturated media are now known well enough for engineering design purposes. There is a sound basis of underlying theory that has been validated by experiment. At the same time there are outstanding problems in the cases of unsaturated media and multiphase flow in heterogeneous media, which are relevant to such topics as the drying of porous materials and enhanced oil recovery.

The sheer bulk of the available material has limited the scope of this book. It has forced us to omit a discussion of convection in unsaturated media and also of geothermal reservoir modeling; references to reviews of these topics are given. We also have excluded mention of several hundred additional papers, including some of our own. We have emphasized reports of experimental work, which are in relatively short supply (and in some areas are still lacking). We also have emphasized simple analysis where this illuminates the physics involved. The excluded material includes some good early work, which has now been superseded, and some recent

numerical work involving complex geometry. Also excluded are papers involving the additional effects of rotation or magnetic fields; we know of no reported experimental work or significant applications of these extensions. We regret that our survey could not be exhaustive, but we believe that this book gives a good picture of the current state of research in this field.

The first three chapters provide the background for the rest of the book. Chapters 4 through 8 form the core material on thermal convection. Our original plan, which was to separate foundational material from applications, proved to be impractical, and these chapters are organized according to geometry and the form of heating. Chapter 9 deals with combined heat and mass transfer and Chap. 10 with convection coupled with change of phase. Geophysical themes involve additional physical processes and have given rise to additional theoretical investigations; these are discussed in Chap. 11.

This book was written while D.A.N. was enjoying the hospitality of the Department of Mechanical Engineering and Materials Science at Duke University, while on Research and Study Leave from the University of Auckland. Financial support for this leave was provided by the University of Auckland, Duke University, and the United States—New Zealand Cooperative Science Program. We are particularly grateful to Dean Earl H. Dowell and Prof. Robert M. Hochmuth, both of Duke University, for their help in making this book project possible.

Linda Hayes did all the work of converting our rough handwritten notes into the current high-quality version on computer disk. She did this most efficiently and with tremendous understanding (i.e., patience!) for the many instances in which we changed our minds and modified the manuscript.

At various stages in the preparation of the manuscript and the figures we were assisted by Linda Hayes, Kathy Vickers, Jong S. Lim, Jose L. Lage, and Laurens Howle. Eric Smith and his team at the Engineering Library of Duke University went to great lengths to make our literature search easier. We are very grateful for all the assistance we have received.

Auckland, New Zealand  
Durham, USA

Donald A. Nield  
Adrian Bejan

# Contents

<b>1 Mechanics of Fluid Flow Through a Porous Medium . . . . .</b>	<b>1</b>
1.1 Introduction . . . . .	1
1.2 Porosity . . . . .	4
1.3 Seepage Velocity and the Equation of Continuity . . . . .	5
1.4 Momentum Equation: Darcy's Law . . . . .	5
1.4.1 Darcy's Law: Permeability . . . . .	5
1.4.2 Deterministic Models Leading to Darcy's Law . . . . .	6
1.4.3 Statistical Models Leading to Darcy's Law . . . . .	7
1.5 Extensions of Darcy's Law . . . . .	8
1.5.1 Acceleration and Other Inertial Effects . . . . .	8
1.5.2 Quadratic Drag: Forchheimer's Equation . . . . .	10
1.5.3 Brinkman's Equation . . . . .	15
1.5.4 Non-Newtonian Fluid . . . . .	18
1.6 Hydrodynamic Boundary Conditions . . . . .	18
1.7 Effects of Porosity Variation . . . . .	25
1.8 Turbulence in Porous Media . . . . .	26
1.9 Fractured Media, Deformable Media, and Complex Porous Structures . . . . .	28
<b>2 Heat Transfer Through a Porous Medium . . . . .</b>	<b>31</b>
2.1 Energy Equation: Simple Case . . . . .	31
2.2 Energy Equation: Extensions to More Complex Situations . . . . .	32
2.2.1 Overall Thermal Conductivity of a Porous Medium . . . . .	32
2.2.2 Effects of Pressure Changes and Viscous Dissipation . . . . .	34
2.2.3 Absence of Local Thermal Equilibrium . . . . .	36
2.2.4 Thermal Dispersion . . . . .	39
2.2.5 Cellular Porous Media . . . . .	42
2.3 Oberbeck-Boussinesq Approximation . . . . .	42

2.4	Thermal Boundary Conditions . . . . .	43
2.5	Hele-Shaw Analogy . . . . .	44
2.6	Bioheat Transfer and Other Approaches . . . . .	45
<b>3</b>	<b>Mass Transfer in a Porous Medium: Multicomponent and Multiphase Flows . . . . .</b>	<b>47</b>
3.1	Multicomponent Flow: Basic Concepts . . . . .	47
3.2	Mass Conservation in a Mixture . . . . .	49
3.3	Combined Heat and Mass Transfer . . . . .	51
3.4	Effects of a Chemical Reaction . . . . .	53
3.5	Multiphase Flow . . . . .	54
3.5.1	Conservation of Mass . . . . .	56
3.5.2	Conservation of Momentum . . . . .	57
3.5.3	Conservation of Energy . . . . .	59
3.5.4	Summary: Relative Permeabilities . . . . .	61
3.6	Unsaturated Porous Media . . . . .	64
3.7	Electrodiffusion Through Porous Media . . . . .	65
3.8	Nanofluids . . . . .	67
<b>4</b>	<b>Forced Convection . . . . .</b>	<b>69</b>
4.1	Plane Wall with Prescribed Temperature . . . . .	69
4.2	Plane Wall with Constant Heat Flux . . . . .	72
4.3	Sphere and Cylinder: Boundary Layers . . . . .	73
4.4	Point Source and Line Source: Thermal Wakes . . . . .	77
4.5	Confined Flow . . . . .	79
4.6	Transient Effects . . . . .	81
4.6.1	Scale Analysis . . . . .	82
4.6.2	Wall with Constant Temperature . . . . .	83
4.6.3	Wall with Constant Heat Flux . . . . .	86
4.6.4	Other Configurations . . . . .	87
4.7	Effects of Inertia and Thermal Dispersion: External Flow . . . . .	88
4.8	Effects of Boundary Friction and Porosity Variation: Exterior Flow . . . . .	90
4.9	Effects of Boundary Friction, Inertia, Porosity Variation, Thermal Dispersion, and Axial Conduction: Confined Flow . . . . .	95
4.10	Local Thermal Nonequilibrium . . . . .	103
4.11	Partly Porous Configurations . . . . .	104
4.12	Transversely Heterogeneous Channels and Pipes . . . . .	107
4.13	Thermal Development . . . . .	109
4.14	Surfaces Covered with Porous Layers . . . . .	110
4.15	Designed Porous Media . . . . .	114
4.16	Other Configurations or Effects . . . . .	117
4.16.1	Effect of Temperature-Dependent Viscosity . . . . .	117
4.16.2	Oscillatory Flows, Counterflows . . . . .	118
4.16.3	Non-Newtonian Fluids . . . . .	119

4.16.4	Bidisperse Porous Media . . . . .	119
4.16.5	Other Flows, Other Effects . . . . .	122
4.17	Heatlines for Visualizing Convection . . . . .	123
4.18	Constructal Tree Networks: Flow Access in Volume-to-Point Flow . . . . .	126
4.18.1	The Fundamental Volume-to-Point Flow Problem . . . . .	127
4.18.2	The Elemental Volume . . . . .	128
4.18.3	The First Construct . . . . .	131
4.18.4	Higher-Order Constructs . . . . .	132
4.18.5	The Constructal Law of Design and Evolution in Nature . . . . .	134
4.19	Constructal Multiscale Flow Structures: Vascular Design . . . . .	137
4.20	Optimal Spacings for Plates Separated by Porous Structures . . . . .	141
<b>5</b>	<b>External Natural Convection . . . . .</b>	<b>145</b>
5.1	Vertical Plate . . . . .	145
5.1.1	Power-Law Wall Temperature: Similarity Solution . . . . .	147
5.1.2	Vertical Plate with Lateral Mass Flux . . . . .	149
5.1.3	Transient Case: Integral Method . . . . .	150
5.1.4	Effects of Ambient Thermal Stratification . . . . .	152
5.1.5	Conjugate Boundary Layers . . . . .	155
5.1.6	Higher-Order Boundary-Layer Theory . . . . .	158
5.1.7	Effects of Boundary Friction, Inertia, and Thermal Dispersion . . . . .	159
5.1.8	Experimental Investigations . . . . .	166
5.1.9	Further Extensions of the Theory . . . . .	169
5.2	Horizontal Plate . . . . .	175
5.3	Inclined Plate, Wedge . . . . .	179
5.4	Vortex Instability . . . . .	181
5.5	Horizontal Cylinder . . . . .	185
5.5.1	Flow at High Rayleigh Number . . . . .	185
5.5.2	Flow at Low and Intermediate Rayleigh Number . . . . .	187
5.6	Sphere . . . . .	189
5.6.1	Flow at High Rayleigh Number . . . . .	189
5.6.2	Flow at Low Rayleigh Number . . . . .	191
5.6.3	Flow at Intermediate Rayleigh Number . . . . .	193
5.7	Vertical Cylinder . . . . .	193
5.8	Cone . . . . .	195
5.9	General Two-Dimensional or Axisymmetric Surface . . . . .	198
5.10	Horizontal Line Heat Source . . . . .	200
5.10.1	Flow at High Rayleigh Number . . . . .	200
5.10.2	Flow at Low Rayleigh Number . . . . .	205

5.11	Point Heat Source . . . . .	208
5.11.1	Flow at High Rayleigh Number . . . . .	208
5.11.2	Flow at Low Rayleigh Number . . . . .	210
5.11.3	Flow at Intermediate Rayleigh Number . . . . .	214
5.12	Other Configurations . . . . .	216
5.12.1	Fins Projecting from a Heated Base . . . . .	216
5.12.2	Flows in Regions Bounded by Two Planes . . . . .	217
5.12.3	Other Situations . . . . .	218
5.13	Surfaces Covered with Hair . . . . .	219
<b>6</b>	<b>Internal Natural Convection: Heating from Below . . . . .</b>	<b>221</b>
6.1	Horton-Rogers-Lapwood Problem . . . . .	221
6.2	Linear Stability Analysis . . . . .	222
6.3	Weak Nonlinear Theory: Energy and Heat Transfer Results . . . . .	227
6.4	Weak Nonlinear Theory: Further Results . . . . .	231
6.5	Effects of Solid–Fluid Heat Transfer . . . . .	238
6.6	Non-Darcy, Dispersion, and Viscous Dissipation Effects . . . . .	240
6.7	Non-Boussinesq Effects . . . . .	243
6.8	Finite-Amplitude Convection: Numerical Computation and Higher-Order Transitions . . . . .	245
6.9	Experimental Observations . . . . .	248
6.9.1	Observations of Flow Patterns and Heat Transfer . . . . .	248
6.9.2	Correlations of the Heat Transfer Data . . . . .	251
6.9.3	Further Experimental Observations . . . . .	256
6.10	Effect of Net Mass Flow . . . . .	257
6.10.1	Horizontal Throughflow . . . . .	257
6.10.2	Vertical Throughflow . . . . .	258
6.11	Effect of Nonlinear Basic Temperature Profiles . . . . .	261
6.11.1	General Theory . . . . .	261
6.11.2	Internal Heating . . . . .	262
6.11.3	Time-Dependent Heating . . . . .	265
6.11.4	Penetrative Convection, Icy Water . . . . .	271
6.12	Effects of Anisotropy . . . . .	272
6.13	Effects of Heterogeneity . . . . .	275
6.13.1	General Considerations . . . . .	275
6.13.2	Layered Porous Media . . . . .	276
6.13.3	Analogy Between Layering and Anisotropy . . . . .	278
6.13.4	Heterogeneity in the Horizontal Direction . . . . .	279
6.13.5	Heterogeneity in Both Horizontal and Vertical Directions . . . . .	283
6.13.6	Strong Heterogeneity . . . . .	283
6.14	Effects of Nonuniform Heating . . . . .	284

6.15	Rectangular Box or Channel . . . . .	286
6.15.1	Linear Stability Analysis, Bifurcation Theory, and Numerical Studies . . . . .	286
6.15.2	Thin Box or Slot . . . . .	291
6.15.3	Additional Effects . . . . .	292
6.16	Cylinder or Annulus . . . . .	294
6.16.1	Vertical Cylinder or Annulus . . . . .	294
6.16.2	Horizontal Cylinder or Annulus . . . . .	296
6.17	Internal Heating in Other Geometries . . . . .	297
6.18	Localized Heating . . . . .	299
6.19	Superposed Fluid and Porous Layers, Partly Porous Configurations . . . . .	303
6.19.1	Onset of Convection . . . . .	304
6.19.2	Flow Patterns and Heat Transfer . . . . .	311
6.19.3	Other Configurations and Effects . . . . .	312
6.20	Layer Saturated with Water Near 4°C . . . . .	313
6.21	Effects of a Magnetic Field or Electric Field, Ferromagnetic Fluid . . . . .	314
6.22	Effects of Rotation . . . . .	315
6.23	Non-Newtonian and Other Types of Fluids . . . . .	318
6.24	Effects of Vertical Vibration and Variable Gravity . . . . .	319
6.25	Bioconvection . . . . .	321
6.26	Constructal Theory of Bénard Convection . . . . .	322
6.26.1	The Many Counterflows Regime . . . . .	323
6.26.2	The Few Plumes Regime . . . . .	325
6.26.3	The Intersection of Asymptotes . . . . .	328
6.27	Bidisperse Porous Media and Cellular Porous Media . . . . .	329
7	<b>Internal Natural Convection: Heating from the Side . . . . .</b>	331
7.1	Darcy Flow Between Isothermal Sidewalls . . . . .	331
7.1.1	Heat Transfer Regimes . . . . .	331
7.1.2	Boundary Layer Regime . . . . .	336
7.1.3	Shallow Layer . . . . .	342
7.1.4	Stability of Flow . . . . .	346
7.1.5	Conjugate Convection . . . . .	347
7.1.6	Non-Newtonian Fluid . . . . .	347
7.1.7	Other Situations . . . . .	348
7.2	Sidewalls with Uniform Flux and Other Thermal Conditions . . . . .	349
7.3	Other Configurations and Effects of Property Variation . . . . .	350
7.3.1	Internal Partitions . . . . .	350
7.3.2	Effects of Heterogeneity and Anisotropy . . . . .	352
7.3.3	Cylindrical or Annular Enclosure . . . . .	355
7.3.4	Spherical Enclosure . . . . .	360

7.3.5	Porous Medium Saturated with Water Near 4°C . . . . .	361
7.3.6	Triangular Enclosure . . . . .	363
7.3.7	Other Enclosures . . . . .	364
7.3.8	Internal Heating . . . . .	365
7.3.9	Bidisperse Porous Media . . . . .	366
7.4	Penetrative Convection . . . . .	366
7.4.1	Lateral Penetration . . . . .	367
7.4.2	Vertical Penetration . . . . .	368
7.4.3	Other Penetrative Flows . . . . .	370
7.5	Transient Effects . . . . .	371
7.6	Departure from Darcy Flow . . . . .	375
7.6.1	Inertial Effects . . . . .	375
7.6.2	Boundary Friction, Variable Porosity, Local Thermal Nonequilibrium, Viscous Dissipation, and Thermal Dispersion Effects . . . . .	378
7.7	Fluid and Porous Regions . . . . .	380
7.8	Sloping Porous Layer or Enclosure . . . . .	383
7.9	Inclined Temperature Gradient . . . . .	389
7.10	Periodic Heating . . . . .	392
7.11	Sources in Confined or Partly Confined Regions . . . . .	393
7.12	Effects of Rotation . . . . .	395
<b>8</b>	<b>Mixed Convection . . . . .</b>	<b>397</b>
8.1	External Flow . . . . .	397
8.1.1	Inclined or Vertical Plane Wall . . . . .	397
8.1.2	Horizontal Wall . . . . .	403
8.1.3	Cylinder or Sphere . . . . .	404
8.1.4	Other Geometries . . . . .	408
8.1.5	Unified Theory . . . . .	409
8.1.6	Other Aspects of External Flow . . . . .	414
8.2	Internal Flow: Horizontal Channel . . . . .	414
8.2.1	Horizontal Layer: Uniform Heating . . . . .	414
8.2.2	Horizontal Layer: Localized Heating . . . . .	416
8.2.3	Horizontal Annulus . . . . .	417
8.2.4	Horizontal Layer: Lateral Heating . . . . .	418
8.3	Internal Flow: Vertical Channel . . . . .	418
8.3.1	Vertical Layer: Uniform Heating . . . . .	418
8.3.2	Vertical Layer: Localized Heating . . . . .	419
8.3.3	Vertical Annulus: Uniform Heating . . . . .	420
8.3.4	Vertical Annulus: Localized Heating . . . . .	421
8.4	Other Geometries and Other Effects . . . . .	423
8.4.1	Partly Porous Configurations . . . . .	423
8.4.2	Jet Impingement . . . . .	423
8.4.3	Other Aspects . . . . .	423

<b>9 Double-Diffusive Convection . . . . .</b>	425
9.1 Vertical Heat and Mass Transfer . . . . .	425
9.1.1 Horton–Rogers–Lapwood Problem . . . . .	425
9.1.2 Nonlinear Initial Profiles . . . . .	429
9.1.3 Finite-Amplitude Effects . . . . .	430
9.1.4 Soret and Dufour Cross-Diffusion Effects . . . . .	433
9.1.5 Flow at High Rayleigh Number . . . . .	436
9.1.6 Other Effects . . . . .	438
9.2 Horizontal Heat and Mass Transfer . . . . .	443
9.2.1 Boundary Layer Flow and External Natural Convection . . . . .	443
9.2.2 Enclosed Porous Medium . . . . .	449
9.2.3 Transient Effects . . . . .	456
9.2.4 Stability of Flow . . . . .	458
9.3 Concentrated Heat and Mass Sources . . . . .	459
9.3.1 Point Source . . . . .	459
9.3.2 Horizontal Line Source . . . . .	462
9.4 Other Configurations . . . . .	462
9.5 Inclined and Crossed Gradients . . . . .	465
9.6 Mixed Double-Diffusive Convection . . . . .	466
9.6.1 Mixed External Convection . . . . .	466
9.6.2 Mixed Internal Convection . . . . .	467
9.7 Nanofluids . . . . .	467
<b>10 Convection with Change of Phase . . . . .</b>	469
10.1 Melting . . . . .	469
10.1.1 Enclosure Heated from the Side . . . . .	469
10.1.2 Scale Analysis . . . . .	475
10.1.3 Effect of Liquid Superheating . . . . .	477
10.1.4 Horizontal Liquid Layer . . . . .	485
10.1.5 Vertical Melting Front in an Infinite Porous Medium . . . . .	488
10.1.6 A More General Model . . . . .	489
10.1.7 Further Studies . . . . .	492
10.2 Freezing and Solidification . . . . .	495
10.2.1 Cooling from the Side . . . . .	495
10.2.2 Cooling from Above . . . . .	498
10.2.3 Solidification of Binary Alloys . . . . .	499
10.3 Boiling and Evaporation . . . . .	506
10.3.1 Boiling and Evaporation Produced by Heating from Below . . . . .	506
10.3.2 Film Boiling and Evaporation . . . . .	512
10.4 Condensation . . . . .	518
10.5 Spaces Filled with Fluid and Fibers Coated with a Phase-Change Material . . . . .	520

<b>11 Geophysical Aspects . . . . .</b>	523
11.1 Snow . . . . .	523
11.2 Patterned Ground . . . . .	525
11.3 Thawing Subsea Permafrost . . . . .	527
11.4 Magma Production and Magma Chambers . . . . .	529
11.5 Diagenetic Processes . . . . .	530
11.6 Oceanic Crust . . . . .	532
11.6.1 Heat Flux Distribution . . . . .	532
11.6.2 Topographical Forcing . . . . .	532
11.7 Geothermal Reservoirs: Injection and Withdrawal . . . . .	534
11.8 Other Aspects of Single-Phase Flow . . . . .	535
11.9 Two-Phase Flow . . . . .	539
11.9.1 Vapor–Liquid Counterflow . . . . .	539
11.9.2 Heat Pipes . . . . .	544
11.9.3 Other Aspects . . . . .	546
11.10 Cracks in Shrinking Solids . . . . .	546
11.11 Carbon Dioxide Sequestration . . . . .	549
11.12 Reaction Scenarios . . . . .	550
11.12.1 Reaction Fronts . . . . .	551
11.12.2 Gradient Reactions . . . . .	552
11.12.3 Mixing Zones . . . . .	553
<b>References . . . . .</b>	555
<b>Index . . . . .</b>	773

# Nomenclature

B	Transition number for electrodiffusion, Eq. (3.95)
$Be$	Bejan number, Eq. (4.145)
$Br$	Brinkman number, Sect. 2.2.2
$C$	Concentration
$c$	Specific heat
$c_a$	Acceleration coefficient
$c_F$	Forchheimer coefficient
$c_p$	Specific heat at constant pressure
$D$	Diameter
$D$	$d/dz$
$D_m$	Solute diffusivity
$D_{CT}$	Thermodiffusion coefficient (Soret coefficient times $D_m$ )
$Da$	Darcy number
$d_p$	Particle diameter
$Ec$	Eckert number, Sect. 2.2.2
$g$	Gravitational acceleration
$Ge$	Gebhart number, Sect. 2.2.2
$H$	Vertical dimension
$\mathbf{i}, \mathbf{j}, \mathbf{k}$	Unit vectors
$Ja$	Jakob number
$K$	Permeability
$k$	Thermal conductivity
$k_m$	Thermal conductivity of the porous medium
$L$	Horizontal dimension
$Le$	Lewis number
$N$	Buoyancy ratio
$Nu$	Nusselt number
$P$	Pressure
$Pe$	Péclet number
$Pr$	Prandtl number

$q'$ , $q''$ , $q'''$	Heat transfer rate per unit length, area, volume, respectively
r. e. v	Representative elementary volume
$Ra$	Thermal Rayleigh (Rayleigh-Darcy) number
$Ra_D$	Solutal Rayleigh number
$Re$	Reynolds number
$r$	Radial coordinate
$Sc$ , $Sh$	Jakob numbers
$Ste$	Stefan number
$s$	Time constant
$T$	Temperature
$t$	Time
$\mathbf{V}$	Intrinsic velocity
$\mathbf{v}$	$(u, v, w)$ , seepage velocity
$x, y, z$	Position coordinates
$\alpha$	Nondimensional wavenumber
$\alpha_{BJ}$	Beavers-Joseph coefficient
$\alpha_m$	Thermal diffusivity of the porous medium
$\beta$	Thermal expansion coefficient
$\beta_C$	Concentration expansion coefficient
$\delta$	Boundary layer thickness
$\zeta$	Inter-phase momentum transfer coefficient
$\eta$	Similarity variable
$\theta$	Angle
$\theta$	Temperature perturbation amplitude
$\lambda$	Exponent in power law variation
$\mu$	Dynamic viscosity
$\tilde{\mu}$	Effective viscosity (Brinkman)
$\nu$	Kinematic viscosity
$\rho$	Density
$\sigma$	Heat capacity ratio, $\sigma = \varphi + (1 - \varphi)(\rho c)_s / (\rho c_P)_f$
$\tau$	Nondimensional time
$\varphi$	Porosity
$\varphi$	Angle
$\psi$	Streamfunction
$\omega$	Frequency
$\chi$	$c_F K^{1/2}$

## Subscripts

$b$	Basic state
$b$	Bulk
$C$	Concentration
$c$	Critical

$D$	Parameter based on length $D$
$e$	Effective
eff	Effective
$f$	Fluid
$g$	Gas
$H$	Horizontal
$L$	Parameter based on length $L$
$l$	Liquid
$m$	Porous medium
$p$	Particle
ref	Reference
$s$	Solid
$V$	Vertical
$w$	Wall
$x$	Parameter based on length $x$
0	Reference
$\infty$	Far field

## Superscripts

' Perturbation



# Chapter 1

## Mechanics of Fluid Flow Through a Porous Medium

### 1.1 Introduction

By a porous medium, we mean a material consisting of a solid matrix with an interconnected void. We suppose that the solid matrix is either rigid (the usual situation) or it undergoes small deformation. The interconnectedness of the void (the pores) allows the flow of one or more fluids through the material. In the simplest situation (“single-phase flow”), the void is saturated by a single fluid. In “two-phase flow,” a liquid and a gas share the void space.

In a natural porous medium, the distribution of pores with respect to shape and size is irregular. Examples of natural porous media are beach sand, sandstone, limestone, rye bread, wood, and the human lung (Fig. 1.1 and Table 1.1). Man-made porous media include ceramics, composite materials, and high-porosity metallic foams. On the pore scale (the microscopic scale), the flow quantities (velocity, pressure, etc.) will be clearly irregular. But in typical experiments, the quantities of interest are measured over areas that cross many pores, and such space-averaged (macroscopic) quantities change in a regular manner with respect to space and time, and hence are amenable to theoretical treatment.

How we treat a flow through a porous structure is largely a question of distance—the distance between the problem solver and the actual flow structure (Bejan 2004a, b). When the distance is short, the observer sees only one or two channels, or one or two open or closed cavities. In this case, it is possible to use conventional fluid mechanics and convective heat transfer to describe what happens at every point of the fluid- and solid-filled spaces. When the distance is large so that there are many channels and cavities in the problem solver’s field of vision, the complications of the flow paths rule out the conventional approach. In this limit, volume-averaging and global measurements (e.g., permeability, conductivity) are useful in describing the flow and in simplifying the description. As engineers focus more and more on designed porous media at decreasing pore scales, the problems tend to fall between the extremes noted above. In this intermediate range, the challenge is not only to describe *coarse* porous structures, but also to *optimize*

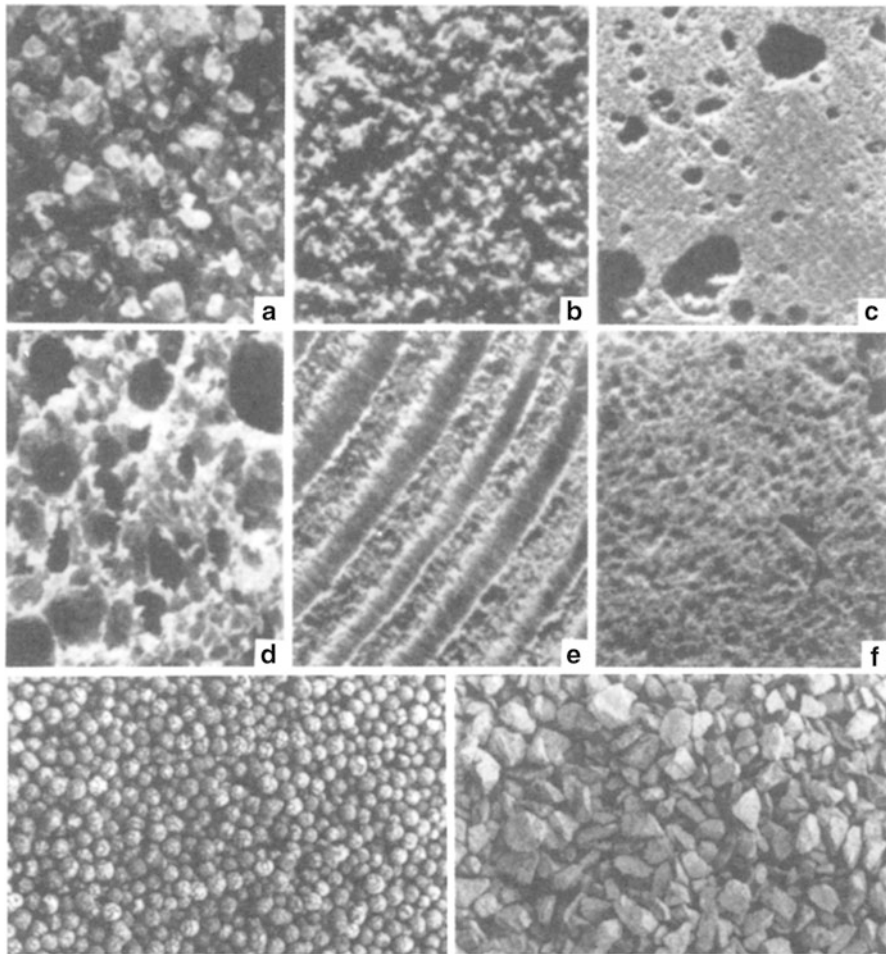


**Fig. 1.1** Top: Examples of natural porous materials: (a) beach sand, (b) sandstone, (c) limestone, (d) rye bread, (e) wood, and (f) human lung (Collins 1961, with permission from Van Nostrand Reinhold). Bottom: Granular porous materials used in the construction industry, 0.5-cm-diameter Liapor® spheres (left) and 1-cm-size crushed limestone (right) (Bejan 1984)

flow elements, and to *assemble* them. The resulting flow structures are *designed* porous media (see Bejan et al. 2004; Bejan 2004b).

The usual way of deriving the laws governing the macroscopic variables is to begin with the standard equations obeyed by the fluid and to obtain the macroscopic equations by averaging over volumes or areas containing many pores. There are two ways to do the averaging: spatial and statistical. In the spatial approach, a macroscopic variable is defined as an appropriate mean over a sufficiently large *representative elementary volume* (r.e.v.); this operation yields the value of that

**Table 1.1** Properties of common porous materials (based on data compiled by Scheidegger 1974; Bejan and Lage 1991)

Material	Porosity $\varphi$	Permeability $K$ (cm $^2$ )	Surface per unit volume (cm $^{-1}$ )
Agar-agar		$2 \times 10^{-10}$ to $4.4 \times 10^{-9}$	
Black slate powder	0.57–0.66	$4.9 \times 10^{-10}$ to $1.2 \times 10^{-9}$	$7 \times 10^3$ to $8.9 \times 10^3$
Brick	0.12–0.34	$4.8 \times 10^{-11}$ to $2.2 \times 10^{-9}$	
Catalyst (Fischer-Tropsch, granules only)	0.45		$5.6 \times 10^5$
Cigarette		$1.1 \times 10^{-5}$	
Cigarette filters	0.17–0.49		
Coal	0.02–0.12		
Concrete (ordinary mixes)	0.1		
Concrete (bituminous)		$1 \times 10^{-9}$ to $2.3 \times 10^{-7}$	
Copper powder (hot- compacted)	0.09–0.34	$3.3 \times 10^{-6}$ to $1.5 \times 10^{-5}$	
Cork board		$2.4 \times 10^{-7}$ to $5.1 \times 10^{-7}$	
Fiberglass	0.88–0.93		560–770
Granular crushed rock	0.45		
Hair (on mammals)	0.95–0.99		
Hair felt		$8.3 \times 10^{-6}$ to $1.2 \times 10^{-5}$	
Leather	0.56–0.59	$9.5 \times 10^{-10}$ to $1.2 \times 10^{-9}$	$1.2 \times 10^4$ to $1.6 \times 10^4$
Limestone (dolomite)	0.04–0.10	$2 \times 10^{-11}$ to $4.5 \times 10^{-10}$	
Sand	0.37–0.50	$2 \times 10^{-7}$ to $1.8 \times 10^{-6}$	150–220
Sandstone (“oil sand”)	0.08–0.38	$5 \times 10^{-12}$ to $3 \times 10^{-8}$	
Silica grains	0.65		
Silica powder	0.37–0.49	$1.3 \times 10^{-10}$ to $5.1 \times 10^{-10}$	$6.8 \times 10^3$ to $8.9 \times 10^3$
Soil	0.43–0.54	$2.9 \times 10^{-9}$ to $1.4 \times 10^{-7}$	
Spherical packings (well shaken)	0.36–0.43		
Wire crimps	0.68–0.76	$3.8 \times 10^{-5}$ to $1 \times 10^{-4}$	29–40

variable at the centroid of the r.e.v. It is assumed that the result is independent of the size of the representative elementary volume. The length scale of the r.e.v. is much larger than the pore scale, but considerably smaller than the length scale of the macroscopic flow domain (Fig. 1.2).

In the statistical approach, the averaging is over an ensemble of possible pore structures that are macroscopically equivalent. A difficulty is that usually the statistical information about the ensemble has to be based on a single sample, and this is possible only if statistical homogeneity (stationarity) is assumed.

If one is concerned only with deriving relationships between the space-averaged quantities and is not concerned about their fluctuation, then the results obtained by using the two approaches are essentially the same. Thus, in this situation, one might as well use the simpler approach, namely, the one based on the r.e.v. An example of its use is given in Sect. 3.5. This approach is discussed at length by Bear and

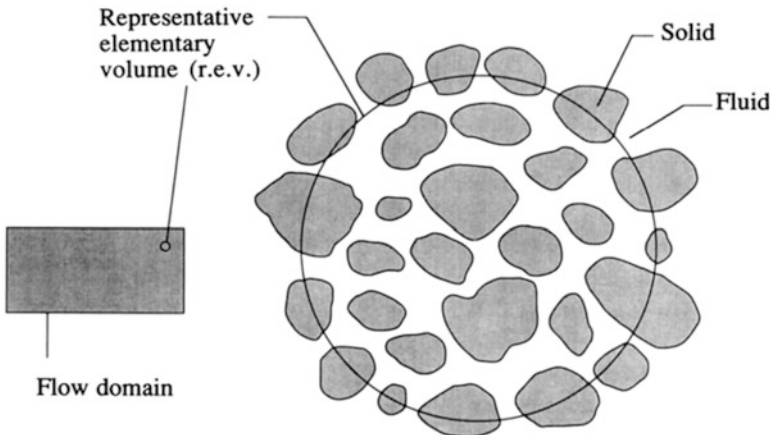


**Fig. 1.2** The representative elementary volume (r.e.v.): the figure illustrates the intermediate size relative to the sizes of the flow domain and the pores

Bachmat (1990). However, a number of problems require a statistical approach (see, e.g., Georgiadis and Catton 1987, 1988; Georgiadis 1991).

For an extensive treatment of the method of volume averaging the reader is referred to Whitaker (1999).

## 1.2 Porosity

The porosity  $\varphi$  of a porous medium is defined as the fraction of the total volume of the medium that is occupied by void space. Thus,  $1 - \varphi$  is the fraction that is occupied by solid. For an isotropic medium, the “surface porosity” (i.e., the fraction of void area to total area of a typical cross section) will normally be equal to  $\varphi$ .

In defining  $\varphi$  in this way, we are assuming that all the void space is connected. If in fact one has to deal with a medium in which some of the pore space is disconnected from the remainder, then one has to introduce an “effective porosity,” defined as the ratio of connected void to total volume.

For natural media,  $\varphi$  does not normally exceed 0.6. For beds of solid spheres of uniform diameter  $\varphi$  can vary between the limits 0.2595 (rhombohedral packing) and 0.4764 (cubic packing). Nonuniformity of grain size tends to lead to smaller porosities than for uniform grains, because smaller grains fill the pores formed by larger grains. For man-made materials such as metallic foams  $\varphi$  can approach the value 1. Table 1.1 shows a compilation of porosities and other properties of common porous materials.

### 1.3 Seepage Velocity and the Equation of Continuity

We construct a continuum model for a porous medium, based on the r.e.v. concept. We introduce a Cartesian reference frame, and consider volume elements that are sufficiently large compared with the pore volumes for reliable volume averages to be obtained. In other words, the averages are not sensitive to the choice of volume element. A distinction is made between an average taken with respect to a volume element  $V_m$  of the medium (incorporating both solid and fluid material) and one taken with respect to a volume element  $V_f$  consisting of fluid only. For example, we denote the average of the fluid velocity over  $V_m$  by  $\mathbf{v} = (u, v, w)$ . This quantity has been given various names, by different authors, such as seepage velocity, filtration velocity, superficial velocity, Darcy velocity, and volumetric flux density. We prefer the term Darcy velocity since it is short and distinctive. Taking an average of the fluid velocity over a volume  $V_f$ , we get the intrinsic average velocity  $\mathbf{V}$ , which is related to  $\mathbf{v}$  by the Dupuit–Forchheimer relationship  $\mathbf{v} = \varphi\mathbf{V}$ .

Once we have a continuum to deal with, we can apply the usual arguments and derive differential equations expressing conservation laws. For example, the conservation of mass is expressed by the continuity equation

$$\phi \frac{\partial \rho_f}{\partial t} + \nabla \cdot (\rho_f \mathbf{v}) = 0 \quad (1.1)$$

where  $\rho_f$  is the fluid density. This equation is derived by considering an elementary unit volume of the medium and equating the rate of increase of the mass of the fluid within that volume,  $\partial(\varphi\rho_f)/\partial t$ , to the net mass flux into the volume,  $-\nabla \cdot (\rho_f \mathbf{v})$ , noting that  $\varphi$  is independent of  $t$ .

### 1.4 Momentum Equation: Darcy's Law

We now discuss various forms of the momentum equation which is the porous-medium analog of the Navier–Stokes equation. For the moment, we neglect body forces such as gravity; the appropriate terms for these can be added easily at a later stage.

#### 1.4.1 Darcy's Law: Permeability

Henry Darcy's (1856) investigations into the hydrology of the water supply of Dijon and his experiments on steady-state unidirectional flow in a uniform medium revealed a proportionality between flow rate and the applied pressure difference. In modern notation this is expressed, in refined form, by

$$u = -\frac{K}{\mu} \frac{\partial P}{\partial x} \quad (1.2)$$

Here,  $\partial P/\partial x$  is the pressure gradient in the flow direction and  $\mu$  is the dynamic viscosity of the fluid. The coefficient  $K$  is independent of the nature of the fluid but it depends on the geometry of the medium. It has dimensions (length)<sup>2</sup> and is called the *specific permeability* or *intrinsic permeability* of the medium. In the case of single-phase flow, we abbreviate this to permeability. The permeabilities of common porous materials are summarized in Table 1.1. It should be noted that in Eq. (1.2),  $P$  denotes an intrinsic quantity, and that Darcy's equation is not a balance of forces averaged over a r.e.v. Special care needs to be taken when adding additional terms such as the one expressing a Coriolis force. One needs to take averages over the fluid phase before introducing a Darcy drag term (see Sect. 1.5.1).

In three dimensions, Eq. (1.2) generalizes to

$$\mathbf{v} = -\mu^{-1} \mathbf{K} \cdot \nabla P, \quad (1.3)$$

where now the permeability  $\mathbf{K}$  is in general a second-order tensor. For the case of an isotropic medium, the permeability is a scalar and Eq. (1.3) simplifies to

$$\nabla P = -\frac{\mu}{K} \mathbf{v}. \quad (1.4)$$

Values of  $K$  for natural materials vary widely. Typical values for soils, in terms of the unit m<sup>2</sup>, are clean gravel  $10^{-7}\text{--}10^{-9}$ , clean sand  $10^{-9}\text{--}10^{-12}$ , peat  $10^{-11}\text{--}10^{-13}$ , stratified clay  $10^{-13}\text{--}10^{-16}$ , and unweathered clay  $10^{-16}\text{--}10^{-20}$ . Workers concerned with geophysics often use as a unit of permeability the *Darcy*, which equals  $0.987 \times 10^{-12}$  m<sup>2</sup>.

Darcy's law has been verified by the results of many experiments. Theoretical backing for it has been obtained in various ways, with the aid of either deterministic or statistical models. It is interesting that Darcy's original data may have been affected by the variation of viscosity with temperature (Lage 1998). A refined treatment of the mass and momentum conservation equations, based on volume averaging, has been presented by Altevogt et al. (2003).

Ochoa-Tapia et al. (2007) showed that, when fractional-order gradients are involved, on volume averaging two new terms appear. One is a traditional convective term induced by spatial porosity gradients and the other is a fractional correction of Brinkman type (see Sect. 1.5.3). A new model based on fractal resistance was proposed by Wu and Yu (2007).

### 1.4.2 Deterministic Models Leading to Darcy's Law

If  $K$  is indeed determined by the geometry of the medium, then clearly it is possible to calculate  $K$  in terms of the geometrical parameters, at least for the case of simple

geometry. A great deal of effort has been spent on this endeavor, and the results are well presented by Dullien (1992).

For example, in the case of beds of particles or fibers, one can introduce an effective average particle or fiber diameter  $D_p$ . The hydraulic radius theory of Carman–Kozeny leads to the relationship

$$K = \frac{D_{p2}^2 \varphi^3}{180(1 - \varphi)^2}, \quad (1.5)$$

where

$$D_{p2} = \frac{\int_0^\infty D_p^3 h(D_p) dD_p}{\int_0^\infty D_p^2 h(D_p) dD_p} \quad (1.6)$$

and  $h(D_p)$  is the density function for the distribution of diameters  $D_p$ . The constant 180 in Eq. (1.5) was obtained by seeking a best fit with experimental results. The Carman–Kozeny equation gives satisfactory results for media that consist of particles of approximately spherical shape and whose diameters fall within a narrow range. The equation is often not valid in the cases of particles that deviate strongly from the spherical shape, broad particle-size distributions, and consolidated media. Nevertheless, it is widely used since it seems to be the best simple expression available. A modified Carman–Kozeny theory was proposed by Liu et al. (1994). A fibrous porous medium was modeled by Davis and James (1996). For randomly packed monodisperse fibers, the experiments of Rahli et al. (1997) showed that the Carman–Kozeny “constant” is dependent on porosity and fiber aspect ratio. The Carman–Kozeny correlation has been applied to compressed expanded natural graphite, an example of a high porosity and anisotropic consolidated medium, by Mauran et al. (2001). Li and Park (1998) applied an effective medium approximation to the prediction of the permeability of packed beds with polydisperse spheres.

### 1.4.3 Statistical Models Leading to Darcy's Law

Many authors have used statistical concepts in the provision of theoretical support for Darcy's law. Most authors have used constitutive assumptions in order to obtain closure of the equations, but Whitaker (1986) has derived Darcy's law, for the case of an incompressible fluid, without making any constitutive assumption. This theoretical development is not restricted to either homogeneous or spatially periodic porous media, but it does assume that there are no abrupt changes in the structure of the medium.

If the medium has periodic structure, then the homogenization method can be used to obtain mathematically rigorous results. The method is explained in detail by Ene and Polievski (1987), Mei et al. (1996), and Ene (1997, 2004). The first authors derive Darcy's law without assuming incompressibility, and they go on to prove that the permeability is a symmetric positive-definite tensor.

## 1.5 Extensions of Darcy's Law

### 1.5.1 Acceleration and Other Inertial Effects

Following Wooding (1957), many early authors on convection in porous media used an extension of Eq. (1.4) of the form

$$\rho_f \left[ \frac{\partial \mathbf{V}}{\partial t} + (\mathbf{V} \cdot \nabla) \mathbf{V} \right] = -\nabla P - \frac{\mu}{K} \mathbf{v} \quad (1.7)$$

which, when the Dupuit–Forchheimer relationship is used, becomes

$$\rho_f \left[ \phi^{-1} \frac{\partial \mathbf{v}}{\partial t} + \phi^{-2} (\mathbf{v} \cdot \nabla) \mathbf{v} \right] = -\nabla P - \frac{\mu}{K} \mathbf{v}. \quad (1.8)$$

This equation was obtained by analogy with the Navier–Stokes equation. Beck (1972) pointed out that the inclusion of the  $(\mathbf{v} \cdot \nabla) \mathbf{v}$  term was inappropriate because it raised the order (with respect to space derivatives) of the differential equation, and this was inconsistent with the slip boundary condition (appropriate when Darcy's law was employed). More importantly, the inclusion of  $(\mathbf{v} \cdot \nabla) \mathbf{v}$  is not a satisfactory way of expressing the nonlinear drag, which arises from inertial effects, since  $(\mathbf{v} \cdot \nabla) \mathbf{v}$  is identically zero for steady incompressible unidirectional flow no matter how large the fluid velocity, and this is clearly in contradiction to experience.

There is a further fundamental objection. In the case of a viscous fluid, a material particle retains its momentum, in the absence of applied forces, when it is displaced from a point A to a neighboring arbitrary point B. But in a porous medium with a fixed solid matrix this is not so, in general, because some solid material impedes the motion and causes a change in momentum. The  $(\mathbf{v} \cdot \nabla) \mathbf{v}$  term is generally small in comparison with the quadratic drag term (see Sect. 1.5.2) and then it seems best to drop it in numerical work. This term needs to be retained in the case of highly porous media. Also, at least the irrotational part of the term needs to be retained in order to account for the phenomenon of choking in high-speed flow of a compressible fluid (Nield 1994b). Nield suggested that the rotational part, proportional to the intrinsic vorticity, be deleted. His argument is based on the expectation that a medium of low porosity will allow scalar entities like fluid speed to be freely advected, but will inhibit the advection of vector quantities like vorticity. It is

now suggested that even when vorticity is being continuously produced (e.g., by buoyancy), one would expect that it would be destroyed by a momentum dispersion process due to the solid obstructions. The claim that the  $(\mathbf{v} \cdot \nabla) \mathbf{v}$  term is necessary to account for boundary layer development is not valid; viscous diffusion can account for this. Formal averaging of the Navier-Stokes equation leads to a  $(\mathbf{v} \cdot \nabla) \mathbf{v}$  term, but this is deceptive. Averaging methods inevitably involve a loss of information with respect to the effects of geometry on the flow.

With the  $(\mathbf{v} \cdot \nabla) \mathbf{v}$  term dropped, Eq. (1.8) becomes

$$\frac{\rho_f}{\phi} \frac{\partial \mathbf{v}}{\partial t} = -\nabla P - \frac{\mu}{K} \mathbf{v}. \quad (1.9)$$

One can now question whether the remaining inertial term (the left-hand side of this equation) is correct. It has been derived on the assumption that the partial derivative with respect to time permutes with a volume average, but in general, this is not valid. The inadequacy of Eq. (1.9) can be illustrated by considering an ideal medium, one in which the pores are identical parallel tubes of uniform circular cross section of radius  $a$ . Equation (1.9) leads to the prediction that in the presence of a constant pressure gradient, any transient will decay like  $\exp[-(\mu\varphi/K\rho_f)t]$ , whereas from the exact solution for a circular pipe (see, e.g., formula (4.3.19) of Batchelor (1967)), one concludes that the transient should decay approximately like  $\exp[-(\lambda_1^2 \mu/a^2 \rho_f)t]$ , where  $\lambda_1 = 2.405$  is the smallest positive root of  $J_0(\lambda) = 0$ , and where  $J_0$  is the Bessel function of the first kind of order zero. In general, these two exponential decay terms will not be the same. It appears that the best that one can do is to replace Eq. (1.9) by

$$\rho_f c_a \cdot \frac{\partial \mathbf{v}}{\partial t} = -\nabla P - \frac{\mu}{K} \mathbf{v}, \quad (1.10)$$

where  $c_a$  is a constant tensor that depends sensitively on the geometry of the porous medium and is determined mainly by the nature of the pore tubes of largest cross sections (since in the narrower pore tubes the transients decay more rapidly). We propose that  $c_a$  be called the “acceleration coefficient tensor” of the porous medium. For the special medium introduced above, in which we have unidirectional flow, the acceleration coefficient will be a scalar,  $c_a = a^2/\lambda_1^2 K$ . If the Carman–Kozeny formula (Eq. 1.5) is valid, and if  $D_{p2}$  can be identified with  $a/\gamma$  where  $\gamma$  is some constant, then

$$c_a = 180\gamma^2(1-\phi)^2/\lambda_1^2\phi^3 = 31.1\gamma^2(1-\phi)^2/\phi^3. \quad (1.11)$$

Liu and Masliyah (2005) present an equation, obtained by volumetric averaging, that does indicate a slower decaying speed than that based on the straight passage model. They also say that the decaying speed is expected to be much faster than that for a medium free from solids, and it is this characteristic that makes the flow in a

porous medium more hydrodynamically stable than that in an infinitely permeable medium and delayed turbulence is expected.

In any case, one can usually drop the time-derivative term completely because in general, the transients decay rapidly. An exceptional situation is when the kinematic viscosity  $v = \mu/\rho_f$  of the fluid is small in comparison with  $K/t_0$  where  $t_0$  is the characteristic time of the process being investigated. This criterion is rarely met in studies of convection. Even for a liquid metal ( $v \sim 10^{-7} \text{ m}^2 \text{ s}^{-1}$ ) and a material of large permeability ( $K \sim 10^{-7} \text{ m}^2$ ), it requires  $t_0 \ll 1 \text{ s}$ . However, it is essential to retain the time-derivative term when modeling certain instability problems: see Vadasz (1999a, b).

For a porous medium in a frame rotating with angular velocity  $\Omega$  with respect to an inertial frame, in Eq. (1.8),  $P$  is replaced by  $P - \rho_f|\Omega \times \mathbf{x}|^2/2$ , where  $\mathbf{x}$  is the position vector, and a term  $\rho_f\Omega \times \mathbf{v}/\varphi$  is added on the left-hand side.

If the fluid is electrically conducting, then in Eq. (1.8)  $P$  is replaced by  $P + |\mathbf{B}|^2/2\mu_m$ , where  $\mathbf{B}$  is the magnetic induction and  $\mu_m$  is the magnetic permeability, and a term  $(\mathbf{B} \cdot \nabla)\mathbf{B}/\varphi \mu_m$  is added to the right-hand side. In most practical cases, the effect of a magnetic field on convection will be negligible, for reasons spelled out in Sect. 6.21.

The solution of the momentum equation and equation of continuity is commonly carried out by using the vector operators div and curl to solve in succession for the rotational and irrotational parts of the velocity field. The accuracy of the numerical solution thus obtained depends on the order of performing the operations. Wooding (2007) showed that taking a certain linear combination of the two solutions produces a solution of optimal accuracy.

### 1.5.2 Quadratic Drag: Forchheimer's Equation

Darcy's equation (1.3) is linear in the seepage velocity  $\mathbf{v}$ . It holds when  $\mathbf{v}$  is sufficiently small. In practice, "sufficiently small" means that the Reynolds number  $Re_p$  of the flow, based on a typical pore or particle diameter, is of order unity or smaller. As  $\mathbf{v}$  increases, the transition to nonlinear drag is quite smooth; there is no sudden transition as  $Re_p$  is increased in the range 1–10. Clearly, this transition is not one from laminar to turbulent flow, since at such comparatively small Reynolds numbers the flow in the pores is still laminar. Rather, the breakdown in linearity is due to the fact that the form drag due to solid obstacles is now comparable with the surface drag due to friction. According to Joseph et al. (1982), the appropriate modification to Darcy's equation is to replace Eq. (1.4) by

$$\nabla P = -\frac{\mu}{K}\mathbf{v} - c_F K^{-1/2} \rho_f |\mathbf{v}| \mathbf{v}, \quad (1.12)$$

where  $c_F$  is a dimensionless form-drag constant. Equation (1.12) is a modification of an equation associated with the names of Dupuit (1863) and Forchheimer (1901);

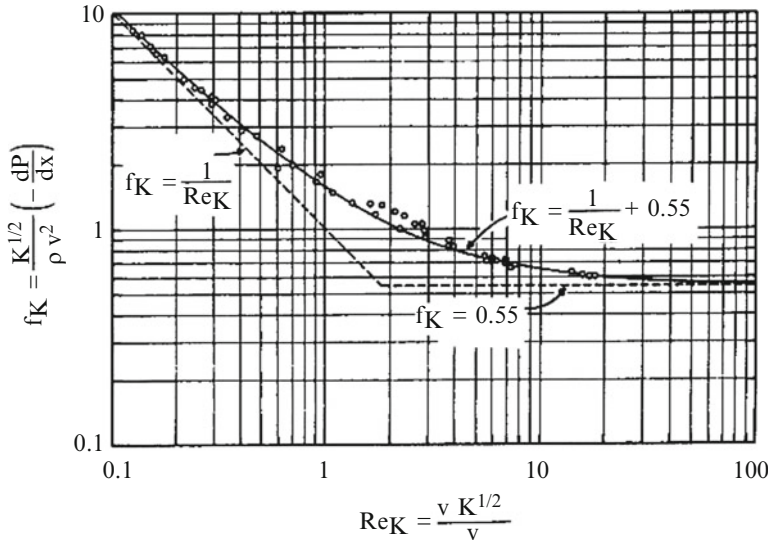


**Fig. 1.3** The transition from the Darcy regime to the Forchheimer regime in unidirectional flow through an isothermal saturated porous medium (Ward 1964)

see Lage (1998). For simplicity, we shall call Eq. (1.12) the Forchheimer equation and refer to the last term as the Forchheimer term, but in fact, the dependence on  $\rho_f K^{-1/2}$  is a modern discovery (Ward 1964). Ward thought that  $c_F$  might be a universal constant, with a value of approximately 0.55, but later it was found that  $c_F$  does vary with the nature of the porous medium, and can be as small as 0.1 in the case of foam metal fibers. Beavers et al. (1973) showed that the bounding walls could have a substantial effect on the value of  $c_F$ , and found that their data correlated fairly well with the expression

$$c_F = 0.55 \left( 1 - 5.5 \frac{d}{D_e} \right), \quad (1.13)$$

where  $d$  is the diameter of their spheres and  $D_e$  is the equivalent diameter of the bed, defined in terms of the height  $h$  and width  $w$  of the bed by

$$D_e = \frac{2wh}{w+h}. \quad (1.14)$$

The numerical calculations of Coulaud et al. (1988) on flow past circular cylinders suggest that  $c_F$  varies as  $\varphi^{-1}$  for  $\varphi$  less than 0.61.

Equation (1.12) is invariant under a rotation of coordinate frame. Kaviany (1995) gives a form for the Forchheimer term (see his Eq. (2.57)), which does not

have this property, and he gives no evidence for his claim that his form is more in accordance with the experimental results.

The transition from the Darcy regime to the Forchheimer regime is illustrated in Fig. 1.3. The data refer to unidirectional isothermal flow with the seepage velocity  $v$  in the direction  $x$ . Plotted on the ordinate is the “friction factor”  $f_K$ , which is based on  $K^{1/2}$  as length scale. The abscissa belongs to the Reynolds number based on  $K^{1/2}$ . Figure 1.3 shows that the transition occurs in the  $Re_K$  range 1–10. At higher Reynolds numbers, the quadratic drag term dominates on the right-hand side of Eq. (1.12), and  $f_K$  becomes the same as  $c_F$ .

Associated with the transition to pore-scale turbulence, the coefficient  $c_F$  varies with velocity. For a *limited range*, one can take  $c_F$  to be linear in velocity. That means that the drag is cubic in velocity. Experiments reported by Lage et al. (1997) show this behavior. Extensive experimental data for flow in packed beds were presented by Achenbach (1995). This sort of cubic variation is distinct from that which occurs for small values of the pore-based Reynolds number. Firdauss et al. (1997) showed that, under fairly general assumptions and for periodic porous media whose period is of the same order as that of the inclusion, the nonlinear correction to Darcy’s law is cubic with respect to the Darcy number. In this case, the quadratic term vanishes. The case of anisotropic media was discussed by Skjetne and Auriault (1999a). However, Lage and Antohe (2000) demonstrated that this mathematically valid cubic extension is irrelevant in practice, and they suggested an alternative parameter, in place of the Reynolds number, to characterize the transition from linearity. A further limit on the applicability of a Forchheimer-type law was noted by Montillet (2004). The validation of Forchheimer’s law for flow through porous media with converging boundaries was discussed by Venkataraman and Rao (2000). An extra term, involving  $|v|^{1/2}v$  (effectively the geometric mean of the two terms on the right-hand side of Eq. (1.12)) was introduced by Hsu and Cheng (1990). They argued that this modification was necessitated by the need to allow for the viscous boundary layer effect at intermediate values of the Reynolds number. The modification is supported by the results of pressure-drop experiments reported by Hsu et al. (1999). However, for practical thermal convection problems, the inclusion of this term in the model leads to relatively little improvement in explanatory power, and so the term is usually neglected.

The transition from Darcy flow (Eq. (1.4)) to Darcy-Forchheimer flow (Eq. (1.12)) occurs when  $Re_K$  is of order  $10^2$ . This transition is associated with the occurrence of the first eddies in the fluid flow, for example, the rotating fluid behind an obstacle or a backward facing step. The order of magnitude  $Re_K \sim 10^2$  is one in a long list of constructal theory results that show that the laminar-turbulent transition is associated with a universal *local Reynolds number* of order  $10^2$  (Bejan 1984, p. 213).

To derive  $Re_K \sim 10^2$  from turbulence, assume that the porous structure is made of three-dimensional random fibers that are so sparsely distributed that  $\varphi \leq 1$ . According to Koponen et al. (1998), in this limit, the permeability of the structure is correlated very well by the expression  $K = 1.39D^2/[e^{10.1(1-\varphi)} - 1]$ , where  $D$  is the fiber diameter. In this limit, the volume-averaged velocity has the same scale as the velocity of the free stream that bathes every fiber. It is well known that vortex

shedding occurs when  $Re_D = uD/v \sim 10^2$  (e.g., Bejan 2000, p. 155). By eliminating  $D$  between the above expressions for  $K$  and  $Re_D$ , we calculate  $Re_K = uK^{1/2}/v$  and find that when eddies begin to appear, the  $Re_K$  value is in the range 100–200 when  $\varphi$  is in the range 0.9–0.99.

Equation (1.12) is the form of Forchheimer's equation that we recommend for use, but for reference, we note that Irmay (1958) derived an alternate equation, for unidirectional flow, of the form

$$\frac{dP}{dx} = -\frac{\beta\mu(1-\phi)^2v}{d_p^2\phi^3} - \frac{\alpha\rho_f(1-\phi)v^2}{d_p\phi^3} \quad (1.15)$$

where  $d_p$  is the mean particle diameter and  $\alpha$  and  $\beta$  are shape factors that must be determined empirically. With  $\alpha = 1.75$  and  $\beta = 150$ , this equation is known as Ergun's equation. The linear terms in Eq. (1.15) and the unidirectional case of Eq. (1.12) can be made identical by writing

$$K = \frac{d_p^2\varphi^3}{\beta(1-\varphi)^2} \quad (1.16)$$

which is Kozeny's equation, but it is not possible at the same time to make the quadratic terms identical, in general. Some authors have forced them to be identical by taking  $c_F = \alpha\beta^{-1/2}\varphi^{-3/2}$ , and they have then used this expression in their numerical computations. It should be appreciated that this is an ad hoc procedure. Either Eq. (1.12) or (1.15) correlates well with available experimental data (see, e.g., Macdonald et al. 1979). A correlation slightly different from that of Ergun was presented by Lee and Ogawa (1994). Papathanasiou et al. (2001) showed that for fibrous material the Ergun equation overpredicts the observed friction factor when the usual Reynolds number (based on the particle diameter) is greater than unity, and they proposed an alternative correlation, based directly on the Forchheimer equation and a Reynolds number based on the square root of the permeability.

For further discussion of the Forchheimer equation, supporting the viewpoint taken here, see Barak (1987) and Hassanizadeh and Gray (1988). They emphasize that the averaging of microscopic *drag forces* leads to a macroscopic nonlinear theory for flow, but the average of microscopic *inertial terms* is negligible in typical practical circumstances. It seems that the need for fluid to flow around solid particles leads to a reduction in the coherence of the fluid momentum pattern, so that on the macroscopic scale there is negligible net transfer of momentum in a direction transverse to the seepage velocity vector. An analytical development based on form drag was given by du Plessis (1994). An analysis of the way in which microscopic phenomena give rise to macroscopic phenomena was presented by Ma and Ruth (1993).

The ratio of the convective inertia term  $\rho\varphi^{-2}(\mathbf{v}\cdot\nabla)\mathbf{v}$  to the quadratic drag term is of order  $K^{1/2}/c_F\varphi^2L$ , where  $L$  is the characteristic length scale. This ratio is normally small, and hence it is expected that the calculations of the heat transfer

which have been made by several authors, who have included both terms in the equation of motion, are not significantly affected by the convective inertia term. This has been confirmed for two cases by Lage (1992) and Manole and Lage (1993). Thus, it is not appropriate to retain the convective inertia term but drop the quadratic drag term.

A momentum equation with a Forchheimer correction was obtained using the method of volume averaging by Whitaker (1996). A generalized Forchheimer equation for two-phase flow based on hybrid mixture theory was proposed by Bennethum and Giorgi (1997). Other derivations have been given by Giorgi (1997) (via matched asymptotic expansions), Chen et al. (2001) (via homogenization), and Levy et al. (1999) (for the case of a thermoelastic medium). A generalized tensor form applicable to anisotropic permeability was derived by Knupp and Lage (1995). An alternative derivation for anisotropic media was given by Wang et al. (1999). An attempt to determine the values of the constants in an Ergun-type equation by numerical simulation for an array of spheres was reported by Nakayama et al. (1995). A reformulation of the Forchheimer equation, involving two Reynolds numbers, was made by Teng and Zhao (2000). Lee and Yang (1997) investigated Forchheimer drag for flow across a bank of circular cylinders. The effective inertial coefficient for a heterogeneous porous medium was discussed by Fourar et al. (2005).

Lage et al. (2005) prefer to work in terms of a form coefficient  $C$  related to  $c_F$  by  $C = c_F L / K^{1/2}$ , where  $L$  is a global characteristic length such as the length of a channel. They introduce a protocol for the determination of  $K$  and  $C$ , using Darcy's law for a porous medium and Newton's law of flow round a bluff body as constitutive equations defining  $K$  and  $C$ , respectively. Their analysis shows that the model equation for measuring  $C$  requires the separation between the viscous-drag effect imposed by the porous medium and the viscous effect of the boundary walls on the measured pressure drop when defining  $K$ . Naakteboren et al. (2012) examined in detail inlet and outlet pressure-drop effects on the determination of permeability and form coefficient. An application to experiments with porous inserts was studied by Wilson et al. (2006).

The structure of the dependence of the Darcy and Forchheimer coefficients on porosity has been examined by Straughan (2010a, b, c). Bussiere et al. (2006) made measurements of these coefficients for silica sand beds. The modeling of form drag in a porous medium saturated by a power-law fluid has been discussed by Nield (2009b) and Tosca et al. (2012). It is recommended that, until further experimental work is carried out, the simple quadratic expression for the form drag be used, on the understanding that the coefficient is not necessarily given by the Ergun formula. Some practical considerations of the application of the Forchheimer equation have been studied by Huang and Ayoub (2008) and Panilov and Fourar (2006).

Care should be taken when modeling high-velocity flow in a heterogeneous medium. Auriault et al. (2007) demonstrated that the Forchheimer law does not generally survive upscaling the flow at the heterogeneity scale where the Forchheimer law is assumed to hold. The macroscopic flow is strongly nonlinear and anisotropic.

### 1.5.3 Brinkman's Equation

An alternative to Darcy's equation is what is commonly known as Brinkman's equation. With inertial terms omitted, this takes the form

$$\nabla P = -\frac{\mu}{K} \mathbf{v} + \tilde{\mu} \nabla^2 \mathbf{v}. \quad (1.17)$$

We now have two viscous terms. The first is the usual Darcy term and the second is analogous to the Laplacian term that appears in the Navier–Stokes equation. The coefficient  $\tilde{\mu}$  is an effective viscosity. Brinkman set  $\mu$  and  $\tilde{\mu}$  equal to each other, but in general, that is not true.

Sometimes, Eq. (1.17) has been referred to as “Brinkman's extension of Darcy's law,” but this is a misleading expression. Brinkman (1947a, b) did not just add another term. Rather, he obtained a relationship between the permeability  $K$  and the porosity  $\varphi$  for an assembly of spheres a “self-consistent” procedure, which is valid only when the porosity is sufficiently large,  $\varphi > 0.6$  according to Lundgren (1972). This requirement is highly restrictive since, as we have noted earlier, most naturally occurring porous media have porosities less than 0.6.

When the Brinkman equation is employed as a general momentum equation, the situation is more complicated. In Eq. (1.17),  $P$  is the intrinsic fluid pressure, so each term in that equation represents a force per unit volume of the *fluid*. A detailed averaging process leads to the result that, for an isotropic porous medium,  $\tilde{\mu}/\mu = 1/\varphi T^*$ , where  $T^*$  is a quantity called the tortuosity of the medium (Bear and Bachmat 1990, p. 177). Thus,  $\tilde{\mu}/\mu$  depends on the geometry of the medium. This result appears to be consistent with the result of Martys et al. (1994), who on the basis of a study in which a numerical solution of the Stokes' equation was matched with a solution of Brinkman's equation for a flow near the interface between a clear fluid and a porous medium, concluded that the value of  $\tilde{\mu}/\mu$  had to exceed unity, and increased monotonically with decreasing porosity. Liu and Masliyah (2005) summarize the current understanding by saying that the numerical simulations have shown that, depending upon the type of porous medium, the effective viscosity may be either smaller or greater than the viscosity of the fluid. On the one hand, straight volume averaging as presented by Ochoa-Tapia and Whitaker (1995a) gives  $\tilde{\mu}/\mu = 1/\varphi$ , greater than unity. On the other hand, analyses such as that by Saez et al. (1991) give  $\tilde{\mu}/\mu$  close to a tortuosity  $\tau$ , defined as  $dx/ds$  where  $s(x)$  is the distance along a curve, a quantity that is less than unity. Liu and Masliyah (2005) suggest that one can think of the difference between  $\tilde{\mu}$  and  $\mu$  as being due to momentum dispersion. They say that it has been generally accepted that  $\tilde{\mu}$  is strongly dependent on the type of porous media as well as the strength of flow. They note that there are further complications if the medium is not isotropic. They also note that it is common practice for  $\tilde{\mu}$  to be taken as equal for  $\mu$  for high porosity cases. This matter has been further examined by Valdes-Parada et al. (2007c), who used employed volume averaging of the Stokes equation with a slip boundary condition.

Experimental checks of Brinkman's theory have been indirect and few in number. Lundgren refers to measurements of flows through cubic arrays of spherical beads on wires, which agree quite well with the Brinkman formula for permeability as a function of porosity. Givler and Altobelli (1994) matched theoretical and observed velocity profiles for a rigid foam of porosity 0.972 and obtained a value of about 7.5 for  $\tilde{\mu}/\mu$ . In our opinion, the Brinkman model is breaking down when such a large value of  $\tilde{\mu}/\mu$  is needed to match theory and experiment. Some preliminary results of a numerical investigation by Gerritsen et al. (2005) suggest that the Brinkman equation is indeed not uniformly valid as the porosity tends to unity.

It was pointed out by Tam (1969) that whenever the spatial length scale is much greater than  $(\tilde{\mu} K/\mu)^{1/2}$ , the  $\nabla^2 v$  term in Eq. (1.17) is negligible in comparison with the term proportional to  $v$ , so that Brinkman's equation reduces to Darcy's equation. Levy (1981) showed that the Brinkman model holds only for particles whose size is of order  $\eta^3$ , where  $\eta (\ll 1)$  is the distance between neighboring particles; for larger particles, the fluid filtration is governed by Darcy's law, and for smaller particles, the flow does not deviate from that for no particles. Durlofsky and Brady (1987), using a Green's function approach, concluded that the Brinkman equation was valid for  $\varphi > 0.95$ . Rubinstein (1986) introduced a porous medium having a very large number of scales, and concluded that it could be valid for  $\varphi$  as small as 0.8.

We conclude that for many practical purposes, there is no need to include the Laplacian term. If it is important that a no-slip boundary condition be satisfied, then the Laplacian term is indeed required, but its effect is significant only in a thin boundary layer whose thickness is of order  $(\tilde{\mu} K/\mu)^{1/2}$ , the layer being thin since the continuum hypothesis requires that  $K^{1/2} \ll L$  where  $L$  is a characteristic macroscopic length scale of the problem being considered. When the Brinkman equation is employed, it usually will be necessary to also account for the effects of porosity variation near the wall (see Sect. 1.7).

There are situations in which some authors have found it convenient to use the Brinkman equation. One such situation is when one wishes to compare flows in porous media with those in clear fluids. The Brinkman equation has a parameter  $K$  (the permeability) such that the equation reduces to a form of the Navier-Stokes equation as  $K \rightarrow \infty$  and to the Darcy equation as  $K \rightarrow 0$ . Another situation is when one wishes to match solutions in a porous medium and in an adjacent viscous fluid. But usage of the Brinkman equation in this way is not without difficulty, as we point out in the following section.

Several authors have added a Laplacian term to Eq. (1.12) to form a "Brinkman-Forchheimer" equation. The validity of this is not completely clear. As we have just seen, in order for Brinkman's equation to be valid, the porosity must be large, and there is some uncertainty about the validity of the Forchheimer law at such large porosity. A scale analysis by Lage (1993a) revealed the distinct regimes in which the various terms in the Brinkman-Forchheimer equation were important or not.

It is possible to derive a Brinkman-Forchheimer equation by formal averaging, but only after making a closure that incorporates some empirical material and that inevitably involves loss of information. Clarifying and correcting earlier work by

Vafai and Tien (1981, 1982), Hsu and Cheng (1990) obtained an equation that in our notation can be written

$$\rho_f \left[ \frac{1}{\varphi} \frac{\partial \mathbf{v}}{\partial t} + \frac{1}{\varphi} \nabla \left( \frac{\mathbf{v} \cdot \mathbf{v}}{\varphi} \right) \right] = -\nabla P + \frac{\mu}{\varphi} \nabla^2 \mathbf{v} - \frac{\mu}{K} \mathbf{v} - \frac{c_F \rho_f}{K^{1/2}} |\mathbf{v}| \mathbf{v} \quad (1.18)$$

For an incompressible fluid,  $\nabla \cdot \mathbf{v} = 0$ , and so  $\varphi^{-1} \nabla(\varphi^{-1} \mathbf{v} \cdot \mathbf{v})$  reduces to  $\varphi^{-1} \mathbf{v} \cdot \nabla(\mathbf{v}/\varphi)$ , and then Eq. (1.21) becomes an easily recognizable combination of Eqs. (1.8), (1.12), and (1.17). The position of the factor  $\varphi$  in relation to the spatial derivatives is important if the porous medium is heterogeneous.

If  $L$  is the appropriate characteristic length scale, the ratio of the last term in Eq. (1.17) to the previous term is of the order of magnitude of  $(\tilde{\mu}/\mu)K/L^2$ , the Darcy number. Authors who assume that  $\tilde{\mu} = \mu$  define the Darcy number to be  $K/L^2$ . The value of  $Da$  is normally much less than unity, but Weinert and Lage (1994) reported a sample of a compressed aluminum foam 1-mm thick, for which  $Da$  was about 8. Nield and Lage (1997) proposed the term "hyperporous medium" for such a material. The flow in their sample was normal to the smallest dimension, and so, unlike in Vafai and Kim (1997), the sample was not similar to a thin screen. When the Brinkman term is comparable with the Darcy term throughout the medium, the  $K$  which appears in Eq. (1.17) can no longer be determined by a simple Darcy-type experiment.

Further work in the spirit of Brinkman has been carried out. For example, Howells (1998) treated flow through beds of fixed cylindrical fibers. Efforts to produce consistency between the Brinkman equation and the lattice Boltzmann method have been reported by Martys (2001). An experimental determination of inertial and viscous contributions in flow in metallic foams was carried out by Madani et al. (2007).

In the case when the fluid is a rarefied gas and the Knudsen number (ratio of the mean free path to a characteristic length) has a large value, velocity slip occurs in the fluid at the pore boundaries. This phenomenon is characteristic of a reduction in viscosity. Hence, in these circumstances one could expect that the Darcy and Brinkman drag terms (the viscous terms) would become insignificant in comparison with the Forchheimer drag term (the form drag term). At very large values of the Knudsen number, a continuum model is not appropriate on the pore scale, but on the REV scale, a continuum model may still be useful.

Various mathematical matters related to stability problems, such as convergence, continuous dependence, and structural stability, for each of the Darcy, Forchheimer, and Brinkman models, have been discussed by Payne and Song (1997, 2000, 2002), Payne and Straughan (1998b, 1999), Payne et al. (1999, 2001), and Song (2002). These discussions have been reviewed by Straughan (2004b). The convergence and continuous dependence for the Brinkman–Forchheimer equations was studied by Liu (2009). Such studies provide assurance that the models are reliable, and so can be used with confidence.

The domain of validity of Brinkman's equation was further examined by Auriault (2009). He concluded that this equation appears to be valid for describing

flows through swarms of fixed particle or fixed beds of fibers at very low concentration, only, and under precise conditions. The effective viscosity is then equal to the viscosity of the fluid. For isotropic and macroscopically homogeneous classical porous media with connected porous matrices, Darcy's law is valid up to a third-order approximation, and for such media, Brinkman's equation has no physical background. The domain of validity of the equation is very restricted. Clear experimental checking is missing. The main difficulty is that are difficult to avoid and the law to describe these (Forchheimer's law) is not exact. There is also a problem involving scaling.

#### 1.5.4 Non-Newtonian Fluid

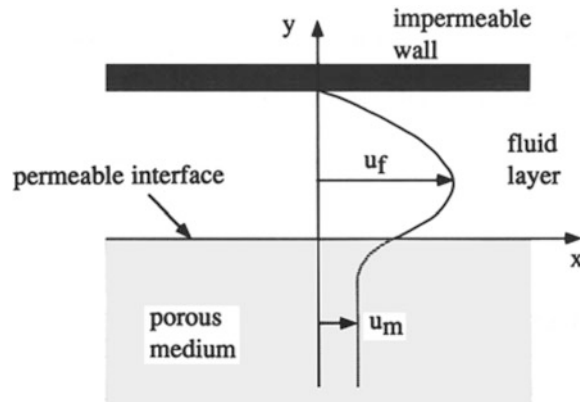
Shenoy (1994) has reviewed studies of flow in non-Newtonian fluids in porous media, with attention concentrated on power-law fluids. He suggested, on the basis of volumetric averaging, that the Darcy term be replaced by  $(\mu^*/K^*)v^{n-1}\mathbf{v}$ , the Brinkman term by  $(\mu^*/\varphi^n)\nabla\{\|0.5\Delta:\Delta\|^{1/2}\}^{n-1}\Delta$  for an Ostwald-de Waele fluid, and the Forchheimer term be left unchanged (because it is independent of the viscosity). Here,  $n$  is the power-law index,  $\mu^*$  reflects the consistency of the fluid,  $K^*$  is a modified permeability, and  $\Delta$  is the deformation tensor. We would replace  $\mu^*$  in the Brinkman term by an equivalent coefficient, not necessarily the same as that in the Darcy term. A similar momentum equation was obtained by Hayes et al. (1996) using volume averaging.

Some wider aspects have been discussed by Shah and Yortsos (1995). Using homogenization theory, they show that the macroscopic power law has the same form as the power law for a single capillary, at low Reynolds numbers (a regime that is reached at low velocities only if  $n < 2$ ). However, the power-law permeability may depend also on the orientation of the pressure gradient. The homogenization method, together with the theory of isotropic tensor function of tensor arguments, was used by Auriault et al. (2002b) to treat anisotropic media. An alternative model was proposed by Liu and Masliyah (1998). Numerical modeling of non-Newtonian fluids in a three-dimensional periodic array was reported by Inoue and Nakayama (1998).

### 1.6 Hydrodynamic Boundary Conditions

In order to be specific, we consider the case where the region  $y < 0$  is occupied by a porous medium, and there is a boundary at  $y = 0$ , relative to Cartesian coordinates  $(x, y, z)$ . If the boundary is impermeable, then the usual assumption is that the normal component of the seepage velocity  $\mathbf{v} = (u, v, w)$  must vanish there, that is,

**Fig. 1.4** Velocity profile for unidirectional flow through a fluid channel bounded by an impermeable wall and a saturated porous medium



$$v = 0 \quad \text{at } y = 0. \quad (1.19)$$

If Darcy's law is applicable, then, since that equation is of first order in the spatial derivatives, only one condition can be applied at a given boundary. Hence, the other components of the velocity can have arbitrary values at  $y = 0$ ; that is, we have slip at the boundary.

If instead of being impermeable the boundary is free (as in the case of a liquid-saturated medium exposed to the atmosphere), then the appropriate condition is that the pressure is constant along the boundary. If Darcy's law is applicable and the fluid is incompressible, this implies that

$$\frac{\partial v}{\partial y} = 0 \quad \text{at } y = 0. \quad (1.20)$$

This conclusion follows because at  $y = 0$ , we have  $P = \text{constant}$  for all  $x$  and  $z$ , so  $\partial P/\partial x = \partial P/\partial z = 0$ , and hence,  $u = w = 0$  for all  $x$  and  $z$ . Hence,  $\partial u/\partial x = \partial w/\partial z = 0$  at  $y = 0$ . Since the equation of continuity

$$\frac{\partial u}{\partial x} + \frac{\partial v}{\partial y} + \frac{\partial w}{\partial z} = 0 \quad (1.21)$$

holds for  $y = 0$ , we deduce the boundary condition (1.20).

If the porous medium is adjacent to clear fluid identical to that which saturates the porous medium, and if there is unidirectional flow in the  $x$  direction (Fig. 1.4), then according to Beavers and Joseph (1967), the appropriate boundary condition is the empirical relationship

$$\frac{\partial u_f}{\partial y} = \frac{\alpha_{BJ}}{K^{1/2}} (u_f - u_m), \quad (1.22)$$

where  $u_f$  is the velocity in the fluid and  $u_m$  is the seepage velocity in the porous medium. It is understood that in Eq. (1.22),  $u_f$  and  $\partial u_f / \partial y$  are evaluated at  $y = 0^+$  and  $u_m$  is evaluated at some small distance from the plane  $y = 0$ , so there is a thin layer just inside the medium over which the transition in velocity takes place.

The quantity  $\alpha_{BJ}$  is dimensionless and is independent of the viscosity of the fluid, but it depends on the material parameters that characterize the structure of the permeable material within the boundary region. In their experiments, Beavers and Joseph found that  $\alpha_{BJ}$  had the values 0.78, 1.45, and 4.0 for Foametal having average pore sizes 0.016, 0.034, and 0.045 in., respectively, and 0.1 for Aloxite with average pore size 0.013 or 0.027 in. More evidence for the correctness of this boundary condition was produced by Beavers et al. (1970, 1974). Some historical details have been recorded by Nield (2009c). Sahraoui and Kaviany (1992) have shown that the value of  $\alpha_{BJ}$  depends on the flow direction at the interface, the Reynolds number, the extent of the clear fluid, and nonuniformities in the arrangement of solid material at the surface.

Some theoretical support for the Beavers–Joseph condition is provided by the results of Taylor (1971) and Richardson (1971), based on an analogous model of a porous medium, and by the statistical treatment of Saffman (1971). Saffman pointed out that the precise form of the Beavers–Joseph condition was special to the planar geometry considered by Beavers and Joseph, and in general was not in fact correct to order  $K$ . Saffman showed that on the boundary

$$u_f = \frac{K^{1/2}}{\alpha_{BJ}} \frac{\partial u_f}{\partial n} + O(K), \quad (1.23)$$

where  $n$  refers to the direction normal to the boundary. In Eq. (1.22),  $u_m$  is  $O(K)$  and thus may be neglected if one wishes.

Jones (1973) assumed that the Beavers–Joseph condition was essentially a relationship involving shear stress rather than just velocity shear, and on this view, Eq. (1.22) would generalize to

$$\frac{\partial u_f}{\partial y} + \frac{\partial v_f}{\partial x} = \frac{\alpha_{BJ}}{K^{1/2}} (u_f - u_m) \quad (1.24)$$

for the situation when  $v_f$  was not zero. This seems plausible, but apparently it has not yet been confirmed. However, Straughan (2004b) has argued that one should give consideration to the Jones version, because it and not the original Beavers–Joseph version is properly invariant under coordinate transformation.

Taylor (1971) observed that the Beavers–Joseph condition can be deduced as a consequence of the Brinkman equation. This idea was developed in detail by Neale and Nader (1974), who showed that in the problem of flow in a channel bounded by a thick porous wall one gets the same solution with the Brinkman equation as one gets with the Darcy equation together with the Beavers–Joseph condition, provided that one identifies  $\alpha_{BJ}$  with  $(\bar{\mu}/\mu)^{1/2}$ .

Near a rigid boundary, the porosity of a bed of particles is often higher than elsewhere in the bed because the particles cannot pack so effectively right at the boundary (see Sect. 1.7). One way of dealing with the channeling effect that can arise is to model the situation by a thin fluid layer interposed between the boundary and the porous medium, with Darcy's equation applied in the medium and with the Beavers–Joseph condition applied at the interface between the fluid layer and the porous medium. Nield (1983) applied this procedure to the porous-medium analog of the Rayleigh–Bénard problem. Alternatively, the Brinkman equation, together with a formula such as Eq. (1.26), can be employed to model the situation.

Haber and Mauri (1983) proposed that the boundary condition  $\mathbf{v} \cdot \mathbf{n} = 0$  at the interface between a porous medium and an impermeable wall should be replaced by

$$\mathbf{v} \cdot \mathbf{n} = K^{1/2} \nabla_t \cdot \mathbf{v}_t, \quad (1.25)$$

where  $\mathbf{v}$  is the velocity inside the porous medium and  $\mathbf{v}_t$  is its tangential component, and where  $\nabla_t$  is the tangential component of the operator  $\nabla$ . Haber and Mauri argue that Eq. (1.25) should be preferred to  $\mathbf{v} \cdot \mathbf{n} = 0$ , since the former accords better with solutions obtained by solving some model problems using Brinkman's equation. For most practical purposes, there is little difference between the two alternatives, since  $K^{1/2}$  will be small compared to the characteristic length scale  $L$  in most situations.

A difficulty arises when one tries to match the solution of Brinkman's equation for a porous medium with the solution of the usual Navier–Stokes equation for an adjacent clear fluid, as done by Haber and Mauri (1983), Somerton and Catton (1982), and subsequent authors. In implementing the continuity of the tangential component of stress, they use equations equivalent to the continuity of  $\mu \partial u / \partial y$  across the boundary at  $y = 0$ . Over the fluid portion of the interface, the clear fluid value of  $\mu \partial u / \partial y$  matches with the intrinsic value of the same quantity in the porous medium, but over the solid portion of the interface, the matching breaks down because there in the clear fluid  $\mu \partial u / \partial y$  has some indeterminate nonzero value while the porous medium value has to be zero. Hence, the average values of  $\mu \partial u / \partial y$  in the clear fluid and in the medium do not match.

Authors who have specified the matching of  $\mu \partial u / \partial y$  have overdetermined the system of equations. This leads to overprediction of the extent to which motion induced in the clear fluid is transmitted to the porous medium. The availability of the empirical constant  $\alpha_{BJ}$  in the alternative Beavers–Joseph approach enables one to deal with the indeterminacy of the tangential stress requirement.

There is a similar difficulty in expressing the continuity of normal stress, which is the sum of a pressure term and a viscous term. Some authors have argued that the pressure, being an intrinsic quantity, has to be continuous across the interface. Since the total normal stress is continuous, that means that the viscous term must also be continuous. Such authors have overdetermined the system of equations. It is true that the pressure has to be continuous on the microscopic scale, but on the macroscopic scale the interface surface is an idealization of a thin layer in which the

pressure can change substantially because of the pressure differential across solid material. In practice, the viscous term may be small compared with the pressure, and in this case, the continuity of total normal stress does reduce to the approximate continuity of pressure. Also, for an incompressible fluid, the continuity of normal stress does reduce to continuity of pressure if one takes the effective Brinkman viscosity equal to the fluid viscosity, as shown by Chen and Chen (1992). Authors who have formulated a problem in terms of stream function and vorticity have failed to deal properly with the normal stress boundary condition (Nield 1997a). For a more soundly based procedure for numerical simulation and for a further discussion of this matter, the reader is referred to Gartling et al. (1996).

Ochoa-Tapia and Whitaker (1995a, b) have expressly matched the Darcy and Stokes equations using the volume-averaging procedure. This approach produces a jump in the stress (but not in the velocity) and involves a parameter to be fitted experimentally. They also explored the use of a variable porosity model as a substitute for the jump condition and concluded that the latter approach does not lead to a successful representation of all the experimental data, but it provides insight into the complexity of the interface region. Kuznetsov (1996a) applied the jump condition to flows in parallel-plate and cylindrical channels partially filled with a porous medium. Kuznetsov (1997b) reported an analytical solution for flow near an interface. Ochoa-Tapia and Whitaker (1998) included inertia effects in a momentum jump condition. Questions about mathematical continuity were discussed by Payne and Straughan (1998a), whose results were improved by Kelliher et al. (2011). Homogenization of wall-slip gas flow was treated by Skjetne and Auriault (1999b). Matching using a dissipation function was proposed by Cieszko and Kubik (1999). Jäger and Mikelić (2000) and Jäger et al. (2001) employed asymptotic analysis to derive matching conditions. Duman and Shavit (2009) showed that the stress-jump could be taken to be zero if one knew the maximum velocity and chose the effective position of the interface accordingly. Deng and Martinez (2005) compared results for one- and two-domain models and found little difference if 1, had a certain value, dependent on the Reynolds and Darcy numbers.

A study of flow in a channel with a fluid layer bounded by a porous layer modeled using the Brinkman equation was made by Rudraiah (1985). Modeling of the interface using a transition layer was introduced by Murdoch and Soliman (1999) and by Goyeau et al. (2003, 2007), and Nield and Kuznetsov (2009c) obtained an analytical solution in closed form of the case where the reciprocal of the permeability varies linearly across a transition layer. Layton et al. (2003) introduced a finite-element scheme that allows the simulation of the coupled problem to be uncoupled into steps involving porous media and fluid flow subproblems. (They also proved existence of weak solutions for the coupled Darcy and Stokes equations.) Numerical treatments of jump conditions include those by Silva and de Lemos (2003a) and Costa et al. (2004a, b). The interfacial region was modeled by Stokes flow in a channel partly filled with an array of circular cylinders beside one wall by James and Davis (2001). Their calculations show that the external flow penetrates the porous medium very little, even for sparse

arrays, with a velocity  $u_m$  about one quarter of that predicted by the Brinkman model. Kubik and Cieszko (2005) employed Lagrange multipliers in their analysis of boundary conditions. Valdes-Parada et al. (2007a, b, 2009a, b) used volume averaging to evaluate momentum jump coefficients. Further numerical work was reported by Discacciati et al. (2002), Miglio et al. (2003a, b), Hanspal et al. (2006), Yu et al. (2007), Siyyam et al. (2007), Chen et al. (2008a), and Costa et al. (2008). The case of heterogeneous porous domains was considered by Das et al. (2005) and Das and Lewis (2007). An investigation using the lattice Boltzmann method was carried out by Bai et al. (2009). A general discussion of one-domain and two-domain models was made by Gobin and Goyeau (2012).

Shavit et al. (2002, 2004) have simulated the interface using a Cantor-Taylor brush configuration to model the porous medium. They also reported the results of particle image velocimetry measurements that showed that the concept of apparent viscosity did not provide a satisfactory agreement. They proposed that the standard Brinkman equation be replaced by a set of three equations.

Salinger et al. (1994a) found that a Darcy-slip finite-element formulation produced solutions that were more accurate and more economical to compute than those obtained using a Brinkman formulation. A further study using a finite-element scheme was reported by Nassehi (1998).

Similar considerations apply at the boundary between two porous media. Conservation of mass requires that the normal component of  $\rho_f v$ , the product of fluid density and seepage velocity, be continuous across the interface. For media in which Darcy's law is applicable only one other hydrodynamic boundary condition can be imposed and that is that the pressure is continuous across the interface. The fluid mechanics of the interface region between two porous layers, one modeled by the Forchheimer equation and the other by the Brinkman equation, were analyzed by Allan and Hamdan (2002).

A range of hydrodynamic and thermal interfacial conditions between a porous medium and a fluid layer were analyzed by Alazmi and Vafai (2001). In general, it is the velocity field that is sensitive to variation in boundary conditions, while the temperature field is less sensitive and the Nusselt number is even less sensitive. Goharzadeh et al. (2005) performed experiments and observed that the thickness of the transition zone is order of the grain diameter, and hence much larger than the square root of the permeability as predicted by some previous theoretical studies. Min and Kim (2005) have used the special two-dimensional model of Richardson (1971) as the basis for an extended analysis of thermal convection in a composite channel.

The homogenization approach has been followed by both Jäger and Mikelić (2009) and Auriault (2010a), who differ the details of their conclusions (see Jäger and Mikelić 2010; Auriault 2010b). The latter states that the experimental conditions of Beavers and Joseph do not show a good separation of scales, and that means that the BJ condition is not transposable to different macroscopic conditions. However, when that separation is good, an intrinsic boundary condition can be obtained using the homogenization technique of multiple scale asymptotic expansions. There is agreement that, as with the Beavers and Joseph approach, the adherence condition of the free fluid is obtained at the first-order approximation, but

according to Auriault, the corrector to the adherence condition is  $O(\varepsilon^2)$ , whereas it is  $O(\varepsilon)$  in the BJ condition, where  $\varepsilon$  is the separation of scales. Auriault notes that an experimental measure of the small corrector is practically out of reach.

Further work on interface conditions has been conducted by Chandesris and Jamet (2006, 2007, 2009a, b), focusing on a transition zone and the upscaling from the mesoscopic to the macroscopic level of description. They emphasized the importance of just where the interface conditions are imposed. The last paper contains a derivation of jump conditions for a turbulence  $k-\varepsilon$  model. Based on a two-step upscaling analysis, Jamet and Chandesris (2009) show that jump parameters can be interpreted as surface-excess quantities, the value of each of which depends linearly on the position of the discontinuous interface and is therefore not an intrinsic property like surface tension. They propose a theoretical approach that allows the introduction of genuine intrinsic interfacial properties, and they propose a best choice for the position of the discontinuous interface. The surface-excess concept was further developed by Chandesris and Jamet (2009c). Zhang and Nepf (2011) reported experimental and numerical work on exchange flow between open water and floating vegetation.

Jamet et al. (2009) showed that the two-domain and discontinuous one-domain approach are equivalent provided that the latter is interpreted in the sense of distributions. In particular, interfacial jumps are introduced in the discontinuous one-domain through Dirac delta functions. Some subtle discretization errors give rise to large variations that can be misinterpreted as the existence of jump parameters.

Carotenuto and Minale (2011) investigated self-similarity in coupled Brinkman/Navier–Stokes flows. They applied their analysis to porous media constituted of patterned cylindrical obstacles modeling a forest, which can freely deflect under the aerodynamic shear exerted by air flowing through and over the forest. A detailed examination of shear flow over a porous layer was made by Chen and Tsao (2012). They applied experimental rheological tests on the velocity profile in proximity to the interface. They found agreement with the prediction of Ochoa-Tapia and Whitaker (1995a, b).

A reexamination of interfacial conditions in the context of binary alloy solidification was made by Bars and Worster (2006). In order to obtain satisfactory agreement between the single- and multi-domain approaches they found it necessary to define a viscous transition zone inside the porous domain, where the Stokes equation still applies, and to impose continuity of pressure and velocities across it. They then found agreement between the two formulations when there is a continuous variation of porosity across the interface between a partially solidified region (mushy zone) and the melt. Nabovati and Amon (2012) applied the lattice-Boltzmann method to simulate the interface with a fibrous medium. Their predicted results were in agreement with both the Beavers-Joseph and Ochoa-Tapia & Whitaker models when appropriate fitting parameters are used.

A situation involving turbulent flow has been examined by Toutant et al. (2009).

Nabovati and Amon (2012) applied the lattice-Boltzmann method to simulate the interface with a fibrous medium. Their predicted results were in agreement with both the Beavers-Joseph and Ochoa-Tapia and Whitaker models when appropriate fitting parameters are used.

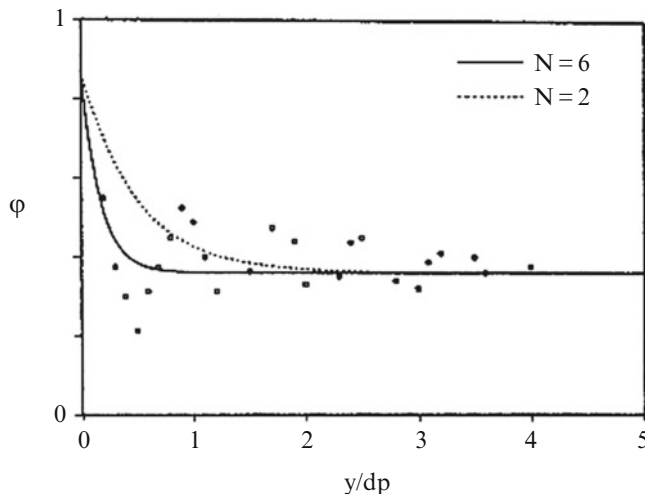


**Fig. 1.5** The variation of porosity near the wall (Cheng et al. 1991, with permission from Kluwer Academic Publishers)

## 1.7 Effects of Porosity Variation

In a porous bed filling a channel or pipe with rigid impermeable walls, there is in general an increase in porosity as one approaches the walls because the solid particles are unable to pack together as efficiently as elsewhere because of the presence of the wall. Experiments have shown that the porosity is a damped oscillatory function of the distance from the wall, varying from a value near unity at the wall to nearly core value at about five diameters from the wall. These oscillations are illustrated by the experimental data (the circles) plotted in Fig. 1.5.

The notion of volume averaging over a r.e.v. breaks down near the wall, and most investigators have assumed a variation of the form (Fig. 1.5).

$$\varphi = \varphi_\infty \left[ 1 + C \exp\left(-N \frac{y}{d_p}\right) \right], \quad (1.26)$$

where  $y$  is the distance from the wall,  $d_p$  is the particle diameter, and  $C$  and  $N$  are empirical constants. Recent experiments have indicated that appropriate values are  $C = 1.4$  and  $N = 5$  or 6 for a medium with  $\varphi_\infty = 0.4$ .

As a consequence of the porosity increase in the vicinity of the wall, the velocity of a flow parallel to the wall increases as the wall is approached and goes through a maximum before it decreases to zero (to satisfy the no-slip condition). In general, this leads to a net increase in volume flux, that is, to the phenomenon called the *channeling effect*.

As Georgiadis and Catton (1987) have pointed out, there also is a more general phenomenon that arises because of porosity variation in association with quadratic drag. To illustrate this, consider the steady fully developed two-dimensional flow through a channel. The unidirectional nondimensional velocity profile  $q(y)$  for flow parallel to the  $x$  axis is the solution of a boundary value problem of the following form (Brinkman–Forchheimer):

$$\frac{d^2q}{dy^2} = \frac{dP}{dx} + Kq + \Lambda|q|q, \quad \text{with } q(\pm 1) = 0. \quad (1.27)$$

The quantities  $K$  and  $\Lambda$  depend on the porosity  $\varphi$  (compare the Irmay-Ergun equation (1.15)). The solution of Eq. (1.27), with the boundary layer term omitted, is

$$q = \frac{(3\alpha)^{1/2}}{\Lambda} - \frac{K}{2\Lambda}, \quad (1.28)$$

where

$$\alpha = -\frac{dP}{dx} \frac{\Lambda}{3} + \frac{K^2}{12}. \quad (1.29)$$

The mean flow rate over the channel cross section is given by the spatial average of Eq. (1.27), and assuming statistical homogeneity, this is equivalent to an ensemble average with  $\varphi$  as the variable. It is easily shown that the function  $q(\varphi)$  of the random variable  $\varphi$  is convex in the interval  $[0,1]$  if the Ergun relationships hold. This implies that for the same pressure gradient along the channel the mean flux is larger when there is a spatial variation of porosity:  $\bar{q}(\phi) > q(\bar{\phi})$ . This means that if we use the average value  $\bar{\varphi}$  of the porosity, we obtain only a lower bound for the flow rate through the packed bed. Georgiadis and Catton (1987) found that in one realistic case  $\bar{q}(\phi)$  could be 9 % greater than  $q(\bar{\phi})$ . Pressure-drop/flow rate measurements therefore would give an effective value for the permeability greater than that otherwise expected. Fu and Huang (1999) showed that random porosity led to a negative correlation between local Nusselt number and near-wall local porosity.

Sakamoto and Kulacki (2008) have examined the effective thermal diffusivity of porous media in the vicinity of a wall.

## 1.8 Turbulence in Porous Media

The nonlinear spectral analysis of Rudraiah (1988) was based on a Brinkman model valid for high porosity only, and so is of questionable use for media in which the solid material inhibits the formation of macroscopic eddies. Masuoka and Takatsu (1996) used a volume averaging procedure to produce a zero-equation model. Nield

(1997c) questioned their basic assumption that the Forchheimer flow resistance and dispersion are caused mainly by turbulent mixing, and that the drag force caused by the molecular stress can be equated to the Darcy term alone. Takatsu and Masuoka (1998) and Masuoka and Takatsu (2002) have further developed their model and have conducted experiments on flow through banks of tubes. They have persisted with their faulty assumption, based on the assumption that the deviation from Darcy's law appears at the same value of the Reynolds number (based on a characteristic particle diameter) as that at which turbulent vortices appear. Nield (1997c) pointed out that the experimental work on which Masuoka and Takatsu relied in fact indicates otherwise. More recent experiments have been conducted by Seguin et al. (1998).

Travkin and Catton (1994, 1995, 1998, 1999), Gratton et al. (1996) and Catton and Travkin (1996) have developed general models in which the solid-phase morphology is emphasized. They have not related their models to critical experiments, and so it is not clear that this refinement is justified from a practical point of view.

Lee and Howell (1991) performed extensive numerical calculations, of forced convective heat transfer from a heated plate, using a volume-averaged  $\kappa$ - $\epsilon$  model. The  $\kappa$ - $\epsilon$  model of Antohe and Lage (1997b), which is more general than the ones introduced by Lee and Howell (1987) and Prescott and Incropera (1995), is promising from a practical aspect. Their analysis leads to the conclusion that, for a medium of small permeability, the effect of the solid matrix is to damp the turbulence, as one would expect. This analysis was further extended by Getachew et al. (2000). Further work with a  $\kappa$ - $\epsilon$  model was reported by Chen et al. (1998a, b) and by Laakkonen (2003). Modeling with one energy equation was performed by Chung et al. (2003). Numerical modeling of composite porous-medium/clear-fluid ducts has been reported by Kuznetsov and Xiong (2003), Kuznetsov (2004a), and Yang and Hwang (2003).

Kuwahara et al. (1996) performed numerical modeling of the turbulent flow within the pores of a porous medium using a spatially periodic array, and obtained some macroscopic characteristics of that flow. Note that this is different from turbulence on a macroscopic scale, because the period length in the simulations (something that is representative of the pore scale) provides an artificial upper bound on the size of the turbulent eddies that can be generated. This was pointed out by Nield (2001b). Further numerical modeling using periodic arrays was conducted by Kuwahara and Nakayama (1998), Kuwahara et al. (1998), Nakayama and Kuwahara (1999, 2000), and Nakayama et al. (2004).

In his discussion of transition to turbulence, Lage (1998) has noted the difference in pressure-drop versus flow-speed relationship between the case of a porous medium that behaves predominantly like an aggregate of conduits (characterized by a balance between pressure drop and viscous diffusion) and the case of a medium that behaves like an aggregate of bluff bodies (characterized by a balance between pressure drop and form drag).

An alternative approach has been extensively developed by de Lemos and coworkers: de Lemos (2004) (review), de Lemos and Braga (2003), de Lemos

and Mesquita (2003), de Lemos and Pedras (2000, 2001), Rocamora and de Lemos (2000), de Lemos and Rocamora (2002), de Lemos and Tofaneli (2004), Pedras and de Lemos (2000, 2001a, b, c, 2003), and Silva and de Lemos (2003b). It is based on volume averages and a double decomposition concept involving both spatial deviations and time fluctuations. To a limited extent, this approach unifies the work of Masuoka, Takatsu, Nakayama, and Kuwahara (who applied a time average followed by a volume average) and Lage and his coworkers and predecessors (who applied the two averages in the opposite order).

Simplified models for turbulence in porous media, or related systems such as vegetation, have been presented by Wang and Takle (1995), Nepf (1999), Macedo et al. (2001), Hoffman and van der Meer (2002), Flick et al. (2003), and Alvarez et al. (2003).

Work on the topic of this section has been reviewed by Lage et al. (2002). A related paper is the study of hydrodynamic stability of flow in a channel or duct occupied by a porous medium by Nield (2003). As one would expect from the conclusions of Antohe and Lage (1997b) cited above, for such flows the critical Reynolds number for the onset of linear instability is very high. Darcy drag, Forchheimer drag, and additional momentum dispersion all contribute to a flattening of the velocity profile in a channel, and thus to increased stability. Also contributing to increased stability is the rapid decay with time noted in Sect. 1.5.1. Work to date indicates that turbulence changes the values of drag coefficients from their laminar flow values but does not qualitatively change convective flows in porous media except when the porosity is high. Further reviews of turbulence in porous media have been made by Vafai et al. (2006a, b) and de Lemos (2005c).

Further numerical modeling using periodic arrays was conducted by Kuwahara and Nakayama (1998), Kuwahara et al. (2006), Nakayama and Kuwahara (1999, 2000, 2005, 2008), and Nakayama et al. (2004). Studies of turbulence in relation to the interface between a porous medium and a clear fluid region have been made by de Lemos (2005b), Assato et al. (2005), and Zhu and Kuznetsov (2005).

Additional work on turbulence in porous media has been reported by Braga and de Lemos (2006, 2008, 2009), Chandesris et al. (2006), de Lemos (2008, 2009), de Lemos and Dorea (2011), de Lemos and Fischer (2008), de Lemos and Saito (2008), de Lemos and Silva (2006), Dorea and de Lemos (2010), Pinson et al. (2006, 2007), and Saito and de Lemos (2006, 2009, 2010). Much of this work has been summarized in the book by de Lemos (2012a, b).

## 1.9 Fractured Media, Deformable Media, and Complex Porous Structures

The subject of flow in fractured media is an important one in the geological context. In addition to continuum models, discrete models have been formulated. In these models, Monte Carlo simulations and various statistical methods are employed, and

the concepts of percolation processes, universal scaling laws, and fractals are basic tools. These matters are discussed in detail by Barenblatt et al. (1990) and Sahimi (1993, 1995). The lattice Boltzmann method is widely employed; see, for example, Maier et al. (1998).

Likewise, little research has been done yet on convection with deformable porous media, although some thermoelastic aspects of this subject have been studied. For example, dual-porosity models (involving two overlapping continua) have been developed by Bai and Roegiers (1994) and Bai et al. (1994a, b, 1996). Another exception is the discussion of the flow over and through a layer of flexible fibers by Fowler and Bejan (1995). Some flows in media formed by porous blocks separated by fissures have been studied by Levy (1990) and Royer et al. (1995), who employed a homogenization method, and also by Lage (1997). There is one published study of convection in a saturated fissured medium, that by Kulacki and Rajen (1991). This paper contains a useful review, an experimental study of heat transfer in an idealized fissured medium, and supporting numerical work. They conclude that one interconnected fissure in every one tenth of the domain is sufficient for an equivalence between a saturated fissure system and a porous medium, and that the assumption that a fissured system can be treated as a porous medium leads to an overestimate (i.e., an upper bound) for the heat transfer.

It is likely that in the future, an increasing use of numerical simulation will be used in the study of complex porous structures, such as geological structures. An interesting development is the finite-element program that has been used by Joly et al. (1996) to study the onset of free convective and the stability of two-dimensional convective solutions to three-dimensional perturbations. Further numerical studies have been reported by Ghorayeb and Firoozabadi (2000a, b, 2001) and by Saghir et al. (2001).

Biological applications have motivated the investigation of other phenomena related to convection in porous media. Khaled and Vafai (2003) surveyed some investigations of diffusion processes within the brain, diffusion during tissue generation, applications of magnetic resonance to the categorization of tissue properties, blood flow in tumors, blood flow in perfusion tissues, bioheat transfer in tissues, and bioconvection. Lage et al. (2004a) have used a porous medium model to investigate the red cell distribution effect on alveolar respiration. Ghosh et al. (2011) used a porous medium model to discuss drug delivery in interior carcinoma.

A model of a bidisperse porous medium proposed by Nield and Kuznetsov (2005c) is discussed in Sect. 4.16.5.

# Chapter 2

## Heat Transfer Through a Porous Medium

### 2.1 Energy Equation: Simple Case

In this chapter we focus on the equation that expresses the first law of thermodynamics in a porous medium. We start with a simple situation in which the medium is isotropic and where radiative effects, viscous dissipation, and the work done by pressure changes are negligible. Very shortly we shall assume that there is local thermal equilibrium so that  $T_s = T_f = T$ , where  $T_s$  and  $T_f$  are the temperatures of the solid and fluid phases, respectively. Here we also assume that heat conduction in the solid and fluid phases takes place in parallel so that there is no net heat transfer from one phase to the other. More complex situations will be considered in Sect. 6.5. The fundamentals of heat transfer in porous media are also presented in Bejan et al. (2004) and Bejan (2004a).

Taking averages over an elemental volume of the medium we have, for the solid phase,

$$(1 - \varphi)(\rho c)_s \frac{\partial T_s}{\partial t} = (1 - \varphi)\nabla \cdot (k_s \nabla T_s) + (1 - \varphi)q''_s \quad (2.1)$$

and, for the fluid phase,

$$\varphi(\rho c_P)_f \frac{\partial T_f}{\partial t} + (\rho c_P)_f \mathbf{v} \cdot \nabla T_f = \varphi \nabla \cdot (k_f \nabla T_f) + \varphi q'''_f. \quad (2.2)$$

Here the subscripts  $s$  and  $f$  refer to the solid and fluid phases, respectively,  $c$  is the specific heat of the solid,  $c_P$  is the specific heat at constant pressure of the fluid,  $k$  is the thermal conductivity, and  $q'''(\text{W/m}^3)$  is the heat production per unit volume.

In writing Eqs. (2.1) and (2.2) we have assumed that the surface porosity is equal to the porosity. This is pertinent to the conduction terms. For example,  $-k_s \nabla T_s$  is the conductive heat flux through the solid, and thus  $\nabla \cdot (k_s \nabla T_s)$  is the net rate of heat conduction into a unit volume of the solid. In Eq. (2.1) this appears multiplied by

the factor  $(1 - \varphi)$ , which is the ratio of the cross-sectional area occupied by solid to the total cross-sectional area of the medium. The other two terms in Eq. (2.1) also contain the factor  $(1 - \varphi)$  because this is the ratio of volume occupied by solid to the total volume of the element. In Eq. (2.2) there also appears a convective term, due to the seepage velocity. We recognize that  $\mathbf{V} \cdot \nabla T_f$  is the rate of change of temperature in the elemental volume due to the convection of fluid into it, so this, multiplied by  $(\rho c_p)_f$ , must be the rate of change of thermal energy, per unit volume of fluid, due to the convection. Note further that in writing Eq. (2.2) use has been made of the Dupuit-Forchheimer relationship  $\mathbf{v} = \varphi \mathbf{V}$ .

Setting  $T_s = T_f = T$  and adding Eqs. (2.1) and (2.2) we have

$$(\rho c)_m \frac{\partial T}{\partial t} + (\rho c)_f \mathbf{v} \cdot \nabla T = \nabla \cdot (k_m \nabla T) + q''_m, \quad (2.3)$$

where

$$(\rho c)_m = (1 - \varphi)(\rho c)_s + \varphi(\rho c_p)_f, \quad (2.4)$$

$$k_m = (1 - \varphi)k_s + \varphi k_f, \quad (2.5)$$

$$q''_m = (1 - \varphi)q''_s + \varphi q''_f \quad (2.6)$$

are, respectively, the overall heat capacity per unit volume, overall thermal conductivity, and overall heat production per unit volume of the medium.

## 2.2 Energy Equation: Extensions to More Complex Situations

### 2.2.1 Overall Thermal Conductivity of a Porous Medium

In general, the overall thermal conductivity of a porous medium depends in a complex fashion on the geometry of the medium. As we have just seen, if the heat conduction in the solid and fluid phases occurs in parallel, then the overall conductivity  $k_A$  is the weighted arithmetic mean of the conductivities  $k_s$  and  $k_f$ :

$$k_A = (1 - \varphi)k_s + \varphi k_f. \quad (2.7)$$

On the other hand, if the structure and orientation of the porous medium is such that the heat conduction takes place in series, with all of the heat flux passing through both solid and fluid, then the overall conductivity  $k_H$  is the weighted harmonic mean of  $k_s$  and  $k_f$ :

$$\frac{1}{k_H} = \frac{1 - \varphi}{k_s} + \frac{\varphi}{k_f}. \quad (2.8)$$

In general,  $k_A$  and  $k_H$  will provide upper and lower bounds, respectively, on the actual overall conductivity  $k_m$ . We always have  $k_H \leq k_A$ , with equality if and only if  $k_s = k_f$ . For practical purposes, a rough and ready estimate for  $k_m$  is provided by  $k_G$ , the weighted geometric mean of  $k_s$  and  $k_f$ , defined by

$$k_G = k_s^{1-\varphi} k_f^\varphi. \quad (2.9)$$

This provides a good estimate so long as  $k_s$  and  $k_f$  are not too different from each other (Nield 1991b). More complicated correlation formulas for the conductivity of packed beds have been proposed. Experiments by Prasad et al. (1989b) showed that these formulas gave reasonably good results provided that  $k_f$  was not significantly greater than  $k_s$ . The agreement when  $k_f \gg k_s$  was not good, the observed conductivity being greater than that predicted. This discrepancy may be due to porosity variation near the walls. Since  $k_m$  depends on  $\varphi$  there is an effect analogous to the hydrodynamic effect already noted in Sect. 1.7. Some of the discrepancy may be due to the difficulty of measuring a truly stagnant thermal conductivity in this case (Nield 1991b).

In the case when the fluid is a rarefied gas and the Knudsen number has a large value, temperature slip occurs in the fluid at the pore boundaries. In these circumstances one could expect that the fluid conductivity would tend to zero as the Knudsen number increases. Then in the case of external heating the heat would be conducted almost entirely through the solid matrix. In the case of just internal heating in the fluid, the situation is reversed as the fluid phase becomes thermally isolated from the solid phase.

Further models for stagnant thermal conductivity have been put forward by Hsu et al. (1994, 1995), Cheng et al. (1999), and Cheng and Hsu (1998, 1999). In particular, Cheng et al. (1999), and also Hsu (2000), contain comprehensive reviews of the subject. Volume averaging was used by Buonanno and Carotenuto (1997) to calculate the effective conductivity taking into account particle-to-particle contact. Experimental studies have been made by Imadojemu and Porter (1995) and Tavman (1996). The former concluded that the thermal diffusivity and conductivity of the fluid played the major role in determining the effective conductivity of the medium. Hsu (1999) presented a closure model for transient heat conduction, while Hsiao and Advani (1999) included the effect of heat dispersion. Hu et al. (2001) discussed unconsolidated porous media, Paek et al. (2000) dealt with aluminum foam materials, and Fu et al. (1998) studied cellular ceramics. Boomsma and Poulikakos studied the effective thermal conductivity of a three-dimensionally structured fluid-saturated metal foam. Carson et al. (2005) obtained thermal conductivity bounds for isotropic porous materials.

A unified closure model for convective heat and mass transfer has been presented by Hsu (2005). He notes that r.e.v. averaging leads to the introduction of new unknowns (dispersion, interfacial tortuosity, and interfacial transfer) whose determination constitutes the closure problem. More experiments are needed to determine some of the coefficients that are involved. His closure relation for the

interfacial force contains all the components due to drag, lift, and transient inertia to the first-order approximation. He concludes that the macroscopic energy equations are expected to be valid for all values of the time scale and Reynolds number, for the case of steady flows. Further investigations are needed for unsteady flows.

So far we have been discussing the case of an isotropic medium, for which the conductivity is a scalar. For an anisotropic medium  $k_m$  will be a second-order tensor. Lee and Yang (1998) modeled a heterogeneous anisotropic porous medium.

A fundamental issue has been raised by Merrikh et al. (2002, 2005a, b) and Merrikh and Lage (2005). This is the question of how the internal regularity of a solid/fluid physical domain affects global flow and heat transfer. These authors have considered a situation (a regular distribution of rectangular solid obstacles in a rectangular box) that is sufficiently simple for a comparison to be made between the results of numerical modeling involving a treatment of the fluid and solid phases considered separately (“continuum model”) and a standard r.e.v.-averaged porous medium (“porous continuum model”). The results for the two models can be substantially different. In other words, the internal regularity can have an important effect. The authors considered situations where the obstacles were separated from the boundary walls, and thus some of the difference is due to a channeling effect. Further contributions have been made by Braga and de Lemos (2005a, b).

The effective thermal conductivity of rough spherical packed beds was studied by Bahrami et al. (2006). Two effective conductivity models for porous media composed of hollow spherical agglomerates were proposed by Yu et al. (2006a). A collocated parameter model was employed by Reddy and Karhikeyan (2009) to estimate the effective thermal conductivity of two-phase materials, a subject also studied by Samantray et al. (2006).

Works on the effective thermal conductivity of saturated porous media have been surveyed by Aichlmayr and Kulacki (2006).

The analogy between dual-phase-lagging and porous-medium conduction was discussed by Wang et al. (2008d). The analogy permits existence, uniqueness, and structural stability results established for the former to be applied to the latter.

A comprehensive review of various models for the effective conductivity was made by Singh (2011), who pointed out that this quantity was dependent not only on the conductivities and volume fractions of the constituents, the morphology of the constituent particles, and the structure of the material but also on interphase interactions. Qu et al. (2012a) introduced an octet-truss lattice unit cell model.

### 2.2.2 Effects of Pressure Changes and Viscous Dissipation

If the work done by pressure changes is not negligible (i.e., the condition  $\beta T(g\beta/c_{pf})L \ll 1$  is not met), then a term  $-\beta T(\partial P/\partial t + \mathbf{v} \cdot \nabla P)$  needs to be added to the left-hand side of Eq. (2.3). Here  $\beta$  is the coefficient of volumetric thermal expansion, defined by

$$\beta = -\frac{1}{\rho} \left( \frac{\partial \rho}{\partial T} \right)_P. \quad (2.10)$$

Viscous dissipation is negligible in natural convection if  $(g\beta/c_P)T \ll 1$ , which is usually the case. If it is not negligible, another term must be added to the right-hand side of Eq. (2.3), as noted first by Ene and Sanchez-Palencia (1982). If Darcy's law holds, that term is  $(\mu/K)\mathbf{v}\cdot\mathbf{v}$  in the case of an isotropic medium, and  $\mu\mathbf{v}\cdot\mathbf{K}^{-1}\cdot\mathbf{v}$  if the medium is anisotropic. To see this, note that the average of the rate of doing work by the pressure, on a unit volume of an r.e.v., is given by the negative of  $\operatorname{div}(P\varphi\mathbf{V}) = \operatorname{div}(P\mathbf{v}) = \mathbf{v}\cdot\operatorname{grad} P$ , since  $\operatorname{div} \mathbf{v} = 0$ . The Forchheimer drag term, dotted with the velocity vector, contributes to the dissipation, despite the fact that the viscosity does not enter explicitly. This apparent paradox was resolved by Nield (2000). The contribution of the Brinkman drag term is currently a controversial topic. Nield (2004b) proposed that the Brinkman term be treated in the same way as the Darcy and Forchheimer terms, so that the total viscous dissipation remains equal to the power of the total drag force. Thus the viscous dissipation  $\varphi$  would then be modeled by

$$\varphi = \frac{\mu}{K} \mathbf{v} \cdot \mathbf{v} + \frac{c_P}{K^{1/2}} |\mathbf{v}|_P \mathbf{v} \cdot \mathbf{v} - \tilde{\mu} \mathbf{v} \cdot \nabla^2 \cdot \mathbf{v}. \quad (2.11)$$

Al-Hadhrami et al. (2003) prefer a form that remains positive and reduces to that for a fluid clear of solid material in the case where the Darcy number tends to infinity. Accordingly, they would add the usual clear fluid term to the Darcy and Forchheimer terms. Nield (2004b) suggested that the Brinkman equation may break down in this limit. In most practical situations the Brinkman term will be small compared with the Darcy term, and so the form of the Brinkman term is then not important. Additional discussion of viscous dissipation in porous media and the validity of the Brinkman equation can be found in Salama (2011a), who included an additional term involving the gradient of the porosity. Salama et al. (2012) compared the effects of various terms on boundary layer flow on a vertical wall.

Nield (2000) noted that scale analysis, involving the comparison of the magnitude of the viscous dissipation term to the thermal diffusion term, shows that viscous dissipation is negligible if  $N \ll 1$ , where  $N = \mu U^2 L^2 / K k_m \Delta T = Br/Da$ , where the Brinkman number is defined by  $Br = \mu U^2 / k_m \Delta T = EcPr$ , where the Eckert number  $Ec$  is defined by  $Ec = U^2 / c_P \Delta T$ . For most situations the Darcy number  $K/L^2$  is small, so viscous dissipation is important at even modest values of the Brinkman number. For forced convection the choice of the characteristic velocity is obvious. For natural convection, scale analysis leads to the estimate  $U \sim (k_m / \rho c_P L) Ra^{1/2}$  and the condition that viscous dissipation is negligible becomes  $Ge = 1$ , where  $Ge$  is the Gebhart number defined by  $Ge = g\beta L / c_P$ . The above comments on forced convection are made on the assumption that the Péclet number  $Pe = \rho c_P UL / k_m$  is not large. If it is large, then the proper comparison is one between the magnitudes of the viscous dissipation term and the convective transport term. This ratio is of order  $Ec/DaRe$ , where the Reynolds number

$Re = \rho UL/\mu$ . Further aspects of the effects of viscous dissipation on the flow in porous media are discussed in the survey by Magyari et al. (2005b).

The question of how the viscous dissipation relates to the pressure work and other non-Boussinesq effects has been the subject of considerable discussion by Costa (2009, 2010), Nield (2007b, 2009a), Barletta (2008), and Nield and Barletta (2010a). Costa argued that the first law of thermodynamics required that the contributions of viscous dissipation and pressure work had to be in balance. Nield and Barletta argued that Costa had misapplied the first law to an unsteady problem which he treated as a steady-state one, and that there are physical situations where the viscous dissipation is significant and the pressure work is not significant.

### 2.2.3 Absence of Local Thermal Equilibrium

Usually it is a good approximation to assume that the solid and fluid phases are in thermal equilibrium but there are situations, such as highly transient problems and some steady-state problems (Nield 1998a), where this is not so. Now this is commonly referred to as local thermal nonequilibrium (LTNE), though Vadasz (2005a, b) prefers the expression lack of thermal equilibrium.

If one wishes to allow for heat transfer between solid and fluid (that is, one no longer has local thermal equilibrium), then one can, following Combarous (1972) and Bories (1987), replace Eqs. (2.1) and (2.2) by

$$(1 - \varphi)(\rho c)_s \frac{\partial T_s}{\partial t} = (1 - \varphi) \nabla \cdot (k_s \nabla T_s) + (1 - \varphi) q_s''' + h(T_f - T_s), \quad (2.12)$$

$$\varphi(\rho c_p)_f \frac{\partial T_f}{\partial t} + (\rho c_p)\mathbf{v} \cdot \nabla T_f = \varphi \nabla \cdot (k_f \nabla T_f) + \varphi q_f''' + h(T_s - T_f), \quad (2.13)$$

where  $h$  is a heat transfer coefficient. See also Eqs. (2.12a) and (2.13a) later in this section. A critical aspect of using this approach lies in the determination of the appropriate value of  $h$ . Experimental values of  $h$  are found in an indirect manner; see, e.g., Polyaev et al. (1996). According to correlations for a porous bed of particle established in Dixon and Cresswell (1979),

$$h = a_{fs} h^*, \quad (2.14)$$

where the specific surface area (surface per unit volume)  $a_{fs}$  is given by

$$a_{fs} = 6(1 - \varphi)/d_p, \quad (2.15)$$

and

$$\frac{1}{h^*} = \frac{d_p}{\text{Nu}_{fs} k_f} + \frac{d_p}{\beta k_s} \quad (2.16)$$

where  $d_p$  is the particle diameter and  $\beta = 10$  if the porous bed particles are of spherical form. The fluid-to-solid Nusselt number  $\text{Nu}_{fs}$  is, for Reynolds numbers (based on  $d_p$ )  $Re_p > 100$ , well correlated by the expression presented in Handley and Heggs (1968):

$$\text{Nu}_{fs} = (0.255/\varphi) Pr^{1/3} Re_p^{2/3}, \quad (2.17)$$

while for low values of  $Re_p$  the estimates of  $\text{Nu}_{fs}$  vary between 0.1 and 12.4, these being based on Miyauchi et al. (1976) and Wakao et al. (1976, 1979). As an alternative to Eq. (2.17), Wakao and Kaguei (1982) proposed the correlation

$$\text{Nu}_{fs} = 2.0 + 1.1 Pr^{1/3} Re_p^{0.6} (\varphi d_p/d_h)^{0.6} \quad (2.17a)$$

Here  $d$  is the pore-scale hydraulic diameter.

Other authors have used alternative expressions for  $h^*$  and  $a_{fs}$  and some of these were considered by Alazmi and Vafai (2000), who found that the various models give closely similar results for forced convection channel flow when the porosity is high or the pore Reynolds number is large or the particle diameters are small. Theoretical and experimental results reported by Grangeot et al. (1994) indicate that  $h^*$  depends weakly on the Péclet number of the flow. This subject is discussed further in Sects. 6.5 and 6.9.2. The topic in the context of turbulence has been discussed by Saito and de Lemos (2005). An experimental study for a metallic packed bed was reported by Carrillo (2005). The effect of different packings was investigated experimentally by Yang et al. (2012b). They found that the formula in Eq. (2.17a) over-predicted their results unless the coefficients 2.0 and 1.1 were replaced by smaller values.

A discussion of further aspects of the two-medium approach to heat transfer in porous media is given by Quintard et al. (1997) and Quintard and Whitaker (2000). Nield (2002a) noted that Eqs. (2.12) and (2.13) are based on the implicit assumption that the thermal resistances of the fluid and solid phases are in series. For the case of a layered medium in a parallel plate channel with fluid/solid interfaces parallel to the  $x$ -direction, he suggested that the appropriate equations in the absence of internal heating are

$$(1 - \varphi) (\rho c)_s \frac{\partial T_s}{\partial t} = (1 - \varphi) \left[ \frac{\partial}{\partial x} \left( k'_s \frac{\partial T_s}{\partial x} \right) + \frac{\partial}{\partial y} \left( k_s \frac{\partial T_s}{\partial y} \right) \right] + h (T_f - T_s), \quad (2.12a)$$

$$\varphi(\rho c_p)_f \frac{\partial T_f}{\partial t} + (\rho c_p) \mathbf{v} \cdot \nabla T_f = \varphi \left[ \frac{\partial}{\partial x} \left( k'_f \frac{\partial T_f}{\partial x} \right) + \frac{\partial}{\partial y} \left( k_f \frac{\partial T_f}{\partial y} \right) \right] + h(T_s - T_f), \quad (2.13a)$$

where  $k'_f = k'_s = k_H$  with  $k_H$  given by Eq. (2.8). Equations (2.12) and (2.13) have to be solved subject to certain applied thermal boundary conditions. If a boundary is at uniform temperature, then one has  $T_f = T_s$  on the boundary. If uniform heat flux is imposed on the boundary, then there is some ambiguity about the distribution of flux between the two phases. Nield and Kuznetsov (1999) argued that if the flux is truly uniform, then it has to be uniform with respect to the two phases, and hence the flux on the r.e.v. scale has to be distributed between the fluid and solid phases in the ratio of the surface fractions; for a homogeneous medium that means in the ratio of the volume fractions, that is in the ratio  $\varphi : (1 - \varphi)$ . This distribution allows the conjugate problem considered by them to be treated in a consistent manner. The consequences of other choices for the distribution were explored by Kim and Kim (2001) and Alazmi and Vafai (2002). The Nield and Kuznetsov (1999) approach is equivalent to Model 1D in Alazmi and Vafai (2002) and is not equivalent to either approach used in Kim and Kim (2001).

The particular case of LTNE in a steady process is discussed by Nield (1998a). Petit et al. (1999) have proposed an LTNE model for two-phase flow. A numerical study of the interfacial convective heat transfer coefficient was reported by Kuwahara et al. (2001). Their results were modified by Pallares and Grau (2010) to produce agreement between the theoretical results for the Nusselt number and experimental data. An application of the method of volume averaging to the analysis of heat and mass transfer in tubes was made by Golfier et al. (2002). An alternative two-equation model for conduction only was presented by Fourie and Du Plessis (2003a, b). Vadasz (2005a) demonstrated that, for heat conduction problems, local thermal equilibrium applies for any conditions that are a combination of constant temperature and insulation. He also questioned whether a linear relationship between the average temperature difference between the phases and the heat transferred over the fluid–solid surface was appropriate in connection with conditions of LTNE. The exclusion of oscillations in the context of conduction with LTNE and an associated paradox were discussed by Vadasz (2005b, 2006b, 2007). (The apparent paradox arises in trying to reconcile the results from two alternative mathematical approaches to modeling the problem.) This work is surveyed by Vadasz (2008b), who also shows the relevance of LTNE to the study of nanofluids and bi-composite media, as well as to the experimental measurement of the effective thermal conductivity of a porous medium via the transient hot wire method.

Rees and Pop (2005) surveyed studies of LTNE with special attention to natural and forced convection boundary layers and on internal natural convection. Their survey complements that by Kuznetsov (1998e) for internal forced convection. The effect of LTNE on conduction in channels with a uniform heat source was investigated by Nouri-Borujerdi et al. (2007b). Several causes of LTNE were

discussed by Virtol et al. (2009). Some microscopic modeling of conduction with LTNE was carried out by Rees (2010).

The topic of LTNE was reviewed by Haji-Sheikh and Minkowycz (2008). They cite references to a number of engineering applications, such as nuclear devices, fuel cells, electronic systems, and micro devices, in the context of rapid transport of heat. They include a discussion of the development of the thermal field with a moving fluid. They summarize experimental results obtained by Nnanna et al. (2004, 2005) which conform to the observation by Vadasz (2005b, 2006b, 2007) that the physical conditions for thermal waves to materialize are not obtainable in a porous slab subject to a combination of constant heat flux and temperature boundary conditions.

When one examines LTNE at the boundary of a porous medium, or at an interface with a fluid clear of solid material, the solution of the differential equation system that arises is undetermined until further information is available to determine how the total heat flux is split between the two phases. Two second order differential equations are involved and so at an interface one needs four boundary conditions, two involving the temperature and two involving the heat flux. The conservation of energy imposes just one heat flux condition, and hence another condition must be sought. For this Yang and Vafai (2010, 2011a, b, c) and Vafai and Yang (2012) introduced five models for what they called “heat flux bifurcation,” but they did not clearly distinguish between them. Nield (2012) argued that this approach was not satisfactory. Rather, one should distinguish between the heat transfer in the bulk of the porous medium (which depends on the interphase heat transfer coefficient) and the heat transfer across the interface (which is affected by what happens on the other side of the interface, i.e., outside the porous medium). For example, if the porous medium is bounded by a solid with high thermal conductivity (effectively a constant-temperature boundary), then one has LTNE at the boundary and one can use the formulation employed by Nield and Kuznetsov (2012c). Much the same is true if the neighboring region is a fluid of high conductivity. If the region is a solid of very low conductivity (an insulating boundary) then there is essentially no boundary flux to be divided between the two phases. More generally, if the solid boundary is controlled by an imposed constant flux, then the natural assumption is that just across the interface in the porous medium the flux is also constant. Thus the splitting occurs so that the flux in the fluid phase is the same as in the solid phase. This means that the interfacial heat transport is divided between the fluid and solid phases in the ratio of  $\varphi$  to  $(1-\varphi)$ . This was the model employed by Nield and Kuznetsov (1999).

### 2.2.4 Thermal Dispersion

A further complication arises in forced convection or in vigorous natural convection in a porous medium. There may be significant thermal dispersion, i.e., heat transfer due to hydrodynamic mixing of the interstitial fluid at the pore scale. In

addition to the molecular diffusion of heat, there is mixing due to the nature of the porous medium. Some mixing is due to the obstructions; the fact that the flow channels are tortuous means that fluid elements starting a given distance from each other and proceeding at the same velocity will not remain at the same distance apart. Further mixing can arise from the fact that all pores in a porous medium may not be accessible to a fluid element after it has entered a particular flow path.

Mixing can also be caused by recirculation caused by local regions of reduced pressure arising from flow restrictions. Within a flow channel mixing occurs because fluid particles at different distances from a wall move relative to one another. Mixing also results from the eddies that form if the flow becomes turbulent. Diffusion in and out of dead-end pores modifies the nature of molecular diffusion. For details, see Greenkorn (1983, p. 190).

Dispersion is thus a complex phenomenon. Rubin (1974) took dispersion into account by generalizing Eq. (2.3) so that the term  $\nabla \cdot (\alpha_m \nabla T)$ , where  $\alpha_m = k_m / (\rho c)_m$  is the thermal diffusivity of the medium, is replaced by  $\nabla \cdot \mathbf{E} \cdot \nabla T$  where  $\mathbf{E}$  is a second-order tensor (the dispersion tensor). In an isotropic medium the dispersion tensor is axisymmetric and its components can be expressed in the form

$$E_{ij} = F_1 \cdot \delta_{ij} + F_2 V_i V_j, \quad (2.18)$$

where  $V_i (= v_i / \varphi)$  is the  $i^{\text{th}}$  component of the barycentric (intrinsic) velocity vector, and  $F_1$  and  $F_2$  are functions of the pore size and the Péclet and Reynolds numbers of the flow.

At any point in the flow field it is possible to express  $\mathbf{E}$  with reference to a coordinate system in which the first axis coincides with the flow direction; when this is done we have

$$\begin{aligned} E_{11} &= \eta_1 U + \alpha_m, \\ E_{22} &= E_{33} = \eta_2 U + \alpha_m, \\ E_{ij} &= 0 \quad \text{for } i \neq j, \end{aligned} \quad (2.19)$$

where  $E_{11}$  is the longitudinal dispersion coefficient,  $E_{22}$  and  $E_{33}$  are the lateral dispersion coefficients, and  $U$  is the absolute magnitude of the velocity vector.

If the Péclet number of the flow is small, then  $\eta_1$  and  $\eta_2$  are small and the molecular thermal diffusivity  $\alpha_m$  is dominant. If the Péclet number of the flow is large, then  $\eta_1$  and  $\eta_2$  are large and almost constant. It is found experimentally that  $\eta_2 = \eta_1/30$ , approximately.

For an account of the treatment of dispersion in anisotropic media in the context of convection, the reader is referred to Tyvand (1977). In the particular case when heat conduction is in parallel, Catton et al. (1988) conclude on the basis of their statistical analysis that the effective thermal conductivity  $k_{zz}^*$  for mass and thermal transport in the  $z$ -direction through a bed of uniform spherical beads, is given by

$$k_{zz}^* = (1 - \varphi) k_s + \varphi \left( \frac{2B}{\pi} \right) Pe k_f \quad (2.20)$$

In this expression  $B$  is a constant introduced by Ergun (empirically,  $B = 1.75$ ) and  $Pe$  is the Péclet number defined by  $Pe = vd_p/\alpha_f(1 - \varphi)$ , where  $d_p$  is the spherical particle diameter and  $\alpha_f$  is the thermal diffusivity of the fluid, defined by  $\alpha_f = k_f/(\rho c_p)_f$ .

Thermal dispersion plays a particularly important role in forced convection in packed columns. The steep radial temperature gradients that exist near the heated or cooled wall were formerly attributed to channeling effects, but more recent work has indicated that thermal dispersion is also involved. For a nearly parallel flow at high Reynolds numbers, the thermal dispersivity tensor reduces to a scalar, the transverse thermal dispersivity. Cheng and his colleagues [see Hsu and Cheng (1990) and the references given in Sect. 4.9] assumed that the local transverse thermal dispersion conductivity  $k'_T$  is given by

$$\frac{k'_T}{k_f} = D_T Pe_d \lambda \frac{u}{u_m}. \quad (2.21)$$

In this equation  $Pe_d$  is a Péclet number defined by  $Pe_d = u_m d_p/\alpha_f$ , in terms of the mean seepage velocity  $u_m$ , the particle diameter  $d_p$ , and fluid thermal diffusivity  $\alpha_f$ , while  $D_T$  is a constant and  $\lambda$  is a dimensionless dispersive length normalized with respect to  $d_p$ . In recent work the dispersive length is modeled by a wall function of the Van Driest type:

$$\lambda = 1 - \exp(-y/\omega d_p). \quad (2.22)$$

The empirical constants  $\omega$  and  $D_T$  depend on the coefficients  $N$  and  $C$  in the wall porosity variation formula [Eq. (1.28)]. The best match with experiments is given by  $D_T = 0.12$  and  $\omega = 1$ , if  $N = 5$  and  $C = 1.4$ . The theoretical results based on this *ad hoc* approach agree with a number of experimental results.

A theoretical backing for this approach has been given by Hsu and Cheng (1990). This is based on volume averaging of the velocity and temperature deviations in the pores in a dilute array of spheres, together with a scale analysis. The thermal diffusivity tensor  $\mathbf{D}$  is introduced as a multiplying constant which accounts for the interaction of spheres. For the case of high pore Reynolds number flow, Hsu and Cheng (1990) found the thermal dispersion conductivity tensor  $\mathbf{k}'$  to be given by

$$\mathbf{k}' = \mathbf{D} k_f \frac{1 - \varphi}{\varphi} Pe_d \quad (2.23)$$

The linear variation with  $Pe_d$  is consistent with most of the existing experimental correlations for high pore Reynolds number flow. At low pore Reynolds number flow, they found

$$\mathbf{k}' = \mathbf{D}^* k_f \frac{1 - \varphi}{\varphi^2} Pe_d^2 \quad (2.24)$$

where  $\mathbf{D}^*$  is another constant tensor. The quadratic dependence on  $Pe_d$  has not yet been confirmed by experiment.

Kuwahara et al. (1996) and Kuwahara and Nakayama (1999) have studied numerically thermal diffusion for a two-dimensional periodic model. A limitation of their correlation formulas as the porosity tends to unity was discussed by Yu (2004) and Nakayama and Kuwahara (2004). A similar model was examined by Souto and Moyne (1997a, b). The frequency response model was employed by Muralidhar and Misra (1997) in an experimental study of dispersion coefficients. The role of thermal dispersion in the thermally developing region of a channel with a sintered porous metal was studied by Hsieh and Lu (2000). Kuwahara and Nakayama (2005) have extended their earlier numerical studies to the case of three-dimensional flow in highly anisotropic porous media. Niu et al. (2006) reported direct measurements of eddy transport and thermal dispersion in a high-porosity matrix. An equation for thermal dispersion-flux transport was introduced by Nakayama et al. (2006).

For further information about dispersion in porous media, the reader is referred to the review by Liu and Masliyah (2005), which deals with the dispersion of mass, heat, and momentum. Rudraiah and Ng (2007) have reviewed dispersion in porous media with and without reaction.

### 2.2.5 Cellular Porous Media

Cellular porous media have the property that to a good approximation the effect of radiation can be modeled using a temperature-dependent thermal conductivity (Viskanta 2009). For a few situations an analytical solution can be obtained. This was done by Nield and Kuznetsov (2010a, c) and Nield and Kuznetsov (2010b) for paradigmatic forced convection, external natural convection, and internal natural convection problems.

## 2.3 Oberbeck-Boussinesq Approximation

In studies of natural convection we add the gravitational term  $\rho_f \mathbf{g}$  to the right-hand side of the Darcy equation (1.4) or its appropriate extension. [Note that in Eq. (1.4) the term  $\nabla P$  denotes an *intrinsic* quantity, so we add the gravitational force per unit

volume of the *fluid*]. For thermal convection to occur, the density of the fluid must be a function of the temperature, and hence we need an equation of state to complement the equations of mass, momentum, and energy. The simplest equation of state is

$$\rho_f = \rho_0[1 - \beta(T - T_0)], \quad (2.25)$$

where  $\rho_0$  is the fluid density at some reference temperature  $T_0$  and  $\beta$  is the coefficient of thermal expansion.

In order to simplify the subsequent analysis, one employs the Boussinesq approximation whenever it is valid. Strictly speaking, one should call this the *Oberbeck-Boussinesq approximation*, since Oberbeck (1879) has priority over Boussinesq (1903), as documented by Joseph (1976). The approximation consists of setting constant all the properties of the medium, except that the vital buoyancy term involving  $\beta$  is retained in the momentum equation. As a consequence the equation of continuity reduces to  $\nabla \cdot \mathbf{v} = 0$ , just as for an incompressible fluid. The Boussinesq approximation is valid provided that density changes  $\Delta\rho$  remain small in comparison with  $\rho_0$  throughout the flow region and provided that temperature variations are insufficient to cause the various properties of the medium (fluid and solid) to vary significantly from their mean values. Johannsen (2003) discussed the validity of the Boussinesq approximation in the case of a bench mark problem known as the Elder problem.

## 2.4 Thermal Boundary Conditions

Once the thermal conductivity in the porous medium has been determined, the application of thermal boundary conditions is usually straightforward. At the interface between two porous media, or between a porous medium and a clear fluid, we can impose continuity of the temperature (on the assumption that we have local thermodynamic equilibrium) and continuity of the normal component of the heat flux. We note that two conditions are required because the equation of energy (2.3) contains second-order derivatives.

The heat flux vector is the sum of two terms: a convective term  $(\rho c_p)_f T \mathbf{v}$  and a conductive term  $-k \nabla T$ . The normal component of the former is continuous because both  $T$  and the normal component of  $\rho_f \mathbf{v}$  are continuous. It follows that the normal component of  $k \nabla T$  also must be continuous. At an impermeable boundary the usual thermal condition appropriate to the external environment can be applied, e.g., one can prescribe either the temperature or the heat flux, or one can prescribe a heat transfer coefficient.

Sahraoui and Kaviany (1993, 1994) have discussed the errors arising from the use of approximations of the effective conductivity near a boundary, due to nonuniformity of the distributions of the solid and fluid phases there. They have

introduced a slip coefficient into the thermal boundary condition to adjust for this, for the case of two-dimensional media.

Ochoa-Tapia and Whitaker (1997, 1998) have developed flux jump conditions applicable at the boundary of a porous medium and a clear fluid. These are based on a nonlocal form of the volume-averaged thermal energy equations for fluid and solid. The conditions involve excess surface thermal energy and an excess nonequilibrium thermal source. Min and Kim (2005) have used the special two-dimensional model of Richardson (1971) in order to obtain estimates of the coefficients that occur in the thermal and hydrodynamic jump conditions. The jump conditions were further analyzed by d'Hueppe et al. (2011). Valdes-Parada et al. (2009b) included the effects of adsorption and a chemical reaction. Betchen et al. (2006) considered a nonequilibrium model. d'Hueppe et al. (2012) discussed the coupling of a two-temperature model with a one-temperature model at a fluid-porous interface.

An analogous mass transfer jump condition was formulated by Valencia-López et al. (2003). The thermal interaction at the interface between a porous medium and an impermeable wall was studied by Kim and Kim (2001). The role of particle-particle contact on effective thermal properties in the interfacial region was examined by Aguilar-Madera et al. (2011b).

## 2.5 Hele-Shaw Analogy

The space between two plane walls a small distance apart constitutes a Hele-Shaw cell. If the gap is of thickness  $h$  and the walls each of thickness  $d$ , then the governing equations for gap-averaged velocity components (parallel to the plane walls) are identical with those for two-dimensional flow in a porous medium whose permeability  $K$  is equal to  $h^3/[12(h + 2d)]$ , for the case where the heat flow is parallel to the plane walls (Hartline and Lister 1977). The Hele-Shaw cell thus provides a means of modeling thermal convection in a porous medium, as in the experiments by Elder (1967a).

For the analogy to hold, the three quantities  $h/\delta$ ,  $Uh^2/v\delta$ , and  $Uh^2/\alpha_f\delta$  must all be small compared with unity. Here  $U$  is the velocity scale and  $\delta$  the smallest length scale of the motion being modeled, while  $v$  and  $\alpha_f$  are the kinematic viscosity and thermal diffusivity of the fluid. These conditions ensure that there is negligible advection of vorticity and rapid diffusion of vorticity and heat across the flow.

The experimental temperature profiles found by Vorontsov et al. (1991) were in good agreement with the theory. Schöpf (1992) extended the comparison to the case of a binary mixture. Specific studies of convection in a Hele-Shaw cell were reported by Cooper et al. (1997), Goldstein et al. (1998), and Gorin et al. (1998).

The Hele-Shaw cell experiments are especially useful for revealing streamline patterns when the walls are made of transparent material. The analogy has obvious limitations. For example, it cannot deal with the effects of lateral dispersion or instabilities associated with three-dimensional disturbances. The discrepancies

associated with these effects have been examined by Kvernvold (1979) and Kvernvold and Tyvand (1981).

Hsu (2005) has compared the governing equations for the averaged flows and heat transfer in Hele-Shaw cells with those of porous media and he observed the following differences: (a) the averaged Hele-Shaw cell is two-dimensional, (b) the interfacial force in the averaged Hele-Shaw flows is contributed entirely from the shear force, and (c) there exists no thermal tortuosity for the averaged Hele-Shaw flows. Thus the Hele-Shaw analogy is good for viscous dominated two-dimensional flow with negligible thermal tortuosity. However, these simplifications help in the verification of closure modeling. Furthermore, a three-dimensional numerical simulation of the convection heat transfer in Hele-Shaw cells may reveal some detailed physics of heat transfer in porous media that are impossible to tackle due to the randomness and the complexity of the microscopic solid geometry. Hsu (2005) illustrates this with results for the case of oscillating flows past a heated circular cylinder. Babuskin and Demin (2006) reported an experimental and theoretical investigation of transient convective regimes. Backhaus et al. (2011) investigated the convective instability and mass transport of diffusion layers. Abdelkareem et al. (2009) performed an experimental study on oscillatory convection in a Hele-Shaw cell due to an unstably heated side.

## 2.6 Bioheat Transfer and Other Approaches

Convective heat transfer in biological tissues involves a special situation. In some cases applications of porous media theory are appropriate (see for example, the surveys by Khanafer et al. (2008a) and Khanafer and Vafai (2009).) Some aspects relevant to biological tissues were discussed by Khanafer et al. (2003), Khaled and Vafai (2003), Yao and Gu (2007), Wood et al. (2007), Mahjoob and Vafai (2009, 2010, 2011), and Wang and Fan (2011) A feature of bioheat transfer is that in many situations there is counterflow. For example, blood flows in adjacent arteries and veins in opposite directions. Nield and Kuznetsov (2008a, 2009a, 2010b) and Kuznetsov and Nield (2009a, b) have modeled forced convection in a porous medium with counterflow. A general set of bioheat transfer equations based on volume averaging theory has been obtained by Nakayama et al. (2011), who applied the bioheat equation to cryoablation therapy for the treatment of malignant cancers.

Direct numerical simulation of heat and fluid flow, using the full Navier–Stokes equations at the pore scale, for regularly spaced square or circular rods or spheres has been conducted by Kuwahara et al. (1994). A direct numerical simulation was applied by He and Georgiadis (1992) to the study of the effect of randomness on one-dimensional heat conduction. Direct numerical simulation has also been employed by Rahimian and Poushaghagy (2002), Yu et al. (2006b), Pourshaghagh et al. (2007), Narasimhan and Raju (2007), Gamrat et al. (2008), and Ma and Zabaras (2008), Lattice gas cellular automata simulations were performed by McCarthy (1994) for flow through arrays of cylinders, and by Yoshino and Inamura (2003)

for flow in a three-dimensional structure. Buikis and Ulanova (1996) have modeled nonisothermal gas flow through a heterogeneous medium using a two-media approach. A diffuse approximation has been applied by Prax et al. (1996) to natural convection. Martins-Costa et al. (1992, 1994), Martins-Costa et al. (1994), and Martins-Costa (1996) have applied the continuous theory of mixtures to the modeling and simulation of heat transfer in various contexts. Modeling of convection in reservoirs having fractal geometry has been conducted by Fomin et al. (2002). Spaid and Phelan (1997) applied lattice Boltzmann methods to model microscale flow in fibrous porous media.

A general discussion of the dynamic modeling of convective heat transfer in porous media was provided by Hsu (2005). Further simulation studies with a lattice Boltzmann model have been reported by Guo and Zhao (2005a, b) (with the viscosity independent or dependent on the temperature), Zhou et al. (2010b) (a problem involving double diffusion), Seta et al. (2006), Rong et al. (2010a), Shokouhmand et al. (2009), Xu et al. (2005, 2008), Wang et al. (2007a), Yan et al. (2006), Zhao et al. (2010a, b), Roussellet et al. (2011), and Vishnampet Ramanathan et al. (2011). Visser et al. (2008a, b) have introduced an artificial compressibility method for buoyancy-driven flow.

Petrasch et al. (2008) described a tomography-based determination of the interfacial heat transfer coefficient in reticulate porous dynamics.

Radiative heat transfer is beyond the scope of this book, but we mention that a review of this subject was made by Howell (2000) and a combined radiation and convection problem was studied by Talukdar et al. (2004).

# Chapter 3

## Mass Transfer in a Porous Medium: Multicomponent and Multiphase Flows

### 3.1 Multicomponent Flow: Basic Concepts

The term “mass transfer” is used here in a specialized sense, namely the transport of a substance that is involved as a component (constituent, species) in a fluid mixture. An example is the transport of salt in saline water. As we shall see below, convective mass transfer is analogous to convective heat transfer.

Consider a batch of fluid mixture of volume  $V$  and mass  $m$ . Let the subscript  $i$  refer to the  $i$ th component (component  $i$ ) of the mixture. The total mass is equal to the sum of the individual masses  $m_i$  so  $m = \sum m_i$ . Hence if the concentration of component  $i$  is defined as

$$C_i = \frac{m_i}{V}, \quad (3.1)$$

then the aggregate density  $\rho$  of the mixture must be the sum of all the individual concentrations,

$$\rho = \sum C_i. \quad (3.2)$$

Clearly the unit of concentration is  $\text{kg m}^{-3}$ . Instead of  $C_i$  the alternative notation  $\rho_i$  is appropriate if one thinks of each component spread out over the total volume  $V$ .

When chemical reactions are of interest, it is convenient to work in terms of an alternative description, one involving the concept of *mole*. By definition, a mole is the amount of substance that contains as many molecules as there are in 12 g of carbon 12. That number of entities is  $6.022 \times 10^{23}$  (Avogadro’s constant). The molar mass of a substance is the mass of one mole of that substance. Hence if there are  $n$  moles in a mixture of molar mass  $M$  and mass  $m$ , then

$$n = \frac{m}{M}. \quad (3.3)$$

Similarly the number of moles  $n_i$  of component  $i$  in a mixture is the mass of that component divided by its molar mass  $M_i$ ,

$$n_i = \frac{m_i}{M_i}. \quad (3.4)$$

The *mass fraction* of component  $i$  is

$$\Phi_i = \frac{m_i}{m} \quad (3.5)$$

so clearly  $\sum \Phi_i = 1$ . Similarly the *mole fraction* of component  $i$  is

$$x_i = \frac{n_i}{n} \quad (3.6)$$

and  $\sum x_i = 1$ .

To summarize, we have three alternative ways to deal with composition: a dimensional concept (concentration) and two dimensionless ratios (mass fraction and mole fraction). These quantities are related by

$$C_i = \rho \Phi_i = \rho \frac{M_i}{M} x_i, \quad (3.7)$$

where the equivalent molar mass ( $M$ ) of the mixture is given by

$$M = \sum M_i x_i. \quad (3.8)$$

If, for example, the mixture can be modeled as an *ideal gas*, then its equation of state is

$$PV = mR_m T \quad \text{or} \quad PV = nRT, \quad (3.9)$$

where the gas constant of the mixture ( $R_m$ ) and the universal gas constant ( $R$ ) are related by

$$R_m = \frac{n}{m} R = \frac{R}{M}. \quad (3.10)$$

The *partial pressure*  $P_i$  of component  $i$  is the pressure one would measure if component  $i$  alone were to fill the mixture volume  $V$  at the same temperature  $T$  as the mixture. Thus

$$P_i V = m_i R_m T \quad \text{or} \quad P_i V = n_i R T. \quad (3.11)$$

Summing these equations over  $i$ , we obtain Dalton's law,

$$P = \sum P_i, \quad (3.12)$$

which states that the pressure of a mixture of gases at a specified volume and temperature is equal to the sum of the partial pressures of the components. Note that  $P_i/P = x_i$ , and so using Eqs. (3.7) and (3.8) we can relate  $C_i$  to  $P_i$ .

The nomenclature we have used in this section applies to a mixture in *equilibrium*, that is, to a fluid batch whose composition, pressure, and temperature do not vary from point to point. In a convection study we are (out of necessity) involved with a *nonequilibrium* mixture which we view as a patchwork of small equilibrium batches: the equilibrium state of each of these batches is assumed to vary only slightly as one moves from one batch to its neighbors.

## 3.2 Mass Conservation in a Mixture

We apply the principle of mass conservation to each component in the mixture. For the moment we use the notation  $\rho_i$  instead of  $C_i$  for the concentration of component  $i$ . In the absence of component generation we must have

$$\frac{\partial \rho_i}{\partial t} + \nabla \cdot (\rho_i \mathbf{V}_i) = 0, \quad (3.13)$$

where  $\mathbf{V}_i$  is the (intrinsic) velocity of particles of component  $i$ . Summing over  $i$ , we obtain

$$\frac{\partial \rho}{\partial t} + \nabla \cdot \left( \sum \rho_i \mathbf{V}_i \right) = 0. \quad (3.14)$$

This is the same as

$$\frac{\partial \rho}{\partial t} + \nabla \cdot (\rho \mathbf{V}) = 0 \quad (3.15)$$

provided that we identify  $\mathbf{V}$  with the mass-averaged velocity,

$$V = \frac{1}{\rho} \sum \rho_i \mathbf{V}_i. \quad (3.16)$$

Motion of a component relative to this mass-averaged velocity is called *diffusion*. Thus,  $\mathbf{V}_i - \mathbf{V}$  is the diffusion velocity of component  $i$ , and

$$\mathbf{j}_i = \rho_i(\mathbf{V}_i - \mathbf{V}) \quad (3.17)$$

is the *diffusive flux* of component  $i$ . Equation (3.13) now gives

$$\frac{\partial \rho_i}{\partial t} + \nabla \cdot (\rho_i \mathbf{V}) = -\nabla \cdot \mathbf{j}_i. \quad (3.18)$$

Reverting to the notation  $C_i$  for concentration, and assuming that the mixture is incompressible, we have

$$\frac{DC_i}{Dt} = -\nabla \cdot \mathbf{j}_i, \quad (3.19)$$

where  $D/Dt = \partial/\partial t + \mathbf{V} \cdot \nabla$ .

For the case of a two-component mixture, Fick's law of mass diffusion is

$$\mathbf{j}_1 = -D_{12}\nabla C_1, \quad (3.20)$$

where  $D_{12}$  is the mass diffusivity of component 1 into component 2 and similarly for  $\mathbf{j}_2$ . In fact,  $D_{12} = D_{21} = D$ . The diffusivity  $D$ , whose units are  $\text{m}^2\text{s}^{-1}$ , has a numerical value which in general depends on the mixture pressure, temperature, and composition. From Eqs. (3.19) and (3.20) we have

$$\frac{DC_1}{Dt} = \nabla \cdot (D\nabla C_1). \quad (3.21)$$

If the migration of the first component is the only one of interest, then the subscript can be dropped. For a homogeneous situation we have

$$\frac{DC}{Dt} = D\nabla^2 C. \quad (3.22)$$

The analogy between this equation and the corresponding energy equation (temperature  $T$ , thermal diffusivity  $\alpha_m$ )

$$\frac{DT}{Dt} = \alpha_m \nabla^2 T \quad (3.23)$$

is obvious. Fourier's law of thermal diffusion  $\mathbf{q} = -k\nabla T$ , where  $\mathbf{q}$  is the heat flux and  $k$  is the thermal conductivity, is analogous to Fick's law of mass diffusion  $\mathbf{j} = -D\nabla C$ .

So far in this chapter we have been concerned with the fluid only, but now we consider a porous solid matrix saturated by fluid mixture. Within the solid there is of course neither flow nor any component of the mixture. *Thus in a porous medium mass transfer is in this respect distinctly different from heat transfer in medium.* Multiplying Eq. (3.21) (with the suffix dropped) by the porosity  $\phi$  we have

$$\varphi \frac{\partial C}{\partial t} + \varphi \mathbf{V} \cdot \nabla C = \varphi \nabla \cdot (D \nabla C).$$

Recalling the Dupuit-Forchheimer relationship  $\mathbf{v} = \varphi \mathbf{V}$ , we see that this equation can be written, if  $\varphi$  is constant, as

$$\varphi \frac{\partial C}{\partial t} + \mathbf{v} \cdot \nabla C = \nabla \cdot (D_m \nabla C), \quad (3.24)$$

where  $D_m = \varphi D$  is the mass diffusivity of the porous medium. Some authors invoke tortuosity and produce a more complicated relationship between  $D_m$  and  $D$ . The diffusive mass flux in the porous medium (rate of flow of mass across unit cross-sectional area of the medium) is

$$\mathbf{j}_m = -D_m \nabla C = \varphi \mathbf{j}. \quad (3.25)$$

This is consistent with the surface porosity of the medium being equal to  $\varphi$ . Equation (3.24) also may be derived directly by using as control volume an element of the medium. If the mass of the substance whose concentration is  $C$  is being generated at a rate  $\dot{m}'''$  per unit volume of the medium, then the term  $\dot{m}'''$  must be added to the right-hand side of Eq. (3.24). The result may be compared with Eq. (2.3).

### 3.3 Combined Heat and Mass Transfer

In the most commonly occurring circumstances the transport of heat and mass (e.g., salt) is not directly coupled, and both Eqs. (2.3) and (3.24) (which clearly are uncoupled) hold without change. In double-diffusive (e.g., thermohaline) convection the coupling takes place because the density  $\rho$  of the fluid mixture depends on both temperature  $T$  and concentration  $C$  (and also, in general, on the pressure  $P$ ). For sufficiently small isobaric changes in temperature and concentration, the mixture density  $\rho$  depends linearly on both  $T$  and  $C$ , and we have approximately

$$\rho = \rho_0 [1 - \beta(T - T_0) - \beta_C(C - C_0)], \quad (3.26)$$

where the subscript zero refers to a reference state,  $\beta$  is the volumetric thermal expansion coefficient,

$$\beta = -\frac{1}{\rho} \left( \frac{\partial \rho}{\partial T} \right)_{P,C}, \quad (3.27)$$

and  $\beta_C$  is the volumetric concentration expansion coefficient,

$$\beta_C = -\frac{1}{\rho} \left( \frac{\partial \rho}{\partial C} \right)_{T,P}. \quad (3.28)$$

Both  $\beta$  and  $\beta_C$  are evaluated at the reference state.

In some circumstances there is direct coupling. This is when cross-diffusion (Soret and Dufour effects) is not negligible. The Soret effect refers to mass flux produced by a temperature gradient, and the Dufour effect refers to heat flux produced by a concentration gradient. For the case of no heat and mass sources we have, in place of Eqs. (2.3) and (3.24),

$$\frac{(\rho c)_m}{(\rho c)_f} \frac{\partial T}{\partial t} + \mathbf{v} \cdot \nabla T = \nabla \cdot (D_T \nabla T + D_{TC} \nabla C), \quad (3.29)$$

$$\varphi \frac{\partial C}{\partial t} + \mathbf{v} \cdot \nabla C = \nabla \cdot (D_C \nabla C + D_{CT} \nabla T), \quad (3.30)$$

where  $D_T (= k_m/(\rho c)_f)$  is the thermal diffusivity,  $D_C (= D_m)$  is the mass diffusivity,  $D_{TC}/D_T$  is the Dufour coefficient, and  $D_{CT}/D_C$  is the Soret coefficient of the porous medium.

The variation of density with temperature and concentration gives rise to a combined buoyancy force, proportional to  $\beta(T - T_0) + \beta_C(C - C_0)$ . The fact that the coefficients of Eq. (3.29) differ from those of Eq. (3.30) leads to interesting effects, such as flows oscillating in time in the presence of steady boundary conditions.

The Soret and Dufour effects are usually minor and can be neglected in simple models of coupled heat and mass transfer. According to Platten and Legros (1984), the mass fraction gradient established under the effect of thermal diffusion is very small. However, it has a disproportionately large influence on hydrodynamic stability relative to its contribution to the buoyancy of the fluid. They also state that in most liquid mixtures the Dufour effect is inoperative, but that this may not be the case in gases. Mojtabi and Charrier-Mojtabi (2000) confirm this by noting that in liquids the Dufour coefficient is an order of magnitude smaller than the Soret effect. They conclude that for saturated porous media, the phenomenon of cross-diffusion is further complicated because of the interaction between the fluid and the porous matrix and because accurate values of the cross-diffusion coefficients are not available.

The thermodiffusion coefficient  $D_{TC}$  and the isothermal diffusion coefficient  $D_T$  were separately measured by Platten and Costeseque (2004) for both a porous medium and the corresponding liquid clear of solid material. They found that the measured value of the ratio of these two quantities (what they call the Soret coefficient) was the same for the clear fluid as for the porous medium to within experimental error.

The thermodynamic irreversibility of coupled heat and mass transfer in saturated porous media is treated based on the method of irreversible thermodynamics in

Bejan et al. (2004). Viskanta (2005) has reviewed studies of combustion and heat transfer in inert porous media.

### 3.4 Effects of a Chemical Reaction

In recent years it has been realized that it is not always permissible to neglect the effects of convection in chemical reactors of porous construction. Suppose that we have a solution of a reagent whose concentration  $C$  is defined as above. If  $m$  is the molar mass of the reagent, then its concentration in moles per unit volume of the fluid mixture is  $C_m = C/m$ . Suppose that the rate equation for the reaction is

$$\frac{d C_m}{d t} = -k C_m^n. \quad (3.31)$$

The integer power  $n$  is the order of the reaction. The rate coefficient  $k$  is a function of the absolute temperature  $T$  given by the Arrhenius relationship

$$k = A \exp\left(-\frac{E}{RT}\right), \quad (3.32)$$

where  $E$  is the activation energy of the reaction (energy per mole),  $R$  is the universal gas constant, and  $A$  is a constant called the preexponential factor.

Assume further that the solid material of the porous medium is inert, that the reaction produces a product whose mass can be ignored, and that there is negligible change in volume. Then the rate of increase of  $C$  due to the reaction is  $m dC_m/dt$ . It follows that Eq. (3.24) is to be replaced by

$$\varphi \frac{\partial C}{\partial t} + \mathbf{v} \cdot \nabla C = \nabla \cdot (D_m \nabla C) - \varphi A m^{1-n} C^n \exp\left(-\frac{E}{RT}\right). \quad (3.33)$$

If the consumption of one mole of reagent causes the heat energy to increase by an amount  $-\Delta H$  due to the reaction, then the increase in energy per unit volume of the fluid mixture is  $(\Delta H)dC_m/dt$ . Thus in place of Eq. (2.3) we have

$$\begin{aligned} & (\rho c)_m \frac{\partial T}{\partial t} + (\rho c)_f \mathbf{v} \cdot \nabla T \\ &= \nabla \cdot (k_m \nabla T) + \dot{m}''' - \varphi A (\Delta H) m^{-n} C^n \exp\left(-\frac{E}{RT}\right). \end{aligned} \quad (3.34)$$

Equation (3.33), for the case of a first-order reaction ( $n = 1$ ), is in accord with the formulation of Kolesnikov (1979). We note that for a zero-order reaction ( $n = 0$ ) the thermal equation (3.34) is decoupled from Eq. (3.33) in the sense

that Eq. (3.34) does not depend explicitly on  $C$  [though  $C$  and  $T$  are still related by Eq. (3.33)].

These equations are appropriate if the reaction is occurring entirely within the fluid. Now suppose that we have a catalytic reaction taking place only on the solid surface of the porous matrix. If the surface porosity is equal to the (volume) porosity  $\phi$ , and if the reaction rate is proportional to the mass of the solid material, then Eqs. (3.33) and (3.34) should be altered by replacing  $\phi A$  by  $(1 - \phi)\rho_s A'$  where  $A'$  is a new constant preexponential factor (compare Gatica et al. 1989).

Recent papers on the effects of chemical reactions include those by Balakotaiah and Portalet (1990a, b); Stroh and Balakotaiah (1991, 1992, 1993); Farr et al. (1991); Gabito and Balakotaiah (1991); Nandakumar and Weinitschke (1992); Salinger et al. (1994b); Nguyen and Balakotaiah (1995); Subramanian and Balakotaiah (1995, 1997); Vafai et al. (1993); Kuznetsov and Vafai (1995b); and Chao et al. (1996).

### 3.5 Multiphase Flow

If two or more miscible fluids occupy the void space in a porous medium, then even if they occupy different regions initially, they mix because of diffusive and other dispersive effects, leading ultimately to a multicomponent mixture such as what we just have been considering. If immiscible fluids are involved, the situation is more complicated. Indeed the complexities are such that, insofar as convection studies are concerned, only the simplest situations have been treated. It invariably has been assumed that Darcy's law is valid. Consequently our discussion of the momentum and energy equations in this section will be comparatively brief. This will enable us to present a derivation of the basic equations using formal averages. We follow the presentation of Cheng (1978) based on volume averaging. For a more extensive treatment the reader is referred to Whitaker (1999).

We consider "two-phase" fluid flow in a porous medium. This means that we actually have three phases: two fluids and the solid matrix. The fluids could well both be liquids, but to simplify the discussion we suppose that we have a liquid phase (which we can label by the suffix l) and a gas phase (suffix g). As in previous chapters the suffix s refers to the solid matrix, which in this section is not necessarily fixed.

We take a representative elementary volume  $V$  occupied by the liquid, gas, and solid, whose interfaces may move with time, so

$$V = V_l(t) + V_g(t) + V_s(t). \quad (3.35)$$

We define the phase average of some quantity  $\psi_\alpha$  as

$$\langle \psi_\alpha \rangle \equiv V^{-1} \int_V \psi_\alpha dV \quad (3.36)$$

where  $\psi_\alpha$  is the value of  $\psi$  in the  $\alpha$  phase ( $\alpha = l, g, s$ ) and is taken to be zero in the other phases. The intrinsic phase average of  $\psi_\alpha$  is defined as

$$\langle \psi_\alpha \rangle^\alpha \equiv V_\alpha^{-1} \int_{V_\alpha} \psi_\alpha dV, \quad (3.37)$$

that is, the integration is carried out over only the  $\alpha$  phase. Since  $\psi_\alpha$  is zero in the other phases, Eq. (3.37) can be rewritten as

$$\langle \psi_\alpha \rangle^\alpha \equiv V_\alpha^{-1} \int_V \psi_\alpha dV. \quad (3.38)$$

Comparing Eqs. (3.36) and (3.38), we see that

$$\langle \psi_\alpha \rangle = \varepsilon_\alpha \langle \psi_\alpha \rangle^\alpha \quad (3.39)$$

where

$$\varepsilon_\alpha = \frac{V_\alpha}{V} \quad (3.40)$$

is the fraction of the total volume occupied by the  $\alpha$  phase. In terms of the porosity  $\phi$  of the medium we have

$$\varepsilon_l + \varepsilon_g = \phi, \quad \varepsilon_s = 1 - \phi. \quad (3.41)$$

We define deviations (from the respective average values, for the  $\alpha$  phase)

$$\tilde{\psi}_\alpha \equiv \psi_\alpha - \langle \psi_\alpha \rangle^\alpha, \quad \tilde{\chi}_\alpha \equiv \chi_\alpha - \langle \chi_\alpha \rangle^\alpha \quad (3.42)$$

and note that in the other phases  $\tilde{\psi}_\alpha$  and  $\tilde{\chi}_\alpha$  are zero. It is easily shown that

$$\langle \psi_\alpha \chi_\alpha \rangle^\alpha = \langle \psi_\alpha \rangle^\alpha \langle \chi_\alpha \rangle^\alpha + \langle \tilde{\psi}_\alpha \tilde{\chi}_\alpha \rangle^\alpha \quad (3.43)$$

and

$$\langle \psi_\alpha \chi_\alpha \rangle = \varepsilon_\alpha \langle \psi_\alpha \rangle^\alpha \langle \chi_\alpha \rangle^\alpha + \langle \tilde{\psi}_\alpha \tilde{\chi}_\alpha \rangle. \quad (3.44)$$

The following theorems are established by integration over an elementary volume.

*Averaging theorem:*

$$\langle \nabla \psi_\alpha \rangle = \nabla \langle \psi_\alpha \rangle + V^{-1} \int_{A_\alpha} \psi_\alpha n_\alpha dS. \quad (3.45)$$

Modified averaging theorem:

$$\langle \nabla \psi_\alpha \rangle = \varepsilon_\alpha \nabla \langle \psi_\alpha \rangle^\alpha + V^{-1} \int_{A_\alpha} \tilde{\psi}_\alpha n_\alpha dS. \quad (3.46)$$

*Transport theorem:*

$$\left\langle \frac{\partial \psi_\alpha}{\partial t} \right\rangle = \frac{\partial}{\partial t} \langle \psi_\alpha \rangle - V^{-1} \int_{A_\alpha} \psi w_\alpha \cdot n_\alpha dS, \quad (3.47)$$

where  $A_\alpha$  denotes the interfaces between the  $\alpha$  phase and the other phases,  $\mathbf{w}_\alpha$  is the velocity vector of the interface, and  $\mathbf{n}_\alpha$  is the unit normal to the interface pointing outward from the  $\alpha$  phase.

### 3.5.1 Conservation of Mass

The microscopic continuity equation for the liquid phase is

$$\frac{\partial \rho_l}{\partial t} + \nabla \cdot (\rho_l \mathbf{V}_l) = 0, \quad (3.48)$$

which can be integrated over an elementary volume to give

$$\left\langle \frac{\partial \rho_l}{\partial t} \right\rangle + \langle \nabla \cdot (\rho_l \mathbf{V}_l) \rangle = 0, \quad (3.49)$$

where  $\rho_l$  and  $\mathbf{V}_l$  are the density and velocity of the liquid. Application of the transport theorem to the first term and the averaging theorem to the second term of this equation, with the aid of Eq. (3.44), leads to

$$\begin{aligned} & \frac{\partial}{\partial t} \left( \varepsilon_l \langle \rho_l \rangle^l \right) + \nabla \cdot \left( \langle \rho_l \rangle^l \langle \mathbf{V}_l \rangle + \langle \tilde{\rho}_l \hat{\mathbf{V}}_l \rangle \right) \\ & + V^{-1} \int_{A_{lg}} \rho_l (\mathbf{V}_l - \mathbf{w}_{lg}) \cdot \mathbf{n}_l dS + V^{-1} \int_{A_{ls}} \rho_l (\mathbf{V}_l - \mathbf{w}_{ls}) \cdot \mathbf{n}_l dS = 0 \end{aligned} \quad (3.50)$$

where  $A_{lg}$  and  $A_{ls}$  are the liquid–gas and liquid–solid interfaces that move with velocities  $\mathbf{w}_{lg}$  and  $\mathbf{w}_{ls}$ . The first integral in Eq. (3.50) represents mass transfer due to a change of phase from liquid to gas, and in general this is nonzero; but the second integral vanishes, since there is no mass transfer across the liquid–solid interface. The dispersive term  $\langle \tilde{\rho}_l \hat{\mathbf{V}}_l \rangle$  is generally small, and we suppose that it can be neglected. Accordingly, Eq. (3.50) reduces to

$$\frac{\partial}{\partial t} \left( \varepsilon_l \langle \rho_l \rangle^l \right) + \nabla \cdot \left( \langle \rho_l \rangle^l \langle \mathbf{V}_l \rangle \right) + V^{-1} \int_{A_{lg}} \rho_l (\mathbf{V}_l - w_{lg}) \cdot \mathbf{n}_l dS = 0. \quad (3.51)$$

Similarly the macroscopic continuity equations for the gas and for the solid are

$$\frac{\partial}{\partial t} \left( \varepsilon_g \langle \rho_g \rangle^g \right) + \nabla \cdot \left( \langle \rho_g \rangle^g \langle \mathbf{V}_g \rangle \right) + V^{-1} \int_{A_{gl}} \rho_g (\mathbf{V}_g - w_{gl}) \cdot \mathbf{n}_g dS = 0 \quad (3.52)$$

and

$$\frac{\partial}{\partial t} (\varepsilon_s \langle \rho_s \rangle^s) + \nabla \cdot (\langle \rho_s \rangle^s \langle \mathbf{V}_s \rangle) = 0. \quad (3.53)$$

The mass gained by change of phase from liquid to gas is equal to the mass lost by change of phase from gas to liquid. Thus the surface integrals in Eqs. (3.51) and (3.52) are equal in magnitude but opposite in sign. The integrals thus cancel each other when Eqs. (3.51)–(3.53) are added to give

$$\begin{aligned} & \frac{\partial}{\partial t} \left[ \varepsilon_l \langle \rho_l \rangle^l + \varepsilon_g \langle \rho_g \rangle^g + \varepsilon_s \langle \rho_s \rangle^s \right] \\ & + \nabla \cdot \left( \langle \rho_l \rangle^l \langle \mathbf{V}_l \rangle^l + \langle \rho_g \rangle^g \langle \mathbf{V}_g \rangle^g + \langle \rho_s \rangle^s \langle \mathbf{V}_s \rangle^s \right) = 0 \end{aligned} \quad (3.54)$$

Note that, for example,  $\langle \mathbf{V}_l \rangle = \varepsilon_l \langle \mathbf{V}_l \rangle^l$  since  $\mathbf{V}_l$  is taken to be zero in the gas and solid phases. If the volumetric liquid and gas saturation,  $S_l$  and  $S_g$ , are defined by

$$S_l = \frac{\mathbf{V}_l}{\mathbf{V}_l + \mathbf{V}_g}, \quad S_g = \frac{\mathbf{V}_g}{\mathbf{V}_l + \mathbf{V}_g} \quad (3.55)$$

so that

$$S_l + S_g = 1, \quad \varepsilon_l = \varphi S_l, \quad \varepsilon_g = \varphi S_g, \quad \text{and} \quad \varepsilon_s = 1 - \varphi, \quad (3.56)$$

then Eq. (3.54) can be rewritten as

$$\begin{aligned} & \frac{\partial}{\partial t} \left[ \varphi S_l \langle \rho_l \rangle^l + \varphi S_g \langle \rho_g \rangle^g + (1 - \varphi) \langle \rho_s \rangle^s \right] \\ & + \nabla \cdot \left( \langle \rho_l \rangle^l \langle \mathbf{V}_l \rangle^l + \langle \rho_g \rangle^g \langle \mathbf{V}_g \rangle^g + \langle \rho_s \rangle^s \langle \mathbf{V}_s \rangle^s \right) = 0 \end{aligned} \quad (3.57)$$

### 3.5.2 Conservation of Momentum

The microscopic momentum equation for the liquid phase is

$$\frac{\partial}{\partial t}(\rho_l \mathbf{V}_l) + \nabla \cdot (\rho_l \mathbf{V}_l \mathbf{V}_l) + \nabla P_l - \nabla \cdot \tau_l - \rho_l \mathbf{f} = 0, \quad (3.58)$$

where  $P_l$ ,  $\tau_l$ , and  $\mathbf{f}$  are, respectively, the pressure, the viscous stress tensor, and the body force per unit mass of the liquid. If the body force is entirely gravitational, then

$$\mathbf{f} = \mathbf{g} = -\nabla \Phi, \quad (3.59)$$

where  $\Phi$  is the gravitational potential. We substitute Eq. (3.59) into Eq. (3.58), integrate the resulting equation over an elementary volume, apply the transport theorem to the first term and the averaging theorem to the second, third, and fourth terms, and use Eq. (3.44). We also make use of the equation of continuity (3.57) and replace  $\nabla \cdot \tau_l$  by  $\mu_l \nabla^2 \langle \mathbf{V}_l \rangle$  (see Gray and O'Neill, 1976). We get

$$\begin{aligned} & \left[ \varepsilon_l \langle \rho_l \rangle^l \frac{\partial}{\partial t} \langle \mathbf{V}_l \rangle^l + \varepsilon_l \langle \rho_l \rangle^l \langle \mathbf{V}_l \rangle \cdot \nabla \langle \mathbf{V}_l \rangle \right. \\ & \quad \left. + V^{-1} \int_{A_{lg}} \rho_l \mathbf{V}_l (\mathbf{V}_l - w_{lg}) \cdot \mathbf{n}_l dS + \nabla \cdot (\langle \rho_l \rangle^l \langle \tilde{\mathbf{V}}_l \tilde{\mathbf{V}}_l \rangle) \right] \\ & \quad + \varepsilon_l \nabla \langle P_l \rangle^l + \varepsilon_l \langle \rho_l \rangle^l \nabla \langle \Phi_l \rangle^l \\ & \quad + V^{-1} \int_{A_{lg}} \left( \tilde{P}_l + \langle \rho_l \rangle^l \tilde{\Phi}_l \right) \mathbf{n}_l dS + V^{-1} \int_{A_{ls}} \left( \tilde{P}_l + \langle \rho_l \rangle^l \tilde{\Phi}_l \right) \mathbf{n}_l dS \\ & \quad - \mu_l \nabla^2 \langle \mathbf{V}_l \rangle - V^{-1} \int_{A_{lg}} \mathbf{n}_l \cdot \tau_l dS - V^{-1} \int_{A_{ls}} \mathbf{n}_l \cdot \tau_l dS = 0, \end{aligned} \quad (3.60)$$

where density gradients at the microscopic level have been assumed to be small compared to the corresponding velocity gradients.

For an isotropic medium, Gray and O'Neill (1976) argued that

$$V^{-1} \int_{A_{lg}} \mathbf{n}_l \cdot \tau_l dS + V^{-1} \int_{A_{ls}} \mathbf{n}_l \cdot \tau_l dS = \mu \varepsilon_l B \left( \langle \mathbf{V}_s \rangle^s - \langle \mathbf{V}_l \rangle^l \right) \quad (3.61)$$

and

$$\begin{aligned} & V^{-1} \int_{A_{lg}} (\tilde{P}_l + \langle \rho_l \rangle^l \tilde{\Phi}_l) n_l dS + V_l^{-1} \int_{A_{ls}} (\tilde{P}_l + \langle \rho_l \rangle^l \tilde{\Phi}_l) \mathbf{n}_l dS \\ & = \mathbf{F} \left( \nabla \langle P_l \rangle^l + \langle \rho_l \rangle^l \nabla \langle \Phi_l \rangle^l \right) \end{aligned} \quad (3.62)$$

where  $B$  and  $F$  are constants that depend on the nature of the isotropic medium. Substituting Eqs. (3.61) and (3.62) into Eq. (3.60) and neglecting the inertia terms

in the square brackets and the term  $\mu \nabla^2 \langle \mathbf{V}_l \rangle$  (compare the discussion in Sect. 1.5) yields

$$\langle \mathbf{V}_l \rangle^l - \langle \mathbf{V}_s \rangle^s = -\frac{k_{sl} K}{\varepsilon_l \mu_l} \left( \nabla \langle P_l \rangle^l + \langle \rho_l \rangle^l \nabla \langle \Phi_l \rangle^l \right), \quad (3.63)$$

where  $k_{sl} K \equiv \varepsilon_l (1 + F)/B$ . Here  $K$  denotes the intrinsic permeability of the porous medium, as defined for one-phase flow. The new quantity  $k_{sl}$  is the relative permeability of the porous medium saturated with liquid. It is a dimensionless quantity.

Similarly, when inertia terms and the term  $\mu_g \nabla^2 \langle \mathbf{V}_g \rangle$  are neglected, the momentum equation for the gas phase is

$$\langle \mathbf{V}_g \rangle^g - \langle \mathbf{V}_s \rangle^s = -\frac{k_{sg} K}{\varepsilon_g \mu_g} \left( \nabla \langle P_g \rangle^g + \langle \rho_g \rangle^g \nabla \langle \Phi_g \rangle^g \right), \quad (3.64)$$

where  $k_{sg}$  denotes the relative permeability of the porous medium saturated with gas. Equations (3.63) and (3.64) are the Darcy equations for a liquid–gas combination in an isotropic porous medium. A similar expression for an anisotropic medium has been developed by Gray and O’Neill (1976). A permeability tensor is involved. They also obtain an expression for flow in an isotropic medium with nonnegligible inertial effects.

### 3.5.3 Conservation of Energy

The microscopic energy equation, in terms of enthalpy for the liquid phase, is

$$\frac{\partial}{\partial t} (\rho_l h_l) + \nabla \cdot (\rho_l h_l \mathbf{V}_l - k_l \nabla T_l) - \left( \frac{\partial P_l}{\partial t} + \mathbf{V}_l \cdot \nabla P_l \right) = 0, \quad (3.65)$$

where  $h_l$  and  $k_l$  are the enthalpy and thermal conductivity of the liquid. In writing this equation we have neglected the viscous dissipation, thermal radiation, and any internal energy generation. Integrating this equation over a representative elementary volume and applying the transport equations to the first and fourth terms, Eqs. (3.44) and (3.45) to the second term, Eq. (3.46) to the third term, and Eq. (3.44) to the fifth term yields, Eq. (3.66)

$$\begin{aligned} & \frac{\partial}{\partial t} \left( \varepsilon_l \langle \rho_l \rangle^l \langle h_l \rangle_l \right) + \nabla \cdot \left( \langle \rho_l \rangle_l \langle h_l \rangle_l \langle \mathbf{V}_l \rangle \right) - \nabla \cdot \left( \varepsilon_l k_l^* \nabla \langle T_l \rangle^l \right) \\ & - \left[ \varepsilon_l \frac{\partial}{\partial t} \left( \langle P_l \rangle^l \right) + \langle \mathbf{V}_l \rangle \cdot \nabla \langle P_l \rangle^l \right] + Q_{lg} + Q'_{lg} + Q'_{ls} = 0, \end{aligned} \quad (3.66)$$

where  $k_l^*$  is the effective thermal conductivity of the liquid in the presence of the solid matrix. This  $k_l^*$  is the sum of the stagnant thermal conductivity  $k_l'$  (due to molecular diffusion) and the thermal dispersion coefficient  $k_l''$  (due to mechanical dispersion), which in turn are defined by

$$-\varepsilon_l k_l' \nabla \langle T_l \rangle^l = -\langle k_l \rangle^l \left( \varepsilon_l \nabla \langle T_l \rangle^l + V^{-1} \int_{A_{lg}} \tilde{T}_l n_l dS + V^{-1} \int_{A_{ls}} \tilde{T}_l \mathbf{n}_l dS \right) \quad (3.67a)$$

and

$$\begin{aligned} -\nabla \cdot (\varepsilon_l k_l'' \nabla \langle T_l \rangle^l) &= \nabla \cdot (\rho_l h_l \tilde{\mathbf{V}}_l) - \langle \tilde{\mathbf{V}}_l \cdot \nabla \tilde{P}_l \rangle \\ &+ V^{-1} \int_{A_{lg}} \tilde{P}_l \tilde{\mathbf{V}}_l \cdot \mathbf{n}_l dS + V^{-1} \int_{A_{ls}} \tilde{P}_l \tilde{\mathbf{V}}_l \cdot \mathbf{n}_l dS. \end{aligned}$$

The integrals in Eq. (3.67a) account for the change in thermal diffusion due to the microstructure of the solid matrix. The terms  $Q_{lg}$ ,  $Q'_{lg}$ , and  $Q'_{ls}$  are given, respectively, by

$$Q_{lg} = V^{-1} \int_{A_{lg}} (\rho_l h_l - \tilde{P}_l) (\mathbf{V}_l - w_{lg}) \cdot \mathbf{n}_l dS \approx V^{-1} \int_{A_{lg}} \rho_l h_l (\mathbf{V}_l - w_{lg}) \cdot \mathbf{n}_l dS, \quad (3.68a)$$

$$Q'_{lg} = V^{-1} \int_{A_{lg}} \mathbf{q} \cdot \mathbf{n}_l dS \quad (3.68b)$$

$$Q'_{ls} = V^{-1} \int_{A_{ls}} \mathbf{q} \cdot \mathbf{n}_l dS = A_{ls} h_l V^{-1} (T_s - T_l), \quad (3.68c)$$

where  $\mathbf{q}$  in Eqs. (3.68b) and (3.68c) is the conduction heat flux across the interface and  $h_l$  in Eq. (3.68c) is defined as the local volume averaged heat transfer coefficient at the liquid–solid interface, which depends on the physical properties of the liquid and its flow rate.

Similarly, the energy equation for the gas phase and for the solid-matrix phase is, respectively,

$$\begin{aligned} \frac{\partial}{\partial t} \left( \varepsilon_g \langle \rho_g \rangle^g \langle h_g \rangle^g \right) + \nabla \cdot \left( \langle \rho_g \rangle^g \langle h_g \rangle^g \langle \mathbf{V}_g \rangle \right) - \nabla \cdot \left( \varepsilon_g k_g^* \nabla \langle T_g \rangle^g \right) \\ - \left( \varepsilon_g \frac{\partial}{\partial t} \langle \rho_g \rangle^g + \langle \mathbf{V}_g \rangle \cdot \nabla \langle P_g \rangle^g \right) + Q_{gl} + Q'_{gl} + Q'_{gs} = 0 \end{aligned} \quad (3.69)$$

and

$$\begin{aligned} \frac{\partial}{\partial t} (\varepsilon_s \langle \rho_s \rangle^s \langle h_s \rangle^s) + \nabla \cdot (\langle \rho_s \rangle^s \langle h_s \rangle^s \langle \mathbf{V}_s \rangle) - \nabla \cdot (\varepsilon_s k_s^* \nabla \langle T_s \rangle^s) \\ - \left( \varepsilon_s \frac{\partial}{\partial t} \langle P_s \rangle^s + \langle \mathbf{V}_s \rangle \cdot \nabla \langle P_s \rangle^s \right) + Q'_{sl} + Q'_{sg} = 0, \end{aligned} \quad (3.70)$$

where  $k_g^*$  and  $k_s^*$  are defined analogously to  $k_l^*$  and similarly for the various  $Q$  terms. Note that

$$Q_{gl} = -Q_{lg}, \quad Q'_{gl} = -Q'_{lg}, \quad Q'_{sl} = -Q'_{ls} \quad (3.71)$$

and

$$Q'_{gs} = V^{-1} \int_{A_{gs}} \mathbf{q} \cdot \mathbf{n}_g dS = A_{gs} h_g V^{-1} (T_s - T_g) = -Q'_{sg} \quad (3.72)$$

where  $h_g$  is the heat transfer coefficient at the gas–solid interface.

The difference between  $P_g$  and  $P_l$  is called the capillary pressure. In many circumstances, including most geophysical situations, the capillary pressure can be neglected, so in this case we have

$$\langle P_l \rangle^l = \langle P_g \rangle^g = \langle P_s \rangle^s = \langle P \rangle. \quad (3.73)$$

Furthermore, we can usually assume local thermodynamic equilibrium and so

$$\langle T_l \rangle^l = \langle T_g \rangle^g = \langle T_s \rangle^s = \langle T \rangle. \quad (3.74)$$

Adding Eqs. (3.66), (3.69), and (3.70) in this case, we get

$$\begin{aligned} \frac{\partial}{\partial t} \left[ \varphi S_l \langle \rho_l \rangle^l \langle h_l \rangle^l + \varphi S_g \langle \rho_g \rangle^g \langle h_g \rangle^g + (1 - \varphi) \langle \rho_s \rangle^s \langle h_s \rangle^s \right] \\ + \nabla \cdot \left[ \langle \rho_l \rangle^l \langle h_l \rangle^l \langle \mathbf{V}_l \rangle + \langle \rho_g \rangle^g \langle h_g \rangle^g \langle \mathbf{V}_g \rangle + \langle \rho_s \rangle^s \langle h_s \rangle^s \langle \mathbf{V}_s \rangle \right] \\ - \nabla \cdot (k \nabla \langle T \rangle) - \left[ \frac{\partial}{\partial t} \langle P \rangle + (\langle \mathbf{V}_l \rangle + \langle \mathbf{V}_g \rangle + \langle \mathbf{V}_s \rangle) \cdot \nabla \langle P \rangle \right] = 0, \end{aligned} \quad (3.75)$$

where  $k = \varphi (S_l k_l^* + S_g k_g^*) + (1 - \varphi) k_s^*$  is the effective thermal conductivity of the porous medium saturated with liquid and gas at local thermal equilibrium, with the heat conduction assumed to be in parallel (see Sect. 2.2.1).

### 3.5.4 Summary: Relative Permeabilities

The governing equations for two-phase flow, for the case of negligible capillary pressure and local thermal equilibrium, are Eqs. (3.57), (3.63), (3.64), and (3.75).

Since  $P$  and  $T$  are independent of phase we can drop the angle brackets in  $\langle P \rangle$  and  $\langle T \rangle$ . Also we note that  $\langle \mathbf{V}_l \rangle$  is just  $\mathbf{v}_l$ , the seepage velocity for the liquid phase, etc. Also, in Eq. (3.57),  $\langle \rho_l \rangle \langle \mathbf{V}_l \rangle^1 = \varepsilon_l^{-1} \langle \rho_l \rangle \langle \mathbf{V}_l \rangle = \langle \rho_l \rangle^1 \langle \mathbf{V}_l \rangle$ , etc. For a gravitational body force we have  $\nabla \Phi_l = \nabla \Phi_g = -\mathbf{g}$ . Thus we can rewrite the four governing equations, with the angle brackets for intrinsic averages dropped, as

$$\frac{\partial}{\partial t} \left[ \varphi S_l \rho_l + \varphi S_g \rho_g + (1 - \varphi) \rho_s \right] + \nabla \cdot (\rho_l \mathbf{v}_l + \rho_g \mathbf{v}_g + \rho_s \mathbf{v}_s) = 0, \quad (3.76)$$

$$\mathbf{v}_l - \frac{\varepsilon_l}{\varepsilon_s} \mathbf{v}_s = -\frac{k_{sl} K}{\mu_l} (\nabla P - \rho_l \mathbf{g}), \quad (3.77)$$

$$\mathbf{v}_g - \frac{\varepsilon_g}{\varepsilon_s} \mathbf{v}_s = -\frac{k_{sg} K}{\mu_g} (\nabla P - \rho_g \mathbf{g}), \quad (3.78)$$

$$\begin{aligned} \frac{\partial}{\partial t} & \left[ \varphi S_l \rho_l h_l + \varphi S_g \rho_g h_g + (1 - \varphi) \rho_s h_s \right] + \nabla \cdot (\rho_l h_l \mathbf{v}_l + \rho_g h_g \mathbf{v}_g + \rho_s h_s \mathbf{v}_s) \\ & - \nabla \cdot (k \nabla T) - \left[ \frac{\partial P}{\partial t} + (\mathbf{v}_l + \mathbf{v}_g + \mathbf{v}_s) \cdot \nabla P \right] = 0. \end{aligned} \quad (3.79)$$

We can now extend Eqs. (3.76) and (3.79) by allowing for source terms  $q_M'''$  (rate of increase of mass per unit volume of the medium) and  $q_E'''$  (rate of increase of energy per unit volume of the medium). At the same time we can introduce  $A_M$  and  $A_E$ , respectively, the mass and energy per unit volume of the medium, and  $\mathbf{F}_M$  and  $\mathbf{F}_E$ , the mass flux and energy flux in the medium. These are given by

$$A_M = \varphi S_l \rho_l + \varphi S_g \rho_g + (1 - \varphi) \rho_s, \quad (3.80)$$

$$A_E = \varphi S_l \rho_l h_l + \varphi S_g \rho_g h_g + (1 - \varphi) \rho_s h_s, \quad (3.81)$$

$$\mathbf{F}_M = \rho_l \mathbf{v}_l + \rho_g \mathbf{v}_g + \rho_s \mathbf{v}_s, \quad (3.82)$$

$$\mathbf{F}_E = \rho_l h_l \mathbf{v}_l + \rho_g h_g \mathbf{v}_g + \rho_s h_s \mathbf{v}_s - k \nabla T. \quad (3.83)$$

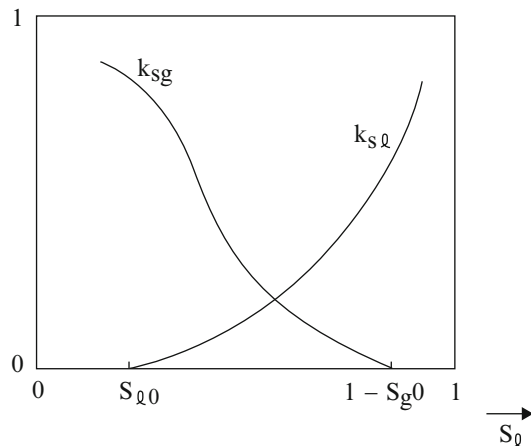
We also write

$$\frac{D^* P}{D t} = \frac{\partial P}{\partial t} + (\mathbf{v}_l + \mathbf{v}_g + \mathbf{v}_s) \cdot \nabla P. \quad (3.84)$$

Thus,  $D^*/Dt$  is a material derivative based on the sum of  $\mathbf{v}_l$ ,  $\mathbf{v}_g$ , and  $\mathbf{v}_s$ , rather than the mass-weighted average of the velocities. The extended forms of the mass equation (3.76) and the energy equation (3.79) are

$$\frac{\partial A_M}{\partial t} + \nabla \cdot \mathbf{F}_M = q_M''' \quad (3.85)$$

**Fig. 3.1** The general form of the relative permeability curves for two-phase flow through a porous medium



and

$$\frac{\partial A_E}{\partial t} + \nabla \cdot \mathbf{F}_E - \frac{D^* P}{D t} = q'''_E. \quad (3.86)$$

We are now confronted with the task of solving the Darcy equations (3.77) and (3.78), the mass equation (3.85), and the energy equation (3.86) subject to appropriate initial and boundary conditions. In many practical situations there will be no source terms ( $q''_M = q'''_E = 0$ ), the solid matrix will be fixed ( $\mathbf{v}_s = 0$ ), and the pressure term  $D^* P/Dt$  will be negligible. Even then the task is not straightforward, because the relative permeabilities are not constant.

It is observed experimentally that in general the relative permeability for the liquid phase  $k_{sl}$  increases in a nonlinear fashion from 0 to 1 as the liquid saturation  $S_l$  increases from 0 to 1, and the functional relationship is not single valued. The value observed as  $S_l$  increases differs from that observed as  $S_l$  decreases, i.e., one has hysteresis. Also,  $k_{sl}$  may not differ from zero until  $S_l$  exceeds some nonzero critical value  $S_{l0}$ . This last behavior is illustrated in Fig. 3.1.

The complications arise because usually one fluid “wets” the solid and adheres to its surfaces, and each fluid can establish its own channels of flow through the medium only to a limited extent. Further, the flow of one fluid can destroy the connectivity of the pores available for the flow of the other fluid. Another factor affecting permeability is the difference in viscosity between fluids; one fluid can act as a lubricant for the other. Also, permeabilities tend to be slightly higher at higher pressure gradients.

In view of this complexity it is fortunate that experience has shown that the main qualitative features of convection flows are not sensitive to the precise form of the relative permeability versus saturation relationship. For several situations, satisfactory results have been reported when use has been made of a simple linear relationship, namely,

$$k_{sl} = S_l, \quad k_{sg} = S_g (= 1 - S_l). \quad (3.87)$$

For the case when the liquid is oil, Corey et al. (1956) proposed the use of the semiempirical formulas

$$k_{sl} = \hat{S}_l^4 \quad \text{and} \quad k_{sg} = (1 - \hat{S}_l)^2 (1 - \hat{S}_l^2), \quad (3.88a)$$

where

$$\hat{S}_l = \frac{S_l - S_{l0}}{1 - S_{l0} - S_g}. \quad (3.88b)$$

The Corey formulas also have been used with water and steam.

A general alternative description of two-phase flow has been proposed by Hassanzadeh and Gray (1993). An experimental study of relative permeabilities and the various flow regimes that arise during steady-state two-phase flow was reported by Avroam and Payatakes (1995). A new model for multiphase, multicomponent transport in capillary porous media, in which the multiple phases are considered as constituents of a multiphase mixture, has been developed by Wang and Cheng (1996). This model is mathematically equivalent to the traditional model but involves a reduced number of model equations. An experimental and theoretical study of two-phase flow and heat transfer was conducted by Jamialahmadi et al. (2005). Some specific situations involving two-phase flows are discussed in Sect. 11.9.

The concept of relative permeability was critiqued by Spanos (2012).

### 3.6 Unsaturated Porous Media

Here we provide introductory references to an important topic that we have not discussed because of lack of space. The modeling of convection in unsaturated porous media, with and without boiling or condensation, has been discussed by Plumb (1991a). The particular topic of drying of porous media has been surveyed by Bories (1991) and Plumb (1991b, 2000). Some additional references to convection in unsaturated porous media are given in the general review by Tien and Vafai (1990a). The subject of multiphase flow and heat transfer in porous media has been reviewed by Wang and Cheng (1997) and Chang and Wang (2002). These papers reveal that convection in unsaturated media is a difficult problem.

One difficulty is that because of instabilities the interface between phases is on the macroscopic scale often far from being a well-defined smooth surface. A second difficulty is caused by the effects of surface tension. This produces a pressure difference that is proportional to the interface curvature on the *pore scale*, something that is completely different from the interface curvature on the macroscopic scale. Since the local pressure difference is affected by contact angle, and this is

dependent on a number of things, there is a fundamental difficulty in calculating the appropriate average pressure difference on the macroscopic scale. A third difficulty is that hysteresis is commonly associated with the advance and recession of a phase interface.

Some recent papers involving the drying of porous media include those by Francis and Wepfer (1996); Daurelle et al. (1998); Lin et al. (1998); Oliveira and Haghghi (1998); Mhimid et al. (1999, 2000); Zili and Ben Nasrallah (1999); Coussot (2000); Landman et al. (2001); Natale and Santillan Marcus (2003); Ploude and Prat (2003); Salagnac et al. (2004); Nganhou (2004); Dayan et al. (2004); Frei et al. (2004); Tao et al. (2005); Erriquible et al. (2006b); Izadifar et al. (2006); Dantas et al. (2007); Lu and Shen (2007); Prat (2007); Sander (2007); Skikiatden and Roberts (2007); Yiotis et al. (2007); Almubarak et al. (2008); Bennamon and Belhamri (2008); Kowalski and Pawlowski (2008); Lehmann et al. (2008); Murugesan et al. (2008); Salagnac et al. (2008); Sghaier et al. (2008); Sinha et al. (2008); Surasani et al. (2008a, b); Mihoubli and Bellagi (2009); Kowalski et al. (2010); Prommas et al. (2010); and Prommas (2011).

Recent papers of other aspects of convection in unsaturated media include those of Yu et al. (1993); Hanamura and Kaviany (1995); Larbi et al. (1995); Zhu and Vafai (1996); Dickey and Peterson (1997); Gibson and Charmchi (1997); Bouddour et al. (1998); Chen et al. (1998a); Figus et al. (1998); Yan et al. (1998); Wang and Cheng (1998); Moya et al. (1999); Peng et al. (2000); Zhao and Liao (2000); Liu et al. (2002); Kacur and Van Keer (2003); Shen et al. (2003); Zili-Ghedira et al. (2003); Jadhav and Pillai (2003); Dos Santos and Mendes (2009a, b); and Najjar and Ben Nasrallah (2009).

### 3.7 Electrodiffusion Through Porous Media

Diffusion is a slow process. When the diffusing species are electrically charged, diffusion can be accelerated by applying externally an electric current or by imposing a gradient of electrical potential. There are many applications at several scales, for example, the delivery of drugs by iontophoresis through the human body and the dechlorination of concrete structures such as bridges contaminated and corroded by sea water.

The basics of diffusion of ionic species through nonreactive and reactive porous media were reviewed most recently in the book by Bejan et al. (2004), based on the work of Frizon et al. (2003) and others. This section is based on the simplest presentation of electrodiffusion through nonreactive porous media, which was made based on scale analysis by Lorente and Ollivier (2006).

Instead of the classical Fick diffusion equation (3.22), the presence of electrical forces requires the use of the more general Nernst-Planck equation

$$\varphi \frac{\partial C_i}{\partial t} = D_i \frac{\partial}{\partial x} \left( \frac{\partial C_i}{\partial x} + z_i \frac{F}{RT} C_i \frac{\partial \psi}{\partial x} \right). \quad (3.89)$$

The subscript  $i$  indicates the ionic species that diffuses through the porous medium,  $z_i$  is the charge number,  $F$  is the Faraday constant,  $R$  is the ideal gas constant,  $T$  is the absolute temperature, and  $\psi$  is the electric potential created by the ionic species. In the same equation,  $C_i$  is the ionic species concentration, and  $D_i$  is the effective diffusion coefficient of the species. For simplicity, we consider time-dependent diffusion in one direction ( $x$ ). The problem is closed by solving Eq. (3.89) in conjunction with the current conservation equation,

$$F \sum_i z_i j_i = j \quad (3.90)$$

where  $j_i$  is the ionic flux through the porous medium,

$$j_i = -D_i \left( \frac{\partial C_i}{\partial x} + z_i \frac{F}{RT} C_i \frac{\partial \psi}{\partial x} \right) \quad (3.91)$$

and  $j$  is the constant current density applied from the outside. The electric potential gradient follows from Eqs. (3.90) and (3.91):

$$\frac{\partial \psi}{\partial x} = -\frac{RT}{F} \frac{j}{F} + \frac{\sum_i z_i D_i \frac{\partial C_i}{\partial x}}{\sum_i z_i^2 D_i C_i}. \quad (3.92)$$

As an example, consider a one-dimensional porous medium (a slab) of thickness  $L$ . Initially the species of interest has  $C_i = 0$  throughout the porous medium ( $0 < x < L$ ). At the time  $t = 0$ , a new concentration level is imposed on one face,  $C_i = \Delta C_i$  at  $x = 0$ , while the  $x = L$  face is maintained at  $C_i = 0$ .

Lorente and Ollivier (2006) established the scales of diffusion in two limits. When the dominant driving force is the concentration gradient, the scales are those of classic diffusion, and the time of diffusion penetration over the distance  $L$  is

$$t_{\text{diff}} \sim \varphi \frac{L^2}{D_i}. \quad (3.93)$$

When electrical effects dominate, the time of diffusion over  $L$  is

$$t_{\text{el}} \sim \varphi \frac{LF}{j} \Delta C_i. \quad (3.94)$$

The transition between the two regimes is described by the new dimensionless group

$$B = \frac{FD\Delta C_i}{Lj} \quad (3.95)$$

which is the ratio of the two characteristic time scales,

$$B \sim \frac{t_{el}}{t_{diff}}. \quad (3.96)$$

Lorente and Ollivier (2006) modeled the same one-dimensional time-dependent electrodiffusion numerically, in a nondimensionalization based on the correct scales revealed by scale analysis. Numerical simulations conducted for practical examples (e.g., the extraction of an ionic species from a contaminated block) validated the predictions based on scale analysis and confirmed the correctness of both methods. Lorente (2007) showed that the constructal law governs the sequence in which this phenomenon selects its diffusion mechanism. At any point in time, the selected mechanism is the one that facilitates flow access. The progress with the constructal law field was reviewed by Bejan and Lorente (2006, 2010, 2011). Auger et al. (2008) used the constructal design philosophy (Bejan and Lorente, 2008) to develop the geometric configuration of electrodes to facilitate ionic access through a finite size porous medium.

### 3.8 Nanofluids

We may regard a nanofluid is being a special sort of multicomponent fluid. Nanofluids are suspensions whose distinctive feature is an unusually small size of particles suspended in a base fluid (which can be water or an organic solvent); nanoparticles' sizes are typically in the range between 1 and 100 nm. They have been extensively studied in recent years because of the possibility that they may lead to enhanced heat transfer. Due to a very small size of suspended nanoparticles, nanofluids form very stable colloidal systems with very little settling, and significant enhancement of effective thermal conductivity in comparison with the base fluid has been observed in some experiments.

Currently two distinct approaches are being investigated. One approach, employed by Tiwari and Das (2007), is to examine the effect of the variation of thermal conductivity and viscosity with nanofluid particle fraction, utilizing expressions obtained using the theory of mixtures, namely

$$\frac{\mu_{eff}}{\mu_f} = \frac{1}{(1 - \eta)^{2.5}}, \quad (3.97)$$

$$\frac{k_{eff}}{k_f} = \frac{(k_p + 2k_f) - \eta(k_f - k_p)}{(k_p + 2k_f) + \eta(k_f - k_p)}. \quad (3.98)$$

Here  $\eta$  denotes the nanoparticle fraction, and  $k_p$  is the conductivity of the nanoparticles. Equation (3.97) was obtained by Brinkman (1952) using ideas due to Einstein, and Eq. (3.98) is the Maxwell-Garnett formula for a suspension of spherical particles that dates back to Maxwell (1904).

An alternative approach is to follow Buongiorno (2006) who, after considering alternative agencies, proposed a model incorporating the effects of Brownian diffusion and the thermophoresis, each of which gives rise to cross-diffusion terms that are in some ways analogous to the Soret and Dufour terms. In the form used by Nield and Kuznetsov (2009d), the equation of mass conservation is unchanged while the other governing equations, for the conservation of momentum, heat, and nanoparticles, are

$$\rho_f \left( \frac{1}{\phi} \frac{\partial \mathbf{v}}{\partial t} + \frac{1}{\phi^2} \mathbf{v} \cdot \nabla \mathbf{v} \right) = -\nabla p + \mu_{\text{eff}} \nabla^2 \mathbf{v} - \frac{\mu}{K} \mathbf{v} \\ + \left[ \eta \rho_p + (1 - \eta) \left\{ \rho_f (1 - \beta(T - T_0)) \right\} \right] \mathbf{g}, \quad (3.99)$$

$$(\rho c)_m \frac{\partial T}{\partial t} + (\rho c)_f \mathbf{v} \cdot \nabla T = \nabla \cdot (k_m \nabla T) \\ + \varphi (\rho c)_p \left[ D_B \nabla \eta \cdot \nabla T + D_T \frac{\nabla T \cdot \nabla T}{T} \right], \quad (3.100)$$

$$\frac{\partial \eta}{\partial t} + \frac{1}{\phi} \mathbf{v} \cdot \nabla \eta = \nabla \cdot \left[ D_B \nabla \eta + D_T \frac{\nabla T}{T} \right]. \quad (3.101)$$

Here  $\rho_p$  is the density of the particles. The new parameters are the Brownian motion coefficient  $D_B$  and the thermophoresis coefficient  $D_T$ . In deriving these equations it has been assumed that the Brownian motion and thermophoresis processes remain coherent while volume averages over a representative elementary volume are taken. In the spirit of the Boussinesq approximation the buoyancy term in Eq. (3.99) has been linearized. Equation (3.101) involves just intrinsic quantities in the sense that the average is being taken over the nanofluid only and the solid matrix is not involved. In writing Eq. (3.100) it has been assumed that in nanofluids the particles are so small that for practical purposes they remain in suspension in a uniform manner and that in a porous medium the nanoparticles are suspended in nanofluid using either surfactant or surface charge technology, something that prevents particles from agglomeration and deposition on the porous matrix.

# Chapter 4

## Forced Convection

The fundamental question in heat transfer engineering is to determine the relationship between the heat transfer rate and the driving temperature difference. In nature, many saturated porous media interact thermally with one another and with solid surfaces that confine them or are embedded in them. In this chapter we analyze the basic heat transfer question by looking only at *forced-convection* situations, in which the fluid flow is caused (forced) by an external agent unrelated to the heating effect. First we discuss the results that have been developed based on the Darcy flow model and later we address the more recent work on the non-Darcy effects. We end this chapter with a review of current engineering applications of the method of forced convection through porous media. Some fundamental aspects of the subject have been discussed by Lage and Narasimhan (2000), and the topic has been reviewed by Lauriat and Ghafir (2000).

### 4.1 Plane Wall with Prescribed Temperature

Perhaps the simplest and most common heat transfer arrangement is the flow parallel to a flat surface that borders the fluid-saturated porous medium. With reference to the two-dimensional geometry defined in Fig. 4.1, we recognize the equations governing the conservation of mass, momentum (Darcy flow), and energy in the flow region of thickness  $\delta_T$ :

$$\frac{\partial u}{\partial x} + \frac{\partial v}{\partial y} = 0, \quad (4.1)$$

$$u = -\frac{K}{\mu} \frac{\partial P}{\partial x}, \quad v = -\frac{K}{\mu} \frac{\partial P}{\partial y}, \quad (4.2)$$

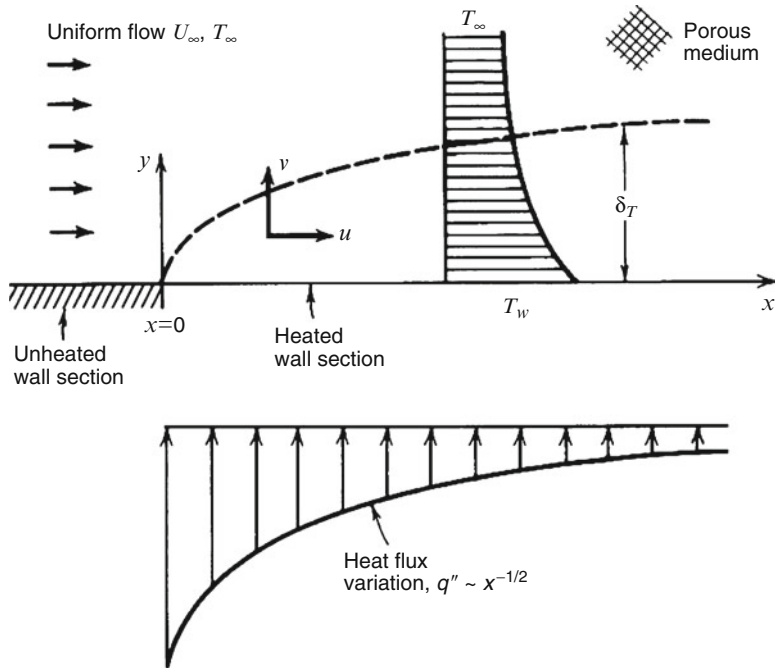


**Fig. 4.1** Parallel flow near an isothermal wall (Bejan 1984)

$$u \frac{\partial T}{\partial x} + v \frac{\partial T}{\partial y} = \alpha_m \frac{\partial^2 T}{\partial y^2}. \quad (4.3)$$

Note the boundary-layer-approximated right-hand side of Eq. (4.3), which is based on the assumption that the region of thickness  $\delta_T$  and length  $x$  is slender ( $\delta_T \ll x$ ). The fluid mechanics part of the problem statement [namely, Eqs. (4.1) and (4.2)] is satisfied by the uniform parallel flow

$$u = U, \quad v = 0. \quad (4.4)$$

The constant pressure gradient that drives this flow ( $-dP/dx = \mu U_\infty / K$ ) is assumed known.

The heat transfer rate between the surface at temperature  $T_w$  and the saturated porous medium at far-field temperature  $T_\infty$  can be determined in several ways. The scale analysis begins with writing  $\Delta T = T_w - T_\infty$  so that the order-of-magnitude counterpart of Eq. (4.3) becomes

$$U_\infty \frac{\Delta T}{x} \sim \alpha_m \frac{\Delta T}{\delta_T^2}. \quad (4.5)$$

From this we can determine the thickness of the thermal boundary layer

$$\delta_T \sim x Pe_x^{-1/2} \quad (4.6)$$

in which  $Pe_x$  is the Péclet number based on  $U_\infty$  and  $x$ :

$$Pe_x = \frac{U_\infty x}{\alpha_m}. \quad (4.7)$$

For the local heat flux  $q''$  we note the scale  $q'' \sim k_m \Delta T / \delta_T$  or the corresponding local Nusselt number

$$Nu_x = \frac{q''}{\Delta T} \frac{x}{k_m} \sim Pe_x^{1/2}. \quad (4.8)$$

Figure 4.1 qualitatively illustrates the main characteristics of the heat transfer region, namely, the boundary-layer thickness that increases as  $x^{1/2}$  and the heat flux that decays as  $x^{-1/2}$ . The exact analytical solution for the same problem can be derived in closed form by introducing the similarity variables recommended by the scale analysis presented above:

$$\eta = \frac{y}{x} Pe_x^{1/2}, \quad \theta(\eta) = \frac{T - T_w}{T_\infty - T_w}. \quad (4.9)$$

In this notation, the energy equation (4.3) and the boundary conditions of Fig. 4.1 become

$$\theta'' + \frac{1}{2} \eta \theta' = 0, \quad (4.10)$$

$$\theta(0) = 0, \quad \theta(\infty) = 1. \quad (4.11)$$

Equation (4.10) can be integrated by separation of variables, and the resulting expressions for the similarity temperature profile and the surface heat flux are (Bejan 1984)

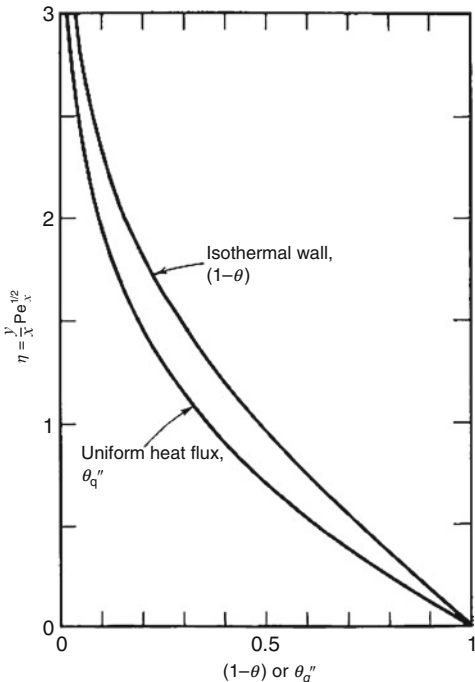
$$\theta = \operatorname{erf}\left(\frac{\eta}{2}\right), \quad (4.12)$$

$$Nu_x = \frac{q''}{T_w - T_\infty} \frac{x}{k_m} = 0.564 Pe_x^{1/2}. \quad (4.13)$$

The overall Nusselt number based on the heat flux  $\bar{q}''$  averaged from  $x = 0$  to a given plate length  $x = L$  is

$$\overline{Nu_L} = \frac{\bar{q}''}{T_w - T} \frac{L}{k_m} = 1.128 Pe_L^{1/2}. \quad (4.14)$$

**Fig. 4.2** The temperature distributions in a forced parallel flow near walls with constant temperature and constant heat flux (Bejan 1984)



Cheng (1977c) found the same  $Nu_x$  result by integrating numerically the equivalent of Eqs. (4.10) and (4.11) for a wider class of problems. The similarity temperature profile (4.12) has been plotted as  $(1-\theta)$  vs.  $\eta$  in Fig. 4.2. The effect of viscous dissipation has been included in the analysis by Magyari et al. (2003b). An experimental study of forced convection over a horizontal plate in a porous medium was reported by Afifi and Berbish (1999). Magyari et al. (2001a) presented some exact analytical solutions for forced convection past a plane or axisymmetric body having a power-law surface distribution. Li et al. (2009) obtained an integral solution for forced convection over an isothermal plate.

## 4.2 Plane Wall with Constant Heat Flux

When the surface heat flux  $q''$  is independent of  $x$ , the temperature difference  $T_w - T_\infty$  increases as  $x$  in the downstream direction. This can be seen by combining the heat flux scale  $q'' \sim k_m(T_w - T_\infty)/\delta_T$  with the  $\delta_T$  scale (4.6), which applies to the constant  $q''$  configuration as well. The similarity solution for the temperature distribution along and near the  $y = 0$  surface was determined numerically by Bejan (1984),

$$T(x, y) - T_\infty = \frac{q''/k_m}{(-d\theta_{q''}/d\eta)_{\eta=0}} \left( \frac{\alpha_m x}{U} \right)^{1/2} \theta_{q''}(\eta), \quad (4.15)$$

in which  $\theta_{q''}(\eta)$  is the similarity temperature profile displayed in Fig. 4.2. The similarity variable  $\eta$  is defined on the ordinate of the figure. Since the calculated slope of the  $\theta_{q''}$  profile at the wall is  $(-d\theta_{q''}/d\eta)_{\eta=0} = 0.886$ , the inverse of the local temperature difference can be nondimensionalized as the local Nusselt number

$$Nu_x = \frac{q''}{T_w(x) - T} \frac{x}{k_m} = 0.886 Pe_x^{1/2}. \quad (4.16)$$

The overall Nusselt number that is based on the average wall temperature  $\bar{T}_w$  (specifically, the temperature averaged from  $x = 0$  to  $x = L$ ) is

$$\overline{Nu_L} = \frac{q''}{\bar{T}_w - T} \frac{L}{k_m} = 1.329 Pe_L^{1/2}. \quad (4.17)$$

We use this opportunity to communicate the exact solution for the problem of heat transfer from an embedded wall with uniform heat flux. The closed-form analytical alternative to the numerical solution (4.15) shown in Fig. 4.2 is

$$\frac{T(x, y) - T_\infty}{q''x/k_m} Pe_x^{1/2} = 2\pi^{-1/2} \exp\left(-\frac{\eta^2}{4}\right) - \eta \operatorname{erfc}\left(\frac{\eta}{2}\right). \quad (4.18)$$

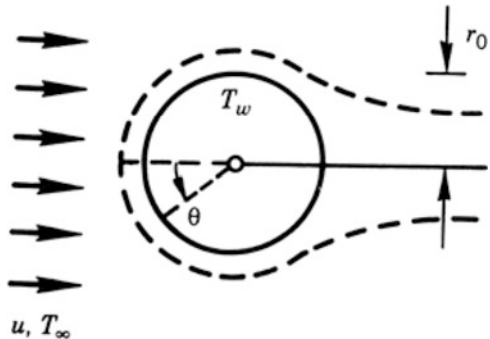
The right-hand side of Eq. (4.18) now replaces the function  $\theta_{q''}/(-d\theta_{q''}/d\eta)_{\eta=0}$  used earlier in (4.15). This exact solution also reveals the exact values of the numerical coefficients that appear in Eqs. (4.16) and (4.17), namely  $0.886 = \pi^{1/2}/2$  and  $1.329 = (3/4)\pi^{1/2}$ .

It is worth reviewing the Nusselt number results (4.13), (4.16), and (4.17) in order to rediscover the order-of-magnitude trend anticipated in Eq. (4.8). All these results are valid if  $\delta_T \ll x$ , i.e., when the Péclet number is sufficiently large so that  $Pe_x^{1/2} \gg 1$ . The effect of variation of viscosity with temperature was studied by Ramirez and Saez (1990) and Ling and Dybbs (1992).

## 4.3 Sphere and Cylinder: Boundary Layers

A conceptually similar forced-convection boundary layer develops over any other body that is imbedded in a porous medium with uniform flow. Sketched in Fig. 4.3 is the thermal boundary-layer region around a sphere or around a circular cylinder that is perpendicular to the uniform flow with volume-averaged velocity  $u$ . The sphere or cylinder radius is  $r_0$ , and the surface temperature is  $T_w$ .

**Fig. 4.3** The forced-convection thermal boundary layer around a sphere or perpendicular cylinder embedded in a porous medium



The distributions of heat flux around the sphere and cylinder were determined by Cheng (1982), who assumed that the flow obeys Darcy's law. With reference to the angular coordinate  $\theta$  defined in Fig. 4.3, Cheng obtained the following expressions for the local peripheral Nusselt number:

Sphere:

$$Nu_\theta = 0.564 \left( \frac{ur_0\theta}{\alpha_m} \right)^{1/2} \left( \frac{3}{2}\theta \right)^{1/2} \sin^2\theta \left( \frac{1}{3}\cos^3\theta - \cos\theta + \frac{2}{3} \right)^{1/2}. \quad (4.19)$$

Cylinder:

$$Nu_\theta = 0.564 \left( \frac{ur_0\theta}{\alpha_m} \right)^{1/2} (2\theta)^{1/2} \sin\theta (1 - \cos\theta)^{1/2}. \quad (4.20)$$

Worth noting in these expressions is the Péclet number based on the swept arc  $r_0\theta$ , namely  $Pe_\theta = u r_0\theta/\alpha_m$ . The local Nusselt number is defined as

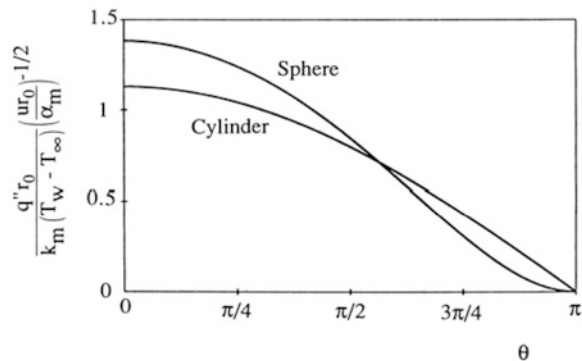
$$Nu_\theta = \frac{q''}{T_w - T_\infty} \frac{r_0\theta}{k_m}. \quad (4.21)$$

The variation of the local heat flux over the cylinder or sphere circumference is illustrated in terms of  $[q''r_0/k_m(T_w - T_\infty)](ur_0/\alpha_m)^{-1/2}$  vs.  $\theta$  in Fig. 4.4.

Equations (4.19) and (4.20) are valid when the boundary layers are distinct (thin), i.e., when the boundary-layer thickness  $r_0 Pe_\theta^{1/2}$  is smaller than the radius  $r_0$ . This requirement can also be written as  $Pe_\theta^{1/2} \gg 1$ , or  $Nu_\theta \gg 1$ .

The conceptual similarity between the thermal boundary layers of the cylinder and the sphere (Fig. 4.3) and that of the flat wall (Fig. 4.1) is illustrated further by the following attempt to correlate the heat transfer results for these three configurations. The heat flux averaged over the area of the cylinder and sphere,  $\bar{q}''$ ,

**Fig. 4.4** The distribution of heat flux over a cylinder or sphere with forced-convection boundary layer



can be calculated by averaging the local heat flux  $q''$  expressed by Eqs. (4.19), (4.20), and (4.21). We have done this on this occasion, and the results are:

Sphere:

$$\overline{Nu_D} = 1.128 Pe_D^{1/2}. \quad (4.22)$$

Cylinder:

$$\overline{Nu_D} = 1.015 Pe_D^{1/2}. \quad (4.23)$$

In these expressions, the Nusselt and Péclet numbers are based on the diameter  $D = 2r_0$ :

$$\overline{Nu_D} = \frac{\overline{q''}}{T_w - T} \frac{D}{k_m}, \quad Pe_D = \frac{uD}{\alpha_m}. \quad (4.24)$$

Remarkable at this stage is the similarity between the  $\overline{Nu_D}$  expressions (4.22) and (4.23), and between this set and the corresponding  $\overline{Nu_L}$  formula for the isothermal flat wall, Eq. (4.14). The correlation of these three results is very successful because in each case the length scale used in the definition of the overall Nusselt number and the Péclet number is the dimension that is aligned with the direction of flow, the diameter in Fig. 4.3, and the length  $L$  in Fig. 4.1.

In an earlier attempt to correlate the overall heat transfer rates for these three configurations, as length scale, we used Lienhard's (1973) "swept" length  $l$ , namely  $l = L$  for the flat wall and  $l = \pi r_0$  for the cylinder and sphere. We found that this length scale does not work nearly as well; in other words, the resulting  $\overline{Nu_l} \sim Pe_l$  expressions change appreciably from one configuration to the next. In defense of Lienhard's length scale, however, it must be said that it was originally proposed for natural convection boundary layers, not forced convection.

The heat transfer by forced convection from a cylinder with elliptic cross section to the surrounding saturated porous medium was analyzed by Kimura (1988a). This geometry bridges the gap between the circular cylinder and the plane wall discussed

in Sect. 4.1. The elliptic cylinder in cross flow is in itself relevant as a model for the interaction between a uniform flow and a circular cylinder that is not perpendicular to the flow direction. The extreme case in which the circular cylinder is parallel to the flow direction was also analyzed by Kimura (1988b).

Murty et al. (1990) investigated non-Darcy effects and found that heat transfer from a cylinder was only weakly dependent on Darcy and Forchheimer numbers for  $Da < 10^{-4}$ ,  $Re < 200$ .

An experimental study of heat transfer from a cylinder embedded in a bed of spherical particles, with cross flow of air, was made by Nasr et al. (1994). Agreement with theory based on Darcy's law and boundary-layer approximations was found to be moderately successful in predicting the data, but improved correlations were obtained with an equation modified to better account for particle diameter and conductivity variations.

For axial flow past a cylinder, an experimental study, with water and glass beads, was carried out by Kimura and Nigorinuma (1991). Their experimental results agreed well with an analysis, similar to that for the flat plate problem but with the curvature taken into account.

Heat transfer from a large sphere embedded in a bed of spherical glass beads was studied experimentally by Tung and Dhir (1993). They concluded that the total rate of heat transfer could be predicted from the equation

$$Nu = Nu_{\text{conduction}} + Nu_{\text{radiation}} + (Nu_{\text{natural}}^3 + Nu_{\text{forced}}^3)^{1/3}, \quad (4.25)$$

where

$$Nu_{\text{forced}} = 0.29 Re^{0.8} Pr^{1/2}, \quad 0.7 \leq Pr \leq 5, \quad Re \leq 2400, \quad (4.26)$$

where  $Re$  is the Reynolds number based on the diameter of the large sphere.

Asymptotic solutions, valid for high or low (respectively)  $Pe$ , for the case of a sphere with either prescribed temperature or prescribed flux, were obtained by Romero (1994, 1995a). Analytical solutions for large Péclet numbers for flow about a cylinder or sphere were reported by Pop and Yan (1998). Numerical simulation of forced convection past a parabolic cylinder was carried out by Haddad et al. (2002). MHD and viscous dissipation effects for flow past a cylinder were studied by El-Amin (2003a). Further analysis of forced convection from a circular cylinder was reported by Al-Sumaily et al. (2012), who studied the effect of local thermal nonequilibrium (LTNE).

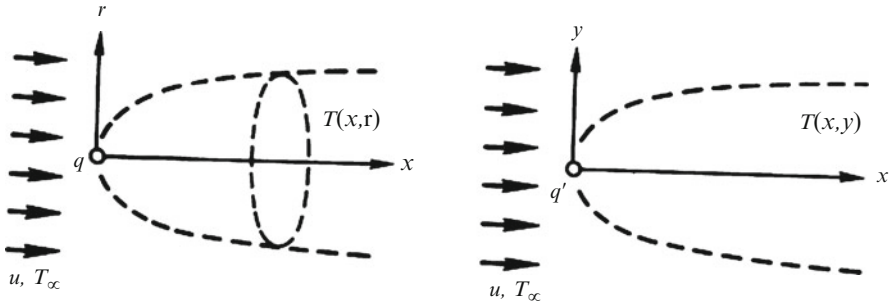


**Fig. 4.5** The thermal wakes behind a point source (left) and behind a line source perpendicular to the uniform flow (right)

#### 4.4 Point Source and Line Source: Thermal Wakes

In the region downstream from the hot sphere or cylinder of Fig. 4.3, the heated fluid forms a thermal wake whose thickness increases as  $x^{1/2}$ . This behavior is illustrated in Fig. 4.5, in which  $x$  measures the distance downstream from the heat source. Seen from the distant wake region, the embedded sphere appears as a point source (Fig. 4.5, left), while the cylinder perpendicular to the uniform flow ( $u, T_\infty$ ) looks like a line source (Fig. 4.5, right).

Consider the two-dimensional frame attached to the line source  $q'$  in Fig. 4.5, right. The temperature distribution in the wake region,  $T(x,y)$ , must satisfy the energy conservation equation

$$u \frac{\partial T}{\partial x} = \alpha_m \frac{\partial^2 T}{\partial y^2}, \quad (4.27)$$

the boundary conditions  $T \rightarrow T_\infty$  as  $y \rightarrow \pm\infty$ , and the integral condition

$$q' = \int_{-\infty}^{\infty} (\rho c_p)_f u (T - T_\infty) dy. \quad (4.28)$$

Restated in terms of the similarity variable  $\eta$  and the similarity temperature profile  $\theta$ ,

$$\eta = \frac{y}{x} Pe_x^{1/2}, \quad \theta(\eta) = \frac{T - T_\infty}{q'/k_m} Pe_x^{1/2}, \quad (4.29)$$

in which  $Pe_x = ux/\alpha_m$ , the problem statement becomes

$$-\frac{1}{2}(\theta + \eta\theta') = \theta'', \quad (4.30)$$

$$\theta \rightarrow 0 \text{ as } \eta \rightarrow \pm\infty \quad (4.31)$$

$$\int_{-\infty}^{\infty} \theta d\eta = 1. \quad (4.32)$$

The solution can be determined analytically,

$$\theta = \frac{1}{2\pi^{1/2}} \exp\left(-\frac{\eta^2}{4}\right). \quad (4.33)$$

In terms of the physical variables, the solution is

$$T - T_{\infty} = 0.282 \frac{q'}{k_m} \left(\frac{\alpha_m}{ux}\right)^{1/2} \exp\left(-\frac{uy^2}{4\alpha_m x}\right). \quad (4.34)$$

In conclusion, the wake temperature distribution has a Gaussian profile in  $y$ . The width of the wake increases as  $x^{1/2}$ , while the temperature excess on the centerline  $[T(x,0) - T_{\infty}]$  decreases as  $x^{-1/2}$ .

The corresponding solution for the temperature distribution  $T(x,r)$  in the round wake behind the point source  $q$  of Fig. 4.5, left is

$$T - T_{\infty} = \frac{q}{4\pi k_m x} \exp\left(-\frac{ur^2}{4\alpha_m x}\right). \quad (4.35)$$

In this case, the excess temperature on the wake centerline decreases as  $x^{-1}$  that is more rapidly than on the centerline of the two-dimensional wake.

Both solutions, Eqs. (4.34) and (4.35), are valid when the wake region is slender, in other words when  $Pe_x \gg 1$ . When this Péclet number condition is not satisfied, the temperature field around the source is dominated by the effect of thermal diffusion, not convection. In such cases, the effect of the heat source is felt in all directions, not only downstream.

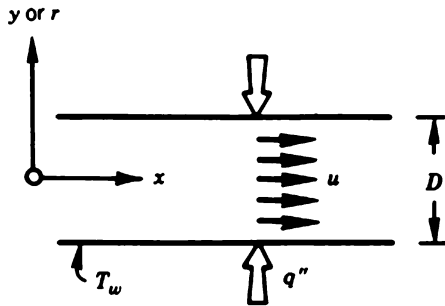
In the limit where the flow ( $u, T_{\infty}$ ) is so slow that the convection effect can be neglected, the temperature distribution can be derived by the classic methods of pure conduction. A steady-state temperature field can exist only around the point source,

$$T(r) - T_{\infty} = \frac{q}{4\pi k_m r}. \quad (4.36)$$

The pure-conduction temperature distribution around the line source remains time-dependent (all the temperatures rise; e.g., Bejan 1993, p. 181). When the time  $t$  is sufficiently long so that  $(x^2 + y^2)/(4\alpha_m t) \ll 1$ , the excess temperature around the line source is well approximated by

$$T(r, t) - T_{\infty} \cong \frac{q'}{4\pi k_m} \left[ \ln\left(\frac{4\alpha_m t}{\sigma r^2}\right) - 0.5772 \right]. \quad (4.37)$$

**Fig. 4.6** Heat transfer to the Darcy flow forced through the porous medium confined by the walls of a channel or duct



In this expression,  $r^2$  is shorthand for  $(x^2 + y^2)$ . We will return to the subject of buried heat sources in Sects. 5.10 and 5.11.

## 4.5 Confined Flow

We now consider the forced-convection heat transfer in a channel or duct packed with a porous material, Fig. 4.6. In the Darcy flow regime the longitudinal volume-averaged velocity  $u$  is uniform over the channel cross section. For this reason, when the temperature field is fully developed, the relationship between the wall heat flux  $q''$  and the local temperature difference ( $T_w - T_b$ ) is analogous to the formula for fully developed heat transfer to “slug flow” through a channel without a porous matrix. The temperature  $T_b$  is the mean or bulk temperature of the stream that flows through the channel (e.g., Bejan 1984, p. 83). The  $T_b$  definition for slug flow reduces to

$$T_b = \frac{1}{A} \int_A T dA \quad (4.38)$$

in which  $A$  is the area of the channel cross section.

In cases where the confining wall is a tube with the internal diameter  $D$ , the relation for fully developed heat transfer can be expressed as a constant Nusselt number (Rohsenow and Choi 1961):

$$Nu_D = \frac{q''(x)}{T_w - T_b(x)} \frac{D}{k_m} = 5.78 \text{ (tube, } T_w = \text{constant}), \quad (4.39)$$

$$Nu_D = \frac{q''}{T_w(x) - T_b(x)} \frac{D}{k_m} = 8 \text{ (tube, } q'' = \text{constant}). \quad (4.40)$$

When the porous matrix is sandwiched between two parallel plates with the spacing  $D$ , the corresponding Nusselt numbers are (Rohsenow and Hartnett 1973)

$$Nu_D = \frac{q''(x)}{T_w - T_b(x)} \frac{D}{k_m} = 4.93 \text{ (parallel plates, } T_w = \text{constant}), \quad (4.41)$$

$$Nu_D = \frac{q''}{T_w(x) - T_b(x)} \frac{D}{k_m} = 6 \text{ (parallel plates, } q'' = \text{constant}). \quad (4.42)$$

The forced-convection results [Eqs. (4.39), (4.40), (4.41), and (4.42)] are valid when the temperature profile across the channel is fully developed, i.e., sufficiently far from the entrance  $x = 0$  (Fig. 4.6). The entrance length, or the length needed for the temperature profile to become fully developed, can be estimated by recalling from Eq. (4.6) that the thermal boundary-layer thickness scales are  $(\alpha_m x/u)^{1/2}$ . By setting  $(\alpha_m x/u)^{1/2} \sim D$  we obtain the thermal entrance length  $x_T \sim D^2 u / \alpha_m$ . Inside the entrance region  $0 < x < x_T$ , the heat transfer is impeded by the forced-convection thermal boundary layers that line the channel walls and can be calculated approximately with the formulas presented in Sects. 4.1 and 4.2.

One important application of the results for a channel packed with a porous material is in the area of heat transfer augmentation. The Nusselt numbers for fully developed heat transfer in a channel without a porous matrix are given by expressions similar to Eqs. (4.39), (4.40), (4.41), and (4.42), except that the saturated porous-medium conductivity  $k_m$  is replaced by the thermal conductivity of the fluid alone,  $k_f$ . The relative heat transfer augmentation effect is indicated approximately by the ratio

$$\frac{h_x(\text{with porous matrix})}{h_x(\text{without porous matrix})} \sim \frac{k_m}{k_f} \quad (4.43)$$

in which  $h_x$  is the local heat transfer coefficient  $q''/(T_w - T_b)$ . In conclusion, a significant heat transfer augmentation effect can be achieved by using a high-conductivity matrix material so that  $k_m$  is considerably greater than  $k_f$ .

An experimental study of forced convection through microporous-enhanced heat sinks was reported by Lage et al. (2004b). An experimental study of flow of CO<sub>2</sub> at supercritical pressure was carried out by Jiang et al. (2004i, j). Correlations for forced convection between two parallel plates or in a circular pipe were obtained by Haji-Sheikh (2004). A numerical study, using a Green's function solution method and dealing with the effects due to a temperature change at the wall and the contributions of frictional heating, was conducted by Haji-Sheikh et al. (2004a). The role of longitudinal diffusion in fully developed forced-convection slug flow in a channel was studied by Nield and Lage (1998). Forced convection in a helical pipe was analyzed by Nield and Kuznetsov (2004b). Curvature of the pipe induces a secondary flow at first order and increases the Nusselt number at second order, while torsion affects the velocity at second order and does not affect the Nusselt number at second order. A numerical study of this problem was made by Cheng and Kuznetsov (2005). Gaseous slip flow in microchannels was studied by Haddad et al. (2006c, 2007b), Hooman (2009), and Hashemi et al. (2011a, b). Flow in rectangular channels was

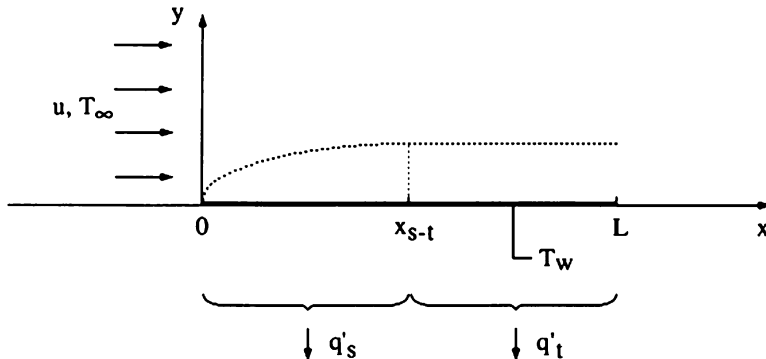


**Fig. 4.7** Forced-convection thermal boundary layer near a plate embedded in a porous medium with steady, parallel, and uniform flow

treated by Haji-Sheikh (2006), Haji-Sheikh et al. (2006), and Hooman (2008c, 2009). Various flow orientations in a packed channel were investigated by Ma et al. (2006).

Analytical solutions for ducts of various shapes (semicircular, sector, super-elliptical, lens-shaped) were reported by Wang (2008, 2010a, b, 2011).

## 4.6 Transient Effects

Most of the existing work on forced convection in fluid-saturated porous media is concerned with steady-state conditions. Notable exceptions are the papers on time-dependent forced-convection heat transfer from an isothermal cylinder (Kimura 1989a) and from a cylinder with uniform heat flux (Kimura 1988c). Nakayama and Ebinuma (1990) studied the forced-convection heat transfer between a suddenly heated plate and a non-Darcy flow that starts initially from rest.

These three papers show that the simplest and perhaps most important forced-convection configuration had been overlooked. In that configuration, the flow through the saturated porous medium is steady, parallel, and uniform (Bejan and Nield, 1991). The flow is driven by a pressure difference that is applied in the  $x$  direction in Fig. 4.7 and can be either a Darcy flow or a non-Darcy flow in which the quadratic drag (Forchheimer effect) plays a role in the overall flow resistance. What distinguishes the Bejan and Nield (1991) configuration from the one analyzed by Nakayama and Ebinuma (1990) is that the flow is and remains steady as the embedded plate is suddenly heated or cooled to a different temperature.

### 4.6.1 Scale Analysis

Consider the uniform flow, with volume-averaged velocity  $u$ , which is parallel to the wall  $y = 0$  shown in Fig. 4.7. The initial temperature of the fluid-saturated porous medium is  $T_\infty$ . Beginning at time  $t = 0$ , the temperature of the wall section  $0 < x < L$  is maintained at a different constant temperature,  $T_w$ . In time, the flow in the fluid-saturated porous medium adjusts to this change by developing a near-wall region wherein the variation from  $T_w$  to  $T_\infty$  is smoothed.

We can develop a feel for the size and history of the near-wall region by examining the order-of-magnitude implications of the energy equation for that region,

$$\sigma \frac{\partial T}{\partial t} + u \frac{\partial T}{\partial x} = \alpha_m \frac{\partial^2 T}{\partial y^2}. \quad (4.44)$$

The temperature boundary conditions are as indicated in Fig. 4.7, specifically

$$T = T_w \quad \text{at} \quad y = 0, \quad (4.45)$$

$$T \rightarrow T_\infty \quad \text{as} \quad y \rightarrow \infty. \quad (4.46)$$

Implicit in the writing of the energy equation (4.42) is the assumption that the near-wall region is slender or boundary-layer-like. To this assumption we will return in Eqs. (4.62), (4.63), (4.64), and (4.65).

One way to perform the scale analysis is by considering the entire boundary-layer region of length  $L$ . The thickness of this thermal boundary layer is denoted by  $\delta$ . If we further write  $\Delta T = T_\infty - T_w$ , we find the following scales for the three terms of Eq. (4.42):

$$\begin{array}{lll} \sigma \frac{\Delta T}{t}, & u \frac{\Delta T}{L}, & \alpha_m \frac{\Delta T}{\delta^2}. \\ \text{thermal} & \text{longitudinal} & \text{transverse} \\ \text{inertia} & \text{convection} & \text{conduction} \end{array} \quad (4.47)$$

At sufficiently short times  $t$ , the transverse heating effect is balanced by the thermal inertia of the saturated porous medium. This balance yields the time-dependent thickness

$$\delta_t \sim \left( \frac{\alpha_m t}{\sigma} \right)^{1/2}. \quad (4.48)$$

As  $t$  increases, the thermal inertia scale decreases relative to the longitudinal convection scale, and the energy equation becomes ruled by a balance between transverse conduction and longitudinal convection. The steady-state boundary-layer thickness scale in this second regime is

$$\delta_s \sim \left( \frac{\alpha_m L}{u} \right)^{1/2}. \quad (4.49)$$

The time of transition  $t_c$ , when the boundary-layer region becomes convective, can be estimated by setting  $\delta_t \sim \delta_s$ :

$$t_c \sim \frac{\sigma L}{u}. \quad (4.50)$$

Not all of the  $L$ -long boundary layer is ruled by the balance between conduction and inertia when  $t$  is shorter than  $T_c$ . When  $t$  is finite, there is always a short enough leading section of length  $x$  in which the energy balance is between transverse conduction and longitudinal convection. In that section of length  $x$  and thickness  $\delta_x$ , the scales of the three terms of Eq. (4.44) are

$$\sigma \frac{\Delta T}{t}, \quad u \frac{\Delta T}{x}, \quad \alpha_m \frac{\Delta T}{\delta_x^2}, \quad (4.51)$$

showing that  $u \Delta T/x \sim \alpha_m \Delta T/\delta_x^2$ , or

$$\delta_x \sim \left( \frac{\alpha_m x}{u} \right)^{1/2} \quad (4.52)$$

when  $\sigma \Delta T/t < u \Delta T/x$ , i.e., when

$$x < \frac{ut}{\sigma}. \quad (4.53)$$

The boundary layer changes from the convective (steady) section represented by Eq. (4.52) to the conductive (time-dependent) trailing section of Eq. (4.48). The change occurs at  $x = x_{s-t}$  where

$$x_{s-t} \sim \frac{ut}{\sigma}. \quad (4.54)$$

### 4.6.2 Wall with Constant Temperature

The two-section structure of the thermal boundary layer is indicated in Fig. 4.7. Its existence was also recognized by Ebinuma and Nakayama (1990b) in the context of transient film condensation on a vertical surface in a porous medium. The chief benefit of this insight is that it enables us to delineate the regions in which two

analytical solutions are known to apply, first the steady leading section where according to Eqs. (4.9), (4.10), (4.11), and (4.12)

$$\frac{T - T_w}{T_\infty - T_w} = \operatorname{erf} \left[ \frac{y}{2} \left( \frac{u}{\alpha_m x} \right)^{1/2} \right] \quad (x < x_{s-t}) \quad (4.55)$$

and farther downstream the time-dependent section where

$$\frac{T - T_w}{T_\infty - T_w} = \operatorname{erf} \left[ \frac{y}{2} \left( \frac{\sigma}{\alpha_m t} \right)^{1/2} \right] \quad (x > x_{s-t}). \quad (4.56)$$

The time-dependent section is no longer present when  $x_{s-t} \sim L$ , i.e., when  $t \sim \sigma L/u$ , in accordance with Eq. (4.50).

We see from the condition (4.52) that the temperature distributions (4.55) and (4.56) match at  $x = x_{s-t}$ . The longitudinal temperature gradient  $\partial T / \partial x$  experiences a discontinuity across the  $x = x_{s-t}$  cut, but this discontinuity becomes less pronounced as  $t$  increases, i.e., as the  $x_{s-t}$  cut travels downstream. It also must be said that neither Eqs. (4.55) nor (4.56) is exact at  $x = x_{s-t}$ , because at that location none of the three effects competing in Eq. (4.45) can be neglected.

The instantaneous heat transfer rate ( $W/m$ ) through the surface of length  $L$  can be deduced by taking the heat transfer rate through the leading (steady-state) section  $0 < x < x_{s-t}$ , cf. Eq. (4.14),

$$q'_s = k_m(T_\infty - T_w) \frac{2}{\pi^{1/2}} \left( \frac{u}{\alpha_m} x_{s-t} \right)^{1/2}, \quad (4.57)$$

and adding to it the contribution made by the time-dependent trailing section  $x_{s-t} < x < L$ :

$$q'_t = (L - x_{s-t}) \frac{k_m(T_\infty - T_w)}{(\pi \alpha_m t / \sigma)^{1/2}}. \quad (4.58)$$

The total heat transfer rate  $q' = q'_s + q'_t$  can be compared with the long-time (steady-state) heat transfer rate of the  $L$ -long plate,

$$q'_{\text{final}} = k(T_\infty - T_w) \frac{2}{\pi^{1/2}} \left( \frac{u}{\alpha_m} L \right)^{1/2}, \quad (4.59)$$

and the resulting expression is

$$\frac{q'}{q'_{\text{final}}} = 1 + \frac{1 - \tau}{2\tau^{1/2}}. \quad (4.60)$$

In this expression  $\tau$  is the dimensionless time

$$\tau = \frac{ut}{\sigma L}. \quad (4.61)$$

According to Eq. (4.50),  $\tau = 1$  marks the end of the time interval in which Eq. (4.60) holds. The beginning of that time interval is dictated by the validity of the assumption that the leading (steady-state) section of the boundary layer is always slender, cf. Eq. (4.49),

$$\left(\frac{\alpha_m x_{s-t}}{u}\right)^{1/2} < x_{s-t}. \quad (4.62)$$

This requirement translates into

$$\frac{ux_{s-t}}{\alpha_m} > 1 \quad (4.63)$$

or, in view of Eqs. (4.54) and (4.61),

$$\tau > \frac{1}{Pe_L}, \quad (4.64)$$

where  $Pe_L$  is the Péclet number based on  $L$ ,

$$Pe_L = \frac{uL}{\alpha_m}. \quad (4.65)$$

At times  $\tau$  shorter than  $1/Pe_L$ , the leading section is not a forced-convection boundary layer, and the entire  $L$  length produces a time-dependent heat transfer rate of type (4.58):

$$q' = L \frac{k_m(T_\infty - T_w)}{(\pi \alpha_m t / \sigma)^{1/2}}. \quad (4.66)$$

The dimensionless counterpart of this estimate is

$$\frac{q'}{q'_{\text{final}}} = \frac{1}{2\tau^{1/2}}. \quad (4.67)$$

In summary, the total heat transfer rate is given by three successive expressions, each for one regime in the evolution of the temperature field near the suddenly heated plate:

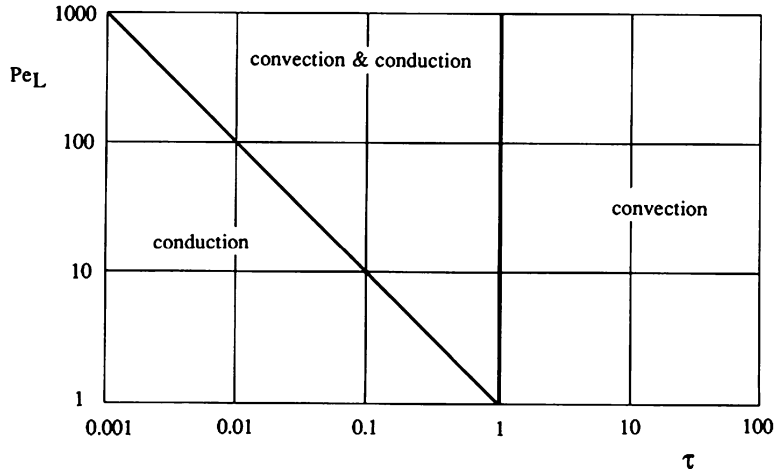


**Fig. 4.8** The  $\tau$ - $Pe_L$  ranges in which the three parts of the solutions (4.66) and (4.68) are applicable

$$\frac{q'}{q'_{\text{final}}} = \begin{cases} \frac{1}{2\tau^{1/2}}, & 0 < \tau < Pe_L^{-1} \\ 1 + \frac{1 - \tau}{2\tau^{1/2}}, & Pe_L^{-1} < \tau < 1 \\ 1, & \tau > 1. \end{cases} \quad (4.68)$$

The domain occupied by each regime is indicated on the  $(Pe_L, \tau)$  plane of Fig. 4.8. The approximate solution (4.66) shows that relative to the long-time result (4.59), the transient heat transfer rate depends on two additional dimensionless groups,  $\tau$  and  $Pe_L$ .

### 4.6.3 Wall with Constant Heat Flux

The thermal boundary layer formed in the vicinity of a plate with sudden heat flux  $q''$  can be described in a way that is analogous to the analysis presented between Eqs. (4.55) and (4.68). The structure shown in Fig. 4.7 is present here as well, and Eqs. (4.54) and (4.61) continue to hold. The upstream portion  $0 < x < x_{s-t}$  closely approximates the steady forced-convection boundary layer with uniform heat flux (Sect. 4.2). The downstream section  $x_{s-t} < x < L$  is dominated by time-dependent conduction into a semi-infinite medium with uniform heat flux at the surface.

The history of the  $L$ -averaged temperature of the wall or of the  $L$ -averaged wall-medium temperature difference  $\bar{\Delta T}$  approaches [cf. Eq. (4.17)] the value

$$\overline{\Delta T}_{\text{final}} = \frac{4}{3\pi^{1/2}} \frac{q''L}{k_m} \left( \frac{uL}{\alpha_m} \right)^{1/2}. \quad (4.69)$$

Expressed in dimensionless form, the  $L$ -averaged temperature difference is

$$\frac{\overline{\Delta T}}{\overline{\Delta T}_{\text{final}}} \cong \begin{cases} \frac{3}{2}\tau^{1/2}, & 0 < Pe_L^{-1} \\ \left(\frac{3}{3} - \frac{\tau}{2}\right)\tau^{1/2}, & Pe_L^{-1} < \tau < 1 \\ 1, & \tau > 1. \end{cases} \quad (4.70)$$

The solutions (4.66) and (4.68) are based on the assumption that  $Pe_L \gg 1$ . For example, Eq. (4.66) shows that the heat transfer ratio  $q'/q'_{\text{final}}$  experiences a change of relative magnitude  $O(Pe_L^{-1})$  at  $\tau = Pe_L^{-1}$ . The same observation applies to the  $\Delta T/\Delta T_{\text{final}}$  ratio of Eq. (4.68).

Unsteady forced convection on a flat plate, with the effect of inertia and thermal dispersion accounted for, was analyzed by Cheng and Lin (2002). The dispersion accelerates the rate of unsteady heat transfer but does not affect the response time to reach a steady state.

#### 4.6.4 Other Configurations

Kimura (1989b) has studied transient forced convection about a vertical cylinder. He obtained analytic solutions for small time (conduction solution) and large time (boundary-layer solution) and numerical results for the general time situation. Thevenin (1995) performed other calculations.

Al-Nimr et al. (1994a, b) investigated numerically convection in the entrance region of either a tube or an annulus, when a timewise step change of wall temperature is imposed, for Darcy and non-Darcy models. A conjugate problem involving concentric annuli was studied numerically by El-Shaarawi et al. (1999). Alkam and Al-Nimr (1998) performed a numerical simulation of transient forced convection in a circular pipe partly filled with a porous substrate. Unsteady forced convection about a sphere was studied numerically by Yan and Pop (1998). Fu et al. (2001) studied experimentally heat transfer in a channel subject to oscillating flow, while Mohamad and Karim (2001) reported experiments in a pipe with core and sheath occupied by different porous materials.

In a series of papers, Kuznetsov (1994, 1995a, b, 1996b, c, d, e, f, 1998e) investigated the effect of LTNE on heat transfer for the problem when a porous bed is initially at a uniform temperature and then suddenly subjected to a step increase of fluid inlet temperature. The locally averaged fluid velocity  $v$  is assumed to be uniform in space and constant in time. The analytical solution obtained by Kuznetsov, using a perturbation method based on the assumption that the fluid-to-solid heat transfer

coefficient is large, shows that the temperature of the fluid ( $T_f$ ) or solid ( $T_s$ ) phase takes the form of an advancing front, while the temperature difference  $T_f - T_s$  takes the form of an advancing pulse. The amplitude of that pulse decreases as the pulse propagates downstream. Kuznetsov treated in turn a one-dimensional semi-infinite region, a one-dimensional finite region, a two-dimensional rectangular region, a circular tube, a concentric tube annulus, and a three-dimensional rectangular box. In the one-dimensional semi-infinite case the wave speed  $v_{\text{wave}}$  is related to the fluid flow speed  $v$  by

$$v_{\text{wave}} = \frac{(\rho c)_f}{\phi (\rho c)_f + (1 - \phi)(\rho c)_s} v. \quad (4.71)$$

In the two-dimensional and three-dimensional cases the amplitude of the pulse also decreases from the central flow region to the walls of the packed bed. Kuznetsov's (1996c) paper deals with a one-dimensional slab with a fluid-to-solid heat transfer coefficient (something whose value is difficult to determine experimentally) that varies about a mean value in a random fashion. He calculated the mean and standard deviation of  $T_f - T_s$ .

The effects of thermal nonequilibrium have been included in numerical simulations by Sözen and Vafai (1990, 1993), Vafai and Sözen (1990a, b), Amiri and Vafai (1994), and Amiri et al. (1995), e.g., in connection with the condensing flow of a gas or longitudinal heat dispersion in a gas flow in a porous bed. They found that the local thermal equilibrium condition was very sensitive to particle Reynolds number and Darcy number, but not to thermophysical properties. Amiri and Vafai (1998) and Wu and Hwang (1998) performed further numerical simulations.

## 4.7 Effects of Inertia and Thermal Dispersion: External Flow

When quadratic drag is taken into account, the Darcy equations (4.2) are replaced by the approximate equations

$$u + \frac{\chi}{v} u^2 = -\frac{K}{\mu} \frac{\partial P}{\partial x}, \quad v = -\frac{K}{\mu} \frac{\partial P}{\partial y} \quad (4.72)$$

for the case when the primary flow is in the  $x$  direction, so  $v/u \ll 1$ . Here  $\chi = c_F K^{1/2}$ , where  $c_F$  was introduced in Eq. (1.12). Eliminating  $P$  from these equations and introducing the stream function  $\Psi$  defined by  $u = \partial \Psi / \partial y$ ,  $v = -\partial \Psi / \partial x$  so that Eq. (4.1) is satisfied, we obtain

$$\frac{\partial^2 \Psi}{\partial y^2} + \frac{\chi}{v} \frac{\partial}{\partial y} \left[ \left( \frac{\partial \Psi}{\partial y} \right)^2 \right] = 0, \quad (4.73)$$

and Eq. (4.3) becomes

$$\frac{\partial \Psi}{\partial y} \frac{\partial T}{\partial x} - \frac{\partial \Psi}{\partial x} \frac{\partial T}{\partial y} = \alpha_m \frac{\partial^2 T}{\partial y^2}. \quad (4.74)$$

If one considers the case where  $T_w = T_\infty + Ax^\lambda$ ,  $U_\infty = Bx^m$ , where  $A, B, \lambda$ , and  $m$  are constants, one finds that a similarity solution is possible if and only if  $m = 0$  and  $\lambda = 1/2$ . One can check that the similarity solution is given by

$$\Psi = (\alpha_m U_\infty x)^{1/2} f(\eta), \quad (4.75)$$

$$T - T_\infty = (T_w - T)\theta(\eta), \quad (4.76)$$

$$\eta = \left( \frac{U_\infty x}{\alpha_m} \right)^{1/2} \frac{y}{x}, \quad (4.77)$$

provided that  $f$  and  $\eta$  satisfy the differential equations

$$f'' + R^* [(f')^2] = 0, \quad (4.78)$$

$$\theta'' = \frac{1}{2} (f'\theta - f\theta'), \quad (4.79)$$

where

$$R^* = \frac{\chi U_\infty}{v}. \quad (4.80)$$

The boundary conditions

$$y = 0 : T = T_w, v = 0, \quad (4.81)$$

$$y \rightarrow \infty : T = T_w, u = U_\infty, \quad (4.82)$$

lead to

$$\theta(0) = 1, f(0) = 0, \theta(\infty) = 0, f'(\infty) = 1. \quad (4.83)$$

The local wall heat flux is

$$q'' = -k_m \left( \frac{\partial T}{\partial y} \right)_{y=0} = -k_m A \left( \frac{B}{\alpha_m} \right)^{1/2} \theta'(0), \quad (4.84)$$

where  $\theta'(0) = -0.886$ . We recognize that this is the case of constant wall heat flux. In nondimensional form this result is precisely the same as Eq. (4.16) and is independent of the value of  $R^*$ . Thus in this case quadratic drag has no effect on the wall heat flux (for fixed  $U_\infty$ ), but it does have the effect of flattening the dimensionless velocity profile (Lai and Kulacki, 1987).

The effect of thermal dispersion in the same case was discussed by Lai and Kulacki (1989a). In the present context it is the transverse component that is important. If one allows for thermal dispersion by adding a term  $Cud_p$  (where  $d_p$  is the mean particle or pore diameter and  $C$  is a numerical constant) to  $\alpha_m$  in the term  $\alpha_m \partial^2 T / \partial y^2$  in Eq. (4.3), then Eq. (4.16) is replaced by

$$Nu_x = 0.886(1 + CPe_d)Pe_x^{1/2}, \quad (4.85)$$

where  $Pe_d = U_\infty d_p / \alpha_m$ . Thus thermal dispersion increases the heat transfer because it increases the effective thermal conductivity in the  $y$  direction.

The effect of quadratic drag in the transient situation for the case of constant wall temperature was examined by Nakayama and Ebinuma (1990), who found that it had the effect of slowing the rate at which a steady-state solution is approached. One can deduce from their steady-state formulas that (as for the constant flux situation) quadratic drag does not affect the  $Nu_x$  ( $Pe_x$ ) relationship, in this book the formula (4.13).

## 4.8 Effects of Boundary Friction and Porosity Variation: Exterior Flow

When one introduces the Brinkman equation in order to satisfy the no-slip condition on a rigid boundary, one runs into a complex problem. The momentum equation no longer has a simple solution, and a momentum boundary-layer problem must be treated. For the purposes of this discussion, we follow Lauriat and Vafai (1991) and take the boundary-layer form of the momentum equation

$$\frac{1}{\phi^2} \left( u \frac{\partial u}{\partial x} + v \frac{\partial u}{\partial y} \right) = \frac{v}{K} (U - u) + \frac{c_F}{K^{1/2}} (U^2 - u^2) + \frac{v}{\phi} \frac{\partial^2 u}{\partial y^2}. \quad (4.86)$$

For the reasons pointed out in Sect. 1.5, we drop the left-hand side of this equation at the outset, and in the last term we replace  $\varphi^{-1}$  by  $\tilde{\mu}/\mu$ . The condition on a plane wall is now

$$u = v = 0, \quad T = T_w \quad \text{for } x > 0, y = 0. \quad (4.87)$$

The remaining equations and boundary conditions are unaltered.

The integral method, as used by Kaviany (1987), provides an approximate solution of the system. If the velocity profile is approximated by

$$u = U_\infty \left[ \frac{3}{2} \frac{y}{\delta} - \frac{1}{2} \left( \frac{y}{\delta} \right)^3 \right], \quad (4.88)$$

one finds that the momentum boundary-layer thickness  $\delta$  is given by

$$\frac{\delta^2}{K/\phi} = \frac{140}{(35 + 48c_F \text{Re}_p)} (1 - e^{-\gamma x^*}), \quad (4.89)$$

where

$$\text{Re}_p = U_\infty K^{1/2} / \nu \quad (4.90)$$

is the pore Reynolds number,

$$\gamma = \left( \frac{70}{13} \frac{1}{\text{Re}_p} + \frac{96}{13} c_F \right) \phi^{3/2}, \quad (4.91)$$

and

$$x^* = \frac{x}{(K/\phi)^{1/2}}. \quad (4.92)$$

The momentum boundary-layer thickness  $\delta$  is almost constant when  $x^* > 5/\gamma$ . Thus the hydrodynamic development length can be taken as

$$x_e = \frac{5}{\gamma} \left( \frac{K}{\phi} \right)^{1/2}, \quad (4.93)$$

and the developed momentum boundary-layer thickness is given by

$$\delta = \left[ \left( \frac{140}{35 + 48c_F \text{Re}_p} \right) \frac{K}{\phi} \right]^{1/2}. \quad (4.94)$$

For the developed region, exact solutions have been obtained by Cheng (1987), Beckermann and Viskanta (1987), and Vafai and Thiyagaraja (1987). They show that the velocity is constant outside a boundary layer whose thickness decreases as  $c_F$  and/or  $\text{Re}_p$  increases, in accordance with Eq. (4.86).

Wall effects caused by nonuniform porosity (Sect. 1.7) have been investigated experimentally by a number of investigators and theoretically by Vafai (1984, 1986), Vafai et al. (1985), and Cheng (1987). The degree to which hydrodynamic wall effects influence the heat transfer from a heated wall depends on the Prandtl number  $Pr$  of the fluid. The ratio of the thermal boundary-layer thickness  $\delta_T$  to the momentum boundary-layer thickness  $\delta$  is of order  $Pr^{-1}$ . For low Prandtl number fluids ( $Pr \rightarrow 0$ ),  $\delta \ll \delta_T$  and the temperature distribution, and hence the heat transfer, is given by the Darcy theory of Sects. 4.1 and 4.2. For a more general case where the inertial effects are taken into account and for a variable wall temperature in the form  $T_w = T_\infty + Ax^p$ , an exact solution was obtained by Vafai and Thiyagaraja (1987) for low Prandtl number fluids in terms of gamma and parabolic cylindrical functions. They found the temperature distribution to be

$$T = T_\infty + A\Gamma(p+1) \times \left\{ 2^{p+1/2} \pi^{-1/2} x^p \exp(-xy^2/x) D_{-(2p+1)}[(4xy^2/x)^{1/2}] \right\}, \quad (4.95)$$

where  $\alpha = U_\infty/8\alpha_m$ . The corresponding local Nusselt number is

$$Nu_x = \frac{\Gamma(p+1)}{\Gamma(p+1/2)} (\text{Re}_p \text{Pr}_e)^{1/2}, \quad Da_x^{-1/4} = \frac{\Gamma(p+1)}{\Gamma(p+1/2)} Pe_x^{1/2}, \quad (4.96)$$

which reduces to Eq. (4.13) when  $p = 0$ .

When the Prandtl number is very large,  $\delta_T \ll \delta$  and so the thermal boundary layer lies completely inside the momentum boundary layer. As  $Pr \rightarrow \infty$  one can assume that the velocity distribution within the thermal boundary layer is linear and given by

$$u = \frac{\tau_w y}{\mu_f}, \quad (4.97)$$

where  $\tau_w$  is the wall stress which is given by

$$\tau_w = \frac{\mu_f U_\infty}{(K/\phi)^{1/2}} \left( 1 + \frac{4}{3} c_F \text{Re}_p \right)^{1/2}. \quad (4.98)$$

This means that the energy equation can be approximated by

$$y \frac{\partial T}{\partial x} = \frac{\alpha_m \mu_f}{\tau_w} \frac{\partial^2 T}{\partial y^2}. \quad (4.99)$$

We now introduce the similarity variables

$$\eta = y \left( \frac{1}{9\xi x} \right)^{1/3}, \quad \theta(\eta) = \frac{T - T_w}{T_\infty - T_w}, \quad (4.100)$$

where

$$\xi = \frac{\alpha_m \mu_f}{\tau_w} = \frac{K}{Re_p Pr_e} \left[ \phi \left( 1 + \frac{4}{3} c_F Re_p \right) \right]^{-1/2} \quad (4.101)$$

and where the *effective* Prandtl number  $Pr_e$  is defined as

$$Pr_e = \frac{v}{\alpha_m}. \quad (4.102)$$

We then have the differential equation system

$$\theta'' + 3\eta^2\theta' = 0, \quad (4.103)$$

$$\theta(0) = 0, \quad \theta(\infty) = 1, \quad (4.104)$$

which has the solution (Beckermann and Viskanta, 1987)

$$\theta = \frac{1}{\Gamma(4/3)} \int_0^\eta e^{-\xi^3} d\xi. \quad (4.105)$$

Hence the local Nusselt number is

$$\begin{aligned} Nu_x &= \frac{k_m (\partial T / \partial y)_{y=0}}{k_m (T_w - T_\infty) / x} = 1.12 \left( \frac{x^2}{9\xi} \right)^{1/3} \\ &= 0.538 \left[ \phi \left( 1 + \frac{4}{3} c_F Re_p \right) \right]^{1/6} \left( \frac{Re_p Pr_e}{Da_x} \right)^{1/3}, \end{aligned} \quad (4.106)$$

and the overall Nusselt number over a length  $L$  from the leading edge becomes

$$\overline{Nu} = 1.68 \left( \frac{L^2}{9\xi} \right)^{1/3}. \quad (4.107)$$

Vafai and Thiyagaraja (1987) compared these analytical results with numerical solutions. They found that the low Prandtl number analytical solution accurately predicts the temperature distribution for a Prandtl number  $Pr_e$  as high as 8, while the

high- $Pr_e$  analytical solution is valid for  $Pr_e$  as low as 100 and possibly for somewhat lower values.

The combined effects of inertia and boundary friction were considered by Kaviany (1987). He expressed his results in terms of a parameter  $\Gamma_x$  defined as the total flow resistance per unit volume (Darcy plus Forchheimer drag) due to the solid matrix, scaled in terms of  $8\rho U_\infty^2/3\varphi x$ . He concluded that the “Darcian regime” where  $Nu_x$  varies as  $Pr_e^{1/2}$  holds when  $\Gamma_x > 0.6 Pr_e$  and the “non-Darcian regime” where  $Nu_x$  varies as  $Pr_e^{1/3}$  holds when  $0.07 < \Gamma_x < 0.6 Pr_e$ . When  $\Gamma_x = 0.07$ , the presence of the solid matrix is not significant. Another study is that by Kumari et al. (1990c).

Vafai et al. (1985) experimentally and numerically investigated the effects of boundary friction and variable porosity. Their experimental bed consisted of glass beads of 5 and 8 mm diameter saturated with water. They found good agreement between observation of the average Nusselt number and numerical predictions when the effect of variable porosity was included (but not otherwise). Cheng (1987) noted that since their experiments were conducted in the range  $100 < Re_p < 900$ , thermal dispersion effects should have been important, and in fact they neglected these. He pointed out that in their numerical work Vafai et al. (1985) used a value of thermal conductivity about three times larger than was warranted, and by doing so they had fortuitously approximated the effect of transverse thermal dispersion.

Further experimental work was undertaken by Renken and Poulikakos (1989). They reported details of thermal boundary-layer thickness, temperature field, and local Nusselt number. Good agreement was found with the numerical results of Vafai et al. (1985) with the effects of flow inertia and porosity variation accounted for.

Some further details on the content of this section can be found in the review by Lauriat and Vafai (1991). Nakayama et al. (1990a) used novel-transformed variables to produce a local similarity solution for flow over a plate. Vafai and Kim (1990) analyzed flow in a composite medium consisting of a fluid layer overlaying a porous substrate that is attached to the surface of a plate. Luna and Mendez (2005) used a Brinkman model to study analytically and numerically the conjugate problem of forced convection on a plate with finite thermal conductivity and with constant heat flux at the extreme boundary.

For the case of cross flow across a cylinder, Fand et al. (1993) obtained empirical correlation expressions for the Nusselt number. For the same geometry, a numerical study was made by Nasr et al. (1995). They reported that the effect of decreasing  $Da$  was an increase in  $Nu$ , but Lage and Nield (1997) pointed out that this is true only if the Reynolds number  $Re$  is held constant. If the pressure gradient is kept constant,  $Nu$  increases with  $Da$ . Nasr et al. (1995) also noted that  $Nu$  increased with increase of either  $Re$  or effective Prandtl number and that the effect of quadratic drag on  $Nu$  is via the product  $Da Re$ .

Heat transfer around a periodically heated cylinder was studied experimentally (with water and glass beads) and numerically by Fujii et al. (1994). They also modeled the effects of thermal dispersion and thermal nonequilibrium.

Conjugate flow around a cylinder with internal heat generation was studied by Kadir et al. (2008).

Unsteady forced convection, produced by small amplitude variations in the wall temperature and free stream velocity, along a flat plate was studied by Hossain et al. (1996).

The effect of viscous dissipation was discussed by Aydin and Koya (2008b,c,d), Rees and Magyari (2008), and Nield (2008a). The effect of variable viscosity and variable Prandtl number was studied by Pantokratoras (2007c).

## 4.9 Effects of Boundary Friction, Inertia, Porosity Variation, Thermal Dispersion, and Axial Conduction: Confined Flow

In porous channels the velocity field generally develops to its steady-state form in a short distance from the entrance. To see this, let  $t_c$  be a characteristic time for development and  $u_c$  a characteristic velocity. During development, the acceleration term is of the same order of magnitude as the Darcy resistance term, so  $u_c/t_c \sim v u_c/K$  and so the development length  $\sim t_c u_c \sim Ku_c/v$ , which is normally small. [Note that, in contrast with the argument used by Vafai and Tien (1981), the present argument holds whether or not the convective inertial term is negligible.] Further, the numerical results of Kaviany (1985) for flow between two parallel plates show that the entrance length decreases linearly as the Darcy number decreases. In this section we assume that the flow is also fully developed thermally.

We start by considering a channel between two plane parallel walls with a distance  $2H$  apart, the boundaries being at  $y = H$  and  $y = -H$ . For fully developed flow the velocity is  $u(y)$  in the  $x$  direction. We suppose that the governing equations are

$$G = \frac{\mu u^*}{K} + \frac{c_F \rho u^{*2}}{K^{1/2}} - \tilde{\mu} \frac{d^2 u^*}{dy^{*2}}, \quad (4.108)$$

$$u^* \frac{\partial T^*}{\partial x^*} = \frac{k_m}{(\rho c_p)_f} \frac{\partial^2 T^*}{\partial y^{*2}}. \quad (4.109)$$

Here the asterisks denote dimensional variables, and  $G$  is the applied pressure gradient. Local thermal equilibrium has been assumed, dispersion is neglected, and it is assumed that the Péclet number is sufficiently large for the axial thermal conduction to be insignificant. We define the dimensionless variables

$$x = \frac{x^*}{H}, \quad y = \frac{y^*}{H}, \quad u = \frac{\tilde{\mu} u^*}{GH^2} \quad (4.110)$$

and write

$$M = \frac{\tilde{\mu}}{\mu}, Da = \frac{K}{H^2}, F = \frac{c_F \rho G H^4}{K^{1/2} \mu^2}. \quad (4.111)$$

Thus  $M$  is a viscosity ratio,  $Da$  is a Darcy number, and  $F$  is a Forchheimer number. Then Eq. (4.108) becomes

$$M \frac{d^2 u}{dy^2} - \frac{u}{Da} - Fu^2 + 1 = 0. \quad (4.112)$$

This equation is to be solved subject to the boundary/symmetry conditions

$$u = 0 \quad \text{at} \quad y = 1, \quad \frac{du}{dy} = 0 \quad \text{at} \quad y = 0. \quad (4.113)$$

When  $F$  is not zero, the solution can be expressed in terms of standard elliptic functions (Nield et al., 1996). When  $F = 0$ , the solution is

$$u = Da \left( 1 - \frac{\cosh Sy}{\cosh S} \right), \quad (4.114)$$

where for convenience we introduce

$$S = \frac{1}{(MDa)^{1/2}}. \quad (4.115)$$

We also introduce the mean velocity  $U^*$  and the bulk mean temperature  $T_m^*$  defined by

$$U^* = \frac{1}{H} \int_0^H u^* dy^*, \quad T_m^* = \frac{1}{HU^*} \int_0^H u^* T^* dy^*. \quad (4.116)$$

We then define further dimensionless variables defined by

$$\hat{u} = \frac{u^*}{U^*}, \quad \hat{T} = \frac{T^* - T_w^*}{T_m^* - T_w^*} \quad (4.117)$$

and the Nusselt number

$$Nu = \frac{2Hq''}{k_m(T_m^* - T_w^*)}. \quad (4.118)$$

Here  $T_w^*$  and  $q''$  are the temperature and heat flux on the wall.

For the case of uniform heat flux on the boundary, the first law of thermodynamics leads to

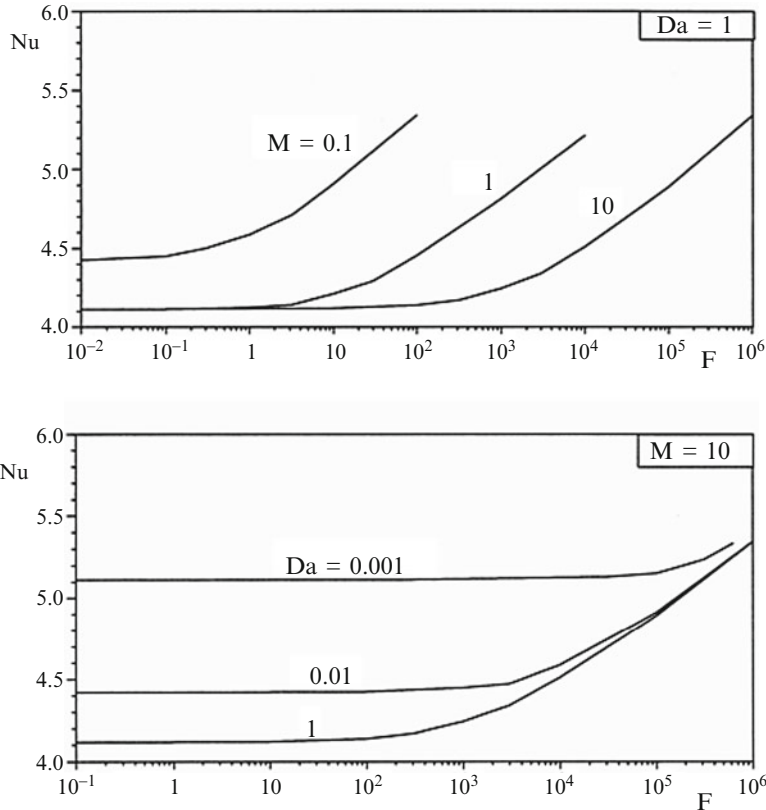


**Fig. 4.9** Effect of the Forchheimer number,  $F$ , on the Nusselt number,  $\text{Nu}$ , for a channel with isoflux boundaries (Nield et al. 1996)

$$\frac{\partial T^*}{\partial x^*} = \frac{dT_m^*}{dx^*} = \frac{q''}{(\rho c_p)_f H U^*} = \text{constant.} \quad (4.119)$$

In this case Eq. (4.109) becomes

$$\frac{d^2 \hat{T}}{dy^2} = -\frac{1}{2} \text{Nu} \hat{u}. \quad (4.120)$$

The boundary conditions for this equation are

$$\hat{T} = 0 \quad \text{at } y = 1, \quad \frac{d\hat{T}}{dy} = 0 \quad \text{at } y = 0. \quad (4.121)$$

For the Brinkman model, with  $u$  given by Eq. (4.114), we have

$$\hat{u} = \frac{S}{S - \tanh S} \left( 1 - \frac{\cosh Sy}{\cosh S} \right), \quad (4.122)$$

$$\hat{T} = \frac{SNu}{S - \tanh S} \left[ \frac{1}{4}(1 - y^2) - \frac{\cosh S - \cosh Sy}{2S^2 \cosh S} \right]. \quad (4.123)$$

The definition of the dimensionless temperature leads to an identity that we call the integral compatibility condition (Nield and Kuznetsov, 2000), namely

$$\int_0^1 \hat{u} \hat{T} dy = 1. \quad (4.124)$$

Substitution from Eqs. (4.122) and (4.123) then leads to

$$Nu = \frac{12S(S - \tanh S)^2}{2S^3 - 15S + 15\tanh S + 3S\tanh^2 S}, \quad (4.125)$$

in agreement with an expression obtained by Lauriat and Vafai (1991). As the Darcy number  $Da$  increases from 0 to  $\infty$ , i.e., as  $S$  decreases from  $\infty$  to 0, the Nusselt number  $Nu$  decreases from the Darcy value 6 [agreeing with Eq. (4.42)] to the clear fluid value  $210/51 = 4.12$ . Thus the effect of boundary friction is to decrease the heat transfer by reducing the temperature gradient at the boundary.

For  $F \neq 0$ , Vafai and Kim (1989) used a boundary-layer approximation in obtaining a closed-form solution. This solution becomes inaccurate for hyperporous media, those for which  $Da > 0.1$ . For such media, the Brinkman term is comparable with the Darcy term throughout the flow (and not just near the walls), and  $K$  can no longer be determined by a simple Darcy-type experiment. A closed-form solution of the Brinkman-Forchheimer equation, valid for all values of  $Da$ , was obtained by Nield et al. (1996). Some typical results are given in Fig. 4.9.

The results of Nield et al. (1996) may be summarized as follows. For each type of thermal boundary condition, the temperature profile is little changed as a result of variation of  $M$ ,  $Da$ , or  $F$ . It is slightly more peaked when  $Da$  is small or when  $F$  is large. On the other hand, the Nusselt number is significantly altered, primarily as a result of the change in velocity profile. The effect of an increase in  $F$  is to produce a more slug-like flow, and because of the way the mean velocity is defined this decreases ( $T_w - T_m$ ) and hence increases  $Nu$ . In particular, for the case of isoflux boundaries, the following holds. When simultaneously  $Da$  is large and  $F$  is small, the velocity profile is approximately parabolic and the Nusselt number is near 70/17 (a lower bound). When either  $Da$  is sufficiently small or  $F$  is sufficiently large, the velocity profile is approximately uniform (apart from a thin boundary layer) and the Nusselt number is near 6 (an upper bound). For the case of isothermal surfaces the story is similar, but the Nusselt numbers are smaller [the reason for this is spelled out in Nield et al. (1996, p. 211)].

For the case of a circular tube, with  $H$  replaced by the radius  $R$  of the tube in the scaling, one finds (Nield et al., 2003b) that the solution can be expressed in terms of modified Bessel functions:

$$\hat{u} = \frac{S[I_0(S) - I_0(Sr)]}{SI_0(S) - 2I_1(S)}, \quad (4.126)$$

$$\hat{T} = \frac{SNu}{SI_0(S) - 2I_1(S)} \left[ \frac{I_0(S)}{4}(1 - r^2) - \frac{I_0(S) - I_0(Sr)}{S^2} \right], \quad (4.127)$$

$$Nu = \frac{8S[SI_0(S) - 2I_1(S)]^2}{(S^3 - 24S)[I_0(S)]^2 + 48I_0(S)I_1(S) + 8S[I_1(S)]^2}. \quad (4.128)$$

When the uniform flux boundary condition is replaced by the uniform temperature condition, one finds that Eq. (4.120) is replaced by

$$\frac{d^2\hat{T}}{dy^2} = -\frac{1}{2}Nu \hat{u}\hat{T}. \quad (4.129)$$

The boundary condition given by Eq. (4.121) still applies. We see that we now have an eigenvalue problem with  $Nu$  as the eigenvalue. Now Eq. (4.124) is satisfied trivially, and instead of this compatibility condition one uses a differential compatibility condition (previously satisfied trivially), namely

$$Nu = -2 \frac{d\hat{T}}{dy}(1). \quad (4.130)$$

Equation (4.130) enables the amplitude of the eigenfunction to be determined. For the case of Darcy flow ( $Da = 0$ ) we have  $\hat{u} = 1$ ,  $\hat{T} = (\pi/2) \cos(\pi y/2)$  and  $Nu = \pi^2/2 = 4.93$ . For other values of  $Da$  the value of  $Nu$  can be found numerically, most readily by expressing the second-order differential equation as two first-order equations and then using a shooting method. Details of the method may be found in Nield and Kuznetsov (2000).

The above results for symmetric heating can be extended to the case of asymmetric heating, using a result established by Nield (2004c). The result applies when the heat flux along each boundary is uniform, or the temperature along each boundary is uniform. With the Nusselt number defined in terms of the mean wall temperature and the mean wall heat flux, the value of the Nusselt number is independent of the asymmetry whenever the velocity profile is symmetric with respect to the midline of the channel. This means that the above results also apply to the case of heating asymmetric with respect to the midline. Further work involving asymmetric heat flux boundary conditions was reported by Mitrovic and Maletić (2006a, b) and Cezmer et al. (2011). Experiments with asymmetrically heated channels filled with glass beads were performed by Jeng et al. (2011).

In the case of a circular tube, Eqs. (4.129) and (4.130) are replaced by

$$\frac{d^2\hat{T}}{dr^2} + \frac{1}{r} \frac{d\hat{T}}{dr} = -Nu \hat{u}\hat{T}, \quad (4.131)$$

$$Nu = -2 \frac{d\hat{T}}{dr}(1). \quad (4.132)$$

For the case  $Da = 0$  one finds that  $Nu = \lambda^2$  where  $\lambda = 2.40483$  is the smallest positive root of the Bessel function  $J_0(x)$  so that  $Nu = (2.40483)^2 = 5.783$  and  $\hat{T} = \lambda J_0(\lambda r)/2J_1(\lambda)$ .

Variable porosity effects in a channel bounded by two isothermal parallel plates and in a circular pipe were examined numerically by Poulikakos and Renken (1987) for the case of a fully developed velocity field. They assumed that the porosity variation had negligible effects on the thermal conductivity, an assumption that breaks down when there is a large difference between the thermal conductivities of the two phases (David et al., 1991). Poulikakos and Renken (1987) found that in the fully developed region the effect of channeling was to produce a Nusselt number increase (above the value based on the Darcy model) of 12% for a parallel plate channel and 22% for a circular pipe.

Renken and Poulikakos (1988) performed an experimental investigation for the parallel plate configuration with the walls maintained at constant temperature, with particular emphasis on the thermally developing region. They also performed numerical simulations incorporating the effects of inertia, boundary friction, and variable porosity. Their experimental and numerical findings agreed on predicting an enhanced heat transfer over that predicted using the Darcy model.

Poulikakos and Kazmierczak (1987) obtained closed-form analytical solutions of the Brinkman equation for parallel plates and a circular pipe with constant heat flux on the walls for the case where there is a layer of porous medium adjacent to the walls and clear fluid interior. They also obtained numerical results when the walls were at constant temperature. For all values of  $Da$  the Nusselt number  $Nu$  goes through a minimum as the relative thickness of the porous region  $s$  varies from 0 to 1. The minimum deepens and is attained at a smaller value of  $s$  as  $Da$  increases. A general discussion of Brinkman, Forchheimer, and dispersion effects was presented by Tien and Hunt (1987). For the Brinkman model and uniform heat flux boundaries, Nakayama et al. (1988) obtained exact and approximate solutions. Analytical studies giving results for small or large Darcy numbers for convection in a circular tube were reported by Hooman and Ranjbar-Kani (2003, 2004).

Hunt and Tien (1988a) have performed experiments that document explicitly the effects of thermal dispersion in fibrous media. They were able to correlate their Nusselt number data, for high Reynolds number flows, in terms of a parameter  $u_a L^{1/2} K^{1/4} / \alpha_m$ , where  $u_a$  is the average streamwise Darcy velocity and  $L$  is a characteristic length. Since this parameter does not depend explicitly on the thermal conductivity, they concluded that dispersion overwhelmed transport from

solid conduction. They were able to explain this behavior using a dispersion conductivity of the form

$$k_d = \rho c_p \gamma K^{1/2} u, \quad (4.133)$$

where  $\gamma$  is a numerical dispersion coefficient, having the empirically determined value of 0.025. An analytical study of the effect of transverse thermal dispersion was reported by Kuznetsov (2000c).

Hunt and Tien (1988b) modeled heat transfer in cylindrical packed beds such as chemical reactors by employing a Forchheimer-Brinkman equation. They allowed the diffusivity to vary across the bed. Marpu (1993) found that the inclusion of axial conduction leads to a significant increase in Nusselt number in the thermally developing region of pipes for Péclet number less than 100. In similar circumstances, the effect of axial dispersion was found by Adnani et al. (1995) to be important for Péclet number less than 10.

Cheng et al. (1991) reviewed methods for the determination of effective radial thermal conductivity and Nusselt number for convection in packed tubes and channels and reanalyzed some of the previous experimental data in the light of their own contributions to thermal dispersion theory with variable porosity effects taken into account. They found that for forced convection in a packed column the average Nusselt number depends not only on the Reynolds number but also on the dimensionless particle diameter, the dimensionless length of the tube, the thermal conductivity ratio of the fluid phase to the solid phase, and the Prandtl number of the fluid. They summarized their conclusions by noting that in their recent work [Cheng et al. (1988), Cheng and Hsu (1986a,b), Cheng and Zhu (1987), Cheng and Vortmeyer (1988), and Hsu and Cheng (1988, 1990)] they had developed a consistent theory for the study of forced convection in a packed column taking into consideration the wall effects on porosity, permeability, stagnant thermal conductivity, and thermal dispersion. These effects become important as the particle/tube diameter ratio is increased. Various empirical parameters in the theory can be estimated by comparison of theoretical and experimental results for the pressure drop and heat transfer, but there is at present a need to perform more experiments on forced convection in packed columns where both temperature distribution and heat flux are measured to enable a more accurate determination of the transverse thermal dispersivity.

Chou et al. (1994) performed new experiments and simulations for convection in cylindrical beds. They concluded that discrepancies in some previous models could be accounted for by the effect of channeling for the case of low Péclet number and the effect of thermal dispersion in the case of high Péclet number. Chou et al. (1992b,c) had reported similar conclusions, on the basis of experiments, for convection in a square channel.

The effect of suction at permeable walls was investigated by Lan and Khodadadi (1993). An experimental study of convection with asymmetric heating was reported by Hwang et al. (1992). Bartlett and Viskanta (1996) obtained analytical solutions

for thermally developing convection in an asymmetrically heated duct filled with a medium of high thermal conductivity.

Lage et al. (1996) performed a numerical study for a device (designed to provide uniform operating temperatures) consisting of a microporous layer placed between two sections of a cold plate. The simulation was based on two-dimensional equations derived from three-dimensional equations by integration over the small dimension of the layer.

For convection in cylindrical beds, Kamiuto and Saitoh (1994) investigated  $Nu_p$ ,  $\kappa$ , and  $\Gamma$ , where  $Nu_p$  and  $Re_p$  are Nusselt and Reynolds numbers based on the particle diameter, while  $\kappa$  is the ratio of thermal conductivity of solid to that of fluid and  $\Gamma$  is the ratio of bed radius to particle diameter. They found that as  $Re_p Pr$  tends to zero,  $Nu_p$  tends to a constant value depending on both  $\kappa$  and  $\Gamma$ , while for large  $Re_p Pr$ , the value of  $Nu_p$  depends on both  $Re_p Pr$  and  $Pr$  but only to a small extend on  $\kappa$ .

For pipes packed with spheres, Varahasamy and Fand (1996) have presented empirical correlation equations representing a body of new experimental data. Experimental studies involving metal foams have been reported by Calmidi and Mahajan (2000), Hwang et al. (2002), and Zhao et al. (2004b). Further experimental and theoretical studies of convection in a circular pipe were conducted by Izadpanah et al. (1998). Extending previous experimental work by Jiang et al. (1999b), Jiang et al. (2004e,f,h) studied numerically and experimentally the wall porosity effect for a sintered porous medium. A similar study of nonsintered material was reported by Jiang et al. (2004g). Sintered materials also were discussed by Kim and Kim (2000). Forced convection in microstructures was discussed by Kim and Kim (1999). Another numerical study in a metallic fibrous material was reported by Angirasa (2002a), and that was followed with an experimental study by Angirasa (2000b). An experimental study with aluminum foam in an asymmetrically heated channel was made by S. J. Kim et al. (2001).

Entropy generation in a rectangular duct was studied by Demirel and Kahraman (1999). For a square duct, a numerical study of three-dimensional flow was reported by Chen and Hadim (1999b). Unsteady convection in a square cylinder was studied numerically by Perng et al. (2011).

The effect of viscous dissipation has been studied numerically by Zhang et al. (1999) for a parallel plate channel and by Yih and Kamioto for a circular pipe. An analytical study of the effects of both viscous dissipation and flow work in a channel, for boundary conditions of uniform temperature or uniform heat flux, was reported by Nield et al. (2004b). These authors specifically satisfied the first law of thermodynamics when treating the fully developed flow. They also considered various models for the contribution from the Brinkman term to the viscous dissipation. Further work involving viscous dissipation was reported by Hung and Tso (2008, 2009).

The effect of axial conduction in channels and tubes was studied by Minkowycz and Haji-Sheikh (2006, 2009) and Haji-Sheikh et al. (2010a,b). The effect of Forchheimer quadratic drag in rectangular ducts was examined by Akyidiz and Siginer (2011).

Some general matters related to the possibility of fully developed convection were discussed by Nield (2006a). An analytical study of heat transfer in Couette flow was made by Kuznetsov (1998c). An analytical treatment of Couette-Poiseuille flow was reported by Aydin and Avci (2011). An analytical study of a conjugate problem, with conduction heat transfer inside the channel walls accounted for, was made by Mahmud and Fraser (2004). Entropy generation in a channel was studied analytically and numerically by Mahmud and Fraser (2005b). Vafai and Amiri (1998) briefly surveyed some of the work done on the topics that here are discussed mainly in Sects. 4.9 and 4.10.

Convection in a hyperporous medium saturated by a rarefied gas, with both velocity slip and temperature slip at the boundaries of a parallel-plate channel or a circular duct, was analyzed by Nield and Kuznetsov (2006a, 2007a) and discussed by Al-Nimr and Haddad (2006). They found that temperature slip leads to decreased transfer, while the effect of velocity slip depends on the geometry and the Darcy number. Shokouhmand et al. (2010) reported results for flow in micro- and nanochannels for a wide range of Knudsen number.

## 4.10 Local Thermal Nonequilibrium

It is now commonplace to employ a two-temperature model to treat forced convection with LTNE. Authors who have done this include Vafai and Tien (1989), Jiang et al. (1998, 1999, 2001, 2002), You and Song (1999), Kim et al. (2000), Kim and Jang (2002), Muralidhar and Suzuki (2001), Nakayama et al. (2001), Mogari (2008), and Hayes et al. (2008). Haddad et al. (2006a, 2007a) studied gas flow in microchannels; Chen and Tsao (2011b) studied the effect of viscous dissipation. Conjugated heat transfer in a double-pipe filled with metallic foam was studied numerically by Du et al. (2010).

Transient and time-periodic convection in a channel has been treated analytically by Al-Nimr and Abu-Hijleh (2002), Al-Nimr and Kiwan (2002), Abu-Hijleh et al. (2004), Khashan et al. (2005), and Forooghi et al. (2011). A further study of transient convection was conducted by Spiga and Morini (1999). An analysis involving a perturbation solution was presented by Kuznetsov (1997d). The specific aspect of LTNE involving steady convective processes was analyzed by Nield (1998a). The modeling of local nonequilibrium in a structured medium was discussed by Nield (2002), and a conjugate problem was analyzed by Nield and Kuznetsov (1999). A problem in a channel with one wall heated was analyzed by Zhang and Huang (2001); see also the note by Magyari and Keller (2002). The departure from local thermal equilibrium due to a rapidly changing heat source was analyzed by Minkowycz et al. (1999). Further analysis was carried out by Lee and Vafai (1999) and Marafie and Vafai (2001). The particular case of various models for constant wall heat flux boundary conditions was discussed by Alazmi and Vafai (2002). The present authors think that the best model is the one where there is uniform flux over the two phases, as employed by Nield and Kuznetsov (1999).

Alazmi and Vafai (2004) showed that thermal dispersion has the effect of increasing the sensitivity of LTNE between the two phases. The case of a non-Newtonian fluid was treated numerically by Khashan and Al-Nimr (2005). Most work on LTNE has been done for confined flows, but Wong et al. (2004) treated finite Péclet number effects in forced convection past a heated cylinder, and Kwan et al. (2008) studied convection past a sphere at finite Péclet number.

The effect of LTNE on minimal resistance of layered systems was treated by Leblond and Gosselin (2008). A general criterion for local thermal equilibrium was proposed by Zhang and Liu (2008) and Zhang et al. (2009).

Celli et al. (2010) studied a steady 2D boundary-layer flow. They noted that when the basic flow is high, the two thermal fields are described accurately using the boundary-layer approximation. They analyzed the resulting parabolic system analytically and numerically and found that the LTNE effects are strongest near the leading edge and equilibrium is attained at large distances.

Fully developed forced convection in a tube was further analyzed by Yang et al. (2011). Imani et al. (2012) numerically simulated convection through an array of disconnected conducting cylindrical fins.

Yang and Vafai (2010, 2011a,b,c) have produced analytical solutions for convection with LTNE based on various alternative boundary conditions. Klinbun et al. (2012) included the effect of LTNE in their study and the effect of a transient electromagnetic field on forced convection in a waveguide filled with porous material. Convection from a circular cylinder was studied by Al-Sumily et al. (2008). Dukhan and Al-Rammahi (2012) made an analytical and experimental study of convection in cylinder occupied by metal foam. Chen and Tsao (2012a) performed a thermal resistance analysis of forced convection with viscous dissipation using an entransy dissipation concept.

## 4.11 Partly Porous Configurations

For complicated geometries numerical studies are needed. The use of porous bodies to enhance heat exchange motivated the early studies of Koh and Colony (1974) and Koh and Stevans (1975). Huang and Vafai (1993,1994a, b, c, d) and Vafai and Huang (1994), using a Brinkman-Forchheimer model, performed studies of a composite system made of multiple porous blocks adjacent to an external wall (either protruding or embedded) or along a wall with a surface substrate. Khanafer and Vafai (2001, 2005) investigated isothermal surface production and regulation for high heat flux applications using porous inserts. Cui et al. (2001) conducted an experimental study involving a channel with discrete heat sources.

Convection in a parallel-plate channel partially filled with a porous layer was studied by Jang and Chen (1992). They found that the Nusselt number is sensitive to the open space ratio and that the Nusselt number is a minimum at a certain porous layer thickness, dependent on Darcy number. A similar study was reported by Tong et al. (1993). Srinivasan et al. (1994) analyzed convection in a spirally

fluted tube using a porous substrate approach. Hadim and Bethancourt (1995) simulated convection in a channel partly filled with a porous medium and with discrete heat sources on one wall. Chikh et al. (1995b, 1998) studied convection in an annulus partly filled with porous material on the inner heated wall and in a channel with intermittent heated porous disks, while Rachidi and Chikh (2001) studied a similar problem. Ould-Amer et al. (1998) studied numerically the cooling of heat-generating blocks mounted on a wall in a parallel-plate channel. Fu et al. (1996) and Fu and Chen (2002) dealt with the case of a single porous block on a heated wall in a channel. Sözen and Kuzay (1996) studied round tubes with porous inserts. Zhang and Zhao (2000) treated a porous block behind a step in a channel. Masuoka et al. (2004) studied experimentally and numerically, with alternative interface conditions considered, the case of a permeable cylinder placed in a wind tunnel of rectangular cross section. Layeghi and Nouri-Borujerdi (2004) discussed forced convection from a cylinder or an array of cylinders in the presence or absence of a porous medium. Huang et al. (2004b) studied numerically the enhancement of heat transfer from multiple heated blocks in a channel using porous covers.

Abu-Hijleh (1997, 2000, 2001b, 2002) numerically simulated forced convection in various geometries with orthotropic porous inserts, while Abu-Hijleh (2003) treated a cylinder with permeable fins. A transient problem involving partly filled channels was studied by Abu-Hijleh and Al-Nimr (2001).

Analytical solutions for some flows through channels with composite materials were obtained by Al-Hadrami et al. (2001a,b). Pipes with porous substrates were treated numerically by Alkam and Al-Nimr (1999a,b, 2001), while parallel-plate channels were similarly treated by Alkam et al. (2001, 2002). A tubeless solar collector and an unsteady problem involving an annulus were likewise treated by Al-Nimr and Alkam (1997a, 1998a). Hamdan et al. (2000) treated a parallel-plate channel with a porous core. W. T. Kim et al. (2003c) studied both a porous core and a porous sheath in a circular pipe. A Green's function method was used by Al-Nimr and Alkam (1998b) to obtain analytical solution for transient flows in parallel-plate channel. Experimental and numerical investigations of forced convection in channels containing obstacles were conducted by Young and Vafai (1998, 1999) and Pavel and Mohamad (2004a, b, c). An analytical solution for the case of an annulus was found by Qu et al. (2012b). A numerical simulation for turbulent flow in a channel was reported by Nimvari et al. (2012).

The limitation of the single-domain approach for the computation of convection in composite channels was exposed by Kuznetsov and Xiong (1999). The effect of thermal dispersion in a channel was analyzed by Kuznetsov (2001). Kuznetsov and Xiong (2000) numerically simulated the effect of thermal dispersion in a composite circular duct.

Kuznetsov (2000a) reviewed a number of analytical studies, including those by Kuznetsov (1998b, 1999a,c, 2001) for flow induced by pressure gradients, and by Kuznetsov (1998d, 2000b) and Xiong and Kuznetsov (2000) for Couette flow. The effect of turbulence on forced convection in a composite tube was discussed by Kuznetsov et al. (2002, 2003b), Kuznetsov (2004a), and Kuznetsov and Becker (2004).

A numerical study of turbulent heat transfer above a porous wall was conducted by Stalio et al. (2004). Convection past a circular cylinder sheathed with a porous annulus, placed perpendicular to a turbulent air flow, was studied numerically and experimentally by Sobera et al. (2003). Hydrodynamically and thermally developing convection in a partly filled square duct was studied numerically using the Brinkman model by Jen and Yan (2005). The effects of a transition layer on forced convection in a channel were studied by Kuznetsov and Nield (2008a). They obtained an analytical solution involving a novel type of Airy function. Chen et al. (2008d) performed a numerical analysis based on stress-jump boundary conditions of flow past a porous square cylinder. Nield and Kuznetsov (2005d) studied the thermal development of flow in partly occupied channel or duct. Multi-plate porous insulation was studied by Lim et al. (2007). Combined convection and radiation in the entry region of circular ducts was studied by Chen and Sutton (2005). An analytical investigation of the effect of viscous dissipation on Couette flow in a channel partly occupied by a porous medium was carried out by Ghazian et al. (2011). A two-equation model was applied to tubes partly filled with metallic foam by Xu et al. (2011). Umapathi et al. (2010) studied generalized Couette flow in a composite channel.

A boundary-layer analysis of unconfined forced convection with a plate and a porous substrate was presented by Nield and Kuznetsov (2003d). A more general analytical investigation of this situation had been presented earlier by Kuznetsov (1999b). The same problem for a wedge was treated by Kuznetsov and Nield (2006a).

Further general studies have been made by Mohais and Bhatt (2009), Huang et al. (2010), Sousa (2005), Yucel and Guven (2007, 2008), Yuan and Chung (2008), Zahi et al. (2008), Zehforoosh and Hossainpour (2008), Bhargavi et al. (2009), Satyamurty and Bhargavi (2010), Bhargavi and Satyamurty (2011), Shokoumand and Sayehvand (2010), Maerefat et al. (2011), Aguiilar-Madera et al. (2011), and Teamah et al. (2011). Turbulent flow has been further studied by Santos and de Lemos (2006), Allouache and Chikh (2008), Saati and Mohamad (2007), and Yang and Hwang (2008). Further studies with porous blocks were conducted by Hooman and Merrikh (2010), Li et al. (2010a), Shuja et al. (2009a,b), Tzeng (2006), and Tzeng et al. (2007). More work on fins or pins has been conducted by Do et al. (2007), Hamdan and Al-Nimr (2010), and Yang et al. (2010b). The case of a centered porous layer was studied by Cekmer et al. (2012). An assessment of local thermal equilibrium in tubes with a porous core or sheath was made by Yang et al. (2012).

Forced convection in a partly filled pipe was simulated numerically by Teamah et al. (2011). Non-Newtonian fluid flow in plane channels with porous blocks was studied by Nebbali and Bouhadef (2011). The effect of LTNE in a partly filled channel was analyzed by Mahmoudi and Maerefat (2011). A similar study was made by Xu et al. (2011a,b) for a tube and a parallel-plate channel. An analytical study of the effect of viscous dissipation in Couette flow in a partly filled channel was made by Ghazian et al. (2011). Experiments in all metallic wire-woven bulk Kagome sandwich panels were made by Joo et al. (2011). Valipour and Ghadi

(2012) investigated numerically forced-convective heat transfer around and through a porous circular cylinder with internal heat generation.

## 4.12 Transversely Heterogeneous Channels and Pipes

Kuznetsov (2000a) reviewed a number of analytical studies, including those by Kuznetsov (1998b, 1999a,c, 2001) for flow induced by pressure gradients, and by Kuznetsov (1998d, 2000b) and Xiong and Kuznetsov (2000) for Couette flow. The effect of turbulence on forced convection in a composite tube was discussed by Kuznetsov et al. (2002, 2003b), Kuznetsov (2004a), and Kuznetsov and Becker (2004). A numerical study of turbulent heat transfer above a porous wall was conducted by Stalio et al. (2004). Convection past a circular cylinder sheathed with a porous annulus, placed perpendicular to a turbulent air flow, was studied numerically and experimentally by Sobera et al. (2003). Hydrodynamically and thermally developing convection in a partly filled square duct was studied numerically using the Brinkman model by Jen and Yan (2005). Chen et al. (2008d) performed a numerical analysis based on stress-jump boundary conditions of flow past a porous square cylinder. Nield and Kuznetsov (2005d) studied the thermal development of flow in partly occupied channel or duct. Multi-plate porous insulation was studied by Lim et al. (2007). Combined convection and radiation in the entry region of circular ducts was studied by Chen and Sutton (2005). An analytical investigation of the effect of viscous dissipation on Couette flow in a channel partly occupied by a porous medium was carried out by Ghazian et al. (2011). A two-equation model was applied to tubes partly filled with metallic foam by Xu et al. (2011). Umapathi et al. (2010) studied generalized Couette flow in a composite channel.

A boundary-layer analysis of unconfined forced convection with a plate and a porous substrate was presented by Nield and Kuznetsov (2003d). A more general analytical investigation of this situation had been presented earlier by Kuznetsov (1999b). The same problem for a wedge was treated by Kuznetsov and Nield (2006a).

Further general studies have been made by Mohais and Bhatt (2009), Huang et al. (2010), Sousa (2005), Yucel and Guven (2007, 2008), Yuan and Chung (2008), Zahi et al. (2008), Zehforoosh and Hossainpour (2008), Bhargavi et al. (2009), Satyamurty and Bhargavi (2010), Bhargavi and Satyamurty (2011), Shokoumand and Sayehvand (2010), Maerefat et al. (2011), Aguiilar-Madera et al. (2011), and Teamah et al. (2011). Turbulent flow has been further studied by Santos and de Lemos (2006), Allouache and Chikh (2008), Saati and Mohamad (2007), and Yang and Hwang (2008). Further studies with porous blocks were conducted by Hooman and Merrikh (2010), Li et al. (2010a), Shuja et al. (2009a,b), Tzeng (2006), and Tzeng et al. (2007). More work on fins or pins has been conducted by Do et al. (2007), Hamdan and Al-Nimr (2010), and Yang et al. (2010b).

Analytical studies on the effect on forced convection, in channels and ducts, of the variation in the transverse direction of permeability and thermal conductivity

were initiated by Nield and Kuznetsov (2000), who used the Darcy model for local thermal equilibrium. Both parallel-plate channels and circular ducts were considered, and walls at uniform temperature and uniform heat flux, applied symmetrically, were treated in turn. Both continuous variation and stepwise variation of permeability and conductivity were treated. For the parallel-plate channel, this work was extended to the Brinkman model by Nield and Kuznetsov (2003d). For the case of a parallel-plate channel with uniform heat flux boundaries, Sundaravadivelu and Tso (2003) extended the basic analysis to allow for the effect of viscosity variations. Asymmetric property variation and asymmetric heating in a parallel-plate channel were considered by Nield and Kuznetsov (2001a). A conjugate problem, with either a parallel-plate channel or a circular duct, was treated by Kuznetsov and Nield (2001). The interaction of thermal nonequilibrium and heterogeneous conductivity was studied by Nield and Kuznetsov (2001b). With application to the experimental results reported by Paek et al. (1999b) in mind, Nield and Kuznetsov (2003a) treated a case of gross heterogeneity and anisotropy using a layered medium analysis. A conjugate problem, involving the Brinkman model and with temperature-dependent volumetric heat inside the solid wall, was treated analytically and numerically by Mahmud and Fraser (2005).

For illustration, we present the results obtained by Nield and Kuznetsov (2000) for the effect of heterogeneity on Nusselt number. We first consider the case where the permeability and thermal conductivity distributions are given by

$$K = K_0 \left\{ 1 + \varepsilon_K \left( \frac{|y^*|}{H} - \frac{1}{2} \right) \right\}, \quad k = k_0 \left\{ 1 + \varepsilon_k \left( \frac{|y^*|}{H} - \frac{1}{2} \right) \right\}. \quad (4.134a,b)$$

Here the boundaries are at  $y^* = -H$  and  $y^* = H$ . The mean values of the permeability and conductivity are  $K_0$  and  $k_0$ , respectively. The coefficients  $\varepsilon_K$  and  $\varepsilon_k$  are each assumed to be small compared with unity. To first order, one finds that for the case of uniform flux boundaries,

$$Nu = 6 \left( 1 + \frac{1}{4} \varepsilon_K - \frac{1}{8} \varepsilon_k \right) \quad (4.135)$$

and for the case of uniform temperature boundaries,

$$Nu = \frac{\pi^2}{2} \left\{ 1 + \frac{2}{\pi^2} (\varepsilon_K - \varepsilon_k) \right\}. \quad (4.136)$$

## 4.13 Thermal Development

In forced convection in a porous medium, hydrodynamic development is not normally of importance. This is because the hydrodynamic development length is readily shown to be of order of magnitude  $(K/\varphi)^{1/2}$ , and usually this is very small compared with the channel width. In contrast, the thermal development length can be much greater.

For the Darcy model one has slug flow, and for the case of walls at uniform temperature the classical Graetz solution for thermal development is applicable. An analysis based on the Brinkman model was reported by Nield et al. (2004a) for both a parallel-plate channel and a circular tube. A finite-element numerical investigation was made by Misirlioglu (2007). The additional effect of a Forchheimer term has not yet been treated, but one would anticipate that since an increase in Forchheimer number would produce a more slug-like flow, the effect of quadratic drag would be similar to that produced by a reduction in Darcy number. The corresponding case where the walls are at uniform heat flux was treated by Nield et al. (2003b). The effect of LTNE was examined by Nield et al. (2002), and the additional effects of transverse heterogeneity were studied by Nield and Kuznetsov (2004). Thermal development in a channel occupied by a non-Newtonian power-law fluid was studied by Nield and Kuznetsov (2005a). In the standard analysis of the Graetz type the axial conduction and viscous dissipation effects are neglected, but in the studies by Nield et al. (2003a) and Kuznetsov et al. (2003c) these effects were included, for the cases of a parallel-plate channel and a circular duct, respectively. For the case of a circular duct, axial conduction effects and viscous dissipation effects were studied numerically by Hooman et al. (2003) and Ranjbar-Kani and Hooman (2004), respectively. A porous medium occupied by a rarefied gas was studied by Kuznetsov and Nield (2009b, 2010f). The case of LTNE was examined by Yang and Liu (2006) and Dukhan (2009b), and thermal nonequilibrium, together with the effect of viscous dissipation, was studied by Chen and Tsao (2011c) (together with viscous dissipation). The effect of viscous dissipation was also studied by Hooman et al. (2006, 2007b) and Tada and Ichimiya (2007b). An entropy generation analysis was performed by Hooman et al. (2008a).

A numerical study of heat transfer in the thermally developing region in an annulus was reported by Hsieh and Lu (1998). Thermally developing forced convection inside ducts of various shapes (including elliptical passages) was analyzed by Haji-Sheikh and Vafai (2004). Haji-Sheikh et al. (2005) illustrated the use of a combination a Green's function solution and an extended weighted residual method to the study of isosceles triangular passages. They noted that their methodology is equally applicable when the boundary conditions are of the first, second, or third kind. A field synergy principle analysis for the case of uniform heat generation was reported by Chen and Tsao (2012b).

The general feature of thermal development is that the Nusselt number increases as one moves from the fully developed region toward the entrance region. It is found that the rate of increase decreases as the Darcy number increases.

## 4.14 Surfaces Covered with Porous Layers

The hair growth on the skin of a mammal is an example of a saturated porous medium where, locally, the solid matrix (hair) is *not* in thermal equilibrium with the permeating fluid (air). A theory for the heat transfer by forced convection through a surface covered with hair has been developed by Bejan (1990a). It was tested subsequently in the numerical experiments of Lage and Bejan (1990). This entire body of work was reviewed by Bejan and Lage (1991) and Bejan (1992b).

The most essential features of the geometry of an actual surface covered with hair are retained in the model presented in Fig. 4.9. The skin surface is connected to a large number of perpendicular strands of hair, the density of which is assumed constant,

$$n = \frac{\text{number of strands of hair}}{\text{unit area of skin surface}}. \quad (4.137)$$

The hair population density  $n$  is related to the porosity of the “hair + air” medium that resides above the skin,

$$\phi = \frac{\text{air volume}}{\text{total volume}} = 1 - nA_s. \quad (4.138)$$

Each strand of hair is modeled as a cylinder with the cross section  $A_s$ .

Parallel to the skin surface and through the porous structure formed by the parallel hair strands flows a uniform stream of air of velocity  $U$ . This stream is driven longitudinally by the dynamic pressure rise formed over that portion of the animal’s body against which the ambient breeze stagnates. The longitudinal length  $L$  swept by the air flow is a measure of the linear size of the animal. The constant air velocity  $U$  is a quantity averaged over the volume occupied by air. It is assumed that the strand-to-strand distances are small enough so that the air flow behaves according to the Darcy law, with apparent slip at the skin surface.

At every point in the two-dimensional ( $x, y$ ) space occupied by the porous medium described above, we distinguish two temperatures: the temperature of the solid structure (the local hair strand),  $T_s$ , and the temperature of air that surrounds the strand,  $T_a$ . Both  $T_s$  and  $T_a$  are functions of  $x$  and  $y$ . The transfer of heat from the skin to the atmosphere is driven by the overall temperature difference ( $T_w - T_\infty$ ), where  $T_w$  is the skin temperature and  $T_\infty$  the uniform temperature of the ambient air that enters the porous structure. The temperature of the interstitial air,  $T_a$ , is equal to the constant temperature  $T_\infty$  in the entry plane  $x = 0$ .

For the solid structure, the appropriate energy equation is the classic conduction equation for a fin (in this case, single strand of hair),

$$k_s A_s \frac{\partial^2 T_s}{\partial y^2} - hp_s (T_s - T_a) = 0, \quad (4.139)$$

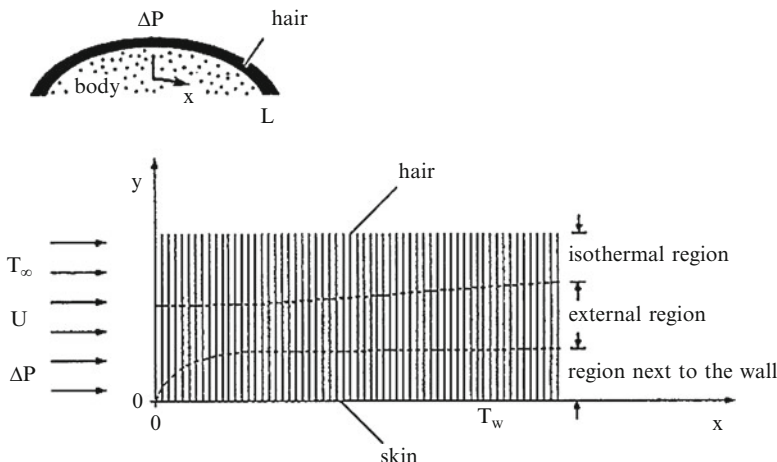


**Fig. 4.10** Two-dimensional model for forced convection through the hair growth near the skin (after Bejan 1990a)

where  $p_s$  is the perimeter of a strand cross section. The thermal conductivity of the strand,  $k_s$ , and the perimeter-averaged heat transfer coefficient,  $h$ , are both constant. The constancy of  $h$  is a result of the assumed low Reynolds number of the air flow that seeps through the hair strands.

The second energy conservation statement refers to the air space alone, in which  $(\rho c_p)$  and  $k_a$  are the heat capacity and thermal conductivity of air:

$$\rho c_p U \frac{\partial^2 T_a}{\partial x^2} = k_a \frac{\partial^2 T_a}{\partial y^2} + nhp_s(T_s - T_a). \quad (4.140)$$

On the left-hand side of this equation, we see only one convection term because the air-space-averaged velocity  $U$  points strictly in the  $x$  direction. The first term on the right-hand side of the equation accounts for air conduction in the transversal direction ( $y$ ). By not writing the longitudinal conduction term  $k_a \partial^2 T_a / \partial x^2$ , we are assuming that the flow region in which the effect of transversal air conduction is important is thin.

The last term in Eq. (4.140) accounts for the “volumetric heat source” effect that is due to the contact between the air stream and the local (warmer) hair strand. Note the multiplicative role of the strand density  $n$  in the makeup of this term: the product  $(np_s)$  represents the total contact area between hair and air, expressed per unit of air volume. The heat source term of Eq. (4.140) is the air-side reflection of the heat sink term (the second term) encountered in the fin conduction equation (4.139).

In an air region that is sufficiently close to the skin, the air stream is warmed up mainly by contact with the skin, i.e., not by the contact with the near-skin area of the hair strands. Consequently, for this region, in Eq. (4.140) the heat source term  $nhp_s(T_s - T_a)$  can be neglected. On the other hand, sufficiently far from the skin most

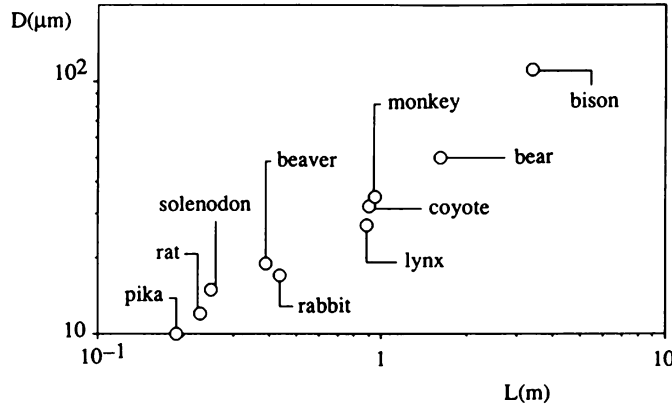


Fig. 4.11 The hair strand diameters and body lengths of ten mammals (Bejan and Lage 1991)

of the heating of the air stream is affected by the hair strands that impede the flow. In the energy balance of this external flow the vertical conduction term can be neglected in Eq. (4.140).

For the details of the heat transfer analysis of the two-temperature porous medium of Fig. 4.10, the reader is referred to the original paper (Bejan, 1990a). One interesting conclusion is that the total heat transfer rate through a skin portion of length  $L$  is minimized when the hair strand diameter assumes the optimal value  $D_{\text{opt}}$  given by

$$\frac{D_{\text{opt}}}{v} \left( \frac{\Delta P}{\rho} \right)^{1/2} = \left( \frac{k_z^2 k_s}{2k_a} \right)^{1/4} \left( \frac{1-\phi}{\phi} \right)^{5/4} \left[ \frac{L}{v} \left( \frac{\Delta P}{\rho} \right)^{1/2} \right]^{1/2}. \quad (4.141)$$

That lowest heat transfer rate is

$$\frac{q'_{\min}}{k_a(T_w - T_\infty)} = \left( 32 \frac{k_s}{k_a} \right)^{1/4} \phi^{3/4} (1-\phi)^{1/4} \left[ \frac{L}{v} \left( \frac{\Delta P}{\rho} \right)^{1/2} \right]^{1/2}. \quad (4.142)$$

These results are based on several additional assumptions, which include a model of type (1.5) for the permeability of the hair matrix

$$K \cong \frac{D^2 \phi^3}{k_z (1-\phi)^2}, \quad (4.143)$$

where the constant  $k_z$  is a number of order  $10^2$ .

Equation (4.142) shows that the minimum heat transfer rate increases with the square root of the linear size of the body covered with hair,  $L^{1/2}$ . The optimal hair

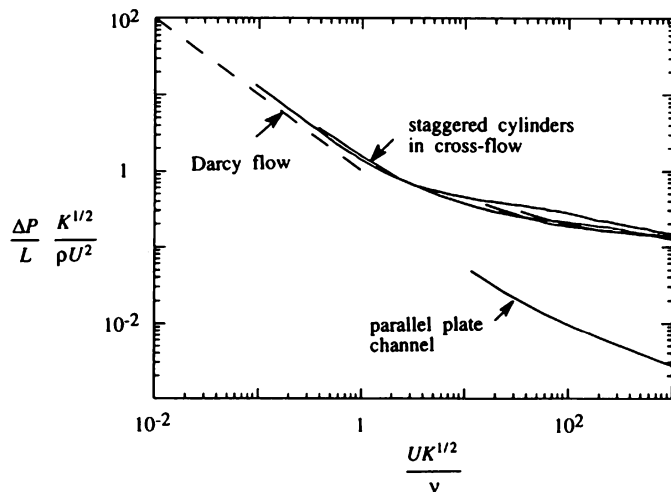


**Fig. 4.12** Porous-medium representation of the classic pressure-drop data for flow through staggered cylinders and stacks of parallel plates (Bejan and Morega 1993)

strand diameter is also proportional to  $L^{1/2}$ . This last trend agrees qualitatively with measurements of the hair sizes of mammals compiled by Sokolov (1982). Figure 4.11 shows the natural hair strand diameters ( $D$ ) of ten mammals, with the length scale of the body of the animal plotted on the abscissa.

The natural design of animal body insulation is an important and visible manifestation of the constructal law of design in nature. Although many natural designs, animate and inanimate (e.g., river basins, lungs), speak loudly of the natural design tendency to facilitate flow access, the design of body insulation seems to contradict this tendency, because it opposes the flow of heat from body to ambient. In fact, there is no contradiction, because what flows in animal design is animal mass on the landscape and the flow of animal mass is facilitated by all the detailed features of animal design, from the *minimization* of fluid flow resistance in lung architecture and vascularized tissues to the *maximization* of heat flow resistance in body insulation (Bejan and Lorente, 2010, 2011, Bejan and Zane, 2012).

More recent studies of surfaces covered with fibers have focused on the generation of reliable pressure drop and heat transfer information for low Reynolds number flow through a bundle of perpendicular or inclined cylindrical fibers (Fowler and Bejan, 1994). There is a general need for data in the low Reynolds number range, as most of the existing results refer to heat exchanger applications (i.e., higher Reynolds numbers). Fowler and Bejan (1995) studied numerically the heat transfer from a surface covered with flexible fibers, which bend under the influence of the interstitial flow. Another study showed that when the effect of radiation is taken into account, it is possible to anticipate analytically the existence of an optimal packing density (or porosity) for minimal heat transfer across the porous cover (Bejan, 1992b).

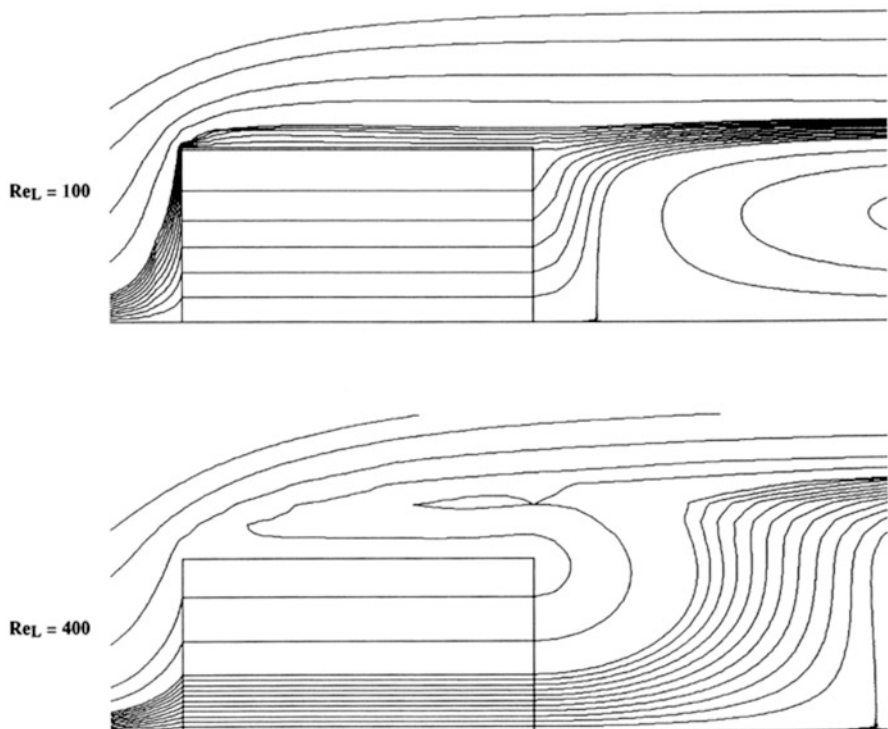


**Fig. 4.13** The flow through and over a stack of rectangular parallel-plate fins attached to a base and modeled as a porous medium (Morega et al. 1995)

Vafai and Kim (1990) and Huang and Vafai (1993, 1994) have shown that a porous coating can alter dramatically the friction and heat transfer characteristics of a surface. This effect was also documented by Fowler and Bejan (1995). Depending on its properties and dimensions, the porous layer can act either as an insulator or as a heat transfer augmentation device. The engineering value of this work is that it makes it possible to “design” porous coatings such that they control the performance of the solid substrate.

## 4.15 Designed Porous Media

A potentially revolutionary application of the formalism of forced convection in porous media is in the field of heat exchanger simulation and design. Heat exchangers are a century-old technology based on information and concepts stimulated by the development of large-scale devices (see, e.g., Bejan, 1993, Chap. 9). The modern emphasis on heat transfer augmentation and the more recent push toward miniaturization in the cooling of electronics have led to the

development of compact devices with much smaller features than in the past. These devices operate at lower Reynolds numbers, where their compactness and small dimensions (“pores”) make them candidates for modeling as saturated porous media.

Such modeling promises to revolutionize the nomenclature and numerical simulation of the flow and heat transfer through heat exchangers. Decreasing dimensions, increasing compactness, and constructal design (Sect. 4.18) make these devices appear and function as *designed porous media* (Bejan, 2004b; Lorente, 2009). This emerging field is outlined in two new books (Bejan, 2004; Bejan et al., 2004).

To illustrate this change, consider Zukauskas’ (1987) classical chart for the pressure drop in cross flow through arrays of staggered cylinders (e.g., Fig. 9.38 in Bejan, 1993). The four curves drawn on this chart for the transverse pitch/cylinder diameter ratios 1.25, 1.5, 2, and 2.5 can be made to collapse into a single curve, as shown in Fig. 4.12 (Bejan and Morega, 1993). The technique consists of treating the bundle as a fluid-saturated porous medium and using the volume-averaged velocity  $U$ , the pore Reynolds number  $UK^{1/2}/v$  on the abscissa, and the dimensionless pressure gradient group  $(\Delta P/L) K^{1/2}/\rho U^2$  on the ordinate.

The effective permeability of the bundle of cylinders was estimated using Eq. (4.143) with  $k_z = 100$  and Zukauskas’ chart. Figure 4.12 shows very clearly the transition between Darcy flow (slope—1) and Forchheimer flow (slope 0). The porous-medium presentation of the array of cylinders leads to a very tight collapse of the curves taken from Zukauskas’ chart. The figure also shows the pressure-drop curve for turbulent flow through a heat exchanger core formed by a stack of parallel plates. An added benefit of Fig. 4.12 is that it extends the curves reliably into the low Reynolds number limit (Darcy flow), where classic heat exchanger data are not available.

This method of presentation (Fig. 4.12) deserves to be extended to other heat exchanger geometries. Another reason for pursuing this direction is that the heat and fluid flow process can be simulated numerically more easily if the heat exchanger is replaced at every point by a porous medium with volume-averaged properties. An example is presented in Fig. 4.13 (Morega et al., 1995). Air flows from left to right along a hot horizontal surface (the electronics module) and through an array of parallel plate fins of rectangular profile (the heat sink). The plate thickness and plate-to-plate spacing are  $t/L = 0.05$  and  $d/L = 0.069$ , where  $L$  is the length of the plate in the flow direction. The Reynolds number  $Re_L$  is based on  $L$  and the approach velocity. The air flows through and over the heat sink. The corresponding temperature field and the effect of changing the Reynolds number are illustrated in Morega et al. (1995). One advantage of the numerical model is that it accounts in a volume-averaged sense for the conduction heat transfer through each plate, longitudinally and transversally. Another advantage comes from the relative simplicity and high computational speed, because in the thermal design and optimization of cooling techniques it is necessary to simulate a large number of geometric configurations such as Fig. 4.13.

Another important application of porous media concepts in engineering is in the optimization of the internal spacings of heat exchangers subjected to overall volume constraints (see Sects. 4.19 and 4.20). Packages of electronics cooled by forced convection are examples of heat exchangers that must function in fixed volumes. The design objective is to install as many components (i.e., heat generation rate) as possible, while the maximum temperature that occurs at a point (hot spot) inside the given volume does not exceed a specified limit. Bejan and Sciubba (1992) showed that a very basic trade-off exists with respect to the number of installed components, i.e., regarding to the size of the pores through which the coolant flows. This trade-off is evident if we imagine the two extremes: numerous components (small pores) and few components (large spacings).

When the components and pores are numerous and small, the package functions as a heat-generating porous medium. When the installed heat generation rate is fixed, the hot spot temperature increases as the spacings become smaller, because in this limit the coolant flow is being shut off gradually. In the opposite limit, the hot spot temperature increases again because the heat transfer contact area decreases as the component size and spacing become larger. At the intersection of these two asymptotes we find an optimal spacing (pore size) where the hot spot temperature is minimal when the heat generation rate and volume are fixed. The same spacing represents the design with maximal heat generation rate and fixed hot spot temperature and volume. Bejan and Sciubba (1992), Bejan (1993), and Morega et al. (1995) developed analytical and numerical results for optimal spacings in applications with solid components shaped as parallel plates. Optimal spacings for cylinders in cross flow were determined analytically and experimentally by Bejan (1995) and Stanescu et al. (1996). The spacings of heat sinks with square pin fins and impinging flow were optimized numerically and experimentally by Ledezma et al. (1996). The latest conceptual developments are outlined in Sect. 4.19.

The dimensionless results developed for optimal spacings ( $S_{\text{opt}}$ ) have generally the form

$$\frac{S_{\text{opt}}}{L} \sim Be_L^{-n} \quad (4.144)$$

where  $L$  is the dimension of the given volume in the flow direction, and  $Be_L$  is the dimensionless pressure drop that Bhattacharjee and Grosshandler (1988) termed the Bejan number,

$$Be_L = \frac{\Delta P \cdot L^2}{\mu_f \alpha_f}. \quad (4.145)$$

In this definition  $\Delta P$  is the pressure difference maintained across the fixed volume. For example, the exponent  $n$  in Eq. (4.144) is equal to 1/4 in the case of laminar flow through stacks of parallel-plate channels. The Bejan number serves as the forced-convection analog of the Rayleigh number used in natural convection (Petrescu, 1994).

Designed porous media are now an active field of research in constructal theory and design. The progress on designed porous media was reviewed by Bejan and Lorente (2006, 2008).

The design of heat transfer processes in porous media is also an important new trend in the wider and rapidly growing field of thermodynamic optimization (Bejan, 1996a). Noteworthy are two optimal-control papers of Kuznetsov (1997a,c), in which the heat transfer is maximized during the forced-convection transient cooling of a saturated porous medium. For example, Kuznetsov (1997a) achieved heat transfer maximization by optimizing the initial temperature of the porous-medium subject to a fixed amount of energy stored initially in the system and a fixed duration of the cooling process.

## 4.16 Other Configurations or Effects

### 4.16.1 Effect of Temperature-Dependent Viscosity

The study of the effect of a temperature-dependent viscosity on forced convection in a parallel-plate channel was initiated by Nield et al. (1999). The original analysis was restricted to small changes of viscosity carried out to first order in Nield et al. (1999) and to second order in Narasimhan et al. (2001b), but the layered medium analysis of Nield and Kuznetsov (2003b) removed this restriction. For the case of a fluid whose viscosity decreases as the temperature increases (the usual situation), it is found that the effect of the variation is to reduce/increase the Nusselt number for cooled/heated walls. The analysis predicts that for the case of small Darcy number the effect of viscosity variation is almost independent of the Forchheimer number, while for the case of large Darcy number the effect of viscosity variation is reduced as the Forchheimer number increases. Within the limitations of the assumptions made in the theory, experimental verification was provided by Nield et al. (1999) and Narasimhan et al. (2001a).

For example, in the case of uniform flux boundaries and Darcy's law, Nield et al. (1999) showed that the mean velocity is altered by a factor  $(1 + N/3)$  and the Nusselt number is altered by a factor  $(1 - 2N/15)$ , where the viscosity variation number  $N$  is defined as

$$N = \frac{q''H}{k} \frac{1}{\mu_0} \left( \frac{d\mu}{dT} \right)_0, \quad (4.146)$$

where the suffix 0 indicates evaluation at the reference temperature  $T_0$ .

The extension to the case where there is a substantial interaction between the temperature dependence of viscosity and the quadratic drag effect was carried out in a sequence of papers by Narasimhan and Lage (2001a,b, 2002, 2003, 2004a). The effect on pump power gain for channel flows was studied by Narasimhan and Lage

(2004b). In these papers the authors developed what they call a Modified Hazen-Dupuit-Darcy model which they then validated with experiments with PAO as the convecting liquid and compressed aluminum-alloy porous foam as the porous matrix. This work on temperature-dependent viscosity was reviewed by Narasimhan and Lage (2005). Further studies on the effect of temperature-dependent viscosity were made by Hooman and Mohebpour (2007) and Hooman and Gurgenci (2008b). The variation of other thermophysical properties was studied by Pantokratoras (2007a,b).

The effects of a magnetic field and temperature-dependent viscosity on forced convection past a flat plate, with a variable wall temperature and in the presence of suction or blowing, were studied numerically by Seddeek (2002, 2005). Entropy generation studies were made by Hooman (2006), Hooman and Gurgenci (2007a), and Hooman et al. (2009).

#### **4.16.2 Oscillatory Flows, Counterflows**

For an annulus and a pipe, Guo et al. (1997a,b) treated pulsating flow. For a completely filled channel, Kim et al. (1994) studied a pulsating flow numerically. Soundalgekhar et al. (1991) studied flow between two parallel plates, one stationary and the other oscillating in its own plane. Hadim (1994a) simulated convection in a channel with localized heat sources.

Sözen and Vafai (1991) analyzed compressible flow through a packed bed with the inlet temperature or pressure oscillating with time about a nonzero mean. They found that the oscillation had little effect on the heat storage capacity of the bed. Paek et al. (1999a) studied the transient cool down of a porous medium by a pulsating flow. Experiments involving steady and oscillating flows were conducted by Leong and Jin (2004, 2005). Reciprocating flows in channels partly filled with a porous medium were studied by Habibi et al. (2011).

An analytical treatment of pulsating flow in a channel or tube was presented by Kuznetsov and Nield (2006b). Pulsating convection from two heat sources mounted with porous blocks was examined by Huang and Yang (2008). Oscillatory flow of a non-Newtonian second-grade fluid was studied by Hayat et al. (2007b). The effect of a periodically oscillating driving force on basic microflows was investigated by Haddad et al. (2006b). Dhahri et al. (2006a) studied pulsating flow in a tube partly filled with a porous medium, while Dhahri et al. (2006b) made a numerical study of reciprocating flow in a pipe. Khanafer et al. (2007) studied the influence of pulsatile blood flow on hyperthermia. An MHD study was reported by Mehmood I (2010). Another flow involving flow oscillation was studied by Byun et al. (2006). Pulsatile flow of a Burger's fluid in a circular pipe was examined by El-Dabe et al. (2010).

Steady counterflow in a parallel-plate channel or a circular tube was studied by Nield and Kuznetsov (2008a) and Kuznetsov and Nield (2009a). The Nusselt number is zero when the net flow is zero. Pulsating counterflow in a channel with small amplitude fluctuations, without phase lag, was treated by Nield and

Kuznetsov (2009a). A similar problem with phase lag was investigated by Nield and Kuznetsov (2010). Pulsating counterflow in a circular tube was considered by Kuznetsov and Nield (2009b).

### 4.16.3 Non-Newtonian Fluids

Boundary-layer flow of a power-law fluid on an isothermal semi-infinite plate was studied by Wang and Tu (1989). The same problem for an elastic fluid of constant viscosity was treated by Shenoy (1992). These authors used a modified Darcy model. A non-Darcy model for a power-law fluid was employed by Shenoy (1993a) and Hady and Ibrahim (1997) for flow past a flat plate, by Alkam et al. (1998) for flow in concentric annuli, and by Nakayama and Shenoy (1993b) and Chen and Hadim (1995, 1998a,b, 1999a) for flow in a channel. These studies showed that in the non-Darcy regime, the effect of increase of power-law index  $n$  is to increase the thermal boundary-layer thickness and the wall temperature and to decrease the Nusselt number; in the Darcy regime the changes are small. As the Prandtl number increases, the Nusselt number increases, especially for shear-thinning fluids ( $n < 1$ ). As  $n$  decreases, the pressure drop decreases.

An elastic fluid was treated by Shenoy (1993b). A viscoelastic fluid flow over a nonisothermal stretching sheet was analyzed by Prasad et al. (2002). An experimental study for heat transfer to power-law fluids under flow with uniform heat flux boundary conditions was reported by Rao (2001, 2002).

A 3D flow in a duct was studied numerically by Nebbali and Bouhadef (2006). Flow over a flat plate of a power-law fluid in a Brinkman medium was analyzed by Pantokratoras and Magyari (2010). The effect of viscous dissipation on flow in a channel occupied by a power-law fluid was studied by Chen and Tsao (2011a). The effect of LTNE in a channel lined with porous layers was examined by Abkar et al. (2010). Attia (2008b) studied the flow of a power-law fluid with a pressure gradient decaying exponentially with time.

### 4.16.4 Bidisperse Porous Media

A bidisperse (or bidispersed—we have opted for the shorter and more commonly used form) porous medium (BDPM), as defined by Z. Q. Chen et al. (2000b), is composed of clusters of large particles that are agglomerations of small particles. Thus there are macropores between the clusters and micropores within them. Applications are found in bidisperse adsorbent or bidisperse capillary wicks in a heat pipe. Since the bidisperse wick structure significantly increases the area available for liquid film evaporation, it has been proposed for use in the evaporator of heat pipes.

A BDPM thus may be looked at as a standard porous medium in which the solid phase is replaced by another porous medium, whose temperature may be denoted by  $T_p$  if local thermal equilibrium is assumed within each cluster. We can then talk about the f-phase (the macropores) and the p-phase (the remainder of the structure). An alternative way of looking at the structure is to regard it as a porous medium in which fractures or tunnels have been introduced. One can then think of the f-phase as being a “fracture phase” and the p-phase as being a “porous phase.”

Questions of interest are how one can determine the effective permeability and the effective thermal conductivity of a bidisperse porous medium. Fractal models for each of these have been formulated by Yu and Cheng (2002a,b). In the first chapter the authors developed two models for the effective thermal conductivity based on fractal geometry and the electrical analogy. Theoretical predictions based on these models were compared with those from a previous lumped-parameter model and with experimental data for the stagnant thermal conductivity reported by Z. Q. Chen et al. (2000). In this chapter a three-dimensional model of touching spatially periodic cubes, which are approximated by touching porous cubes, was used; Cheng and Hsu (1999b) had previously used a two-dimensional model. On the basis of their experiments, Z. Q. Chen et al. (2000) concluded that, when the ratio of solid/fluid thermal conductivity is greater than 100, the effective thermal conductivity of a bidisperse porous medium is smaller than that of a monodisperse porous medium saturated with the same fluid, because of the contact resistance at the microscale and the higher porosity for the bidisperse medium in comparison with the monodisperse one.

Extending the Brinkman model for a monodisperse porous medium, Nield and Kuznetsov (2005a) proposed to model the steady-state momentum transfer in a BDPM by the following pair of coupled equations for  $\mathbf{v}^*_f$  and  $\mathbf{v}^*_p$ , where the asterisks denote dimensional variables,

$$\mathbf{G} = \left( \frac{\mu}{K_f} \right) \mathbf{v}^*_f + \zeta (\mathbf{v}^*_f - \mathbf{v}^*_p) - \tilde{\mu}_f \nabla^{*2} \mathbf{v}^*_f \quad (4.147)$$

$$\mathbf{G} = \left( \frac{\mu}{K_p} \right) \mathbf{v}^*_p + \zeta (\mathbf{v}^*_p - \mathbf{v}^*_f) - \tilde{\mu}_p \nabla^{*2} \mathbf{v}^*_p. \quad (4.148)$$

Here  $\mathbf{G}$  is the negative of the applied pressure gradient,  $\mu$  is the fluid viscosity,  $K_f$  and  $K_p$  are the permeabilities of the two phases, and  $\zeta$  is the coefficient for momentum transfer between the two phases. The quantities  $\tilde{\mu}_f$  and  $\tilde{\mu}_p$  are the respective effective viscosities. From Eqs. (4.147) and (4.148),  $\mathbf{v}^*_p$  can be eliminated to give

$$\begin{aligned} & \tilde{\mu}_f \tilde{\mu}_p \nabla^{*4} \mathbf{v}^*_f - [\tilde{\mu}_f(\zeta + \mu/K_p) + \tilde{\mu}_p(\zeta + \mu/K_f)] \nabla^{*2} \mathbf{v}^*_f \\ & + [\zeta \mu(1/K_f + 1/K_p) + \mu^2/K_f K_p] \mathbf{v}^*_f = \mathbf{G}(2 + \mu/K_p) \end{aligned} \quad (4.149)$$

and  $\mathbf{v}^*_p$  is given by the same equation with subscripts swapped. For the special case of the Darcy limit one obtains

$$\mathbf{v}^*_f = \frac{(\mu/K_p + 2\zeta)\mathbf{G}}{\mu^2/K_f K_p + \zeta\mu(1/K_f + 1/K_p)}, \quad (4.150)$$

$$\mathbf{v}^*_p = \frac{(\mu/K_f + 2\zeta)\mathbf{G}}{\mu^2/K_f K_p + \zeta\mu(1/K_f + 1/K_p)}. \quad (4.151)$$

Thus the bulk flow is given by

$$\mathbf{G} = (\mu/K)\mathbf{v}^*, \quad (4.152)$$

where

$$\mathbf{v}^* = \varphi\mathbf{v}^*_f + (1 - \varphi)\mathbf{v}^*_p, \quad (4.153)$$

$$K = \frac{\varphi K_f + (1 - \varphi)K_p + 2(\zeta/\mu)K_f K_p}{1 + (\zeta/\mu)(K_f + K_p)}. \quad (4.154)$$

Thus, in this case, the effect of the coupling parameter  $\zeta$  merely is to modify the effective permeabilities of the two phases via the parameter  $\zeta/\mu$ .

Nield and Kuznetsov (2005b) treated forced convection in a parallel-plate channel occupied by a BDPM, using a two-temperature model similar to Eqs. (6.54) and (6.55) in this book. Nield and Kuznetsov (2004c) extended the analysis to the case of a conjugate problem with plane solid slabs bounding the channel. They found that the effect of the finite thermal resistance due to the slabs is to reduce both the heat transfer to the porous medium and the degree of LTNE. An increase in the value of the Péclet number leads to decrease in the rate of exponential decay in the downstream direction but does not affect the value of a suitably defined Nusselt number. The case of thermally developing convection in a BDPM was treated by Kuznetsov and Nield (2006c). The case of asymmetric heating of a channel was studied by Kuznetsov and Nield (2010a). Heat transfer in a BDPM has been reviewed by Nield and Kuznetsov (2005c). A three-velocity three-temperature model of a tri-disperse porous medium was applied by Nield and Kuznetsov (2011). The hydrodynamic aspect of bi-disperse porous media in the context of thermal management has been studied by Narasimhan et al. (2012).

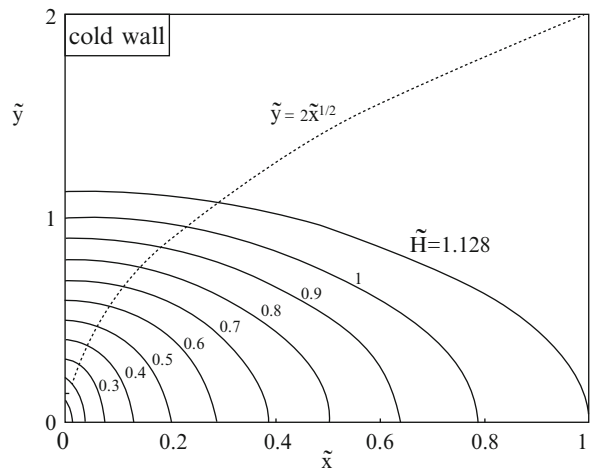
Grosan et al. (2010) studied flow through a spherical porous medium embedded in another porous medium.

#### 4.16.5 Other Flows, Other Effects

Non-Darcy boundary-layer flow over a wedge was studied using three numerical methods by Hossain et al. (1994). An application to the design of small nuclear reactors was discussed by Aithal et al. (1994). Convection with Darcy flow past a slender body was analyzed by Romero (1995b), while Sattar (1993) analyzed boundary-layer flow with large suction. The effect of blowing or suction on forced convection about a flat plate was also treated by Yih (1998d,e). The interaction with radiation in a boundary layer over a flat plate was studied by Mansour (1997). A porous medium heated by a permeable wall perpendicular to the flow direction was studied experimentally by Zhao and Song (2001). The boundary layer at a continuously moving surface was analyzed by Nakayama and Pop (1993) and Khan and Pop (2011). The effect of liquid evaporation on forced convection was studied numerically by Shih and Huang (2002).

Convection in an asymmetrically heated sintered porous channel was investigated by Hwang et al. (1995). Various types of sintered and unsintered heat sinks were compared experimentally by Tzeng and Ma (2004). Convection in a sintered porous channel with inlet and outlet slots was studied numerically by Hadim and North (2005). Sung et al. (1995) investigated flow with an isolated heat source in a partly filled channel. Conjugate forced convection in cross flow over a cylinder array with volumetric heating in the cylinders was simulated by Wang and Georgiadis (1996). Heat transfer for flow perpendicular to arrays of cylinders was examined by Wang and Sangani (1997). An internally finned tube was treated as a porous medium by Shim et al. (2002). Forced convection in a system of wire screen meshes was examined experimentally by Ozdemir and Ozguc (1997). The effect of anisotropy was examined experimentally by Yang and Lee (1999); numerically by S. J. Kim et al. (2001), Nakayama et al. (2002), and Kim and Kuznetsov (2003); and analytically by Degan et al. (2002). The effect of fins in a heat exchanger was studied numerically by S. J. Kim et al. (2000, 2002) and by Kim and Hyun (2005). Forced convection in a channel with a localized heat source using fibrous materials was studied numerically by Angirasa and Peterson (1999). A numerical investigation with a random porosity model was made by W. S. Fu et al. (2001). Experimental studies involving a rectangular duct heated only from the top wall were conducted by Demirel et al. (1999, 2000). A thermodynamic analysis of heat transfer in an asymmetrically heated annular packed bed was reported by Demirel and Kahraman (2000). A laboratory investigation of the cooling effect of a coarse rock layer and a fine rock layer in permafrost regions was reported by Yu et al. (2004). Forced convection in a rotating channel was examined experimentally by Tzeng et al. (2004). Experiments involving a confined slot jet were conducted by Jeng and Tzeng (2007a,b). Other experiments were performed by Noh et al. (2006), Tzeng (2007), Tzeng and Jeng (2006), Jeng et al. (2006, 2010), and Leong et al. (2010). Heat sinks involving nanofluids were studied by Ghazvini and Shokoumand (2009) and Ghazvini et al. (2009). The forced convection of nanofluids was also studied by Maghrebi et al. (2012).

**Fig. 4.14** The heatlines of the boundary layer near a cold isothermal wall (Morega and Bejan 1994)



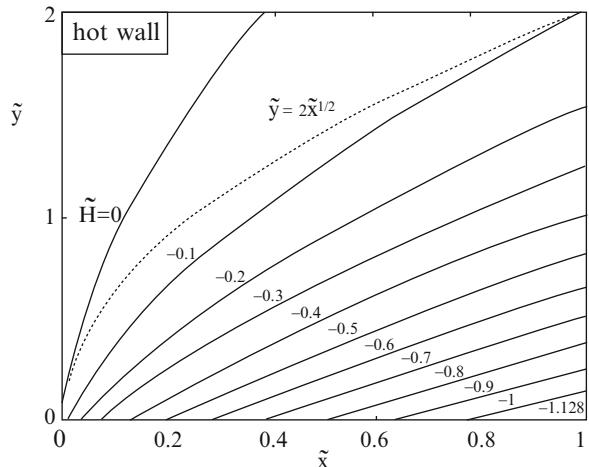
Flow, thermal, and entropy generation characteristics inside a porous channel with viscous dissipation were discussed by Mahmud and Frazer (2005) and Hooman et al. (2007). A similar problem with wavy enclosures filled with microstructures was studied by Mahmud et al. (2007). Further entropy studies were made by Abbasssi (2007), Hooman (2007), Hooman and Ejlali (2007), Hooman and Haji-Sheikh (2007), and Hooman et al. (2007a, 2008b). Other studies were made by Hooman (2008a), Hooman and Gorji-Bandpy (2006, 2007b), Hooman and Merrikh (2006), Ichimiya et al. (2009), Jiang and Lu (2006, 2007), Lu et al. (2006), and Kamisli (2009).

Forced convection in structured packed beds with spherical or ellipsoidal particles was studied computationally by Yang et al. (2010a). Their results were compared with experimental data by Yang et al. (2012). The effect of radiation in cylindrical packed beds was examined by Yee and Kamiuto (2005). Forced convection in parallel flow multilayer microchannels was treated by Saidi and Khiabani (2007). Flow through a channel with wire mesh packing was studied by Dyga (2010). The effect of viscous dissipation in an anisotropic channel with oblique principal axes was studied by Mobedi et al. (2010). A problem with heat generation was studied by Prakash et al. (2012).

## 4.17 Heatlines for Visualizing Convection

The concepts of heat function and heatlines were introduced for the purpose of visualizing the true path of the flow of energy through a convective medium (Kimura and Bejan, 1983; Bejan, 1984). The heat function accounts simultaneously for the transfer of heat by conduction and convection at every point in the medium. The heatlines are a generalization of the flux lines used routinely in the field of

**Fig. 4.15** The heatlines of the boundary layer near a hot isothermal wall (Morega and Bejan 1994)



conduction. The concept of heat function is a spatial generalization of the concept of Nusselt number, i.e., a way of indicating the magnitude of the heat transfer rate through any unit surface drawn through any point on the convective medium.

The heatline method was extended to several configurations of convection through fluid-saturated porous media (Morega and Bejan, 1994). To illustrate the method, consider the uniform flow with thermal boundary layer, which is shown in Fig. 4.1. The heat function  $H(x,y)$  is defined such that it satisfies identically the energy equation for the thermal boundary layer, Eq. (4.3). The  $H$  definition is in this case

$$\frac{\partial H}{\partial y} = (\rho c_p) u(T - T_{\text{ref}}), \quad (4.155)$$

$$-\frac{\partial H}{\partial x} = (\rho c_p) v(T - T_{\text{ref}}) - k_m \frac{\partial T}{\partial y}, \quad (4.156)$$

where the reference temperature  $T_{\text{ref}}$  is a constant. The flow field ( $u, v$ ) and the temperature field ( $T$ ) are furnished by the solutions to the convective heat transfer problem. It was pointed out in Trevisan and Bejan (1987a) that  $T_{\text{ref}}$  can have any value and that a heatline pattern can be drawn for each  $T_{\text{ref}}$  value. The most instructive pattern is obtained when  $T_{\text{ref}}$  is set equal to the lowest temperature that occurs in the convective medium that is being visualized. This choice was made in the construction of Figs. 4.14 and 4.15. In both cases the heat function can be obtained analytically. When the wall is colder ( $T_w$ ) than the approaching flow ( $T_\infty$ ) (Fig. 4.14), the nondimensionalized heat function is

$$\tilde{H}(\tilde{x}, \tilde{y}) = \tilde{x}^{1/2} \left[ \eta \operatorname{erf}\left(\frac{\eta}{2}\right) + \frac{2}{\pi^{1/2}} \exp\left(-\frac{\eta^2}{4}\right) \right], \quad (4.157)$$

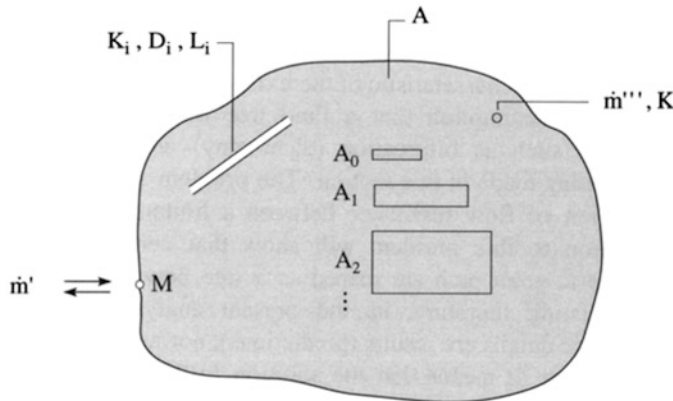


**Fig. 4.16** The two-dimensional flow between one point (M) and a finite-size volume (A)

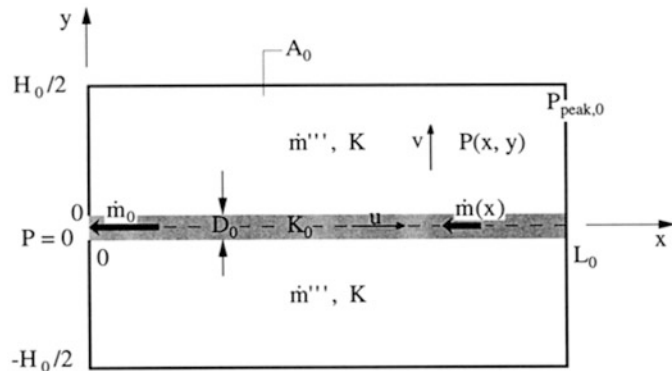
where  $\tilde{H} = H/[k_m(T_\infty - T_w)Pe_L^{1/2}]$ ,  $Pe_L = U_\infty L/\alpha_m$ ,  $\tilde{x} = x/L$ , and  $\eta = y(U_\infty/\alpha_m x)^{1/2}$ . In these expressions,  $L$  is the length of the  $y = 0$  boundary. Figure 4.14 shows that the  $H = \text{constant}$  curves visualize several features of convection near a cold wall. The energy that is eventually absorbed by the wall is brought into the boundary layer ( $\tilde{y} \cong 2\tilde{x}^{1/2}$ ) by fluid from upstream of the cold section of the wall. The heatlines that enter the wall are denser near  $\tilde{x} = 0$ , that is, the heat flux is more intense. Finally, the value of the heat function increases along the wall, because the wall absorbs the heat released by the fluid. The trailing-edge  $\tilde{H}$  value matches the total heat transfer rate through the wall, Eq. (4.14).

Figure 4.15 shows the corresponding pattern of heatlines when the wall is warmer than the approaching fluid,

$$\tilde{H}(\tilde{x}, \tilde{y}) = \tilde{x}^{1/2} \left[ \eta \operatorname{erfc} \left( \frac{\eta}{2} \right) - \frac{2}{\pi^{1/2}} \exp \left( -\frac{\eta^2}{4} \right) \right]. \quad (4.158)$$

The heatlines come out of the wall at an angle because, unlike in Fig. 4.14, the gradient  $\partial H/\partial y$  is not zero at the wall. Above the wall, the heatlines are bent even more by the flow because the effect of transversal conduction becomes weaker. The higher density of heatlines near  $\tilde{x} = 0$  indicates once again higher heat fluxes. The  $\tilde{H}$  value at the wall decreases in the downstream direction because the wall loses heat to the boundary layer.

Morega and Bejan (1994) displayed the heatlines for two additional configurations: boundary layers with uniform heat flux and flow through a porous layer held between parallel isothermal plates. As in Figs. 4.14 and 4.15, the heatlines for cold walls are unlike the heatlines for configurations with hot walls. In other words, unlike the patterns of isotherms that are used routinely in convection heat transfer (e.g., Fig. 7.4), the heatline patterns indicate the true direction of heat flow and distinguish between cold walls and hot walls.



**Fig. 4.17** The smallest volume element, with volumetric flow through the  $K$  porous medium and “channel” flow along a high-permeability layer ( $K_0$ )

Costa (2003) has reported a study of unified streamline, heatline, and massline methods of visualization of two-dimensional heat and mass transfer in anisotropic media. His illustrations include a problem involving natural convection in a porous medium.

Heatlines and masslines are now spreading throughout convection research as the proper way to visualize heat flow and mass flow. This method of visualization is particularly well suited for computational work and should be included in commercial computational packages. The growing activity based on the heatline method is reviewed in Bejan (2004a) and Costa (2005, 2006). The method is expanding vigorously, for example, in natural convection and mass transfer (Zhao et al., 2007; Basak and Roy, 2008; Dalal and Das, 2008; Basak et al., 2009; Singh et al., 2012).

## 4.18 Constructal Tree Networks: Flow Access in Volume-to-Point Flow

It was discovered recently that by reducing systematically the thermal resistance between one point and a finite-size volume (an infinity of points), it is possible to predict a most common natural structure that previously was considered nondeterministic: the tree network (Bejan, 1996b, 1997a,b; Ledezma et al., 1997). Tree network patterns abound in nature, in both animate and inanimate systems (e.g., botanical trees, lightning, neural dendrites, dendritic crystals). The key to solving this famous problem was the optimization of the shape of each finite-size element of the flow volume such that the flow resistance of the element is minimal. The optimal structure of the flow—the tree network—then was *constructed* by putting together the shape-optimized building blocks. This construction of multiscale,

hierarchical geometry became the starting point of the *constructal theory* of design and evolution in nature (Bejan, 1997, 2000; Bejan and Zane, 2012).

The deterministic power of constructal theory is an invitation to new theoretical work on natural flow structures that have evaded determinism in the past. This section is about one such structure: the dendritic shape of the low-resistance channels that develop in natural fluid flows between a volume and one point in heterogeneous media (Bejan, 1997b,c; Errera and Bejan, 1999; Bejan et al., 2004). Examples of volume-to-point fluid flows are the bronchial trees, the capillary vessels, and the river drainage basins and deltas.

The deterministic approach outlined in this section is based on the proposition that a naturally occurring flow structure—its geometric form—is the end result of a process of geometric optimization. The objective of the optimization process is to construct the path (or assembly or paths) that provides minimal resistance to flow, or, in an isolated system, maximizes the rate of approach to equilibrium.

### 4.18.1 The Fundamental Volume-to-Point Flow Problem

Consider the fundamentals of evolutionary design toward less and less fluid flow resistance between one point and a finite-size volume (an infinity of points). For simplicity we assume that the volume is two-dimensional and represented by the area  $A$  (Fig. 4.16). The total mass flow rate  $\dot{m}'$  (kg/sm) flows through the point  $M$  and reaches (or originates from) every point that belongs to  $A$ . We also assume that the volumetric mass flow rate  $\dot{m}'''$  (kg/sm<sup>3</sup>) that reaches all the points of  $A$  is distributed uniformly in space, hence  $\dot{m}' = \dot{m}'''A$ .

The space  $A$  is filled by a porous medium saturated with a single-phase fluid with constant properties. The flow is in the Darcy regime. If the permeability of the porous medium is uniform throughout  $A$ , then the pressure field  $P(x, y)$  and the flow pattern can be determined uniquely by solving the Poisson-type problem associated with the point sink or point source configuration of Fig. 4.16. This classic problem is not the subject of this section.

Instead, we consider the more general situation where the space  $A$  is occupied by a nonhomogeneous porous medium composed of a material of low permeability  $K$  and a number of layers (e.g., cracks, filled, or open) of much higher permeabilities ( $K_1, K_2, \dots$ ). The thicknesses ( $D_1, D_2, \dots$ ) and lengths ( $L_1, L_2, \dots$ ) of these layers are not specified.

For simplicity we assume that the volume fraction occupied by the high-permeability layers is small relative to the volume represented by the  $K$  material. There is a very large number of ways in which these layers can be sized, connected, and distributed in order to collect and channel  $\dot{m}'$  to the point  $M$ . In other words, there are many designs of composite materials ( $K, K_1, K_2, \dots$ ) that can be installed in  $A$ : our objective is to find not only the internal architecture of the composite that minimizes the overall fluid flow resistance but also a *strategy* for the geometric optimization of volume-to-point flows in general.

The approach we have chosen is illustrated in Fig. 4.16. We regard  $A$  as a patchwork of rectangular elements of several sizes ( $A_0, A_1, A_2, \dots$ ). We will show that the shape (aspect ratio) of each such element can be optimized for minimal flow resistance. The smallest element ( $A_0$ ) contains only low-permeability material and one high-permeability layer ( $K_0, D_0$ ), Fig. 4.17. Each successively larger volume element ( $A_i$ ) is an assembly of elements of the preceding size ( $A_{i-1}$ ), which act as tributaries to the collecting layer ( $K_i, D_i, L_i$ ) that defines the assembly. We will show that the optimally shaped assemblies can be arranged like building blocks to collect the volumetric flow  $\dot{m}'''$  and transform it into the single stream  $\dot{m}'$  at the point  $M$ .

Before presenting the analysis, it is worth commenting on the reasons for doing it and how it fits next to the vast amount of work that has been done in the same field. A general characteristic of the existing studies is that they begin with the often tacit assumption that a fluid tree network exists. Geometric details such as bifurcation (dichotomy) are assumed. No such assumptions are being made in this section. The problem solved in this section is the minimization of flow resistance between a finite-size volume and one point. The solution to this problem will show that certain portions of the optimized volume-to-point path are shaped as a tree network. In other words, unlike in the existing literature, in the present analysis the tree and its geometric details are results (predictions), not assumptions. This is a fundamental difference. It means that the solution to the volume-to-point flow problem sheds light on the universal design principle that serves as origin for the formation of fluid tree networks in nature.

### 4.18.2 The Elemental Volume

In Fig. 4.17 the smallest volume  $A_0 = H_0 L_0$  is fixed, but its shape  $H_0/L_0$  may vary. The flow,  $\dot{m}'_0 = \dot{m}''' A_0$ ,  $A_0$  is collected from the  $K$  medium by a layer of much higher permeability  $K_0$  and thickness  $D_0$ . The flow is driven toward the origin  $(0, 0)$  by the pressure field  $P(x, y)$ . The rest of the rectangular boundary  $H_0 \times L_0$  is impermeable. Since the flow rate  $\dot{m}'_0$  is fixed, to minimize the flow resistance means to minimize the peak pressure ( $P_{\text{peak}}$ ) that occurs at a point inside  $A_0$ . The pressure at the origin is zero.

The analysis is greatly simplified by the assumptions that were mentioned already ( $K \ll K_0, D_0 \ll H_0$ ), which, as we will show in Eq. (4.156), also mean that the optimized  $A_0$  shape is such that  $H_0$  is considerably smaller than  $L_0$ . According to these assumptions, the flow through the  $K$  domain is practically parallel to the  $y$  direction,

$$P(x, y) \cong P(y) \quad \text{for } H_0/2 > |y| > D_0/2 \quad (4.159)$$

while the flow through the  $K_0$  layer is aligned with the layer itself  $P(x, y) \cong P(x)$  for  $|y| < D_0/2$ . Symmetry and the requirement that  $P_{\text{peak}}$  be minimum dictate that

the  $A_0$  element be oriented such that the  $K_0$  layer is aligned with the  $x$  axis. The mass flow rate through this layer is  $\dot{m}'(x)$ , with  $\dot{m}'(0) = \dot{m}'_0$  at the origin  $(0, 0)$ , and  $\dot{m}'(L_0) = 0$ . The  $K$  material is an isotropic porous medium with flow in the Darcy regime,

$$v = \frac{K}{\mu} \left( -\frac{\partial P}{\partial y} \right). \quad (4.160)$$

In this equation  $v$  is the volume-averaged velocity in the  $y$  direction (Fig. 4.17). The actual flow is oriented in the opposite direction. The pressure field  $P(x, y)$  can be determined by eliminating  $v$  between Eq. (4.151) and the local mass continuity condition

$$\frac{\partial v}{\partial y} = \frac{\dot{m}'''}{\rho} \quad (4.161)$$

and applying the boundary conditions  $\partial P / \partial y = 0$  at  $y = H_0/2$  and  $P = P(x, 0)$  at  $y \cong 0$  (recall that  $D_0 \ll H_0$ ):

$$P(x, y) = \frac{\dot{m}''' v}{2K} (H_0 y - y^2) + P(x, 0). \quad (4.162)$$

Equation (4.162) holds only for  $y \geq 0$ . The corresponding expression for  $y \leq 0$  is obtained by replacing  $H_0$  with  $-H_0$  in Eq. (4.162).

The pressure distribution in the  $K_0$  material, namely  $P(x, 0)$ , is obtained similarly by assuming Darcy flow along a  $D_0$ -thin path near  $y = 0$ ,

$$u = \frac{K_0}{\mu} \left( -\frac{\partial P}{\partial x} \right), \quad (4.163)$$

where  $u$  is the average velocity in the  $x$  direction. The flow proceeds toward the origin, as shown in Fig. 4.17. The mass flow rate channeled through the  $K_0$  material is  $\dot{m}'(x) = -rD_0 u$ . Furthermore, mass conservation requires that the mass generated in the infinitesimal volume slice  $(H_0 dx)$  contributes to the  $\dot{m}'(x)$  stream:  $\dot{m}''' H_0 dx = -d\dot{m}'$ . Integrating this equation away from the impermeable plane  $x = L_0$  (where  $\dot{m}' = 0$ ) and recalling that  $\dot{m}'_0 = \dot{m}''' H_0 L_0$ , we obtain

$$\dot{m}(x) = \dot{m}''' H_0 (L_0 - x) = \dot{m}_0 \left( 1 - \frac{x}{L_0} \right). \quad (4.164)$$

Combining these equations, we find the pressure distribution along the  $x$  axis

$$P(x, 0) = \frac{\dot{m}'_0 v}{D_0 K_0} \left( x - \frac{x^2}{2L_0} \right). \quad (4.165)$$

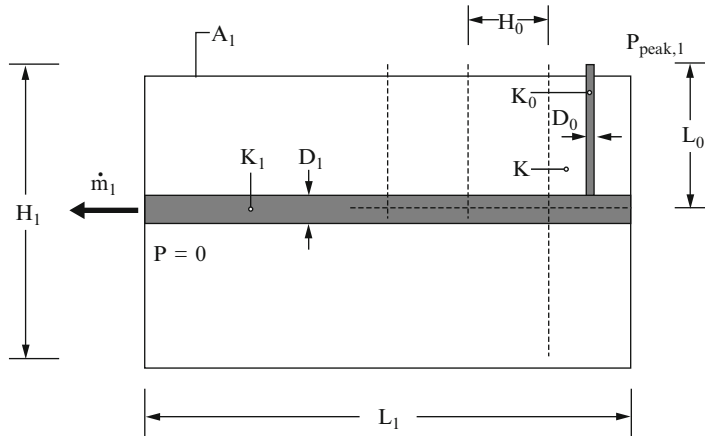


**Fig. 4.18** The first assembly ( $A_1$ ) of elements of size  $A_0$  and the new high-permeability layer  $K_1$

**Table 4.1** The optimized geometry of the elemental area  $A_0$  and the subsequent assemblies when the channel permeabilities are unrestricted (note:  $C_i = K_i \phi_i$ )

$i$	$H_i/L_i$	$\tilde{H}_i$	$\tilde{L}_i$	$n_i = A_i/A_{i-1}$	$\Delta \tilde{P}_i$
0	$2C_0^{-1/2}$	$2^{1/2}C_0^{-1/4}$	$2^{-1/2}C_0^{1/4}$	—	$\frac{1}{2}C_0^{-1/2}$
1	$(2C_0/C_1)^{1/2}$	$2^{1/2}C_0^{1/4}$	$C_0^{-1/4}C_1^{1/2}$	$(2C_1)^{1/2}$	$(2C_0C_1)^{-1/2}$
2	$(2C_1/C_2)^{1/2}$	$2C_0^{-1/4}C_1^{1/2}$	$2^{1/2}C_0^{-1/4}C_2^{1/2}$	$2(C_2/C_0)^{1/2}$	$(2C_1C_2)^{-1/2}$
$i \geq 2$	$(2C_{i-1}/C_i)^{1/2}$	$2^{i/2}C_0^{-1/4}C_{i-1}^{1/2}$	$2^{(i-1)/2}C_0^{-1/4}C_i^{1/2}$	$2(C_1/C_{i-2})^{1/2}$	$(2C_{i-1}C_i)^{-1/2}$

Equations (4.162) and (4.165) provide a complete description of the  $P(x, y)$  field. The peak pressure occurs in the farthest corner ( $x = L_0$ ,  $y = H_0/2$ ):

$$P_{\text{peak},0} = \dot{m}'_0 v \left( \frac{H_0}{8KL_0} + \frac{L_0}{2K_0 D_0} \right). \quad (4.166)$$

This pressure can be minimized with respect to the shape of the element ( $H_0/L_0$ ) by noting that  $L_0 = A_0/H_0$  and  $\phi_0 = D_0/H_0 \ll 1$ . The number  $\phi_0$  is carried in the analysis as an unspecified parameter. For example, if the  $D_0$  layer was originally a crack caused by the volumetric shrinking (e.g., cooling, drying) of the  $K$  medium, then  $D_0$  must be proportional to the thickness  $H_0$  of the  $K$  medium. The resulting geometric optimum is described by

$$\frac{H_0}{L_0} = 2(\tilde{K}_0 \phi_0)^{-1/2} \quad \tilde{L}_0 = 2^{-1/2}(\tilde{K}_0 \phi_0)^{1/4} \quad (4.167)$$

$$\tilde{H}_0 = 2^{1/2}(\tilde{K}_0 \phi_0)^{-1/4} \quad \Delta \tilde{P}_0 = \frac{1}{2}(\tilde{K}_0 \phi_0)^{-1/2}. \quad (4.168)$$

The nondimensionalization used in Eqs. (4.146) and (4.147) and retained throughout this section is based on using  $A_0^{1/2}$  as length scale and  $K$  as permeability scale:

$$(\tilde{H}_i, \tilde{L}_i) = \frac{(H_i, L_i)}{A_0^{1/2}}, \tilde{K}_i = \frac{K_i}{K}, \quad (4.169)$$

$$\Delta\tilde{P}_i = \frac{P_{\text{peak},i}}{\dot{m}''' A_i v / K}, \phi_i = \frac{D_i}{H_i}. \quad (4.170)$$

At the optimum, the two terms on the right side of Eq. (4.166) are equal. The shape of the  $A_0$  element is such that the pressure drop due to flow through the  $K$  material is equal to the pressure drop due to the flow along the  $K_0$  layer. Note also that the first of Eq. (4.168) confirms the assumptions made about the  $D_0$  layer at the start of this section: high permeability ( $\tilde{K}_0 \gg 1$ ) and small volume fraction ( $\phi_0 \ll 1$ ) mean that the optimized  $A_0$  shape is slender,  $H_0 \ll L_0$ , provided that  $\tilde{K}_0 \gg \phi_0^{-1}$ .

### 4.18.3 The First Construct

Consider next the immediately larger volume  $A_1 = H_1 L_1$  (Fig. 4.18) which can contain only elements of the type optimized in the preceding section. The streams  $\dot{m}'_0$  collected by the  $D_0$ -thin layers are now united into a larger stream  $\dot{m}'_1$  that connects  $A_1$  with the point  $P = 0$ . The  $\dot{m}'_1$  stream is formed in the new layer ( $K_1, D_1, L_1$ ).

The problem of optimizing the shape of the  $A_1$  rectangle is the same as the  $A_0$  problem that we just solved. First, we note that when the number of  $A_0$  elements assembled into  $A_1$  is large, the composite material of Fig. 4.18 is analogous to the composite of Fig. 4.17, provided that the permeability  $K$  of Fig. 4.17 is replaced by an equivalent (volume averaged) permeability ( $K_{e1}$ ) in Fig. 4.18. The  $K_{e1}$  value is obtained by writing that the pressure drop across an  $A_0$  element [Eq. (4.168)] is equal to the pressure drop over the distance  $H_1/2$  in the  $K_{e1}$  medium [this second pressure drop can be read off Eq. (4.162) after replacing  $H_0$  with  $H_1$ ,  $y$  with  $H_1/2$ , and  $K$  with  $K_{e1}$ ]. The result is  $K_{e1} = K_0 \phi_0$ ; this value is then used in place of  $K_0$ , in an analysis that repeats the steps executed in Eqs. (4.166), (4.167), and (4.168) for the  $A_0$  optimization problem.

A clearer alternative to this analysis begins with the observation that the peak pressure ( $P_{\text{peak},1}$ ) in Fig. 4.18 is due to two contributions—the flow through the upper-right corner element ( $P_{\text{peak},0}$ ) and the flow along the ( $K_1, D_1$ ) layer:

$$P_{\text{peak},1} = \dot{m}''' A_0 \frac{v}{K} \frac{1}{2} (\tilde{K}_0 \phi_0)^{-1/2} + \dot{m}'_1 v \frac{L_1}{2K_1 D_1}. \quad (4.171)$$

This expression can be rearranged by using the first of Eq. (4.168) and  $H_1 = 2L_0$ :

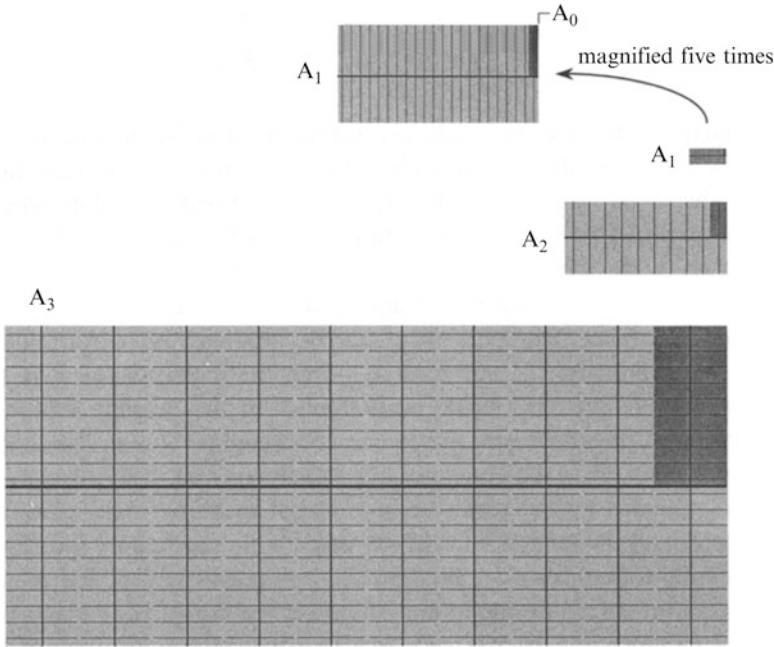


**Fig. 4.19** Composite medium tree architecture for minimal volume-to-point flow resistance when  $C_0 = 100$  and  $C_i/C_{i-1} = 10$  for  $i = 1, 2$ , and  $3$

$$\frac{P_{\text{peak},1}}{\dot{m}''A_1v/K} = \frac{1}{4\tilde{K}_0\phi_0} \frac{H_1}{L_1} + \frac{1}{2\tilde{K}_1\phi_1} \frac{L_1}{H_1}. \quad (4.172)$$

The corner pressure  $P_{\text{peak},1}$  can be minimized by selecting the  $H_1/L_1$  shape of the  $A_1$  rectangle. The resulting expressions for the optimized geometry ( $H_1/L_1, \tilde{H}_1, \tilde{L}_1$ ) are listed in Table 4.1. The minimized peak pressure ( $\Delta\tilde{P}_1$ ) is divided equally between the flow through the corner  $A_0$  element and the flow along the collecting ( $K_1, D_1$ ) layer. In other words, as in the case of the  $A_0$  element, the geometric optimization of the  $A_1$  assembly is ruled by a principle of *equipartition* of pressure drop between the two main paths of the assembly (Lewins, 2003).

#### 4.18.4 Higher-Order Constructs

The assembly and area shape optimization procedure can be repeated for larger assemblies ( $A_2, A_3, \dots$ ). Each new assembly ( $A_i$ ) contains a number ( $n_i$ ) of assemblies of the immediately smaller size ( $A_{i-1}$ ), the flow of which is collected by a new high-permeability layer ( $K_i, D_i, L_i$ ). As in the drawing shown in Fig. 4.17

for  $A_1$ , it is assumed that the number of constituents  $n_i$  is sensibly larger than 2. The analysis begins with the statement that the maximum pressure difference sustained by  $A_i$  is equal to the pressure difference across the optimized constituent ( $A_{i-1}$ ) that occupies the farthest corner of  $A_i$ , and the pressure drop along the  $K_i$  central layer:

$$P_{\text{peak},i} = P_{\text{peak},i-1} + \dot{m}'_i v \frac{L_i}{2K_i D_i}. \quad (4.173)$$

The geometric optimization results are summarized in Table 4.1, in which we used  $C_i = \tilde{K}_i \phi_i$  for the dimensionless flow conductance of each layer. The optimal shape of each rectangle  $H_i \times L_i$  is ruled by the pressure-drop equipartition principle noted in the optimization of the  $A_0$  and  $A_1$  shapes.

Beginning with the second assembly, the results fall into the pattern represented by the recurrence formulas listed for  $i \geq 2$ . If these formulas were to be repeated *ad infinitum* in both directions—toward large  $A_i$  and small  $A_i$ —then the pattern formed by the high-permeability paths ( $K_i, D_i$ ) would be a fractal. Natural tree-shaped flows and those predicted by constructal theory are not fractal. In the present solution to the volume-to-point flow problem, the construction begins with an element of finite size  $A_0$  and ends when the given volume ( $A$ ) is covered. Access to the infinity of points contained by the given volume is not made by making  $A_0$  infinitely small. Instead, all the points of the given volume are reached by a diffusive flow that bathes  $A_0$  *volumetrically*, because the permeability  $K$  of the material that fills  $A_0$  is the lowest of all the permeabilities of the composite porous medium. Constructal theory is the clearest statement that the geometry of nature is not fractal (Bejan, 1997c) and the first theory that predicts the multitude of natural flow structures that could be described as “fractal-like” structures (Poirier, 2003; Rosa et al., 2004).

Figure 4.19 illustrates the minimal-resistance architecture recommended by the results of Table 4.1. At each level of assembly, the calculated number of constituents  $n_i$  was rounded off to the closest even number. The optimal design of the composite porous medium contains a tree network of high-permeability layers ( $K_0, K_1, K_2, \dots$ ), where the interstitial spaces are filled with low-permeability material ( $K$ ). The actual shape of the tree depends on the relative size of the flow conductance parameters  $C_i$ . The conductance increase ratio  $C_i/C_{i-1}$  is essentially equal to the permeability ratio  $K_i/K_{i-1}$ , because the volume fraction ( $\phi_i \ll 1$ ) is expected to vary little from one assembly to the next, cf. the comment made above Eq. (4.167). In other words, the conductance parameters  $C_i$  can be specified independently because the porous-medium characteristics of the materials that fill the high-permeability channels have not been specified.

Several trends are revealed by constructions such as Fig. 4.19. When the conductance ratio  $C_i/C_{i-1}$  is large, the number  $n_i$  is large, the optimal shape of each assembly is slender ( $H_i/L_i < 1$ ), and the given volume is covered “fast,” i.e., in a few large steps of assembly and optimization. When the ratio  $C_i/C_{i-1}$  is large but decreases from one assembly to the next, the number of constituents decreases and the shape of each new assembly becomes closer to square.

Combining the limit  $C_i/C_{i-1} \rightarrow 1$  with the  $n_i$  formula of Table 4.1, we see that the number *two* (i.e., dichotomy, bifurcation, pairing) emerges as a result of geometric optimization of volume-to-point flow. Note that the actual value  $n_i = 2$  is not in agreement with the  $n_i > 2$  assumption that was made in Fig. 4.18 and the analysis that followed. This means that when  $C_i/C_{i-1} \sim 1$  is of order 1, the analysis must be refined by using, for example, a Fig. 4.18 in which the length of the  $(K_1, D_1)$  layer is not  $L_1$  but  $(n_1/2-1)H_0 + H_0/2$ . In this new configuration the right-end tip of the  $(K_1, D_1)$  layer is absent because the flow rate through it would be zero. To illustrate this feature of the tree network, in Fig. 4.19 the zero-flow ends of the central layers of all the assemblies have been deleted.

#### 4.18.5 The Constructal Law of Design and Evolution in Nature

The point-to-volume resistance can be minimized further by varying the angle between tributaries ( $D_{i-1}$ ) and the main channel ( $D_i$ ) of each new volume assembly. This optimization principle is well known in physiology where the work always begins with the assumption that a tree network of tubes *exists*. It can be shown numerically that the reductions in flow resistance obtained by optimizing the angles between channels are small relative to the reductions due to optimizing the shape of each volume element and assembly of elements. In this section we fixed the angles at  $90^\circ$  and focused on the optimization of volume shape. It is the optimization of shape subject to volume constraint—the consistent use of this principle at every volume scale—that is responsible for the emergence of a tree network between the volume and the point. We focused on the optimal shapes of building blocks because our objective was to discover a single optimization principle that can be used to explain the origin of tree-shaped networks in natural flow systems. The objective was to find the physics principle that was missing in the treelike images generated by assumed fractal algorithms.

In summary, we solved in general terms the fundamental fluid mechanics problem of minimizing the flow resistance between one point and a finite-size volume. A single optimization principle—the optimization of the shape of each volume element such that its flow resistance is minimized—is responsible for all the geometric features of the point-to-volume flow path. One of these features is the geometric structure—the tree network—formed by the portions with higher permeabilities ( $K_0, K_1, \dots$ ). The interstices of the network, i.e., the infinity of points of the given volume, are filled with material of the lowest permeability ( $K$ ) and are touched by a flow that diffuses through the  $K$  material.

The most important conclusion is that the larger picture, the optimal overall performance, structure, and working mechanism can be described in a purely deterministic fashion, that is, if the resistance-minimization principle is recognized as law. This law can be stated as follows (Bejan, 1996, 1997a):

For a finite-size system to persist in time (to live), it must evolve in such a way that it provides easier access (less resistance) to the imposed currents that flow through it.

This statement has two parts. First, it recognizes the natural tendency of imposed global currents to construct paths (shapes, structures) for better access through constrained open systems. The second part accounts for the evolution of the structure, which occurs in an identifiable direction that can be aligned with time itself. Small size and shapeless flow (diffusion) are followed in time by larger sizes and organized flows (streams). The optimized complexity continues to increase in time. Optimized complexity must not be confused with maximized complexity.

How important is the constructal approach to the minimal-resistance design, i.e., this single geometric optimization principle that allows us to anticipate the tree architecture seen in so many natural systems? In contemporary physics a significant research volume is being devoted to the search for universal design principles that may explain organization in animate and inanimate systems. In this search, the tree network is recognized as the symbol of the challenge that physicists and biologists face (Kauffman, 1993, pp. 13 and 14): “Imagine a set of identical round-topped hills, each subjected to rain. Each hill will develop a particular pattern of rivulets which branch and converge to drain the hill. Thus the particular branching pattern will be unique to each hill, a consequence of particular contingencies in rock placement, wind direction, and other factors. The particular history of the evolving patterns of rivulets will be unique to each hill. But viewed from above, the statistical features of the branching patterns may be very similar. Therefore, we might hope to develop a theory of the statistical features of such branching patterns, if not of the particular pattern on one hill.”

The constructal approach outlined in this section is an answer to the challenge articulated so well by Kauffman. It introduces an engineering flavor in the current debate on natural organization, which until now has been carried out in physics and biology. By training, engineers begin the design of a device by first understanding its purposes. The size of the device is always finite, never infinitesimal. The device must function (i.e., fulfill its purpose) subject to certain constraints. Finally, to analyze (describe) the device is not sufficient: to optimize it, to construct it, and to make it work are the ultimate objective. All these features—purpose, finite size, constraints, optimization, and construction—can be seen in the network constructions reported in this section. The resulting tree networks are entirely deterministic, and consequently they represent an alternative worthy of consideration in fields outside engineering. The progress in this direction is summarized in Bejan (1997c, 2000), Bejan and Lorente (2008, 2010, 2011), and Bejan and Zane (2012).

The short discussion here is confined to hydrodynamic aspects. For conduction, convection, turbulence, and other flows with structure, the reader is referred to the new books that review the growing interest in constructal theory (Bejan, 2000; Rosa et al., 2004; Bejan et al., 2004). For example, constructal trees were designed for chemically reactive porous media by Azoumah et al. (2004) and Zhou et al. (2008). The constructal law was used to predict the basic features and dimensions of Bénard convection and nucleate boiling (Nelson and Bejan, 1998), the sand

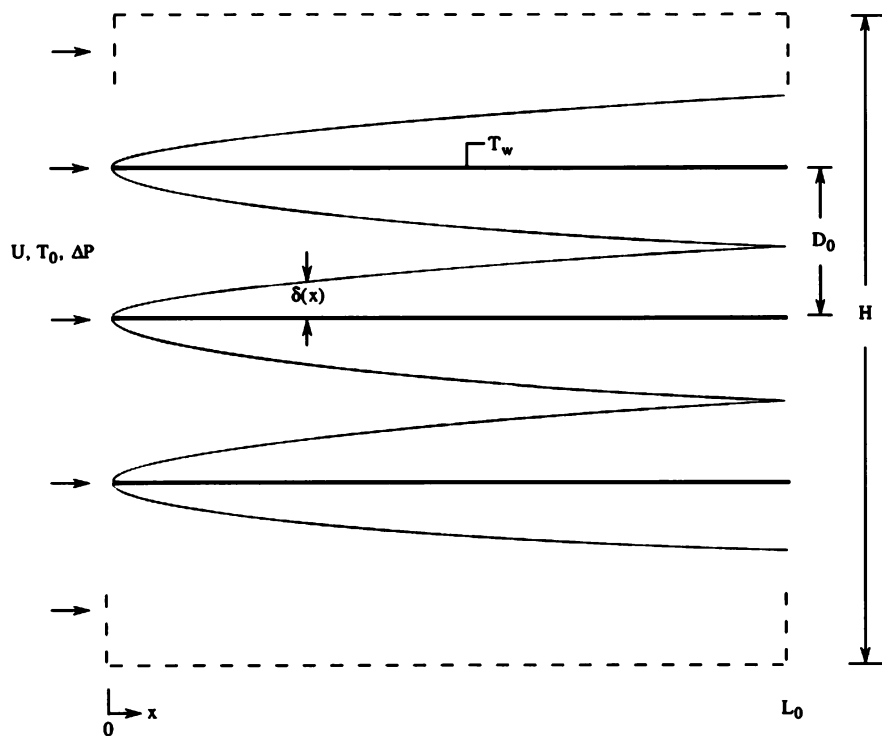


**Fig. 4.20** Optimal package of parallel plates with one spacing (Bejan and Fautrelle 2003)

size and beachface slope (Reis and Gama, 2010), and dust particle clusters (Reis et al., 2006).

The place of the constructal law as a self-standing law in thermodynamics is firmly established (Bejan and Lorente, 2004). The constructal law is distinct from the second law. For example, with respect to the time evolution of an isolated thermodynamic system, the second law states that the system will proceed toward a state of equilibrium ("nothing moves," maximum entropy at constant energy). In this second-law description, the system is a black box, without configuration.

With regard to the same isolated system, the constructal law states that the currents that flow in order to bring the system to equilibrium will seek and develop paths of maximum access. In this way, the system develops its flow configuration, which endows the system with the ability to approach its equilibrium the fastest.

The constructal law is the law of design generation, whereas the second law is the law of entropy generation. The constructal law can be stated in several equivalent ways: a principle of flow access maximization (or efficiency increase), as in the original statement quoted above, a principle of flow compactness maximization (miniaturization), and a principle of flow territory maximization, as in the spreading of river deltas, living species, and empires (Bejan and Lorente, 2004).

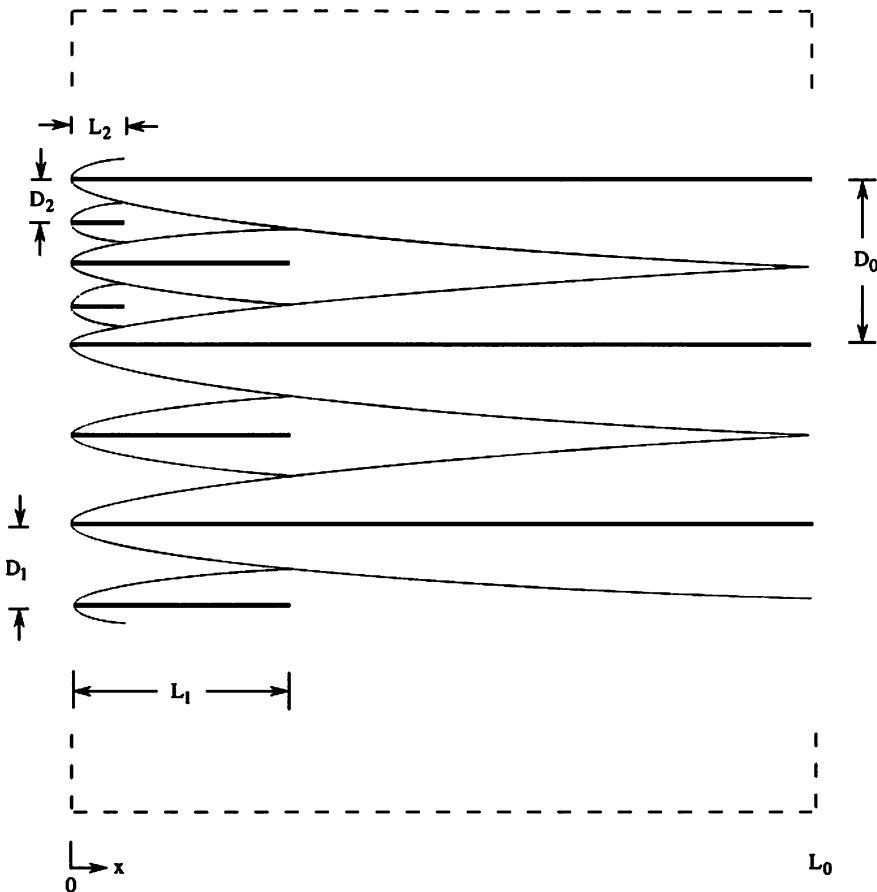


**Fig. 4.21** Optimal multiscale package of parallel plates (Bejan and Fautrelle 2003)

In sum, constructal theory originated from the design of porous and complex flow structures and now unites engineering, physics, biology, and social organization (Poirier, 2003; Rosa et al., 2004; Reis, 2006; Bejan and Lorente, 2006, 2010, 2011; Bejan and Zane, 2012).

## 4.19 Constructal Multiscale Flow Structures: Vascular Design

The tree-shaped flow structures of Sect. 4.18 are examples of “designed” porous structures with multiple length scales, which are organized hierarchically and distributed nonuniformly. These advances are reviewed in Bejan and Lorente (2008). Another class of designed porous media stems from an early result of

constructal theory: the prediction of optimal spacings for the internal flow structure of volumes that must transfer heat and mass to the maximum (Bejan, 2000; Sect. 4.15). Optimal spacings have been determined for several configurations, for example, arrays of parallel plates (e.g., Fig. 4.20). In each configuration, the reported optimal spacing is a single value, that is, a *single length scale* that is distributed uniformly through the available volume.

Is the stack of Fig. 4.20 the best way to pack heat transfer into a fixed volume? It is, but only when a single length scale is to be used, that is, if the structure is to be *uniform*. The structure of Fig. 4.20 is uniform, because it does not change from  $x = 0$  to  $x = L_0$ . At the most, the geometries of single-spacing structures vary periodically, as in the case of arrays of cylinders and staggered plates.

Bejan and Fautrelle (2003) showed that the structure of Fig. 4.20 can be improved if more length scales ( $D_0, D_1, D_2, \dots$ ) are available. The technique consists of placing more heat transfer in regions of the volume  $HL_0$  where the boundary layers are thinner. Those regions are situated immediately downstream of the entrance plane  $x = 0$ . Regions that do not work in a heat transfer sense either must be put to work or eliminated. In Fig. 4.20, the wedges of fluid contained between the tips of opposing boundary layers are not involved in transferring heat. They can be involved if heat-generating blades of shorter lengths ( $L_1$ ) are installed on their planes of symmetry. This new design is shown in Fig. 4.21.

Each new  $L_1$  blade is coated by Blasius boundary layers with the thickness  $\delta(x) \cong 5x(Ux/v)^{-1/2}$ . Because  $\delta$  increases as  $x^{1/2}$ , the boundary layers of the  $L_1$  blade merge with the boundary layers of the  $L_0$  blades at a downstream position that is approximately equal to  $L_0/4$ . The approximation is due to the assumption that the presence of the  $L_1$  boundary layers does not significantly affect the downstream development ( $x > L_0/4$ ) of the  $L_0$  boundary layers. This assumption is made for the sake of simplicity. The order-of-magnitude correctness of this assumption comes from geometry: the edges of the  $L_1$  and  $L_0$  boundary layers must intersect at a distance of order

$$L_1 \cong \frac{1}{4}L_0. \quad (4.174)$$

Note that by choosing  $L_1$  such that the boundary layers that coat the  $L_1$  blade merge with surrounding boundary layers at the downstream end of the  $L_1$  blade, we once more invoke the maximum packing principle of constructal theory. We are being consistent as constructal designers, and because of this every structure with merging boundary layers will be optimal, no matter how complicated.

The wedges of isothermal fluid ( $T_0$ ) remaining between adjacent  $L_0$  and  $L_1$  blades can be populated with a new generation of even shorter blades,  $L_2 \cong L_1/4$ . Two such blades are shown in the upper-left corner of Fig. 4.21. The length scales become smaller ( $L_0, L_1, L_2$ ), but the shape of the boundary-layer region is the same for all the blades, because the blades are all swept by the same flow ( $U$ ). The merging and expiring boundary layers are arranged according to the algorithm

$$L_i \cong \frac{1}{4} L_{i-1}, D_i \cong \frac{1}{2} D_{i-1} \quad (i = 1, 2, \dots, m), \quad (4.175)$$

where we show that  $m$  is finite, not infinite. In other words, as in all the constructal tree structures, the image generated by the algorithm is not a fractal [cf. Bejan (1997c, p. 765)]. The sequence of decreasing length scales is finite, and the smallest size ( $D_m, L_m$ ) is known, as shown in Bejan and Fautrelle (2003) and Bejan et al. (2004). The global thermal conductance of the multiscale package is

$$\frac{q'}{k\Delta T} \cong 0.36 \frac{H}{L_0} Be^{1/2} \left(1 + \frac{m}{2}\right)^{1/2} \quad (4.176)$$

where  $q'$  is the total heat transfer rate installed in the package ( $W/m$ , per unit length in the direction perpendicular to Fig. 4.21),  $k$  is the fluid thermal conductivity, and  $\Delta T$  is the temperature difference between the plates (assumed isothermal) and the fluid inlet. The dimensionless pressure and difference is

$$Be = \frac{\Delta PL_0^2}{\mu\alpha}, \quad (4.177)$$

where  $\mu$  and  $\alpha$  are the fluid viscosity and thermal diffusivity.

Bejan and Fautrelle (2003) also showed that the optimized complexity increases with the imposed pressure difference ( $Be$ ),

$$2^m \left(1 + \frac{m}{2}\right)^{1/4} \cong 0.17 Be^{1/4}. \quad (4.178)$$

As  $Be$  increases, the multiscale structure becomes more complex *and* finer. The monotonic effect of  $m$  is accompanied by diminishing returns: each smaller length scale ( $m$ ) contributes to global performance less than the preceding length scale ( $m-1$ ). The validity of the novel design concept sketched in Fig. 4.21 was demonstrated through direct numerical simulations and optimization for multiscale parallel plates (Bello-Ochende and Bejan, 2004) and multiscale parallel cylinders in cross flow (Bello-Ochende and Bejan, 2005a). A related natural convection situation was treated by Bello-Ochende and Bejan (2005b).

Forced convection was used in Bejan and Fautrelle (2003) only for illustration, that is, as a language in which to describe the new concept. A completely analogous multiscale structure can be deduced for laminar natural convection. The complete analogy that exists between optimal spacings in forced and natural convection was described by Petrescu (1994). In brief, if the structure of Fig. 4.20 is rotated by 90° counterclockwise and if the flow is driven upward by the buoyancy effect, then the role of the overall pressure difference  $\Delta P$  is played by the difference between two hydrostatic pressure heads, one for the fluid column of height  $L_0$  and temperature  $T_0$

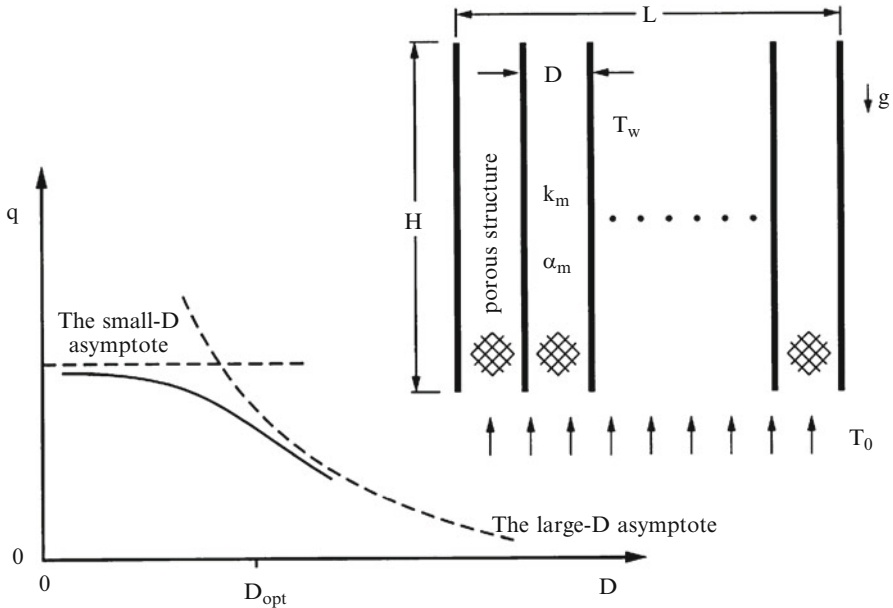


**Fig. 4.22** Volume filled with vertical heat-generating plates separated by a fluid-saturated porous medium and the effect of the channel spacing on the global thermal conductance (Bejan 2004a)

and the other for the  $L_0$  fluid column of temperature  $T_w$ . If the Boussinesq approximation applies, the effective  $\Delta P$  due to buoyancy is

$$\Delta P = \rho g \beta \Delta T L_0, \quad (4.179)$$

where  $\beta$  is the coefficient of volumetric thermal expansion and  $g$  is the gravitational acceleration aligned vertically downward (against  $x$  in Fig. 4.20). By substituting the  $\Delta P$  expression (4.179) into the  $Be$  definition (4.177), we find that the dimensionless group that replaces  $Be$  in natural convection is the Rayleigh number  $Ra = g \beta \Delta T L_0^3 / (\alpha v)$ . Other than the  $Be \rightarrow Ra$  transformation, all the features that are due to the generation of multiscale blade structure for natural convection should mirror, at least qualitatively, the features described for forced convection in this section. The validity of the constructal multiscale concept for volumes packed with natural convection is demonstrated numerically in da Silva and Bejan (2005).

The hierarchical multiscale flow architecture constructed in this section is a theoretical comment on fractal geometry. Fractal structures are generated by assuming (postulating) certain algorithms. In much of the current fractal literature, the algorithms are selected such that the resulting structures resemble flow structures observed in nature. For this reason, fractal geometry is descriptive, not predictive (Bejan, 1997c; Bradshaw, 2001). Fractal geometry is not a theory (Bejan and Zane, 2012).

The most recent advances on designed porous media are being dedicated to the development of vascularized materials with new functionalities distributed throughout the volume: self-healing, self-cooling, mechanical strength, etc. This movement is reviewed in Bejan and Lorente (2006, 2008). Chief examples are the vascular design of solid plates permeated by fluids that provide self-healing (the fusing of internal fissures) and the volumetric cooling of plates subjected to intense heating under steady and unsteady conditions (Lorente and Bejan, 2006, 2009a,b; Kim et al., 2006, 2009b; Zhang et al., 2009; Combelles et al., 2009, 2012; Ordonez et al., 2003; Lee et al., 2008, 2009a-c; Zeng et al., 2010; Cho et al., 2010a,b; Xu et al., 2008; Wang et al., 2006, 2007c, 2009a,b; Moreno et al., 2006; Rocha et al., 2009; Revellin et al., 2009; Kim et al., 2006, 2007, 2008d,e, 2009). Vascular designs that provide both cooling and mechanical strength were developed by Wang et al. (2010a) and Cetkin et al. (2011a,b).

## 4.20 Optimal Spacings for Plates Separated by Porous Structures

Taking the concept of Fig. 4.20 even closer to traditional porous media, consider the optimization of spacings between plates that sandwich a porous medium (Bejan, 2004a). For example, the channels may be occupied by a metallic foam such that the saturated porous medium has a thermal conductivity ( $k_m$ ) and a thermal diffusivity ( $\alpha_m$ ) that are much higher than their pure fluid properties ( $k_f$ ,  $\alpha_f$ ). We consider both natural convection and forced convection with Boussinesq incompressible fluid and assume that the structures are fine enough that Darcy flow prevails in all cases. The analysis is another application of the intersection of asymptotes method (Lewis, 2003).

The natural convection configuration is shown in Fig. 4.22. This time each  $D$ -thin space is filled with the assumed fluid-saturated porous structure. The width in the direction perpendicular to Fig. 4.22 is  $W$ . The effective pressure difference that drives the flow is due to buoyancy:

$$\Delta P = \rho H g \beta (T_w - T_0). \quad (4.180)$$

This  $\Delta P$  estimate is valid in the limit where the spacing  $D$  is sufficiently small so that the temperature in the channel porous medium is essentially the same as the plate temperature  $T_w$ . In this limit, the heat current extracted by the flow from the  $H \times L$  volume is  $q = \dot{m} c_p (T_w - T_0)$ , with  $\dot{m} = \rho U L W$  and Darcy's law,  $U = K \Delta P / \mu H$ , where  $K$  is the permeability of the structure. In conclusion, the total heat transfer rate in the small- $D$  limit is independent of the spacing  $D$ ,

$$q = \rho c_p (T_w - T_0) L W (K \Delta P) / \mu H. \quad (4.181)$$

In the opposite limit,  $D$  is large so that the natural convection boundary layers that line the  $H$ -tall plates are distinct. The heat transfer rate from one boundary layer is  $\bar{h}HW(T_w - T_0)$ , where  $\bar{h}H/k = 0.888 Ra_H^{-1/2}$  and  $Ra_H$  is the Rayleigh number for Darcy flow,  $Ra_H = Kg\beta H(T_w - T_0)/\alpha_m v$ . The number of boundary layers in the  $H \times L$  volume is  $2L/D$ . In conclusion, the total heat transfer rate decreases as  $D$  increases,

$$q = 1.78(L/D)Wk(T_w - T_0)Ra_H^{1/2}. \quad (4.182)$$

For maximal thermal conductance  $q/(T_w - T_0)$ , the spacing  $D$  must be smaller than the estimate obtained by intersecting asymptotes (4.181) and (4.182),

$$D_{\text{opt}}/H \lesssim 1.78 Ra_H^{-1/2}. \quad (4.183)$$

The simplest design that has the highest possible conductance is the design with the fewest plates (i.e., the one with the largest  $D_{\text{opt}}$ ); hence  $D_{\text{opt}}/H \cong 1.78 Ra_H^{-1/2}$  for the recommended design. Contrary to Fig. 4.22, however,  $q$  does not remain constant if  $D$  decreases indefinitely. There exists a small enough  $D$  below which the passages are so tight (tighter than the pores) that the flow is snuffed out. An estimate for how large  $D$  should be so that Eq. (4.183) is valid is obtained by requiring that the  $D_{\text{opt}}$  value for natural convection when the channels are filled only with fluid,  $D_{\text{opt}}/H \cong 2.3 [g\beta H^3(T_w - T_0)/\alpha_f v]^{-1/4}$  must be smaller than the  $D_{\text{opt}}$  value of Eq. (4.171). We find that this is true when

$$\frac{H^2}{K} \frac{\alpha}{\alpha_f} > Ra_H \quad (4.184)$$

in which, normally,  $\alpha/\alpha_f \gg 1$  and  $H^2/K \gg 1$ .

The forced-convection configuration can be optimized similarly (Bejan, 2004a). The flow is driven by the imposed  $\Delta P$  through parallel-plate channels of length  $L$  and width  $W$ . It is found that the forced-convection asymptotes have the same behavior as in Fig. 4.22. The highest conductance occurs to the left of the intersection of the two asymptotes, when

$$D_{\text{opt}}/L \lesssim 2.26 Be_p^{-1/2} \quad (4.185)$$

and where  $Be_p$  is the porous medium Bejan number,  $Be_p = (\Delta P K)/\mu\alpha_m$ . This forced-convection optimization is valid when the  $D_{\text{opt}}$  estimate for the channel with pure fluid is smaller than the  $D_{\text{opt}}$  value provided by Eq. (4.185) when

$$\frac{L^2}{K} \frac{\alpha}{\alpha_f} > Be_p. \quad (4.186)$$

In summary, Eqs. (4.183) and (4.185) provide estimates for the optimal spacings when the channels between heat-generating plates are filled with a fluid-saturated porous structure. The relevant dimensionless groups are  $Ra_H$ ,  $Be_p$ ,  $K/H^2$ ,  $K/L^2$ , and  $\alpha_m/\alpha_f$ . The symmetry between Eqs. (4.183) and (4.185) and between Eqs. (4.184) and (4.186) reinforces Petrescu's (1994) argument that the role of the Bejan number in forced convection is analogous to that of the Rayleigh number in natural convection.

These results are most fundamental and are based on a simple model and a simple analysis: Darcy flow and the intersection of asymptotes method. The same idea of geometry optimization deserves to be pursued in future studies of “designed porous media” based on more refined models and more accurate methods of flow simulation.

# Chapter 5

## External Natural Convection

Numerical calculation from the full differential equations for convection in an unbounded region is expensive, and hence approximate solutions are important. For small values of the Rayleigh number  $Ra$ , perturbation methods are appropriate. At large values of  $Ra$  thermal boundary layers are formed, and boundary-layer theory is the obvious method of investigation. This approach forms the subject of much of this chapter. We follow to a large extent the discussion by Cheng (1985a), supplemented by recent surveys by Pop and Ingham (2000, 2001) and Pop (2004).

### 5.1 Vertical Plate

We concentrate our attention on convection in a porous medium adjacent to a heated vertical flat plate, on which a thin thermal boundary layer is formed when  $Ra$  takes large values. Using the standard order-of-magnitude estimation, the two-dimensional boundary-layer equations take the form

$$\frac{\partial u}{\partial x} + \frac{\partial v}{\partial y} = 0, \quad (5.1)$$

$$u = -\frac{K}{\mu} \left[ \frac{\partial P'}{\partial x} - \rho g \beta (T - T_\infty) \right], \quad (5.2)$$

$$\frac{\partial P'}{\partial y} = 0, \quad (5.3)$$

$$\sigma \frac{\partial T}{\partial t} + u \frac{\partial T}{\partial x} + v \frac{\partial T}{\partial y} = \alpha_m \frac{\partial^2 T}{\partial y^2}. \quad (5.4)$$

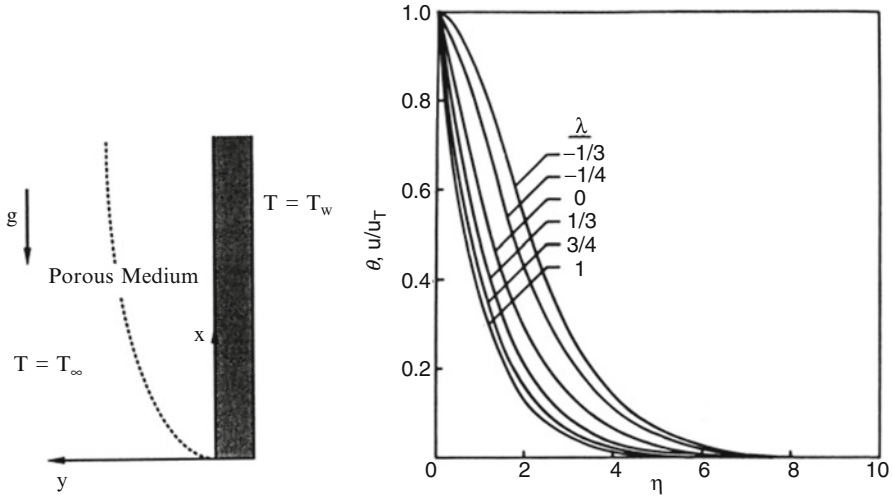


**Fig. 5.1** Dimensionless temperature and vertical velocity vs. the similarity variable for natural convection adjacent to a vertical heated surface (Cheng and Minkowycz 1977)

Here the subscript  $\infty$  denotes the reference value at a large distance from the heated boundary, and  $P'$  denotes the difference between the actual static pressure and the local hydrostatic pressure. It has been assumed that the Oberbeck-Boussinesq approximation and Darcy's law are valid. For later convenience of comparison, the  $x$  axis has been taken in the direction of the main flow (in this case vertically upward, Fig. 5.1, left) and the  $y$  axis normal to the boundary surface and into the porous medium. Near the boundary, the normal component of seepage velocity ( $v$ ) is small compared with the other velocity component ( $u$ ), and derivatives with respect to  $y$  of a quantity are large compared with derivatives of that quantity with respect to  $x$ . Accordingly no term in  $v$  appears in Eq. (5.3), and the term in  $\partial^2 T / \partial x^2$  has been omitted from Eq. (5.4).

Eliminating  $P'$  between Eqs. (5.2) and (5.3) and introducing the stream function  $\Psi$  defined by

$$u = \frac{\partial \Psi}{\partial y}, \quad v = -\frac{\partial \Psi}{\partial x}, \quad (5.5)$$

we reduce Eqs. (5.1, 5.2, 5.3, and 5.4) to the pair

$$\frac{\partial^2 \Psi}{\partial y^2} = \frac{g \beta K}{v} \frac{\partial T}{\partial y}, \quad (5.6)$$

$$\frac{\partial^2 T}{\partial y^2} = \frac{1}{\alpha_m} \left( \sigma \frac{\partial T}{\partial t} + \frac{\partial \Psi}{\partial y} \frac{\partial T}{\partial x} - \frac{\partial \Psi}{\partial x} \frac{\partial T}{\partial y} \right). \quad (5.7)$$

This pair of equations must be solved subject to the appropriate boundary conditions.

### 5.1.1 Power-Law Wall Temperature: Similarity Solution

We now concentrate our attention on the situation when the wall temperature  $T_w$  is a power function of distance along the plate, because in this case, a similarity solution can be obtained. Accordingly, we take

$$T_w = T_\infty + Ax^\lambda, \quad x \geq 0. \quad (5.8)$$

For  $x < 0$  we suppose that either there is no plate or that  $T_w = T_\infty$  on the plate. The set of boundary conditions then is

$$y = 0 : v = 0, \quad T = T_\infty + Ax^\lambda, \quad x \geq 0, \quad (5.9)$$

$$y \rightarrow \infty : u = 0, \quad T = T_\infty. \quad (5.10)$$

One can easily check that a steady-state solution of Eqs. (5.6, 5.7, 5.8, 5.9, and 5.10) is given by

$$\Psi = \alpha_m (Ra_x)^{1/2} f(\eta), \quad (5.11)$$

$$\frac{T - T_\infty}{T_w - T_\infty} = \theta(\eta), \quad (5.12)$$

where

$$\eta = \frac{y}{x} Ra_x^{1/2}, \quad (5.13)$$

$$Ra_x = \frac{g \beta K (T_w - T_\infty) x}{\nu \alpha_m}, \quad (5.14)$$

provided that the functions  $f(\eta)$  and  $\theta(\eta)$  satisfy the ordinary differential equations

$$f'' - \theta' = 0, \quad (5.15)$$

$$\theta'' + \frac{(1 + \lambda)}{2} f \theta' - \lambda f' \theta = 0, \quad (5.16)$$

and the boundary conditions

$$f(0) = 0, \quad \theta(0) = 1, \quad (5.17)$$

$$f'(\infty) = 0, \quad \theta(\infty) = 0. \quad (5.18)$$

**Table 5.1** Values of  $\eta_T$  and  $-\theta'(0)$  for various values of  $\lambda$  for the heated vertical plate problem (after Cheng and Minkowycz 1977)

$\lambda$	$\eta_T$	$-\theta'(0)$	$\overline{Nu}/\overline{Ra}^{1/2}$	
-1/3	7.2	0		Isothermal
-1/4	6.9	0.162	0.842	
0	6.3	0.444	0.888	
1/4	5.7	0.630	1.006	
1/3	5.5	0.678	1.044	
1/2	5.3	0.761	1.118	
3/4	4.9	0.892	1.271	
1	4.6	1.001	1.416	

In terms of the similarity variable  $\eta$ , the seepage velocity components are

$$u = u_r f'(\eta), \quad (5.19)$$

$$v = \frac{1}{2} \left[ \frac{\alpha_m g \beta K (T_w - T_\infty)}{v x} \right]^{1/2} [(1 - \lambda) \eta f' - (1 + \lambda) f], \quad (5.20)$$

where the characteristic velocity  $u_r$  is defined by

$$u_r = \frac{g \beta K (T_w - T_\infty)}{v}. \quad (5.21)$$

Integrating Eq. (5.15) and using Eq. (5.18) we get

$$f' = \theta. \quad (5.22)$$

This implies that the normalized vertical velocity  $u/u_r$  and the normalized temperature  $\theta$  are the same function of  $\eta$ . Their common graph is shown in Fig. 5.1. Another implication is that in this context, Eqs. (5.2) and (5.3) formally may be replaced by

$$u = \frac{g \beta K}{v} (T - T_\infty). \quad (5.23)$$

From Eq. (5.13) we see that the boundary-layer thickness  $\delta$  is given by

$$\frac{\delta}{x} = \frac{\eta_T}{Ra_x^{1/2}}, \quad (5.24)$$

where  $\eta_T$  is the value of  $\eta$  at the edge of the boundary layer, conventionally defined as that place where  $\theta$  has a value 0.01. Values of  $\eta_T$ , for various values of  $\lambda$ , are given in Table 5.1. For the case of constant wall temperature ( $\lambda = 0$ ),  $\delta$  is proportional to  $x^{1/2}$ .

The local surface heat flux at the heated plate is

$$q'' = -k_m \left( \frac{\partial T}{\partial y} \right)_{y=0} = k_m A^{3/2} \left( \frac{g \beta K}{v \alpha_m} \right)^{1/2} x^{(3\lambda-1)/2} [-\theta'(0)]. \quad (5.25)$$

Clearly  $\lambda = 1/3$  corresponds to uniform heat flux. In dimensionless form, Eq. (5.25) is

$$\frac{Nu_x}{Ra_x^{1/2}} = -\theta'(0), \quad (5.26)$$

where the local Nusselt number is defined by  $Nu_x = hx/k$  and where  $h$  is the local heat transfer coefficient  $q''/(T_w - T_\infty)$ . The values of  $[-\theta'(0)]$  also are listed in Table 5.1. In particular, we note that  $[-\theta'(0)] = 0.444$  when  $\lambda = 0$ .

The total heat transfer rate through a plate of height  $L$ , expressed per unit length in the direction perpendicular to the plane  $(x,y)$ , is

$$L \bar{q}'' = q' = \int_0^L q''(x) dx = k_m A^{3/2} \left( \frac{g \beta K}{v \alpha_m} \right)^{1/2} \left( \frac{2}{1 + 3\lambda} \right) L^{(1+3\lambda)/2} [-\theta'(0)]. \quad (5.27)$$

This result can be rewritten as

$$\frac{\overline{Nu}}{\overline{Ra}^{1/2}} = \frac{2(1 + \lambda)^{3/2}}{1 + 3\lambda} [-\theta'(0)], \quad (5.28)$$

where  $\lambda$  and  $Ra$  are based on the  $L$ -averaged temperature difference

$$\begin{aligned} \overline{Nu} &= \frac{q'}{k_m (\overline{T_w - T_\infty})}, & \overline{Ra} &= \frac{g \beta K L (\overline{T_w - T_\infty})}{v \alpha_m}, \\ (\overline{T_w - T_\infty}) &= \frac{1}{L} \int_0^L (T_w - T_\infty) dx. \end{aligned} \quad (5.29)$$

Xu (2004) has treated the same problem by means of homotopy analysis.

### 5.1.2 Vertical Plate with Lateral Mass Flux

If the power-law variation of wall temperature persists but now we have an imposed lateral mass flux at the wall given by  $v = ax^n$ , ( $x = 0$ ), then a similarity solution exists for the case  $n = (\lambda-1)/2$ . Equations (5.11, 5.12, 5.13, 5.14, 5.15, 5.16, 5.17, and 5.18) apply, with the exception that Eq. (5.17) is replaced by

$$f(0) = f_w = 2a(\alpha_m g \beta K A / v)^{-1/2} (1 + \lambda)^{-1}. \quad (5.30)$$

The thermal boundary-layer thickness is still given by Eq. (5.24) but now  $\eta_T$  is an increasing function of the injection parameter  $f_w$  (Cheng 1977b). This problem has applications to injection of hot water in a geothermal reservoir. The practical case of constant discharge velocity at uniform temperature has been treated by different methods by Merkin (1978) and Minkowycz and Cheng (1982).

The solution for the related problems where the heat flux (rather than the temperature) is prescribed at the wall can be deduced from the present solution via a certain change of variables (Cheng 1977a) or obtained directly. Of course we already have the solution for constant prescribed heat flux, with the wall temperature related to the heat flux, via the parameter  $A$  with  $\lambda = 1/3$ , through Eqs. (5.8) and (5.25). From Eq. (5.24) we see that the boundary-layer thickness is proportional to  $x^{1/3}$  in this case.

Similarity solutions for a vertical permeable surface were developed by Chaudhary et al. (1995a, b) for the class with heat flux proportional to  $x^\mu$  and mass flux proportional to  $x^{(\mu-1)/3}$ , where  $\mu$  is a constant. Some series solutions were obtained by Kechil and Hashim (2008).

### 5.1.3 Transient Case: Integral Method

For transient natural convection in a porous medium, similarity solutions exist for only a few unrealistic wall temperature distributions. For more realistic boundary conditions, approximate solutions can be obtained using an integral method. Integrating Eq. (5.4) across the thermal boundary layer and using Eqs. (5.1) and (5.2), we obtain

$$\sigma \frac{\partial}{\partial t} \int_0^\infty \Phi(x, y, t) dy + \frac{g \beta K}{v} \frac{\partial}{\partial x}, \quad (5.31)$$

where  $\Phi = T - T_\infty$ . The Karman-Pohlhausen integral method involves assuming an explicit form of  $\Phi$  that satisfies the temperature boundary conditions, namely  $\Phi = T_w - T_\infty$  at  $y = 0$  and  $\Phi \rightarrow 0$  as  $y \rightarrow \infty$ . The integrals in Eq. (5.31) are then determined, and the resulting equation for the thermal boundary-layer thickness  $\delta$  becomes a first-order partial differential equation of the hyperbolic type which can be solved by the method of characteristics.

For the case of a step increase in wall temperature, Cheng and Pop (1984) assume that the temperature distribution is of the form

$$\Phi = (T_w - T_\infty) \operatorname{erfc}(\zeta), \quad (5.32)$$

where  $\zeta = y/\delta(x, t)$ . The results of the method of characteristics show that during the interval before the steady state is reached one has

$$\delta = 2 \left( \frac{\alpha_m t}{\sigma} \right)^{1/2}, \quad (5.33)$$

$$\frac{T - T_\infty}{T_w - T_\infty} = \operatorname{erfc} \left[ \frac{y}{2} \left( \frac{\sigma}{\alpha_m t} \right)^{1/2} \right] = \frac{vu}{g\beta K(T_w - T_\infty)}, \quad (5.34)$$

$$q''_w = k \left( \frac{\sigma}{\pi \alpha_m t} \right)^{1/2} (T_w - T_\infty), \quad (5.35)$$

for  $t < T_{ss}$ , with  $t_{ss} = \sigma x^2 / \alpha_m K_1 Ra_x$  ( $K_1 = 2 - 2^{1/2} = 0.5857$ ), denoting the time at which steady state is reached. This time interval is related to the propagation of the leading edge effect, which is assumed to travel with the local velocity. In Eq. (5.34),  $u$  is the  $x$  component of the seepage velocity.

Equations (5.33, 5.34, and 5.35) are independent of  $x$  and are similar in form to the solution for the transient heat conduction problem. During the initial stage when the leading edge effect is not being felt, heat is transferred by transient one-dimensional heat conduction. After the steady state is reached, we have

$$\frac{\delta}{x} = \frac{2.61}{Ra_x^{1/2}}, \quad (5.36)$$

$$\frac{T - T_\infty}{T_w - T_\infty} = \operatorname{erfc} \left( \frac{K_1^{1/2} y Ra_x^{1/2}}{2x} \right) = \frac{vu}{g\beta K(T_w - T_\infty)}, \quad (5.37)$$

$$q''_w = \frac{k(T_w - T_\infty)}{x} K_1 / \pi Ra_x^{1/2}. \quad (5.38)$$

Equation (5.38) can be written in dimensionless form as

$$\frac{Nu_x}{Ra_x^{1/2}} = 0.431, \quad (5.39)$$

which compares favorably with the exact similarity solution where the constant is equal to 0.444 (see Table 5.1). Comparison of Eq. (5.36) with Eq. (5.24) for  $\lambda = 0$  shows that the integral method considerably underestimates the steady-state thermal boundary-layer thickness. This is due to the error in the assumed temperature profile in the integral-method formulation.

For flow past a suddenly cooled wall, similarity solutions were obtained by Ingham et al. (1982) for the case of small and large dimensionless times, and these were joined by a numerical solution. A detailed study of the transient problem for the case where the wall temperature varies as  $x^\lambda$  was made by Ingham and Brown (1986). They found that for  $\lambda < -1/2$  no solution of the unsteady boundary-layer

equations was possible, and that for  $-1/2 < \lambda < 1$  the parabolic partial differential equation governing the flow is singular. For  $-1/2 < \lambda < -1/3$  the velocity achieves its maximum value within the boundary layer (instead of on the boundary).

For the case  $\lambda = 0$ , Haq and Mulligan (1990a) have integrated the unsteady boundary-layer equations numerically. Their results confirm that during the initial stage, before the effects of the leading edge are influential at a location, heat transfer is governed by conduction. They show that in a Darcian fluid the local Nusselt number decreases with time monotonically to its steady-state value. The effect of inertia was considered by Chen et al. (1987). They found that the effect of quadratic drag increases the momentum and thermal boundary-layer thicknesses and reduces the heat transfer rate at all times (cf. Sect. 5.1.7.2).

The situation where the permeability varies linearly along the plate was treated by Mehta and Sood (1992a). As one would expect, they found that increase in permeability results in higher rate of heat transfer at the wall and in decreased time to reach the steady state at any location on the plate.

The case of wall heating at a rate proportional to  $x^\lambda$  was examined by Merkin and Zhang (1992). The similarity equations that hold in the limit of large  $t$  were shown to have a solution only for  $\lambda > -1$ . Numerical solutions were obtained for a range of possible values of  $\lambda$ .

Harris et al. (1996, 1997a, b) have treated the case of a jump to a uniform flux situation and the case where the surface temperature or the surface heat flux suddenly jumps from one uniform value to another. Pop et al. (1998a) reviewed work on transient convection heat transfer in external flow. Techniques for solving the boundary-layer equations that arise in such circumstances were discussed by Harris and Ingham (2004). Khadrawi and Al-Nimr (2005) have examined the effect of the local inertial term for a domain partly filled with porous material. The Brinkman model was employed in the numerical study by Kim et al. (2004a).

### 5.1.4 Effects of Ambient Thermal Stratification

When the porous medium is finite in the  $x$  and  $y$  directions, the discharge of the boundary layer into the rest of the medium leads in time to thermal stratification. If the temperature profile at “infinity” is as in Fig. 5.2, and if  $T_0 - T_{\infty,0}$  remains fixed, then as the positive temperature gradient  $\gamma = dT_\infty/dx$  increases, and the average temperature difference between the wall and the porous medium decreases. Thus we should expect a steady decrease in the total heat transfer rate as  $\gamma$  increases. We apply the integral method to the solution of this problem (Bejan 1984).

The Darcy law relation Eq. (5.6) integrates to give

$$T = \frac{v}{g\beta K} u + \text{function}(x). \quad (5.40)$$

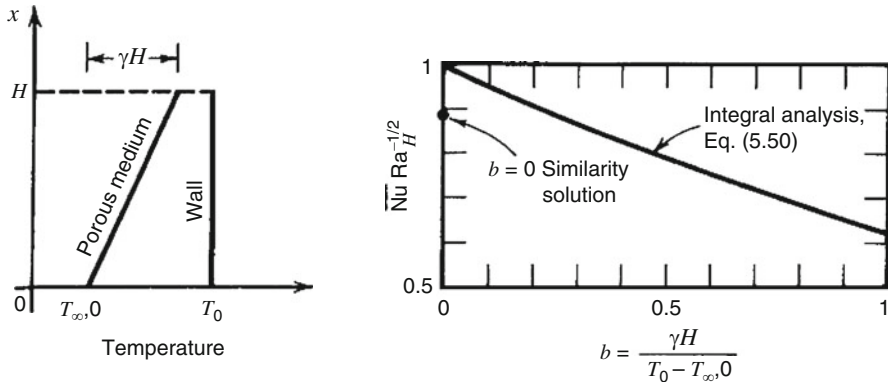


**Fig. 5.2** Heat transfer from a vertical isothermal wall to a linearly stratified porous medium (Bejan 1984)

We assume a vertical velocity profile of the form

$$u = u_0(x) \exp\left[-\frac{y}{\delta_T(x)}\right]. \quad (5.41)$$

Then, using Eq. (5.40) and the temperature boundary conditions

$$T(x, 0) = T_0, \quad T(x, \infty) = T_{\infty,0} + \gamma x, \quad (5.42)$$

we see that the corresponding temperature profile is

$$T(x, y) = (T_0 - T_{\infty,0} - \gamma x) \exp(-y/\delta_T) + T_{\infty,0} + \gamma x, \quad (5.43)$$

and the maximum (wall) vertical velocity is

$$u_0 = \frac{g \beta K}{v} (T_0 - T_{\infty,0} - \gamma x). \quad (5.44)$$

The integral form of the boundary-layer energy equation, obtained by integrating Eq. (5.4) from  $y = 0$  to  $y = \infty$ , is

$$v(x, \infty) T(x, \infty) + \frac{d}{dx} \int_0^\infty u T dy = -\alpha_m \left( \frac{\partial T}{\partial y} \right)_{y=0}, \quad (5.45)$$

where  $T(x, \infty) = T_{\infty,0} + \gamma x$ , and from the mass conservation equation,

$$v(x, \infty) = -\frac{d}{dx} \int_0^\infty u dy. \quad (5.46)$$

Substituting the assumed  $u$  and  $T$  profile into the energy integral equation (5.46) yields

$$\frac{d\delta_*}{dx_*} = \frac{2}{\delta_*(1 - bx_*)}, \quad (5.47)$$

in terms of the dimensionless quantities

$$b = \frac{\gamma H}{T_0 - T_{\infty,0}}, \quad x_* = \frac{x}{H}, \quad \delta_* = \frac{\delta_T}{H} \left[ \frac{g\beta H^3 (T_0 - T_{\infty,0})}{\nu \alpha_m} \right]^{1/2}. \quad (5.48)$$

Integrating Eq. (5.47), with  $\delta_*(0) = 0$ , we obtain

$$\delta_*(x_*) = \left[ -\frac{4}{b} \ln(1 - bx_*) \right]^{1/2}. \quad (5.49)$$

As  $b \rightarrow 0$  this gives the expected result  $\delta_* \sim x_*^{1/2}$ . The average Nusselt number (over the wall height  $H$ ) is given by

$$\frac{\overline{Nu}}{Ra_H^{1/2}} = \int_0^1 \frac{(1 - bx_*) dx_*}{[-(4/b) \ln(1 - bx_*)]^{1/2}}, \quad (5.50)$$

where  $\overline{Nu}$  and  $Ra_H$  are based on the maximum (i.e., *starting*) temperature difference

$$\overline{Nu} = \frac{q'' H}{k(T_0 - T_{\infty,0})}, \quad Ra_H = \frac{g\beta K H}{\nu \alpha_m} (T_0 - T_{\infty,0}). \quad (5.51)$$

Equation (5.50) is plotted in Fig. 5.2. As expected,  $Nu/Ra_H^{1/2}$  decreases monotonically as  $b$  increases. The above approximate integral solution gives  $Nu/Ra_H^{1/2} = 1$  at  $b = 0$ , whereas the similarity solution value for this quantity is 0.888, a discrepancy of 12.5%.

The same phenomenon was studied numerically, without the boundary-layer approximation, by Angirasa and Peterson (1997b) and Ratish Kumar and Singh (1998). The case of a power-law variation of wall temperature was discussed by Nakayama and Koyama (1987c) and Lai et al. (1991b). The stratification problem has also been treated by Tewari and Singh (1992) and (with quadratic drag effects included) by Singh and Tewari (1993). In their study of an isothermal surface with stratification on the Brinkman-Forchheimer model, Chen and Lin (1995) found that a flow reversal is possible in certain circumstances. The same model, with the effect of variable porosity and thermal dispersion included, was employed by Hung et al. (1999). The case of variable wall heat flux was analyzed by Hung and Chen (1997). An MHD problem was analyzed by Chamkha (1997g).

### 5.1.5 Conjugate Boundary Layers

When one has a vertical wall between two porous media (or between a porous medium and a fluid reservoir) and a temperature difference exists between the two systems, we may have a pair of conjugate boundary layers, one on each side of the wall, with neither the temperature nor the heat flux specified on the wall but rather to be found as part of the solution of the problem. Bejan and Anderson (1981) used the Oseen linearization method to analytically solve the problem of a solid wall inserted in a porous medium. They found that the coefficient in the  $Nu/Ra_H^{1/2}$  proportionality decreases steadily as the wall thickness parameter  $\omega$  increases, where  $\omega$  is defined as

$$\omega = \frac{W}{H} \frac{k_m}{k_w} Ra_H^{1/2}. \quad (5.52)$$

In this dimensionless group  $W$  and  $H$  are the width and height of the wall cross section,  $k_m$  and  $k_w$  are the conductivities of the porous medium and wall material, respectively, and  $Ra_H$  is the Rayleigh number based on  $H$  and the temperature difference between the two systems,  $\Delta T = T_{\infty 2} - T_{\infty 1}$ . The overall Nusselt number  $\lambda$  is based on the wall-averaged heat flux  $\bar{q}''$  and the overall temperature difference  $\Delta T$ ,

$$\overline{Nu} = \frac{\bar{q}'' H}{k_m \Delta T}. \quad (5.53)$$

The variation of  $\overline{Nu}/Ra_H^{1/2}$  with  $\omega$  is shown in Fig. 5.3. In the limit of negligible wall thermal resistance ( $\omega \rightarrow 0$ ), the overall Nusselt number reduces to

$$\overline{Nu} = 0.383 Ra_H^{1/2}. \quad (5.54)$$

The case of wall between a porous medium and a fluid reservoir was solved by Bejan and Anderson (1983). Their heat transfer results are reproduced in Fig. 5.4. The value of dimensionless group

$$B = \frac{k_m Ra_H^{1/2}}{k_a Ra_{Ha}^{1/4}} \quad (5.55)$$

determines whether the conjugate problem is dominated by porous medium convection (small  $B$ ) or pure fluid convection (large  $B$ ). Here  $k_a$  and  $Ra_{Ha}$  represent the fluid conductivity and Rayleigh number on the side of the pure fluid (which typically is air).

Pop and Merkin (1995) showed that the boundary-layer equations can be made dimensionless so that the thermal conductivity ratio is scaled out of the problem,

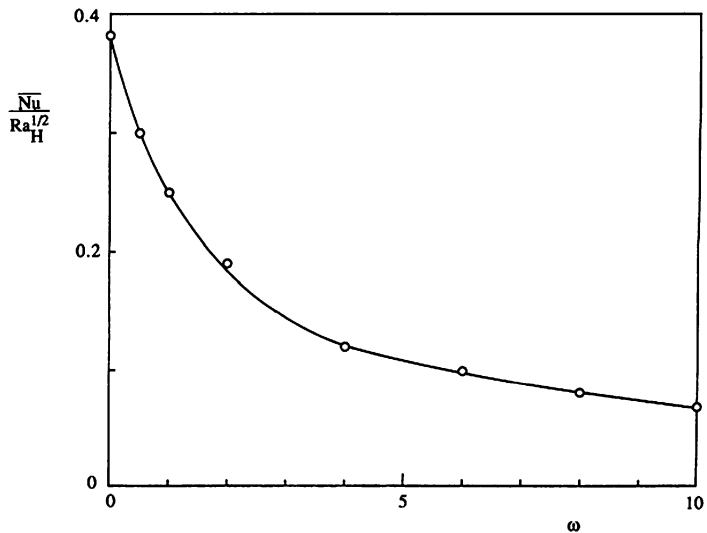


**Fig. 5.3** Heat transfer through a vertical partition inserted in a fluid-saturated porous medium (Bejan and Anderson 1981; Bejan 1984)

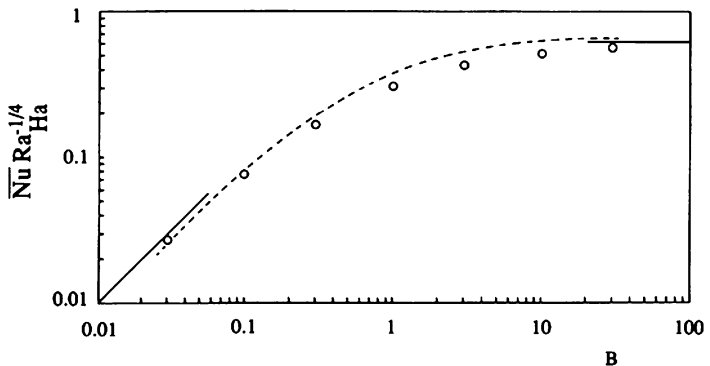


**Fig. 5.4** Heat transfer through the interface between a porous medium and a fluid reservoir (Bejan and Anderson 1983; Bejan 1984)

and thus, just one solution of the transformed nonsimilar boundary-layer equations need be computed. This they did by a finite-difference scheme.

The above analysis of Bejan and Anderson is limited to the case of a thin plate. The thin plate assumption was dropped by Vynnycky and Kimura (1994). They considered a wall of thickness  $a$  and with a segment of height  $b$  conducting and the remainder insulating; the aspect ratio is  $\lambda = a/b$ . They constructed an approximate one-dimensional solution based on the assumption of a boundary layer of thickness  $\delta$ . The average boundary heat flux is given by

$$q'' = k_w \frac{(T_c - \bar{T}_b)}{a} = k_m \frac{\bar{T}_h - T_\infty}{\delta}, \quad (5.56)$$

where  $\bar{T}_b$  is the average interface temperature and  $T_c$  is the constant temperature at the far side of the conducting wall. If  $Ra$  denotes the Rayleigh number based on  $T_c - T_\infty$  and  $Ra^*$  that is based on  $\bar{T}_b - T_\infty$ , and  $\bar{\theta}_b = (T - T_\infty)/(T_c - T_\infty)$ , so that  $Ra^* = Ra\bar{\theta}_b$ , then

$$\frac{\delta}{b} = 1.126(Ra^*)^{-1/2}, \quad (5.57)$$

from the isothermal entry in Table 5.1. Combining Eqs. (5.56) and (5.57), one has

$$\sigma_c X^3 + X^2 - 1 = 0, \quad (5.58)$$

where  $X = \bar{\theta}_b^{1/2}$  and  $\sigma_c = \lambda Ra^{1/2}/1.126k$ , where  $k = k_w/k_m$ . The quantity  $\sigma_c$  may be regarded as a conjugate Biot number. Conjugate effects are small if  $\sigma_c \ll 1$ . For a given  $\sigma_c$ , Eq. (5.58) is readily solved to give  $\bar{\theta}_b$ , and then the average Nusselt number can be obtained from

$$\overline{Nu} = \frac{q'' a}{k_m(T_c - T_\infty)} = 0.888 \frac{\bar{T}_b - T_\infty}{T_c - T_\infty} (Ra^*)^{1/2} = 0.888 \bar{\theta}_b^{3/2} Ra^{1/2}. \quad (5.59)$$

Vynnycky and Kimura (1994) showed that this formula agrees well with numerical computations in typical cases.

Kimura et al. (1997) show how the same ideas can be applied to the problem of a wall between two reservoirs, the extension (to a thick partition) of the work of Bejan and Anderson (1983). Kimura and Pop (1992b, 1994) treated convection around a cylinder or a sphere in a similar fashion. A transient one-dimensional model for conjugate convection from a vertical conducting slab was developed by Vynnycky and Kimura (1995). They obtained analytical solutions for two parameter regimes, (i)  $Ra \gg 1$ ,  $\gamma \ll Ra$ , and (ii)  $\gamma \gg 1$ ,  $Ra \ll \gamma$ , where  $\gamma = [(\rho c)_m/(\rho c)_f](\alpha_w/\alpha_m)$ . Regime (i) implies that the temperature and velocity within the boundary layer adjust themselves instantaneously to conditions in the conducting plate, and time dependency arises through variation of the conjugate boundary temperature. The value of  $\gamma$  affects the development but not the steady state. Regime (ii) corresponds to the case where conduction dominates convection in the early stages of flow development in the porous medium. Vynnycky and Kimura (1995) also checked their analytical solutions against numerical solutions.

The case of conjugate natural convection heat transfer between two porous media at different temperatures separated by a vertical wall was treated by Higuera and Pop (1997). They obtained asymptotic and numerical solutions. The corresponding case for a horizontal wall was examined by Higuera (1997). Conjugate convection from vertical fins was studied numerically by Vaszi et al. (2003). A transient problem involving a vertical plate subjected to a sudden change in surface heat flux was analyzed by Shu and Pop (1998). Another transient problem involving the cooling of

a thin vertical plate was analyzed by Méndez et al. (2004). The topic of conjugate natural convection in porous media was reviewed by Kimura et al. (1997).

### 5.1.6 Higher-Order Boundary-Layer Theory

The above boundary-layer theory arises as a first approximation for large values of Rayleigh number, when expansions are made in terms of the inverse one-half power of the Rayleigh number. At this order, the effects of entrainment from the edge of the boundary layer, the axial heat conduction, and the normal pressure gradient are all neglected.

The magnitudes of these effects have been investigated using higher-order asymptotic analysis by Cheng and Chang (1979), Chang and Cheng (1983), Cheng and Hsu (1984), and Joshi and Gebhart (1984). They found that the ordering of the eigenfunction terms in the perturbation series was dependent on the wall temperature parameter  $\lambda$ . They also found that the coefficients of the eigenfunctions cannot be determined without a detailed analysis of the leading edge effect. Therefore, they truncated the perturbation series at the term where the leading edge effect first appeared. They found that the effect of entrainments from the edge of the thermal boundary layer was of second order while those of axial heat conduction and normal pressure gradient were of third order. For the case of the isothermal vertical plate with  $\lambda = 0$ , the second-order corrections for both the Nusselt number and the vertical velocity are zero, and the leading edge effect appears in the third-order terms. For other values of  $\lambda$ , both the second- and third-order corrections in the Nusselt number are positive and the leading edge effect appears in the fourth-order terms.

The slight increase in the surface heat flux in the higher-order theories is mainly due to the fact that entrainments from the outer flow induce a flow parallel to the heated surface. The higher-order theory has a profound effect on the velocity profiles but has a relatively small effect on the temperature distribution, and hence on the surface heat flux. Figure 5.5 illustrates the higher-order effects on the local Nusselt number  $Nu_x$ . It is evident that for small wall temperature variations ( $\lambda = 1/3$ ) the boundary-layer theory is quite accurate even at small Rayleigh numbers.

Pop et al. (1989) have shown that for the case of uniform wall heat flux the leading edge effects enter the second and subsequent order problems. They cause an increase of the streamwise vertical velocity near the outer edge of the boundary layer and a consequent increase in heat transfer rate by an amount comparable with entrainment effects, the combination producing a 10% increase at  $Ra_x = 100$  and a greater amount at smaller  $Ra_x$ .

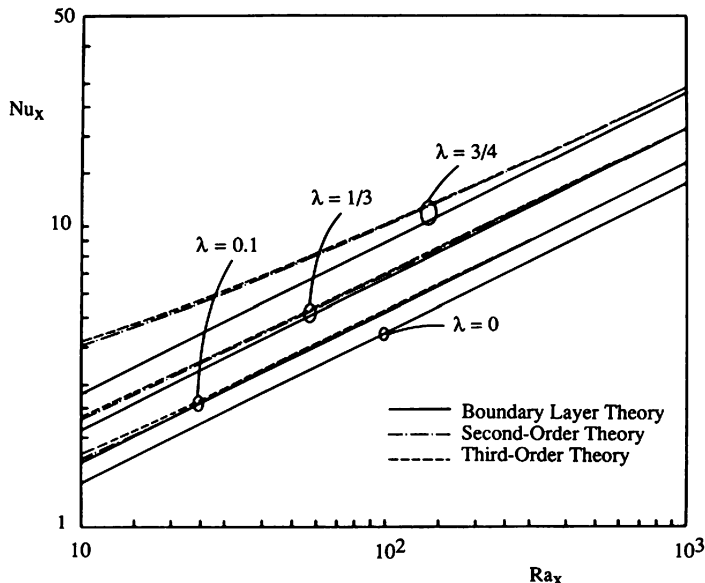


**Fig. 5.5** Higher-order theoretical values of local Nusselt number vs. local Rayleigh number for natural convection about a vertical flat plate in a porous medium (Cheng and Hsu 1984)

### 5.1.7 Effects of Boundary Friction, Inertia, and Thermal Dispersion

So far in this chapter it has been assumed that Darcy's law is applicable, and the effects of the no-slip boundary condition, inertial terms, and thermal dispersion are negligible. We now show that all of these effects are important only at high Rayleigh numbers. The effects of boundary friction and inertia tend to decrease the heat transfer rate while that of thermal dispersion tends to increase the heat transfer rate.

#### 5.1.7.1 Boundary Friction Effects

To investigate the boundary friction effect, Evans and Plumb (1978) made some numerical calculations using the Brinkman equation. They found that the boundary effect is negligible if the Darcy number  $Da$  ( $Da = K/L^2$ , where  $L$  is the length of the plate) is less than  $10^{-7}$ . For higher values of  $Da$ , their numerical results yield a local Nusselt number slightly smaller than those given by the theory based on Darcy's law.

Hsu and Cheng (1985b) and Kim and Vafai (1989) have used the Brinkman model and the method of matched asymptotic expansions to reexamine the problem.

Two small parameters that are related to the thermal and viscous effects govern the problem. For the case of constant wall temperature, these are  $\varepsilon_T = Ra^{-1/2}$  and  $\varepsilon_v = Da^{1/2}$ , where  $Ra$  is the Rayleigh number based on plate length  $L$  and temperature difference  $T_w - T_\infty$ , and  $Da$  is the Darcy number  $K/L^2\varphi$ . For the case of constant wall heat flux,  $\varepsilon_T = Ra^{-1/3}$ , where  $Ra$  is now the Rayleigh number based on  $L$  and the heat flux  $q''_w$ ; here we concentrate on the case of constant  $T_w$ . Cases (a)  $\varepsilon_v \ll \varepsilon_T$  and (b)  $\varepsilon_v \gg \varepsilon_T$  must be treated separately.

In geophysical and engineering applications it is usually case (a) that applies. Dimensional analysis shows that three layers are involved: the inner momentum boundary layer with a constant thickness of  $O(\varepsilon_v)$ ; the middle thermal layer with a thickness of  $O(\varepsilon_T)$ , which is inversely proportional to the imposed temperature difference; and the outer potential region of  $O(1)$ . The asymptotic analysis of Hsu and Cheng (1985b) gives the local Nusselt number in the form

$$Nu_x = C_1 Ra_x^{1/2} - C_2 Ra_x Da_x^{1/2}, \quad (5.60)$$

where  $Da_x = K/x^2$  is the local Darcy number, and the constants  $C_1$  and  $C_2$  are related to the dimensionless temperature gradients at the wall appearing in the first-order and second-order problems. The values of these constants depend on the wall temperature. Equation (5.60) can be rewritten as

$$Nu_x/Ra_x^{1/2} = C_1 - C_3 P_{nx}, \quad (5.61)$$

where  $C_3 = C_2/C_1$  and  $P_{nx}$  is the local no-slip parameter given by

$$P_{nx} = Ra_x^{1/2} Da_x^{1/2} = \left[ \frac{g \beta K^2 (T_w - T_\infty)^{1/2}}{\nu \alpha_m x} \right]. \quad (5.62)$$

Equation (5.61) is plotted in Fig. 5.6. It is clear that the deviation from Darcy's law becomes appreciable at high local Rayleigh numbers only for high local Darcy numbers (i.e., near the leading edge) and for large wall temperature variations. This conclusion is in accordance with the numerical results of Evans and Plumb (1978) and is confirmed by further calculations by Hong et al. (1987).

For case (b) where  $\varepsilon_v \gg \varepsilon_T$ , Kim and Vafai (1989) find that the local Nusselt number  $Nu_x$  is given by

$$Nu_x = 0.5027 Da_x^{-1/4} Ra_x^{1/4} = 0.5027 (Ra_f \phi)^{1/4}, \quad (5.63)$$

where  $Ra_f$  is the standard Rayleigh number for a viscous fluid (independent of permeability), as expected for a very sparse medium. Numerical studies using the Brinkman model were conducted by Beg et al. (1998) and Gorla et al. (1999b). The last study included the effect of temperature-dependent viscosity applied to the plume above a horizontal line source (either isolated or on an adiabatic vertical wall) as well as to a vertical wall with uniform heat flux.

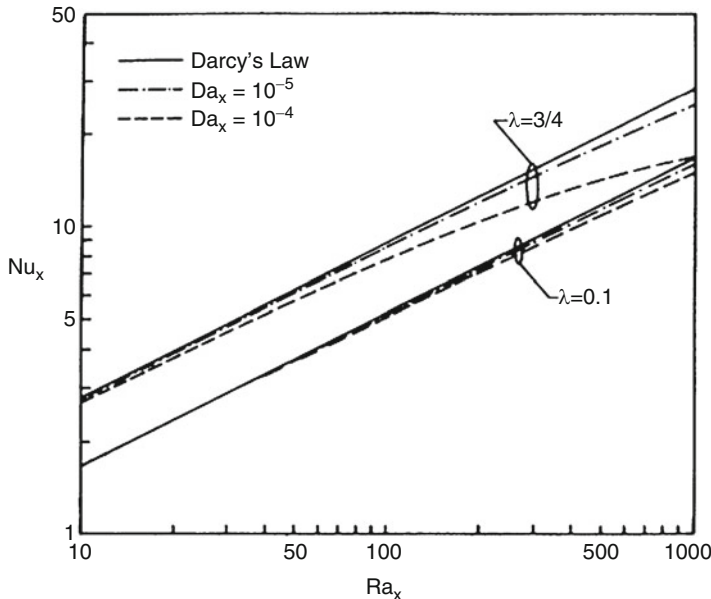


**Fig. 5.6** Boundary effects on the local Nusselt number for natural convection about a vertical surface in a porous medium (Hsu and Cheng 1985b, with permission from Pergamon Press)

### 5.1.7.2 Inertial Effects

Forchheimer's equation with a quadratic drag term was introduced into the boundary-layer theory by Plumb and Huenefeld (1981). Equation (5.23) is replaced by

$$u + \frac{\chi}{v} u^2 = \frac{g \beta K}{v} (T - T_{\infty}), \quad (5.64)$$

in which the coefficient  $\chi$  has the units [m] and represents the group  $c_F K^{1/2}$  seen earlier on the right-hand side of Eq. (1.12). In place of Eq. (5.15), one now has

$$f'' + Gr^*(f'^2)' - \theta' = 0, \quad (5.65)$$

where

$$Gr^* = \frac{g \beta \chi K (T_w - T_{\infty})}{v^2}. \quad (5.66)$$

It is clear that a similarity solution exists if and only if the Grashof number  $Gr^*$  is a constant, which requires that  $T_w$  is constant. Plumb and Huenefeld's results are displayed in Fig. 5.7, which as expected shows that the effect of quadratic drag is to slow down the buoyancy-induced flow and so retard the heat transfer rate.

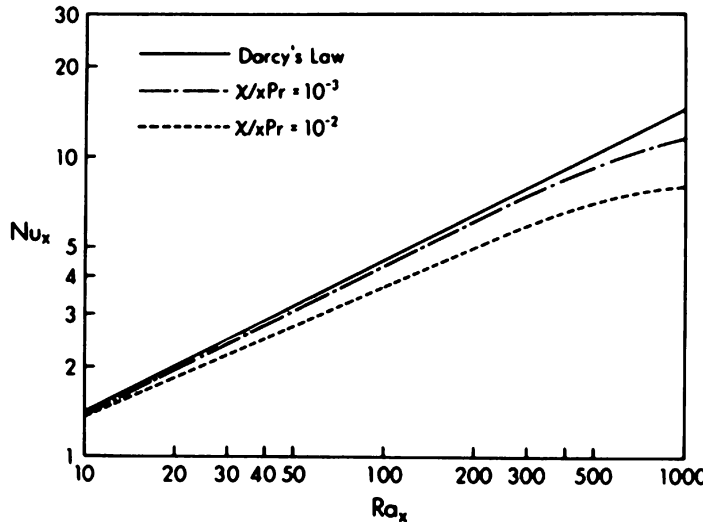


**Fig. 5.7** Non-Darcy inertial effects on the local Nusselt number for natural convection about a vertical surface in a porous medium (Cheng 1985a, with permission from Hemisphere Publishing Corporation)

The alternative analysis of Bejan and Poulikakos (1984) is based on the observation that at sufficiently large Rayleigh numbers, and hence large velocities, the quadratic term on the left-hand side of Eq. (5.60) will dominate the linear term. Scale analysis then indicates that the boundary-layer thickness  $\delta$  is of the order

$$\delta \sim H R a_{\infty}^{-1/4}, \quad (5.67)$$

where  $H$  is a characteristic length scale and the “large Reynolds number limit” Rayleigh number  $R a_{\infty}$  is defined as

$$R a_{\infty} = \frac{g \beta K H^2 (T_w - T_{\infty})}{\chi \alpha_m^2}. \quad (5.68)$$

The introduction of the nondimensional variables

$$\begin{aligned} x_* &= \frac{x}{H}, & y_* &= \frac{y}{H} R a_{\infty}^{1/4}, \\ u_* &= \frac{u H}{\alpha_m R a_{\infty}^{1/2}}, & v_* &= \frac{v H}{\alpha_m R a_{\infty}^{1/4}}, \\ \theta &= \frac{T - T_{\infty}}{T_w - T_{\infty}}, \end{aligned} \quad (5.69)$$

yields

$$u_* \frac{\partial \theta}{\partial x_*} + v_* \frac{\partial \theta}{\partial y_*} = \frac{\partial^2 \theta}{\partial y_*^2}, \quad (5.70)$$

$$G \frac{\partial u_*}{\partial y_*} + \frac{\partial (u_*^2)}{\partial y_*} = \frac{\partial \theta}{\partial y_*}, \quad (5.71)$$

where  $G$  is the new dimensionless group

$$G = v[\chi g \beta K(T_w - T_\infty)]^{-1/2} = (Gr^*)^{-1/2}. \quad (5.72)$$

The Forchheimer regime corresponds to  $G \rightarrow 0$ . Then Eq. (5.71) and the outer condition  $\theta \rightarrow 0$  as  $y \rightarrow \infty$  yields

$$u_* = \theta^{1/2}. \quad (5.73)$$

The appropriate similarity variable is

$$\eta = \frac{y_*}{x_*^{1/2}}. \quad (5.74)$$

The dimensionless streamfunction  $\Psi$  defined by  $u_* = \partial \Psi / \partial y_*$ ,  $v_* = -\partial \Psi / \partial x_*$  is now given by

$$\Psi = x_*^{1/2} F(\eta), \quad (5.75)$$

where

$$F(\eta) = \int_0^\eta \theta^{1/2} d\eta. \quad (5.76)$$

The boundary-layer equations reduce to the system

$$\theta^{1/2} = F', \quad -\frac{1}{2} F \theta' = \theta'', \quad (5.77)$$

with the conditions

$$\theta(0) = 1, F(0) = 0, \quad \text{and} \quad \theta \rightarrow 0 \quad \text{as} \quad \eta \rightarrow \infty. \quad (5.78)$$

This system is readily integrated using a shooting technique. One finds that  $\theta'(0) = -0.494$ , and so the local Nusselt number becomes

$$Nu_x = \frac{q'' x}{(T_w - T_\infty) k_m} = 0.494 Ra_{\infty,x}^{1/4}. \quad (5.79)$$

On the right-hand side,  $Ra_{\infty x}$  is obtained from expression (5.68) for  $Ra_{\infty}$  by replacing  $H$  by  $x$ . This formula for  $Nu_x$  differs radically from its Darcy counterpart, listed in Table 5.1,  $Nu_x = 0.444 Ra_x^{1/2}$ .

The case of uniform heat flux can be treated similarly. One now finds that the boundary-layer thickness is

$$\delta \sim HRa_{\infty*}^{-1/5}, \quad (5.80)$$

where  $Ra_{\infty*}$  is the flux-based Rayleigh number for the large Reynolds number limit,

$$Ra_{\infty*} = \frac{g\beta KH^3 q''}{\chi \alpha_m^2 k_m}. \quad (5.81)$$

The corresponding local Nusselt number is

$$Nu_x = \frac{q''x}{(T_w - T_{\infty})k_m} = 0.804 Ra_{\infty*x}^{1/5} \quad (5.82)$$

For intermediate values of the Forchheimer parameter, similarity solutions do not exist, but nonsimilarity results have been obtained by Bejan and Poulikakos (1984), Kumari et al. (1985) (including the effect of wall mass flux), Hong et al. (1985), Chen and Ho (1986), Hong et al. (1987) (including the effects of nonuniform porosity and dispersion), and Kaviany and Mittal (1987) (for the case of high permeability media). The combination of effects of inertia and suction on the wall was analyzed by Banu and Rees (2000) and by Al-Odat (2004a) for an unsteady situation. The combined effect of inertia and spanwise pressure gradient was examined by Rees and Hossain (1999). In this case the resulting flow is three-dimensional but self-similar, and the boundary-layer equations are supplemented by an algebraic equation governing the magnitude of the spanwise velocity field. It was found that the inertial effects serve to inhibit the spanwise flow near a heated surface.

### 5.1.7.3 Thermal Dispersion Effects

Following Cheng (1985a), one can introduce the effects of thermal dispersion by expressing the heat transfer per unit volume, by conduction and dispersion, in the form

$$\frac{\partial}{\partial x} \left( (k_m + k'_x) \frac{\partial T}{\partial x} \right) + \frac{\partial}{\partial y} \left( (k_m + k'_y) \right) \frac{\partial T}{\partial y}.$$

With  $x$  denoting the streamwise direction,  $k'_x$  and  $k'_y$  are the longitudinal and transverse thermal dispersion coefficients, respectively. Cheng (1981a) assumed that the dispersion coefficients were proportional to the velocity components and to the Forchheimer coefficient  $\chi$ , so

$$k'_x = a_L \frac{\chi}{v} |u|, \quad k'_y = a_T \frac{\chi}{v} |v|, \quad (5.83a)$$

where  $a_L$  and  $a_T$  are constants found by matching with experimental data. With this formulation, Cheng found that the effect of thermal dispersion was to decrease the surface heat flux.

On the other hand, Plumb (1983) assumed that the longitudinal coefficient was negligible and the transverse coefficient was proportional to the streamwise velocity component

$$k'_x = 0, \quad k'_y = C \rho c_p u d. \quad (5.83b)$$

In the  $k'_y$  expression,  $d$  is the grain diameter, and  $C$  is a constant found by matching experimental heat transfer data. In this formulation the surface heat flux is given by

$$q''_w = - \left[ (k + k'_y) \frac{\partial T}{\partial y} \right]_{y=0} = - [k + C \rho c_p u(x, 0) d] \frac{\partial T}{\partial y}(x, 0). \quad (5.84a)$$

The second term inside the square brackets of the last term is always positive since  $u(x, 0)$  is positive. In dimensionless form this equation is

$$\frac{Nu_x}{Ra_x^{1/2}} = -[1 + CRa_d f'(0)] \theta'(0), \quad (5.84b)$$

where

$$\theta = \frac{T - T_\infty}{T_w - T_\infty}, \quad f'(\eta) \frac{u}{u_r}, \quad Ra_d = \frac{g \beta K (T_w - T_\infty) d}{\nu \alpha_m}. \quad (5.85)$$

The dimensionless velocity slip on the wall  $f'(0)$  and the dimensionless temperature gradient at the wall  $\theta'(0)$  are functions of  $Gr^*$  and  $CRa_d$ . Plumb's numerical results are shown in Figs. 5.8 and 5.9. They show that both inertial and dispersion effects tend to decrease the temperature gradient at the wall but the combined effects either may increase or decrease the Nusselt number.

Hong and Tien (1987) included the effect of a Brinkman term to account for the no-slip boundary condition. As expected, this substantially reduces the dispersion effect near the wall.

The combined effect of dispersion and radiation was studied by Abbas (2008). The effect of thermal dispersion was further studied by Abbas et al. (2009).

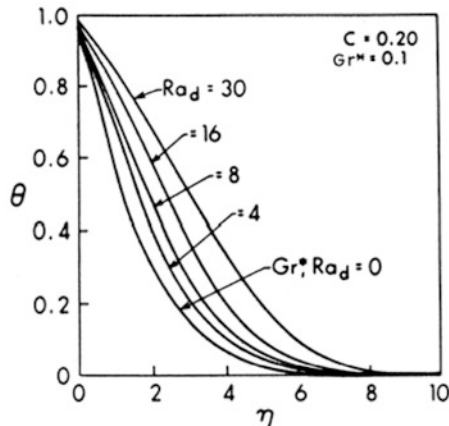


**Fig. 5.8** Combined effects of inertia and thermal dispersion on dimensionless temperature profiles for natural convection adjacent to a vertical heated surface (Plumb 1983)

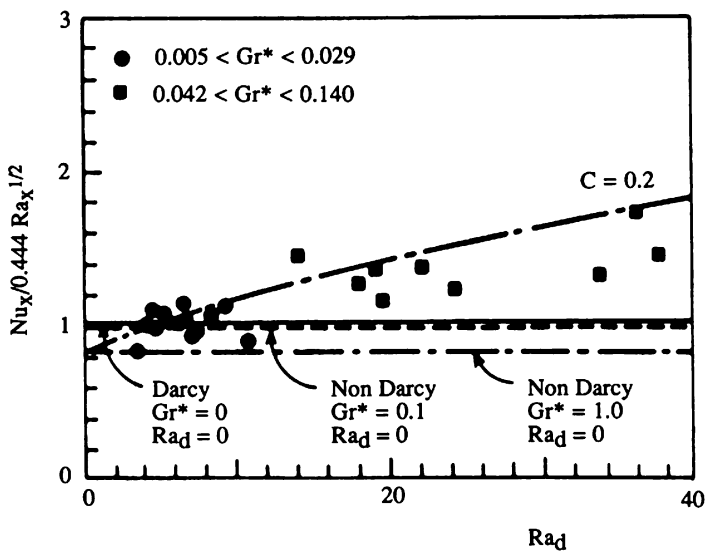


**Fig. 5.9** Combined effects of inertia and thermal dispersion on the local Nusselt number for natural convection adjacent to a vertical heated surface (Plumb 1983)

### 5.1.8 Experimental Investigations

Evans and Plumb (1978) investigated natural convection about a plate embedded in a medium composed of glass beads with diameters ranging from 0.85 to 1.68 mm. Their experimental data, which is shown in Figs. 5.10 and 5.11, is in good agreement with the theory for  $Ra_x < 400$ . When  $Ra_x > 400$ , temperature fluctuations were observed, and the Nusselt number values became scattered.

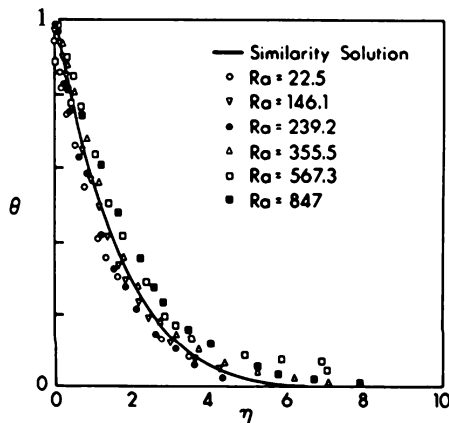


**Fig. 5.10** Dimensionless temperature profiles for natural convection about an isothermal vertical heated surface (Evans and Plumb 1978)

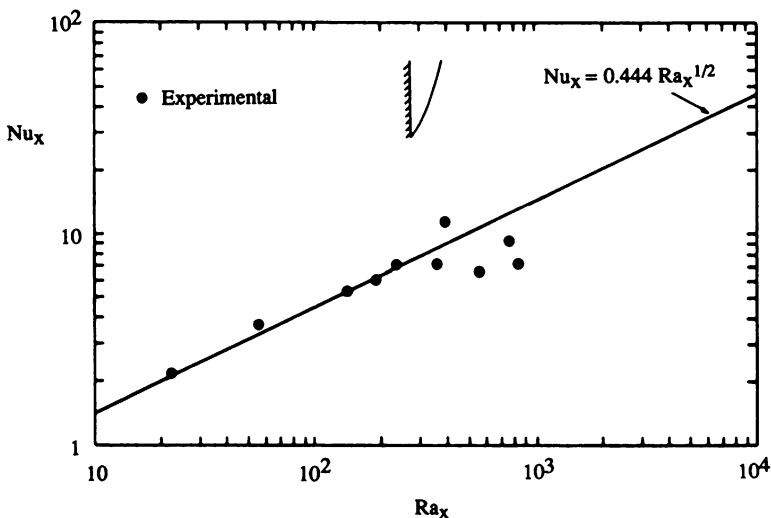


**Fig. 5.11** Local Nusselt number vs. local Rayleigh number for natural convection about an isothermal vertical heated surface (Evans and Plumb 1978)

Similar experiments were undertaken by Cheng et al. (1981) with glass beads of 3-mm diameter in water. They observed that temperature fluctuations began in the flow field when the non-Darcy Grashof number  $Gr^*$  attained a value of about 0.017. They attributed the fluctuations to the onset of non-Darcian flow. After the onset of temperature fluctuations the experimentally determined Nusselt number began to level off and deviate from that predicted by the similarity solution based on Darcy's law. The decrease in  $Nu_x$  was found to be substantially larger than that predicted by

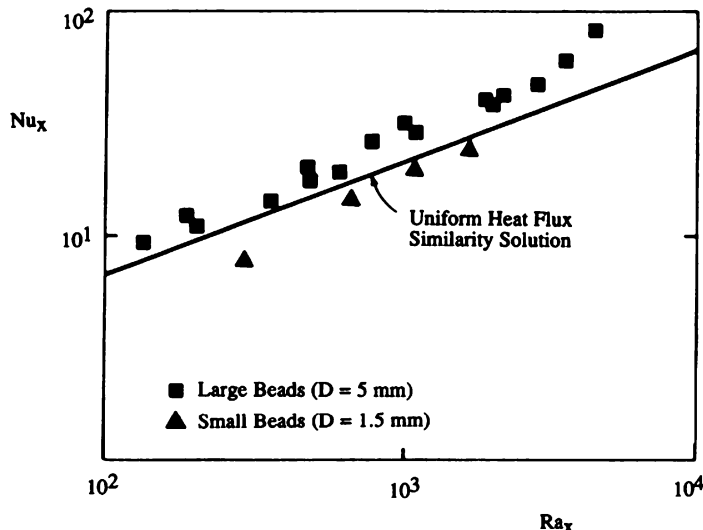


**Fig. 5.12** Local Nusselt number vs. local Rayleigh number for a vertical surface with uniform heat flux (Huenefeld and Plumb 1981)

Plumb and Huenefeld's (1981) theory. Cheng (1981a) originally attributed the decrease in  $Nu_x$  to the effect of thermal dispersion, but in Cheng (1985a) he announced that this attribution was erroneous. The discrepancy remains ill understood.

Huenefeld and Plumb (1981) performed experiments on convection about a vertical surface with uniform heat flux, the medium being glass beads saturated with water. They observed that temperature fluctuations occurred when the non-Darcy Grashof number  $Gr^*$  attained a value of about 0.03. Their results are illustrated in Fig. 5.12. The experimental data for the larger beads (diameter 5 mm) are above the predicted values from the Darcy theory, while those of the smaller beads (diameter 1.5 mm) are below the predicted values.

Kaviany and Mittal (1987) performed experiments with high permeability polyurethane foams saturated with air. Except when the permeability was relatively low, they found good agreement between their results and calculations made using a Brinkman-Forchheimer formulation. In their experiments inertial effects were not significant because the Rayleigh numbers were not very high.

Imadojemu and Johnson (1991) reported results of experiments with water-saturated glass beads or irregular-shaped gravel. They found that they were unable to obtain an effective correlation of the form  $\lambda = A Ra^n$ . Rather, they found that  $A$  and  $n$  varied with the medium and with the heat flux. The mass transfer coefficients found experimentally by Rahman et al. (2000) were found to agree closely with those predicted using a Brinkman model. Rahman and Badr (2002) repeated this experimental work for the case of a vertical wavy surface.

### 5.1.9 Further Extensions of the Theory

#### 5.1.9.1 Particular Analytical Solutions

The homotopy analysis method has been used by Liao and Pop (2004) to obtain explicit analytical solutions of similarity boundary-layer equations. The case of a vertical plate with wall temperature (relative to ambient) varying as  $x^{-1/3}$  (i.e., the case  $m = -1/3$ ) yields a hyperbolic tangent solution that was shown by Magyari et al. (2003c) to belong to a one-parameter family of multiple solutions that can be expressed in terms of Airy functions. Magyari and Keller (2004b) obtained exact analytical solutions for the cases  $m = 1$  and  $m = -1/3$  for the backward boundary layer that arises over a cooled (but upward projecting) vertical plate. Some existence and uniqueness results pertaining to the classic boundary equations were reported by Belhachmi et al. (2000, 2001). Belhachmi et al. (2003) suggested two complementary numerical methods to compute similarity solutions. Magyari and Keller (2000) obtained some special exact analytical solutions for the extended problem where there is variable lateral mass flux. Further special analytical solutions, for unsteady convection for the cases of exponential and power-law time dependence of the surface temperature, were obtained by Magyari et al. (2004).

#### 5.1.9.2 Non-Newtonian Fluids

Non-Newtonian fluid flow has been treated by Chen and Chen (1988a), Haq and Mulligan (1990b), Pascal (1990), Shenoy (1992, 1993a), Hossain and Nakayama (1994), El-Hakiem and El-Amin (2001b), El-Amin (2003a), El-Amin et al. (2003), Kim (2001a, b), and Hassanien et al. (2004e, 2005). Of these papers, those by Kim (2001a) and El-Amin (2003a) included the effect of a magnetic field.

Transient convection in an anisotropic medium was studied by Degan et al. (2007a). Transient MHD convection with a micropolar fluid was examined by Al-Odat and Damseh (2008). The case of oscillatory flow of a polar fluid was treated by Patil (2008), while the case of a conducting couple stress fluid was investigated by Shantha and Shanker (2010). An unsteady MHD flow of a micropolar fluid with radiation was studied by Abdelkhaled (2008b). The effect of a chemical reaction was treated by Chamkha et al. (2010c). A third-grade viscoelastic fluid was studied by Khani et al. (2009). Hady et al. (2011) studied the influence of yield stress on the flow of a non-Newtonian nanofluid. Rosali et al. (2012) studied micropolar fluid flow toward a stretching/shrinking sheet in a porous medium with suction.

#### 5.1.9.3 Local Thermal Nonequilibrium

The classical Cheng-Minkowycz theory was extended to a two-temperature model by Rees and Pop (2000c), using a model introduced by Rees and Pop (1999).

The effect of local thermal nonequilibrium (LTNE) was found to modify substantially the behavior of the flow relative to the leading edge, where the boundary layer is composed of two distinct asymptotic regions. At increasing distances from the leading edge the difference between the temperatures of the solid and fluid phases decreases to zero, i.e., thermal equilibrium is attained. Mohamad (2001) independently treated the same problem. In commenting on this paper Rees and Pop (2002) emphasized the importance of undertaking a detailed asymptotic analysis of the leading edge region in order to obtain boundary conditions for the solid-phase temperature field that are capable of describing accurately its behavior outside the computational domain.

Rees (2003) solved numerically the full equations of motion and thus investigated in detail how the elliptical terms in the governing equations are manifested. In general it is found that at any point in the flow the temperature of the solid phase is higher than that of the fluid phase, and thus the thermal field of the solid phase is of greater extent than that of the fluid phase. The extension to the Brinkman model was made by Haddad et al. (2004), while Haddad et al. (2005a, b) reconsidered flow with the Darcy model. Rees et al. (2003a) considered forced convection past a heated horizontal circular cylinder. Rees and Pop (2005) reviewed work on LTNE in porous media convection. The case of Hiemenz flow was studied by Kokubun and Fachini (2011).

#### **5.1.9.4 Volumetric Heating due to Viscous Dissipation, Radiation, or Otherwise**

Volumetric heating due to the effect of viscous dissipation was analyzed by Magyari and Keller (2003a, b, c). In their first two papers they observed that the opposing effect of viscous dissipation allows for a parallel boundary-layer flow along a cold vertical plate. In their third paper they considered a quasiparallel flow involving a constant transverse velocity directed perpendicularly toward the wall. They observed that even in the case where the wall temperature equals the ambient temperature thermal convection is induced by the heat released by the viscous dissipation. They examined in detail the resulting self-sustaining wall jets. The development of the asymptotic viscous profile that results was studied by Rees et al. (2003b). The vortex instability of the asymptotic dissipation profile was analyzed by Rees et al. (2005a). The case of an exponential wall temperature was studied by Magyari and Rees (2005). The general effect of viscous dissipation, which reduces heat transfer, was investigated by Murthy and Singh (1997a), who also took thermal dispersion effects into account. The effect of variable permeability was added by Hassani et al. (2005). A survey of work on the effect of viscous dissipation was made by Magyari et al. (2005b). Further contributions were made by Modather et al. (2007), Badruddin et al. (2006b, c), Makinde and Moitsheki (2008), Zueco (2008), Mohamed and Abo-Dahab (2009), Mohamed et al. (2010), El-Amin and Ebrahem (2006), and El-Amin et al. (2010). The case of an exponential distribution was studied by Magyari and Rees (2006).

Volumetric heating due to the absorption of radiation was studied by Chamkha (1997a), Takhar et al. (1998), Mohammadien et al. (1998) (see Pantokratoras 2007a, b, 2008a), Mohammadien and El-Amin (2000), Raptis (1998), Raptis and Perdikis (2004), Hossain and Pop (2001), El-Hakiem (2001a), El-Hakiem and El-Amin (2001a), Chamkha et al. (2001), Mansour and El-Shaer (2001), Mansour and Gorla (2000a, c), Israel-Cookey et al. (2003), and Rashad (2009a, b) (see Pantokratoras (2009a)). Some more general aspects of volumetric heating were considered by Chamkha (1997d), Bakier et al. (1997), Postelnicu and Pop (1999), Postelnicu et al. (2000), and Ali (2007). Further work on a heat-generating porous medium was reported by Merkin (2008, 2009, 2012) and Mealey and Merkin (2008). The combined effect of volumetric heat source with power-law dependence on the local temperature and horizontal throughflow was studied by Postelnicu et al. (2009).

### 5.1.9.5 Anisotropy and Heterogeneity

Anisotropic permeability effects have been analyzed by Ene (1991) and Rees and Storesletten (1995). The latter found that the boundary-layer thickness was altered, and a spanwise fluid drift induced, by the anisotropy. As Storesletten and Rees (1998) demonstrated, anisotropic thermal diffusivity produces no such drift. An analytical and numerical study of the effect of anisotropic permeability was reported by Vasseur and Degan (1998).

The effect of variable permeability, enhanced within a region of constant thickness, was treated analytically and numerically by Rees and Pop (2000a). They found that near the leading edge the flow is enhanced, and the rate of heat transfer is much higher than in the uniform permeability case. Further downstream the region of varying permeability is well within the boundary layer, and in this case the flow and heat transfer is only slightly different from that in the uniform case. Convection over a wall covered with a porous substrate was analyzed by Chen and Chen (1996). Convection from an isothermal plate in a porous medium layered in a parallel fashion, with discrete changes in either the permeability or the diffusivity of the medium, was studied by Rees (1999). He supplemented his numerical work with an asymptotic analysis of the flow in the far-downstream limit.

Further work on heterogeneous media was done by Singh (2008), Singh and Gorla (2010), and Singh et al. (2011c).

### 5.1.9.6 Wavy Surface

The case of a wavy surface has been analyzed by Rees and Pop (1994a, 1995a, b, 1997). In the last paper they considered the full governing equations and derived the boundary-layer equations in a systematic way. They found that, for a wide range of values of the distance from the leading edge, the boundary-layer equations for the

three-dimensional flow field are satisfied by a two-dimensional similarity solution. An MHD problem was studied by Mahdy (2009).

### 5.1.9.7 Time-Dependent Gravity or Time-Dependent Heating

The effect of g-jitter was analyzed by Rees and Pop (2000b, 2003) for the cases of small and large amplitudes. Their numerical and asymptotic solutions show that the g-jitter effect is eventually confined to a thin layer embedded within the main boundary layer, but it becomes weak at increasing distances from the leading edge. The case of time-periodic surface temperature oscillating about a constant mean was studied by Jaiswal and Soundalgekar (2001). The more general case of oscillation about a mean that varies as the  $n$ th power of the distance from the leading edge was analyzed by Hossain et al. (2000). They considered low- and high-frequency limits separately and compared these with a full numerical solution, for  $n \leq 1$ . They noted that when  $n = 1$ , the flow is self-similar for any prescribed frequency of modulation. Temperature oscillations also were studied using a Forchheimer model by El-Amin (2004b). A vertical wall with suction varying in the horizontal direction and with a pulsating wall temperature was studied by Chaudhary and Sharma (2003). A nonequilibrium model was used by Saeid and Mohamad (2005a) in their numerical study of the effect of a sinusoidal plate temperature oscillation with respect to time about a nonzero mean.

### 5.1.9.8 Other Thermal Boundary Conditions

The case of surface heating with a boundary condition of the third kind was studied by Lesnic et al. (1999) and Pop et al. (2000). They obtained fully numerical, asymptotic, and matching solutions. A further contribution was made by Nazar et al. (2006).

In the case of a prescribed inverse linear surface heat flux, Magyari (2006) investigated an apparent paradox. Temperature-dependent boundary conditions were studied by Merkin and Pop (2010). Cimpean et al. (2006) considered temperature distribution involving a ramp between two levels.

### 5.1.9.9 Other Aspects

A comprehensive listing of similarity solutions, including some for special transient situations, was presented by Johnson and Cheng (1978). The cases of arbitrary wall temperature and arbitrary heat flux have been treated using a Merk series technique by Gorla and Zinalabedini (1987) and Gorla and Tornabene (1988).

Merkin and Needham (1987) have discussed the situation where the wall is of finite height and the boundary layers on each side of the wall merge to form a buoyant wake. Singh et al. (1988) have studied the problem when the prescribed

wall temperature is oscillating with time about a nonzero mean. Zaturska and Banks (1987) have shown that the boundary-layer flow is stable spatially.

The asymptotic linear stability analysis of Lewis et al. (1995) complements the direct numerical simulation of Rees (1993) in showing that the flow is stable at locations sufficiently close to the leading edge. In the asymptotic regime also the wave disturbances decay, but the rate of decay decreases as the distance downstream of the leading edge increases.

The effect of temperature-dependent viscosity has been examined theoretically by Jang and Leu (1992), for a steady flow, and by Mehta and Sood (1992b) and Rao and Pop (1994), for a transient flow. An MHD problem was studied by Afifi (2007b) and Pantokratoras (2006).

For the case of prescribed heat flux, Kou and Huang (1996a, b) have shown how three cases are related by a certain transformation, and Wright et al. (1996) treated another special case. Ramanaiah and Malarvizhi (1994) have shown how three situations are related. Nakayama and Hossain (1994) have shown that both local-similarity and integral methods perform excellently for a non-isothermal plate. A perturbation approach to the nonuniform heat flux situation was used by Seetharamu and Dutta (1990) and Dutta and Seetharamu (1993). Braudean et al. (1996, 1997a) have given an analytical and numerical treatment for a periodically heated and cooled vertical or horizontal plate. For a vertical plate, a row of counter-rotating cells forms close to the surface, but when the Rayleigh number increases above about 40, the cellular flow separates from the plate. For a horizontal plate the separation does not occur.

Merkin and Needham (1987) have discussed the situation where the wall is of finite height, and the boundary layers on each side of the wall merge to form a buoyant wake. Singh et al. (1988) have studied the problem when the prescribed wall temperature is oscillating with time about a nonzero mean.

Seetharamu and Dutta (1990) used a perturbation approach to treat the case of arbitrary wall temperature. Herwig and Koch (1990) examined the asymptotic situation when the porosity tends to unity. Ramanaiah and Malarvizhi (1991) presented some exact solutions for certain cases. Chandrasekhara et al. (1992) and Chandrasekhara and Nagaraju (1993) have treated a medium with variable porosity, with surface mass transfer or radiation. The effect of variable porosity was also studied by Attia (2007b). Pop and Herwig (1992) presented an asymptotic approach to the case where fluid properties vary, while Na and Pop (1996) presented a new accurate numerical solution of the Cheng-Minkowycz equation equivalent to (5.15, 5.16, 5.17, and 5.18). Rees (1997b) discussed the case of parallel layering, with respect to either permeability or thermal diffusivity, of the medium. The numerical solution of the nonsimilar boundary-layer equations was supplemented by an asymptotic analysis of the flow in the far downstream limit. Rees (1997b) examined the three-dimensional boundary layer on a vertical plate where the surface temperature varies sinusoidally in the horizontal direction. The effect of an exothermic reaction was studied by Minto et al. (1998).

The study of the influence of higher-order effects, on convection in a wedge bounded by a uniformly heated plane and one cold or insulated, by Storesletten and

Rees (1998), revealed that generally instability occurs too close to the leading edge for the basic flow to be represented adequately either by the leading-order boundary-layer theory used in previous chapters, or even by the most accurate higher-order theory obtained using matched expansions.

The effect of lateral mass flux was studied analytically and numerically by Dessaux (1998). Unsteady convection was studied by Al-Nimr and Massoud (1998), and also with the effect of a magnetic field by Helmy (1998). Convection along a vertical porous surface consisting of a bank of parallel plates with constant gaps was studied experimentally by Takatsu et al. (1997). A problem involving Hall current and a slip condition was studied by Hayat et al. (2007a). A nonlinear variation of density with temperature was investigated by Prasad et al. (2011). Stagnation point flow with a fluid having a density maximum was treated by Merkin and Kumaran (2011). Temperature-dependent properties were examined by Vajravelu et al. (2011). The effect of viscous dissipation in a transient situation was studied by Salama et al. (2011) and El-Amin et al. (2012). Another transient situation, involving suction and blowing and variable viscosity, was studied by Husnain et al. (2012). A problem with two isothermally heated elements on an adiabatic vertical plate was treated numerically by Saied (2006b).

The effect of thermophoresis particle deposition was studied by Bakier and Mansour (2007), Rashad (2008), and Damseh and Duwairi (2008). The case of a nanofluid was examined by Gorla and Chamkha (2011). The case of icy water was investigated by Kumaran and Pop (2006).

A bidisperse porous medium was studied by Nield and Kuznetsov (2008b, 2011c) and Rees et al. (2008b).

An entrainment theorem relating to a permeable plate was proved by Magyari and Rees (2006). Exponentially decaying boundaries were examined by Liao and Magyari (2006) as limiting cases of algebraically ones. Consequences of the transition invariance on the Darcy natural convection were investigated by Magyari (2010a).

Despite the fact that a stretching sheet has a negligible effect on flow in a practical porous medium, papers on this topic have been published by Abel et al. (2010a, b, 2011), Attia (2007a), Boutros et al. (2006), Damseh et al. (2008), Dash et al. (2008), Hamad and Pop (2011) (see the discussion by Magyari (2011a, c)) and Pop (2011), Kiwan and Ali (2008), Liu (2006), Mahmoud and Megahed (2006), Noor and Hashim (2010), Pal and Hiremath (2010), Rahman and Sattar (2006), Sajid et al. (2009), Tamayol et al. (2010), Senapati and Dhal (2011), Singh et al. (2011b), Hayat et al. (2011b), and Abou-zeid (2011). Other studies involving a moving wall are those by Chaudhary and Jain (2010), Beg et al. (2008b), and Khan et al. (2011) (who considered MHD convection with an oscillating plate).

**Table 5.2** Values of  $\eta_T$  and  $-\theta'(0)$  for various values of  $\lambda$  for an upward-facing heated horizontal plate (Cheng and Chang 1976)

$\lambda$	$\eta_T$	$-\theta'(0)$
0	5.5	0.420
1/2	5.0	0.816
1	4.5	1.099
3/2	4.0	1.351
2	3.7	1.571

## 5.2 Horizontal Plate

For high Rayleigh number natural convection flow near the edge of an upward-facing heated plate, a similarity solution was obtained by Cheng and Chang (1976), for the case of a power-law wall temperature distribution given by Eq. (5.8). This leads to the formulas

$$\frac{\delta}{x} = \frac{\eta_T}{Ra_x^{1/3}}, \quad (5.86)$$

$$\frac{Nu_x}{Ra_x^{1/3}} = -\theta'(0), \quad (5.87)$$

$$\frac{\overline{Nu}}{Ra^{1/3}} = \frac{3(1 + \lambda)^{4/3}}{(1 + 4\lambda)} [-\theta'(0)], \quad (5.88)$$

for the thermal boundary-layer thickness  $\delta$ , the local Nusselt number  $Nu_x$ , and the overall Nusselt number  $\overline{Nu}$ . Table 5.2 lists values of  $\eta_T$  and  $[-\theta'(0)]$  for selected values of  $\lambda$ . It should be noted that in practice the assumption of quiescent flow outside the boundary layer on an upward-facing heated plate is unlikely to be justified, and such a boundary layer is better modeled as a mixed convection problem.

One would expect a natural convection boundary layer to form on a cooled plate facing upward, or on a warm plate facing downward. This situation was analyzed by Kimura et al. (1985). Relative to a frame with  $x$  axis horizontal and  $y$  axis vertically upward, we suppose that the plate is at  $-l \leq x \leq l$ ,  $y = 0$  and is at constant temperature  $T_w$ , ( $T_w < T_\infty$ ). The plate length is  $2l$ .

The mass and energy equations (5.1) and (5.4) still stand, but now the Darcy equations are

$$u = -\frac{K}{\mu} \frac{\partial P'}{\partial x}, \quad (5.89)$$

$$v = -\frac{K}{\mu} \left[ \frac{\partial P'}{\partial y} + \rho g \beta (T_\infty - T) \right]. \quad (5.90)$$

Eliminating  $P'$  we get

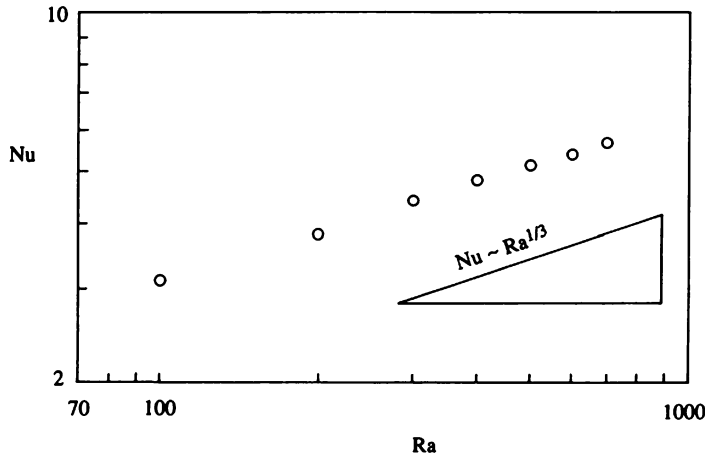


**Fig. 5.13** Nusselt number vs. Rayleigh number for convection on a cooled horizontal plate of finite length facing upward (Kimura et al. 1985)

$$\frac{\partial u}{\partial y} = \frac{g\beta K}{\nu} \frac{\partial}{\partial x} (T_\infty - T). \quad (5.91)$$

The boundary conditions are

$$\begin{aligned} y = 0 : v &= 0 \quad \text{and} \quad T = T_w, \\ y \rightarrow \infty : u &= 0, \quad T = T_\infty \quad \text{and} \quad \frac{\partial T}{\partial y} = 0. \end{aligned} \quad (5.92)$$

The appropriate Rayleigh number is based on the plate half-length  $l$

$$Ra = \frac{g\beta Kl(T_\infty - T_w)}{\nu \alpha_m}. \quad (5.93)$$

Scaling analysis indicates that the boundary-layer thickness must be of order

$$\delta \sim lRa^{-1/3}. \quad (5.94)$$

The Nusselt number defined by

$$Nu = \frac{q'}{k_m(T_\infty - T_w)}, \quad (5.95)$$

in which  $q'[\text{W/m}]$  is the heat transfer rate into the whole plate, is of order

$$Nu \sim Ra^{1/3}. \quad (5.96)$$

This is in contrast to the  $\lambda \sim Ra^{1/2}$  relationships for a vertical plate. Kimura et al. (1985) solved the boundary-layer equations approximately using an integral method. Their numerical results shown in Fig. 5.13 confirm the theoretical trend (5.92).

Ramaniah and Malarvizhi (1991) noted a case in which an exact solution could be obtained. Wang et al. (2003c) reported an explicit, totally analytic, and uniformly valid solution of the Cheng-Chang equation that agreed well with numerical results. Modifications of the Cheng and Chang (1976) analysis include those made by Chen and Chen (1987) for a non-Newtonian power-law fluid, by Lin and Gebhart (1986) for a fluid whose density has a maximum as the temperature is varied, by Minkowycz et al. (1985b) for the effect of surface mass flux, and by Vedhanayagam et al. (1987) for the effects of surface mass transfer and variation of porosity. The combination of power-law fluid and thermal radiation was considered by Mohammadien and El-Amin (2001).

Ingham et al. (1985a) studied the transient problem of a suddenly cooled plate. Harris et al. (2000) studied analytically and numerically the transient convection induced by a sudden change in surface heat flux.

Merkin and Zhang (1990a) showed that for the case of wall temperature proportional to  $x^m$ , a solution of the similarity equations is possible only for  $m > -2/5$ . For a non-Newtonian power-law fluid, Mehta and Rao (1994) treated the case of a power-law wall temperature, and Chamkha (1997c) studied the case of uniform wall heat flux, while the effect of surface mass flux was added by Gorla and Kumari (2003). Pop and Gorla (1991) studied a heated horizontal surface, the fluid being a gas whose thermal conductivity and dynamic viscosity are proportional to temperature. They obtained a similarity solution for the case of constant wall temperature. The effect of temperature-dependent viscosity also was studied by Kumari (2001a, b) and by Postelnicu et al. (2001) for the case of internal heating already treated by Postelnicu and Pop (1999). Similarity solutions for convection adjacent to a horizontal surface with an axisymmetric temperature distribution were given by Cheng and Chau (1977), and El-Amin et al. (2004) added the effects of a magnetic field and lateral mass flux. Lesnic et al. (2000, 2004) studied analytically and numerically the case of a thermal boundary condition of mixed type (Newtonian heat transfer). The case of wall temperature varying as a quadratic function of position was studied, as a steady or unsteady problem, by Lesnic and Pop (1998a).

The singularity at the edge of a downward-facing heated plate was analyzed by Higuera and Weidman (1995) and the appropriate boundary condition deduced. They considered both constant temperature and constant flux boundary conditions, and they treated a circular disk as well as an infinite strip. They also gave solutions for a slightly inclined plate maintained at constant temperature. Convection below a downward-facing heated horizontal surface also was treated numerically by Angirasa and Peterson (1998b). Convection from a heated upward-facing finite horizontal surface was studied numerically by Angirasa and Peterson (1998a). Two-dimensional flows were found for  $40 \leq Ra \leq 600$ , and the correlation

$\lambda = 3.092 Ra^{0.272}$  was obtained. At higher Rayleigh numbers the flow becomes three-dimensional with multiple plume formation and growth.

Rees and Bassom (1994) found that waves grow beyond a nondimensional distance 28.90 from the leading edge, whereas vortices grow only beyond 33.47. This stability analysis was based on a parallel-flow approximation. Because of the inadequacy of this approximation, Rees and Bassom (1993) performed numerical simulations of the full time-dependent nonlinear equations of motion. They found that small-amplitude disturbances placed in the steady boundary-layer propagated upstream much faster than they were advected downstream. With the local growth rate depending on the distance downstream, there is a smooth spatial transition to convection. For the problem where the temperature of the horizontal surface is instantaneously raised above the ambient, they found a particularly violent fluid motion near the leading edge. A strong thermal plume is generated, which is eventually advected downstream. The flow does not settle down to a steady or time-periodic state. The evolving flow field exhibits a wide range of dynamic behavior including cell merging, the ejection of hot fluid from the boundary layer, and short periods of relatively intense fluid motion accompanied by boundary-layer thinning and short-wavelength waves.

Rees (1996a) showed that when the effects of inertia are sufficiently large, the leading-order boundary-layer theory is modified, and he solved numerically the resulting nonsimilar boundary-layer equations. He showed that near the leading edge inertia effects then dominate, but Darcy flow is reestablished further downstream. The effects of inertia in the case of a power-law distribution of temperature were analyzed by Hossain and Rees (1997).

The Brinkman model was employed by Rees and Vafai (1999). They showed that for a constant temperature surface, both the Darcy and Rayleigh numbers can be scaled out of the boundary-layer equations leaving no parameters to vary. They studied these equations using both numerical and asymptotic methods. They found that near the leading edge the boundary layer has a double-layer structure: a near-wall layer where the temperature adjusts from the wall temperature to the ambient and where Brinkman effects dominate and an outer layer of uniform thickness that is a momentum adjustment layer. Further downstream, these layers merge, but the boundary layer eventually regains a two-layer structure; in this case a growing outer layer exists, which is identical to the Darcy flow case for the leading-order term and an inner layer of constant thickness resides near the surface where the Brinkman term is important.

Convection induced by a horizontal wavy surface was analyzed by Rees and Pop (1994b). They focused their attention on the case where the waves have an  $O(Ra^{-1/3})$  amplitude, where  $Ra$  is based on the wavelength and is assumed large. They found that a thin near-wall boundary layer develops within the basic boundary layer as the downstream distance is increased, and they gave an asymptotic analysis that determines the structure of this layer. They found that when the wave amplitude is greater than approximately  $0.95 Ra^{-1/3}$ , localized regions of reversed flow occur at the heated surface.

The case of a sinusoidally (lengthwise) heated and cooled horizontal surface was studied by Bradean et al. (1995a), when at large distances from the plate there is either constant temperature or zero heat flux. Bradean et al. (1996, 1997a) examined cases of unsteady convection from a horizontal (or vertical) surface that is suddenly heated and cooled sinusoidally along its length. They obtained an analytical solution valid for small times and any value of  $Ra$ , and a numerical solution matching this to the steady-state solution (when this exists). The flow pattern is that of a row of counterrotating cells situated close to the surface. When the surface is vertical and for  $Ra > 40$  (approximately), two recirculating regions develop at small times at the point of collision of two boundary layers that flow along the surface. However, for  $40 < Ra < 150$  the steady-state solution is unstable, and at very large time the solution is periodic in time. When the surface is horizontal, the collision of convective boundary layers occurs without separation. As time increases, the height of the cellular flow pattern increases and then decreases to its steady-state value. The heat penetrates infinitely into the porous medium, and the steady state is approached later in time as the distance from the surface increases.

Numerical and similarity solutions for the boundary layer near a horizontal surface with nonuniform temperature and mass injection or withdrawal were reported by Chaudhary et al. (1996). In their study the temperature and mass flux varied as  $x^\mu$  and  $x^{(\mu-2)/3}$ , respectively, where  $\mu$  is a constant. The conjugate problem of boundary-layer natural convection and conduction inside a horizontal plate of finite thickness was solved numerically by Lesnic et al. (1995). The conjugate problem for convection above a cooled or heated finite plate was studied numerically by Vaszi et al. (2001a, 2002a).

Flow over a rotating disk was studied by Attia (2006a, b, c, 2008a). A rotating system was also treated by Guria et al. (2010). Flow over a stretching surface was examined by Mehmood (2008). Postelnicu (2007b) studied the effects of thermophoresis particle deposition. The case of a porous medium saturated by a nanofluid containing microorganisms (bioconvection) was treated by Aziz et al. (2012).

### 5.3 Inclined Plate, Wedge

Again we take the  $x$  axis along the plate and the  $y$  axis normal to the plate. In the boundary-layer regime  $\partial T/\partial x \ll \partial T/\partial y$ , and the equation obtained by eliminating the pressure between the two components of the Darcy equation, reduces to

$$\frac{\partial^2 \Psi}{\partial y^2} = \frac{g_x \beta K}{v} \frac{\partial T}{\partial y}, \quad (5.97)$$

where  $g_x$  is the component of  $g$  parallel to the plate. This is just Eq. (5.6) with  $g$  replaced by  $g_x$ . With this modification, the analysis of Sect. 5.1 applies to the

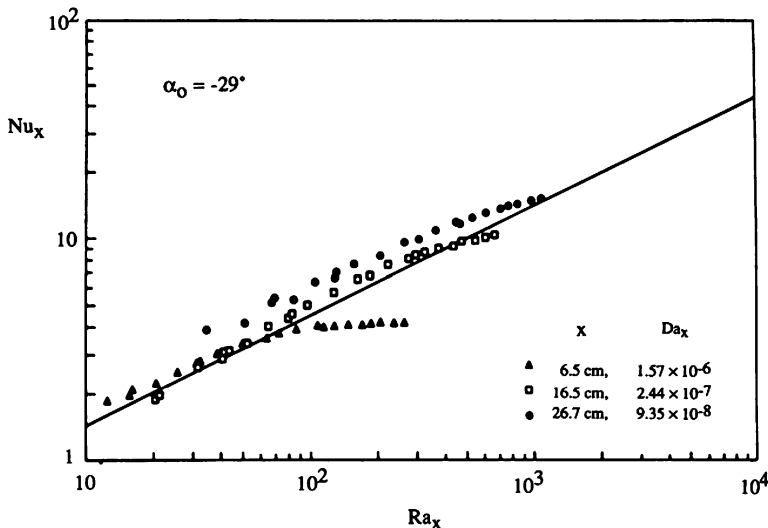


**Fig. 5.14** Local Nusselt number vs. local Rayleigh number for a downward-facing heated inclined plate (Lee 1983; Cheng 1985a, with permission from Hemisphere Publishing Corporation)

inclined plate problem unless the plate is almost horizontal, in which case  $g_x$  is small compared with the normal component  $g_y$ .

The case of small inclination to the horizontal was analyzed by Ingham et al. (1985b) and Rees and Riley (1985). Higher-order boundary-layer effects, for the case of uniform wall heat flux, were incorporated by Ingham and Pop (1988). Jang and Chang (1988d) performed numerical calculations for the case of a power function distribution of wall temperature. They found that, as the inclination to the horizontal increases, both the velocity and temperature boundary-layer thicknesses decrease, and the rate of surface heat transfer increases. Jang and Chang (1989) have analyzed the case of double diffusion and density maximum.

In their experiments on natural convection from an upward-facing inclined isothermal plate to surrounding water-filled glass beads, Cheng and Ali (1981) found that large amplitude temperature fluctuations exist in the flow field at high Rayleigh numbers, presumably because of the onset of vortex instability. Cheng (1985a) also reported on experiments by himself, Fand, and Lee for a downward-facing isothermal plate with inclinations of  $29^\circ$  and  $45^\circ$ . Their results are presented in Fig. 5.14, which shows a leveling off of the local Nusselt number  $Nu_x$  from the  $Ra_x^{1/2}$  dependence at high values of the local Rayleigh number  $Ra_x$ .

The effect of lateral surface mass flux, with a power-law variation of lateral surface velocity and wall temperature, was studied by Dwiek et al. (1994). The use of a novel inclination parameter enabled Pop and Na (1997) to describe all cases of horizontal, inclined, and vertical plates by a single set of transformed boundary-

layer equations. Hossain and Pop (1997) studied the effect of radiation. Shu and Pop (1997) obtained a numerical solution for a wall plume arising from a line source embedded in a tilted adiabatic plane. MHD convection with thermal stratification was studied by Chamkha (1997e) and Takhar et al. (2003a, b). The effects of variable porosity and solar radiation were discussed by Chamkha et al. (2002). The effects of lateral mass flux and variable permeability were analyzed by Rabadi and Hamdan (2000). Conjugate convection from a slightly inclined plate was studied analytically and numerically by Vaszi et al. (2001b). Lesnic et al. (2004) studied analytically and numerically the case of a thermal boundary condition of mixed type (Newtonian heat transfer) on a nearly horizontal surface.

The linear stability of a thermal boundary layer with suction in an anisotropic porous medium was discussed by Rees and Storesletten (2002). The effects of inertia and nonparallel flow were incorporated in the analysis of Zhao and Chen (2002). These effects stabilize the flow.

Variations on this theme have been studied by Ferdows et al. (2009), Kayhani et al. (2011a, b), Hassanien and Eliaw (2007) (effect of variable permeability), Mansour et al. (2010b) (MHD and chemical reaction effects), Salem (2009, 2010) (temperature-dependent viscosity), and El-Kabeir et al. (2008a, b) (MHD, unsteady, stretching surface).

For flow over a wedge (and a cone), Al-Harbi (2005) studied numerically the effects of variable viscosity and thermal radiation, and for a wedge with suction/injection. Muhammin et al. (2010b) studied the effect of a magnetic field.

## 5.4 Vortex Instability

For an inclined or a horizontal upward-facing heated surface embedded in a porous medium, instability leading to the formation of vortices (with axes aligned with the flow direction) may occur downstream as the result of the top-heavy situation. Hsu et al. (1978) and Hsu and Cheng (1979) applied linear stability analysis for the case of a power-law variation of wall temperature, on the assumption that the basic state is the steady two-dimensional boundary-layer flow discussed above. They showed that the length scale of vortex disturbances is less than that for the undisturbed thermal boundary layer, and as a result certain terms in the three-dimensional disturbance equations are negligible.

The simplified equations for the perturbation amplitudes were solved on the basis of local-similarity assumptions (the disturbances being allowed to have a weak dependence in the streamwise direction). It was found that the critical value for the onset of vortex instability in natural convection about an inclined isothermal surface with inclination  $\alpha_0$  to the vertical is given by

$$Ra_{x,a} \tan^2 \alpha_0 = 120.7, \quad (5.98)$$

where

$$Ra_{x,a} = \frac{g\beta K(T_w - T_\infty)(\cos \alpha_0)x}{v\alpha_m}. \quad (5.99)$$

It follows that the larger the inclination angle with respect to the vertical, the more susceptible the flow to vortex instability, and in the limit of zero inclination angle (vertical heated surface) the flow is stable to this type of disturbance.

For the case of a horizontal heated plate, a similar analysis shows that the critical value is  $Ra_x = 33.4$ , where  $Ra_x$  is defined as in Eq. (5.14). More precise calculations, including pressure and salinity effects, and including the effect of the normal component of the buoyancy force in the main flow, were made by Jang and Chang (1987, 1988a). Chang and Jang (1989a, b) examined the non-Darcy effects. The effect of inertia is to destabilize the flow to the vortex mode of disturbance, while the other non-Darcy terms lead to a stabilizing effect. The effect of inertia was also considered by Lee et al. (2000) in their study involving an inclined plate. Jang and Chen (1993a, b, 1994) studied the effect of dispersion (which stabilizes the vortex mode) and the channeling effect of variable porosity (which destabilizes it). The effect of variable viscosity was studied by Jang and Leu (1993) and Leu and Jang (1993). Nield (1994c) pointed out that their implication that this property variation produced a destabilizing effect was invalid. Jang and Lie (1992) and Lie and Jang (1993) treated a mixed convection flow. For a horizontal plate, Hassaniene et al. (2004b, c) considered the effect of variable permeability for the case of variable wall temperature and the effect of inertia in the case of surface mass flux.

The above studies have been made on the assumption of parallel flow. Bassom and Rees (1995) pointed out the inadequacy of this approach and reexamined the problem using asymptotic techniques that use the distance downstream as a large parameter. The parallel-flow theories predict that at each downstream location there are two possible wave numbers for neutral stability, and one of these is crucially dependent on non-parallelism within the flow. The nonparallel situation and inertial effects have been treated analytically and numerically by Zhao and Chen (2002, 2003) for the case of horizontal and inclined plates. They found that the nonparallel flow model predicts a more stable flow than the parallel-flow model. They also noted that as the inclination relative to the horizontal increases, or the inertia effect as measured by a Forchheimer number increases, the surface heat transfer rate decreases and the flow becomes more stable.

Comprehensive and critical reviews of thermal boundary-layer instabilities were made by Rees (1998, 2002c). In the first study he pointed out an inconsistency in the analysis of Jang and Chang (1988a, 1989) and Jang and Lie (1992) that negates their claim that their analysis is valid for a wide range of inclinations; rather, it applies for a near-horizontal surface only. Rees (1998) also noted that the analysis of Jang and Chen (1993a, b) involves a nongeneric formula for permeability variation. The basic difficulty is that a contradiction is entertained by asserting simultaneously that  $x$ , the nondimensional streamwise distance, is

asymptotically large (so that the boundary-layer approximation is valid) and that finite values of  $x$  are to be computed as a result of approximating the stability equations, and in general this critical value of  $x$  is far too small for the boundary-layer approximation to be valid.

One way out of the impasse is to carry out fully elliptic simulations. This was the avenue taken by Rees and Bassom (1993) in their description of wave instabilities in a horizontal layer. The second way out is to consider heated surfaces that are very close to the vertical but which remain upward facing. In such cases the critical distance recedes to large distances from the leading edge, and therefore instability arises naturally in a regime where the boundary-layer approximation is valid. This was the avenue taken by Rees (2001, 2002a) in his study of the linear and nonlinear evolution of vortex instabilities in near-vertical surfaces. Rees found that even under these favorable circumstances the concept of neutral stability is difficult to define. The reason is that the evolution of vortices is governed by a parabolic partial differential equation system rather than an ordinary differential equation system. As a result the point at which instability is “neutral” depends on whether instability is defined as the value of  $x$  at which the thermal energy has a local minimum as  $x$  increases or where the surface rate of heat transfer or the maximum disturbance temperature has minima. Whenever vortices grow, they attain a maximum strength and then decay again, and there is an optimum disturbance amplitude that yields the largest possible response downstream. When applied to developing flows such as boundary layers, these three criteria yield different results. In addition of the wavelength of the vortex, the location of the initiating disturbance and its shape also alter the critical value of  $x$ .

The linear and nonlinear evolution of vortex instabilities in near-vertical surfaces was studied by Rees (2001, 2002a). He found that the strength of the resulting convection depends not only on the wavelength of the vortex disturbance but also on the amplitude of the disturbance and its point of introduction into the boundary layer. Whenever vortices grow, they attain a maximum strength and then decay again. There is an optimum disturbance amplitude that yields the largest possible response downstream. The later study by Rees (2004b) involved the destabilizing of an evolving vortex using subharmonic disturbances. He found that the onset of the destabilization is fairly sudden, but its location depends on the size of the disturbance. Rees also looked at the evolution of isolated thermal vortices. He found then that developing vortices induce a succession of vortices outboard of the current local pattern until the whole spanwise domain is filled with a distinctive wedge-shaped pattern.

The effect of variable permeability, for the case of a horizontal or inclined plate, was studied by Elaiw (2008), Elaiw and Ibrahim (2008), and Elaiw et al. (2007, 2009) and discussed by Rees and Pop (2010). The effect of a magnetic field was examined by Jang and Hsu (2007, 2009b).

For the case of uniform surface suction, the nonlinear development of vortex instabilities has been studied by Rees (2009b), for the case where the Péclet number based on the external velocity is sufficiently large. He found that the

resulting thermal boundary layer develops in a nonsimilar manner until it attains an asymptotic state which is independent of the streamwise coordinate,  $x$ , when it is dominated by surface suction. For sufficiently large but moderate  $Ra$  this boundary layer becomes unstable to streamwise vortex disturbance, and he used a parabolic solver to determine how such disturbances, when placed very close to the leading edge, evolve with  $x$ . He defined neutral stability to be when a suitable energy functional ceases to decay/grow as  $x$  increases. He thus mapped out a neutral curve based on the behavior of this function. He then extended his linearized analysis into the nonlinear domain and ascertained the effect of different magnitudes of disturbances. He found that a rich variety of vortex patterns, including wavy vortices and abrupt changes in perceived wavelength, something that is sometimes sensitively dependent on the values of the governing parameters.

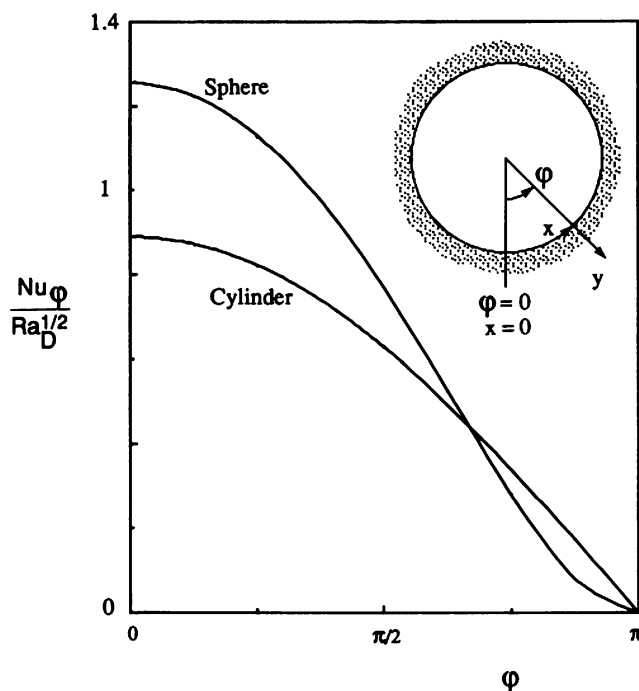


**Fig. 5.15** Local Nusselt number variation for high Rayleigh number natural convection over a horizontal cylinder and a sphere

## 5.5 Horizontal Cylinder

### 5.5.1 Flow at High Rayleigh Number

We now consider steady natural convection about an isothermal cylinder, at temperature  $T_w$  and with radius  $r_0$ , embedded in a porous medium at temperature  $T_\infty$ . We choose a curvilinear orthogonal system of coordinates, with  $x$  measured along the cylinder from the lower stagnation point (in a plane of cross section),  $y$  measured radially (normal to the cylinder), and  $\varphi$  the angle that the  $y$  axis makes with the downward vertical. This system is presented in Fig. 5.15.

If curvature effects and the normal component of the gravitational force are neglected, the governing boundary-layer equations are

$$\frac{\partial^2 \Psi}{\partial y^2} = \frac{g\beta K}{v} \sin \phi \frac{\partial}{\partial y} (T - T_\infty) \quad (5.100)$$

$$\alpha_m \frac{\partial^2 T}{\partial y^2} = \frac{\partial \Psi}{\partial y} \frac{\partial T}{\partial x} - \frac{\partial \Psi}{\partial x} \frac{\partial T}{\partial y}. \quad (5.101)$$

It is easily checked that the solutions of Eqs. (5.100) and (5.101), subject to the boundary conditions (5.9) and (5.10) with  $\lambda = 0$ , are given by

$$\Psi = \left[ \frac{g\beta K}{v} (T_w - T_\infty) \alpha_m r_0 \right]^{1/2} (1 - \cos \phi)^{1/2} f(\eta), \quad (5.102)$$

$$T - T_\infty = (T_w - T_\infty) \theta(\eta), \quad (5.103)$$

$$\eta = \left[ \frac{g\beta K (T_w - T_\infty)}{v \alpha_m r_0} \right]^{1/2} \frac{y \sin \phi}{(1 - \cos \phi)^{1/2}}, \quad (5.104)$$

where  $f$  and  $\theta$  satisfy Eqs. (5.15, 5.16, 5.17, and 5.18) with  $\lambda = 0$ . Accordingly, the local surface heat flux is

$$q''_w = -k_m \left( \frac{\partial T}{\partial y} \right)_{=0} = 0.444 k_m (T_w - T_\infty)^{3/2} \left( \frac{g\beta K}{v_m r_0} \right)^{1/2} \frac{\sin \varphi}{(1 - \cos \varphi)^{1/2}}, \quad (5.105)$$

which can be expressed in dimensionless form as

$$\frac{Nu_\phi}{Ra_D^{1/2}} = 0.628 \frac{\sin \phi}{(1 - \cos \phi)^{1/2}}, \quad (5.106)$$

where

$$Nu_\varphi = \frac{q''_w D}{k_m(T_w - T_\infty)} \quad (5.107)$$

and

$$Ra_D = \frac{g\beta K(T_w - T_\infty)D}{\nu\alpha_m}, \quad (5.108)$$

with  $D$  denoting the diameter of the cylinder. This result is plotted in Fig. 5.15. The average surface heat flux is

$$\bar{q}'' = \frac{1}{\pi} \int_0^\pi q''_w(\phi) d\phi = 0.565 k_m (T_w - T_\infty)^{3/2} \left( \frac{g\beta K}{\nu\alpha_m D} \right)^{1/2}, \quad (5.109)$$

which in dimensionless form is

$$\frac{Nu}{Ra_D^{1/2}} = 0.565, \quad (5.110)$$

where

$$\overline{Nu} = \frac{\bar{q}'' D}{k} (T_w - T_\infty). \quad (5.111)$$

The present problem is a special case of convection about a general two-dimensional heated body analyzed by Merkin (1978). The generalization to a non-Newtonian power-law fluid was made by Chen and Chen (1988b) and for the Forchheimer model by Kumari and Jayanthi (2004).

The conjugate steady convection from a horizontal circular cylinder with a heated core was investigated by Kimura and Pop (1992b). The method of matched asymptotic expansions was applied by Pop et al. (1993a) to the transient problem with uniform temperature. They found that vortices then form at both sides of the cylinder. An extension of this work to a cylinder of arbitrary cross section was reported by Tyvand (1995). For the circular cylinder, a numerical treatment was reported by Bradean et al. (1997b), and further work on transient convection was discussed by Bradean et al. (1998a). They found that, as convection becomes more dominant, a single hot cell forms vertically above the cylinder and then rapidly moves away. Free convection about a cylinder of elliptic cross section was treated by Pop et al. (1992b). Transient convection about a cylinder with constant surface flux heating was dealt with by Pop et al. (1996). A problem involving unsteady convection driven by an  $n$ th-order irreversible reaction was examined by Nguyen et al. (1996). Natural and forced convection around line sources of heat and heated cylinders was analyzed by Kurdyumov and Liñán (2001). Convection near the stagnation point of a two-dimensional cylinder, with the surface temperature oscillating about a mean above ambient, was analyzed by

Merkin and Pop (2000). An analysis of soil heating systems was made by Ngo and Lai (2009). The case of local thermal nonequilibrium was studied by Saied (2006a) and Cheng (2007b), who extended his study of cylinders of elliptic cross section (Cheng 2006b). The nonlinear development of vortex instabilities with uniform suction was studied by Rees (2009b). The effect of variable permeability was examined by Elaiw (2008), Elaiw and Ibrahim (2008), and Elaiw et al. (2007, 2009). The effect of a magnetic field was studied by Jang and Hsu (2007, 2009). A cylinder wrapped with a porous layer was studied by Ait Saada et al. (2007) and Bhattacharyya and Singh (2009). Unsteady flow over a cylinder was treated by Kumari and Nath (2009c). The case of a nanofluid and a cylinder of elliptic cross-section was studied by Cheng (2012c).

Empirical heat transfer correlation equations, with viscous dissipation taken into account, were reported by Fand et al. (1994). Experiments on heat transfer from a cylinder were conducted by Jamin and Mohamad (2008).

### 5.5.2 Flow at Low and Intermediate Rayleigh Number

The experimental results obtained by Fand et al. (1986) on heat transfer in a porous medium consisting of randomly packed glass spheres saturated by either water or silicone oil suggested the division of the Rayleigh number range into a low  $Ra$  (and hence low Reynolds number  $Re$ ) Darcy range and a high  $Ra$  Forchheimer range. Fand et al. (1986) proposed the following correlation formulas: For ( $0.001 < Re_{\max} = 3$ ),

$$Nu Pr^{0.0877} = 0.618 Ra^{0.698} + 8.54 \times 10^6 Ge \operatorname{sech} Ra, \quad (5.112)$$

while for ( $3 < Re_{\max} = 100$ ),

$$Nu Pr^{0.0877} = 0.766 Ra^{0.374} \left( \frac{C_1 D}{C_2} \right)^{0.173}. \quad (5.113)$$

In these correlations,

$$\begin{aligned} Re_{\max} &= \frac{D v_{\max}}{V}, & Nu &= \frac{hD}{k_m}, & Pr &= \frac{\mu c_p}{k_m}, & Ge &= \frac{g \beta D}{c_p}, \\ Ra &= \frac{g \beta K D (T_w - T_\infty)}{v \alpha_m}, \end{aligned} \quad (5.114)$$

where  $D$  is the diameter of the cylinder,  $v_{\max}$  is the maximum velocity,  $h$  is the heat transfer coefficient, and  $C_1$  and  $C_2$  are the dimensional constants appearing in Forchheimer's equation expressed in the form

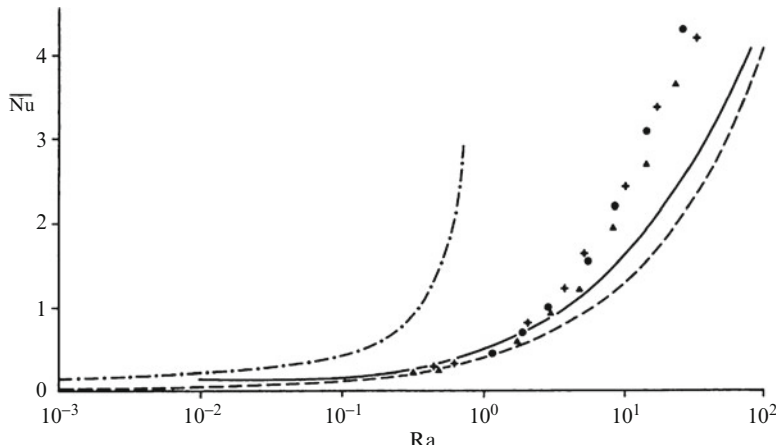


**Fig. 5.16** The variation of the mean Nusselt number with Rayleigh number. - - - numerical solution; - - - - boundary layer solution; - - - - small Rayleigh number solution; •, △, +, experimental results using spheres of diameter 2, 3, and 4 mm, respectively (Ingham and Pop 1987c, with permission from Cambridge University Press)

$$-\frac{dP}{dx} = C_1 \mu u + C_2 \rho u^2. \quad (5.115)$$

The correlation formulas (5.112) and (5.113) may be compared with the Darcy model boundary-layer formula

$$Nu = 0.565 Ra^{1/2} \quad (5.116)$$

and the Forchheimer model boundary-layer formula found by Ingham and quoted by Ingham and Pop (1987c)

$$Nu \propto Ra^{1/4} \left( \frac{vD\chi}{\alpha_m K} \right)^{1/2}. \quad (5.117)$$

The effect of  $d/D$ , the ratio of particle diameter to cylinder diameter, was investigated experimentally by Fand and Yamamoto (1990). They noted that the reduction in the heat transfer coefficient due to wall porosity variation increases with  $d/D$ .

Ingham and Pop (1987c) performed finite-difference calculations for streamlines, isotherms, and Nusselt numbers for  $Ra$  up to 400. Their results for an average Nusselt number  $\bar{Nu}$  defined by

$$\overline{Nu} = -\frac{1}{2\pi} \int_0^{2\pi} \left. \frac{\partial \Theta}{\partial r} \right|_{r=1} d\theta \quad (5.118)$$

are given in Fig. 5.16. The dimensionless temperature difference is defined as  $\Theta = (T - T_\infty) / (T_w - T_\infty)$ .

## 5.6 Sphere

### 5.6.1 Flow at High Rayleigh Number

With the  $x$  and  $y$  axes chosen in a vertical diametral plane of the sphere, and with  $x$  measured along the sphere from the lower stagnation point and  $y$  measured radially outward from the surface (Fig. 5.15), the governing boundary-layer equations are

$$\frac{1}{r} \frac{\partial^2 \Psi}{\partial y^2} = \frac{g\beta K \sin \phi}{v} \frac{\partial}{\partial y} (T - T_\infty), \quad (5.119)$$

$$\alpha_m \frac{\partial^2 T}{\partial y^2} = \frac{1}{r} \left( \frac{\partial \Psi}{\partial y} \frac{\partial T}{\partial x} - \frac{\partial \Psi}{\partial x} \frac{\partial T}{\partial y} \right). \quad (5.120)$$

The streamfunction  $\psi$  is defined by

$$ru = \frac{\partial \Psi}{\partial y}, \quad rv = -\frac{\partial \Psi}{\partial x}, \quad (5.121)$$

where  $r = r_0 \sin \varphi$  and  $r_0$  is the radius of the sphere. Again, the boundary conditions are given by Eqs. (5.9) and (5.10), with  $\lambda = 0$ . The problem admits the similar solution (Cheng 1985a)

$$\Psi = \alpha_m \left[ \frac{g\beta K(T_w - T_\infty)r_0^3}{v\alpha_m} \left( \frac{\cos^3 \phi}{3} - \cos \phi + \frac{2}{3} \right) \right]^{1/2} f(\eta), \quad (5.122)$$

$$\frac{T - T_\infty}{T_w - T_\infty} = \theta(\eta), \quad (5.123)$$

$$\eta = \frac{y}{r_0} \left[ \frac{g\beta K(T_w - T_\infty)r_0}{v\alpha_m} \right]^{1/2} \frac{\sin^2 \phi}{[(\cos^3 \phi)/3 - \cos \phi + 2/3]^{1/2}}, \quad (5.124)$$

where  $f$  and  $\theta$  satisfy Eqs. (5.15, 5.16, 5.17, and 5.18) with  $\lambda = 0$ . Accordingly the local surface heat flux is given by

$$q''_w = 0.444k_m(T_w - T_\infty)^{3/2} \left( \frac{g\beta K}{v\alpha_m r_0} \right)^{1/2} \frac{\sin^2 \varphi}{[(\cos^3 \varphi)/3 - \cos \varphi + 2/3]^{1/2}} \quad (5.125)$$

which in dimensionless form is

$$\frac{Nu_\phi}{Ra_D^{1/2}} = 0.628 \frac{\sin^2 \phi}{[(\cos^3 \phi)/3 - \cos \phi + 2/3]^{1/2}}. \quad (5.126)$$

This result is plotted in Fig. 5.15, which shows that the local heat transfer rate for a sphere is higher than that for a horizontal cylinder except near the upper stagnation point. The average surface heat flux is

$$\begin{aligned} \bar{q}'' &= \frac{1}{4\pi r_0^2} \int_0^\pi 2\pi r_0^2 q''_w(\varphi) \sin \varphi d\varphi \\ &= \frac{0.888}{3^{1/2}} k_m (T_w - T_\infty)^{3/2} \left( \frac{g\beta K}{v\alpha_m r_0} \right)^{1/2} \end{aligned} \quad (5.127)$$

which in dimensionless form reduces to

$$\frac{Nu}{Ra_D^{1/2}} = 0.724. \quad (5.128)$$

This problem is a special case of the natural convection about a general axisymmetric heated body embedded in a porous medium, analyzed by Merkin (1979). The extension to include the effect of normal pressure gradients on convection in a Darcian fluid about a horizontal cylinder and a sphere has been provided by Nilson (1981). The extension to a non-Newtonian power-law theory was made by Chen and Chen (1988b).

Conjugate steady convection from a solid sphere with a heated core of uniform temperature was investigated by Kimura and Pop (1994). The transient problem, where either the temperature or the heat flux of the sphere is suddenly raised and subsequently maintained at a constant value, was treated numerically for both small and large values of the Rayleigh number by Yan et al. (1997).

The analogous problem of convective mass transfer from a sphere was studied experimentally by Rahman (1999). MHD convection over a permeable sphere with internal heat generation was analyzed by Yih (2000a) and Beg et al. (2009d). Chamkha et al. (2011) studied the case of a nanofluid. Mukhopadhyay (2008) examined flow over a sphere in the presence of a heat source/sink near a stagnation point. Moghimi et al. (2011) studied heat generation/absorption effects with an MHD flow.

### 5.6.2 Flow at Low Rayleigh Number

This topic was first studied by Yamamoto (1974). When  $Ra$  is small, we can use a series expansion in powers of  $Ra$ . Using a spherical polar coordinate system  $(r, \theta, \varphi)$  and a Stokes streamfunction  $\psi$ , we can write the governing equations in nondimensional form, for the case of constant surface temperature  $T_w$ ,

$$\frac{1}{\sin \theta} \frac{\partial^2 \Psi}{\partial r^2} + \frac{1}{r^2} \frac{\partial}{\partial \theta} \left( \frac{1}{\sin \theta} \frac{\partial \Psi}{\partial \theta} \right) = Ra \left( \cos \theta \frac{\partial \Theta}{\partial r} + r \sin \theta \frac{\partial \Theta}{\partial r} \right). \quad (5.129)$$

$$\frac{\partial \Psi}{\partial \theta} \frac{\partial \Theta}{\partial r} - \frac{\partial \Psi}{\partial r} \frac{\partial \Theta}{\partial \theta} = \sin \theta \frac{\partial}{\partial r} \left( r^2 \frac{\partial \Theta}{\partial r} \right) + \frac{\partial}{\partial \theta} \left( \sin \theta \frac{\partial \Theta}{\partial \theta} \right). \quad (5.130)$$

In these equations we have used the definitions

$$\Theta = \frac{T - T_\infty}{T_w - T_\infty}, \quad Ra = \frac{g \beta K a (T_w - T_\infty)}{\nu \alpha_m}, \quad (5.131)$$

and  $r$  is the nondimensional radial coordinate scaled with  $a$ , the radius of the sphere. The boundary and symmetry conditions are

$$\begin{aligned} r = 1 : \quad \Theta = 1, \quad \frac{\partial \Psi}{\partial \theta} = 0, \\ r \rightarrow \infty : \quad \Theta = 0, \quad \frac{\partial \Psi}{\partial \theta} = 0, \quad \frac{\partial \Psi}{\partial r} = 0, \\ \theta = 0, \quad \pi : \frac{\partial \Theta}{\partial \theta} = 0, \quad \frac{\partial \Psi}{\partial r} = 0, \quad \frac{\partial}{\partial \theta} \left( \frac{1}{\sin \theta} \frac{\partial \Psi}{\partial \theta} \right) = 0. \end{aligned} \quad (5.132)$$

The solution is obtained by writing

$$(\Psi, \Theta) = (\Psi_0, \Theta_0) + Ra(\Psi_1, \Theta_1) + Ra^2(\Psi_2, \Theta_2) + \dots, \quad (5.133)$$

substituting and solving in turn the problems of order 0,1,2, ... in  $Ra$ . One finds that

$$\Psi_0 = 0, \quad \Theta_0 = \frac{1}{r}, \quad (5.134)$$

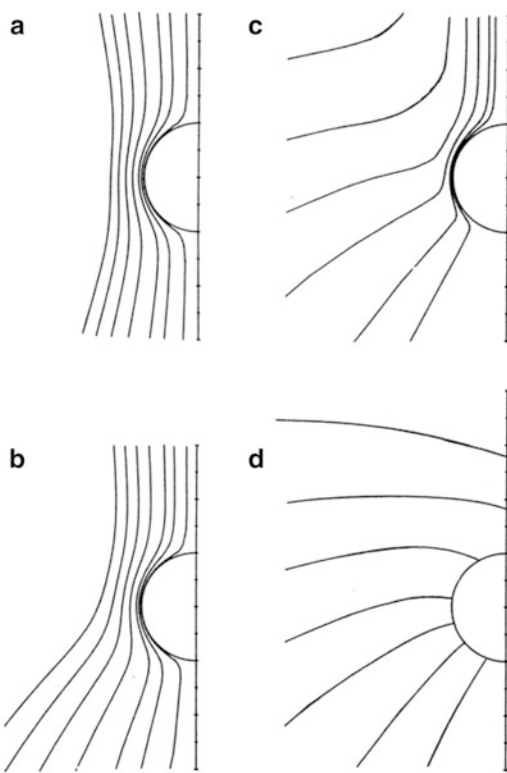
$$\Psi_1 = \frac{1}{2} (r - r^{-1}) \sin^2 \theta, \quad \Theta_1 = \frac{1}{4} (2r^{-1} - 3r^{-2} + r^{-3}) \cos \theta, \quad (5.135)$$

$$\Psi_2 = \frac{1}{24} (4r - 9 + 6r^{-1} - r^2) \sin^2 \theta \cos \theta, \quad (5.136)$$

**Table 5.3** The overall Nusselt number for an isothermal sphere embedded in a porous medium (Pop and Ingham 1990)

$\frac{1}{2}Ra_D$	Boundary-layer solution	Numerical solution
1	0.5124	2.1095
10	1.6024	2.8483
20	2.2915	3.2734
40	3.2407	3.9241
70	4.2870	5.0030
100	5.1240	5.8511
150	6.2756	7.0304
200	7.2464	8.2454

**Fig. 5.17** The streamlines in the vicinity of a sphere: (a)  $Ra = 1$ , (b)  $Ra = 10$ , (c)  $Ra = 100$ , and (d) asymptotic solution (Pop and Ingham 1990, with permission from Hemisphere Publishing Corporation)



$$\begin{aligned}\Theta_2 = & -\frac{13}{180}r^{-1} + \frac{11}{240}r^{-3}\ln r + \frac{31}{224}r^{-3} - \frac{13}{144}r^{-4} \\ & + \frac{27}{1,120}r^{-5} + \left( \frac{5}{48}r^{-1} - \frac{3}{8}r^{-2} + \frac{11}{80}r^{-3}\ln r \right. \\ & \left. + \frac{223}{672}r^{-3} - \frac{1}{12}r^{-4} + \frac{5}{224}r^{-5} \right) \cos 2\theta.\end{aligned}\quad (5.137)$$

**Table 5.4** Values of the constant  $C'$  in Eq. (5.139) for various values of the power-law exponent  $\lambda$  (Cheng 1985a)

$\lambda$	$C'$
0	0.30
1/4	0.23
1/3	0.21
1/2	0.20
3/4	0.17
1	0.15

Working from the second-order approximation  $\Psi = Ra \Psi_1 + Ra^2 \Psi_2$ , Ene and Polievski (1987) found that, whereas for  $Ra < 3$  the streamline pattern was unicellular, for  $Ra > 3$  a second cell appears below the sphere. This is apparently an artifact of their solution, resulting from the nonconvergence of the series for  $Ra > 3$ . No second cell was found by Pop and Ingham (1990).

For convection around a sphere that is suddenly heated and subsequently maintained at a constant heat flux or constant temperature, asymptotic solutions were obtained by Sano and Okihara (1994), Sano (1996), and Ganapathy (1997).

### 5.6.3 Flow at Intermediate Rayleigh Number

In addition to obtaining a second-order boundary-layer theory for large  $Ra$ , Pop and Ingham (1990) used a finite-difference scheme to obtain numerical results for finite values of  $Ra$ . Their results are shown in Table 5.3 and Fig. 5.17. They expressed their heat transfer results in terms of a mean Nusselt surface  $\overline{Nu}$  defined by

$$\overline{Nu} = -\frac{1}{2} \int_0^\pi \left( \frac{\partial \Theta}{\partial r} \right)_{r=1} \sin \theta d\theta, \quad (5.138)$$

## 5.7 Vertical Cylinder

For the problem of natural convection about a vertical cylinder with radius  $r_0$ , power-law wall temperature, and embedded in a porous medium, similarity solutions do not exist. An approximate solution was obtained by Minkowycz and Cheng (1976). For a given value of the power-law exponent  $\lambda$ , Eq. (5.8), they found that the ratio of local surface heat flux of a cylinder ( $q''_c$ ) to that of a flat plate ( $q''$ ) is a nearly linear function of a curvature parameter  $\xi$

$$\frac{q''_c}{q''} = 1 + C' \xi, \quad (5.139)$$

where

$$\xi = \frac{2x}{r_0 Ra_x^{1/2}}, \quad (5.140)$$

where  $x$  denotes the vertical coordinate along the axis of the cylinder and  $q''$  is given by Eq. (5.25). The values of the positive constant  $C'$  are given in Table 5.4.

The ratio of average heat fluxes  $\bar{q}''_c/\bar{q}''$  turns out to be independent of  $\lambda$  and is given approximately by

$$\frac{\bar{q}''_c}{\bar{q}''} = 1 + 0.26\xi_L, \quad (5.141)$$

where  $\xi_L = 2L/r_0 Ra_L^{1/2}$ , and  $L$  is the height of the cylinder. The average heat flux for the vertical plate ( $\bar{q}''$ ) is given by Eq. (5.27).

A detailed solution was obtained by Merkin (1986). Magyari and Keller (2004a) showed that the flow induced by a nonisothermal vertical cylinder approaches the shape of Schlichting's round jet as the porous radius tends to zero. The effects of surface suction or blowing were examined by Huang and Chen (1985); suction increases the rate of heat transfer. The transient problem has been analyzed by Kimura (1989b).

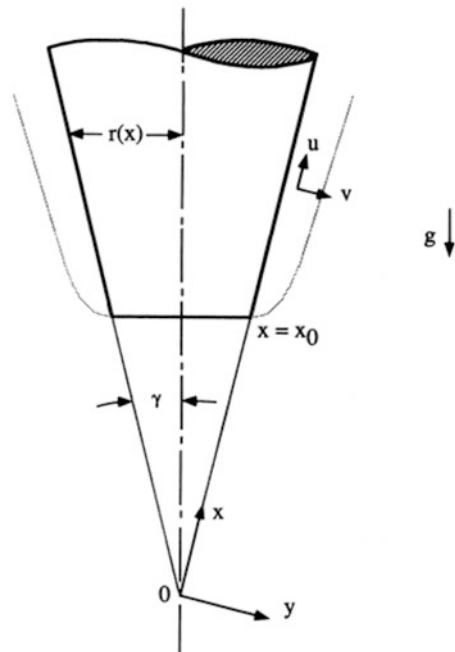


**Fig. 5.18** Coordinate system for the boundary layer on a heated frustum of a cone (Cheng et al. 1985)

Asymptotic analyses and numerical calculations for this problem were reported by Bassom and Rees (1996). They showed that when  $\lambda < 1$ , the asymptotic flowfield for the leading edge of the cylinder takes on a multiple layer structure. However, for  $\lambda > 1$ , only a simple single layer is present far downstream, but a multiple layer structure exists close to the leading edge of the cylinder.

The effects of surface suction or blowing were examined by Huang and Chen (1985); suction increases the rate of heat transfer. Inertial effects and those of suction were analyzed by Hossain and Nakayama (1993). The case of suction with a non-Newtonian fluid (for a vertical plate or a vertical cylinder) was investigated by Pascal and Pascal (1997). The transient problem has been analyzed by Kimura (1989b), while Libera and Poulikakos (1990) and Pop and Na (2000) have treated a conjugate problem. The effect of thermal stratification was added by Chen and Horng (1999) and Takhar et al. (2002). An analogous mass transfer problem was studied experimentally by Rahman et al. (2000). The effect of local thermal nonequilibrium was investigated by Rees et al. (2003a) and Shakeri et al. (2012). The effect of radiation was studied numerically by Yih (1999e). The problem with thermophoresis was examined by Chamkha et al. (2004), while El-Hakiem included the effects of radiation and temperature-dependent viscosity.

## 5.8 Cone

We consider an inverted cone with semiangle  $\gamma$  and take axes in the manner indicated in Fig. 5.18. The boundary layer develops over the heated frustum  $x = x_0$ . In terms of the streamfunction  $\psi$  defined by

$$u = \frac{1}{r} \frac{\partial \Psi}{\partial y}, \quad v = -\frac{1}{r} \frac{\partial \Psi}{\partial x}, \quad (5.142)$$

the boundary-layer equations are

$$\frac{1}{r} \frac{\partial^2 \Psi}{\partial y^2} = \frac{g\beta K}{v} \frac{\partial T}{\partial y}, \quad (5.143)$$

$$\frac{1}{r} \left( \frac{\partial \Psi}{\partial y} \frac{\partial T}{\partial x} - \frac{\partial \Psi}{\partial x} \frac{\partial T}{\partial y} \right) = \alpha_m \frac{\partial^2 T}{\partial y^2}. \quad (5.144)$$

For a thin boundary layer we have approximately  $r = x \sin \gamma$ . We suppose that either a power law of temperature or a power law of heat flux is prescribed on the frustum. Accordingly, the boundary conditions are

$$y \rightarrow \infty : u = 0, \quad T = T_\infty.$$

**Table 5.5** Values of  $\theta'(0)$  and  $\hat{\theta}(0)$  for calculating the local Nusselt number on a vertical cone embedded in a porous medium (Cheng et al. 1985)

$\lambda$	$\theta'(0)$	$\hat{\theta}(0)$
0	-0.769	1.056
1/3	-0.921	0.992
1/2	-0.992	0.965

$$y = 0, \quad x_0 \leq x < \infty : u = 0, \quad \text{and either} \quad T = T_w = T_\infty + (x - x_0)^\lambda \quad (5.145)$$

or

$$-k_m \frac{\partial T}{\partial y} \Big|_{y=0} = q''_w = A(x - x_0)^\lambda.$$

For the case of a full cone ( $x_0 = 0$ ) a similarity solution exists. In the case of prescribed  $T_w$ , we let

$$\Psi = \alpha_m r Ra_x^{1/2} f(\eta), \quad (5.146)$$

$$T - T_\infty = (T_w - T_\infty) \theta(\eta), \quad (5.147)$$

$$\eta = \frac{y}{x} Ra_x^{1/2}, \quad (5.148)$$

where

$$Ra_x = \frac{g \beta K \cos \gamma (T_w - T_\infty) x}{\nu \alpha_m}. \quad (5.149)$$

The dimensionless momentum and energy equations are

$$f' = \theta, \quad (5.150)$$

$$\theta'' + \left( \frac{\lambda + 3}{2} \right) f \theta' - \lambda f' \theta = 0, \quad (5.151)$$

with boundary conditions

$$f(0) = 0, \quad \theta(0) = 1, \quad \theta(\infty) = 0. \quad (5.152)$$

The local Nusselt number is given by

$$Nu_x = Ra_x^{1/2}[-\theta'(0)], \quad (5.153)$$

for which computed values of  $\theta'(0)$  are given in Table 5.5.

The case of a cone with prescribed uniform heat flux  $q''_w$  is handled similarly. We begin with the dimensionless variables

$$\Psi = \alpha_m r \hat{Ra}_x^{1/3} f(\hat{\eta}), \quad (5.154)$$

$$T - T_\infty = \frac{q''_w x}{k_m} \hat{Ra}_x^{-1/3} \hat{\theta}(\hat{\eta}). \quad (5.155)$$

$$\hat{\eta} = \frac{y}{x} \hat{Ra}_x^{1/3}, \quad (5.156)$$

where the Rayleigh number is based on heat flux,

$$\hat{Ra}_x = \frac{g \beta K \cos \gamma q''_w x^2}{\nu \alpha_m k_m}. \quad (5.157)$$

The governing equations become

$$\hat{f}' = \hat{\theta}, \quad (5.158)$$

$$\hat{\theta}'' + \left( \frac{\lambda+5}{2} \right) \hat{f}' \hat{\theta}' - \left( \frac{2\lambda+1}{3} \right) \hat{f}' \hat{\theta} = 0, \quad (5.159)$$

subject to

$$\hat{f}'(0) = 0, \quad \hat{\theta}'(0) = -1, \quad \hat{\theta}(\infty) = 0. \quad (5.160)$$

The local Nusselt number solution to this problem is

$$Nu_x = \hat{Ra}_x^{1/3} [\hat{\theta}(0)]^{-1}, \quad (5.161)$$

with the computed values of  $\hat{\theta}(0)$  given in Table 5.5. The local Nusselt number is defined in the usual way:  $Nu_x = q''_w x / k_m (T_w - T_\infty)$ . Note that in the present (constant  $q''$ ) configuration the cone temperature  $T_w$  is a function of  $x$ .

No similarity solution exists for the truncated cone, but Cheng et al. (1985) obtained results using the local nonsimilarity method. Pop and Cheng (1986) included the curvature effects that become important when the cone is slender. Vasantha et al. (1986) treated non-Darcy effects for a slender frustum, and Nakayama et al. (1988a) have also considered inertial effects.

A cone with a point heat source at the apex was considered by Afazal and Salam (1990). Pop and Na (1994, 1995) studied convection on an isothermal wavy cone or frustum of a wavy cone, for large  $Ra$ , under the assumption that the wavy surface has amplitude and wavelength of order one. They presented results for the effect of the sinusoidal surface on the wall heat flux.

Rees and Bassom (1991) examined convection in a wedge-shaped region bounded by two semi-infinite surfaces, one heated isothermally and the other insulated. For the particular cases (i) a vertical heated surface with a wedge angle of  $\pi$ , and (ii) a horizontal upward-facing surface with a wedge angle of  $3\pi/2$ , the equations on the Darcy model reduce to the classic ordinary differential equations.

Non-Darcy hydromagnetic convection over a cone or wedge was studied by Chamkha (1996). Other MHD studies were conducted by Mahdy et al. (2008) for a wavy cone, by Mahmoud and Megahed (2009) for a non-Newtonian fluid, and by Seddeek (2007) for a cone or wedge with radiation. Variable viscosity and thermal conductivity effects on convection from a cone or wedge were studied numerically by Hassani et al. (2003b). For convection over a cone, the effect of uniform lateral mass flux was studied by Yih (1997a, b, 1998b) for the case of Newtonian or non-Newtonian fluids and with a Forchheimer effect by Kumari and Jayanthi (2005) for a non-Newtonian fluid. Mahmoud (2011) included the effect of variable viscosity of a power-law fluid. Convection over a horizontal cone was studied by Kumari and Nath (2010). The homotopy analysis method was applied to a vertical cone by Sohouli et al. (2008, 2009). The case of a vertical cone with a power-law fluid and viscous dissipation was treated numerically by Mahmoud (2012).

## 5.9 General Two-Dimensional or Axisymmetric Surface

Nakayama and Koyama (1987a) have shown how it is possible to obtain similarity solutions to the boundary-layer equations for flow about heated two-dimensional or axisymmetric bodies of arbitrary shape provided that the wall temperature is a power function of a variable  $\xi$ , which is a certain function of the streamwise coordinate  $x$ . Then the governing equations reduce to those for a vertical flat plate. They thus generalized Merkin's (1979) results for the isothermal case.

A simple analysis of convection about a slender body of revolution with its axis vertical was given by Lai et al. (1990c). In terms of cylindrical polar coordinates with  $x$  in the axial direction and  $r$  in the radial direction, the governing boundary-layer equations are

$$\frac{\partial}{\partial r} \left( \frac{1}{r} \frac{\partial \Psi}{\partial r} \right) = \frac{g\beta K}{v} \frac{\partial T}{\partial r}, \quad (5.162)$$

$$\frac{\partial \Psi}{\partial r} \frac{\partial T}{\partial x} - \frac{\partial \Psi}{\partial x} \frac{\partial T}{\partial r} = \alpha_m \frac{\partial}{\partial r} \left( r \frac{\partial T}{\partial r} \right). \quad (5.163)$$

The boundary conditions at the body surface [ $r = R(x)$ ] and far from the surface ( $r \rightarrow \infty$ ) are, respectively,

$$T = T_w(x) = T_\infty + Ax^\lambda, v = 0, \quad (5.164)$$

$$T = T_\infty, \quad u = 0. \quad (5.165)$$

Suitable similarity variables are defined by

$$\eta = Ra_x \left( \frac{r}{x} \right)^2, \quad (5.166)$$

$$\Psi = \alpha_m x f(\eta), \quad (5.167)$$

$$T - T_\infty = (T_w - T_\infty) \theta(\eta), \quad (5.168)$$

where

$$Ra_x = \frac{g\beta K(T_w - T_\infty)x}{v\alpha_m}. \quad (5.169)$$

If we set  $\eta = a_{nc}$ , where  $a_{nc}$  is a numerically small constant, we have prescribed the surface of a slender body, given by

$$r = \left( \frac{v\alpha_m a_{nc}}{g\beta K A} \right)^{1/2} x^{(1-\lambda)/2}. \quad (5.170)$$

This represents a cylinder when  $\lambda = 1$ , a paraboloid when  $\lambda = 0$  and a cone when  $\lambda = -1$ . The resulting equations are

$$2f' = \theta, \quad (5.171)$$

$$2\eta\theta'' + (2+f)\theta' - \lambda f'\theta = 0 \quad (5.172)$$

with boundary conditions

$$\eta = a_{nc} : \quad \theta = 1, f + (\lambda - 1)\eta f' = 0, \quad (5.173)$$

$$\eta \rightarrow \infty : \theta = 0, \quad f' = 0. \quad (5.174)$$

These equations can be easily solved numerically, and the local Nusselt number is then given by

$$\frac{Nu}{Ra^{1/2}} = -2a_{nc}^{1/2}\theta'(a_{nc}). \quad (5.175)$$

Inertial effects were examined by Ingham (1986) and Nakayama et al. (1989, 1990). The effects of a stratified medium were discussed by Nakayama and Koyama (1989) and those of viscous dissipation by Nakayama and Pop (1989). Convection from a nonisothermal axisymmetric surface was analyzed by Mehta and Sood (1994). Flow of non-Newtonian power-law fluids over nonisothermal bodies of arbitrary shape was studied by Nakayama and Koyama (1991) and also, for the case of permeable bodies, by Wang et al. (2002). Certain wall temperature distributions lead to similarity solutions. A general transformation procedure, for the transient problem and the Forchheimer model, was presented by Nakayama et al. (1991). With this the local-similarity assumption was adapted to produce solutions for a range of geometries. Power-law fluid flow, with or without yield stress, was also discussed by Yang and Wang (1996). Power-law fluids were also treated by El-Amin et al. (2011b) and Abdel-Gaied and Eid (2011). Similarity solutions for convection due to internal heating were obtained by Bagai (2003, 2004) for the cases of constant or variable viscosity. Unsteady stagnation point flow over a three-dimensional body was studied by Hassanien et al. (2006). A problem with variable viscosity, a non-Newtonian fluid and internal heat generation was studied by Bagai and Nishad (2012).

## 5.10 Horizontal Line Heat Source

### 5.10.1 Flow at High Rayleigh Number

#### 5.10.1.1 Darcy Model

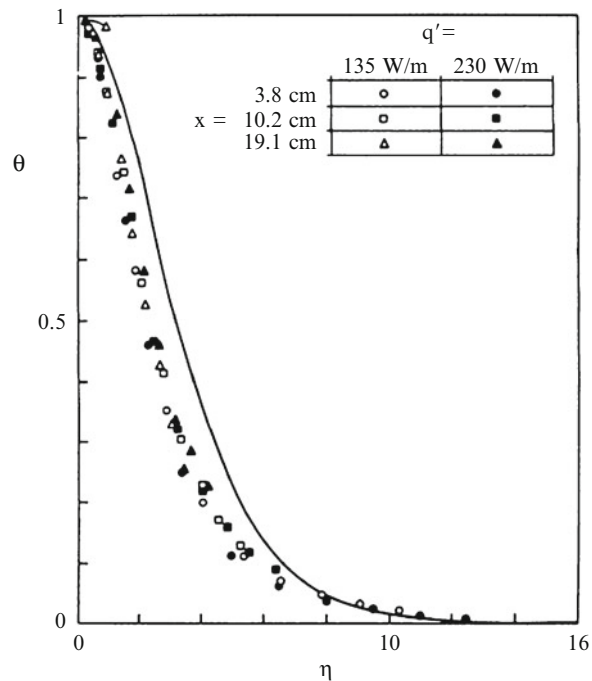
At high Rayleigh number, the flow about a horizontal line source of heat takes the form of a vertical plume. For steady flow the governing boundary-layer equations are again Eqs. (5.6) and (5.7). The boundary conditions (5.10) still apply, but Eq. (5.9) is replaced by the symmetry conditions

$$y = 0 : \frac{\partial^2 \Psi}{\partial y^2} = \frac{\partial T}{\partial y} = 0. \quad (5.176)$$

We now have a homogeneous system of equations, and a nontrivial solution exists only if a certain constraint holds. In the present problem this arises from the global conservation of energy and takes the form

$$q' = \rho_\infty c_p \int_{-\infty}^{\infty} \frac{\partial \Psi}{\partial y} (T - T_\infty) dy, \quad (5.177)$$

**Fig. 5.19** Dimensionless temperature profiles for plume rise above a horizontal line source of heat in a porous medium (Lee 1983; Cheng 1985a, with permission from Hemisphere Publishing Corporation)



where  $q'$  is the prescribed heat flux per unit length and  $c_p$  is the specific heat of the convected fluid at constant pressure. Consistent with the boundary-layer approximation, the axial heat conduction term is omitted from Eq. (5.173).

It is easily checked that the solution of the present problem is (Wooding 1963)

$$\Psi = \alpha_m \hat{Ra}_x^{1/3} f(\eta), \quad (5.178)$$

$$T - T_\infty = \frac{q'}{\rho_\infty c_p \alpha_m} \hat{Ra}_x^{-1/3} \theta(\eta), \quad (5.179)$$

$$\eta = \frac{y}{x} \hat{Ra}_x^{1/3}, \quad (5.180)$$

where

$$\hat{Ra}_x = g \beta K q' x / \mu \alpha_m^2 c_p. \quad (5.181)$$

The functions  $f$  and  $\theta$  satisfy the differential equations

$$f' - \theta = 0, \quad (5.182)$$

$$\theta'' + \frac{1}{3}(f\theta)' = 0, \quad (5.183)$$

the boundary conditions

$$f(0) = \theta'(0) = 0, \quad (5.184)$$

$$f'(\pm\infty) = \theta(\pm\infty) = 0, \quad (5.185)$$

and the constraint

$$\int_{-\infty}^{\infty} f'(\eta)\theta(\eta)d\eta = 1. \quad (5.186)$$

The nontrivial solution of Eqs. (5.182, 5.183, 5.184, 5.185 and 5.186) is

$$\Psi = \alpha_m \hat{R} a_x^{1/3} B \tanh\left(\frac{B\eta}{6}\right), \quad (5.187)$$

$$T - T_\infty = \frac{q}{\rho_\infty c_p \alpha_m} \hat{R} a_x^{-1/3} \frac{B^2}{6} \operatorname{sech}^2\left(\frac{B\eta}{6}\right), \quad (5.188)$$

where  $B = (9/2)^{1/3} = 1.651$ . The dimensionless temperature profile  $\theta(\eta)$  is illustrated in Fig. 5.19.

The problem of a line source situated at the vertex of a solid wedge, together with higher-order boundary-layer effects, was analyzed by Afzal (1985). The effect of material anisotropy on convection induced by point or line sources was studied by Rees et al. (2002). They showed that the path of the plume centerline is strongly affected by the anisotropy and the presence of impermeable bounding surfaces. A line source situated in an anisotropic medium also was studied by Degan and Vasseur (2003). They noted that the minimum (maximum) intensity of the plume is attained if the medium is oriented with its principal axis with high permeability parallel (perpendicular) to the vertical.

Bassom et al. (2001) examined the effects of asymmetrically placed boundaries on convective plumes, while Rees et al. (2008c) studied the linear vortex instability of a near-vertical line-source plume, the source being embedded in a flat plate that is aligned at a small angle to the horizontal.

### 5.10.1.2 Forchheimer Model

When quadratic drag is taken into account, Eq. (5.23) is replaced by

$$u + \frac{\chi}{v} u^2 = \frac{\beta K}{v} (T - T_\infty), \quad (5.189)$$

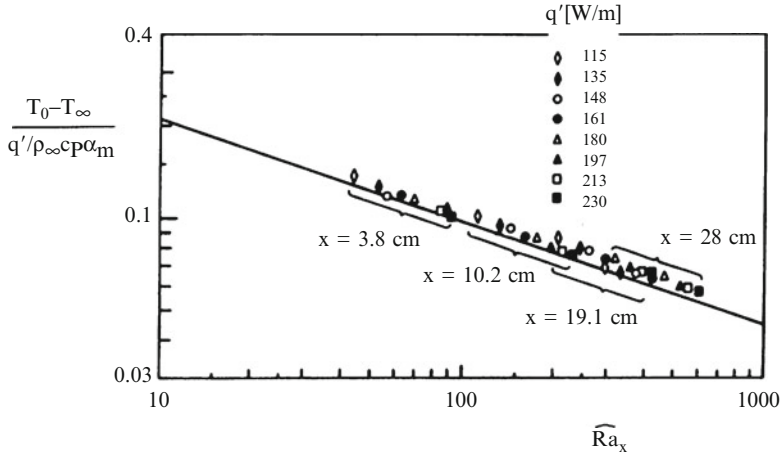


**Fig. 5.20** Dimensionless temperature vs. local Rayleigh number for plume rise above a horizontal line source of heat in a porous medium (Lee 1983; Cheng 1985a, with permission from Hemisphere Publishing Corporation)

where  $u = \partial\Psi/\partial y$ . Following Ingham (1988), we introduce nondimensional quantities defined by

$$x = Xl, \quad y = Yl \left( \frac{Fo}{\hat{Ra}} \right)^{1/5}, \quad (5.190)$$

$$\Psi = \alpha_m \left( \frac{\hat{Ra}}{Fo} \right)^{1/5} \Psi, \quad T - T_\infty = \frac{\chi a_m^2}{g \beta K l^2} \left( \frac{\hat{Ra}}{Fo} \right)^{4/5} \Theta, \quad (5.191)$$

$$\hat{Ra} = \frac{g \beta K l q'}{\nu \alpha_m k_m}, \quad Fo = \frac{\chi \alpha_m}{\nu l}, \quad (5.192)$$

where  $l$  is a characteristic length scale. Substitution into Eq. (5.189) and the steady-state form of Eq. (5.7) gives

$$\left( \frac{\partial \Psi}{\partial Y} \right)^2 = \Theta, \quad (5.193)$$

$$\frac{\partial \Psi}{\partial Y} \frac{\partial \Theta}{\partial X} - \frac{\partial \Psi}{\partial X} \frac{\partial \Theta}{\partial Y} = \frac{\partial^2 \Theta}{\partial Y^2}, \quad (5.194)$$

when a term  $\hat{Ra}^{-2/5} Fo^{-3/5} \partial \Psi / \partial Y$  in Eq. (5.193) has been neglected. Since the boundary-layer thickness is of order  $l(Fo/\hat{Ra})^{1/5}$ , we are requiring that  $\hat{Ra} Fo^{-1} \gg 1$  and  $\hat{Ra}^{2/5} Fo^{3/5} \gg 1$ . The boundary conditions and the source energy constraint are

$$\begin{aligned} Y = 0 : \frac{\partial^2 \Psi}{\partial Y^2} &= 0, \frac{\partial \Theta}{\partial Y} = 0, \\ Y \rightarrow \infty : \frac{\partial \Psi}{\partial Y} &\rightarrow 0, \Theta \rightarrow 0, \\ \int_{-\infty}^{\infty} \frac{\partial \Psi}{\partial Y} \Theta dY &= 1. \end{aligned} \quad (5.195)$$

We now introduce the similarity transformation

$$\Psi = X^{2/5}f(\eta), \quad \Theta = X^{-2/5}g(\eta), \quad \eta = Y/X^{3/5}, \quad (5.196)$$

and then the system (5.193, 5.194, and 5.195) becomes

$$(f')^2 = g, \quad (5.197)$$

$$g'' = -\frac{2}{5}(f'g + fg'), \quad (5.198)$$

$$g'(0) = 0, f'(\infty) = 0, \quad \int_{-\infty}^{\infty} f'g d\eta = 1. \quad (5.199)$$

These equations have the analytical solution

$$f = C \tanh \frac{C}{10}\eta, \quad g = \frac{C^4}{100} \operatorname{sech}^4 \frac{C}{10}\eta, \quad (5.200)$$

where  $C = (8 \times 10^{3/2}/3)^{1/4} = 3.03$ . Comparison of Eq. (5.200) with Eq. (5.188) shows that a  $\operatorname{sech}^2$  function is replaced by a  $\operatorname{sech}^4$  function and this means that the Forchheimer model leads to a more sharply peaked temperature profile than does the Darcy model.

This conclusion is in accordance with the experiments reported by Cheng (1985a), carried out by himself, Fand, and Chui, on the plume rise from a horizontal line source of heat embedded in 3-mm-diameter glass beads saturated with silicone oil. Their results are presented in Figs. 5.19 and 5.20. The work of Ingham (1988) was extended by Rees and Hossain (2001) to intermediate distances from the source by computing the smooth transition between the inertia-dominated and the inertia-free regimes.

An experimental and analytic study of the buoyant plume above a concentrated heat source in a stratified porous medium was made by Masuoka et al. (1986). In experiments with a two-layer system two kinds of glass spheres of different diameter were employed, with water as the saturating fluid. They found that their similarity solution broke down near the interface.

The effect of dispersion was added by Lai (1991b). The wall plume was studied by Leu and Jang (1994) using a Brinkmann-Forchheimer model. The wall plume has

a lower peak velocity and a higher maximum temperature than the corresponding free plume. The case of a non-Newtonian power-law fluid was examined by Nakayama (1993b).

Masuoka et al. (1995b) reported an experimental and analytical study of the effects of a horizontal porous layer on the development of the buoyant plume arising from a line heat source in an infinite fluid space. They observed an expansion of the plume at the lower interface and a contraction at the upper interface of the permeable layer. Their theoretical model incorporated the Beavers-Joseph slip boundary condition, and they interpreted the fairly good agreement between their experimental and numerical results as confirming the validity of that condition.

A problem that leads to curved plume paths was studied by Brambles and Rees (2007).

### 5.10.2 Flow at Low Rayleigh Number

Following Nield and White (1982) we introduce polar coordinates  $(r, \theta)$  with origin at the source and the plane  $\theta = 0$  horizontal. The seepage velocity is  $(v_r, v_\theta)$ . The equations for mass conservation, Darcy flow, and transient energy conservation are

$$\frac{\partial}{\partial r}(rv_r) + \frac{\partial v_\theta}{\partial \theta} = 0, \quad (5.201)$$

$$v_r = -\frac{K}{\mu} \left( \frac{\partial P}{\partial r} + \rho g \sin \theta \right), \quad (5.202)$$

$$v_\theta = -\frac{K}{\mu} \left( \frac{1}{r} \frac{\partial P}{\partial \theta} + \rho g \cos \theta \right), \quad (5.203)$$

$$\frac{1}{\alpha_m} \left( \sigma \frac{\partial T}{\partial t} + v_r \frac{\partial T}{\partial r} + \frac{v_\theta}{r} \frac{\partial T}{\partial \theta} \right) = \frac{\partial^2 T}{\partial r^2} + \frac{1}{r} \frac{\partial T}{\partial r} + \frac{1}{r^2} \frac{\partial^2 T}{\partial \theta^2}. \quad (5.204)$$

Introducing the streamfunction  $\Psi(r, \theta)$  by

$$v_r = \frac{1}{r} \frac{\partial \Psi}{\partial \theta}, \quad v_\theta = -\frac{\partial \Psi}{\partial r} \quad (5.205)$$

and eliminating the pressure between the two Darcy equations, we obtain, in nondimensional form,

$$r_* \frac{\partial^2 \Psi_*}{\partial r_*^2} + \frac{\partial \Psi_*}{\partial r_*} + \frac{1}{r_*} \frac{\partial^2 \Psi_*}{\partial \theta^2} = \hat{Ra} \left( \sin \theta \frac{\partial T_*}{\partial \theta} - r_* \cos \theta \frac{\partial T_*}{\partial r_*} \right). \quad (5.206)$$

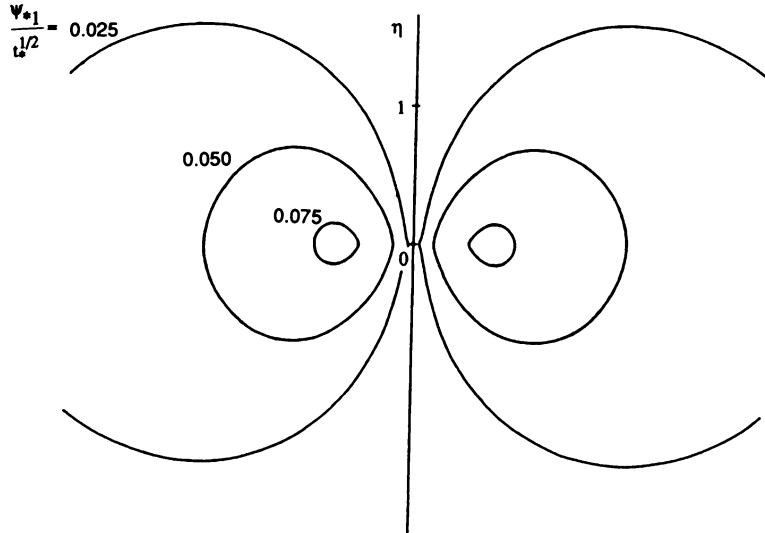


**Fig. 5.21** Streamlines drawn at constant increments of  $\psi_{*1}/t_*^{1/2}$ , for transient natural convection around a horizontal line heat source (Nield and White 1982)

$$\frac{\partial T_*}{\partial t_*} + \frac{1}{r_*} \left( \frac{\partial \Psi_*}{\partial \theta} \frac{\partial T_*}{\partial r_*} - \frac{\partial \Psi_*}{\partial r_*} \frac{\partial T}{\partial \theta} \right) = \frac{\partial^2 T_*}{\partial r_*^2} + \frac{1}{r_*} \frac{\partial T_*}{\partial r_*} + \frac{1}{r_*^2} \frac{\partial^2 T_*}{\partial \theta^2}, \quad (5.207)$$

where

$$t_* = \frac{t \alpha_m}{K \sigma}, \quad r_* = \frac{r}{K^{1/2}}, \quad T_* = \frac{(T - T_\infty) k_m}{q'}, \quad \Psi_* = \frac{\Psi}{\alpha_m}, \quad (5.208)$$

$$\hat{Ra} = \frac{g \beta K^{3/2} q'}{v \alpha_m k_m}. \quad (5.209)$$

The initial conditions, boundary conditions, and energy balance constraint are

$$t = 0 : v_r = v_\theta = 0, \quad T = T_\infty, \quad (5.210)$$

$$r \rightarrow \infty : v_r = v_\theta = 0, \quad T = T_\infty, \quad (5.211)$$

$$\theta = \pm \frac{\pi}{2} : v_\theta = \frac{\partial v_r}{\partial \theta} = \frac{\partial T}{\partial \theta} = 0, \quad (5.212)$$

$$\lim_{r \rightarrow 0} \left[ -k_m (2\pi r) \frac{\partial T}{\partial r} \right] = q'. \quad (5.213)$$

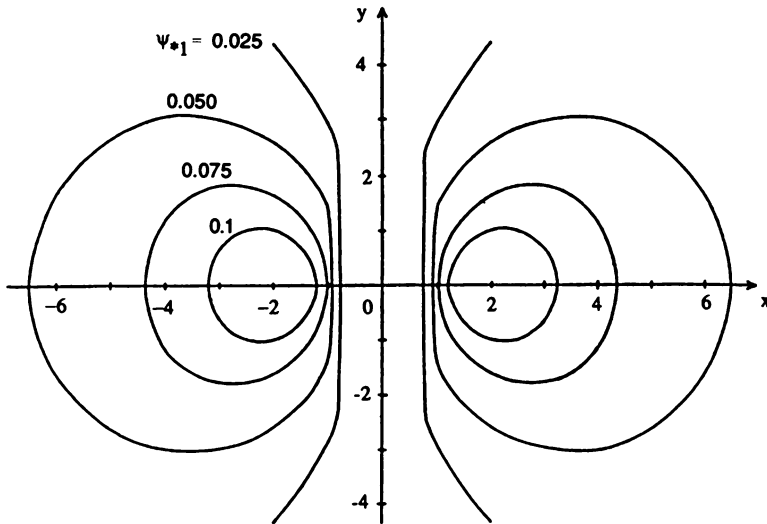


**Fig. 5.22** Streamlines drawn at constant increments of  $\psi_{*1}$ , for transient natural convection around a pair of line heat sources of equal strength, at  $(1,0)$  and  $(-1,0)$  at time  $\tau_* = 1$  (Nield and White 1982)

The last equation implies that  $T$  is of order  $\ln r$  as  $r \rightarrow 0$ , and Eq. (5.204) then implies that  $v_r$  is of order  $r^{-1} \ln r$  and  $v_\theta$  is of order  $r^{-1}$ . The above conditions are readily put in nondimensional form.

For sufficiently small values of  $Ra$  we can expand  $\Psi_*$  and  $T_*$  as power series in  $Ra$

$$(\Psi_*, T_*) = (\Psi_{*0}, T_{*0}) + Ra(\Psi_{*1}, T_{*1}) + Ra^2(\Psi_{*2}, T_{*2}) + \dots \quad (5.214)$$

When we substitute the above equations, collect the terms of the same power of  $Ra$ , and solve in terms the problems of order 0, 1, 2, ... in  $Ra$ , we find the zero-order conduction solution

$$\Psi_{*0} = 0, \quad T_{*0} = -\frac{1}{4\pi} \text{Ei}(-\eta^2), \quad (5.215)$$

with

$$\eta = \frac{r_*}{2t_*^{1/2}}, \quad (5.216)$$

and then the first-order solution

$$\Psi_{*1} = \frac{t_*^{1/2}}{4\pi} \cos \theta \left[ \frac{\exp(-\eta^2) - 1}{\eta} + \eta \text{Ei}(-\eta^2) \right], \quad (5.217)$$

$$T_{*1} = t_*^{1/2} \frac{\sin \theta}{16\pi^2} \left\{ (\ln \eta)[(\gamma - 2)\eta - \eta^3] + \eta(\ln \eta)^2 + \eta \frac{2-\gamma}{2} + \eta^3 \frac{3-\gamma}{2} + \dots \right\}, \quad (5.218)$$

where  $\gamma = 0.5772 \dots$  is Euler's constant. In Fig. 5.21 a set of streamlines  $\psi_*/t_*^{1/2}$  have been plotted. We see that the flow pattern for small Rayleigh numbers consists of an expanding vortex whose radius increases with time as  $t_*^{1/2}$  and whose core is situated at  $\eta = 0.567$  in the horizontal plane containing the source.

Since the momentum equation is linear, we can superpose solutions for sources and use the method of images to deduce the flow field due to the presence of a line source near an insulated vertical wall. We assume that the insulated vertical wall is given by the  $y$  axis of a Cartesian system and the line source is located at  $x = d, y = 0$ . The flow field is equivalent to that produced by a pair of line sources, of equal strength, positioned at  $x = \pm d, y = 0$ . The expression for  $\psi_{*1}$  is now

$$\Psi_{*1} = \frac{\tau^{1/2}}{4\pi} (S_+ + S_-), \quad (5.219)$$

where

$$S_{\pm} = \frac{2\tau^{1/2}(X \pm 1)}{(X \pm 1)^2 + Y^2} \left\{ \exp \left[ -\frac{(X \pm 1)^2 + Y^2}{4\tau} \right] - 1 \right\} - \frac{X \pm 1}{2\tau^{1/2}} \int_{[(X \pm 1)^2 + Y^2]/4\tau}^{\infty} \frac{\exp(-\xi)}{\xi} d\xi, \quad (5.220)$$

where  $\tau = t\alpha_m/d$ ,  $X = x/d$ ,  $Y = y/d$ . From this expression the streamlines were plotted in Fig. 5.22. Since the energy equation is nonlinear, it is not possible to superpose the solutions for  $T_{*1}$ . Degan et al. (2005) studied the effects of anisotropy.

## 5.11 Point Heat Source

### 5.11.1 Flow at High Rayleigh Number

Following Wooding (1963) and Bejan (1984), we consider the slender plume above a point source of constant strength, placed at an impermeable horizontal boundary. We take cylindrical polar coordinates  $(r, \theta, z)$  with the origin at the source and the  $z$  axis vertically upward. The problem has axial symmetry, and the seepage velocity  $(v_r, 0, v_z)$  is given in terms of a Stokes streamfunction  $\Psi$  by

$$v_r = \frac{1}{r} \frac{\partial \Psi}{\partial z}, \quad v_z = -\frac{1}{r} \frac{\partial \Psi}{\partial r}. \quad (5.221)$$

The boundary-layer equations for momentum and energy and the boundary conditions are

$$\frac{1}{r} \frac{\partial^2 \Psi}{\partial r^2} = - \frac{g \beta K}{v} \frac{\partial T}{\partial r}, \quad (5.222)$$

$$\frac{\partial \Psi}{\partial z} \frac{\partial T}{\partial r} - \frac{\partial \Psi}{\partial r} \frac{\partial T}{\partial z} = \alpha_m \frac{\partial}{\partial r} \left( r \frac{\partial T}{\partial r} \right), \quad (5.223)$$

$$r = 0 : \frac{\partial \Psi}{\partial z} = \frac{\partial T}{\partial r} = 0, \quad (5.224)$$

$$r \rightarrow \infty : \frac{\partial \Psi}{\partial r} = 0, \quad T = T_\infty, \quad (5.225)$$

$$z = 0 : \frac{\partial \Psi}{\partial r} = 0. \quad (5.226)$$

If  $q$  [W] is the strength of the source, energy conservation requires that

$$q = \int_0^\infty \rho_\infty c_p v_z (T - T_\infty) 2\pi r dr. \quad (5.227)$$

These equations admit the similarity solution

$$\Psi = -\alpha_m z f(\eta), \quad (5.228)$$

$$T - T_\infty = \frac{q}{k_m r} \tilde{Ra}^{-1/2} \theta(\eta), \quad (5.229)$$

$$\eta = \tilde{Ra}^{1/2} \frac{r}{z}, \quad (5.230)$$

where  $\tilde{Ra}$  is the Rayleigh number based on source strength

$$\tilde{Ra} = \frac{g \beta K q}{v \alpha_m k_m}. \quad (5.231)$$

The functions  $f$  and  $\theta$  satisfy the differential equations

$$f'' - \theta' = 0, \quad (5.232)$$

$$\eta^2 \theta'' + \eta(f-1)\theta' + (1-f+\eta f')\theta = 0, \quad (5.233)$$

the boundary conditions

$$f(0) = \theta(0) = 0, \quad (5.234)$$

$$f''(\infty) = f'(\infty) = \theta(\infty) = 0, \quad (5.235)$$

and the constraint

$$\int_0^\infty \frac{f'\theta}{\eta} d\eta = \frac{1}{2\pi}. \quad (5.236)$$

When the boundary conditions (5.231) are utilized, Eq. (5.228) integrates to give  $f' = \theta$ , and so Eq. (5.229) becomes

$$\frac{d}{d\eta} \left( f'' - \frac{f'}{\eta} + \frac{ff'}{\eta} \right) = 0. \quad (5.237)$$

Integrating this equation and invoking Eq. (5.230), we have

$$ff' = f' - \eta f''. \quad (5.238)$$

The solution satisfying the boundary conditions is

$$f = \frac{(C\eta)^2}{1 + (C\eta/2)^2}, \quad (5.239)$$

and the constraint (5.236) requires that  $C = \pi^{-1/2}/4 = 0.141$ . Wooding (1985) has extended the boundary-layer equations to account for large density differences, dispersion, and convection in the presence of tidal oscillations.

Lai (1990b) showed that a similarity solution could be found for the case of a power-law variation of centerline temperature. The problem was treated using the Forchheimer model by Degan and Vasseur (1995). As one would expect, inertial effects tend to reduce the buoyancy-induced flow. Inertial effects, together with those of thermal dispersion, also were discussed by Leu and Jang (1995). The case of a non-Newtonian power-law fluid was examined by Nakayama (1993a). Higuera and Weidman (1998) noted that the case of natural convection far downstream of a heat source on a solid wall led to a parameter free differential equation problem. Zhang et al. (2010) studied transient and steady convection from a heat source embedded in a thermally stratified layer.

### 5.11.2 Flow at Low Rayleigh Number

We now consider a point heat source of strength  $q$  [W] in an unbounded domain. We introduce spherical polar coordinates  $(r, \theta, \varphi)$ , with  $\theta$  the “colatitude” and  $\varphi$  the “longitude,” and with the line  $\theta = 0$  vertically upward. We have an axisymmetric

problem with no dependence on  $\varphi$ . The equations for mass conservation, Darcy flow, and transient energy conservation are

$$\frac{\partial}{\partial r}(r^2 v_r \sin \theta) + \frac{\partial}{\partial \theta}(r v_\theta \sin \theta) = 0, \quad (5.240)$$

$$v_r = -\frac{K}{\mu} \left( \frac{\partial P}{\partial r} + \rho g \cos \theta \right), \quad (5.241)$$

$$v_\theta = -\frac{K}{\mu} \left( \frac{1}{r} \frac{\partial P}{\partial \theta} - \rho g \sin \theta \right), \quad (5.242)$$

$$\frac{1}{\alpha_m} \left( \sigma \frac{\partial T}{\partial t} + v_r \frac{\partial T}{\partial r} + \frac{v_\theta}{r} \frac{\partial T}{\partial \theta} \right) = \frac{1}{r^2} \frac{\partial}{\partial r} \left( r^2 \frac{\partial T}{\partial r} \right) + \frac{1}{r^2 \sin \theta} \frac{\partial}{\partial \theta} \left( \sin \theta \frac{\partial T}{\partial \theta} \right). \quad (5.243)$$

Introducing the Stokes streamfunction  $\Psi(r, \theta)$  by

$$v_r = \frac{1}{r^2 \sin \theta} \frac{\partial \Psi}{\partial \theta}, \quad v_\theta = -\frac{1}{r \sin \theta} \frac{\partial \Psi}{\partial r} \quad (5.244)$$

and eliminating the pressure between the two Darcy equations, we get, in nondimensional variables,

$$\frac{1}{r_*^2} \frac{\partial}{\partial \theta} \left( \frac{1}{\sin \theta} \frac{\partial \Psi_*}{\partial \theta} \right) + \frac{1}{\sin \theta} \frac{\partial^2 \Psi_*}{\partial r_*^2} = \tilde{Ra} \left( \cos \theta \frac{\partial T_*}{\partial \theta} + r_* \sin \theta \frac{\partial T_*}{\partial r_*} \right), \quad (5.245)$$

$$\begin{aligned} & \frac{\partial T_*}{\partial t_*} + \frac{1}{r_*^2 \sin \theta} \left( \frac{\partial \Psi_*}{\partial \theta} \frac{\partial T_*}{\partial r_*} - \frac{\partial \Psi_*}{\partial r_*} \frac{\partial T_*}{\partial \theta} \right) \\ &= \frac{1}{r_*^2} \frac{\partial}{\partial r_*} \left( r_*^2 \frac{\partial T_*}{\partial r_*} \right) + \frac{1}{r_*^2 \sin \theta} \frac{\partial}{\partial \theta} \left( \sin \theta \frac{\partial T_*}{\partial \theta} \right), \end{aligned} \quad (5.246)$$

where

$$\begin{aligned} t_* &= \frac{t \alpha_m}{K \sigma}, \quad r_* = \frac{r}{K^{1/2}}, \quad T_* = \frac{(T - T_\infty) k_m K^{1/2}}{q} \\ \Psi_* &= \frac{\Psi}{\alpha_m K^{1/2}}, \quad \tilde{Ra} = \frac{g \beta K q}{\nu \alpha_m k_m}. \end{aligned} \quad (5.247)$$

The initial conditions for this transient problem are

$$t = 0 : v_r = v_\theta = 0, \quad T = T_\infty.$$

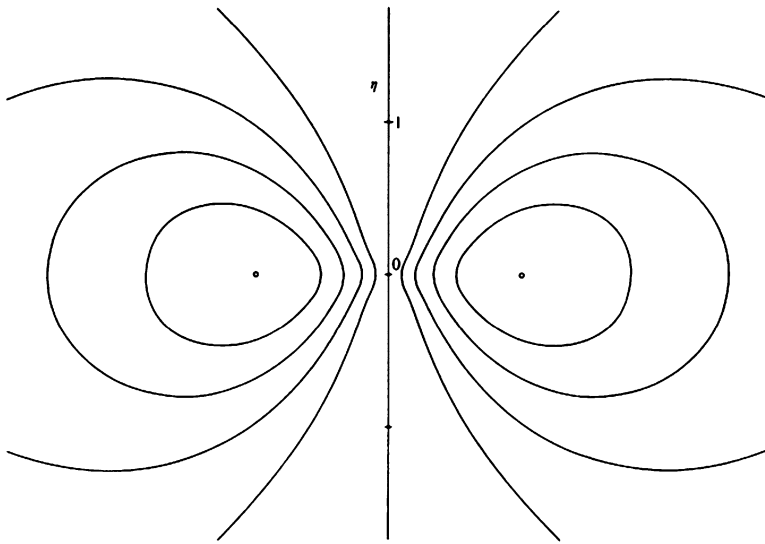


**Fig. 5.23** Transient natural convection flow pattern about a point heat source. The lines correspond to equal increments of  $\psi_{*1}/t^{1/2}$  \* (Bejan 1978, 1984)

The appropriate boundary conditions are

$$\begin{aligned} r \rightarrow \infty : \quad v_r = v_\theta = 0, \quad T = T_\infty, \\ \theta = 0, \pi : \quad v_\theta = \frac{\partial v_r}{\partial \theta} = \frac{\partial T}{\partial \theta} = 0, \end{aligned} \quad (5.248)$$

together with the fact that  $v_r$ ,  $v_\theta$ , and  $T$  are of order  $1/r$  as  $r \rightarrow 0$ . This is required by the balance of terms in the above differential equations, together with the energy balance constraint

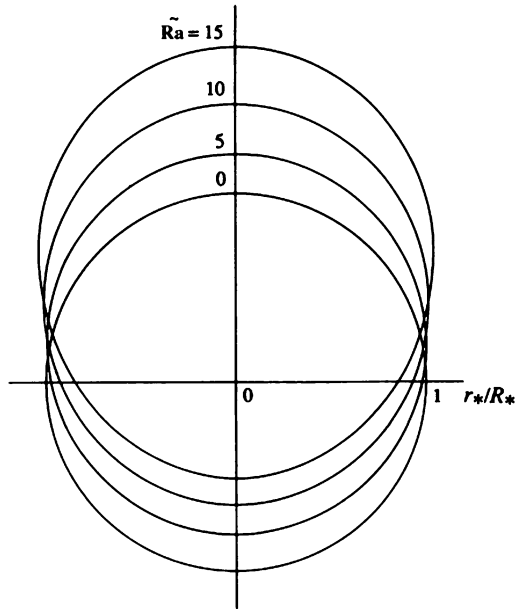
$$\lim_{r \rightarrow 0} \left[ -k_m (4\pi r^2) \frac{\partial T}{\partial r} \right] = q. \quad (5.249)$$

The above conditions are readily put in nondimensional form. For sufficiently small values of  $\tilde{Ra}$  we can expand  $\Psi_*$  and  $T_*$  as power series in  $\tilde{Ra}$

$$(\Psi_*, T_*) = (\Psi_{*0}, T_{*0}) + \tilde{Ra}(\Psi_{*1}, T_{*1}) + \dots \quad (5.250)$$

We can then substitute into the above equations and equate terms in like powers of  $\tilde{Ra}$ , thus obtaining subproblems at order  $\tilde{Ra}_0$ ,  $\tilde{Ra}_1$ , and  $\tilde{Ra}_2$ . The zero-order problem yields the conduction solution

**Fig. 5.24** Steady temperature distribution around a point heat source; the lines represent the  $(4\pi R_*)\theta = 1$  isotherm, for increasing values of  $\tilde{Ra}$  (Bejan 1978, 1984)



$$T_{*0} = \frac{1}{4\pi r} \operatorname{erfc} \eta, \quad (5.251)$$

$$\Psi_{*0} = 0, \quad (5.252)$$

where  $\eta = r_*/2t_*^{1/2}$ . The first-order problem yields (Bejan 1978)

$$\Psi_{1*} = \frac{1}{8\pi} t_*^{1/2} \sin^2 \theta \left( 2\eta \operatorname{erfc} \eta + \frac{1}{\eta} \operatorname{erf} \eta - \frac{2}{\pi^{1/2}} e^{-\eta^2} \right), \quad (5.253)$$

$$T_{*1} = \frac{\cos \theta}{64\pi^2 t_*^{1/2}} \left( \frac{1}{\eta} - \frac{4}{3\pi^{1/2}} + \frac{6}{5\pi^{1/2}} \eta^2 - \frac{16}{45\pi} \eta^3 - \frac{152}{315\pi^{1/2}} \eta^4 + \dots \right). \quad (5.254)$$

Figure 5.23, based on Eq. (5.253), shows that as soon as the heat source is turned on a vortex ring forms about the source. The radius of the core of the vortex is given by  $\eta = 0.881$ , i.e., the physical radius grows with time as the group  $1.762(\alpha_m t/\sigma)^{1/2}$ .

Unlike the line-source problem of Sect. 5.1.9.2, the present point source problem has a steady-state small  $\tilde{Ra}$  solution with

$$\Psi_* = \frac{r_*}{8\pi} \left[ \sin^2 \theta \tilde{Ra} + \frac{1}{24\pi} \sin \theta \sin 2\theta \tilde{Ra}^2 - \frac{5}{18432\pi^3} (8\cos^4 \theta - 3) \tilde{Ra}^3 + \dots \right], \quad (5.255)$$

$$T_* = \frac{1}{4\pi r_*} \left[ 1 + \frac{1}{8\pi} \cos \theta \tilde{Ra} + \frac{5}{768\pi^2} \cos 2\theta \tilde{Ra}^2 + \frac{1}{55,296\pi^3} \cos \theta (47\cos^2 \theta - 30)\tilde{Ra}^3 + \dots \right]. \quad (5.256)$$

This solution gives valid results for source strength Rayleigh numbers  $\tilde{Ra}$  up to about 20. The temperature field is illustrated in Fig. 5.24 in which a curve represents the isothermal surface  $T_* = 1/4\pi R_*$ , where  $R_*$  is a fixed nondimensional distance from the origin. The figure shows that the warm region, originally spherical about the point source, shifts upward and becomes elongated like the flame of a candle as  $\tilde{Ra}$  increases.

Whereas Bejan (1978) used the source condition (5.249), which requires the heat flux to be uniformly distributed over an isothermal source, Ene and Polievski (1987) took

$$\lim_{r \rightarrow 0} \int_{S_r} \left( -k_m \frac{\partial T}{\partial r} \right) d\sigma = q, \quad (5.257)$$

where  $S_r$  is the sphere of radius  $r$ . Equation (5.257) implies that  $\partial T / \partial r$  varies with  $\theta$  in a special way (determined by the overall problem) as  $r \rightarrow 0$ . It appears to be the more appropriate condition. Both Eqs. (5.249) and (5.257) are based on the assumption that the convective heat transport at the source is negligible (compare Eq. (5.264)).

Hickox (1981) has utilized the fact that the momentum equation is linear in  $Ra$  to investigate certain other geometries by superposing sources. Ganapathy and Purushothaman (1990) discussed the case of an instantaneous point source. The Brinkman term affects the solution at radial distances up to  $O(K^{1/2})$  from the source, where at small times it slows the rate of momentum transfer. Purushothaman et al. (1990) dealt with a pulsating point heat source. Ganapathy (1992) treated an instantaneous point source which is enveloped by a solid sphere that is itself surrounded by a porous medium.

### 5.11.3 Flow at Intermediate Rayleigh Number

For the steady situation Hickox and Watts (1980) obtained results for arbitrary values of  $\tilde{Ra}$ , for both the semi-infinite region considered by Wooding and Bejan and the infinite region. For the infinite region, with spherical polar coordinates and the streamfunction defined as in Eq. (5.244), one can put

$$\eta = \cos \theta, \quad \Psi = \alpha_m r f(\eta), \quad T - T_\infty = \frac{\alpha_m}{gK\beta} \frac{g(\eta)}{r}. \quad (5.258)$$

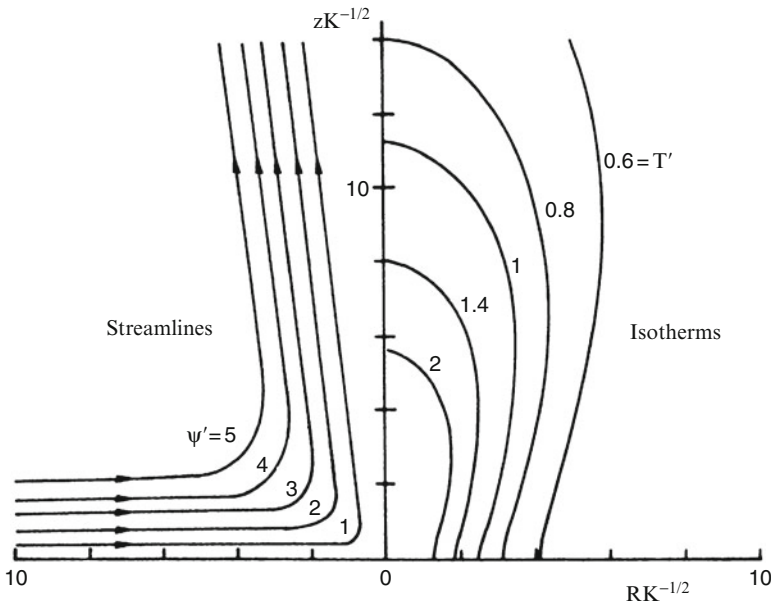


**Fig. 5.25** Streamlines and isotherms for a point source at the base of a semi-infinite region,  $Ra = 10$ ,  $\Psi' = \Psi/\alpha_m K^{1/2}$ , and  $T' = (T - T_\infty) g \beta K^{3/2} / v \alpha_m$  (Hickox and Watts 1980)

The problem reduces to the solution of the differential equations

$$f'' = -(\eta g)', \quad (5.259)$$

$$(fg)' = g'' - (\eta^2 g')', \quad (5.260)$$

subject to the symmetry and boundary conditions

$$f(1) = 0, \quad f(-1) = 0, \quad (5.261)$$

$$g, g' \text{ bounded as } \eta \rightarrow \pm 1, \quad (5.262)$$

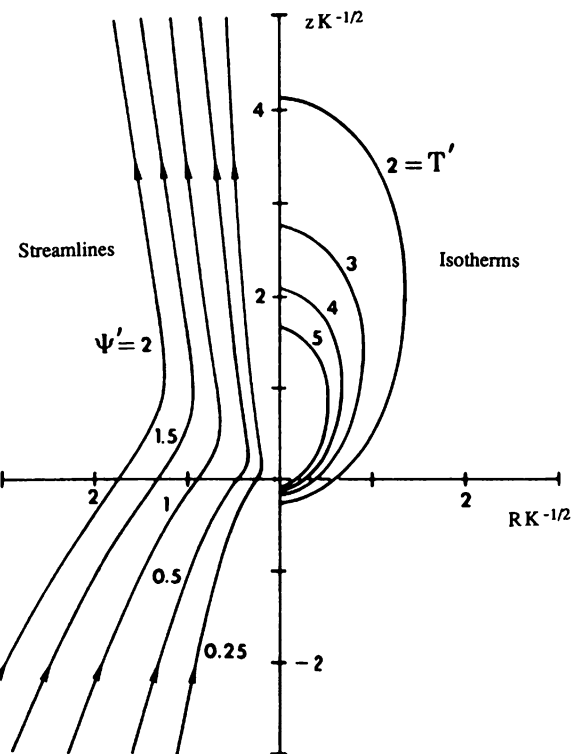
and the constraint

$$\int_{-1}^1 (1 - f') g d\eta = 2\pi \tilde{Ra}. \quad (5.263)$$

The last equation arises from the requirement that the energy flux, integrated over a sphere centered at the origin, should equal  $q$ , so

$$\int_0^\pi \left[ (\rho c_p)_f v_r (T - T_\infty) - k_m \frac{\partial T}{\partial r} \right] 2\pi r^2 \sin \theta d\theta = q. \quad (5.264)$$

**Fig. 5.26** Streamlines and isotherms for a point source in an infinite region,  $Ra = 10$ ,  $\Psi'$  and  $T'$  defined as in Fig. 5.25 (Hickox and Watts 1980)



Hickox and Watts (1980) integrated Eqs. (5.259, 5.260, 5.261, 5.262, and 5.263) numerically. They treated the semi-infinite region in a similar fashion, but using a different similarity transformation. Some representative plots of isotherms and streamlines are presented in Figs. 5.25 and 5.26.

## 5.12 Other Configurations

### 5.12.1 Fins Projecting from a Heated Base

The problem of high Rayleigh number convection about a long vertical thin fin with a heated base can be treated as a conjugate conduction-convection problem. Various geometries have been considered. Pop et al. (1985) obtained a similarity solution for a vertical plate fin projecting downward from a heated horizontal plane base at constant temperature for the case of the conductivity-fin thickness product varying as a power function of distance from a certain specified origin. They also

dealt with the similar problem of a vertical plate extending from a heated horizontal cylindrical base at constant temperature.

Pop et al. (1986) used a finite-difference numerical method for the former geometry but with constant conductivity and fin thickness, and Liu and Minkowycz (1986) investigated the influence of lateral mass flux in this situation. Gill and Minkowycz (1988) examined the effects of boundary friction and quadratic drag. Hung et al. (1989) have incorporated non-Darcy effects in their study of a transient problem. The above studies all have been of a vertical plate fin. The case of a vertical cylindrical fin was analyzed by Liu et al. (1987b); again the effect of lateral mass flux was included. Convection from a slender needle, for the case where the axial wall thickness varies as a power function of distance from the leading edge, was analyzed by Peng et al. (1992).

Conjugate convection about a vertical plate fin was studied by Hung (1991) using the Brinkman-Forchheimer model. Chen and Chiou (1994) added the effects of thermal dispersion and nonuniform porosity. Conjugate convection of a non-Newtonian fluid about a vertical plate was studied by Pop and Nakayama (1994), while the corresponding problem for a vertical cylindrical fin was treated by Hossain et al. (1995). Further work on conjugate convection from vertical plate fins was reported by Vaszi et al. (2002b, 2004) and Pop and Nakayama (1999).

Further work involving fins was conducted by Kiwan (2007a, b), Seyf and Layeghi (2010), and Gorla and Bakier (2011).

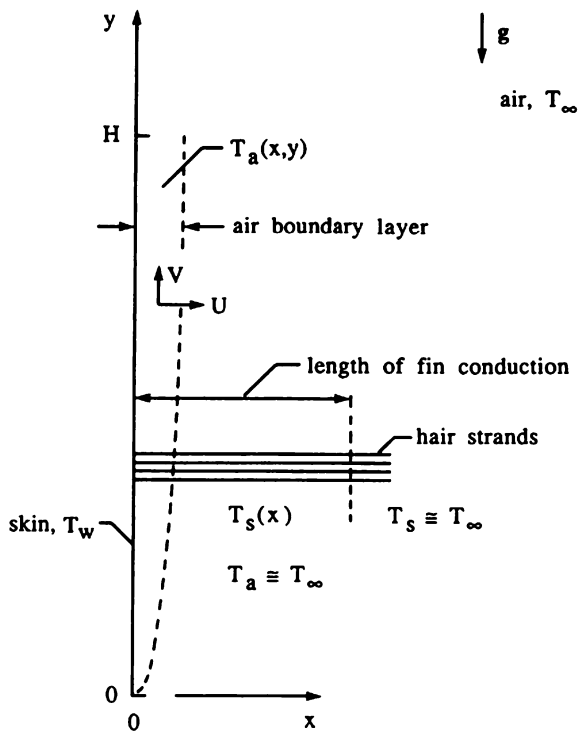
### **5.12.2 *Flows in Regions Bounded by Two Planes***

The Darcy flow in a corner region bounded by a heated vertical wall and an insulated inclined wall was analyzed by Daniels and Simpkins (1984), while Riley and Rees (1985) analyzed the non-Darcy flow in the exterior region bounded by a heated inclined wall and an inclined wall that was either insulated or cooled. In each of these two publications the heated wall was at constant temperature. Hsu and Cheng (1985a) analyzed the Darcy flow about an inclined heated wall with a power law of variation of temperature and an inclined unheated isothermal wall.

The particular case of the Darcy flow in the “stably heated” corner between a cold horizontal wall and a hot vertical wall situated above the horizontal wall (or between a hot horizontal wall and a cold vertical wall situated below the horizontal wall) was studied by Kimura and Bejan (1985). Their scale analysis and numerical solutions showed that the single-cell corner flow becomes increasingly more localized as the Rayleigh number increases. At the same time the mass flow rate engaged in natural convection and the conduction-referenced Nusselt number increase.

Liu et al. (1987a) found a local-similarity solution for flow in the corner formed by two mutually perpendicular vertical plates for the case when both plates are at the same constant wall temperature. Earlier solutions by Liu and Ismail (1980) and Liu and Guerra (1985) (the latter with an arbitrary angle between the vertical plates)

**Fig. 5.27** Vertical skin area, air boundary layer, and hair strands that act as fins (Bejan 1990b)



had been obtained under an asymptotic suction assumption. Two other problems involving perpendicular planes were studied by Ingham and Pop (1987a, b). Pop et al. (1997) performed calculations for convection in a Darcian fluid in a horizontal L-shaped corner, with a heated isothermal vertical plate joined to a horizontal surface that is either adiabatic or held at ambient temperature.

### 5.12.3 Other Situations

The problem of the cooling of a circular plate situated in the bottom plane boundary of a semi-infinite region was analyzed as a boundary-layer problem by McNabb (1965). The boundary-layer flow near the edge of a horizontal circular dish in an unbounded region was studied by Merkin and Pop (1989). A numerical study on various models of convection in open-ended cavities was reported by Ettefagh et al. (1991).

The subject of conjugate natural convection in porous media has been reviewed by Kimura et al. (1997). They discussed various configurations including slender bodies, rectangular slabs, horizontal cylinders, and spheres. Three-dimensional

stagnation point convection on a surface on which heat is released by an exothermic reaction was analyzed by Pop et al. (2003). The topic of chemically driven convection in porous media was reviewed by Pop et al. (2002); other relevant papers include those by Mahmood and Merkin (1998) and Merkin and Mahmood (1998). The effect of local thermal nonequilibrium or g-jitter on convective stagnation point flow was analyzed by Rees and Pop (1999, 2001). Convection from a cylinder covered with an orthotropic porous layer in cross flow was investigated numerically by Abu-Hijleh (2001a).

Convection in a triangular cavity filled with a porous medium saturated with a nanofluid, and with a flush mounted heater on a wall, was studied by Sun and Pop (2011).

## 5.13 Surfaces Covered with Hair

The two-temperature porous medium model described in Sect. 4.10 was also used in the theoretical study of natural convection heat transfer from surfaces covered with hair (Bejan 1990b). With reference to a vertical surface (Fig. 5.27) the boundary-layer equations for energy conservation and Darcy flow are written as

$$\rho c_p \left( U \frac{\partial T_a}{\partial x} + V \frac{\partial T_a}{\partial y} \right) = k_a \frac{\partial^2 T_a}{\partial x^2} + nh p_s (T_s - T_a), \quad (5.265)$$

$$\frac{\partial V}{\partial x} = \frac{g \beta K}{v \phi} \frac{\partial T_a}{\partial x}. \quad (5.266)$$

The porosity  $\varphi$  appears in the denominator in Eq. (5.266), because in this model  $V$  is the air velocity averaged only over the space occupied by air. The rest of the notation is defined in Fig. 5.27 and Sect. 4.10. For example,  $n$  is the hair density (strands/m<sup>2</sup>).

The boundary-layer heat transfer analysis built on this model showed that the total heat transfer rate through a skin area of height  $H$  is minimized when the hair strand diameter reaches the optimal value

$$\frac{D_{\text{opt}}}{H} = \left( \frac{1 - \phi}{0.444} \right)^{1/2} \left( \frac{k_s}{k_a} \frac{f_2}{\phi f_1 R_{af}} \right)^{1/4}. \quad (5.267)$$

The  $R_{af}$  factor in the denominator is the Rayleigh number for natural convection in open air,  $R_{af} = g \beta H^3 (T_w - T_\infty) / v \alpha_a$ . The minimum heat transfer rate that corresponds to  $D_{\text{opt}}$  is

$$\frac{q'_{\min}}{k_a(T_w - T_\infty)} = 1.776(1 - \phi)^{1/2} \left( \phi f_1 f_2 \frac{k_s}{k_a} Ra_f \right)^{1/4}. \quad (5.268)$$

The factors  $f_1$  and  $f_2$  are both functions of porosity and result from having modeled the permeability and strand-air heat transfer coefficient by

$$K = D^2 f_1(\phi), \quad h = \frac{k_a}{D} f_2(\phi). \quad (5.269)$$

It is important to note that since  $Ra_f$  is proportional to  $H^3$ , Eq. (5.267) states that the optimal strand diameter is proportional to  $H^{1/4}$ . The theoretical results for a vertical surface covered with hair were tested in an extensive series of numerical experiments (Lage and Bejan 1991).

Analogous conclusions are reached in the case where instead of the vertical plane of Fig. 5.27, the skin surface has the shape of a long horizontal cylinder of diameter  $D_o$ . The optimal hair strand diameter is

$$\frac{D_{\text{opt}}}{D_o} = 1.881(1 - \phi)^{1/2} \left( \frac{k_s}{k_a} \frac{f_2}{\phi f_1 Ra_{fo}} \right)^{1/4}, \quad (5.270)$$

where  $Ra_{fo} = g\beta D_o^3 (T_w - T_\infty) / v\alpha_a$ . In the case where the body shape approaches a sphere of diameter  $D_o$ , the optimal hair strand diameter has a similar form,

$$\frac{D_{\text{opt}}}{D_o} = 2.351(1 - \phi)^{1/2} \left( \frac{k_s}{k_a} \frac{f_2}{\phi f_1 Ra_{fo}} \right)^{1/4}. \quad (5.271)$$

Equations (5.270) and (5.271) show that  $D_{\text{opt}}$  increases as  $D_o^{1/4}$ . Combined with Eq. (5.267), they lead to the conclusion that when the heat transfer mechanism is boundary-layer natural convection, the optimal hair strand diameter increases as the vertical dimension of the body ( $H$ , or  $D_o$ ) raised to the power 1/4.

# Chapter 6

## Internal Natural Convection: Heating from Below

### 6.1 Horton-Rogers-Lapwood Problem

We start with the simplest case, that of zero flow through the fluid-saturated porous medium. For an equilibrium state, the momentum equation is satisfied if

$$-\nabla P + \rho_f \mathbf{g} = \mathbf{0}. \quad (6.1)$$

Taking the curl of each term yields

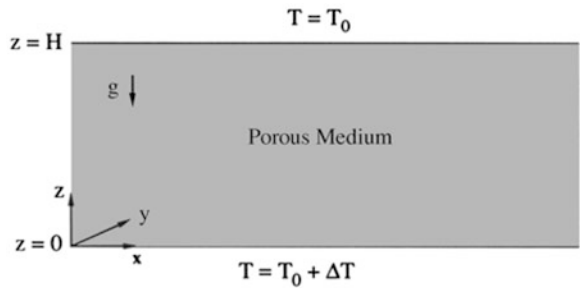
$$\nabla \rho_f \times \mathbf{g} = \mathbf{0}. \quad (6.2)$$

If the fluid density  $\rho_f$  depends only on the temperature  $T$ , then this equation implies that  $\nabla T \times \mathbf{g} = \mathbf{0}$ . We conclude that a necessary condition for equilibrium is that the temperature gradient is vertical (or zero). Intra-pore convection may increase effective conductivity of the medium. We thus have a special interest in the problem of a horizontal layer of a porous medium uniformly heated from below. This problem, the porous-medium analog of the Rayleigh-Bénard problem, was first treated by Horton and Rogers (1945) and independently by Lapwood (1948).

With reference to Fig. 6.1, we take a Cartesian frame with the  $z$ -axis vertically upward. We suppose that the layer is confined by boundaries at  $z = 0$  and  $z = H$ , the lower boundary being at uniform temperature  $T_0 + \Delta T$  and the upper boundary at temperature  $T_0$ . We thus have a layer of thickness  $H$  and an imposed adverse temperature gradient  $\Delta T/H$ . We suppose that the medium is homogeneous and isotropic, that Darcy's law is valid, and that the Oberbeck-Boussinesq approximation is applicable, and we also make the other standard assumptions (local thermal equilibrium, negligible heating from viscous dissipation, negligible radiative effects, etc.). The appropriate equations are, cf. (1.1), (1.10), (2.3), and (2.20),

$$\nabla \cdot \mathbf{v} = \mathbf{0}, \quad (6.3)$$

**Fig. 6.1** The Horton-Rogers-Lapwood problem: infinite horizontal porous layer heated from below



$$c_a \rho_0 \frac{\partial \mathbf{v}}{\partial t} = -\nabla P - \frac{\mu}{K} \mathbf{v} + \rho_f \mathbf{g}, \quad (6.4)$$

$$(\rho c)_m \frac{\partial T}{\partial t} + (\rho c_p)_f \mathbf{v} \cdot \nabla T = k_m \nabla^2 T, \quad (6.5)$$

$$\rho_f = \rho_0 [1 - \beta(T - T_0)]. \quad (6.6)$$

The reader is reminded that  $\mathbf{v}$  is the seepage velocity,  $P$  is the pressure,  $\mu$  the dynamic viscosity,  $K$  the permeability,  $c$  the specific heat,  $k_m$  the overall thermal conductivity, and  $\beta$  the thermal volume expansion coefficient.

We observe that (6.3), (6.4), (6.5), and (6.6) have a basic steady-state solution, which satisfies the boundary conditions  $T = T_0 + \Delta T$  at  $z = 0$  and  $T = T_0$  at  $z = H$ . That solution is

$$\mathbf{v}_b = 0, \quad (6.7)$$

$$T_b = T_0 + \Delta T \left(1 - \frac{z}{H}\right), \quad (6.8)$$

$$P_b = P_0 - \rho_0 g \left[z + \frac{1}{2} \beta \Delta T \left(\frac{z^2}{H} - 2z\right)\right]. \quad (6.9)$$

It describes the “conduction state,” one in which the heat transfer is solely by thermal conduction.

## 6.2 Linear Stability Analysis

We now examine the stability of this solution and assume that the perturbation quantities (those with primes) are small. We write

$$\mathbf{v} = \mathbf{v}_b + \mathbf{v}', \quad T = T_b + T', \quad P = P_b + P'. \quad (6.10)$$

When we substitute into (6.3), (6.4), and (6.5) and neglect second-order small quantities, we obtain the linearized equations (note  $\mathbf{v}' = (u', v', w')$ ):

$$\nabla \cdot \mathbf{v}' = 0, \quad (6.11)$$

$$c_a \rho_0 \frac{\partial \mathbf{v}'}{\partial t} = -\nabla P' - \frac{\mu}{K} \mathbf{v}' - \beta \rho_0 T' \mathbf{g}, \quad (6.12)$$

$$(\rho c)_m \frac{\partial T'}{\partial t} - (\rho c_p)_f \frac{\Delta T}{H} w' = k_m \nabla^2 T'. \quad (6.13)$$

Nondimensional variables are introduced by choosing  $H$ ,  $\sigma H^2/\alpha_m$ ,  $\alpha_m/H$ ,  $\Delta T$ , and  $\mu \alpha_m/K$  as scales for length, time, velocity, temperature, and pressure, respectively. Here  $\alpha_m$  is a thermal diffusivity defined by

$$\alpha_m = \frac{k_m}{(\rho c_p)_f} = \frac{k_m}{k_f} \alpha_f, \quad (6.14a)$$

where  $\alpha_f = k_f/(\rho c_p)_f$  is the thermal diffusivity of the fluid phase. It is convenient to define the *heat capacity ratio*

$$\sigma = \frac{(\rho c)_m}{(\rho c_p)_f} \quad (6.14b)$$

and put

$$\hat{x} = \frac{x}{H}, \quad \hat{t} = \frac{\alpha_m t}{\sigma H^2}, \quad \hat{v} = \frac{H v'}{\alpha_m}, \quad \hat{T} = \frac{T}{\Delta T}, \quad \hat{P} = \frac{K P'}{\mu \alpha_m}, \quad (6.15)$$

with  $\hat{x} = (x, y, z)$ . Substituting (6.11), (6.12), and (6.13), we get

$$\nabla \cdot \hat{\mathbf{v}} = 0, \quad (6.16)$$

$$\gamma_a \frac{\partial \hat{v}}{\partial \hat{t}} = -\nabla \hat{P} - \hat{v} + Ra \hat{T} \mathbf{k}, \quad (6.17)$$

$$\frac{\partial \hat{T}}{\partial \hat{t}} - \hat{w} = \nabla^2 \hat{T}, \quad (6.18)$$

where  $\mathbf{k}$  is the unit vector in the  $z$  direction and

$$Ra = \frac{\rho_0 g \beta K \Delta T}{\mu \alpha_m}, \quad Pr_m = \frac{\mu}{\rho_0 \alpha_m}, \quad \gamma_a = \frac{c_a K}{\sigma Pr_m H^2}. \quad (6.19)$$

In (6.19)  $Ra$  is the Rayleigh-Darcy number (or Rayleigh number, for short),  $Pr_m$  is an overall Prandtl number, and  $\gamma_a$  is a nondimensional acceleration coefficient. In most practical situations the Darcy number  $K/H^2$  will be small and as a consequence  $\gamma_a$  also will be small. Accordingly we take  $\gamma_a = 0$  unless otherwise specified. Note that the Rayleigh-Darcy number is the product of the Darcy number and the usual Rayleigh number for a clear viscous fluid.

Operating on (6.17) twice with curl, using (6.16), and taking only the  $z$  component of the resulting equation, we obtain

$$(1 + \gamma_a \partial/\partial t) \nabla^2 \hat{w} = Ra \nabla_H^2 \hat{T}, \quad (6.20)$$

where  $\nabla_H^2 = \partial^2/\partial x^2 + \partial^2/\partial y^2$ . Equations (6.18) and (6.20) contain just two dependent variables,  $\hat{w}$  and  $\hat{T}$ . Since the equations are linear, we can separate the variables. Writing

$$(\hat{w}, \hat{T}) = [W(\hat{z}), \theta(\hat{z})] \exp(st + il\hat{x} + im\hat{y}) \quad (6.21)$$

and substituting into (6.18) and (6.20), we obtain

$$(D^2 - \alpha^2 - s)\theta = -W, \quad (6.22)$$

$$(1 + \gamma_a s)(D^2 - \alpha^2)W = -\alpha^2 Ra \theta, \quad (6.23)$$

where

$$D \equiv \frac{d}{d\hat{z}} \quad \text{and} \quad \alpha = (l^2 + m^2)^{1/2}. \quad (6.23')$$

In these equations  $\alpha$  is an overall horizontal wavenumber. This pair of ordinary differential equations forms a fourth-order system, which must be solved subject to four appropriate boundary conditions.

Various types of boundaries can be considered. If both boundaries are impermeable and are perfect thermal conductors, then we must have  $w' = 0$  and  $T' = 0$  at  $z = 0$  and  $z = H$ , and so

$$W = \theta = 0 \quad \text{at } \hat{z} = 0 \quad \text{and} \quad \hat{z} = 1. \quad (6.24)$$

The homogeneous equations (6.22) and (6.24) form an eigenvalue system in which  $Ra$  may be regarded as the eigenvalue. In order for the solution to remain bounded as  $x, y \rightarrow \infty$ , the wavenumbers  $l$  and  $m$  must be real, and hence, the overall wavenumber  $\alpha$  must be real. In general  $s$  can be complex,  $s = s_r + i\omega$ . If  $s_r > 0$ , then perturbations of the form (6.21) grow with time, that is, we have instability. The case  $s_r = 0$  corresponds to marginal stability. In general  $\omega$  gives the frequency of oscillations, but in the present case it is easily proven that  $\omega = 0$  when

$s_r > 0$ , so when the disturbances grow with time they do so monotonically. In other words, the so-called principle of exchange of stabilities is valid.

For the case of marginal stability we can put  $s = 0$  in (6.22) and (6.23), which become

$$(D^2 - \alpha^2)\theta = -W, \quad (6.25)$$

$$(D^2 - \alpha^2)W = -\alpha^2 Ra \theta. \quad (6.26)$$

Eliminating  $\theta$  we have

$$(D^2 - \alpha^2)^2 W = \alpha^2 Ra W, \quad (6.27)$$

with

$$W = D^2 W = 0 \quad \text{at } \hat{z} = 0 \quad \text{and} \quad \hat{z} = 1. \quad (6.28)$$

We see immediately that  $W = \sin(j\pi\hat{z})$  is a solution, for  $j = 1, 2, 3, \dots$ , if

$$Ra = \frac{(j^2\pi^2 + \alpha^2)^2}{\alpha^2}. \quad (6.29)$$

Clearly  $Ra$  is a minimum when  $j = 1$  and  $\alpha = \pi$ , that is, the critical Rayleigh number is  $Ra_c = 4\pi^2 = 39.48$  and the associated critical wavenumber is  $\alpha_c = \pi$ . For the higher-order modes ( $j = 2, 3, \dots$ ),  $Ra_j = 4\pi^2 j^2$  and  $\alpha_{cj} = j\pi$ . An alternative to the derivation of critical Rayleigh number is constructal theory (Nelson and Bejan 1998; Bejan 2000), which yields  $Ra_c = 12\pi = 37.70$  (see Sect. 6.26).

In conclusion, for  $Ra < 4\pi^2$ , the conduction state remains stable. When  $Ra$  is raised above  $4\pi^2$ , instability appears as convection in the form of a cellular motion with horizontal wavenumber  $\pi$ .

In this way linear stability theory predicts the size of the convection cells, but it says nothing about their horizontal planform because the eigenvalue problem is degenerate. The  $(x, y)$  dependence can be given by any linear combination of terms of the form  $\exp(ilx + imy)$  where  $l^2 + m^2 = \alpha^2$ . In particular, dependence on  $\sin\alpha x$  corresponds to convection rolls whose axes are parallel to the  $y$ -axis, dependence on  $\sin(\alpha x/\sqrt{2}) \sin(\alpha y/\sqrt{2})$  corresponds to cells of square planform, and dependence on  $\cos\alpha x + 2\cos(\alpha x/2)\cos(\sqrt{3}\alpha y/2)$  corresponds to cells of hexagonal planform. In each case the nondimensional horizontal wavelength is  $2\pi/\alpha_c = 2$ . Since the height of the layer is 1, this wavelength is the width of a pair of counterrotating rolls of square vertical cross section. Further, linear theory does not predict whether, in a hexagonal cell, fluid rises in the center and descends near the sides or vice versa; nonlinear theory is needed to predict which situation will occur.

Equation (6.29) has been obtained for the case of impermeable conducting boundaries. For other boundary conditions the eigenvalue problem must in general

be solved numerically, but there is one other case when a numerical calculation is not necessary. It is made possible by the fact that the critical wavenumber is zero, and so an expansion in powers of  $\alpha^2$  works.

That special case is when both boundaries are perfectly insulating, that is, the heat flux is constant on the boundaries. When the boundaries are also impermeable, we have

$$W = D\theta = 0 \text{ at } \hat{z} = 0 \quad \text{and} \quad \hat{z} = 1. \quad (6.30)$$

Writing

$$(W, \theta, Ra) = (W_0, \theta_0, Ra_0) + \alpha^2(W_1, \theta_1, Ra_1) + \dots, \quad (6.31)$$

substituting (6.25), (6.26), and (6.30) and equating powers of  $\alpha^2$ , we obtain in turn systems of various orders. For the zero-order system we find that

$$D^2W_0 = 0, \quad D^2\theta_0 + W_0 = 0,$$

$$W_0 = D\theta_0 = 0 \quad \text{at } \hat{z} = 0, 1.$$

This system has the solution  $W_0 = 0$ ,  $\theta_0 = \text{constant}$ , and without loss of generality we can take  $\theta_0 = 1$ . The order  $\alpha^2$  system is

$$D^2W_1 = W_0 - Ra_0\theta_0 = -Ra_0, \quad D^2\theta_1 + W_1 = \theta_0 = 1,$$

$$W_1 = D\theta_1 = 0 \quad \text{at } \hat{z} = 0, 1.$$

With the arbitrary factor suitably chosen, these equations yield in succession

$$W_1 = -\frac{1}{2}Ra_0(\hat{z}^2 - \hat{z}),$$

$$\left\langle 1 + \frac{1}{2}Ra_0(\hat{z}^2 - \hat{z}) \right\rangle = 0,$$

This implies that  $Ra_0 = 12$ . From the order  $\alpha^4$  system,  $Ra_1$  can be calculated. It turns out to be positive, so it follows that  $Ra_c = 12$ ,  $\alpha_c = 0$ .

More generally, one can impose boundary conditions

$$DW - K_l W = 0, \quad D\theta - L_l \theta \quad \text{at } \hat{z} = 0, \quad (6.32)$$

$$DW + K_u W = 0, \quad D\theta + L_u \theta = 0 \quad \text{at } \hat{z} = 1.$$

The subscripts l and u refer to lower and upper boundaries, respectively. Here  $L_l$  and  $L_u$  are Biot numbers, taking the limit values 0 for an insulating boundary and  $\infty$  for a conducting boundary. The coefficients  $K_l$  and  $K_u$  take discrete values, 0 for a

**Table 6.1** Values of the critical Rayleigh number  $Ra_c$  and the corresponding critical wavenumber  $\alpha_c$  for various boundary conditions (after Nield 1968)

$K_l$	$K_u$	$L_l$	$L_u$	$Ra_c$	$\alpha_c$
IMP	IMP	CON	CON	$39.48 = 4\pi^2$	$3.14 = \pi$
IMP	IMP	CON	CHF	27.10	2.33
IMP	IMP	CHF	CHF	12	0
IMP	FRE	CON	CON	27.10	2.33
IMP	FRE	CHF	CON	17.65	1.75
IMP	FRE	CON	CHF	$9.87 = \pi^2$	$1.57 = \pi/2$
IMP	FRE	CHF	CHF	3	0
FRE	FRE	CON	CON	12	0
FRE	FRE	CON	CHF	3	0
FRE	FRE	CHF	CHF	0	0

The terms free, conducting, and insulating are equivalent to constant pressure, constant temperature, and constant heat flux, respectively

*IMP* impermeable ( $K = \infty$ ); *FRE* free ( $K = 0$ ); *CON* conducting ( $L = \infty$ ); *CHF* constant heat flux ( $L = 0$ )

boundary at constant pressure (as for the porous medium bounded by fluid), and  $\infty$  for an impermeable boundary. Critical values for various combinations are given in Table 6.1 after Nield (1968), with a correction. (The traditional term “insulating” refers to perturbations. This is somewhat confusing terminology, so following Rees (2000) we now refer to this as the constant heat flux condition. Also, strictly speaking, the constant-pressure condition refers to a hydrostatic situation in the exterior region.) As one would expect,  $Ra_c$  and  $\alpha_c$  both decrease as the boundary conditions are relaxed. Calculations for intermediate values of the Biot numbers  $L_l$  and  $L_u$  were reported by Wilkes (1995). The onset of gas convection in a moist porous layer with the top open to the atmosphere was analyzed by Lu et al. (1999). They found that the critical Rayleigh number was then less than the classical value of  $\pi^2$ . The open-top problem for a vertical fault was analyzed by Malkovsky and Pek (2004).

Tyvand (2002) demonstrated that the open boundary condition, traditionally known as the constant-pressure boundary condition, corresponds to requiring that the surrounding fluid is hydrostatic. Just as the kinematic condition on an impermeable boundary is  $\mathbf{n} \cdot \mathbf{v} = 0$ , the condition on an open boundary is  $\mathbf{v} \times \mathbf{n} = 0$ . The effect of conducting boundary plates, which lead to a conjugate convection-conduction problem, was studied by Mojtabi and Rees (2011) and Saleh et al. (2011b).

## 6.3 Weak Nonlinear Theory: Energy and Heat Transfer Results

The nonlinear nondimensional perturbation equations are

$$\gamma_a \frac{\partial \mathbf{v}}{\partial t} = -\nabla P - \mathbf{v} + Ra T \mathbf{k}, \quad (6.33)$$

$$\frac{\partial T}{\partial t} - w + \mathbf{v} \cdot \nabla T = \nabla^2 T \quad (6.34)$$

in which, for convenience, we have dropped the carets. These equations can be compared with the linear sets (6.17) and (6.18).

We can obtain equations involving energy balances by multiplying (6.33) and (6.34) by  $\mathbf{v}$  and  $\theta$ , respectively, and averaging over the fluid layer. We use the notation

$$\langle f \rangle = \int_0^1 \bar{f} dz,$$

where the bar denotes an average over  $(x, y)$  values at a given value of  $z$ . Using the fact that all expressions that can be written as a divergence vanish because of the boundary conditions and because contributions from the sidewalls become negligible in the limit of an infinitely extended layer, we obtain

$$\frac{1}{2} \gamma_a \frac{\partial}{\partial t} \langle \mathbf{v} \cdot \mathbf{v} \rangle = \langle Ra wT \rangle - \langle \mathbf{v} \cdot \mathbf{v} \rangle, \quad (6.35)$$

$$\frac{1}{2} \frac{\partial}{\partial t} \langle T^2 \rangle = \langle wT \rangle - \langle |\nabla T|^2 \rangle. \quad (6.36)$$

For steady or statistically stationary convection, the left-hand sides of these two equations are zero. Then (6.35) expresses the balance between the work done by the buoyancy force and the viscous dissipation, while (6.36) represents a similar relationship between the convective heat transfer and the entropy production by convection.

That  $\langle wT \rangle$  represents the convective part of the heat transport can be demonstrated as follows. The horizontal mean of (6.34) is

$$\frac{\partial \bar{T}}{\partial t} + \frac{\partial}{\partial z} (\bar{wT}) = \frac{\partial^2 \bar{T}}{\partial z^2}. \quad (6.37)$$

For a steady temperature field, integration with respect to  $z$  and use of the boundary conditions give

$$\frac{\partial \bar{T}}{\partial z} = \bar{wT} - \langle wT \rangle. \quad (6.38)$$

Since the normal component of the velocity ( $w$ ) vanishes at the boundary, the entire heat flux is transported by conduction at the boundary. Thus the expression

$$-\left. \frac{\partial \bar{T}}{\partial z} \right|_{z=1} = \langle wT \rangle$$

represents the convective contribution to the heat transport. The Nusselt number  $Nu$  is defined as the ratio of the heat transports with and without convection. Therefore we conclude that

$$Nu = 1 + \langle wT \rangle. \quad (6.39)$$

From (6.35) it follows that under stationary conditions  $\langle wT \rangle = 0$  and so  $Nu = 1$ . Also, under the same conditions, we see from (6.35) to (6.36) that

$$Ra = \frac{\langle |v|^2 \rangle \langle |\nabla T|^2 \rangle}{\langle WT \rangle^2} \quad (6.40)$$

The right-hand side has a positive minimum value, and it follows that steady or statistically stationary convection can exist only above a certain positive value of  $Ra$ . The right-hand side can be interpreted as a functional of the trial fields  $v$  and  $T$ . When this functional is minimized subject to the constraints of the continuity equation (6.16) and the boundary conditions, the energy stability limit  $Ra_E$  is obtained. No steady or statistically stationary form of convection is possible for  $Ra < Ra_E$ ; further details on this are given by Joseph (1976). The Euler equations corresponding to the variational problem that determine  $Ra_E$  turn out to be mathematically identical to the linearized steady version of (6.16), (6.17), and (6.18). Thus finite-amplitude “subcritical instability” is not possible, and the criterion  $Ra = Ra_c$  provides not only a sufficient condition for instability but also a necessary one.

We also note that the total nondimensional mean temperature gradient  $\partial \bar{T}_{\text{total}} / \partial z$  is given by

$$\frac{\partial \bar{T}_{\text{total}}}{\partial z} = -1 + \overline{wT} - \langle wT \rangle \quad (6.41)$$

and that it is related to the conduction-referenced Nusselt number,

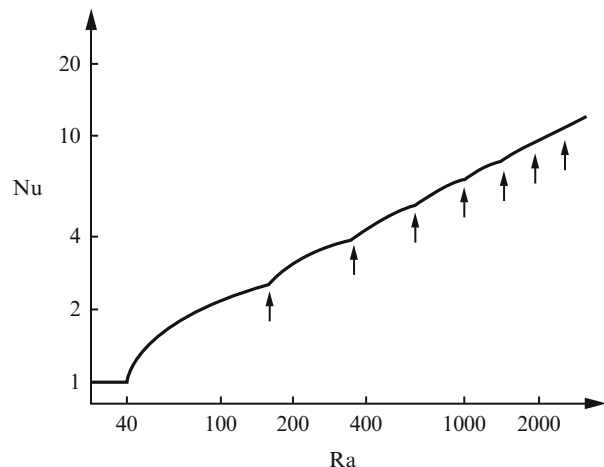
$$Nu = - \left| \frac{\partial \bar{T}_{\text{total}}}{\partial z} \right|_{z=0}. \quad (6.42)$$

We also note that the effect of convection is to increase the temperature gradient near each boundary and decrease it in the remainder of the layer.

From (6.34) in the steady case we have

$$\int_0^1 \overline{wT} \frac{\partial \bar{T}_{\text{total}}}{\partial z} dz = \langle T \nabla^2 T \rangle$$

**Fig. 6.2** The theoretical relationship  $Nu(Ra)$  given by (6.45) (Bories 1987, with permission from Kluwer Academic Publishers)



and after using (6.41),

$$\langle wT \rangle + \langle T\nabla^2 T \rangle = \int_0^1 (\overline{wT})^2 dz - \langle wT \rangle^2. \quad (6.43)$$

If we now substitute for  $w$  and  $T$  the solutions of the linearized equations, we obtain an expression for the amplitude  $A$  of the disturbances corresponding to the  $j$ th mode,

$$A = (Ra - Ra_{cj})^{1/2}. \quad (6.44)$$

At the same time we can compute the Nusselt number from (6.39).

If we assume that the various modes contribute independently to the Nusselt number, we then obtain

$$Nu = 1 + \sum_{j=1}^{\infty} k_j \left( 1 - \frac{Ra_{cj}}{Ra} \right), \quad (6.45)$$

where  $Ra_{cj} = 4j^2\pi^2$ ,  $k_j = 2$  for  $Ra > Ra_{cj}$ , and  $k_j = 0$  for  $Ra < Ra_{cj}$ , for the case of two-dimensional rolls. As Rudraiah and Srimani (1980) showed, other planforms lead to smaller values of  $k_1$  and hence may be expected to be less favored at slightly supercritical Rayleigh numbers. The Nusselt number relationship (6.45) is plotted in Fig. 6.2. It predicts values of  $Nu$  that generally are lower than those observed. It leads to the asymptotic relationship  $Nu \rightarrow (2/3\pi) Ra^{1/2}$  as  $Ra \rightarrow \infty$  (Nield 1987b). Similar results for the case of constant-flux boundaries rather than isothermal boundaries were obtained by Salt (1988). As expected, this change leads to an increase in  $Nu$ , the change becoming smaller as  $Ra$  increases (because more and more modes then contribute).

Expression (6.45) may be compared with the result of Palm et al. (1972), who performed a perturbation expansion in powers of a perturbation parameter  $\zeta$  defined by

$$\zeta = \left(1 - \frac{Ra_c}{Ra}\right)^{1/2}.$$

Their sixth-order result is

$$Nu = 1 + 2\lambda \left[ \zeta^2 + \left(1 - \frac{17}{24}\lambda\right)\zeta^4 + \left(1 - \frac{17}{24}\lambda + \frac{191}{288}\right)\lambda^2 \right] \zeta^6, \quad (6.46)$$

where  $\lambda = (1 - \zeta^6)^{-1}$ . Equation (6.46) predicts well the observed heat transfer for  $Ra/Ra_c < 5$ .

Using a variational formulation based on the Malkus hypothesis that the physical realizable solution is the one that maximizes the heat transport (see also Sect. 6.24), Busse and Joseph (1972) and Gupta and Joseph (1973) obtained upper bounds on  $Nu$ . These were found to be in good agreement with the experimental data of Combarous and Le Fur (1969) and Buretta and Berman (1976) for  $Ra$  values up to 500 (see Sect. 6.9). Further work on bounds on heat transport was reported by Doering and Constantin (1998), Vitanov (2000), Wei (2007), and Wen et al. (2012).

An expansion in powers of  $(Ra - Ra_c)^{1/2}$  to order 34 was carried out by Grundmann and Mojtabi (1995) and Grundmann et al. (1996). They thus computed with great precision the values of  $Nu$  at a few values of  $Ra$ .

## 6.4 Weak Nonlinear Theory: Further Results

We briefly outline the perturbation approach that is applicable to convection in both clear fluids and in porous media. It has been presented in detail by Busse (1985). The analysis starts with the series expansions

$$\mathbf{v} = \varepsilon[\mathbf{v}^{(0)} + \varepsilon\mathbf{v}^{(1)} + \varepsilon^2\mathbf{v}^{(2)} + \dots], \quad (6.47)$$

$$Ra = Ra_c + \varepsilon Ra^{(1)} + \varepsilon^2 Ra^{(2)} + \dots \quad (6.48)$$

and analogous expressions for  $T$  and  $P$ , and involves the successive solutions of linear equations corresponding to each power of  $\varepsilon$ . These expressions are substituted into (6.16), (6.17), and (6.18). Since only steady solutions are examined, the  $\partial/\partial t$  terms vanish, and in the order  $\varepsilon^1$  problem we have the same equations as for the linear problem treated in Sect. 6.2. The general solution to that problem is expressed as

$$w^{(0)} = f(z, \alpha) \sum_n c_n \exp(i\mathbf{k}_n \cdot \mathbf{r}), \quad (6.49)$$

where  $\mathbf{r}$  is the position vector and the horizontal wavenumber vectors  $\mathbf{k}_n$  satisfy  $|\mathbf{k}_n| = \alpha$  for all  $n$ .

In the order  $\varepsilon^2$  and higher-order problems, inhomogeneous linear equations arise, and the solvability condition determines the coefficients  $Ra^{(n)}$  and provides constraints on the choice of coefficients  $c_n$ . In this fashion possible solutions, representing two-dimensional rolls and hexagons, are determined. There still exist many such solutions. The stability of each of these is examined by superposing arbitrary infinitesimal disturbances  $\tilde{\mathbf{v}}, \tilde{T}$  on the steady solution  $\mathbf{v}, T$ . By subtracting the steady equations from the equations for  $\mathbf{v} + \tilde{\mathbf{v}}, T + \tilde{T}$ , the following stability problem is obtained:

$$\sigma \gamma_a \tilde{\mathbf{v}} = -\nabla \tilde{P} + Ra \tilde{T}k - \tilde{\mathbf{v}}, \quad (6.50a)$$

$$\tilde{\sigma} \tilde{T} + \tilde{\mathbf{v}} \cdot \nabla T + \mathbf{v} \cdot \tilde{T} = \tilde{w} + \nabla^2 \tilde{T}, \quad (6.50b)$$

$$\nabla \cdot \tilde{\mathbf{v}} = 0, \quad (6.50c)$$

$$\tilde{w} = \tilde{T} = 0 \quad \text{at } \hat{z} = 0.1. \quad (6.50d)$$

These equations are based on the observation that since the stability problem is linear, the time dependence can be assumed to be of the form  $\exp(\tilde{\sigma}t)$ . The steady solution is unstable when an eigenvalue  $\tilde{\sigma}$  with a positive real part exists.

The eigenvalue problem (6.50) can be solved by expanding  $\tilde{\mathbf{v}}, \tilde{T}$ , and  $\tilde{\sigma}$  as power series in  $\varepsilon$  analogous to (6.47). By considering coefficients up to  $\tilde{\sigma}^{(2)}$  in the series for  $\tilde{\sigma}$ , one can demonstrate that all steady solutions are unstable with the exception of two-dimensional rolls. Moreover, it is found that at small but finite values of  $Ra - Ra_c$  rolls corresponding to a finite range of wavenumbers are stable.

The main conclusion to be drawn from such results is that a spectrum of different steady convection modes is physically realizable and the asymptotic state of a convection layer in general will depend on the initial conditions.

Although two-dimensional rolls are favored when the physical problem has vertical symmetry about the midplane, it is found that hexagons are favored when there is a significant amount of asymmetry, whether it is due to different boundary conditions at top and bottom or due to property variations with temperature or other heterogeneities. Hexagons also are favored when the basic temperature profile is not linear, as when convection is produced by a volume distribution of heat sources rather than by heating from below. Two-dimensional rolls rarely have been observed in experiments on Horton-Rogers-Lapwood (HRL) convection, even in circumstances when they might have been expected (as in one experiment reported by Lister (1990)).

The direction of motion in a hexagonal cell is influenced by property variations. Other things being equal, motion at the center of a cell is in the direction of increasing kinematic viscosity. In liquids the kinematic viscosity decreases as the temperature increases, so the liquid rises in the center of a cell. In gases the reverse

is the case, so gas sinks in the center of a cell. Further reading on this is provided by Joseph (1976, p. 112).

We conclude this section with the results of a study of the stability of convection rolls to three-dimensional disturbances made by Joseph and Nield and reported in Joseph (1976, Chapter XI). The various types of possible disturbances are graphically labeled as parallel rolls, cross rolls, sinuous (or zigzag) rolls, and varicose rolls. Joseph and Nield found that the sinuous rolls and the cross rolls are the ones that effectively restrict the range  $\alpha_1(\varepsilon) < \alpha(\varepsilon) < \alpha_2(\varepsilon)$  for which the convection rolls of wavenumber  $\alpha(\varepsilon)$  are stable. For the case of impermeable conducting boundaries, the stability boundary for cross rolls in the neighborhood of the critical point  $(\alpha_c, Ra_c)$ , where  $\alpha_c = \pi$ ,  $Ra_c = 4\pi^2$ , is given by

$$\frac{Ra}{Ra_c} - 1 = \frac{10}{3} \left( \frac{\alpha}{\alpha_c} - 1 \right)^2 \quad (6.51)$$

and that for the sinuous rolls is given by

$$\frac{Ra}{Ra_c} - 1 = \frac{12}{19^{1/2}} \left( 1 - \frac{\alpha}{\alpha_c} \right)^{1/2}, \quad \alpha < \alpha_c. \quad (6.52)$$

For comparison, the neutral curve for the basic conduction solution is

$$\frac{Ra}{Ra_c} - 1 = \left( \frac{\alpha}{\alpha_c} - 1 \right)^2. \quad (6.53)$$

Equation (6.52) determines the lower limit of the range of wavenumbers for stable rolls and (6.51) the upper limit for  $Ra$  values near  $Ra_c$  (Fig. 6.3).

For larger values of  $Ra$ , numerical calculations are necessary to determine the range of wavenumbers for stability. In this way Straus (1974) calculated a balloon-shaped curve in the  $(\alpha, Ra)$  plane. The points situated inside the balloon correspond to stable rolls (Fig. 6.4).

The stability of two-dimensional convection has been analyzed further by De la Torre Juárez and Busse (1995) for  $Ra$  values up to 20 times the critical. Some of their results are displayed in Figs. 6.5, 6.6, and 6.7. In Fig. 6.5, the Nusselt number is plotted against  $Ra$  for fixed  $\alpha = \alpha_c$ . At  $Ra = 391 \pm 1$ , the steady solution becomes unstable and is replaced by an oscillatory solution with a higher Nusselt number; the frequency also is given in the figure. At  $Ra = 545$ , this even solution becomes unstable. For a given Rayleigh number, the Nusselt number varies with the wavenumber as shown in Fig. 6.6. The results of stability analysis are shown in Fig. 6.7. This figure shows that there is an oscillatory instability predicted for small wavenumbers  $\alpha \sim \alpha_c$ . This oscillatory state has been observed in experiments with Hele-Shaw cells.

De la Torre Juárez and Busse also carried out direct numerical integrations in time of the solutions in the unstable regions. They found that the Eckhaus instability

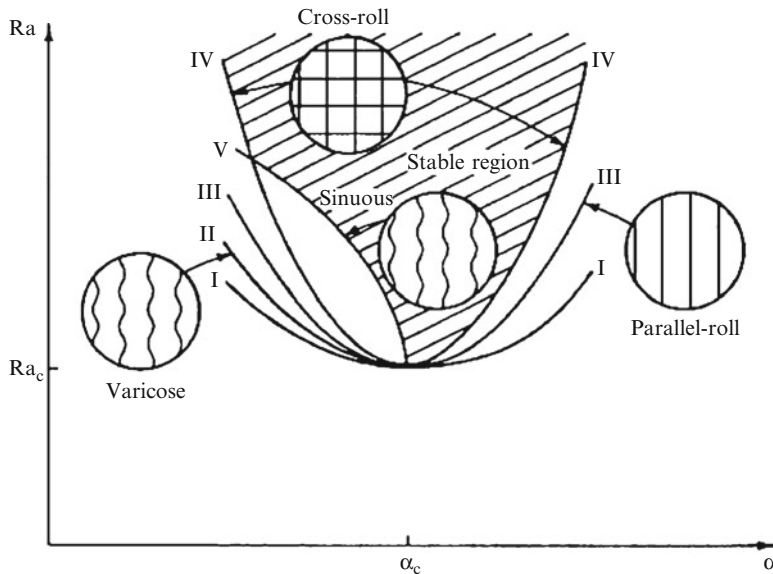


**Fig. 6.3** Sketch of parabolic approximations of  $(\alpha, Ra)$  projections of nonlinear neutral curves for roll convection, valid in a neighborhood of  $(\alpha_c, Ra_c)$ . The neutral curve for the rest state with a constant temperature gradient is shown as I. Curves II, III, IV, and V are nonlinear neutral curves for different convection disturbances. Sinuous and varicose instabilities occur only when  $\alpha < \alpha_c$  (Joseph 1976, with permission from Springer Verlag)

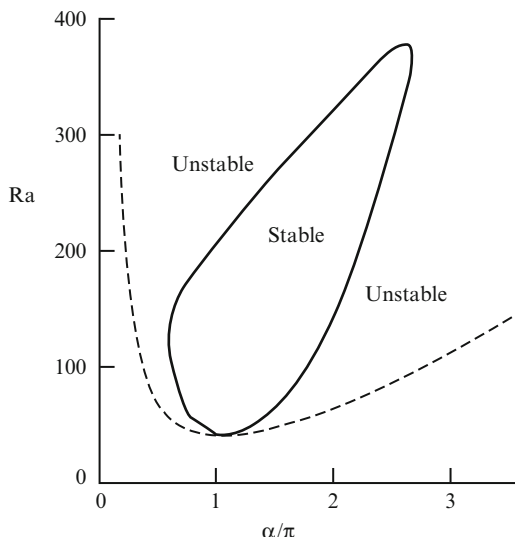


**Fig. 6.4** Regions of stable and unstable two-dimensional rolls. The dashed line is the neutral stability curve obtained from the linear stability analysis (Straus 1974, with permission from Cambridge University Press)

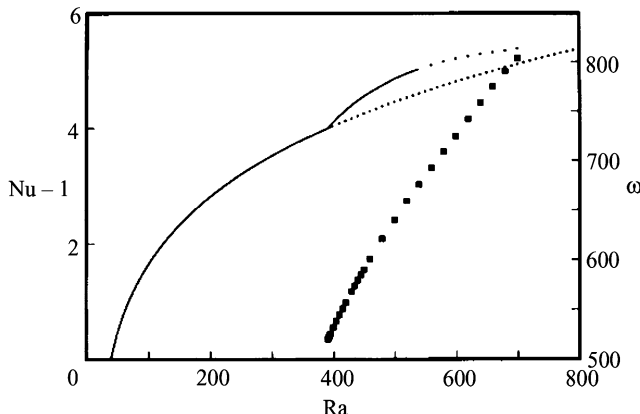


**Fig. 6.5** Average value of the Nusselt number of the steady and oscillatory solutions as a function of the Rayleigh number for a fixed wavenumber  $\alpha = \alpha_c$ . The unstable stationary solutions are represented by dots. The frequency of the oscillatory solutions is denoted by squares (De la Torre Juarez and Busse 1995, with permission from Cambridge University Press)

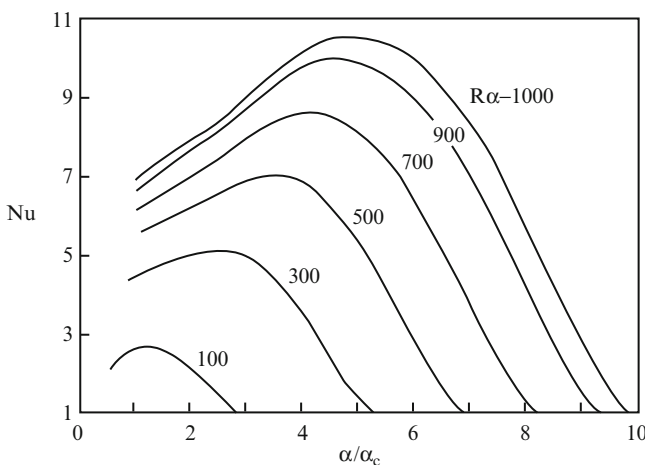


**Fig. 6.6** Value of the Nusselt number of the steady solutions as a function of the wavenumber  $\alpha$  for different values of the Rayleigh number (De la Torre Juarez and Busse 1995, with permission from Cambridge University Press)

limiting the band of stable wavenumbers at low supercritical Rayleigh numbers is replaced by a sideband instability corresponding to odd-parity perturbations as the Rayleigh number increases. This instability leads to a 3:1 jump in the wavelength. A third instability of oscillatory character occurs at high wavenumbers, which is also related to a 3:1 resonance mechanism and tends to change the wavelength by a

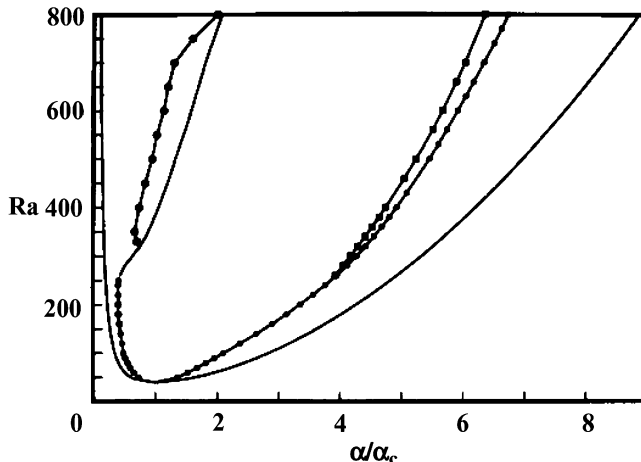


**Fig. 6.7** Regions of stability of the steady solutions as a function of the Rayleigh number and the wavenumber. The neutral curve is the outer solid line; the Eckhaus instability is plotted as a line with solid circles; the transitions to the different oscillatory instabilities are plotted as a solid line with squares at high wavenumbers and as a solid line at low wavenumbers; the stability limits of the stationary oscillatory solutions are plotted as a solid line with open circles (De la Torre Juarez and Busse 1995, with permission from Cambridge University Press)

finite amount. The fourth instability yields an oscillatory state of even parity for low wavenumbers and for Rayleigh numbers above  $\text{Ra} = 218$ . In the region where even oscillatory solutions exist, they lose stability through the growth of odd oscillatory modes. In one case the odd modes grow while the existing even oscillatory solution persists, yielding a non-centrosymmetric state with several temporal frequencies. In a second case, occurring at  $\text{Ra}$  above 790, steady convection bifurcates into a regular oscillatory state where the odd modes dominate the even modes; this is related to an asymmetry between the rising hot and the falling cold plumes.

Nisse and Neél (2005) have investigated the stability of rolls with intermediate wavelength (those not unstable to the cross roll, Eckhaus, and zigzag instabilities). They proved that such rolls are spectrally stable.

The effect of quadratic drag was studied by Rees (1996b). He found that rolls with a wavenumber less than the critical value are no longer unconditionally unstable. Also the Eckhaus (parallel-roll) and zigzag (sinuous) stability bounds are less restrictive than in the absence of quadratic drag, but the opposite is true for the cross-roll instability.

The results discussed so far in this section have been based on the assumption that the porous medium is bounded by impermeable isothermal (perfectly conducting) planes. Riahi (1983) has shown that when the boundaries have finite thermal conductivity, the convection phenomenon is different. He found that cells of square planform are preferred in a bounded region  $\Gamma$  of the  $(\lambda_b, \lambda_t)$  space, where  $\lambda_b$  and  $\lambda_t$  are the ratios of the thermal conductivities of the lower and upper boundaries to that of the fluid and two-dimensional rolls are favored only outside  $\Gamma$ .

For the case of uniform heat flux on the boundaries, Néel and Lyubimov (1995) proved the existence of periodic solutions for a class of nonlinear regular vector fields.

The results in this section bear on the choice of wavenumber to use in numerical simulations. Since the theory does lead to a unique value and since the Malkus hypothesis (that the selected wavenumber which maximizes heat transfer) is now known to be unsatisfactory, Nield (1997b) has suggested that in most cases it is probably satisfactory to take  $\alpha = \alpha_c$  in the simulations.

Adomian's decomposition method and weak nonlinear theory were compared by Vadasz (1999a), who explained the experimental observation of hysteresis from steady convection to chaos to steady state (see also Auriault 1999; Vadasz 1999b). The Adomian method was further used by Vadasz and Olek (1999a, 2000a) to discuss convection for low and moderate Prandtl number, and its application to the solution of the Lorenz equations was investigated by Vadasz and Olek (2000b). Weak turbulence in small and moderate Prandtl number convection was reviewed and elucidated by Vadasz (2003). The computational recovery of the homoclinic orbit was discussed by Vadasz and Olek (1999b), while the compatibility of analytical and computational solutions was discussed by Vadasz (2001b). The question of whether the transitions involved in porous media natural convection could be smooth was examined by Vadasz et al. (2005). The results of their examination suggest that the transitions inevitably are sudden. The phenomenon of hysteresis was studied by Vadasz (2006a). A comprehensive review of the subject of weak turbulence and transitions to chaos was made by Vadasz (2006b). The Vadasz-Olek model was examined as a system of coupled oscillators by Magyari (2010c). The "butterfly effect" in a porous slab was studied by Magyari (2006b). The case of Cattaneo heat flux was studied by Straughan (2010b). The selection of steady states was analyzed by Tsybulin et al. (2006) and Tsybulin and Karasozen (2008).

An unconditional stability result for the case of a cubic dependence of density on temperature, with the Forchheimer equation, was obtained by Carr (2003). Previously Gentile and Rionero (2000) had studied global nonlinear stability for penetration with fluids of cubic density. Further work on oscillatory convection regimes was reported by Holzbecher (2001), while Holzbecher (2004b) treated a mixed boundary condition appropriate for open-top enclosures. He noted that at 16.51 the critical Rayleigh number is then much lower than the classical value. Holzbecher (2005a) studied both free and forced convective flows for open-top enclosures. Co-symmetric families of steady states and their collision were investigated by Karasozen and Tsybulin (2004).

A review of some aspects of nonlinear convection was made by Rudraiah et al. (2003). A comprehensive review of other matters, including methods for calculating eigenvalues, is contained in the books by Straughan (2004b, 2008). Recent work on the analytical transition to weak turbulence and chaotic natural convection was surveyed by Vadasz (2008a).

A Legendre spectral element for eigenvalues was introduced by Hill and Straughan (2006). The effect of conducting boundaries was studied by Rees

and Mojtabi (2011). Their aim was to identify the identity of the post-critical convection patterns as a function of the thicknesses and conductivities of the bounding plates relative to the porous layer. They presented regions in parameter space where convection in the form of rolls is unstable and within which cells with square planform form the preferred pattern.

## 6.5 Effects of Solid–Fluid Heat Transfer

At sufficiently large Rayleigh numbers, and hence sufficiently large velocities, one can expect that local thermal equilibrium will break down so that the temperatures  $T_s$  and  $T_f$  in the solid and fluid phases are no longer identical. Instead of a single energy equation (2.3) or (6.5), one must revert to the pair of equations (2.1) and (2.2). Following Bories (1987), we consider the case of constant conductivities  $k_s$  and  $k_f$  and no heat sources, but we modify (2.1) and (2.2) by allowing for heat transfer between the two phases. Accordingly we have

$$(1 - \varphi)(\rho c)_s \frac{\partial T_s^*}{\partial t^*} = k_{es} \nabla^{*2} T_s^* - h(T_s^* - T_f^*), \quad (6.54)$$

$$\varphi(\rho c_P)_f \frac{\partial T_f^*}{\partial t^*} + (\rho c_P)_f \mathbf{v}^* \cdot \nabla^* T_f^* = k_{ef} \nabla^{*2} T_f^* - h(T_f^* - T_s^*). \quad (6.55)$$

In these equations asterisks denote dimensional quantities, and  $h$  is a heat transfer coefficient, while  $k_{es}$  and  $k_{ef}$  are effective conductivities. In the purely thermal conduction limit,  $k_{es} = (1 - \varphi)k_s$  and  $k_{ef} = \varphi k_f$ . Equations (6.3), (6.4), and (6.6) still stand. We choose  $H$  for length scale,  $(\rho c)_m H^2/k_m$  for timescale,  $k_m/(\rho c_P)_f H$  for velocity scale,  $\Delta T$  for temperature scale, and  $\mu k_m/K(\rho c_P)_m$  for pressure scale. Then (6.54) and (6.55) take nondimensional forms:

$$(1 - \varphi M)(1 + \Lambda) \frac{\partial T_s}{\partial t} = \nabla^2 T_s - \Lambda \chi(T_s - T_f), \quad (6.56)$$

$$\varphi M(1 + \Lambda^{-1}) \frac{\partial T_f}{\partial t} + (1 + \Lambda^{-1}) \mathbf{v} \cdot \nabla T_f = \nabla^2 T_f - \chi(T_f - T_s), \quad (6.57a)$$

where

$$M = \frac{(\rho c_P)_f}{(\rho c)_m}, \quad \Lambda = \frac{k_{ef}}{k_{es}}, \quad \chi = \frac{hH^2}{\varphi k_f}. \quad (6.57b)$$

Combarnous (1972) calculated the Nusselt number  $Nu$  as a function of  $Ra$ ,  $\Lambda$ , and  $\chi$ . He found that for a given value of  $\Lambda$ ,  $Nu$  is an increasing value of  $\chi$  which tends, when  $h \rightarrow \infty$ , toward the value given in the local equilibrium model.

This trend is expected because the limit corresponds to perfect transfer between solid and fluid phase.

When the parameter  $\chi$  defined in (6.58) is maintained constant,  $Nu$  tends toward the local equilibrium value as  $\Lambda$  increases, that is, as the contribution of heat conduction by the solid phase becomes negligible. When heat conduction through the solid phase becomes very large, the Nusselt number decreases; in fact,  $Nu \rightarrow 1$  as  $\Lambda \rightarrow 0$ .

The computed temperature distributions show that  $|T_s - T_f|$  takes relatively large values in the upper part of the upward current and the lower part of the downward current. This illustrates the role of the solid phase as a heat exchanger. Another point follows from the fact that  $\chi$  is the product of a local heat transfer factor  $hd_p^2/\varphi k_f$  and  $(H/d_p)^2$ , where  $d_p$  is the pore scale. When the scale factor  $H/d_p$  is large, the porous medium behaves as a thorough blend of solid and fluid phases. When it is small, the porous medium is effectively more heterogeneous.

Banu and Rees (2002) demonstrated that both the critical Rayleigh number and the wavenumber are modified by thermal nonequilibrium. For intermediate values of the interphase heat transfer coefficient, the critical wavenumber is always greater than  $\pi$ , the classic value. Postelnicu and Rees (2003) incorporated form drag and boundary effects. For the case of stress-free boundaries, they obtained the expression

$$Ra = \frac{(\pi^2 + \alpha^2)^2}{\alpha^2} [1 + Da(\pi^2 + \alpha^2)] \left[ \frac{(\pi^2 + \alpha^2) + \chi(1 + \gamma)}{(\pi^2 + \alpha^2 + \gamma\chi)} \right], \quad (6.58)$$

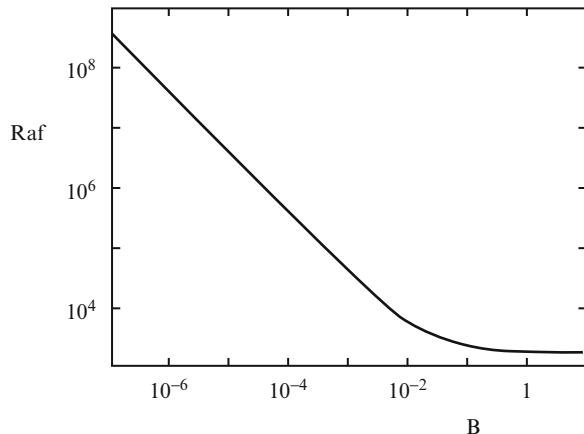
where  $\gamma = \phi\Lambda/(1 - \phi)$ . The critical Rayleigh number is obtained on minimization with respect to variation of  $\alpha$ . Clearly  $Ra_c$  is an increasing function of  $Da$ , and for  $Da = 0$ , it is an increasing function of  $\chi$  from the base value  $4\pi^2$  with the amount of increase decreasing as  $\gamma$  increases.

The case of isoflux boundary conditions was studied by Barletta and Rees (2012a) for the case of boundary walls of high conductivity. Their linear perturbation analysis led to a one-dimensional eigenvalue problem which they solved numerically to determine a neutral stability condition. They obtained analytical solutions for the limit of small wavenumbers and in the region where the solid conductivity is much larger than the fluid conductivity. They found that the critical wavenumber is zero only when the interphase heat transfer coefficient is sufficiently large.

Boundary effects were also considered by Malashetty et al. (2005a). The situation where there is heat generation in the solid phase in a square enclosure was studied numerically by Baytas (2003, 2004a). An anisotropic layer was considered by Malashetty et al. (2005b).

Global nonlinear stability was studied by Straughan (2006). Chaotic convection was treated by Sheu (2006).

**Fig. 6.8** Critical fluid Rayleigh number  $Ra_f = Ra H^2/K$  vs. the Brinkman coefficient  $B = (\tilde{\mu}/\mu)K/H^2 = (\tilde{\mu}/\mu)$ .  $Da = \tilde{D}a$ . The figure illustrates the transition from the Darcy limit to the clear fluid limit (Walker and Homsy 1977)



Further work on local thermal nonequilibrium has been conducted by Khashan et al. (2006), Postelnicu (2008), and Shivakumara et al. (2010b, c). Vadasz (2012) has studied a layer heated from below via a constant heat flux.

## 6.6 Non-Darcy, Dispersion, and Viscous Dissipation Effects

Corresponding to the Darcy equation (6.17), the linear Brinkman equation is

$$\gamma_a \frac{\partial v}{\partial t} = -\nabla P - v + \tilde{D}a \nabla^2 v + Ra \theta k. \quad (6.59)$$

Here  $\tilde{D}a$  is a Darcy number defined by

$$\tilde{D}a = \frac{\tilde{\mu}}{\mu} \frac{K}{H^2} = \frac{\tilde{\mu}}{\mu} \frac{K}{d_p^2} \left( \frac{d_p}{H} \right)^2 \quad (6.60)$$

and  $d_p$  is a characteristic length on the pore scale. From the Carman-Kozeny equation (1.5), we see that  $K/d_p^2$  is of the order of unity unless  $\varphi$  is close to 1. Also  $\tilde{\mu}/\mu$  is of the order of unity, while  $d_p/H$  is small if the porous medium is properly represented by a continuum. It follows that  $\tilde{D}a$  is normally very small, and thus the Brinkman term is important only in boundary layers where  $\nabla^2 v$  is large. In conclusion, in naturally occurring media the net effect of the Brinkman term is to alter the critical Rayleigh number by a small amount. An apparent exception to this statement was reported by Lebon and Cloot (1986); they failed to distinguish between a constant-pressure boundary and a stress-free boundary. Detailed calculations are given by Walker and Homsy (1977), and Fig. 6.8. The Darcy result holds if the Darcy number  $Da = K/H^2 < 10^{-3}$ . For  $Da > 10$ ,  $Ra \sim 1,708 Da$ ,

**Table 6.2** Approximate values showing the dependence of Nusselt number  $Nu$  and nondimensional r.m.s. velocity  $\bar{Q}$  on the Rayleigh number  $Ra$  (Nield and Joseph 1985)

$Ra$	$Nu$	$\bar{Q}$
$10^2$	3	15
$3 \times 10^2$	6	40
$10^3$	10	100
$3 \times 10^3$	14	200
$10^4$	20	340

the clear fluid limit. Rees (2002b) performed a perturbation analysis for small Darcy number (defined to include the viscosity ratio) and obtained the approximation

$$Ra_c = 4\pi^2 + 8\pi^2 Da^{1/2} + [8\pi^4 + 12\pi^2 + 4\pi^3 3^{1/2} \tanh(3^{1/2}\pi/2)] Da, \quad (6.60a)$$

$$a_c = \pi + \pi Da^{1/2}. \quad (6.60b)$$

The Forchheimer equation that replaces (6.17) is

$$\gamma_a \frac{\partial \mathbf{v}}{\partial t} = -\nabla P - \mathbf{v} - F|\mathbf{v}|\mathbf{v} + Ra \theta \mathbf{k}, \quad (6.61)$$

where  $F$  is a Forchheimer coefficient defined by

$$F = \frac{c_F \rho_f K^{1/2} \alpha_m}{\mu H}, \quad Q = \frac{c_F}{Pr_f} \frac{k_m}{k_f} \left( \frac{K}{H^2} \right)^{1/2} Q. \quad (6.62)$$

In these equations  $Pr_f = \mu/\rho_f \alpha_f$  is the Prandtl number of the fluid, and  $Q$  is a Péclet number expressing the ratio of a characteristic velocity of the convective motion to the velocity scale  $\alpha_m/H$  (with which we are working). In particular, if we take  $Q$  to be the r.m.s. average  $\bar{Q}$ , then we can use information given by Palm et al. (1972) to deduce that (see Table 6.2):

$$\bar{Q} = [Ra(Nu - 1)]^{1/2}. \quad (6.63)$$

We can conclude that the Forchheimer term can be significant, even for modest Rayleigh numbers, for thin layers of media for which  $Pr_f(k_f/k_m)$  is small. For example, if we take the values  $c_F = 0.1$ ,  $K = 10^{-3} \text{ cm}^2$ ,  $H = 1 \text{ cm}$ , which are appropriate for a 1-cm-thick layer of a medium of metallic fibers, and the value  $Ra = 300$  that is typical for a transition to oscillatory convection (Sect. 6.8), then

quadratic drag is significant if  $Pr_f k_f/k_m$  is of order 0.1 or smaller. In other situations rather large Rayleigh numbers are needed before quadratic drag becomes important.

The effect of quadratic drag was shown by Nield and Joseph (1985) to cause the nose of the bifurcation curve in the  $(Ra, \varepsilon)$  plane to be sharpened; the standard pitchfork bifurcation is modified to straight lines intercepting the zero amplitude axis. Here  $\varepsilon$  is a measure of the amplitude of the disturbance. He and Georgiadis (1990) confirmed the sharpening. Rees (1996b) undertook a third-order analysis that showed that at higher Rayleigh numbers, the usual square root behavior is restored. He also developed a full weakly nonlinear stability analysis and found that inertia causes some wavenumbers less than the critical value to regain stability, but the cross-roll instability is more effective and reduces the stable wavenumber range. The effect of quadratic drag on higher-order transitions was studied numerically by Strange and Rees (1996). They expressed their results in terms of a parameter  $G = F/Q$ . They found that at Rayleigh numbers below a second critical value, a steady cellular pattern exists, but the amplitude of the motion and the corresponding rate of heat transfer decrease sharply as  $G$  increases. At the second critical Rayleigh number, whose value increases almost linearly with  $G$ , the preferred mode of convection is time periodic. The mechanism of Kimura et al. (1986), where waves orbit each cell, also applies when quadratic drag is present.

Néel (1998) considered how a horizontal pressure gradient affects convection in the presence of inertia and boundary friction effects. Her formulation leads to a cubic (rather than quadratic) drag term, and she found that this inertial effect leads to an increase in the critical Rayleigh number.

We saw in Sect. 2.2.3 that the effect of thermal dispersion was to increase the effective conductivity of the porous medium. Instead of (6.18), we now have

$$\frac{\partial T}{\partial t} - \hat{w} = \nabla \cdot [(1 + D^*) \nabla \hat{T}], \quad (6.64)$$

where  $D^*$  is the ratio of dispersive to stagnant conductivity. According to the model for a packed bed of beads adopted by Georgiadis and Catton (1988),  $D^* = Di \text{lv}_l$ , where

$$Di = \frac{Cd_b}{(1 - \varphi)H}. \quad (6.65)$$

Here  $d_b$  is the mean bead diameter, and  $C$  is a dispersion coefficient whose value depends on the type of packing. Georgiadis and Catton performed calculations with the value  $C = 0.36$ , which was chosen to give the best fit to experimental data.

Since the term  $D^* \nabla T = Di |v| \nabla T$  is of second order, it is clear that dispersion does not affect the critical Rayleigh number but it does have nonlinear effects that decrease the overall Nusselt number significantly for coarse materials (Neichloss and Dagan 1975). Kvernvold and Tyvand (1980) showed that dispersion expands the stability balloon of Straus (1974) (Fig. 6.4), that is, it causes two-dimensional

rolls to remain stable to cross-roll instabilities for Rayleigh numbers larger than those in the absence of dispersion. The effect of dispersion associated with the natural flow of aquifers was studied by Hassanzadeh et al. (2009).

The effect of viscous dissipation and inertia on hexagonal cell formation was studied by Magyari et al. (2005b). They show that when viscous dissipation is present the temperature profile loses its up/down symmetry when convection occurs, and this causes hexagonal cells rather than parallel rolls to occur in the case of a layer of infinite horizontal extent. This is because the lack of symmetry allows two rolls, whose axes are at  $60^\circ$  to one another, to interact and reinforce a roll at  $60^\circ$  to each of them, thus providing the hexagonal pattern. Hexagonal convection is subcritical, that is, it appears at Rayleigh numbers below  $4\pi^2$ . However, when  $Ra$  is sufficiently above  $4\pi^2$ , the rolls are reestablished as the preferred pattern of convection. When the Forchheimer terms are included, the range of Rayleigh numbers over which hexagons exist and are stable decreases, and the hexagons are eventually extinguished. This result is qualitatively similar to that resulting when the layer is tilted at increasing angles from the horizontal, although there are two main orientations of hexagonal solutions in this case. The rolls that form when hexagons are destabilized are longitudinal rolls that may be regarded as streamwise vortices like those considered by Rees et al. (2005).

Further work on the effect of viscous dissipation, in situations involving either horizontal throughflow or vertical throughflow, was carried out by Barletta et al. (2009a, b, 2010a, b, 2011b). In the case where a boundary is adiabatic, the instability can arise even in the absence of bottom heating. The effect of bottom heating was added by Barletta and Storesletten (2010b). The case of an open boundary with a prescribed temperature gradient was examined by Barletta and Storesletten (2010a). The case of local thermal nonequilibrium was studied by Barletta and Celli (2011). Transverse heterogeneity effects in the case of dissipation-induced instability were treated by Barletta et al. (2011a).

## 6.7 Non-Boussinesq Effects

So far we have neglected the work done by pressure changes. When we allow for this, we replace (6.5) by

$$(\rho c)_m \frac{\partial T}{\partial t} + (\rho c_P)_f \mathbf{v} \cdot \nabla T + \beta T \left( \frac{\partial P}{\partial t} + \mathbf{v} \cdot \nabla P \right) = k_m \nabla^2 T, \quad (6.66)$$

where the coefficient of thermal expansion  $\beta$  and isothermal compressibility  $\beta_P$  are given by

$$\beta = -\frac{1}{\rho} \left( \frac{\partial \rho}{\partial T} \right)_P, \quad (6.67)$$

$$\beta_P = \frac{1}{\rho} \left( \frac{\partial \rho}{\partial P} \right)_T . \quad (6.68)$$

The basic steady-state solution is given by the hydrostatic equations

$$v_b = 0, \quad T_b = T_0 + \Delta T \left( 1 - \frac{z}{H} \right), \quad \frac{dP_b}{dz} = -\rho_b g, \quad (6.69a, b, c)$$

$$\frac{d\rho_b}{dz} = \beta_{Pb}\rho_b \frac{dP_b}{dz} - \beta_b\rho_b \frac{dT_b}{dz} = -\beta_{Pb}\rho_b^2 g + \beta_b\rho_b \frac{\Delta T}{H}. \quad (6.69d)$$

The two-dimensional linearized time-independent perturbation equations are

$$\frac{\partial u'}{\partial x} + \frac{\partial w'}{\partial z} + w' \left( \beta_b \frac{\Delta T}{H} - \beta_{Pb}\rho_b g \right) = 0, \quad (6.70)$$

$$\rho_b w' \left( -c_{Pb} \frac{\Delta T}{H} + \beta_b T_b g \right) = k_m \left( \frac{\partial^2 T'}{\partial x^2} + \frac{\partial^2 T'}{\partial z^2} \right), \quad (6.71)$$

$$\frac{\partial P'}{\partial x} + \mu_b \frac{u'}{K} = 0, \quad (6.72)$$

$$\frac{\partial P'}{\partial z} + \mu_b \frac{w'}{K} = -\rho' g, \quad (6.73)$$

$$\rho' = \beta_{Pb}\rho_b P' - \beta_b\rho_b T'. \quad (6.74)$$

In the Boussinesq approximation, the term  $-\beta_b\rho_b T'$  in the equation for  $\rho'$  is retained, but otherwise  $\beta_b$  and  $\beta_{Pb}$  are set equal to zero, while  $\rho_b$ ,  $c_{Pb}$ ,  $T_b$ , and  $\mu_b$  are regarded as constants. As a second approximation, one also can retain the term  $\beta_b T_b g$  in (6.71), the left-hand side of which can be written as  $\rho_b c_{Pb}(\beta_b T_b g/c_{Pb} - \Delta T/H)w'$ .

The end result is that the critical Rayleigh number value is the same as before, provided that in the definition of Rayleigh number, one replaces the applied temperature gradient  $\Delta T/H$  by the difference between that and the adiabatic gradient  $\beta_b T_b g/c_{Pb}$ . Thus the prime effect of compressibility is stabilizing, and the other non-Boussinesq effects have only a comparatively minor effect on the critical Rayleigh number. Details for the case when the fluid is water are discussed by Straus and Schubert (1977) and for the case of an ideal gas by Nield (1982). For a moist ideal gas of 100% humidity, flow and heat transfer are strongly coupled. Zhang et al. (1994), using a perturbation analysis, showed that  $Ra_c$  then depends heavily on the vapor pressure; the moist gas is much less stable than a dry gas because of the large latent heat carried by the former. A rarefied gas was considered by Parthiban and Patil (1996), but their analysis is flawed (see Nield 2001c).

A finite-amplitude analysis was reported by Staufer et al. (1997). The impact of thermal expansion on transient convection was studied by Vadasz (2001c, d).

It is usually a straightforward adjustment to allow for the variations of fluid properties with temperature. This is exemplified by the numerical investigations of Gartling and Hickox (1985). The effect of viscosity variation was explicitly examined by Kassoy and Zebib (1975), Zebib and Kassoy (1977), Blythe and Simpkins (1981), and Patil and Vaidyanathan (1981). Morland et al. (1977) examined variable property effects in an elastic porous matrix. Nonlinear stability analysis for the case of temperature-dependent viscosity was reported by Richardson and Straughan (1993) and Qin and Chadam (1996), incorporating Brinkman and inertial terms, respectively. Payne and Straughan (2000b) addressed the Forchheimer equation and obtained unconditional nonlinear stability bounds close to the linear stability ones using a viscosity linear in the temperature. They also extended the analysis to a viscosity quadratic in temperature and to a penetrative convection situation. For the Forchheimer model, nonlinear stability was analyzed using Lyapunov's direct method by Capone (2001).

Nield (1996) showed that the effect of temperature-dependent viscosity on the onset of convection was generally well taken into account provided the Rayleigh number was defined in terms of the viscosity at the average temperature. (An exception occurs when very large temperature differences are involved (Kassoy and Zebib 1975).) This result is in accord with concept of effective Rayleigh number  $Ra_{\text{eff}}$  introduced by Nield (1994c); for this parameter the quantities appearing in the numerator of  $Ra$  are replaced by their arithmetic mean values, and those that appear in the denominator are replaced by their harmonic-mean values. Capone and Rionero (1999) conducted a nonlinear stability study with time-dependent viscosity. A detailed theoretical and numerical study of the effect of temperature-dependent viscosity was reported by Lin et al. (2003). Further work on the effect of temperature-dependent viscosity was reported by Hooman and Gurgenci (2008a, c) and Rong et al. (2010b) (using a lattice Boltzmann method).

The effect of pressure work was studied by Nield and Barletta (2009).

## 6.8 Finite-Amplitude Convection: Numerical Computation and Higher-Order Transitions

Starting with Holst and Aziz (1972), the governing equations for natural convection have been solved using a range of numerical techniques (finite differences, finite element, spectral method). Out of necessity, these calculations must be made in a finite domain, so a preliminary decision must be made about conditions on lateral boundaries. It is presumed that these vertical boundaries are placed to coincide at the cell boundaries, where the normal (i.e., horizontal) component of velocity and the normal component of heat flux are both zero.

Caltagirone et al. (1981) performed calculations using the spectral method and obtained the following results:

- (a) For  $Ra < 4\pi^2$ , the perturbation induced by initial conditions decreased, and the system tended to the pure-conduction solution, as expected.
- (b) For  $4\pi^2 < Ra < 240\text{--}300$ , the initial perturbation developed to give a stable convergent solution that does not depend on the intensity or nature of this perturbation. Various stable convective rolls were observed: counterrotating rolls (two-dimensional), superposition of counterrotating rolls (three-dimensional), and polyhedral cells (three-dimensional).
- (c) For  $Ra > 240\text{--}300$ , a stable regime was not reached.

Transition to the fluctuating convection regime is characterized by an increase of heat transfer relative to the stable solutions. The oscillations appear to be caused by the instability of the thermal boundary layers at the horizontal boundaries. The existence of the oscillating state had been deduced from a stability analysis of finite-amplitude two-dimensional solutions by Straus (1974), whose results are illustrated in Fig. 6.3. It was also demonstrated through numerical calculations by Horne and O'Sullivan (1974a). The oscillations have been shown by Caltagirone (1975) and Horne and Caltagirone (1980) to be associated with the continuous creation and disappearance of cells.

Or (1989) has extended the computations to the situation where the viscosity is allowed to be temperature dependent. The vertical asymmetry thereby introduced makes mixed modes significant. Or (1989) also examined stability with respect to a class of disturbances that have a  $\pi/2$  phase shift relative to the basic state. He found little difference in transition parameters for the in-phase and phase-shifted oscillatory instabilities. It is noteworthy that the temperature dependence of viscosity provides a mechanism for generating a mean flow.

Further studies of higher-order transitions have been made by Aidun (1987), Aidun and Steen (1987), Kimura et al. (1986, 1987), Caltagirone et al. (1987), Steen and Aidun (1988), and Caltagirone and Fabrie (1989). The last study, based on a pseudospectral method, concluded that in a two-dimensional square cavity, the following sequence occurs: From the second bifurcation, occurring at  $Ra = 390$ , the flow becomes periodic. Between 390 and 600, the phenomenon is single periodic and only the frequency  $f_2$  incommensurable with  $f_1$  introduces a quasiperiodic regime  $QP_1$ . When  $Ra$  increases further, the flow again becomes periodic (state  $P_2$ ) up to  $Ra = 1,000$ , where the appearance of frequencies  $f_2$  and  $f_3$  gives a second quasiperiodic regime  $QP_2$ .

The second regime  $QP_2$  can be maintained up to  $Ra = 1,500$ , after which the single convecting roll splits up into two unsteady convecting rolls by entering a chaotic restructuring regime. This sequence is subject to hysteresis as  $Ra$  is lowered. The frequency  $f_1$  varies as  $Ra^2$ ,  $f_2$  as  $Ra^{5/2}$ , and  $f_3$  as  $Ra^{3/2}$ .

The periodic window between  $Ra = 600$  and 1,000 corresponds to third-order locking of the oscillators corresponding to  $f_1$  and  $f_2$ . The oscillators spring up and develop within the thermal boundary layer near the horizontal walls, and the evolution with  $Ra^2$  of  $f_1$  corroborates the fact that the observed instabilities are due to the loss of stability in the boundary layer. The earlier study by Kimura et al.

(1987) revealed a rather different picture; for example, the second quasiperiodic regime was not found, and  $f_1$  varied as  $Ra^{7/8}$ . The work of Kladias and Prasad (1990) suggests that when non-Darcy effects are taken into account, the second quasiperiodic regime does not exist.

Kladias and Prasad (1989b, 1990) have made numerical studies of oscillatory convection using a Brinkman-Forchheimer equation. They found that whereas the channeling effect (due to porosity variation) substantially reduced the critical Rayleigh number for the onset of steady convection, the opposite occurred with the critical Rayleigh number for the transition to oscillatory convection. This is primarily due to the fact that the core of the cavity becomes more or less stagnant, whereas the thermal activity and fluid motion is concentrated within thin boundary layers along the walls. While the effects of mean porosity and specific heat ratio are insignificant for steady convection, they are quite significant in the random fluctuating regime. In a square cavity, steady convection is characterized by a single cell, but the flow pattern for fluctuating convection is complex and dependent on the fluid Prandtl number  $Pr_f$ . For example, four cells can exist with pairs on the diagonals alternately attaching and detaching with time. This results in a large variation in Nusselt number with time. Generally an increase in  $Pr_f (> 10)$  increases the amplitude of fluctuation, whereas a decrease in  $Pr_f (< 0.1)$  results in a more stable flow. Otero et al. (2004) have studied numerically the case of infinite Darcy-Prandtl number and high Rayleigh number. Their results include a derivation of an upper bound on the heat transport:  $Nu \leq 0.0297 \times Ra$ .

For the special case of constant flux imposed on the horizontal boundaries, the situation is markedly different. The analytical and numerical study of Kimura et al. (1995) revealed that the unicellular setup when  $Ra$  exceeds 12 remains a stable mode as the aspect ratio  $A$  increases, in contrast to the constant-temperature case where multicellular convection is the preferred mode for  $A > 2^{1/2}$ . Further, the unicellular flow remains as  $Ra$  increases to 311.53, above which nonoscillatory longitudinal disturbances can grow. At sufficiently large  $Ra$  (above about 640 for  $A = 8$ , with a critical frequency  $f = 22.7$ ), there is a transition to oscillatory flow, according to the numerical calculations; linear stability theory predicts a Hopf bifurcation with transverse disturbances at  $Ra = 506.07$  with frequency  $f = 22.1$ .

Vadasz and Olek (1998) have shown that when a Darcy equation with timewise inertia term is taken, and with suitable scaling, the system of partial differential equations can be approximated by the same famous system of ordinary equations treated by Lorenz but with different values of the parameters. Their work described for centrifugally driven convection extends to the gravitational situation.

Further numerical studies using a unified finite approach exponential-type scheme have been reported by Llagostera and Figueiredo (1998) and Figueiredo and Llagostera (1999). Bilgen and Mbaye (2001) have treated a cavity with warm bottom and warm top and with additional lateral cooling.

Large-scale thermal convection was studied by Goldobin and Shklyaeva (2008). Scenarios of unsteady regimes were examined by Govorukhin and Shevchenko (2006).

This discussion of finite-amplitude convection is continued in Sect. 6.15.1.

## 6.9 Experimental Observations

### 6.9.1 *Observations of Flow Patterns and Heat Transfer*

Qualitative results for two-dimensional free convection were obtained using the Hele-Shaw cell analogy by Elder (1967a) and Bories (1970a, b). In a Hele-Shaw cell the isothermal lines can be observed by interferometry by using the fact that the refractive index of a liquid is a function of density and so of temperature. The streamlines can be visualized by stroboscopy, that is, by using light diffracted from aluminum particles suspended in the liquid. These experiments confirmed the theoretical value for the critical wavenumber and the fact that the wavenumber increases with  $Ra$  in accordance with calculations based on the Malkus hypothesis.

Direct visualization of three-dimensional flow in a porous medium was made by Bories and Thirriot (1969). They observed the accumulation of aluminum scattered on a thin liquid layer overlying the medium. The cells appeared to have approximately hexagonal cross section (away from the lateral boundaries) with the fluid rising in the center of each cell. The observations were checked by in situ temperature recordings. For slightly supercritical Rayleigh number values, the dimensions of the cells were about the same as those predicted by linear theory. Howle et al. (1997) reported further visualization studies.

Many authors have performed experimental work in layers bounded by impermeable isothermal planes using conventional experimental cells (Schneider 1963; Elder 1967a, b; Katto and Masuoka 1967; Combarous and Le Fur 1969; Bories 1970a; Combarous 1970; Yen 1974; Kaneko et al. 1974; Buretta and Berman 1976). These have been concerned largely with heat transfer, but some experimenters have measured temperatures in the median plane of the layer in order to observe the boundaries of convective cells. In experiments reported by Combarous and Bories (1975) it was found that the cells were not as regular as those obtained with a fluid clear of solid material. Again, polygons were observed away from the lateral boundaries; the cell sizes were consistent with linear theory, and the wavenumber increased slightly with Rayleigh number. This change of wavenumber is consistent with the observations in a Hele-Shaw cell (see two paragraphs above), but it is in the opposite direction to that found in experiments with a clear fluid. Nield (1997b) tentatively ascribed the difference as an effect of dispersion.

The experimental heat transfer results of several of these workers, together with curves showing results from the upper bound analysis of Gupta and Joseph (1973) and the numerical calculations of Straus (1974) and Combarous and Bia (1971), are displayed in Fig. 6.9. The theoretical results are in agreement with experimental results for glass-water, glass-oil, and heptane-sand systems but considerably overestimate the heat transfer for steel-oil, lead-water, and ethanol-sand systems. Possible reasons for this discrepancy are discussed below.

We note that the theoretical critical Rayleigh number  $Ra_c \approx 40$  (defined as the  $Ra$  value for which  $Nu$  departs from the value 1) is confirmed by numerous

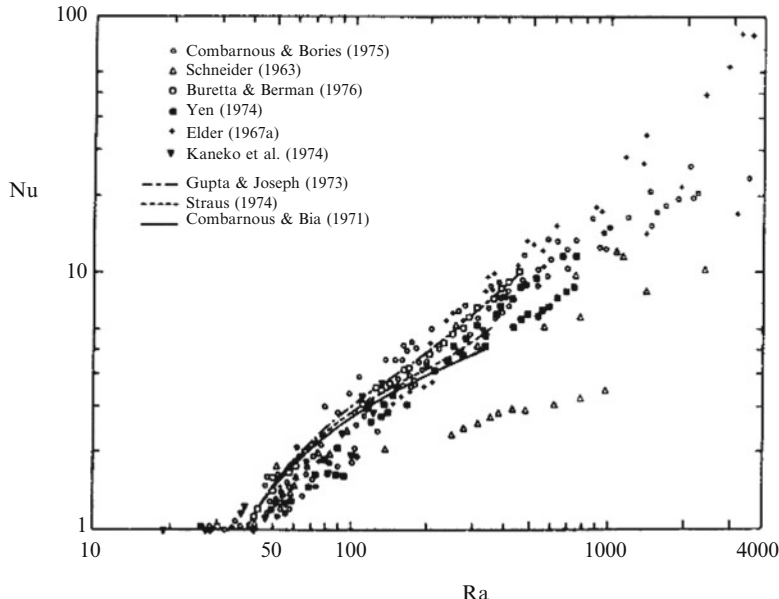


**Fig. 6.9** Compilation of experimental, analytical, and numerical results of Nusselt number vs. Rayleigh number for convective heat transfer in a horizontal layer heated from below (Cheng 1978, with permission from Academic Press)

experiments. A precise test for  $Ra_c$  was made by Katto and Masuoka (1967), who used nitrogen as the saturating fluid in order to reduce the temperature difference required for a large variation in Rayleigh number and thus reduce the effect of property variation with temperature. Both the kinematic viscosity and thermal diffusivity of a gas are almost inversely proportional to the pressure, and so  $Ra$  can be varied through a large range by varying the pressure. Katto and Masuoka found satisfactory agreement between theory and experiment. Kaneko et al. (1974) observed  $Ra_c \approx 28$  for ethanol-sand systems, but it is likely that the reduction in  $Ra_c$  was due to a nonlinear basic temperature profile (see Sect. 6.11). Close et al. (1985) found that  $Ra_c$  remains near 40 even when the layer depth is as small as two particle diameters.

When  $Ra$  is slightly supercritical,  $Nu$  increases linearly with  $Ra$ . For some systems (e.g., glass-water), the range of linearity is quite extensive, and for these, Elder (1967a) proposed the correlation

$$Nu = \frac{Ra}{40}. \quad (6.75)$$

An extensive investigation, using glass beads, lead spheres, and sand as solids and silicone oil and water as fluids, was carried out by Combarious and Le Fur (1969). This study showed that when the Rayleigh number reaches 240–280, there

was a noticeable increase in the slope of the  $Nu$  vs.  $Ra$  curve. Caltagirone et al. (1971) noted that it was apt to call the new regime the “fluctuating convective state” since the temperature field was continually oscillating. This fluctuating state also was observed in Hele-Shaw cell experiments by Horne and O’Sullivan (1974a). The transition is in accord with the numerical results discussed in Sect. 6.8. We recall that the transition is caused by instability of boundary layers at the horizontal boundaries and that the fluctuating state is one in which convection cells continually appear and disappear, the number of cells doubling and halving.

Lein and Tankin (1992a) used the Christiansen filter concept to visualize the convection in test sections with different aspect ratios. They found that the width-to-height ratio of the convection cells did not vary with  $Ra$  for an impermeable upper boundary, but it did increase significantly for a permeable upper boundary.

Further experiments were conducted by Kazmierczak and Muley (1994). They found an increased heat transfer for a “clear top layer” compared with that for a completely packed layer, the increase being due to channeling and which Nield (1994a) showed was consistent with predictions based on the model of a clear fluid layer on top of the porous-medium layer (Sect. 6.19.1). They also did experiments with the bottom wall temperature changed cyclically and found that the modulation could either increase or decrease the heat transfer.

Using magnetic resonance imaging, a noninvasive technique that yields quantitative velocity information, Shattuck et al. (1997) examined the onset of convection in a bed packed with monodisperse spheres in circular rectangular and hexagonal planforms. Disordered media, prepared by pouring spheres into a container, are characterized by regions of close packing separated by grain barriers and isolated defects that lead to locally larger porosity and permeability, and so to spatial variations in  $Ra$ . The authors found that stable localized convective regions exist for  $Ra < Ra_c$ , and these remain as pinning sites for convection patterns in the ordered regions as  $Ra$  increases above  $Ra_c$  up to  $5Ra_c$ , the highest value studied in such media. In ordered media, with deviations from close packing only near the vertical walls, stable localized convection appears at  $0.5Ra_c$  in the wall regions. Different stable patterns are observed in the bulk for the same  $Ra$  after each recycling below  $Ra_c$ , even for similar patterns of small rolls in the wall regions. As expected, roll-like structures are observed that relax rapidly to stable patterns between  $Ra_c$  and  $5Ra_c$ , but the observed wavenumber was found to be  $0.7\pi$  instead of the  $\pi$  predicted from linear stability theory. As  $Ra$  grows above  $Ra_c$ , it was found that the volume of upflowing to the volume of downflowing regions decreases and leads to a novel time-dependent state, rather than the expected cross rolls; this state begins at  $6Ra_c$  and is observed up to  $8Ra_c$ , the largest  $Ra$  studied, and is probably linked to departures from the Boussinesq approximation. Further, it was found that the slope ( $S$ ) of the Nusselt number curve is 0.7 rather than the predicted value of 2. (For comparison, Elder (1967a) found  $S = 1$ . Howle et al. (1997) found a slope between 0.53 and 1.35, depending on the medium, while Close et al. (1985) found that  $S$  decreases as  $d/H$  increases.) Further experiments involving nuclear magnetic resonance plus numerical simulations were reported by Weber et al. (2001), Kimmich et al. (2001), and Weber and Kimmich (2002).

In related work, Howle et al. (1997) used a modified shadowgraphic technique to observe pattern formation at the onset of convection. They found that for ordered porous media, constructed from grids of overlapping bars, convective onset is characterized by a sharp bifurcation to straight parallel rolls whose orientation is determined by the number of bar layers,  $N_b$ ; for odd  $N_b$  the roll arc is perpendicular to the direction of the top and bottom bars, but for even  $N_b$  they are at  $45^\circ$  to the bars. In a disordered system, produced by stacking randomly drilled disks separated by spaces, a rounded bifurcation to convection, with localized convection near onset, is observed, and the flow patterns take on one of several different cellular structures after each recycling through onset. The observations suggest that the mechanism of Zimmermann et al. (1993) (involving spatial fluctuations in  $Ra$ ) and of Braester and Vadasz (1993) (involving continuous spatial variations of permeability and thermal diffusivity) may both be operating. Howle (2002) has reviewed work on convection in ordered and disordered porous layers.

### 6.9.2 Correlations of the Heat Transfer Data

The outstanding question posed by the experimental results is how one can best explain the spread of points in the  $Nu$  vs.  $Ra$  plot (Fig. 6.6). There are two theoretical approaches to the matter. The first explanation, put forward by Combarous (1972), elaborated by Combarous and Bories (1974), and modified by Chan and Banerjee (1981), is based on the effect of solid–fluid heat transfer (see Sect. 6.5). A drawback to using this approach is that it is difficult to make an independent assessment of the heat transfer coefficient  $h$ . It turns out that this theory predicts some but not all of the observed reduction in  $Nu$  values (below those predicted from the simple Darcy local thermal equilibrium model).

For this reason Prasad et al. (1985) decided that the solid–fluid heat transfer model was of limited use. They proposed the use of an effective conductivity:

$$k_e = \omega k_f + (1 - \omega)k_m, \quad (6.76)$$

where  $(1 - \omega)$  is the ratio obtained by dividing the overall pure-conduction heat transfer estimate by the total heat transfer rate. This procedure, which is based on the argument that somehow or other the influence of the porous-medium conductivity  $k_m$  decreases and that of the fluid-phase conductivity  $k_f$  increases, is quite successful in correlating the data, but it is ad hoc.

The second explanation is that put forward by Somerton (1983), Catton (1985), and Georgiadis and Catton (1986). These authors showed that the data spread can be substantially reduced by taking into account the effect of fluid inertia (the quadratic drag) which inevitably becomes increasingly important as  $Ra$  increases. Jonsson and Catton (1987) presented a power-law correlation of  $Nu$  in terms of  $Ra$  and  $Pr_e$ , where  $Pr_e$  is an effective Prandtl number that can be defined, in terms of the quantities that appear in (6.62), by

$$Pr_e = \frac{Pr_f}{c_F} \frac{k_f}{k_m} \left( \frac{K}{H^2} \right)^{1/2}. \quad (6.77)$$

Close (1986) suggested that the data be brought in line with theory by means of the formula

$$\frac{Nu}{Nu_i} = 1.572 \times 10^{-2} \times Ra_f^{0.344} \left( \frac{k_f}{k_s} \right)^{0.227} \left( \frac{H}{d_p} \right)^{0.446} \left( \frac{\varphi}{1-\varphi} \right)^{0.496} Pr_f^{0.279}, \quad (6.78)$$

where  $Nu_i$  is given by expression (6.45) and  $Ra_f$  is a standard (non-Darcy) Rayleigh number based on the properties of the fluid and a layer thickness  $d_p$  (the pore diameter). Formula (6.78) is successful for  $Nu < 10$ , but there are discrepancies for  $Nu > 10$ . Close noted that the near equality of the exponents of  $k_f/k_s$  and  $Pr_f$  in (6.78) meant that Somerton's claim that it is neglect of inertial terms rather than solid–fluid heat transfer that causes the spread of data is not necessarily correct, and it is likely that both are involved.

Wang and Bejan (1987) strengthened the case for the inertial explanation by introducing the dimensionless group

$$Pr_p = Pr_e \frac{H^2}{K} \quad (6.79)$$

which arises naturally from the following scale analysis. At large  $Ra$  the quadratic drag term dominates over the linear term in the Forchheimer equation

$$\mathbf{v} + \frac{\chi}{v} |\mathbf{v}| \mathbf{v} = \frac{K}{\mu} (-\nabla P + \rho_f g), \quad (6.80)$$

where  $\chi = c_F K^{1/2}$  and  $v = \mu/\rho_f$ . The flow consists of a core counterflow plus boundary layers as shown in Fig. 6.10. In the core the vertical inertia scales as  $\chi v^2/v$ , and the boundary term scales as  $(K/\mu)\rho g \beta \Delta T$ , so the momentum balance requires

$$\frac{\chi}{v} v^2 \sim \frac{K}{\mu} \rho g \beta \Delta T. \quad (6.81)$$

The energy equation (Bejan 1984) is a balance between upward enthalpy flow gradient ( $v \Delta T/H$ ) and lateral thermal diffusion between the two branches of the counterflow  $\alpha_m \Delta T/L^2$ , so

$$v \frac{\Delta T}{H} \sim \alpha_m \frac{\Delta T}{L^2}. \quad (6.82)$$

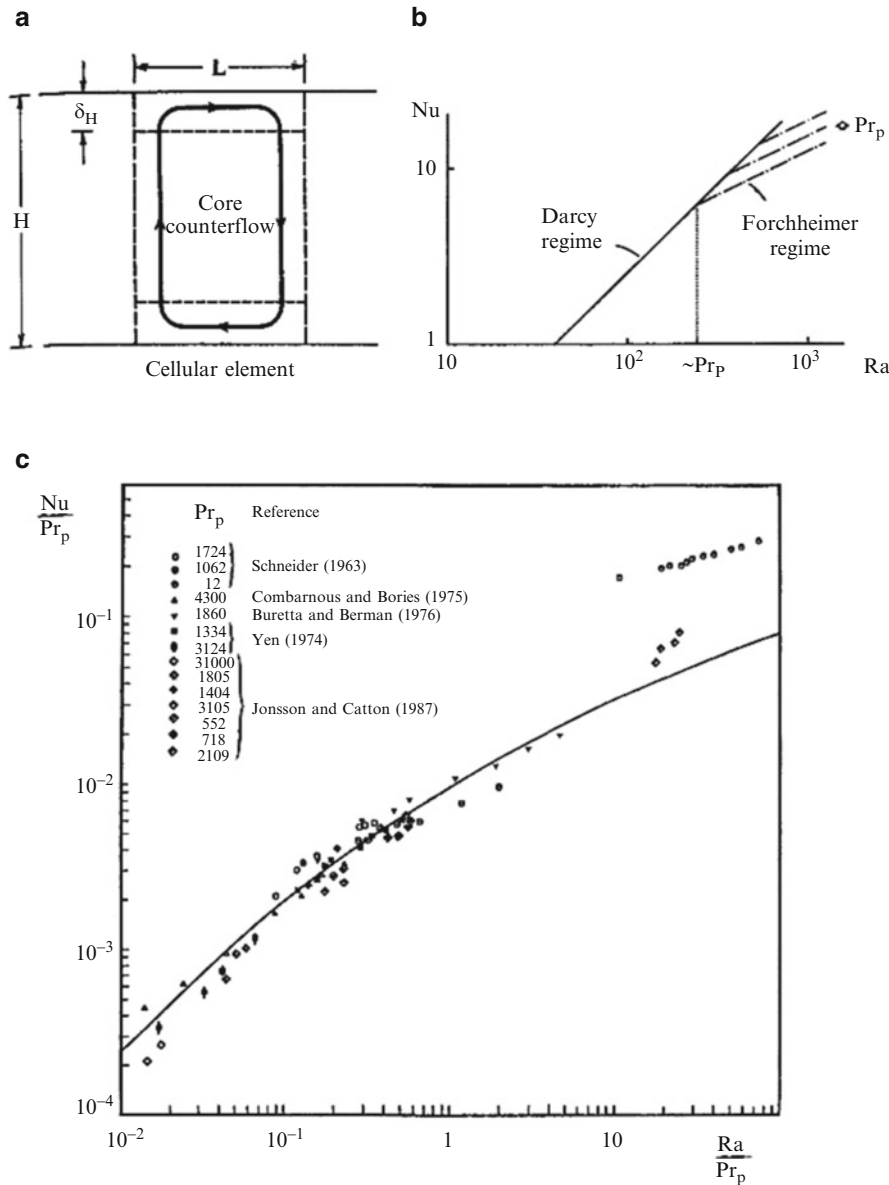


**Fig. 6.10** (a) Convective roll dimensions. (b) The asymptotes of the function  $Nu(Ra, \text{Pr}_p)$  suggested by scale analysis. (c) Heat transfer data, for convective heat transfer in a horizontal layer heated from below (Wang and Bejan 1987)

The balance between vertical enthalpy flow through the core ( $\rho v L c_p \Delta T$ ) and vertical thermal diffusion through the end region of height  $\delta_H$  and width  $L$  requires

$$\rho v L c_p T \sim k_e L \Delta T / \delta_H. \quad (6.83)$$

The scales that emerge as solutions to the systems (6.81), (6.82), and (6.83) are

$$L \sim (\alpha_m H)^{1/2} \left( \frac{\chi}{g \beta K \Delta T} \right)^{1/4}, \quad (6.84)$$

$$v \sim \left( \frac{g \beta K \Delta T}{\chi} \right)^{1/2}, \quad (6.85)$$

$$\delta_H \sim \alpha_m \left( \frac{\chi}{g \beta K \Delta T} \right)^{1/2}. \quad (6.86)$$

We note in passing that these equations imply that  $L/H$  varies as  $Ra^{-1/4}$  and  $v$  varies as  $Ra^{1/2}$ . The heat transfer rate in the Forchheimer flow limit therefore must scale as

$$Nu \sim \frac{H}{\delta_H} \sim (Ra \Pr_p)^{1/2}. \quad (6.87)$$

In contrast, heat flow in the Darcy flow limit scales as

$$Nu \sim \frac{1}{40} Ra. \quad (6.88)$$

Thus the transition from Darcy to Forchheimer flow occurs at the intersection of (6.87) and (6.88),

$$Ra \sim \Pr_p \quad (6.89)$$

from which we deduce

$$\frac{Nu}{\Pr_p} \sim \frac{1}{40} \frac{Ra}{\Pr_p}, \quad 40 < Ra < \Pr_p, \quad (6.90)$$

$$\frac{Nu}{\Pr_p} \sim \left( \frac{Ra}{\Pr_p} \right)^{1/2}, \quad Ra > \Pr_p. \quad (6.91)$$

An important feature of (6.90) and (6.91) is that they are both of the form  $Nu/\Pr_p = f(Ra/\Pr_p)$ . This motivates the plotting of  $Nu/\Pr_p$  against  $Ra/\Pr_p$  to produce the graph shown in the lower part of Fig. 6.10. The agreement is good, with the notable exception of Schneider's (1963) data for  $\Pr_p = 12$  in the top right corner of the figure. A line through this subset of data has the correct slope but is clearly too high, and possibly the deduced  $\Pr_p$  value of 12 is not correct. With this subset ignored, Wang and Bejan obtained the correlation

$$Nu = \left\{ \left( \frac{Ra}{40} \right)^n + [c(Ra Pr_p)^{1/2}]^n \right\}^{1/n}, \quad (6.92a)$$

where  $n$  and  $c$  are two empirical constants,

$$n = -1.65 \quad \text{and} \quad c = 1896.4. \quad (6.92b)$$

The simplicity of (6.92) in comparison with (6.78) is obvious.

We note that Kladias and Prasad (1989a, b, 1990) published the results of numerical calculations of the Nusselt number in which they have investigated the effects of Darcy number, Prandtl number, and conductivity ratio. They presented their results in terms of a fluid Rayleigh number and a fluid Prandtl number. We find this unhelpful for our present purpose, which is to summarize how the various effects act in concert rather than in isolation. Kladias and Prasad made an important advance by showing that allowance for porosity variations brings the computed Nusselt numbers in better agreement with experimental observations. However, their (1989b) claim that  $Ra_c$  increases as  $Pr$  decreases was refuted by Lage et al. (1992), who showed numerically that  $Ra_c$  is independent of  $Pr$ , as the linear stability analysis indicates. (As Rees (2000) pointed out, this result is obvious when the momentum equation is scaled so that  $Pr$  appears only in the nonlinear terms, but it is not so obvious with other scalings.) Lage et al. proposed the correlation (accurate to within 2%)

$$\frac{Nu - 1}{Ra/Ra_c - 1} = [(C_1 Pr^2)^{-m} + C_2^{-m}]^{-m}, \quad (6.93a)$$

where

$$\varphi = 0.4, \quad C_1 = 172 Da^{-0.516}, \quad C_2 = 0.295 Da^{-0.121}, \quad m = 0.4, \quad (6.93b)$$

$$\varphi = 0.7, \quad C_1 = 30 Da^{-0.501}, \quad C_2 = 1.21 Da^{-0.013}, \quad m = 0.7. \quad (6.93c)$$

On the basis of scale analysis, Lage (1993a) obtained the following general scale for the Nusselt number:

$$Nu \sim \frac{(L/H)}{2} \left\{ \frac{\sigma}{\tau} + \frac{-\Pi + [\Pi^2 + 2\varphi^2 Ra Pr E]^{1/2}}{2E} \right\}^{1/2}, \quad (6.94a)$$

where

$$E = 1 + \varphi JA(Pr) Pr + \frac{0.143 \varphi^{1/2}}{Da^{1/2}}, \quad (6.94b)$$

$$\Pi = \frac{\varphi}{\tau} + \frac{\varphi^2 Pr}{Da} + \frac{\phi JA(Pr) Pr \sigma}{\tau} \quad (6.94c)$$

and the function  $A(Pr)$  takes the value 1 for  $Pr \geq 1$  and  $Pr^{-1}$  for  $Pr < 1$ , and  $L$  and  $H$  are horizontal and vertical length scales, respectively, while  $\tau$  is the characteristic time and  $J$  denotes the viscosity ratio  $\mu/\mu_{\text{eff}}$ . The coefficient 0.143 arises from the assumption that  $c_F$  takes a form proposed by Ergun (1952). As Rees (2000) pointed out, the criterion for the onset of convection depends on  $Da/\varphi$  rather than just  $Da$ , and this dependence also may be observed in (6.94a, b, c). Additional experimental work has been reported by Ozaki and Inaba (1997).

Vadasz (2010b) derived analytical solutions which confirmed the experimental and numerical results revealing a widespread dispersion of heat flux data in natural convection in porous media. He used the weak nonlinear method of solution to evaluate the heat flux in a porous layer heated from below and subject to weak boundary and domain imperfections. Previously little attention had been paid to the effect that the lower branch of the imperfect bifurcation curve has on the average heat flux. The results presented by Vadasz demonstrate the latter effect and explain the reason behind the dispersion of data. The comparison of his results with existing experimental and numerical data confirms the findings. In addition he showed that the latter effect is shown to be essential in one's ability to control heat transfer enhancement via natural convection in porous metal foams, for example.

### 6.9.3 Further Experimental Observations

Experiments by Lister (1990) in a large porous slab (3 m in diameter, 30 cm thick), using two quite different media (a matrix of rubberized curled coconut fiber and clear polymethylmethacrylate beads), have revealed several new phenomena. With the clear beads it was possible to visually observe the flows at the upper boundary. The boundary conditions were symmetrical (both impermeable and conducting), and so rolls were to be expected. Lister found that convection began in a hexagonal pattern and there was only a slight tendency to form rolls at slightly supercritical Rayleigh numbers.

Lister suggested that the asymmetry of the onset (one boundary maintained at a constant temperature, the other slightly heated) and the shape of the apparatus (hexagonal) could both be involved in the appearance of hexagons rather than rolls. At higher Rayleigh numbers the pattern of convection became very complex, irregular, and three-dimensional, without developing any obvious temporal instabilities. The visualization provided direct confirmation that the horizontal wavenumber of the convection cells increased with the Rayleigh number, approximately as  $(Ra + C)^{0.5}$ , where  $C$  is a constant.

The  $Nu$  vs.  $Ra$  curves obtained with the two media were substantially different. This conclusion was unexpected. The only feature that they had in common was a central section where the slope on a log/log graph was slightly over 0.5. On the graph for the fiber experiment this section was preceded by a slope close to 1 and followed by a slope close to 0.33. This last value is about the same as other experimenters have observed for convection in a clear liquid, so the result is expected because the fiber-filled medium had a porosity close to 100%.

The temperature measured at a point in the fill 25 mm below the top boundary was unsteady at conditions representative of the upper two segments of the graph.

On the other hand, the Nusselt number for the bead fill jumps upward just above onset (where  $Ra = 4\pi^2$ ), rapidly settles to a slope of 0.52, and then gradually breaks upward again to a slope greater than 1 at the highest values (about 2,000) for  $Ra$  reached in the experiment. Lister reported that increases in conductivity and permeability close to the boundary were not large enough to cause this increase in slope. He concluded that a new phenomenon, lateral thermal dispersion, appears to be responsible.

The phenomenon becomes important when the boundary layers become comparable in size with the diffusion length of the lateral dispersion, namely the bead size. The pores between beads are interlacing channels, that is, they continually join and separate again, occasionally juxtaposing flows that would otherwise be separated by a substantial thermal-diffusion distance. This greatly enhances interchannel thermal contact, and the use of beads with an irregular shape (they were slightly rounded short cylinders of 3 mm diameter and length in Lister's experiment) means that there will be some actual flow exchange between channels. In this way the effective thermal diffusivity can be raised but only if the flow velocity is sufficient to juxtapose channel streamlines more frequently than they would diffuse into equilibrium with each other by conduction. This means that lateral thermal dispersion has no effect on heat transfer at the onset of convection nor when the pores are sufficiently fine.

Davidson et al. (2009) reported experiments in water-saturated reticulated vitreous carbon foam.

## 6.10 Effect of Net Mass Flow

### 6.10.1 Horizontal Throughflow

On the Darcy model, if the basic flow is changed from zero velocity to a uniform flow in the  $x$  direction with speed  $U$ , then the eigenvalue problem of linear stability analysis is not altered if dispersion is negligible, since all the equations involved are invariant to a change to coordinate axes moving with speed  $U$ , a result noted by Prats (1966). Now some degeneracy is removed in that now longitudinal rolls (i.e., rolls with axes parallel to the  $x$ -axis) are favored over other patterns of convection; in other words, such disturbances grow faster than other disturbances for the same Rayleigh number and overall horizontal wavenumber.

On the Forchheimer model the situation is different, as Rees (1998) pointed out. Now, for the usual boundary conditions

$$Ra_c = \pi^2 [(1 + F)^{1/2} + (1 + 2F)^{1/2}]^2, \quad (6.95a)$$

where  $F$  is given by (6.62) with the Péclet number  $Q$  based on the throughflow. The critical wavenumber is given by

$$\alpha_c = \pi \left( \frac{1 + 2F}{1 + F} \right)^{1/4}. \quad (6.95b)$$

Rees noted that this result provides a means of testing the validity of (1.12) compared with, for example, (2.57) of Kaviany (1995). Kubitscheck and Weidman (2003) have analyzed a problem where the bottom wall is heated by forced convection. Delache et al. (2002) have studied the effect of inertia and transverse aspect ratio on the pattern of flow. Time-periodic convective patterns have been studied numerically and analytically by Néel (1998) and Dufour and Néel (1998, 2000). Here various end-wall boundary conditions are imposed and the resulting flow patterns investigated. They found an entry effect whereby increasing flow rates yield increasing distances before strong travel-wave convection is obtained. A nonlinear instability study using the Brinkman model was performed by Lombardo and Mulone (2003). Further nonlinear analysis was carried out by Delache et al. (2007) and Delache and Quarzazi (2008). An experimental study related to aquifer thermal energy storage was performed by Nakagano et al. (2002). Numerical simulations related to diagenesis in layers of sedimentary rock were reported by Raffensperger and Vlassopoulos (1999), but it appears that they ignored the possibility of longitudinal rolls. The case of constant-flux boundary conditions was treated by Park et al. (2006). The effects of viscous heating and an applied horizontal temperature gradient were studied by Nield and Barletta (2010b) and Barletta and Nield (2010). The effect of viscous heating with icy water was investigated by Storesletten and Barletta (2009). A viscoelastic fluid was studied by Hirata and Ouarzazi (2010a, b), and a power-law fluid was examined by Barletta and Nield (2011a). The effect of local thermal nonequilibrium was investigated by Postelnicu (2007a, 2010b). The analytical development of a disturbed matrix eigenvalue problem was applied by Ben Hamed and Bennacer (2008). The onset of convection in horizontally partitioned porous layers was studied by Genc and Rees (2011). The effects of combined horizontal and vertical heterogeneity on the onset of stability with horizontal throughflow were examined by Nield and Kuznetsov (2011f). The case of a channel subject to symmetrical wall heat fluxes was studied by Barletta (2012). Variable viscosity effects on the viscous dissipation instability were treated by Barletta and Nield (2012b).

### 6.10.2 Vertical Throughflow

The effect of net mass flow with mean speed  $U$  in the  $z$  direction was studied by Sutton (1970) and Homsy and Sherwood (1976). This effect is more significant because this alters the dimensionless temperature gradient from  $-1$  to  $F(z)$  where

$$F(z) = -\frac{Pe \exp(Pe z)}{\exp(Pe) - 1}, \quad (6.96)$$

where  $Pe$  is the Péclet number for the flow,

$$Pe = \frac{UH}{\alpha_m}. \quad (6.97)$$

Equation (6.26) is unchanged, but (6.25) is replaced by

$$(D^2 - \alpha^2 - Pe D)\hat{\theta} = F(z)\hat{W}. \quad (6.98)$$

Before discussing quantitative results, we consider some qualitative ones. When  $Pe$  is large, the effect of the throughflow is to confine significant thermal gradients to a thermal boundary layer at the boundary toward which the throughflow is directed. The effective vertical length scale  $L$  is then the small boundary layer thickness rather than the thickness  $H$  of the porous medium, and so the effective Rayleigh number, which is proportional to  $L$ , is much less than the actual Rayleigh number  $Ra$ . Larger values of  $Ra$  thus are needed before convection begins. Thus the effect of large throughflow is stabilizing.

Within the bulk of the medium, a large part of the heat transport can be effected by the throughflow alone, and the value of the temperature gradient at which convection cells are required is increased. The effective Rayleigh number is largely independent of the boundary conditions at the boundary from which the throughflow comes.

The situation for small values of  $Pe$  is more complex. The case of insulating boundaries is readily amenable to approximate analysis. On the assumption that the effect of  $Pe$  does not appreciably alter the shape of the eigenfunctions, one can obtain analytical formulas for the critical Rayleigh number for various combinations of boundary conditions.

For example, for the case in which both boundaries are impermeable and insulating, Nield (1987a) obtained the formula

$$Ra_c = \frac{2Pe^2}{Pe \coth(Pe/2) - 2}. \quad (6.99)$$

Clearly  $Ra_c$  is an even function of  $Pe$ , and for positive  $Pe$  is an increasing function of  $Pe$ . Hence throughflow is stabilizing for all values of  $Pe$ , and the direction of flow does not matter. For small values of  $Pe$ , we have

$$Ra_c = 12 + \frac{1}{5}Pe^2. \quad (6.100)$$

On the other hand, when the lower boundary is impermeable and insulating and the upper boundary is insulating and free (at constant pressure),

$$Ra_c = \frac{2Pe[\exp(Pe) - 1]}{2Pe + 2 + (Pe)^2 \exp(Pe)}. \quad (6.101)$$

For small values of  $Pe$ ,

$$Ra_c = 3\left(1 - \frac{1}{8}Pe\right) \quad (6.102)$$

showing that the case of downflow ( $Pe < 0$ ) is stabilizing and that upflow of small magnitude is destabilizing. A similar picture is painted by the numerical results for conducting boundaries by Jones and Persichetti (1986).

For symmetrical situations, where the lower and upper boundaries are of the same type,  $Ra_c$  is an even function of  $Pe$ , and throughflow is stabilizing by a degree that is independent of the flow direction. When the boundaries are of different types, throughflow in one direction is clearly destabilizing for small values of  $Pe$  since  $dRa_c/dPe$  at  $Pe = 0$  is not zero. The destabilization occurs when the throughflow is away from the more restrictive boundary. The throughflow then decreases the temperature gradient near the restrictive boundary and increases it in the rest of the medium. Effectively the applied temperature drop acts across a layer of smaller thickness, but the stabilizing effect of this change is more than made up by the destabilization produced by changing the effective boundary condition to a less restrictive one. A similar phenomenon, arising when the vertical symmetry is removed by the temperature dependence of viscosity or by some nonuniformity of the permeability, was found by Artem'eva and Stroganova (1987). Khalili and Shivakumara (1998, 2003), Shivakumara (1999), and Khalili et al. (2002) have extended the linear stability theory to consider the effects of internal heat generation and anisotropy and also boundary and inertial effects. A study of the stability of the solutions given by linear stability theory, together with a numerical study to confirm the findings, was conducted by Zhao et al. (1999b).

Wu et al. (1979) have used numerical methods to study the case of maximum density effects with vertical throughflow, while Quintard and Prouvost (1982) studied throughflow with viscosity variations that lead to Rayleigh-Taylor instability. The nonlinear stability analysis of Riahi (1989) for the case of large  $Pe$  shows that subcritical instability exists and this is associated with up hexagons, which are stable for amplitude  $\epsilon$  satisfying  $|\epsilon| = 0.35$ . For  $|\epsilon| = 0.4$ , squares too are stable, and the realized flow pattern depends on initial conditions. A general nonlinear analysis was reported by van Duijn et al. (2002). Their predictions were in good agreement with the results of laboratory experiment with Hele-Shaw cells of Wooding et al. (1997a, b). A transient problem was studied by Pieters and van Duijn (2006). Global stability was studied by Hill (2007) and Hill et al. (2007) (penetrative convection).

Nield and Kuznetsov (2011g) analyzed the effect of vertical throughflow on the onset of convection in a rectangular box. The effect of strong vertical throughflow was studied by Nield and Kuznetsov (2011f). Double-diffusive convection in a heterogeneous vertical cylinder was treated by Kuznetsov and Nield (2012c).

## 6.11 Effect of Nonlinear Basic Temperature Profiles

### 6.11.1 General Theory

Nonlinear basic temperature profiles can arise in various ways, notably by rapid heating or cooling at a boundary or by a volumetric distribution of heat sources. When the former is the case, the profile is time-dependent, but one can investigate instability on the assumption that the profile is quasistatic, that is, it does not change significantly on the timescale of the growth of small disturbances. It is found that with a curved temperature profile, it is possible for the critical Rayleigh number to be less than that for a linear profile. Indeed, in the case of the parabolic profile arising from a uniform volume distribution of sources, the critical value  $Ra_c$  can be arbitrarily small. But when the profiles are restricted to ones in which the gradient does not change sign, the question of which profile leads to the least  $Ra_c$  is not trivial. The question can be answered readily for the case of insulating (constant heat flux) boundaries because then an analytic expression for  $Ra_c$  can be found.

The problem is to minimize  $Ra_c$  with respect to the class of nondimensional adverse temperature gradients  $f(\hat{z})$  satisfying

$$f(\hat{z}) \geq 0, \quad \langle f(\hat{z}) \rangle = 1, \quad (6.103)$$

where  $\langle f(\hat{z}) \rangle$  denotes the integral off( $\hat{z}$ ) with respect to  $\hat{z}$ , from  $\hat{z} = 0$  to  $\hat{z} = 1$ . Nield (1975) shows that the problem reduces to maximizing  $\langle W_0 \theta_0 \cdot f(\hat{z}) \rangle$  where  $W_0$  and  $\theta_0$  are normalized eigenfunctions. For example, in the case of impermeable insulating boundaries, it is found that  $W_0 = \hat{z} - \hat{z}^2$ ,  $\theta_0 = 1$ , and

$$Ra_c = \frac{2}{\langle (\hat{z} - \hat{z}^2) f(\hat{z}) \rangle}. \quad (6.104)$$

The expression  $(\hat{z} - \hat{z}^2)$  has its maximum when  $\hat{z} = 1/2$ , and consequently the function  $f(\hat{z})$ , which minimizes  $Ra_c$  subject to the constraints (6.103), is the Dirac delta function:

$$f(\hat{z}) = \delta\left(\hat{z} - \frac{1}{2}\right).$$

The corresponding minimum value is  $Ra_c = 8$ . This may be compared with the value  $Ra_c = 12$  for the linear temperature profile. More generally, the step-function temperature profile whose gradient is  $f(\hat{z}) = \delta(\hat{z} - \varepsilon)$  gives

$$Ra_c = \frac{2}{\varepsilon - \varepsilon^2}. \quad (6.105)$$

For piecewise linear temperature profiles whose gradient is of the form

$$f(\hat{z}) = \begin{cases} \varepsilon^{-1}, & 0 \leq \hat{z} < \varepsilon, \\ 0, & \varepsilon < \hat{z} \leq 1, \end{cases} \quad (6.106)$$

one finds that

$$Ra_c = \frac{12}{3\varepsilon - 2\varepsilon^2}. \quad (6.107)$$

The case of the linear temperature profile is given by  $\varepsilon = 1$ ,  $Ra_c = 12$ , as expected. As  $\varepsilon$  varies the minimum of expression (6.107) is attained at  $\varepsilon = 3/4$ , and then  $Ra_c = 32/3$ . Nield (1975) showed that this provides the minimum for  $Ra_c$  subject to

$$f(z) \geq 0, \quad df/d\hat{z} \leq 0 \text{ (almost everywhere)}, \quad \langle f(\hat{z}) \rangle = 1. \quad (6.108)$$

An extension of the above theory, incorporating the Brinkman term, was made by Vasseur and Robillard (1993). An extension to the case of permeable boundaries was reported by Thangaraj (2000).

### 6.11.2 Internal Heating

When a volumetric heat source  $q'''$  is present, (6.5) is replaced by

$$(\rho c)_m \frac{\partial T}{\partial t} + (\rho c_p)_f \mathbf{v} \cdot \nabla T = k_m \nabla^2 T + q'''. \quad (6.109)$$

The steady state is given by

$$\mathbf{v}_b = 0 \quad \text{and} \quad k_m \nabla^2 T_b = -q'''. \quad (6.110)$$

If  $q'''$  is constant, then the basic steady-state temperature distribution is parabolic:

$$T_b = -\frac{q''' z^2}{2k_m} + \left( \frac{q''' H}{2k_m} - \frac{\Delta T}{H} \right) z + T_0 + \Delta T. \quad (6.111)$$

In place of (6.13), one has

$$(\rho c)_m \frac{\partial T'}{\partial t} + (\rho c)_f \left| \frac{q'''}{2k_m} (H - 2z) - \frac{\Delta T}{H} \right| w' = k_m \nabla^2 T'. \quad (6.112)$$

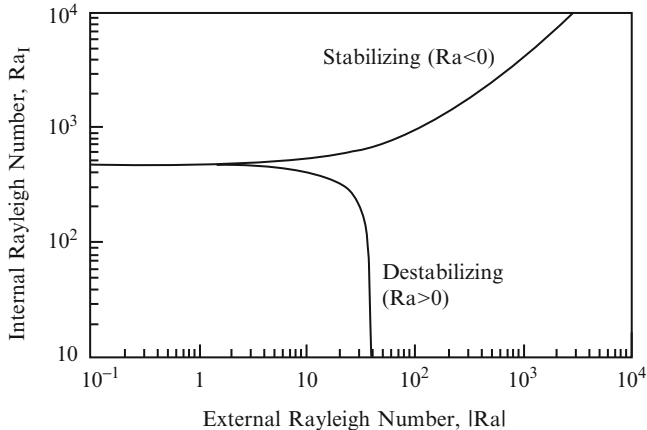


**Fig. 6.11** Critical internal Rayleigh number vs. external Rayleigh number for stabilizing and destabilizing temperature differences (Gasser and Kazimi 1976)

Equations (6.11) and (6.12) still stand. If instead of  $\Delta T$  we now choose  $Ra\Delta T$  as temperature scale, then in terms of the new nondimensional variables, one has, for monotonic instability,

$$\nabla^2 \hat{w} = \nabla_H^2 \hat{T}, \quad (6.113)$$

$$\nabla_H^2 \hat{T} = [Ra_I(1 - 2\hat{z}) - Ra]\hat{w}, \quad (6.114)$$

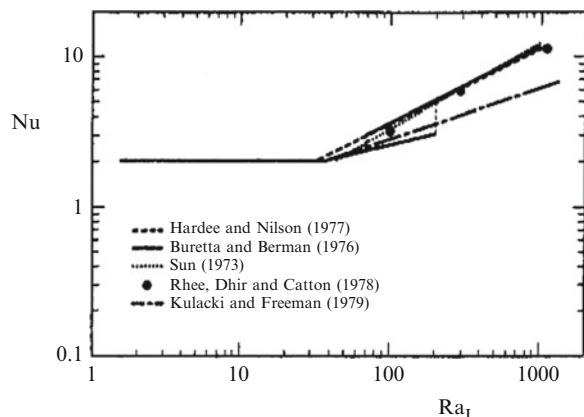
where  $\hat{T} = Ra\hat{T}$ . The new nondimensional parameter is the internal Rayleigh number  $Ra_I$  defined by

$$Ra_I = \frac{H^2 q'''}{2k_m \Delta T} Ra = \frac{g \beta K H^3 q'''}{2\nu \alpha_m k_m}. \quad (6.115)$$

We can refer to the original  $Ra$  as the external Rayleigh number, to distinguish it from the internal Rayleigh number  $Ra_I$ .

Equations (6.113) and (6.114), which now contain a nonconstant coefficient, may be solved numerically by using, for example, the Galerkin method. The stability boundary in the  $(Ra, Ra_I)$  plane (Fig. 6.11) was calculated by Gasser and Kazimi (1976) for the case of impermeable conducting boundaries. When  $Ra_I = 0$ , the critical value of  $Ra$  is  $4\pi^2$ . When  $Ra = 0$ , the critical value of  $Ra_I$  is 470. Changing the thermal boundary condition at the lower boundary has a marked effect on the critical value of  $Ra_I$ ; Buretta and Berman (1976) gave the estimate 32.8 for the case of an insulating lower boundary. Within experimental error, this was in agreement with their experiments, which involved a copper sulfate solution saturating a bed of spherical glass beads.

**Fig. 6.12** Comparison of heat transfer results for internal heating (Kulacki and Freeman 1979)



These experiments by Buretta and Berman revealed an interesting effect. Their  $Nu$  vs.  $Ra$  diagram showed a bifurcation into two branches with different slopes. There was also a jump from the lower branch to the upper at some  $Ra$  value that increased with bead size. Subsequent experiments by Hardee and Nilson (1977), Rhee et al. (1978), and Kulacki and Freeman (1979) failed to reproduce the jump. The data obtained by Kulacki and Freeman tended to correlate with the lower branch of Buretta and Berman's curve, but those of the other experimenters tended to correlate with the upper branch (Fig. 6.12). It appears that the discrepancy is still unresolved, but it may be related to the unusual bifurcation structure found by He and Georgiadis (1990), which arises from the effect of hydrodynamic dispersion in the case of uniform volumetric heating.

Various authors have made analytical or numerical extensions of the problem. Kulacki and Ramchandani (1975) varied the thermal boundary conditions. Tveitereid (1977) carried out a nonlinear stability analysis. He found that down hexagons (downward flow in the centers of the cells) were stable for  $Ra$  up to  $8Ra_c$ , up hexagons were stable for all values of  $Ra$ , and two-dimensional rolls were stable for  $3Ra_c < Ra < 7Ra_c$ . His computed  $Nu$  vs.  $Ra$  curves correlated quite well with the upper branch of Buretta and Berman's curve. Rudraiah et al. (1980, 1982b) carried out calculations of  $Ra_{lc}$  for various boundary conditions using the Brinkman equation. A nonlinear (energy) stability analysis was carried out by Ames and Cobb (1994), who thereby estimated the  $Ra$  band for possible subcritical instabilities.

Somerton et al. (1984) performed calculations that indicated that the wavenumber for convection decreases with increasing internal Rayleigh number. Kaviany (1984a) discussed a transient case when the upper surface temperature is decreasing linearly with time. Hadim and Burmeister (1988, 1992) have modeled a solar pond by allowing  $q'''$  to vary exponentially with depth, including the effect of vertical throughflow. Rionera and Straughan (1990) added the effect of gravity varying in the vertical direction. Their analysis, based on the energy method, revealed the possibility of subcritical convection. Stubos and Buchlin (1993) numerically simulated the transient behavior of a liquid-saturated core debris bed

with internal dissipation. Parthiban and Patil (1995) have extended the theory to the case of inclined gradients (see Sect. 7.9). A bifurcation study employing the Brinkman model was carried out by Choi et al. (1998).

The problem with a fluid undergoing a zero-order exothermic reaction was analyzed by Malashetty et al. (1994): the chemical reaction leads to increased instability. With determination of the conditions for the spontaneous combustion of a coal stockpile in mind, Bradshaw et al. (1991) used an approximate analysis to obtain convection patterns. They found that down hexagons and two-dimensional rolls are the stable planforms, and using a continuation procedure they obtained a simple criterion for the point of ignition in the layer, one given by a Frank-Kamenetskii parameter exceeding 5.17.

Lu and Zhang (1997) studied the onset of convection in a mine waste dump, in which there is active oxidation of pyritic materials, the rock being filled with moist gas. They took into account the effects of compressibility, latent heat, and a volumetric heat source varying exponentially with depth. Royer and Flores (1994) presented a novel way of dealing with Darcy flow in an anisotropic and heterogeneous medium. The combination of internal heat sources and vertical throughflow was treated by Yoon et al. (1998). A study involving external radiative incidence and imposed downward convection was reported by Liu (2003). A general study of radiative heat transfer was reported by Park et al. (1996).

The case where the volumetric heating is due to the selective absorption of radiation was studied by Hill (2003, 2004a, b), employing both linear and nonlinear stability analysis and also numerically, for each of the Darcy, Forchheimer, and Brinkman models. Convection with a non-Newtonian (power law) fluid at a large internal Rayleigh number was treated numerically by Kim and Hyun (2004).

Transient effects and heat transfer correlations for turbulent heat transfer were reported by Kim and Kim (2002) and Kim et al. (2002a, b). Jiménez-Islas et al. (2004) conducted a numerical study of natural convection with grain in cylindrical silos.

The effect of thermal nonequilibrium was studied by Baytas (2007), Nouri-Borujerdi et al. (2007c), and Saravanan (2009b), who treated a density maximum. Low Prandtl number chaotic convection was studied by Jawat and Hashim (2010). A problem involving a layer of gas underlying a layer of oil was investigated by Kim et al. (2007). Steady finite Rayleigh number flows were examined by Mealey and Merkin (2009). The effects of anisotropy were included in a study of unsteady convection by Slimi et al. (2005).

### 6.11.3 Time-Dependent Heating

The case where the temperature imposed on the lower boundary is timewise periodic was analyzed by Chhuon and Caltagirone (1979). The thermal boundary conditions are now  $T = T_0$  at  $z = H$  and

$$T = T_0 + \Delta T(1 + \beta \sin \omega^* t) \quad \text{at } z = 0. \quad (6.116)$$

For the basic state the nondimensional equations, expressed in terms of the same scales as in Sect. 6.2, are  $v_b = 0$  and

$$\frac{\partial \hat{T}_b}{\partial \hat{t}} = \frac{\partial^2 \hat{T}_b}{\partial \hat{z}^2}, \quad (6.117)$$

$$\hat{T}_b = 1 \quad \text{at } \hat{z} = 1, \quad (6.118)$$

$$\hat{T}_b = 1 + \beta \sin \omega \hat{t} \quad \text{at } \hat{z} = 0, \quad (6.119)$$

$$\omega = \frac{\sigma H^2}{\alpha_m} \omega^*. \quad (6.120)$$

The solution of the system of equations (6.117), (6.118), (6.119), and (6.120) is

$$\hat{T}_b = (1 - \hat{z}) + \beta \alpha(\hat{z}) \sin(\omega t + \varphi(\hat{z})), \quad (6.121)$$

where

$$\alpha(\hat{z}) = |q|, \quad \varphi(\hat{z}) = \operatorname{Arg} q,$$

$$q(\hat{z}) = \frac{\sinh[k(1+i)(1-\hat{z})]}{\sinh[k(1+i)]}, \quad k = \left(\frac{\omega}{2}\right)^{1/2}. \quad (6.122)$$

If we take perturbations on this steady state and, instead of (6.23), take

$$(\hat{w}, \hat{T}) = [W(\hat{z}, \hat{t}), \theta(\hat{z}, \hat{t})] \exp(il\hat{x} + im\hat{y}) \quad (6.123)$$

we obtain

$$\frac{\partial \theta}{\partial \hat{t}} = (D^2 - \alpha^2)\theta - W \frac{\partial \hat{T}_b}{\partial \hat{z}}, \quad (6.124)$$

$$\gamma_a \frac{\partial}{\partial \hat{t}} (D^2 - \alpha^2)W = -Ra \alpha^2 \theta - (D^2 - \alpha^2)W. \quad (6.125)$$

In the case of impermeable isothermal boundaries the boundary conditions are

$$W = \theta = 0 \quad \text{at } \hat{z} = 0 \quad \text{and} \quad \hat{z} = 1. \quad (6.126)$$

Chhuon and Caltagirone then set  $\gamma_a = 0$ , solved the systems ((6.124), (6.125), and (6.126)) using the Galerkin method, and examined the stability of solutions of the resulting ordinary differential equations using the Floquet theory. In this way

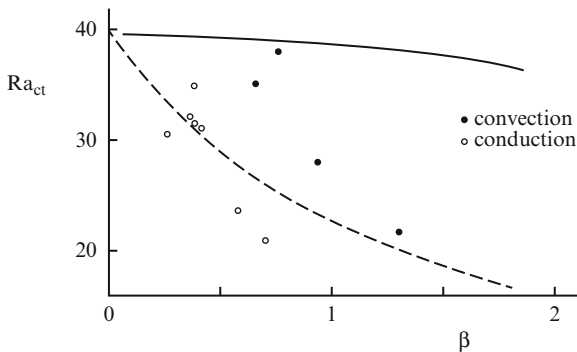


**Fig. 6.13** Critical Rayleigh numbers vs. amplitude for frequency  $f = 4.23$ ; •, ◦ experiment; —— linear theory; and —— Floquet theory (Chhuon and Caltagirone 1979)

they obtained the value of a critical Rayleigh number  $Ra_{ct}$  as a function of wavenumber  $\alpha$ , amplitude  $\beta$ , and frequency  $f = 2\pi/\omega$ . They also performed experiments and compared their observations with their Floquet theory calculations and with calculations based on linear theory by Caltagirone (1976a), shown in Fig. 6.13.

In comparing the theories there is the problem that for the linear theory the stability criterion taken was  $a(t) < 0$ ,  $a(t)$  being the amplitude of the temperature perturbation. Both theories give the frequency range 1–100 as that over which  $Ra_{ct}$  varies significantly, but whereas in the Floquet theory  $Ra_{ct}$  varies only slightly with  $f$ , in the linear theory  $Ra_{ct}$  varies from 40 as  $f \rightarrow \infty$  to  $40/(\beta + 1)$  at  $f = 0$ . Both theories predict destabilization from the stationary case. The Floquet theory breaks down when  $f \rightarrow 0$ , since the critical Rayleigh numbers must necessarily approach  $4\pi^2/(\beta + 1)$ .

As Fig. 6.13 shows, convective phenomena are observed for Rayleigh numbers between those given by the two theories. Additional numerical calculations by Chhuon and Caltagirone showed that during part of the period of oscillation, the effect of convection is that the initial perturbation is attenuated considerably and then it increases. At high frequencies both theories agree that the temperature oscillation has no effect on the stability of the layer.

The Brinkman model was employed by Rudraiah and Malashetty (1990). They concluded that modulation could advance or delay the onset of convection according to whether the variation of top and bottom temperatures was in phase or out of phase. An extension to the Forchheimer model was made by Malashetty and Wadi (1999), while Malashetty and Basavaraja (2002) combined an oscillatory wall temperature with an oscillatory gravitational field. Néel and Nemrouch (2001) examined the stability of a layer with an open top and a pulsating temperature imposed at the upper boundary, using the Darcy model. The case of an oscillatory thermal condition at the top was also studied numerically by Holzbecher (2004c).

The effect of temperature modulation on the onset of convection in a Hele-Shaw cell was studied by Souhar et al. (2011).

Other authors have been concerned with situations where the imposed surface temperature varies monotonically with time. Now amplification of disturbances inevitably occurs at some stage, and the interest is in determining an onset time by which the growth factor has reached some specified criterion, say 1,000. Caltagirone (1980) investigated the case when the lower surface is subjected to a sudden rise in temperature. He used linear theory, energy-based theory, and a two-dimensional numerical model. Kaviany (1984a) made a theoretical and experimental investigation of a layer with a lower surface temperature increasing linearly with time. His second paper (Kaviany 1984b) involved both time-dependent cooling of the upper surface and uniform internal heating. An alternative treatment of this problem was reported by Yoon et al. (1992), following on from Yoon and Choi (1989). They predicted an onset time  $\tau_c$  given by

$$\tau_c = 6.55(Da Ra)^{-2/3}, \quad (6.127)$$

where  $Da = K/\varphi H^2$ , and found that the experimental data of Kaviany (1984b) indicated that the convection is detectable at time  $4\tau_c$ . The fact that this onset time is significantly larger than  $t_c$  suggests that the fastest growing modes will be the ones that are observed. A study of the most unstable disturbance corresponding to momentary instability, based on an optimization over the range of possible initial conditions, was made by Green (1990). A prediction of the time required for the onset of convection in a porous-medium saturated with oil with a layer of gas underlying the oil was made by Rashidi et al. (2000). Propagation theory was employed by Kim et al. (2004b) to study the onset of convection in a transient situation with a suddenly applied constant heat flux at the bottom of the layer. A further theoretical study was reported by Kim and Kim (2005). Linear and global stability analyses of the extension of the Caltagirone (1980) problem to the case of an anisotropic medium were made by Ennis-King et al. (2005), for both thin and thick slabs. For a thick slab they found that the increase of  $\tau_c$  as  $\gamma$  (the ratio of vertical permeability to horizontal permeability) decreases is given approximately by  $(1 + \sqrt{\gamma})^4/16\gamma^2$ . Their study is applicable to the geological storage of carbon dioxide, for which the timescale can vary from less than a year (for high-permeability formations) to decades or centuries (for low-permeability ones).

The topic of the previous paragraph, in the context of an unsteady boundary layer formed when the temperature or solute at a plane boundary is changed instantaneously to a new level, was discussed in detail in the review paper by Rees et al. (2008d). In this situation the thermal/solutal field which then forms is unsteady, and it spreads outward uniformly by diffusion. When the less dense fluid lies below the more dense fluid, the evolving system is stable at first but eventually becomes unstable, and so one is interested in determining the critical time at which the system is deemed to be unstable. Many methods have been used to do this, with varying results illustrated in Table 6.3. We now briefly discuss these methods in turn.

The quasistatic assumption is made by assuming that all time derivatives in the eigenvalue problems are zero. If this is done before a similarity coordinate transformation, then one has propagation theory (case QS1), while if it is done afterward,

**Table 6.3** Critical times and wavenumbers obtained by different methods

Case	$\tau_c$	$t_c$	$k_c$	References
QS1	12.9439	167.544	0.06963	Selim and Rees (2007a)
QS2	7.4559	55.590	0.05834	Rees et al. (2008d)
QS3	12.43	154.5	0.0736	Yoon and Choi (1989)
QS4	7.27	52.85	0.07428	Kim et al. (2003)
LR1	46.5520	2261.2	0.06607	Tan et al. (2003)
LR2	9.8696	97.409	0.07958	Rees et al. (2008d)
ES1*	~9.6	~96		Caltagirone (1980)
ES2*	~5.5	~30		Ennis-King et al. (2005)
AT1	8.9018	79.242	0.07807	Selim and Rees (2007a)
AT2*	~8.9	~80		Caltagirone (1980)
AT3a*	8.7	75	0.066	Ennis-King et al. (2005)
AT3b	10.56	111.5	0.0752	Ennis-King et al. (2005)
AT4	12.1	147	0.07	Riaz et al. (2006)
AT5*	8.671	75.19	0.06529	Xu et al. (2006)
AT6*	7.75	60	0.05	Hassanzadeh et al. (2006)

Results marked with an asterisk are extrapolated from finite thickness calculations (after Rees et al. 2008d). Here  $\tau = t^{1/2}$ , where  $t$  is the time scaled in terms of the thermal/solutal diffusion time  
*QS* quasistatic; *LR* local Rayleigh number; *ES* energy stability; *AT* amplitude theory

one has the frozen time method (case QS2). Each method involves an essentially arbitrary strong constraint on which disturbances are allowable. The results of Yoon and Choi (1989) (QS3) were obtained using propagation theory applied to a finite layer, which gives deep-pool results when the Rayleigh number is large. Kim et al. (2003a) (QS4) employ propagation theory with a stress-free boundary condition applied at the lower surface.

The local Rayleigh number analysis (cases LR1 and LR2) is a rough and ready method which uses the basic HRL results with a Rayleigh number based on the current thickness of the boundary layer. Hence it gives just ballpark estimates. The large value for the critical time obtained by Tan et al. (2003) is obviously anomalous, and in fact Nield (2004a) pointed out that their work is flawed in a number of respects.

The idea behind energy stability analysis (cases ES1 and ES2) is to find a time before which no disturbances grow. Variational methods are used to find the earliest time before which an appropriately defined energy functional is stationary. In Table 6.3 the results for case ES1 have been obtained by extrapolating the results of Caltagirone (1980) for a finite layer. Ennis-King et al. (2005) extended Caltagirone's results to anisotropic media. Their isotropic results are at variance with Caltagirone's in predicting a much earlier time, and currently there is insufficient information to resolve the matter.

The amplitude method (case AT) (also called dominant-mode analysis) uses solutions of the full parabolic disturbance equations. It is necessary to specify the initial perturbation whose evolution is then determined. This has been undertaken using either Galerkin methods for a finite thickness layer (Caltagirone 1980; Ennis-King et al. 2005; Xu et al. 2005) or in the deep-pool context by Galerkin methods

(Ennis-King et al. 2005) or by finite difference methods (Selim and Rees 2007a). A means of determining the amplitude of the evolving perturbation also has to be defined, and various options have been used in the literature. In all cases the chosen measure is evaluated at each time step, and the times at which the time derivative is zero are noted together with the wavenumber  $k$ . Hassanzadeh et al. (2006) used the same methodology as Ennis-King et al. (2005) and Xu et al. (2006) but varied the initial conditions and the boundary conditions.

For further discussion and critical comment on this complicated matter, the reader is referred to Rees et al. (2008d). They conclude tentatively that the results of Caltagirone (1980) and Selim and Rees (2007a) should be regarded as definitive, at least for amplitude theory. Rees et al. (2008d) also draw attention in this context to the studies of anisotropy by Ennis-King et al. (2005), of ramped heating by Kim and Kim (2005) and Hassanzadeh et al. (2006), of internal heat sources by Kim et al. (2002a), and of local thermal nonequilibrium by Nouri-Borujerdi et al. (2007c). Generally it was found that the critical time decreases as the degree of LTNE increases. This may be attributed to the fact that the convecting fluid does not have to impart heat to the solid phase, and thus to the fluid's experience of what might be called a thermal drag.

We add that Kim and Choi (2007) and Kim (2010) have employed a modified energy theory (they call it relaxed energy stability analysis). They obtained the values  $t_c = 83.72$  and  $k_c = 0.067$ . We note that this value for the critical time is consistent with the results of Caltagirone (1980) and Selim and Rees (2007a).

The possibility of feedback control of the conduction state was demonstrated theoretically by Tang and Bau (1993). The temperature perturbation  $\theta$  at some horizontal cross section is monitored. The controller momentarily modifies the perturbation temperature distribution of the heated base in proportion to a linear combination of  $\theta_0$  and its time derivative. Thus the controller slightly reduces/increases the bottom temperature at locations where the fluid tends to ascend/descend. Once the disturbance has disappeared, the bottom temperature is restored to its nominal value. This simple procedure suppresses the first even mode and so delays the onset of convection until the first odd mode is unstable, giving a fourfold increase in the critical Rayleigh number. More general issues were discussed by Bau (1993). The feedback control of chaotic convection was studied by Vadasz (2010a), Mahmud and Hashim (2010, 2011), and Roslan et al. (2011).

The effects of a sinusoidal temperature distribution, as a wave with wavelength that of the incipient Bénard cells superimposed on the hot temperature of the lower plate, were studied numerically by Mamou et al. (1996). For a given value of  $Ra$ , the cells move with the imposed wave if the velocity of the latter remains below a critical value, but at higher velocity, the cell motion is irregular and fluctuates. Ganapathy and Purushothaman (1992) had analyzed previously a similar problem with a moving thermal boundary condition at the upper surface. The effects of adding small-amplitude traveling thermal waves, of the same amplitude and phase at the top and bottom boundaries, were examined by Banu and Rees (2001). At sufficiently low Rayleigh number  $Ra$ , the induced flow follows the motion of the thermal wave, but at higher  $Ra$ , this form of convection breaks

down, and there follows a regime where the flow travels more slowly on the average and does not retain the forcing periodicity. At much higher  $Ra$  (or for large wave speeds at moderate  $Ra$ ), two very different timescales appear in the numerical simulations. Hossain and Rees (2003) treated the variant problem where the sidewalls have the same cold temperature as the upper surface. Now the flow becomes weaker as the Darcy number decreases from the pure fluid limit toward the Darcy flow limit, and the number of cells that form in the cavity varies primarily with the aspect ratio and is always even due to the symmetry imposed by the cold sidewalls.

The onset of convection induced by volumetric heating, with the source strength varying exponentially with depth and also varying with time, was analyzed by Nield (1995); he added a term

$$q''' e^{\beta(z/H-1)} [1 + \varepsilon e^{i\omega(t-t'')}] \quad (6.128)$$

to the right-hand side of (6.5) and showed that for the case of conducting boundaries, instability occurs when

$$Ra + Ra_I f(\beta) [4\pi^2 \varepsilon (16\pi^2 + \omega^2)^{-1/2} - 1] > 4\pi^2, \quad (6.129)$$

where  $f(\beta) = 2(1 - e^{-\beta})/(4\pi^2 + \beta^2)$ ,  $Ra_I$  is given by (6.115), and  $\omega$  is given by (6.120), the most unstable conduction-state temperature profile occurring at the end of the cooling phase of a cycle if  $\beta$  is positive. Nield also gave results for other thermal boundary conditions. He also investigated the case of square-wave periodic heating, both for a steady state and the transient situation after the heating is suddenly switched on. He showed that the square-wave time-periodic source leads to a more unstable situation than a sinusoidal time-periodic source of the same amplitude and that transient on-off heating leads to greater instability than the corresponding steady state.

### 6.11.4 Penetrative Convection, Icy Water

Mamou et al. (1999) used linear stability analysis with the Brinkman model to study the onset of convection in a rectangular porous cavity saturated by icy water. They also obtained numerical results for finite-amplitude convection. These results indicate that subcritical convection is possible when the upper stable layer extends over more than one half of the cavity depth and demonstrate the existence of multiple solutions for a certain parameter range. Penetrative convection in a horizontally isotropic porous layer was investigated by Carr and de Putter (2003) using alternatively an internal heat sink model or a quadratic temperature law. They performed linear and nonlinear stability analyses and showed that their two models led to the same predicted instability boundaries. Carr and Straughan (2003)

numerically calculated the onset of convection in two-layer system with icy water underlying a porous medium with patterned ground in mind. Straughan (2004a) studied an interesting resonant situation. He showed that there is a parametric range in which the convection may switch from the lower part of the layer to being prominent in the upper part of the layer. The continuous dependence on the heat source in resonant natural convection was investigated by Straughan (2011a). Mahidjiba et al. (2000b, c, 2002, 2003) applied linear stability analysis to an anisotropic porous medium saturated with icy water. They introduced an inversion parameter  $\gamma$  and an orientation  $\theta$  of the principal axes. They found that the presence of a stable layer near the upper boundary for  $\gamma < 2$  changes drastically the critical Rayleigh number, and an asymptotic situation is reached when  $\gamma \leq 1$ . For that asymptotic solution, and with  $\theta = 0^\circ$  or  $90^\circ$ , the incipient flow field consists of primary convective cells near the lower boundary with superposed layers of secondary cells. For  $0^\circ < \theta < 90^\circ$ , primary and secondary cells coalesce to form obliquely elongated cells.

## 6.12 Effects of Anisotropy

The material in this section and the next is based on the review by McKibbin (1985). The criterion for the onset of convection in a layer with anisotropic permeability and which has impermeable upper and lower boundaries was obtained by Castinel and Combarous (1974, 1975). They also reported results from experiments using glass fiber materials saturated with water. The experimental values of  $Ra_c$  agreed reasonably well with the predictions.

Epherre (1975) allowed both permeability and thermal conductivity to be anisotropic. If one defines  $Ra$  in terms of the vertical permeability  $K_V$  and the vertical thermal conductivity  $k_V$  of the medium, so that

$$Ra = \frac{g\beta K_V H \Delta T}{\nu \alpha_V}, \quad (6.130)$$

where  $\alpha_V = k_V/(\rho c_P)_f$ , then the critical value of  $Ra$  for the onset of two-dimensional convection (rolls) of cell width/depth ratio  $L$  is

$$Ra_c(L) = \frac{\pi^2(\xi + L^2)(\eta + L^2)}{\xi L^2}, \quad (6.131)$$

where  $\xi = K_H/K_V$  and  $\eta = k_H/k_V$ . The subscript H refers to quantities measured in the horizontal direction. As  $L$  varies, the minimum value of  $Ra$  is attained when  $L = L_c = (\xi\eta)^{1/4}$ ,

$$Ra_{c,\min} = \pi^2 \left[ 1 + \left( \frac{\eta}{\xi} \right)^{1/2} \right]^2. \quad (6.132)$$

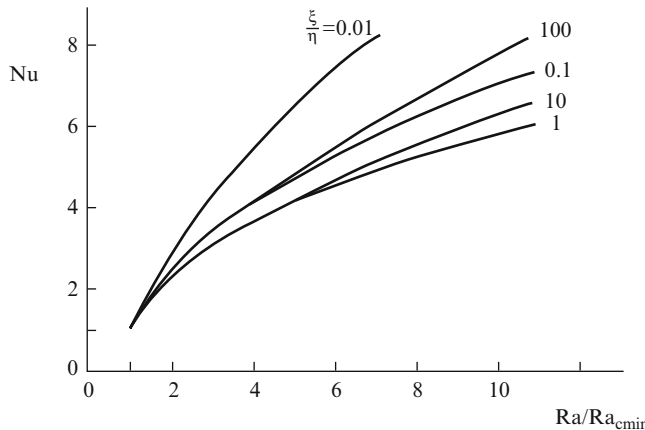


**Fig. 6.14** Nusselt number vs.  $Ra/Ra_{c,\min}$  for various anisotropy ratios  $\xi/\eta$  (McKibbin 1985; after Kvernold and Tyvand 1979)

These analyses were extended by Kvernold and Tyvand (1979) to steady finite-amplitude convection. They found that for two-dimensional flow the Nusselt number  $Nu$  depends on  $\xi$  and  $\eta$  only in the ratio  $\xi/\eta$ . They also found that if  $Nu$  is graphed as a function of  $Ra/Ra_c$ , the various curves start out from the point (1,1) at the same slope, which is equal to 2.0 (Fig. 6.14). Nield (1997b) pointed out that (6.132) is equivalent to  $Ra_{Ec} = 4\pi^2$ , where  $Ra_E$  is an equivalent Rayleigh number defined as in (6.19) but with  $K/\alpha_m$  replaced by the square harmonic-mean square root of  $K_V/\alpha_V$  and  $K_H/\alpha_H$ , and in Fig. 6.14, the quantity  $Ra/Ra_{c,\min}$  is equivalent to  $Ra_E/4\pi^2$ .

Wooding (1978) noted that in a geothermal system with a ground structure composed of many successively laid down strata of different permeabilities, the overall horizontal permeability may be up to ten times as large as the vertical component. He extended the linear analysis to three-dimensional convection in a layer in which the permeability is anisotropic and also may vary with depth. He treated both impermeable and free (constant-pressure) upper boundaries. As expected, the free boundaries yield a smaller  $Ra_c$  than the impermeable boundaries, but the difference becomes small when  $\xi = K_H/K_V$  becomes large because then vertical flow is more difficult than horizontal flow.

A study of the fraction  $r$  of the total flow that recirculates within an anisotropic layer at the onset of convection was conducted by McKibbin et al. (1984). It was extended by McKibbin (1986a) to include a condition of the form  $P + \lambda \partial P / \partial n = 0$  at the upper boundary, where  $\lambda$  is a parameter taking the limiting values 0 for a constant-pressure boundary and  $\infty$  for an impermeable boundary. He found that there is always some recirculation of the fluid within the porous layer provided that  $\lambda$  is finite (Fig. 6.15a). In the case  $\lambda = 0$ , there is a stagnation point on the surface as well as in the interior of the layer (Fig. 6.15b). McKibbin calculated  $Ra_c$ ,  $L_c$ ,  $\sigma_*$ , and  $r$  for various values of  $\lambda$ , as functions of  $\xi/\eta$ . The results show that the recirculation diminishes as  $\xi/\eta \rightarrow 0$  and there is full recirculation as  $\xi/\eta \rightarrow \infty$ .

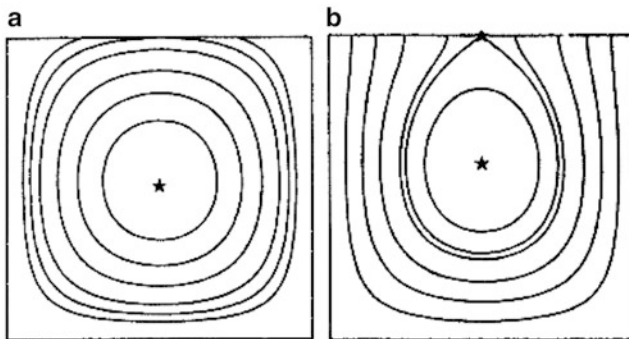


**Fig. 6.15** Streamline patterns at the onset of convection in an anisotropic layer with a kinematic boundary condition of the form  $P + \lambda \partial P / \partial n = 0$  at the upper surface, for the case  $\xi = 2$ ,  $\eta = 1$ , and  $L = 1$ . (a)  $\lambda = 1$ , recirculating fraction of flow = 0.869; (b)  $\lambda = 0$ , recirculating fraction of flow = 0.290. The stagnation point is marked with an asterisk (McKibbin 1985; after McKibbin 1986a)

Here  $\sigma_*$  is the slope coefficient which appears in the heat transfer relationship (for slightly supercritical conditions):

$$Nu = 1 + \sigma_* \left( \frac{Ra}{Ra_c} - 1 \right). \quad (6.133)$$

The effects of dispersion, in addition to anisotropic permeability, were studied by Tyvand (1977, 1981). He found that the combined effects of anisotropy and dispersion may be much stronger than the separate effects.

Tyvand and Storesletten (1991) have analyzed the situation when the anisotropic permeability is transversely isotropic, but the orientation of the longitudinal principal axes is arbitrary. The flow patterns now have either a tilted plane of motion or tilted cell walls if the transverse permeability is larger or smaller than the longitudinal permeability. Storesletten (1993) treated a corresponding problem where there is anisotropic thermal diffusivity. Zhang et al. (1993) studied numerically convection in a rectangular cavity with inclined principal axes of permeability.

A nonlinear stability analysis of the situation of Tyvand and Storesletten (1991), but with a quadratic density law, was conducted by Straughan and Walker (1996a). They obtained the dramatic result that, in contrast to the Boussinesq situation, the effect of anisotropy is to make the bifurcation into convection occur via an oscillatory instability.

The effect of anisotropy of the dispersive part of the effective thermal conductivity tensor, with a Forchheimer term included in the momentum equation, was investigated using numerical simulation by Howle and Georgiadis (1994), for two-dimensional steady cellular convection. They used the formula of Lage et al. (1992) (6.93) to determine experimental values of  $Ra_c$  and then plotted  $Nu$  vs.  $Ra/Ra_c$ , thereby greatly reducing the divergence of experimental results found for the usual

$Nu$  vs.  $Ra$  plot. They found that dispersion increased the net heat transfer after a Rayleigh number  $\sim 100\text{--}200$ , and as the degree of anisotropy is increased, the wall averaged Nusselt number is decreased.

Joly and Bernard (1995) have computed values of  $Ra_c$  for an anisotropic porous medium bounded by anisotropic impermeable domains. Qin and Kaloni (1994) computed  $Ra_c$  values for the case of anisotropic permeability on the Brinkman model. A numerical study of the effects of anisotropic permeability and layering in seafloor hydrothermal systems was made by Rosenberg et al. (1993).

Linear stability analysis was applied to a conjugate problem with solid boundary plates by Gustafson and Howle (1999), and the results compared favorably with experiment. Mahidjiba et al. (2000c) applied linear and weak nonlinear analyses to a layer of finite lateral extent, and Mamou et al. (1998a) treated a layer for the case of constant heat flux on the boundaries. The effects of anisotropy on convection in both horizontal and inclined layers were studied by Storesletten (2004). The effects of nonuniform thermal gradient and transient effects were studied by Degan and Vasseur (2003), who studied a layer heated from the bottom with a constant heat flux and with the other surfaces insulated. The effect of radiative transfer was studied by Devi et al. (2002).

Anisotropy effects in general have been reviewed by Storesletten (1998). The later survey by Storesletten (2004) discussed various models for the anisotropy. It was noted that for horizontal layers, anisotropy affects the critical Rayleigh number and the critical wavenumber, but even the inclusion of three-dimensional anisotropy does not lead to any essentially new flow patterns at the onset of convection, provided that one of the principal axes of anisotropy is normal to the layer. When none of the principal axes are vertical, then new flow patterns, either with tilted plane of motion or with tilted as well as curved lateral walls, appear. For inclined layers, anisotropy has a strong influence on the preferred flow structure at the onset of convection. When the permeability is transversely isotropic, there are two cases. A permeability minimum in the longitudinal direction leads to longitudinal rolls for all inclinations. A permeability maximum in the longitudinal direction leads to transverse rolls when the inclination is less than a critical value and longitudinal rolls when the inclination is greater than that critical value. In the general case with anisotropy both in permeability and thermal diffusivity, either longitudinal rolls are favored for all inclinations or there is a transition from transverse rolls at lower inclinations to longitudinal rolls at higher inclinations via oblique rolls.

## 6.13 Effects of Heterogeneity

### 6.13.1 General Considerations

Extending previous work by Donaldson (1962), McKibbin (1983) calculated the criterion for the onset of convection and estimates of preferred cell width and heat

transfer for two-dimensional convection in a system consisting of a permeable layer overlying an impermeable layer, the base of the impermeable layer being isothermal. McKibbin's results showed that, compared with a homogeneous permeable system of the same total depth, the presence of the impermeable layer increases the overall temperature difference required for instability, as well as reducing the subsequent heat flux when convection occurs. The critical value of a Rayleigh number based on the parameters of the permeable stratum is decreased by the presence of the impermeable layer because of the relaxation of the thermal boundary condition at the base of the permeable stratum.

The marginal stability for a layer in which the thermal conductivity and the reciprocal of the permeability both vary linearly with depth (to an arbitrary extent) was studied by Green and Freehill (1969). Ribando and Torrance (1976) carried out numerical calculations of finite-amplitude convection for an exponential variation with depth of the ratio  $\mu/K$  of viscosity to permeability. As expected, the strongest convection takes place in regions of small  $\mu/K$ . A more general formulation of the onset problem where both the group  $\mu/K$  and the thermal diffusivity vary with depth was made by Rubin (1981). A further study is that by Malkovski and Pek (1999).

### **6.13.2 Layered Porous Media**

Studies of convection in general layered systems have been made by several investigators, starting with Rana et al. (1979). The most comprehensive are those by McKibbin and O'Sullivan (1980, 1981), who studied both the onset of convection and subsequent heat transfer for a multilayered system bounded below by an isothermal impermeable surface and above by an isothermal surface that was either impermeable or at constant pressure. Two-dimensional flow patterns and associated values of  $Ra_c$ , cell width, and initial slope  $\sigma_*$  of the Nusselt number graph were calculated for two- and three-layer systems over a range of layer thickness and permeability ratios. The results show that significant permeability differences are required to force the layered system into an onset mode different from that for a homogeneous system. They also show that increasing contrasts ultimately lead to transition from "large-scale" convection (occurring through the entire system) to "local" convection confined mainly to fewer layers. Another conclusion is that  $\sigma_*$  depends strongly on the cell width (Fig. 6.16). An experimental study, using a Hele-Shaw cell modeling a three-layered system, by Ekholm (1983) yielded results in qualitative agreement with the theory of McKibbin and O'Sullivan (1980). The assumption of two-dimensionality used by many authors was examined by Rees and Riley (1990), who found criteria governing when the preferred flow patterns are three-dimensional and presented detailed results of the ranges of stable wavenumbers.

Gjerde and Tyvand (1984) studied a layer with permeability  $K(z)$  of the form  $K(z) = K_V/(1 + a \sin N\pi z)$ , where  $K_V$ ,  $a$ , and  $N$  are constants. They found that local convection never occurs in this smoothly stratified model.

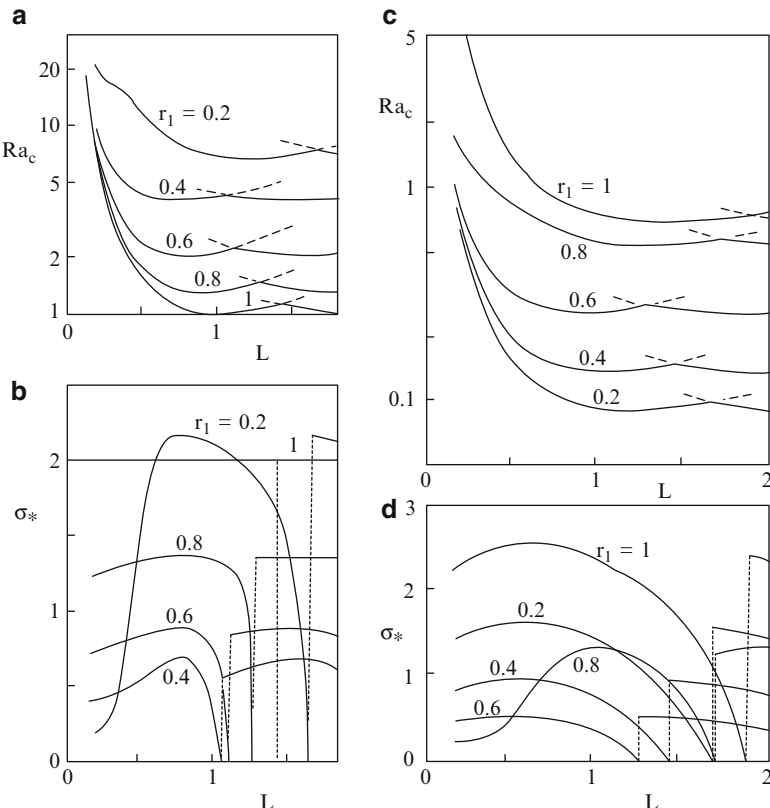


**Fig. 6.16** Variation of  $Ra_c$  and  $\sigma^*$  with system width  $L$  for two-layer systems. The lower layer occupies a fraction  $r_1$  of the total depth, and the permeability contrast between upper and lower layers is  $K_2/K_1$ . (a, b) Closed top,  $K_2/K_1 = 0.1$  and (c, d) open top,  $K_2/K_1 = 10$  (McKibbin 1985; after McKibbin and O'Sullivan 1981)

Masuoka et al. (1988) made a numerical and theoretical examination of convection in layers with peripheral gaps. Hickox and Chu (1990) numerically simulated a geothermal system using a model involving three horizontal layers of finite horizontal extent. Delmas and Arquis (1995) reported an experimental and numerical investigation of convection in a layer with solid conductive inclusions.

For permeability fields that are anisotropic, layered, or both, Rosenberg and Spera (1990) performed time-dependent numerical simulations in a two-dimensional square box. They found that the time to steady state was proportional to the square root of the kinetic energy. Their heat transfer results were consistent with previous results.

Masuoka et al. (1991, 1994, 1995a) made experimental and theoretical studies of the use of a thermal screen, consisting of a row of heat pipes with a very high effective thermal conductivity placed part way up the layer, in improving the insulation effect of a porous layer. The screen suppresses the onset of convection by making the temperature field more uniform.

Leong and Lai (2001) investigated the feasibility of using a lumped system approach using an effective Rayleigh number, on the basis of numerical calculations with two layers. Their results were generally anticipated by Nield (1994c). A similar study for a layered vertical porous annulus was made by Ngo and Lai (2000). Leong and Lai (2004) studied two or four layers in a rectangular cavity whose aspect ratio was either 0.2 or 5.0. They found that the convection is always initiated in the more permeable sublayer and this convection penetrates to the less permeable sublayer as the Rayleigh number is further increased.

The effect of vertically stratified porosity was studied by Rionero (2011). The effects of local thermal nonequilibrium and nonuniform basic temperature gradient on the onset of convection in a heterogeneous medium were treated by Sivasankaran et al. (2011). The effect of vertical heterogeneity on the onset of convection in the case of a prescribed horizontal temperature gradient was studied by Barletta et al. (2012).

The onset of convection in a horizontal layer whose permeability is a continuous periodic function of the horizontal coordinate was studied by Rees and Tyvand (2009). They employed Floquet theory to determine the favored two-dimensional mode of convection and used a matrix eigenvalue method to find the critical Rayleigh number. They supplemented this by a multi-scale analysis of the large period limit and a brief consideration of the anisotropic limit for very short periods.

The onset of convection in porous layers with multiple horizontal thin impermeable partitions was investigated by Rees and Genc (2011) using linear stability analysis. They treated the cases of two and three sublayers explicitly, and they investigated the general case. They found that the neutral stability curves tend to form themselves into natural groups of  $N$  members when there are  $N$  sublayers. When the disturbance wavenumber  $k$  is large, each member of any group lies within an  $O(k^{-1})$  distance of all other members but an  $O(1)$  distance of other groups. When the number of sublayers is large, the system tends to one with critical Rayleigh number 12 and critical wavenumber zero (as for a single porous layer with constant-flux boundaries). They also used an asymptotic analysis to determine the critical wavenumber and its associated wavenumber when the number of sublayers is large.

### 6.13.3 *Analogy Between Layering and Anisotropy*

Wooding (1978) noted that there is a correspondence between layering and anisotropy in porous media. In a system in which the permeability  $K$  varies with the vertical coordinate  $z$ , the average horizontal and vertical permeabilities, in a layer of thickness  $H$ , are given by

$$\bar{K}_H = \frac{1}{H} \int_0^H K(z) dz, \quad \bar{K}_V = H / \int_0^H \frac{dz}{K(z)} \quad (6.134)$$

and so, since the arithmetic mean exceeds the harmonic mean,

$$\xi = \frac{\bar{K}_H}{\bar{K}_V} > 1. \quad (6.135)$$

A similar result applies for thermal conductivity. It implies that layering implies anisotropy with  $\xi > 1$ ,  $\eta > 1$ . The result holds whether the layering is continuous or not, but the question is whether or not a transition to local convection will cause the analogy to break down. McKibbin and Tyvand (1982) explored this question. They concluded that the analogy is likely to be reliable in a continuously layered system and also in a discretely layered system provided that the contrast between the layers is not too great.

McKibbin and Tyvand (1983, 1984) studied systems in which every second layer is very thin. If these thin layers have very small permeability (i.e., the layers are “sheets”), convection is large scale except when the sheets are almost impermeable. If the thin layers have very high permeability (i.e., the layers are “cracks”), then local convection is almost absent, so the analogy is more likely to be reliable for modeling. However, there is one feature of the crack problem that has no counterpart in the anisotropic model: There is a strong horizontal flow in the cracks (Fig. 6.17) and this affects the analogy.

#### 6.13.4 Heterogeneity in the Horizontal Direction

The configuration where the porous medium consists of a number of homogeneous vertical slabs or columns of different materials is more difficult to study in comparison with the horizontally layered problem, and so far few studies have been published. McKibbin (1986b) calculated critical Rayleigh numbers, streamlines, and the variation of heat flux across the surface for a few examples involving inhomogeneity of permeability and thermal conductivity. His results are shown in Figs. 6.18, 6.19, and 6.20. Here  $Ra_i$  denotes the Rayleigh number for material  $i$ ,

$$Ra_i = \frac{g \beta K_i H \Delta T}{\nu \alpha_{m i}}. \quad (6.136)$$

$L$  is the horizontal to vertical aspect ratio of the entire system and  $r_i$  is the fraction of the total width occupied by material  $i$ .

Figure 6.18 shows that as the permeability contrast increases, so does  $Ra_{1c}$ , indicating, as expected, that a larger overall temperature gradient is required to destabilize the conductive state of the system. One example of the streamline flow pattern is illustrated in Fig. 6.19a. Here the small amount of flow in the less permeable layer is reflected in the small and almost even increase in heat transfer

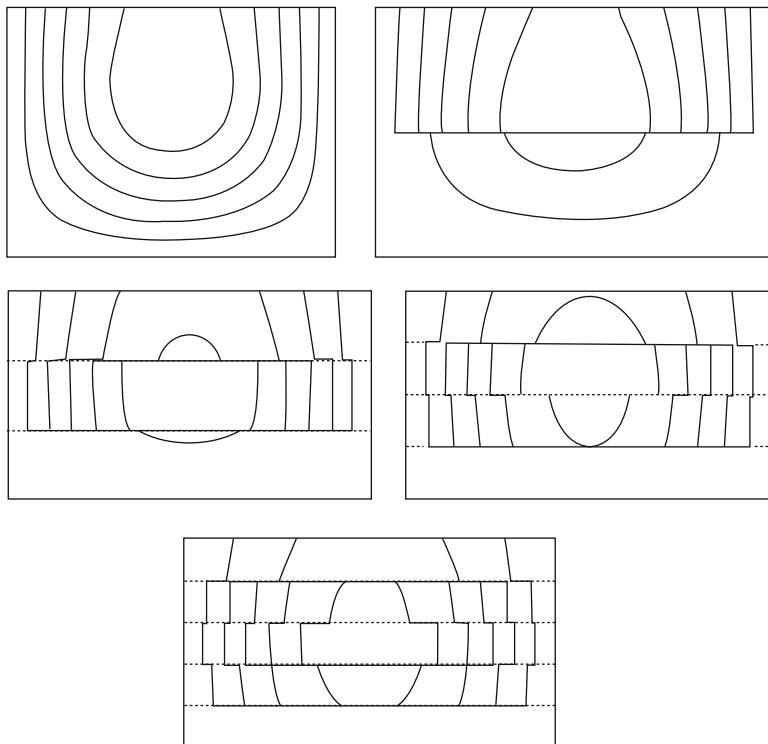


**Fig. 6.17** Streamlines at onset of convection in a system with thin, very permeable layers (cracks). The ratio of the thickness of each crack to that of the intervening material layers is 0.02, and the equivalent induced anisotropy in each case is  $\xi = 10$  (McKibbin and Tyvand 1984, with permission from Pergamon Press)

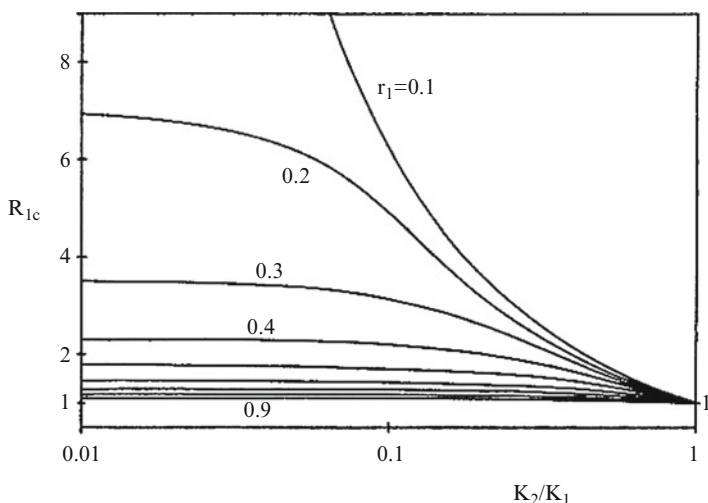


**Fig. 6.18** The critical Rayleigh number  $R_{1c} = Ra_{1c}/4\pi^2$  for a two-layer system with  $L = 1$ ,  $r_1 = 0.1$  (0.1) 0.9, and  $0.01 = K_2/K_1 = 1.0$  (McKibbin 1986b, with permission from Kluwer Academic Publishers)

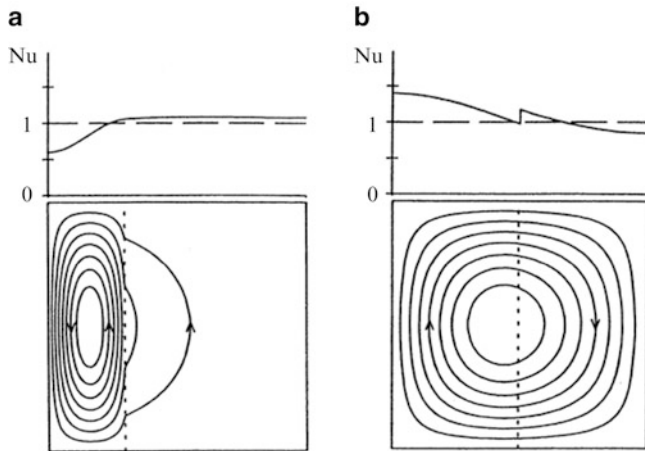


**Fig. 6.19** Streamline patterns at the onset of convection and typical Nusselt number at the surface, for slightly supercritical flow. In each case the overall aspect ratio  $L = 1$ . The subscripts 1 and 2 indicate regions numbered from *left* to *right*.  $R = Ra/4\pi^2$ , where  $Ra$  is the Rayleigh number. (a) Permeability ratio  $K_2/K_1 = 0.1$ ,  $R_{1c} = 3.132$ ,  $R_{2c} = 0.313$ ; (b) thermal conductivity ratio  $k_2/k_1 = 1.2$ ,  $R_{1c} = 1.084$ ,  $R_{2c} = 0.903$  (McKibbin 1986b, with permission from Kluwer Academic Publishers)

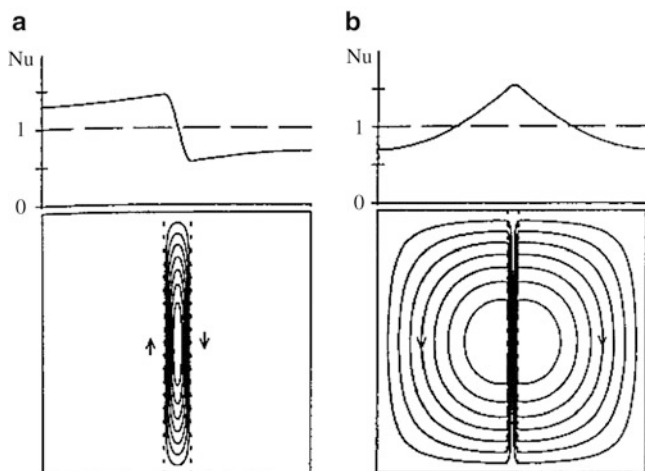


**Fig. 6.20** Streamline patterns and Nusselt number at the surface for the case of a centrally placed narrow stratum, permeability ratio  $K_2/K_1 = 100$  and  $K_3 = K_1$ . (a)  $r_2 = 0.1$ ,  $R_{1c} = 0.267$ ,  $R_{2c} = 26.7$ ; (b)  $r_2 = 0.04$ ,  $R_{1c} = 0.665$ ,  $R_{2c} = 66.5$ , where  $R = Ra/4\pi^2$  (McKibbin 1986b, with permission from Kluwer Academic Publishers)

at the surface due to convection. At the same time, the stronger flow in the more permeable section has a marked effect on the surface heat flux. Figure 6.19b illustrates a small thermal conductivity contrast. The strength of flow is slightly greater in the less conductive region. The jump in heat flux is due to the greater conductivity of material 2.

In the case of a thin, more permeable stratum cutting an otherwise homogeneous medium, as the thin stratum becomes more permeable, there is a sudden transition from approximately square flow cells to a flow pattern where a very strong flow takes place up (or down) the permeable fault. For a narrower fault the permeability contrast needed for transition is greater. An example is shown in Fig. 6.20. The contrast between the flow patterns and the surface heat flux patterns is remarkable. This is different from the case of horizontal layering, where the spatial distribution of surface heat flux remains basically the same for all configurations, even though permeability and/or conductivity contrasts are great (McKibbin and Tyvand 1984).

An approximate analysis of convective heat transport in vertical slabs or columns of different permeabilities was made by Nield (1987b). He took advantage of the fact that when Darcy's law is applicable, one can superpose solutions of the eigenvalue problem for a single slab to obtain a feasible solution of the equations for the overall problem with the slabs placed side by side. This is, of course, an artificial flow since extra constraints have been imposed on the eigenvalue problem. In general, the actual flow will be one in which the convection induced in one slab will penetrate into adjacent slabs; one would expect that the actual flow would be more efficient at transporting heat than the artificial flow. This procedure leads to a lower bound for the true overall heat flux and an upper bound on a critical Rayleigh number.

Nield discussed some sample situations and also established a general result. If the heat transfer is given by  $Nu = g(Ra)$ , then for sufficiently large values of  $Ra$ , the second derivative  $g''(Ra)$  is usually negative. It then follows that if  $Ra$  is supercritical everywhere, then for small and gradual variations in  $Ra$  with horizontal position, the effect of inhomogeneity is to decrease the heat flux by a factor

$$1 + \left[ \frac{g''(\bar{R}a)}{2g(\bar{R}a)} \right] \sigma_{Ra}^2 \quad (6.137)$$

relative to that for an equivalent homogeneous layer with the same Rayleigh number average  $\bar{R}a$ . In the above expression,  $\sigma_{Ra}^2$  is the variance of the Rayleigh number distribution. In particular, if we take  $g(Ra) = \alpha Ra^\beta$ , where  $0 < \beta < 1$ , then the reduction factor is

$$1 - \frac{1}{2} \beta(1 - \beta) \frac{\sigma_{Ra}^2}{Ra^2}. \quad (6.138)$$

Gounot and Caltagirone (1989) analyzed the effect of periodic variations in permeability. They showed that short-scale fluctuations had the same effect on

stability as anisotropy. As expected, the variability causes the critical Rayleigh number based on the mean permeability to be raised and the Nusselt numbers to be lowered relative to the homogeneous values.

Vadasz (1990) used weakly nonlinear theory to obtain an analytic solution of the bifurcation problem for a heterogeneous medium for the case of heat leakage through the sidewalls. He showed that if the effective conductivity function  $k_m(x, y, z)$  is not of the form  $f(z)h(x, y)$ , then horizontal temperature gradients (and hence natural convection) always must be present. A comprehensive study of convection in a layer with small spatial variations of permeability and effective conductivity was made by Braester and Vadasz (1993). For certain conductivity functions a motionless state is possible, and the stability of this was examined using weak nonlinear theory. A smooth transition through the critical Rayleigh number was found. Heterogeneity of permeability plays a relatively passive role compared with heterogeneity of thermal conductivity. For a certain range of supercritical  $Ra$ , symmetry of conductivity function produces symmetry of flow.

Convective stability for a horizontal layer containing a vertical porous segment having different properties was studied by Wang (1994). Convection in a rectangular box with a fissure protruding part way down from the top was treated numerically by Debeda et al. (1995).

### 6.13.5 *Heterogeneity in Both Horizontal and Vertical Directions*

In a series of papers Nield and Kuznetsov (2007b, c, d, e, 2008d), with the aid of a two-dimensional Galerkin method, obtained analytical results for the case of weak heterogeneity in both the horizontal and vertical directions. (The cases of a bidisperse medium and an anisotropic medium were considered in turn, and in one paper, the case of constant-flux boundaries was treated.) A related problem, involving an enclosure of varying width or height, was studied by Nield and Kuznetsov (2007f) with the same methodology. Transient convection was examined by Nield and Kuznetsov (2007g), while Nield and Kuznetsov (2011e) added the effect of vertical throughflow. This work was surveyed by Nield (2008c). A case involving moderate heterogeneity was treated by Nield and Kuznetsov (2008c).

### 6.13.6 *Strong Heterogeneity*

Nield and Simmons (2007) discussed the applicability of a Rayleigh number as a criterion for determining the onset of convection in a strongly heterogeneous medium. In such a medium a single Rayleigh number based on averaged quantities is no longer useful, and so Nield et al. (2010b) and Kuznetsov et al. (2010) introduced a stability exploration package for strong heterogeneity. This computer package examines in turn various possible sub-domains of a porous medium.

Simmons et al. (2010) discussed the geologic implications of these results. The case of a transient basic temperature profile was examined by Kuznetsov et al. (2011). The case of strong throughflow was studied by Kuznetsov and Nield (2012b) and Nield and Kuznetsov (2012b).

## 6.14 Effects of Nonuniform Heating

O'Sullivan and McKibbin (1986) have performed a perturbation analysis and numerical calculations to investigate the effect of small nonuniformities in heating on convection in a horizontal layer. They found that  $O(\varepsilon^3)$  variations in heating of the bottom generally produce variations of the same order in convection amplitude. However, if the distribution of the heating nonuniformity happens to have a wavelength equal to the wavelength of the preferred convection mode, then  $O(\varepsilon^3)$  variations in heating produce an  $O(\varepsilon)$  effect on the amplitude of convection at Rayleigh numbers within  $O(\varepsilon^2)$  of the critical Rayleigh number  $Ra_c$ . This produces a smoothing of the  $Nu$  vs.  $Ra$  curve in the vicinity of the critical Rayleigh number, as shown in Fig. 6.21.

Rees and Riley (1989a) and Rees (1990), using weakly nonlinear theory, have considered in turn the consequences of excitation of near-resonant wavelength, nonresonant wavelength, and long-wavelength forms. When the modulations on the

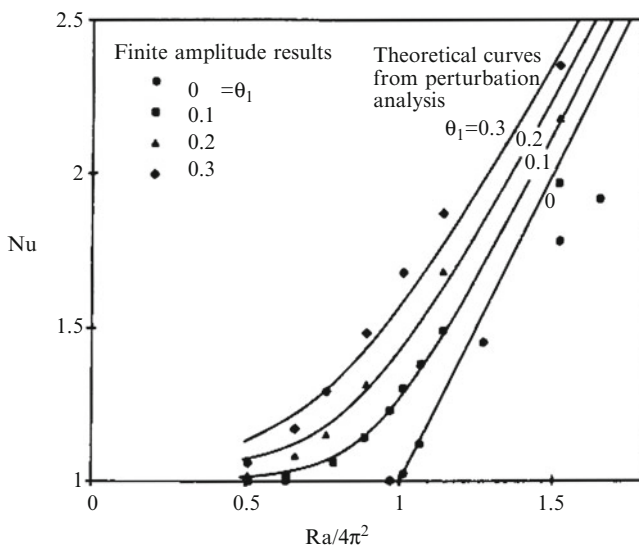


**Fig. 6.21** Effect of nonuniform heating on heat transfer. The calculations refer to a two-dimensional square container (length-to-height ratio = 1) with impermeable top and bottom and with insulated sidewalls. The dimensionless temperature distribution on the bottom is assumed to be  $T(x, 0) = 1 + \theta_1 \cos \pi x$ , ( $0 \leq x \leq 1$ ) (O'Sullivan and McKibbin 1986)

upper and lower boundaries are in phase, at the near-resonant wavelength, steady rolls with spatially deformed axes or spatially varying wavenumbers evolve. Rolls with a spatially varying wavenumber also evolve when the modulations are  $\pi$  out of phase. For a wide range of nonresonant wavelengths, a three-dimensional motion with a rectangular planform results from a resonant interaction between a pair of oblique rolls and the boundary forcing. Symmetric modulations of large wavelength can result in patterns of transverse and longitudinal rolls that do not necessarily have the same periodicity as the thermal forcing, but the most unstable transverse roll does have the same periodicity. For certain ranges of values of modulation wavelength, the first mode to appear as  $Ra$  is increased is a rectangular cell of large-aspect-ratio planform. This mode is a linear superposition of two rolls equally aligned at a small angle away from the direction of the longitudinal roll.

The effect of slightly nonuniform heating at the bottom a parallelopipedic box on the onset of convection was analyzed by Néel (1992). Depending on the symmetry or otherwise of the heating, the nonuniformity can change, for a particular choice of aspect ratios, the predicted pattern of steady convection or even result in oscillatory convection.

A perturbation method was employed by Riahi (1993a) to study three-dimensional convection resulting when a nonuniform temperature with amplitude  $L^*$  is prescribed at the lower wall. When the wavelength  $\gamma_{bn}$  of the  $n$ th mode of modulation is equal to the critical wavelength  $\gamma_c$  for all  $n$ , regular or nonregular solutions in the form of multimodal pattern convection can become preferred in some range of  $L^*$ , provided the wave vectors of such pattern are contained in the set of wave vectors representing the boundary temperature. There can be critical values  $L_c^*$  of  $L^*$  below which the preferred pattern is different from the one for  $L^* > L_c^*$ . For  $\gamma_{bn}$  equal to a constant different from  $\gamma_c$ , some three-dimensional solution in the form of multimodal convection can be preferred, even if the boundary modulation is one-dimensional, provided that the wavelength of the modulation is not too small. There are qualitatively similar results when the location (rather than the temperature) of the bottom boundary (and hence the depth) is modulated.

Riahi (1996) then extended his analysis to the case of a continuous finite bandwidth of modes. He found that the results were qualitatively similar to those for the discrete case. He also noted that large-scale flow structures are quite different from the small-scale flow structures in a number of cases and in particular they can exhibit kinks and can be nonmodal in nature. The resulting flow patterns can be affected accordingly, and they can provide quite unusual and nonregular three-dimensional preferred patterns. In particular, they are multiples of irregular rectangular patterns, and they can be nonperiodic.

Rees and Riley (1986) conducted a two-dimensional simulation of convection in a symmetric layer with wavy boundaries. In this case the onset of convection is abrupt and is delayed by the presence of the nonuniformity. However, the onset of time-periodic flow takes place at much smaller Rayleigh numbers than those corresponding to the uniform layer. The mechanism generating unsteady flow is no longer a thermal boundary layer instability but rather a cyclical interchange between two distinct modes that support each other via the imperfection, and its

onset is not a Hopf bifurcation. At relatively high amplitudes of the wavy surface, the basic flow may bifurcate directly to unsteady flow. Also, Riahi (1999), Ratish Kumar et al. (1997, 1998), Ratish Kumar (2000), and Ratish Kumar and Shalini (2003b, 2004c) have studied convection in a cavity with a wavy surface. The undulations generally lead to a reduced heat transfer.

Yoo and Schultz (2003) analyzed the small Rayleigh number convection in a layer whose lower and upper walls have sinusoidal temperature distributions with a phase difference. They found that for a given wavenumber, an out-of-phase configuration yields minimum heat transfer on the walls and that maximum heat transfer occurs at the wavenumber value 2.286 with an in-phase configuration. Capone and Rionero (2003) considered the nonlinear stability of a vertical steady flow driven by a horizontal periodic temperature gradient.

## 6.15 Rectangular Box or Channel

### 6.15.1 Linear Stability Analysis, Bifurcation Theory, and Numerical Studies

In a horizontal layer, with vertical heating, the lateral boundaries of the convection cells are vertical, and there is no heat transfer across them. This means that, assuming that slip is allowed on a rigid wall, an impermeable insulating barrier can be placed at a cell boundary without altering the flow. Consequently,  $Ra_c$  remains at  $4\pi^2$  (for the case of impermeable conducting horizontal boundaries) if the nondimensional width and breadth ( $L_x/H = h_1$  and  $L_y/H = h_2$ , for the box  $0 = x = L_x$ ,  $0 = y = L_y$ ,  $0 = z = H$ ) of a rectangular box are integral multiples of  $2\pi/\alpha_c$ . For other values of width and breadth, the value of  $Ra_c$  is raised above  $4\pi^2$ . This is because the minimization of  $(\pi^2 + \alpha^2)^2/\alpha^2$ , where  $\alpha^2 = l^2 + m^2$ , is now over discrete values of the wavenumbers  $l$  and  $m$  rather than over continuous values. Eigenmodes are represented by the stream functions

$$\Psi_{pqr} = \sin p\pi \frac{\hat{x}}{h_1} \sin q\pi \frac{\hat{y}}{h_2} \sin r\pi \hat{z} \quad (6.139)$$

for integers  $p$ ,  $q$ , and  $r$ . The corresponding Rayleigh numbers are

$$Ra_{pqr} = \pi^2 \left( b + \frac{r^2}{b} \right)^2, \quad (6.140)$$

where

$$b = \left[ \left( \frac{p}{h_1} \right)^2 + \left( \frac{q}{h_2} \right)^2 \right]^{1/2}. \quad (6.141)$$

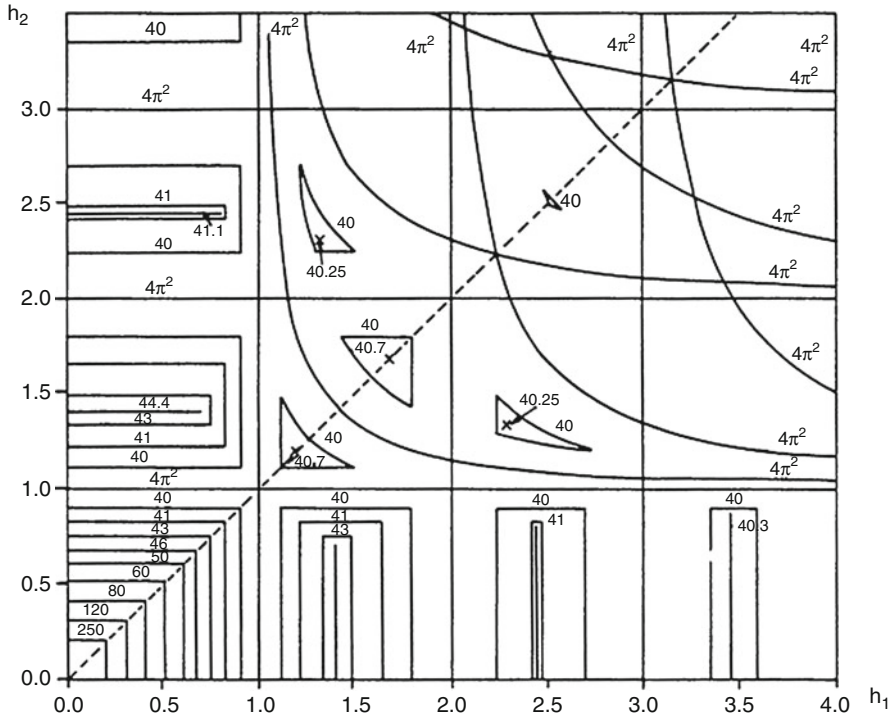


**Fig. 6.22** Variation of the critical Rayleigh number  $Ra_c$  in an enclosed three-dimensional porous medium as a function of  $h_1$  and  $h_2$  (Beck 1972)

Thus the critical Rayleigh number is given by

$$Ra_c = \pi^2 \min_{(p, q, r)} \left( b + \frac{r^2}{b} \right)^2 = \pi^2 \min_{(p, q)} \left( b + \frac{1}{b} \right)^2. \quad (6.142)$$

The minimization problem over the sets of nonnegative integers  $p$  and  $q$  for a set of values  $h_1$  and  $h_2$  has been solved by Beck (1972), and the results are displayed in Figs. 6.22 and 6.23. Figure 6.22 shows that the value of  $Ra_c$  rapidly approaches  $4\pi^2$  as either  $h_1$  or  $h_2$  becomes large so that the lateral walls have little effect on the critical Rayleigh number except in tall boxes with narrow bases, for which  $h_1 \ll 1$  and  $h_2 \ll 1$ . The preferred cellular mode  $(p, q)$  as a function of  $(h_1, h_2)$  is shown in Fig. 6.23. Note the symmetry with respect to the line  $h_1 = h_2$ . The modal exchange between the rolls  $(p, 0)$  and  $(p + 1, 0)$  occurs at  $h_1 = [p(p + 1)]^{1/2}$ . Two-dimensional rolls are preferred when the height is not the smallest dimension (i.e., when  $h_1 < 1$  or  $h_2 < 1$ ) and that a roll that has the closest approximation to a square cross section is preferred.

Using techniques of bifurcation theory, Riley and Winters (1989) have investigated the mechanics of modal exchanges as  $Ra$  and  $h_1 \equiv h$  vary, for a two-dimensional

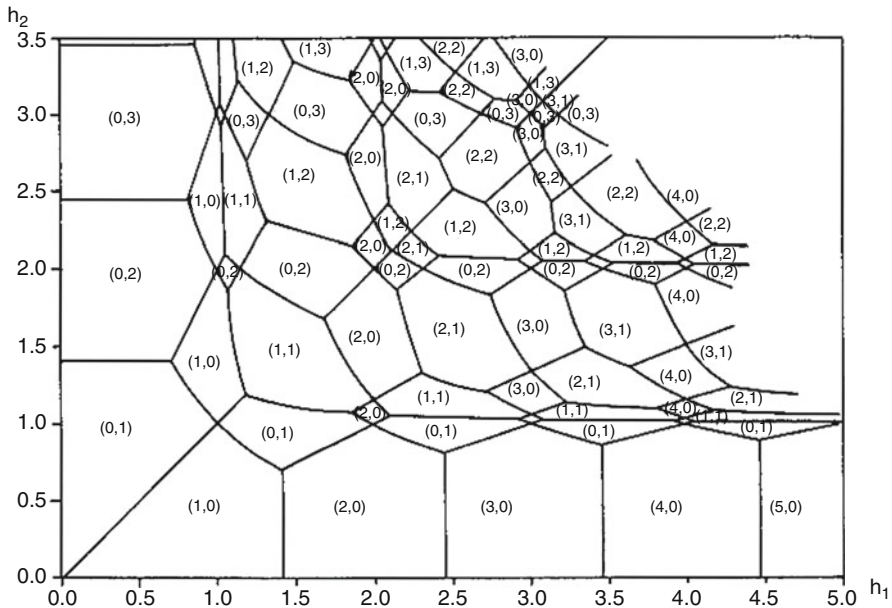


**Fig. 6.23** Preferred cellular mode  $(p, q)$  as a function of  $h_1$  and  $h_2$  in a three-dimensional box filled with a porous medium (Beck 1972)

cavity. They use a synthesis of degree theory, symmetry arguments, and continuation methods. They show that as  $h$  increases for fixed  $Ra$ , primary bifurcations (from conduction states) occur and then secondary bifurcations. At a secondary bifurcation, a previously unstable mode can regain stability. Thus the behavior of physical bifurcations is intimately connected with that of unphysical ones, and the stability boundary for one-cell flows turns out to be quite complicated. Impey et al. (1990) extended the work of Riley and Winters (1989) to include the effects of small tilt and small sidewall heat flux.

Beck's work has been extended to other types of boundary conditions. Tewari and Torrance (1981) considered the case of a permeable upper boundary; their results are as expected. A general feature is that when both breadth and width become small,  $\alpha_c$  becomes large and  $Ra_c \sim \alpha_c^2$ . In this case the perturbation quantities  $w$  and  $\theta$  vary only slowly with the vertical coordinate  $z$ , and the horizontal components are negligible. When the lateral boundaries are not insulating, new features appear. Chelghoum et al. (1987) found that if lateral boundaries are conducting rather than insulating,  $Ra_c$  is raised and two-dimensional rolls (modes of type  $(p, 0)$  and  $(0, q)$ ) are eliminated in favor of modes of type  $(p, 1)$  and  $(1, q)$ , and when  $h_1$  and  $h_2$  are not small, the modal picture is complicated.

Convection in rectangular boxes has been the topic of many numerical studies. Some of this work has been referred to in Sect. 6.8. For the two-dimensional case, Horne and O'Sullivan (1978a) and Horne and Caltagirone (1980) reported studies

of oscillatory convection, while Schubert and Straus (1982), for a square cavity, found a succession of transitions as  $Ra$  is increased.

The three-dimensional case has been studied by Horne (1979), Straus and Schubert (1979, 1981), and Caltagirone et al. (1981). A noteworthy discovery was that different steady structures develop with time, the final form depending on the initial conditions. An analytical study by Steen (1983) has complemented and corrected results of the numerical studies. The top and bottom of the box are taken to be isothermal and the sides insulated. Steen showed that for a cubic box, convection first occurs at  $Ra = 4\pi^2$ , and then a two-dimensional roll cell grows to a finite-amplitude pattern with  $Ra$  increasing. Immediately above criticality, it is the only stable pattern; the three-dimensional state found by Zebib and Kassoy (1978) is unstable. Another three-dimensional pattern comes into existence as a linear mode grows at  $Ra = 4.5\pi^2$ . It remains unstable from birth until  $Ra = 4.87\pi^2$ , when it gains stability and begins to compete with the two-dimensional pattern. These two- and three-dimensional patterns remain the only stable states up to a value of  $Ra$  (about  $1.5Ra_c$ ) when other modes become important. Steen calculated that, provided all disturbances of unit norm are equally likely, there is a 21% chance that the three-dimensional pattern will be selected at  $Ra = 50$ .

Other work on pattern selection and bifurcation in rectangular boxes has been reported by Steen (1986), Kordylewski and Borkowska-Pawlak (1983), Borkowska-Pawlak and Kordylewski (1982, 1985), Kordylewski et al. (1987), Vincourt (1989a, b), and Néel (1990a, b). The study by Riley and Winters (1991) focused on the destabilization, through Hopf bifurcations (leading to time-periodic convection), of the various stable convective flow patterns. There is a complex evolution of the Hopf bifurcation along the unicellular branch as the aspect ratio  $h$  increases. Steady unicellular flow is stable for a range of  $Ra$  values that is  $(4\pi^2, 390.7)$  at  $h = 1$  and becomes increasingly narrow and finally disappears when  $h$  exceeds 2.691. Riley and Winters also obtained an upper stability bound for steady multicellular flows. They found that stable  $m$  cells exist only for  $h < 2.691m$ .

An argument of Howard type, based on the Bénard-Rayleigh instability in boundary layers at the top and bottom surfaces, leads to the asymptotic scaling laws  $Nu \sim Ra$  and  $f \sim Ra^2$  for the mean Nusselt number and the characteristic frequency  $f$ . For convection in a square, Graham and Steen (1994) computationally studied the regime from  $Ra = 600$  to 1,250. They found that as  $Ra$  increases, a series of traveling waves with spatial wavenumber  $n$  appear, each born at a Hopf bifurcation. Modal interactions of these lead to quasiperiodic mixed modes (whose complicated behavior was studied by Graham and Steen (1992)). The  $Ra$  range studied is characterized by thermal plumes and overall follows the asymptotic scaling behavior, but the plumes drive resonant instabilities that lead to windows of quasiperiodic, subharmonic, or weakly chaotic behavior. The plume formation is disrupted in these windows, causing deviations from the simple scaling behavior. The instability is essentially a phase modulation of the plume formation process. Graham and Steen argue that each instability corresponds to a parametric resonance between the timescale for plume formation and the characteristic convection timescale of the flow. Graham et al. (1992) observed a diagonal oscillation in

**Table 6.4** Values of the critical Rayleigh number  $Ra_c$  for various lateral boundary conditions, for the onset of convection in a rectangle of height  $H$  and width  $L$

Left-hand wall	Right-hand wall	$Ra_c$
IMP/INS	IMP/INS	$\pi^2 \min[(nH/L) + (L/nH)]^2$
FRE/CON	FRE/CON	$\pi^2 \min[(nH/L) + (L/nH)]^2$
IMP/CON	IMP/CON	$4\pi^2[1 + H^2/L^2]$
FRE/INS	FRE/INS	$4\pi^2[1 + H^2/L^2]$
IMP/INS	FRE/CON	$\pi^2 \min[(nH/2L) + (2L/nH)]^2$
IMP/INS	IMP/CON	$4\pi^2[1 + H^2/4L^2]$
FRE/CON	IMP/CON	$4\pi^2[1 + H^2/4L^2]$
FRE/CON	FRE/INS	$4\pi^2[1 + H^2/4L^2]$
IMP/INS	FRE/INS	$4\pi^2[1 + H^2/4L^2]$
FRE/INS	IMP/CON	See Rees and Tyvand (2004c)

The top and bottom are assumed impermeable and conducting (after Tyvand 2002)

*IMP* impermeable (closed); *FRE* free (open); *CON* conducting; *INS* insulating

Hele-Shaw slots. A computational comparison between classic Galerkin and approximate inertial manifold methods was made by Graham et al. (1993). Extensions of this work involving Gevrey regularity were conducted by Ly and Titi (1999) and Oliver and Titi (2000). A stability analysis based on a generalized integral transform technique involving transitions in the number of cells was carried out by Alves et al. (2002).

Rees and Tyvand (2004a, b) considered convection in cavities with conducting boundaries. In this case linear stability analysis leads to a Helmholtz equation that governs the critical Rayleigh number and makes it independent of the orientation of the porous cavity. They numerically solved the eigenvalue equation for cavities of various shapes. Rees and Tyvand (2004c) found that for a two-dimensional cavity with one lateral wall thermally conducting and the other thermally insulating and open, the mode of onset of convection is oscillatory in time, corresponding to a disturbance traveling as a wave through the box from the impermeable wall to the open wall. A further study of convection in a cavity with an open sidewall, now with various sets of boundary conditions treated in turn, was studied by Nygård and Tyvand (2011b).

General surveys of this subject have been done by Rees (2000), Tyvand (2002), and Straughan (2004b). Straughan (2001a) has discussed the calculations of eigenvalues associated with porous convection. In particular, Tyvand (2002) considered a two-dimensional rectangular container with closed and conducting top and bottom and with various combinations of kinematic and thermal boundary conditions on the left- and right-hand walls. His results for the values of the critical Rayleigh number are presented in Table 6.4. The corresponding streamline patterns may be found in Tyvand (2002). For a three-dimensional box with general lateral boundary conditions, no simple analytical solution is possible.

Following earlier work by Schubert and Straus (1979) and Horne and O'Sullivan (1978a), three-dimensional convection in a cube was treated by Kimura et al.

(1989). They found a transition from a symmetric steady state ( $S$ ) to a partially nonsymmetric steady state ( $S'$ , vertical symmetry only) at  $Ra$  about 550. At  $Ra$  of 575, the flow became oscillatory ( $P^{(1)}$ ) with a single frequency that increased with  $Ra$ . It became quasiperiodic at a value of  $Ra$  between 650 and 680, returned to a simple periodic state in a narrow range about  $Ra = 725$ , and then became quasiperiodic again. Thus the three-dimensional situation was similar to the two-dimensional one, except for the higher critical  $Ra$  at the onset of oscillations (575 vs. 390) and a corresponding higher frequency (175 vs. 82.5) and except for the transition  $S \rightarrow S'$ ; however, this was dependent on step size, and it was possible that it might not occur prior to  $S \rightarrow P^{(1)}$  for sufficiently small steps in  $Ra$ . They also noted that the (time-averaged) Nusselt number for the three-dimensional flows was generally greater than that for the two-dimensional flows.

The transition from steady to oscillatory convection in a cube was found by Graham and Steen (1991) to occur at  $Ra = 584$  and to involve a traveling wave instability in which seven pairs of thermal blobs circulate around the cube. They also observed a correspondence between the three-dimensional convection and two-dimensional flow in a box of square planform but with aspect ratio  $2^{-1/2}$ .

Further numerical calculations for convection in a cube were performed by Stamps et al. (1990). For the case of insulated vertical sides, they found simply periodic oscillations with frequency  $f \propto Ra^{3.6}$  appearing for  $Ra$  between 550 and 560 and irregular fluctuations once  $Ra$  exceeded a value between 625 and 640. When heat is transferred through the vertical sides of the cube, three different flow patterns could occur, depending on  $Ra$  and the rate of heat transfer. Sezai (2005) used the Brinkman-Forchheimer model in his treatment of a cube with impermeable adiabatic walls. He carried out computations for  $Ra$  up to 1,000. He observed a total of ten steady-flow patterns, of which five show oscillatory behavior for some Rayleigh-number range.

The general topic of oscillatory convection in a porous medium has been reviewed by Kimura (1998). Analysis of the onset of convection in a sector-shaped box (analogous to that of Beck (1972) for a rectangular box) was reported by Wang (1997). The case of a box with a rigid top or a constant-pressure top and with constant-flux bottom heating was analyzed by Wang (1999b, 2002).

### 6.15.2 Thin Box or Slot

Geological faults can be modeled by boxes that are short in one horizontal dimension but long in the other two dimensions. Convection in such boxes has been studied by Lowell and Shyu (1978), Lowell and Hernandez (1982), Kassoy and Zebib (1978), and Murphy (1979). Lowell and Shyu (1978) were concerned with the effect of a pair of conducting lateral boundaries (the other pair being insulated). Lowell and Hernandez (1982) used finite-difference techniques to investigate finite-amplitude convection. They found that in containers with prescribed wall temperatures, the flow was weakly three-dimensional but with the general appearance of two-dimensional transverse rolls. In containers bounded by impermeable blocks of finite

thermal conductivity, a flow pattern similar to that for containers with prescribed wall temperatures tended to be set up, but asymmetrical initial perturbations tended to give rise to slowly evolving flows. Kassoy and Zebib (1978) studied the development of an isothermal slug flow entering the fault at large depth. An entry solution and the subsequent approach to the fully developed flows were obtained for the case of large Rayleigh number.

Convection in a thin vertical slot has been analyzed by Kassoy and Cotte (1985), Weidman and Kassoy (1986), and Wang et al. (1987). They found that the appearance of slender fingerlike convection cells is characteristic of motion in this configuration, and the streamline pattern is extremely sensitive to the value of  $Ra$ . For the case of large wavenumber and insulated sidewalls, Lewis et al. (1997) present asymptotic analyses for weakly nonlinear and highly nonlinear convection. They found that three separate nonlinear regimes appear as the Rayleigh number increases but convection remains unicellular. On the other hand, for the case of perfectly conducting boundaries and with a linearly decreasing temperature profile imposed at the sidewalls, Rees and Lage (1996) found that for all cell ratios, the onset problem is degenerate in the sense that any combinations of an odd mode and an even mode is destabilized simultaneously at the critical Rayleigh number. This degeneracy persists even into the nonlinear regime. For the case of particular linear distributions of temperature on the vertical walls, Storesletten and Pop (1996) obtained an analytical solution. Some implications for hydrothermal circulation for hydrothermal circulation along mid-ocean ridges or for the thermal regime in crystalline basements and for heat recovery experiments were discussed by Rabinowicz et al. (1999) and Tournier et al. (2000).

### 6.15.3 Additional Effects

The effect of large-scale dependence of fluid density on heat transfer has been numerically investigated by Marpu and Satyamurty (1989). Nilsen and Storesletten (1990) have analyzed two-dimensional convection in horizontal rectangular channels with the lateral walls (as well as the horizontal boundaries) permeable and conducting. They have treated both isotropic and anisotropic media. They showed that  $Ra_c$  depends on the anisotropy-aspect ratios  $\xi$  and  $\eta$  defined by

$$\xi = \frac{K_H}{K_V} \left( \frac{H}{L} \right)^2, \quad \eta = \frac{\alpha_{mH}}{\alpha_{mV}} \left( \frac{H}{L} \right)^2, \quad (6.143)$$

where  $K_H$  and  $K_V$  are the horizontal and vertical permeabilities,  $\alpha_{mH}$  and  $\alpha_{mV}$  are the horizontal and vertical thermal diffusivities, and  $L$  and  $H$  are the horizontal and vertical dimensions of the channel.

For the case  $\xi = \eta$ , which includes the isotropic situation,

$$Ra_c = 4\pi^2(1 + \xi). \quad (6.144)$$

This may be compared with the result  $Ra_c = 4\pi^2$  for insulating walls; as expected, the effect of conductivity of the walls is stabilizing. There are two possible cell patterns, each with symmetrical streamlines. For  $n = 2, 3, 4, \dots$ , they consist of  $n$  and  $n + 1$  cells, respectively, if

$$(n - 1)^2 - 1 < \xi^{-1} \leq n^2 - 1. \quad (6.145)$$

The conclusion of weakly nonlinear stability analysis is that both structures are stable against two-dimensional perturbations. Compositions of this pair of flow patterns are possible, so the flow is not uniquely determined by the boundary conditions.

The situation is similar for the case  $\xi \neq \eta$ , but now there is only a single steady-flow pattern (stable against two-dimensional disturbances) which consists of  $n$  cells if  $\xi < \eta$  and  $n + 1$  cells if  $\xi > \eta$ , where

$$(n - 1)^2 - 1 < (\xi\eta)^{-1/2} < n^2 - 1. \quad (6.146)$$

The problem of convection induced by internal heat generation in a box was given a theoretical and experimental treatment by Beukema and Bruin (1983).

The theory in this section has been based on the assumption that the sidewalls are perfectly insulating. Vadasz et al. (1993) showed that for perfectly conducting sidewalls, convection occurs regardless of the Rayleigh number and regardless of whether the fluid is heated from below, except for a particular sidewall temperature variation. When there is no temperature difference between the sidewalls, and with heating from below, a subcritical flow results mainly near the sidewalls, and this amplifies and extends over the entire domain under supercritical conditions. The authors treated cases with heating from above as well as heating from below.

Weak nonlinear theory was applied by Vadasz and Braester (1992) to the case of imperfectly insulated sidewalls. There is now a smooth transition of the amplitude of convection with increase of  $Ra$  from subcritical values, but a three-branch bifurcation develops at higher  $Ra$  values, with two branches stable. For slightly supercritical  $Ra$ , the amplitude and direction of the convection currents are uniquely determined by the heat leakage through the lateral walls. In this situation there is weak convection at relatively low Rayleigh numbers, and this grows sharply in strength near the classical critical Rayleigh number; a second stable flow exists within the weakly nonlinear regime if the Rayleigh number is sufficiently large.

Convection in a square box with a wavy bottom was studied numerically by Murthy et al. (1997). They found flow separation and attachment on the walls of the box for  $Ra$  around 50 and above, with the manifestation of cycles of unicellular and bicellular clockwise and counterclockwise flows. The counterflow on the wavy wall hinders heat transfer into the system by an amount that increases with wave amplitude or wavenumber. The case of a box with a heated bottom with sinusoidal variation of temperature was studied by Khandelwal et al. (2012).

The effect of harmonic oscillation of the gravitational acceleration was studied numerically by Khallouf et al. (1996). Numerical studies involving a transient situation or an oscillating boundary were reported by Jue (2001a, b).

The onset of convection in a box or cylinder with sidewalls that are partly conducting and partly penetrative was studied by Nygård and Tyvand (2010, 2011a). Barletta and Storesletten (2012) carried out a three-dimensional study of a box with partially conducting lateral walls.

## 6.16 Cylinder or Annulus

### 6.16.1 Vertical Cylinder or Annulus

Following Wooding (1959), for the case of a thin circular cylinder, one can assume that  $\theta$  and  $w$  are independent of  $z$ , and then (6.17) gives

$$\frac{dP}{dz} = Ra \hat{T} - \hat{w} = C, \quad (6.147)$$

where  $C$  is a “separation of variables” constant that can be taken as zero. For marginal stability, (6.18) reduces to

$$\nabla_H^2 \hat{T} = -\hat{w}. \quad (6.148)$$

Eliminating  $\hat{w}$  from (6.145) to (6.146) gives

$$\nabla_H^2 \hat{T} + Ra \hat{T} = 0. \quad (6.149)$$

The solutions of this equation, which are periodic functions of  $\varphi$  and are finite at  $\hat{r} = 0$ , where  $(\hat{r}, \varphi)$  are polar coordinates, have the form

$$\hat{T}_n = C_n J_n(\lambda \hat{r}) \cos n\varphi \quad (n = 0, 1, 2, \dots), \quad (6.150)$$

where  $\lambda = Ra^{1/2}$  and  $J_n$  is the Bessel function of order  $n$ . The eigenvalues for this problem are determined by the temperature boundary conditions. For example, if we have an insulated surface at  $\hat{r} = r_0/H$ , so that  $\partial \hat{T} / \partial \hat{r} = 0$ , then

$$J'_n \left( \lambda \frac{r_0}{H} \right) = 0. \quad (6.151)$$

The smallest possible value of  $\lambda$  is attained when  $n = 1$  (corresponding to flow antisymmetric with respect to a diameter), and the critical Rayleigh number is

$$Ra_c = \lambda_1^2 \frac{H^2}{r_0^2} = 3.390 \frac{H^2}{r_0^2}. \quad (6.152)$$

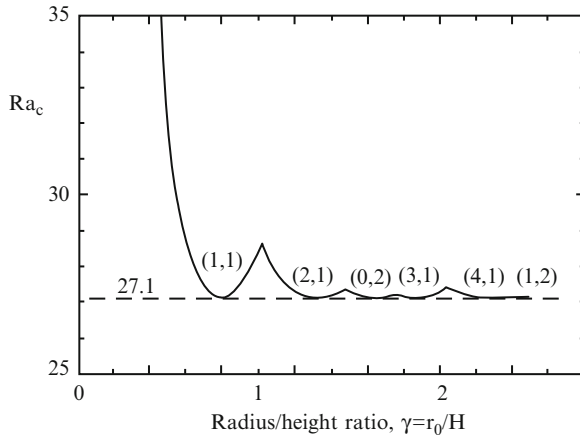


**Fig. 6.24** Critical Rayleigh number and the preferred convective modes  $(m, p)$  at the onset of convection in a vertical cylinder. The temperature perturbation is of the form  $\theta = \Theta(z)J_m(Z_{mp}r/\gamma) \cos m\varphi$ , where  $Z_{mp}$  is the  $p$ th zero of  $J_m(x)$ . The *dashed line* indicates the value for an infinite horizontal layer with isothermal boundaries, the lower impermeable and the upper permeable (Bau and Torrance 1982b)

This can be written as  $\tilde{Ra}_c = 3.390$ , where

$$\tilde{Ra} = Ra \frac{r_0^2}{H^2} = \frac{g \beta K r_0^2 \Delta T}{H \nu \alpha_m}. \quad (6.153)$$

Further analysis of convection in a vertical cylinder was reported by Zebib (1978) and Bories and Deltour (1980) (who considered the effects of finite conduction in the surrounding medium) for the case of impermeable boundaries and by Bau and Torrance (1982b) for the case of a permeable upper boundary. The variation of  $Ra_c$  vs. aspect (radius to height) ratio  $\gamma$  for the latter case is shown in Fig. 6.24. The preferred mode is asymmetric except for a limited range of  $\gamma$ . Experiments by Bau and Torrance (1982b) for situations with  $\gamma$  in the range 0.2–0.3 confirmed the prediction that the mode of onset of convection was asymmetric. Their heat transfer data for moderately supercritical convection was in accord with their calculations. When  $Ra$  reached a value  $5.5Ra_c$ , there was a transition to oscillatory convection (like that occurring in a horizontal layer).

Convection in the annulus between vertical coaxial cylinders was analyzed by Bau and Torrance (1981). Again the preferred mode of convection is asymmetric. Experiments with this geometry, with constant heat flux on the inner cylinder and constant temperature on the outer and with a permeable, constant-pressure upper surface, were reported by Reda (1983). The measured distribution of temperature was in accord with numerical predictions. These results are pertinent to the design of nuclear waste repositories.

A numerical and experimental study of two-dimensional convection was reported by Charrier-Mojtabi et al. (1991). The experiments, in which the Christiansen effect was employed for visualization, were in good agreement with the numerical results.

The onset of convection in a cylindrical enclosure with constant-flux bottom heating and either an impermeable or permeable top was analyzed by Wang (1998b, 1999c). Convection in a cylindrical enclosure filled by a heat-generating porous medium was studied numerically by Das et al. (2003). Tyvand (2002) noted that the lateral boundary conditions employed in the papers by Zebib (1978), Bau and Torrance (1982b), and Wang (1998b) are identical and that the transformation  $(Ra/4\pi^2, \pi x, \pi y) \rightarrow (Ra/27.21, 2.33x, 2.33y)$  allows one to deduce the results of the second and third papers from the results of the first. The same transformation allows the results of Tewari and Torrance (1981) to be deduced from those of Beck (1972). Tyvand (2002) also studied convection in a vertical hexagonal cylinder with impermeable boundaries, a conducting top and bottom, and insulating lateral walls.

Bringedal et al. (2011) combined linear stability analysis with high-order numerical simulations using pseudospectral methods to examine convection cells and their preferred planform in a vertical annulus. They found that variations in the Rayleigh number affect the convection modes and their stability in a complex manner. They identified some stable secondary modes and some overlapping stability regimes.

Barletta and Storesletten (2011a) studied the onset of convective rolls in a circular porous duct with external heat transfer to a thermally stratified environment. Experimental work with water-saturated metal foam was conducted by Kathare et al. (2008). Kim et al. (2008b) considered the onset of convection in a liquid-saturated cylindrical porous layer supported by a gas layer. Kuznetsov and Nield (2012c) studied the onset of double-diffusive convection in a vertical cylinder occupied by a heterogeneous porous medium with vertical throughflow.

### 6.16.2 Horizontal Cylinder or Annulus

Lyubimov (1975) considered Rayleigh-Bénard convection in a circular horizontal porous cylinder, but he did continue the analysis to identify preferred modes and the critical Rayleigh number. Storesletten and Tveitereid (1987) analyzed two-dimensional convective motion in a circular horizontal cylinder. They calculated  $Ra_c$  to be 46.265, where  $Ra$  is now defined as

$$Ra = \frac{g \beta \Delta T K r_0}{\nu \alpha_m}, \quad (6.154)$$

where  $r_0$  is the radius of the cylinder and  $\Delta T$  is the temperature difference across the vertical diameter. At moderately supercritical Rayleigh numbers, they found two steady-flow patterns, consisting of two or three cells, respectively, both structures being stable. The first mode involves two counterrotating cells with strictly vertical

motions (upward or downward) in the middle. The second mode consists of three cells: one dominating central roll occupying most of the areas, flanked by two smaller rolls. In their numerical study, Robillard et al. (1993) obtained 46.6 as the critical value. The situation for a cylinder of length  $L$  with insulated ends was studied by Storesletten and Tveitereid (1991). For  $L > 0.86$ , a unique three-dimensional flow appears at the onset of convection, while for  $L < 0.86$ , the flow is two-dimensional with two or three rolls, each flow being stable, but with thermal forcing, the flow is uniquely determined. The effect of weak rotation was studied by Zhao et al. (1996).

A bifurcation study of two-dimensional convection was made by Bratsun and Lyubimov (1995). The degeneracy (infinite number of solutions) is removed when fluid seeps through the boundaries either vertically or horizontally. At large  $Ra$ , a quasiperiodic solution branches from a limit cycle for both types of seepage. The reduction of heat transfer in horizontal eccentric annuli, involving a transition from tetracellular to bicellular flow patterns, was studied numerically by Barbosa Mota and Saatdjian (1997). A numerical treatment of a horizontal annulus filled with an anisotropic porous medium was reported by Aboubi et al. (1998). Convection in a thin horizontal shell of finite length with impermeable walls was examined by Tyvand (2002), who also considered a similar problem with a thin spherical shell.

## 6.17 Internal Heating in Other Geometries

In Sect. 6.11.2 we discussed internal heating in an infinite horizontal layer. We now discuss internal heating in other geometrical configurations.

Blythe et al. (1985a) analyzed two-dimensional convection driven by uniformly distributed heat sources within a rectangular cavity whose vertical sidewalls are isothermal and whose horizontal boundaries are adiabatic. In the limit of large internal Rayleigh number  $Ra_I$  (defined in (6.114)), they found that boundary layers of thickness of order  $Ra_I^{-1/3}$  formed on the sidewalls, the internal core being stratified in the vertical direction. Further work on this geometry is the numerical studies by Haajizadeh et al. (1984) and Prasad (1987). The latter obtained heat transfer results for  $Ra_I$  up to  $10^4$  and for aspect ratios  $A$  in the range 0.5–20. These authors reported unicellular flow for the entire range of  $Ra_I$  and  $A$  and stratification in the upper layers of the cavity. Prasad (1987) also examined the effect of changing the boundary conditions on the horizontal walls from adiabatic to isothermally cooled.

Banu et al. (1998) noted that in the situation described by Blythe et al. (1985a), the upper part of the cavity is unstably stratified, and so the flow described by Blythe et al. is unlikely to be realized in practice. The numerical study of Banu et al. (1998) showed that incipient unsteady flow occurs at values of  $Ra_I$  that are highly dependent on the aspect ratio of the cavity. The convective instabilities of the time-dependent motion are confined to the top of the cavity, and for tall thin cavities the critical  $Ra_I$  is proportional to the inverse third power of the aspect ratio. For a shallow cavity the flow may become chaotic and it loses left/right symmetry. In this situation downward-pointing plumes are generated whenever there is sufficient room near the top of the cavity and subsequently travel toward the nearer sidewall.

Vasseur et al. (1984) discussed convection in the annular space between horizontal concentric cylinders. Their calculations showed that at small  $Ra_I$  values a more or less parabolic temperature profile is established across the annulus, resulting in two counterrotating vortices (both with axes centered on the horizontal midplane) in each half cavity. Under the effect of weak and moderate convection, the maximum temperature within the porous medium can be considerably higher than that induced by pure conduction. At large  $Ra_I$  values, the flow structure consists of a thermally stratified core and two boundary layers, with a thickness and heat transfer rate of the order of  $Ra_I^{-1/3}$  and  $Ra_I^{1/3}$ , respectively. Now, the inner radius replaces  $H$  in the definition of  $Ra_I$ .

Numerical studies of two-dimensional convection in a horizontal annulus with flow across a permeable outer or inner boundary were reported by Burns and Stewart (1992) and Stewart and Burns (1992), while the case where both boundaries are permeable was treated by Stewart et al. (1994).

Convection in a vertical cylinder of finite height was studied by Stewart and Dona (1988). They took the bottom to be adiabatic and the remaining boundaries isothermal. Their numerical results for height ( $H$ ) to radius ( $R$ ) ratio 2 showed compression of isotherms near the top and side of the cylinder as  $Ra_I$  increased. They defined  $Ra_I$  with  $R^2H$  replacing  $H^3$  in (6.115). They found that single-cell flow occurred until  $Ra_I$  was about 7,000. At higher  $Ra_I$  a smaller reverse flow region formed near the top and axis, and the transition was accompanied by the position of maximum temperature moving off the axis. Dona and Stewart (1989) treated the same problem but including the effects of quadratic drag and the variation of density and viscosity with temperature for  $Ra_I$  values up to 7,000. For such values the property variations have a significant effect, but the effect of quadratic drag is small.

Prasad and Chui (1989) made a numerical study of convection in a vertical cylinder with the vertical wall isothermal and the horizontal boundaries either adiabatic or isothermally cooled. When the horizontal walls are insulated, the flow in the cavity is unicellular, and the temperature field in the upper region is highly stratified. However, if the top boundary is cooled, there may exist a multicellular flow and an unstable thermal stratification in the upper region of the cylinder. Under the influence of weak convection, the maximum temperature in the cavity can be considerably higher than that induced by pure conduction (as in the horizontal annulus problem mentioned above). The local heat flux on the wall is generally a strong function of  $Ra_I$ , the aspect ratio, and the wall boundary conditions.

The effect of water density maximum on heat transfer in a vertical cylinder, with adiabatic bottom and isothermal sides and top, was modeled numerically by Weiss et al. (1991). A linear stability analysis of convection in a vertical annulus was presented by Saravanan and Kandaswamy (2003a).

Weinitschke et al. (1990) and Islam and Nandakumar (1990) have conducted studies of two-dimensional bifurcation phenomena in rectangular ducts with uniform heat generation. Multiple steady states appear as the internal Rayleigh number is increased up to several thousand. In the second paper the evaluation with time of these multiple states is examined. The solution structure is complicated. The effect of tilt was treated by Ryland and Nandakumar (1992). A bifurcation study

of convection generated by an exothermic chemical reaction was made by Islam (1993). Heat and mass transfer in a semi-infinite cylindrical enclosure, with permeable or impermeable boundaries, were treated by Van Dyne and Stewart (1994). A numerical study using the Brinkman model for eccentric or oval enclosures was reported by Das et al. (2003).

A problem related to astrophysics was studied by Zhang et al. (2005a). This problem is concerned with pore water convection within carbonaceous chondrite parent bodies. These are modeled as spherical bodies within which the gravitational field is radial and varies with radial distance and the viscosity is allowed to vary with temperature. The linear stability analysis leads to the determining of a critical Rayleigh number as a function of the central temperature. Zhang et al. (2005) found that the nonlinearity from the viscosity-temperature dependence removed a degeneracy in the azimuthal variation of the mode of convection.

The effect of asymmetry on steady convection in a vertical torus was studied by Adrian and Nicoleta (2005). Kandaswamy et al. (2008b) investigated transient convection in icy water with internal heat generation. Muthamilselvan et al. (2010) studied convection in a lid-driven heat-generating cavity with various boundary conditions. Grosan et al. (2009) examined magnetic field and internal heat generation effects in a rectangular cavity.

## 6.18 Localized Heating

Numerical calculations are called for in more complex situations, as when only part of the bottom boundary of a container is heated. The prototypical problem is convection in a rectangular cavity of height  $H$  and width  $2L$ , of which the central section (of the bottom) of width  $2D$  is heated. One can define the aspect ratio of the half cavity  $A$  and the heated length fraction  $s$  by

$$A = \frac{L}{H}, \quad s = \frac{D}{L}. \quad (6.155)$$

The boundaries are assumed to be impermeable. Various thermal boundary conditions can be considered in turn (see Table 6.5). If, for example, one considers the boundary conditions of Prasad and Kulacki (1986), and the nondimensional variables are taken to be

$$X = \frac{x}{H}, \quad Y = \frac{y}{H}, \quad \theta = \frac{T - T_c}{T_h - T_c}, \quad \Psi = \frac{\Psi}{\alpha_m}, \quad \tau = \frac{\alpha_m t}{\sigma H^2} \quad (6.156)$$

then one has to solve

$$\frac{1}{A^2} \frac{\partial^2 \Psi}{\partial X^2} + \frac{\partial^2 \Psi}{\partial Y^2} = Ra \frac{\partial \theta}{\partial X}, \quad (6.157)$$

**Table 6.5** Thermal boundary conditions for localized heating in a rectangular cavity

	Central bottom	Outer bottom	Sides	Top
Elder (1967a, b)	$T = T_h$	$T = T_c$	$T = T_c$	$T = T_c$
Horne and O'Sullivan (1974a, 1978b)	$T = T_h$	$T = T_c$	$\frac{\partial T}{\partial n} = 0$	$T = T_c$
Prasad and Kulacki (1986, 1987) and Robillard et al. (1988)	$T = T_h$	$\frac{\partial T}{\partial n} = 0$	$\frac{\partial T}{\partial n} = 0$	$T = T_c$
Rajen and Kulacki (1987)	$\frac{\partial T}{\partial n} = -\frac{q''}{k_m}$	$\frac{\partial T}{\partial n} = 0$	$\frac{\partial T}{\partial n} = 0$	$T = T_c$
El-Khatib and Prasad (1987)	$T = T_h$	$T = T_c$	$T = T_c + \frac{y}{H}(T_t - T_c)$	$T = T_t$

$$\frac{\partial \theta}{\partial \tau} + \frac{\partial \Psi}{\partial X} \frac{\partial \theta}{\partial Y} - \frac{\partial \Psi}{\partial Y} \frac{\partial \theta}{\partial X} = \frac{\partial^2 \theta}{\partial X^2} + A^2 \frac{\partial^2 \theta}{\partial Y^2} \quad (6.158)$$

subject to appropriate initial conditions (for the nonsteady problem) and the boundary conditions:

$$\begin{aligned} \theta &= 1 && \text{for } 0 \leq |X| < s, Y = 0, \\ \frac{\partial \theta}{\partial Y} &= 0 && \text{for } s < |X| \leq 1, Y = 0, \\ \theta &= 0 && \text{for } Y = 1, \\ \frac{\partial \theta}{\partial X} &= 0 && \text{for } X = -1 \text{ or } 1. \end{aligned} \quad (6.159)$$

This system is readily solved using finite differences. Because of the symmetry of the problem, computations need be made for only the right half of the domain.

The pioneering numerical and experimental study by Elder (1967a) for steady convection demonstrated that more than one cell exists in the half cavity for  $s = 1.5$  and the Nusselt number is a function of  $s$  and the number of cells. Elder (1967b) also studied the transient problem. He noted (see Fig. 6.25) an alternation between periods of slow gradual adjustment and periods of rapid change of flow patterns.

The numerical results of Horne and O'Sullivan (1974a) for time-dependent boundary conditions indicate that when the lower boundary is partially heated, the system is self-restricting and it settles down into a steady multicellular flow or a periodic oscillatory flow, depending on  $Ra$  and the amount of boundary that is heated. At high  $Ra$ , oscillatory flow is the norm. Typical flow patterns are shown in Fig. 6.26. Approximately mushroom-shaped isotherms predominate. The effects of temperature-dependent viscosity and thermal expansion coefficient on the temperature and flow fields were studied by Horne and O'Sullivan (1978b). They found that in some cases the acceleration of the flow in certain areas, due to a decrease in viscosity, causes localized thermal instabilities.

Further numerical calculations were reported by Prasad and Kulacki (1986, 1987). For the case  $D/H > 1$ , they noted the appearance at small  $Ra$  of a circulation near the heated segment and the development of further cells as  $Ra$  increases. Further increase of  $Ra$  does not increase the number of cells, but it strengthens existing cells and leads to the formation of boundary layers.

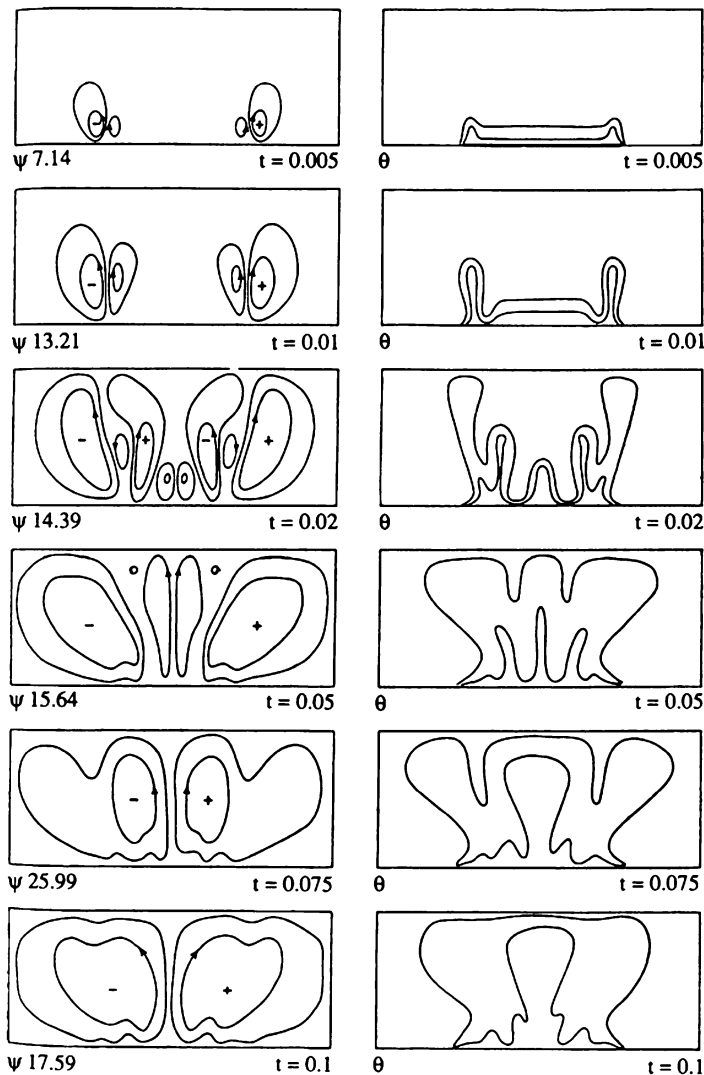
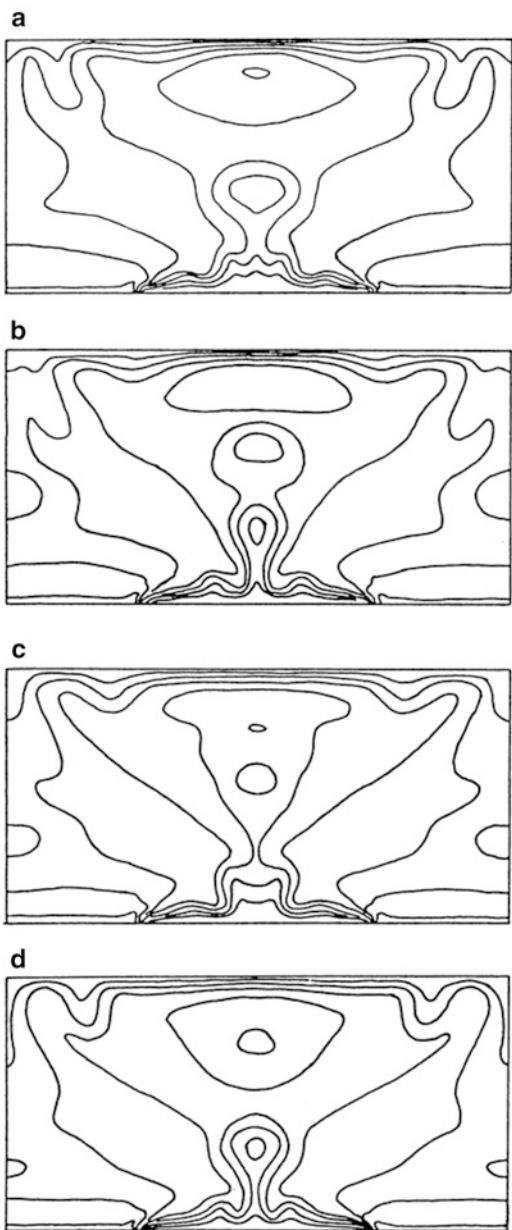


**Fig. 6.25** Streamlines and isotherms for a localized heater problem at various times;  $Ra = 400$ ,  $A = 2$ ,  $s = 0.5$  (Elder 1967b, with permission from Cambridge University Press)

The outermost cell extends to the sidewall. Within the inner cells, plumes are formed at large  $Ra$ , the isotherms taking the characteristic mushroom shape (as with uniform heating). Because Prasad and Kulacki considered only the steady problem, they did not observe any oscillatory behavior.

Prasad and Kulacki (1986, 1987) also made calculations of heat transfer rates. As expected, the local Nusselt number has peaks where hot fluid rises. The peak value increases with the size of heat source until a new cell is formed. The overall

**Fig. 6.26** Plots of computed isotherms during a single oscillation for a localized heating problem;  $Ra = 750$ ,  $A = 1$ ,  $s = 0.5$  (Horne and O'Sullivan 1974a, with permission from Cambridge University Press)



Nusselt number based on the heated segment ( $Nu_s$ ) decreases with  $s$  (for fixed  $Ra > 1,000$ ) until  $s = 0.4$  and then remains steady, the steadiness indicating that the heat transfer rate is then proportional to the area of the heat source. The overall Nusselt number based on the entire cavity width ( $Nu_L$ ) increases monotonically with  $s$ . Both overall Nusselt numbers increase with  $Ra$ , the rate of increase being

approximately uniform (on a log–log scale) when  $Ra > 100$ , the boundary layer regime. In this regime, the slope of the  $\ln(Nu_L)$  vs.  $\ln(Ra)$  curve increases gradually with  $s$ . When  $s$  is close to 1, the overall Nusselt numbers increase rapidly with  $Ra$  in the vicinity of  $Ra = 40$ , as expected.

El-Khatib and Prasad (1987) extended the calculations to include the effects of linear thermal stratification, expressed by the parameter

$$S = \frac{T_t - T_c}{T_h - T_c}. \quad (6.160)$$

See the last line of Table 6.3 for definitions of  $T_t$ ,  $T_c$ , and  $T_h$ . El-Khatib and Prasad did calculations for  $A = 1$ ,  $s = 0.5$ ,  $0 = S = 10$ , and  $Ra$  up to 1,000. They found that an increase in  $S$  for a fixed  $Ra$  reduces the convective velocities and hence the energy lost by the heat source. In fact, for sufficiently large  $S$ , at least part of the heated segment may gain energy. A similar situation pertains to the top surface. For  $S > 1$  the energy gained by the upper surface is almost independent of  $Ra$ .

Rajen and Kulacki (1987) reported experimental and numerical results for  $A = 16$  or 4.8, and  $s = 1$ , 1/2, or 1/12, with the boundary conditions given in Table 6.3. Their observations of Nusselt number values were in very good agreement with the predicted values.

Robillard et al. (1988) performed calculations for the case when the heat source is not symmetrically positioned. Merkin and Zhang (1990b) treated numerically a similar situation. A variant of the Elder short-heater problem with a spatially sinusoidal distribution along the hot plate was studied numerically by Saeid (2005). A fluid-superposed porous layer locally heated from below was studied by Bagchi and Kulacki (2011). The effect of variable viscosity on convection in a horizontal porous channel with a partly heated or cooled bottom wall was treated by Pop et al. (2008). Partly heated surfaces were also treated by Pakdee and Rattanadecho (2006, 2009). Linear stability analysis was applied by Hong et al. (2008) to a layer subject to time-dependent heating. The effect of a nonlinear concentration profile, and initial and boundary conditions, on the stability of a horizontal layer was studied by Hassanzadeh et al. (2006).

Impulsively heated layers were examined by Kohl et al. (2008). Nield and Kuznetsov (2010d) studied a transient temperature profile in a heterogeneous medium. The nonmodal growth of perturbations was studied by Rapaka et al. (2008), while Rapaka et al. (2009) investigated the onset of convection over a transient base state in anisotropic and layered media.

## 6.19 Superposed Fluid and Porous Layers, Partly Porous Configurations

Convection in a system consisting of a horizontal layer of porous medium and a superposed clear fluid layer has been modeled in two alternative ways. In the two-domain approach, the porous medium and clear fluid are considered separately, and

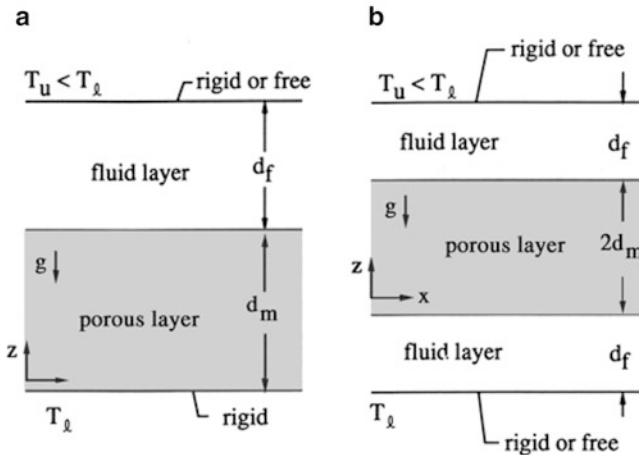


**Fig. 6.27** Composite fluid-layer porous-layer systems

the pair of solutions is coupled using matching conditions at the interface. In the single-domain approach, the fluid is considered as a special case of a porous medium, the latter being modeled using a Brinkman-Forchheimer equation. The second approach is subject to the caveat about use of the Brinkman equation mentioned in Sect. 1.6, but in most situations discussed in this section, the two approaches are expected to yield qualitatively equivalent results for the global temperature and velocity fields. An exception is when the depth of the porous layer is not large in comparison with the particle/pore diameter.

### 6.19.1 Onset of Convection

#### 6.19.1.1 Formulation

We start by considering a porous layer of depth  $d_m$  superposed by clear fluid of depth  $d_f$ , the base of the porous medium being at temperature  $T_1$  and the top of the clear fluid region at temperature  $T_u$  (Fig. 6.27a). We suppose that flow in the porous medium is governed by Darcy's equation and that in the clear fluid by the Navier-Stokes equation. The combined system has a basic steady-state conduction solution given by

$$V = 0, \quad T = T_b \equiv T_u - \beta_f(z - d_m - d_f), \quad P = P_b \quad \text{for the fluid}, \quad (6.161)$$

$$v_m = 0, \quad T_m = T_{bm} \equiv T_1 - \beta_m z, \quad P_m = P_{bm} \quad \text{for the porous layer}. \quad (6.162)$$

Here  $\beta_f$  and  $\beta_m$  are the temperature gradients. Continuity of temperature and heat flux at the interface requires that

$$T_u + \beta_f d_f = T_l - \beta_m d_m = T_i \quad \text{and} \quad k_f \beta_f = k_m \beta_m, \quad (6.163\text{a, b})$$

where  $T_i$  is the interface temperature, and hence

$$\beta_f = \frac{k_m(T_l - T_u)}{k_m d_f + k_f d_m}, \quad \beta_m = \frac{k_f(T_l - T_u)}{k_m d_f + k_f d_m}. \quad (6.164\text{a, b})$$

In terms of perturbations from the conduction state,  $T' = T - T_b$ ,  $P' = P - P_b$ , etc., the linearized perturbation equations in time-independent form are

$$\nabla \cdot \mathbf{V}' = 0, \quad (6.165\text{a})$$

$$\frac{1}{\rho_0} \nabla P' = v \nabla^2 \mathbf{V}' + g \beta T' \mathbf{k}, \quad (6.165\text{b})$$

$$\beta_f w' + \alpha_f \nabla^2 T' = 0, \quad (6.165\text{c})$$

$$\nabla \cdot \mathbf{v}'_m = 0, \quad (6.166\text{a})$$

$$\frac{1}{\rho_0} \nabla P'_m = -\frac{v}{K} \mathbf{v}'_m + g \beta T'_m \mathbf{k}, \quad (6.166\text{b})$$

$$\beta_m w'_m + \alpha_m \nabla^2 T'_m = 0. \quad (6.166\text{c})$$

In the fluid layer, appropriate nondimensional variables are

$$\hat{x} = \frac{(x - d_m k)}{d_f}, \quad \hat{V} = \frac{d_f \mathbf{V}'}{\alpha_f}, \quad \hat{P} = \frac{d_f^2 P'}{\mu \alpha_f}, \quad \hat{T} = \frac{T'}{\beta_f d_f}. \quad (6.167)$$

Substituting (6.163) and dropping the carets, we have for the fluid layer

$$\nabla \cdot \mathbf{V} = 0, \quad (6.168\text{a})$$

$$\nabla P = \nabla^2 \mathbf{V} + Ra_f T \mathbf{k}, \quad (6.168\text{b})$$

$$w + \nabla^2 T = 0, \quad (6.168\text{c})$$

where

$$Ra_f = \frac{g \beta \beta_f d_f^4}{v \alpha_f}. \quad (6.169)$$

Eliminating  $P$ , we reduce the equations for the fluid layer to

$$\nabla^4 w + Ra \nabla_H^2 T = 0, \quad (6.170a)$$

$$w + \nabla^2 T = 0. \quad (6.170b)$$

Here  $\nabla_H^2$  denotes the horizontal Laplacian as in (6.20). Similarly, for the porous medium, we put

$$\hat{x}_m = \frac{x}{d_m}, \quad \hat{v}_m = \frac{d_m v'}{\alpha_m}, \quad \hat{P}_m = \frac{K P'_m}{\mu \alpha_m}, \quad \hat{T}_m = \frac{T'_m}{\beta_m d_m}. \quad (6.171)$$

Substituting (6.162), dropping the carets, and eliminating  $P_m$ , we have for the porous medium

$$\nabla_m^2 w_m - Ra_m \nabla_{Hm}^2 T_m = 0, \quad (6.172a)$$

$$w_m + \nabla_m^2 T_m = 0, \quad (6.172b)$$

where

$$Ra_m = \frac{g \beta \beta_m K d_m^2}{\nu \alpha_m}. \quad (6.173)$$

We now separate the variables by letting

$$\begin{Bmatrix} w \\ T \end{Bmatrix} = \begin{Bmatrix} W(z) \\ \theta(z) \end{Bmatrix} f(x, y), \quad \begin{Bmatrix} w_m \\ T_m \end{Bmatrix} = \begin{Bmatrix} w_m(z_m) \\ \theta_m(z_m) \end{Bmatrix} f_m(x_m, y_m), \quad (6.174)$$

where

$$\nabla_H^2 f + \alpha^2 f = 0, \quad \nabla_{Hm}^2 f_m + \alpha_m^2 f_m = 0. \quad (6.175)$$

Since the dimensional horizontal wavenumber must be the same for the fluid layer and the porous medium if matching is to be achieved, the nondimensional horizontal wavenumbers  $\alpha$  and  $\alpha_m$  are related by  $\alpha/d_f = \alpha_m/d_m$ , and so

$$\alpha_m = \hat{d} \alpha, \quad \text{where } \hat{d} = d_m/d_f. \quad (6.176)$$

The reader should not be confused by the use (in this section only) of the symbol  $\alpha_m$  for both thermal diffusivity and horizontal wavenumber. He or she should note that Chen and Chen (1988c, 1989) have used  $\hat{d}$  to denote  $d_f/d_m$ . Equations (6.164) and (6.166) yield

$$(D^2 - \alpha^2)^2 W - Ra_f \alpha^2 \theta = 0, \quad (6.177a)$$

$$(D^2 - \alpha_m^2)\theta + W = 0 \quad (6.177b)$$

and

$$(D_m^2 - \alpha_m^2)W_m + Ra_m \alpha_m^2 \theta_m = 0, \quad (6.178a)$$

$$(D_m^2 - \alpha_m^2)\theta_m + W_m = 0, \quad (6.178b)$$

where  $D = d/dz$  and  $D_m = d/dz_m$ . We match the solutions of (6.177) and (6.178) at the fluid/porous-medium interface by invoking the continuity of temperature, heat flux, normal velocity (note that it is the Darcy velocity and not the intrinsic velocity which is involved), and normal stress. The Beavers-Joseph condition supplies the fifth matching condition. Thus we have at  $z_m = 1$  (or  $z = 0$ ),

$$T = \varepsilon_T T_m, \quad \frac{\partial T}{\partial z} = \frac{\partial T_m}{\partial z_m}, \quad \varepsilon_T w = w_m, \quad (6.179a, b, c)$$

$$\varepsilon_T \hat{d}^3 Da \left( 3 \nabla_H^2 \frac{\partial w}{\partial z} + \frac{\partial^3 w}{\partial z^3} \right) = - \frac{\partial w_m}{\partial z_m}, \quad (6.179d)$$

$$\varepsilon_T \hat{d} \left( \frac{\partial w}{\partial z} - \Delta \frac{\partial^2 w}{\partial z^2} \right) = - \frac{\partial w_m}{\partial z_m}, \quad (6.179e)$$

where  $\varepsilon_T = \beta_m d_m / \beta_f d_f = k_f d_m / k_m d_f = \hat{d}/\hat{k}$ ,

$$Da = \frac{K}{d_m^2}, \quad \Delta = \hat{d} \frac{Da^{1/2}}{\alpha_{BJ}}, \quad \hat{d} = \frac{d_m}{d_f}, \quad \hat{k} = \frac{k_m}{k_f}. \quad (6.180)$$

Equation (6.179d) is derived from the condition

$$-P + 2\mu \frac{\partial w}{\partial z} = -P_m \quad (6.181)$$

and (6.179e) is derived from the Beavers-Joseph condition

$$\frac{\partial u}{\partial z} = \frac{\alpha_{BJ}}{K^{1/2}} (u - u_m). \quad (6.182)$$

The remaining boundary conditions come from the external conditions. For example, if the fluid-layer/porous-medium system is bounded above and below by rigid conducting boundaries, then one has

$$w = \frac{\partial w}{\partial z} = T = 0 \text{ at } z = 1, \\ w_m = T_m = 0 \text{ at } z_m = 0. \quad (6.183a, b, c)$$

The tenth-order systems (6.176) and (6.178) now can be solved subject to the ten constraints (6.179) and (6.180). Note that the fluid Rayleigh number  $Ra_f$  and the Rayleigh-Darcy number  $Ra_m$  are related by

$$Ra_m = \hat{d}\varepsilon_T^2 Da Ra_f = \hat{d}^4 \hat{k}^{-2} Da Ra_f. \quad (6.184)$$

Hence the critical Rayleigh-Darcy number  $Ra_m$  can be found as a function of four parameters,  $\hat{d}$ ,  $\hat{k}$ ,  $Da$ , and  $\alpha_{BJ}$ , or, alternatively,  $\hat{d}$ ,  $\varepsilon_T$ ,  $Da$ , and  $\Delta$ .

### 6.19.1.2 Results

As in Sect. 6.2, the case of constant heat flux boundaries yields a closed form for the stability criterion. The critical wavenumber is zero, and the stability criterion for the case of a free top and an impermeable bottom is given by (Nield 1977)

$$\begin{aligned} & \varepsilon_T \{ 3 + 24\Delta + Da \hat{d}^2 [84 + 384\hat{d} + 300\varepsilon_T \hat{d} + 720\Delta d(1 + \varepsilon_T)] \} Ra_{fc} \\ & + \hat{d}^2 [320 + 960\Delta + Da \hat{d}^2 (960 + 240\hat{d}) \\ & + \varepsilon_T^{-1} (300 + 720\Delta + 720Da \hat{d}^2)] Ra_{mc} \\ & = [960 + 2,880\Delta + 2,880Da \hat{d}^2 (1 + \hat{d})] (\varepsilon_T + \hat{d}^2). \end{aligned} \quad (6.185)$$

If we let  $\hat{d} \rightarrow \infty$  with  $\varepsilon_T$ ,  $Da$ , and  $\Delta$  finite, (6.185) gives  $Ra_{mc} \rightarrow 12$ , the expected value for a porous medium between two impermeable boundaries.

A similar analysis has been performed for a system consisting of a porous-medium layer of thickness  $2d_m$  sandwiched between two fluid layers, each of thickness  $d_f$  (Fig. 6.24b). The following stability criteria have been obtained.

Rigid top and rigid bottom (Nield 1983):

$$\begin{aligned} & \varepsilon_T [8 + 18\Delta + (15 + 45\Delta)\varepsilon_T] Ra_{fc} + \left\{ 120(1 + \Delta)\hat{d}^2 + 180\hat{d} + 60\frac{\hat{d}}{\varepsilon_T} \right. \\ & \left. + \frac{1}{Da} \left[ \left( \frac{30 + 120\Delta}{\hat{d}} \right) + \left( \frac{15 + 45\Delta}{\hat{d}\varepsilon_T} \right) \right] \right\} Ra_{mc} = 360(1 + \Delta)(\varepsilon_T + \hat{d}^2). \end{aligned} \quad (6.186)$$

Free top and free bottom (Pillatsis et al. 1987):

$$\begin{aligned} & \varepsilon_T [192 + 360\Delta(1 + 2\hat{d}) + 720Da \hat{d}^3 + 300\hat{d}] Ra_{fc} \\ & + \hat{d}^2 \left\{ 480 + \left( \frac{60}{Da \hat{d}^4} \right) [5 + 8\hat{d} + 12\Delta(1 + 2\hat{d}) + 24\hat{d}^3 Da] \right\} Ra_{mc} \\ & = 1,440(\varepsilon_T + \hat{d}^2). \end{aligned} \quad (6.187)$$

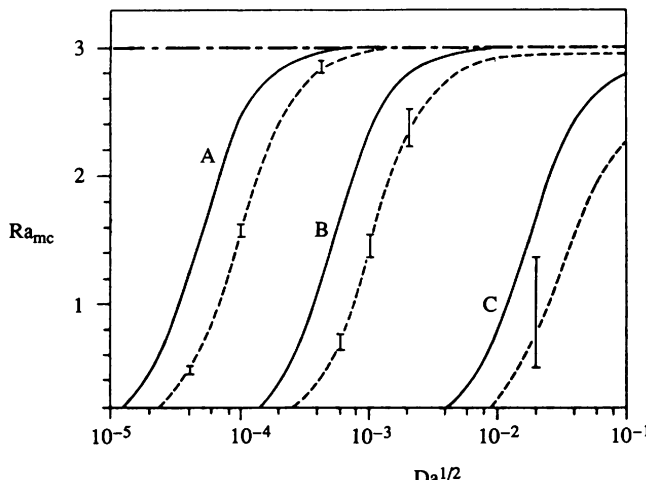


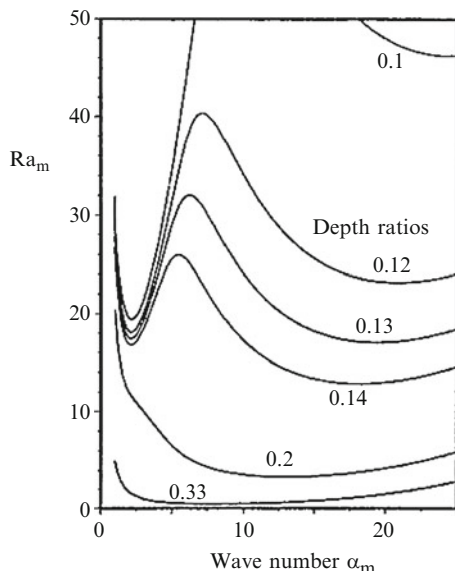
**Fig. 6.28** Critical Rayleigh number for a porous layer sandwiched between two fluid layers (Fig. 6.24b) for the constant-flux case. (a)  $\hat{d} = d_m/d_f = 500$ , (b)  $\hat{d} = 100$ , (c)  $\hat{d} = 10$ ;  $k_f/k_m = 1$  and  $= 0.05$  for all curves; — rigid boundaries, - - - free boundaries, and  $- \cdot - Ra_{mc} = 3$  corresponding to the case of a porous layer alone. The vertical bars denote the range of  $Ra_{mc}$  when the conductivity ratio  $k_f/k_m$  is varied from 10 to 0.1 (Pillatsis et al. 1987)

As  $\hat{d} \rightarrow 0$  (with  $\Delta \rightarrow 0$ ), (6.186) and (6.187) yield  $Ra_{fc} = 45$  and 7.5, the critical Rayleigh numbers for a fluid layer of depth  $2d_f$  between rigid-rigid and free-free boundaries, respectively. As  $\hat{d} \rightarrow \infty$  they yield  $Ra_{mc} = 3$ , the critical Rayleigh-Darcy number for a porous layer of depth  $2d_m$  between impermeable boundaries. These results are as expected. Figure 6.28 shows the results of calculations based on (6.186) and (6.187).

For isothermal boundaries, the critical wavenumber is no longer zero, and numerical calculations are needed. Pillatsis et al. (1987) and Taslim and Narusawa (1989) have employed power series in  $z$  to obtain the stability criterion. They treated the fluid/porous-medium, the fluid/porous-medium/fluid, and the porous-medium/fluid/porous-medium situations. The results are in accord with expectations. A rigid boundary at the solid-fluid interface suppresses the onset of convection compared with a free boundary. The presence of a fluid layer increases instability in the porous medium, and  $\alpha_{mc}$  decreases as the effect of the fluid layer becomes more significant, as it does when the fluid layer thickens. The parameter  $\alpha_{BJ}$  has a significant effect only when the Darcy number is large. The effect of the Jones modification to the Beavers-Joseph condition is minimal.

Nield (1994a) has shown that the above theory is consistent with observations of increased heat transfer due to channeling reported by Kazmierczak and Muley (1994). Further calculations by Chen and Chen (1988) show that the marginal stability curves are bimodal for a fluid/porous-medium system with  $d_f/d_m$  small (Fig. 6.29). The critical wavenumber jumps from a small to a large value as  $d_f/d_m$

**Fig. 6.29** Marginal stability curves for a fluid-superposed porous layer heated from below for isothermal rigid boundaries, with the thermal conductivity ratio  $k_f/k_m = 0.7$ ,  $Da = 4 \times 10^{-6}$ , and  $\alpha_{BJ} = 0.1$ , for various values of the depth ratio  $d_f/d_m$  (Chen and Chen 1988)



increases from 0.12 to 0.13. Chen and Chen noted that the change correlated with a switch from porous-layer-dominated convection to fluid-layer-dominated convection. Numerical calculations for supercritical convection by Kim and Choi (1996) are in good agreement with the predictions from linear stability theory.

The experiments of Chen and Chen (1989) generally confirmed the theoretical predictions. They employed a rectangular enclosure with 3-mm glass beads and a glycerin-water solution of varying concentrations to produce a system with  $0 \leq d_f/d_m \leq 1$ . They observed that  $Ra_{mc}$  does decrease significantly as  $d_f/d_m$  increases. They also estimated the size of convective cells from temperature measurements. They found that the cells were three-dimensional and that the critical wavenumber increased eightfold when  $d_f/d_m$  was increased from 0.1 to 0.2.

Somerton and Catton (1982) used the Brinkman equation. Their results are confined to high Darcy numbers,  $K/(d_f + d_m)^2 > 37 \times 10^{-4}$ , and thick fluid layers,  $d_f/d_m = 0.43$ . Vasseur et al. (1989) also employed the Brinkman equation in their study of a shallow cavity with constant heat flux on the external boundaries. An extra isothermal condition at the interface mentioned in their paper was in fact not used in the calculations.

A nonlinear computational study, using a Brinkman-Forchheimer equation, was made by Chen and Chen (1992). The effect of rotation on the onset of convection was analyzed by Jou et al. (1996). The effect of vertical throughflow was treated by Chen (1991). The effect of anisotropy was studied by Chen et al. (1991) and Chen and Hsu (1991) and that of viscosity variation by Chen and Lu (1992b). A fluid layer sandwiched between two porous layers of different permeabilities was analyzed by Balasubramanian and Thangaraj (1998). The case where the bottom boundary is heated by a constant flux was analyzed by Wang (1999a), who found

that the critical Rayleigh number for the porous layer increases with the thickness of the solid layer, a result opposite to that when the heating is at constant temperature. Reacting fluid and porous layers were analyzed by McKay (1998a). The effect of property variation was incorporated by Straughan (2002). A comparison of the one- and two-domain approaches to handling the interface was made by Valencia-Lopez and Ochoa-Tapia (2001). Significant differences between the predicted overall average Nusselt numbers were found when the Rayleigh and Darcy numbers were large enough. The characteristic-based split algorithm was used in the numerical study of interface problems by Massarotti et al. (2001).

### 6.19.2 Flow Patterns and Heat Transfer

Heat transfer rates for a fluid-layer/porous-layer system were calculated by Somerton and Catton (see Catton 1985) using the power integral method. Both streamlines and heat transfer rates were calculated by numerical integration of the time-dependent equations by Poulikakos et al. (1986) and Poulikakos (1987a). Laboratory experiments, in a cylindrical cavity heated from below, have been reported by Catton (1985), Prasad et al. (1989a), and Prasad and Tian (1990). Prasad and his colleagues performed both heat transfer and flow visualization experiments, the latter with transparent acrylic beads and a liquid matched for index of refraction. There is qualitative agreement between calculations and observations. For example, in a cell of aspect ratio and  $d_f/d_m = 1$ , there is a transition from a two-cell pattern to a four-cell pattern with an increase in Rayleigh number or Darcy number. In the two-cell pattern, the flow extends well into the porous layer, while in the four-cell pattern, the flow is concentrated in the fluid layer.

Once convection starts, the Nusselt number  $Nu$  always increases with Rayleigh number for fixed  $\eta$ , where  $\eta$  denotes the fraction of the depth occupied by the porous medium. For small particle size  $\gamma$  and/or small Rayleigh number,  $Nu$  decreases monotonically with  $\eta$ ; otherwise, the dependence of  $Nu$  on  $\eta$  is complex. The complexity is related to the variation in the number of convection cells that occur. In general,  $Nu$  depends on at least six parameters:  $Ra$ ,  $Pr$ ,  $\gamma$ ,  $k_m/k_f$ ,  $\eta$ , and  $A$ .

Further experiments, involving visualization as well as heat transfer studies, were made by Prasad et al. (1991). They found that flow channels through large voids produce highly asymmetric and complicated flow structures. Also,  $Nu$  first decreases from the fluid heat transfer rates with an increase in  $\eta$  and reaches a minimum at  $\eta_{min}$ . Any further increase in porous layer height beyond  $\eta_{min}$  augments the heat transfer rate, and the  $Nu$  curves show peaks. Prasad (1993) observed the effects of varying thermal conductivity and Prandtl number.

Even more complicated is the situation when one has volumetric heating of the porous medium as well as an applied vertical temperature gradient. This situation was studied numerically, using the Brinkman equation, by Somerton and Catton (1982) and Poulikakos (1987a, b); the latter also included the Forchheimer term. Poulikakos studied convection in a rectangular cavity whose bottom was either

isothermal or adiabatic. For the aspect ratio  $H/L = 0.5$ , he noted a transition from two to four cells as  $Ra_l$  and  $Da$  increase. Related experiments were reported by Catton (1985) and others. Further experimental and numerical work was conducted by Schulenberg and Müller (1984). Serkitjjs (1995) conducted experimental (and numerical) work on convection in a layer of polystyrene pellets, of spherical or cylindrical shape, below a layer of air. He found that the occurrence of natural convection in the air space has only a marginal effect on heat transfer in the porous medium. A numerical study of transient convection in a rectangular cavity was reported by Chang and Yang (1995).

The subject of this section was extensively reviewed by Prasad (1991). Further complexity arises if chemical reactions are involved. Examples are found in the papers by Hunt and Tien (1990) and Viljoen et al. (1990).

More recently nonlinear stability studies have been carried out by Hill and Straughan (2009a) and Hill and Carr (2010a, b).

### **6.19.3 Other Configurations and Effects**

A hydrothermal crystal growth system was modeled by Chen et al. (1999b), on the assumption that the growth process is quasisteady. A similar system was modeled by Popov et al. (2006). The flow through a fluid-sediment interface in a benthic chamber was computed by Basu and Khalili (1999). The addition of vertical throughflow was studied by Khalili et al. (2003). Horizontal throughflow of Poiseuille type was studied by Chang (2006), Chang et al. (2006), and by Hill and Straughan (2008, 2009b). Convective instability in a layer saturated with oil and a layer of gas underlying it was analyzed by Kim et al. (2003a).

Convection in a square cavity partly filled with a heat-generating porous medium was studied analytically and numerically by Kim et al. (2001a). Convection induced by the selective absorption of radiation was analyzed by Chang (2004). Penetrative convection resulting from internal heating was studied by Carr (2004). It was found that a heat source in the fluid layer has a destabilizing effect on the porous medium, but one in the fluid has a stabilizing effect on the fluid, while the effects on their respective layers depend strongly on the overall temperature difference and the strength and type of heating in the opposite layer. It also was found that the initiating cell pattern is not necessarily the strongest one. A horizontal plane Couette flow problem was analyzed by Chang (2005).

A surface tension (Marangoni) effect on the onset of convection was analyzed by Nield (1998c). A similar situation was treated by Hennenberg et al. (1997), Rudraiah and Prasad (1998), Straughan (2001b), Desaive et al. (2001), and Saghir et al. (2002, 2005b) using the Brinkman model. The last authors reported numerical studies for the combined buoyancy and surface tension situation. Kozak et al. (2004) included the effect of evaporation at the free surface. Straughan (2004b) pointed out that the results of Chen and Chen (1988) lend much support for the two-layer model of Nield (1998c). Further studies of Marangoni convection have

been made by Shivakumara et al. (2006b, 2009a, 2010a, 2011a, 2012b), Liu et al. (2008a), and Zhao et al. (2008e, 2010c, 2011b).

Further studies of the effect of interface boundary conditions were made by Hirata et al. (2007a, b, 2009b). The stability problem has been investigated using integral transforms by Hirata et al. (2006). The double-diffusive problem was treated by Hirata et al. (2009a). A problem involving heat generation was studied by Jimenez-Islas et al. (2009). A cavity with porous layers on the top and bottom walls was examined by Chen et al. (2009a). Experimental work with superposed metal foam and water layers was conducted by Kathare et al. (2009). Alloui and Vasseur (2010) studied the case of Neumann boundary conditions at the horizontal walls. The effect of a magnetic field was included by Banjer and Abdullah (2012). Throughflow effects were studied by Suma et al. (2012).

A layer of a porous medium sandwiched by two fluid layers was used by Nield (1983) to investigate the limitations of the Brinkman equation. A similar model was used by Bogorodskii and Nagurnyi (2000) in the context of under-ice meltwater puddles. They demonstrated that the melting of Arctic ice was accelerated by the fact that melting occurred at the lower boundary.

Gobin and Goyeau (2008) reviewed the topic of convection in partly porous media.

## 6.20 Layer Saturated with Water Near 4°C

Poulikakos (1985b) reported a theoretical investigation of a horizontal porous layer saturated with water near 4°C, when the temperature of the top surface is suddenly lowered. The onset of convection has been studied using linear stability analysis (Sun et al. 1970) and time-dependent numerical solutions of the complete governing equations (Blake et al. 1984). In both studies, the condition for the onset of convection is reported graphically or numerically for a series of discrete cases. The numerical results of Blake et al. (1984) for layers with  $T_c = 0^\circ\text{C}$  on the top and  $5^\circ\text{C} = T_h = 8^\circ\text{C}$  on the bottom can be used to derive (Bejan 1987)

$$\frac{gKH}{\nu\alpha_m} > 1.25 \times 10^5 \exp[\exp(3.8 - 0.446T_h)] \quad (6.188)$$

as an empirical dimensionless criterion for the onset of convection. In this criterion the bottom temperature  $T_h$  is expressed in degrees Celsius.

Finite-amplitude heat and fluid flow results for Rayleigh numbers  $g\gamma K(T_h - T_c)^2 H / \nu\alpha_m$  of up to  $10^4$  (i.e., about 50 times greater than critical) have also been reported by Blake et al. (1984). In the construction of this, Rayleigh number  $\gamma$  is the coefficient in the parabolic model for the density of cold water,  $\rho = \rho_{\text{ref}} [1 - \gamma (T - 3.98^\circ\text{C})^2]$ , namely  $\gamma = 8 \times 10^{-6} (\text{ }^\circ\text{C})^{-2}$ .

Nonlinear changes in viscosity (as well as density) were treated numerically by Holzbecher (1997). He found that a variety of flow patterns (e.g., two or four cells in

a two-dimensional square domain) are possible, depending on the choice of maximum and minimum temperatures. Mixed boundary conditions were treated by Mahidjiba et al. (2006). Convection in a cavity was studied by Eswaramurthi et al. (2008).

## 6.21 Effects of a Magnetic Field or Electric Field, Ferromagnetic Fluid

Despite the near absence of experimental work (the case of a mushy layer is an exception) and a general lack of practical applications (the case of ferromagnetic fluids is an exception), a large number of theoretical papers, including those by Patil and Rudraiah (1973), Rudraiah and Vortmeyer (1978), and Rudraiah (1984), have been published on magnetohydrodynamic convection in a horizontal layer. The simplest case is that of an applied vertical magnetic field and electrically conducting boundaries. Oscillatory convection is a possibility under certain circumstances, but this is ruled out if the thermal diffusivity is smaller than the magnetic resistivity, and this condition is met by a large margin under most terrestrial conditions. On the Darcy model, for the case of thermally conducting impermeable boundaries, the Rayleigh number at the onset of nonoscillatory instability for disturbances of dimensionless wavenumber  $\alpha$  is given by

$$Ra = \frac{(\pi^2 + \alpha^2)(\pi^2 + \alpha^2 + Q\pi^2)}{\alpha^2}, \quad (6.189)$$

where

$$Q = \frac{\sigma B^2 K}{\mu}. \quad (6.190)$$

Here  $B$  is the magnetic induction and  $\sigma$  is the electrical conductivity. The parameter  $Q$  has been called the Chandrasekhar-Darcy number; it is the Darcy number  $K/H^2$  times the usual Chandrasekhar number, which in turn is the square of the Hartmann number. Some workers use a Hartmann-Darcy number equal to  $Q^{1/2}$ . It is clear that the effect of the magnetic field is stabilizing. The critical Rayleigh number again is found by taking a minimum as varies. Because of the practical difficulties of achieving a large magnetic field,  $Q$  is almost always much less than unity, and so the effect of the magnetic field is negligible. Bergman and Fearn (1994) discussed an exceptional situation, namely convection in a mushy zone at the Earth's inner-outer core boundary. They concluded that the magnetic field may be strong enough to act against the tendency for convection to be in the form of chimneys, and that is confirmed by the experimental work of Bergman et al. (1999).

The case of a ferrofluid with a magnetic-field-dependent viscosity has been extensively studied, starting with Vaidyanathan et al. (1991) with a Darcy model. The Brinkman model was used by Vaidyanathan et al. (2002a), Sunil et al. (2004a), and Nanjundappa et al. (2010, 2011c) (with internal heat generation). A nonlinear analysis was performed by Qin and Chadam (1995), Sunil and Mahajan (2008b, 2009b), and Sunil et al. (2009b). Various boundary conditions were considered by Shivakumara et al. (2009b). Penetrative convection was studied by Nanjundappa et al. (2011a). The case of thermal nonequilibrium was treated by Lee et al. (2011), Srivastava et al. (2011, 2012) (anisotropy), Shivakumara et al. (2011f), and Sunil et al. (2010a) (nonlinear stability).

The effect of rotation was studied by Sekar and Vaidyanathan (1993), Vaidyanathan et al. (2002c), Desaive et al. (2004), Sunil et al. (2006b) (micropolar fluid), and Sunil and Mahajan (2009a) (nonlinear stability). Penetrative ferroconvection was studied by Lee and Shivakumar (2011) and by Nanjundappa et al. (2012) (via internal heating in a layer with constant heat flux at the lower boundary).

An anisotropic medium was studied by Ramanathan and Surendra (2003), Ramanathan and Suresh (2004), and Nanjundappa et al. (2011b).

The effect of dust particles on ferroconvection was added by Sunil et al. (2004c, 2005b, c, d, 2006a, 2010c) and by Mittal and Rana (2009) who treated a micropolar fluid.

The problem for the case of the Brinkman model and isoflux boundaries was treated by Alchaar et al. (1995a). In this paper and in Bian et al. (1996a), the effect of a horizontal magnetic field was studied, but these treatments are incomplete because only two-dimensional disturbances were considered, and so the most unstable disturbance may have been overlooked.

Further studies of MHD convection have been reported by Goel and Agrawal (1998) for a viscoelastic dusty fluid, by Sunil and Singh (2000) for a Rivlin-Ericksen fluid, by Sunil et al. (2003a) with throughflow and rotation effects, by Shivakumara et al. (2010d) for a nanofluid, by Krakov and Nikiforov (3D convection patterns in a cube), and by Idris and Hashim (2010) (chaos with a low Prandtl number fluid).

Electroconvection problems were studied by Rudraiah et al. (2007) (thermal modulation), Bhaduria (2007a) (thermal modulation and rotation), Rudraiah and Gyathri (2009) (thermal modulation), and Shivakumara et al. (2011g) (rotation).

## 6.22 Effects of Rotation

The subject of flow in rotating porous media has been reviewed in detail by Vadasz (1997a, 1998b, 2000a, 2002), whose treatment is followed here. On the Darcy model, constant density flow in a homogeneous porous medium is irrotational, and so the effect of rotation on forced convection is normally unimportant. For natural

convection the situation is different. For a homogeneous medium the momentum equation (with Forchheimer and Brinkman terms omitted) can be written in the dimensionless form

$$\frac{Da}{\varphi Pr} \frac{\partial \mathbf{v}}{\partial t} = -\nabla p - Ra T \nabla(\mathbf{e}_g \cdot \mathbf{X}) + Ra_\omega T \mathbf{e}_\omega \times (\mathbf{e}_\omega \times \mathbf{X}) + \frac{1}{Ek} \mathbf{e}_\omega \times \mathbf{v}. \quad (6.191)$$

Here  $\mathbf{e}_g$  and  $\mathbf{e}_\omega$  are unit vectors in the direction of gravity and rotation, respectively, and  $\mathbf{X}$  is the position vector. The new parameters are the rotational Rayleigh number  $Ra_\omega$  and the Ekman-Darcy number  $Ek$  defined by

$$Ra_\omega = \left( \frac{\omega^2 H}{g} \right) Ra, \quad Ek = \frac{\varphi \mu}{2\omega \rho K}, \quad (6.192)$$

where  $\omega$  is the dimensional angular velocity of the coordinate frame with respect to which motion is measured. Normally  $Ek \gg 1$  and then the Coriolis term is negligible, but it can cause secondary flow in an inhomogeneous medium. Generally the Coriolis effect is analogous to that of anisotropy (Palm and Tyvand 1984). The appearance of the porosity in the expression for  $Ek$  should be noted because some authors have overlooked this factor. This error was pointed out by Nield (1999), who also discussed the analogy between (1) Darcy flow in an isotropic porous medium with a magnetic or rotation effect present and (2) flow in a medium with anisotropic permeability.

For the case  $Ra/Ra_\omega \ll 1$ , that is, when the centrifugal force dominates over gravity, Vadasz (1992, 1994b) considered a two-dimensional problem for a rectangular domain with heating from below and rotation about a vertical boundary. He first showed that for small height-to-breadth aspect ratio  $H/L$ , the Nusselt number is given approximately by

$$Nu = \frac{1}{24} (H/L) Ra_\omega. \quad (6.193)$$

He then relaxed this condition, reduced the problem to that of solving an ordinary differential equation, and found that  $Nu$  increases faster with  $Ra_\omega$  than (6.191) would indicate.

The Coriolis effect on the HRL problem has been investigated by several authors. On the Darcy model, one finds that the critical Rayleigh number is given by

$$Ra_c = \pi^2 [(1 + Ek^{-2})^{1/2} + 1]^2. \quad (6.194)$$

Using the Brinkman model, Friedrich (1983) performed a linear stability analysis and a nonlinear numerical study. On this model, convection sets in as an oscillatory

instability for a certain range of parameter values. Patil and Vaidyanathan (1983) dealt with the influence of variable viscosity on linear stability. A nonlinear energy stability analysis was performed by Qin and Kaloni (1995). A study of the heat transfer produced in nonlinear convection was made by Riahi (1994), following the procedure of Gupta and Joseph (1973). In terms of a Taylor-Darcy number  $Ta$  defined by  $Ta = 4/Ek^2$ , he found the following results. For  $Ta \ll O(1)$ , the rotational effect is not significant. For  $O(1) \ll Ta \ll O(Ra^{1/2} \log Ra)$ , the Nusselt number  $Nu$  decreases with increasing  $Ta$  for a given  $Ra$ . For  $O(Ra^{1/2} \log Ra) \ll Ta \ll O(Ra)$ ,  $Nu$  is proportional to  $(Ra/Ta) \log (Ra/Ta)$ . For  $Ta = O(Ra)$ ,  $Nu$  becomes  $O(1)$  and the convection is inhibited entirely by rotation for  $Ta > Ra/\pi^2$ .

The weak nonlinear analysis of Vadász (1998b) showed that, in contrast to the clear fluid case, overstable convection is possible for all values of  $Pr$  (not just  $Pr < 1$ ) and that the critical wavenumber in the plane containing the streamlines for stationary convection is dependent on rotation. It also showed that the effect of viscosity is destabilizing for high rotation rates. As expected, there is a pitchfork bifurcation for stationary convection, and a Hopf bifurcation for overstable convection and rotation retards heat transfer (except for a narrow range of small values of  $\varphi Pr/Da$ , where rotation enhances the heat transfer associated with overstable convection). Bounds on convective heat transfer in a rotating porous layer were obtained by Wei (2004). A sharp nonlinear threshold for instability was obtained by Straughan (2001c). Bresch and Sy (2003) presented some general mathematical results for convection in rotating porous media.

A study of Coriolis effects on the filtration law in rotating porous media was made by Auriault et al. (2002a). Alex and Patil (2000a) analyzed an anisotropic medium. Desaive et al. (2002) included a study of Kuppers-Lortz instability for the case of Coriolis effects. Vadász and Govender (2001) and Govender (2003a, c) treated in turn the Coriolis effect for monotonic convection and oscillating convection induced by gravity and centrifugal forces, each in a rotating porous layer distant from the axis of rotation.

Various non-Newtonian fluids have been considered. A Rivlin-Ericksen fluid was analyzed by Krishna (2001). A micropolar fluid was treated by Sharma and Kumar (1998). An electrically conducting couple-stress fluid was studied by Sunil et al. (2002). A couple-stress fluid was also treated by Shivakumara et al. (2011h). A viscoelastic fluid was studied by Kang et al. (2011) and by Kumar and Bhaduria (2011a) (anisotropy).

The effect of thermal modulation was studied by Bhaduria (2007d), Bhaduria and Suthar (2009), and Malashetty and Swamy (2007c). Modulation of rotation frequency was treated by Suthar et al. (2009, 2011). The effect of anisotropy was included in the studies by Govender (2006a, b), Govender and Vadász (2007) (thermal nonequilibrium), Malashetty and Swamy (2007c), Saravanan (2009a) (MHD), Saravanan and Brindha (2011) (nonlinear stability), and by Vanishree and Siddheshwar (2010).

The effect of local thermal nonequilibrium was also studied by Malashetty et al. (2007) and Malashetty and Swamy (2010a).

Shivakumara et al. (2009c, 2011b, d) included in turn some bifurcation analysis, throughflow and quadratic drag effects, and a ferromagnetic fluid. Falsaperla et al.

(2010, 2011) studied a case with prescribed heat flux and then inertial effects. A nanofluid was considered by Bhaduria and Agarwal (2011b). A nonlinear magnetic field was studied by Allehiany and Abdullah (2009). A further nonlinear stability analysis was performed by Babu et al. (2012).

## 6.23 Non-Newtonian and Other Types of Fluids

The onset of convection in a horizontal layer of a medium saturated with a micropolar fluid was studied by Sharma and Gupta (1995). Coupling between thermal and micropolar effects may introduce oscillatory motions. A nonlinear analysis with a micropolar medium was reported by Siddheshwar and Krisna (2003). The MHD problem with a micropolar fluid was studied by Sharma and Kumar (1997). The corresponding problem with a non-Newtonian power-law fluid, with constant-flux boundary conditions, was treated analytically and numerically by Amari et al. (1994). The effect of suspended particles was treated by Mackie (2000). Viscoelastic fluids were studied by Prakash and Kumar (1999a), Sri Krishna (2001), and Yoon et al. (2003, 2004), and also by Prakash and Kumar (1999a, b) for the case of variable gravity, Sharma and Kango (1999) for the MHD case, and by Kumar (1999) with the addition of suspended particles, while Kim et al. (2003b) conducted a nonlinear analysis.

A viscoelastic fluid has been studied by Kumar and Singh (2006) and Bertola and Cafaro (2006) (as initial-value problems), by Fu et al. (2007) (square box), by Idris and Hashim (2011) (cubic temperature profile), by Malashetty and Swamy (2007d) (anisotropy), by Malashetty et al. (2006b) (thermal modulation), by Niu et al. (open-top layer), by Sheu et al. (2008) (chaotic convection), by Sheu (2011) (nanofluid), by Shivakumara and Sureshkumar (2007) (throughflow), by Shivakumara et al. (2006a, 2011i), (local thermal nonequilibrium, thermal modulation), and by Zhang et al. (cylinder).

Oldroyd-B fluids were examined by Malashetty et al. (2006a) (thermal nonequilibrium), by Niu et al. (2010b) (Newtonian heating), by El-Sayed (2008) (electroconvection), and by Zhang et al. (2008) (nonlinear stability).

The onset of convection in a power-law fluid has some anomalous features that were discussed by Nield (2011b, c).

Couple-stress fluids were studied by Malashetty et al. (2009b) and Shivakumara (2010). Maxwell fluids were treated by Tan and Masuoka (2007), Malashetty and Kulkarni (2009) (thermal nonequilibrium), and Yin et al. (2012) (constant-flux heating). A second-grade fluid, with Hall current and rotation, was studied by Hayat et al. (2008a). A Green-Naghdi fluid with thermal nonequilibrium was analyzed by Straughan (2010a).

Other papers involving non-Newtonian fluids have been mentioned in the previous section.

A nanofluid was studied by Kuznetsov and Nield (2011b), Bhaduria and Agarwal (2011a), Agarwal and Bhaduria (2011) (thermal nonequilibrium, rotation), and Agarwal et al. (2011).

## 6.24 Effects of Vertical Vibration and Variable Gravity

The subject of thermovibrational convection is of current interest in connection with the study of the behavior of materials in a microgravity environment as on a spacecraft, where residual accelerations ( $g$ -jitter) may have undesirable effects. The term thermovibrational convection refers to the appearance of a mean flow in a fluid-filled cavity having temperature heterogeneities. In this case, by proper selection of frequency and amplitude of vibration, one may observe significant modifications in the stability threshold of convective motions in the direction of increased stability. Historically, there have been two schools of thought on treating this type of problem. The first group applies linear stability analysis to the system of hydrodynamic equations in its original form and thus obtains a set of coupled linear differential equations with periodic coefficients. The second group applies the time-averaging method, and now a periodic coefficient does not appear explicitly in the governing equations. In this approach, which is valid for the case of high frequency and small amplitude, the temperature, pressure, and velocity fields may be decomposed into two parts, the first of which varies slowly with time, while the second part varies rapidly with time and has a zero mean over a vibrational period. This method leads to substantial simplifications in the mathematical formulation and even in some cases provides us with analytical relationships for the onset of convection. It enables a more in-depth analysis of the control parameters and consequently a better understanding of vibrational effect. The validity of the time-averaged method has been proved mathematically as well as experimentally (cf. Gershuni and Lyubimov 1998). Several theoretical papers, including those of Zenkovskaya (1992), Zenkovskaya and Rogovenko (1999) (who considered a variable direction of vibration and found that only the vertical vibration always has a stabilizing effect), and Bardan and Mojtabi (2000), have been published on thermovibrational convection in porous media by applying this method. The simplest case is that of an infinite horizontal porous layer with height  $H$  that undergoes a vertical vibration of sinusoidal form, which is characterized by amplitude ( $b$ ) and frequency ( $\omega$ ). As a first step, the simultaneous effects of vibration and gravitational acceleration may be considered; the vibration vector is parallel to the gravitational acceleration. The boundaries of the layer are kept at constant but different temperatures. Adopting the Darcy model, the Rayleigh number at the onset of stationary convection can be expressed as

$$Ra = \frac{(\pi^2 + \alpha^2)^2}{\alpha^2} + Ra_v \frac{\alpha^2}{\alpha^2 + \pi^2}, \quad (6.195)$$

where

$$Ra_v = \frac{(RRa)^2}{2B\omega^{*2}} \quad (6.196)$$

and  $\alpha$  is the dimensionless wavenumber.

Here  $R$  is an acceleration ratio ( $b\omega^2/g$ ),  $B$  may be considered as a sort of inverse Darcy-Prandtl number ( $B = a^*K/\nu\sigma H^2$ ), and  $\omega^*$  is the dimensionless frequency. The stability diagram in the  $Ra_c$ - $R$  plane reveals that vibration increases the stability threshold and reduces the critical wavenumber. Another interesting result obtained from (6.195) is that under microgravity conditions, the layer is linearly/ininitely stable. It was shown mathematically by Zenkovskaya (1992) that the transition toward an oscillatory convection in this case is not possible. This problem was also treated by Pedram Razi et al. (2002) by using the direct method. In these papers, the authors showed that the stability analysis led to a Mathieu equation. An analogy between the stability behaviors of the thermofluid problem with that of an inverted pendulum under the effect of vertical vibration was made (cf. Pedram Razi et al. 2005). It may be recalled that vertical vibration may stabilize an inverted pendulum, which is in an unstable position. Based on a scale analysis reasoning, the domain of validity of time-averaged method was found. Pedram Razi et al. explained why the transient term should be kept in the momentum equation at high frequency. In addition, they argued that the time-averaged method only gives the harmonic response and they predicted the existence of a subharmonic response. Thus these studies bridged the gap between the two schools of thought on thermovibrational problems. The outcome of these analyses can be interpreted in the context of constructal theory (Bejan 2000) as follows: Among the many combinations between frequency and amplitude of vibration, it is the high frequency and small amplitude that provide the stabilizing effect.

The finite-amplitude case was studied by Bardan and Mojtabi (2000), Mojtabi (2002), Bardan et al. (2004), and Pedram Razi et al. (2005). Their weakly nonlinear analysis shows that the bifurcation at the transition point is of the supercritical pitchfork type. Mojtabi et al. (2004) examined the case of variable directions of vibration in the limiting case of high frequency and small amplitude. They concluded that when the direction of vibration is perpendicular to the temperature gradient, the vibration has a destabilizing effect. They also predicted the onset of convection in microgravity conditions. Charrier-Mojtabi et al. (2006) revisited the horizontal layer and confined cavity problems and found a relationship between the stability analyses of these two problems via a Mathieu equation. A summary of new predictive high-frequency thermovibrational modes was made by Pedram Razi et al. (2009).

The alternative school of thought is represented by the papers by Malashetty and Padmavathi (1997, 1998) (who included Brinkman and Forchheimer effects) and Govender (2004b, 2005c, d, f). The latter presented the results of both linear and weak nonlinear analyses with emphasis on the transition from synchronous to subharmonic motions, and he treated the cases of low frequency and a layer heated from above. Govender's linear stability analysis was performed with the aid of Mathieu stability charts and showed that gravity modulation stabilizes the convection for the region of synchronous solutions but slowly destabilizes it for the regions of subharmonic solutions. The transition from synchronous to subharmonic solutions occurs at the value 1,225 (approximately) of the frequency scaled in terms of layer depth and thermal conductivity. Govender

found that his numerical results revealed that increasing the frequency of vibration causes the amplitude of the convection to approach zero. This work was extended to the case of solidifying mushy layers by Pillay and Govender (2005). A review of work on natural convection in gravity-modulated porous layers was made by Govender (2008b).

The effect of anisotropy was studied by Malashetty and Basavaraja (2003), Saravanan and Purusothaman (2009), Saravanan and Arunkumar (2010), and Saravanan and Sivakumar (2010). Govender (2007) noted an analogy between a gravity-modulated layer heated from below and an inverted pendulum with an oscillating pivot point. In addition he noted that a roll cell behaves in a manner similar to a very long pendulum. The Brinkman model was employed by Saravanan and Sivakumar (2010). The case of a Maxwell fluid was studied by Malashetty and Begum (2011b). The effect of local thermal nonequilibrium was treated by Saravanan and Sivakumar (2011b). The effects of nonuniform temperature gradient and local thermal nonequilibrium were examined by Lee et al. (2011a). Anisotropy and variable viscosity effects were studied by Siddheshwar et al. (2012). A nonlinear stability analysis for the case of a rotating anisotropic medium was reported by Bhaduria et al. (2012a), while Bhaduria et al. (2012b) included the effect of internal heating. Convection in a cylindrical porous layer was studied by Govender (2006c). The case of a binary fluid has been extensively studied, and this work is surveyed in Sect. 9.1.6.4.

Herron (2001) analyzed the onset of convection in a porous medium heated internally and with the gravitational field varying with distance through the layer. He proved that oscillatory is not possible as long as the gravity field and the integral of the heat sources have the same sign. Kim et al. (2005) studied the transient convection resulting from a sudden imposition of gravity. The influence of vibrations on the convective stability of reaction fronts was studied by Aatif et al. (2010) and (for quasiperiodic modulation) by Allali et al. (2012). The effect of couple stress was examined by Saravanan and Premalatha (2012).

Thermal vibration convection in a porous medium saturated by either a pure or binary fluid was surveyed by Pedram Razi et al. (2008).

## 6.25 Bioconvection

Bioconvection is concerned with pattern formation in suspensions of microorganisms, such as bacteria and algae, due to up swimming of the microorganisms. The microorganisms are denser than water and on the average, they swim upward. When they congregate, the system becomes top-heavy and instability as convection may result. Microorganisms respond to various stimuli. Gravitaxis refers to swimming in the opposite sense as gravity. Gyrotaxis is swimming directed by the balance between the torque due to gravity acting on a bottom-heavy cell and the torque due to viscous forces arising from local shear flows. Oxytaxis corresponds to swimming up an oxygen concentration gradient.

Kuznetsov and coworkers have analyzed various aspects of bioconvection in a porous medium, sufficiently sparse so that the microorganisms can swim freely. Gravitaxis was considered by Kuznetsov and Jiang (2001, 2003) and Kuznetsov and Avramenko (2003a) with and without cell deposition and declogging. Further studies of gravitaxis were conducted by Nguyen et al. (2004) and Nguyen-Quang et al. (2005). A falling plume involving the bioconvection of oxytactic bacteria was treated by Kuznetsov et al. (2003a, 2004). The stability of oxytactic bioconvection was treated by Kuznetsov and Avramenko (2003c). The oxytactic situation with superposed fluid and porous layers was studied by Avramenko and Kuznetsov (2005). A falling plume was also studied numerically by Becker et al. (2004). Gyrotaxis was studied by Kuznetsov and Avramenko (2002, 2003b, 2005), Nield et al. (2004c), and Avramenko and Kuznetsov (2004). Work on bioconvection in porous media was reviewed by Kuznetsov (2005, 2008).

The effect of vertical throughflow in the case of gyrotactic organisms and superposed fluid and porous layers was studied by Avramenko and Kuznetsov (2006). The effect of vertical vibration was treated by Kuznetsov (2006b). Thermo-bioconvection was studied by Kuznetsov (2006a, c).

Gravitactic bioconvection was further investigated by Nguyen-Quang (2008) for an anisotropic medium and by Nguyen-Quang et al. (2008) for the case of double diffusion. Experimental work involving a protozoan culture was reported by Nguyen-Quang et al. (2009). This work was reviewed by Nguyen-Quang et al. (2011).

The effect of a nanofluid was studied by Kuznetsov (2012a, b), and Kuznetsov and Bubnovich (2012) (simultaneous gyrostatic and oxytactic microorganisms).

## 6.26 Constructal Theory of Bénard Convection

In this section we take a closer look at the phenomenon of convection in a porous layer heated from below. Our objective is to show that most of the features of the flow can be determined based on a simple method: the intersection of asymptotes (Bejan 1984; Nelson and Bejan 1998). This method was originally used for the optimization of spacings for compact cooling channels for electronics (Bejan 1984); see also Lewins (2003) and Bejan et al. (2004).

Assume that the system of Fig. 6.30 is a porous layer saturated with fluid and that if present the flow is two-dimensional and in the Darcy regime. The height  $H$  is fixed, and the horizontal dimensions of the layer are infinite in both directions. The fluid has nearly constant properties such that its density-temperature relation is described well by the Boussinesq linearization. The volume-averaged equations that govern the conservation of mass, momentum, and energy are

$$\frac{\partial u}{\partial x} + \frac{\partial v}{\partial y} = 0, \quad (6.197)$$

$$\frac{\partial u}{\partial y} - \frac{\partial v}{\partial x} = - \frac{Kg\beta}{v} \frac{\partial T}{\partial x}, \quad (6.198)$$

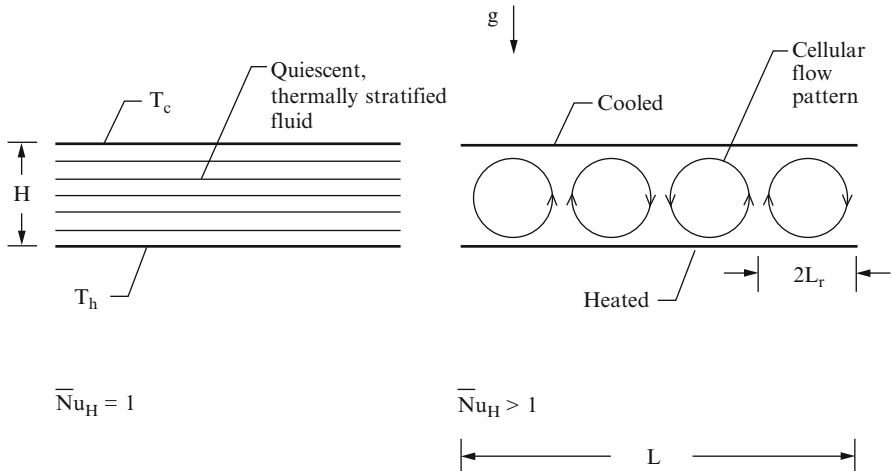


**Fig. 6.30** Horizontal porous layer saturated with fluid and heated from below (Nelson and Bejan 1998)

$$u \frac{\partial T}{\partial x} + v \frac{\partial T}{\partial y} = \alpha \left( \frac{\partial^2 T}{\partial x^2} + \frac{\partial^2 T}{\partial y^2} \right). \quad (6.199)$$

The horizontal length scale of the flow pattern ( $2L_r$ ), or the geometric aspect ratio of one roll, is unknown. The method consists of analyzing two extreme flow configurations—many counterflows vs. few plumes—and intersecting these asymptotes for the purpose of maximizing the global thermal conductance of the flow system, that is, by invoking the constructal law (Bejan 1997c, 2000).

### 6.26.1 The Many Counterflows Regime

In the limit  $L_r \rightarrow 0$ , each roll is a very slender vertical counterflow (Fig. 6.31). Because of symmetry, the outer planes of this structure ( $x = \pm L_r$ ) are adiabatic: They represent the center planes of the streams that travel over the distance  $H$ . The scale analysis of the  $H \times (2L_r)$  region indicates that in the  $L_r/H \rightarrow 0$  limit, the horizontal velocity component  $u$  vanishes. This scale analysis is not shown because it is well known as the defining statement of fully developed flow. Equations (6.197), (6.198), and (6.199) reduce to

$$\frac{\partial v}{\partial x} = \frac{Kg\beta}{v} \frac{\partial T}{\partial x}, \quad (6.200)$$

$$v \frac{\partial T}{\partial y} = \alpha_m \frac{\partial^2 T}{\partial x^2} \quad (6.201)$$

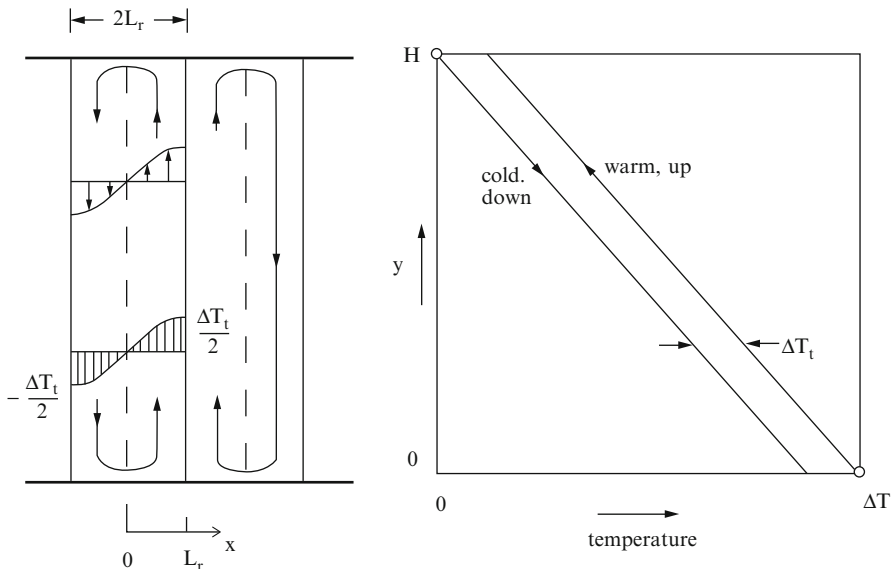


**Fig. 6.31** The extreme in which the flow consists of many vertical and slender counterflows (Nelson and Bejan 1998)

which can be solved exactly for  $v$  and  $T$ . The boundary conditions are  $\partial T/\partial x = 0$  at  $x = \pm L_r$ , and the requirement that the extreme (corner) temperatures of the counterflow region are dictated by the top and bottom walls,  $T(-L_r, H) = T_c$  and  $T(L_r, 0) = T_h$ . The solution is given by

$$v(x) = \frac{\alpha_m}{2H} \left[ Ra_H - \left( \frac{\pi H}{2L_r} \right)^2 \right] \sin\left(\frac{\pi x}{2L_r}\right), \quad (6.202)$$

$$T(x, y) = \frac{v}{Kg\beta} v(x) + \frac{v}{Kg\beta} \left( 2 \frac{y}{H} - 1 \right) \frac{\alpha_m}{2H} \left[ Ra_H - \left( \frac{\pi H}{2L_r} \right)^2 \right] + (T_h - T_c) \left( 1 - \frac{y}{H} \right), \quad (6.203)$$

where the porous-medium Rayleigh number  $Ra_H = Kg\beta H(T_h - T_c)/(\alpha_m v)$  is a specified constant. The right side of Fig. 6.31 shows the temperature distribution along the vertical boundaries of the flow region ( $x = \pm L_r$ ): The vertical temperature gradient  $\partial T/\partial y$  is independent of altitude. The transversal (horizontal) temperature difference ( $\Delta T_t$ ) is also a constant,

$$\Delta T_t = T(x = L_r) - T(x = -L_r) = \frac{v}{Kg\beta} \frac{\alpha_m}{H} \left[ Ra_H - \left( \frac{\pi H}{2L_r} \right)^2 \right]. \quad (6.204)$$

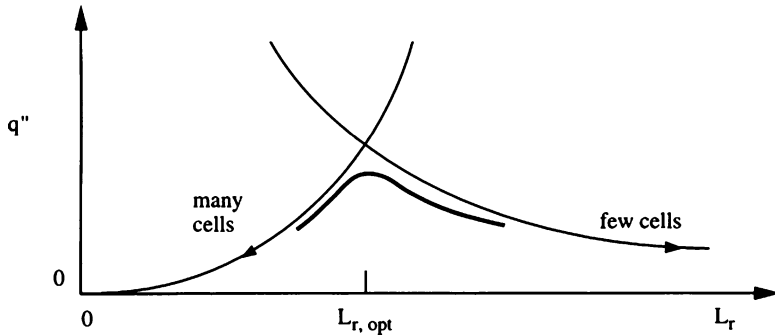


**Fig. 6.32** The intersection of asymptotes method: the geometric maximization of the thermal conductance of a fluid-saturated porous layer heated from below (Nelson and Bejan 1998)

The counterflow convects heat upward at the rate  $q'$ , which can be calculated using (6.202) and (6.203):

$$q' = \int_{-L}^L (\rho c_p)_f v T \, dx. \quad (6.205)$$

The average heat flux convected in the vertical direction,  $q'' = q'/(2L_r)$ , can be expressed as an overall thermal conductance

$$\frac{q''}{\Delta T} = \frac{k_m}{8H Ra_p} \left[ Ra_p - \left( \frac{\pi H}{2L_r} \right)^2 \right]^2. \quad (6.206)$$

This result is valid provided the vertical temperature gradient does not exceed the externally imposed gradient,  $(-\partial T/\partial y) < \Delta T/H$ . This condition translates into

$$\frac{L_r}{H} > \frac{\pi}{2} Ra_p^{-1/2} \quad (6.207)$$

which in combination with the assumed limit  $L_r/H \rightarrow 0$  means that the domain of validity of (6.206) widens when  $Ra_H$  increases. In this domain the thermal conductance  $q''/\Delta T$  decreases monotonically as  $L_r$  decreases (cf. Fig. 6.32).

### 6.26.2 The Few Plumes Regime

As  $L_r$  increases, the number of rolls decreases, and the vertical counterflow is replaced by a horizontal counterflow in which the thermal resistance between  $T_h$  and  $T_c$  is dominated by two horizontal boundary layers, as in Fig. 6.33. Let  $\delta$  be the

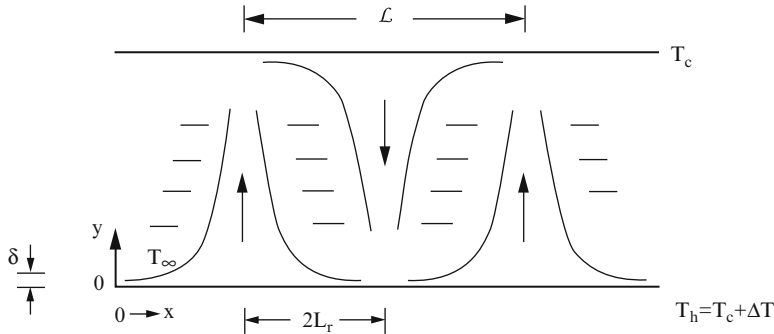


**Fig. 6.33** The extreme in which the flow consists of a few isolated plumes (Nelson and Bejan 1998)

scale of the thickness of the horizontal boundary layer. The thermal conductance  $q''/\Delta T$  can be deduced from the heat transfer solution for natural convection boundary layer flow over a hot isothermal horizontal surface facing upward or a cold surface facing downward. The similarity solution for the horizontal surface with power-law temperature variation (Cheng and Chang 1976) can be used to develop an analytical result, as we show at the end of this section.

A simpler analytical solution can be developed in a few steps using the integral method. Consider the slender flow region  $\delta \times (2L_r)$ , where  $\delta \ll 2L_r$ , and integrate (6.197), (6.198), and (6.199) from  $y = 0$  to  $y \rightarrow \infty$ , that is, into the region just above the boundary layer. The surface temperature is  $T_h$ , and the temperature outside the boundary layer is  $T_\infty$  (constant). The origin  $x = 0$  is set at the tip of the wall section of length  $2L_r$ . The integrals of (6.197) and (6.199) yield

$$\frac{d}{dx} \int_0^\infty u(T - T_\infty) dy = -\alpha \left( \frac{\partial T}{\partial y} \right)_{y=0}. \quad (6.208)$$

The integral of (6.198), in which we neglect  $\partial v / \partial x$  in accordance with boundary layer theory, leads to

$$u_0(x) = \frac{Kg\beta}{v} \frac{d}{dx} \int_0^\infty T dy, \quad (6.209)$$

where  $u_0$  is the velocity along the surface,  $u_0 = u(x, 0)$ . Reasonable shapes for the  $u$  and  $T$  profiles are the exponentials

$$\frac{u(x, y)}{u_0(x)} = \exp \left[ -\frac{y}{\delta(x)} \right] = \frac{T(x, y) - T_\infty}{T_h - T_\infty} \quad (6.210)$$

which transform (6.208) and (6.209) into

$$\frac{d}{dx}(u_0\delta) = \frac{2\alpha}{\delta}, \quad (6.211)$$

$$u_0 = \frac{Kg\beta}{\nu} (T_h - T_\infty) \frac{d\delta}{dx}. \quad (6.212)$$

These equations can be solved for  $u_0(x)$  and  $\delta(x)$ ,

$$\delta(x) = \left[ \frac{9\alpha\nu}{Kg\beta(T_h - T_\infty)} \right]^{1/3} x^{2/3}. \quad (6.213)$$

The solution for  $u_0(x)$  is of the type  $u_0 \sim x^{-1/3}$ , which means that the horizontal velocities are large at the start of the boundary layer and decrease as  $x$  increases. This is consistent with the geometry of the  $H \times 2L_r$  roll sketched in Fig. 6.33, where the flow generated by one horizontal boundary layer turns the corner and flows vertically as a relatively narrow plume (narrow relative to  $2L_r$ ), to start with high velocity ( $u_0$ ) a new boundary layer along the opposite horizontal wall.

The thermal resistance of the geometry of Fig. 6.33 is determined by estimating the local heat flux  $k(T_h - T_\infty)/\delta(x)$  and averaging it over the total length  $2L_r$ :

$$q'' = \left( \frac{3}{4} \right)^{1/3} \frac{k_m \Delta T}{H} \left( \frac{T_h - T_\infty}{\Delta T} \right)^{4/3} Ra_H^{1/3} \left( \frac{H}{L_r} \right)^{2/3}. \quad (6.214)$$

The symmetry of the sandwich of boundary layers requires  $T_h - T_\infty = (1/2)\Delta T$ , such that

$$\frac{q''}{\Delta T} = \frac{3^{1/3} k}{4H} Ra_H^{1/3} \left( \frac{H}{L_r} \right)^{2/3}. \quad (6.215)$$

The goodness of this result can be tested against the similarity solution for a hot horizontal surface that faces upward in a porous medium and has an excess temperature that increases as  $x^\lambda$ . The only difference is that the role that was played by  $(T_h - T_\infty)$  in the preceding analysis is now played by the excess temperature averaged over the surface length  $2L_r$ . If we use  $\lambda = 1/2$ , which corresponds to uniform heat flux, then it can be shown that the solution of Cheng and Chang (1976) leads to the same formula as (6.215), except that the factor  $3^{1/3} = 1.442$  is replaced by  $0.816(3/2)^{4/3} = 1.401$ . Equation (6.215) is valid when the specified  $Ra_H$  is such that the horizontal boundary layers do not touch. We write this geometric condition as  $\delta(x = 2L_r) < H/2$ , and using (6.213), we obtain

$$\frac{L_r}{H} < \frac{1}{24} Ra_H^{1/2}. \quad (6.216)$$

Since in this analysis  $L_r/H$  was assumed to be very large, we conclude that the  $L_r/H$  domain in which (6.215) is valid becomes wider as the specified  $Ra_H$  increases. The important feature of the “few rolls” limit is that the thermal conductance decreases as the horizontal dimension  $L_r$  increases. This second asymptotic trend has been added to Fig. 6.32.

### 6.26.3 The Intersection of Asymptotes

Figure 6.32 presents a bird’s-eye view of the effect of flow shape on thermal conductance. Even though we did not draw completely  $q''/\Delta T$  as a function of  $L_r$ , the two asymptotes tell us that the thermal conductance is maximum at an optimal  $L_r$  value that is close to their intersection. There is a family of such curves, one curve for each  $Ra_H$ . The  $q''/\Delta T$  peak of the curve rises, and the  $L_r$  domain of validity around the peak becomes wider as  $Ra_H$  increases. Looking in the direction of small  $Ra_H$  values, we see that the domain vanishes (and the cellular flow disappears) when the following requirement is violated:

$$\frac{1}{24}HRa_H^{1/2} - \frac{\pi}{2}HRa_H^{-1/2} \geq 0. \quad (6.217)$$

This inequality means that the flow exists when  $Ra_H \geq 12\pi = 37.70$ . This conclusion is extraordinary: It agrees with the stability criterion for the onset of two-dimensional convection (6.29), namely  $Ra_H > 4\pi^2 = 39.5$ , which was derived based on a lengthier analysis and the assumption that a flow structure exists: the initial disturbances (Horton and Rogers 1945; Lapwood 1948).

We obtain the optimal shape of the flow,  $2L_{r,\text{opt}}/H$ , by intersecting the asymptotes (6.206) and (6.215):

$$\pi^2 \left( \frac{H}{2L_{r,\text{opt}}} Ra_p^{-1/2} \right)^2 + 2^{5/6} 3^{1/6} \left( \frac{H}{2L_{r,\text{opt}}} Ra_p^{-1} \right)^{1/3} = 1. \quad (6.218)$$

Over most of the  $Ra_H$  domain where (6.217) is valid, (6.218) is approximated well by its high  $Ra_H$  asymptote:

$$\frac{2L_{r,\text{opt}}}{H} \cong \pi Ra_p^{-1/2}. \quad (6.219)$$

The maximum thermal conductance is obtained by substituting the  $L_{r,\text{opt}}$  value in either (6.215) or (6.206). This estimate is an upper bound because the intersection is above the peak of the curve. In the high  $Ra_H$  limit (6.219), this upper bound assumes the analytical form

$$\left( \frac{q''}{\Delta T} \right)_{\max} \frac{H}{k} < \frac{3^{1/3}}{2^{4/3} \pi^{2/3}} Ra_p^{2/3}. \quad (6.220)$$

Toward lower  $Ra_H$  values the slope of the  $(q''/\Delta T)_{\max}$  curve increases such that the exponent of  $Ra_H$  approaches 1. This behavior is in excellent agreement with the large volume of experimental data collected for Bénard convection in saturated porous media (Cheng 1978). The less-than  $-1$  exponent of  $Ra_H$  in the empirical  $Nu$  ( $Ra_H$ ) curve, and the fact that this exponent decreases as  $Ra_H$  increases, has attracted considerable attention from researchers during the last two decades, as we showed earlier in this chapter.

The intersection of asymptotes method and its applications are reviewed in Bejan (2012).

## 6.27 Bidisperse Porous Media and Cellular Porous Media

Bidisperse porous media (BDPM) have been introduced in Sect. 4.16.4. In the context of the HRL problem, these were studied by Nield and Kuznetsov (2006b) and Straughan (2009). Their results were extended to a tridisperse porous medium by Kuznetsov and Nield (2011a).

Radiative transfer in cellular porous materials was overviewed by Viskanta (2009). A noteworthy feature of these materials is that often one can, to a good approximation, treat the radiation term as an additional thermal conduction term with temperature-dependent conductivity. In general this complication prevents an analytical treatment, but in the case of the HRL problem, an analytical solution was obtained by Nield and Kuznetsov (2010a).

# Chapter 7

## Internal Natural Convection: Heating from the Side

Enclosures heated from the side are most representative of porous systems that function while oriented vertically, as in the insulations for buildings, industrial cold-storage installations, and cryogenics. As in the earlier chapters, we begin with the most fundamental aspects of the convection heat transfer process when the flow is steady and in the Darcy regime. Later, we examine the special features of flows that deviate from the Darcy regime, flows that are time dependent, and flows that are confined in geometries more complicated than the two-dimensional rectangular space shown in Fig. 7.1. Some of the topics of this chapter have been reviewed by Oosthuizen (2000).

### 7.1 Darcy Flow Between Isothermal Sidewalls

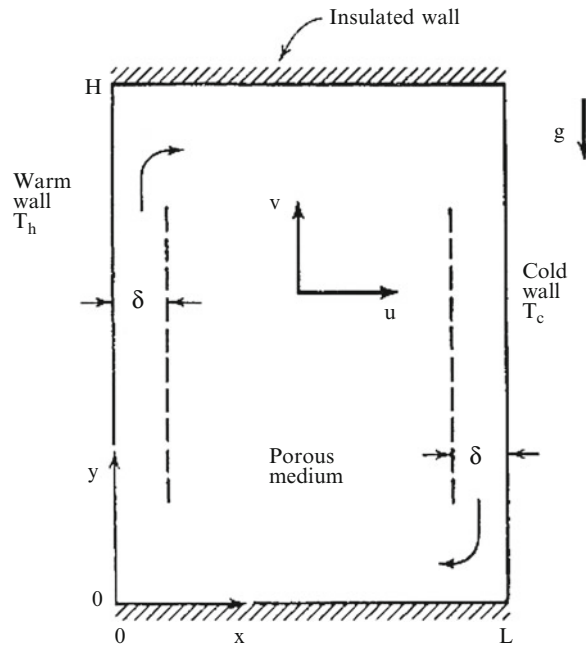
#### 7.1.1 Heat Transfer Regimes

Consider the basic scales of the clockwise convection pattern maintained by the side-to-side heating of the porous medium defined in Fig. 7.1. In accordance with the homogeneous porous medium model, we begin with the equations for the conservation of mass, Darcy flow, and the conservation of energy in the  $H \times L$  space:

$$\frac{\partial u}{\partial x} + \frac{\partial v}{\partial y} = 0, \quad (7.1)$$

$$u = -\frac{K}{\mu} \frac{\partial P}{\partial x}, \quad (7.2)$$

**Fig. 7.1** Two-dimensional rectangular porous layer held between differently heated sidewalls (Bejan 1984)



$$v = -\frac{K}{\mu} \left( \frac{\partial P}{\partial y} + \rho g \right), \quad (7.3)$$

$$u \frac{\partial T}{\partial x} + v \frac{\partial T}{\partial y} = \alpha_m \left( \frac{\partial^2 T}{\partial x^2} + \frac{\partial^2 T}{\partial y^2} \right). \quad (7.4)$$

Note that in contrast to the system used in Sect. 5.1, the  $y$  axis is now vertically upward. By eliminating the pressure  $P$  between (7.2) and (7.3) and by invoking the Boussinesq approximation  $\rho \cong \rho_0[1 - \beta(T - T_0)]$  in the body force term  $\rho g$  of (7.3), we obtain a single equation for momentum conservation:

$$\frac{\partial u}{\partial y} - \frac{\partial v}{\partial x} = -\frac{Kg\beta}{\nu} \frac{\partial T}{\partial x}. \quad (7.5)$$

In this equation  $\nu$  is the kinematic viscosity  $\mu/\rho_0$ , which is assumed constant along with the other properties, the permeability  $K$ , the coefficient of volumetric thermal expansion  $\beta$ , and the porous medium thermal diffusivity  $\alpha_m = k_m/(\rho c_p)_f$ .

The three equations (7.1), (7.4), and (7.5) hold in the entire domain  $H \times L$  subject to the boundary conditions indicated in the figure. The four walls are impermeable, and the side-to-side temperature difference is  $T_h - T_c = \Delta T$ . Of special interest are the scales of the vertical boundary layers of thickness  $\delta$

and height  $H$ . In each  $\delta \times H$  region, the order-of-magnitude equivalents of (7.1), (7.4), and (7.5) are

Mass:

$$\frac{u}{\delta} \sim \frac{y}{H}, \quad (7.6)$$

Energy:

$$\left( u \frac{\Delta T}{\delta}, v \frac{\Delta T}{H} \right) \sim \left( \alpha_m \frac{\Delta T}{\delta^2}, \alpha_m \frac{\Delta T}{H^2} \right), \quad (7.7)$$

Momentum:

$$\left( \frac{u}{H}, \frac{v}{\delta} \right) \sim \frac{Kg\beta}{v} \frac{\Delta T}{\delta}. \quad (7.8)$$

To begin with, the mass balance (7.6) shows that the two scales on the left-hand side of (7.7) are of the same order, namely  $v\Delta T/H$ . On the right-hand side of (7.7), the second scale can be neglected in favor of the first, because the  $\delta \times H$  region is a boundary layer (i.e., slender),

$$\delta \ll H. \quad (7.9)$$

In this way, the energy conservation statement (7.7) reduces to a balance between the two most important effects, the conduction heating from the side, and the convection in the vertical direction,

$$\frac{v \frac{\Delta T}{H}}{\text{longitudinal convection}} \sim \frac{\alpha_m \frac{\Delta T}{\delta^2}}{\text{lateral conduction}}. \quad (7.10)$$

Turning our attention to the momentum scales (7.8), we see that the mass balance (7.6) implies that the ratio between  $(u/H)$  and  $(v/\delta)$  is of the order  $(\delta/H)^2 \ll 1$ . We then neglect the first term on the left-hand side of (7.8) and find that the momentum balance reduces to

$$\frac{v}{\delta} \sim \frac{Kg\beta}{v} \frac{\Delta T}{\delta}, \quad (7.11)$$

Equations (7.10), (7.11), and (7.6) imply that the scales of the vertical boundary layer (Bejan 1985) are

$$v \sim \frac{Kg\beta}{v} \Delta T \sim \frac{\alpha_m}{H} Ra, \quad (7.12)$$

$$\delta \sim HRa^{-1/2}, \quad (7.13)$$

$$u \sim \frac{\alpha_m}{H} Ra^{1/2}, \quad (7.14)$$

where  $Ra$  is the Rayleigh number based on height,

$$Ra = \frac{g\beta KH\Delta T}{\nu\alpha_m}. \quad (7.15)$$

The total heat transfer rate from one sidewall to the other is simply

$$q' \sim k_m H \frac{\Delta T}{\delta} \sim k_m \Delta T R a^{1/2}. \quad (7.16)$$

This heat transfer rate is expressed per unit length in the direction perpendicular to the plane  $H \times L$ . It can be nondimensionalized as the overall Nusselt number

$$Nu = \frac{q'}{q'_c} \sim \frac{k_m \Delta T R a^{1/2}}{k_m H \Delta T / L} \sim \frac{L}{H} R a^{1/2}, \quad (7.17)$$

in which  $q'_c = k_m H \Delta T / L$  is the true heat transfer rate in the pure-conduction limit (i.e., in the absence of convection).

Two requirements must be met if the results (7.12), (7.13), (7.14), (7.15), and (7.17) are to be valid. First, the vertical boundary layers must be *slender*, which in view of (7.9) and (7.13) means

$$Ra \gg 1. \quad (7.18)$$

Second, the vertical boundary layers must be *distinct*, that is, thinner than the layer itself,  $\delta \ll L$ . This second requirement can be rewritten (cf. (7.13)) as

$$Ra^{1/2} \gg \frac{H}{L}. \quad (7.19)$$

The domain  $Ra, H/L$  in which the vertical boundary layers are distinct is indicated to the right of the rising dash line in Fig. 7.2.

The fluid completes its clockwise circulation in Fig. 7.1 by flowing along the horizontal boundaries. Whether or not these horizontal jets are distinct (thinner than  $H$ ) can be determined using the scaling results (7.12), (7.13), and (7.14). The volumetric flow rate of the horizontal jet is the same as that of the vertical boundary layer, namely  $v\delta$ . The two horizontal jets form a counterflow that carries energy by convection from left to right in Fig. 7.1, at the rate

$$q'_{(-)} \sim v\delta(\rho c_p)_f \Delta T. \quad (7.20)$$

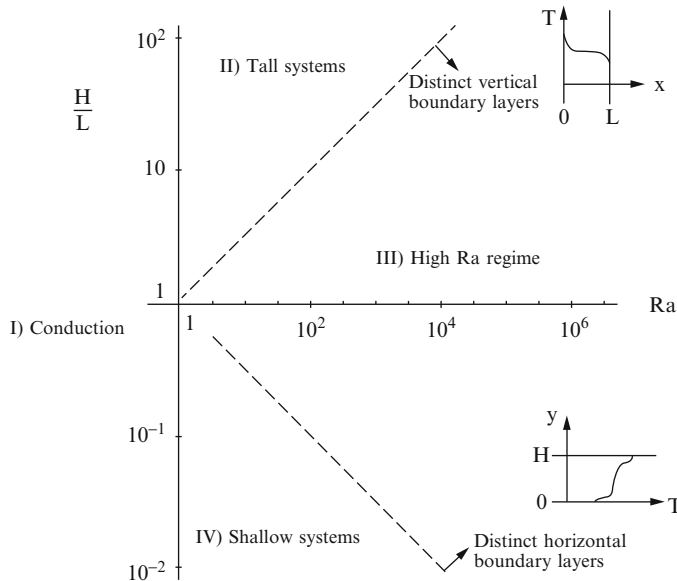


**Fig. 7.2** The four heat transfer regimes for natural convection in a two-dimensional porous layer heated from the side (Bejan 1984)

The heat transfer rate by thermal diffusion between these two jets, from top to bottom in Fig. 7.2, is

$$q'_{(\downarrow)} \sim k_m L \frac{\Delta T}{H}. \quad (7.21)$$

One horizontal jet travels the entire length of the porous layer ( $L$ ) without experiencing a significant change in its temperature when the vertical conduction rate (7.21) is small relative to the horizontal convection rate (7.20). The inequality  $q'_{(\downarrow)} \ll q'_{(\rightarrow)}$  yields

$$\frac{H}{L} \gg Ra^{-1/2} \quad (7.22)$$

as the criterion for the existence of distinct horizontal layers. The parametric domain in which (7.22) is valid is indicated to the right of the descending dash line in Fig. 7.2. The structure of the horizontal layers contains additional features that have been analyzed systematically by Daniels et al. (1982).

Figure 7.2 summarizes the four regimes that characterize the heat transfer through a porous layer heated from the side. The results derived in this section recommend the adoption of the following heat transfer scales:

I. Pure conduction (no distinct boundary layers):

$$Nu \cong 1, \quad q' \cong k_m H \frac{\Delta T}{L}. \quad (7.23)$$

II. Tall layers (distinct horizontal boundary layers only):

$$Nu \tilde{>} 1, \quad q' \tilde{>} k_m H \frac{\Delta T}{L}. \quad (7.24)$$

III. High  $Ra$  convection (distinct vertical and horizontal boundary layers):

$$Nu \sim \frac{L}{H} Ra^{1/2}, \quad q' \sim k_m H \frac{\Delta T}{H}. \quad (7.25)$$

IV. Shallow layers (distinct vertical boundary layers only):

$$Nu \tilde{<} \frac{L}{H} Ra^{1/2}, \quad q' \tilde{<} k_m H \frac{\Delta T}{\delta}. \quad (7.26)$$

In the remainder of this section we focus on regimes III and IV, in which the heat transfer rate can be significantly greater than the heat transfer rate associated with pure conduction. A more detailed classification of the natural convection regimes that can be present in a porous layer heated from the side was developed by Blythe et al. (1983).

### 7.1.2 Boundary Layer Regime

Weber (1975b) developed an analytical solution for the boundary layer regime by applying the Oseen linearization method. The focus of the analysis is the vertical boundary layer region along the left wall in Fig. 7.1, for which the momentum and energy equations are

$$\frac{\partial^2 \Psi_*}{\partial x_*^2} = \frac{\partial T_*}{\partial x_*}, \quad (7.27)$$

$$\frac{\partial \Psi_*}{\partial x_*} \frac{\partial T_*}{\partial y_*} - \frac{\partial \Psi_*}{\partial y_*} \frac{\partial T_*}{\partial x_*} = \frac{\partial^2 T_*}{\partial x_*^2}. \quad (7.28)$$

These equations involve the stream function  $\Psi$  now defined by  $u = -\partial \Psi / \partial y$  and  $v = \partial \Psi / \partial x$  and the dimensionless variables

$$x_* = \frac{x}{H} Ra^{1/2}, \quad y_* = \frac{y}{H}, \quad (7.29)$$

$$\Psi_* = \frac{\Psi}{\alpha_m Ra^{1/2}}, \quad T_* = \frac{T - (T_h + T_c)/2}{T_h - T_c}. \quad (7.30)$$

The solution begins with treating  $\partial\Psi_*/\partial y_*$  (the entrainment velocity) and  $\partial T_*/\partial y_*$  as functions of  $y_*$  only. This leads to the exponential profiles

$$\Psi_* = \Psi_\infty(1 - e^{-\lambda x_*}), \quad (7.31)$$

$$T_* = T_\infty + \left(\frac{1}{2} - T\right)e^{-\lambda x_*}, \quad (7.32)$$

in which the core temperature  $T_\infty$ , the core stream function  $\Psi_\infty$ , and the boundary layer thickness  $1/\lambda$  are unknown functions of  $y_*$ . These unknowns are determined from three conditions, the equations obtained by integrating (7.27) and (7.28) across the boundary layer,

$$\lambda \Psi_\infty = \frac{1}{2} - T_\infty, \quad (7.33)$$

$$\frac{d}{dy_*} \left[ \frac{1}{2\lambda} \left( \frac{1}{2} - T_\infty \right)^2 \right] + \Psi \frac{dT_\infty}{dy_*} = \lambda \left( \frac{1}{2} - T_\infty \right), \quad (7.34)$$

and the centrosymmetry of the entire flow pattern. The latter implies that  $\Psi_\infty$  must be an even function of  $z = y_* - 1/2$  and that  $T_\infty$  must be an odd function of altitude  $z$ . Note that  $z$  is measured away from the horizontal midplane of the rectangular space. The solution is expressed by

$$\psi_* = C(1 - q^2) \left\{ 1 - \exp \left[ -\frac{x_*}{2C(1 + q)} \right] \right\}, \quad (7.35)$$

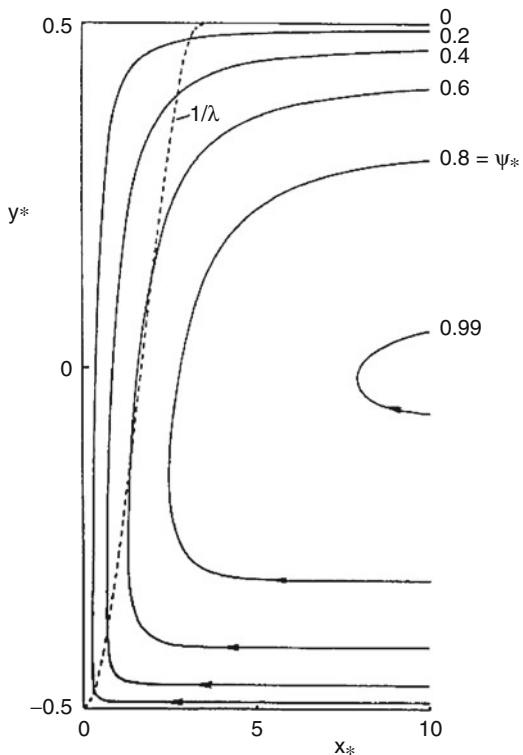
$$T_* = \frac{1}{2} \left\{ q + (1 - q) \exp \left[ -\frac{x_*}{2C(1 + q)} \right] \right\}, \quad (7.36)$$

where  $q$  is an implicit odd function of  $z$ :

$$z = C^2 \left( q - \frac{1}{3} q^3 \right). \quad (7.37)$$

Weber (1975b) determined the constant  $C$  by invoking the impermeable top and bottom conditions  $\Psi_* = 0$  at  $z = \pm 1/2$  and obtained  $C = 3^{1/2}/2 = 0.866$ . The patterns of streamlines and isotherms that correspond to this solution were drawn later by Bejan (1984) and are reproduced in Figs. 7.3 and 7.4. These figures show a vertical boundary layer flow that discharges itself horizontally into a thermally

**Fig. 7.3** The streamlines near the heated wall in the boundary layer regime (Bejan 1984)



stratified core region. The total heat transfer rate between the two sidewalls can be expressed as the conduction-referenced Nusselt number defined in (7.17), now given by

$$Nu = 0.577 \frac{L}{H} Ra^{1/2}. \quad (7.38)$$

The agreement between Weber's solution (7.38) and the order-of-magnitude prediction (7.17) is evident. Figure 7.5 shows a comparison between (7.38) and experimental and numerical data collected from three sources (Schneider 1963; Klarsfeld 1970; Bankvall 1974). The proportionality between  $Nu$  and  $(L/H)Ra^{1/2}$  anticipated from (7.17) and (7.38) appears to be correct in the high Rayleigh number limit. It is important to also note that the boundary layer theory (7.38) consistently overpredicts the Nusselt number, especially at high Rayleigh numbers.

Bejan (1979) showed that the discrepancy between theory and empirical results can be attributed to the way in which the constant  $C$  was determined for the solutions (7.35), (7.36), and (7.37). His alternative was to simultaneously invoke the impermeable and adiabatic wall conditions at  $z = \pm 1/2$ . This was approximately accomplished

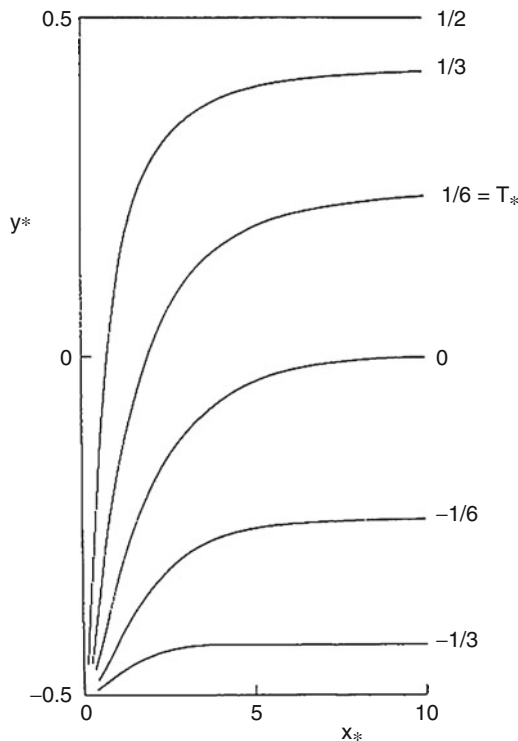


**Fig. 7.4** The isotherms near the heated wall in the boundary layer regime (Bejan 1984)

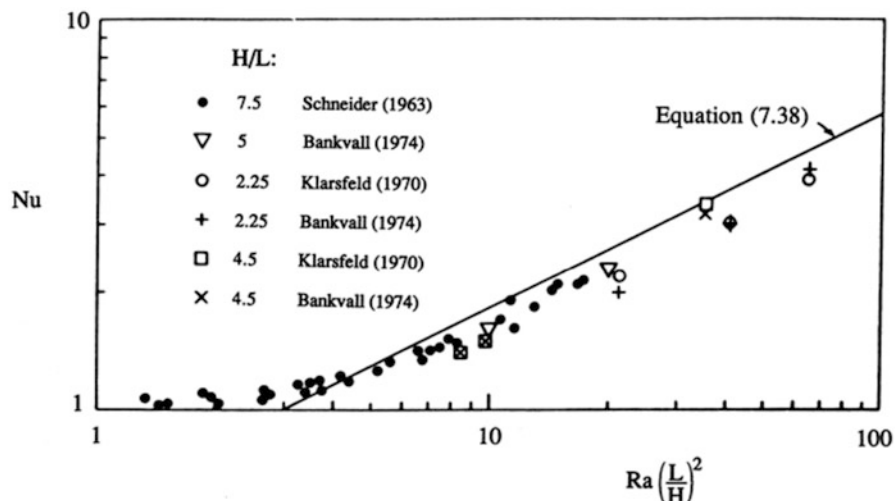


**Fig. 7.5** Theoretical, numerical, and experimental results for the heat transfer rate through a porous layer heated from the side (Bejan 1984)

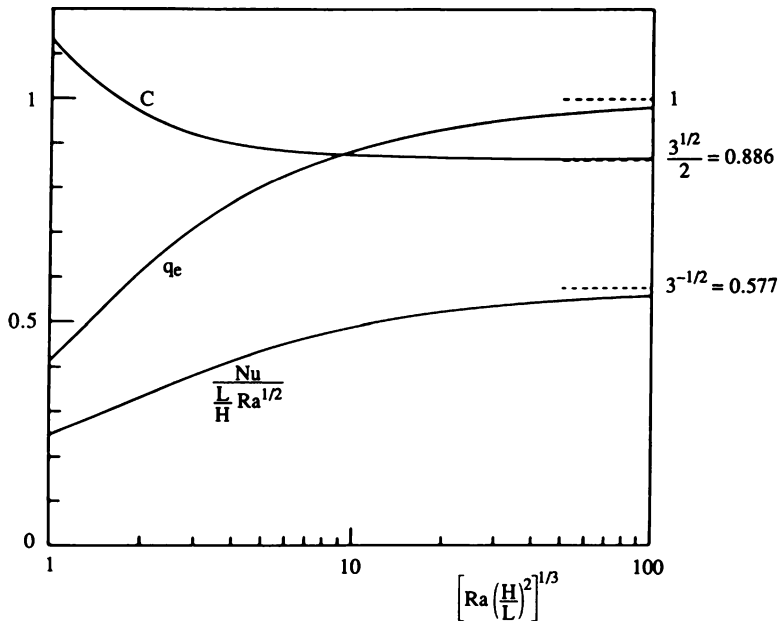


**Fig. 7.6** The effect of the group  $Ra(H/L)^2$  on the solution for boundary layer natural convection in a porous layer heated from the side (Bejan 1979)

by setting the total vertical energy flow rate (convection + conduction) equal to zero at the top and the bottom of the porous layer. The  $C$  value that results from this condition is given implicitly by

$$C = (1 - q_e^2)^{-2/3} Ra^{-1/6} \left( \frac{H}{L} \right)^{-1/3} \quad (7.39)$$

in which  $q_e$  is itself a function of  $C$ ,

$$\frac{1}{2} = C^2 \left( q_e - \frac{1}{3} q_e^3 \right). \quad (7.40)$$

Figure 7.6 shows the emergence of  $Ra(H/L)^2$  as a new dimensionless group that differentiates between various boundary layer regimes. The constant  $C$  approaches Weber's value  $3^{1/2}/2$  as this new group approaches infinity. The same figure shows that the Nusselt number is generally below the value calculated with (7.38), where  $0.577 = 3^{-1/2}$ . An alternative presentation of this heat transfer information is given in Fig. 7.7, which shows that in the boundary layer regime,  $Nu$  depends not only on  $Ra(L/H)^2$ , cf. (7.17), but also on the aspect ratio  $H/L$ . This secondary effect is a reflection of the new group  $Ra(H/L)^2$  identified in Fig. 7.6.

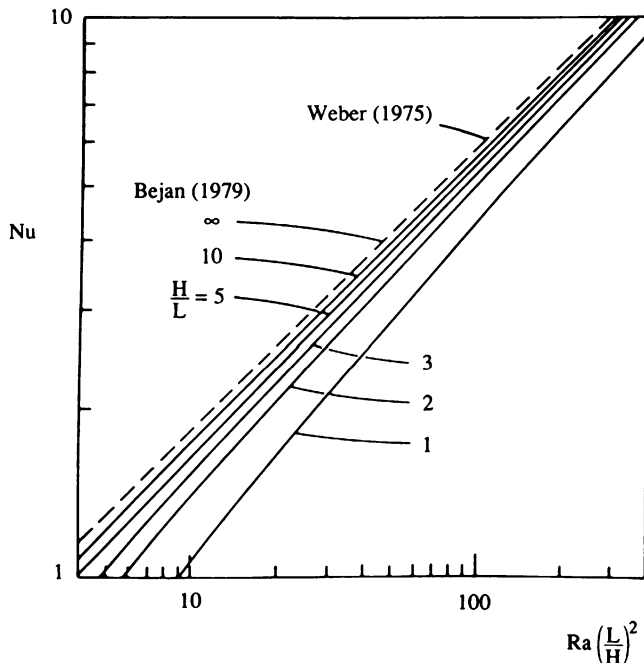


**Fig. 7.7** The heat transfer rate in the boundary layer regime ( $Nu > 1$ ) in a porous layer heated from the side (Bejan 1979)

An integral boundary layer solution that incorporates the same zero vertical energy flow condition was reported by Simpkins and Blythe (1980). The structure of the vertical boundary layer region near the top and bottom corners—neglected in the work reviewed here—was analyzed by Blythe et al. (1982). A numerical study of high  $Ra$  convection, yielding correlations for the heat transfer rate, was reported by Shiralkar et al. (1983). For tall cavities, Rao and Glakpe (1992) proposed a correlation of the form  $Nu = 1 + a(Ra)L/H$ , for  $H/L > H_m(Ra)$ , where  $a(Ra)$  and  $H_m(Ra)$  are quantities determined numerically. Ansari and Daniels (1993, 1994) treated flow in tall cavities, taking into account the nonlinear flow that occurs near each end of the cavity. Their second study, which was concerned with the case of  $Ra$  and aspect ratio large and of the same order, led to the prediction of a position of minimum heat transfer across the cavity. A further study using a boundary domain integral method was reported by Jecl and Skerget (2000). Another study involving a tall cavity was made by Ben Yedder and Erchiqui (2009).

Masuoka et al. (1981) performed experiments with glass beads and water, the results of which were in agreement with a boundary layer analysis extended to take account of the vertical temperature gradient in the core and the apparent wall-film thermal resistance which is caused by a local increase in porosity near the wall.

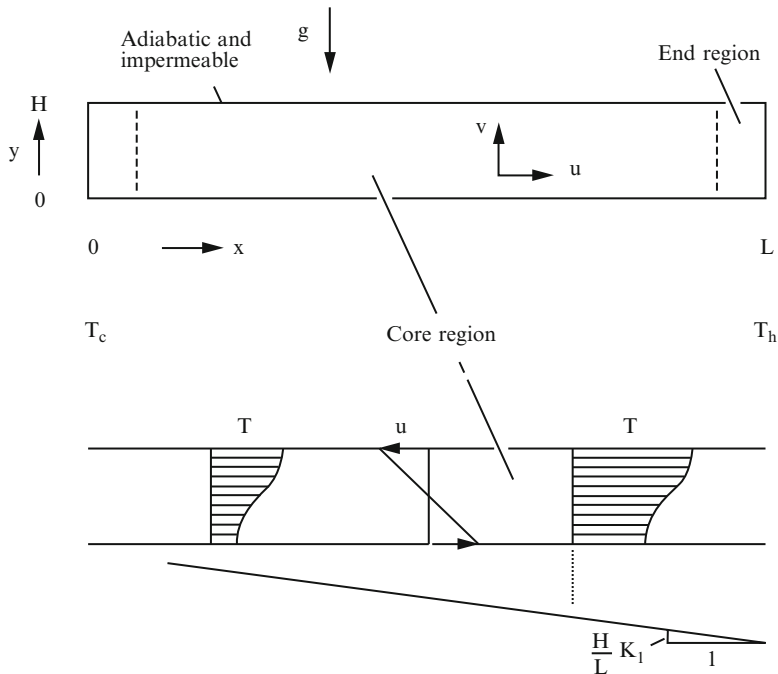


**Fig. 7.8** The structure of a horizontal porous layer subjected to an end-to-end temperature difference (Bejan and Tien 1978)

### 7.1.3 Shallow Layer

Like the high  $Ra$  regime III described in the preceding subsection, the natural convection in shallow layers (regime IV, Fig. 7.2) also can be characterized by heat transfer rates that are considerably greater than the heat transfer rate in the absence of a buoyancy effect. Regime IV differs from regime III in that the horizontal boundary layers are not distinct. The main characteristics of natural convection in a shallow layer are presented in Fig. 7.8: the vertical end layers are distinct and a significant temperature drop is registered across the “core,” that is, along the horizontal counterflow that occupies most of the length  $L$ .

The first studies of natural convection in shallow porous layers were published independently by Bejan and Tien (1978) and Walker and Homsy (1978). These studies showed that in the core region, the circulation consists of a purely horizontal counterflow:

$$u = -\frac{\alpha_m}{H} Ra \frac{H}{L} K_1 \left( y_* - \frac{1}{2} \right) \quad (7.41)$$

$$v = 0, \quad (7.42)$$

in which  $y_* = y/H$ . As shown in the lower part of Fig. 7.8, the core temperature varies linearly in the horizontal direction, while the degree of vertical thermal stratification is independent of  $x$ ,

$$\frac{T - T_c}{T_h - T_c} = K_1 \frac{x}{L} + K_2 + Ra \left( \frac{H}{L} \right)^2 K_1^2 \left( \frac{y_*^2}{4} - \frac{y_*^3}{6} \right). \quad (7.43)$$

The conduction-referenced Nusselt number for the total heat transfer rate from  $T_h$  to  $T_c$  is

$$Nu = \frac{q'}{k_m \Delta T / L} = K_1 + \frac{1}{120} K_1^3 \left( Ra \frac{H}{L} \right)^2. \quad (7.44)$$

Parameters  $K_1$  and  $K_2$  follow from matching the core flows (7.41), (7.42), and (7.43) to the vertical boundary layer flows in the two end regions. Bejan and Tien (1978) determined the function  $K_1(H/L, Ra)$  parametrically by matching the core solution to integral solutions for the end regions. Their result is given implicitly by the system of equations

$$\frac{1}{120} \delta_e Ra^2 K_1^3 \left( \frac{H}{L} \right)^3 = 1 - K_1, \quad (7.45)$$

$$\frac{1}{2} K_1 \frac{H}{L} \delta_e (\delta_e^{-2} - 1) = 1 - K_1, \quad (7.46)$$

in which  $\delta_e$  is the ratio end-region thickness/ $H$ . The Nusselt number based on this  $K_1$  function and (7.44) has been plotted in Fig. 7.9, next to the numerical results published subsequently by Hickox and Gartling (1981), who also reported representative patterns of streamlines and isotherms. Additional patterns can be seen in the paper by Daniels et al. (1986). In the infinitely shallow layer limit  $H/L \rightarrow 0$ , the horizontal counterflow accounts for the entire temperature drop from  $T_h$  to  $T_c$  and  $K_1$  approaches 1. In the same limit,  $Nu$  also approaches 1, cf. (7.44), with  $K_1 = 1$ :

$$Nu = 1 + \frac{1}{120} \left( Ra \frac{H}{L} \right)^2, \quad \left( \frac{H}{L} \rightarrow 0 \right). \quad (7.47)$$

It is important to note that the shallow-layer solution of Fig. 7.9 and (7.44), (7.45), (7.46), (7.47) approaches a proportionality of type  $Nu \sim (L/H)Ra^{1/2}$  as  $Ra$  increases, which is in agreement with the scaling law (7.17). That proportionality (Bejan and Tien 1978),

$$Nu = 0.508 \frac{L}{H} Ra^{1/2} \quad (Ra \rightarrow \infty), \quad (7.48)$$

is nearly identical to Weber's (1975b) solution (7.38) for the high  $Ra$  regime. In conclusion, the  $Nu(Ra, H/L)$  solution represented by (7.44), (7.45), (7.46), (7.47), and (7.48) and Fig. 7.9 is adequate for heat transfer calculations in both

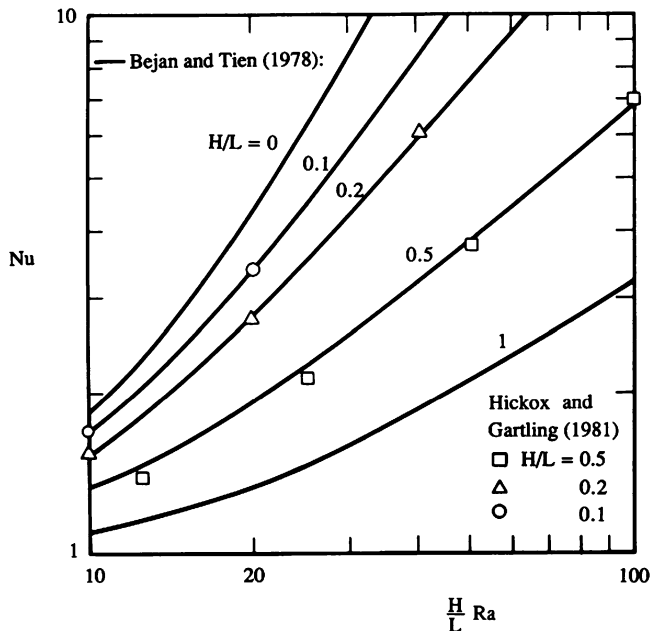


**Fig. 7.9** The heat transfer rate in a shallow porous layer with different temperatures (Bejan 1984)

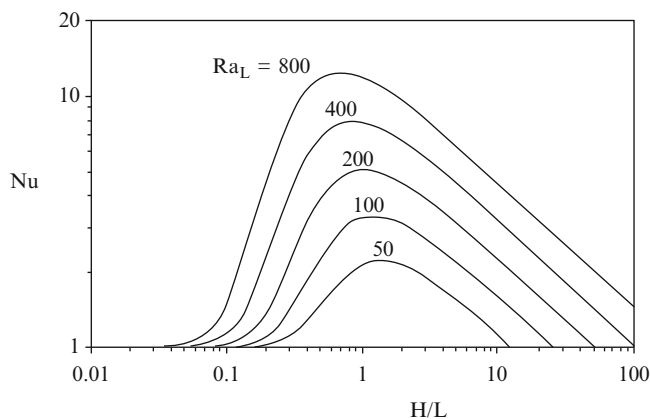


**Fig. 7.10** The effect of the height of the enclosure on the heat transfer rate through a porous layer heated from the side

shallow and tall layers, at low and high Rayleigh numbers. This conclusion is stressed further in Fig. 7.10, which shows the full effect of the aspect ratio when the Rayleigh number based on the horizontal dimension  $Ra_L = g\beta KL\delta T/\nu\alpha_m$  is fixed (Bejan 1980). The heat transfer rate reaches a maximum when the rectangular domain is nearly square.

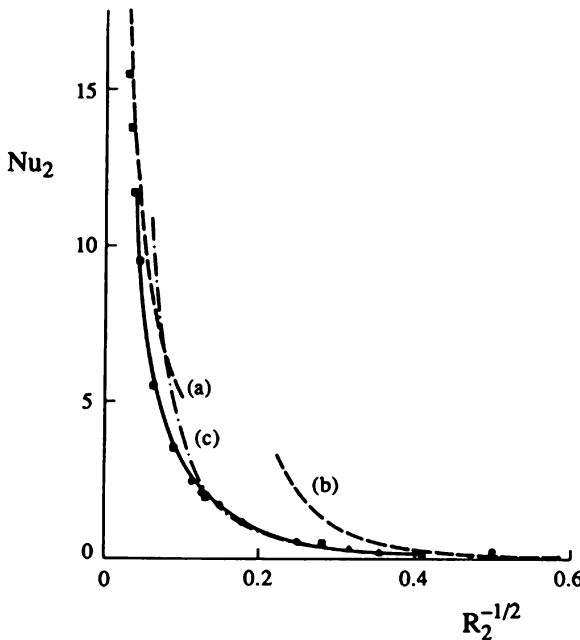


**Fig. 7.11** Variation of  $Nu_2 = NuH_2/L_2$  vs.  $R_2^{-1/2} = Ra^{-1/2}L/H$ . The solid line defines the merged-layer solution. Dashed lines show the asymptotic solutions (a)  $Nu_2 \sim 0.515R_2^{1/2}$ , (b)  $Nu_2 \sim R_2^2/120$ , and (c)  $Nu_2 \sim R_2^2/120(1 - 3\sigma_1 R_2)$  where  $\sigma_1 \approx -0.07$ . Results from numerical solutions by Hickox and Gartling (1981) and Prasad and Kulacki (1984b) are shown for various values of  $Ra$  and  $L/H$ : filled squares  $L/H = 2$ ; filled circles  $L/H = 5$ ; and filled triangles  $L/H = 10$  (Daniels et al. 1989)

This conclusion is relevant to the design of vertical double walls filled with fibrous or granular insulation held between internal horizontal partitions with the spacing  $H$ . In this design, the wall-to-wall spacing  $L$  is fixed while the number and positions of the horizontal partitions can change. The conclusion that the maximum heat transfer rate occurs when  $H$  is of order  $L$  also holds when the enclosure does not contain a porous matrix. In that case, the vertical spacing between partitions that corresponds to the maximum heat transfer rate is given approximately by  $H/L \sim 0.1-1$  (Bejan 1980).

Blythe et al. (1985b) and Daniels et al. (1989) have analyzed the merged-layer regime which is defined by  $L/H \rightarrow \infty$  at fixed  $R_2 = Ra H^2/L^2$ . In this limit the boundary layers on the horizontal walls merge and completely fill the cavity. The regime is characterized by a nonparallel core flow that provides the dominant structure over a wide range of  $R_2$  values. The use of  $R_2$  leads to the heat transfer correlation shown in Fig. 7.11. Further studies of shallow cavity flow, incorporating a stably stratified medium, were made by Daniels (2006, 2007). Hill (2006) also studied horizontal convection.

### 7.1.4 Stability of Flow

Gill (1969) showed that linear stability analysis using the Darcy equation with no inertial terms leads to the prediction that the basic flow produced by differential heating of the walls of a vertical slab of infinite height is stable. Georgiadis and Catton (1985) claimed that instability was predicted when one included the time-wise acceleration term in the momentum equation, but Rees (1988) showed that their analysis contained an error. The nonlinear analysis of Straughan (1988) predicts that the basic flow is stable provided that the initial disturbance is smaller than a certain threshold that is proportional to the inverse of the Rayleigh number.

The situation is dramatically changed when boundary friction is accounted for by means of the Brinkman equation. Kwok and Chen (1987) performed a linear stability analysis that led to predicted values  $Ra_c = 308.0$ ,  $\alpha_c = 2.6$  if viscosity variations are ignored and  $Ra_c = 98.3$ ,  $\alpha_c = 1.6$  if viscosity variations are taken into account. However, an extremely large (and perhaps physically unrealistic) temperature difference is required for instability according to linear stability theory. In their experiment they observed a value 66.2 for the critical Rayleigh number  $Ra_c$ , which is based on the width  $L$ . They did not measure the critical vertical wavenumber  $\alpha_c$ . The instability appears to be related to the fact that the basic vertical velocity profile is no longer linear. The disagreement between predicted and observed values of  $Ra_c$  presumably is due to the effect of porosity variation. A nonlinear analysis on the Brinkman model was performed by Qin and Kaloni (1993) for rigid or stress-free boundaries.

Riley (1988) has studied the effect of spatially periodic boundary imperfections. He found that out-of-phase imperfections enhance the heat transfer significantly.

The stability problem that arises for a rotating medium occupying a vertical slot, for which there is a horizontal body force due to the centrifugal acceleration and a positive temperature gradient in the same direction, was studied analytically by Vadasz (1994a). Convection in the form of superposed convection cells appears when a centrifugal Rayleigh number exceeds a certain value. Govender and Vadasz (1995) have shown that there is an analogy between this problem and natural convection in an inclined layer subject only to gravity. The results of experiments in a Hele-Shaw cell by Vadasz and Heerah (1998) showed qualitative agreement with the theory.

Rees and Lage (1996) considered a rectangular container where the impermeable bounding walls are held at a temperature that is a linearly decreasing function of height, the local temperature drop across the container being zero. They considered containers of finite aspect ratio and those of asymptotically large aspect ratio. For both cases, they found that modes bifurcate in pairs as the linear stability equations admit an infinite set of double eigenvalues. They analyzed the weakly nonlinear evolution of the primary pair of eigenmodes and found that the resulting steady-state flow is dependent on the form of the initial disturbance. For asymptotically tall boxes, their numerical and asymptotic analysis produced no evidence of persistently unsteady flow.

Kimura (1992) numerically studied convection in a square cavity with the upper half of a vertical wall cooled and the lower half heated, so that a cold current descends and fans out over a rising hot current. The unstable layer so formed appears to be associated with the onset of oscillations at  $Ra = 200$ . The effects of temperature-dependent thermal diffusivity and viscosity were included in a nonlinear stability analysis by Flavin and Rionero (1999).

The effect of local thermal nonequilibrium on the stability of convection in a vertical channel, heated and cooled from the sides, was investigated by Rees (2011). His energy stability analysis showed that the system remains unconditionally stable to small-amplitude disturbances. Further stability analysis in terms of stratification parameters was performed by Bahloul (2006).

### 7.1.5 Conjugate Convection

Conjugate convection in a rectangular cavity surrounded by walls of high relative thermal conductivity was examined by Chang and Lin (1994a). They reported that wall heat conduction effects decrease the heat transfer rate. The heat transfer through a vertical partition separating porous-porous or porous-fluid reservoirs at different temperatures was studied by Kimura (2003) on the basis of a simple one-dimensional vertically averaged model on the assumption that there is a linear increase in temperature in both of the reservoirs and the partition. He obtained results that are in general agreement with experiment. The steady-state heat transfer characteristics of a thin vertical strip with internal heat generation placed in a porous medium was studied by Méndez et al. (2002). A conjugate convection problem involving a thin vertical strip of finite length, placed in a porous medium, was studied by Martínez-Suásteegui et al. (2003) using numerical and asymptotic techniques. A conjugate convection problem in a square cavity with horizontal conductive walls of finite thickness was studied numerically by Baytas et al. (2001). Mohamad and Rees (2004) have examined numerically conjugate convection in a porous medium attached to a wall held at a constant temperature. Conjugate convection in a vertical layer of a box sandwiched by walls of finite thickness was studied by Saeid (2007a, d, 2008), with the last paper treating thermal non-equilibrium. Unsteady convection in a square enclosure was examined by Aleshkova and Sheremet (2010). A steady-state problem was studied by Al-Amiri et al. (2008).

### 7.1.6 Non-Newtonian Fluid

Convection in a rectangular cavity filled by a non-Newtonian power-law fluid was studied theoretically and numerically by Getachew et al. (1996). They employed scaling arguments to delineate heat transfer regimes analogous to those discussed in

Sect. 7.1.1 and verified their results using numerical calculations. A numerical study on the Brinkman-Forchheimer model was carried out by Hadim and Chen (1995). A further numerical study, using the boundary element method, was reported by Jecl and Skerget (2003). A numerical study of flow involving a couple-stress fluid was published by Umapathi and Malashetty (1999), but the authors did not explain how the couple stress is maintained on the scale of a representative elementary volume. The effect of the macroscopic inertial term was highlighted by Abuzaid et al. (2005). Beg et al. (2008a) investigated the case of a third grade viscoelastic fluid. Hayat et al. (2011c) treated a Maxwell fluid with MHD and radiation effects.

### 7.1.7 Other Situations

Convective heat transfer through porous insulation in a vertical slot with leakage of mass at the walls was analyzed by Burns et al. (1977). The effects of pressure stratification on multiphase transport across a vertical slot were studied by Tien and Vafai (1990b). The sidewall heating in shallow cavities with icy water was treated by Leppinen and Rees (2004). They considered a case in which the density maximum occurs somewhere between the sidewalls, and they treated the situation using asymptotic analysis valid in the limit of vanishing aspect ratio and Rayleigh number of  $O(1)$ . In this case the flow is divided into two counterrotating cells whose size depends on the temperature giving the density maximum and the temperatures of the sidewalls. Icy water was treated in terms of heatlines by Varol et al. (2010b). The heatline approach was also employed by Kaluri et al. (2009), Kaluri and Basak (2010b), and Waheed (2009). A study of entropy production for an MHD situation was made by Mahmud and Fraser (2004b). Further studies involving entropy production were carried out by Kaluri and Basak (2010a, 2011a). Thermal convection in a vertical slot with a spatially periodic thermal boundary condition was analyzed by Yoo (2003). Numerical studies of various problems involving lateral heating of square cavities were reported by Nithiarasu et al. (1999a, b, 2002). The effect of local thermal nonequilibrium was included in the studies by Rees et al. (2008a) (with injection of hot fluid), Slimi (2009) (with radiation), Vadasz (2011c) and Foudi et al. (2012) (experimentally). 3D convection in a vertical channel was studied by Guria et al. (2009). A problem involving sinusoidal g-jitter was investigated by Ghosh and Ghosh (2009). Developing convective gas flow in an open-ended vertical channel was treated by Haddad et al. (2005b). The lattice Boltzmann method was applied to an open-ended square cavity by Haghshenas et al. (2010). A partly open cavity was examined by Oztop et al. (2011b). For system of equations modeling differentially heated sidewalls and with a thermal source, Akyildiz et al. (2012) have obtained some existence, uniqueness, and concavity results. The effect of anisotropy in a rectangular slab was studied by Chandra and Samurty (2012). The feedback control of flows in a square enclosure with nonuniform internal heating was treated by Saleh et al. (2012). Costa et al. (2012) studied convection in square enclosures under the influence of a magnetic field induced by two parallel vertical electric currents.

## 7.2 Sidewalls with Uniform Flux and Other Thermal Conditions

In the field of thermal insulation engineering, a more appropriate description for the side heating of the porous layer is the model where the heat flux  $q''$  is distributed uniformly along the two sidewalls. In the high Rayleigh number regime (regime III, Fig. 7.2), the overall Nusselt number is given by (Bejan 1983b)

$$Nu = \frac{q''H}{k_m H \overline{\Delta T} / L} = \frac{1}{2} \left( \frac{L}{H} \right)^{4/5} Ra_*^{2/5}. \quad (7.49)$$

In this  $Nu$  definition,  $\overline{\Delta T}$  is the height-averaged temperature difference that develops between the two sidewalls,  $(\bar{T}_h - \bar{T}_c)$ , while  $Ra_*$  is the Rayleigh number based on heat flux,

$$Ra_* = \frac{g \beta K H^2 q''}{\nu \alpha_m k_m}. \quad (7.50)$$

Formula (7.49) is based on a matched boundary layer analysis that combines Weber's (1975b) approach with the zero energy flow condition for the top and bottom boundaries of the enclosure (Bejan 1979). The solution obtained also showed that:

- (a) The vertical boundary layers have a constant thickness of order  $HRa_*^{-1/3}$ .
- (b) The core region is motionless and linearly stratified, with a vertical temperature gradient equal to  $(q''/k_m)Ra_*^{-1/5}(H/L)^{2/5}$ .
- (c) The temperature of each sidewall increases linearly with altitude at the same rate as the core temperature, and so the local temperature difference between the sidewalls is independent of altitude.
- (d) In any horizontal cut through the layer, there exists an exact balance between the net upflow of enthalpy and the net downward heat conduction.

The conditions that delineate the parametric domain in which (7.49) and regime III are valid are  $Ra_*^{-1/3} < H/L < Ra_*^{1/3}$ . This solution and the special flow features revealed by it are supported by numerical experiments performed in the range  $100 = Ra = 5,000$  and  $1 = H/L = 10$ , which also are reported in Bejan (1983b).

The heat transfer by Darcy natural convection in a two-dimensional porous layer with uniform flux along one side and uniform temperature along the other side was investigated numerically by Prasad and Kulacki (1984a). Their set of thermal boundary conditions is a cross between those of Weber (1975b) and Bejan (1983b). The corresponding heat transfer process in a vertical cylindrical annulus with uniform heat flux on the inner wall and uniform temperature on the outer wall was studied experimentally by Prasad et al. (1986) and numerically by Prasad (1986). Dawood and Burns (1992) used a multigrid method to deal with three-dimensional convective heat transfer in a rectangular parallelepiped. Convection in a square

cavity, with one sidewall heated and the other cooled, with the heated wall assumed to have a spatial sinusoidal temperature variation about a constant mean value, was treated numerically by Saeid and Mohamad (2005b).

An analytical and numerical study of the multiplicity of steady states that can arise in a shallow cavity was made by Kalla et al. (1999). The linear stability of the natural convection that arises in either a tall or shallow cavity was analyzed by Prud'homme and Bougerara (2001) and Prud'homme et al. (2003). Inverse problems, requiring the determination of an unknown sidewall flux, were treated by Prud'homme and Jasmin (2001) and Prud'homme and Nguyen (2001). Various boundary conditions were examined by Basak et al. (2006) and Zahmatkesh (2008). The effect of radiation was included by Badruddin et al. (2006b, 2007b) (with viscous dissipation and thermal nonequilibrium). A problem involving discrete heating was studied by Sivasankaran et al. (2011). An experimental study of the dynamic behavior of a porous medium submitted to a wall heat flux in view of the thermal energy storage by sensible heat was carried out by Dhifaoui et al. (2007). Sakamoto and Kulacki (2007) reported measurements of heat transfer coefficients in steady convection on a vertical constant-flux plate. Various asymmetric boundary conditions were studied by Zueco et al. (2011a, b).

## 7.3 Other Configurations and Effects of Property Variation

### 7.3.1 Internal Partitions

The effect of horizontal and vertical internal partitions on natural convection in a porous layer with isothermal sidewalls was investigated numerically by Bejan (1983a). As an example, Fig. 7.12 shows the effect of a horizontal partition on the flow and temperature fields in regime III. In Fig. 7.12a the partition is absent and natural circulation is clearly in the boundary layer regime. When the horizontal midlevel partition is complete, the heat transfer rate decreases in predictable fashion as the height of each vertical boundary layer drops from  $H$  in Fig. 7.12a to  $H/2$  in Fig. 7.12c. With the horizontal partition in place, the Nusselt number continues to scale as in (7.17); however, this time  $H/2$  replaces  $H$ , and the Rayleigh number is based on  $H/2$ .

The insulation effect of a complete midplane vertical partition is illustrated in Fig. 7.13. The partition reduces the overall heat transfer rate by more than 50% as the Rayleigh number increases and vertical boundary layers form along all the vertical boundaries. This change can be expected in an order-of-magnitude sense: relative to the original system (without partitions), which has only two vertical boundary layers as thermal resistances between  $T_h$  and  $T_c$ , the partitioned system ( $Nu_v$  in Fig. 7.13) has a total of four thermal resistances. The two additional resistances are associated with the conjugate boundary layers that form on the two sides of the partition.

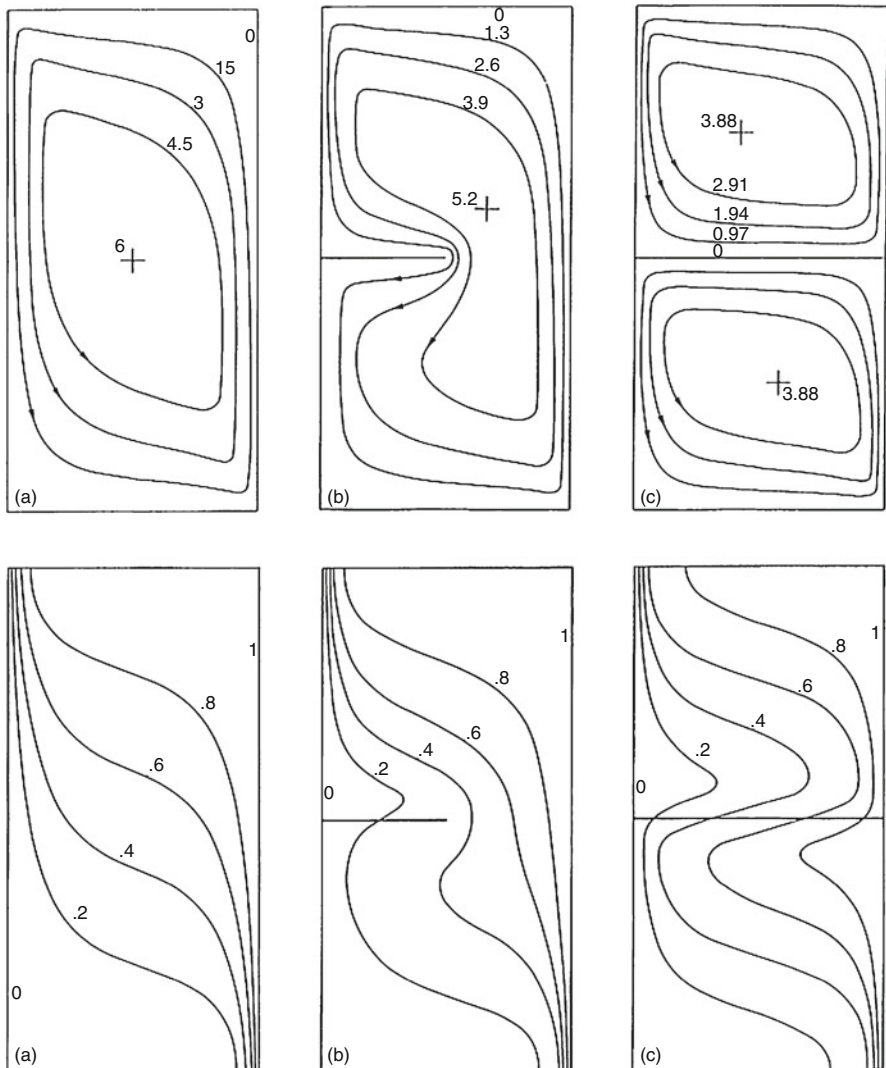


**Fig. 7.12** Streamlines and isotherms in a porous layer with a horizontal diathermal partition ( $Ra = 400, H/L = 2$ ) (Bejan 1983a)

The thermal insulation effect associated solely with the conjugate boundary layers has been documented in Bejan and Anderson (1981) and in Sect. 5.1.5 of this book. Mbaye and Bilgen (1992, 1993) have studied numerically steady convection in a solar collector system that involves a porous wall. Analysis of variable-spaced embedded plates was conducted by Beithou (2008).

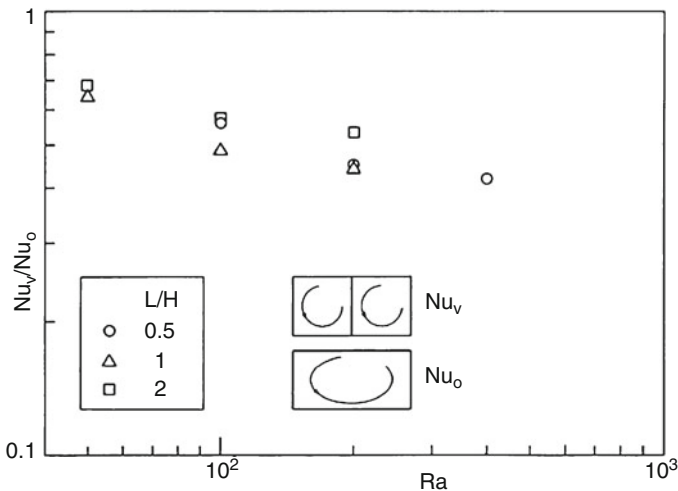


**Fig. 7.13** The reduction in overall heat transfer rate caused by a vertical diathermal partition (Bejan 1983a)

### 7.3.2 Effects of Heterogeneity and Anisotropy

The preceding results apply to situations in which the saturated porous medium can be modeled as homogeneous. Poulikakos and Bejan (1983a) showed that the nonuniformity of permeability and thermal diffusivity can have a dominating effect on the overall heat transfer rate. For example, if the properties vary so much that the porous layer can be modeled as a vertical sandwich of vertical sublayers of different permeability and diffusivity (Fig. 7.14a), an important parameter is the ratio of the peripheral sublayer thickness ( $d_1$ ) to the thermal boundary layer thickness ( $\delta_1$ ) based on the properties of the  $d_1$  sublayer. Note that according to (7.14),  $\delta_1$  scales as  $HRa_1^{-1/2}$ , where  $Ra_1 = g\beta K_1 H(T_h - T_c)/\nu\alpha_{m,1}$  and the subscript 1 represents the properties of the  $d_1$  sublayer.

If the sublayer situated next to the right wall ( $d_N$ ) has the same properties as the  $d_1$  sublayer, and if  $\delta_1 < d_1$  and  $\delta_N < d_N$ , then the overall heat transfer rate can be estimated with the methods of Sect. 7.1 provided both  $Nu$  and  $Ra$  are based on the properties of the peripheral layers. An example of this kind is illustrated numerically in Fig. 7.15, where there are only three sublayers ( $N = 3$ ), and the permeability of the core is five times greater than the permeability of the peripheral sublayers. The permeable core seems to “attract” the flow; this property renders the streamlines and isotherms almost horizontal and results in a vertically stratified core.

When the porous medium inhomogeneity is such that the  $H \times L$  system resembles a sandwich of  $N$  horizontal sublayers (Fig. 7.14b), the overall Nusselt number in the convection-dominated regime is approximated by the correlation (Poulikakos and Bejan 1983a)

**Fig. 7.14** Layered porous media heated from the side: vertical sublayers (a) and horizontal sublayers (b)

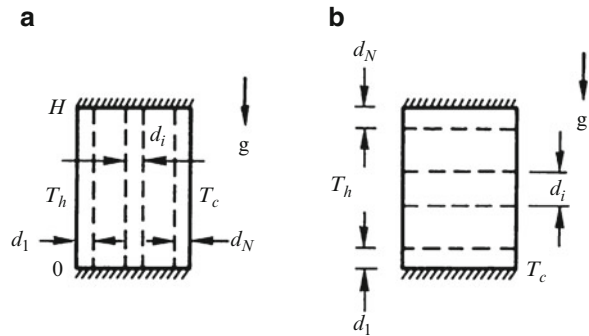
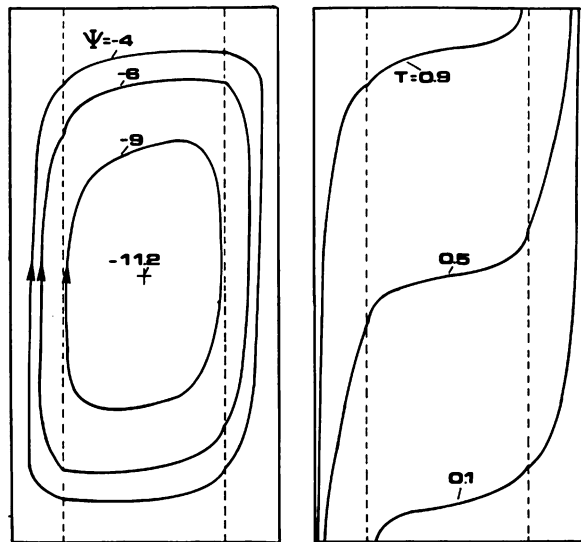


**Fig. 7.15** Streamlines and isotherms in a sandwich of three vertical porous layers heated from the side ( $Ra_1 = 200$ ,  $H/L = 2$ ,  $K_2/K_1 = 5$ ,  $K_1 = K_3$ ,  $N = 3$ , and  $\alpha_{m,1} = \alpha_{m,2} = \alpha_{m,3}$ )  
(Poulikakos and Bejan 1983a)



$$Nu \sim 2^{-3/2} Ra_1^{1/2} \frac{L}{H} \sum_{i=1}^N \frac{k_i}{k_1} \left( \frac{K_i d_i \alpha_{m,i}}{K_1 d_1 \alpha_{m,1}} \right)^{1/2}, \quad (7.51)$$

where both  $Nu$  and  $Ra_1$  are based on the properties of the bottom sublayer ( $d_1$ ). This correlation was tested numerically in systems that contain two sublayers ( $N = 2$ ). A sample of the computed streamlines and isotherms is presented in Fig. 7.16, for a case in which the upper half of the system is five times more permeable than the lower half. This is why the upper half contains most of the circulation. The discontinuity exhibited by the permeability  $K$  across the horizontal midplane causes cusps in the streamlines and the isotherms. The effect of nonuniformities in the thermal diffusivity of the porous medium in the two configurations of Fig. 7.14 also has been documented by Poulikakos and Bejan (1983a). A boundary layer analysis for a medium vertically layered in permeability was reported by Masuoka (1986).

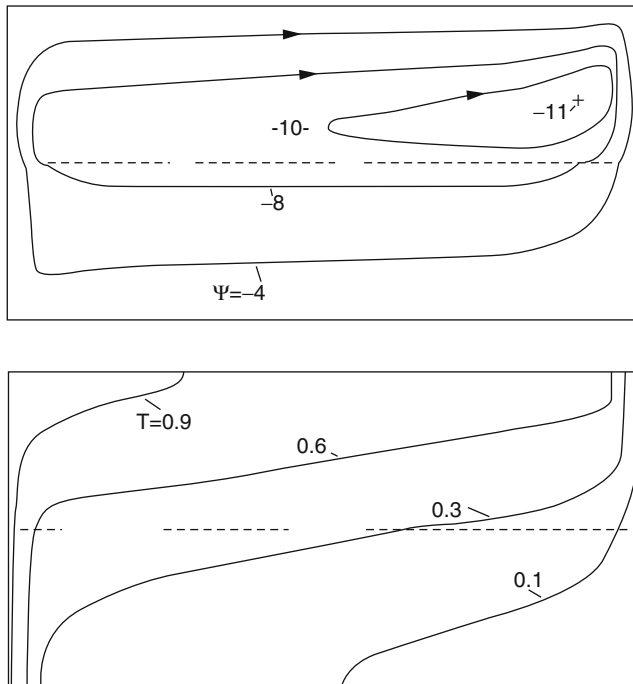


**Fig. 7.16** Streamlines and isotherms in a sandwich of two horizontal porous layers heated from the side ( $Ra_1 = 150$ ,  $H/L = 0.5$ ,  $K_2/K_1 = 5$ ,  $N = 2$ , and  $\alpha_{m,1} = \alpha_{m,2}$ ) (Poulikakos and Bejan 1983a)

In all the geometries discussed so far in this chapter, the walls that surrounded the saturated porous medium were modeled as impermeable. As a departure from the classic problem sketched in Fig. 7.8, the heat transfer through a shallow porous layer with both end surfaces permeable was predicted by Bejan and Tien (1978). Their theory was validated by subsequent laboratory measurements and numerical solutions conducted for  $Ra$  values up to 120 (Haajizadeh and Tien 1983).

Lai and Kulacki (1988c) discussed convection in a rectangular cavity with a vertical permeable interface between two porous media of permeabilities  $K_1$ ,  $K_2$  and thermal conductivity  $k_1$ ,  $k_2$ , respectively. The first medium was bounded by a heated face at constant heat flux and the second was bounded by a cooled isothermal face. The results of their calculations are generally in line with our expectations based on the material discussed in Sect. 6.13, but their finding of the existence of a second recirculating cell when  $K_1/K_2 < 1$ ,  $k_1/k_2 < 1$  is very surprising. A similar situation was treated numerically by Merrikh and Mohamad (2002). A cavity with variable porosity and Darcy number was studied by Oliveski and Macrzak (2008).

Ni and Beckermann (1991a) have computed the flow in an anisotropic medium occupying a square enclosure. The horizontal permeability is denoted by  $K_x$  and the vertical permeability by  $K_y$ , and  $k_x$ ,  $k_y$  are the corresponding thermal conductivities.

Relative to the situation when the medium is isotropic with permeability  $K_x$  and thermal conductivity  $k_x$ , large  $K_y/K_x$  causes channeling along the vertical (isothermal) walls, a high flow intensity, and consequently a higher heat transfer rate  $Nu$  across the enclosure. Similarly, small  $K_y/k_x$  causes channeling along the horizontal (adiabatic) boundaries and a smaller  $Nu$ . Large  $k_y/k_x$  causes a higher flow intensity and a smaller  $Nu$ , but small  $k_y/k_x$  has very little effect on the heat transfer pattern. The effect of anisotropy has also been treated by Kumar and Bera (2009) (with nonuniform heating of the bottom wall) and by Krishna et al. (2009) (with a finite heat source at the bottom wall).

Non-Boussinesq variable-property effects were studied numerically by Peirotti et al. (1987) for the case of water or air. They found that these had a considerable impact on  $Nu$ . Kimura et al. (1993) presented an analysis, based on a perturbation method for small  $Ra$ , a rectangular cavity with anisotropy of permeability and thermal diffusivity. A numerical study for a rectangular cavity with a wall conduction effect and for anisotropic permeability and thermal diffusivity was performed by Chang and Lin (1994b). Degan et al. (1995) have treated analytically and numerically a rectangular cavity, heated and cooled with constant heat flux from the sides, with principal axes for permeability oblique to gravity and those for thermal conductivity aligned with gravity. They found that a maximum (minimum) heat transfer rate is obtained if the high permeability axis is parallel (perpendicular) to gravity and that a large thermal conductivity ratio causes a higher flow intensity but a lower heat transfer. Degan and Vasseur (1996, 1997) and Degan et al. (1998a, b) presented a boundary layer analysis for the high  $Ra$  version of this problem and a numerical study on the Brinkman model. Egorov and Polezhaev (1993) made a comprehensive theoretical (Darcy model) and experimental study for the anisotropic permeability problem. They found good agreement between their numerical results and experimental data for multilayer insulation. Vasseur and Robillard (1998) reviewed the anisotropy aspects. The case of icy water was studied by Zheng et al. (2001). Further theoretical work, supplemented by experiments with a Hele-Shaw cell, was reported by Kimura and Okajima (2000) and Kimura et al. (2000).

Marvel and Lai (2010a, b) studied in turn anisotropic and heterogeneous media with nonuniform layering. Singh et al. (2011) analyzed asymmetric/heating/cooling of the walls of a vertical channel for unsteady hydromagnetic flow.

### 7.3.3 *Cylindrical or Annular Enclosure*

#### 7.3.3.1 *Horizontal Cylinder*

Related to the two-dimensional convection phenomenon discussed so far in this chapter is the heat transfer through a porous medium confined by a horizontal cylindrical surface (Fig. 7.17a). The disk-shaped ends of the system are maintained at different temperatures. A parametric solution for heat transfer in this geometry was reported by Bejan and Tien (1978). The corresponding phenomenon in the

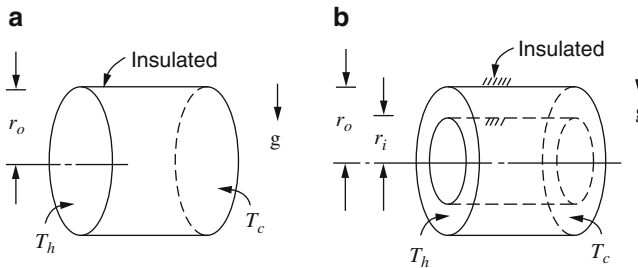


**Fig. 7.17** Confined porous medium with different end temperature: horizontal cylindrical enclosure (a) and horizontal cylindrical enclosure with annular cross section (b)

porous medium between two horizontal concentric cylinders with different temperatures (Fig. 7.17b) was analyzed by Bejan and Tien (1979). A further investigation was made by Siraev and Yakushin (2008).

### 7.3.3.2 Vertical Cylinder

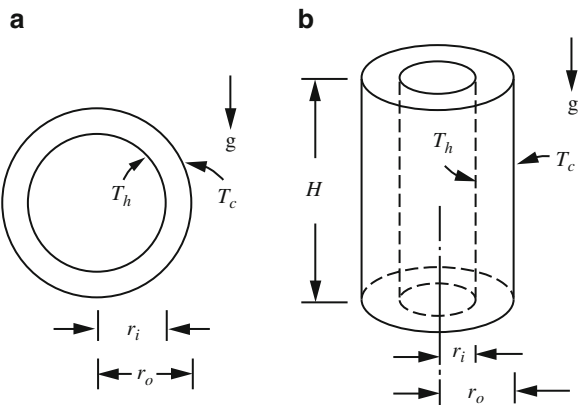
Rao and Wang (1991) studied both low and high  $Ra$  convection induced by internal heat generation in a vertical cylinder. Convection at large  $Ra$  is characterized by a homogeneous upward flow in the central part of the cylinder and a thin downward boundary layer at the cooled wall, with the effect of curvature of the boundary being negligible. This means that after introduction of a change of variable, the results can be applied to enclosures with other than circular boundaries. Chang and Hsiao (1993) studied numerically convection in a vertical cylinder filled with an anisotropic medium with uniform high temperature on all boundaries except the cooler bottom. Lyubimov (1993) summarized earlier Soviet work on the bifurcation analysis of two-dimensional convection in a cylinder of arbitrary shape, with the temperature specified on the boundary. The onset of convection in a vertical cylinder with a conducting wall was analyzed by Haugen and Tyvand (2003). Transient convection in a vertical cylinder with suddenly imposed or time-periodic wall heat flux was studied numerically by Slimi et al. (1998) and Amara et al. (2000). Transient convection in a vertical channel with the effect of radiation was studied numerically by Slimi et al. (2004).

Further studies for a vertical cylinder were conducted by Ameziani et al. (2008), Degan et al. (2007b) (with anisotropy), Tada and Ichimiya (2007a), and Zueco et al. (2009b) (network numerical analysis, magneto-micropolar fluid).

### 7.3.3.3 Horizontal Annulus

A basic configuration in the field of thermal insulation engineering is the horizontal annular space filled with fibrous or granular material (Fig. 7.18a). In this configuration the heat transfer occurs between the two concentric cylindrical surfaces of radii

**Fig. 7.18** Radial heat transfer: horizontal cylindrical annulus or spherical annulus (a) and vertical cylindrical annulus (b)



$r_i$  and  $r_o$ , unlike in Fig. 7.17b where the cylindrical surfaces were insulated. Experimental measurements and numerical solutions for the overall heat transfer rate in the geometry of Fig. 7.18a have been reported by Caltagirone (1976b), Burns and Tien (1979), and Facas and Farouk (1983). The data of Caltagirone (1976b) in the range  $1.19 \leq r_o/r_i \leq 4$  were correlated by Bejan (1987) on the basis of the scale-analysis procedure described in Bejan (1984, p. 194):

$$Nu = \frac{q'}{q'_c} \cong 0.44 Ra_{r_i}^{1/2} \frac{\ln(r_o/r_i)}{1 + 0.916(r_i/r_o)^{1/2}}. \quad (7.52)$$

In the definition of the overall Nusselt number, the denominator is the conduction heat transfer rate  $q'_c = 4\pi k_m (T_h - T_c) / \ln(r_o/r_i)$ . The Rayleigh number is based on the inner radius,  $Ra_{r_i} = g\beta K_r (T_h - T_c) / \nu \alpha_m$ . The correlation (7.52) is valid in the convection-dominated regime, that is, when  $Nu \gg 1$ .

Transitions in the flow field in a horizontal annulus have been analyzed using a Galerkin method by Rao et al. (1987, 1988). As  $Ra$  is increased, two-dimensional modes with one, two, and three cells on each side of the annulus appear in succession, and the average Nusselt number increases with the number of cells. The extra cells appear near the top of the annulus. Three-dimensional modes also are possible with secondary flows in which the streamlines form a coaxial double helix, and these produce enhancement of the overall heat transfer resulting from a higher maximum local heat transfer rate in the upper part of the annulus.

Himasekhar and Bau (1988b) made a detailed bifurcation analysis for radii ratio values, 2,  $2^{1/2}$ ,  $2^{1/4}$ , and  $2^{1/8}$ . Barbosa Mota and Saatdjian (1994, 1995) reported accurate numerical solutions for the Darcy model. For a radius ratio above 1.7 and for Rayleigh numbers above a critical value, they observed a closed hysteresis curve, indicating two possible solutions (two- or four-cell pattern) depending on initial conditions. For a radius ratio below 1.7 and as  $Ra$  is increased, the number of cells in the annulus increases without bifurcation and no hysteresis is observed. For very small radius ratios, steady-state regimes containing 2, 4, 6, and 8 cells are obtained in succession. For a radius ratio of 2, they found good agreement with experiment.

Charrier-Mojtabi and Mojtabi (1994, 1998) and Charrier-Mojtabi (1998) have numerically investigated both two- and three-dimensional flows for the Darcy model. They found that three-dimensional spiral flows are described in the vicinity of the transition from two-dimensional unicellular flows. They determined numerically the bifurcation points between two-dimensional unicellular flows and either two-dimensional multicellular flows or three-dimensional flows. Linear and non-linear stability analyses were also performed by Charrier-Mojtabi and Mojtabi (1998). These show that subcritical instability becomes increasingly likely as the radius ratio increases away from the value unity. For the cases of either isothermal or convective boundary conditions, Rajamani et al. (1995) studied the effects of both aspect ratio and radius ratio. They found that  $Nu$  always increases with radius ratio and  $Ra$  and it exhibits a maximum when the aspect ratio is about unity, the maximum shifting toward lesser aspect ratios as  $Ra$  increases.

For the case of the Darcy model and small dimensionless gap width  $\varepsilon = (r_i - r_o)/r_i$ , Mojtabi and Charrier-Mojtabi (1992) obtained an approximate analytical solution leading to the formula

$$Nu = 1 + \frac{17}{40320} Ra^2 (\varepsilon^2 - \varepsilon^3), \quad (7.53)$$

where

$$Ra = g\beta K(T_i - T_o)(r_i - r_o)/\nu\alpha_m. \quad (7.54)$$

A development up to order  $\varepsilon^{15}$  was given by Charrier-Mojtabi and Mojtabi (1998). Convection in a horizontal annulus with vertical eccentricity has been analyzed by Bau (1984a, c) for small  $Ra$  and by Himasekhar and Bau (1986) for large  $Ra$  for the case of steady two-dimensional flow. At low  $Ra$  there is an optimum eccentricity that minimizes the heat transfer, but generally the heat transfer decreases with eccentricity, independently of whether the heated inner cylinder is centered below or above the axis of the cooled outer cylinder. Highly accurate computations for this problem were reported by Barbosa Mota et al. (1994). A transient convection problem in an elliptical horizontal annulus was reported by Chen et al. (1990). A further numerical study of convection in such annuli was reported by Mota et al. (2000).

Conjugate convection in a horizontal annulus was studied by Kimura and Pop (1991, 1992a). In their first paper they had isothermal boundaries but with a jump in heat flux at the fluid–solid interface, while in their second paper they used a Forchheimer model to study the case of the inner surface maintained at one temperature and the outer at a lower temperature.

Effects of rotation about the axis of a horizontal annulus were studied by Robillard and Torrance (1990) and Aboubi et al. (1995a). The former treated weak rotation, which generates a circulation relative to the solid matrix and thereby reduces the overall heat transfer. The latter examined the effect of a centrifugal force field for the case when the outer boundary is heated by a constant heat flux

while the inner boundary is insulated. They performed a linear stability analysis and finite amplitude calculations which indicated the existence of multiple solutions differing by the number of cells involved.

Pan and Lai (1995, 1996) studied convection in a horizontal annulus with two subannuli for different permeabilities. They corrected (by satisfying the interface conditions more closely) the work by Muralidhar et al. (1986), thereby producing better agreement with experimental data. They noted that using a harmonic average permeability gives a better approximation to  $Nu$  than does an arithmetic average. Convection in a horizontal annulus with azimuthal partitions was studied numerically by Nishimura et al. (1996). Aboubi et al. (1995b) studied numerically convection in a horizontal annulus filled with an anisotropic medium, with principal axes of permeability inclined to the vertical. Three-dimensional anisotropy was incorporated into the model studied by Bessonov and Brailovskaya (2001). Convective flow driven by a constant vertical temperature gradient in a horizontal annulus was analyzed by Scurtu et al. (2001).

The case of a medium of variable permeability was treated by Aldoss (2009). A partly filled horizontal annulus was studied by Khanafer et al. (2008), Kiwan and Zeitoun (2008) (fins), and Saada et al. (2009, 2010). Gas convection was examined by Ramazanov (2010). Unsteady convection was considered by Kumari and Nath (2008).

### 7.3.3.4 Vertical Annulus

The heat transfer through an annular porous insulation oriented vertically (Fig. 7.18b) was investigated numerically by Havstad and Burns (1982), Hickox and Gartling (1985), and Prasad and Kulacki (1984c, 1985), and experimentally by Prasad et al. (1985). Havstad and Burns (1982) correlated their results with the five-constant empirical formula

$$Nu \cong 1 + a_1 \left[ \frac{r_i}{r_o} \left( 1 - \frac{r_i}{r_o} \right) \right]^{a_2} Ra_{r_o}^{a_4} \left( \frac{H}{r_o} \right)^{a_5} \exp \left( -a_3 \frac{r_i}{r_o} \right), \quad (7.55)$$

in which

$$\begin{aligned} a_1 &= 0.2196, \quad a_4 = 0.9296, \\ a_2 &= 1.334, \quad a_5 = 1.168 \\ a_3 &= 3.702, \quad Ra_{r_o} = g\beta Kr_o(T_h - T_c)/\nu\alpha_m \end{aligned} \quad (7.56)$$

The overall Nusselt number is defined as in (7.52),  $Nu = q/q_c$ , where  $q_c = 2\pi k_m H(T_h - T_c)/\ln(r_o/r_i)$ . The above correlation fits the numerical data in the range  $1 = H/r_o = 20$ ,  $0 = Ra_{r_o} < 150$ ,  $0 < r_i/r_o = 1$ , and  $1 < Nu < 3$ .

For the convection-dominated regime (high Rayleigh numbers and  $Nu \gg 1$ ), the scale analysis of the boundary layers that form along the two cylindrical surfaces of Fig. 7.18b recommends the following correlation (Bejan 1987):

$$Nu = c_1 \frac{\ln(r_o/r_i)}{c_2 + r_o/r_i} \frac{r_o}{H} Ra^{1/2}. \quad (7.57)$$

The Nusselt number is defined as in (7.52), and the Rayleigh number is based on height,  $Ra = g\beta KH(T_h - T_c)/v\alpha_m$ . Experimental and numerical data are needed in the convection regime ( $Nu \gg 1$ ) in order to determine the constants  $c_1$  and  $c_2$ . Havstad and Burns' (1982) data cannot be used because they belong to the intermediate regime  $1 < Nu < 3$  in which the effect of direct conduction from  $T_h$  to  $T_c$  is not negligible.

The experimental and numerical study of Reda (1986) treated a two-layered porous medium in a vertical annulus, with constant heat flux on the inner cylinder and constant temperature on the outer. Quasisteady convection in a vertical annulus, with the inner wall heated by a constant heat flux and the other walls adiabatic, was treated analytically and numerically by Hasnaoui et al. (1995). Also for a vertical annulus, Marpu (1995), Dharma Rao et al. (1996), and Satya Sai et al. (1997a) reported on numerical studies on the Brinkman-Forchheimer model. An asymptotic analysis for a shallow vertical annulus was presented by Pop et al. (1998b) and Leppinen et al. (2004). Passive heat transfer augmentation in an annulus was studied by Iyer and Vafai (1999). The effect of local thermal nonequilibrium in convection in a vertical annulus was studied by Deibler and Bortolozzi (1998) and Bortolozzi and Deibler (2001). A numerical study of transient convection in a vertical annulus was reported by Shivakumara et al. (2002). Convection in a vertical annulus with an isothermal outer boundary and with a mixed inner boundary condition was treated by Jha (2005). Conjugate convection from a vertical cylindrical fin in a cylindrical enclosure was studied numerically by Naidu et al. (2004b). Convection in an elliptical vertical annulus was studied numerically by Saatdjian et al. (1999). The Brinkman model was employed by Rossi di Schio et al. (2011). Discrete heating was investigated by Sankar et al. (2011b). An anisotropic medium was studied by Thansekhar et al. (2009).

Badruddin et al. (2006a) studied the effect of thermal nonequilibrium. The effect of viscous dissipation and radiation was studied by Badruddin et al. (2007a). The use of porous inserts in a vertical annulus was treated by Kiwan and Alzahrany (2008). Heat generation in a porous annulus was studied by Reddy and Narasimhan (2010). The case of an annulus between square cylinders was treated by Badruddin et al. (2012).

### 7.3.4 Spherical Enclosure

Another geometry that is relevant to the design of thermal insulations is the porous medium shaped as a spherical annulus (Fig. 7.18a). Heat is transferred radially between the two spherical walls that hold the porous material. Numerical heat

transfer results for discrete values of the Rayleigh number and the geometric ratio  $r_i/r_o$  have been reported graphically by Burns and Tien (1979). From that set, the data that correspond to the convection-dominated regime were correlated based on scale analysis by Bejan (1987),

$$Nu = \frac{q}{q_c} \cong 0.756 Ra_{r_i}^{1/2} \frac{1 - r_i/r_o}{1 + 1.422(r_i/r_o)^{3/2}}. \quad (7.58)$$

The definitions used in (7.58) are  $q_c = 4\pi k_m(T_h - T_c)/(r_i^{-1} - r_o^{-1})$  and  $Ra_{r_i} = g\beta K r_i (T_h - T_c)/\nu\alpha_m$ . The correlation (7.56) agrees within two percent with Burns and Tien's (1979) data for the convection regime represented by  $Nu \gtrsim 1.5$ .

It is interesting to note that the scaling-correct correlation (7.58) can be restated in terms of the Rayleigh number based on insulation thickness,

$$Ra_{r_o-r_i} = \frac{g\beta K (r_o - r_i)(T_h - T_c)}{\nu\alpha_m}. \quad (7.59)$$

The resulting expression that replaces (7.58) is

$$Nu \cong 0.756 Ra_{r_o-r_i}^{1/2} \frac{[r_i/r_o - (r_i/r_o)^2]^{1/2}}{1 + 1.422(r_i/r_o)^{3/2}}. \quad (7.60)$$

This form can be differentiated to show that when  $Ra_{r_o-r_i}$  is fixed, the overall heat transfer rate ( $Nu$ ) reaches a maximum value when  $r_i/r_o = 0.301$ . The existence of such a maximum was noted empirically by Burns and Tien (1979). An explanation for this maximum is provided by the boundary layer scale analysis on which the correlation (7.58) is based (Bejan 1987). This maximum is the spherical-annulus analog of the maximum found in Fig. 7.10 for the heat transfer through a two-dimensional layer heated from the side. Future studies may show that similar  $Nu$  maxima occur in the cylindrical-annulus configurations of both Fig. 7.18a, b, when the Rayleigh number based on porous layer thickness  $Ra_{r_o-r_i}$  is constant. Convection in spherical annular sectors defined by an adiabatic radial wall was studied numerically by Baytas et al. (2002). Prakash et al. (2010) performed an analysis of convection, diffusion, and reaction inside a spherical porous pellet in the presence of oscillatory flow.

### 7.3.5 Porous Medium Saturated with Water Near 4°C

One class of materials that departs from the linear-density model used in the Boussinesq approximation (7.5) are the porous media saturated with cold water. The density of water at atmospheric pressure exhibits a maximum near 4°C. The natural convection in a cold-water saturated medium confined by the rectangular

enclosure of Fig. 7.1 was described by Poulikakos (1984). As the equation of state in the Boussinesq approximation, he used

$$\rho_m - \rho = \gamma \rho_m (T - T_m)^2 \quad (7.61)$$

with  $T_m = 3.98^\circ\text{C}$  and  $\gamma \cong 8 \times 10^{-6} \text{ K}^{-2}$  for pure water at atmospheric pressure. This parabolic density model is valid at temperatures ranging from 0 to  $10^\circ\text{C}$ . Bejan (1987) showed that in the convection-dominated regime, the Nusselt number correlation must have the form

$$Nu = c_3 \frac{L/H}{Ra_{\gamma h}^{-1/2} + c_4 Ra_{\gamma c}^{-1/2}}, \quad (7.62)$$

where the two Rayleigh numbers account for how  $T_h$  and  $T_c$  are positioned relative to the temperature of the density maximum  $T_m$ :

$$Ra_{\gamma h} = \frac{g\gamma KH(T_h - T_m)^2}{\nu\alpha_m}, \quad Ra_{\gamma c} = \frac{g\gamma KH(T_m - T_c)^2}{\nu\alpha_m}. \quad (7.63)$$

The overall Nusselt number  $Nu$  is referenced to the case of pure conduction,  $Nu = q'/q'_c$ .

Poulikakos (1984) reported numerical  $Nu$  results in tabular form for the convection-dominated regime, primarily for the case  $T_c = 0^\circ\text{C}$ ,  $T_h = 7.96^\circ\text{C}$ . By relying on these data, Bejan (1987) showed that when  $T_c$  and  $T_h$  are positioned symmetrically around  $T_m$  (i.e., when  $Ra_{\gamma h} = Ra_{\gamma c}$ ), the correlation (7.62) reduces to

$$Nu \cong 0.26 \frac{L}{H} Ra_{\gamma h}^{1/2}. \quad (7.64)$$

In other words, this set of data indicates that in this case the two constants that appear in the general correlation (7.60) must satisfy the relationship  $c_3 \cong 0.26(1 + c_4)$  in which, by symmetry,  $c_4 = 1$ . More experimental data for the high Rayleigh number range with asymmetric heating ( $Ra_{\gamma h} \neq Ra_{\gamma c}$ ) are needed in order to determine  $c_3$  uniquely. A numerical study of convection in a rectangular cavity saturated by icy water, with various boundary thermal boundary conditions on the sidewalls, was reported by Benhadji et al. (2003). The numerical study by Baytas et al. (2004) treated the case of a square cavity and a more complicated density state equation. The case where one vertical wall is heated differentially by an isothermal discrete heater and the other vertical wall is cooled to a constant temperature, with adiabatic horizontal walls, was studied numerically by Saeid and Pop (2004c). The case of variable sidewall temperatures was treated by Kandaswamy and Eswaramurthi (2008). The effect of thermal nonequilibrium was studied by Saeid (2007c).

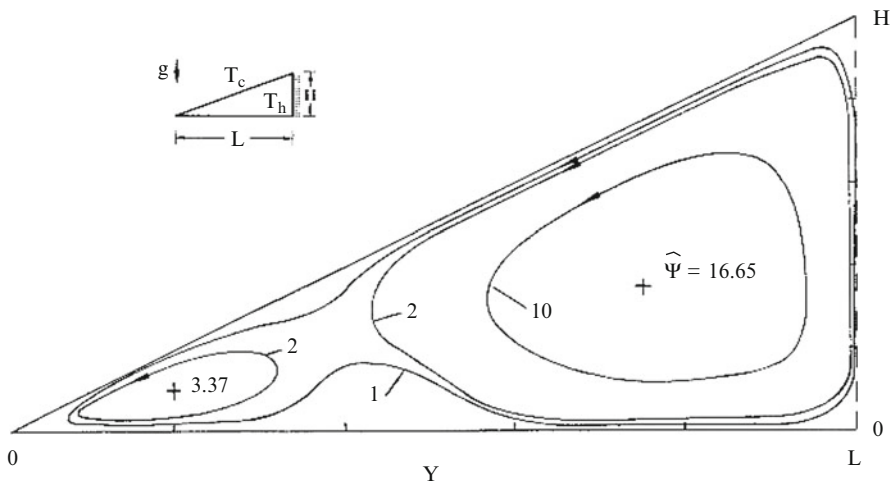


**Fig. 7.19** The flow pattern in an attic-shaped porous medium cooled the inclined wall ( $H/L = 0.5$ ,  $Ra = 1,000$ ) (Poulikakos and Bejan 1983b)

### 7.3.6 Triangular Enclosure

In a saturated porous medium confined by a wedge-shaped impermeable enclosure cooled along the sloped wall (Fig. 7.19), the convective flow consists of a single cell. Like all the flows in porous media heated or cooled from the side, this particular flow exists even in the limit  $Ra \rightarrow 0$ . The flow intensifies as the Rayleigh number based on height ( $Ra$ ) increases. The bottom wall is heated, while the vertical wall is insulated.

The numerical solutions reported by Poulikakos and Bejan (1983b) show the development of a Bénard-type instability at sufficiently high Rayleigh numbers. This instability is due to the heated bottom wall. In an enclosure with the aspect ratio  $H/L = 0.2$ , the instability occurs in the vicinity of  $Ra \sim 620$ . This critical Rayleigh number increases as  $H/L$  increases. Convection in trapezoidal enclosures was simulated using parallel computation by Kumar and Kumar (2004). An overview of natural and forced convection in an attic space was made by Wahlgren (2007).

Other triangular enclosures were studied by Basak et al. (2008a, b, c, 2010a, b, c, d) (isosceles and right-angled, heatline approach), Oztop and Pop (2008, 2009) (wall conduction, icy water), Varol (2011) (centered conducting body), Varol and Oztop (2009) (embedded thin plate), and Varol et al. (2006, 2008b, c, d, h, 2009a, b, c, d, e, f) (inclined enclosure, partitioned enclosure, conjugate problem, square divided diagonally). A triangular enclosure with a fin attached was treated by Varol et al. (2007a, b). Anandalakshmi et al. (2011) and Basak et al. (2012) studied heatline-based management and entropy generation within a right-angled triangular enclosure with various thermal conditions on the walls.

### 7.3.7 Other Enclosures

For the case of very small Rayleigh number, Philip (1982a, b, 1988) has obtained exact solutions for the flow pattern for a variety of two-dimensional (rectangular, elliptical, triangular, etc.) and axisymmetric (cylindrical, toroidal) cavities, for the case of uniform horizontal temperature gradient (which is radial for the axisymmetric situation). These were obtained under the assumption of negligible convective heat transfer and so are of limited use on their own. They may be useful as the first stage in a perturbation analysis. Campos et al. (1990) studied numerically on the Brinkman model convection in a vertical annular enclosure partly filled with a vertical annular volume occupied by a porous medium. Asako et al. (1992) and Yamaguchi et al. (1993) reported numerical solutions with a Darcy model for three-dimensional convection in a vertical layer with a hexagonal honeycomb core that is either conducting or adiabatic. Chen and Wang (1993a, b) performed a convection instability analysis for a porous enclosure with either a horizontal or vertical baffle projecting partway into the enclosure. Lai (1993a, b, 1994) has performed calculations for the effects of inserting baffles of various sorts (radial and circumferential in horizontal annuli or pipes). Shin et al. (1994), with the aid of a transformation to bicylindrical coordinates, studied numerically two-dimensional convection in a segment of a circle, with the boundary inclined to the vertical.

Convection in a cavity with a dome (circular, elliptical, parabolic, etc.) on top was treated numerically by Das and Morsi (2003, 2005). Conjugate convection heat transfer from a vertical cylindrical fin in a cylindrical enclosure was treated numerically by Naidu et al. (2004a). A numerical solution procedure to study convection in a two-dimensional enclosure of arbitrary geometry was presented by Singh et al. (2000). Convection in an inclined trapezoidal enclosure with cylindrical top and bottom surfaces was studied numerically by Baytas and Pop (2001). Further work on trapezoidal enclosures was done by Basak et al. (2009a) (inclined enclosures), Basak et al. (2009b, c, 2010a) (nonuniform bottom heating, various inclinations), Mamun et al. (2010b), Saleh et al. (2007a) (inclined magnetic field), Varol (2010) (divided cavities), Varol et al. (2008f, 2010a) (inclined enclosure, maximum density effects), and Al-Azmi (2011). Numerical investigations of convection in insulating layers in attics were carried out by Shankar and Hagentoft (2000). Convection in embankments built in permafrost has been modeled by Goering and Kumar (1996), Goering (2003), Jiang et al. (2004d), Sun et al. (2005a, b, 2007, 2009), Lai et al. (2006a, b), and Zhang et al. (2005b, 2006a, b, 2007b, 2009b). Convection in a porous toroidal thermosiphon has been studied numerically by Jiang and Shoji (2002). Convection in a thin porous elliptical ring, located in an impermeable rock mass and subject to an inclined geothermal gradient, was treated by Ramazanov (2000). Fluid flow and heat transfer in partly divided cavities was studied numerically by Jue (2000). Convection in a reentrant rectopolygonal cavity was studied numerically and experimentally by Phanikumar and Mahajan (2002). Radiative effects on a MHD flow between infinite parallel plates with time-dependent suction were studied analytically by Alagoa et al. (1999). Convection from a wavy wall in a thermally stratified enclosure was treated numerically by Ratish Kumar and Shalini (2004a). Natural convection in a cavity with

wavy vertical walls was studied by Misirlioglu et al. (2005) and Srinivas and Muthuraj (2010b) (MHD flow with slip effects and temperature-dependent heat source). Convection driven by differential heating of the upper surface of a rectangular cavity was studied numerically and analytically by Daniels and Punpocha (2004, 2005). The case of a square cavity where one vertical wall is heated differentially by an isothermal discrete heater and the other vertical wall is cooled to a constant temperature, with adiabatic horizontal walls, was studied numerically by Saeid and Pop (2005b). A two-temperature model was applied by Sanchez et al. (2005b) to a problem with symmetrically connected fluid and porous layers. A square enclosure with nonuniformly heated walls was investigated by Basak et al. (2007). A rectangular enclosure was studied by Varol et al. (2007c, 2008g). A non-Newtonian power-law fluid was treated numerically by Hadim (2006). Convection in a horizontal elliptical annulus was studied numerically and experimentally by Sakr and Berbisch (2012).

Enclosures with wavy walls were studied by Ratish Kumar and Shalini (2003a), Misirlioglu et al. (2006a, b) (heat generation, inclined enclosure), Sultana and Hyder (2007), Chen et al. (2008c), Varol and Oztop (2008) (inclined solar collectors), Khanafer et al. (2009), Tiwari and Singh (2010), and Mansour et al. (2011b) (with thermal nonequilibrium). The case of a rhombic annulus was treated by Moukalled and Darwiche (2010). A study of local thermal nonequilibrium in porous heat sinks using fin theory was made by Jeng et al. (2006). An enclosure problem where the left wall is at constant flux, the right wall is adiabatic and there is a heat sink on the top wall was studied by Villemure et al. (2008). A conical cylinder was examined by Ahmed et al. (2009). A parallelogrammic enclosure was studied by Han and Hyun (2008). A vertical layer with two thermal sources was studied by Saeid (2006b). Support vector mechanics was applied to a cavity with discrete sources by Varol et al. (2008a). Open-ended (or partly capped) cavities were studied by Weidman and Medina (2008) and Wang (2009). Kaluri and Basak (2011b) studied energy generation in discretely heated square cylinders. Entropy generation in rhombic enclosures was studied by Anandalakshmi and Basak (2012). Optimal convection in a space between a vertical polygonal duct and a heated core was examined by Wang (2012).

### 7.3.8 Internal Heating

Steady natural convection in a two-dimensional cavity with uniform heat generation was simulated numerically by Du and Bilgen (1992) for the case of adiabatic horizontal walls and isothermal vertical walls at different temperatures. A further numerical treatment was reported by Das and Sahoo (1999). Steady convection in a rectangular enclosure with the top and one sidewall cold and the other non-isothermal and with the bottom heated at constant temperature was studied numerically by Hossain and Wilson (2002). Convection in a two-dimensional vertical cylinder with either (1) insulated top and bottom and cooled lateral walls or (2) all walls isothermally cooled was given a numerical treatment by Jiménez-Islas et al. (1999). A transient convection problem with sidewall heating was studied by Jue (2003). A dual reciprocity boundary element method was applied to a differentially

and internally heated rectangular enclosure by Sarler (2000) and Sarler et al. (2000a, b, 2004a, b). A numerical and experimental study of three-dimensional convection in an anisotropic medium in a rectangular cavity was carried out by Suresh et al. (2005). Internal heat generation in a tall cavity was studied by Ansari (2007). Barletta et al. (2008b) treated the effect of viscous heating in a vertical circular duct. Natural convection in metal foam strips was studied by Hetsroni et al. (2008). Convection in a partly heat-generating rod bundle inside an enclosure was treated by Krishna et al. (2010). The effect of a magnetic field was introduced by Revnic et al. (2011). Ejlali and Hooman (2011) studied the cooling of a coal stockpile.

### 7.3.9 Bidisperse Porous Media

Convection in a bidisperse porous medium enclosure was studied by Narasimhan and Reddy (2010, 2011a, b), Revnic et al. (2009), and Jamalud-Din et al. (2010) (using a network model and numerical simulations inside an enclosure with distributed solid blocks).

## 7.4 Penetrative Convection

In this section we turn our attention to buoyancy-driven flows that only partially penetrate the enclosed porous medium. One basic configuration in which this flow can occur is shown in Fig. 7.20a. The saturated porous medium is a two-dimensional layer of height  $H$  and length  $L$ , confined by a rectangular boundary. Three of the walls are impermeable and at the same temperature (e.g.,  $T_c$ ), while

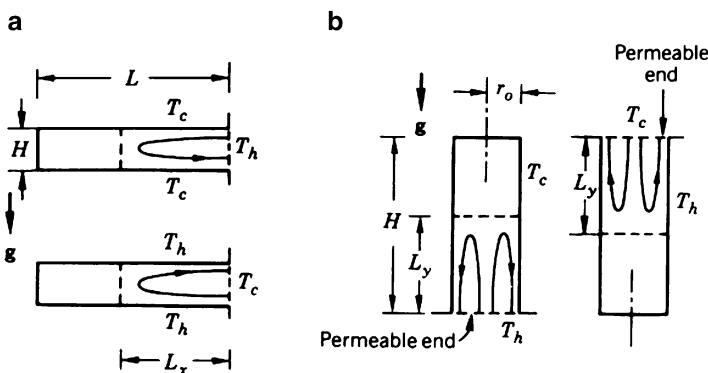


**Fig. 7.20** Lateral penetration (a) and vertical penetration (b) of natural convection into an isothermal porous space with one and permeable

one of the sidewalls is permeable and in communication with a fluid reservoir of a different temperature,  $T_h$ . In Fig. 7.20b the same layer is oriented vertically. In both cases, natural convection penetrates the porous medium over a length dictated by the Rayleigh number alone and not by the geometric ratio of the layer,  $H/L$  (Bejan 1980, 1981). The remainder of the porous layer contains essentially stagnant and isothermal fluid.

### 7.4.1 Lateral Penetration

First consider the horizontal layer of Fig. 7.20a, in which the lateral penetration distance  $L_x$  is unknown. According to (7.1), (7.4), and (7.5), the order-of-magnitude balances for mass, energy, and momentum are

Mass:

$$\frac{u}{L_x} \sim \frac{v}{H}, \quad (7.65)$$

Energy:

$$u \frac{\Delta T}{L_x} \sim \alpha_m \frac{\Delta T}{H^2}, \quad (7.66)$$

Momentum:

$$\frac{u}{H} \sim \frac{Kg\beta}{v} \frac{\Delta T}{L_x}. \quad (7.67)$$

In writing balances we have assumed that the penetration length  $L_x$  is greater than the vertical dimension  $H$ . The temperature difference  $\Delta T$  is shorthand for  $T_h - T_c$ .

Equations (7.65), (7.66), and (7.67) can be solved easily for the unknown scales  $u$ ,  $v$ , and  $L_x$ . For example, the penetration length is (Bejan 1981)

$$L_x \sim H Ra^{1/2}, \quad (7.68)$$

in which  $Ra$  is the Darcy-modified Rayleigh number based on  $H$  and  $\Delta T$ . The corresponding heat transfer rate  $q'$  [W/m] between the lateral fluid reservoir  $T_h$  and the  $T_c$  boundary of the porous medium scales as

$$q' \sim (\rho c_p)_f u H \Delta T \sim k_m \Delta T Ra^{1/2}. \quad (7.69)$$

The heat transfer rate  $q'$  is expressed per unit length in the direction normal to the plane of Fig. 7.20a. All these results demonstrate that the actual length of the porous layer ( $L$ ) has no effect on the flow and the heat transfer rate:  $L_x$  as well as  $q'$  are set by the Rayleigh number. The far region of length  $L - L_x$  is isothermal and filled with stagnant fluid.

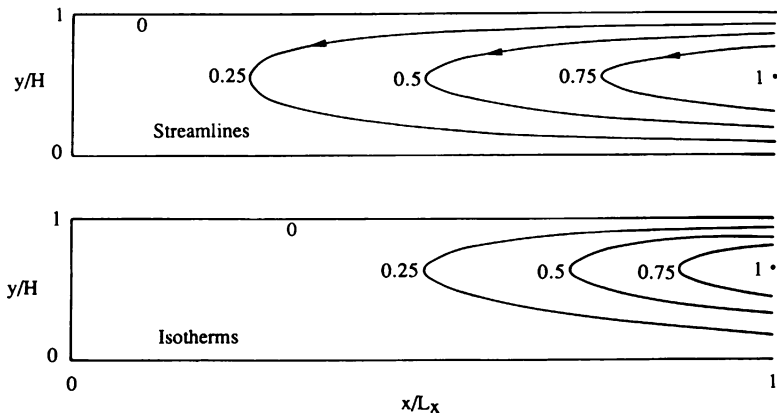


**Fig. 7.21** Streamlines and isotherms in the region of lateral penetration into a two-dimensional porous layer (Bejan 1981)

The actual flow and temperature fields associated with the lateral penetration phenomenon have been determined analytically as a similarity solution (Bejan 1981). Figure 7.21 shows the dimensionless stream function and temperature for only the region of length  $L_x$ . The penetration length and heat transfer rate predicted by this solution are

$$L_x = 0.158 H Ra^{1/2}, \quad (7.70)$$

$$q' = 0.319 k_m \Delta T Ra^{1/2}. \quad (7.71)$$

The results presented in this subsection are valid when  $L_x < L$  and  $L_x \gg H$ , which translates into the following  $Ra$  range:

$$1 \ll Ra < \frac{L}{H}. \quad (7.72)$$

In the same paper, Bejan (1981) also documented the lateral penetration in an anisotropic porous medium in which the principal thermal conductivities are different and aligned with the  $x$  and  $y$  axes,  $k_{m,x} \neq k_{m,y}$ . He also showed that a similar partial penetration phenomenon occurs when the temperature of each of the two horizontal walls (Fig. 7.20a) varies linearly from  $T_h$  at one end to  $T_c$  at the other.

#### 7.4.2 Vertical Penetration

In the vertical two-dimensional layer of Fig. 7.20b, it is the bottom or the top side that is permeable and in communication with a fluid reservoir of different temperature. In Chap. 6 we saw that in porous layers heated from below or cooled from

above, convection is possible only above a critical Rayleigh number. In the configuration of Fig. 7.20b, however, fluid motion sets in as soon as the smallest  $\Delta T$  is imposed between the permeable horizontal boundary and the vertical walls. This motion is driven by the horizontal temperature gradient of order  $\Delta T/L$ .

If we write  $L_y$  for the unknown distance of vertical penetration and if we assume that  $L_y \gg L$ , we obtain the following order-of-magnitude balances:

Mass:

$$\frac{u}{L} \sim \frac{v}{L_y}, \quad (7.73)$$

Energy:

$$u \frac{\Delta T}{L} \sim \alpha_m \frac{\Delta T}{L^2}, \quad (7.74)$$

Momentum:

$$\frac{v}{L} \sim \frac{Kg\beta}{v} \frac{\Delta T}{L}. \quad (7.75)$$

The vertical penetration distance that results from this system of equations is (Bejan 1984)

$$L_y \sim L Ra_L, \quad (7.76)$$

in which  $Ra_L$  is the Rayleigh number based on the thickness  $L$ :  $Ra_L = g\beta KL\Delta T/v\alpha_m$ . The scale of the overall heat transfer rate  $q'$  [W/m] through the permeable side of the porous layer is

$$q' \sim (\rho c_p)_f v L \Delta T \sim k_m \Delta T R a_L. \quad (7.77)$$

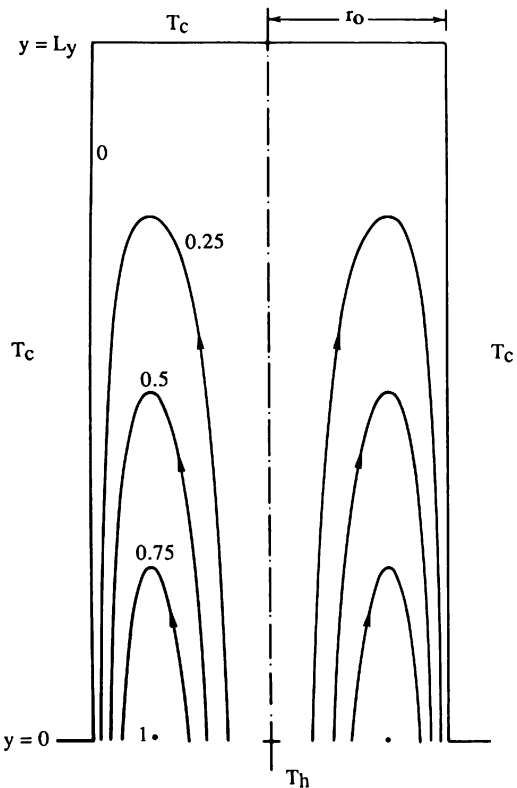
Once again, the physical extent of the porous layer ( $H$ ) does not influence the penetrative flow, as long as  $H$  is greater than the penetration distance  $L_y$ . The latter is determined solely by the transversal dimension  $L$  and the imposed temperature difference  $\Delta T$ . The vertical penetration distance and total heat transfer rate are proportional to the Rayleigh number based on the thickness  $L$ .

The vertical penetration of natural convection also was studied in the cylindrical geometry of Fig. 7.22, as a model of certain geothermal flows or the flow of air through the grain stored in a silo (Bejan 1980). The vertical penetration distance and the total heat transfer rate  $q$  [W] are

$$\frac{L_y}{r_o} = 0.0847 R a_{r_o}, \quad (7.78)$$

$$q = 0.255 r_o k_m \Delta T R a_{r_o}, \quad (7.79)$$

**Fig. 7.22** Streamlines in the region of vertical penetration into a cylindrical space filled with porous medium (Bejan 1980)



where  $r_o$  is the radius of the cylindrical cavity filled with saturated porous material and  $Ra_{r_o}$  is the Rayleigh number based on radius,  $Ra_{r_o} = g\beta K r_o \Delta T / \nu \alpha_m$ . Figure 7.22 shows the streamlines in the region of height  $L_y$ , which is penetrated by natural convection. The region of height  $H - L_y$ , which is situated above this flow and is not shown in Fig. 7.22, is isothermal and saturated with motionless fluid.

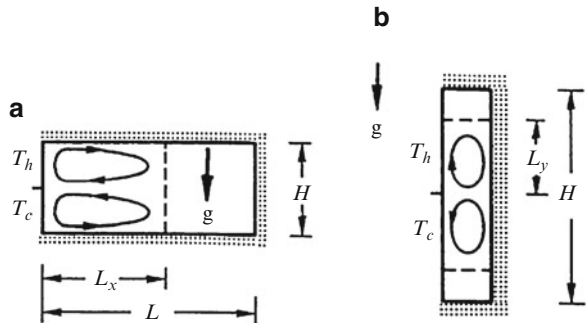
The results presented in this subsection are valid when the penetrative flow is slender,  $L_y \gg (L, r_o)$ , and when  $L_y$  is shorter than the vertical dimension of the confined porous medium,  $L_y < H$ . These restrictions limit the Rayleigh number domain that corresponds to these flows:

$$1 \ll Ra_{(L, r_o)} < \frac{H}{(L, r_o)}. \quad (7.80)$$

#### 7.4.3 Other Penetrative Flows

Two types of penetrative flows that are related to those of Fig. 7.20a, b are presented in Fig. 7.23. Poulikakos and Bejan (1984a) showed that in a porous medium that is heated and cooled along the same vertical wall, the flow penetration can be either

**Fig. 7.23** Incomplete horizontal penetration (a) and vertical penetration (b) in a porous layer heated and cooled along the same vertical side



horizontal (Fig. 7.23a) or vertical (Fig. 7.23b). In the case of horizontal penetration, the penetration distance  $L_x$  and the total heat transfer rate  $q'$  are of the same order as in (7.66) and (7.67). These scales are valid in the range  $1 \ll Ra < L/H$ , the Rayleigh number  $Ra$  being based on height. The scales of vertical penetration in Fig. 7.23b are different,

$$L_y \sim H \left( \frac{L}{H} \right)^{2/3} Ra^{-1/3}, \quad (7.81)$$

$$q' \sim k_m (T_h - T_c) \left( \frac{L}{H} Ra \right)^{1/3}. \quad (7.82)$$

in which  $Ra$  is again based on  $H$ . These scales are valid when  $Ra > H/L$ . The two penetrative flows of Fig. 7.23 occur only when the heated section is situated above the cooled section of the vertical wall. When the positions of the  $T_h$  and  $T_c$  sections are reversed, the buoyancy-driven flow fills the entire  $H \times L$  space (Poulikakos and Bejan 1984a).

In a semi-infinite porous medium bounded from below or from above by a horizontal wall with alternating zones of heating and cooling (Fig. 7.24), the buoyancy-driven flow penetrates to a distance  $L_y$  into the medium (Poulikakos and Bejan 1984b). This distance scales as  $\lambda Ra_\lambda^{1/2}$ , where  $\lambda$  is the spacing between a heated zone and the adjacent cooled zone and  $Ra_\lambda = g\beta K \lambda (T_h - T_c) / \nu \alpha_m$ . Figure 7.24 shows a sample of the numerical results that have been developed for the range  $1 \leq Ra_\lambda \leq 100$ .

## 7.5 Transient Effects

The work reviewed in the preceding sections dealt with steady-state conditions in which the flow is slow enough to conform to the Darcy model. In this section, we drop the steady-flow restriction and examine the time scales and evolution of the

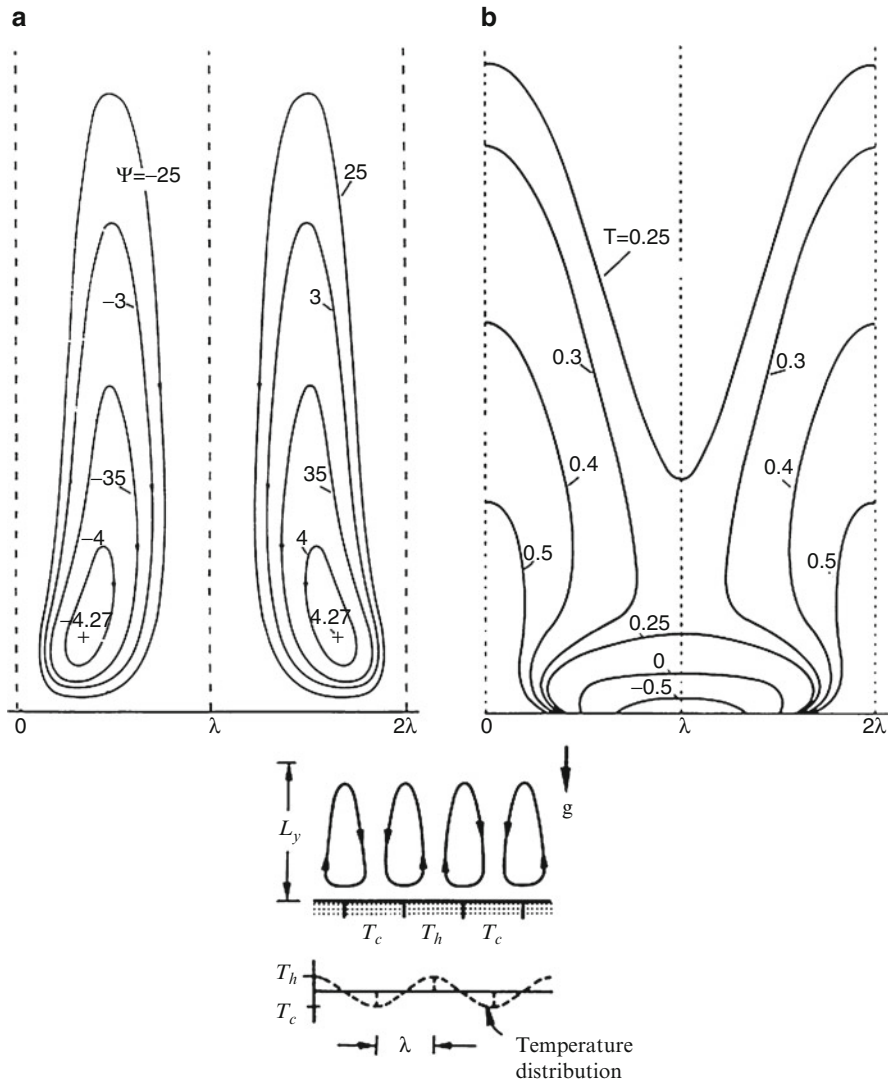


**Fig. 7.24** Streamlines and isotherms for the vertical penetration of natural convection in a semi-infinite porous medium bounded by a horizontal wall with alternating hot and cold spots ( $Ra_\lambda = 100$ ) (Poulikakos and Bejan 1984b)

buoyancy-driven flow. The equations that govern the conservation of mass, momentum, and energy in Fig. 7.1 are, in order, (7.1), (7.5), and, in place of (7.4),

$$\sigma \frac{\partial T}{\partial t} + u \frac{\partial T}{\partial x} + v \frac{\partial T}{\partial y} = \alpha_m \left( \frac{\partial^2 T}{\partial x^2} + \frac{\partial^2 T}{\partial y^2} \right). \quad (7.83)$$

Consider the two-dimensional saturated porous medium shown in Fig. 7.1, which is initially isothermal at  $T_{\text{avg}} = (T_h + T_c)/2$  and saturated with motionless fluid. At the time  $t = 0$ , the temperatures of the two sidewalls are changed to  $T_h = T_{\text{avg}} + \Delta T/2$  and  $T_c = T_{\text{avg}} - \Delta T/2$ , while the top and bottom walls remain insulated. All the walls are impermeable. Of special interest is the time needed by the flow and heat transfer to reach steady state, that is, the time interval after which the flow regimes described in Sect. 7.1 become valid. This basic transient convection problem was studied by Poulikakos and Bejan (1983c).

By focusing on the vertical boundary layer that develops along the left-hand side of the rectangular system of Fig. 7.1, we note that initially the time-dependent thickness of this boundary layer  $\delta(t)$  grows by pure conduction. With respect to the region of thickness  $\delta$  and height  $H$ , the energy equation (7.83) dictates a balance between the side heating effect and the thermal inertia of the saturated porous medium,

$$\sigma \frac{\Delta T}{t} \sim \alpha_m \frac{\Delta T}{\delta^2}. \quad (7.84)$$

This balance yields the well-known penetration distance of pure conduction:

$$\delta \sim \left( \frac{\alpha_m t}{\sigma} \right)^{1/2}. \quad (7.85)$$

The growth of the conduction layer gives rise to a horizontal temperature gradient of order  $\partial T / \partial x \sim \Delta T / \delta$ . This development makes the buoyancy term in the momentum balance (7.5) finite. In fact, the scales of the three terms appearing in (7.5) are

$$\left( \frac{u}{H}, \frac{v}{\delta} \right) \sim \frac{Kg\beta}{v} \frac{\Delta T}{\delta}. \quad (7.86)$$

The mass conservation scaling (7.6) shows that the ratio of the two scales on the left-hand side of (7.86) is

$$\frac{u/H}{v/\delta} \sim \left( \frac{\delta}{H} \right)^2, \quad (7.87)$$

in other words, that  $u/H$  is negligible relative to  $v/\delta$ . In conclusion, the momentum balance reduces to (7.11), and the vertical velocity scale turns out to be identical to the scale listed in (7.12) for the steady state. An interesting feature of the transient flow is that the vertical velocity scale is independent of time. The vertical flow rate however,  $v\delta$ , grows in time as  $t^{1/2}$ .

As soon as fluid motion is present, the energy equation (7.83) is ruled by the competition among three different scales:

$$\begin{array}{ccc} \sigma \frac{\Delta T}{t}, & v \frac{\Delta T}{H} & \sim \alpha_m \frac{\Delta T}{\delta^2}, \\ \text{Inertia} & \text{Convection} & \text{Conduction}. \\ (t^{-1}) & (t^0) & (t^{-1}) \end{array} \quad (7.88)$$

The time dependence of each scale also is shown. Since the lateral conduction effect is always present, the convection scale eventually overtakes inertia on the left-hand side of (7.88). The time  $t$  when this changeover takes place, that is, when the vertical boundary layer becomes convective, is given by

$$\sigma \frac{\Delta T}{t} \sim v \frac{\Delta T}{H}, \quad (7.89)$$

which in view of the  $v$  scale (7.12) yields

$$t \sim \frac{\sigma}{\alpha_m} H^2 Ra^{-1}. \quad (7.90)$$

It is easy to verify that the boundary layer thickness (7.85), which corresponds to (and after) this time, is the steady-state scale determined earlier in (7.13). In conclusion, this transient-convection analysis reconfirms the criterion (7.19) for distinct vertical boundary layers.

By following the same approach, Poulikakos and Bejan (1983c) traced the development of the horizontal boundary layers along the top and bottom walls of the enclosure. They found that the horizontal layers become “developed” earlier than the vertical layers when the enclosure is tall enough so that

$$\frac{H}{L} > Ra^{1/6}. \quad (7.91)$$

The criterion for distinct horizontal boundary layers turns out to be the same as the inequality (7.22). In summary, the analysis of the time-dependent development of natural circulation in the two-dimensional system of Fig. 7.1 provides an alternative way to construct the four-regime map seen earlier in Fig. 7.2.

A comprehensive study of transient convection between parallel vertical plates on the Brinkman-Forchheimer model has been carried out by Nakayama et al. (1993). They obtained asymptotic solutions for small and large times and a bridging numerical solution for intermediate times. An MHD problem with suction or injection on one plate was treated by Chamkha (1997b). For convection in a rectangular enclosure, Lage (1993b) used scale analysis to obtain general heat transfer correlations. A further numerical study was reported by Merrikh and Mohamad (2000). An analytic study using Laplace transforms was conducted by Jha (1997). The effect of variable porosity was examined by Paul et al. (2001). Saeid and Pop (2004a, b) considered a transient problem arising from the sudden heating of one sidewall and the sudden cooling of the other, with and without the effect of viscous dissipation. They found that the heat transfer was reduced as a result of the dissipation. Convection in a non-Newtonian power-law fluid was studied numerically by Al-Nimr et al. (2005).

A transient problem for convection between two concentric spheres was studied by Pop et al. (1993b). They obtained solutions, valid for short time, of the Darcy

and energy equations using the method of matched asymptotic expansions. Nguyen et al. (1997b) treated a similar problem with a central fluid core surrounded by a porous shell. They performed numerical calculations on the Brinkman model. They found remarkable effects along the porous medium-fluid interface, but the overall heat flux was sensitive only to the ratio of thermal conductivity of the solid matrix to that of the fluid.

Transient convection in a vertical annulus for various thermal boundary conditions was studied by Al-Nimr and Darabseh (1995) for the Brinkman model. Transient convection in a horizontal annulus, with the inner and outer cylinders maintained at uniform temperatures, was examined by Pop et al. (1992a). They used the method of matched asymptotic expansions to obtain a solution valid for short times. Sundfor and Tyvand (1996) studied convection in a horizontal cylinder with a sudden change in wall temperature. An investigation of the effect of local thermal nonequilibrium was reported by Ben Nasrallah et al. (1997). Further numerical studies of the effect of local thermal nonequilibrium were carried out by Khadrawi and Al-Nimr (2003b) and Krishnan et al. (2004). A hybrid numerical-analytical solution for two-dimensional transient convection in a vertical cavity, based on a generalized transform technique, was presented by Alves and Cotta (2000). Similar three-dimensional studies were made by Neto et al. (2002, 2004) and Cotta et al. (2005). Convection in a square cavity with oscillating wall temperature was studied by Saeid (2006c). The case of an impulsive change of temperature on a sidewall was treated by Kumari and Nath (2009b). Another unsteady problem with side heating was examined by Aldabbagh et al. (2008). A situation arising in the storage of granular material was studied by Avila-Acevedo and Tsotsas (2008). A vibration effect on heat transfer and entropy generation in an elliptical cavity was investigated by Mahmud and Frazer (2006). The effects of strong compressibility with a near-critical fluid were studied by Soboleva (2008).

## 7.6 Departure from Darcy Flow

### 7.6.1 Inertial Effects

The behavior of the flow and heat transfer process changes substantially as the flow regime departs from the Darcy limit. The effect of the quadratic drag on the heat transfer through the most basic configuration that opened this chapter (Fig. 7.1) was demonstrated by Poulikakos and Bejan (1985). In place of the momentum equation (7.5), they used the Forchheimer modification of Darcy's law,

$$\frac{\partial}{\partial y}(Bu) - \frac{\partial}{\partial x}(Bv) = -\frac{g\beta K}{v} \frac{\partial T}{\partial x}. \quad (7.92)$$

**Table 7.1** The scales of the vertical natural convection boundary layer in a porous layer heated from the side (Poulikakos and Bejan 1985)

	Forchheimer regime $G \ll 1$	Darcy regime $G \gg 1$
Boundary layer thickness	$HRa_{\infty}^{-1/4}$	$HRa^{-1/2}$
Vertical velocity	$\frac{\alpha_m}{H} Ra_{\infty}^{1/2}$	$\frac{\alpha_m}{H} Ra$
Heat transfer rate	$k_m \Delta T Ra_{\infty}^{1/2}$	$k_m \Delta T Ra^{1/2}$

This follows from (1.12) by eliminating the pressure between the  $x$  and  $y$  momentum equations and by writing

$$B = 1 + \frac{\chi}{v} (u^2 + v^2)^{1/2}. \quad (7.93)$$

The Forchheimer term coefficient  $\chi$  has the units [m] and is used as shorthand for the group  $c_F K^{1/2}$ , where  $c_F$  is defined by (1.12). The same notation was used in (5.64), in the analysis of the flow near a single vertical wall.

Poulikakos and Bejan (1985) analyzed the Darcy-Forchheimer convection phenomenon using three methods: scale analysis, a matched boundary layer analysis, and case-by-case numerical finite-difference simulations. The main results of the scale analysis for the convection regime III are summarized in Table 7.1, next to the scales derived for the Darcy limit in Sect. 7.1.1. The transition from Darcy flow to Forchheimer flow, that is, to a flow in which the second term dominates on the right-hand side of (7.93), takes place when the dimensionless number  $G$  is smaller than  $O(1)$ ,

$$G = v[\chi g \beta K(T_h - T_c)]^{-1/2}. \quad (7.94)$$

In the Forchheimer regime  $G \ll 1$ , the appropriate Rayleigh number is the large Reynolds number limit version encountered already in (5.64),

$$Ra_{\infty} = \frac{g \beta K H^2 (T_h - T_c)}{\chi \alpha_m^2}. \quad (7.95)$$

The important heat transfer conclusion of the scale analysis is that the overall (conduction-referenced) Nusselt number defined in (7.17) scales as  $(L/H)Ra_{\infty}^{1/4}$  in the limit in which the effect of inertia dominates. A more accurate estimate was provided by an analytical solution in which Oseen linearized solutions for the two vertical boundary layers were matched to the same stratified core (Poulikakos and Bejan 1985):

$$Nu = 0.889 \frac{L}{H} Ra_{\infty}^{1/4} \quad (G \ll 1). \quad (7.96)$$

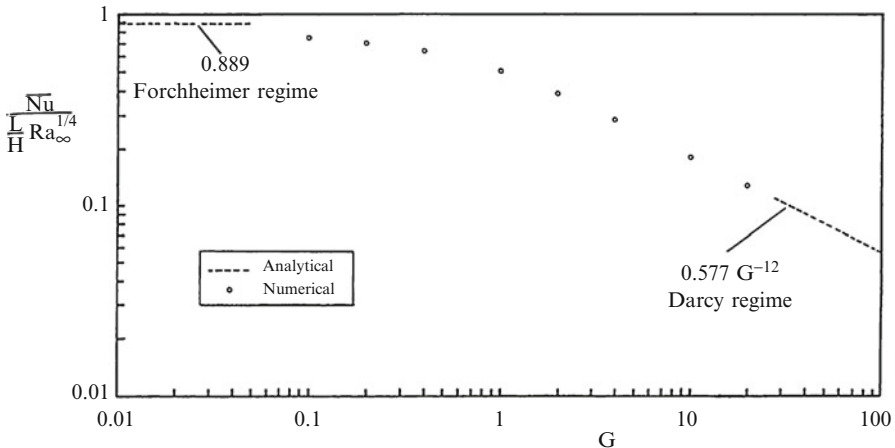


**Fig. 7.25** Numerical results for the total heat transfer rate through a porous layer heated from the side, in the intermediate Darcy-Forchheimer range ( $H/L = 2$ ,  $Ra = 4,000$ , and  $1.6 \times 10^5 \leq Ra_{\infty} \leq 1.6 \times 10^9$ ) (Poulikakos and Bejan 1985)

This solution is the Forchheimer regime counterpart of the Oseen linearized solution derived by Weber (1975b) for the Darcy limit, namely (7.38). By intersecting (7.96) with (7.38), we learn that the transition from Darcy flow to Forchheimer flow occurs when  $Ra_{\infty}^{1/2} \sim Ra$ , which is another way of saying  $G \sim O(1)$ . In fact the group  $G$  defined in (7.94) is the same as the ratio  $Ra_{\infty}^{1/2} \sim Ra$ .

Figure 7.25 shows Poulikakos and Bejan's (1985) finite-difference calculations for the overall heat transfer rate in the intermediate regime represented by  $0.1 \leq G \leq 10$ . In these calculations, the momentum equation contained the Darcy and Forchheimer terms shown in (7.92) and (7.93). The numerical data agree well with Weber's formula in the Darcy limit  $G \rightarrow \infty$ . In the opposite limit, the numerical data fall slightly below the theoretical asymptote (7.96). This behavior has been attributed to the fact that the group  $(H/L) Ra_{\infty}^{-1/4}$ , whose smallness describes the goodness of the boundary layer approximation built into the analysis that produced (7.96), increases steadily as  $G$  decreases at constant  $Ra$  (note that in Fig. 7.25  $Ra = 4,000$ ). In other words, constant- $Ra$  numerical experiments deviate steadily from the boundary layer regime as  $G$  decreases. Indeed, Poulikakos and Bejan (1985) found better agreement between their  $G < 1$  numerical data and (7.96) when the Rayleigh number was higher,  $Ra = 5,000$ .

In a subsequent numerical study, Prasad and Tuntomo (1987) contributed additional numerical results for natural convection in the configuration treated by Poulikakos and Bejan (1985), which confirmed the reported theoretical scaling trends. Specifically, Prasad and Tuntomo included the Darcy and Forchheimer terms in the momentum equation and covered the range  $1 \leq H/L \leq 20$ ,  $10 \leq Ra \leq 10^4$ . They also pointed out that the progress toward the inertia-dominated regime ( $G \rightarrow 0$  in Fig. 7.25) is accompanied by a proportional increase in the pore Reynolds number. This can be shown here by using the volume-averaged vertical

velocity scale listed in Table 7.1,  $v \sim (\alpha_m/H) Ra_\infty^{1/2}$ . The corresponding pore velocity scale is  $v_p = v/\varphi \sim (\alpha_m/\varphi H) Ra_\infty^{1/2}$ . The pore Reynolds number is

$$Re_p = \frac{v_p D_p}{v}, \quad (7.97)$$

in which  $D_p$  is the pore size. This Reynolds number can be rewritten in terms of  $G$  and the particle size  $d_p$  by invoking (7.94) and (1.13):

$$Re_p \sim \frac{D_p}{d_p} \frac{\beta^{1/2}}{c_F} \frac{(1 - \varphi)}{\varphi^{5/2} G}. \quad (7.98)$$

Taking  $\beta = 150$ ,  $c_F \cong 0.55$ ,  $D_p/d_p \sim O(1)$ , and  $\varphi = 0.7$  as representative orders of magnitude in (7.96), the pore Reynolds number becomes approximately

$$Re_p \sim \frac{C}{G}, \quad (7.99)$$

where  $C$  is a dimensionless coefficient of order 10.

This last  $Re_p$  expression reconfirms the notion that the effect of inertia becomes important when  $Re_p \sim O(10)$ , because  $G < 1$  is the inertia-dominated domain revealed by Poulikakos and Bejan's (1985) theory. The pore Reynolds number domain  $Re_p > 300$ , in which the flow becomes turbulent (Dybbs and Edwards 1984), corresponds to the range  $G < 0.03$  at constant  $Ra$ . Prasad and Tuntomo (1987), however, went too far when they claimed that "the Forchheimer extended Darcy equation of motion will become invalid when  $G$  decreases below 0.1. The flow is then unsteady and chaotic" (p. 311). Their assertion is incorrect, because quadratic drag is a macroscopic phenomenon that does not change qualitatively when the flow in the pores becomes turbulent.

A numerical study of convection in a square cavity using the Forchheimer model was conducted by Saeid and Pop (2005a). They confirmed the expectation that inertial effects slow down the convection currents and reduce the Nusselt number for a fixed value of the Rayleigh number.

### 7.6.2 Boundary Friction, Variable Porosity, Local Thermal Nonequilibrium, Viscous Dissipation, and Thermal Dispersion Effects

The effects of boundary friction incorporated in the Brinkman model has been studied by several authors, starting with Chan et al. (1970). For the shallow porous layer, with isothermal lateral walls and adiabatic top and bottom, the top being either rigid or free, Sen (1987) showed that the Brinkman term does not significantly affect the heat transfer rate until the Darcy number  $Da = K/H^4$  exceeds  $10^{-1/4}$ , and then the Nusselt

number  $Nu$  decreases as  $Da$  increases. As one would expect, the reduction is smaller for the case of a free upper surface than that of a rigid upper surface. Also, for a shallow cavity with various combinations of rigid or free upper and lower boundaries, Vasseur et al. (1989) studied the case of lateral heating with uniform heat flux, exploiting the fact that in this situation there is parallel flow in the core.

For cavities with aspect ratios of order unity, Tong and Subramanian (1985) performed a boundary layer analysis, and Tong and Orangi (1986) carried out numerical calculations. Vasseur and Robillard (1987) studied the boundary layer regime for the case of uniform heat flux. The vertical cavity case was treated numerically by Lauriat and Prasad (1987). Again the chief result is that, because of the reduction in velocity near the wall, the Nusselt number  $Nu$  decreases as  $Da$  increases, the effect increasing as  $Ra$  increases. The variation porosity near the wall partly cancels the boundary friction effect. Numerical studies of this effect were conducted by Nithiarasu et al. (1997a, 1998) and Marcondes et al. (2001).

The combined effects of boundary friction and quadratic drag were studied numerically by Beckermann et al. (1986), David et al. (1988, 1991), Lauriat and Prasad (1989), and Prasad et al. (1992) for rectangular cavities; by Kaviany (1986) and Murty et al. (1989) for horizontal annuli (concentric and eccentric, respectively); and by David et al. (1989) for vertical annuli. The studies by David et al. (1988, 1989) included the effect of variable porosity, which increases the rate of heat transfer. The last paper reported excellent agreement between the numerical results and experimental data obtained by Prasad et al. (1985) for water-glass media at high Rayleigh numbers and large particle sizes. Extensive reviews of the topic of boundary friction, quadratic drag, and variable porosity were made by Prasad and Kladias (1991) and Lauriat and Prasad (1991). These authors noted that there remained a discrepancy between theory and experiment for the case of media with a highly conductive solid matrix, such as steel beads. The theoretical values were some 20–25% too high.

The comparative numerical studies of a heated square cavity on Darcy, Brinkman, and Brinkman-Forchheimer models by Misra and Sarkar (1995) confirmed that boundary friction and quadratic drag lead to a reduction in heat transfer. Further numerical studies were conducted by Satya Sai et al. (1997b), Jecl et al. (2001), and Jecl and Škerget (2004). Sathiyamoorthy et al. (2007) studied the situation where one or both sidewalls were linearly heated. An MHD problem was treated by Sathiyamoorthy (2011). A thin fin on the left-hand heated wall was added by Sathiyamoorthy and Narasimman (2011), while Sathiyamoorthy et al. (2011) studied the case of a sinusoidally heated bottom wall with linearly heated sidewall and the top wall adiabatic.

The case of local thermal nonequilibrium (together with variable porosity and thermal dispersion) was treated by Alazmi and Vafai (2000), Mohamad (2000), Al-Amiri (2002), Baytas and Pop (2002), and Kayhani et al. (2011b). For a square enclosure heated at the left wall, the maximum difference between the fluid- and solid-phase temperatures occurs in the bottom left and upper right corners.

Rees (2004a) showed that the effect of viscous dissipation could result in single-cell convection being replaced by a two-cell flow as the dissipation parameter increases. At higher values of this parameter, the maximum temperature within the cavity begins to exceed the highest boundary temperature and subsequently the flow becomes time periodic.

Thermal dispersion effects were studied numerically by Beji and Gobin (1992) and de Medeiros et al. (2006) on the Brinkman-Forchheimer model. These cause a significant increase in the overall heat transfer, and when they are included, a better agreement with the experimental data is obtained, particularly when the thermal conductivities of the fluid and the solid matrix are similar.

## 7.7 Fluid and Porous Regions

Several authors, all using the Brinkman equation, have calculated the flow in a laterally heated rectangular container partly filled by clear fluid and partly with a porous medium saturated by that fluid. In most of these studies the porous medium forms a vertical layer; the interface either can be impermeable to fluid or permeable. Sathe et al. (1987) reported experimental results for a box divided in two with a vertical impermeable partition bounding the porous medium, which agreed with calculations made by Tong and Subramanian (1986). Sathe and Tong (1989) compared these results with calculations by Sathe et al. (1988) for the same problem with a permeable interface and with results for a cavity completely filled with porous medium and with a partitioned cavity containing solely clear fluid. Heat transfer is reduced by the presence of porous material having the same thermal conductivity as the fluid and by the presence of a partition. At low  $Da$  ( $=10^{-4}$ ) the first mechanism is more prominent while for high  $Da$  the second produces a greater insulating effect. The differences become accentuated at large  $Ra$ . Experiments by Sathe and Tong (1988) confirmed that partly filling an enclosure with porous medium may reduce the heat transfer more than totally filling it.

The case of a rectangular cavity with a porous medium occupying the lower half, the interface being permeable, was studied numerically by Nishimura et al. (1986). The results agreed well with previous experiments by those authors. As one would expect, most of the flow and the heat transfer occurs in the fluid region.

The most comprehensive study available of flow and temperature fields is that by Beckermann et al. (1988). They performed calculations and experiments for the configurations shown in Fig. 7.26. In the experiments the beads were of glass or aluminum and the fluid was water or glycerin. A sample result is illustrated in Fig. 7.27. In all cases investigated, the temperature profiles indicated strong convection in the fluid layer but little in the porous layer. Figure 7.27 illustrates a situation with large beads of high thermal conductivity. For smaller aluminum beads (smaller Darcy number) there is less flow in the porous layer. For the case of glass beads (of small thermal conductivity) the situation is accentuated; for small beads there is almost no flow in the porous layer, but for large beads there is a substantial amount of flow at the top and bottom of the porous layer, with the eddy centers in the fluid layer displaced toward the upper right and lower left corners.

A configuration similar to that of Fig. 7.27 is the vertical slot filled with air and divided along its vertical midplane by a permeable screen (Zhang et al. 1991a, b). The screen is a venetian blind system made out of horizontal plane strips that can be

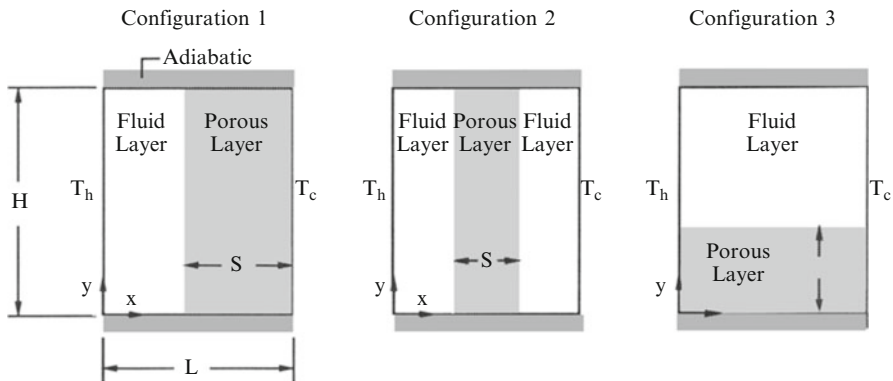


**Fig. 7.26** Definition sketch for fluid and porous regions in a vertical cavity

rotated. In the nearly “closed” position, the strips almost touch and the airflow that leaks through it behaves as in Darcy or Forchheimer flow. On both sides of the partition, the air circulation is driven by the temperature difference maintained between the two vertical walls of the slender enclosure. Zhang et al. showed numerically that there exists a ceiling value for the airflow conductance through the screen: above this value the screen pressure drop does not have a perceptible effect on the overall heat transfer rate. This ceiling value can be used for design purposes, for example, in the calculation of the critical spacing that can be tolerated between two consecutive strips in the screen.

Du and Bilgen (1990) performed a numerical study of heat transfer in a vertical rectangular cavity partially filled with a vertical layer of uniform heat-generating porous medium and with lateral heating. They varied the aspect ratio of the cavity and the thickness and position of the porous layer.

Structures with solid walls separating cavities filled with porous materials and spaces filled with air are being contemplated in the advanced design of cavernous bricks and walls of buildings (Vasile et al. 1998; Lorente et al. 1996, 1998; Lorente and Bejan 2002).

A numerical treatment of convection in a fluid-filled square cavity with differentially heated vertical walls covered by thin porous layers was studied numerically by Le Breton et al. (1991). They showed that porous layers having a thickness of the order of the boundary layer thickness were sufficient to reduce the overall Nusselt number significantly (by an amount that increased with increase of  $Ra$ ) and thicker porous layers produced only a small additional decrease in heat transfer.

Three-dimensional convection in a rectangular enclosure containing a fluid layer overlying a porous layer was treated numerically on the Brinkman model by Singh et al. (1993). A comparison study of the Darcy, Brinkman, and Brinkman-Forchheimer models was carried out by Singh and Thorpe (1995). Convection in a rectangular cavity with a porous medium occupying half the lateral distance from heated to cooled wall was studied both theoretically (with an anisotropic medium incorporated) and experimentally (using perforated plates for the solid matrix which allowed flow

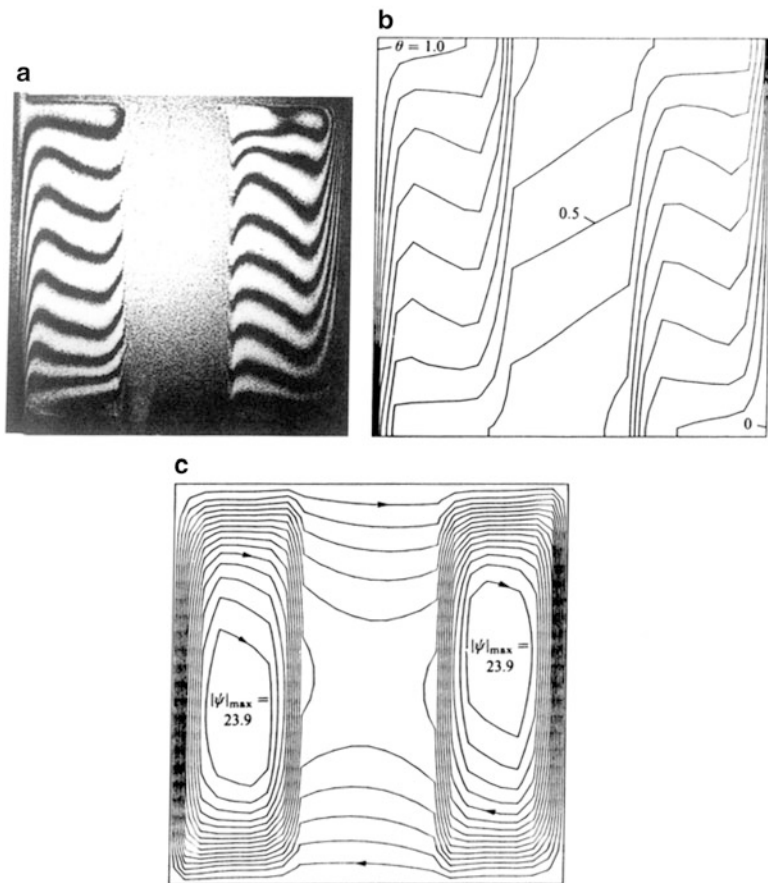


**Fig. 7.27** Experimental and predicted results for the configuration 2 shown in Fig. 7.26, with water and 6.35-mm aluminum breads: (a) photograph of interference fringe patterns, (b) predicted isotherms (equal increments), and (c) predicted streamlines (equal increments).  $S/L = 0.33$ ,  $Ra_f = 3.70 \times 10^6$ ,  $Da_L = 1.534 \times 10^{-5}$ ,  $Pr_f = 6.44$ , and  $K_m/K_f = 37.47$  (Beckermann et al. 1988, with permission from Cambridge University Press)

visualization with the aid of dye) by Song and Viskanta (1994). Convection in a partly filled inclined rectangular enclosure, with uniform or localized heating of the bottom, was studied by Naylor and Oosthuizen (1995). They found that flow patterns were sensitive to small angles of inclination to the horizontal and that dual solutions were possible. Masuoka et al. (1994) investigated the channeling effect (due to porosity variation) with a model involving a thin fluid layer adjacent to a vertical porous medium layer. They found that convection was generally enhanced by the channeling effect, but for weak convection it is reduced by the thermal resistance near the wall.

A study that involves turbulence is that by Chen et al. (1998b). They applied a  $\kappa-\epsilon$  model to the fluid part of a partly filled enclosure. They found that when the flow is turbulent in the fluid region, the heat transfer in the porous region is

dominated by convection and the penetration of the fluid into the porous region is more intensive than in the case of laminar flow.

A closed-form solution for natural convection in a rectangular cavity including a layer of porous medium adjacent to the heated side, with uniform heat flux from the sides, was obtained by Weisman et al. (1999). Mercier et al. (2002) obtained analytical expressions for a developing flow in similar circumstances. Fully developed convection in partly filled open-ended vertical channels was analyzed by Al-Nimr and Haddad (1999a); see also Nield (2001a). MHD convection in such channels was analyzed by Al-Nimr and Hader (1999b).

Paul and Singh (1998) studied convection in partly filled vertical annuli. An analytical study of convection in a partly filled vertical channel was performed by Paul et al. (1998). A numerical study of transient convection in a partly filled vertical channel was studied numerically by Paul et al. (1999). Transient convection in various domains partly filled with porous media was investigated analytically using Laplace transforms by Al-Nimr and Khadrawi (2003). Further studies of convection in partly filled vertical channels were made by Khadrawi and Al-Nimr (2003a), Singh and Gorla (2008), and Singh et al. (2011a) (Brinkman-Forchheimer model, transient effects). Pseudosteady-state convection inside a spherical container partly filled with a porous medium was studied numerically by Zhang et al. (1999a, b). Conjugate convection in a partly filled horizontal annulus was investigated by Aldoss et al. (2004). A two-temperature model was applied by Sanchez et al. (2005a, b) to a problem with symmetrically connected fluid and porous layers. Convection in an annulus with a porous sleeve was studied by Leong and Lai (2006). Saada et al. (2007) studied convection around a solid horizontal cylinder wrapped with a layer of fibrous or porous material. Convection in an open-ended inclined channel was treated by Kiwan and Khadier (2008). Avtar and Srivastava (2006) modeled the convective flow of fluid in the anterior chamber of the eye as a region partly filled by a porous medium. Free-convective Couette flow in a composite channel was studied by Jha et al. (2011). Natural convection in a composite metal-foam inclined parallel-plates channel was investigated numerically by Piller and Stalio (2012). They noted that when non-Darcy and dispersion effects are negligible the overall Nusselt number is independent of the inclination. Heat transfer between natural convection in a porous medium and forced convection in a clear fluid, separated by an impermeable vertical wall of finite thickness and height, was studied by Mosaad (2012).

## 7.8 Sloping Porous Layer or Enclosure

The topic of this section has features discussed in Chap. 6 as well as those noted in this chapter. We shall concentrate our attention on convection in the rectangular box shown in Fig. 7.28. Unless otherwise specified, the plane  $z = 0$  is heated and the plane  $z = H$  is cooled, and the other faces of the box are insulated. (Thus  $\varphi = \pi$  corresponds to a box heated from above.)

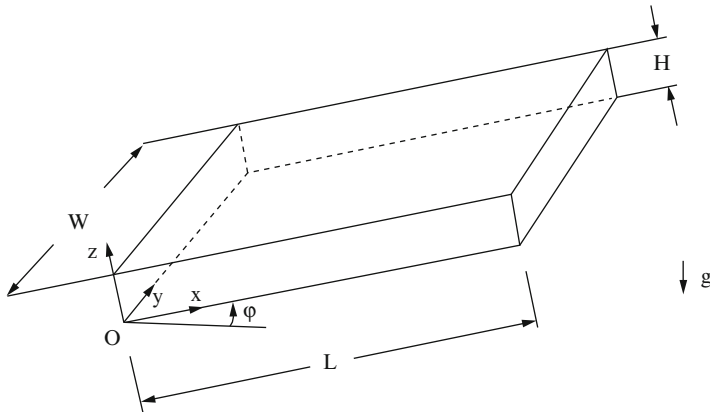


**Fig. 7.28** Definition sketch for a tilted box.  $Oy$  is horizontal and  $\varphi$  measures the inclination of  $Ox$  above the horizontal

We first consider the extension of the Horton-Rogers-Lapwood problem. The thermal boundary conditions are as in Sect. 6.1, namely  $T = T_o + \Delta T$  at  $z = 0$  and  $T = T_o$  at  $z = H$ . The differential equations (6.3), (6.4), (6.5), and (6.6) have the basic steady-state solution given by (6.8) and (6.9) and (in place of (6.7))

$$v_b = \frac{g\beta K \Delta T}{v} \left( \frac{1}{2} - \frac{z}{H} \right) \sin \varphi i, \quad (7.100)$$

This describes a unicellular flow with an upward current near the hot plate and a downward current near the cold plate.

The perturbation equation (6.16) is unchanged, but (6.17) and (6.18) are replaced by

$$\gamma_a \frac{\partial v}{\partial \hat{t}} = -\nabla \hat{P} - \hat{v} + Ra \hat{T} (\sin \varphi i + \cos \varphi k), \quad (7.101)$$

$$\frac{\partial \hat{T}}{\partial \hat{t}} + (Ra \sin \varphi) \left( \frac{1}{2} - \hat{z} \right) \frac{\partial \hat{T}}{\partial \hat{x}} - \hat{w} = \nabla^2 \hat{T} \quad (7.102)$$

and instead of (6.22) and (6.23), we now have

$$\left[ D^2 - a^2 - s - ik(Ra \sin \varphi) \left( \frac{1}{2} - \hat{z} \right) \right] \theta = -W, \quad (7.103)$$

$$(1 + \gamma_a s)(D^2 - a^2)W = -Ra[a^2(\cos \varphi)\theta + ik(\sin \varphi)D\theta]. \quad (7.104)$$

Eliminating  $W$ , one gets

$$(1 + \gamma_a s)(D^2 - a^2)(D^2 - a^2 - s)\theta - Ra \alpha^2(\cos \varphi)\theta \quad (7.105)$$

$$-ik Ra \sin \varphi \left\{ (1 + \gamma_a s) \left[ \left( \frac{1}{2} - \hat{z} \right) (D^2 - \alpha^2) \theta - 2D\theta \right] + D\theta \right\} = 0.$$

For the case of conducting impermeable boundaries,

$$\theta = D^2\theta = 0 \quad \text{at } \hat{z} = 0 \text{ and } \hat{z} = 1. \quad (7.106)$$

The system (7.105) and (7.106) can be solved by the Galerkin method (Caltagirone and Bories 1985), but an immediate result can be obtained for the case  $k = 0$ , because then the eigenvalue problem reduces to that for the horizontal layer but with  $Ra$  replaced by  $Ra \cos \varphi$ . This case corresponds to longitudinal rolls (with axes up the slope) superposed on the basic flow, that is, longitudinal helicoidal cells. A detailed examination shows that the basic unicellular flow is indeed stable for  $Ra \cos \varphi = 4\pi^2$ . Caltagirone and Bories found that convection appears in the form of polyhedral cells for small inclinations  $\varphi$  and as longitudinal helicoidal cells for larger values of  $\varphi$ , for the range  $4\pi^2 < Ra \cos \varphi < 240-280$ . When  $Ra \cos \varphi$  exceeds 240–280 for small  $\varphi$ , one has a transition to a fluctuating regime characterized by the continuous creation and disappearance of cells (as for the horizontal layer), while for larger  $\varphi$  the transition is to oscillating rolls whose boundaries are no longer parallel planes. Experiments by Bories and Combarous (1973), with a medium composed of glass beads and water, produced general agreement with the theory. The situation is summarized in Fig. 7.29. However, Nield (2011a) pointed out that the region marked (B) in the figure was incorrectly labeled. The theory does not predict that polyhedral cells should be expected in a layer with small slope.

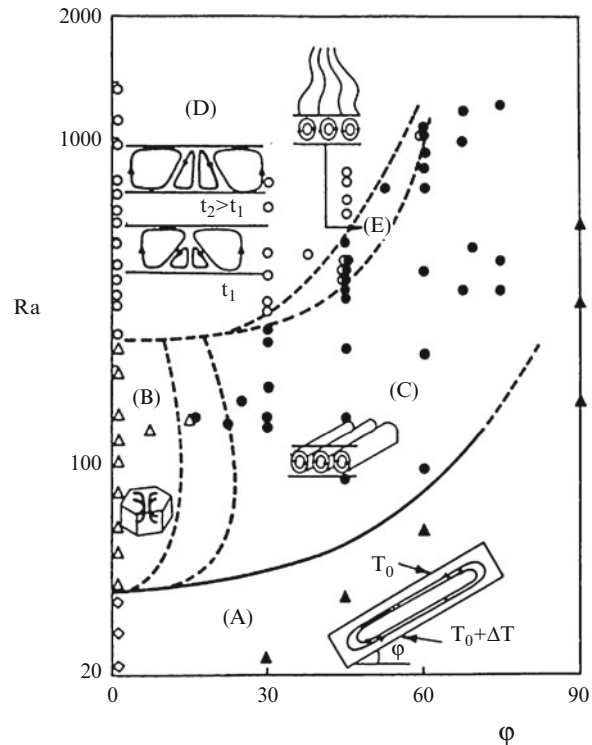
Additional experimental results reported by Hollard et al. (1995) were in agreement with the prediction (based on scale analysis) of Bories (1993) that the inclination angle  $\varphi_t$  for the transition between polyhedral cells (or transverse rolls) and longitudinal rolls is given by solving the equation

$$Ra \sin \varphi = 2^{3/2} M (Ra \cos \varphi - 4\pi)^{1/2}, \quad (7.107)$$

where  $M = 0.82$ ,  $2^{3/2}$ , or  $2$ , for hexagonal cells, transverse roll, or square cells, respectively. Hollard et al. (1995) also investigated the transition between the stationary and nonstationary flows by means of a spectral analysis of the temperature field.

In the above discussion we have assumed that the inclination  $\varphi$  is fixed prior to the experiment. When one changes  $\varphi$  with  $Ra$  held constant, one observes hysteresis with respect to flow pattern transition (Kaneko et al. 1974), but the overall heat transfer appears to be almost independent of flow pattern. As predicted by the analysis of Weber (1975a), the Nusselt number correlates well with  $Ra \cos \varphi$ . End effects modify the transition criteria, increasing the domain of stability of the basic flow (Jaffrenou et al. 1974).

**Fig. 7.29** The different types of convective motion experimentally observed in a tilted porous layer: (A) unicellular flow, (B) polyhedral cells, (C) longitudinal stable coils, (D) fluctuating regime, and (E) oscillating longitudinal coils (Combarious and Bories 1975, with permission from Academic Press)



Inaba et al. (1988) performed experiments using media of several different materials for  $0^\circ \leq \varphi \leq 180^\circ$ ,  $5 \leq L/H \leq 32.7$ , and  $0.074 \leq d_p/H \leq 1.0$ , where  $d_p$  is the particle diameter. These and previous experiments indicated the existence of a maximum heat transfer rate at  $\varphi = 45\text{--}60^\circ$  for  $Ra = 350$ . This motivates the following correlation formulas of Inaba et al. (1988), in which  $Pr = v/\alpha_m$ .

For  $60 \leq Ra \cos(\varphi - 60^\circ) \leq 4.5 \times 10^2$ ,  $0^\circ \leq \varphi \leq 15^\circ$ ,

$$Nu = 0.053 Pr^{0.13} \left( \frac{d_p}{H} \right)^{-0.20} [Ra \cos(\varphi - 60^\circ)]^{0.72}. \quad (7.108)$$

For  $60 \leq Ra \cos(\varphi - 60^\circ) \leq 4.5 \times 10^2$ ,  $15^\circ \leq \varphi \leq 120^\circ$ ,

$$Nu = 0.024 Pr^{0.13} \left( \frac{L}{H} \right)^{-0.34} [Ra \cos(\varphi - 60^\circ)]^{0.52}. \quad (7.109)$$

For  $4.5 \times 10^2 \leq Ra \cos \varphi \leq 3 \times 10^4$ ,  $0 \leq \varphi \leq 60^\circ$ ,

$$Nu = 0.067 Pr^{0.13} \left( \frac{d_p}{H} \right)^{-0.65} (Ra \cos \varphi)^{0.52}. \quad (7.110)$$

For  $4.5 \times 10^2 \leq Ra \sin \varphi \leq 3 \times 10^4$ ,  $60^\circ \leq \varphi \leq 120^\circ$ ,

$$Nu = 0.062 Pr^{0.13} \left( \frac{L}{H} \right)^{-0.52} (Ra \sin \varphi)^{0.46}. \quad (7.111)$$

The case of large  $L/H$ ,  $W/H$  was examined numerically by Moya et al. (1987). They found that for small  $\varphi$ , multiple solutions were possible. In addition to “natural” unicellular convection with flow up the heated wall and down the cooled wall, there also can exist an “antinatural” motion with circulation in the opposite direction. A bifurcation study by Riley and Winters (1990) shows that the appearance of the antinatural mode is associated with an isola. The various modal exchanges that occur as the aspect ratio of the tilted cavity varies were studied by Impey and Riley (1991).

There are further complications when  $L/H$  and  $W/H$  are of order unity. Pien and Sen (1989) showed by numerical calculation that there was hysteresis in the transition from an upslope roll pattern to a cross-slope roll pattern as  $\varphi$  is varied, the Nusselt number being affected.

Detailed studies of the onset of convection in an inclined layer heated from below were reported by Rees and Bassom (1998, 2000). They included a full numerical solution of the linearized disturbance equations, and the results were used to motivate various asymptotic analyses. They found that at large Rayleigh numbers, a two-dimensional instability only can arise when the angle that the layer makes with the horizontal is less than or equal to  $31.30^\circ$ , while the maximum inclination below which this instability may be possible is the slightly greater value  $31.49^\circ$ , which corresponds to a critical Rayleigh number of 104.30.

So far in our discussion, the heated and cooled boundaries have been isothermal. Problems involving constant-flux heating have also been considered. For  $90^\circ < \varphi < 180^\circ$  and the limit  $L/H \rightarrow \infty$ , an analytic parallel-flow solution was obtained by Vasseur et al. (1987). This solution is a good predictor of  $Nu$  for  $L/H = 4$ . Sen et al. (1987, 1988) have investigated the multiple steady states that occur when  $\varphi$  is small and all four faces of a rectangular enclosure are exposed to uniform heat fluxes, opposite faces being heated and cooled, respectively. Vasseur et al. (1988) showed that in the case  $90^\circ < \varphi < 180^\circ$ , the maximum temperature within the porous medium can be considerably higher than that induced by pure conduction. In this case the convection is considerably decreased when  $L/H$  is either very large or very small. A further study of constant-flux heating was made by Alex and Patil (2000b), using the Brinkman model.

The effect of the Brinkman boundary friction on heat transfer in an inclined box or layer was first calculated by Chan et al. (1970) and later by Vasseur et al. (1990). The additional effects of viscous dissipation were studied analytically by Malashetty et al. (2001). Flow in between concentric-inclined cylinders was studied numerically and experimentally by Takata et al. (1982) for isothermal heating and by Wang and Zhang (1990) for constant flux on the inner cylinder.

The problem for a non-Newtonian (power-law) fluid was studied by Bian et al. (1994a, b). For a Newtonian fluid, the effect of a magnetic field was examined by Alchaar et al. (1995b) and Bian et al. (1996b). Because they considered two-dimensional disturbances only, their treatment may be incomplete.

The quasisteady convection produced by heating one side of a porous slab was studied by Robillard and Vasseur (1992). The case of a porous layer adjacent to a wall of finite thickness was investigated by Mbaye et al. (1993). A porous layer with an off-center diathermal partition was examined by Jang and Chen (1989). A numerical solution for convection in a cavity with a discrete heat source on one wall was obtained by Hsiao et al. (1994). An experimental investigation of a layer bounded by impervious domains of finite thermal conductivity in the presence of a vertical temperature gradient was conducted by Chevalier et al. (1996). The expected transition from two-dimensional to three-dimensional convection, as  $Ra$  increases, was found. A further numerical and experimental study of this configuration was reported by Chevalier et al. (1999).

Convection and dispersion in a reservoir with tilted fractures was studied theoretically and experimentally by Luna et al. (2004) under the assumption that the fluid thermal conductivity is very small compared with the rock conductivity.

A novel approach to convection in anisotropic-inclined porous layers, which is able to deal with nonsymmetric multilayered systems, was presented by Trew and McKibbin (1994). The method involves the numerical summation of a series. A further study of the effect of anisotropic permeability on convection flow patterns was made by Storesletten and Tveitereid (1999). A layer anisotropic with respect to both permeability and diffusivity was analyzed by Rees and Postelnicu (2001) and Postelnicu and Rees (2001); the second paper was concerned with small angles to the horizontal. They found that often there is a smooth rather than an abrupt transition between longitudinal and transverse rolls as the governing parameters are varied. The effect of anisotropy also was studied numerically by Cserepes and Lenkey (2004) for the case of an unconfined aquifer. The effect of the Forchheimer drag was added by Rees et al. (2006a). They found that in general the critical Rayleigh number increases substantially as the form drag effects strengthen but the wavenumber increases by only a small amount. They supplemented their numerical study by a brief asymptotic analysis of the case where the Forchheimer terms dominate, and they showed that then the critical Rayleigh number increases in direct proportion to the form drag parameter.

The effects of variable porosity and thermal dispersion were investigated numerically by Hsiao (1998). An analytical and experimental study of low Rayleigh number convection in long tilted fractures, embedded in an impermeable solid subjected to a vertical temperature gradient, was reported by Medina et al. (2002). Detailed numerical calculations for steady-state convection in an inclined porous cavity were made by Baytas and Pop (1999) and calculations of entropy generation were reported by Baytas (2004b) and Baytas and Baytas (2005). MHD problems were studied numerically by Khanafer and Chamkha (1998) and Khanafer et al. (2000).

The case of volumetric heating in a porous bed adjacent to a fluid layer in an inclined enclosure was investigated numerically by Chen and Lin (1997). In this case multiple steady-state solutions are possible. The effect of a magnetic field was added by Mansour et al. (2010a) and by Al-Badawi and Duwairi (2010). The combined effects of inclination, anisotropy, and internal heat generation on the linear stability of the basic parallel flow were analyzed by Storesletten and Rees (2004). They found that the preferred motion at the onset of convection depends strongly on the anisotropy ratio  $\xi = K_L/K_T$ . When  $\xi < 1$  the preferred motion is longitudinal rolls for all inclinations. When  $\xi > 1$  transverse rolls are preferred for small inclinations but at high inclinations longitudinal rolls are preferred, while at intermediate inclinations the preferred roll orientation varies smoothly between these two extremes. The case of an anisotropic medium with oblique principal axes was examined by Rees et al. (2006b). They found that when the principal axes are not aligned with the coordinate directions and when the ratios of principal permeabilities or diffusivities are not too small or too large, there is always a smooth transition in the orientation of the most dangerous mode of instability as the inclination increases from the horizontal, but in the more extreme cases there may be sudden changes in orientation, Rayleigh number, and wavenumber.

Convection in tilted cylindrical cavities embedded in rocks subject to a uniform temperature gradient was studied theoretically by Sanchez et al. (2005a, b). Passive dispersion in symmetrically interconnected layers was studied by Sanchez and Medina (2006).

Weak 2D convective plumes in a sloping porous layer were studied by McKibbin (2009), while convection in layered sloping warm-water aquifers was treated by McKibbin et al. (2011), and the instability of this flow was examined by McKibbin (2012). The linear stability of the problem with isoflux boundaries was analyzed by Rees and Barletta (2011). The effect of viscous dissipation on the onset of convection in an inclined layer was studied by Nield et al. (2011).

Oztop (2007) studied convection in partly cooled inclined rectangular enclosures. Wang et al. (2007b) and Shedadeh and Duwairi studied numerically the effect of a magnetic field. Time-periodic boundary conditions were treated by Wang et al. (2008a, b, 2010b). Entropy variation for a case of unsteady convection with radiation was treated by Slimi (2006). Further studies of convection in tilted cavities were carried out by Báez and Nicolás (2006, 2007).

## 7.9 Inclined Temperature Gradient

We now discuss an extension to the Horton-Rogers-Lapwood problem. We suppose that a uniform horizontal temperature gradient  $\beta_H$  is imposed on the system, in addition to the vertical temperature gradient  $\Delta T/H$ . The boundary conditions used in Sect. 6.1 are now replaced by

$$T = T_o + \Delta T - \beta_H x \text{ at } z = 0, \quad T = T_o - \beta_H x \text{ at } z = H. \quad (7.112)$$

The basic steady-state solution, in nondimensional form, is now given by

$$u_b = \hat{\beta}_H Ra \left( \hat{z} - \frac{1}{2} \right), \quad (7.113)$$

$$T_b = \frac{T_o}{\Delta T} + 1 - \hat{\beta}_H \hat{x} - \hat{z} - \frac{1}{12} \hat{\beta}_H^2 Ra (\hat{z} - 3\hat{z}^2 + 2\hat{z}^3), \quad (7.114)$$

where

$$\hat{\beta}_H = \frac{\beta_H H}{\Delta T}. \quad (7.115)$$

Equation (6.23) is unchanged, but (6.22) is replaced by

$$(D^2 - \alpha^2 - s - ilu_b)\theta + i\hat{\beta}_H \left( \frac{l}{\alpha^2} \right) DW - WDT_b = 0. \quad (7.116)$$

The system (6.22), (6.24), and (7.116) can be solved using the Galerkin method. Some approximate results based on a low-order approximation and with  $\gamma_a$  assumed negligible were obtained by Nield (1991a). He found that longitudinal stationary modes ( $l = 0, s = 0$ ) are the most unstable modes. For the first such mode, the critical values are

$$\alpha_1 = \pi, \quad Ra_1 = 4\pi^2 + \frac{Ra_H^2}{4\pi^2}, \quad (7.117)$$

where the horizontal Rayleigh number  $Ra_H$  is defined by

$$Ra_H = \hat{\beta}_H Ra = \frac{g\beta K H^2 \beta_H}{\nu \alpha_m}. \quad (7.118)$$

For small  $\hat{\beta}_H$ , (7.117) agrees with the approximation obtained by Weber (1974), namely

$$Ra = 4\pi^2 (1 + \hat{\beta}_H^2). \quad (7.119)$$

For the second mode, the critical values are

$$\alpha_2 = 2\pi, \quad Ra_2 = 16\pi^2 + \frac{Ra_H^2}{16\pi^2}. \quad (7.120)$$

We see that  $Ra_2 > Ra_1$  for  $Ra_H < 8\pi^2$ , but  $Ra_2 < Ra_1$  when  $Ra_H > 8\pi^2$ . Thus there is a transition from the first mode to the second as  $Ra_H$  increases.

The effect of increasing  $Ra_H$  is stabilizing because it distorts the basic temperature profile away from the linear one and ultimately changes the sign of its slope in the center of the channel. More accurate results, reported by Nield (1994d), showed that as  $Ra_H$  increases, the critical value of  $Ra$  reaches a maximum and passes through zero. This means that the Hadley flow becomes unstable, even in the absence of an applied vertical gradient, when the circulation is sufficiently intense. The flow pattern changes from a single layer of cells to two or more superimposed layers of cells (superimposed on the Hadley circulation) as  $Ra_H$  increases. Yet more accurate results, together with the results of a nonlinear energy stability analysis, were reported by Kaloni and Qiao (1997). Two very accurate methods for determining the eigenvalues and eigenfunctions involved with such problems were discussed by Straughan and Walker (1996b).

Direct numerical simulations of supercritical Hadley circulation, restricted to transverse secondary flow, were performed by Manole and Lage (1995) and Manole et al. (1995). The results are in general accord with the linear stability analysis. Beyond a threshold value of  $Ra_H$  the Hadley circulation evolves to a time-periodic flow, and the vertical heat transfer increases. The secondary flow emerges in the form of a traveling wave aligned with the Hadley flow direction. At low supercritical values of  $Ra$ , this traveling wave is characterized by the continuous drifting of two horizontal layers of cells that move in opposite directions. As  $Ra$  increases, the traveling wave becomes characterized by a single layer of cells drifting in the direction opposite to the applied horizontal temperature gradient. The extension to the anisotropic case, or to include the effect of internal heat sources, was made by Parthiban and Patil (1993, 1995).

Nield (1990) also investigated the effect of adding a net horizontal mass flux  $Q$  in the  $x$  direction. This is destabilizing, and at sufficiently large values of  $Q$ , instability is possible in the absence of a vertical temperature gradient.  $Q$  also has the effect of smoothing out the transition from one mode to the next. More accurate results and a supplementary nonlinear analysis were reported by Qiao and Kaloni (1997). In this connection, new computational methods described by Straughan and Walker (1996b) are useful. The effect of vertical throughflow was incorporated by Nield (1998b). This study was extended to include absolute and convective instabilities by Brevdo (2009) and Brevdo and Ruderman (2009a, b). The effect of a gravitational field varying with distance in the layer and with the additional effects of vertical throughflow, or volumetric heating with or without anisotropy, was analyzed by Alex et al. (2001), Alex and Patil (2002a, b), and Parthiban and Patil (1997). Nonlinear instability studies, for the cases of vertical throughflow and variable gravity, were conducted by Qiao and Kaloni (1998) and Kaloni and Qiao (2001). Horizontal mass flux and variable gravity effects were considered by Saravanan and Kandaswamy (2003b). The topic of this section has been reviewed by Lage and Nield (1998).

The linear instability of the Darcy-Hadley flow in an inclined layer was studied by Barletta and Rees (2012b). They found that longitudinal modes are selected. They treated three regimes: (1) upward cooling, (2) upward heating, and (3) buoyancy balanced. In regime 3, the basic state is one of zero velocity and vertical temperature

gradient. In regime 1, with fixed  $Ra_H$ , increasing the inclination angle  $\phi$  leads to a destabilizing effect. When  $\phi$  exceeds a value that depends of  $Ra_H$ , the basic solution becomes unstable for every  $Ra$ . In regime 2, increasing  $\phi$  leads to stabilization.

The effect of viscous dissipation on the Hadley-Prats problem (with horizontal throughflow) was studied by Barletta and Nield (2010). The effect of vertical heterogeneity on the Hadley flow was investigated by Barletta and Nield (2012). The case of a horizontal temperature gradient with asymmetric thermal boundary conditions was studied by Barletta and Rossi di Schio (2012).

## 7.10 Periodic Heating

Lage and Bejan (1993) showed that when an enclosed saturated porous medium is heated periodically from the side, the buoyancy-induced circulation resonates to a well-defined frequency of the pulsating heat input. The resonance is characterized by maximum fluctuations in the total heat transfer rate through the vertical midplane of the enclosure. Lage and Bejan (1993) demonstrated this principle for an enclosure filled with a clear fluid and an enclosure filled with a fluid-saturated porous medium. They showed that the resonance frequency can be anticipated based on theoretical grounds by matching the period of the pulsating heat input to the period of the rotation (circulation) of the enclosed fluid. Below we outline Lage and Bejan's (1993) scale analysis of the resonance frequency in the Darcy and Forchheimer flow regimes.

Consider the two-dimensional configuration of Fig. 7.1 and assume that the flow is in the Darcy regime. The period of the fluid wheel that turns inside the enclosure is

$$w \sim \frac{4H}{V}, \quad (7.121)$$

where  $V$  is the scale of the peripheral velocity of the wheel and  $4H$  is the wheel perimeter in a square enclosure. The velocity scale is given by (7.12),

$$V \sim \frac{\alpha_m}{H} \overline{Ra}, \quad (7.122)$$

where  $\overline{Ra} = g\beta KH(\bar{T}_h - T_c)/(V\alpha_m)$  is the Darcy-modified Rayleigh number based on the average side-to-side temperature difference  $(\bar{T}_h - T_c)$ . The hot-side temperature ( $T_h$ ) varies in time because the heat flux through that wall is administered in pulses that vary between  $q''_M$  (maximum) and zero. The cold-side temperature ( $T_c$ ) is fixed.

The  $V$  scale can be restated in terms of the flux Rayleigh number  $Ra_* = g\beta KH^2 q''_M/(V\alpha_m k_m)$  by noting that  $\overline{Ra} = Ra_*/\overline{Nu}$ , where in accordance with (7.49),

$$\overline{Nu} = \frac{q''_M H}{k(\bar{T}_h - T_c)} \sim Ra_*^{2/5}. \quad (7.123)$$

Combining the relations listed between (7.121) and (7.123) we obtain  $V \sim (\alpha_m/H)$   $Ra_*^{3/5}$  and the critical period for resonance (Lage and Bejan 1993):

$$w \sim 4 \frac{H^2}{\alpha_m} Ra_*^{-3/5} \text{(Darcy).} \quad (7.124)$$

At higher Rayleigh numbers, when the Forchheimer term ( $\chi/v$ )  $V^2$  is greater than the Darcy term ( $V$ ) on the left side of (7.90), the vertical velocity scale is (cf. Table 7.1)

$$V \sim \frac{\alpha_m}{H} Ra_\infty^{1/2}. \quad (7.125)$$

In this expression,  $Ra_\infty = g\beta KH^2(\bar{T}_h - T_c)/(\chi\alpha_m^2)$  is the Forchheimer-regime Rayleigh number. Next, we introduce the flux Rayleigh number for the Forchheimer regime,  $Ra_{\infty*} = g\beta KH^3 q''_M/(\chi\alpha_m^2 k_m)$ , and note that  $Ra_\infty = Ra_{\infty*}/\overline{Nu}$  and  $\overline{Nu} \sim Ra_{\infty*}^{1/5}$ . These relations produce the following scaling law for the critical period (Lage and Bejan 1993):

$$w \sim 4 \frac{H^2}{\alpha_m} Ra_{\infty*}^{-2/5} \text{(Forchheimer).} \quad (7.126)$$

Three findings were extended and strengthened by subsequent numerical and theoretical studies of the resonance phenomenon. Antohe and Lage (1994) generalized the preceding scale analysis and produced a critical-frequency scaling law that unites the Darcy and Forchheimer limits ((7.124) and (7.126)) with the clear fluid limit, which had been treated separately in Lage and Bejan (1993). The effect of the pulse amplitude was investigated more recently by Antohe and Lage (1996), who showed that the convection intensity within the enclosure increases linearly with the heating amplitude. The convection intensity decreases when the fluid Prandtl number increases or decreases away from a value of order one (Antohe and Lage 1997a).

The corresponding phenomenon in forced convection was analyzed theoretically and numerically by Morega et al. (1995). Their study covered both the clear fluid (all  $Pr$  values) and saturated porous medium limits of the flow parallel to a plane surface with pulsating heating. The critical heat pulse period corresponds to the time scale of one sweep over the surface, that is, the time of boundary layer renewal.

The effect of local thermal nonequilibrium was studied by Khadrawi et al. (2005).

## 7.11 Sources in Confined or Partly Confined Regions

The problem of nuclear waste disposal has motivated a large number of studies of heat sources buried in the ground. An early review of the subject is that by Bau (1986a, b).

The analyses of Bau (1984b) for small  $Ra$  and Farouk and Shayer (1988) for  $Ra$  up to 300 apply to a cylinder in the semi-infinite region bounded by a permeable plane. This geometry is applicable to the experiments conducted by Fernandez and Schrock (1982). The numerical work is aided by a preliminary transformation to bicylindrical coordinates.

Himasekhar and Bau (1987) obtained analytical and numerical solutions for convection induced by isothermal hot or cold pipes buried in a semi-infinite medium with a horizontal impermeable surface subject to a Robin thermal boundary condition. Himasekhar and Bau (1988a) made a theoretical and experimental study of convection around a uniform-flux cylinder embedded in a box. They found a transition from a two-dimensional steady flow to a three-dimensional oscillatory flow as the Rayleigh number increased. A similar problem with a sheath of different permeability surrounding the pipe was examined numerically by Ngo and Lai (2005). Hsiao et al. (1992) studied two-dimensional transient convection numerically on the Brinkman-Forchheimer model with thermal dispersion and nonuniform porosity allowed for. The effects of these two agencies increase the predicted heat flux, bringing it more in line with experimental data. Murty et al. (1994) used the Brinkman-Forchheimer model to study numerically convection around a buried cylinder using a penalty function method. Muralidhar (1992) summarized some analytical and numerical results for the temperature distribution around a cylinder (or an array of cylinders), for free or forced convection, with temperature or heat flux prescribed on the cylinder and Darcy's law assumed. Muralidhar (1993) made a numerical study of heat and mass transfer for buried cylinders with prescribed heat flux and leach rates. He obtained the temperature and concentration distributions on the surface of the containers under a variety of conditions. The case of a buried elliptic heat source with a permeable surface was studied numerically on the Darcy model by Facas (1995b). An ellipse with its minor axis horizontal yields much higher heat transfer rates than one with its major axis horizontal. The heat transfer depends little on the burial depth. A numerical study using the Brinkman-Forchheimer model of steady and transient convection from a corrugated plate of finite length placed in a square enclosure was performed by Hsiao and Chen (1994) and Hsiao (1995).

Anderson and Glasser (1990) fitted experimental steady-state temperature measurements in a porous medium containing a buried heater to a theoretical model of vertical cylindrical source of finite height placed in a box with a pyramid lid, with a constant heat transfer coefficient at the upper free surface. They derived a simple one-dimensional model relating power input to surface temperature irrespective of the values of permeability, source size, and depth, and they showed that this was useful in monitoring the self-heating in stockpiles of coal, for example, and was consistent with the experiments.

Numerical modeling on the Brinkman-Forchheimer model, of convection around a horizontal circular cylinder, was carried out by Christopher and Wang (1993). They found that the presence of an impermeable surface above the cylinder significantly alters the flow field and reduces the heat transfer from the cylinder, while recirculating zones may develop above the cylinder, creating regions of low

and high heat transfer rates. As expected, the Forchheimer term reduces the flow velocity and heat transfer, especially for the case of large  $Da$ .

Facas (1994, 1995a) has investigated numerically on the Darcy model convection around a buried pipe with two horizontal baffles attached and with a permeable bounding surface. They handled the complicated geometry using a body-fitted curvilinear coordinate system.

The case of a horizontal line heat source placed in an enclosure of rectangular cross section was studied numerically on the Darcy model by Desrayaud and Lauriat (1991). Their results indicated that the heat fluxes transferred to the walls and the source temperature vary strongly with the thermal conductivity of the sidewalls and the convective boundary condition at the ground. Further, for burial depths larger than the width of the cavity, the flow may be unstable to small disturbances and as a result the thermal plume may be deflected toward one of the sidewalls.

Oosthuizen and Naylor (1996a) studied numerically heat transfer from a cylinder placed on the vertical centerline of a square enclosure partially filled with a porous medium. Oosthuizen and Paul (1992), Oosthuizen (1995), and Oosthuizen and Naylor (1996b) used a finite element method to study heat transfer from a heated cylinder buried in a frozen porous medium in a square container, the flow being steady, two-dimensional, and with Darcy's law applicable and with either uniform temperature or heat flux specified on the cylinder and with one or more of the walls of the enclosure held at some subfreezing point temperature (or temperatures).

The inverse determination of a heat source from natural convection in a cavity was investigated by Wong and Xie (2011), while Sankar et al. (2011a) studied convection in a cavity with partly thermally active sidewalls.

## 7.12 Effects of Rotation

The problem of stability of free convection in a rotating porous slab with lateral boundaries at different temperatures and rotation about a vertical axis so that the temperature gradient is collinear with the centrifugal body force was treated analytically by Vadasz (1994a, 1996a, b), first for a narrow slab adjacent to the center of rotation and then distant from the center of rotation. In the limit of infinite distance from the axis of rotation, the problem is analogous to that of gravitational buoyancy-induced convection with heating from below, the critical value of the centrifugal Rayleigh number  $Ra_{\omega 0}$  (defined as in (6.190)) being  $4\pi^2$  for the case of isothermal boundaries. At finite distance from the axis of rotation, a second centrifugal Rayleigh number  $Ra_{\omega 1}$  (one proportional to that distance) enters the analysis. The stability boundary is given by the equation  $(Ra_{\omega 1}/7.81\pi^2) + (Ra_{\omega 0}/4\pi^2) = 1$ . The convection appears in the form of superimposed rolls.

The case where the axis of rotation is within the slab so that the centrifugal body force alternates in direction was treated by Vadasz (1996b). He found that the flow pattern was complex and that the critical centrifugal Rayleigh number and

wavenumber increase significantly as the slab's cold wall moves significantly away from the rotation axis. This leads eventually to unconditional stability when the slab's hot wall coincides with the rotation axis. Unconditional stability is maintained when the axis of rotation moves away from the porous domain, so that the imposed temperature gradient opposes the centrifugal acceleration. Centrifugal convection with a magnetic fluid was analyzed by Saravanan and Yamaguchi (2005).

A further extension in which gravity as well as centrifugal forces is taken was made by Vadasz and Govender (1998). They considered a laterally heated vertical slab far away from the axis of rotation and calculated critical values of  $Ra_{\omega 0}$  for various values of a gravitational Rayleigh number  $Ra_g$ .

A related problem involving a slowly rotating (large Ekman number) long box heated above and rotating about a vertical axis was analyzed by Vadasz (1993). Now the applied temperature gradient is orthogonal to the centrifugal body force and the interest is on the Coriolis effect. Vadasz employed an expansion in terms of small aspect ratio and small reciprocal Ekman number. He showed that secondary flow in a plane orthogonal to the leading free convection plane resulted. The controlling parameter is  $Ra_{\omega}/Ek$ . The Coriolis effect in a long box subject to uniform heat generation was investigated analytically by Vadasz (1995). A nonlinear analysis using the Adomian decomposition method was employed by Olek (1998). An MHD study incorporating the effect of Hall current was done by Singh and Kumar (2009).

# Chapter 8

## Mixed Convection

### 8.1 External Flow

#### 8.1.1 Inclined or Vertical Plane Wall

We already have discussed one form of mixed convection in a horizontal layer, namely, the onset of convection with throughflow when the heating is from below (see Sect 6.10). In this chapter, we discuss some more general aspects of mixed convection. Since we have dealt with natural convection and forced convection in some detail, our treatment of mixed convection in a porous medium [first treated by Wooding (1960)] can be brief. It is guided by the surveys by Lai et al. (1991a) and Lai (2000). We endorse the statement by Lai (2000) that despite the increased volume of research in this field, experimental results are still very few. In particular experimental data on thermal dispersion are very scarce, and this is hindering the study of the functional relationship between effective thermal conductivity and thermal dispersion.

We start with a treatment of boundary layer flow on heated plane walls inclined at some nonzero angle to the horizontal. The foundational study is that by Cheng (1977c). This configuration is illustrated in Fig. 8.1. The boundary layer equations [compare Eqs. (5.5) and (5.6)] for steady flow are

$$\frac{\partial^2 \Psi}{\partial y^2} = \pm \frac{g_x \beta K}{v} \frac{\partial T}{\partial y} \quad (8.1)$$

$$\frac{\partial \Psi}{\partial y} \frac{\partial T}{\partial x} - \frac{\partial \Psi}{\partial x} \frac{\partial T}{\partial y} = \frac{\partial}{\partial y} \left( \alpha_m \frac{\partial T}{\partial y} \right). \quad (8.2)$$

Here  $\pm g_x$  is the component of  $\mathbf{g}$  in the positive  $x$  direction, i.e., the direction of the stream velocity  $\mathbf{U}_\infty$  at infinity. The Plus sign corresponds to the case where the buoyancy force has a component “aiding” the general flow and the Minus

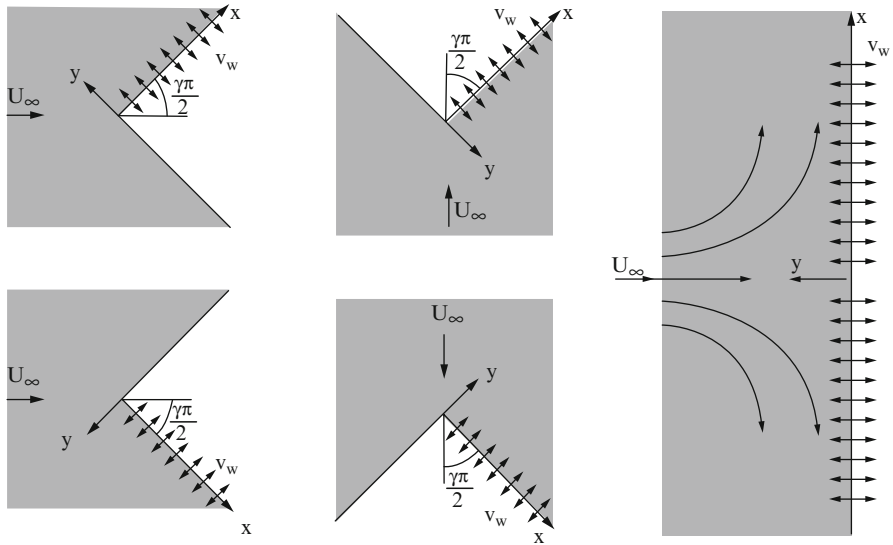


**Fig. 8.1** Definition sketch for mixed convection over an inclined surface

sign to the “opposing” case. We seek a similarity solution and allow for suction/injection at the wall. Hence we take as boundary conditions the set

$$y = 0 : \quad T = T_\infty \pm Ax^\lambda, \quad v = -\frac{\partial \Psi}{\partial x} = ax^n, \quad (8.3)$$

$$y \rightarrow \infty : \quad T = T_\infty, u = \frac{\partial \Psi}{\partial y} = U_\infty = Bx^m, \quad (8.4)$$

where  $A$ ,  $a$ , and  $B$  are constants. The exponent  $m$  is related to the angle of inclination  $\gamma\pi/2$  (to the incident free-stream velocity) by the relation  $\gamma = 2m/(m+1)$ .

We find that a similarity solution does exist if  $\lambda = m$  and  $n = (m-1)/2$ . The range of possibilities includes the cases

$\lambda = m = 0, n = -1/2$  (vertical isothermal wall, injection  $\propto x^{-1/2}$ )

$\lambda = m = 1/3, n = -1/3$  (wall at  $45^\circ$  inclination, constant heat flux)

$\lambda = m = 1, n = 0$  (stagnation flow normal to vertical wall (Fig. 1.1e), linear temperature variation, uniform injection)

With the similarity variables

$$\eta = \left( \frac{U_\infty x}{\alpha_m} \right)^{1/2} \frac{y}{x}, \quad f(\eta) = \frac{\Psi}{(\alpha_m U_\infty x)^{1/2}}, \quad \theta(\eta) = \frac{T - T_\infty}{T_w - T_\infty} \quad (8.5)$$

and the wall suction parameter

$$f_w = -2a/(m+1)(\alpha_m B)^{1/2}, \quad (8.6)$$

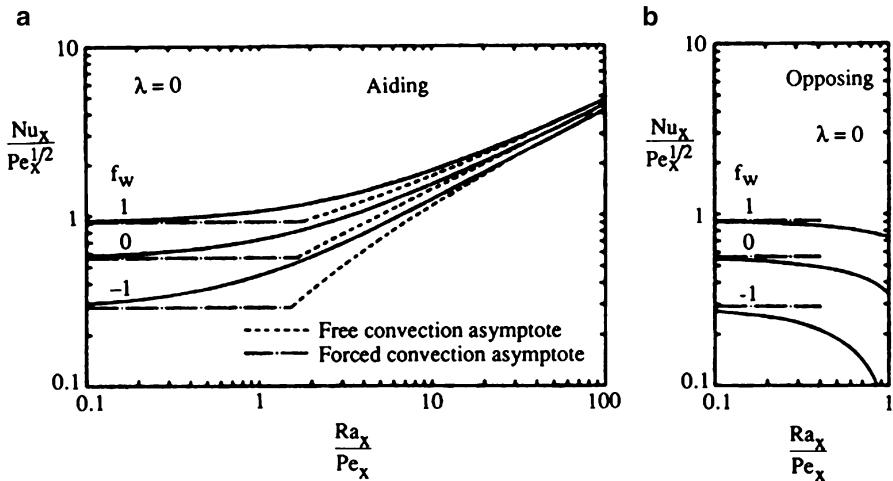


**Fig. 8.2** Nusselt numbers for aiding and opposing flow with injection and suction on a vertical flat plate (Lai and Kulacki 1990d)

we obtain the system

$$f'' = \pm \frac{Ra_x}{Pe_x} \theta', \quad (8.7)$$

$$\theta'' = -\frac{\lambda + 1}{2} f \theta' + \lambda f' \theta \quad (8.8)$$

$$\theta(0) = 1, \quad f(0) = f_w, \quad \theta(\infty) = 0, \quad f'(\infty) = 1. \quad (8.9)$$

The numbers  $Ra_x$  and  $Pe_x$  are defined in Eq. (8.14). The quantity  $Ra/Pe$  has been called the mixed convection parameter by Holzbecher (2004a). For the case when this parameter is in the range  $[-3/2.0]$  and the plate temperature varies inverse-linearly with distance, exact dual solutions were obtained by Magyari et al. (2001b). Such solutions were first investigated by Merkin (1985). A special case that leads to a self-similar solution was studied by Magyari et al. (2002).

A positive  $f_w$  indicates withdrawal of fluid. The case of forced convection corresponds to letting  $Ra_x \rightarrow \infty$ . The case of natural convection requires a different similarity variable. Lai and Kulacki (1990d) obtained and solved these equations. Their results for the Nusselt number are shown in Fig. 8.2 for the case  $\lambda = 0$ . Those for  $\lambda = 1/3$  and  $\lambda = 1$  are qualitatively similar; the effect of increasing  $\lambda$  is to raise the Nusselt number slightly. The case of adiabatic surfaces was analyzed by Kumari et al. (1988c).

The effects of flow inertia and thermal dispersion were studied by Lai and Kulacki (1988a). Now Eq. (8.1) is replaced by

$$\frac{\partial^2 \Psi}{\partial y^2} + \frac{\chi}{v} \frac{\partial}{\partial y} \left( \frac{\partial \Psi}{\partial y} \right)^2 = \pm \frac{g_x \beta K}{v} \frac{\partial T}{\partial y}, \quad (8.10)$$

where  $\chi = c_F K^{1/2}$ , and in Eq. (8.2)  $\alpha_m$  is replaced by  $\alpha_e$ , the sum of a molecular diffusivity  $\alpha_0$  and a dispersive term  $\alpha' = Cud_p$ , where  $d_p$  is the mean pore diameter and  $C$  is a constant. We treat an isothermal vertical plate, and we suppose that there is no suction. Equations (8.7)–(8.9) thus are replaced by

$$f'' + Fo_x Re_x [(f')^2]' = \pm \frac{Ra_x}{Pe_x} \theta', \quad (8.11)$$

$$\theta'' + \frac{1}{2} f \theta' + CPe_d (f'' \theta' + f' \theta'') = 0, \quad (8.12)$$

$$\theta(0) = 1, \quad f(0) = 0, \quad \theta(\infty) = 0, \quad f'(\infty) = 1, \quad (8.13)$$

where

$$Fo_x = \frac{c_F K^{1/2}}{x}, \quad Re_x = \frac{U_\infty x}{v}, \quad Pe_x = \frac{U_\infty x}{\alpha_m}, \quad Pe_d = \frac{U_\infty d_p}{\alpha_m}, \quad (8.14)$$

$$Ra_x = \frac{g_x \beta K x (T_w - T_\infty)}{v \alpha_m}, \quad Ra_d = \frac{g_x \beta K d_p (T_w - T_\infty)}{v \alpha_m}.$$

The local Nusselt number  $Nu_x$  is given by

$$\frac{Nu_x}{Pe_x^{1/2}} = \left( \frac{Ra_x}{Pe_x^{1/2}} \right)^{1/2} \{ -[1 + CRa_d f'(0)] \theta'(0) \}. \quad (8.15)$$

The results of the calculations of Lai and Kulacki (1988a) are shown in Figs. 8.3 and 8.4. The effect of quadratic drag is to reduce the aiding or opposing effect of buoyancy in increasing  $Nu_x/Pe_x^{1/2}$ , while that of thermal dispersion is (as expected) to increase the heat transfer. Non-Darcy effects also were treated by Gorin et al. (1988), Kodah and Al-Gasem (1998), Tashtoush and Kodah (1998), Elbashbeshy and Bazid (2000b) with variable surface heat flux, Elbashbeshy (2003) with suction or injection, and Murthy et al. (2004a) with suction or injection and the effect of radiation. The effect of variable permeability was studied by Mohammadien and El-Shaer (2004).

For a vertical surface, higher-order boundary layer theory (for Darcy flow) has been developed by Merkin (1980) and Joshi and Gebhart (1985). Merkin pointed out that in the case of opposing flow there is separation of the boundary layer

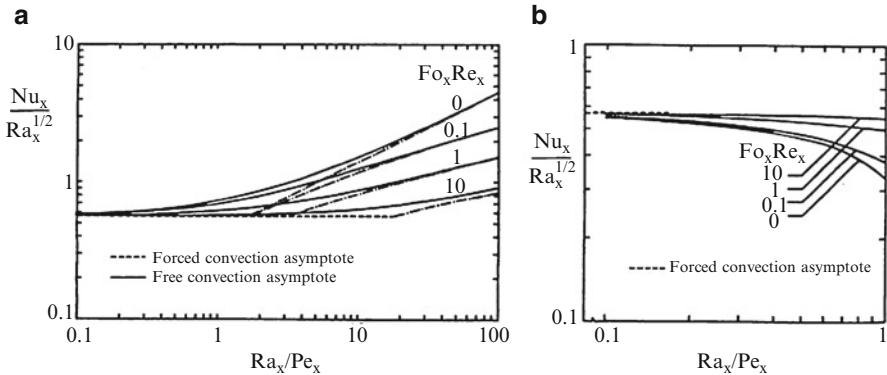


**Fig. 8.3** Nusselt numbers for aiding and opposing flow on a vertical plate with inertia effects (Lai and Kulacki 1988a)

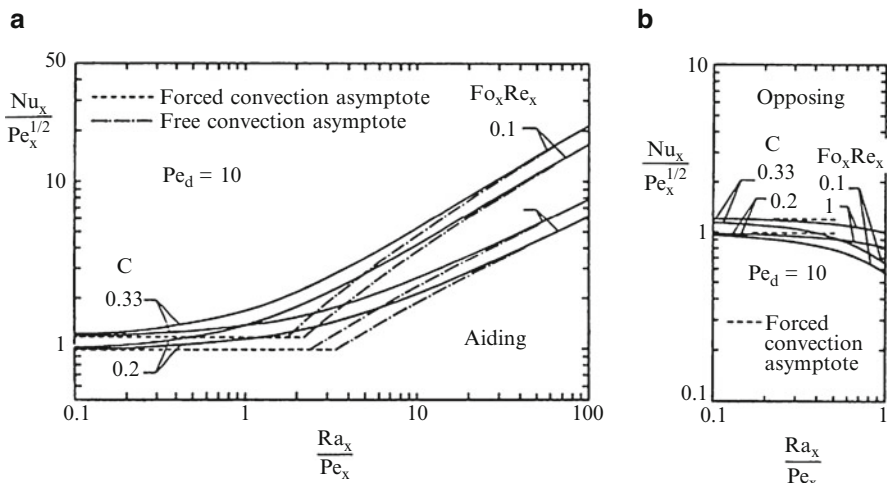


**Fig. 8.4** Nusselt numbers for aiding and opposing flow on a vertical plate with inertia and dispersion effects (Lai and Kulacki 1988a)

downstream of the leading edge. Ranganathan and Viskanta (1984) included the effects of inertia, porosity variation, and blowing at the surface. They reported the rather unexpected result that porosity variation affected the Nusselt number by no more than 1%. Chandrasekhara and Namboodiri (1985) have studied the effect of variation of permeability and conductivity. Lai and Kulacki (1990c) have examined the effect of viscosity variation with temperature. They found that for liquids the Nusselt number values are greater than those for the constant viscosity case and for gases the reverse holds. Ramaniah and Malarvizhi (1990) have obtained a similarity solution for the combination of lateral mass flux and inertia when the linear Darcy drag term is negligible in comparison with the quadratic drag.

Chen and Chen (1990a) have studied the combined effects of quadratic drag, boundary friction, thermal dispersion, and nonuniform porosity and the consequent nonuniform conductivity for the case of aiding flow on a vertical surface. As expected, boundary friction reduces the velocity at the wall, inertia generally reduces the velocity, thermal dispersion has negligible effect on the velocity, and nonuniform porosity substantially increases the velocity just out from the wall. The temperature gradient at the wall is reduced by boundary friction and quadratic drag and increased by variable porosity; the overall effect is reduction. Consequently, the local Nusselt number is reduced by boundary friction and quadratic drag and increased by variable porosity; the overall effect is little change. The local Nusselt number  $Nu_x$  is increased about threefold by thermal dispersion. The effect of increase of  $Ra_x/Pe_x$  is to increase  $Nu_x$  and increase the amount of channeling. The effects of thermal dispersion and stratification were considered by Hassanien et al. (1998), while Hassanien and Omer (2002) considered the effect of variable permeability. Further work on variable porosity was done by Pal and Mondal (2009, 2010a) (radiation, MHD, stretching sheet).

The case of a non-Newtonian power-law fluid has been treated by Wang et al. (1990b), Nakayama and Shenoy (1992, 1993a), Gorla and Kumari (1996, 1998, 1999a, b, c), Kumari and Gorla (1996), Gorla et al. (1997), Mansour and Gorla (2000b), Ibrahim et al. (2000), and El-Hakiem (2001a, b), while Shenoy (1992) studied flow of an elastic fluid.

The magnetohydrodynamic case was examined by Aldoss et al. (1995), Chamkha (1998), and Oztop et al. (2011a). The effect of suction (which increases heat transfer) was treated by Hooper et al. (1994b) and Weidman and Amberg (1996). Conjugate convection was studied by Pop et al. (1995b) and Shu and Pop (1999). Stagnation point flow with suction or injection was treated by Yih (1999i). Further work on stagnation point flow was reported by Asghar et al. (2008) (some exact solutions), Ishak et al. (2008a), Bachok et al. (2010a), and Rohni et al. (2012a). The last authors studied unsteady convection with suction and temperature effects. In this connection Magyari (2012) found that the solutions bifurcated into a non-denumerable infinity of solutions, with the corresponding Nusselt number becoming indeterminate. This he interpreted as a further insufficiency of the boundary layer approximation.

Comprehensive nonsimilarity solutions were presented by Hsieh et al. (1993a, b). Jang and Ni (1992) considered convection over an inclined plate. For a vertical plate, numerical work on non-Darcy models has been reported by Takhar et al. (1990), Lai and Kulacki (1991a), Yu et al. (1991), Shenoy (1993a), Chen et al. (1996), Kodah and Duwairi (1996), and Takhar and Beg (1997). The numerical studies by Gorla et al. (1996) and Chen (1997a) have discussed the effect of such things as thermal dispersion, porosity variation, and variable conductivity. Thermal dispersion and viscous dissipation was discussed by Murthy and Singh (1997b) and Murthy (1998, 2001). The case of the plate temperature oscillating with time about a nonzero mean was studied by Vighnesan et al. (2001). Volumetric heating due to radiation was discussed by Bakier (2001a, b). The case of a piecewise heated wall was studied by Saeid and Pop (2005c). A stratified fluid was treated by Ishak et al. (2008b). Variable viscosity was examined by Chin et al. (2007). An anisotropic medium was studied by

Bachok et al. (2010b). The effect of viscous dissipation was treated by Aydin and Koya (2006, 2008a). For comment on the second paper, see Rees and Magyari (2008) and Nield (2008a). The DTM-Pade method was applied to an inclined plate by Rashidi et al. (2010). This chapter was discussed by Magyari (2011b). An inclined plate with radiation and a magnetic field was studied by Aydin and Kaya (2011) (MHD) and Moradi et al. (2012).

Transient convection resulting from a sudden change in wall temperature was studied by Harris et al. (1998, 1999, 2002). The last paper allowed for a thermal capacity effect. They made a complete analysis of the steady-state solution (large times), obtained a series solution for small times, and then linked the two by a numerical solution for intermediate times. Transient convection near stagnation point flow was treated by Nazar et al. (2003) and, using a homotopy analysis method that produces accurate uniformly valid series solutions, by Cheng et al. (2005). A transient problem involving suction or injection was studied by Al-Odat (2004b). Various aspects of the solutions of the boundary layer equations were studied by Guedda (2005a), Brigi and Hoernel (2006), and Magyari and Aly (2006a, b). Some exact solutions for the case of unsteady flow with temperature slip were found by Fang et al. (2012) and Merkin et al. (2012).

### 8.1.2 Horizontal Wall

For horizontal surfaces the situation is similar to that for vertical surfaces, but now  $Ra_x/Pe_x^{3/2}$  replaces  $Ra_x/Pe_x$  as a measure of buoyancy to nonbuoyancy effects. Cheng (1977d) provided similarity solutions for the cases of (a) horizontal flat plate at zero angle of attack with constant heat flux and (b) stagnation point flow about a horizontal flat plate with wall temperature  $T_w$  varying as  $x^2$ .

Minkowycz et al. (1984) dealt with  $T_w$  varying as  $x^\lambda$  for arbitrary  $\lambda$ , using the local nonsimilarity method. Chandrasekhara (1985) extended Cheng's results to the case of variable permeability (which increases the heat transfer rate). Lai and Kulacki (1987, 1989a, b) treated quadratic drag (for uniform  $U_x$  with  $T_w$  varying as  $x^{1/2}$ ), thermal dispersion, and flow injection/withdrawal, respectively. As in the case of the vertical wall,  $Nu_x$  is decreased by inertial effects and substantially increased by thermal dispersion effects; it is also enhanced by withdrawal of fluid across the surface. Chandrasekhara and Nagaraju (1988) and Bakier and Gorla (1996) included the effect of radiation. Kumari et al. (1990a) treated quadratic drag and extended the work of Lai and Kulacki (1987) to obtain some nonsimilarity solutions. The singularity associated with certain outer velocity profiles was investigated by Merkin and Pop (1997). Some new similarity solutions for specific outer velocity and wall temperature distributions were reported by Magyari et al. (2003a).

Ramaniah et al. (1991) and Elbashbeshy (2001) examined the effect of wall suction or injection. For the Forchheimer model, Yu et al. (1991) presented a universal similarity transformation. For the case of variable wall flux, calculations on the Brinkman model were performed by Aldoss et al. (1994b), while Chen

(1996) used the Brinkman-Forchheimer model and also included the effects of porosity variation and thermal dispersion. On the Darcy model and for various thermal boundary conditions, Aldoss et al. (1993a, b, 1994a) presented nonsimilarity solutions for a comprehensive set of circumstances. A comprehensive analysis on the Brinkman-Forchheimer model was presented by Chen (1997b). The effect of velocity-dependent dispersion was studied by Thiele (1997). Nonsimilarity solutions were obtained for the case of variable surface heat flux by Duwairi et al. (1997) and Chen (1998a) and for the case of variable surface temperature by Chen (1998b). Non-Newtonian fluids were treated by Kumari et al. (1997), Gorla et al. (1998), and Kumari and Nath (2004a). The effect of radiative flux was added by Kumari and Nath (2004b). The effect of temperature-dependent viscosity was discussed by Kumari (2001a). Convection above or below a horizontal plate was discussed by Lesnic and Pop (1998b).

Renken and Poulikakos (1990) presented experimental results of mixed convection about a horizontal isothermal surface embedded in a water-saturated bed of glass spheres. They measured the developing thermal boundary layer thickness and the local surface heat flux.

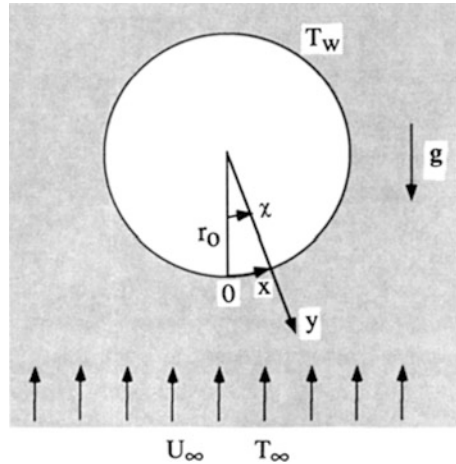
The onset of vortex instability for horizontal and inclined impermeable surfaces was studied by Hsu and Cheng (1980a, b). They found that the effect of the external flow is to suppress the growth of vortex disturbances in both aiding and opposing flows. For the inclined surfaces, aiding flows are more stable than opposing flows (for the same value of  $Ra_x/Pe_x$ ). For the horizontal surfaces, stagnation point aiding flows are more stable than parallel aiding flows. A case of unsteady convection near a stagnation point was analyzed by Nazar and Pop (2004). Jang et al. (1995) showed that the effect of blowing at the surface is to decrease Nu and make the flow more susceptible to vortex instability, while suction results in the opposite. The effect of variable permeability was treated by Hassanien et al. (2003c, 2004a). The effect of surface mass flux was studied by Murthy and Singh (1997c), together with thermal dispersion effects, and by Hassanien et al. (2004c) and Hassanien and Omer (2005). Entropy generation in non-Newtonian fluids was examined by Khan and Gorla (2011a).

The above theoretical papers have dealt with walls of infinite length. The case of a wall of finite length was studied analytically and numerically, on the Darcy model, by Vynnycky and Pop (1997). They observed flow separation for both heating and cooling.

### ***8.1.3 Cylinder or Sphere***

For an isothermal sphere or a horizontal cylinder in the presence of an otherwise uniform vertically flowing stream, Cheng (1982) obtained boundary layer equations in the form

**Fig. 8.5** Definition sketch for mixed convection over a horizontal cylinder or a sphere



$$\frac{1}{r^n} \frac{\partial^2 \Psi}{\partial y^2} = \frac{g \beta K}{v} \sin\left(\frac{x}{r_0}\right) \frac{\partial T}{\partial y}, \quad (8.16)$$

$$\frac{1}{r^n} \left( \frac{\partial \Psi}{\partial y} \frac{\partial T}{\partial x} - \frac{\partial \Psi}{\partial x} \frac{\partial T}{\partial y} \right) = \alpha_m \frac{\partial^2 T}{\partial y^2}, \quad (8.17)$$

where

$$u = \frac{1}{r^n} \frac{\partial \Psi}{\partial y}, \quad v = -\frac{1}{r^n} \frac{\partial \Psi}{\partial x}. \quad (8.18)$$

In these equations,  $n = 0$  for a horizontal cylinder,  $n = 1$  for a sphere, and  $r = r_0 \sin(x/r_0)$  where  $r_0$  is the radius of the sphere or cylinder. These apply when  $x$  is measured from the lower stagnation point and  $y$  is in the normal (radial) direction. This configuration is sketched in Fig. 8.5.

The appropriate boundary conditions are

$$y = 0 : \quad T = T_w, \quad \frac{\partial \Psi}{\partial x} = 0, \quad (8.19)$$

$$y \rightarrow \infty : \quad T = T_\infty, \quad \frac{1}{r^n} \frac{\partial \Psi}{\partial y} = U(x) = U_\infty A_n \sin\left(\frac{x}{r_0}\right), \quad (8.20)$$

where  $U(x)$  is the tangential velocity on the surface (given by potential theory), so  $A_0 = 2$  and  $A_1 = 3/2$ . The introduction of nondimensional variables defined by

$$\Psi = \alpha r_0^n (A_n U_\infty r_0 / \alpha_m) G_n(\chi) f(\eta), \quad (8.21)$$

$$\theta = \frac{T - T_\infty}{T_w - T_\infty}, \quad (8.22)$$

$$\eta = (A_n U_\infty r_0 / \alpha_m)^{1/2} (y/r_0) H_n(\chi), \quad (8.23)$$

where

$$\begin{aligned} \chi &= x/r_0, & G_0(\chi) &= (1 - \cos \chi)^{1/2}, & G_1(\chi) &= \left( \frac{\cos^3 \chi}{3} - \cos \chi + \frac{2}{3} \right)^{1/2}, \\ H_0(\chi) &= \sin \chi / G_0(\chi), & H_1(\chi) &= \sin^2 \chi / G_1(\chi) \end{aligned} \quad (8.24)$$

reduces the problem to finding the solution of

$$f'' = \frac{Ra}{Pe} \theta', \quad \theta'' = -\frac{1}{2} f \theta', \quad (8.25)$$

$$f(0) = 0, \quad \theta(0) = 1, \quad f'(\infty) = 1, \quad \theta(\infty) = 0, \quad (8.26)$$

which is the set [Eqs. (8.7)–(8.9)] for  $\lambda = 0, f_w = 0$ . Here  $Ra$  and  $Pe$  are based on  $r_0$ . Thus the solution for an isothermal sphere or horizontal cylinder can be deduced from that for a vertical plate.

Following the same approach, Huang et al. (1986) obtained the solution for the constant heat flux case. Minkowycz et al. (1985a) obtained approximate solutions for a nonisothermal cylinder or sphere using the local nonsimilarity method. Kumari et al. (1987) made more precise calculations for flow about a sphere. Badr and Pop (1988) considered aiding and opposing flows over a horizontal isothermal cylinder using a series expansion plus a finite-difference scheme. They found that for opposing flows there exists a recirculating flow zone just above the cylinder. For a similar situation, Badr and Pop (1992) studied the effect of varying the stream direction.

For horizontal cross flow over a horizontal cylinder below an impermeable horizontal surface, Oosthuizen (1987) performed a numerical study. He found that the presence of the surface has a negligible effect on heat transfer when the depth of the cylinder is greater than three times its diameter. The heat transfer is a maximum when the depth of the axis is about 0.6 times the diameter. The presence of the surface increases local heat transfer coefficients on the upper upstream quarter of the cylinder and decreases it on the upper downstream quarter, while buoyancy increases it on the upper upstream quarter and decreases it on the lower downstream quarter. The experiments by Fand and Phan (1987) were confined to finding correlations for overall Nusselt number data for horizontal cross flow over a horizontal cylinder. A horizontal cylinder was also studied by Hassanien and Rashed (2010, 2011) (variable viscosity and thermal conductivity) and Kumari and Pop (2009) (bidisperse medium).

The problem of longitudinal flow past a vertical cylinder was analyzed by Merkin and Pop (1987), who found that a solution of the boundary layer equations was possible only when  $Ra/Pe = -1.354$  and that there is a region of reversed flow when  $Ra/Pe < -1$ . Here the minus sign indicates opposing flow. Reda (1988) performed experiments and a numerical analysis (without a boundary layer approximation) for opposing flow along a vertical cylinder of finite length. He found that buoyancy-induced upflow disappeared when  $|Ra/Pe| = 0.5$ . Ingham and Pop (1986a, b) analyzed the boundary layers for longitudinal flow past a vertical cylinder and horizontal flow past a vertical cylinder. For the case of a permeable vertical thin cylinder, an exact solution was found by Magyari et al. (2005a). A three-dimensional problem involving the combined effects of wake formation and buoyancy on convection with cross flow about a vertical cylinder was numerically simulated by Li and Kimura (2005).

Inertial effects on heat transfer along a vertical cylinder, with aiding or opposing flows, were analyzed by Kumari and Nath (1989a). As expected, their results show that inertial effects reduce heat transfer. Heat transfer still increases with buoyancy increase for aiding flows and decreases for opposing flows. Kumari and Nath (1990) have studied inertial effects for aiding flow over a nonisothermal horizontal cylinder and a sphere. For a vertical cylinder, numerical studies on the Brinkman-Forchheimer model, with the effects of porosity variation and transverse thermal dispersion included, were reported by Chen et al. (1992) and for conjugate convection by Chen and Chen (1991), while nonsimilarity solutions were found by Hooper et al. (1994a) and Aldoss et al. (1996); the magnetohydrodynamic case was treated by Aldoss (1996), and Kumari et al. (1993) included the effect of thermal dispersion. A problem involving variable surface heat flux was analyzed by Pop and Na (1998). Further numerical studies by Zhou and Lai (2002) revealed that oscillatory flows occur for opposing flows at high Grashof number to Reynolds number ratios. The case of a non-Newtonian fluid was discussed by Mansour et al. (1997). A numerical simulation was performed by Li and Kimura (2005). Kaya (2011) studied a conjugate problem with convection about a vertical slender hollow cylinder embedded in a porous medium of high porosity.

The double-diffusive and MHD problem for an unsteady (oscillatory or uniform acceleration) vertical flow over a horizontal cylinder and a sphere was analyzed by Kumari and Nath (1989b). MHD convection from a horizontal cylinder was also treated by Aldoss and Ali (1997). A substantial study of convection from a suddenly heated horizontal cylinder was reported by Braden et al. (1998b). A correction to their results was pointed out by Diersch (2000). The Brinkman model was applied to the case of a horizontal cylinder by Nazar et al. (2003b).

For convection over a sphere, Tung and Dhir (1993) performed experiments and Nguyen and Paik (1994) carried out further numerical work. The latter considered variable surface temperature and variable surface heat flux conditions, and they noted that recirculation was possible when the forcing flow opposed the flow induced by buoyancy, as in the case of cylinders. Unsteady convection around a sphere at low Péclet numbers for the case of sudden heating was analyzed by Sano and Makizono (1998). Unsteady mass transport from a sphere at finite Péclet

numbers was studied by Feng and Michaelides (1999). Transient conjugate convection from a sphere with pure saline water was treated numerically by Paik et al. (1998). Radiation effects on convection over a nonisothermal sphere or cylinder were studied by Duwairi (2006). The case of a vertical cylinder with a nanofluid was studied by Gorla et al. (2011).

### 8.1.4 Other Geometries

Introducing a general transformation, Nakayama and Koyama (1987b) showed that similarity solutions are possible for two-dimensional or axisymmetric bodies of arbitrary shape provided the external free-stream velocity varies as the product of the streamwise component of the gravitational force and the wall-ambient temperature difference. Examples are when  $T_w - T_\infty$  varies as the same power function as  $U_\infty$  for a vertical wedge or a vertical cone. In these cases the problem can be reduced to the vertical plate problem solved by Cheng (1977c).

Invoking the slender body assumption, Lai et al. (1990c) have obtained similarity solutions for two other problems, namely, accelerating flow past a vertical cylinder with a linear temperature variation along the axis and uniform flow over a paraboloid of revolution at constant temperature. They found that  $Nu_x/Pe_x^{1/2}$  decreases with an increase in the dimensionless radius of a cylinder, but for paraboloids of revolution, this is so only when  $Ra_x/Pe_x$  is not too large.

Chen and Chen (1990b) have studied the flow past a downward projecting plate fin in the presence of a vertically upward free stream, incorporating the effects of quadratic drag, boundary friction, variable porosity, and thermal dispersion. A vertical cylindrical fin was investigated by Gill et al. (1992) and Aly et al. (2003).

For mixed convection in the thermal plume over a horizontal line heat source, Cheng and Zheng (1986) obtained a local similarity solution. They performed calculations for the thermal and flow fields and for heat transfer with the effects of transverse thermal dispersion and quadratic drag included. Further studies of this problem were reported by Lai (1991c) and Pop et al. (1995a). A line heat source embedded at the leading edge of a vertical adiabatic surface was examined by Jang and Shiang (1997). A heat source/sink effect on MHD convection in stagnation flow on a vertical plate was studied numerically by Yih (1998a).

Vargas et al. (1995) employed three different methods of solution for mixed convection on a wedge in a porous medium with Darcy flow. The methods were local nonsimilarity, finite elements in a boundary layer formulation, and finite elements in a formulation without boundary layer approximations. For wedges with uniform wall temperature in the range  $0.1 \leq Ra_x/Pe_x \leq 100$ , the three methods produced results that are in very good agreement. New solutions were reported for wedges with half angles of  $45^\circ$ ,  $60^\circ$ , and  $90^\circ$ . Convection over a wedge also has been treated by Kumari and Gorla (1997) for the case of a nonisothermal surface, by Mansour and Gorla (1998) and Mansour and El-Shaer (2004) for the case of a power-law fluid with radiation, by Gorla and Kumari (2000) for a non-Newtonian fluid and with

variable surface heat flux, and by Hassanien (2003) for variable permeability and with variable surface heat flux. Studies for the entire regime were carried out by Ibrahim and Hassanien (2000) for variable permeability and a nonisothermal surface and by Yih (2001a) with a radiation effect included. Transient convection resulting from impulsive motion from rest and a suddenly imposed wedge surface temperature was studied numerically by Bhattacharyya et al. (1998). Steady MHD convection with variable permeability, surface mass transfer, and viscous dissipation was investigated by Kumari et al. (2001). Further work with a wedge was done by Al-Odat et al. (2005) (radiation) and Khan and Gorla (2010a, b, c, 2011) (icy water, power-law fluid). A second law analysis for a non-Newtonian fluid was reported by Gorla et al. (2012).

Ingham and Pop (1991) treated a cylinder embedded to a wedge. Oosthuizen (1988b) studied a horizontal plate buried beneath an impermeable horizontal surface. Kimura et al. (1994) investigated heat transfer to ultralarge-scale heat pipes placed in a geothermal reservoir. Thermal dispersion effects on non-Darcy convection over a cone were studied by Murthy and Singh (2000). MHD convection from a rotating cone was studied by Chamkha (1999). The effect of radiation on convection from an isothermal cone was studied by Yih (2001b). The entire regime for convection about a cone was investigated by Yih (1999g). The case of a cone with radiation and variable permeability was studied by El-Amin et al. (2011a).

A special geometry was considered in the early numerical and experimental study by Jannot et al. (1973). Heat transfer over a continuously moving plate was treated numerically by Elbashbeshy and Bazid (2000a).

### 8.1.5 Unified Theory

We now present the unified theory of Nakayama and Pop (1991) for mixed convection on the Forchheimer model about plane and axisymmetric bodies of arbitrary shape. The boundary layer equations are

$$\frac{1}{r^*} \frac{\partial r^* u}{\partial x} + \frac{\partial v}{\partial y} = 0, \quad (8.27)$$

$$\frac{v}{K} u + \frac{c_F}{K^{1/2}} u^2 = \frac{v}{K} u_\infty + \frac{c_F}{K^{1/2}} u_\infty^2 + g_x \beta (T - T_\infty), \quad (8.28)$$

$$u \frac{\partial T}{\partial x} + v \frac{\partial T}{\partial y} = \alpha_m \frac{\partial^2 T}{\partial y^2}, \quad (8.29)$$

with the boundary conditions

$$y = 0 : \quad v = 0, \quad T = T_w(x), \quad (8.30a)$$

$$y = \infty : \quad u = u_\infty(x) \text{ or } T = T_\infty, \quad (8.30b)$$

where

$$r^* = \begin{cases} 1, & \text{planebody,} \\ r(x), & \text{axisymmetric body} \end{cases} \quad (8.31)$$

and

$$g_x = g \left[ 1 - \left( \frac{dr}{dx} \right)^2 \right]^{1/2}. \quad (8.32)$$

For the case of axisymmetric bodies, it is assumed that the body radius  $r(x)$  is large relative to the boundary layer thickness, so the transverse radial pressure gradient is negligible. Horizontal flat surfaces are excluded here; these require separate treatment.

The convective inertia term has been dropped from Eq. (8.28) because a scaling argument shows that the influence of this term is felt only very close to the leading edge, except for flow in highly permeable media. Nakayama (1995, 1998) also argued that for most porous materials the viscous boundary layer is confined for almost the entire surface to a thin layer close to the wall, so that the temperature distribution is essentially free from boundary viscous effects, and hence it is reasonable to drop the Brinkman term. However, Rees (private communication) noted that the analysis reported in Rees and Vafai (1999) for a uniformly heated horizontal plate indicates that the situation is more complicated, at least at intermediate values of  $x$ , than implied by Nakayama and Pop. Eq. (8.28) gives

$$u = \frac{v}{2c_F K^{1/2}} \left\{ \left[ (1 + 2Re_K)^2 + 4Gr_K \left( \frac{T - T_\infty}{T_w - T_\infty} \right) \right]^{1/2} - 1 \right\}, \quad (8.33)$$

where

$$Re_K(x) = c_F K^{1/2} u_\infty(x)/v, \quad (8.34)$$

and

$$Gr_K(x) = c_F K^{3/2} g_x(x) \beta [T_w(x) - T_\infty]/v^2. \quad (8.35)$$

From Eqs. (8.30a) and (8.33), the wall velocity is

$$u_w = \frac{v}{2c_F K^{1/2}} \left\{ \left[ (1 + 2Re_K)^2 + 4Gr_K \right]^{1/2} - 1 \right\}, \quad (8.36)$$

Nakayama and Pop (1991) argued that it is this velocity, which depends on both external flow, that essentially determines convective heat transfer from the wall, and they introduced a modified Péclet number,

$$Pe_x^* = \frac{u_w x}{\alpha_m} = Pe_x \frac{\left[ (1 + 2Re_K)^2 + 4Gr_K \right]^{1/2} - 1}{2Re_K}, \quad (8.37)$$

since the usual Péclet number is defined by

$$Pe_x = \frac{u_\infty x}{\alpha_m}. \quad (8.38)$$

The energy equation (8.29) yields the scaling

$$u_w \frac{T_w - T_\infty}{x} \sim \alpha_m \frac{T_w - T_\infty}{\delta_T^2}, \quad (8.39)$$

where  $\delta_T$  is the thermal boundary layer thickness. Hence one expects that, for all convection modes,

$$Nu_x \sim \frac{x}{\delta_T} \sim Pe_x^{*1/2}, \quad (8.40)$$

where the local Nusselt number is defined as

$$Nu_x = \frac{q'' x}{k_m(T_w - T_\infty)}. \quad (8.41)$$

Nakayama and Pop (1991) also define

$$Ra_x^* = \frac{K^{1/4} [g_x \beta (T_w - T_\infty)]^{1/2} x}{c_F^{1/2} \alpha_m} \quad (8.42)$$

and then identify the following regimes:

Regime I (Forced convection regime):

$$Nu_x^2 \sim Pe_x^* = Pe_x \quad \text{for} \quad Re_K + Re_K^2 \gg Gr_K. \quad (8.43a)$$

Regime II (Darcy natural convection regime):

$$Nu_x^2 \sim Pe_x^* = Ra_x \quad \text{for} \quad Re_K \ll Gr_K \ll 1. \quad (8.43b)$$

Regime III (Forchheimer natural convection regime):

$$Nu_x^2 \sim Pe_x^* = Ra_x \quad \text{for} \quad Re_K + Re_K^2 \ll Gr_K \quad \text{and} \quad Gr_K \gg 1. \quad (8.43c)$$

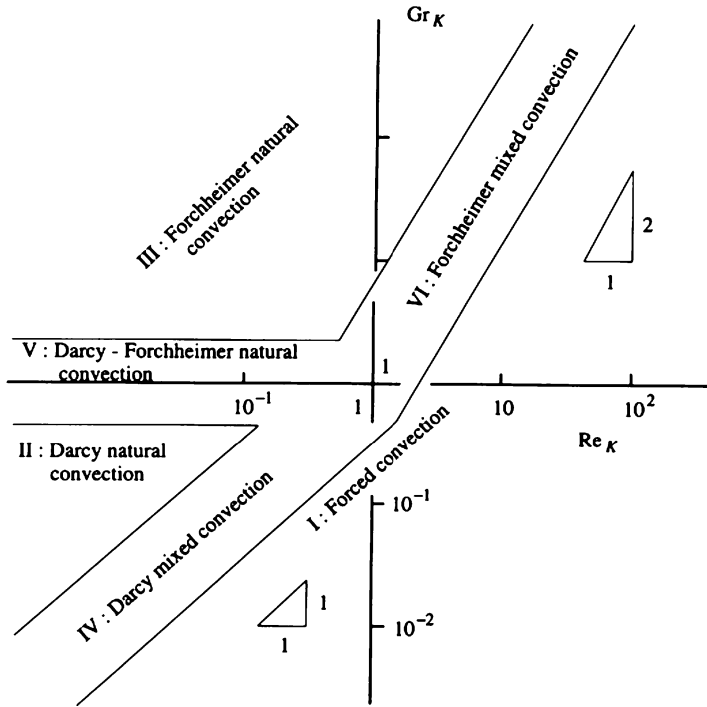


**Fig. 8.6** Convection flow regime map (Nakayama and Pop 1991, with permission from Pergamon Press)

Regime IV (Darcy mixed convection regime):

$$Nu_x^2 \sim Pe_x^* = Pe_x + Ra_x \quad \text{for } Re_K \sim Gr_K \ll 1. \quad (8.43d)$$

Regime V (Darcy-Forchheimer natural convection regime):

$$Nu_x^2 \sim Pe_x^* = Ra_x \frac{(1 + 4Gr_K)^{1/2} - 1}{2Gr_K} \quad \text{for } Gr_K \sim 1 \text{ and } Re_K \ll 1. \quad (8.43e)$$

Regime VI (Forchheimer mixed convection regime):

$$Nu_x^2 \sim Pe_x^* = (Pe_x^2 + Ra_x^{*2})^{1/2} \quad \text{for } Gr_K \sim Re_K \gg 1. \quad (8.43f)$$

The situation is summarized in Fig. 8.6. The three macroscale parameters  $Pe_x$ ,  $Ra_x$ ,  $Ra_x^*$  and the two microscale parameters  $Re_K$ ,  $Gr_K$  are related by

$$\frac{Ra_x}{Pe_x} = \frac{Gr_K}{Re_K}, \quad \frac{Ra_x}{Ra_x^*} = Gr_K^{1/2}. \quad (8.44)$$

Nakayama and Pop (1991) then introduce the general transformations

$$f(x, \eta) = \frac{\Psi}{\alpha_m r^* (Pe_x^* I)^{1/2}}, \quad (8.45)$$

$$\theta(x, \eta) = \frac{T - T_\infty}{T_w - T_\infty}, \quad (8.46)$$

$$\eta = \frac{y}{x} \left( \frac{Pe_x^*}{I} \right)^{1/2}, \quad (8.47)$$

where

$$I = \frac{\int_0^x (T_w - T_\infty)^2 u_w r^{*2} dx}{(T_w - T_\infty)^2 u_w r^{*2} x}. \quad (8.48)$$

The momentum and energy equations reduce to

$$f = \frac{\int_0^\eta \left[ (1 + 2Re_K)^2 + 4Re_K \theta \right]^{1/2} d\eta - \eta}{\left[ (1 + 2Re_K)^2 + 4Re_K \theta \right]^{1/2} - 1}, \quad (8.49)$$

and

$$\theta'' + \left( \frac{1}{2} - m_T I \right) f \theta' - m_T I \theta f' = I x \left( f' \frac{\partial \theta}{\partial x} - \theta' \frac{\partial f}{\partial x} \right), \quad (8.50)$$

where

$$m_T(x) = \frac{d \ln(T_w - T_\infty)}{d \ln x} = \frac{x}{(T_w - T_\infty)} \frac{dT_w}{dx}. \quad (8.51)$$

The transformed boundary conditions are

$$\eta = 0 : \quad \theta = 1, \quad (8.52a)$$

$$\eta \rightarrow \infty : \quad \theta = 0. \quad (8.52b)$$

Once the set of equations (8.49) and (8.50) subject to (8.52a) and (8.52b) have been solved, the local Nusselt number may be evaluated from

$$Nu_x = -\theta'(x, 0) \left( \frac{Pe_x^2}{I} \right)^{1/2}. \quad (8.53)$$

Nakayama and Pop (1991) then proceed to consider regimes I through VI in turn, seeking similarity solutions. In general these exist if and only if  $T_w - T_\infty$  is a power function of the downstream distance variable  $\xi$ . They recover various results

reported above in Chap. 4 (forced convection; regime I) and Chap. 5 (natural convection; regimes II, III, and V). For their other results, the reader is referred to the original paper and also the reviews by Nakayama (1995, 1998). These reviews include related material on the cases of convection over a horizontal plane, convection from line or point heat sources (Nakayama 1993b, 1994), and also a study of forced convection over a plate on the Brinkman-Forchheimer model (Nakayama et al. 1990a).

### ***8.1.6 Other Aspects of External Flow***

The case of icy water was studied by Ling et al. (2007a,b, 2009), Pantokratoras (2009b) (sinusoidal surface temperature distribution), and by Guedda et al. (2011) (MHD). Other MHD studies were conducted by Damseh (2006); Damseh and Tahat (2009) (thermophoresis particle deposition); Sharma et al. (2007 (heat source/sink)); El-Kabeir et al. (2007) (moving wall, unsteady flow), with comment by Pantokratoras (2009a, b); Elgazery and Elazem (2009) (non-Newtonian fluid, unsteady flow); Srinivas and Muthuraj (2010a) (radiation); Pal (2010) (variable porosity); Rashad et al. (2010); Singh et al. (2010) (rotating system); Makinde and Aziz (2010) (convective boundary condition); and El-Amin and Sun (2011) (thermal dispersion).

The effect of variable viscosity was examined by Jayanthi and Kumari (2006, 2007) (regular fluid, non-Newtonian fluid). Further work involving a stretching sheet was done by Hayat et al. (2008b, 2010a, b), Mukhopadhyay (2009) (radiation, unsteady flows), and Pal and Mondal (2011c) (radiation).

Further work on stagnation point flow was conducted by Harris et al. (2009), Hayat et al. (2009, 2010a), and Hassanien and Al-Arabi (2009) (radiation, variable viscosity, unsteady flow). The effect of thermal dispersion was examined by Sobha et al. (2010). The combined effects of thermophoresis and electrophoresis on particle deposition onto a vertical plate were studied by Tsai and Huang (2010). The thermophoresis effect was also studied by Duwairi and Damseh (2008a) and Seddeek (2006) (viscous dissipation). Transient convection with internal heat generation and oscillating temperature was treated by Duwairi et al. (2007). The effect of a temperature slip boundary condition was studied by Merkin et al. (2012).

## **8.2 Internal Flow: Horizontal Channel**

### ***8.2.1 Horizontal Layer: Uniform Heating***

The problem of buoyancy-induced secondary flows in a rectangular duct filled with a saturated porous medium through which an axial flow is maintained was

examined experimentally by Combarous and Bia (1971) for the case of a large horizontal to vertical aspect ratio denoted by  $A$ . As predicted by linear stability theory (see Section 6.10), the axial flow did not affect the critical Rayleigh number for the onset of convective secondary flow nor the heat transfer. For Péclet numbers  $Pe$  less than about 0.7, cross rolls rather than longitudinal rolls were usually (but not always) the observed secondary motion. For larger values of  $Pe$ , longitudinal rolls were always observed.

Islam and Nandakumar (1986) made a theoretical investigation of this problem. They used the Brinkman equation for steady fully developed flow and assumed negligible axial conduction, a constant rate of heat transfer per unit length, and an axially uniform heat flux, thus reducing the problem to a two-dimensional one that they solved numerically. Since axial conduction was neglected, their solutions are valid for large  $Pe$  values only. To save computational effort they assumed symmetry about the vertical midline of the duct, thus permitting only an even number of buoyancy-induced rolls. In our opinion this assumption is probably not justified; for the aspect ratios used ( $0.6 < A < 3$ ), we would expect that the physically significant solution would sometimes be a single-vortex roll. They treated two cases: bottom heating and heating all around the periphery. For each case they found a transition from a two-vortex pattern to a four-vortex pattern as the Grashof number  $Gr$  increased, with both two- and four-vortex solutions existing in a certain range of  $Gr$ . Further investigations by Nandakumar et al. (1987) indicated that the number of possible solutions depends sensitively on the aspect ratio. Islam and Nandakumar (1988) extended their analysis by including quadratic drag.

For a rectangular channel, Chou et al. (1992a) reported experimental and numerical work on the Brinkman-Forchheimer model and with variable porosity and thermal dispersion allowed for, while Chou and Chung (1995) allowed for the effect of variation of effective thermal conductivity. Hwang and Chao (1992) investigated numerically the case of finite wall conductivity. Chou et al. (1994) studied numerically the effect of thermal dispersion in a cylindrical tube. Islam (1992) investigated numerically the time evolution of the multicellular flows. His results show the presence of periodic, quasiperiodic, and chaotic behavior for increasingly high Grashof numbers (or Rayleigh numbers). An MHD problem was studied by Takhar and Ram (1994). Llagostera and Figueiredo (2000) numerically simulated mixed convection in a two-dimensional horizontal layer with a cavity of varying depth on the bottom surface and heated from below. Yokoyama et al. (1999) studied numerically and experimentally convection in a duct whose cross-section has a sudden expansion with heating on the lower downstream section. The onset of vortex instability in a layer, heated below with a stepwise change on the bottom boundary and with thermal dispersion, was studied using propagation theory by Chung et al. (2002). A spatiotemporal instability was studied using linear and weakly nonlinear theory by Chung et al. (2009). Unsteady convection involving internal heating and a moving lid was studied numerically by Khanafer and Chamkha (1999). A stability analysis of dual adiabatic flows was made by Barletta and Rees (2009). They examined the effect of viscous dissipation in a layer with adiabatic and impermeable boundaries. They found that there exist two stationary and parallel solutions for each

prescribed pair of Gebhart and Péclet number values if the Gebhart number is less than a certain limit. Their linear stability analysis revealed that one of the branches in the dual solution space is more stable than the other.

### 8.2.2 Horizontal Layer: Localized Heating

Prasad et al. (1988) and their colleagues have conducted a series of two-dimensional numerical studies to examine the effects of a horizontal stream on buoyancy-induced velocity and temperature fields in a horizontal porous layer discretely heated over a length  $D$  at the bottom and isothermally cooled at the top. The heated portion consisted of one or more sections of various sizes (nondimensional length  $A = D/H$ ), and the heating was either isothermal or uniform flux. Darcy's equation was used. The computations were carried out for the range  $1 \leq Ra \leq 500$ ,  $0 \leq Pe \leq 50$ , the Rayleigh and Péclet numbers being based on the layer height. The domain was taken sufficiently long so that at the exit the flow could be assumed parallel and axial conduction could be neglected.

The results for the case of a single source of length  $A = 1$  indicate that when the forced flow is weak ( $Pe$  small) a thermal plume rises above the heat source and a pair of counterrotating cells is generated above the source, the upstream cell being higher than the downstream one. The temperature field is approximately symmetric, fore and aft. As  $Pe$  is increased, the isotherms lose their symmetry, the strength of the two recirculating cells becomes weaker, and the convective rolls and plume move downstream, the downstream roll being weaker than the upstream one. This is so for small values of  $Ra$ , but when  $Ra = 500$ , there are two pairs of convective rolls along side each other.

The overall Nusselt number  $Nu$  increases monotonically with  $Pe$  as long as  $Ra = 10$ , the increase being significant when  $Pe > 1$ , but for  $Ra = 100$ , the Nusselt number goes through a minimum before increasing when forced convection becomes dominant. The apparent reason for the decrease initially is because the enhancement in heat transfer by an increase in forced flow is not able to compensate for the reduction in buoyancy-induced circulation.

Further studies (Lai et al. 1987a) indicated that  $Nu$  is increased significantly if the heat source is located on an otherwise isothermally cooled (rather than adiabatic) bottom surface, because this results in stronger buoyancy effects, but the effect is small if either buoyancy or forced convection dominates the other. Additional investigation (Lai et al. 1987b) revealed that flow structure, temperature field, and heat transfer coefficients change significantly with the size of the heat source. If  $Ra$  is small, only two recirculating cells are produced, one near the leading edge and the other at the trailing edge of the heat source. At large  $Ra$ , the number of cells increases with the size of the source. All are destroyed by sufficient increase in forced flow. The transient problem has been discussed by Lai and Kulacki (1988b).

The extension to multiple heat sources was undertaken by Lai et al. (1990a). For the convective regime, each source behaves more or less independently and the

contributions to heat transfer are approximately additive. With the introduction of forced flow, interaction occurs. Ultimately as  $Pe$  increases, the buoyancy cells weaken and disappear, but at certain intermediate values of  $Ra$  and  $Pe$ , the flow becomes oscillatory as cells are alternately generated and destroyed. A similar phenomenon was observed in the case of a long heat source. In general, the dependence of  $Nu$  on  $Ra$  and  $Pe$  for multiple sources is similar to that for a single source. The minimum in  $Nu$  that occurs at intermediate values of  $Pe$  is accentuated for large numbers of heat sources and tends to be associated with the oscillatory behavior; both effects involve an interaction between forcing flow and buoyancy.

Experiments performed by Lai and Kulacki (1991b) corroborated to a large extent the numerical results. In particular the observed overall Nusselt number data agreed quite well with the predicted values. When an effective thermal conductivity was introduced, the experimental data were correlated by

$$\frac{Nu_D}{Pe_D^{0.5}} = \left[ 1.895 + 0.200 \left( \frac{Ra_D}{Pe_D^{1.5}} \right) \right]^{0.375}, \quad (8.54)$$

where the subscript  $D$  denotes numbers based on the heater length  $D$ . This is very close to the correlation obtained from the numerical solutions,

$$\frac{Nu_D}{Pe_D^{0.5}} = \left[ 1.917 + 0.210 \left( \frac{Ra_D}{Pe_D^{1.5}} \right) \right]^{0.372}. \quad (8.55)$$

The experiments also verified the occurrence of oscillatory behavior. This was observed by recording the fluctuations in temperatures. A precise criterion for the appearance of oscillatory flow could not be determined, but the data available show that  $Ra_D$  has to exceed 10. A numerical study of oscillatory convection was reported by Lai and Kulacki (1991c). The experimental and numerical study by Yokoyama and Kulacki (1996) of convection in a duct with a sudden expansion just upstream of the heated region showed that the expansion had very little effect on the Nusselt number. A problem involving uniform axial heating and peripherally uniform wall temperature was studied numerically by Chang et al. (2004).

### 8.2.3 Horizontal Annulus

The problem of mixed convection in a horizontal annulus with isothermal walls, the inner heated and the outer cooled, was studied by Muralidhar (1989). His numerical results for radius ratio  $r_o/r_i = 2$  and  $Ra = 500$ ,  $Pe = 10$  indicate that forced convection dominates in an entry length  $x < (r_o - r_i)$ . Buoyancy increases the rate at which boundary layers grow and it determines the heat transfer rate once the annular gap is filled by the boundary layer on each wall.

Vanover and Kulacki (1987) conducted experiments in a porous annulus with  $r_o/r_i = 2$ , with the inner cylinder heated by constant heat flux and the outer cylinder isothermally cooled. The medium consisted of 1- and 3-mm glass beads saturated

with water. In terms of  $Pe$  and  $Ra$  based on the gap width ( $r_o - r_i$ ) and the temperature scale  $q''(r_o - r_i)/k_m$ , their experimental data covered the range  $Pe < 520$  and  $Ra < 830$ . They found that when  $Ra$  is large the values of  $Nu$  for mixed convection may be lower than the free convection values. They attributed this to restructuring of the flow as forced convection begins to play a dominant role. Muralidhar (1989) did not observe this phenomenon since he dealt only with  $Pe = 10$ . Vanover and Kulacki obtained the following correlations:

$$\text{Mixed convection } (6 < Pe < 82) : Nu = 0.619 Pe^{0.177} Ra^{0.092} \quad (8.56)$$

$$\text{Forced convection } (Pe > 180) : Nu = 0.117 Pe^{0.657} \quad (8.57)$$

where the overall Nusselt number is normalized with its conduction value  $Nu_c = 1.44$  for an annulus with  $r_o/r_i = 2$ . Convection within a heat-generating horizontal annulus was studied numerically by Khanafar and Chamkha (2003).

### 8.2.4 Horizontal Layer: Lateral Heating

The flow produced by an end-to-end pressure difference and a horizontal temperature gradient in a horizontal channel was studied by Haajizadeh and Tien (1984) using perturbation analysis and numerical integration. The parameters are the Rayleigh number  $Ra$ , the channel aspect ratio  $L$  (length/height), and the dimensionless end-to-end pressure difference  $P$  which is equivalent to a Péclet number. Their results show that in the range  $Ra^2/L^3 \leq 50$  and  $P \leq 1.5$ , the heat transfer enhancement due to the natural convection and the forced flow can be simply added together. Even a small rate of throughflow has a significant effect on the temperature distribution and heat transfer across the channel. For  $P/Ra \geq 0.2$  the contribution of the natural convection to the Nusselt number is negligible.

## 8.3 Internal Flow: Vertical Channel

### 8.3.1 Vertical Layer: Uniform Heating

Hadim and Govindarajan (1988) calculated solutions of the Brinkman-Forchheimer equation for an isothermally heated vertical channel and examined the evolution of mixed convection in the entrance region. Viscous dissipation effects were analyzed by Ingham et al. (1990), for the cases of symmetric and asymmetrically heated walls. Further calculations on the Brinkman-Forchheimer model were performed by Kou and Lu (1993a, b) for various cases of thermal boundary conditions, by Chang and Chang (1996) for the case of a partly filled channel, by Chen et al. (2000a) for the case of uniform heat flux on the walls, and by Hadim (1994b) for the development of convection in a channel inlet. Umavathi et al. (2005) included the effect of viscous

dissipation in their numerical and analytic study using the Brinkman-Forchheimer model and with various combinations of boundary conditions. They noted that viscous dissipation enhances the flow reversal in the case of downward flow and counters the flow in the case of upward flow. Pantokratoras (2008c) pointed out that this publication needed a corrigendum. An MHD convection problem with heat generation or absorption was studied numerically by Chamkha (1997f). The effect of local thermal nonequilibrium was investigated by Saeid (2004) and Khandelwal and Bera (2012). An experimental study for the case of asymmetric heating of the opposing walls was conducted by Pu et al. (1999). The results indicated the existence of three convection regimes: natural convection,  $105 < Ra/Pe$ ; mixed convection,  $1 < Ra/Pe < 105$ ; and forced convection,  $Ra/Pe < 1$ . Multiple solutions associated with the case of a linear axial temperature distribution were observed by Mishra et al. (2002).

A linear stability analysis of the mixed convection flow was reported by Chen and Chung (1998) and Chen (2004). It was found that the fully developed shear flow can become unstable under only mild heating conditions in the case of large Darcy number values (1 and  $10^{-2}$ ), and the critical Rayleigh number drops steeply when the Reynolds number reaches a threshold value that depends on the values of the Darcy and Forchheimer numbers. The critical Rayleigh number increases substantially for  $Da = 10^{-4}$ . For the case of an anisotropic channel, a linear stability analysis was conducted by Bera and Khalili (2002b). The convective cells may then be unicellular or bicellular. Further studies of stability were made by Bera and Khalili (2006, 2007) (influence of Prandtl number, dependence on permeability) and Kumar et al. (2010b).

For an anisotropic channel, aiding mixed convection was studied by Degan and Vasseur (2002). The effect of viscous dissipation was analyzed by Al-Hadrami et al. (2002). For the case of wall temperature decreasing linearly with height, they found that at any value of the Rayleigh number, there were two solutions mathematically, but only one of them is physically acceptable. The effects of a porous manifold on thermal stratification in a liquid storage tank, an unsteady problem, were treated numerically by Yee and Lai (2001). Problems involving multiple porous blocks were studied by Bae et al. (2004) and Huang et al. (2004a). The optimal mixed convection for maximal energy recovery in a solar wall was studied by Boutin and Gosselin (2009). An experimental study of flow-assisted mixed convection in high porosity foams was reported by Kamath et al. (2011). The case of boundary conditions of the third kind was treated numerically by Umavathi and Veershetty (2012) and Umavathi et al. (2012b) (volumetric heat source.) Convection in a long vertical channel containing porous and fluid layers bounded by a corrugated wall and a smooth wall was studied by Umavathi et al. (2012a).

### **8.3.2 Vertical Layer: Localized Heating**

Lai et al. (1988) performed a numerical study of the case when the heat source is a strip of height  $H$  (equal to the layer width) on an otherwise adiabatic vertical wall. The other wall was isothermally cooled; aiding or opposing Darcy flow was considered.

In the absence of a forced flow, a convection cell extends from near the bottom edge of the source to well above the top edge, and the higher the Rayleigh number  $Ra$ , the larger is its extent and the stronger the circulation. When the forced flow is weak, buoyancy forces generally dominate the velocity field, but the acceleration caused by buoyancy forces deflects the main flow toward the heat source, so the circulation zone is pushed to the cold wall side. One consequence is that the vertical velocity in a thin layer on the heated segment increases. The aiding flow reattaches to the cold wall far downstream.

An increase in  $Pe$  moves the convective cell upward and this delays the separation of the main flow from the cold wall. When  $Pe$  becomes large, the strength of the circulation decreases substantially, the reattachment point moves upstream, and the center of the cell is pushed toward the cold wall. At a sufficiently high Péclet number ( $Pe > 10$ ), the main flow does not separate from the cold wall and the effects of buoyancy forces become negligible.

The opposite trends are present when the forced flow is downward (opposing). When the main flow is weak, there is a circulation in the hot wall region and the main flow is directed toward the cold wall. As  $Pe$  increases, both the separation and reattachment points move closer to the heat source, so that circulation is confined to the neighborhood of the source and the heat transfer is reduced from its free convection value. As  $Pe$  increases further, the circulation disappears and the heat transfer coefficient increases with  $Pe$ .

For both aiding and opposing flows, the average Nusselt number  $Nu$  increases with  $Ra$ , it being greater for aiding flows than for opposing flows. It increases monotonically with  $Pe$  for aiding flows, but for opposing flows it decreases with  $Pe$  until a certain value (which increases with  $Ra$  and increases from then on). The boundary layer formula for an isothermally heated vertical flat plate overpredicts the values of  $Nu$  for a channel if the flow is aiding and underpredicts them if the flow is opposing, the error being small in the forced convection regime. Further numerical work was reported by A. Hadim and Chen (1994a, b) and H. A. Hadim (1994a, b). A theoretical study of convection in a thin vertical duct with suddenly applied localized heating on one wall was reported by Pop et al. (2004). Kumar et al. (2005) studied numerically the case of a micropolar fluid. A problem involving discrete heat sources was studied by Bensouici and Bessiah (2010). The effects of viscous dissipation and pressure work were examined by Barletta et al. (2007), Barletta and Nield (2009a,b), and Magyari (2009a,b).

### 8.3.3 Vertical Annulus: Uniform Heating

Muralidhar (1989) has performed calculations for aiding Darcy flow in a vertical annulus with height to gap ratio = 10 and  $r_o/r_i = 2$ , for  $Ra < 100$ ,  $Pe < 10$ , with isothermal heating and cooling on the inner and outer walls, respectively. As expected, the average Nusselt number  $Nu$  increases with  $Ra$  and/or  $Pe$ . Muralidhar found a sharp change in  $Nu$  as  $Pe$  changed from 0 to 1. According to

him, the circulation that exists at  $Pe = 0$  is completely destroyed when  $Pe > 0$  and is replaced by thin thermal boundary layers that give rise to large heat transfer rates. Hence, the jump in Nu from  $Pe = 0$  to  $Pe = 1$  is essentially a phenomenon related to inlet conditions of flow, and the jump can be expected to reduce as the length of the vertical annulus is reduced.

Parang and Keyhani (1987) solved the Brinkman equation for fully developed aiding flow in an annulus with prescribed constant heat flux  $q_i''$  and  $q_o''$  on the inner and outer walls, respectively. They found that the Brinkman term has a negligible effect if  $Da/\varphi = 10^{-5}$ . For larger values of  $Da/\varphi$ , it had a significant effect, which is more pronounced at the outer wall where the temperature is raised and the Nusselt number is reduced, the relative change increasing with  $Gr/Re$ .

In their experimental and numerical study, Clarksean et al. (1988) considered an adiabatic inner cylinder and an isothermally heated outer wall, with a radius ratio of about 12. Their numerical and experimental data showed the Nusselt number to be proportional to  $(Ra/Pe)^{-0.5}$  in the range  $0.05 < Ra/Pe < 0.5$ , wherein heat transfer is dominated by forced convection.

Choi and Kulacki (1992b) performed experimental and numerical work (on the Darcy model) that agreed in showing that Nu increases with either  $Ra$  or  $Pe$  when the imposed flow aids the buoyancy-induced flow, while when the imposed flow is opposing, Nu goes through a minimum as  $Pe$  increases. They noted that under certain circumstances, Nu for a lower  $Ra$  may exceed that for a higher  $Ra$  value. Good agreement was found between predicted and measured Nusselt numbers, which are correlated by expressing  $Nu/Pe^{1/2}$  in terms of  $Ra/Pe^{3/2}$ .

Further numerical work, including non-Darcy effects, was reported by Kwendakwema and Boehm (1991), Choi and Kulacki (1993), Jiang et al. (1996), Kou and Huang (1997) (for various thermal boundary conditions), and also Du and Wang (1999). The experimental and numerical work of Jiang et al. (1994), for an inner wall at constant heat flux and the outer wall adiabatic, was specifically concerned with the effect of thermal dispersion and variable properties. Choi and Kulacki (1992a) reviewed work in this area. Density inversion with icy water was studied numerically by Char and Lee (1998) using the Brinkman-Forchheimer model. The effect of thermal nonequilibrium was studied by Ahmed et al. (2011).

### 8.3.4 Vertical Annulus: Localized Heating

Choi et al. (1989) have made calculations based on the Darcy model for convection in a vertical porous annulus, when a finite heat source (of height  $H$  equal to the annulus gap) is located on the inner wall. The rest of the inner wall is adiabatic and the outer wall is cooled at a constant temperature. They found that for both aiding and opposing flows, the strength of the circulation decreases considerably as the radius ratio  $\gamma = (r_o - r_i)/r_i$  increases (with  $Ra$  and  $Pe$  fixed). Under the same circumstances, the center of the cell moves toward the cold wall. The variations in Nu as  $Ra$  and  $Pe$  change are similar to those for the vertical layer channel. As  $\gamma$

increases,  $\text{Nu}$  increases toward the asymptotic value appropriate for a vertical cylinder. The following correlations were found.

Isothermal source, aiding flow:

$$\frac{\text{Nu}}{\text{Pe}^{0.5}} = (3.373 + \gamma^{0.566}) \left( 0.0676 + 0.0320 \frac{\text{Ra}}{\text{Pe}} \right)^{0.489}. \quad (8.58)$$

Isothermal source, opposing flow:

$$\frac{\text{Nu}}{\text{Pe}^{0.5}} = (2.269 + \gamma^{0.511}) \left( 0.0474 + 0.0469 \frac{\text{Ra}}{\text{Pe}} \right)^{0.509}. \quad (8.59)$$

Constant-flux source, aiding flow:

$$\frac{\text{Nu}}{\text{Pe}^{0.5}} = (7.652 + \gamma^{0.892}) \left( 0.0004 + 0.0005 \frac{\text{Ra}}{\text{Pe}^2} \right)^{0.243}. \quad (8.60)$$

Constant-flux source, opposing flow:

$$\frac{\text{Nu}}{\text{Pe}^{0.5}} = (4.541 + \gamma^{0.787}) \left( 0.0017 + 0.0021 \frac{\text{Ra}}{\text{Pe}^2} \right)^{0.253}, \quad (8.61)$$

where  $\text{Nu}$ ,  $\text{Ra}$ , and  $\text{Pe}$  are defined in terms of the annular gap and either the temperature difference (for the isothermal source) or the temperature scale  $q''H/k_m$  (for the constant-flux source). Nield (1993) noted that the final exponents in Eqs. (8.31)–(8.34) are better replaced by 1/2, 1/2, 1/4, and 1/4, since  $\text{Nu}$  should be independent of  $\text{Pe}$  as  $\text{Ra}$  tends to infinity. For the same reason, the final exponents in Eqs. (8.27) and (8.28) should be 1/3.

The numerical and experimental study performed by Reda (1988) qualitatively supports the observations of Choi et al. (1989). In Reda's experiment, the medium extended vertically from  $z/\Delta r = 0\text{--}4$  and the heater from  $z/\Delta r = 1.9\text{--}3.1$ , where  $\Delta r = r_o - r_i$ , the remainder of the inner wall being insulated, and the outer wall isothermally cooled. The forced flow was downward. Since the radius ratio was large ( $r_o/r_i$  approximately equal to 23), the effects of the outer wall on the temperature and flow fields were small. Reda found that buoyancy-induced circulation disappeared when  $\text{Ra}/\text{Pe}$  is approximately equal to 0.5, independent of the source length or power input.

The effects of quadratic drag and boundary friction were studied by Choi and Kulacki (1990). Their numerical results show that quadratic drag has a negligible effect on  $\text{Nu}$ , but boundary friction significantly changes the flow and temperature fields near the boundary and in highly porous media, as expected. For aiding flows,

the reduction of  $Nu$  becomes pronounced as either  $Ra$  or  $Pe$  increases. For opposing flows, the interaction is complex. The effect of a radially varying magnetic field was studied by Barletta et al. (2008a, c).

## 8.4 Other Geometries and Other Effects

### 8.4.1 Partly Porous Configurations

Mixed convection in a partly filled channel was numerically simulated by Jaballah et al. (2006, 2008) (regular, irregular heating). Jaballah et al. (2012) employed a thermal nonequilibrium model to study a channel partly filled with multiple porous layers. Further studies were carried out by Kumar et al. (2009b, 2010a), Malashetty et al. (2005a, b) (inclined channel), Moraga et al. (2010) (vented enclosure, unsteady flow), and Huang and Chen (2012).

Convection in a channel with heated porous blocks of various shapes was studied by Guerrouddj and Kahalerras (2010). Convection in a vertical annulus with porous layers was studied by Zahrani and Kiwan (2009). A vertical channel with a nanofluid was treated by Hajipour and Dehkordi (2012).

### 8.4.2 Jet Impingement

Jet impingement cooling of a horizontal surface in a confined porous medium was studied by Saeid and Mohamad (2006). Saeid and Pop (2006) treated periodic mixed convection in a horizontal porous layer heated from below by an isoflux heater. Further work involving jets was done by Saeid (2007b), Wong and Saeid (2009a, b, c, d, e, f), Wong et al. (2009), Marafie et al. (2008), and Sivasamy et al. (2010a, b, 2011). Aspects studied by these authors include the effect of local thermal nonequilibrium, a conjugate solid layer of finite thickness, and unsteady convection of a confined jet in a fluid-superposed medium. Rosali et al. (2011) studied stagnation point flow past a vertical plate with prescribed heat flux.

### 8.4.3 Other Aspects

Lid-driven flow was studied by Kandaswamy et al. (2008c), Oztop (2006), Oztop and Varol (2009), Vishnuvardhanarao and Das (2008, 2009, 2010), and Kumari and Nath (2011) (with internal heat generation). The effect of solid cylinder rotating within a square cavity was studied by Misirlioglu (2006).

A square duct with suction on a boundary was investigated by Kumar et al. (2010d), Murthy et al. (2010a,b), and Ratish Kumar and Murthy (2010a). Vented square enclosures were also studied by Mahmud and Pop (2006) and Ghazanfarian and Abbassi (2007). Convection in an obstructed open-ended cavity was studied by Shi and Vafai (2010). Convection in a vertical pipe was treated by Kumar et al. (2010d).

Mixed convection between inclined plates was studied by Cimpean et al. (2009) (fully developed convection) and Barletta et al. (2008c). Barletta et al. (2008a) studied mixed convection with heating effects in a vertical porous annulus with a radially varying magnetic field, while Barletta et al. (2009c) found closed form solutions for mixed convection with a magnetohydrodynamic effect in a vertical porous annulus surrounding an electric cable. Basak et al. (2011) and Ramakrishna et al. (2012) used a finite element-based heatline approach to study convection in a square cavity with various wall thermal boundary conditions. Kumar et al. (2009b) investigated numerically convection in a cavity with various non-Darcy models. Hayat et al. (2011a) studied Falkner-Skan wedge flow of a power-law fluid. The combined effects of magnetic field and thermal dispersion on a non-Darcy mixed convection were studied by Oztop et al. (2011a).

Experimental studies of mixed convection in a vertical duct were carried out by Venugopal et al. (2010a, b) and Jiang et al. (2006b, 2008) ( $\text{CO}_2$  at supercritical pressure).

# Chapter 9

## Double-Diffusive Convection

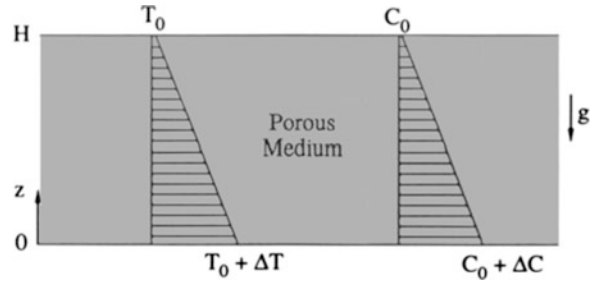
In this chapter, we turn our attention to processes of combined (simultaneous) heat and mass transfer that are driven by buoyancy. The density gradients that provide the driving buoyancy force are induced by the combined effects of temperature and species concentration nonuniformities present in the fluid-saturated medium. The present chapter is guided by the review of Trevisan and Bejan (1990), which began by showing that the conservation statements for mass, momentum, energy, and chemical species are the equations that have been presented here in Chaps. 1, 2, and 3. In particular, the material in Sect. 3.3 is relevant. The new feature is that beginning with Eq. (3.26), the buoyancy effect in the momentum equation is represented by two terms, one due to temperature gradients and the other to concentration gradients. Useful review articles on double-diffusive convection include those by Mojtabi and Charrier-Mojtabi (2000, 2005), Mamou (2002b), and Diersch and Kolditz (2002).

### 9.1 Vertical Heat and Mass Transfer

#### 9.1.1 Horton–Rogers–Lapwood Problem

The interesting effects in double-diffusive (or thermohaline, if heat and salt are involved) convection arise from the fact that heat diffuses more rapidly than a dissolved substance. Whereas a stratified layer involving a single-component fluid is stable if the density decreases upward, a similar layer involving a fluid consisting of two components, which can diffuse relative to each other, may be dynamically unstable. If a fluid packet of such a mixture is displaced vertically, it loses any excess heat more rapidly than any excess solute. The resulting buoyancy may act either to increase the displacement of the particle, and thus cause monotonic instability, or reverse the direction of the displacement and so cause oscillatory instability, depending on whether the solute gradient is destabilizing and the temperature gradient is stabilizing or vice versa.

**Fig. 9.1** Infinite horizontal porous layer with linear distributions of temperature and concentration



The double-diffusive generalization of the Horton–Rogers–Lapwood problem was studied by Nield (1968). In terms of the temperature  $T$  and the concentration  $C$ , we suppose that the density of the mixture is given by Eq. (3.26):

$$\rho_f = \rho_0 [1 - \beta(T - T_0) - \beta_C(C - C_0)]. \quad (9.1)$$

In this equation,  $\beta_C = -\rho_f^{-1} \partial \rho_f / \partial C$  is a concentration expansion coefficient analogous to the thermal expansion coefficient  $\beta = -\rho_f^{-1} \partial \rho_f / \partial T$ . We assume that  $\beta_C$  and  $\beta$  are constants. In most practical situations,  $\beta_C$  will have a negative value.

As shown in Fig. 9.1, we suppose that the imposed conditions on  $C$  are

$$C = C_0 + \Delta C \text{ at } z = 0 \quad \text{and} \quad C = C_0 \text{ at } z = H. \quad (9.2)$$

The conservation equation for chemical species is

$$\varphi \frac{\partial C}{\partial t} + \mathbf{v} \cdot \nabla C = D_m \nabla^2 C, \quad (9.3)$$

and the steady-state distribution is linear:

$$C_s = C_0 + \Delta C \left(1 - \frac{z}{H}\right). \quad (9.4)$$

Proceeding as in Sect. 6.2, choosing  $\Delta C$  as concentration scale and putting  $\hat{C} = C'/\Delta C$  and writing

$$\hat{C} = \gamma(z) \exp(st + il\hat{x} + im\hat{y}), \quad (9.5)$$

we obtain

$$\left[ \text{Le}^{-1}(D^2 - \alpha^2) - \frac{\varphi}{\sigma} s \right] \gamma = -W. \quad (9.6)$$

In place of Eq. (6.23), we now have, if  $\gamma_a$  is negligible,

$$(D^2 - \alpha^2)W = -\alpha^2 Ra(\theta + N\gamma), \quad (9.7)$$

while Eq. (6.22) remains unchanged, namely,

$$(D^2 - \alpha^2 - s)\theta = -W. \quad (9.8)$$

The nondimensional parameters that have appeared are the Rayleigh and Lewis numbers

$$Ra = \frac{g\beta KH\Delta T}{v\alpha_m}, \quad Le = \frac{\alpha_m}{D_m}, \quad (9.9)$$

and the buoyancy ratio

$$N = \frac{\beta_C \Delta C}{\beta \Delta T}. \quad (9.10)$$

If both boundaries are impermeable, isothermal (conducting), and isosolutal (constant  $C$ ), then Eqs. (9.6)–(9.8) must be solved subject to

$$W = \theta = \gamma = 0 \quad \text{at} \quad \hat{z} = 0 \quad \text{and} \quad \hat{z} = 1. \quad (9.11)$$

Solutions of the form

$$(W, \theta, \gamma) = (W_0, \theta_0, \gamma_0) \sin j\pi\hat{z} \quad (9.12)$$

are possible if

$$J(J+s)(J+\Phi s) = Ra \alpha^2 (J + \Phi s) + Ra_D \alpha^2 (J + s), \quad (9.13)$$

where

$$J = j^2\pi^2 + \alpha^2, \quad \Phi = \frac{\varphi}{\sigma} Le, \quad Ra_D = NLeRa = \frac{g\beta_C KH\Delta C}{vD_m}. \quad (9.14)$$

At marginal stability,  $s = i\omega$ , where  $\omega$  is real, and the real and imaginary parts of Eq. (9.13) yield

$$J^2 - \Phi\omega^2 = (Ra + Ra_D)\alpha^2, \quad (9.15)$$

$$\omega[J^2(1 + \Phi) - (\Phi Ra + Ra_D)\alpha^2] = 0. \quad (9.16)$$

This system implies either  $\omega = 0$  and

$$Ra + Ra_D = \frac{J^2}{\alpha^2}, \quad (9.17)$$

or

$$\Phi Ra + Ra_D = (1 + \Phi) \frac{J^2}{\alpha^2}, \quad (9.18)$$

and

$$\Phi \frac{\omega^2}{\alpha^2} = \frac{J^2}{\alpha^2} - (Ra + Ra_D). \quad (9.19)$$

Since  $J^2/\alpha^2$  has the minimum value  $4\pi^2$ , attained when  $j = 1$  and  $\alpha = \pi$ , we conclude that the region of stability in the  $(Ra, Ra_D)$  plane is bounded by the lines

$$Ra + Ra_D = 4\pi^2, \quad (9.20)$$

$$\Phi Ra + Ra_D = 4\pi^2(1 + \Phi), \quad (9.21)$$

Equation (9.20) represents the boundary for monotonic or stationary instability, and Eq. (9.21) is the boundary for oscillatory instability with frequency  $\omega$  given by

$$\Phi \frac{\omega^2}{\pi^2} = 4\pi^2 - (Ra + Ra_D). \quad (9.22)$$

Clearly the right-hand side of Eq. (9.22) must be nonnegative in order to yield a real value for  $\omega$ .

If  $\Phi = 1$ , then the lines (9.20) and (9.21) are parallel, with the former being nearer the origin. Otherwise they intersect at

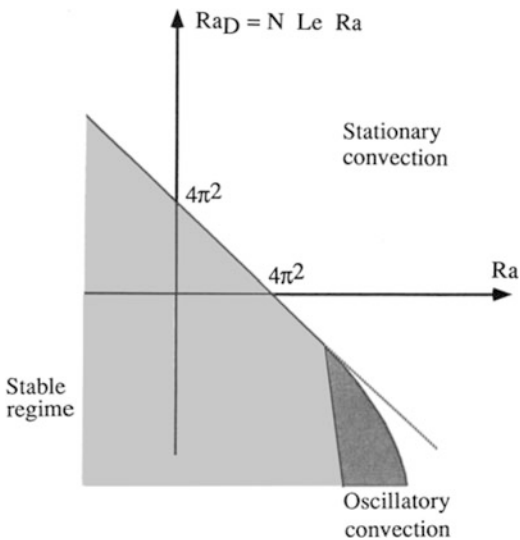
$$Ra = \frac{4\pi^2\Phi}{\Phi - 1}, \quad Ra_D = \frac{4\pi^2}{1 - \Phi}. \quad (9.23)$$

Illustrated in Fig. 9.2 is the case  $\Phi > 1$ , which corresponds to  $Le > \sigma/\Phi$ .

The cases of other combinations of boundary conditions can be treated in a similar manner. If the boundary conditions on the temperature perturbation  $\theta$  are formally identical with those of the solute concentration perturbation  $\gamma$ , then the monotonic instability boundary is a straight line:

$$Ra + Ra_D = Ra_c. \quad (9.24)$$

**Fig. 9.2** The stability and instability domains for double-diffusive convection in a horizontal porous layer



One can interpret  $Ra$  as the ratio of the rate of release of thermal energy to the rate of viscous dissipation of energy and a similar interpretation applies to  $Ra_D$ . When the thermal and solutal boundary conditions are formally identical, the eigenfunctions of the purely thermal and purely solutal problems are identical, and consequently the thermal and solutal effects are additive. When the two sets of boundary conditions are different, the coupling between the thermal and solutal agencies is less than perfect, and one can expect that the monotonic instability boundary will be concave toward the origin, since then  $Ra + Ra_D \geq Ra_c$  with equality occurring only when  $Ra = 0$  or  $Ra_D = 0$ .

When  $Ra$  and  $Ra_D$  are both positive, the double-diffusive situation is qualitatively similar to the single-diffusive one. When  $Ra$  and  $Ra_D$  have opposite signs, there appear interesting new phenomena: multiple steady-and unsteady-state solutions, subcritical flows, periodic or chaotic oscillatory flows, traveling waves in relatively large-aspect-ratio enclosures, and axisymmetric flow structures. Such phenomena arise generally because the different diffusivities lead to different timescales for the heat and solute transfer. But similar phenomena can arise even when the thermal and solutal diffusivities are nearly equal because of the factor  $\Phi/\sigma$  (often called the normalized porosity). This is because heat is transferred through both the fluid and solid phases, but the solute is necessarily transported through the fluid phase only since the porous matrix material is typically impermeable.

Experiments with a Hele-Shaw cell by Cooper et al. (1997, 2001) and Pringle et al. (2002) yielded results in agreement with the theory.

### 9.1.2 Nonlinear Initial Profiles

Since the diffusion time for a solute is relatively large, it is particularly appropriate to discuss the case when the concentration profile is nonlinear, the basic concentration distribution being given by

$$C_s = C_0 + \Delta C[1 - F_c(\hat{z})]. \quad (9.25)$$

The corresponding nondimensional concentration gradient is  $f_c(\hat{z}) = F'_c(\hat{z})$  and satisfies  $\langle f'_c(\hat{z}) \rangle = 1$ , where the angle brackets denote the vertical average. Then, in place of Eq. (9.6), one now has

$$\left[ Le^{-1}(D^2 - \alpha^2) - \frac{\varphi}{\sigma} s \right] \gamma = -f_c(\hat{z}) W. \quad (9.26)$$

In the case of impermeable conducting boundaries, the Galerkin method of solution (trial functions of the form  $\sin l\pi\hat{z}$  with  $l = 1, 2, \dots$ ) gives us the first approximation to the stability boundary for monotonic instability:

$$Ra + 2Ra_D \langle f_c(\hat{z}) \sin^2 \pi^2 \hat{z} \rangle = 4\pi^2. \quad (9.27)$$

For example, for the cosine profile with  $F_c(\hat{z}) = (1 - \cos \pi \hat{z})/2$  and hence with  $f_c = (\pi/2) \sin \pi \hat{z}$ , we get

$$Ra + \frac{4}{3} Ra_D = 4\pi^2. \quad (9.28)$$

Similarly, for the step-function concentration, with  $F_c(\hat{z}) = 0$  for  $0 \leq \hat{z} < 1/2$  and  $F_c(\hat{z}) = 1$  for  $1/2 < \hat{z} \leq 1$ , so that  $f_c(\hat{z}) = \delta(\hat{z} - 1/2)$ , we have

$$Ra + Ra_D = 4\pi^2. \quad (9.29)$$

The approximation leading to this result requires that  $|Ra_D|$  be small.

### 9.1.3 Finite-Amplitude Effects

Experiments in viscous fluids have shown that monotonic instability, associated with warm salty water above cool fresh water, appears in the form of “fingers” that grow downward from the upper part of the layer. More generally, fingering occurs when the faster diffusing component is stabilizing and the slower diffusing component is destabilizing. This situation is referred to as the fingering regime. On the other hand, oscillatory instability, associated with warm salty water below cool fresh water, gives rise to a series of convecting layers that form in turn, each on top of its predecessor. This situation is referred to as the diffusive regime.

In the case of a porous medium, the questions are whether the fingers form fast enough before they are destroyed by dispersive effects and whether their width is large enough compared to the grain size for Darcy’s law to be applicable. Following earlier work by Taunton et al. (1972), these questions were examined by Green

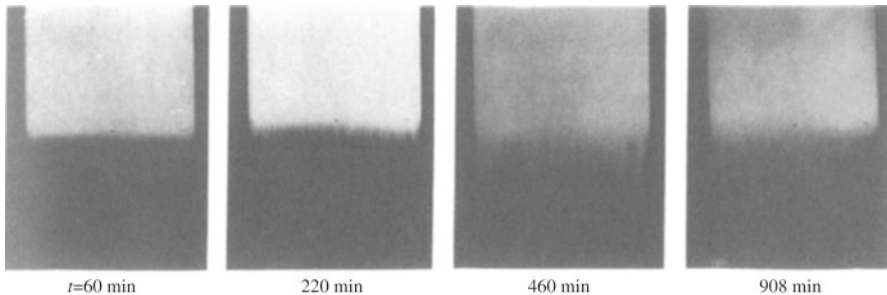


**Fig. 9.3** A series of pictures of finger growth. Dyed sugar solution (*light color*) overlies heavier salt solution (Imhoff and Green 1988, with permission from Cambridge University Press)

(1984), who, on the basis of his detailed analysis, predicted that fluxes associated with double-diffusive fingering may well be important, but horizontal dispersion may limit the vertical coherence of the fingers. In their visualization and flux experiments using a sand-tank model and a salt–sugar system, Imhoff and Green (1988) found that fingering did indeed occur, but it was quite unsteady, in contrast to the quasisteady fingering observed in a viscous fluid (Fig. 9.3). Despite the unsteadiness, good agreement was attained with the theoretical predictions. Imhoff and Green (1988) concluded that fingering could play a major role in the vertical transport of contaminants in groundwater. (It should be noted that fingering can also arise from Rayleigh–Taylor instability, and the hydrological situation can be complex (Xie et al. 2012)).

That layered double-diffusive convection is possible in a porous medium was shown by Griffiths (1981). His experiments with a two-layer convecting system in a Hele-Shaw cell and a porous medium of glass spheres indicated that a thin “diffusive” interface is maintained against diffusive thickening, despite the lack of inertial forces. The solute and thermal buoyancy fluxes are approximately in the ratio  $r = \varphi Le^{-1/2}$ . Griffiths explained the behavior of the heat flux in terms of a coupling between purely thermal convection within each convecting layer and diffusion through the density interface. Further experiments in a Hele-Shaw cell by Pringle and Glass (2002) explored the influence of concentration at a fixed buoyancy ratio.

Rudraiah et al. (1982a) applied nonlinear stability analysis to the case of a porous layer with impermeable, isothermal, and isosolutal boundaries. They reported Nusselt and Sherwood numbers for  $Ra$  values up to 300 and  $Ra_D$  values up to 70. Their results show that finite-amplitude instability is possible at subcritical values of  $Ra$ .

Brand and Steinberg (1983a, b) and Brand et al. (1983) have obtained amplitude equations appropriate for the onset of monotonic instability and oscillatory instability and also for points in the vicinity of the lines of monotonic and oscillatory instability. Brand et al. (1983) found an experimentally feasible example of a codimension-two bifurcation (an intersection of monotonic and oscillatory instability boundaries). Brand and Steinberg (1983b) predicted that the Nusselt number and

also the “Froude” (Sherwood) number should oscillate with a frequency twice that of the temperature and concentration fields. Small-amplitude nonlinear solutions in the form of standing and traveling waves and the transition to finite-amplitude overturning convection, as predicted by bifurcation theory, were studied by Knobloch (1986). Rehberg and Ahlers (1985) reported heat transfer measurements in a normal-fluid  $\text{He}^3\text{-}\text{He}^4$  mixture in a porous medium. They found a bifurcation to steady or oscillatory flow, depending on the mean temperature, in accordance with theoretical predictions.

Murray and Chen (1989) have extended the linear stability theory, taking into account effects of temperature-dependent viscosity and volumetric expansion coefficients and a nonlinear basic salinity profile. They also performed experiments with glass beads in a box with rigid isothermal lower and upper boundaries. These provide a linear basic-state temperature profile, but only allow a nonlinear and time-dependent basic-state salinity profile. With distilled water as the fluid, the convection pattern consisted of two-dimensional rolls with axes parallel to the shorter side. In the presence of stabilizing salinity gradients, the onset of convection was marked by a dramatic increase in heat flux at a critical temperature difference  $\Delta T$ . The convection pattern was three-dimensional, whereas two-dimensional rolls are observed for single-component convection in the same apparatus. When  $\Delta T$  was then reduced from supercritical to subcritical values, the heat flux curve completed a hysteresis loop.

For the case of uniform flux boundary conditions, Mamou et al. (1994) have obtained both analytical asymptotic and numerical solutions, the latter for various aspect ratios of a rectangular box. Both uniform flux and uniform temperature boundary conditions were considered by Mamou and Vasseur (1999) in their linear and nonlinear stability, analytical, and numerical studies. They identified four regimes dependent on the governing parameters: stable diffusive, subcritical convective, oscillatory, and augmenting direct regimes. Their results indicated that steady convection can arise at Rayleigh numbers below the supercritical value for linear stability, indicating the development of subcritical flows. They also demonstrated that in the overstable regime, multiple solutions can exist. Also, their numerical results indicate the possible occurrence of traveling waves in an infinite horizontal enclosure.

A nonlinear stability analysis using the Lyapunov direct method was reported by Lombardo et al. (2001) and Lombardo and Mulone (2002). A numerical study of the governing and perturbation equations, with emphasis on the transition from steady to oscillatory flows and with an acceleration parameter taken into consideration, was conducted by Mamou (2003). The numerical and analytic study by Mbaye and Bilgen (2001) demonstrated the existence of subcritical oscillatory instabilities. The numerical study by Mohamad et al. (2004) for convection in a rectangular enclosure examined the effect of varying the lateral aspect ratio. Schoofs et al. (1999) discussed chaotic thermohaline convection in the context of low-porosity hydrothermal systems. Schoofs and Spera (2003) in their numerical study observed that increasing the ratio of chemical buoyancy to thermal buoyancy, with the latter kept fixed, led to a transition from steady to chaotic convection with a stable limit cycle

appearing at the transition. The dynamics of the chaotic flow is characterized by transitions between layered and nonlayered patterns as a result of the spontaneous formation and disappearance of gravitationally stable interfaces. These interfaces temporally divide the domain in layers of distinct solute concentration and lead to a significant reduction of kinetic energy and vertical heat and solute fluxes. A scale analysis, supported by numerical calculations, was presented by Bourich et al. (2004c) for the case of bottom heating and a horizontal solutal gradient. The case of mixed boundary conditions (constant temperature and constant mass flux, or vice versa) was studied numerically by Mahidjiba et al. (2000a). They found that when the thermal and solute effects are opposing the convection, patterns differ markedly from the classic Bénard ones.

The linear stability for triply diffusive convection was studied by Tracey (1996). For certain parameter values, complicated neutral curves were found, including a heart-shaped disconnected oscillatory curve, and it was concluded that three critical Rayleigh numbers were involved. The energy method was used to obtain an unconditional nonlinear stability boundary and to identify possible regions of subcritical instability.

Mulone and Straughan described an operative method to obtain necessary and sufficient stability conditions. An extension to the case of systems with spatially dependent coefficients (such as the case of a concentration-based internal heat source) was made by Hill and Malashetty (2012). Falsaperla et al. (2012) studied rotating porous media under general boundary conditions. Peterson et al. (2010) performed a multi-resolution simulation of double-diffusive convection. Umla et al. (2010) examined roll convection of binary fluid mixtures. Global stability for penetrative convection was studied by Hill (2008). A differential equation approach to obtain global stability for radiation-induced convection was introduced by Hill (2009). Lo Jacono et al. (2010) studied the origin and properties of time-independent spatially localized convection, computing using numerical continuation different types of single- and multi-pulse states. Rionero (2012) reexamined global nonlinear stability in double-diffusive convection in the light of hidden symmetries. Diaz and Brevdo (2011, 2012) examined the absolute/convective instability dichotomy at the onset of convection with either horizontal or vertical solutal and inclined thermal gradients and with horizontal through flow.

#### **9.1.4 Soret and Dufour Cross-Diffusion Effects**

In the case of steep temperature gradients, the cross-coupling between thermal diffusion and solutal diffusion may no longer be negligible. The tendency of a solute to diffuse under the influence of a temperature gradient is known as the Soret effect.

In its simplest expression, the conservation equation for  $C$  now becomes

$$\varphi \frac{\partial C}{\partial t} + \mathbf{v} \cdot \nabla C = D_m \nabla^2 C + D_{CT} \nabla^2 T, \quad (9.30)$$

where the Soret coefficient  $D_{CT}$  is treatable as a constant. If the Soret parameter  $S$  is defined as

$$S = -\frac{\beta_C D_{CT}}{\beta D_m}, \quad (9.31)$$

then the equation for the marginal state of monotonic instability in the absence of an imposed solutal gradient is

$$Ra = \frac{4\pi^2}{1 + S(1 + Le)}. \quad (9.32)$$

The corresponding equation for marginal oscillatory instability is

$$Ra = \frac{4\pi^2(\sigma + \varphi Le)}{Le(\varphi + \sigma S)}. \quad (9.33)$$

The general situation, with both cross-diffusion and double-diffusion (thermal and solutal gradients imposed), was analyzed by Patil and Rudraiah (1980). Taslim and Narusawa (1986) showed that there is an analogy between cross-diffusion (Soret and Dufour effects) and double-diffusion in the sense that the equations can be put in mathematically identical form.

The linear analysis of Lawson et al. (1976), based on the kinetic theory of gases and leading to a Soret effect, was put forward to explain the lowering of the critical Rayleigh number in one gas due to the presence of another. This effect was observed in a binary mixture of helium and nitrogen by Lawson and Yang (1975). Lawson et al. (1976) observed that the critical Rayleigh number may be lower or greater than for a pure fluid layer depending upon whether thermal diffusion induces the heavier component of the mixture to move toward the cold or hot boundary, respectively. Brand and Steinberg (1983a) pointed out that with the Soret effect, it is possible to have oscillatory convection induced by heating from above. Rudraiah and Siddheshwar (1998) presented a weak nonlinear stability analysis with cross-diffusion taken into account.

The experimental and numerical study of Benano-Melly et al. (2001) was concerned with Soret coefficient measurement in a medium subjected to a horizontal thermal gradient. The onset of convection in a vertical layer subject to uniform heat fluxes along the vertical walls was treated analytically and numerically by Joly et al. (2001). The Soret effect also was included in the numerical study by Nejad et al. (2001). Sovran et al. (2001) studied analytically and numerically the onset of Soret-driven convection in an infinite horizontal layer with an applied vertical temperature gradient. They found that for a layer heated from above, the motionless solution is infinitely linearly stable in  $N > 0$ , while a stationary bifurcation occurs in  $N < 0$ . For a layer heated from below, the onset of convection is steady or oscillatory depending on whether  $N$  is above or below a certain value that depends

on  $Le$  and the normalized porosity. The numerical study of Faruque et al. (2004) of the situation where fluid properties vary with temperature, composition, and pressure showed that for lateral heating, the Soret effect was weak, but with bottom heating, the Soret effect was more pronounced.

Further studies of Soret convection, building on studies discussed in Sect. 1.9, were reported by Jiang et al. (2004a, b, c) and by Saghir et al. (2005a). Attention has been placed on thermogravitational convection, a topic treated by Estebe and Schott (1970). This refers to a coupling effect when a fluid mixture saturating a vertical porous cavity in a gravitational field is exposed to a uniform horizontal thermal gradient, and thermodiffusion produces a concentration gradient that leads to species separation. The porous media situation has been considered by Jamet et al. (1992) and Marcoux and Charrier-Mojtabi (1998). The numerical results of Marcoux and Mojtabi show the existence of a maximum separation corresponding to an optimal Rayleigh number as expected, but there remains a difference between the numerical results for that optimal value and experimental results of Jamet et al. (1992). The study by Jiang et al. (2004b) concentrated on the two-dimensional simulation of thermogravitation convection in a laterally heated vertical column with space-dependent thermal, molecular, and pressure diffusion coefficients taken as functions of temperature using the irreversible thermodynamics theory of Shukla and Firoozabadi. The numerical results reveal that the lighter fluid component migrates to the hot side of the cavity, and as the permeability increases, the component separation in the thermal diffusion process first increases, reaches a peak, and then decreases. Jiang et al. (2004b) reported values of a separation ratio for a methane and n-butane mixture. Further studies of separation have been made by Er-Raki et al. (2008a, b) (vertical enclosure), Elhajjar et al. (2008, 2009, 2010) (horizontal or inclined cell), Bennacer et al. (2009) (multi-domain separation), and Charrier-Mojtabi et al. (2011) (horizontal slot submitted to a heat flux). Jiang et al. (2004c) explicitly investigated the effect of heterogeneous permeability, something that strongly affects the Soret coefficient. Saghir et al. (2005a) have reviewed some aspects of thermodiffusion in porous media.

Soret-driven convection in a shallow enclosure and with uniform heat (or both heat and mass) fluxes was studied analytically and numerically by Bourich et al. (2002, 2004e, f, 2005) and Er-Raki et al. (2005). Depending on the values of  $Le$  and  $N$ , subcritical stationary convection may or may not be possible, and parallel convective flow may or may not be possible. Convection in a shallow enclosure was also studied by Bourich et al. (2005a, b).

Enclosures heated and salted from the sides were studied by Er-Raki et al. (2006a, 2007, 2011). In this situation, subcritical convection is possible.

An analytical and numerical study of convection in a horizontal layer with uniform heat flux applied at the horizontal walls, and with or without constant mass flux at those walls, was reported by Bahloul et al. (2003) and Boutana et al. (2004). A structural stability result was reported by Straughan and Hutter (1999).

Abbasi et al. (2011) studied the thermodiffusion of carbon dioxide in various binary mixtures. Theoretical predictions of effective thermodiffusion coefficients were made by Davarzani et al. (2010). A ternary mixture was examined by Jaber et al. (2008). Heterogeneous media were analyzed numerically by Jiang et al. (2006a). A doubly

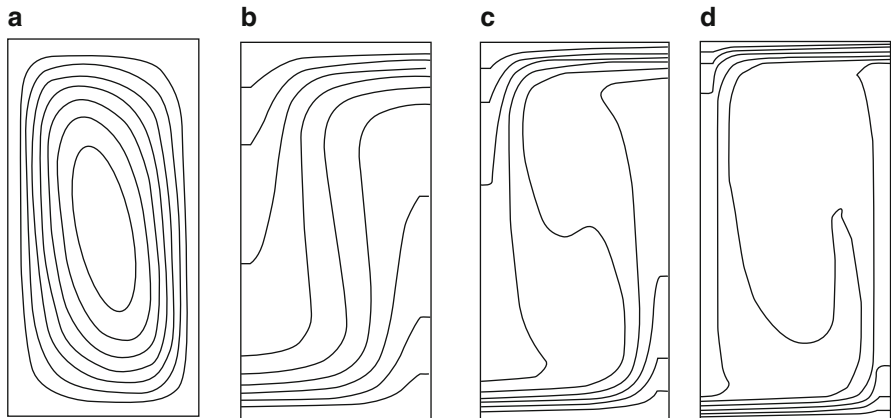


**Fig. 9.4** Two-dimensional numerical simulation for heat-transfer-driven ( $N = 0$ ) convection in a horizontal porous layer ( $Ra = 200$ ,  $H/L = 1.89$ ). (a) Streamlines; (b) isotherms, also isosolutal lines for  $Le = 1$ ; (c) isosolutal lines for  $Le = 4$ ; and (d) isosolutal lines for  $Le = 20$  (Trevisan and Bejan 1987b)

stratified medium was studied by Narayana and Murthy (2007). Nonlinear convection due to compositional and thermal buoyancy was treated by Tagare and Babu (2007). A strongly endothermic chemical reaction system was studied by Li et al. (2006a). Saravanan and Jegajoth (2010) examined a stationary fingering stability with coupled molecular diffusion and thermal nonequilibrium. Soret-driven convection in a cavity with perfectly conducting boundaries was analyzed by Lyubimov et al. (2011). Soret-driven convection in a horizontal layer in the presence of a heat or concentration source was studied by Goldobin and Lyubimov (2007). An analytical and numerical stability analysis of Soret-driven convection in a horizontal layer was made by Charrier-Mojtabi et al. (2007). A square cavity heated and salted from below was studied by Khadiri et al. (2010). A square cavity with icy fluid was treated by Alloui et al. (2010a). The effect of anisotropy on linear and nonlinear convection in a horizontal layer was examined by Gaikwad et al. (2009a, b), while Gaikwad and Prasad (2011) studied the case of a couple-stress fluid. A study of stationary and oscillatory convection of binary fluids was made by Augustin et al. (2010). The effects of rotation and anisotropy were included by Gaikwad and Kousar (2012). Ouattara et al. (2012) studied the effect of conducting boundary plates.

### 9.1.5 Flow at High Rayleigh Number

The interaction between the heat transfer and mass transfer processes in the regime of strong convection was investigated on the basis of a two-dimensional model by Trevisan and Bejan (1987b). They used scale analysis to back up their numerical work. Figure 9.4 shows the main characteristics of the flow, temperature, and concentration fields in one of the rolls that form. This particular flow is heat-transfer-driven in the sense that the dominant buoyancy effect is one due to

temperature gradients ( $N = 0$ ). The temperature field (Fig. 9.4b) shows the formation of thermal boundary layers in the top and bottom end-turn regions of the roll. The concentration field is illustrated in Fig. 9.4b–d. The top and bottom concentration boundary layers become noticeably thinner as  $Le$  increases from 1 to 20.

The overall Nusselt numbers  $Nu$  and overall Sherwood number  $Sh$  are defined by

$$Nu = \frac{\bar{q}''}{k_m \Delta T / H}, \quad Sh = \frac{\bar{j}}{D_m \Delta C / H}, \quad (9.34)$$

where  $\bar{q}''$  and  $\bar{j}$  are the heat and mass fluxes averaged over one of the horizontal boundaries. In heat-transfer-driven convection,  $|N| \ll 1$ , it is found that the Nusselt number scales are

$$Nu = (Ra / 4\pi^2)^{1/2}. \quad (9.35)$$

In the same regime, the mass transfer scales are

$$Sh \approx Le^{1/2} (Ra / 4\pi^2)^{7/8} \quad \text{if } Le > (Ra / 4\pi^2)^{1/4}, \quad (9.36a)$$

$$Sh \approx Le^2 (Ra / 4\pi^2)^{1/2} \quad \text{if } (Ra / 4\pi^2)^{-1/4} < Le < (Ra / 4\pi^2)^{1/4}, \quad (9.36b)$$

$$Sh \approx 1 \quad \text{if } Le < (Ra / 4\pi^2)^{1/4}. \quad (9.36c)$$

The scales of mass-transfer-driven flows,  $|N| \gg 1$ , can be deduced from these by applying the transformation  $Ra \rightarrow Ra_D$ ,  $Nu \rightarrow Sh$ ,  $Sh \rightarrow Nu$ , and  $Le \rightarrow Le^{-1}$ . The results are

$$Sh \approx (Ra_D / 4\pi^2)^{1/2}, \quad (9.37)$$

and

$$Nu \approx Le^{-1/2} (Ra_D / 4\pi^2)^{7/8} \quad \text{if } Le < (Ra_D / 4\pi^2)^{-1/4}, \quad (9.38a)$$

$$Nu \approx Le^{-2} (Ra_D / 4\pi^2)^{1/2} \quad \text{if } (Ra_D / 4\pi^2)^{-1/4} < Le < (Ra_D / 4\pi^2)^{1/4}, \quad (9.38b)$$

$$Nu \approx 1 \quad \text{if } Le > (Ra_D / 4\pi^2)^{1/4}. \quad (9.38c)$$

These estimates agree well with the results of direct numerical calculations.

Rosenberg and Spera (1992) performed numerical simulations for the case of a fluid heated and salted from below in a square cavity. As the buoyancy ratio  $N$  increases, the dynamics changes from a system that evolves to a well-mixed steady state, to one that is chaotic with large-amplitude fluctuations in composition, and

finally to one that evolves to a conductive steady state. Their correlations for  $Nu$  and  $Sh$  were in good agreement with the results of Trevisan and Bejan (1987b).

Sheridan et al. (1992) found that their experimentally measured heat transfer data correlated well with  $Nu \sim (Ra Da N)^{0.294} Ja^{-0.45}$ . Here  $Ja$  is the Jakob number, defined by  $Ja = c_p \Delta T / h_{fg} \Delta m$ , where  $h_{fg}$  is the enthalpy of evaporation and  $m$  is the saturated mass ratio (vapor/gas).

### 9.1.6 Other Effects

#### 9.1.6.1 Dispersion

If a net horizontal flow is present in the porous layer, it will influence not only the vertical solutal gradient but also the phenomenon of solute dispersion. Thermal dispersion also can be affected. In most applications,  $\alpha_m$  is greater than  $D_m$ , and as a consequence, the solutal dispersion is more sensitive to the presence of through flow. The ultimate effect of dispersion is that the concentration distribution becomes homogeneous.

The stability implications of the anisotropic mass diffusion associated with an anisotropic dispersion tensor were examined by Rubin (1975) and Rubin and Roth (1978, 1983). The dispersion anisotropy reduces the solutal stabilizing effect on the inception of monotonic convection and at the same time enhances the stability of the flow field with respect to oscillatory disturbances. Monotonic convection appears as transverse rolls with axes perpendicular to the direction of the horizontal net flow, while oscillatory motions are associated with longitudinal rolls (axes aligned with the net flow), the rolls of course being superposed on that net flow.

Certain geological structures contain some pores and fissures of large sizes. In such cavernous media, even very slow volume-averaged flows can deviate locally from the Darcy flow model. The larger pores bring about an intensification of the dispersion of solute and heat and because of the high-pore Reynolds numbers,  $Re_p$ , the effect of turbulence within the pores. Rubin (1976) investigated the departure from the Darcy flow model and its effect on the onset of convection in a horizontal layer with horizontal through flow. This study showed that in the case of laminar flow through the pores ( $Re_p \ll 1$ ), the net horizontal flow destabilizes the flow field by enhancing the effect of solutal dispersion. A stabilizing effect is recorded in the intermediate regime ( $Re_p \approx 1$ ). In the inertial flow regime ( $Re_p \gg 1$ ), the stability characteristics become similar to those of monodiffusive convection, the net horizontal flow exhibiting a stabilizing effect.

#### 9.1.6.2 Anisotropy and Heterogeneity

The onset of thermohaline convection in a porous layer with varying hydraulic resistivity ( $r = \mu/K$ ) was investigated by Rubin (1981). If one assumes that the

dimensionless hydraulic resistivity  $\xi = r/r_0$  varies only in the vertical direction and only by a relatively small amount, the linear stability analysis yields the monotonic marginal stability condition:

$$Ra + Ra_D = \pi^2 (\xi_H^{1/2} + \xi_V^{1/2})^2. \quad (9.39)$$

In this equation,  $\xi_H$  and  $\xi_V$  are the horizontal and vertical mean resistivities

$$\xi_H = \left( \int_0^1 \frac{d\hat{z}}{\xi} \right)^{-1}, \quad \xi_V = \int_0^1 \xi d\hat{z}, \quad (9.40)$$

and so  $\xi_H \leq \xi_V$ . The right-hand side of Eq. (9.39) can be larger or smaller than  $4\pi^2$  depending on whether  $Ra$  is based on  $\xi_V$  or  $\xi_H$ . A similar conclusion is reached with respect to the onset of oscillatory motions.

The Galerkin method has been used by Rubin (1982a) in an analysis of the effects of nonhomogeneous hydraulic resistivity and thermal diffusivity on stability. The effect of simultaneous vertical anisotropy in permeability (hydraulic resistivity), thermal diffusivity, and solutal diffusivity was investigated by Tyvand (1980) and Rubin (1982b).

Chen (1992) and Chen and Lu (1992b) analyzed the effect of anisotropy and inhomogeneity on salt-finger convection. They concluded that the critical Rayleigh number for this is invariably higher than that corresponding to the formation of plumes in the mushy zone during the directional solidification of a binary solution (see Sect. 10.2.3). A numerical study of double-diffusive convection in layered anisotropic porous media was made by Nguyen et al. (1994).

Viscosity variations and their effects on the onset of convection were considered by Patil and Vaidyanathan (1982), who performed a nonlinear stability analysis using the Brinkman equation, assuming a cosine variation for the viscosity. The variation reduces the critical Rayleigh number based on the mean viscosity. Bennacer (2004) treated analytically and numerically a two-layer (one anisotropic) situation with vertical through mass flux and horizontal through heat flux.

### 9.1.6.3 Brinkman Model

The effect of porous-medium coarseness on the onset of convection was documented by Poulikakos (1986). With the Brinkman equation, the critical Rayleigh number for the onset of monotonic instability is given by

$$Ra + Ra_D = \frac{(\alpha_c^2 + \pi^2)^2}{\alpha_c^2} [(\alpha_c^2 + \pi^2) \tilde{D}a + 1], \quad (9.41)$$

where the critical dimensionless horizontal wave number ( $\alpha_c$ ) is given by

$$\alpha_c^2 = \frac{(\pi^2 \tilde{D}a + 1)^{1/2} (9\pi^2 \tilde{D}a + 1)^{1/2} - \pi^2 \tilde{D}a - 1}{4\tilde{D}a}. \quad (9.42)$$

In terms of the effective viscosity  $\tilde{\mu}$  introduced in Eq. (1.17), the Darcy number  $\tilde{D}a$  is defined by

$$\tilde{D}a = \frac{\tilde{\mu}}{\mu} \frac{K}{H^2}. \quad (9.43)$$

Nonlinear energy stability theory was applied to this problem by Guo and Kaloni (1995b). Fingering convection, with the Forchheimer term as well as the Brinkman term taken into account, was treated numerically by Chen and Chen (1993). With  $Ra$  fixed, they found a transition from steady to time-periodic (and then to quasiperiodic) convection as  $Ra_D$  increases. An analytical solution based on a parallel-flow approximation and supported by numerical calculations was presented by Amahmid et al. (1999a). They showed that there is a region in the  $(N, Le)$  plane where a convective flow of this type is not possible for any  $Ra$  and Da values. A linear and nonlinear stability analysis leading to calculations of Nusselt numbers, streamlines, isotherms, and isohalines was presented by Shivakumara and Sumithra (1999). Further work with the Brinkmann model and a horizontal cavity was done by Alloui et al. (2010b). The ultimate boundedness and stability of triply diffusive mixtures in rotating layers was studied by Capone and de Luca (2012).

#### 9.1.6.4 Additional Effects

The situation in which one of the components undergoes a slow chemical reaction was analyzed by Patil (1982), while a convective instability that is driven by a fast chemical reaction was studied by Steinberg and Brand (1983). Further work involving chemical reactions was carried out by Subramanian (1994), Malashetty et al. (1994), and Malashetty and Gaikwad (2003). The effect of a third diffusing component was treated by Rudraiah and Vortmeyer (1982), Poulikakos (1985c), and Tracey (1998), who obtained some unusual neutral stability curves, including a closed approximately heart-shaped oscillatory curve disconnected from the stationary neutral curve, and thus requiring three critical values of  $Ra$  to describe the linear stability criteria. For certain values of parameters, the minima on the oscillatory and stationary curves occur at the same Rayleigh number but different wavenumbers. Kalla et al. (2001a) studied a situation involving imposed vertical heat and mass fluxes and a horizontal heat flux that they treated as a perturbation leading to asymmetry of the bifurcation diagram. Multiple steady-state solutions, with different heat and mass transfer rates, were found to coexist. Two- and three-dimensional multiple steady states were studied by Khadiri et al. (2011). Multiple steady states in an enclosure partly heated and fully salted from below were examined by Alloui et al. (2009b). In their analytical studies, Masuda et al. (1999, 2002) found that there is a range of buoyancy ratios  $N$  for which there is an oscillation between two

types of solution, temperature dominated and concentration dominated. Some mathematical aspects were studied by Rionero (2007, 2010) and Lin and Payne (2007). The boundary-domain integral method was used by Kramer et al. (2007) and Jeci et al. (2009). The Brinkman model was used by Wang and Tan (2009). The case of strong exothermic chemical reaction with local thermal nonequilibrium was studied by Boursi et al. (2012).

The effect of rotation was included by Chakrabarti and Gupta (1981) and Rudraiah et al. (1986), and for anisotropic media by Patil et al. (1989, 1990), and Malashetty and Begum (2011a), while the effect of thermal nonequilibrium was added by Malashetty et al. (2008), Malashetty and Heera (2008a, b, 2009), Malashetty et al. (2009a), and Chen et al. (2011). Anisotropy was also treated by Malashetty and Swamy (2010b). The effects of magnetic field and compressibility were studied by Sunil (1994, 1999, 2001), while Khare and Sahai (1993) combined the effects of a magnetic field and heterogeneity. Chamkha and Al-Naser (2002) studied numerically MHD convection in a binary gas. The effect of a magnetic field was also studied by Ramanbason and Vasseur (2007) and Bourich et al. (2009) (external shear stress). MHD, anisotropy, and Soret effects together were examined by Srivastava et al. (2012).

Papers on MHD convection with a non-Newtonian fluid are those by Sharma and Kumar (1996), Sharma and Thakur (2000), Sharma and Sharma (2000), Sharma and Kishor (2001), Sharma et al. (2001), and Sunil et al. (2001). Papers involving a rotating non-Newtonian fluid are those by Sharma et al. (1998, 1999a) and Sharma and Rana (2001, 2002). Non-Newtonian fluids permeated with suspended particles have been studied by Sharma et al. (1999b), Sunil et al. (2003c, 2004d), and Sharma and Sharma (2004). Other papers on a non-Newtonian fluid are those by Awad et al. (2010) (Maxwell fluid), Kumar and Bhaduria (2001c) (rotation), Malashetty et al. (2009c, e, 2010b, 2011), (viscoelastic fluid with rotation, anisotropy), Kumar and Bhaduria (2011b) (viscoelastic fluid, thermal nonequilibrium), Malashetty and Kollur (2011) (couple-stress fluid, anisotropy), Malashetty et al. (2010a) (couple-stress fluid), Wang and Tan (2008c, 2011) (Maxwell fluid, cross-diffusion), and Narayana et al. (2012) (Maxwell fluid). A viscoelastic fluid with local thermal nonequilibrium was examined by Malashetty et al. (2012). Gupta and Sharma (2008) examined a compressible Rivlin–Eriksen fluid in the presence of rotation and Hall effects. The combination of couple-stress fluid, magnetic field, and rotation was studied by Singh and Kumar (2011).

A ferromagnetic fluid was treated by Sekar et al. (1998) (rotation) and Sunil et al. (2004b, 2005a, b, c), Divya et al. (2005), Sunil and Sharma (2005), Sunil and Mahajan (2008a, 2009a, b), and Sunil et al. (2005a, b, 2007, 2009a, 2010b). These papers covered both linear and nonlinear stability and the various effects of rotation, micropolar fluid, magnetic-field-dependent viscosity, suspended dust particles, and local thermal nonequilibrium.

The effect of vertical through flow was studied by Shivakumara and Khalili (2001), Shivakumara and Nanjundappa (2006) (quadratic drag), Shivakumara and Sureshkumar (quadratic drag, Oldroyd B fluid), and Pieters and Schutteelaars (2008) (nonlinear dynamics) and that of horizontal through flow by Joulin and

Ouarzazi (2000) and Lyubimov et al. (2008a). Convection in an enclosure with partial or localized heating and salting was studied by Zhao et al. (2008b, c). Turbulent convection was treated by Tofaneli and de Lemos (2009).

Subramanian and Patil (1991) combined anisotropy with cross-diffusion. The critical conditions for the onset of convection in a doubly diffusive porous layer with internal heat generation were documented by Selimos and Poulikakos (1985). The effect of heat generation or absorption was also studied by Chamkha (2002). Heat generation with anisotropy was studied by Bhaduria (2012). Lin (1992) studied numerically a transient problem.

The effect of temporally fluctuating temperature on instability was analyzed by Ouarzazi and Bois (1994), Quarzazi et al. (1994), McKay (1998b, 2000), Ramazanov (2002), and Malashetty and Basavaraja (2004). The last study included the effect of anisotropy. The studies by McKay make use of Floquet theory. He demonstrated that the resulting instability may be synchronous, subharmonic, or at a frequency unrelated to the heating frequency.

The effect of modulated temperature at the boundaries was considered by Bhaduria (2007b, c), Bhaduria and Sherani (2008b), and Bhaduria and Srivastava (2010) (MHD).

The effect of vertical vibration was studied analytically and numerically by Sovran et al. (2000, 2002) and Jounet and Bardan (2001). Depending on the governing parameters, vibrations are found to delay or advance the onset of convection, and the resulting convection can be stationary or oscillatory. An intensification of the heat and mass transfers is observed at low frequency for sufficiently high vibration frequency. The onset of Soret-driven convection with a vertical variation of gravity was analyzed by Alex and Patil (2001) and Charrier-Mojtabi et al. (2004, 2005). The latter considered also horizontal vibration and reported that for both monotonic and oscillatory convection, the vertical vibration has a stabilizing effect, while the horizontal vibration has a destabilizing effect on the onset of convection. A further study of the effect of vibration was made by Strong (2008a). The effect of vibration on a system with a horizontal layer of clear fluid overlying a horizontal porous layer was studied by Lyubimov et al. (2008b).

Heterogeneity effects were also studied by Alloui 2009a, Jaber and Saghir (2011), and Kuznetsov and Nield (2008b). The effects of chemical reaction with double dispersion were examined by El-Amin et al. (2008). A strong endothermic chemical reaction with local thermal nonequilibrium was investigated by Li et al. (2007). The onset of convection driven by a catalytic surface reaction was studied by Postelnicu (2009) and Scott and Straughan (2011); in the latter paper, it was shown that if the reaction parameter exceeds a certain value, then convection appears as oscillatory (rather than stationary) convection. Scott (2012a,b) studied the case of a layer with an exothermal surface reaction at the lower boundary, with and without the Soret effect. Prichard and Richardson (2007) studied the effect of temperature-dependent solubility. The effect of viscous dissipation was examined by Barletta and Nield (2011b). Tipping points for convection with a Cattaneo–Christov fluid were studied by Straughan (2011b). Malashetty and Swamy (2011)

investigated convection in a rotating anisotropic porous layer saturated by a viscoelastic fluid. The case of a viscoelastic fluid was also examined by Swamy et al. (2012). The effect of rotation was also studied by Saravanan and Keerthana (2012). Shivakumara et al. (2011j) treated linear and nonlinear stability with a couple-stress fluid.

The problem of convection in groundwater below an evaporating salt lake was studied in detail by Wooding et al. (1997a, b) and Wooding (2007). Now the convection is driven by the evaporative concentration of salts at the land surface, leading to an unstable distribution of density, but the evaporative groundwater discharge dynamically can stabilize this saline boundary layer. The authors investigated the nature, onset, and development (as fingers or plumes) of the convection. They reported the result of linear stability analysis, numerical simulation, and laboratory experimentation using a Hele-Shaw cell. The results indicate that in typical environments, convection will predominate in sediments whose permeability exceeds about  $10^{-14} \text{ m}^2$ , while below this threshold the boundary layer should be stabilized, resulting in the accumulation of salts at the land surface. A numerical model simulating this situation was presented by Simmons et al. (1999). A related problem involving the evaporation of groundwater was studied analytically and numerically by Gilman and Bear (1996). The groundwater flow pattern in the vicinity of a salt lake also has been studied numerically by Holzbecher (2005b). A numerical study of convection above a salt dome was made by Holzbecher et al. (2010). A stability aspect of hot springs was studied by Bera et al. (2011). The onset of convection in groundwater wells was examined by Love et al. (2007). The onset of convection in under-ice melt ponds was studied by Hirata et al. (2012). Convection due to a wavy horizontal surface was investigated by Narayana and Sibanda (2012). Kuznetsov and Nield (2012c) studied the onset of double-diffusive convection in a vertical cylinder occupied by a heterogeneous porous medium with vertical through flow. The effect of g-jitter with a viscoelastic fluid and local thermal non-equilibrium was studied by Suthar et al. (2012). Convection in a cavity for the case of a density maximum was treated by MuthamilSelvan and Das (2012).

## 9.2 Horizontal Heat and Mass Transfer

### 9.2.1 Boundary Layer Flow and External Natural Convection

The most basic geometry for simultaneous heat and mass transfer from the side is the vertical wall embedded in a saturated porous medium. Specified at the wall are the uniform temperature  $T_0$  and the uniform concentration  $C_0$ . The temperature and concentration sufficiently far from the wall are  $T_\infty$  and  $C_\infty$ .

The Darcy flow driven by buoyancy in the vicinity of the vertical surface can have one of the four two-layer structures shown in Fig. 9.5. The thicknesses  $\delta$ ,  $\delta_T$ ,

**Fig. 9.5** The four regimes of boundary layer heat and mass transfer near a vertical surface embedded in a porous medium (Bejan and Khair 1985)

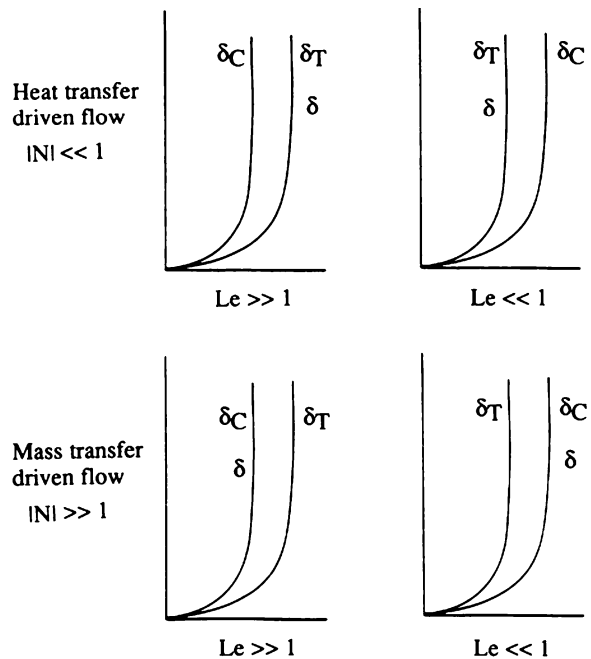


**Table 9.1** The flow, heat, and mass transfer scales for the boundary layer near a vertical wall embedded in a porous medium (Bejan 1984; Bejan and Khair 1985)

Driving mechanism	$v$	$Nu$	$Sh$	$Le$ domain
Heat transfer ( $ N  \ll 1$ )	$(\alpha_m/H) Ra$	$Ra^{1/2}$	$(Ra Le)^{1/2}$	$Le \gg 1$
Mass transfer ( $ N  \gg 1$ )	$(\alpha_m/H) Ra N $	$(Ra N )^{1/2}$	$(Ra N Le)^{1/2}$	$Le \ll 1$
	$(\alpha_m/H) Ra N $	$Le^{-1/2}(Ra N )^{1/2}$	$(Ra N Le)^{1/2}$	$Le \gg 1$

and  $\delta_C$  indicate the velocity, thermal, and concentration boundary layers. The relative size of these three thicknesses is determined by the combination ( $N, Le$ ).

The heat and mass transfer from the vertical surface was determined first based on scale analysis (Bejan 1984, pp. 335–338) and later based on the boundary layer similarity method (Bejan and Khair 1985). The results of the scale analysis are summarized in Table 9.1. Each row in this table corresponds to one of the quadrants of the ( $N, Le$ ) domain covered by Fig. 9.5. The  $v$  scale represents the largest vertical velocity, which in Darcy flow occurs right at the wall. By writing this time  $\bar{q}''$  and  $\bar{j}$  for the heat and mass fluxes averaged over the wall height  $H$ , the overall Nusselt and Sherwood numbers are defined as

$$Nu = \frac{\bar{q}''}{k_m(T_0 - T_\infty)/H}, \quad Sh = \frac{\bar{j}}{D_m(C_0 - C_\infty)/H}. \quad (9.44)$$

The similarity solution to the same problem was obtained by Bejan and Khair (1985) by selecting the nondimensional similarity profiles recommended by the scale analysis (Table 9.1):

$$u = -\frac{\alpha_m}{x} Ra_x f'(\eta), \quad (9.45)$$

$$v = -\frac{\alpha_m}{2x} Ra_x^{1/2} (f - \eta f'), \quad (9.46)$$

$$\theta(\eta) = \frac{T - T_\infty}{T_0 - T_\infty}, \quad \eta = \frac{y}{x} Ra_x^{1/2}, \quad (9.47)$$

$$c(\eta) = \frac{C - C_\infty}{C_0 - C_\infty}. \quad (9.48)$$

In this formulation,  $x$  is the distance measured along the wall, and the Rayleigh number is defined by  $Ra_x = g\beta Kx(T_0 - T_\infty)/\nu\alpha_m$ . The equations for momentum, energy, and chemical species conservation reduce to

$$f'' = -\theta' - Nc', \quad (9.49)$$

$$\theta'' = \frac{1}{2} f\theta', \quad (9.50)$$

$$c'' = \frac{1}{2} fc'Le, \quad (9.51)$$

with the boundary conditions  $f = 0$ ,  $\theta = 1$ ,  $c = 1$  at  $\eta = 0$ , and  $(f, \theta, c) \rightarrow 0$  as  $\eta \rightarrow \infty$ . Equations (9.49)–(9.51) reinforce the conclusion that the boundary layer phenomenon depends on two parameters,  $N$  and  $Le$ .

Figure 9.6 shows a sample of vertical velocity and temperature (or concentration) profiles for the case  $Le = 1$ . The vertical velocity increases, and the thermal boundary layer becomes thinner as  $|N|$  increases. The same similarity solutions show that the concentration boundary layer in heat-transfer-driven flows ( $N = 0$ ) becomes thinner as  $Le$  increases, in good agreement with the trend anticipated by scale analysis.

The effect of wall inclination on the two-layer structure was described by Jang and Chang (1988b, c). Their study is a generalization of the similarity solution approach employed by Bejan and Khair (1985). The heat and mass transfer scales that prevail in the extreme case when the embedded  $H$ -long surface is horizontal are summarized in Table 9.2. A related study was reported by Jang and Ni (1989), who considered the transient development of velocity, temperature, and concentration boundary layers near a vertical surface.

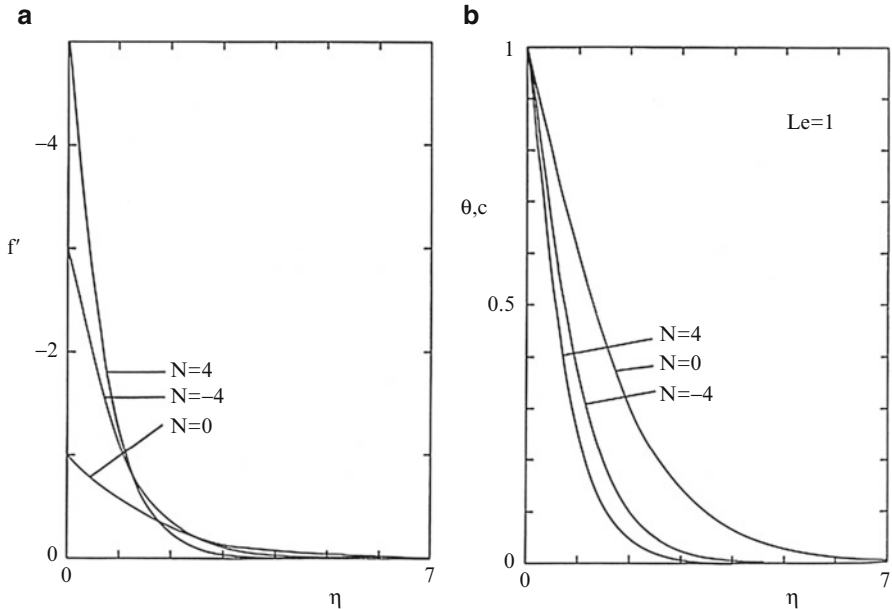


**Fig. 9.6** The buoyancy ratio effect on the  $Le = 1$  similarity profiles for boundary layer heat and mass transfer near a vertical wall embedded in a porous medium. (a) Velocity profiles and (b) temperature and concentration profiles (Bejan and Khair 1985)

**Table 9.2** The flow, heat, and mass transfer scales for the boundary layer near a horizontal wall embedded in a saturated porous medium (Jang and Chang 1988b)

Driving mechanism	$u$	$Nu$	$Sh$	$Le$ domain
Heat transfer $( N  \ll 1)$	$(\alpha_m/H)Ra^{2/3}$	$Ra^{1/3}$	$Ra^{1/3}Le^{1/2}$	$Le \gg 1$
Mass transfer $( N  \gg 1)$	$(\alpha_m/H) Ra^{2/3}Le^{-1/3}$	$Ra^{1/3}$	$Ra^{1/3}Le$	$Le \ll 1$
	$(\alpha_m/H) \times (Ra N )^{2/3}Le^{-1/3}$	$(Ra N )^{-1/3}Le^{-1/6}$	$(Ra N Le)^{1/3}$	$Le \ll 1$
	$(\alpha_m/H) \times (Ra N )^{2/3}Le^{-1/3}$	$(Ra N )^{-1/3}Le^{-2/3}$	$(Ra N Le)^{1/3}$	$Le \gg 1$

The effect of flow injection on the heat and mass transfer from a vertical plate was investigated by Lai and Kulacki (1991d) (see also the comments by Bejan (1992a)). Raptis et al. (1981) showed that an analytical solution is possible in the case of an infinite vertical wall with uniform suction at the wall-porous-medium interface. The resulting analytical solution describes flow, temperature, and concentration fields that are independent of altitude ( $y$ ). This approach was extended to the unsteady boundary layer flow problem by Raptis and Tzivanidis (1984). For the case of a non-Newtonian (power-law fluid), an analytical and numerical treatment was given by Rastogi and Poulikakos (1995). The case of a thermally stratified medium was studied numerically by Angirasa et al. (1997). Nonsimilar solutions for the case of two prescribed thermal and solutal boundary conditions were obtained by Aly and Chamkha (2010).

The physical model treated by Bejan and Khair (1985) was extended to the case of a boundary of arbitrary shape by Nakayama and Hossain (1995). A further scale analysis of natural convection boundary layers driven by thermal and mass diffusion was made by Allain et al. (1992), who also made some corroborating numerical investigations. They noted the existence of flows that are heat driven even though the amplitude of the solutal convection is dominant.

An analytical–numerical study of hydrodynamic dispersion in natural convection heat and mass transfer near vertical surfaces was reported by Telles and Trevisan (1993). They considered flows due to a combination of temperature and concentration gradients and found that four classes of flows are possible according to the relative magnitude of the dispersion coefficients.

For convection over a vertical plate, the Forchheimer effect was analyzed by Murthy and Singh (1999); dispersion effects were studied by Khaled and Chamkha (2001), Chamkha and Quadri (2003), and El-Amin (2004a), and the effect of double stratification was discussed by Bansod et al. (2002) and Murthy et al. (2004b). Using homotopy analysis and the Forchheimer model, an analytic solution was obtained by Wang et al. (2003a). The effect of thermophoresis particle deposition was analyzed by Chamkha and Pop (2004). Three-dimensional flow was treated by Singh (2005), Chamkha et al. (2006a), Duwairi and Damseh (2008b, 2009) (radiation, mixed convection), and Partha (2008, 2009) (cross-diffusion). The case of power-law non-Newtonian fluids was treated numerically by Jumar and Majumdar (2000, 2001). A non-Newtonian fluid with yield stress was studied by Hirata et al. (2010) (chemical reaction and cross-diffusion) and Ibrahim et al. (2010). A viscoelastic fluid and permeability periodic in the longitudinal direction was treated by Choudhury and Dey (2010). A polar fluid with chemical reaction and internal heat generation was studied by Patil and Kulkarni (2008) (for comment, pointing out an error in modeling viscous dissipation, see Rees (2009a)). The case of density depending on temperature and concentration in a nonlinear manner was studied by Patha (2010) and Beg et al. (2009c) (time dependence, radiation). A power-law fluid with yield stress, with cross-diffusion, was considered by Cheng (2006c, 2011b). Cheng (2007a,c, 2009a) studied a vertical wavy surface with a power-law fluid. Radiation and a non-Newtonian fluid were studied by El-Hakiem (2009). An inclined wavy surface was treated by Cheng (2010b). A corrugated surface with cross-diffusion was studied by Ratish Kumar and Murthy (2010b). Flow over a wedge with a chemical reaction was investigated by Kandaswamy and Palanima (2007), Kandaswamy et al. (2008a), and Muhammin et al. (2009a) (MHD, mixed convection, thermophoresis). Cross-diffusion was also studied by Patha et al. (2006), Salem (2006b) (viscoelastic fluid), Postelnicu (2007c, 2010a) (chemical reaction, stagnation point flow), Tsai and Huang (2009a), Narayana et al. (2009) (power-law fluid with yield stress), Tai and Char (2010) (non-Newtonian fluid, radiation), Tak et al. (2010) (MHD, radiation), and Ratish Kumar and Murthy (2010b) (wavy boundary). A doubly stratified medium was studied by Narayana and Murthy (2006), Ratish Kumar and Shalini (2005a, b) (wavy boundary), Srinivasacharya and RamReddy (2010), and Srinivasacharya et al. (2011). The combination of wavy boundary, double stratification and Soret and Dufour effects

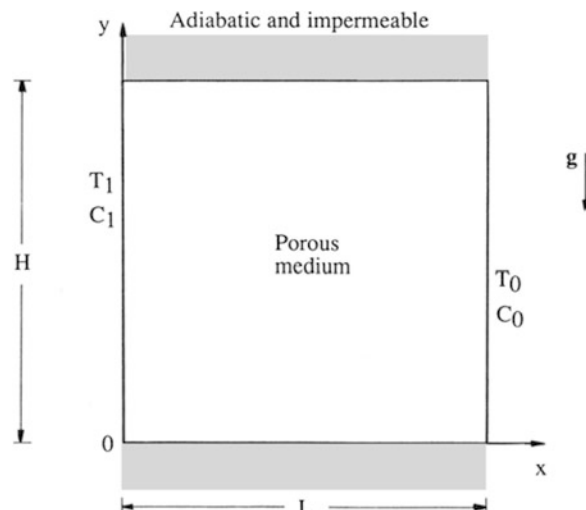
was studied by Ratish Kumar and Murthy (2012). Convection past a curved surface with variable permeability was treated by Mohammadein and Al Shear (2011).

MHD convection was treated for a vertical plate by Cheng (1999, 2005), Chamkha and Khaled (2000c, d), Acharya et al. (2000), Jang and Hsu (2009a) (Hall effect), Makinde (2009a, 2011a, 2012) (radiation, chemical reaction, stagnation point flow), and Makinde and Sibande (2008), and by Postelnicu (2004) with Soret and Dufour effects; for a cone or wedge by Chamkha et al. (2000); with heat generation or absorption effects for a cylinder or a cone by Chamkha and Quadri (2001, 2002); and for unsteady convection past a vertical plate by Kamel (2001) and Takhar et al. (2003a, b) and Hayat et al. (2010c). MHD convection of a micropolar fluid over a vertical moving plate was studied by Kim (2004). MHD convection for the case where the permeability oscillates with time about a nonzero mean was analyzed by Hassanien and Allah (2002). A transient MHD situation was studied by Prasad and Reddy (2008), Al-Odat et al. (2009), and Singh and Kumar (2010). MHD convection for a non-Newtonian fluid obeying the Eyring-Powell mode was studied by Eldabe et al. (2008). The combined effects of MHD, temperature-dependent viscosity, and cross-diffusion were treated by Afifi (2007a). The effects of MHD, radiation, and variable viscosity on convection from a vertical truncated cone were studied by Mandy et al. (2010). Unsteady MHD convection was examined numerically by Sharma et al. (2010).

Convection over a wavy vertical plate or cone was studied by Cheng (2000c, d), Ratish Kumar and Shalini (2004b), and Narayana and Murthy (2010) (cross-diffusion). Convection from a wavy wall in a thermally stratified enclosure with mass and thermal stratification was treated numerically by Ratish Kumar and Shalini (2005a, b). A vertical wavy wall with double stratification was also studied by Neagu (2011). A cone, truncated or otherwise, with variable wall temperature and concentration was analyzed by Yih (1999a, d) and Cheng (2000a). A vertical cone was also treated by Kumari and Nath (2009a), Awad et al. (2011) (cross-diffusion), and Cheng (2009c, d, f, 2010d, 2011a) (non-Newtonian fluid, cross-diffusion, variable wall temperature and concentration, variable wall heat and mass fluxes). A truncated cone was studied by Chamkha et al. (2006b) (icy water) Cheng (2007c) (nonsimilar solutions), Cheng (2007c, 2008, 2009b,e, 2010a) (non-Newtonian fluid, wavy wall, variable viscosity), Mahdy (2010) (chemical reaction, variable viscosity), and Kairi and Murthy (2011).

Convection above a near-horizontal surface and convection along a vertical permeable cylinder were analyzed by Hossain et al. (1999a, b). A vertical cylinder was also treated by Cheng (2010c), El-Aziz (2007) (MHD, permeable surface), and Singh and Chandarki (2009). A horizontal permeable cylinder was considered by Yih (1999f). Flow over a horizontal cylinder was also studied by El-Kabeir et al. (2008a, b) (MHD, cross-diffusion, non-Newtonian fluid) and Zueco et al. (2009a). Li and Lai (1998), Bansod (2003), and Bansod et al. (2005) reexamined convection from horizontal plates. Also for a horizontal plate, Wang et al. (2003b) obtained an analytical solution for Forchheimer convection with surface mass flux and thermal dispersion effects, Bansod and Jadhav employed an integral treatment, and Narayana and Murthy (2008) studied the effect of cross-diffusion. Flow over a

**Fig. 9.7** Enclosed porous medium subjected to heat and mass transfer in the horizontal direction



stretching sheet was studied by Abel et al. (2001) (viscoelastic fluid), Salem (2006b) (viscoelastic fluid), Mansour et al. (2008a, b) (chemical reaction, thermal stratification, MHD, cross-diffusion), Aly et al. (2011) (cross-diffusion), Beg et al. (2009a) (MHD, cross-diffusion), Pal and Chatterjee (2010) (MHD, micropolar fluid, non-uniform heat source, thermal radiation), Pal and Mondal (2010b) (MHD, radiation), Pal and Mondal (2012b) (MHD, Forchheimer drag, nonuniform heat source/sink, variable viscosity), Abdou (2010) (temperature-dependent viscosity), Rahman and Al-Lawatia (2010) (chemical reaction, micropolar fluid), Chamkha et al. (2010b) (unsteady flow, chemical reaction), Kandaswamy et al. (2010a) (thermophoresis, temperature-dependent viscosity), Chamkha and Aly (2011) (stagnation point flow, polar fluid, cross-diffusion), and Huang et al. (2011) (inclined surface, chemical reaction). A moving surface with MHD unsteady flow, a micropolar fluid, and radiation was studied by Kumar et al. (2010c). An impulsively started surface with radiation was investigated by Beg et al. (2009e). An oscillating plate with a magnetic field was studied by Chaudhary and Jain (2007a). The effects of magnetic field, micropolar fluid, radiation, variable permeability, and slip flow were considered by Chaudhary and Jain (2007b). An MHD flow with oscillatory suction was studied by Das et al. (2009). Unsteady MHD convection with Dufour and Soret effects was treated numerically by Al-Odat and Al-Ghamdi (2012).

### 9.2.2 Enclosed Porous Medium

As the simplest configuration of simultaneous heat and mass transfer in an enclosed porous medium consider the two-dimensional system defined in Fig. 9.7. The

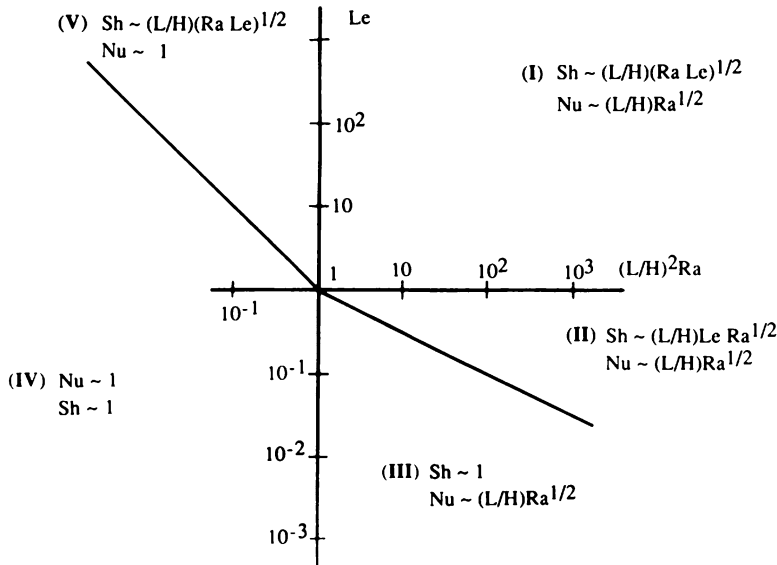


**Fig. 9.8** The heat and mass transfer regimes when the buoyancy effect in the system of Fig. 9.7 is due mainly to temperature gradients,  $|N| \ll 1$  (Trevisan and Bejan 1985)

uniform temperature and concentration are maintained at different levels along the two sidewalls. The main engineering challenge is the calculation of the overall heat and mass transfer rates expressed by Eq. (9.44).

Relative to the single-wall problem (Fig. 9.5), the present phenomenon depends on the geometric aspect ratio  $L/H$  as an additional dimensionless group next to  $N$  and  $Le$ . These groups account for the many distinct heat and mass transfer regimes that can exist. Trevisan and Bejan (1985) identified these regimes on the basis of scale analysis and numerical experiments. Figure 9.8 shows that in the case of heat-transfer-driven flows ( $|N| \ll 1$ ), there are five distinct regimes, which are labeled I–V. The proper  $Nu$  and  $Sh$  scales are listed directly on the  $[Le (L/H)^2 Ra]$  subdomain occupied by each regime.

Five distinct regimes also are possible in the limit of mass-transfer-driven flows,  $|N| \gg 1$ . Figure 9.9 shows the corresponding Nusselt and Sherwood number scales and the position of each regime in the plane  $[Le (L/H)^2 Ra|N|]$ . Had we used the plane  $[Le^{-1} (L/H)^2 Ra|N|Le]$  then the symmetry with Fig. 9.8 would have been apparent. The  $Nu$  and  $Sh$  scales reported in Figs. 9.8 and 9.9 are correct within a numerical factor of order 1. Considerably more accurate results have been developed numerically and reported in Trevisan and Bejan (1985).

The most striking effect of varying the buoyancy ratio  $N$  between the extremes represented by Figs. 9.8 and 9.9 is the suppression of convection in the vicinity of  $N = -1$ . In this special limit, the temperature and concentration buoyancy effects are comparable in size but have opposite signs. Indeed, the flow disappears completely if  $Le = 1$  and  $N = -1$ . This dramatic effect is illustrated in Fig. 9.10,

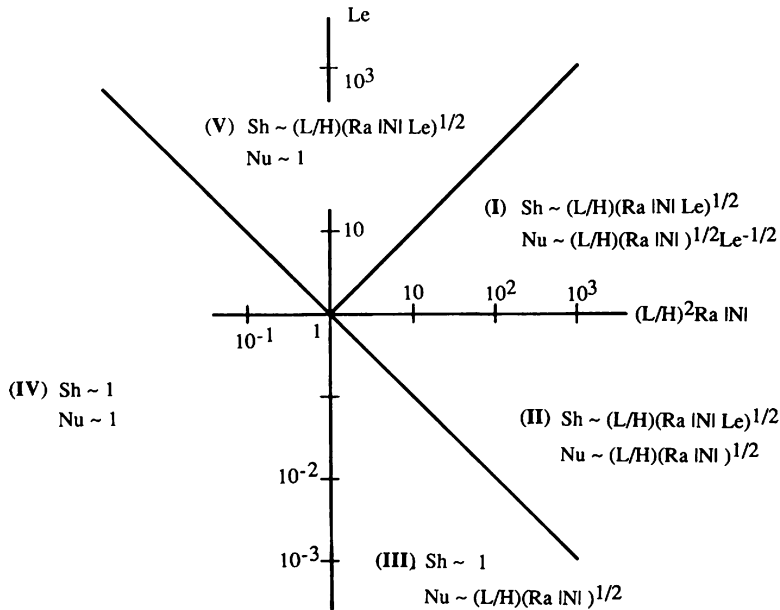


**Fig. 9.9** The heat and mass transfer regimes when the buoyancy effect in the system of Fig. 9.7 is due mainly to concentration gradients,  $|Nl| \gg 1$  (Trevisan and Bejan 1985)

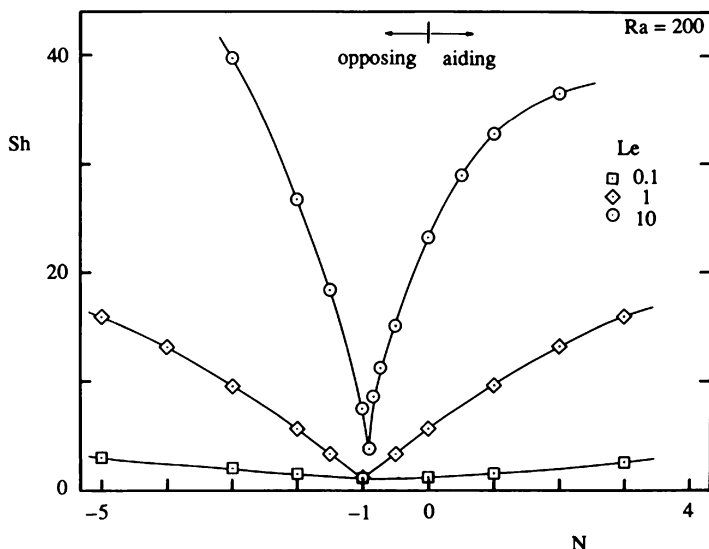


**Fig. 9.10** The effect of the buoyancy ratio on the overall mass transfer rate through the enclosed porous medium shown in Fig. 9.7 ( $Ra = 200, H/L = 1$ ) (Trevisan and Bejan 1985)

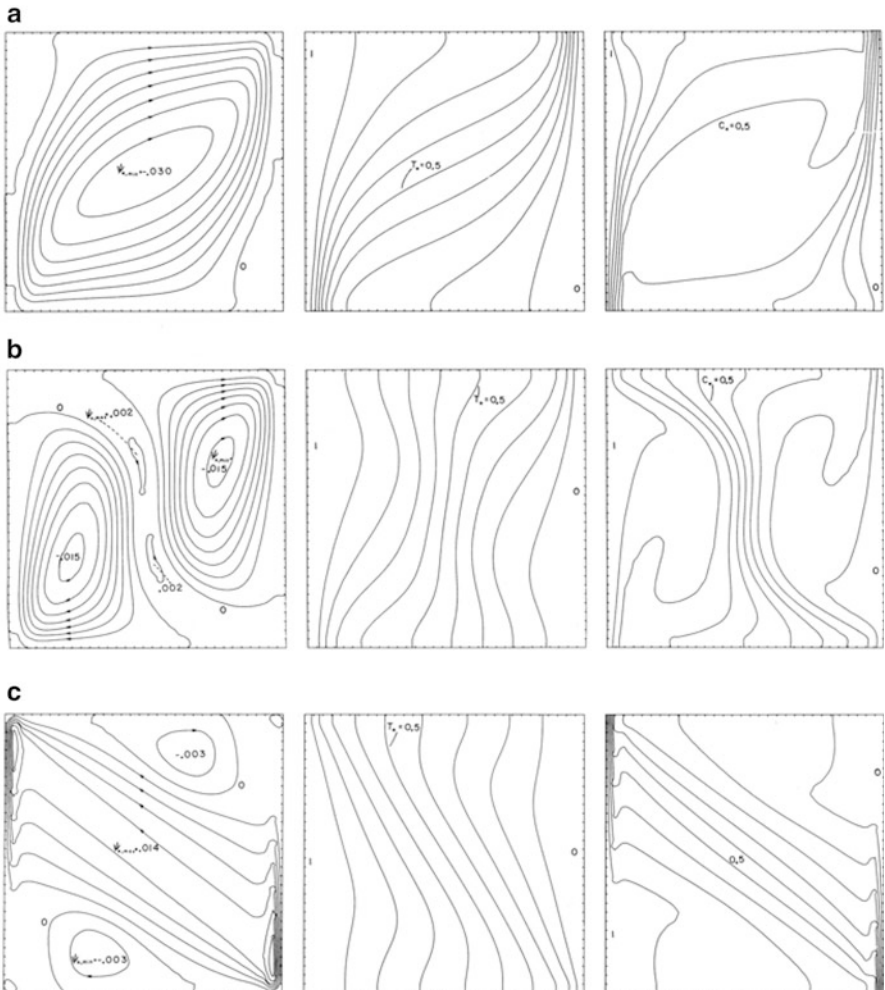


**Fig. 9.11** Streamlines, isotherms, and isosolutal lines for natural convection in the enclosed porous medium of Fig. 9.7, showing the flow reversal that occurs near  $N = -1$  ( $Ra = 200$ ,  $Le = 10$ ,  $H/L = 1$ ). (a)  $N = -0.85$ ; (b)  $N = -0.9$ ; and (c)  $N = -1.5$  (Trevisan and Bejan 1985)

which shows how the overall mass transfer rate approaches the pure diffusion level ( $Sh = 1$ ) as  $N$  passes through the value  $-1$ .

When the Lewis number is smaller or greater than 1, the passing of  $N$  through the value  $-1$  is not accompanied by the total disappearance of the flow. This aspect is illustrated by the sequence of streamlines, isotherms, and concentration lines displayed in Fig. 9.11. The figure shows that when  $N$  is algebraically greater than approximately  $-0.85$ , the natural convection pattern resembles the one that would be expected in a porous layer in which the opposing buoyancy effect is not the dominant driving force. The circulation is reversed at  $N$  values lower than

approximately  $-1.5$ . The flow reversal takes place rather abruptly around  $N = -0.9$ , as is shown in Fig. 9.11b. The core, which exhibited temperature and concentration stratification at  $N$  values sufficiently above and below  $-0.9$ , is now dominated by nearly vertical constant  $T$  and  $C$  lines. This feature is consistent with the tendency of both  $Nu$  and  $Sh$  to approach their pure diffusion limits (e.g., Fig. 9.10).

A compact analytical solution that documents the effect of  $N$  on both  $Nu$  and  $Sh$  was developed in a subsequent paper by Trevisan and Bejan (1986). This solution is valid strictly for  $Le = 1$  and is based on the constant-flux model according to which both sidewalls are covered with uniform distributions of heat flux and mass flux. The overall Nusselt number and Sherwood number expressions for the high Rayleigh number regime (distinct boundary layers) are

$$Nu = Sh = \frac{1}{2} \left( \frac{H}{L} \right)^{1/5} Ra_*^{2/5} (1 + N)^{2/5}, \quad (9.52)$$

where  $Ra_*$  is the heat-flux Rayleigh number defined by  $Ra_* = g\beta KH^2 q''/\nu\alpha_m k_m$ . These theoretical  $Nu$  and  $Sh$  results agree well with numerical simulations of the heat and mass transfer phenomenon.

Another theoretical result has been developed by Trevisan and Bejan (1986) for the large Lewis numbers limit in heat-transfer-driven flows ( $|N| \ll 1$ ). In this limit, the concentration boundary layer can be described by means of a similarity solution, leading to the following expression for the overall Sherwood number:

$$Sh = 0.665 \left( \frac{L}{H} \right)^{1/10} Le^{1/2} Ra_*^{3/10}. \quad (9.53)$$

The mass flux  $j$  used in the  $Sh$  definition,  $Sh = jH/D_m \Delta C$ , is constant, while  $\Delta C$  is the resulting concentration–temperature difference between the two sidewalls. Equation (9.53) is also in good agreement with numerical experiments.

It has been shown that the constant-flux expressions (9.52) and (9.53) can be recast in terms of dimensionless groups ( $Ra, Nu, Sh$ ) that are based on temperature and concentration differences. This was done in order to obtain approximate theoretical results for the configuration of Fig. 9.7, in which the sidewalls have constant temperature and concentrations (Trevisan and Bejan 1986). Similarly, appropriately transformed versions of these expressions can be used to anticipate the  $Nu$  and  $Sh$  values in enclosures with mixed boundary conditions, that is, constant  $T$  and  $j$ , or constant  $q''$  and  $C$  on the same wall. Numerical simulations of the convective heat and mass transfer across enclosures with mixed boundary conditions are reported by Trevisan and Bejan (1986).

An analytical and numerical study of convection in vertical slots due to prescribed heat flux at the vertical boundaries was made by Alavyoon (1993), whose numerical results showed that of any value of  $Le > 1$ , there exists a minimum aspect

ratio  $A$  below which the concentration field in the core region is rather uniform and above which it is linearly stratified in the vertical direction. For  $Le > 1$ , the thermal layers at the top and bottom of the enclosure are thinner than their solutal counterparts. In the boundary layer regime and for sufficiently large  $A$ , the thicknesses of the vertical boundary layers of velocity, concentration, and temperature were found to be equal. The case of opposing fluxes was studied by Alavyoon et al. (1994). They found that at sufficiently large values of  $Ra$ ,  $Le$ , and  $A$ , there is a domain of  $N$  in which one obtains oscillating convection, while outside this domain the solution approaches steady-state convection.

Numerical simulations based on an extension to the Brinkman model for the case of cooperating thermal and solutal buoyancy forces in the domain of positive  $N$  and for  $Le > 1$  were reported by Goyeau et al. (1996a). The Brinkman model was also employed by Mamou et al. (1998a).

The studies reviewed in this subsection are based on the homogeneous and isotropic porous-medium model. The effect of medium heterogeneity on the heat and mass transfer across an enclosure with constant-flux boundary conditions is documented by Mehta and Nandakumar (1987). They show numerically that the  $Nu$  and  $Sh$  values can differ from the values anticipated based on the homogeneous porous-medium model.

For the case  $N = -1$ , a purely diffusive solution exists for suitable geometry and boundary conditions. Charrier-Mojtabi et al. (1997, 1998) have studied this case for a rectangular slot with constant temperature imposed on the sidewalls. The onset of convection, for which  $\gamma = Le \theta$  occurs when  $Ra |Le - 1|$ , exceeds a certain critical value, depending on the aspect ratio  $A$ . The critical value is 184.06 for a square cavity ( $A = 1$ ) and 105.33 for a vertical layer of infinite extent; the corresponding critical wavenumber has the value 2.51. For  $A = 1$ , they also performed numerical simulations, the results of which confirmed the linear instability results. They observed that the bifurcation to convection was of the transcritical type and that the bifurcation diagrams indicated the existence of both symmetrical and asymmetrical subcritical and supercritical solutions.

A numerical study for a square cavity, comparing the Darcy, Forchheimer, and Brinkman models, was made by Karimi-Fard et al. (1997). They found that  $Nu$  and  $Sh$  increase with  $Da$  and decrease with increase of a Forchheimer parameter. The quadratic drag effects are almost negligible, but the boundary effect is important. A further numerical study, for the case of opposing buoyancy effects, was reported by Angirasa and Peterson (1997a). Effects of porosity variation were emphasized in the numerical study by Nithiarasu et al. (1996). Three-dimensional convection in a cubic or rectangular enclosure with opposing horizontal gradients of temperature and concentration was studied numerically by Sezai and Mohamad (1999) and Mohamad and Sezai (2002). A numerical treatment with a random porosity model was reported by Fu and Ke (2000).

The various studies for the case  $N = -1$  have demonstrated that there exists a threshold for the onset of monotonic convection, such that oscillatory convection occurs in a narrow range of values of  $Le$  (close to 1, applicable for many gases) depending on the normalized porosity. For the case of an infinite layer, the wavelength

at the onset of stationary convection is independent of the Lewis number, but this is not so for overstability. When the Lewis number is close to unity, the system remains conditionally stable provided that the normalized porosity is less than unity. For a vertical enclosure with constant heat and solute fluxes, the particular case  $N = -1 + \varepsilon$  case (where  $\varepsilon$  is a very small positive number) was studied by Amahmid et al. (2000). In this situation, multiple unicellular convective flows are predicted.

A non-Newtonian fluid was studied theoretically and numerically by Getachew et al. (1998), Benhadji and Vasseur (2003), and Ben Khelifa et al. 2012). An electrochemical experimental method was demonstrated by Chen et al. (1999a, b). An inverse method, leading to the determination of an unknown solute concentration on one wall given known conditions for temperature and concentration on the remaining faces, was reported by Prud'homme and Jiang (2003). A numerical study of the effect of thermal stratification on convection in a square enclosure was made by Ratish Kumar et al. (2002).

Analytical and numerical studies of convection in a vertical layer were reported by Amahmid et al. (1999b, c, 2000, 2001), Bennacer et al. (2001b), Mamou et al. (1998a) and Mamou (2002a). A vertical layer or slot was also treated by Dash et al. (2010) (second-order fluid), Li et al. (2006b) (transient convection, gas diffusion), Rawat et al. (2009) (transient convection, MHD, micropolar fluid, variable thermal conductivity, heat source), Zhao et al. (2007b) (thermal and solutal source), and Liu et al. (2008b) (concentrated energy and solute sources). The effect of evaporation was added by Asbik et al. (2002) in their numerical treatment. Convection in a square cavity, or a horizontal layer with the Soret effect included, under crossed heat and mass fluxes, was studied analytically and numerically by Bennacer et al. (2001a, 2003b). Entropy production in a square cavity was treated by Mchirgui et al. (2012). Convection in a vertically layered system, with a porous layer between two clear layers, was studied by Mharzi et al. (2000). Anisotropic cavities were studied analytically and numerically by Tobbal and Bennacer (1998), Bera et al. (1998, 2000), Bera and Khalili (2002a), and Muasovi and Shahnazari (2008). Three algebraic analytical solutions were presented by Cai et al. (2003). The effect of a magnetic field was studied by Robillard et al. (2006) and Ahmed and Zueco (2011) (rotation, Hall current). Bahloul et al. (2006) investigated convection in tall vertical annuli. Cheng (2006a) studied a vertical annulus with asymmetric wall temperatures and concentrations. Akbal and Baytas (2008) investigated the effects of nonuniform porosity on convection in a cavity with a partly permeable wall. A cavity with icy water was studied by Kandaswamy et al. (2008a), Sivasankaran et al. (2008), and Eswaramurthi and Kandaswamy (2009). Unusual oscillations in a box with opposing heat and mass fluxes on the vertical walls were investigated numerically by Masuda et al. (2008, 2010). El-Sayed et al. (2011) studied the effect of chemical reaction with a non-Newtonian fluid in a vertical peristaltic tube. Sankar et al. (2012) treated convection from a discrete heat and solute source in a vertical annulus.

### 9.2.3 Transient Effects

Another basic configuration in which the net heat and mass transfer occurs in the horizontal direction is the time-dependent process that evolves from a state in which two (side-by-side) regions of a porous medium have different temperatures and species concentrations. In time, the two regions share a counterflow that brings both regions to a state of thermal and chemical equilibrium. The key question is how parameters such as  $N$ ,  $Le$ , and the height-length ratio of the two-region ensemble affect the time scale of the approach to equilibrium. These effects have been documented both numerically and on the basis of scale analysis by Zhang and Bejan (1987).

As an example of how two dissimilar adjacent regions come to equilibrium by convection, Fig. 9.12 shows the evolution of the flow, temperature, and concentration fields of a relatively high Rayleigh number flow driven by thermal buoyancy effects ( $N = 0$ ). As the time increases, the warm fluid (initially on the left-hand side) migrates into the upper half of the system. The thermal barrier between the two thermal regions is smoothed gradually by thermal diffusion. Figure 9.12c, d show that as the Lewis number decreases, the sharpness of the concentration dividing line disappears, as the phenomenon of mass diffusion becomes more pronounced.

In the case of heat-transfer-driven flows, the timescale associated with the end of convective mass transfer in the horizontal direction is

$$\hat{t} = \frac{\varphi}{\sigma} \left( \frac{L}{H} \right)^2 Ra^{-1} \quad \text{if} \quad Le Ra > \frac{\varphi}{\sigma} \left( \frac{L}{H} \right)^2, \quad (9.54)$$

$$\hat{t} = \frac{\varphi}{\sigma} \left( \frac{L}{H} \right)^2 Le \quad \text{if} \quad Le Ra < \frac{\varphi}{\sigma} \left( \frac{L}{H} \right)^2. \quad (9.55)$$

The dimensionless time  $\hat{t}$  is defined as

$$\hat{t} = \frac{\alpha_m t}{\sigma H^2}. \quad (9.56)$$

Values of  $\hat{t}$  are listed also on the side of each frame of Fig. 9.12. The time criteria (9.54)–(9.56) have been tested numerically along with the corresponding timescales for approach to thermal equilibrium in either heat-transfer-driven or mass-transfer-driven flows.

The transient problem for the case of a vertical plate, with a simultaneous step change in wall temperature and wall concentration, was treated numerically using a Brinkman–Forchheimer model by Jang et al. (1991). They found that the time to reach steady state decreases with increase of  $Da$  or magnitude of the buoyancy ratio  $N$ , increases with increase of the inertia coefficient  $c_F$ , and passes through a

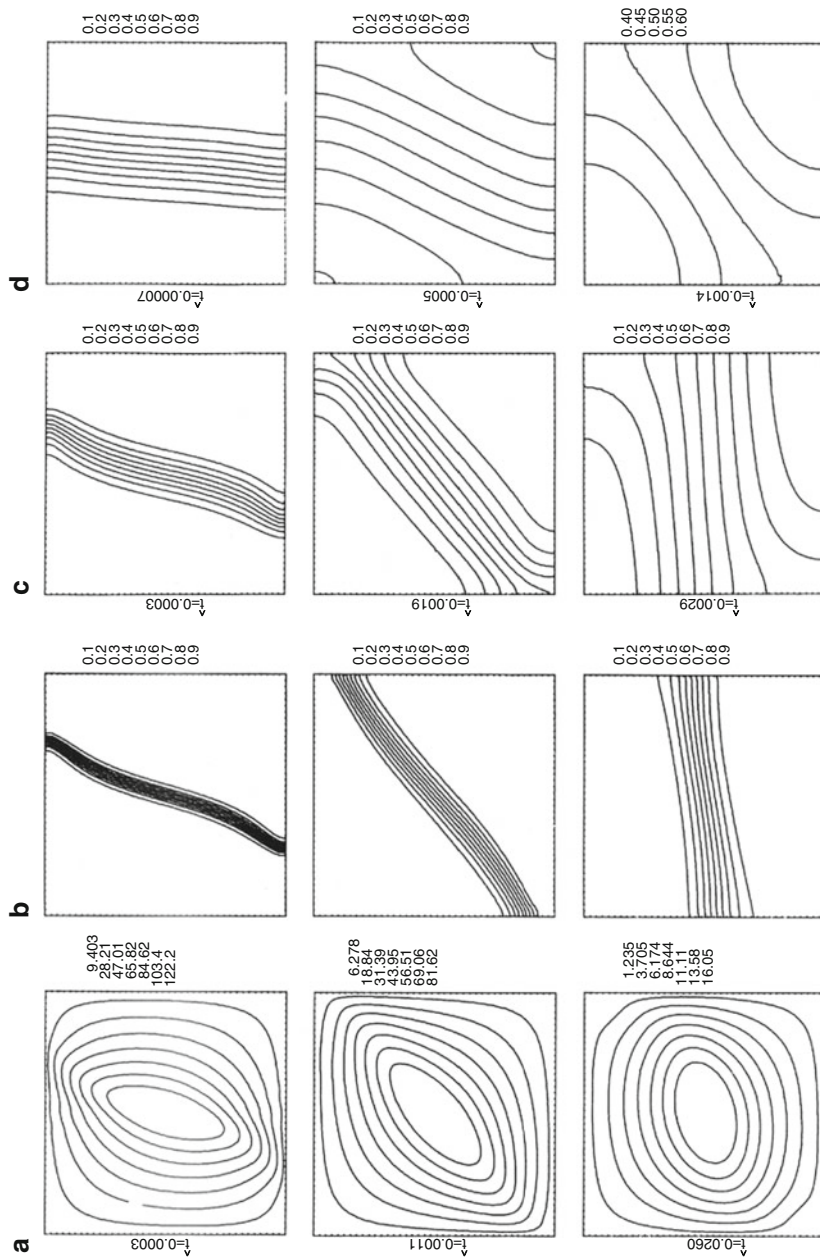


**Fig. 9.12** The horizontal spreading and layering of thermal and chemical deposits in a porous medium ( $N = 0$ ,  $Ra = 1,000$ ,  $H/L = 1$ ,  $\sigma\phi/\sigma = 1$ ). (a) Streamlines; (b) isotherms, or isosolutal lines for  $Le = 1$ ; (c) isosolutal lines for  $Le = 0.1$ ; and (d) isosolutal lines for  $Le = 0.01$  (Zhang and Bejan 1987)

minimum as  $Le$  increases through the value 1. Earlier Pop and Herwig (1990) had shown that when just the concentration was suddenly changed at an isothermal vertical plate, the local Sherwood number decreases with time and approaches its steady-state value. Cheng (2000b) analyzed a problem involving transient heat and mass transport from a vertical plate on which the temperature and concentration are power functions of the streamwise coordinate. The influence of fluctuating thermal and mass diffusion on unsteady MHD buoyancy-driven convection past a vertical plate with variable wall heat and mass fluxes was studied by Pal and Talukdar (2012).

Milne and Butler (2007) carried out a numerical investigation of the effects of compositional and thermal buoyancy on transient plumes in a porous layer.

#### 9.2.4 Stability of Flow

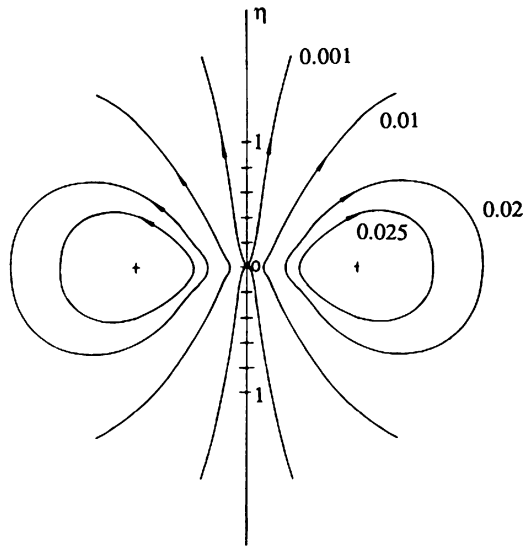
The stability of the steady Darcy flow driven by differential heating of the isothermal walls bounding an infinite vertical slab with a stabilizing uniform vertical salinity gradient was studied independently by Gershuni et al. (1976, 1980) and Khan and Zebib (1981). Their results show disagreement in some respects. We believe that Gershuni et al. are correct. The flow is stable if  $|Ra_D|$  is less than  $Ra_{D1} = 2.486$  and unstable if  $|Ra_D| > Ra_{D1}$ . The critical wavenumber  $\alpha_c$  is zero for  $Ra_{D1} < |Ra_D| < Ra_{D2}$ , where  $Ra_{D2} \approx 52$  for the case  $N = 100$ ,  $\sigma = 1$ , and nonzero for  $|Ra_D| > Ra_{D2}$ . As  $|Ra_D| \rightarrow \infty$ , either monotonic or oscillatory instability can occur depending on the values of  $N$  and  $\sigma$ . If, as in the case of aqueous solutions,  $N$  and  $N/\sigma$  are fairly large and of the same order of magnitude, then monotonic instability occurs, and the critical values are

$$Ra_c = \frac{2\pi^{1/2}}{|N - 1|} |Ra_D|^{3/4}, \quad \alpha_c = \left(\frac{\pi}{2}\right)^{1/2} |Ra_D|^{1/4}. \quad (9.57)$$

Mamou et al. (1995a) have demonstrated numerically the existence of multiple steady states for convection in a rectangular enclosure with vertical walls. Mamou et al. (1995b) studied analytically and numerically convection in an inclined slot. Again multiple solutions were found. Convection in an inclined cavity with a temperature-dependent heat source or sink was studied by Chamkha and Al-Mudhaf (2008).

Two-dimensional convection produced by an endothermic chemical reaction and a constant heat flux was examined by Basu and Islam (1996). They identified various routes to chaos. The onset of convection in a rectangular cavity with balanced heat and mass fluxes applied to the vertical walls was analyzed by Marcoux et al. (1999a). An analytical and numerical study of a similar situation was reported by Mamou et al. (1998d).

**Fig. 9.13** The time-dependent flow field around a suddenly placed point source of heat and mass ( $A = 1$ ) (Poulikakos 1985a, with permission from Pergamon Press)



## 9.3 Concentrated Heat and Mass Sources

### 9.3.1 Point Source

Poulikakos (1985a) considered the transient flow as well as the steady flow near a point source of heat and mass in the limit of small Rayleigh numbers based on the heat source strength  $q[W]$ ,  $\tilde{R}a = g\beta Kq/v\alpha_m k_m$ . The relative importance of thermal and solutal buoyancy effects is described by the “source buoyancy ratio”:

$$N_s = \frac{\beta_C m / D_m}{\beta q / k_m}, \quad (9.58)$$

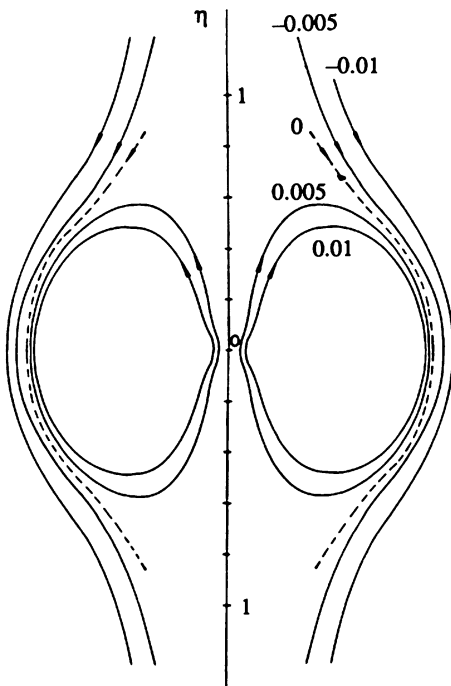
in which  $m[\text{kg}/\text{s}]$  is the strength of the mass source.

Figure 9.13 shows Poulikakos' (1985a) pattern of streamlines for the time-dependent regime. The curves correspond to constant values of the special group  $\Psi^* t^{*-1/2}(1-N_s)$ , in which

$$\Psi^* = \frac{\Psi}{\alpha_m} K^{-1/2}, \quad t^* = \frac{\alpha_m t}{\sigma K}, \quad (9.59)$$

and where  $\Psi[\text{m}^3/\text{s}]$  is the dimensional streamfunction. The radial coordinate  $\eta$  is defined by

**Fig. 9.14** The effect of a small Lewis number (or small  $A$ ) on the transient flow near a point source of heat and mass ( $N = 0.5, A = 0.1$ ) (Poulikakos 1985a, with permission from Pergamon Press)



$$\eta = \frac{r}{2} \left( \frac{\sigma}{\alpha_m t} \right)^{1/2}, \quad (9.60)$$

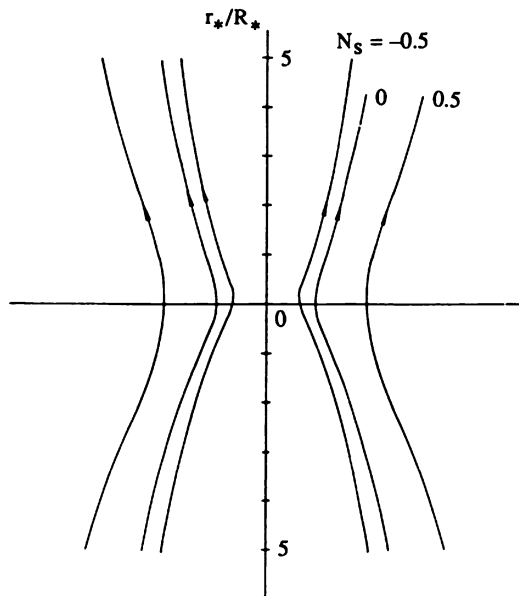
showing that the flow region expands as  $t^{1/2}$ . Figure 9.13 represents the special case  $A = 1$ , where  $A$  is shorthand for

$$A = \left( \frac{\varphi}{\sigma} \text{Le} \right)^{1/2}. \quad (9.61)$$

Poulikakos (1985a) showed that the  $A$  parameter has a striking effect on the flow field in cases where the two buoyancy effects oppose one another ( $N_s > 0$  in his terminology). Figure 9.14 illustrates this effect for the case  $N = 0.5$  and  $A = 0.1$ ; when  $A$  is smaller than 1, the ring flow that surrounds the point source (seen also in Fig. 9.13) is engulfed by a far-field unidirectional flow. The lines drawn on Fig. 9.14 correspond to constant values of the group  $2\pi\Psi^* t^{*-1/2}$ .

In the steady state and in the same small- $\tilde{Ra}$  limit, the flow, temperature, and concentration fields depend only on  $\tilde{Ra}$ ,  $N_s$ , and  $Le$ . Figure 9.15 shows the migration of one streamline as the buoyancy ratio  $N_s$  increases from  $-0.5$  to  $0.5$ , that is, as the buoyancy effects shift from a position of cooperation to one of competition. When the buoyancy effects oppose one another,  $N = 0.5$ , the vertical flow field is wider

**Fig. 9.15** The steady-state flow near a point source of heat and mass ( $\tilde{Ra} = 5$ ,  $Le = 1$ ) and the effect of the source buoyancy ratio (Poulikakos 1985a, with permission from Pergamon Press)



and slower. The curves drawn in Fig. 9.15 correspond to  $\Psi^* = RaR_*/8\pi$ , where  $R_* = R/K^{1/2}$  and  $R$  is a reference radial distance. Asymptotic analytical solutions for the steady-state temperature and concentration fields also are reported by Poulikakos (1985a). Ganapathy (1994a) treated the same problem using the Brinkman model. For the case of large Rayleigh numbers, a boundary layer analysis was carried out by Nakayama and Ashizawa (1996). They showed that for large  $Le$ , the solute diffuses some distance from the plume centerline and the mass transfer influences both velocity and temperature profiles over a wide range. For large  $Le$ , the solute diffuses within a narrow region along the centerline. A strongly peaked velocity profile then appears for positive buoyancy ratio  $N$ , while a velocity defect emerges along the centerline for negative  $N$ .

A finite element model for a leaking third species migration from a heat source buried in a porous medium was demonstrated by Nithiarasu (1999). An inverse problem, the determination from temperature measurement of an unknown volumetric heat source that is a function of the solute concentration, was discussed by Prud'homme and Jasmin (2003) and Jasmin and Prud'homme (2005). Hill (2005) has considered the linear and nonlinear stability of a layer in which there is a concentration-dependent internal volumetric heat source.

### 9.3.2 Horizontal Line Source

The corresponding heat and mass transfer processes in the vicinity of a horizontal line source were analyzed by Larson and Poulikakos (1986). The source buoyancy ratio in this case is

$$N_s' = \frac{\beta_C m'/D_m}{\beta q'/k_m}, \quad (9.62)$$

where  $q'$  [ $\text{W/m}$ ] and  $m'$  [ $\text{kg/m/s}$ ] are the heat and mass source strengths. All the features described in the preceding sections also are present in the low Rayleigh number regime of the line source configuration. The Rayleigh number for the line source is based on the heat source strength  $q'$ :

$$\hat{Ra} = \frac{g\beta K^{3/2} q'}{\nu \alpha_m k_m}. \quad (9.63)$$

In addition to developing asymptotic solutions for the transient and steady states, Larson and Poulikakos (1986) illustrated the effect of a vertical insulated wall situated in the vicinity of the horizontal line source. An analysis using the Brinkman model was reported by Ganapathy (1994b).

The high Rayleigh number regime was studied by Lai (1990a). He obtained a similarity solution and made calculations for a range of  $Le$  and  $N$  values. For the special case  $Le = 1$ , he obtained a closed form solution analogous to that given by Eqs. (5.192)–(5.196). The study of Nakayama and Ashizawa (1996) mentioned in the previous section covered the case of a line source also.

## 9.4 Other Configurations

The double-diffusive case of natural convection over a sphere was analyzed by Lai and Kulacki (1990a), while Yücel (1990) has similarly treated the flow over a vertical cylinder and Lai et al. (1990b) the case of a slender body of revolution. Non-Darcy effects on flow over a two-dimensional or axisymmetric body were treated by Kumari et al. (1988a, b), and Kumari and Nath (1989c, d) have dealt with the case where the wall temperature and concentration vary with time. A numerical study of convection in an axisymmetric body was reported by Nithiarasu et al. (1997b). Flow over a horizontal cylinder, with the concentration gradient being produced by transpiration, was studied by Hassan and Mujumdar (1985). Natural convection in a horizontal shallow layer induced by a finite source of chemical constituent was given a numerical treatment by Trevisan and Bejan (1989).

Convection in a vertical annulus was studied analytically and numerically by Marcoux et al. (1999b); numerically by Beji et al. (1999), who analyzed the effect of curvature on the value of  $N$  necessary to pass from clockwise to anticlockwise rolls; and analytically and numerically by Bennacer (2000). The effect of thermal diffusion for this case was studied numerically and analytically by Bennacer and Lakhal (2005). An analytical and numerical study of the separation of the components in a binary mixture in a vertical annulus with uniform heat fluxes at the walls was conducted by Bahloul et al. (2004b). Convection in a partly porous vertical annulus was studied numerically by Benzeghiba et al. (2003). Convection from a discrete heat and solute source in a vertical annulus was treated by Sankar et al. (2012b). A problem involving a vertical enclosure with two isotropic or anisotropic porous layers was studied numerically by Bennacer et al. (2003a), while convection in a partly filled rectangular enclosure was studied numerically by Goyeau and Gobin (1999), Singh et al. (1999), and Younsi et al. (2001). A horizontal annulus was treated by Al-Amiri et al. (2006) (pulsating heating) and Alloui and Vasseur (2011) (centrifugal force field). Flow over a sphere with radiation, MHD, and porosity variation was studied by Prasad et al. (2012).

The onset of convection in an inclined layer has been studied using linear stability analysis numerically by Karimi-Fard et al. (1998, 1999), who obtained parameter ranges for which the first primary bifurcation is a Hopf bifurcation (oscillatory convection). The same problem was studied numerically by Mamou et al. (1998c) and Mamou (2004) using a finite element method and by Chamkha and Al-Naser (2001) using a finite-difference method.

The composite fluid layer over a porous substrate was studied theoretically by Chen (1990), who extended to a range of  $Ra_m$  (the thermal Rayleigh number in the porous medium as defined in Eq. (6.167)), the calculations initiated by Chen and Chen (1988c) for the salt-finger situation. For small  $Ra_m$  ( $= 0.01$ ), there is a jump in  $\alpha_c$  as the depth ratio  $\hat{d} = d_f/d_m$  increases (the jump is fivefold as  $\hat{d}$  increases between 0.2 and 0.3). For large  $Ra_m$  ( $= 1$ ), there is no sudden jump. Convection occurs primarily in the fluid layer if  $\hat{d}$  is sufficiently large. When this is so, multicellular convection occurs for sufficiently large  $Ra_m$ . The cells are superposed, and their number increases with increase of  $Ra_m$ . For  $\hat{d} < 0.1$ , the critical  $Ra_{Dm}$  (the solutal Rayleigh number for the porous-medium layer) and  $\alpha_{cm}$  decrease as  $\hat{d}$  increases, but when multicellular convection occurs, the critical  $Ra_{Dm}$  remains almost constant as  $\hat{d}$  is increased for fixed  $Ra_m$ . Zhao and Chen (2001) returned to the same problem but used a one-equation model rather than a two-equation model. They found that the two models predicted quantitative differences in the critical conditions and flow streamlines at the onset of convection, and they noted that carefully conducted experiments were needed to determine which model gave the more realistic results. A further study of the composite problem was conducted by Gobin and Goyeau (2012), in the context of a general discussion of the validity of one-domain and two-domain approaches.

Goyeau et al. (1996b) studied numerically for  $N > 0$ , the effect of a thin layer of low permeability medium, which suppresses the convective mass transfer. Further numerical studies were reported by Gobin et al. (1998, 2005).

Transient double-diffusive convection in a fluid/porous layer composite was studied by Kazmierczak and Poulikakos (1989, 1991) numerically and then experimentally. The system considered was one containing a linear stabilizing salt distribution initially and suddenly heated uniformly from below at constant flux. In the experiments it was possible to visually observe the flow in the fluid layer but not in the porous layer. In all the experiments  $\hat{d} = 1$ , and most of the convective flow took place in the fluid layer. In general, a series of mixed layers formed in turn, starting with one just above the porous layer as time increased, as one would expect if the porous matrix was absent. A corresponding numerical study, with the system cooled through its top boundary (adjacent to the solid layer), was conducted by Rastogi and Poulikakos (1993). A numerical study involving two layers of contrasting permeabilities was conducted by Saghir and Islam (1999). A transient problem involving double-diffusive convection from a heated cylinder buried in a saturated porous medium was studied numerically by Chaves et al. (2005).

An experimental study with a clear liquid layer below a layer at porous medium was performed by Rastogi and Poulikakos (1997). They took the initial species concentration of the porous layer to be linear and stable and that in the clear fluid uniform and the system initially isothermal and then cooled from above. Al-Farhan and Turan studied a layer bounded by walls of finite thickness. Baytas et al. (2009) treated an enclosure filled by a step type porous layer. Further work on fluid/porous regions was performed by Alloui et al. (2008).

Sandner (1986) performed experiments, using salt water and glass beads in a vertical cylindrical porous bed. In his experiments, the salt concentration was initially uniform. When the system was heated at the bottom, a stabilizing salinity gradient developed, due to the Soret effect. Some related work is discussed in Sect. 10.5.

Natural convection in a trapezoidal enclosure was studied numerically by Nguyen et al. (1997a) (anisotropy) and Younsi (2009) (MHD). A forced convection flow around a porous-medium layer placed downstream on a flat plate was studied numerically and experimentally by Lee and Howell (1991). Convection in a parallelogramic enclosure was studied numerically by Costa (2004). A transient problem, involving a smaller rectangular cavity containing initially cold fresh fluid located in the corner of a larger one containing hot salty fluid, was studied numerically by Saghir (1998). Inclined triangular enclosures were studied by Chamkha et al. (2010d) (fins, heat generation/absorption) and Mansour et al. (2011a) (unsteady convection, heat source/sink, sinusoidal boundary conditions). The effects of MHD, radiation, and variable viscosity on convection from a vertical truncated cone were studied by Mandy et al. (2010). A vertical truncated cone with Soret and Dufour effects was studied by Cheng (2012a).

Melnikov and Shevtsova (2011) studied separation of a binary fluid in a fluid-porous-fluid system. Kalita and Dass (2011) investigated higher-order compact simulation of double-diffusive convection in a vertical annulus. Srinivasacharya and RamReddy (2011a) treated convection of a doubly stratified micropolar fluid on a vertical wall. Salama et al. (2011) studied a vertical wall with thermophoresis, radiation, and heat generation. Convection from a discrete heat and solute source in a vertical porous annulus was studied by Sankar et al. (2012). The case of a 2D rectangular cavity with uniform and constant heat and solute mass fluxes imposed on the horizontal walls and with impermeable and adiabatic vertical walls was studied by Bennisaad and Ouarzaa (2012).

## 9.5 Inclined and Crossed Gradients

The effects of horizontal gradients on thermosolutal stability, for the particular case where the horizontal thermal and solutal gradients compensate each other as far as density is concerned, was studied theoretically by Parvathy and Patil (1989) and Sarkar and Phillips (1992a, b). The more general case for arbitrary inclined thermal and solutal gradients was treated by Nield et al. (1993) and independently but in a less detailed manner by Parthiban and Patil (1994). Even when the gradients are coplanar the situation is complex. The effect of the horizontal gradients may be to either increase or decrease the critical vertical Rayleigh number, and the favored mode may be oscillatory or nonoscillatory and have various inclinations to the plane of the applied gradients according to the signs of the gradients. The horizontal gradients can cause instability even in the absence of any vertical gradients. The noncoplanar case was also treated by Nield et al. (1993). A nonlinear stability analysis was presented by Guo and Kaloni (1995a). Their main theorem was proved for the coplanar case. Kaloni and Qiao (2000) extended this analysis to the case of horizontal mass flow. A linear instability analysis for the extension where there is net horizontal mass flow was reported by Manole et al. (1994).

The case of horizontal temperature and vertical solutal gradients was investigated numerically by Mohamad and Bennacer (2001, 2002) and both analytically and numerically by Kalla et al. (2001b). Bennacer et al. (2004, 2005) analyzed convection in a two-layer medium with the lower one thermally anisotropic and submitted to a uniform horizontal heat flux and a vertical mass flux.

Mansour et al. (2004, 2006) studied numerically the Soret effect on multiple solutions in a square cavity with a vertical temperature gradient and a horizontal concentration gradient. Bourich et al. (2004a) showed that the multiplicity of solutions is eliminated if the buoyancy ratio  $N$  exceeds some critical value that depends on  $Le$  and  $Ra$ . A similar problem with a partly heated lower wall was treated by Bourich et al. (2004b). A vertical slot heated from below and with horizontal concentration gradients was studied analytically and numerically by Bahloul et al. (2004a). Convection in a shallow cavity was treated by Bahloul et al. (2007). Further work with a shallow layer was performed by Mansour et al.

(2007, 2008) and Narayana et al. (2008). A numeral study of an anisotropic porous medium was conducted by Oueslati et al. (2006). Absolute/convective stability for the case of Soret-driven convection with inclined thermal and solute gradients was studied by Brevdo and Cirpa (2012).

## 9.6 Mixed Double-Diffusive Convection

### 9.6.1 *Mixed External Convection*

Similarity solutions also can be obtained for the double-diffusive case of Darcy mixed convection from a vertical plate maintained at constant temperature and concentration (Lai 1991a). The relative importance of buoyancy and forcing effects is critically dependent on the values of  $Le$  and  $N$ . Kumari and Nath (1992) studied convection over a slender vertical cylinder, with the effect of a magnetic field included. Another study of mixed convection was made by Yücel (1993). Darcy–Forchheimer convection over a vertical plate was studied by Jumar et al. (2001), and a similar problem with double dispersion was analyzed by Murthy (2000). For convection about a vertical cylinder, the entire mixed convection regime was covered by Yih (1998g). The effect of transpiration on mixed convection past a vertical permeable plate or vertical cylinder was treated numerically by Yih (1997a, b, 1999h). For thermally assisted flow, suction increases the local surface heat and mass transfer rates. Mixed convection in an inclined layer has been analyzed by Rudraiah et al. (1987). The effect of radiation was considered by Murthy et al. (2005), Salem (2006a) (viscous dissipation), and Pal and Talukdar (2010) (MHD and chemical reaction). The effects of viscous dissipation, quadratic drag, and chemical reaction were considered by Mahdy and Chamkha (2010). Thermal diffusion, MHD, and heat generation were studied by Abdel-Rahman (2008). MHD and cross-diffusion effects were treated by Shateyi et al. (2010). A transient problem with MHD and chemical reaction was studied by Pal and Talukdar (2011). The combination of chemical reaction, polar fluid, and internal heat generation was examined by Patil et al. (2012).

Mixed convection over a vertical plate, a wedge, or a cone with variable wall temperature and concentration was analyzed by Yih (1998c, f, 1999b, c, 2000b). Similar studies for MHD convection and a vertical plate were reported by Chamkha and Khaled (1999, 2000a, b) and Chamkha (2000). The effects of variable viscosity and thermal conductivity on mixed convection over a wedge, for the cases of uniform heat flux and uniform mass flux, were analyzed by Hassanien et al. (2003a). A wedge with the effects of a magnetic field and chemical reaction was studied by Muhammin et al. (2009a, b) (variable viscosity, thermophoresis), Kandaswamy and Muhammin (2010b), and Kandaswamy et al. (2008d), and Kandaswamy et al. 2010b (variable viscosity, thermophoresis). A vertical wedge with Soret and Dufour effects was studied by Cheng (2012b).

The influence of lateral mass flux on mixed convection over inclined surfaces was analyzed by Singh et al. (2002) and Bansod et al. (2005). Mixed convection over a vertical plate with viscosity variation was analyzed by Chamkha and Khanafer (1999). The case of a vertical plate with transverse spatially periodic suction that produces a three-dimensional flow was analyzed by Sharma (2005).

Convection over a vertical stretching surface was studied by Hayat et al. (2010a) (viscoelastic fluid, cross-diffusion), Pal and Chatterjee (2011) (micropolar fluid, cross-diffusion, MHD), Pal and Mondal (2010a, b, 2012a) (chemical reaction, cross-diffusion, MHD, nonuniform source, variable viscosity), Tsai and Huang (2009b) (Hiemenz flow, cross-diffusion), Rashad and El-Khabeir (2010) (unsteady flow), Kandaswamy and Muhammin (2010a) (MHD, variable viscosity, thermophoresis), and Shateyi and Motwa (2011) (MHD, radiation). The effect of cross-diffusion was also treated by Chamkha and Ben-Nakhi (2008) (MHD), Sallam (2010), Mandy (2010) (non-Newtonian fluid), Makinde (2011b) (MHD) and Srinivasacharya and RamReddy (2011b). A non-Newtonian fluid was also examined by Chamkha and Al-Humoud (2007) and Kairi and Murthy (2010) (double dispersion).

### 9.6.2 *Mixed Internal Convection*

A numerical study of mixed convection with opposing flow in a rectangular cavity with horizontal temperature and concentration gradients was reported by Younsi et al. (2002a, b), who noted that for a certain combination of  $Ra$ ,  $Le$ , and  $N$  values, the flow has a multicellular structure. Mixed convection driven by a moving lid of a square enclosure was studied numerically by Khanafer and Vafai (2002) for the case of insulated vertical walls and horizontal at different constant temperature and concentration. Convection in a vertical wavy channel with traveling thermal waves was examined by Muthuraj and Srinivas (2010). A nonuniformly heated vertical channel with heat sources and dissipation was studied numerically by Nath et al. (2010). Couette flow of an MHD viscoelastic fluid was treated by Eldabe and Sallam (2005). Srinivas and Muthuraj (2011) studied the effects of MHD, chemical reaction, peristalsis, and the special variation of porosity for flow in a vertical channel with asymmetric boundary conditions. Convection in a vertical pipe with local thermal non-equilibrium was studied by Bera et al. (2012).

## 9.7 Nanofluids

The reader is referred to Sect. 3.7.

The Horton–Rogers–Lapwood problem was treated by Nield and Kuznetsov (2009d), Kuznetsov and Nield (2010c, d, e) (using first the Darcy model, then the Brinkman model, and then including the effect of local thermal nonequilibrium),

Nield and Kuznetsov (2011d) (vertical throughflow), Sheu (2011) (viscoelasticity), Bhaduria and Agarwal (2011a, b), Agarwal et al. (2011) (rotation and anisotropy), Agarwal and Bhaduria (2011) (rotation and thermal non-equilibrium) and Agarwal et al. (2012) (nonlinear transport). In these chapters, the significant effects were those of Brownian motion and thermophoresis. The effect of rotation was added by Chand and Rana (2012). An alternative model, incorporating the effects of conductivity and viscosity variation and with cross-diffusion also included, was examined by Nield and Kuznetsov (2012a). The effect of rotation was studied by Chand and Rana (2012). Bioconvection with both gyrotactic and oxytactic microorganisms was investigated by Kuznetsov and Bubnovich (2012). Boundary and internal source effects were treated by Yadav et al. (2012).

The Cheng–Minkowycz problem was studied by Nield and Kuznetsov (2009b, 2011a). The case of a heated upward facing horizontal flat plate was considered by Uddin et al. (2012). Mixed convection over the surface of a horizontal cylinder was examined by Nazar et al. (2011). The case of a vertical truncated cone and a non-Newtonian fluid was treated by Cheng (2012d). Mixed convection from a horizontal plate with Forchheimer drag, but considering only the effect of the volume fraction parameter, was investigated by Rosca et al. (2012). Mixed convection over a wedge with radiation effects was studied by Chamkha et al. (2012). A wedge with thermal stratification was studied by Kandaswamy et al. (2012). Double-diffusion effects with prescribed fluxes on a vertical plate were examined by Khan and Aziz (2011). Mixed convection with viscous heating in a vertical channel was studied by Memari et al. (2011). Khanafer and Vafai (2011) discussed the thermophysical characteristics of nanofluids.

Heat transfer augmentation by means of nanofins was investigated by Vadasz (2011a, b).

# Chapter 10

## Convection with Change of Phase

In the examples of forced and natural convection discussed until now, the fluid that flowed through the pores did not experience a change of phase, no matter how intense the heating or cooling effect. In this chapter, we turn our attention to situations in which a change of phase occurs, for example, melting or evaporation upon heating and solidification or condensation upon cooling.

### 10.1 Melting

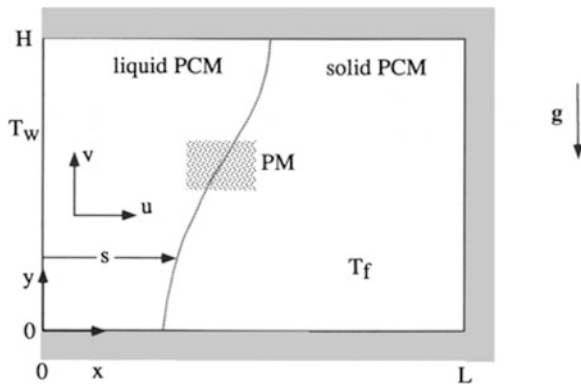
#### 10.1.1 *Enclosure Heated from the Side*

The first analysis of melting dominated by natural convection in a porous matrix saturated with a phase-change material and heated from the side was performed by Kazmierczak et al. (1986). Their study was based on a simple model in which (a) the liquid flow was assumed to be slow enough to conform to the Darcy regime and (b) the melting front that separates the region saturated with solid from the region saturated with liquid was modeled as a surface (i.e., as a region of zero thickness and at the melting point).

These modeling assumptions also have been made in the simplest studies of the geometry illustrated in Fig. 10.1 (Jany and Bejan 1988a), in which the porous medium is confined by an impermeable boundary and is heated through one of its sidewalls. On the problem considered by Kazmierczak et al. (1986), we will focus in Sect. 10.1.5 because that problem is in one way more general than the configuration addressed in this section.

Consider the two-dimensional system illustrated schematically in Fig. 10.1. Initially, the walls are all insulated, and the cavity is filled with porous medium (*PM*) and phase-change material (*PCM*) in the solid state, both at the fusion temperature  $T_f$ .

**Fig. 10.1** Melting in a two-dimensional porous medium heated from the side (after Jany and Bejan 1988a)



For times  $t = 0$ , the left vertical wall is heated and maintained at constant temperature,  $T_w$ , so that  $T_w > T_f$ . In the domain occupied by liquid PCM, the conservation of mass, momentum, and energy is governed by the equations

$$\frac{\partial u}{\partial x} + \frac{\partial v}{\partial y} = 0, \quad (10.1)$$

$$u = -\frac{K}{\mu} \frac{\partial P}{\partial x}, \quad (10.2)$$

$$v = -\frac{K}{\mu} \left( \frac{\partial P}{\partial y} + \rho g [1 - \beta (T - T_f)] \right), \quad (10.3)$$

$$\sigma \frac{\partial T}{\partial t} + u \frac{\partial T}{\partial x} + v \frac{\partial T}{\partial y} = \alpha_m \left( \frac{\partial^2 T}{\partial x^2} + \frac{\partial^2 T}{\partial y^2} \right). \quad (10.4)$$

Equations (10.1)–(10.4) are based on the following assumptions: (1) two-dimensional flow, (2) Darcy flow model [see also assumption (a) above], (3) local thermodynamic equilibrium between PCM and PM, (4) negligible viscous dissipation, (5) isotropic PM, and (6) constant thermophysical properties, with the exception of the assumed linear relation between density and temperature in the buoyancy term of Eq. (10.3) (the Oberbeck-Boussinesq approximation). The boundary conditions for Eqs. (10.1)–(10.4) are

$$y = 0; \quad y = H : \quad v = 0, \quad \frac{\partial T}{\partial y} = 0, \quad (10.5)$$

$$x = 0 : \quad u = 0, \quad T = T_w, \quad (10.6)$$

$$x = L : \quad u = 0, \quad \frac{\partial T}{\partial x} = 0, \quad (10.7)$$

$$x = s(<L) : u = 0, T = T_f, \quad (10.8)$$

$$\frac{\partial s}{\partial t} = -\frac{\alpha_m c_P}{h_{sf}} \left( \frac{\partial T}{\partial x} - \frac{\partial s}{\partial y} \frac{\partial T}{\partial y} \right), \quad (10.9)$$

where  $h_{sf}$  is the latent heat of melting of the phase-change material. Equation (10.9) represents the energy balance at the interface between the liquid and solid saturated regions while neglecting the difference between the densities of liquid and solid at the melting point.

The melting process was simulated numerically by Jany and Bejan (1988a), based on the streamfunction formulation  $u = \partial \Psi / \partial y$ ,  $v = -\partial \Psi / \partial x$  and in terms of the following dimensionless variables:

$$\Theta = \frac{T - T_f}{T_w - T_f}, \quad X = \frac{x}{H}, \quad Y = \frac{y}{H}, \quad (10.10)$$

$$S = \frac{s}{H}, \quad U = u \frac{H}{\alpha_m}, \quad V = v \frac{H}{\alpha_m}, \quad (10.11)$$

$$\Psi = \frac{\Psi}{\alpha_m}, \quad \text{Fo} = \frac{\alpha_m t}{H^2}. \quad (10.12)$$

The transformed, dimensionless equations involve the Fourier number  $\text{Fo}$ , the aspect ratio  $L/H$ , and the Rayleigh and Stefan numbers defined below:

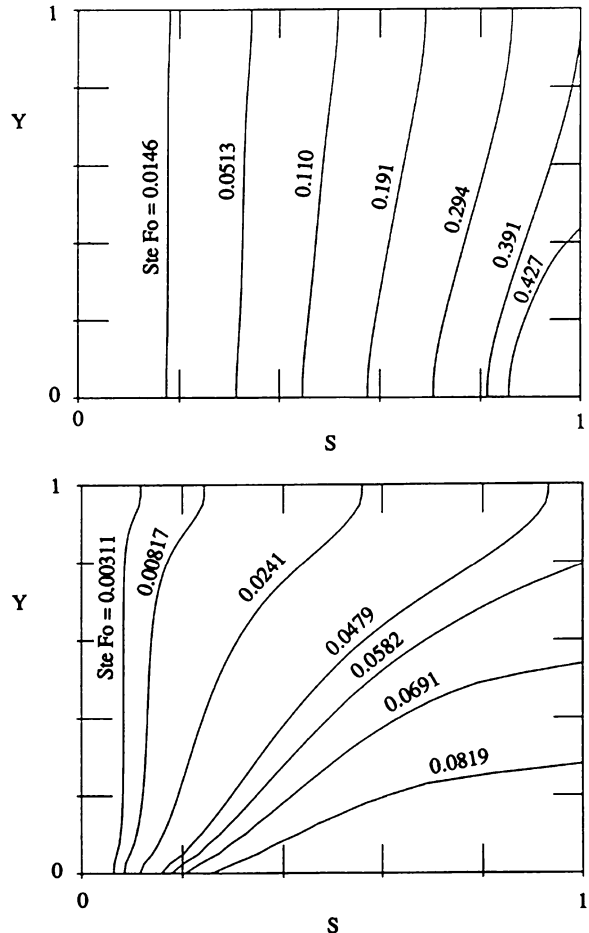
$$\text{Ra} = \frac{g \beta K H (T_w - T_f)}{\nu \alpha_m}, \quad \text{Ste} = \frac{c_P (T_w - T_f)}{h_{sf}}. \quad (10.13)$$

They assumed that in the case of small Stefan numbers, the interface moves relatively slowly, so that  $\partial S / \partial \text{Fo} \ll U, V$ . Therefore, it was reasonable to assume that the liquid flow is not disturbed by the interface motion. Said another way, the interface motion results from a fully developed state of natural convection in the liquid. This “quasistationary front” approximation implies a fixed melting domain [ $S = S(Y)$ ] during each time interval, hence a stepwise motion of the interface. Details of the finite-difference numerical procedure are presented in Jany and Bejan (1988a,b).

Figure 10.2 shows the evolution of the melting front in a square cavity. Because of the quasistationary front assumption, the Stefan and Fourier numbers appear always as a product,  $\text{Ste} \text{Fo}$ . The two-graph sequence of Fig. 10.2 illustrates the strong influence of natural convection on the melting velocity and on the melting front shape. The deviation from the pure heat conduction (vertical interfaces) increases with the dimensionless time ( $\text{Ste} \text{Fo}$ ) and with the Rayleigh number.

The transition from a heat transfer regime dominated by conduction to one dominated by convection is illustrated in Fig. 10.3. Isotherms are plotted for a square domain for each of the Rayleigh numbers, 12.5 and 800. The existence of distinct

**Fig. 10.2** The evolution of the melting front ( $L/H = 1$ ). Top:  $\text{Ra} = 12.5$ ; bottom:  $\text{Ra} = 800$  (Jany and Bejan 1988a)



boundary layers is evident in Fig. 10.3 (right), while the nearly equidistant isotherms of Fig. 10.3 (left) suggest a heat transfer mechanism dominated by conduction.

For the same values of Rayleigh number, Fig. 10.4 shows the transition of the flow field from the conduction-dominated regime to the boundary layer (convection) regime. The flow pattern is qualitatively similar to what is found in cavities without porous matrices. However, the velocity and flow rate scales depend greatly on the properties of the fluid-saturated porous medium. These scales are addressed in the next subsection.

An important quantitative measure of the intensity of the flow and heat transfer process is the overall Nusselt number, which is defined as

$$Nu = \frac{q'}{k_m (T_w - T_f)} = - \int_0^1 \left( \frac{\partial \Theta}{\partial X} \right)_{x=0} dY. \quad (10.14)$$

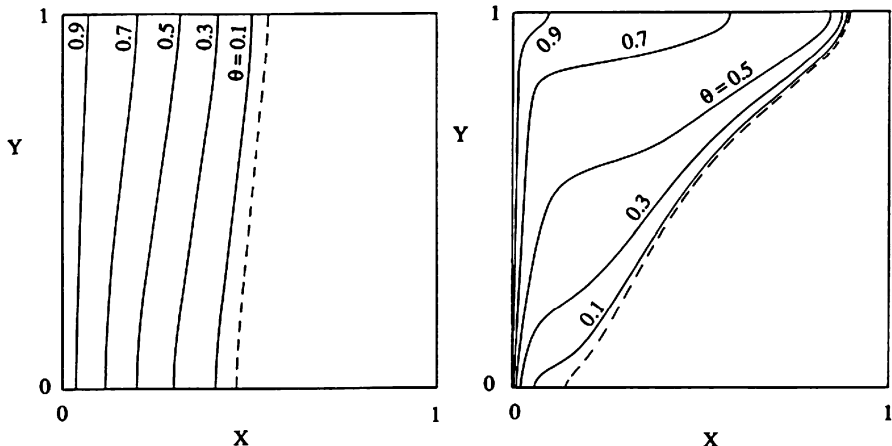


**Fig. 10.3** Patterns of isotherms in the melting process of Fig. 10.1 ( $L/H = 1$ ). *Left:*  $Ra = 12.5$ ,  $Ste\;Fo = 0.125$ ; *right:*  $Ra = 800$ ,  $Ste\;Fo = 0.0452$  (Jany and Bejan 1988a)

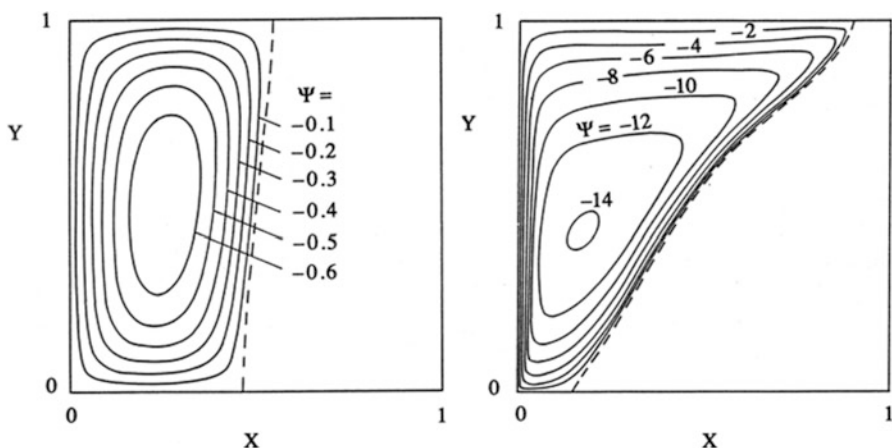


**Fig. 10.4** Patterns of streamlines in the melting process of Fig. 10.1 ( $L/H = 1$ ). *Left:*  $Ra = 12.5$ ,  $Ste\;Fo = 0.125$ ; *right:*  $Ra = 800$ ,  $Ste\;Fo = 0.0452$  (Jany and Bejan 1988a)

The numerator in this definition,  $q'$ , is the heat transfer rate per unit length measured in the direction perpendicular to the  $(x,y)$  plane. The results of this calculation are shown in Fig. 10.5 as Nu versus the time number  $Ste\;Fo$  for different Rayleigh numbers and  $L/H = 1$ . The “knee” point marked on each curve represents the first arrival of the liquid–solid interface at the right vertical wall. This figure shows that the Nusselt number departs significantly from the pure-conduction solution ( $Ra = 0$ ) as the Rayleigh number increases above approximately 50. At  $Ra$  values of order 200 and higher, the  $Nu(Ste\;Fo)$  curve has a minimum at “short times,” that is, before the melting front reaches the right wall.

**Fig. 10.5** The Nusselt number as a function of time and Rayleigh number ( $L/H = 1$ ) (Jany and Bejan 1988a)

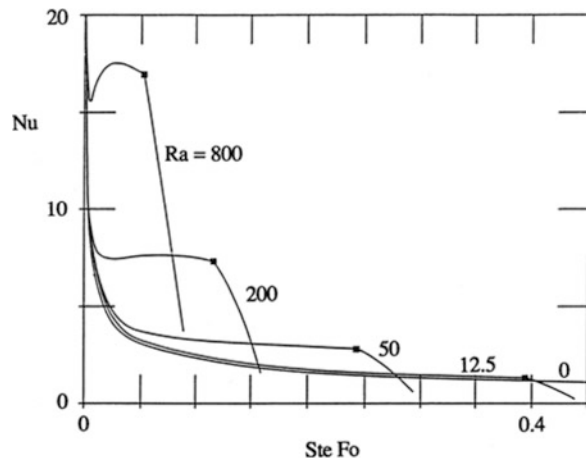
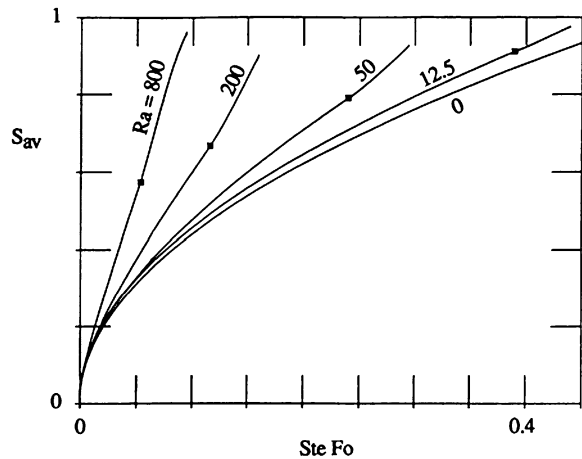


**Fig. 10.6** The average melting front location as a function of time and Rayleigh number ( $L/H = 1$ ) (Jany and Bejan 1988a)



Another overall measure of the evolution of the melting process is the melt fraction or the mean horizontal dimensionless position of the melting front:

$$S_{av} = \int_0^1 S dY. \quad (10.15)$$

This quantity is also a measure of the total energy storage and is related to  $Nu$  by

$$\frac{dS_{av}}{d(Ste Fo)} = Nu. \quad (10.16)$$

Numerical  $S_{av}$  results are presented in Fig. 10.6 for a square cavity at five different Ra values. The melting process is accelerated as Ra increases. On the other hand, the  $S_{av}(Ste Fo)$  curves collapse onto a single curve as  $Ste Fo$  approaches zero.

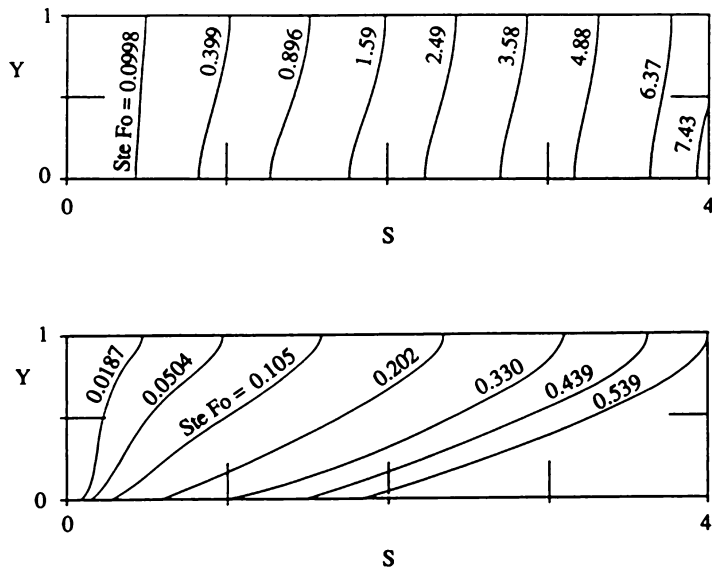


**Fig. 10.7** The evolution of the melting front in a shallow rectangular porous medium ( $L/H = 4$ ). *Top:*  $\text{Ra} = 12.5$ ; *bottom:*  $\text{Ra} = 800$  (Jany and Bejan 1988a)

Similar results are revealed by calculations involving rectangular cavities. Figure 10.7 shows the evolution of the melting front in a shallow space ( $L/H = 4$ ) for the Ra values 12.5 and 800. For example, it is evident that the Ra = 12.5 solution represents a case dominated by conduction. Also worth noting is the severe tilting of the liquid–solid interface during the convection-dominated case Ra = 800.

### 10.1.2 Scale Analysis

The numerical results have features that are similar to those encountered in the classical problem of melting in a cavity without a porous matrix (Jany and Bejan 1988b). In the present problem, it is convenient to identify first the four regimes I–IV whose main characteristics are sketched in Fig. 10.8. The “conduction” region (I) is ruled by pure thermal diffusion and covered by the classical Neumann solution

$$\Theta(\text{Fo}) = 1 - \frac{\text{erf}(X/2 \text{Fo}^{1/2})}{\text{erf}(C)}, \quad S(\text{Fo}) = 2C \text{Fo}^{1/2}, \quad (10.17)$$

where  $C$  is the root of the equation

$$\frac{C \text{erf}(C)}{\exp(-C^2)} = \frac{\text{Ste}}{\pi^{1/2}}. \quad (10.18)$$

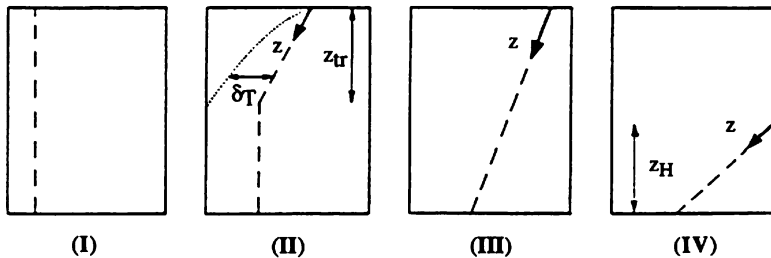


**Fig. 10.8** The four regimes for the scale analysis of melting in a porous medium heated from the side (Jany and Bejan 1988a)

The “transition” regime (II) is where the flow carves its own convection-dominated zone in the upper part of the liquid region, while the lower part remains ruled by conduction. The “convection” regime (III) begins when the convection-dominated zone of the preceding regime fills the entire height  $H$ . Finally, the arrival of the liquid–solid interface at the right vertical wall marks the beginning of the “variable-height” regime (IV).

The scales of regimes I and II become apparent if we focus on the transition regime II, where  $z_{tr}$  is the height of the convection-dominated upper zone. The boundary layer thickness scale in this upper zone is (e.g., Bejan 1984, p. 392)

$$\delta_T \sim z_{tr} Ra_{z_{tr}}^{-1/2} \sim z_{tr} \left( Ra \frac{z_{tr}}{H} \right)^{-1/2}. \quad (10.19)$$

where  $Ra_{z_{tr}} = g\beta K z_{tr} (T_w - T_f)/\nu\alpha_m$ . The convection-dominated zone is such that at its lower extremity,  $\delta_T$  is of the same order as the width of the conduction-dominated zone of height  $(H - z_{tr})$ , in other words,

$$z_{tr} \left( Ra \frac{z_{tr}}{H} \right)^{-1/2} \sim H (\text{Ste Fo})^{1/2}, \quad (10.20)$$

which means that  $z_{tr} \sim H \text{ Ra Ste Fo}$ .

The scale of the overall Nusselt number is obtained by adding the conduction heat transfer integrated over the height  $(H - z_{tr})$  to the convection heat transfer integrated over the upper portion of height  $z_{tr}$ . The result is

$$\text{Nu} \sim (H - z_{tr}) s^{-1} + \int_0^{z_{tr}} \delta_T^{-1} dz \sim (\text{Ste Fo})^{-1/2} + \text{Ra} (\text{Ste Fo})^{1/2} \quad (10.21)$$

or in terms of the average melting front location [Eqs. (10.15) and (10.16)],

$$S_{av} \sim (\text{Ste Fo})^{1/2} + \text{Ra} (\text{Ste Fo})^{3/2}. \quad (10.22)$$

The transition regime II expires when  $z_{tr}$  becomes of order  $H$ , that is, at a time of order  $\text{Ste Fo} \sim Ra^{-1}$ .

The most striking feature of this set of scaling results is the  $Nu$  minimum revealed by Eq. (10.21). Setting  $\partial Nu / \partial (\text{Ste Fo}) = 0$ , we find that the minimum occurs at a time of order:

$$(\text{Ste Fo})_{\min} \sim Ra^{-1}, \quad (10.23)$$

and that the minimum Nusselt number scale is

$$Nu_{\min} \sim Ra^{1/2}. \quad (10.24)$$

The  $Nu_{\min}$  scale is supported very well by the heat transfer data of Fig. 10.5, in which the actual values obey the relationship  $Nu_{\min} \cong 0.54 Ra^{1/2}$  in the  $Ra$  range 200–1200 (Jany and Bejan 1988a).

In the convection regime III, the heat transfer and the melting front progress are controlled by the two thermal resistances of thickness  $\delta_T$ :

$$Nu \sim \int_0^H \delta_T^{-1} dz \sim Ra^{1/2}, \quad (10.25)$$

$$S_{av} \sim Ra^{1/2} \text{Ste Fo}. \quad (10.26)$$

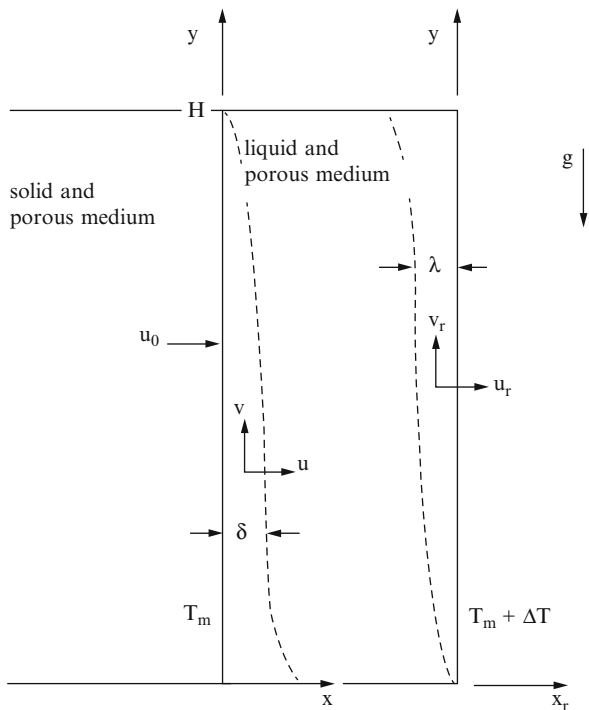
The convection regime begins at a time of order  $\text{Ste Fo} \sim Ra^{-1}$  and expires when the melting front reaches the right wall (at the “knee” points in Figs. 10.5 and 10.6). In the entire  $Ra$  domain 12.4–800, the  $Nu/Ra^{1/2}$  ratio during the convection regime is roughly equal to 0.5. It is interesting that the value of  $Nu/Ra^{1/2}$  is extremely close to what we expect in the convection regime in a rectangular porous medium, namely, 0.577 (Weber 1975b).

The scales of melting and natural convection during the variable-height regime IV are discussed in Jany and Bejan (1988a).

### 10.1.3 Effect of Liquid Superheating

In this section, we review a theoretical solution to the problem of melting in the presence of natural convection in a porous medium saturated with a phase-change material (Bejan 1989). The porous medium is held in a rectangular enclosure, which is being heated from the side (Fig. 10.9 or Fig. 10.1). The porous medium is initially saturated with solid phase-change material; its initial temperature is uniform and equal to the melting point of the phase-change material. The heating from the side consists of suddenly raising the sidewall temperature and maintaining it at a constant level above the melting point.

**Fig. 10.9** The boundary layer regime in the melt region of a porous medium heated from the right (Bejan 1989)



We begin with the analysis of the convection-dominated regime. The main features of the temperature distribution in the liquid space are the two distinct boundary layers that line the heated wall and the solid–liquid interface. The core region of the liquid space is thermally stratified: its temperature is represented by the unknown function  $T_c(y)$ . The horizontal boundary layers that line the top and bottom walls and the details of the flow in the four corners are being neglected.

The analysis consists of first obtaining temperature and flow field solutions for the two vertical boundary layer regions and then meshing these solutions with a third (unique) solution for the core region. The key results of the analytical solution are

$$\tilde{\delta} = A (1 - \tau) (1 + \tau^2 Ste)^{-1/2}, \quad (10.27)$$

$$\tilde{\lambda} = A \tau (1 + \tau^2 Ste)^{-1/2}, \quad (10.28)$$

$$\tilde{y} = \frac{A^2}{4 Ste} \left[ \frac{\tau (1 + \tau Ste)}{1 + \tau^2 Ste} - \frac{\tan^{-1} (\tau Ste^{1/2})}{Ste^{1/2}} \right], \quad (10.29)$$

where  $A$  depends only on the Stefan number

$$A = 2 \text{Ste}^{1/2} \left[ 1 - \frac{\tan^{-1}(\text{Ste}^{1/2})}{\text{Ste}^{1/2}} \right]^{-1/2}. \quad (10.30)$$

The dimensionless variables  $\tilde{\delta}$ ,  $\tilde{\lambda}$ , and  $\tau$  represent the thickness of the cold boundary layer, the thickness of the warm boundary layer, and the temperature in the core region (cf. Fig. 10.9):

$$(\tilde{\delta}, \tilde{\lambda}) = \frac{(\delta, \lambda)}{H} Ra^{1/2}, \quad (10.31)$$

$$\tau = \frac{T_c - T_m}{\Delta T}, \quad \tilde{y} = \frac{y}{H}. \quad (10.32)$$

The left-hand side of Fig. 10.10 shows the solution obtained for the cold boundary layer thickness. The function  $\tilde{\delta}(\tilde{y})$  increases monotonically in the flow direction (downward); its bottom value  $\tilde{\delta}(0)$  is finite. The cold boundary layer thickness increases substantially as the Stefan number increases.

Figure 10.11 illustrates the manner in which the core temperature distribution responds to changes in the Stefan number. The core temperature distribution is symmetric about the midheight level only when  $\text{Ste} = 0$ . The core temperature decreases at all levels as  $\text{Ste}$  increases above zero. Said another way, the average core temperature in the melting and natural convection problem (finite  $\text{Ste}$ ) is always lower than the average core temperature in the pure natural convection problem ( $\text{Ste} = 0$ ).

The thickness of the warm boundary layer has been plotted on the right-hand side of Fig. 10.10. We learn in this way that the warm boundary layer becomes thinner as the Stefan number increases. The  $\text{Ste}$  effect on the warm layer, however, is less pronounced than on the boundary layer that descends along the solid–liquid interface.

The useful feature of this analytical solution is the ability to predict the rate at which the melting and natural convection process draws heat from the right wall of the system. This heat transfer rate through the right-hand side of Fig. 10.9 is

$$q_r' = k_m \int_0^H \left( \frac{\partial T}{\partial x} \right)_{x_r=0} dy \quad (10.33)$$

or, as an overall Nusselt number,

$$Nu_r = \frac{q_r'}{k_m \Delta T} = Ra^{1/2} F_r(\text{Ste}), \quad (10.34)$$

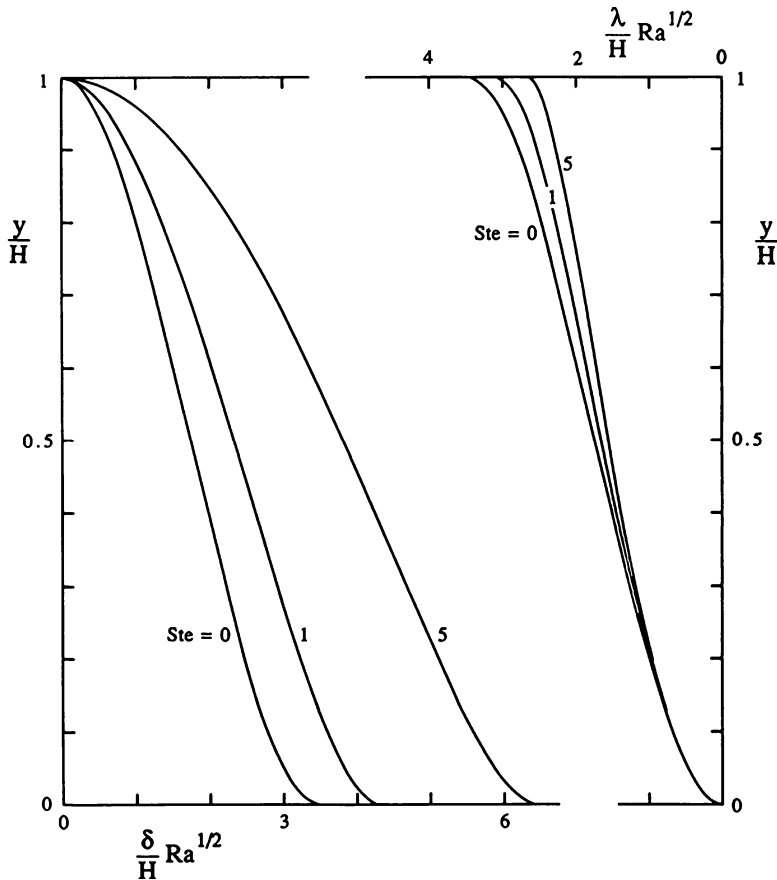


**Fig. 10.10** The thicknesses of the cold (left) boundary layer and the warm (right) boundary layer (Bejan 1989)

with

$$F_r = \int_0^1 \frac{1 - \tau}{\tilde{\lambda}} d\tilde{y} = \frac{Ste^{3/4}}{[Ste^{1/2} - \tan^{-1}(Ste^{1/2})]^{1/2}} \times \left\{ \frac{(Ste - 1)(Ste + 1)^{1/2} - 2Ste}{Ste(Ste + 1)} + Ste^{-3/2} \ln [Ste^{1/2} + (Ste + 1)^{1/2}] \right\}. \quad (10.35)$$

The approximate proportionality  $Nu_r \sim \text{Ra}^{1/2}$  that is revealed by Eq. (10.34) is expected from the scale analysis shown in the preceding section. The new aspect unveiled by the present solution is the effect of the Stefan number. Representative  $F_r$  values constitute the top curve in Fig. 10.12. These values show that the heat transfer rate in the quasi-steady regime increases gradually as the Stefan number increases.

**Fig. 10.11** The core temperature distribution in the boundary layer regime (Bejan 1989)

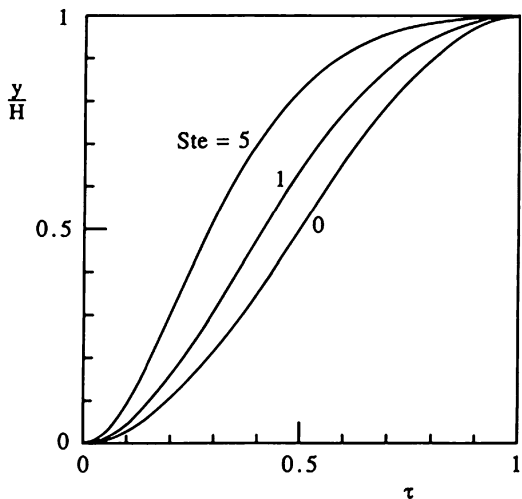
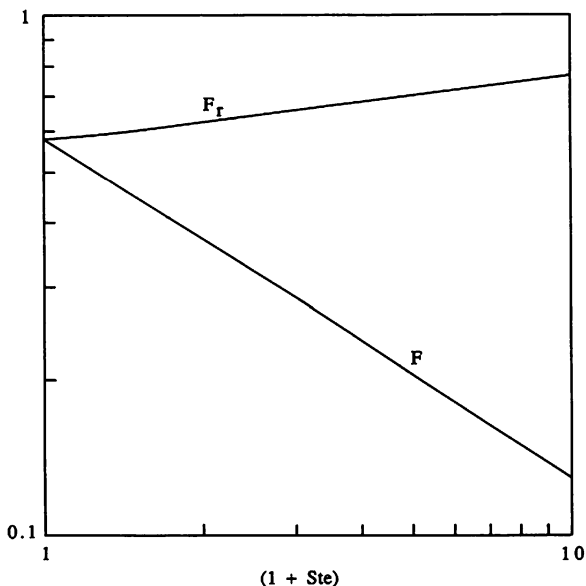


**Fig. 10.12** The effect of liquid superheating on melting in the convection-dominated regime (Bejan 1989)



One quantity of interest on the cold side of the liquid-saturated region is the overall heat transfer rate into the solid–liquid interface

$$q' = k_m \int_0^H \left( \frac{\partial T}{\partial x} \right)_{x=0} dy \quad (10.36)$$

or the left-hand side Nusselt number

$$Nu = \frac{q'}{k_m \Delta T} = Ra^{1/2} F(Ste), \quad (10.37)$$

with

$$F = \int_0^1 \frac{\tau}{\delta} d\tilde{y} = \frac{Ste^{-3/4}}{[Ste^{1/2} - \tan^{-1}(Ste^{1/2})]^{1/2}} \times \left\{ \ln \left[ Ste^{1/2} + (Ste + 1)^{1/2} \right] - \left( \frac{Ste}{Ste + 1} \right)^{1/2} \right\}. \quad (10.38)$$

The behavior of  $F(Ste)$  is illustrated in Fig. 10.12. We see that the left-hand side Nusselt number decreases dramatically as the Stefan number increases.

In summary, the effect of increasing the Stefan number is to accentuate the difference between the heat transfer administered to the right wall ( $Nu_r$ ) and the heat transfer absorbed by the solid–liquid interface ( $Nu$ ). The difference between the two heat transfer rates is steadily being spent on raising the temperature of the newly created liquid up to the average temperature of the liquid-saturated zone.

Another quantity that can be anticipated based on this theory is the average melting rate. Writing  $u_0$  for the local rate at which the solid–liquid interface migrates to the left in Fig. 10.9 and  $\tilde{u}_0$  for the nondimensional counterpart,

$$\tilde{u}_0 = \frac{u_0}{\alpha_m/H} Ra^{-1/2} = Ste \frac{\tau}{\delta} \quad (10.39)$$

leads to

$$\tilde{u}_{0,av} = Ste \int_0^1 \frac{\tau}{\delta} d\tilde{y} = Ste F. \quad (10.40)$$

The function  $\tilde{u}_{0,av}$  depends only on the Stefan number, as is shown by Fig. 10.12.

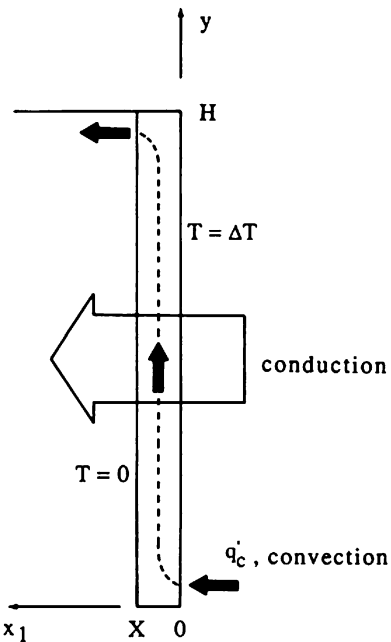
In closing, it is worth commenting on the use of  $(1 + Ste)$  as abscissa in Fig. 10.12. This choice has the effect of making the  $F$  and  $F_r$  curves appear nearly straight in the logarithmic plane, improving in this way the accuracy associated with reading numerical values directly off Fig. 10.12. This observation leads to two very simple formulas:

$$F_r \cong 3^{-1/2} (1 + 1.563 Ste)^{0.107}, \quad (10.41)$$

$$F \cong 3^{-1/2} (1 + 0.822 Ste)^{-0.715}, \quad (10.42)$$

which approach within 0.5 % the values calculated based on Eqs. (10.35) and (10.38).

**Fig. 10.13** Combined conduction and convection during the earliest stages of melting due to heating from the side (Bejan 1989)



In the very beginning of the melting process, the liquid-saturated region is infinitely slender and the heat transfer mechanism is that of pure conduction. With reference to the slender liquid zone sketched in Fig. 10.13, the history of the thickness  $X$  is described by the well-known Neumann solution [Eqs. (10.17) and (10.18)], which can be written here as

$$X = 2\Lambda (\alpha_m f)^{1/2}, \quad \frac{\exp(-\Lambda^2)}{\operatorname{erf}(\Lambda)} = \pi^{1/2} \frac{\Lambda}{Ste}. \quad (10.43)$$

According to the same solution, the excess temperature of the liquid-saturated porous medium depends on  $t$  and  $x_1$  (and not on  $y$ ), where  $x_1$  is chosen such that it increases toward the left in Fig. 10.13 (note that here  $T = 0$  on the melting front),

$$T = \Delta T \left[ 1 - \frac{1}{\operatorname{erf}(\Lambda)} \operatorname{erf} \frac{x_1}{2(\alpha_m t)^{1/2}} \right]. \quad (10.44)$$

The overall heat transfer rate delivered through the heated wall ( $q'_r$ , or  $\text{Nu}_r$ ) is also well known. For example, in the limit  $\text{Ste} = 0$ , the overall Nusselt number decays as

$$\text{Nu}_r = 2^{-1/2} \tau^{-1/2}, \quad \tau = \frac{\alpha_m t}{H^2} \text{Ste}. \quad (10.45)$$

Bejan (1989) showed that it is possible to develop an analytical transition from the short-times Nusselt number (10.45) to the long-times expression of the quasi-steady regime (10.34). In other words, it is possible to develop a heat transfer theory that holds starting with  $\tau = 0$  and covers the entire period during which the heat transfer mechanism is, in order, pure conduction, conduction and convection, and finally convection.

This theoretical development is based on the observation that even in the limit  $\tau \rightarrow 0$  when the liquid region approaches zero thickness, there is liquid motion in the liquid-saturated region. The incipient convective heat transfer contribution is

$$q'_c = \int_0^X \rho c_f v T \, dx = \rho c_f \frac{g \beta K \Delta T}{v} \Delta T X B, \quad (10.46)$$

where the function  $B(Ste)$  is the integral

$$B(Ste) = \int_0^1 \left[ \frac{\int_0^A \operatorname{erf}(m) \, dm}{A \operatorname{erf}(A)} - \frac{\operatorname{erf}(nA)}{\operatorname{erf}(A)} \right] \left[ 1 - \frac{\operatorname{erf}(nA)}{\operatorname{erf}(A)} \right] \, dn. \quad (10.47)$$

This function was evaluated numerically. In the conduction regime, the effect of  $q'_c$  on the overall heat transfer rate is purely additive because the top and bottom ends of the liquid-zone temperature field (the only patches affected by the flow) are negligible in height when compared with the rest of the system (height  $H$ ). Therefore, the instantaneous total heat transfer rate through the right wall is

$$q'_r = k_m H \left( -\frac{\partial T}{\partial x_1} \right)_{x_1=0} + q'_c, \quad (10.48)$$

where the first term on the right-hand side accounts for the dominant conduction contribution. Employing the  $Nu_r$  notation defined in Eq. (10.34), expression (10.48) translates into

$$Nu_r = G_0 \tau^{-1/2} + G_c Ra \tau^{1/2}. \quad (10.49)$$

The functions  $G_0$  and  $G_c$  depend only on the Stefan number

$$G_0 = \frac{Ste^{1/2}}{\pi^{1/2} \operatorname{erf}(A)}, \quad G_c = 2AB Ste^{-1/2}, \quad (10.50)$$

and are presented in Fig. 10.14. The Stefan number has a sizeable effect on both  $G_0$  and  $G_c$ . For fixed values of  $\tau$  and  $Ra$ , the effect of increasing the Stefan number is to diminish the relative importance of the convection contribution to the overall Nusselt number.

In view of the reasoning on which Eq. (10.49) is based, we must keep in mind that this  $Nu_r$  expression cannot be used beyond the moment  $\tau$  when the second (convection) term begins to outweigh the first (conduction) term. This condition,

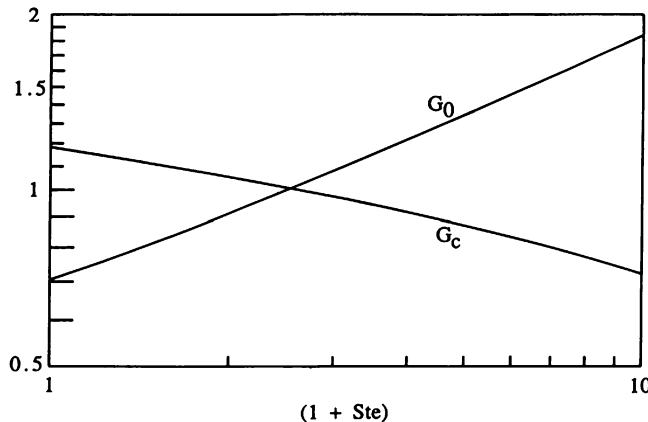


**Fig. 10.14** The effect of liquid superheating on the combined conduction and convection regime (Bejan 1989)

$$G_0 \tau^{-1/2} > G_c Ra \tau^{1/2}, \quad (10.51)$$

yields the following time criterion for the domain of validity of Eq. (10.49):

$$\tau Ra < \frac{G_0}{G_c}. \quad (10.52)$$

The solid lines of Fig. 10.15 show the Nusselt number history predicted by Eq. (10.49) all the way up to the time limit (10.52). That limit, or the point of expiration of each solid curve, is indicated by a circle. Plotted on the ordinate is the group  $Nu, Ra^{-1/2}$ : this group was chosen in order to achieve a Ra correlation of the Nusselt number in the convection limit.

The horizontal dash lines of Fig. 10.15 represent the Nusselt number values that prevail at long times in the boundary layer regime [Eq. (10.34)]. It is remarkable that two different and admittedly approximate theories [Eqs. (10.34) and (10.49)] provide a practically continuous description for the time variation of the overall Nusselt number. Only when  $Ste$  increases above 5 does a mismatch of a few percentage points develop between the  $Nu, Ra^{-1/2}$  values predicted by the two theories at the transition time (10.52).

#### 10.1.4 Horizontal Liquid Layer

In the convection-dominated regime, the melting front acquires a characteristic shape, the dominant feature of which is a horizontal layer of melt that grows along the top boundary of the phase-change system. The slenderness of the horizontal layer increases with the time and Rayleigh number (Figs. 10.2–10.4, 10.7).

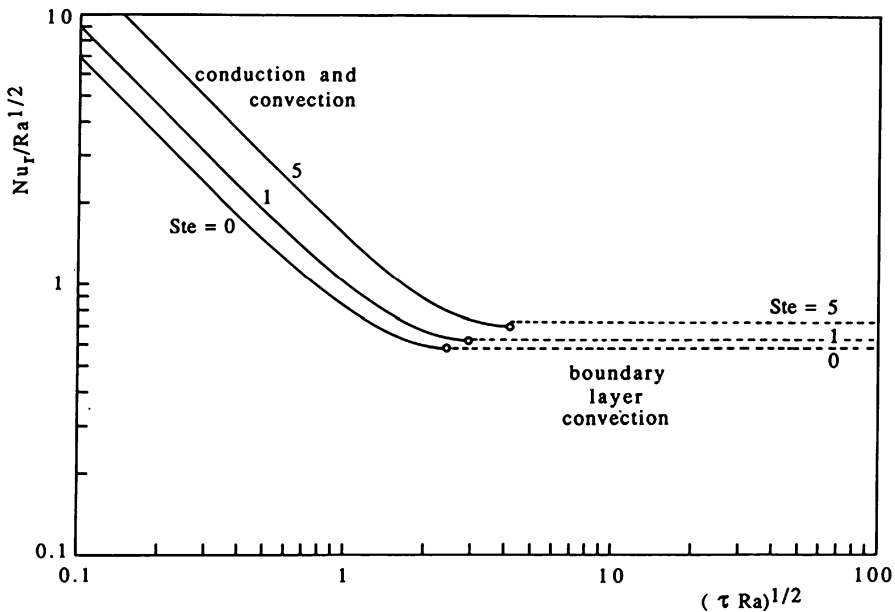


**Fig. 10.15** The evolution of the Nusselt number during the conduction, mixed, and convection regimes (Bejan 1989)

With these images in mind, the liquid-saturated region can be viewed as the union of two simpler regions, an upper zone that is a horizontal intrusion layer and a lower zone that houses a vertical counterflow (as in Fig. 10.9). These two zones are labeled  $A_2$  and  $A_1$  in Fig. 10.16.

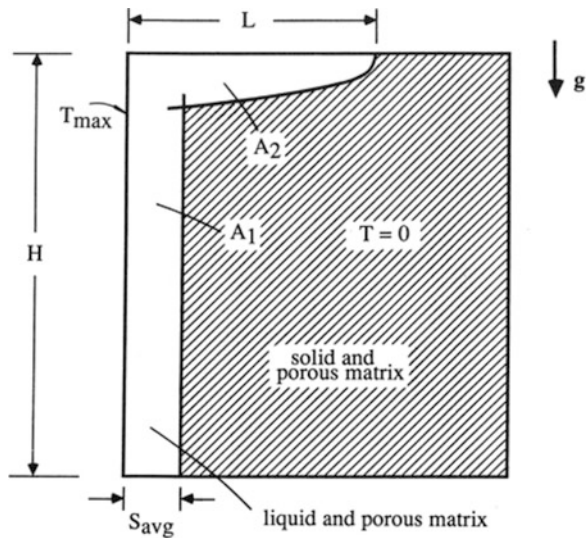
It is possible to describe the shape and propagation of the horizontal intrusion layer by means of a similarity solution of the boundary layer type (Bejan et al. 1990). In addition to the features of the Darcy flow model described in Sect. 10.1.1, this similarity solution was based on the assumption that the depth of the intrusion layer ( $\delta$ ) is considerably smaller than the distance of horizontal penetration of the leading edge ( $L$ ). The melting speed  $U = dL/dt$  was assumed small relative to the horizontal velocity in the liquid-saturated region: this particular assumption holds in the limit  $Ste \ll 1$ . Finally, it was assumed that the melting front shape is preserved in time, that is, in a frame attached to the leading edge of the intrusion.

The main result of the intrusion layer analysis is the theoretical formula

$$\frac{L}{H} = 0.343 Ra^{1/2} (Ste Fo)^{3/4} \quad (10.53)$$

that describes the evolution of the length of horizontal penetration  $L(t)$ . This formula agrees very well with the  $L(t)$  read off numerical plots such as those of Fig. 10.7 (bottom), in the Ra range 200–800.

**Fig. 10.16** Two-zone model ( $A_1 + A_2$ ) for the melt region of a rectangular system heated from the side (Bejan et al. 1990)



Another result of the intrusion layer analysis is that the volume (area  $A_2$  in Fig. 10.16) of the upper region of the liquid-saturated porous medium increases with both Ra and Ste Fo as

$$\frac{A_2}{H^2} = 0.419 Ra^{1/2} (Ste Fo)^{5/4}. \quad (10.54)$$

This estimate can be added to the one for area  $A_1$ , which accounts for the regime of boundary layer convection in the vertical slot (cf. Eq. (10.34) and Fig. 10.12) at Ste = 0:

$$\frac{A_1}{H^2} = 0.577 Ra^{1/2} Ste Fo, \quad (10.55)$$

in order to calculate the total cross-sectional area of the region saturated by liquid:

$$\frac{A_1 + A_2}{H^2} = 0.577 Ra^{1/2} Ste Fo \left[ 1 + 0.725 (Ste Fo)^{1/4} \right]. \quad (10.56)$$

The relative effect of the horizontal intrusion layer on the size of the melt region is described by the group  $(Ste Fo)^{1/4}$ . When the order of magnitude of the group  $(Ste Fo)^{1/4}$  is greater than 1, the size of the melt fraction is ruled by the horizontal intrusion layer. When this group is less than 1 (as in the numerical experiments of Sect. 10.1.1), the melt fraction is dominated by the boundary layer convection that erodes the nearly vertical portion of the two-phase interface (area  $A_1$ ).

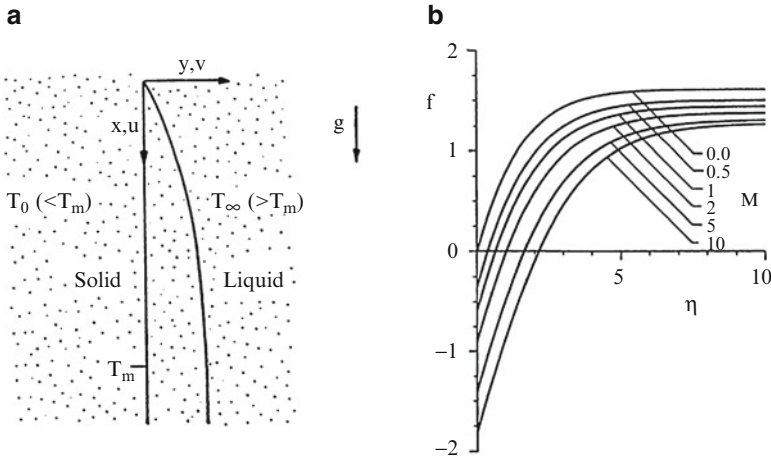


**Fig. 10.17** The dimensionless streamfunction for boundary layer convection on the liquid side of a vertical melting front in a porous medium (Kazmierczak et al. 1986, with permission from Hemisphere Publishing Corporation)

### 10.1.5 Vertical Melting Front in an Infinite Porous Medium

Kazmierczak et al.'s (1986) analysis of melting with natural convection applies to the configuration shown on the left-hand side of Fig. 10.17. The melting front is vertical and at the melting point  $T_m$ . The coordinate system  $x-y$  is attached to the melting front: in it, the porous medium flows to the right, with a melting (or blowing) velocity across the  $x$ -axis. The melting front is modeled as a vertical plane.

The geometry of Fig. 10.17 is more general than in the systems analyzed until now because the temperature of the solid region is below the melting point,  $T_0 < T_m$ . On the right-hand side of the melting front, the liquid is superheated,  $T_\infty > T_m$ . A vertical boundary layer flow on the liquid side smooths the transition from  $T_m$  to  $T_\infty$ . Because of the presence of solid subcooling, the Stefan number  $\text{Ste}$  of Eq. (10.13) is now replaced by the “superheating and subcooling” number

$$M = \frac{c_f (T_\infty - T_m)}{h_{sf} + c_s (T_m - T_0)}, \quad (10.57)$$

where  $c_f$  and  $c_s$  are the specific heats of the liquid and solid.

The flow and temperature field on the liquid side of the melting front was determined in the form of a similarity solution. Figure 10.17 shows the dimensionless streamfunction profile  $f(\eta)$ , which is defined by

$$\Psi = \alpha_m Ra_x^{1/2} f(\eta), \quad \eta = \frac{y}{x} Ra_x^{1/2}, \quad (10.58)$$

and  $\text{Ra}_x = g\beta K(T_\infty - T_m)x/\nu\alpha_m$ . The streamfunction is defined in the usual way, by writing  $u = \partial\Psi/\partial y$  and  $v = -\partial\Psi/\partial x$ . The figure shows that the number  $M$  can have a sizeable impact on the flow. The limit  $M = 0$  corresponds to the case of natural convection near a vertical impermeable plate embedded in a fluid-saturated porous medium (Cheng and Minkowycz 1977), discussed earlier in Chap. 5, Sect. 5.1.

The superheating and subcooling parameter  $M$  also has an effect on the local heat transfer flux through the melting front ( $q''_x$ ) and on the melting rate  $v(x,y) = 0$ . The two are related by

$$\frac{x}{\alpha_m} v(x, 0) = MNu_x, \quad (10.59)$$

where  $Nu_x$  is the local Nusselt number ( $q''_x$ )  $x/k_m(T_\infty - T_m)$ . It was found that the Nusselt number varies in such a way that the ratio  $Nu_x/\text{Ra}_x^{1/2}$  is a function of  $M$  only. Originally that function was calculated numerically and tabulated in Kazmierczak et al. (1986). It was shown more recently (Bejan 1989) that the same numerical results are correlated within 1 % by an expression similar to Eqs. (10.41) and (10.42):

$$\frac{Nu_x}{Ra_x^{1/2}} = 0.444 (1 + 0.776 M)^{-0.735}. \quad (10.60)$$

Combining Eqs. (10.59) and (10.60), we note that the melting velocity  $v(x,0)$  increases with  $M$  and that its rate of increase decreases as  $M$  becomes comparable with 1 or greater.

Kazmierczak et al. (1986) also treated the companion phenomenon of boundary layer natural convection melting near a perfectly horizontal melting front in an infinite porous medium. They demonstrated that the same parameter  $M$  has a significant effect on the local heat flux and melting rate.

### 10.1.6 A More General Model

An alternative to the Darcy flow model (outlined in Sect. 10.1.1 and used in all the studies discussed until now) was developed by Beckermann and Viskanta (1988a). One advantage of this general model is that the resulting governing equations apply throughout the porous medium, that is, in both the liquid-saturated region and the solid region. Because of this feature, the same set of equations can be solved in the entire domain occupied by the porous medium, even in problems with initial solid subcooling (i.e., time-dependent conduction in the solid). Another advantage of this model is that it can account for the inertia and boundary friction effects in the flow of the liquid through the porous matrix.

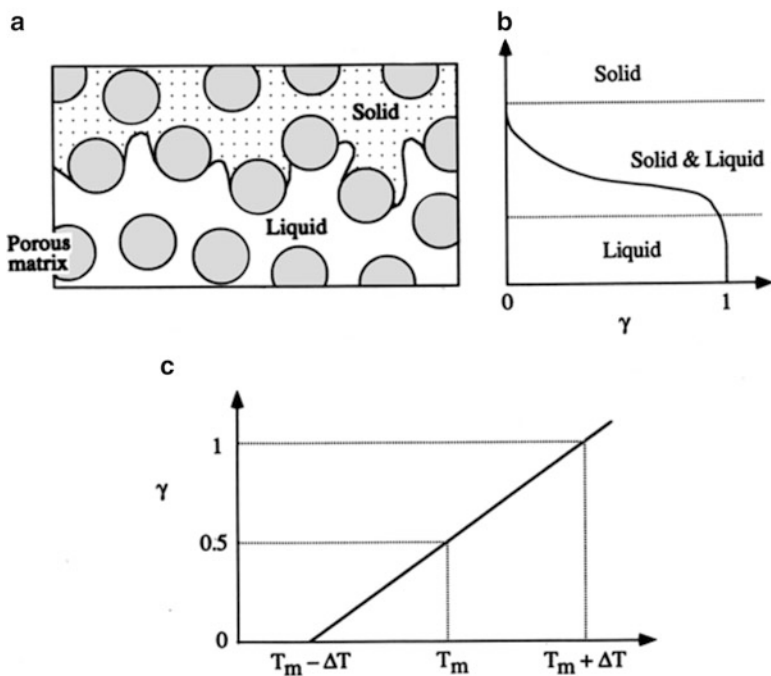


**Fig. 10.18** A more general model for melting in a saturated porous medium: (a) element used for volume averaging; (b) the coexistence of liquid and solid in the pores in the phase-change region; and (c) the assumed variation of the liquid fraction with the local temperature (after Beckermann and Viskanta 1988a)

The model is based on the volume averaging of the microscopic conservation equations. In accordance with Fig. 10.18a, the saturated porous medium is described by three geometric parameters, two of which are independent:

$$\varepsilon = \frac{V_f}{V}, \text{ pore fraction in volume element (previously labeled } \varphi) \quad (10.61)$$

$$\gamma(t) = \frac{V_1(t)}{V_f}, \text{ liquid fraction in pore space} \quad (10.62)$$

$$\delta(t) = \frac{V_1(t)}{V} \varepsilon \gamma, \text{ liquid fraction in volume element.} \quad (10.63)$$

Next, the melting “front” actually can have a finite width even when the phase-change substance has a well-defined melting point  $T_m$  because the phase-change region can be inhabited at the same time by solid and liquid in the pores (Fig. 10.18b). The liquid fraction  $\gamma$  varies from 0 to 1 across this region, while the average temperature of the saturated porous medium in this zone is  $T_m$  (Fig. 10.18c).

In addition to these ideas, Beckermann and Viskanta's (1988a) model is based on the assumptions that the flow and temperature fields are two-dimensional, the properties of the solid matrix and the phase-change material (liquid or solid) are homogeneous and isotropic, local thermal equilibrium prevails, the porous matrix and the solid phase-change material are rigid, the liquid is Boussinesq incompressible and the properties of the liquid and solid phases are constant, the dispersion fluxes due to velocity fluctuations are negligible, and the solid and liquid phases of the phase-change material have nearly the same density  $\rho$ . Under these circumstances, the volume-averaged equations for mass and momentum conservation become

$$\nabla \cdot \mathbf{u} = 0, \quad (10.64)$$

$$\frac{\rho}{\delta} \frac{\partial \mathbf{u}}{\partial t} + \frac{\rho}{\delta^2} (\mathbf{u} \cdot \nabla) \mathbf{u} = -\nabla P + \frac{\mu_l}{\delta} \nabla^2 \mathbf{u} - \left( \frac{\mu_l}{K} + \frac{\rho c_F}{K^{1/2}} |\mathbf{u}| \right) \mathbf{u} - \rho \mathbf{g} \beta (T - T_{ref}), \quad (10.65)$$

where  $\mathbf{u}$  is the Darcian velocity  $\mathbf{u} = \delta \mathbf{u}_l$  and  $\mathbf{u}_l$  is the average liquid velocity through the pore.

The third group on the right-hand side of Eq. (10.65) accounts for the Darcy term and the Forchheimer inertia correction, in which  $c_F \cong 0.55$  (Ward 1964). For a bed of spherical beads of diameter  $d$ , the permeability  $K$  can be calculated with the Kozeny-Carman relation (1.16), in which  $d_p = d$  and  $\varphi = \delta$ . The permeability is therefore equal to  $K(\delta = \varepsilon)$  in the liquid-saturated region,  $K(\delta = 0) = 0$  in the solid region, and takes in-between values in the phase-change region (Fig. 10.18b).

The volume-averaged equation for energy conservation is (Beckermann and Viskanta 1988a)

$$\overline{\rho c} \frac{\partial T}{\partial t} + \rho c_l (\mathbf{u} \cdot \nabla T) = \nabla \cdot (k_{\text{eff}} \nabla T) - \varepsilon \rho \Delta h \frac{\partial \gamma}{\partial t}, \quad (10.66)$$

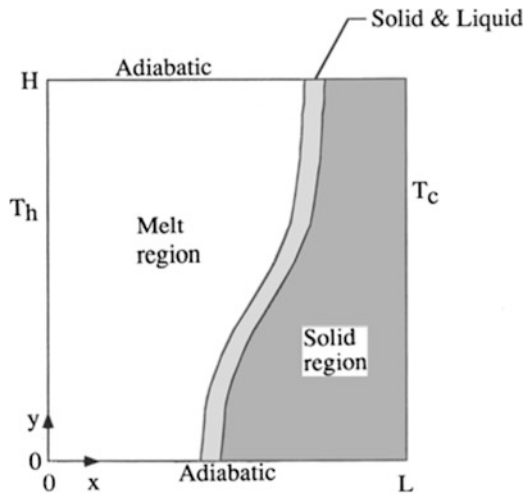
in which  $c_l$  is the liquid specific heat,  $\Delta h$  is the latent heat of melting (labeled  $h_{sf}$  in the preceding sections), and  $\overline{\rho c}$  is the average thermal capacity of the saturated porous medium

$$\overline{\rho c} = \varepsilon \rho [\gamma c_l + (1 - \gamma) c_s] + (1 - \varepsilon) (\rho c)_m. \quad (10.67)$$

The subscript  $( )_m$  refers to properties of the solid matrix. The effective thermal conductivity  $k_{\text{eff}}$  can be estimated using Veinberg's (1967) model:

$$k_{\text{eff}} + \varepsilon k_{\text{eff}}^{1/3} \frac{k_m - k_{ls}}{k_{ls}^{1/3}} - k_m = 0, \quad (10.68)$$

**Fig. 10.19** The finite thickness of the melting front according to the model of Fig. 10.18 (after Beckermann and Viskanta 1988a)



where  $k_{ls}$  is the average conductivity of the phase-change material (liquid and solid phases):

$$k_{ls} = \gamma k_l + (1 - \gamma) k_s. \quad (10.69)$$

The above model was used by Beckermann and Viskanta (1988a) in the process of numerically simulating the evolution of the melting process in the porous-medium geometry shown in Fig. 10.19. The two sidewalls are maintained at different temperatures,  $T_h$  and  $T_c$ . Because of the mixed region recognized in Fig. 10.18b, the melting front is a region of finite thickness in Fig. 10.19. These numerical simulations agreed with a companion set of experimental observations in a system consisting of spherical glass beads ( $d = 6$  mm) and gallium ( $T_m = 29.78^\circ\text{C}$ ). The numerical runs were performed for conditions in which the Rayleigh number  $\text{Ra}$  varied from 9.22 to 11.52. Because of the low  $\text{Ra}$  range, the calculated shape of the melting region was nearly plane and vertical, resembling the melting front shapes exhibited here in Fig. 10.2 (top). In the same numerical runs, the Darcy term dominated the Forchheimer and Brinkman terms on the right-hand side of Eq. (10.65).

### 10.1.7 Further Studies

Kazmierczak et al. (1988) analyzed the melting process in a porous medium in which the frozen phase-change material (PCM) is not the same substance as the warmer liquid that saturates the melt region. They considered a vertical melting front and showed the formation of a liquid counterflow along the melting front. Adjacent to the solid is the liquid formed as the PCM melts: in this first layer, the

liquid rises along the solid–liquid interface. The second layer bridges the gap between the first layer (liquid *PCM*) and the warmer dissimilar liquid that drives the melting process. In this outer boundary layer, the dissimilar liquid flows downward. The corresponding problem in which the heat transfer in the dissimilar fluid is by forced convection was considered by Kazmierczak et al. (1987).

Zhang (1993) performed a numerical study on the Darcy model of an ice–water system in a rectangular cavity heated laterally, using the Landau transformation to immobilize the interface and a finite-difference technique. He reported that local maximum and minimum average Nusselt numbers occur at heating temperatures of 5°C and 8°C, respectively. If the heating temperature is less than 8°C, the melt region is wider at the bottom than at the top, while the reverse is true for higher heating temperatures. The numerical study of Sasaguchi (1995) was concerned with a cavity with one heated sidewall and three insulated walls, a transient problem. The further numerical study by Zhang et al. (1997) dealt with the case of anisotropic permeability with the principal axes oriented at an angle  $\theta$  to the gravity vector. The effect of a magnetic field on melting from a vertical plate was treated by Tashtoush (2005) using the Forchheimer model.

The research discussed so far in this chapter has dealt with heating from the side. Zhang et al. (Zhang et al. 1991a, Zhang et al. 1991b) have made a theoretical investigation of the melting of ice in a cavity heated from below. They found that the convection that arises in the unstable layer can penetrate into the stable region but cannot reach the melting front, and this results in a flatter solid–liquid interface than that produced in the absence of a stable layer. They also found that in transition from onset to final state, the convection pattern passes through several intermediate forms, each change being accompanied by a sudden increase (which is followed by a subsequent decline) in the heat transfer rate and in the displacement velocity of the solid–liquid interface. Zhang and Nguyen (1990, 1994) have found that melting from above is more effective than melting from below when the heating temperature is between 0°C and 8°C, convection arises earlier, the melting process is faster, and the total melt at steady state is thicker. The time for the onset of convection is a minimum and the heat transfer rate is a maximum when the upper boundary is at 6°C, and at this temperature, the heat transfer rate is a maximum. Hguyen (sic) and Zhang (1992) studied the penetrative convection that occurs during the melting of a layer of ice heated either above or below. They found that convection starts to play an increasingly important role as the melt thickness attains a certain value corresponding to the critical Rayleigh number for the onset of convection. The new convection cells have an approximately square form. As time passes, these cells become more slender and suddenly break up sequentially. The breaking up process is quite short and is associated with a sharp jump in the curve of Nusselt number versus time.

The melting of ice has also been considered by Kazmierczak and Poulikakos (1988). They dealt with both vertical and horizontal interfaces. Plumb (1994a) developed a simple model for convective melting of particles in a packed bed with throughflow and solved it numerically in one dimension to predict melting rates for a single substance and a system in which the liquid phase at elevated

temperature enters a packed bed of the solid phase at the melting temperature. He found that the thickness of the melting zone increases with Péclet number and Prandtl number for systems dominated by convection.

Melting around a horizontal cylinder was studied numerically on the Darcy model by Christopher and Wang (1994). They found that heat transfer from the cylinder is minimized at some value of the burial depth that is a function of Ra and the dimensionless phase-change temperature. The influence of density inversion on thawing round a cylinder was treated by Smith (2006). Chang and Yang (1996) studied numerically, on the Brinkman-Forchheimer model, the melting of ice in a rectangular enclosure. They noted that as time goes on, heat transfer on the hot side decreases and that on the cold side increases. A lattice Boltzmann simulation on natural convection-dominated melting in a rectangular cavity was performed by Gao and Chen (2011).

Ellinger and Beckerman (1991) reported an experimental study of melting of a pure substance (*n*-octadecane) in a rectangular enclosure that is partially occupied by horizontal or vertical layers of a relatively high thermal conductivity medium (glass or aluminum beads). They found that though such a porous layer may cause a faster movement of the solid–liquid interface, the effect of low permeability causes a reduction in melting and heat transfer rates compared with the case without the porous layer. Tong et al. (1996) demonstrated the enhancement of heat transfer by inserting a metal matrix into a phase-change material. Pak and Plumb (1997) studied numerically and experimentally the melting of a mixture that consists of melting and nonmelting components, with heat applied to the bottom of the bed. Thermosolutal convection was examined by Oueslati et al. (2008b). Lafdi et al. (2007) performed experiments on the influence of foam porosity and pore size on the melting of phase-change materials.

Mixed convection with melting from a vertical plate was analyzed by Bakier (1997) and Gorla et al. (1999a). They noted that the melting phenomenon decreases the local Nusselt number at the solid–liquid surface. Horizontal forced and mixed convection with local thermal nonequilibrium melting was studied experimentally and theoretically by Hao and Tao (2003a,b). The topic of local thermal nonequilibrium melting was further addressed by Harris et al. (2001) and Agwu Nnanna et al. (2004). Transient mixed convection was studied by Cheng and Lin (2006, 2007, 2009). The effect of radiation with a non-Newtonian fluid was treated by Chamkha et al. (2010a).

The topic of metal foams was passive control systems as surveyed by Krishnan et al. (2008). In particular, they discussed the two-temperature model employed by Krishnan et al. (2005).

Hong et al. (2007) studied the onset of buoyancy-driven convection in a porous medium heated from below. An analysis of melting under pulsed heating was carried out by Krishnan et al. (2007). A numerical simulation of melting via a modified temperature-transforming model was undertaken by Damronglerd and Zhang (2006).

A related problem, involving a phase-change front at the interface between a diminishing solid volume and an increasing fluid volume, has been treated by

Rocha et al. (2001) and Bejan et al. (2004). This involves a layer of porous medium impregnated by solid methane hydrate material. The clathrate (endowed with a lattice) hydrates are solid crystals of water and methane at sufficiently high pressures and low temperatures. When the layer is depressurized suddenly on its lower plane, the methane hydrate material progressively dissociates into methane gas plus liquid water. Further studies of melting with volume change, of phase-change materials in metal foams, were made by Yang and Garimella (2010) (with volume change) and Li et al. (2012). Tian and Zhao (2011) reported a numerical investigation of heat transfer in phase-change material embedded in porous metals.

## 10.2 Freezing and Solidification

### 10.2.1 Cooling from the Side

#### 10.2.1.1 Steady State

In a study that deals with both freezing and melting, Oosthuizen (1988a) considered the steady state in the two-dimensional configuration of Fig. 10.20. The porous medium is heated from the left and cooled from the right in such a way that the melting point of the phase-change material falls between the temperatures of the two sidewalls,  $T_h > T_m > T_c$ .

In the steady state, the freezing front takes up a stationary position and the freezing and melting at the front ceases. This is why in the steady state, the latent heat of the phase-change material ( $h_{sf}$ ) does not play a role in the heat transfer process or in deciding the position and shape of the melting front. The heat transfer from  $T_h$  to  $T_c$  is one of conjugate convection and conduction: specifically, convection through the zone saturated with liquid and conduction through the zone with pores filled by solid phase-change material.

Oosthuizen (1988a) relied on the finite-element method in order to simulate the flow and heat transfer through the entire  $H \times L$  domain of Fig. 10.20. The porous-medium model was the same as the one outlined in the first part of Sect. 10.1.1. The parametric domain covered by this study was  $0 = \text{Ra} = 500$ ,  $0.5 = H/L = 2$ , and  $1 = k_F/k_U = 3$ . The thermal conductivities  $k_F$  and  $k_U$  refer to the frozen and the unfrozen zones. They are both of type  $k_m$ , that is, thermal conductivities of the saturated porous medium. The Rayleigh number is defined as  $\text{Ra} = g\beta KH(T_h - T_c)/v\alpha_m$ .

Besides  $\text{Ra}$ ,  $H/L$ , and  $K_U$ , the fourth dimensionless group that governs the steady state is the dimensionless temperature difference ratio:

$$\theta_c = \frac{T_m - T_c}{T_h - T_c}, \quad (10.70)$$

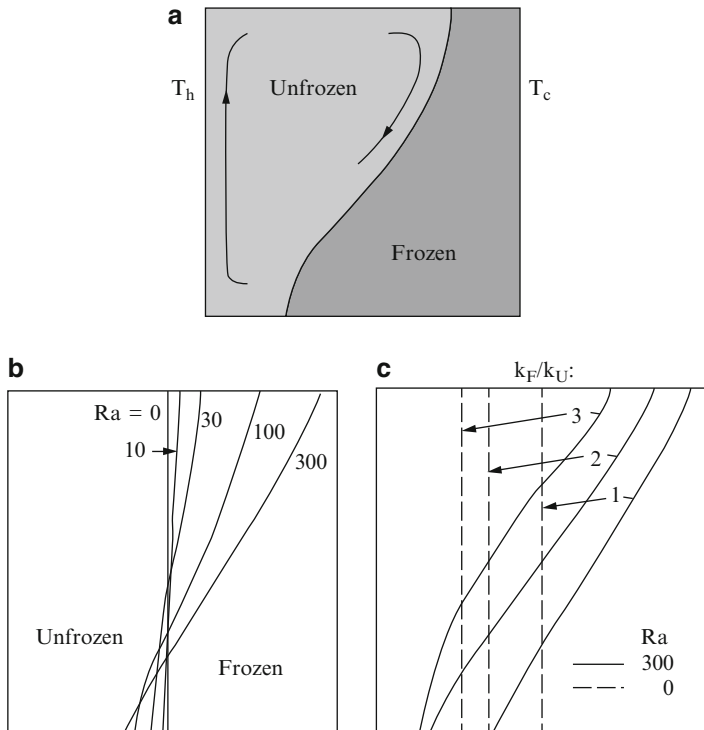


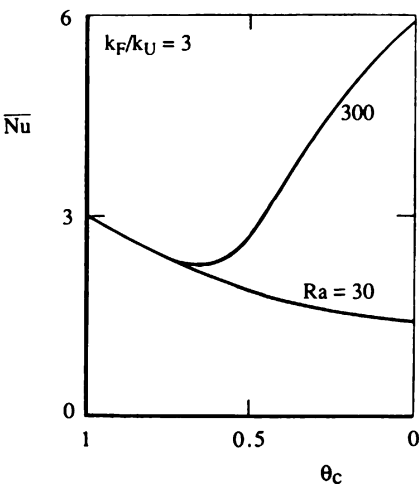
**Fig. 10.20** (a) Steady-state convection and heat transfer in a porous medium with differentially heated sidewalls. (b) The effect of  $\text{Ra}$  on the freezing front ( $\theta_c = 0.5$ ,  $k_F = k_U$ ). (c) The effect of  $k_F/k_U$  on the freezing front ( $\theta_c = 0.5$ ) (Oosthuizen 1988a)

which describes the position of  $T_m$  relative to  $T_h$  and  $T_c$ . Figure 10.20b shows the effect of increasing the Rayleigh number when  $k_F = k_U$  and  $\theta_c = 0.5$ . In this case, in the absence of natural convection ( $\text{Ra} = 0$ ), the melting front constitutes the vertical midplane of the  $H \times L$  cross section. The melting front becomes tilted, S-shaped, and displaced to the right as  $\text{Ra}$  increases. The effect of natural convection is important when  $\text{Ra}$  exceeds approximately 30.

The effect of the conductivity ratio  $k_F/k_U$  is illustrated in Fig. 10.20c, again for the case when  $T_m$  falls right in the middle of the temperature interval  $T_c - T_h$  (i.e., when  $\theta_c = 0.5$ ). The figure shows that when the conductivity of the frozen zone is greater than that of the liquid-saturated zone ( $k_F/k_U > 1$ ), the frozen zone occupies a greater portion of the  $H \times L$  cross section. The effect of the  $k_F/k_U$  ratio is felt at both low and high Rayleigh numbers.

The melting-point parameter  $\theta_c$  has an interesting effect, which is illustrated in Fig. 10.21. The ordinate shows the value of the overall Nusselt number, which is the ratio of the actual heat transfer rate to the pure-conduction estimate,  $Nu = q'/[k_U(T_h - T_c)/L]$ . On the abscissa, the  $\theta_c$  parameter decreases from  $\theta_c = 1$  (or  $T_m = T_c$ ) to  $\theta_c = 0$  (or  $T_m = T_h$ ). The figure shows that when  $k_F/k_U > 1$ , there

**Fig. 10.21** The effect of the melting-point parameter  $\theta_c$  on the overall heat transfer rate through the system of Fig. 10.20a  
(Oosthuizen 1988a)



exists an intermediate  $\theta_c$  value for which the overall heat transfer rate is minimum. This effect is particularly evident at high Rayleigh numbers, where convection plays an important role in the unfrozen zone.

### 10.2.1.2 Other Studies

Weaver and Viskanta (1986) experimented with a cylindrical capsule (7.3 cm diameter, 15.9 cm length) filled with spherical beads and distilled water. Freezing was initiated by cooling the outer wall of the capsule. Experiments were conducted using either glass beads or aluminum beads, with the capsule oriented vertically or horizontally. Weaver and Viskanta (1986) complemented their measurements with a computational solution in which the heat transfer process was modeled as one-dimensional pure conduction. The computed thickness of the frozen zone agreed well with the experimental data for the combination of glass beads and distilled water, in which the difference between thermal conductivities is small. The agreement was less adequate when the aluminum beads were used. These observations lead to the conclusion that the effective porous-medium thermal conductivity model is adequate when the solid matrix and pore material have similar conductivities and that the local thermal equilibrium model breaks down when the two conductivities differ greatly.

The breakdown of the local thermal equilibrium assumption was studied further by Chellaiah and Viskanta (1987, 1989a). In the first of these experimental studies, Chellaiah and Viskanta examined photographically the freezing of water or water-salt solutions around aluminum spheres aligned inside a tube surrounded by a pool of the same phase-change material. They found that the freezing front advances faster inside the tube. When water was used, they found that the leading aluminum

sphere is covered at first by a thin layer of ice of constant thickness. This layer was not present when the phase-change material was a water-salt solution.

In their second study of freezing of water, Chellaiah and Viskanta (1989a) showed that the water is supercooled (i.e., its temperature falls below the freezing point) before freezing is initiated. The degree of supercooling was considerably smaller than the one observed in the freezing of water in the absence of the porous matrix (glass or aluminum beads).

Chellaiah and Viskanta (1989b, 1990a, b) found good agreement between calculations using the Brinkman-Forchheimer equation and experiments using water and glass beads in a rectangular enclosure suddenly cooled from the side. They investigated the effects of imposed temperature difference and the superheat defined by  $S = c_P(T_h - T_f)/h_{sf}$ , where  $T_f$  is the fusion temperature. For small  $S$ , the flow is weak and the interface is almost planar. The larger  $S$  convection modifies the shape of the interface. Further numerical results for lateral transient freezing were reported by Sasaki et al. (1990). A further numerical and experimental study was performed by Sasaki and Aiba (1992).

A boundary layer solution, appropriate for high Rayleigh number, for freezing on the exterior of a vertical cylinder was obtained numerically by Wang et al. (1990a, b). Transient freezing about a horizontal cylinder was studied numerically by Bian and Wang (1993). Experiments with an inclined bed of packed spheres were performed by Yang et al. (1993a, b).

A generalized formulation of the Darcy-Stefan problem, one valid for irregular geometries with irregular subregions and not requiring the smoothness of the temperature, was proposed by Rodrigues and Urbano (1999). A comprehensive theoretical and experimental study of lateral freezing with an aqueous salt solution as the fluid, and taking into account anisotropy and the formation of dendrite arrays, was made by Song and Viskanta (2001). They found that the porous matrix phase affected the freezing of the aqueous salt solution by offering an additional resistance to the motion of the fluid and migration of separate crystals. The amount of macrosegregation was found to be mainly controlled by the porous matrix permeability in the direction of gravity, while macrosegregation was decreased when the permeabilities of the porous matrix phase and/or dendrite arrays were decreased. Natural convection between vertical plates, with solidification taking place on one plate, was studied by Lipnicki and Weigand (2008).

### **10.2.2 Cooling from Above**

Experiments on layers cooled from above were performed by Sugawara et al. (1988). They employed water and beads of either glass or steel. Their main interest was in predicting the onset of convection. Experimental and numerical work was reported by Lein and Tankin (1992b). The experimental work involved visualization. The authors reported that the convection process is controlled by the mean Rayleigh number and weakens as the freezing process proceeds. They examined

results for various aspect ratios, and they found that these agreed reasonably well with the formula of Beck (1972) (Fig. 6.20). A nonlinear stability analysis was presented by Karcher and Müller (1995). The analysis shows that due to the kinematic conditions at the solid/liquid interface, hexagons having upflow in the center are stable near the onset of convection, but for sufficiently supercritical Rayleigh numbers, rolls are the only stable mode. The transition from hexagons to rolls is characterized by a hysteresis loop. A numerical study of a superheated fluid-saturated porous medium in a rectangular cavity, with the bottom and sidewalls insulated and the top wall maintained at a constant temperature below the freezing point, was reported by Zhang and Nguyen (1999). A substantial numerical and experimental study was reported by Kimura (2005). The onset of buoyancy-driven convection in a layer of a porous medium solidified from above in a time-dependent situation was studied by Kim et al. (2009a, b).

### 10.2.3 *Solidification of Binary Alloys*

When a binary mixture solidifies from a solid boundary, the planar solidification front often becomes unstable due to constitutional undercooling and the result is a mushy layer, separating the completely liquid phase from the completely solid phase. The mushy layer has been modeled as a reactive porous medium. A feature of the mushy zone is that it contains columnar solid dendrites, and so the porous medium is anisotropic. One principal axis for the anisotropic permeability is commonly, but not necessarily, approximately aligned with the temperature gradient.

The solidification of aqueous solutions of binary substances (notably ammonium chloride) is analogous in many ways to the solidification of metallic alloys, so experiments are often done with aqueous solutions. A pioneering study of solidification in a vertical container was carried out by Beckermann and Viskanta (1988b). Fundamental experimental work on solidification produced by cooling from the side in a rectangular cavity has been performed by Choi and Viskanta (1993) and Matsumoto et al. (1993, Nakayama et al. 1995), while Cao and Poulikakos (1991a, b) and Choi and Viskanta (1992) observed solidification with cooling from above and Song et al. (1993) observed cooling from below. Okada et al. (1994) did experiments on solidification around a horizontal cylinder.

The simplest model for the momentum equation, Darcy's law, was introduced in this context by Mehrabian et al. (1970). Subsequent modeling has been based on either a mixture theory in which the mushy zone is viewed as an overlapping continuum (e.g., Bennon and Incropera 1987) or on volume averaging (e.g., Beckermann and Viskanta 1988b; Ganesan and Poirier 1990—the latter were more explicit about underlying assumptions). The second approach requires more work, but in relating macroscopic effects to microscopic effects, it leads to greater insight about the physical processes involved. The averaging approach also allows the incorporation of the effects of thermal or chemical nonequilibrium or a moving

solid matrix (Ni and Beckermann (1991b)). Felicelli et al. (1991) investigated the effect of spatially varying porosity but found that that had no significant effect on the convection pattern. They did find that the effect of remelting in part of the mushy zone was important. Poirier et al. (1991) showed that for relatively large solidification rate and/or thermal gradients, the effects of heat of mixing need to be incorporated in the energy equation. Using the mixture continuum model modified to include the effect of shrinkage induced flow, Chiang and Tsai (1992) analyzed solidification in a two-dimensional rectangular cavity with riser. For the same geometry, Schneider and Beckermann (1995) used numerical simulation to compare two types (Scheil and lever rule) of microsegregation models; the predicted macrosegregation patterns were found to be similar although the predicted eutectic fraction is significantly higher with the Scheil model. They noted that the predicted pattern is sensitive to the permeability function assumed in the model.

Ni and Incropera (1995a,b) produced a new model that retains the computational convenience of the mixture continuum model while allowing for the inclusion of important features of the volume-average two-phase model. They relaxed several assumptions inherent in the original formulation of the two-phase model, making it possible to account for the effects of solutal undercooling, solidification shrinkage, and solid movement.

The effect of anisotropy of permeability has been investigated by Sinha et al. (Sinha et al. 1992, Sinha et al. 1993) and Yoo and Viskanta (1992). A three-phase model, in which the release of dissolved gas from the alloy is taken into account, was developed by Kuznetsov and Vafai (1995a).

Prescott and Incropera (1995) introduced the effect of turbulence in the context of stirring produced by an oscillating magnetic field. Their results indicate that turbulence decreases the propensity for channel development and macrosegregation by enhancing mixing and reducing the effective Lewis number from a large value to near unity. For modeling the turbulence, they employed an isotropic low-Reynolds number  $k$ - $\epsilon$  model. The turbulence is produced via a shear-production source term. They carried out numerical calculations for comparison with experiments with a lead-tin alloy. The turbulence occurs in the liquid and near the liquidus interface; it is strongly damped in the mushy zone. Prescott and Incropera remark that turbulence can survive in the mush only in regions with porosity about 0.99 or higher, and there slurry conditions are likely to occur in practice. However, this assumption may be an artifact of an assumption of the model (Lage 1996), and turbulence may penetrate further into the mushy layer than this model predicts.

Compositional convection can occur in a mushy layer cooled from below when unstable density gradients are formed as a result of rejection of the lighter component of the mixture upon solidification. There is an interaction among convection, heat transfer, and solidification that can lead to the formation of "chimneys" or localized channels devoid of solid through which buoyant liquid rises. An analytical investigation of chimneys was made by Roberts and Loper (1983), who used equations formulated by Hills et al. (1983). Observations of chimneys led to stability analyses. Fowler (1985a, b) modeled the mushy layer as a nonreacting porous layer, while the linear stability analysis of Worster (1992) included the

effects of the interaction of convection and solidification. Linear stability analysis had been applied previously by Nandapurkar et al. (1989). Worster identified two direct modes of convective instability: one driven from a narrow compositional boundary layer about the mush-liquid interface and the other driven from the interior of the mushy layer. The graph of Rayleigh number versus wave number has two minima. The boundary layer mode results in fine-scale convection in the melt above the mushy layer and leaves the interstitial fluid in the mushy layer virtually stagnant. The mushy-layer model causes perturbations to the solid fraction of the mushy layer that are indicative of a tendency to form chimneys. Good quantitative agreement was found with the experimental results of Tait and Jauport (1992) for the onset of the mushy-layer mode of convection. These authors and Tait et al. (1992) discussed geophysical implications of their experimental results.

The linear stability analysis of Emms and Fowler (1994) involved a time-dependent basic state that included the effect of finger-type convection in the liquid. However, their analysis indicated that the onset of convection in the mushy layer is little affected by vigorous convection in the melt.

Worster's (1991, 1992) analysis was extended by Chen et al. (1994) to the case of oscillatory modes. They found that when stabilizing thermal buoyancy is present in the liquid, the two steady modes of convection can separate by way of an oscillatory instability. They noted that the oscillatory instability occurred only when the buoyancy ratio (thermal to solutal) in the liquid region was nonzero, so they associated the oscillatory instability with the interaction of the double-diffusive convection in the liquid region with the mushy-layer convective mode. Their results showed that the steady modes became unstable before the oscillatory mode. Chen et al. (1994) also performed experiments with ammonium chloride solution which confirmed that during the progress of solidification, the melt in the mush is in a thermodynamic equilibrium state except at the melt-mush interface where most of the solidification occurs.

A weakly nonlinear analysis based on the assumption that the mushy layer is decoupled from the overlying liquid layer and the underlying solid layer was performed by Amberg and Homsy (1993). They made progress by considering the case of small growth Péclet number, small departures from the eutectic point, and infinite Lewis number. Their analysis, which revealed the structure of possible nonlinear, steady convecting states in the mushy layer, was extended by Anderson and Worster (1995) to include additional physical effects and interactions in the mushy layer. They employed a near-eutectic approximation and considered the limit of large far-field temperature, so that their model involved small deviations from the classic HRL problem. The effects of asymmetries in the basic state and the nonuniform permeability lead to transcritically bifurcating convection with hexagonal planform. They produced a set of amplitude equations that described the evolution of small-amplitude convecting states associated with direct modes of instability. Analysis of these revealed that either two-dimensional rolls or hexagons can be stable, depending on the relative strengths of different physical mechanisms. They determined how to adjust the control parameters to minimize the degree of subcriticality of the bifurcation and hence render the system more stable globally.

Moreover, their work suggested the possibility of an oscillatory mode of instability despite the lack of any stabilizing thermal buoyancy, in contrast with the results of Chen et al. (1994).

The linear instability analysis of Anderson and Worster (1996) was designed to investigate this new oscillatory instability. Their model contained no double-diffusive effects and no region in which a statically stable density gradient exists. They considered the limit of large Stefan number, which incorporates a key balance for the existence of the oscillatory instability. They discovered that the mechanism underlying the oscillatory instability involves a complex interaction between heat transfer, convection, and solidification. Further work on the oscillatory modes of nonlinear convection has been reported by Riahi (2002b, 2004). The modes take the form of two- and three-dimensional traveling and standing waves. For most of the parameter range studied, supercritical simple traveling waves are stable. Riahi (1998a) examined the structure of an unsteady convecting mushy layer. He identified four regimes corresponding to high or low Prandtl number melt and strongly or weakly dependent flow. He found that strongly time-dependent flow can lead to nonvertical chimneys, and for weakly time-dependent flow of a low Prandtl number melt, vertical chimneys are possible only when the chimneys have small radius.

Some of the experimental results reported by Chen (1995) confirm the theoretical predictions, while others reveal phenomena not observed hitherto.

The effects of rotation about a vertical axis were included in the linear stability analysis of Lu and Chen (1997). They noted that very high rotation rates were necessary to significantly increase the critical Rayleigh number, but smaller rates could change the most critical convection mode. They found their results to be sensitive to the value of a buoyancy ratio defined as  $\Gamma\alpha_t/(\alpha_s - \Gamma\alpha_t)$ , where  $\alpha_t$ ,  $\alpha_s$  are the thermal, solutal expansion coefficients, respectively, and  $\Gamma$  is the slope of the solidus. The effect of rotation also was studied by Guba and Boda (1998), Riahi (1993b, 1997), Sayre and Riahi (1996, 1997), and Riahi and Sayre (Riahi and Sayre 1996a, b). The latter investigated nonlinear natural convection under a high-gravity environment, where the rotation axis is inclined to the high-gravity vector. They found that for some particular moderate rotation range, the vertical velocity in the chimneys decreases rapidly with increasing rotation rate and appears to have opposite signs across some rotation-dependent vertical level. Inclined rotation was also studied by Chung and Chen (2000).

The study by Guba (2001) concentrated on the way rotation controls the bifurcating convection with various planforms. Govender and Vadasz (2002a,b) have reported a weak nonlinear analysis of moderate Stefan number stationary convection in rotating layers. Further linear stability studies were made by Govender and Vadasz (2002c), Maharaj and Govender (2005a, b), and Govender (2003b, 2005a–c, g, 2008). The results show that generally the oscillatory mode is the most dangerous mode for intermediate values of the Stefan number at sufficiently large Taylor number values, while the stationary mode is the most dangerous for very small and very large values of the Stefan number. Further finite-amplitude studies of convection have been carried out by Govender (2003d,e, 2004c) to

consider factors such as large Stefan number or small variations in retardability. Other studies by Riahi (2003a, b) on effects of rotation have dealt with oscillatory modes of convection and with nonlinear steady convection. Some aspects of the topic were reviewed by Riahi (1998b, 2002a).

A numerical study of the effects of rotation was made by Neilson and Incropera (1993). They found that slow, steady rotation had insignificant effect on channel formation, but with intermittent rotation corresponding to successive spin-up and spin-down of the mold in their numerical study, channel nucleation was confined to the centerline and outer radius of the casting. They attributed the elimination of channels from the core of the casting to the impulsive change in angular frequency associated with spin-up and its effect on establishing an Ekman layer along the liquidus front, the front being washed by flow within the layer, thereby eliminating the perturbations responsible for channel nucleation.

Further work involving the effects of rotation has been reported by Riahi (2005, 2006b, 2007a, b) and Okhuysen and Riahi (2008)

A flow-focusing instability, driven by expansion or contraction upon solidification, was analyzed by Chiarelli and Worster (1995), and comparisons were made with acid-etching instabilities in porous rocks. They concluded that though the potential for instability exists, it is unlikely to occur in practice.

For the case of unidirectional solidification, Krane and Incropera (1996) performed a scaling analysis that showed that Darcy's law was adequate in the mushy zone except in the region near the liquidus isotherm and that advection dominates the solute transport throughout the mush, though in the denser regions of the solid–liquid region, the liquid velocities are so small as to have a negligible effect of macrosegregation.

The review by Worster (1997) contains a summary of a theory of an ideal mushy layer. When use is made of the linear liquidus relationship

$$T = T_E + \Gamma (C - C_E), \quad (10.71)$$

where  $\Gamma$  is a constant and the subscript  $E$  refers to the eutectic point, the equation of state (9.1) reduces to

$$\rho_f = \rho_0 + \beta^* (C - C_0), \quad (10.72)$$

where

$$\beta^* = -\beta\Gamma - \beta_C. \quad (10.73)$$

Consequently, an appropriate Rayleigh number is

$$\text{Ra}_m = \frac{\rho_0 g \beta^* K_0 \Delta C}{\mu V} = \frac{\rho_0 g \beta^* K_0 L \Delta C}{\mu \alpha_m}, \quad (10.74)$$

where  $K_0$  is a reference permeability and  $V$  is the rate of solidification and the thermal length scale  $L$  is defined by  $L = \alpha_m/V$ . Convection in the ideal mushy layer is governed by  $\text{Ra}_m$  together with a Stefan number and a compositional ratio. Experimental results such as those by Bergman et al. (1997) confirm that  $\text{Ra}_m$  is indeed a governing parameter.

Worster's (1997) review also includes a discussion of explanations of why chimneys may or not form. The explanation of Worster and Kerr (1994) is that interfacial undercooling causes a strengthening of the boundary layer mode of convection, which retards growth of the mushy layer, increases its solid fraction, and decreases the compositional contract across it. These three effects combine to reduce  $\text{Ra}_m$ , and as time progresses,  $\text{Ra}_m$  may reach a maximum less than that required for chimneys to form. Worster (1997) also mentions experiments related to the formation of a mushy zone in sea ice (Wettlaufer et al. 1997), as well as applications to solidifying magmas and the molten outer core of the Earth. The topic of sea ice was discussed in detail by Feltham et al. (2006), Notz and Worster (2009), and Hunke et al. (2011). The development of chimneys has been further studied numerically by Schulze and Worster (1998, 1999) and by Emms (1998). An alternative model for mush-chimney convection was proposed by Loper and Roberts (2001).

Further work on plume formation in mushy layers has been reported by Chung and Chen (2000a) and Chung and Worster (2002). Chung and Chen (2000b) studied convection in directionally solidifying alloys under inclined rotation. The effect of initial solutal concentration on the evolution of the convection pattern during the solidification of a binary mixture was examined experimentally by Skudarnov et al. (2002). An experimental study of the solidification of a ternary alloy was reported by Thompson et al. (2003). A model for the diffusion-controlled solidification of ternary alloys was described by Anderson (2003). A morphological instability due to a forced flow in the melt was analyzed by Feltham and Worster (1999) and Chung and Chen (2001). An alternative hybrid model of a mushy zone has been proposed by Mat and Ilegbusi (2002). An experimental study of the suppression of natural convection by an additive to increase the viscosity of the fluid was reported by Nishimura and Wakamatsu (2000). Convection in ternary alloys was further examined by Anderson and Schulze (2005) and Anderson et al. (2010). Magnetic resonance studies were reported by Aussillous et al. (2006).

Further complexities of alloy solidification are discussed in the reviews by Beckermann and Viskanta (1993), Beckermann and Wang (1995), and Prescott and Incropera (1996). Experimental work has been reported by Solomon and Hartley (1998). A numerical investigation of the macrosegregation during the thin strip casting of carbon steel was made by Kuznetsov (1998a). Another convective instability problem involving solidification was analyzed using linear stability theory by Hwang (2001). An expository article on the solidification of fluids was presented by Worster (2000). Adnani and Hsiao (2005) have reviewed transport phenomena in liquid composites modeling processes and their roles in process control and optimization.

Roberts et al. (2003) have considered the convective instability of a plane mushy layer that advances as heat is withdrawn at a uniform rate from the bottom of an alloy. They assumed that the solid that forms is composed entirely of the denser

constituent, making the residual liquid compositionally buoyant and thus prone to convective motion. They focused on the large-scale mush mode of instability, quantified the minimum critical Rayleigh number, and determined the structure of the convective modes of motion within the mush and the associated deflections of the mush-melt and mush-solid boundaries.

The effect of a magnetic field has been studied by Bhatta et al. (2010). Numerical modeling of convection in a reactive porous medium with a mobile mush-liquid interface was conducted by Butler et al. (2006). Further studies of the onset of convection were reported by Hwang and Choi (2008, 2009). The implications of interfacial conditions were discussed by Le Bars and Worster (2006a), while Le Bars and Worster (2006b) carried out finite-element single-domain simulation and presented new benchmark solutions. Guba and Worster (2006a) studied natural convection in laterally solidifying mushy regions, and Guba and Worster (2006b) further studied nonlinear oscillatory convection. The effect of vertical vibration in a cylindrical layer was studied by Govender (2011). Gravity modulation was treated by Pillay and Govender (2005, 2007) and Srivastava and Bhaduria (2011). The effect of shear flow was considered by Neufeld and Wettlaufer (2008, 2011). A nonlinear evolution approach to the subject was reported by Riahi (2010) and Bhatta et al. (2012) (for an active layer), while Riahi (2006a) investigated the effect of permeability in a dendrite layer. Some experiments on steady-state mushy layer were reported by Peppin et al. (2007, 2008). The simulation of directional solidification, thermochemical convection, and chimney formation in a Hele-Shaw cell was reported by Katz and Worster (2008). Convection forced by sidewall heat losses was studied by Roper et al. (2007), while Roper et al. (2011) studied localization of convection in mushy layers with weak background flow. Saija et al. (2011) discussed the modeling of freckle segregation with mesh adaptation. The linear stability of solutal convection in a mushy layer subjected to gravity modulation was studied by Srivastava and Bhaduria (2011). A variational principle for solidification problems, involving maximal potential energy transport, was presented by Wells et al. (2010). The topic of flows involving phase change has been surveyed by Huppert and Worster (2012). The influence of inertia on channel segregation during columnar solidification was studied by Kumar et al. (2012). Finite-sample-size effects were studied by Zhong et al. (2012). A problem involving transient natural convection was investigated numerically by Cheng et al. (2012). The effect of a vertical magnetic field on nonlinear convection was examined by Riahi (2012).

A related problem involving dissolution-driven convection was investigated by Hallworth et al. (2005). They considered experimentally and theoretically the heating from above of an initially homogeneous layer of solid crystals, saturated liquid, and glass ballotini. The heat flux causes crystals at the top of the layer to dissolve, forming liquid that, being more concentrated, drives convection in the lower layer. Mixing of this concentrated liquid into the lower layer leads to precipitation, thereby releasing latent heat that raises the temperature of the lower layer. There results a three-layered system: clear fluid, clear fluid plus close-packed ballotini, and a mixture of solid crystals, ballotini, and saturated liquid. The theoretical model used is based on the concept that the heat supplied from above is used entirely for the dissolution of solid crystals at the upper boundary of the

lower layer. The resulting compositional convection redistributes the dissolved salt uniformly through the lower layer where it partly recrystallizes to restore chemical equilibrium. The crystallization leads to a gradual and uniform increase in both the solid fraction and the temperature of the lower layer.

## 10.3 Boiling and Evaporation

### 10.3.1 *Boiling and Evaporation Produced by Heating from Below*

When boiling begins in a fluid-saturated porous medium heated from below, a two-layer system is formed with a liquid region overlying a two-phase region, as sketched in Fig. 10.22. Experiments by Sondergeld and Turcotte (1977) and Bau and Torrance (1982a) have shown that the liquid regime temperature profile may be conductive or convective, but the two-phase region is essentially isothermal at the saturation temperature. The two-phase region may be liquid dominated or vapor dominated. Heat is transported across the two-phase region by vertical counterpercolation of liquid and vapor; liquid evaporates on the heating surface, and vapor condenses at the interface between the liquid and two-phase regions. Experiments have indicated that thermal convection in the liquid region may occur before the onset of boiling or after the onset of boiling. Visualization experiments (Sondergeld and Turcotte 1978) reveal that after the onset of convection, the liquid region streamlines penetrate the two-phase region. The convection in the liquid region is in the form of polyhedral cells whose dimensions vary with the heat flux.

With the liquid region overlying the two-phase region, there are two mechanical mechanisms for instability: buoyancy and gravitational instability, the latter due to the heavier liquid region overlying the lighter two-phase region. The gravitational instability differs from the classical Rayleigh-Taylor instability of superposed fluids because the interface is now permeable and therefore permits both heat and mass transfer across it. Schubert and Straus (1977) noted that convection also can be driven by a phase-change instability mechanism. If steam and water stay in thermal equilibrium, then thermal perturbations lead to pressure variations that tend to move the fluid against the frictional resistance of the medium. Because of conservation of mass, horizontal divergence is accompanied by vertical contraction and phase change takes place so that the vertical forces stay in balance. In a porous medium containing saturated liquid or a liquid-vapor mixture, convection occurs more readily by the phase-change mechanism than it would with ordinary liquid driven by buoyancy. Phase-change-driven convection is concentrated toward the bottom of the porous layer, and the cells are narrow in comparison with their depth. The model used by Schubert and Straus (1977) is valid only for a mixture with small amounts of steam.

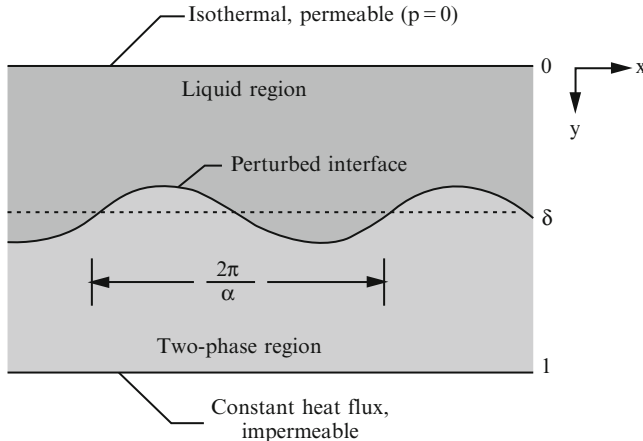


**Fig. 10.22** Definition sketch for boiling produced by heating from below

Schubert and Straus (1980) also considered the stability of a vapor-dominated system with a liquid region overlying a dry vapor region. Their analysis predicts that such systems are stable provided that the permeability is sufficiently small. The stability arises because when liquid penetrates the interface, that interface is distorted so the system remains on the Clapeyron curve, and this results in a pressure gradient that acts to restore equilibrium.

O'Sullivan (1985b) described some numerical experiments modeling a geothermal reservoir in which the level of heat input at the base of a layer is varied. As the heat input is increased, the flow changes from conduction to single-phase convection, then to convection with an increasingly larger boiling zone, and finally to an irregular oscillatory two-phase convection.

The onset of two-dimensional roll convection in the configuration of Fig. 10.22 was studied using linear stability analysis by Ramesh and Torrance (1990). They assumed that the relative permeabilities of liquid and vapor were linear functions of the liquid saturation  $S$ . Their analysis reveals that the important parameters are the Rayleigh numbers  $\text{Ra}$  and  $\text{Ra}_{2\varphi}$  in the liquid and two-phase regions and the dimensionless heat flux  $Q_b$  at the lower boundary. The parameters are defined by

$$\begin{aligned} \text{Ra} &= \frac{g \beta_l K H (T_s - T_0)}{\nu_l \alpha_{ml}}, & \text{Ra}_{2\varphi} &= \frac{(1 - \bar{\rho}_v) K H}{\nu_l \alpha_{ml}}, \\ Q_b &= \frac{q''_b H}{k_m (T_s - T_0)}, \end{aligned} \quad (10.75)$$

where  $q''_b$  is the heat flux at the lower boundary,  $T_s$  is the saturation temperature,  $T_0$  is the temperature at the top boundary,  $\bar{\rho}_v$  is the ratio of vapor to liquid densities, while  $\lambda$  (see Fig. 10.23) is defined to be  $h_{fg}/[c_P(T_s - T_0)]$ , where  $h_{fg}$  is the latent heat.

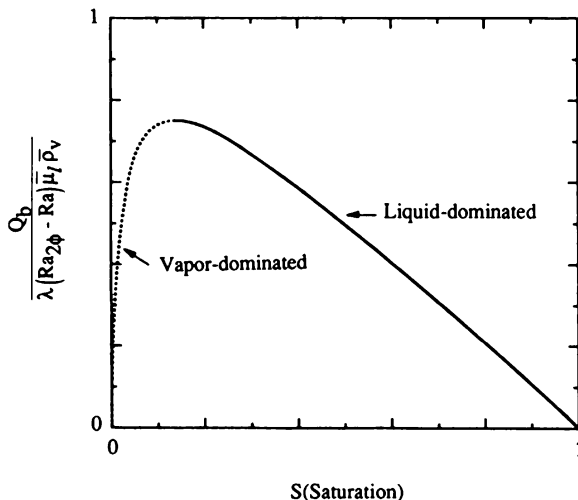


**Fig. 10.23** The relationship between bottom heat transfer rate and saturation for the basic state in a steam-water system (Ramesh and Torrance 1990, with permission from Pergamon Press)

For sufficiently large  $Q_b$ , there is dryout of the liquid phase region in the two-phase region. For smaller values of  $Q_b$ , there are two  $S$  values for each value of  $Q_b$  (Fig. 10.23). The smaller value ( $S < 0.17$  for water) corresponds to a vapor-dominated system and the larger value to a liquid-dominated system. For a liquid-dominated system, the solution map (for water) is shown in Fig. 10.24. The picture is approximate because it is based on a single wave number,  $\alpha = \pi$ . We are primarily interested in values  $Q_b = 1$  because  $1/Q_b$  is the ratio of the mean depth of the interface to the total depth of the medium.

The onset of boiling is indicated by the curve  $ABE$ . For  $Q_b$  values above this curve, boiling occurs with a liquid layer overlying a two-phase zone. For  $Q_b$  values below  $ABE$ , boiling does not occur. The onset of convection in the liquid is denoted by the curve  $CBD$ ; convection occurs only to the right of this curve. Its nose defines the critical Rayleigh number as  $Q_b$  varies for  $\alpha = \pi$ . (As  $Q_b$  and  $\alpha$  both vary, the minimum value of Ra is 14.57, attained at  $Q_b = 1.35$ ,  $\alpha = 1.9$ .) In laboratory experiments, boiling occurs when the temperature at the bottom reaches the saturation temperature  $T_s$ . The branch  $AB$  corresponds to  $Q_b = 1$  and represents the onset of boiling before the onset of convection, while the branch  $BE$  represents the onset of boiling after convection already exists within a liquid-filled layer.

We consider experiments conducted on a porous medium with constant properties by varying the bottom heat flux. At low Ra (as indicated by line 1-1'), the liquid region is conductive before and after the onset of boiling. This is consistent with the experiments of Bau and Torrance (1982a) on low-permeability porous beds ( $K = 11 \times 10^{-12} \text{ m}^2$ ). At higher Ra (as indicated by line 2-2'), the liquid region is conductive before the onset of boiling but becomes convective

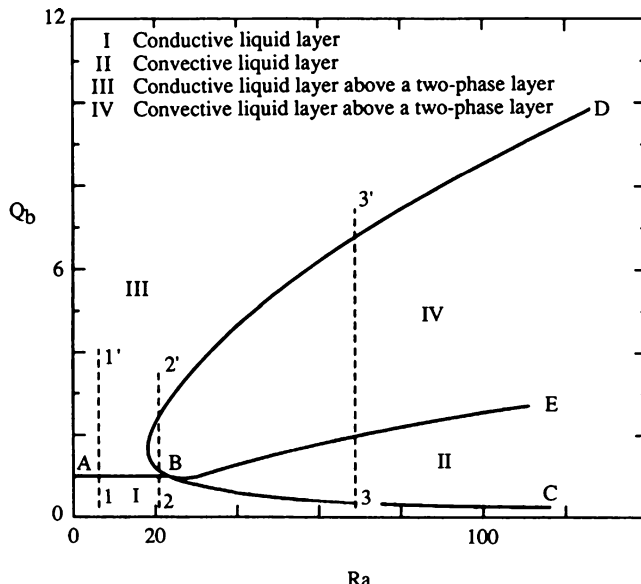


**Fig. 10.24** Map of conductive and convective solutions in  $(\text{Ra}, Q_b)$  parameter space for liquid-dominated two-phase systems, for the nondimensional wave number  $\alpha = \pi$  (Ramesh and Torrance 1990, with permission from Pergamon Press)

almost immediately when boiling starts, which is in agreement with the observations of Sondergeld and Turcotte (1977), ( $K = 70 \times 10^{-12} \text{ m}^2$ ). For large  $\text{Ra}$  (as indicated by line 3-3'), the liquid region becomes convective before the onset of boiling and stays convective after the onset of boiling, which is consistent with the experiments of Bau and Torrance (1982c) on high-permeability beds ( $K = 1600 \times 10^{-12} \text{ m}^2$ ). They observed that at large heat fluxes the liquid region reverts back to a conductive state, which is consistent with Fig. 10.24.

For vapor-dominated systems, the density difference between the liquid and two-phase regions is large, and as we noted above, we can expect gravitational instability to dominate over buoyancy effects. If the buoyancy effects are negligible ( $\text{Ra} = 0$ ), the stability diagram shown in Fig. 10.25 is obtained. This applies for water with  $T_0 = 30^\circ\text{C}$ ,  $T_s = 100^\circ\text{C}$ . For  $\alpha = \pi$ , the minimum value of  $\text{Ra}_{2\varphi}$  is 18.95, occurring for  $Q_b = 1.4$ .

The minimum value of  $S$  on the curve  $BD$  in Fig. 10.24 is approximately equal to 0.98. The maximum value of  $S$  on the curve in Fig. 10.25 is about 0.02. We conclude that if the rest-state value of  $S$  lies in the range 0.02 to 0.98, then the rest state is stable according to linear theory.

However, the numerical study of Ramesh and Torrance (1993) indicates that finite-amplitude instability is possible in this range. This study involved convection and boiling in a two-dimensional rectangular region with length-to-height aspect ratio equal to 2. In order to model experiments in a Hele-Shaw cell, a volumetric

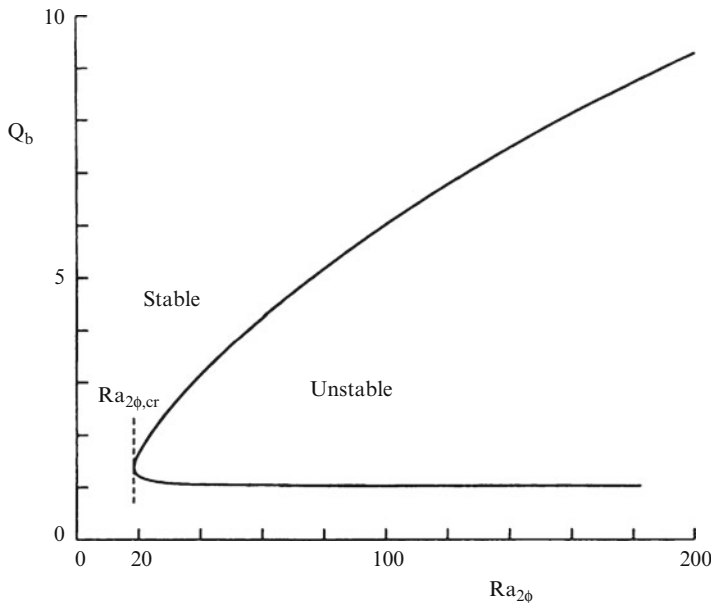


**Fig. 10.25** Neutral stability curve for vapor-dominated systems, for  $\text{Ra} = 0$ ,  $\alpha = \pi$  (Ramesh and Torrance 1990, with permission from Pergamon Press)

cooling term (to take account of heat losses from the front and back walls of the cell) was allowed for in equations for the temperature and saturation. The results indicate three solution regimes: conduction dominated, steady convection dominated, and oscillatory convection. In some cases, the solutions exhibit a dependence on initial conditions and perturbations. As Figure 10.26 indicates, the finite-amplitude solutions agree with the linear stability analysis.

Ramesh and Torrance (1993) also reported that their numerical results agree with prior laboratory experiments, including those of Echaniz (1984) on the oscillatory convection, which is observed for high-permeability beds (i.e., high  $\text{Ra}$ ). Such solutions are generated numerically for high  $\text{Ra}$  by introducing asymmetric perturbations into a one-dimensional initial conduction field (initial symmetric disturbances lead to steady-state solutions). The time period in oscillations decreases with increase of  $Q_b$ . Heat transfer rates are drastically increased by the onset of oscillatory convection. Echaniz (1984) concluded that the oscillations are caused by thermals (pairs of small vortices) that originate at the heating surface where the cold fluid descends, grows, and then disappears either at the top boundary or in the two-phase region.

Ramesh and Torrance (1993) also showed that when steady convection had its onset after the onset of boiling, the preferred computed convective mode is two cells symmetric about the centerline. The interface moves up as the heat flux is increased and is depressed in the center (indicating downflow of cold fluid there) and raised at the sides (or vice versa). The center of the cell lies in the liquid region,

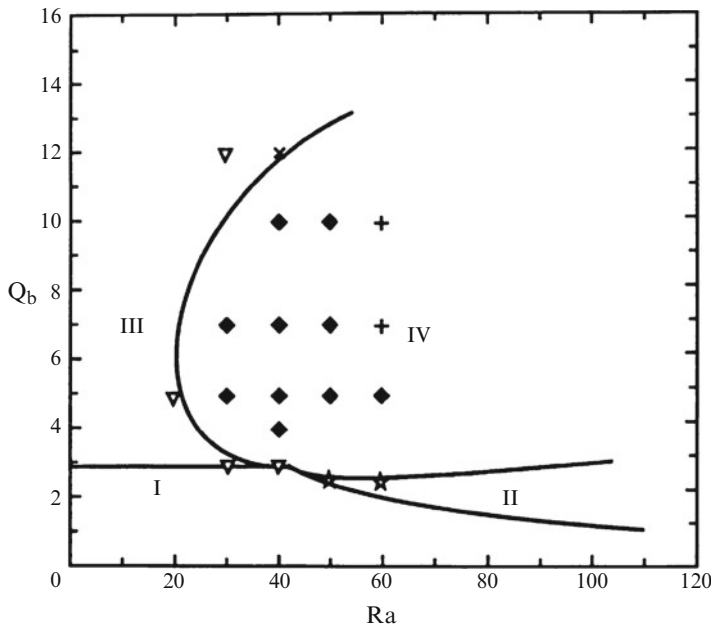


**Fig. 10.26** Comparison of numerical solutions (symbols) and linear stability theory (solid lines) in  $Ra$ - $Q_b$  parameter space. I, II, III, and IV denote four solution regimes: I, a conductive liquid layer—no boiling; II, a convective liquid layer—no boiling; III, a conductive liquid layer overlying a two-phase layer; IV, a convective liquid layer overlying a two-phase layer. The numerically observed solutions are as follows: square, steady convective liquid layer—no boiling; triangle, steady conductive liquid layer over a two-phase layer; solid diamond, steady convective liquid layer overlying a two-phase layer; addition symbol, steady or oscillatory convective liquid layer, overlying a two-phase layer; multiplication symbol, steady conductive or steady convective liquid layer overlying a two-phase layer (Ramesh and Torrance 1993, with permission from Cambridge University Press)

where the buoyancy production term is present. When the onset of convection precedes that of boiling, the stable two-cell convection pattern is retained after boiling if  $Ra$  is low, but at larger  $Ra$ , a transition from a two-cell to a four-cell structure occurs, in qualitative agreement with the experiment of Tewari (1982). [The stable three cells also observed by Tewari (1982), not replicated in the computations, may have been due to experimental nonuniformities.] The steady-state heat flux  $Q_{\text{top}}$  for the numerical two-cell solutions was found to vary with heat-flux Rayleigh number  $Ra_f$  ( $=Ra$   $Q_b$ ) according to  $Q_{\text{top}} \propto Ra_f^{0.6}$ , in approximate accord with the experimental correlation  $Nu \propto Ra_f^{0.5}$  reported by Echaniz (1984).

In connection with the testing of a new two-phase mixture model introduced by Wang and Beckermann (1993), Wang et al. (1994a, b) have made a numerical study of boiling in a layer of a capillary porous medium heated from below. Their numerical procedure employs a fixed grid and avoids tracking explicitly the moving interface between the liquid and two-phase regions. Also on the new mixture model, Wang and Beckermann (1995) performed a two-phase boundary layer analysis, and

Easterday et al. (1995) studied numerically and experimentally two-phase flow and heat transfer in a horizontal porous formation with horizontal water throughflow and partial heating from below. The latter found that the resulting two-phase structure and flow patterns are strongly dependent on the water inlet velocity and the bottom heat flux. They reported qualitative agreement between numerical and experimental results. Wang et al. (1994a) studied numerically transient natural convection and boiling in a square cavity heated from below. They observed boiling-induced natural convection, flow transition from a unicellular to a bicellular pattern with the onset of boiling, and flow hysteresis as the bottom heat flux first increases and then decreases. This subject has been reviewed by Wang (1998a). A numerical study of boiling with mixed convection in a vertical porous layer was made by Najjari and Ben Nasrallah (2002), while Najjari and Ben Nasrallah (2005) similarly studied the effect of aspect ratio on natural convection in a rectangular cavity. Najjari and Ben Nasrallah (2006, 2008) treated mixed convection in a discretely heated layer and the effects of latent heat storage on heat transfer in a forced flow in a layer. A three-dimensional simulation of phase-change heat transfer in an asymmetrically heated channel was carried out by Li et al. (2010b), while Li et al. (2010c, d) examined some transient situations. Li and Leong (2011) performed an experimental and numerical study of single and two-phase flow and heat transfer in aluminum foams. Damronglerd and Zhang (2006) studied transient fluid flow and heat transfer in a layer with partial heating and evaporation at the upper surface.

Stommelen et al. (1992) noted that large-amplitude oscillations are observed in a boiling porous medium with high heat fluxes, and they presented a simplified linear stability analysis that they carried out to determine the stability criterion.

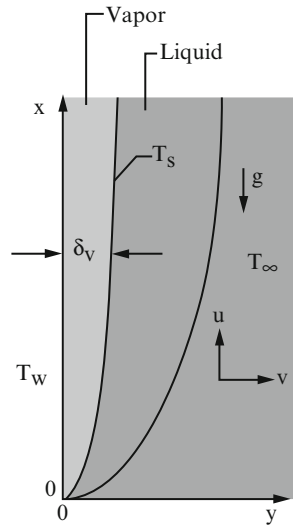
For discussion of some wider aspects of boiling and two-phase flow in porous media, the reader is referred to the reviews by Dhir (1994, 1997).

### **10.3.2 Film Boiling and Evaporation**

It was observed by Parmentier (1979) that, because of the nature of the  $(P,T)$  phase diagram, the thin film of water vapor that forms adjacent to a vertical surface is separated from the liquid water by a sharp interface with no mixed region in between. The assumption that the vapor and liquid form adjacent boundary layers (as in Fig. 10.26), with a stable smooth interface, is mathematically convenient and has been adopted in most theoretical studies of film boiling. In reality, the interface may be wavy or unsteady, due to the formation and detachment of bubbles.

If one assumes, following Cheng and Verma (1981), that the Oberbeck-Boussinesq approximation and Darcy's law are applicable and variables are defined as in Fig. 10.27, then the governing equations for the region saturated with superheated vapor (subscript  $v$ ),  $y < \delta_v$ , are

**Fig. 10.27** Definition sketch for film boiling



$$\frac{\partial u_v}{\partial x} + \frac{\partial v_v}{\partial y} = 0, \quad (10.76)$$

$$u_v = -\frac{K}{\mu} (\rho_v - \rho_\infty) g, \quad (10.77)$$

$$u_v \frac{\partial T_v}{\partial x} + v_v \frac{\partial T_v}{\partial y} = \alpha_m \frac{\partial^2 T_v}{\partial y^2}, \quad (10.78)$$

while those for the region filled with subcooled liquid (subscript *l*),  $y > \delta_v$ , are

$$\frac{\partial u_l}{\partial x} + \frac{\partial v_l}{\partial y} = 0, \quad (10.79)$$

$$u_l = \frac{\rho g \beta_{l\infty} K (T_l - T_\infty)}{\mu_l}, \quad (10.80)$$

$$u_l \frac{\partial T_l}{\partial x} + v_l \frac{\partial T_l}{\partial y} = \alpha_{ml} \frac{\partial^2 T_l}{\partial y^2}. \quad (10.81)$$

The boundary conditions are

$$y = 0 : \quad v_v = 0, \quad T_v = T_w, \quad (10.82)$$

$$y \rightarrow \infty : \quad u_l = 0, \quad T_l = T_\infty, \quad (10.83)$$

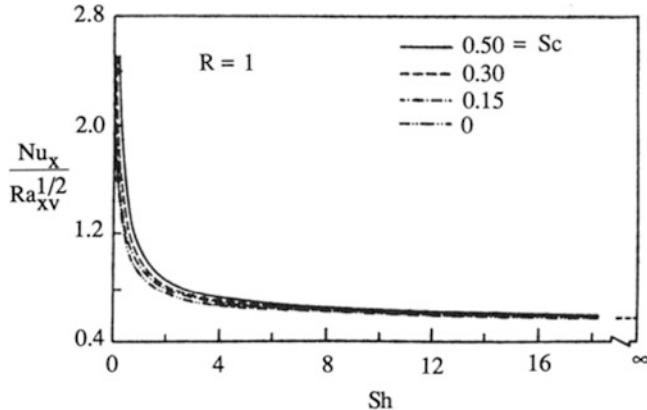


**Fig. 10.28** Heat transfer results for film boiling (Cheng and Verma 1981, with permission from Pergamon Press)

where the saturation temperature  $T_s$  satisfies  $T_w > T_s = T_\infty$ . At the vapor–liquid interface  $y = \delta_v$ , we have

$$T_v = T_s = T_l, \quad (10.84)$$

$$\rho_v \left( v_v - u_v \frac{d\delta_v}{dx} \right) = \rho_l \left( v_l - u_l \frac{d\delta_v}{dx} \right) = \dot{m}_\delta, \quad (10.85)$$

$$-k_{mv} \frac{\partial T_v}{\partial y} = \dot{m}_\delta h_{fv} - k_{ml} \frac{\partial T_l}{\partial y}, \quad (10.86)$$

where  $k_m$  is the effective thermal conductivity of the porous medium and  $h_{fv}$  is the latent heat of vaporization of the liquid at  $T_s$ . Equation (10.86) states that the energy crossing the interface is partly used to evaporate liquid at a rate  $\dot{m}_\delta$ .

We introduce the streamfunctions  $\Psi_v$ ,  $\Psi_l$  defined by

$$u_v = \frac{\partial \Psi_v}{\partial y}, \quad v_v = -\frac{\partial \Psi_v}{\partial x}, \quad (10.87)$$

$$u_l = \frac{\partial \Psi_l}{\partial y}, \quad v_l = -\frac{\partial \Psi_l}{\partial x}, \quad (10.88)$$

and the similarity variables defined by

$$\eta_v = (\text{Ra}_{xv})^{1/2} y/x, \quad \eta_l = (\text{Ra}_{xl})^{1/2} (y - \delta_v)/x, \quad (10.89)$$

$$\Psi_v = \alpha_{mv} (\text{Ra}_{xv})^{1/2} f_v(\eta_v), \quad \Psi_l = \alpha_{ml} (\text{Ra}_{xl})^{1/2} f_l(\eta_l), \quad (10.90)$$

$$T_v - T_s = (T_w - T_s) \theta_v(\eta_v), \quad T_l - T_s = (T_s - T_\infty) \theta_l(\eta_l), \quad (10.91)$$

where

$$\text{Ra}_{xv} = \frac{(\rho - \rho_v) g K x}{\mu_v \alpha_{mv}}, \quad \text{Ra}_{xl} = \frac{\rho g \beta_l K (T_s - T_\infty) x}{\mu_l \alpha_{ml}}. \quad (10.92)$$

We then have

$$f'_v = 1, \quad f'_l = \theta, \quad (10.93)$$

$$2\theta''_v + f_v \theta'_v = 0, \quad 2\theta''_l + f_l \theta'_l = 0, \quad (10.94)$$

$$f_v(0) = 0, \quad f'_l(\infty) = 0, \quad (10.95)$$

$$\theta_v(0) = 1, \quad \theta_l(\infty) = 0, \quad (10.96)$$

and at the interface, which is given by  $y = \delta_v$ , and therefore by

$$\eta_v = \eta_{v\delta} = \text{Ra}_{xv}^{1/2} \delta_v / x, \quad \eta_l = 0, \quad (10.97)$$

we have

$$\theta_v(\eta_{v\delta}) = 0, \quad \theta_l(0) = 0, \quad (10.98)$$

$$f_l(0) = -\frac{\dot{m}_\delta 2 x^{1/2}}{\rho [\alpha_{ml} \rho_\infty g \beta_l K (T_s - T_\infty) / \mu_l]^{1/2}} = \frac{R}{Sc^{1/2}} \eta_{v\delta}, \quad (10.99)$$

$$Sh \theta'_v(\eta_{v\delta}) = \frac{Sc^{3/2}}{R} \theta'_l(0) - \frac{\eta_{v\delta}}{2}. \quad (10.100)$$

Here,

$$Sc = c_{Pl} (T_s - T_\infty) / h_{fv}, \quad Sh = c_{Pv} (T_w - T_s) / h_{fv} \quad (10.101)$$

are “Jakob numbers” measuring, respectively, the degree of subcooling of the fluid and the superheating of the vapor, and  $R$  is defined by

$$R = \frac{\rho_v}{\rho_\infty} \left[ \frac{\mu_l \alpha_{mv} (\rho_\infty - \rho_v) c_{Pl}}{\mu_v \alpha_{ml} \rho_\infty \beta_l h_{fv}} \right]^{1/2}. \quad (10.102)$$

Equation (10.99), which is related to the rate of evaporation, determines  $\eta_{v\delta}$ . The remaining equations in  $f_v$ ,  $\theta_v$ ,  $f_l$ , and  $\theta_l$  constitute a sixth-order eigenvalue problem. Those in  $f_v$ ,  $\theta_v$  have the exact solution

$$f_v = \eta_v, \quad \theta_v = 1 - \frac{\operatorname{erf}(\eta_v/2)}{\operatorname{erf}(\eta_{v\delta}/2)}, \quad (10.103)$$

while those in  $f_l$ ,  $\theta_l$  reduce to the problem discussed in Chap. 5, Sect. 5.1.2 if the values of  $\eta_{v\delta}$ ,  $R$ , and  $Sc$  are prescribed.

We define the local Nusselt number  $Nu_x$  in terms of the wall heat flux  $q_w''$ , so

$$Nu_x = \frac{q_w'' x}{k_{mv} (T_w - T_s)}, \quad (10.104)$$

and then

$$\frac{Nu_x}{Ra_{xv}^{1/2}} = -\theta'_v(0) = \frac{1}{\pi^{1/2} \operatorname{erf}(\eta_{v\delta}/2)}. \quad (10.105)$$

The value of  $\theta'_v(0)$  can be obtained numerically, and results are shown in Fig. 10.27. In particular, we have the asymptotic result

$$\frac{Nu_x}{Ra_{xv}^{1/2}} \rightarrow 0.564 \text{ as } Sh \rightarrow \infty. \quad (10.106)$$

Results for other geometrical configurations are readily attained (Cheng et al. 1982). For example, for a horizontal cylinder of diameter  $D$ , we have Eq. (5.120), modified by the replacement of the coefficient 0.628 with the expression  $2^{1/2}[-\theta'_v(0)]$ . Likewise, Eq. (5.122), similarly modified, applies for a sphere of diameter  $D$ . For a cone of half-angle  $\alpha$  with axis vertical and vertex downward,

$$\frac{Nu_x}{Ra_{xv}^{1/2}} = 3^{1/2} [-\theta'_v(0)], \quad (10.107)$$

where now  $g \cos \alpha$  replaces  $g$  in the definition of  $Ra_{xv}$ , while for a wedge, the same applies except that the factor  $3^{1/2}$  is absent.

Nakayama et al. (1987) have extended the boundary layer theory to general two-dimensional and axisymmetric bodies. They show that an accurate approximate formula is

$$\frac{Nu_x}{(Ra/I)^{1/2}} = \left\{ \pi^{-1} + \left[ \left( 2Sh + \left( 0.444 \frac{Sc}{R_n} \right)^2 \right)^{1/2} - 0.444 \frac{Sc}{R_n} \right]^{-2} \right\}^{1/2}, \quad (10.108)$$

where

$$R_n = \frac{\rho_v \alpha_{mv}}{\rho_l \alpha_{ml}} \left[ \frac{\alpha_{ml} v_l (\rho_l - \rho_v)}{\alpha_{mv} v_v \rho_v \beta_v (T_s - T_\infty)} \right]^{1/2}, \quad (10.109)$$

$$I(x) = \frac{\int_0^x g_x r^*{}^2 dx}{g_x r^*{}^2 x}, \quad (10.110)$$

$$r^* = \begin{cases} 1 & \text{for plane flow,} \\ r(x) & \text{for axisymmetric flow,} \end{cases} \quad (10.111)$$

$$g_x = g \left[ 1 - \left( \frac{dr}{dx} \right)^2 \right]^{1/2}. \quad (10.112)$$

Here,  $r(x)$  defines the surface, where  $x$  is measured along the surface from a stagnation point. Thus, for example,  $I = 1$  for a vertical plate and  $I = 1/3$  for a vertical cone pointing downward.

Subcooled forced convection film boiling over a vertical plate was analyzed by Nakayama and Koyama (1988b), and similarity solutions for the vertical plate, horizontal circular cylinder, and sphere were found by Nakayama and Koyama (1988a). A theoretical and experimental study of film boiling over a sphere or a horizontal cylinder was performed by Orozco et al. (1988). Film boiling of a binary mixture over a vertical plate was studied analytically and experimentally (with good agreement between the results) by Essome and Orozco (1991). A theoretical study of mixed convection film boiling of a binary mixture over a horizontal cylinder was reported by Orozco and Zhu (1993). The effect of liquid evaporation on mixed convection from a vertical plate was treated by Shih et al. (2005). A mixed convection problem with a non-Newtonian fluid was studied by Shih et al. (2008).

Heat and mass transfer together were studied by Leu et al. (2006, 2009), while Leu et al. (2011) examined non-Darcy effects and inlet conditions on forced convection.

An analytical study was made by Kokubun and Fachini (2012) of Hiemenz (stagnation point) flow with the aim of modeling heat supplied to a low-volatility fluid in a porous medium by a hot impinging gas, something applicable to the steam injection process for oil recovery. They included the effect of local thermal nonequilibrium required by their assumption of high rates of heat transfer between gas and solid and between liquid and solid. They thus extended the previous study (with thermal equilibrium) by Zhao (1999).

## 10.4 Condensation

Several authors have used a one-dimensional model to analyze condensation in porous media. For example, Vafai and Sarkar (1986, 1987) have reported a transient analysis of moisture migration and condensation in porous and partially porous enclosures, and Sözen and Vafai (1990) have analyzed the transient forced convective condensing flow of a gas through a packed bed, with quadratic drag effects incorporated. A two-dimensional transient model was employed by Vafai and Whitaker (1986) to study the accumulation and migration of moisture in an insulation material; this involved a porous slab.

The only problem that has been studied in depth is that of film condensation. This problem is analogous to that of film boiling, discussed in the previous section. The roles of the liquid and the vapor are reversed, and heating is replaced by cooling, but the mathematical analysis is the same provided that the liquid/vapor interface remains sharp, that is, there is no intervening two-phase region, provided that capillary effects are negligible. In the literature, the analysis has been developed in parallel with that discussed in Chap. 5. Hence, our discussion will be brief.

The original study by Cheng (1981b) for steady condensation outside a wedge or cone embedded in a porous medium filled with a dry saturated vapor was extended by Cheng and Chui (1984) to the transient situation. Liu et al. (1984) extended the analysis to treat general two-dimensional and axisymmetric bodies and to allow for the effect of lateral mass flux.

White and Tien (1987) employed the Brinkman equation to account for boundary friction and also the effect of variable porosity at the wall. Lai and Kulacki (1989b) allowed for the effect of temperature-dependent viscosity; this can significantly increase the heat transfer rate if the wall temperature is close to the saturation temperature. Ebinuma and Nakayama (1990a, b, 1997) have included the effect of quadratic drag for the transient problem (the additional drag increases the time required to reach the steady state) and the transient problem with lateral mass flux. Li and Wang (1998) investigated analytically the influence of an effective thermal conductivity change adjacent to the cooling wall. The effect of a transient suction effect at the porous layer interface was studied by Ma and Wang (1998). The effect of suction on condensation on a finite-sized horizontal flat medium was studied theoretically by Wang et al. (2003d). A further study incorporating non-Darcian effects was reported by Masoud et al. (2000).

The effects of surface tension on film condensation were analyzed by Majumdar and Tien (1990a, b). Now, the thermodynamics of phase equilibria requires the existence of a two-phase zone lying between the liquid and vapor regions. In this zone, solutions of the conservation equations indicate a boundary layer profile for the capillary pressure. Majumdar and Tien considered various models for the boundary conditions. They concluded that the best results are attained if one assumes that there is no shear at the interface between liquid and the two-phase zone. Results obtained using this model are shown in Fig. 10.29. The parameter  $R_\sigma$ , the Rayleigh number  $\text{Ra}$ , and the Jakob number  $\text{Ja}$  are defined here by

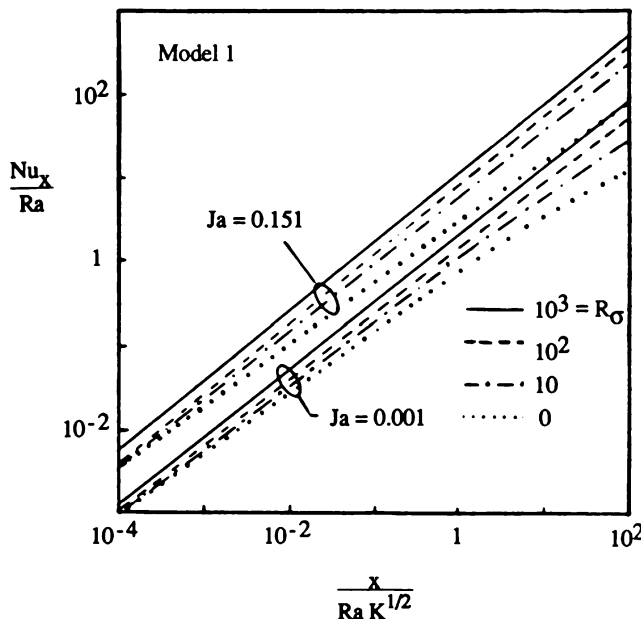


**Fig. 10.29** Heat transfer results for film condensation (Majumdar and Tien 1990a, b)

$$\begin{aligned}
 R_\sigma &= \frac{\sigma^* (K \varphi)^{1/2}}{\mu_l \alpha_m}, & Ra &= \frac{g (\rho_l - \rho_v) K^{3/2}}{\mu_l \alpha_m}, \\
 Ja &= \frac{c_p (T_s - T_w)}{h_f g}, & &
 \end{aligned} \tag{10.113}$$

where  $\sigma^*$  is the surface tension and the other quantities are as in Sect. 10.3.2.

Condensation on a vertical surface was investigated experimentally and numerically by Chung et al. (1992). Their numerical model assumed a distinct two-phase zone existing between liquid and vapor zones and included the effect of vapor flow in that two-phase zone. Their experiments were performed for steam condensing in packed beds of glass beads of three different sizes. They reported good agreement between numerical and experimental results. They found that the calculated liquid film thicknesses are of the order of the diameter of the glass beads.

Nakayama (1991) used the Forchheimer model in his analytical treatment of film condensation in the presence of both gravity and externally forced flow. He introduced a similarity transformation involving a modified Péclet number based on the resultant velocity of the condensate. Microscale Grashof and Reynolds numbers based on the square root of the permeability govern the delineation of four limiting regions, namely, (1) Darcy forced convection, (2) Forchheimer forced convection, (3) Darcy natural convection, and (4) Forchheimer natural convection.

An experimental and numerical investigation on the Brinkman model of condensation of a downward flowing vapor on a horizontal cylinder embedded in a vapor-saturated porous medium was carried out by Orozco (1992). Good agreement was found between predicted and measured values of Nu and condensate thickness.

Renken and Aboye (1993a,b) have reported numerical and experimental studies of film condensation within thin inclined porous coatings. The experiments involved a condensate region overlaying metallic permeable coating adhered to an isothermal copper block. Reduced gravity measurements were obtained by condensing saturated steam containing small concentrations of noncondensables on surfaces with effective body forces between 0.3 and 1 g. They also investigated the effects of surface subcooling. The presence of the coating enhanced the heat transfer substantially. The previous work of Renken et al. (1989) involved a numerical study of a porous coating on a vertical surface. The subsequent work by Renken et al. (1994) involved further numerical investigation on the Brinkman-Forchheimer model or coatings on inclined surfaces. Experiments on forced convection past porous coatings placed parallel to saturated steam flow were reported by Renkin and Raich (1996).

Wang and Beckermann (1995) performed a two-phase boundary layer analysis based on a two-phase mixture model for buoyancy-driven two-phase flow (condensing or boiling) in capillary porous media. They used the solution to reveal the capillary effect.

For film condensation on a vertical plate, Al-Nimr and Alkam (1997a) obtained closed-form expressions for the condensate film thickness and flow rate and for the convective heat transfer coefficient. They found that the liquid film thickness is proportional to  $x^{1/4}$  in a thin porous domain as the permeability tends to infinity, but it is proportional to  $x^{1/2}$  in a thick porous domain as the permeability tends to zero. Masoud et al. (2000) extended this analysis to a transient problem. The effect of thermal dispersion was studied by Asbik et al. (2007).

Char and Lin (2001) and Char et al. (2001) treated conjugate film condensation in natural and mixed convection between two porous media separated by a vertical plate. Further conjugate problems were studied by Mosaad (1999) and Bautista et al. (2008). Heat and mass transfer with condensation in a fibrous insulation slab was studied experimentally and analytically by Murata (1995). Forced convection film condensation on a vertical porous-layer-coated surface was studied analytically by Toda et al. (1998) and by Asbik et al. (2003). Entropy generation was studied by Bin-Mansoor et al. (2005).

## 10.5 Spaces Filled with Fluid and Fibers Coated with a Phase-Change Material

It has been shown that polyethylene glycols (polyols) can be bonded stably on fibrous materials and that the resulting composites—the “thermally active” fibers—exhibit reproducible energy storage and release properties (e.g., Vigo and Bruno

1987). The energy storage and release is due to the large latent heat of melting and crystallization of the polyols affixed to the fibers. A fundamental model for heat transfer through a space filled with polyol-coated fibers surrounded by air was described by Lim et al. (1993), who also reviewed the applications of this new class of materials. In this model, the fibers *and* the phase-change material (polyol, liquid or solid) constitute the matrix of the porous medium, while air is the fluid that flows through the interstitial spaces.

It is worth noting that this model differs fundamentally from the one used in earlier studies of melting and solidification in porous media (e.g., Sect. 10.1.1). In the earlier studies, the melted phase-change material was the fluid that filled the pores, and therefore, there was no flow through regions saturated with solid phase-change material. In the model for spaces filled with thermally active fibers, the fluid (air) flows through the entire matrix regardless of whether the polyol coatings are liquid or solid.

The model of Lim et al. (1993) is based on the homogeneous porous medium and local thermal equilibrium assumptions. The composition of the porous medium is described by the porosity,  $\varphi$  (about 80 %), and the fraction of the matrix occupied by polyol,  $\varepsilon$  (about 20 %). This means that a unit volume is distributed in the following proportions:  $\varphi = \text{air}$ ,  $(1 - \varphi) = \text{matrix (fibers and polyol)}$ ,  $(1 - \varphi)\varepsilon = \text{polyol}$ , and  $(1 - \varphi)(1 - \varepsilon) = \text{fibers}$ . The average heat capacity of the porous medium is

$$(\rho c)_m = \varphi (\rho c_P)_a + (1 - \varphi) [\varepsilon (\rho c)_P + (1 - \varepsilon) (\rho c)_f], \quad (10.114)$$

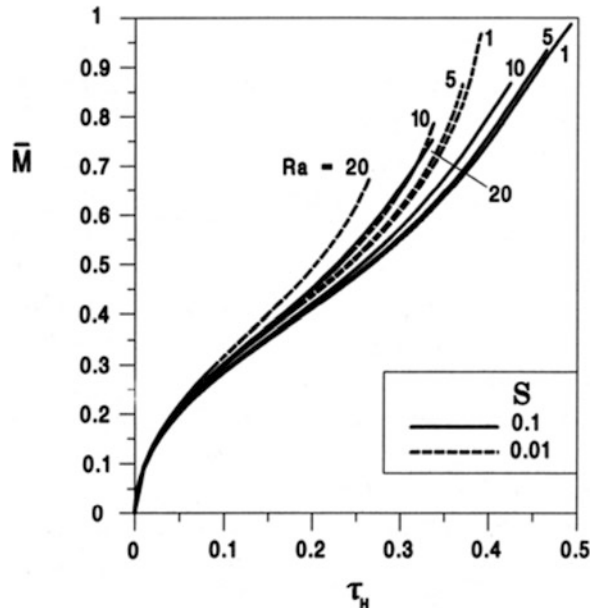
in which the subscripts  $m$ ,  $a$ ,  $p$ , and  $f$  refer to the averaged porous medium, air, polyol, and fibers.

Lim et al. (1993) applied the model to melting and freezing in three configurations, which were analyzed numerically: one-dimensional conduction, one-dimensional convection, and two-dimensional natural convection due to heating or cooling from the side. In each case, the focus was on the relation between the time of complete melting or solidification of the polyol coatings and the various dimensions and external parameters of the enclosure. For example, in a two-dimensional space with time-dependent melting by natural convection (Fig. 10.1), the time-dependent flow and heat transfer is ruled by four independent groups:  $\text{Ra} = g\beta KH(T_h - T_i)/\nu\alpha_m$ ,  $H/L$ ,  $S = (1 - \varphi)\varepsilon \rho_p\lambda/(\rho c)_m(T_h - T_i)$ , and  $\theta_m = (T_m - T_i)/(T_h - T_i)$  where  $T_h$ ,  $T_i$ ,  $T_m$ , and  $\lambda$  are the temperature of the heated sidewall, the uniform initial temperature of the system, the melting temperature, and the latent heat of melting. Note that in the corresponding configuration of Sect. 10.1.1, the phenomenon was described by only two independent groups,  $\text{Ra}$  and  $H/L$ .

The shape and evolution of the melting front has the same features as in Fig. 10.2. Several effects are presented in condensed form in Fig. 10.30, which shows the average position of the melting front

$$\overline{M}(\tau_H) = \frac{1}{H} \int_0^H \frac{s}{L} dy \quad (10.115)$$

**Fig. 10.30** The effect of Ra and the latent heat on the evolution of the average melting front position in a space filled with fibers coated by a phase-change material (Lim et al. 1993)



versus the dimensionless time  $\tau_H = \alpha_m t / \sigma H^2$ , where  $\sigma$  is the heat capacity ratio  $\sigma = (\rho c)_m / (\rho C_P)_a$ . The dimensions  $s(y, t)$ ,  $H$ , and  $L$  are defined in Fig. 10.1. Each of the curves plotted in Fig. 10.30 is terminated at the time when the melting front has traveled the distance  $L$  along the top of the enclosure. The inflection of each curve is considerably more pronounced than in Fig. 10.6.

The effect of the latent heat parameter  $S$  is also shown in Fig. 10.30. A larger latent heat (larger  $S$ ) means a longer time until the coating melts on the fibers located the farthest from the heated wall. The melting times decrease sensibly as the Rayleigh number becomes greater than approximately 5. The effects of changing  $\theta_m$  and  $H/L$  are further documented in Lim et al. (1993).

The solidification process in the same two-dimensional configuration is analogous to the melting process discussed until now. In solidification, the  $H \times L$  region is initially isothermal ( $T_i$ ), and all the fibers are coated with liquid polyol,  $T_i > T_m$ . The temperature of one of the sidewalls is lowered suddenly to  $T_c$ , which is lower than  $T_m$ . The movement of the solidification front is similar to that of Fig. 10.2: the shape of the front can be visualized by imagining the mirror image of Fig. 10.2, where the role of mirror is played by one of the horizontal walls. Figure 10.30 continues to be valid subject to the new definitions  $\text{Ra} = \gamma \beta K H (T_i - T_c) / v \alpha_m$  and  $\theta_m = (T_i - T_m) / (T_i - T_c)$ .

Further work on convection in composite systems with phase-change material has been performed by Mbaye and Bilgen (2006) and Nayak et al. (2006).

# Chapter 11

## Geophysical Aspects

Most of the studies of convection in porous media published before 1970 were motivated by geophysical applications, and many published since have geophysical ramifications; see, for example, the reviews by Cheng (1978, 1985b). On the other hand, geothermal reservoir modeling involves several features that are outside the scope of this book. Relevant reviews include those by Donaldson (1982), Grant (1983), O’Sullivan (1985a), Bodvarsson et al. (1986), Bjornsson and Stefansson (1987), McKibbin (1998, 2005), and O’Sullivan et al. (2000, 2001). An important book dealing with geological fluid dynamics is that by Phillips (2009). In this book, the emphasis is on flow patterns and specifically geological processes, involving dissolution, chemical reaction, and deposition. Some examples are discussed below in Sect. 11.12.

In this chapter, we discuss a number of topics that involve additional physical processes or have led to theoretical developments beyond those that we have already covered.

### 11.1 Snow

It is not uncommon for an unstable air density gradient to be found in a dry snow cover, because the base is often warmer than the upper surface. The geothermal heat flux, the heat release due to seasonal lag, and the release of heat if the soil freezes are factors that tend to keep the bottom boundary of a snow cover near 0°C. In contrast, the upper boundary is usually near the ambient air temperature, which in cold climates can be below 0 °C for long periods of time.

When the unstable air density gradient within the snow becomes sufficiently great, convection occurs, and the rate of transport of both heat and vapor increases, and the snow undergoes metamorphosis. For example, a strong vertical temperature gradient favors the growth of ice particles. These may grow to 1 or 2 cm in diameter. As the particles increase in size, their number decreases so rapidly that the density of the snow decreases, relative to that in the absence of a temperature gradient.

At the same time, there is a change in the shape of ice crystals. The strength of the snow against shear stresses is lowered, and on sloping terrain, this can lead to slab avalanches.

Thermal convection has been observed in snow both in laboratory experiments and in the field. These experiments indicate that natural convection should be fairly common under subarctic conditions.

The particular feature of convection in snow that distinguishes it from convection in other porous media is the fact that the energy balance is significantly affected by the phase change due to the transport of water vapor from particle to particle in snow. This has been studied by Palm and Tveitereid (1979). Their analysis was refined by Powers et al. (1985). The latter assume that the Boussinesq approximation is valid and that the equation of state for vapor at saturation can be taken as

$$\rho_v = \rho_0 \exp[B(T - T_0)]. \quad (11.1)$$

The heat flux is incremented by  $L\mathbf{j}_v$ , where  $L$  is the latent heat and  $\mathbf{j}_v$  is the diffusive flux of vapor, given by  $\mathbf{j}_v = -D_{\text{eff}}\nabla\rho_v$  where  $D_{\text{eff}}$  is an effective mass diffusivity. At the same time, there is an additional energy transport term resulting from the convection of vapor (for details, see Powers et al. 1985). As a consequence, one ends up with an energy equation in the form

$$[L\rho_v B + (\rho c_p)_a] \mathbf{v} \cdot \nabla T = \nabla \cdot [(k_m + LD_{\text{eff}}\rho_v B) \nabla T], \quad (11.2)$$

where the subscript  $a$  denotes air and  $\mathbf{v}$  is the mass-averaged seepage velocity (which is approximately equal to the air velocity because the density of vapor is much less than that of air). If the various coefficients in Eq. (11.2) can be approximated by constant values, this takes the form

$$\mathbf{v} \cdot \nabla T = \alpha_e \nabla^2 T, \quad (11.3)$$

where

$$\alpha_e = \alpha_m \left( \frac{1 + \gamma}{1 + a\gamma} \right), \quad (11.4)$$

where in turn

$$\alpha_m = \frac{k_m}{(\rho c_p)_a}, \gamma = \frac{LD_{\text{eff}}}{k_m} \left( \frac{d\rho_v}{dT} \right), a = \frac{\alpha}{D_{\text{eff}}}. \quad (11.5)$$

We see that the primary effect of the diffusion of water vapor (which arises from the variation of saturation vapor density with temperature) is to change the value of the effective thermal diffusivity.

To Eq. (11.3), we can add the equations of continuity, momentum, and state:

$$\nabla \cdot \mathbf{v} = 0, \quad (11.6)$$

$$-\nabla P - \frac{\mu}{K} \mathbf{v} + \rho_a \mathbf{g} = 0, \quad (11.7)$$

$$\rho_a = \rho_0 [1 - \beta(T - T_0)], \quad (11.8)$$

and appropriate boundary conditions to formulate a variant of the Horton-Rogers-Lapwood problem. Powers et al. (1985) solved this system for the two-dimensional case using finite differences and calculated the heat transfer for Rayleigh numbers just above critical. They treated various types of boundary conditions, and they briefly discussed the case of inclined layers.

We note that the effect of water vapor is destabilizing if  $\alpha > 1$  and stabilizing if  $\alpha < 1$ . In practice, the value of  $\alpha$  can vary widely, but typical values are in the range of 0.5–2. This means that the critical Rayleigh number is in the range 25–35 for the case of an isothermal permeable top and an isothermal impermeable bottom boundary.

Sommerfeld and Rocchio (1993) reported experiments on the permeability of snow. They noted that while calculated Rayleigh numbers have exceeded those thought critical for natural convection in snow, field experiments by Sturm and Johnson (1991) indicate that extreme thermal gradients are necessary for even intermittent convection. Sturm and Johnson, however, concluded that convection occurred almost continuously during two of the three winters during which they made their experiments.

Comparing the results of a numerical model with a field experiment where air was forced through a natural snowpack, Albert (1995) concluded that the airflow through the pack was sufficient to produce advection-dominated heat transfer throughout most of the pack. Aspects of the convective instability of air in snow cover treated as a two-layered system were discussed by Zhekamukhov and Zhekamukhova (2002). A nonequilibrium treatment of heat and mass transfer in alpine snowcovers was reported by Bartelt et al. (2004).

## 11.2 Patterned Ground

There are many places in arctic or mountainous regions where the surface of the ground takes the form of a regular pattern of circles, stripes, or polygons. These are made prominent because of the segregation of stones and fines resulting from diurnal, seasonal, or other recurrent freeze-thaw cycles in water-saturated soils. These patterns also are found underwater, in shallow lakes, or near shores. The diameter of sorted polygons may vary from 0.1 to 10 m. A variety of photographs is included in the article by Krantz et al. (1988).

When frozen soil thaws, the potential for convection exists because of the density inversion for water between 0 and 4 °C. More dense water at a few degrees above its freezing point can overlie less dense water at 0 °C. But convection currents alone are too weak to move either the stones or the soil.

Ray et al. (1983) provided the following explanation of the formation of patterned ground. Once gravitationally induced convection occurs, it typically forms hexagonal cells in horizontal ground and roll cells or helical coils in sloped terrain. These regular cellular flow patterns can then be impressed on the underlying ice front, because in areas of downflow, the warmer descending water causes extra melting, whereas in areas of upflow, the rising cooler water hinders melting of the ice front. Consequently, the ice level is lowered under descending currents and raised over ascending currents, relative to the mean level. Thus, a pattern of regularly spaced peaks and troughs is formed on the underlying ice front that mirrors the cellular convection patterns in the thawed layer. This pattern is transferred to the ground surface through the process of mechanisms such as frost push or frost pull. The width of the flow cell at the onset of convection then determines the width  $W$  of the observed stone patterns. The height  $H$  of the thawed layer at the onset of convection is assumed to correspond to the sorting depth  $D$ . Linear instability theory thus predicts the value of  $W/D$ . This tallies well with observations (Gleason et al. 1986). The model also provides an explanation for the transition from polygons on horizontal ground to stripes on sloped terrain.

The direction of fluid circulation determines whether the stones concentrate over the ice troughs or peaks. Gleason et al. (1986) report results of weakly nonlinear stability theory that shows that under most conditions, the determining temperature-dependent property for convection arising from thawing frozen soil is the coefficient of thermal expansion. This decreases from  $3.5 \times 10^{-5}$  per degree Celsius to zero as the temperature increases from 0 to 4 °C, and this decrease implies cell circulation with upflow in the cell center and downflow along the polygonal borders. The underlying ice front then should have isolated ice peaks and continuous polygonal troughs. If stones tend to concentrate over troughs during sorting, this would lead to stone-bordered polygons. In fact these are the most frequently observed patterns. If kinematic viscosity were the dominant temperature-dependent property, then the decrease in kinematic viscosity as the temperature increases would imply the opposite direction of circulation, and this would lead to stone pits. These are occasionally observed.

Rock conducts heat better than soil does. Thus, if in the freeze following the thaw period wherein the convection was initiated, the sorting process moves some stones over the convection-induced ice troughs, then during the next thaw period, the conductive heat transfer will be largest in precisely those regions. Thus, heat conduction will act to accentuate the previous pattern.

George et al. (1989) state that three conditions are believed to be essential for the formation of stone polygons: the existence of freeze-thaw cycles within the soil, the saturation of the soil with water for at least part of the year, and the presence of an impermeable ice barrier underlying the active layer. Once these conditions are satisfied, the formation of polygonal ground follows a five-step process. Stone polygons have been grown in the laboratory by reproducing these five steps, namely, (1) permeability enhancement as the result of the formation of needle ice and frost heaving in the soil, (2) onset of buoyancy-driven convection in the water-saturated soil, (3) formation of a tessellated surface in the permafrost, (4) genesis of polygonal ground through frost heaving, and (5) perpetuation of the hexagonal pattern.

Gleason et al. (1986) claimed that the two forms of convection cells that can occur in sloped terrain have widely different width-to-depth ratios, 2.7 for two-dimensional rolls (which occur for small downslope flow) and 3.8 for helical coils (which occur for large downslope flow). They have not published the analysis that leads to these values. We would expect the values to be practically the same. The value 2.7 would correspond to an impermeable conducting bottom and a permeable conducting top surface.

George et al. (1989) also have extended the theoretical analysis of the onset of convection in several respects. Whereas Ray et al. (1983) approximated the density vs. temperature relationship by a linear expression, George et al. (1989) worked with a more accurate parabolic expression. George et al. (1989) also allowed for a permeability that varies linearly with depth, and they contributed a nonlinear analysis based on the method of energy. They found that their theoretical predictions of  $W/D$  agreed well with field studies when a constant-flux condition is imposed at the upper boundary and an upwardly stratified permeability is chosen. Theoretical extensions to include the effects of solar radiation, phase change, cubic density law, and overlying water have been made by McKay (1992, 1996) and McKay and Straughan (1991, 1993), respectively. In particular, McKay (1992) presented a linear analysis involving Floquet theory, a nonlinear energy analysis, and extensive numerical results.

Experimental work together with the results of a theoretical investigation of heterogeneity effects was reported by Zimmerman et al. (1998). The mathematical aspects of the pattern formation were emphasized in the review by Straughan (2004b). The self-organization aspect of the phenomenon was discussed by Kessler and Werner (2003)

## 11.3 Thawing Subsea Permafrost

During the ice age (18,000 years ago), the sea level was some 100 m lower than it is at present, and the lower ambient temperatures led to substantial permafrost forming around arctic shores. With the rise of sea levels, the permafrost has responded to the relatively warm and salty sea, which has created a thawing front and a layer of salty sediments beneath the seabed. Those off the coast of Alaska have been extensively studied. It is believed that convection is taking place in the layer between the seabed and the permafrost. (This belief is based on the fact that although conduction appears to be the dominant heat transfer mechanism, the molecular diffusion of salt is too slow to explain the observed rate of thawed layer development. Also the salinity Rayleigh number is supercritical, salinity gradients in the thawed layer are small except for a boundary layer near the bottom, and the pure water pressure is different from hydrostatic.) A buoyancy mechanism is provided by the release of relatively fresh and therefore buoyant water liberated by thawing at the base of the layer.

The analysis of Swift and Harrison (1984) is of interest because of the way in which they were able to replace a moving boundary (Stefan) problem with one essentially on a fixed domain, using the facts that the convection is salt dominated and the climatic interface advance is slow (2–5 cm/year). The argument is as follows.

On the moving boundary  $z = D$ , Stefan conditions hold for the temperature and salinity fields. At  $z = D$ ,

$$L_V \frac{dD}{dt} = -k_m \frac{\partial T}{\partial z} \Big|_{D-} \quad \text{and} \quad S(D) \frac{dD}{dt} = -\alpha_s \frac{\partial S}{\partial z} \Big|_{D-}, \quad (11.9a, b)$$

where  $S$  is the salinity,  $k_m$  the thermal conductivity,  $L_V$  is the latent heat per unit volume of the salty thawed layer, and  $\alpha_s$  is the diffusivity of salt. Because salinity is the driving mechanism, the temperature profile can be assumed linear throughout, and hence, the temperature gradient can be replaced by  $[T(D) - T_0]/D$ , where  $T_0$  is the seabed temperature. The requirement for phase equilibrium is that  $S(D)$  is proportional to  $T(D)$ , and so we can write  $S(D)/S_r = T(D)/T_0$ , where  $S_r$  is the salinity of water that would begin to freeze at temperature  $T_0$ . Here  $T(D) < T_0 < 0$ , and so  $S(D) > S_r$ . Now  $dD/dt$  can be eliminated from Eqs. (11.9a) and (11.9b), and we end up with the nonlinear boundary condition:

$$\frac{\partial S}{\partial z} = \frac{k_m T_0}{L_v \alpha_s D} S \left( \frac{S}{S_r} - 1 \right) \quad \text{at } z = D. \quad (11.10)$$

The other boundary conditions are the usual ones, and the problem is reduced to a standard linear stability problem on a fixed domain.

Swift and Harrison (1984) went on to solve this problem numerically for solute Rayleigh numbers 1,750 and 17,500 (which we recall are well in excess of the critical value for the onset of convection, which is about 40). Galdi et al. (1987) reexamined this problem, using both linear and nonlinear analysis. They used an energy method to determine a critical Rayleigh number below which convection cannot develop. Payne et al. (1988) also have applied an energy method to this problem. They assumed that the downward permafrost interface movement is negligible, and they allowed the density to vary quadratically with temperature.

Subsequent studies have shown that salt fingering may play a major role in the thawing of the permafrost. The salt gradient is produced partly by salts rejected during sea ice growth producing concentrated brine near the seabed and partly by salts rejected during sediment freezing near the seabed causing the formation of a concentrated brine layer within the deeper and yet unfrozen sediments. Gosink and Baker (1990) report theoretical, laboratory, and field investigations. The theoretical ones are based on timescale balances related to the result of Wooding (1959) that convective instability in the form of fingering takes place when the magnitude of the salinity Rayleigh number exceeds a certain critical value (3.390 in the case of a vertical cylinder, the Rayleigh number being based on the radius of the cylinder;

compare Sect. 6.16.1). The results of Gosink and Baker suggest that downward salt fingering will occur at Prudhoe Bay whenever the density gradient in the thawed subsea sediments exceeds  $6.2 < 10^{-5} \text{ g cm}^{-4}$ . The maximum predicted velocity of fingering is about 2 m/day, and this is consistent with estimates made from measurements of pressure gradients and numerical modeling in the thawing permafrost. The energy dissipated by viscous force in the thawed layer balances the energy added to the layer by the salt fingers caused by concentrated brines at the seabed.

Hutter and Straughan (1997) have employed a realistic equation of state and have imposed a linear temperature gradient. For this case, they have developed linear and fully nonlinear stability analyses. They found that the refinements to the equation of state led to a reduction in critical Rayleigh number. An unconditional nonlinear stability bound (close to that of linear theory) was found by Budu (2001). A further study was carried out by Hutter and Straughan (1999). Their multiscale perturbation analysis verified the observed thaw rates with a parabolic-in-time phase boundary retreat and enabled an investigation of possible currents induced by the ocean circulation overlying the thawed permafrost layer. Their analysis indicates that the phase boundary beneath the seabed and below the thawing layer has a parabolic shape, something that is observed in practice. The topic of this section has been reviewed by Straughan (2004b), who concludes that the nonlinear stability thresholds will be extremely close to the linear instability ones for any practical choice of the density equation of state.

## 11.4 Magma Production and Magma Chambers

In general, the flow of magma can be treated like that of a viscous fluid subject to the Navier–Stokes equation, but there are two situations where Darcy’s equation is applicable. The first is when crystallization leads to a porous structure near the walls of a magma chamber. The second is when a partial melt is formed during magma genesis and the melt products tend to concentrate along interconnected grain boundaries. Lowell (1985) has applied double-diffusive stability analysis to each of these situations.

The partial melt problem involves a layer whose thickness varies with time, and so the associated boundary condition is of Stefan type. Lowell (1985) obtains an approximate expression for the critical thermal Rayleigh number

$$Ra_C = 4\pi^2 \left( 1 - \frac{Q^2}{2\pi^2} \right), \quad (11.11)$$

where  $Q$  is determined as the root of

$$\pi^{1/2} Q \operatorname{erf}(Q) \exp(Q^2) = \operatorname{Ste}, \quad (11.12)$$

where the Stefan (or Jakob) number  $\text{Ste} = \Delta T c_p / \varphi L_h$ . Here  $\Delta T$  is the difference between the basal temperature of the layer and the eutectic temperature (the starting temperature for the melting process),  $c_p$  is the specific heat of the solid/melt mixture,  $\varphi$  is the melt fraction (porosity), and  $L_h$  the latent heat. In the present context,  $Q$  is a small parameter, so the dynamics of the melt front can be decoupled from the double-diffusive effects. Thus, the basic stability results of Nield (1968) are applicable. The critical thickness can vary from about 800 m to a few centimeters, depending on the composition of the magma. Lowell concluded that convective processes will tend to homogenize the melt before it separates from the source zone, but the vigor of mixing is dependent upon the composition of the source.

Lowell's (1985) other problem concerns the structure of the porous boundary layer that forms as a result of side-wall crystallization in a convecting magma chamber. His examination of the steady-state boundary layer equations shows that the structure may be one of two types. If upon crystallization at the wall, the residual melt fraction has negative compositional buoyancy, or if the negative thermal buoyancy at the cold wall exceeds the positive compositional buoyancy of the residual melt, then the flow across the whole boundary layer will be downward. Then if the residual melt fraction has negative compositional buoyancy, the magma chamber will become stratified as the result of the accumulation of a layer of dense cold liquid on the floor, while if the melt fraction has positive compositional buoyancy, the boundary layer fluid will tend to be remixed into the interior of the magma chamber. If, on the other hand, the positive compositional buoyancy exceeds the negative thermal buoyancy, counterflowing boundary layers will occur and the compositional buoyancy liquid will tend to be fractionated toward the top of the magma chamber.

## 11.5 Diagenetic Processes

Diagenetic processes involve reactions between pure water and mineral phases during which unstable minerals are dissolved and more stable phases are precipitated, resulting in changes in porosity and permeability. If fluid flow is involved, then the dissolution and precipitation occur in different parts of the medium. Davis et al. (1985) have computed the flow pattern and the resulting diagenetic contours (of  $\mathbf{v} \cdot \nabla T$ ) for convection in a folded porous layer (sand) bounded by an impermeable medium (shale) heated from below and held at a constant temperature above. (Following Dr. James Wood, the quantity  $\mathbf{v} \cdot \nabla T$  has been called the rock alteration index by Phillips (2009), who discusses its use in a number of related situations.) They assumed that the dip angles are small and the convection is weak, so that the temperature field can be uncoupled from the fluid flow. Their results are shown in Fig. 11.1. The direction of circulation, and hence the region of precipitation, depends on whether the conductivity of the porous medium ( $k_m$ ) is less than or greater than the conductivity of the impermeable

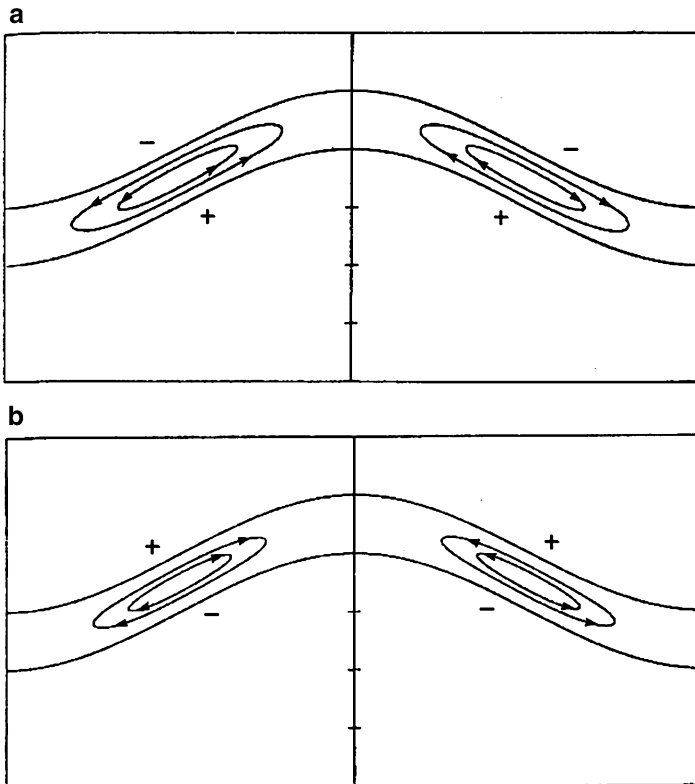


**Fig. 11.1** Streamlines in a folded porous layer. In (a) the thermal conductivity ratio  $k_m/k_s$  is 0.8, where  $m$  refers to the porous layer (sandstone) and  $s$  to the surrounding impermeable material (shale). In (b) the ratio is 1.25. The + signs denote the loci of maximum precipitation of quartz and the - signs the loci of maximum dissolution (Davis et al. 1985, with permission from the *American Journal of Science*)

medium ( $k_s$ ). If  $k_m/k_s < 1$ , the precipitation of quartz takes place on the lower flanks of the porous layer, because the solubility increases with temperature, and hence, the material is leached from the porous matrix in regions where the fluid is being heated and precipitated in regions where it is cooled.

The rate of mass transfer is radically increased if the critical Rayleigh number is exceeded and multicellular convection occurs. Palm (1990) has modified the analysis which Palm and Tveitereid (1979) developed for convection in snow (see Sect. 11.1) to slightly supercritical two-dimensional flow in a sloping layer in order to determine the rate of change of mean porosity  $\bar{\varphi}$  (averaged with respect to the upslope coordinate). Palm (1990) showed that

$$\frac{\partial \bar{\varphi}}{\partial t} = 4\pi \frac{\rho_w}{\rho s} \frac{dC_s}{dT} \Big|_T \alpha_m \frac{\Delta T}{H^2} \frac{Ra - Ra_c}{Ra} \sin\left(\frac{2\pi z}{H}\right), \quad (11.13)$$

where  $\rho_w$  is the density of water while  $C_s$  is the mass fraction of the transported material in water, in his case silica quartz, and  $\rho_s$  is its density. The other quantities are as in Sect. 7.8. We note that the maximal changes in porosity occur at  $z = (1/4)H$  and  $z = (3/4)H$ . This work was applied to the sedimentary basin under the North Sea by Bjørlykke et al. (1988).

The book by Phillips (1991, Chap. 7) contains further extensions. Phillips presents detailed analysis of convective flow at small Rayleigh number in submerged banks of slowly varying thickness or in compact platforms or reefs. He also treats flow patterns at intermediate Rayleigh number and scale ratio.

A computation of porosity redistribution resulting from thermal convection in slanted porous layers was made by Gouze et al. (1994). Implications for hydrothermal circulation at midocean ridges, resulting from permeability changes due to diagenesis in the fractured crust, were studied by Fontaine et al. (2001).

## 11.6 Oceanic Crust

### 11.6.1 Heat Flux Distribution

Measurements of heat flow on the ocean floor near the Galapagos spreading center have revealed a spatial periodicity with a wavelength of about 7 km, peaks of 12 HFU (where  $1 \text{ HFU} \equiv 1 \mu \text{ cal cm}^{-2} \text{ s}^{-1}$  is the “heat flux unit”), and troughs of 2 HFU, that is, a peak to trough ratio of 6. Ribando et al. (1976) calculated this ratio for various values of a Rayleigh number  $Ra$  based on heat flux, for the cases of permeable and impermeable upper boundary, and for exponentially decreasing and constant permeability. The heat flux distributions for permeable and impermeable tops are similar, and in the parameter range of interest, the peak to trough ratio is not sensitive to whether the permeability is constant or exponentially decreasing, taking the value 6 for  $Ra = 100$ . For a cell depth of 3.5 km, this corresponds to a permeability of  $4.5 \times 10^{-12} \text{ cm}^2$ , in accordance with other estimates of the permeability of oceanic basalts.

### 11.6.2 Topographical Forcing

Convection in oceanic crust has motivated studies of convection initiated by topography giving rise to horizontal temperature gradients and also of the extent to which topography influences the wavelength of convection cells produced by vertical temperature gradients. Lowell (1980) studied the first aspect. He assumed that the topography is two-dimensional, of uniform wavelength  $L$  and amplitude  $d$ , with  $d/L \ll 1$ , as shown in Fig. 11.2. This allows the temperature boundary condition to be changed from  $T = 0$  at the surface to

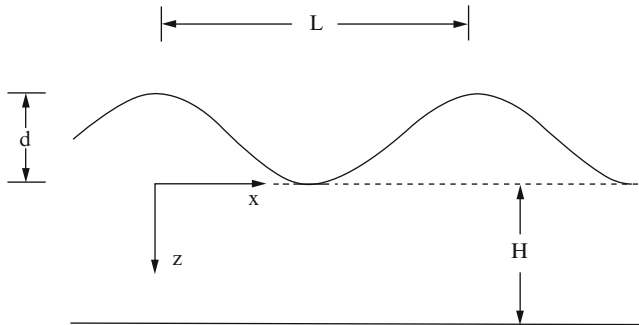


**Fig. 11.2** Definition sketch for low amplitude, wavelike crustal topography

$$T = \frac{d\Delta T}{2H} (1 + \cos kx) \text{ at } z = 0, \quad (11.14)$$

where  $k = 2\pi/L$ . The other boundary conditions are taken as

$$\frac{\partial w}{\partial z} = 0 \text{ at } z = 0, \quad \text{and} \quad w = T = 0 \text{ at } z = H \quad (11.15)$$

The linearized momentum and energy equations for steady flow take the form

$$\nabla^2 w = \frac{g\beta K}{v} \frac{\partial^2 T}{\partial x^2}, \quad (11.16)$$

$$\nabla^2 T = \frac{\Delta T}{H\alpha_m} w. \quad (11.17)$$

This system of equations can be solved iteratively. The first-order solution is

$$T_1 = \frac{d\Delta T}{2H} \left[ 1 + \cos kx \frac{\sinh k(h-z)}{\sinh kh} - \frac{z}{H} \right], \quad (11.18)$$

$$w_1 = -\frac{g\beta K d\Delta T}{4vH \sinh kh} \cos kx [(1 + kh \tanh kh) \sinh k(H-z) - k(H-z) \cosh k(H-z)]. \quad (11.19)$$

The last equation shows that the fluid descends at topographic troughs and ascends beneath topographic peaks as expected. The vertical velocity is proportional to the topographic amplitude  $d$ , but the convective heat flux  $\rho c_p w_1 T_1$  is proportional to  $d^2$ . Lowell (1980) also analyzed the case when the topography is covered with a layer of sediment.

The extent to which boundary topography can control the pattern of convection in a porous layer was examined by Hartline and Lister (1981). Their experiments using a Hele-Shaw cell indicate that for supercritical values of  $Ra$ , the topography does not control the convection pattern except when the topographic wavelength is comparable to the depth of water penetration, the nondimensional wave number  $2\pi H/L$  taking values between 2.5 and 4.8. We note that this range brackets  $\pi$ , the critical wave number for a slab with planar, isothermal, and impermeable boundaries. Topographies within this range control the circulation pattern perfectly, with downwelling under troughs and upwelling aligned with peaks. Other topographies do not force the pattern, although in some cases the convection wave number may be a harmonic of the topographic wave number. Unforced convection cells wander and vary in size. Hartline and Lister (1981) conclude that where the submarine circulation correlates with bottom topography, it may be because the topographic wavelength is comparable to the depth to which water penetrates the porous crust.

## 11.7 Geothermal Reservoirs: Injection and Withdrawal

Geothermal reservoir modeling has motivated many numerical studies of problems involving the withdrawal and injection of fluids. It is often convenient to formulate such problems in terms of pressure and temperature. For example, Cheng and Teckchandani (1977) studied the transient response in a liquid-dominated geothermal reservoir resulting from sudden heating and the withdrawal of fluids. They considered a two-dimensional rectangular reservoir confined by caprock at the top, heated by bedrock from below, and recharged continuously through vertical boundaries from the sides, with withdrawal from either a centrally placed line sink or a vertical plane sink. The characteristic feature is the contraction of isotherms in the neighborhood of the sink (see Fig. 11.3). Oscillatory convection starts at  $Ra = 200$ , a lower Rayleigh number than in the absence of cold water recharge from the sides.

In other studies, the withdrawal and recharge of fluid has been through a permeable top. The numerical results of Horne and O'Sullivan (1974b) showed that fluid withdrawal can increase or decrease the rate of heat transfer from the bottom (heated) surface depending on its position relative to the heat source. A two-temperature model was used by Turcotte et al. (1977) to simulate hot springs. Fluid is assumed to enter an upper permeable boundary at ambient temperature. That leaving is at a temperature greater than ambient temperature. At large  $Ra$ , the significant temperature differences between fluid and solid are restricted to a thin layer near the upper boundary. Further work on this topic has been reviewed by Cheng (1978, 1985b).

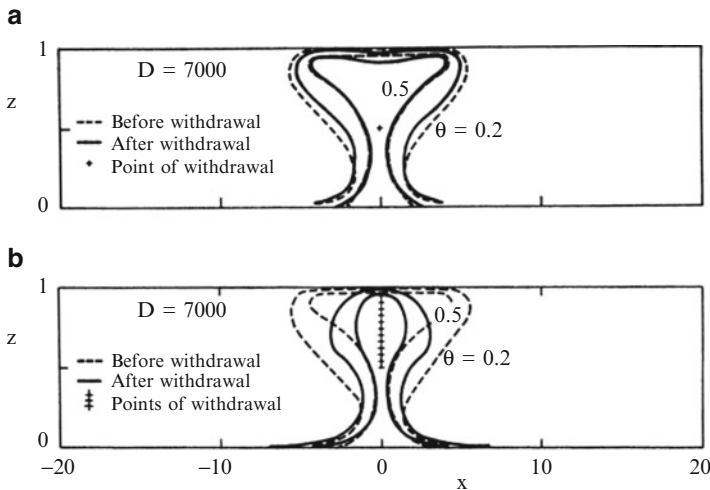


**Fig. 11.3** Contraction of isotherms in a geothermal reservoir resulting from fluid withdrawal from (a) a point sink and (b) a vertical line sink. Here  $\theta$  is the nondimensional temperature, and  $D = Ra/\beta\Delta T$  (Cheng and Teckchandani 1977)

## 11.8 Other Aspects of Single-Phase Flow

In the vicinity of the fluid critical point, the intensity of natural convective circulation can increase dramatically. Dunn and Hardee (1981) presented laboratory data that show that in a porous medium, heat transfer rates can increase by a factor of 70 in the vicinity of the critical point. They also showed that the conditions for this type of superconvection are compatible with expected geological conditions above magma bodies in the Earth's crust. Numerical experiments on convective heat transfer at near-critical conditions were reported by Cox and Pruess (1990). The heat transfer rates obtained in the simulations were considerably smaller than those reported by Dunn and Hardee (1981). Cox and Pruess suggested that possible causes of the discrepancy are the effects of pressure variation, channeling, and vertical asymmetry of the temperature field. Ingebritsen and Hayba (1994) observed that singularities in the equations of state of water at its critical point could be avoided by switching to a pressure-enthalpy formulation. Their numerical simulations showed that there was little near-critical enhancement in heat transfer for systems in which flow is driven by fixed pressure drops. However, in density-driven systems, there can be an enhancement of heat transfer by a factor  $10^2$  or more, with convection occurring in narrow cells, if the permeability is sufficiently high. The restriction to high permeability environments within a fairly narrow pressure-enthalpy window indicates that superconvection may be quite rare in natural near-magma systems.

In order to discuss convective flow patterns in ground water near salt domes, Evans and Nunn (1989) made some calculations of double-diffusive convection. They did not invoke the Boussinesq approximation. They found that along a salt flank, the flow can be either up or down, the sense of direction depending mainly on the value of the buoyancy ratio  $N$  [defined in Eq. (9.10)] and how sharply the isotherms are pulled up near the salt dome. These factors depend in turn on the regional salinity variation, the time since diapirism, and the thermal conductivity of water-saturated sediments.

A time-dependent numerical model of heat transfer across a thickening conductive boundary layer, between a crystallizing magma chamber and a single-pass hydrothermal system in the ocean crust, was developed by Lowell and Burnell (1991) and applied to seafloor black smokers. General discussions of submarine hydrothermal systems were presented by Lowell (1991) and Lowell et al. (1995), Wilcock (1998), and Jupp and Schultz (2000, 2004). High Rayleigh number convection in an open top porous layer (or Hele-Shaw cell) heated from below was studied by Cherkaoui and Wilcock (1999, 2001).

Convection in a mushy zone at the Earth's inner-outer core boundary was discussed by Bergman and Fearn (1994). They concluded that the magnetic field may be strong enough to act against the tendency for convection to be in the form of narrow chimneys.

The interaction of thermally driven convective circulation in a steeply dipping fault zone and groundwater flow through the surrounding rock that is driven by a regional topographic gradient was examined by López and Smith (1995). Three-dimensional thermoconvection in an anisotropic-inclined sedimentary layer was numerically simulated by Ormond and Genton (1993).

Numerical modeling was used by Mullis (1995) to check the usefulness of the analytical solution given by Eq. (7.100). He found that for a homogeneous aquifer, this solution is a good approximation provided that the inclination of the layer is replaced by the inclination of the isotherms. He also numerically modeled convection in wedges and lenses.

A general discussion based on numerical simulation of the patterns of flow induced by geothermal sources in deep ground was presented by Holzbecher and Yusa (1995). A geological thermosyphon, where the convection in a closed loop is coupled to conduction in the surrounding earth, was simulated numerically by Paterson and Schlanger (1992). They found that at a Rayleigh number above 1, convection leads to a temperature reduction near the source.

The problem of confinement of nuclear wastes in places like Yucca Mountain in which the temperature and humidity inside emplacement drifts are of interest has led to new numerical simulations by Webb et al. (2003) and Itamura et al. (2004). An analytical assessment of the impact of covers on the onset of air convection in mine wastes was reported by Lu (2001).

Studies of the successive formation and evolution of layered structures in porous media resulting from heating a compositionally stable stratified fluid from below were made by Schoofs et al. (1998, 2000a). Thermochemical convection in and between intracratonic basins was studied by Schoofs et al. (2000b). The depletion

of a brine layer at the base of ridge-crest hydrothermal systems was simulated by Schoofs and Hansen (2000). Numerical simulations of midocean ridge hydrothermal circulation including the phase separation of seawater were made by Kawada et al. (2004). A comprehensive study of NaCl–H<sub>2</sub>O convection in the Earth's crust was reported by Geiger et al. (2005) who employed a novel finite element–finite volume numerical method. They allowed for phase separation. To characterize the onset of convection with a non-Boussinesq situation, they introduced a fluxibility parameter (a scaled energy flux) and a local Rayleigh number. Further studies of midocean ridges and seafloor spreading were carried out by Lowell (2007) and Wilson and Ruppel (2007). Coupled process models of fluid flow and heat transfer in hydrothermal systems in three dimensions were presented by Kuhn and Gessner (2009). Numerical simulation of magmatic hydrothermal systems was reviewed by Ingebritsen et al. (2010).

Using finite-element numerical modeling, Zhao et al. (1997, 1998a, 1999c, d, 2000a, 2001a, b) have treated a range of situations. Zhao et al. (1998b, 1999a) studied high Rayleigh number steady-state heat transfer in media heated from below. The first paper dealt with the effect of geological inhomogeneity with both heat and mass transfer and the second with the effect of medium thermoelasticity, mineralization, and deformable media. Zhao et al. (2003a) transformed a magma solidification problem with a moving boundary into a problem without the moving boundary but with an equivalent heat source. Kissling and Weir (2005) proposed an explanation of the spatial distribution of the geothermal fields in the Taupo Volcanic Zone (TVZ), New Zealand, while Kissling et al. (2009) modeled convective flows in a TVZ-like zone with a brittle/ductile transition. Fluid flows through some geological discontinuities were studied by Ingham et al. (2006).

Steady-state heat transfer through midcrustal vertical cracks with upward throughflow in hydrothermal systems was analyzed by Zhao et al. (2002). The onset of convective flow in three-dimensional fluid-saturated faults was analyzed by Zhao et al. (2003a, b, 2004a, 2005). Further interesting studies of thermohaline convection, involving layering or plume separation, have been carried out by Oldenburg and Pruess (1998, 1999). Additional work on the numerical simulation of double-diffusive convection with rock alteration was reported by Zhao et al. (2006a, b). This work is summarized in the book by Zhao et al. (2008a). Zhao et al. (2011a; b) reported a computational simulation of convective flow in the Earth's crust with consideration of dynamic crust-mantle interactions.

Convection in continental faulted rifts was modeled by McLellan et al. (2010). Simmons et al. (2008) investigated various modes of convection in fractured porous media. Nield et al. (2008c) studied episodic convection beneath an evaporating salt lake. This followed work by Massmann et al. (2006) on a theoretical analysis of mixed convection in a stably stratified fresh surface water saline groundwater discharge zone. Van Dam et al. (2009) documented the occurrence in the field of natural convection in groundwater. Further evidence of natural convection in groundwater was found by Stevens et al. (2009) in field-based experiments near wind-tidal flats. Voss et al. (2010) established a three-dimensional benchmark for

variable-density flow and transport simulation by matching semi-analytic stability modes for steady unstable convection in an inclined porous box. The importance of anisotropy and layered heterogeneity in brackish aquifers in the variable-density modeling of multiple-cycle aquifer storage and recovery was pointed out by Ward et al. (2008). Various aspects of groundwater flow in fractured rock were studied by Graf and Therrien (2007a, b, 2009).

The influence of free convection on soil salinization in arid regions was studied by Gilman and Bear (1996). Their paper contains a linear stability analysis. A numerical technique useful for such problems was supplied by Payne and Straughan (2000a). Straughan (2004b) notes that a nonlinear energy theory for this problem is lacking, but Payne et al. (1999) have used energy-like techniques to derive continuous dependence and convergence results for the basic equations arising from the Gilman and Bear (1996) theory. Numerical modeling of reaction-induced cavities in a porous rock was conducted by Ormond and Ortoleva (2000). Solute transport in a peat moss layer produced by buoyancy-driven flow was discussed by Rappoldt et al. (2003). Thermal convection in faulted extensional sedimentary basins was simulated by Simms and Garven (2004). Phase separation together with convection in hydrothermal systems was studied by Emmanuel and Berkovitz (2006a, 2007b). Continuous time random walks were applied to heat transfer in porous media by Emmanuel and Berkovitz (2007a), while Emmanuel and Berkovitz (2006b) studied the suppression and stimulation of seafloor hydrothermal convection by exothermic mineral hydration. Ritchie and Prichard (2011) studied natural convection and the evolution of a reactive porous medium.

Highly heterogeneous geologic systems recently have received special attention from Simmons et al. (2001) and Prasad and Simmons (2003). They pointed out that in many geologic systems, hydraulic properties such as the hydraulic conductivity of the system under consideration can vary by many orders of magnitude and sometimes rapidly over small spatial scales. Geologic systems, characterized by fractured rock environments or lenticular mixes of sand and clay, are common in many hydrogeologic systems. Such heterogeneity occurs over many spatial scales, and variable-density flow phenomena may be triggered, grow, and decay over a very large mix of different spatial and temporal scales. Dense plume problems in these geologic environments in general are expected to be inherently transient in nature and often may involve sharp plume interfaces whose spatiotemporal development is very sensitive to initial conditions. Importantly, the onset of instability in transient, sharp interface problems is controlled by very local conditions in the vicinity of the evolving boundary layer and not by the global layer properties or some average property of that macroscopic layer. Simmons et al. (2001) and Prasad and Simmons (2003) pointed out that any averaging process is likely to remove the very structural controls and physics that are important in controlling the onset, growth, and/or decay of instability in a highly heterogeneous system. These authors, together with Schincariol et al. (1997), reported that in the case of dense plume migration in highly heterogeneous environments, the application of an average global Rayleigh number based upon average hydraulic conductivity of the medium was problematic. In these cases, an average Rayleigh number appears

to be unable to predict the onset of instability accurately because the system is characterized by unsteady flows and large amplitude perturbations. For statistically equivalent geologic systems, and hence average global  $Ra$ , dense plume behavior was observed by Simmons et al. (2001) and Prasad and Simmons (2003) to vary between highly unstable to highly stable. Heterogeneity effects on a possible salinity-driven natural convective flow in low-permeability strata were studied by Sharp and Shi (2009).

Travis and Schubert (2005) studied hydrothermal convection in carbonaceous chondrite parent bodies. The stability of thermal convection in the porous methane-soaked regolith of Titan was investigated by Czechowski and Kossacki (2009).

## 11.9 Two-Phase Flow

### 11.9.1 Vapor–Liquid Counterflow

For a geothermal field, the solid (rock) is at rest and the gas is the vapor. With subscript  $v$  (for vapor) replacing  $g$ , Eqs. (3.77) and (3.78) reduce to

$$v_l = -\frac{k_l K}{\mu_l} (\nabla P - \rho_l g) \quad (11.20)$$

$$v_v = -\frac{k_v K}{\mu_v} (\nabla P - \rho_v g). \quad (11.21)$$

Here, it is assumed that  $K$  is constant. Likewise, Eqs. (3.82) and (3.83) reduce to

$$J_M = \rho_l v_l + \rho_v v_v, \quad (11.22)$$

$$J_E = \rho_l h_l v_l + \rho_v h_v v_v - k \nabla T \quad (11.23)$$

Under the two-phase conditions, the pressure  $P$  and temperature  $T$  are functionally related through the saturation line relation  $T = T_{\text{sat}}(P)$ . It is customary to take the  $z$ -axis in the vertically downward direction. In the absence of source terms and with the pressure term there negligible, Eqs. (3.85) and (3.86) give for vertical flow

$$\frac{\partial A_M}{\partial t} + \frac{\partial J_M}{\partial z} = 0, \quad (11.24)$$

$$\frac{\partial A_E}{\partial t} + \frac{\partial J_E}{\partial z} = 0, \quad (11.25)$$

where  $A_M(P, S)$ ,  $A_E(P, S)$ ,  $J_M(P, \partial P / \partial z, S)$ , and  $J_E(P, \partial P / \partial z, S)$  and  $S$  is the liquid saturation. The relative permeabilities  $k_l(S)$  and  $k_v(S)$  are assumed to be monotonic increasing and decreasing, respectively, and to satisfy the conditions

$$k_l(S) = 0 \quad \text{for } 0 < S < S_* \quad (11.26)$$

$$k_v(S) = 0 \quad \text{for } S^* < S < 1, \quad (11.27)$$

where  $S_*$  and  $1 - S^*$  denote the residual liquid saturation and vapor saturation, respectively. From Eqs. (11.20), (11.21), (11.22), (11.23), and (11.24), it follows that for the case of negligible conduction,

$$J_M = -F + G_M \quad (11.28)$$

$$J_E = -hF + G_E \quad (11.29)$$

where the gravitational terms are

$$G_M = \left( \frac{\rho_l^2 K k_l}{\mu_l} + \frac{\rho_v^2 K k_v}{\mu_v} \right) g, \quad (11.30)$$

$$G_E = \left( \frac{\rho_l^2 K k_l h_l}{\mu_l} + \frac{\rho_v^2 K k_v h_v}{\mu_v} \right) g, \quad (11.31)$$

The mass mobility  $F$  is given by

$$F = K \left( \frac{\rho_l k_l}{\mu_l} + \frac{\rho_v k_v}{\mu_v} \right), \quad (11.32)$$

and the flowing enthalpy  $h$  is given by

$$h(P, S) = \frac{\rho_l k_l h_l / \mu_l + \rho_v k_v h_v / \mu_v}{\rho_l k_l / \mu_l + \rho_v k_v / \mu_v}. \quad (11.33)$$

Substituting Eqs. (11.28) and (11.29) into (11.24) and (11.25) and eliminating second derivatives of the pressure, one obtains a first-order wave equation of the form

$$\frac{\partial S}{\partial t} + c \frac{\partial S}{\partial z} = f_l(S, P, \partial P / \partial t, \partial P / \partial z), \quad (11.34)$$

where  $f_l$  is a forcing term and the wave speed  $c$  (whose reciprocal is an eigenvalue of the differential system) is given by

$$c = \frac{1}{E_s} \left( \frac{\partial h}{\partial S} J_M - \frac{\partial G}{\partial S} \right), \quad (11.35)$$

where, in turn, for the case of negligible conduction,

$$G = hG_M - G_E, \quad (11.36)$$

$$E_S = \frac{\partial A_E}{\partial S} - h \frac{\partial A_M}{\partial S}. \quad (11.37)$$

Equation (11.34) may be analyzed by the standard method of characteristics. Rankine-Hugoniot equations, expressing conservation of mass and energy, relate the shock velocity to changes in densities and flows:

$$U = \frac{[J_M]}{[A_M]} = \frac{[J_E]}{[A_E]}, \quad (11.38)$$

where [] denotes a jump across the shock. It can be verified that for the case of zero conduction, the second equality in the last equation is equivalent to the continuity of a volumetric flux vector  $J_Q$  given by

$$J_Q = -\frac{K}{\mu} \left( \frac{\partial P}{\partial z} - \rho g \right), \quad (11.39)$$

where  $\mu$  and  $\rho$  are defined by

$$\frac{1}{\mu} = \frac{k_l}{\mu_l} + \frac{k_v}{\mu_v}, \quad \frac{\rho}{\mu} = \frac{k_l \rho_l}{\mu_l} + \frac{k_v \rho_v}{\mu_v}. \quad (11.40)$$

On the basis of analysis and numerical simulations, Kissling et al. (1992b) concluded that although the phases can travel in opposite directions (counterflow), information travels either up or down, depending on the sign of the wave speed  $c$ . Wave speed, saturation, and other quantities are defined on a two-sheeted surface over the mass-energy flow plane, with the sheets overlapping in the counterflow region. [For counterflow, there are either two or zero solutions of Eq. (11.34), for the case of zero conduction.] Most saturations are of the wetting type, that is, they leave the environment more saturated after their passage. In fact, when the flow is horizontal, all shocks are wetting, but in vertical two-phase flow, there also exist drying shocks for sufficiently small mass and energy flows.

A general analytical treatment of three-dimensional flow was given by Weir (1991). He showed that when both phases were mobile, the generalization of Eq. (11.34) is of the form

$$\frac{\partial S}{\partial t} + c \cdot \nabla S = f, \quad (11.41)$$

where

$$\mathbf{c} = \frac{1}{E_S} \left( \frac{\partial h}{\partial S} \mathbf{J}_M - \frac{\partial G}{\partial S} \mathbf{k} \right), \quad (11.42)$$

where  $\mathbf{k}$  is the unit vector in the  $z$ -direction. Weir (1991) showed that at each point in space, flows are essentially two-dimensional, in the sense that  $\mathbf{J}_M$ ,  $\mathbf{J}_E$ ,  $\mathbf{J}_Q$ , and  $\mathbf{c}$  all lie in a vertical plane. Here  $\mathbf{J}_Q$  is the vector generalization of the scalar in Eq. (11.39). Further, gravity establishes a vertical hierarchy; the volumetric, energy, and mass flux vectors (listed in descending order) can never point below a lower member of this triple.

For a one-dimensional horizontal two-phase flow, Eqs. (11.41) and (11.42) give, analogous to Eqs. (11.34) and (11.35) with zero gravity,

$$\frac{\partial S}{\partial t} + c \frac{\partial S}{\partial x} = f_1(S, P, \partial P / \partial t, \partial P / \partial x), \quad (11.43)$$

where

$$c = - \frac{F}{E_S} \frac{\partial h}{\partial S} \frac{\partial P}{\partial x}. \quad (11.44)$$

Equation (11.44) is formally similar to the Buckley-Leverett equation (of oil recovery theory) describing isothermal flow of a two-component single-phase fluid in a porous medium when capillarity can be ignored. However, in the present situation, the saturation equation (11.44) is strongly coupled to the nonlinear diffusion equation, for  $P$ , obtained by eliminating  $\partial S / \partial t$  from the conservation equations:

$$\frac{\partial P}{\partial t} - D \frac{\partial^2 P}{\partial x^2} = f_2(S, P, \partial S / \partial x, \partial P / \partial x), \quad (11.45)$$

where

$$D = - \frac{\frac{E_S F}{\partial M} \frac{\partial E}{\partial P}}{\frac{\partial S}{\partial S} \frac{\partial P}{\partial P} - \frac{\partial E}{\partial S} \frac{\partial M}{\partial P}} \quad (11.46)$$

Kissling et al. (1992a) solved Eqs. (11.45) and (11.43) in turn under the assumption that pressure disturbances diffuse to steady state faster than saturation changes convect. They performed numerical simulations for a block of porous material with pressure and saturation given constant values at the ends of the block. When pressure diffusion occurs much faster than saturation convection, the numerical results can be described in terms of either saturation expansion fans or isolated saturation shocks. When pressure diffusion and saturation convection occur on the same timescale, initial simple shock profiles evolve into multiple shocks.

In the work discussed so far, conduction has been neglected. Weir (1994a) has shown that this is certainly valid for sufficiently high temperatures and sufficiently high permeabilities. Young (1993b) has shown that even when conduction has been included, the geothermal saturation wave speed is formally identical to the Buckley-Leverett wave speed when the latter is written as the saturation derivative of a volumetric flow.

For the case of two-phase brine mixtures, one has to add an equation expressing conservation of salt. Young (1993a) presented a model in which the flows are described by a parabolic equation for the pressure with a derivative coupling to a pair of equations for saturation and salt concentration. He showed that the wave-speed matrix for the hyperbolic part of the coupled system is formally identical to the corresponding matrix in the polymer flood model for oil recovery. Indeed, for a class of strongly diffusive hot brine models, the wave phenomena in geothermal reservoirs can be predicted from the polymer flood model.

The two-phase geothermal theory has been extended by Weir (1994b) to the case where nonreacting chemical transport (e.g., of CO<sub>2</sub>) is added. He derived a natural factorization of the system of equations into diffusive and wave equations. Each wave equation allows for the corresponding variable to be discontinuous or equivalently for shock propagation to occur. In general, there now are more than the usual two (vapor- and liquid-dominated) saturations for a given mass, energy, and chemical flux in steady flow.

A further extension of the theory to the case of withdrawal of fluid at a constant rate was made by Young and Weir (1994). They defined a parameter  $\alpha$ ,

$$\alpha = \frac{\mu_v W}{Kg\rho_l(\rho_l - \rho_v)}, \quad (11.47)$$

where  $W$  is the rate of withdrawal (mass per unit area per unit time). They concluded that for large  $\alpha$ , fluid withdrawal is a mining process, a vapor-dominated zone spreads out from the production level, and production enthalpies tend toward steam values. For small  $\alpha$ , gravity predominates and buoyancy forces can lead to the formation of a steam bubble that escapes from the production boundary and rises toward the surface. Then production enthalpy may remain at the liquid value over long periods. In addition, certain saturation ranges at the sink may be forbidden as a consequence of the constant rate boundary condition, and then, saturation shocks also may occur.

A more general study of vapor–liquid counterflow is that of Satik et al. (1991). They considered a situation in which the counterflow is inclined to the vertical, and their analysis included capillarity, heat conduction, and Kelvin effects (the lowering of the vapor pressure due to capillarity). They treated a three-zone model in which the counterflow zone is sandwiched between two zones (one containing mainly vapor and one containing mainly liquid) in which there is no flow. They found that the critical heat flux (above which dryout occurs) increases with decreasing permeability and that a threshold permeability exists below which steady states may not exist. In this context, the critical heat flux is dependent on the pressure and the

temperature and so is not precisely defined. As special cases of their general theory, they considered what they called the “heat pipe” and “geothermal” problems. In the former, the flow is driven by capillary pressure, and the Kelvin effects are of significance only over a narrow boundary layer at the vapor-phase boundary. In the latter, the flow is driven by gravity.

The effect of capillary heterogeneity induced by variation in permeability was analyzed by Stubos et al. (1993b). They found that the heterogeneity acts as a spatially varying body force that may enhance or diminish gravity effects on heat pipes. A detailed numerical investigation of a transient problem involving a self-heated porous bed was conducted by Stubos et al. (1997). Another investigation of a heterogeneous medium, one involving oscillatory instability, was made by Xu and Lowell (1998).

For the axially symmetric problem of constant-strength heat source embedded in an infinite homogeneous medium with uniform initial conditions, Doughty and Pruess (1990, 1992) obtained a similarity solution in terms of the variable  $r/t^{1/2}$ . In their second paper, they included an air component and investigated vapor-pressure lowering, pore-level phase change effects, and an effective continuum representation of fractured porous media.

A model taking into account latent heat, vertical flow, and heat conduction terms, and so involving a new parameter representing a combination of those quantities, was presented by Pestov (1997, 1998).

### 11.9.2 Heat Pipes

A heat pipe is a system in which a very efficient heat transfer process is effected by vapor–liquid counterflow and associated evaporation and condensation effects with transfer of latent heat. Vapor and liquid may flow in opposite directions due to gravity or capillary action or both. If heat is injected into such a system, the liquid phase will vaporize, causing pressurization of the vapor phase and vapor flow away from the heat source. In cooler regions, the vapor condenses and deposits its latent heat. In the case of a heat pipe depending on capillary action, this sets up a saturation profile, with liquid-phase saturations increasing away from the heat source and capillary forces then cause backflow of the liquid toward the heat source.

For a vertical heat pipe, McGuinness et al. (1993) showed that the steady-state values of  $J_E$  and  $\partial P/\partial z$  are given by

$$\frac{J_E}{K} \left( \frac{\mu_l}{\rho_l k_l} + \frac{\mu_v}{\rho_v k_v} \right) = \frac{J_M}{K} \left( \frac{\mu_l h_l}{\rho_l k_l} + \frac{\mu_v h_v}{\rho_v k_v} \right) - g(h_v - h_l)(\rho_l - \rho_v), \quad (11.48)$$

$$\frac{\partial P}{\partial z} \left( \frac{\rho_l k_l}{\mu_l} + \frac{\rho_v k_v}{\mu_v} \right) = -\frac{J_M}{K} + \left( \frac{\rho_l^2 k_l}{\mu_l} + \frac{\rho_v^2 k_v}{\mu_v} \right). \quad (11.49)$$

If the simplification  $k_l + k_v = 1$  is assumed (this is a good approximation in many situations), the value of the wave speed that appears in Eq. (11.34) is, for the case  $J_M = 0$  (which is appropriate for a heat pipe),

$$c = A \left( \frac{\mu_l k_v^2}{\rho_l} - \frac{\mu_v k_l^2}{\rho_v} \right), \quad (11.50)$$

where  $A$ , defined by

$$A = \frac{k(\partial k_l / \partial S)g(\rho_l - \rho_v)}{(k_l \mu_v + k_v \mu_l)(k_l \mu_v / \rho_v + k_v \mu_l / \rho_l)}, \quad (11.51)$$

is always positive. Hence,  $c$  is normally negative for a steady liquid-dominated pipe ( $k_v \approx 0$ ) and normally positive for a steady vapor-dominated pipe ( $k_l \approx 0$ ). This fixes the direction of information flow and hence tells one at which end of the pipe one should impose flux values in numerical simulations of geothermal systems and at which end one should specify the saturation and pressure. For the vapor-dominated solution, the pressure and saturation should be fixed at depth and the heat and mass flux specified at the top. These boundary conditions are appropriate for a laboratory heat pipe, but they are questionable for geothermal systems.

An extension of this work was made by McGuinness (1996), who pointed out that the three-zone model used by Satik et al. (1991) limits the possible range of heat flow values through the heat pipe and also limits solutions to those with a smooth transition from pure vapor to pure liquid. The single-zone model of McGuinness allowed these restrictions to be removed. He used a singular perturbation approach (valid for  $K > 10^{-15}$  m<sup>2</sup>, so that the heat flow is convection dominated), allowing for capillary boundary layers in the temperature-saturation phase plane. He found that in the geothermal context and with heat flow that is dominated by convection, phase-plane trajectories of temperature vs. saturation track zero-capillarity (gravity-driven) solutions (one liquid-dominated and one vapor-dominated) when they exist. Which of the two solutions is selected depends on the boundary conditions. In the case of bottom heating, it is the liquid-dominated solution that should be selected. Whereas the work of Satik et al. (1991) suggested that only the vapor-dominated solution is typically obtained, the results of McGuinness (1996) explain why Bau and Torrance (1982a) and others obtained only liquid-dominated solutions in their laboratory experiments. McGuinness (1996) also calculated bounds (maxima) for the lengths of heat pipes in cases where previous work had predicted unbounded lengths.

The theory of two-phase convection, and in particular the theory of heat pipes, is currently controversial. The work of Satik et al. (1991) and Stubos et al. (1993a, b) was developed in the context of laboratory experiments, and care needs to be exercised in extending their theory to geothermal systems. For further discussion, the reader is referred to Young (1996a, b, 1998a, b).

The quadratic drag (Forchheimer) effect was included in the analysis by Zhu and Vafai (1999). The dynamics of submarine geothermal heat pipes was investigated by Bai et al. (2003). A further study of the stability of heat pipes in vapor-dominated systems was reported by Amili and Yortsos (2003).

### **11.9.3 Other Aspects**

A numerical investigation of two-phase fluid flow and heat transfer in a porous medium heated from the side was conducted by Waite and Amin (1999). A general local thermal nonequilibrium model for two-phase flows with phase change in porous media was proposed by Duval et al. (2004). Two-phase flow in porous-channel heat sinks was studied by Peterson and Chang (1997, 1998). Buoyancy effects together with phase change have been discussed by Zhao et al. (1999e, 2000b). A review of several aspects of liquid and vapor flow in superheated rock was made by Woods (1999). Geiger et al. (2006a, b) studied multiphase thermohaline convection in the Earth's crust, combining a new finite element–finite volume solution technique with a new equation of state for NaCl–H<sub>2</sub>O. Nasrabadi et al. (2006) studied two-phase multicomponent diffusion and convection for reservoir initialization.

## **11.10 Cracks in Shrinking Solids**

The earth's crust is a cracked porous medium with multiple scales, which result from erosion and from periodic shrinking due to volumetric cooling and drying. In spite of the apparent diversity of crack sizes and locations, there is pattern. For example, wet soil exposed to the sun and the wind becomes drier, shrinks superficially, and develops a network of cracks. The loop in the network has a characteristic length scale. The loop is round, more like a hexagon or a square, not slender. The loop is smaller (i.e., cracks are denser) when the wind blows harder, that is, when the drying rate is higher.

The characteristic scales of cracks in volumetrically shrinking solids were recently deduced from constructal theory (Bejan et al. 1998; Bejan 2000). They were deduced by invoking the constructal law: the maximization of access for the mass transfer from wet and cracked soil to the ambient. In Bejan et al. (1998), the model was a heat transfer analog in which a one-dimensional solid slab of thickness  $L$  is initially at the high temperature  $T_H$  and has the property of shrinking on cooling. The coolant is a single-phase fluid of temperature  $T_L$ .

The question is how to maximize the thermal contact between the solid and the fluid or how to minimize the overall cooling time. This objective makes it necessary to allow the fluid to flow through the solid. In Fig. 11.4, the cracks are spaced uniformly, but their spacing  $R$  is arbitrary. The channel width  $D$  increases in time,

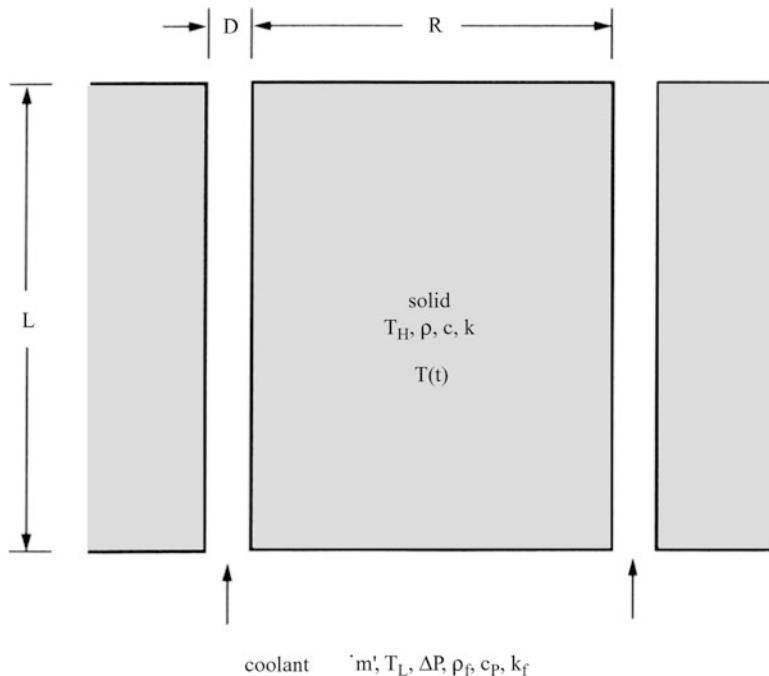


**Fig. 11.4** Cracks in a shrinking solid cooled by forced convection (Bejan et al. 1998)

as each solid piece \$R\$ shrinks. The fluid is driven by the pressure difference \$\Delta P\$, which is maintained across the solid thickness \$L\$. The imposed \$\Delta P\$ is an essential aspect of the channel spacing selection mechanism. For example, in the air cooling of a hot solid layer, the scale of \$\Delta P\$ is set at \$(1/2)\rho\_f U\_\infty^2\$, where \$\rho\_f\$ and \$U\_\infty\$ are the density and the free-stream velocity, respectively, of the external air flow.

To examine the effect of the channel spacing \$R\$ on the time needed for cooling the solid, we consider the asymptotes \$R \rightarrow 0\$ and \$R \rightarrow \infty\$. The approach is known as the intersection of asymptotes method (Lewis 2003). When the number of channels per unit length is large, the spacing \$R\$ is small and so is the eventual shrinkage that is experienced by each \$R\$ element. This means that when \$R \rightarrow 0\$, we can expect \$D \rightarrow 0\$ and laminar flow through each \$D\$-thin channel, such that the channel mass flow rate is \$m' = \rho\_f D U \sim \rho\_f D^3 \Delta P / (\mu L)\$. In the same limit, \$R\$ is small enough so that the solid conduction is described by the lumped thermal capacitance model. The solid piece \$R\$ has a single temperature \$T\$, which decreases in time from the initial level \$T\_H\$ to the inlet temperature of the fluid \$T\_L\$. This cooling effect is governed by the energy balance \$\rho c R L (dT/dt) = -q'\$, where \$\rho\$ and \$c\$ are the density and the specific heat, respectively, of the solid. The cooling effect (\$q'\$) provided by the flow through the channel is represented well by \$q' = m' c\_p (T - T\_L)\$, where \$c\_p\$ is the specific heat of the coolant. We obtain the order-of-magnitude statement

$\rho c RL(\Delta T/t) \sim m'c_p \dot{\Delta T}$ , where  $\Delta T$  is the scale of the instantaneous solid excess temperature  $T - T_L$ . Finally, by using the scale, we find the cooling time scale:

$$t \sim \frac{\rho c}{\rho_f c_p} \frac{\mu R L^2}{D^3 \Delta P} \quad (R \rightarrow 0) \quad (11.52)$$

In the opposite limit,  $R$  is large and the shrinkage (the channel width  $D$ ) is potentially very large in proportion to  $R$ . The fluid present at one time in the channel is mainly isothermal at the inlet temperature  $T_L$ . The cooling of each solid side of the crack is ruled by one-dimensional thermal diffusion into a semi-infinite medium. The cooling time in this regime is the same as the time of thermal diffusion:

$$t \sim \frac{R^2}{\alpha} \quad (R \rightarrow \infty), \quad (11.53)$$

where  $\alpha = k/(\rho c)$  and  $k$  is the thermal conductivity of the solid.

To summarize, in the limit  $R \rightarrow 0$ , the cooling time is proportional to  $R/D^3$  or  $R^{-2}$  because we expect a proportionality between  $D$  and  $R$ , namely,  $D/R \sim \beta \Delta T \ll 1$ , where  $\Delta T \sim T_H - T_L$  and  $\beta$  is the coefficient of thermal contraction of the solid. In the opposite limit,  $R \rightarrow \infty$ , the cooling time is proportional to  $R^2$ . Put together, these proportionalities suggest that the cooling time possesses a sharp minimum with respect to  $R$  or the channel density. Intersecting the two asymptotes, we find that the optimal crack distance for fastest cooling

$$R_{opt} \sim \left[ \frac{k}{k_f} \frac{\alpha_f v L^2}{U_\infty^2 (\beta \Delta T)^3} \right]^{1/4}. \quad (11.54)$$

The optimal crack distance decreases as the external pressure (or flow) is intensified. This is in accord with observations that mud cracks become denser when the wind speed increases. The  $R_{opt}$  result predicts a higher density of cracks (a smaller  $R_{opt}$ ) as the solid excess temperature  $\Delta T$  increases, again in agreement with observations.

An important geometric aspect of the  $R_{opt}$  scale is that the optimal distance between consecutive cracks must increase as  $L^{1/2}$ . This is relevant to predicting the length scale of the lattice of vertical cracks formed in a horizontal two-dimensional surface cooled (or dried) from above, under the influence of external forced convection. As the air flow direction changes locally from time to time and as the material (its graininess) is such that cracks may propagate in more than one direction, we arrive at the problem of cooling a two-dimensional terrain (area  $A$ , when seen from above) with cracks of length  $L$  and associated area elements of width  $R_{opt}$ .

Figure 11.5 shows the two extremes in which  $L$  may find itself in relation to  $R_{opt}$ . First, when  $L$  is considerably shorter than  $R_{opt}$ , it is impossible to cover the area  $A$  exclusively with patches of size  $L \times R_{opt}$ . The reason is that when two cracks of

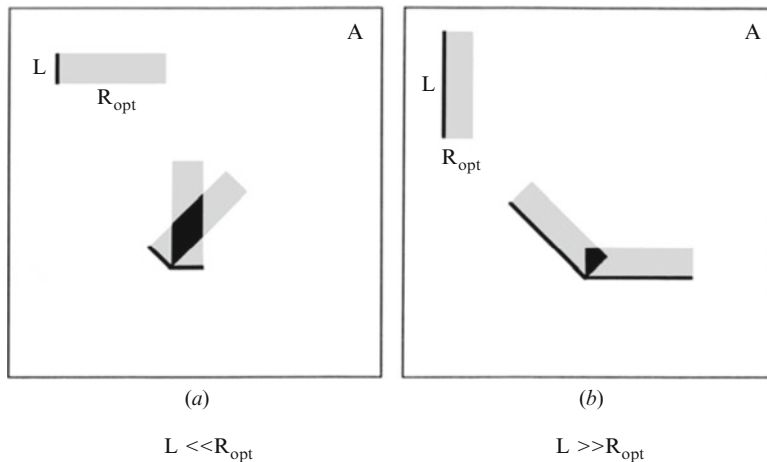


**Fig. 11.5** Two extremes in covering a two-dimensional solid ( $A$ ) with cracks ( $L$ ) and optimally shaped volume elements ( $L \times R_{\text{opt}}$ ) (Bejan et al. 1998)

length  $L$  are joined at an angle, the elemental area  $\sim L^2$  trapped between them is too small to accommodate the amount of ideally cooled solid material. When  $L$  is considerably longer than  $R_{\text{opt}}$ , any lattice of cracks will fail to cover the area  $A$  completely. Now the trapped elemental area ( $\sim L^2$ ) is considerably larger than the amount of ideally cooled solid ( $\sim LR_{\text{opt}}$ ): most of the interior of the area element of size  $L^2$  would require a cooling time that is considerably longer than the minimum time determined in the preceding analysis.

In conclusion, maximum access for the global heat current is achieved by covering the  $A$  cross section with  $L \times R_{\text{opt}}$  elements, in which  $L \sim R_{\text{opt}}$ . The optimal pattern is one with relatively round or square loops, not slender loops. Combining  $L \sim R_{\text{opt}}$  with the  $R_{\text{opt}}$  expression, we find the optimal length scale of the loop in the network of cracks that will minimize the cooldown time:  $R_{\text{opt}} \sim (\alpha_f v k / k_f)^{1/2} / [U_\infty (\beta \Delta T)^{3/2}]$ . Once again, in agreement with observations, the lattice length scale  $R_{\text{opt}}$  must decrease as the wind speed and the initial excess temperature increase.

Further geophysical applications of constructal theory are explored in Bejan et al. (2005).

## 11.11 Carbon Dioxide Sequestration

The important practical problem of the storage of excess carbon dioxide in response to global warming has motivated a number of recent studies. Of special interest is the convection that may be induced in native saline water as  $\text{CO}_2$  dissolves into it near the  $\text{CO}_2$ -brine interface.

The modeling of convective mixing in CO<sub>2</sub> storage has been discussed by Hassanzadeh et al. (2005, 2006, 2007), Preuss and Zhang (2008), and Ghesmat et al. (2011a, b). Ennis-King and Paterson (2003, 2005, 2007), Ennis-King et al. (2005), Riaz et al. (2006), and Xu et al. (2006) studied the coupling of geochemical reaction with convective mixing. This and some related work has been discussed in Sect. 6.11.3 in the context of unsteady boundary layers. Linear stability analysis was also applied by Javaheri et al. (2009, 2010), Wessel-Berg (2009), and Andres and Cardoso (2011). Slim and Ramakrishnan (2010) have studied the onset and cessation of dissolution-driven convection in a time-dependent situation. This situation was re-examined by Kim and Choi (2012), who compared the stability characteristics obtained with and without the quasi-steady state approximation for the problem of an initially quiescent layer, kept isothermal while a solute diffuses due to an impulse change in concentration at an upper boundary.

Green and Ennis-King (2010) investigated the effect of vertical heterogeneity on the long-term migration of CO<sub>2</sub> in saline aquifers. The effect of dispersion on the onset of convection during CO<sub>2</sub> sequestration was investigated by Hidalgo and Carrera (2009). Laboratory flow experiments for visualizing carbon-dioxide-induced, density-driven brine convection were conducted by Kneafsey and Pruess (2010). High-resolution simulation and characterization of density-driven flow in CO<sub>2</sub> storage in saline aquifers were carried out by Pau et al. (2010), following on from related work by Farajzadeh et al. (2007). Yang et al. (2011a, b) numerically simulated the convective stability of the short-term storage of CO<sub>2</sub>. Javadpour and Nicot (2011) studied the effect of nanoparticles on enhanced storage and sequestration in the context of commingled disposal of depleted uranium and CO<sub>2</sub>. The effect of heterogeneity on the character of density-driven convection of carbon dioxide overlying a brine layer was investigated by Farajzadeh et al. (2011) and Ranganathan et al. (2012). Moghaddam et al. (2012) quantified density-driven natural convection as a dissolution mechanism in CO<sub>2</sub> sequestration (see the discussion by Emami Maybodi (2012)). Natural convection in a layer with two miscible phases was studied experimentally by Suekane et al. (2012).

Work on carbon dioxide storage in saline aquifers was surveyed by Michael et al. (2009).

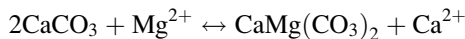
## 11.12 Reaction Scenarios

In Sect. 11.5, we have discussed one example of a flow-controlled chemical reaction. In this section, we follow Chap. 5 of Phillips (2009) and discuss various other geological scenarios that involve changes in composition due to flow-controlled reaction resulting from the fact that the rates of reaction (such as dissolution, combination, or replacement) may be limited by the rate at which the flow can deliver dissolved solutes to the reaction site. For example, when dissolved contaminants in a

surface aquifer are absorbed, or react with, the enclosing matrix, a patch of contaminant moves considerably more slowly than does the interstitial fluid.

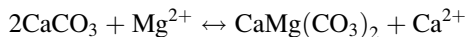
### 11.12.1 Reaction Fronts

We illustrate this phenomenon by an example. Consider the calcite-dolomite replacement reaction



that occurs when seawater, rich in magnesium, seeps through a calcite bed. The pattern of decreasing magnesium ion  $\text{Mg}^{2+}$  in solution is set up within the time that it takes for the individual fluid elements to move through the matrix a distance of two or three times the equilibration length, that is, over a span of a few to a few tens of years. Then the distribution of concentration of the  $\text{Ca}^{2+}$  in solution produced in the reaction also stabilizes, being essentially zero at the entry point, increasing with increasing path length, and ultimately reaching equilibrium with the matrix after a travel distance of the order of the equilibration length.

Consider the calcite-dolomite replacement reaction



that occurs when seawater, rich in magnesium, seeps through a calcite bed. The pattern of decreasing magnesium ion  $\text{Mg}^{2+}$  in solution is set up within the time that it takes for the individual fluid elements to move through the matrix a distance of two or three times the equilibration length, that is, over a span of a few to a few tens of years.

Suppose that one has an initially pristine water-saturated permeable region and that at some initial instant, a uniform stream of chemically distinct water enters the region and as it percolates through, it begins to dissolve or react with the solid matrix. The incoming fluid infiltrates into the region at the mean interstitial fluid velocity  $\bar{v}$  and gradually tends toward a local equilibrium with the solid phase. Within a contact time  $\gamma^{-1}$ , where  $\gamma$  is the kinetic rate constant, and during this time, the fluid elements have moved a distance (called the equilibration length):

$$l_E = \bar{v}/\gamma.$$

Near the boundary, the incoming fluid is far from saturation, and the rate of dissolution of the matrix (or generation of reactant) is greater, but it decreases with distance from the interface as the interstitial fluid approaches saturation. An order-of-magnitude estimate of the time needed to develop a separate front is given by considering the amount of water it takes to flush the products of reaction from the

slice of the matrix adjacent to the boundary with thickness  $l_E$  and unit cross-sectional area. If  $2s_0$  is the number of moles of calcite per unit volume initially in the solid medium, then the number per unit area in the slice is

$$2s_0 l_E \approx 2s_0 \bar{v} / \gamma.$$

Half of the calcium has to be removed from the reaction site in the form of aqueous Ca with concentration (number of moles of Ca per unit mass of water)  $c_0$ . This requires a volume  $V$  per unit cross-sectional area such that  $c_0 V = s_0 l_E$ , so that  $V = (s_0/c_0)l_E$ , which is very much greater than the equilibration length. Since the transport velocity is  $\varphi\bar{v}$  where  $\phi$  is the porosity, the requisite volume  $V$  of water per unit cross-sectional area is supplied in time  $T$  such that  $c_0 V = s_0 l_E$ . Consequently, the time needed for a front to form is

$$T \sim \frac{V}{\phi\bar{v}} = \frac{s_0}{c_0} \frac{l_E}{\phi\bar{v}} \sim \frac{s_0}{\phi\gamma c_0}.$$

This is independent of the mean interstitial fluid velocity since the equilibration length is proportional to  $\bar{v}$ . Now  $s_0$  is the number of moles of the solid reactant, calcite, per unit volume, and  $c_0$  is the number of moles in aqueous solution, smaller by a factor of order  $10^{-5}$ – $10^{-6}$ . Thus,  $s_0/c_0 \sim 10^{-5}$ – $10^{-6}$ , the porosity  $\phi \sim 0.2$ – $0.3$ , and the reaction rate  $\gamma \sim 1 \text{ yr}^{-1}$  with much scatter. The time for the formation of a reaction front is then estimated to be about  $10^5$ – $10^6$  yr, a huge multiple of the time that it takes for the fluid element to travel a distance equal to the equilibration length.

### 11.12.2 Gradient Reactions

The equilibrium concentration of a solute is generally a function of temperature and (to some extent) total pressure, and this means that if the temperature and total pressure vary spatially in a region, then so does the local concentration of dissolved species. Even if there is local equilibrium if the fluid is at rest, when interstitial fluids move through the matrix, the fluid elements find themselves in regions of different temperature and pressure, and for the fluid to move toward a new local equilibrium with the matrix, reactions must occur between the fluid and the surrounding matrix. In general, the concentration of solute in each fluid element must change at a rate proportional to (1) the interstitial fluid velocity, (2) the variation of equilibrium concentration with temperature (for example), and (3) the spatial temperature gradient along the flow path. This is called the gradient reaction scenario, identified by Wood and Hewett (1982). It has a number of characteristics that distinguish it from the passage of a reaction front in a porous medium. Reaction occurs throughout the region simultaneously but more rapidly

along cracks or fractures that provide effective flow paths across isotherms. Gradient reactions can be expected particularly in geothermal regions where the temperature field may provide both the buoyancy distribution that drives the flow and the spatial temperature gradient that alters the equilibrium concentration along flow paths. Reactions proceed more slowly in relatively less permeable inclusions where the interstitial flow is reduced. A consequence is that a gradient reaction may slowly modify the mineral composition in a region. For example, in a closed circulating flow, the processes of dissolution in some regions and deposition in others can redistribute minerals spatially along the flow paths.

### ***11.12.3 Mixing Zones***

Alterations in mineral composition or precipitation or dissolution can also occur by the mixing of different interstitial waters, though in a porous medium this is a slower process than in a fluid clear of solid material. The usual sequence of turbulent eddy sizes is inhibited in a classical permeable medium, but fractures can provide pathways for rapid flow and local mixing. Simple mixing of water types inside a permeable region occurs predominantly in a few particular flow situations, such as freshwater-saltwater interfaces. When the equilibrium concentrations of a solute are different in fresh and saline waters, their mixture may produce dissolution or deposition.

# References

- Aatif, H., Allali, K. and El Karouni, K. 2010 Influence of vibrations on convective instability of reaction fronts in porous media. *Math. Modell. Natur. Phen.* **5**, 123–137. [6.24]
- Abbas, I. A. 2008 Combined effect of thermal dispersion and radiation on free convection in a fluid saturated, optically thick porous medium. *Forsch. Ingen. Engng. Res.* **72**, 135–144. [5.1.7.3]
- Abbas, I. A., El-Amin, M. F. and Salama, A. 2009 Effect of thermal dispersion on the free convection in a fluid saturated porous medium. *Int. J. Heat Fluid Flow* **30**, 229–236. [5.1.7.3]
- Abbasi, A., Saghir, M. Z. and Kawaji, M. 2011 Study of thermodiffusion of carbon dioxide in binary mixtures of n-butane and carbon dioxide and n-dodecane and carbon dioxide in porous media. *Int. J. Therm. Sci.* **50**, 124–132. [9.1.4]
- Abbassi, H. 2007 Entropy generation analysis in a uniformly heated microchannel heat sink. *Energy* **32**, 1932–1947. [4.16.5]
- Abdel-Gaied, S. M. and Eid, M. R. 2011 Natural convection of non-Newtonian power-law fluid over axisymmetric and two-dimensional bodies of arbitrary shape in fluid-saturated porous media. *Appl. Math. Mech. (English ed.)* **32**, 179–188. [5.9]
- Abdelkareem, A. H., Kimura, S., Kiwata, T. and Komatsu, N. 2009 Experimental study on oscillatory convection in a Hele-Shaw cell due to unstably heated side. *Transp. Porous Media* **76**, 363–375. [2.5]
- Abdelkhalek, M. M. 2008b Radiation and dissipation effect on unsteady MHD micropolar flow, past an infinite vertical plate in porous medium with time dependent suction. *Indian J. Phys. Proc. Indian Assoc. Cult. Sci.* **82**, 415–434. [5.1.9.2]
- Abdel-Rahman, G. M. 2008 Thermal diffusion and MHD effects on combined free-forced convection and mass transfer of a viscous fluid flow through a porous medium with heat generation. *Chem. Engng. Tech.* **31**, 554–559. [9.6.1]
- Abdel-Rahman, G. M. 2010 Thermal-diffusion and MHD for Soret and Dufour's effect on Hiemenz flow and mass transfer of fluid flow though porous medium onto a stretching surface. *Physica B* **405**, 2560–2569. [9.1.4]
- Abdou, M. M.M. 2010 Effect of radiation with temperature dependent viscosity and thermal conductivity on unsteady stretching sheet through porous media. *Nonlinear Anal. Modell. Control* **15**, 257–270. [9.2.1]
- Abel, M. S. and Ueera, P. H. 1998 Viscoelastic fluid flow and heat transfer in a porous medium over a stretching sheet. *Int. J. Nonlinear Mech.* **33**, 531–540.s
- Abel, M. S., Khan, S. K. and Prasad, K. V. 2001 Convective heat and mass transfer in a viscoelastic fluid flow through a porous medium over a stretching sheet. *Int. J. Numer. Meth. Heat Fluid Flow* **11**, 779–792. [9.2.1]
- Abel, M. S., Mahesha, N. and Malipatel, S. B. 2011 Heat transfer due to MHD slip flow of a second-grade liquid over a stretching sheet through a porous medium with non-uniform heat source/sink. *Chem. Engng. Commun.* **198**, 191–213. [5.1.9.9]

- Abel, M. S., Nandeppanavar, M. M. and Malipatil, S. B. 2010a Heat transfer in a second grade fluid through a porous medium from a permeable stretching sheet with non-uniform heat source/sink. *Int. J. Heat Mass Transfer* **53**, 1788–1795. [5.1.9.9]
- Abel, M. S., Nandeppanavar, M. M. and Malkhed, M. B. 2010b Hydromagnetic boundary layer flow and heat transfer in a fluid over a continuously moving permeable stretching surface with nonuniform heat source/sink embedded in fluid saturated porous medium. *Chem. Engng. Commun.* **197**, 633–655. [5.1.9.9]
- Abkar, M., Forooghi, P., Abbassi, A. and Aghdam, M. M. 2010 Heat transfer of non-Newtonian fluid flow in a channel lined with porous layers under thermal nonequilibrium conditions. *J. Porous Media* **13**, 235–246. [4.16.3]
- Aboubi, K., Robillard, L. and Bilgen, E. 1995a Convective heat transfer in an annular porous layer with centrifugal force field. *Numer. Heat Transfer A* **28**, 375–38. [7.3.3]
- Aboubi, K., Robillard, L. and Bilgen, E. 1995b Natural convection in horizontal annulus filled with an anisotropic porous medium. *Proc. ASME/JSM Thermal Engineering Joint Conf.* Vol. 3, 415–422. [7.3.3]
- Aboubi, K., Robillard, L. and Vasseur, P. 1998 Natural convection in horizontal annulus filled with an anisotropic porous medium. *Int. J. Numer. Meth. Heat Fluid Flow* **8**, 689–702. [6.16.2]
- Abou-zeid, M. Y. 2011 Magnetohydrodynamic boundary layer heat transfer to a stretching sheet including viscous dissipation and internal heat generation in a porous medium. *J. Porous Media* **14**, 1007–1008. [5.1.9.9]
- Abu-Hijleh, B. A. K. 1997 Convection heat transfer from a laminar flow over a 2-D backward facing step with asymmetric and orthotropic porous floor segments. *Numer. Heat Transfer A* **31**, 325–335. [4.11]
- Abu-Hijleh, B. A. K. 2000 Heat transfer from a 2D backward facing step with isotropic porous floor segments. *Int. J. Heat Mass Transfer* **43**, 2727–2737. [4.11]
- Abu-Hijleh, B. A. K. 2001a Natural convection heat transfer from a cylinder covered with an orthotropic porous layer in cross-flow. *Numer. Heat Transfer A* **40**, 767–782. [5.12.3]
- Abu-Hijleh, B. A. K. 2001b Laminar forced convection heat transfer from a cylinder covered with an orthotropic porous layer in cross-flow. *Int. J. Numer. Meth. Heat Fluid Flow* **11**, 106–120. [4.11]
- Abu-Hijleh, B. A. K. 2002 Entropy generation due to cross-flow heat transfer from a cylinder covered with an orthotropic porous layer. *Heat Mass Transfer* **39**, 27–40. [4.11]
- Abu-Hijleh, B. A. K. 2003 Enhanced forced convection heat transfer from a cylinder using permeable fins. *ASME J. Heat Transfer* **125**, 804–811. [4.11]
- Abu-Hijleh, B. A. K. and Al-Nimr, M. A. 2001 The effect of the local inertial term on the fluid flow in channels partially filled with porous material. *Int. J. Heat Mass Transfer* **44**, 1565–1572. [4.11]
- Abu-Hijleh, B. A. K., Al-Nimr, M. A. and Hader, M. A. 2004 Thermal equilibrium in transient forced convection porous channel flow. *Transport Porous Media* **57**, 49–58. [4.10]
- Abuzaid, M. M., Al-Nimr, M. A. and Aldoss, T. K. 2005 Effect of the macroscopic local inertial term on the non-Newtonian free-convection flow in channels filled with porous materials. *J. Porous Media* **8**, 419–430. [7.1.6]
- Acharya, M., Dash, G. C. and Singh, L. P. 2000 Magnetic effects on the free convection and mass transfer flow through porous medium with constant suction and constant heat. *Indian J. Pure Appl. Math.* **31**, 1–18. [9.2.1]
- Achenbach, E. 1995 Heat and flow characteristics of packed beds. *Expt. Thermal Fluid Science* **10**, 17–27. [1.5.2]
- Adnani, P., Catton, I. and Abdou, M. A. 1995 Non-Darcian forced convection in porous media with anisotropic dispersion. *ASME J. Heat Transfer* **117**, 447–451. [4.9]
- Adnani, S. G. and Hsiao, K. T. 2005 Transport phenomena in liquid composites molding processes and their roles in process control and optimization. *Handbook of Porous Media* (ed. K. Vafai), 2nd ed., Taylor and Francis, New York, pp. 573–606. [10.2.3]

- Adrian, P. and Nicoleta, S. 2005 Effect of asymmetry on the steady convection in a vertical torus filled with a porous medium. *Strojnicki Vestnik—J. Mech. Engng.* **51**, 501–508. [6.17]
- Afazal, N. and Salam, M. Y. 1990 Natural convection from point source embedded in Darcian porous medium. *Fluid Dyn. Res.* **6**, 175–184. [5.8]
- Afifi, A. A. 2007 a Effects of temperature-dependent viscosity with Soret and Dufour numbers on non-Darcy MHD free convective heat and mass transfer past a vertical surface embedded in a porous medium. *Transp. Porous Media* **66**, 391–401. [9.2.1]
- Afifi, A. A. 2007b Effects of variable viscosity on non-Darcy MHD free convection along a non-isothermal vertical surface in a thermally stratified porous medium. *Appl. Math. Modell.* **31**, 1621–1634. [5.1.9,9]
- Afifi, R. I. and Berbish, N. S. 1999 Experimental investigation of forced convection heat transfer over a horizontal flat plate in a porous medium. *J. Engng. Appl. Sci.* **46**, 693–710. [4.1]
- Afzal, N. 1985 Two-dimensional buoyant plume in porous media: higher-order effects. *Int. J. Heat Mass Transfer* **28**, 2029–2041. [5.10.1.1]
- Agarwal, S. and Bhaduria, B. S. 2011 Natural convection in a nanofluid saturated rotating porous layer with thermal non-equilibrium model. *Transp. Porous Media* **90**, 627–654. [6.23, 9.7]
- Agarwal, S., Bhaduria, B. S. and Siddheshwar, P. G. 2011 Thermal instability of a nanofluid saturating a rotating anisotropic porous medium *Spec. Top. Rev. Porous Media* **2**, 53–64. [6.23]
- Agarwal, S., Saceti, N. M., Chanran, P., Bhaduria, B. S. and Singh, A. K. 2012 Nonlinear convective transport in a binary nanofluid saturated porous layer. *Transp. Porous Media* **93**, 29–49. [9.7]
- Aguilar-Madera C. G., Valdes-Parada, F. J., Goyeau, B. and Ochoa-Tapia, J. A. 2011a Convective heat transfer in a channel partially filled with a porous medium. *Int. J. Therm. Sci.* **50**, 1355–1368. [4.11]
- Aguilar-Madera, C. G., Valdes-Parada, F. J., Goyeau, B. and Ochoa-Tapia, J. A. 2011b Effective thermal properties at the fluid-porous medium interfacial region: Role of the particle-particle contact. *Rev. Mexicana Ing. Quim.* **10**, 375–386. [2.4]
- Agwu Nnanna, A. G., Haji-Sheikh, A. and Harris, K. T. 2004 Experimental study of local thermal non-equilibrium phenomena during phase change in porous media. *Int. J. Heat Mass Transfer* **43**, 4365–4375. [10.1.7]
- Ahmad, S. and Pop, I. 2010 Mixed convection boundary layer flow from a vertical plate embedded in a porous medium filled with nanofluids. *Int. Comm. Heat Mass Transfer* **37**, 987–991. [8.1.6]
- Ahmed, N. J. S., Badruddin, I. A., Kaneshan, J., Zainal, Z. A. and Ahamaed, K. S. N. 2011 Study of mixed convection in an annular vertical cylinder filled with saturated porous medium, using thermal non-equilibrium model. *Int. J. Heat Mass Transfer* **54**, 3822–3825. [8.3.3]
- Ahmed, N. J. S., Badruddin, I. A., Zainal, Z. A., Khaleed, H. M. T. and Kaneshan, J. 2009 Heat transfer in a conical cylinder with porous medium. *Int. J. Heat Mass Transfer* **52**, 3070–3078. [7.3.7]
- Ahmed, S. and Zueco, J. 2011 Modeling of heat and mass transfer in a rotating vertical porous channel with Hall current. *Chem. Engng. Comm.* **198**, 1294–1308. [9.4]
- Aichlmayr, H. T. and Kulacki, F. A. 2006 The effective thermal conductivity of saturated porous media. *Adv. Heat Transfer* **39**, 377–460. [2.2.1]
- Aidun, C. K. 1987 Stability of convection rolls in porous media. *ASME HTD* **94**, 31–36. [6.8]
- Aidun, C. K. and Steen, P. H. 1987 Transition of oscillatory convective heat transfer in a fluid-saturated porous medium. *AIAA J. Thermophys. Heat Transfer* **1**, 268–273. [6.8]
- Ait Saada, M., Chikh, S. and Campo, A. 2007 Natural convection around a horizontal solid cylinder wrapped with a layer of fibrous or porous material. *Int. J. Heat Fluid Flow* **28**, 483–495. [5.5.1]
- Aithal, S. M., Aldemir, T. and Vafai, K. 1994 Assessment of the impact of neutronic/ thermal-hydraulic coupling in the design and performance of nuclear reactors on the design and performance of nuclear reactors for space propulsion. *Nuclear Tech.* **106**, 187–202. [4.16.5]
- Akbal, S. and Baytas, F. 2008 Effects on non-uniform porosity on double diffusive natural convection in a porous cavity with partially permeable wall. *Int. J. Therm. Sci.* **47**, 875–885. [9.2.2]

- Akyildiz, F. T. and Signer, D. A. 2011 Nonlinear Forchheimer effect on the forced convection in porous-saturated ducts of rectangular cross section. *J. Porous Media* **14**, 81–90. [4.9]
- Akyildiz, F. T., Signer, D. A., Vajravelu, K. and Van Gorder, R. A. 2012 Natural convection heat transfer of a viscous liquid in a vertical porous channel. *J. Engng. Math.* **74**, 61–71. [7.1.7]
- Alagoa, K. D., Tay, G. and Abbey, T. M. 1999 Radiative and free-convection effects of a MHD flow through porous medium between infinite parallel plates with time-dependent suction. *Astrophys. Space Science* **260**, 455–468. [7.3.7]
- Al-Amiri, A. M. 2002 Natural convection in porous enclosures: The application of the two-energy model. *Numer. Heat Transfer A* **41**, 817–834. [7.6.2]
- Al-Amiri, A. M., Khanafer, K. and Lightstone, M. F. 2006 Unsteady numerical simulation of double diffusive convection heat transfer in a pulsating horizontal heating annulus. *Heat Mass Transfer* **42**, 1007–1015. [9.4]
- Al-Amiri, A. M., Khanafer, K. and Pop, I. 2008 Steady-state conjugate natural convection in a fluid-saturated porous cavity. *Int. J. Heat Mass Transfer* **51**, 4260–4275. [7.1.5]
- Alavyoon, F. 1993 On natural convection in vertical porous enclosures due to prescribed fluxes of heat and mass at the vertical boundaries. *Int. J. Heat Mass Transfer* **36**, 2479–2498. [9.2.2]
- Alavyoon, F., Masuda, Y. and Kimura, S. 1994 On the natural convection in vertical porous enclosures due to opposing fluxes of heat and mass prescribed at the vertical walls. *Int. J. Heat Mass Transfer* **37**, 195–206. [9.2.2]
- Al-Azmi, B. A. 2011 Natural convection in a trapezoidal enclosure filled with a non-Darcy porous medium. *J. Porous Media* **14**, 467–480. [7.3.7]
- Alazmi, B. and Vafai, K. 2000 Analysis of variants within the porous media transport models. *ASME J. Heat Transfer* **122**, 303–326. [7.6.2]
- Alazmi, B. and Vafai, K. 2001 Analysis of fluid flow and heat transfer interfacial conditions between a porous medium and a fluid layer. *Int. J. Heat Mass Transfer* **44**, 1735–1749. [1.6]
- Alazmi, B. and Vafai, K. 2002 Constant wall heat flux boundary conditions in porous media under local thermal non-equilibrium conditions. *Int. J. Heat Mass Transfer* **45**, 3071–3087. [2.2.3, 4.10]
- Alazmi, B. and Vafai, K. 2004 Analysis of variable porosity, thermal dispersion and local thermal nonequilibrium on free surface flows through porous media. *ASME J. Heat Mass Transfer* **126**, 389–399. [4.10]
- Al-Badawi, Y. M. and Duwairi, H. M. 2010 MHD natural convection with Joule and viscous heating effects in iso-flux porous medium-filled enclosures. *Appl. Math. Mech. English ed.* **31**, 1105–1112. [7.8]
- Albert, M. R. 1995 Advective-diffusive heat transfer in snow. *ASME Int. Mech. Cong. Expos.*, San Francisco, Paper 95-Wa/HT-44. [11.1]
- Alchaar, S., Vasseur, P. and Bilgen, E. 1995a Effects of a magnetic field on the onset of convection in a porous medium. *Heat Mass Transfer* **30**, 259–267. [6.21]
- Alchaar, S., Vasseur, P. and Bilgen, E. 1995b Hydromagnetic natural convection in a tilted rectangular porous enclosure. *Numer. Heat Transfer A* **27**, 107–127. [7.8]
- Aldabbagh, L. B. Y., Manesh, H. F. and Mohamad, A. A. 2008 Unsteady natural convection inside a porous enclosure heated from the side. *J. Porous Media* **11**, 73–83. [7.5]
- Aldoss, T. K. 1996 MHD mixed convection from a vertical cylinder embedded in a porous medium. *Int. Comm. Heat Mass Transfer* **23**, 517–530. [8.1.3]
- Aldoss, T. K. 2009 Natural convection from a horizontal annulus filled with porous medium of variable permeability. *J. Porous Media* **12**, 715–724. [7.3.3]
- Aldoss, T. K. and Ali, Y. D. 1997 MHD mixed convection from a horizontal cylinder in a porous medium. *JSME Int. J. Ser. B* **40**, 290–295. [8.1.3]
- Aldoss, T. K., Alkam, M. and Shatarah, M. 2004 Natural convection from a horizontal annulus partially filled with a porous medium. *Int. Comm. Heat Mass Transfer* **31**, 441–452. [7.7]
- Aldoss, T. K., Alnimir, M. A., Jarrahr, M. A. and Alshaer, B. J. 1995 Magnetohydrodynamic mixed convection from a vertical plate embedded in a porous medium. *Numer. Heat Transfer A* **28**, 635–645. [8.1.1]

- Aldoss, T. K., Chen, T. S. and Armaly, B. F. 1993a Nonsimilarity solutions for mixed convection from horizontal surfaces in a porous medium — variable surface heat flux. *Int. J. Heat Mass Transfer* **36**, 463–470. [8.1.2]
- Aldoss, T. K., Chen, T. S. and Armaly, B. F. 1993b Nonsimilarity solutions for mixed convection from horizontal surfaces in a porous medium — variable wall temperature. *Int. J. Heat Mass Transfer* **36**, 471–477. [8.1.2]
- Aldoss, T. K., Chen, T. S. and Armaly, B. F. 1994a Mixed convection over nonisothermal horizontal surfaces in a porous medium — the entire regime. *Numer. Heat Transfer A* **25**, 685–701. [8.1.2]
- Aldoss, T. K., Jarrah, M. A. and Al-Sha'er, B. J. 1996 Mixed convection from a vertical cylinder embedded in a porous medium: non-Darcy model. *Int. J. Heat Mass Transfer* **39**, 1141–1148. [8.1.3]
- Aldoss, T. K., Jarrah, M. A. and Duwairi, H. M. 1994b Wall effect on mixed convection flow from horizontal surfaces with a variable heat flux. *Canad. J. Chem. Engng.* **72**, 35–42. [8.1.2]
- Aleshkova, I. A. and Sheremet, M. A. 2010 Unsteady conjugate convection in a square enclosure filled by a porous medium. *Int. J. Heat Mass Transfer* **53**, 5364–5372. [7.1.5]
- Alex, S. M. and Patil, P. R. 2000a Thermal instability in an anisotropic rotating porous medium. *Heat Mass Transfer* **36**, 159–163. [6.22]
- Alex, S. M. and Patil, P. R. 2000b Thermal instability in an inclined isotropic porous medium. *J. Porous Media* **3**, 207–216. [7.8]
- Alex, S. M. and Patil, P. R. 2001 Effect of variable gravity field on Soret driven thermosolutal convection in a porous medium. *Int. Comm. Heat Mass Transfer* **28**, 509–518. [9.1.6.4]
- Alex, S. M. and Patil, P. R. 2002a Effect of a variable gravity field on convection in an isotropic porous medium with internal heat source and inclined temperature gradient. *ASME J. Heat Transfer* **124**, 144–150. [7.9]
- Alex, S. M. and Patil, P. R. 2002b Effect of a variable gravity field on thermal instability in a porous medium with inclined temperature gradient and vertical throughflow. *J. Porous Media* **5**, 137–147. [7.9]
- Alex, S. M., Patil, P. R. and Venakrishnan, K. S. 2001 Variable gravity effects on thermal instability in a porous medium with internal heat source and inclined temperature gradient. *Fluid Dyn. Res.* **29**, 1–6. [7.9]
- Al-Farhany, K. and Turan, A. 2011 Non-Darcy effects on conjugate double-diffusive natural convection in a variable porous layer sandwiched by finite thickness walls. *Int. J. Heat Mass Transfer* **54**, 2868–2879. [9.4]
- Al-Hadhrami, A. K., Elliot, L. and Ingham, D. B. 2002 Combined free and forced convection in vertical channels of porous media. *Transport in Porous Media* **49**, 265–289. [8.3.1]
- Al-Hadhrami, A. K., Elliot, L. and Ingham, D. B. 2003 A new model for viscous dissipation in porous media across a range of permeability values. *Transport in Porous Media* **53**, 117–122. [2.2.2]
- Al-Hadhrami, A. K., Elliot, L., Ingham, D. B. and Wen, X. 2001a Fluid flows through two-dimensional channels of composite materials. *Transport Porous Media* **45**, 283–302. [4.11]
- Al-Hadhrami, A. K., Elliot, L., Ingham, D. B. and Wen, X. 2001b Analytical solutions of fluid flows through composite channels. *J. Porous Media* **4**, 149–163. [4.11]
- Al-Harbi, S. M. 2005 Numerical study of natural convection heat transfer with variable viscosity and thermal radiation from a cone and wedge in porous media. *Appl. Math. Comput.* **170**, 64–75. [5.3, 5.8]
- Ali, M. E. 2007 The effect of lateral mass flux on the natural convection boundary layers induced by a heated vertical plate embedded in a saturated porous medium with internal heat generation. *Int. J. Therm. Sci.* **46**, 157–163. [5.1.9.4]
- Alkam, M. K. and Al-Nimr, M. A. 1998 Transient non-Darcian forced convection flow in a pipe partially filled with a porous material. *Int. J. Heat Mass Transfer* **41**, 347–356. [4.6.4]
- Alkam, M. K. and Al-Nimr, M. A. 1999a Improving the performance of double-pipe heat exchangers by using porous substrates. *Int. J. Heat Mass Transfer* **42**, 3609–3618. [4.11]

- Alkam, M. K. and Al-Nimr, M. A. 1999b Solar collectors with tubes partially filled with porous substrates. *ASME J. Solar Energy* **121**, 20–24. [4.11]
- Alkam, M. K. and Al-Nimr, M. A. 2001 Transient flow hydrodynamics in circular channels partially filled with a porous material. *Heat Mass Transfer* **37**, 133–137. [4.11]
- Alkam, M. K., Al-Nimr, M. A. and Hamdan, M. O. 2001 Enhancing heat transfer in parallel-plate channels by using porous media. *Int. J. Heat Mass Transfer* **44**, 931–938. [4.11]
- Alkam, M. K., Al-Nimr, M. A. and Hamdan, M. O. 2002 On forced convection in channels partially filled with porous substrates. *Heat Mass Transfer* **38**, 337–342. [4.11]
- Alkam, M. K., Al-Nimr, M. A. and Mousa, Z. 1998 Forced convection of non-Newtonian fluids in porous concentric annuli. *Int. J. Numer. Meth. Heat Fluid Flow* **8**, 703–716. [4.16.3]
- Allain, C., Cloitre, M. and Mongruel, A. 1992 Scaling in flows driven by heat and mass convection in a porous medium. *Europhys. Lett.* **20**, 313–318. [9.2.1]
- Allali, K., Belhaq, M. and El Karouni, K. 2012 Influence of quasi-periodic gravitational modulation on convective instability of reaction fronts in porous media. *Comm. Nonlinear Sci. Numer. Simul.* **17**, 1586–1596. [6.24]
- Allan, F. M. and Hamdan, M. H. 2002 Fluid mechanics of the interface region between two porous layers. *Appl. Math. Comput.* **128**, 37–43. [1.6]
- Allehiany, F. M. and Abdullah, A. A. 2009 Bénard convection in a horizontal porous layer permeated by a non-linear magnetic fluid under the influence of both magnetic field and Coriolis forces. *Appl. Math. Inform. Sci.* **3**, 59–77. [6.22]
- Allouache, N. and Chikh, S. 2008 Numerical modeling of turbulent flow in an annular heat exchanger partly filled with a porous substrate. *J. Porous Media* **11**, 617–632. [4.11]
- Alloui, Z. and Vasseur, P. 2011 Natural convection induced by a centrifugal force field in a horizontal annular porous layer saturated with a binary fluid. *Transp. Porous Media* **88**, 169–185. [9.4]
- Alloui, Z. and Vasseur, P. 2010 Convection in superposed fluid and porous layers. *Acta Mech.* **214**, 245–260. [6.19.3]
- Alloui, Z., Bennacer, R. and Vasseur, P. 2009a Variable permeability effect on convection in binary mixtures saturating a porous layer. *Heat Mass Transfer* **45**, 1117–1127. [9.1.6.2]
- Alloui, Z., Dufau, L., Beji, H. and Vasseur, P. 2009b Multiple steady states in a porous enclosure partially heated and fully salted from below. *Int. J. Therm. Sci.* **48**, 521–534. [9.1.6.4]
- Alloui, Z., Fekri, M., Beji, H. and Vasseur, P. 2008 Natural convection in a horizontal binary fluid bounded by thin porous layers. *Int. J. Heat Fluid Flow* **24**, 1154–1163. [9.4]
- Alloui, Z., Robillard, L. and Vasseur, P. 2010a Density maximum effect on Soret-induced natural convection in a square porous cavity. *Fluid Dyn. Res.* **42**, #055507. [9.1.4]
- Alloui, Z., Vasseur, P., Robillard, L. and Bahoul, A. 2010b Onset of double diffusive convection in a horizontal Brinkman cavity. *Chem. Engng. Comm.* **197**, 387–399. [9.1.6.3]
- Almubarak, A. A., Al-Saeedi, J. N. and Shoukry, M. 2008 The effect of a boundary layer on drying mechanisms of beach and desert sand. *European J. Soil. Sci.* **59**, 807–816. [3.6]
- Al-Nimr, M. A. and Abu-Hijleh, B. A. 2002 Validation of thermal equilibrium assumption in transient forced convection flow in porous channel. *Transport in Porous Media* **49**, 127–138. [4.10]
- Al-Nimr, M. A. and Alkam, M. K. 1997a Film condensation on a vertical plate embedded in a porous medium. *J. Appl. Energy* **56**, 47–57. [10.4]
- Al-Nimr, M. A. and Alkam, M. K. 1997b Unsteady non-Darcian forced convection analysis in an annulus partially filled with a porous material. *ASME J. Heat Transfer* **119**, 799–804. [4.11]
- Al-Nimr, M. A. and Alkam, M. K. 1998a A modified tubeless solar collector partially filled with porous substrate. *Renewable Energy* **13**, 165–173. [4.11]
- Al-Nimr, M. A. and Alkam, M. K. 1998b Unsteady non-Darcian fluid flow in parallel-plates channels partially filled with porous materials. *Heat Mass Transfer* **33**, 315–318. [4.11]
- Al-Nimr, M. A. and Darabseh, T. T. 1995 Analytical solution for transient laminar free convection in open-ended vertical concentric porous annuli. *ASME J. Heat Transfer* **117**, 762–764. [7.5]

- Al-Nimr, M. A. and Haddad, O. M. 1999a Fully developed free convection in open-ended vertical channels partially filled with porous material. *J. Porous Media* **2**, 179–204. [7.7]
- Al-Nimr, M. A. and Haddad, O. M. 2006 Comments on ‘Forced convection with slip-flow in a channel or duct occupied by a hyper-porous medium saturated by a rarefied gas’. *Transp. Porous Media* **67**, 165–167. [4.9]
- Al-Nimr, M. A. and Hader, M. A. 1999b MHD free convection flow in open-ended vertical porous channels. *Chem. Engng. Sci.* **54**, 1883–1889. [7.7]
- Al-Nimr, M. A. and Khadrawi A. F. 2003 Transient free convection fluid flow in domains partially filled with porous media. *Transport in Porous Media* **51**, 157–172. [7.7]
- Al-Nimr, M. A. and Kiwan, S. 2002 Examination of the thermal equilibrium assumption in periodic forced convection in a porous channel. *J. Porous Media* **5**, 35–40. [4.10]
- Al-Nimr, M. A. and Massoud, S. 1998 Unsteady free convection flow over a vertical flat plate immersed in a porous medium. *Fluid Dyn. Res.* **23**, 153–160. [5.1.9.9]
- Al-Nimr, M. A., Aldoss, T. and Abuzaid, M. M. 2005 Effect of the macroscopic local inertial term on the non-Newtonian free-convection flow in channels filled with porous materials. *J. Porous Media* **8**, 421–430. [7.5]
- Al-Nimr, M. A., Aldoss, T. and Naji, M. I. 1994a Transient forced convection in the entrance region of a porous tube. *Canad. J. Chem. Engng.* **72**, 249–255. [4.6.4]
- Al-Nimr, M. A., Aldoss, T. and Naji, M. I. 1994b Transient forced convection in the entrance region of porous concentric annuli. *Canad. J. Chem. Engng.* **72**, 1092–1096. [4.6.4]
- Al-Odat, M. Q. 2004a Nonsimilar solutions for unsteady free convection from a vertical plate embedded in a non-Darcy porous medium. *Int. Comm. Heat Mass Transfer* **31**, 377–386. [5.1.7.2]
- Al-Odat, M. Q. 2004b Transient non-Darcy mixed convection along a vertical surface in porous medium with suction or injection. *Appl. Math. Comput.* **156**, 679–694. [8.1.1]
- Al-Odat, M. Q. and Al-Ghamdi, A. 2012 Numerical investigation of Dufour and Soret effects on unsteady MHD natural convection flow past vertical plate embedded in non-Darcy porous medium. *Appl. Math. Mech-English ed.* **33**, 195–210. [9.2.1]
- Al-Odat, M. Q. and Damseh, R. A. 2008 Viscous dissipation and joule heating effects on transient non-Darcy magnetodynamic convection flow of micropolar fluids past a vertical moving plate. *J. Porous Media* **11**, 85–100. [5.1.9.2]
- Al-Odat, M. Q., Al-Azab, T. A., Al-Hasan, M. and Shannak, B. A. 2009 Transient MHD double-diffusive natural convection over a vertical surface embedded in a non-Darcy porous medium. *Math. Problems Engng.* #758046. [9.2.1]
- Al-Odat, M. Q., Al-Hussein, F. M. S. and Damseh, R. A. 2005 Influence of radiation on mixed convection over a wedge in non-Darcy porous medium. *Forsch. Ingen.—Engng Research* **69**, 209–215. [8.1.4]
- Al-Sumaily, G. F., Nakayama, A., Sheridan, J. and Thompson, M. C. 2012a The effect of porous media particle size on forced convection from a circular cylinder without assuming local thermal equilibrium between phases. *Int. J. Heat Mass Transfer* **55**, 3366–3378. [4.3, 4.10]
- Al-Sumaily, G. P., Sheridan, J. and Thompson, M. C. 2012b Analysis of forced convection heat transfer from a circular cylinder embedded in a porous medium. *Int. J. Therm. Sci.* **51**, 121–131. [4.3].
- Altevogt, A. S., Rolston, D. E. and Whitaker, S. 2003 New equations for binary gas transport in porous media; part 1: equation development. *Adv. Water Res.* **26**, 695–715. [1.4.1]
- Alvarez, G., Bournet, P. E. and Flick, D. 2003 Two-dimensional simulation of turbulent flow and transfer through stacked spheres. *Int. J. Heat Mass Transfer* **46**, 2459–2469. [1.8]
- Alves, L. S. de B. and Cotta, R. M. 2000 Transient natural convection inside porous cavities: hybrid numerical-analytical solution and symbolic-numerical computation. *Num. Heat Transfer A* **38**, 89–110. [7.5]
- Alves, L. S. de B., Cotta, R. M. and Pontes, J. 2002 Stability analysis of natural convection in porous cavities through integral transforms. *Int. J. Heat Mass Transfer* **45**, 1185–1195. [6.15.1].

- Aly, A. M. and Chamkha, A. 2010 Non-similar solutions for heat and mass transfer from a surface embedded in a porous medium for two prescribed thermal and solutal boundary conditions. *Int. J. Chem. Reactor Engng.* **8**, #A56. [9.2.1]
- Aly, A. M., Mansour, M. A. and Chamkha, A. 2011 Effects of Soret and Dufour numbers on free convection over isothermal and adiabatic stretching surfaces embedded in porous media. *J. Porous Media* **14**, 67–72.[9.2.1]
- Aly, E. H., Elliott, L. and Ingham, D. B. 2003 Mixed convection boundary-layer flow over a vertical surface embedded in a porous medium. *European J. Mech. B/Fluids* **22**, 529–543. [8.1.1]
- Amahmid, A., Hasnaoui, M. and Douamna, S. 2001 Analytic and numerical study of double-diffusive parallel flow induced in a vertical porous layer subjected to constant heat and mass fluxes. *Strojnicki Vestnik-J. Mech. Engng.* **47**, 501–505. [9.2.2]
- Amahmid, A., Hasnaoui, M. and Vasseur, P. 1999c Étude analytique et numérique de la convection naturelle dans une couche poreuse de Brinkman doublement diffusive. *Int. J. Heat Mass Transfer* **42**, 2991–3005. [9.2.2]
- Amahmid, A., Hasnaoui, M., Mamou, M. and Vasseur, P. 1999a Double-diffusive parallel flow induced in a horizontal Brinkman porous layer subjected to constant heat and mass fluxes: analytical and numerical studies. *Heat Mass Transfer* **35**, 409–421. [9.1.6.3]
- Amahmid, A., Hasnaoui, M., Mamou, M. and Vasseur, P. 1999b Boundary layer flows in a vertical porous enclosure induced by opposing buoyancy forces. *Int. J. Heat Mass Transfer* **42**, 3599–3608. [9.2.2]
- Amahmid, A., Hasnaoui, M., Mamou, M. and Vasseur, P. 2000 On the transition between aiding and opposing double-diffusive flows in a vertical porous cavity, *J. Porous Media* **3**, 123–137. [9.2.2]
- Amanifard, N. and Hagh, A. K. 2008 A numerical study of drying porous media. *Korean J. Chem. Engng* **25**, 191–198.[3.6]
- Amara, T., Slimi, K. and Ben Nasrallah, S. 2000 Free convection in a vertical cylindrical enclosure. *Int. J. Thermal Sci.* **39**, 616–634. [7.3.3]
- Amari, B., Vasseur, P. and Bilgen, E. 1994 Natural convection of non-Newtonian fluids in a horizontal porous layer. *Wärme-Stoffübertrag.* **29**, 185–193. [6.23]
- Amberg, G. and Homsy, G. M. 1993 Nonlinear analysis of buoyant convection in binary solidification with application to channel formation. *J. Fluid Mech.* **252**, 79–98. [10.2.3]
- Ames, K. A. and Cobb, S. S. 1994 Penetrative convection in a porous medium with internal heat sources. *Int. J. Engng Sci.*, **32**, 95–106. [6.11.2]
- Ameziani, D. E., Bouhadef, K., Bennacer, R. and Rahli, O. 2008 Analysis of the chimney natural convection in a vertical porous cylinder. *Numer. Heat Transfer A* **54**, 47–66.[7.3.3]
- Amili, P. and Yortsos, Y. C. 2003 Stability of heat pipes in vapor-dominated systems. *Int. J. Heat Mass Transfer* **47**, 1233–1246. [11.9.2]
- Amiri, A. and Vafai, K. 1994 Analysis of dispersion effects and non-thermal equilibrium non-Darcian, variable porosity incompressible flow through porous media. *Int. J. Heat Mass Transfer* **37**, 939–954. [4.6.4]
- Amiri, A. and Vafai, K. 1998 Transient analysis of incompressible flow through a packed bed. *Int. J. Heat Mass Transfer* **41**, 4259–4279. [4.6.4]
- Amiri, A., Vafai, K. and Kuzay, T. M. 1995 Effects of boundary conditions on non-Darcian heat transfer through porous media and experimental comparisons. *Numer. Heat Transfer A* **27**, 651–664. [4.6.4]
- Anandalakshmi, R. and Basak, T. 2012 Analysis of energy management via entropy generation approach during natural convection in porous rhombic enclosures. *Chem. Engng. Sci.* **79**, 75–93. [7.3.7]
- Anandalakshmi, R., Kaluri, R. S. and Basak, T. 2011 Heatline based thermal management for natural convection within right-angled porous triangular enclosures with various thermal conditions on walls. *Energy* **36**, 4879–4896.[7.3.6]

- Anderson, D. M. 2003 A model for diffusion-controlled solidification of ternary alloys in mushy layers. *J. Fluid Mech.* **483**, 165–197. [10.2.3]
- Anderson, D. M. and Worster, M. G. 1995 Weakly nonlinear analysis of convection in mushy layers during solidification of binary alloys. *J. Fluid Mech.* **302**, 307–331. [10.2.3]
- Anderson, D. M. and Worster, M. G. 1996 A new oscillatory instability in a mushy layer during the solidification of binary alloys. *J. Fluid Mech.* **307**, 245–267. [10.2.3]
- Anderson, D. M., McFadden, G. B., Coriell, S. R. and Murray, B. T. 2010 Convective instabilities during solidification of an ideal ternary alloy in a mushy layer. *J. Fluid Mech.* **647**, 309–333. [10.2.2]
- Anderson, D. M., Schulze, T. P. 2005 Linear and nonlinear convection in solidifying ternary alloys. *J. Fluid Mech.* **545**, 213–243. [10.2.3]
- Anderson, P. and Glassner, D. 1990 Thermal convection and surface temperatures in porous media. *Int. J. Heat Mass Transfer* **33**, 1321–1330. [7.11]
- Andres, J. T. H. and Cardoso, S. S. S. 2011 Onset of convection in a porous medium in the presence of chemical reaction. *Phys. Rev. E* **83**, #046312. [11.1]
- Angirasa, D. 2002a Forced convection heat transfer in metallic fibrous materials. *ASME J. Heat Transfer* **124**, 739–745. [4.9]
- Angirasa, D. 2002b Experimental investigation of forced convection heat transfer augmentation with metallic fibrous materials. *Int. J. Heat Mass Transfer* **45**, 919–922. [4.9]
- Angirasa, D. and Peterson, G. P. 1997a Combined heat and mass transfer by natural convection with opposing buoyancy effects in a fluid saturated porous medium. *Int. J. Heat Mass Transfer* **40**, 2755–2733. [9.2.2]
- Angirasa, D. and Peterson, G. P. 1997b Natural convection heat transfer from an isothermal vertical surface to a fluid saturated thermally stratified porous medium. *Int. J. Heat Mass Transfer* **40**, 4329–4335. [5.1.4]
- Angirasa, D. and Peterson, G. P. 1998a Upper and lower Rayleigh number bounds for two-dimensional natural convection over a finite horizontal surface situated in a fluid-saturated porous medium. *Numer. Heat Transfer A* **33**, 477–493. [5.2]
- Angirasa, D. and Peterson, G. P. 1998b Natural convection below a downward facing heated horizontal surface in a fluid-saturated porous medium. *Numer. Heat Transfer A* **34**, 301–311. [5.2]
- Angirasa, D. and Peterson, G. P. 1999 Forced convection heat transfer augmentation in a channel with a localized heat source using fibrous materials. *ASME J. Electr. Pack.* **121**, 1–7. [4.16.5]
- Angirasa, D., Peterson, G. P. and Pop, I. 1997 Combined heat and mass transfer by natural convection in a saturated thermally stratified porous medium. *Numer. Heat Transfer A* **31**, 255–272. [9.2.1]
- Ansari, A. 2007 Internal heat generation in a tall cavity filled with a porous medium. *J. Porous Media* **10**, 585–599. [7.3.8]
- Ansari, A. and Daniels, P. G. 1993 Thermally driven tall cavity flows in porous media. *Proc. Roy. Soc. Lond. A.* **433**, 163–181. [7.1.2]
- Ansari, A. and Daniels, P. G. 1994 Thermally driven tall cavity flows in porous media: the convective regime. *Proc. Roy. Soc. Lond. A.* **444**, 375–388. [7.1.2]
- Antohe, B. V. and Lage, J. L. 1994 A dynamic thermal insulator: inducing resonance within a fluid saturated porous medium heated periodically from the side. *Int. J. Heat Mass Transfer* **37**, 771–782. [7.10]
- Antohe, B. V. and Lage, J. L. 1996 Amplitude effect on convection induced by tile-periodic heating. *Int. J. Heat Mass Transfer* **39**, 1121–1133. [7.10]
- Antohe, B. V. and Lage, J. L. 1997a The Prandtl number effect on the optimum heating frequency of an enclosure filled with fluid or with a saturated porous medium. *Int. J. Heat Mass Transfer* **40**, 1313–1323. [7.10]
- Antohe, B. V. and Lage, J. L. 1997b A general two-equation macroscopic turbulence model for incompressible flow in porous media. *Int. J. Heat Mass Transfer* **40**, 3013–3024. [1.8]

- Arquis, E. and Caltagirone, J. 1984 Sur les conditions hydrodynamiques au voisinage d'une interface milieu fluide-milieu poreux: application à la convection naturelle. *C. R. Acad. Sc., Sér. II* **299**, 1–4. [6.19.1.1]
- Artem'eva, E. L. and Stroganova, E. V. 1987 Stability of a nonuniformly heated fluid in a porous horizontal layer. *Fluid Dyn.* **21**, 845–848. [6.10.2]
- Asako, Y., Nakamura, H., Yamaguchi, Y. and Fagri, M. 1992 Three-dimensional natural convection in a vertical porous layer with a hexagonal honeycomb core. *ASME J. Heat Transfer* **114**, 924–927. [7.3.7]
- Asbib, M., Chaynane, R., Boushaba, H., Zeghamti, B. and Khmou, A. 2003 Analytic investigation of forced convection film condensation on a vertical porous-layer coated surface. *Heat Mass Transfer* **40**, 143–155. [10.4]
- Asbib, M., Sadki, H., Hajar, M., Zeghamti, B. and Khmou, A. 2002 Numerical study of laminar mixed convection in a vertical saturated porous enclosure: The combined effect of double diffusion and evaporation. *Numer. Heat Transfer A* **41**, 403–420. [9.2.2]
- Asbib, M., Zeghamti, B., Louahlia-Gualos, H. and Yan, W. M. 2007 The effect of thermal dispersion on free convection film condensation on a vertical plate with a thin porous layer. *Transp. Porous Media* **67**, 335–352. [10.4]
- Asghar, S., Mushtaq, M. and Kara, A. H. 2008 Exact solutions for mixed convection flow near a stagnation point on a vertical surface in a porous medium. *J. Porous Media* **11**, 415–419. [8.1.1]
- Assato, M., Pedras, M. H. J. and de Lemos, M. J. S. 2005 Numerical solution of turbulent channel flow past a backward-facing step with a porous insert using linear and nonlinear  $k - \varepsilon$  models. *J. Porous Media* **8**, 13–29. [1.8]
- Attia, H. A. 2006a On the effectiveness of uniform suction and injection on unsteady rotating disk flow in porous medium with heat transfer. *Comput. Mat. Sci.* **38**, 240–244. [5.2]
- Attia, H. A. 2006b Rotating disk flow in a porous medium. *J. Porous Media* **9**, 789–798. [5.2]
- Attia, H. A. 2006c Unsteady flow and heat transfer of viscous incompressible fluid with temperature-dependent viscosity due to a rotating disc in a porous medium. *J. Phys. A* **39**, 979–991. [5.2]
- Attia, H. A. 2007a On the effectiveness of porosity on stagnation point flow towards a stretching surface with heat generation. *Comput. Mat. Sci.* **38**, 741–745. [5.1.9.9]
- Attia, H. A. 2007b On the effectiveness of porosity on stagnation point flow with heat transfer over a permeable surface. *J. Porous Media* **10**, 625–651. [5.1.9.9].
- Attia, H. A. 2008a Rotating disk flow and heat transfer through a porous medium of a non-Newtonian fluid with suction and injection. *Comm. Nonlinear Sci. Numer. Simul.* **13**, 1571–1580. [5.2]
- Attia, H. A. 2008b Time varying flow of a power law fluid in a porous medium between parallel porous plates with heat transfer under an exponentially decaying pressure gradient. *J. Porous Media* **11**, 487–495. [4.16.3]
- Auger, J., Yssorche-Cubaynes, M. P., Lorente, S., Cussigh, F. and Demillecamp, L. 2008 Ionic access through porous media with distributed electrodes. *J. Applied Physics* **104**, #184913. [3.7]
- Augustin, M., Umla, R., Huke, B. and Lucke, M. 2010 Stationary and oscillatory convection of binary fluids in a porous medium. *Phys. Rev. E* **82**, #056303. [9.1.4]
- Auriault, J. L. 1999 Comments on the paper “Local and global transitions to chaos and hysteresis in a porous layer heated from below” by P. Vadasz. *Transport in Porous Media* **37**, 247–249. [6.4]
- Auriault, J. L. 2009 On the domain of validity of Brinkman's equation. *Transp. Porous Media* **79**, 215–223. [1.5.3]
- Auriault, J. L. 2010a About the Beavers and Joseph boundary condition. *Transp. Porous Media* **83**, 257–266. [1.6]
- Auriault, J. L. 2010b Reply to the comments on “About the Beavers and Joseph boundary condition”. *Transp. Porous Media* **83**, 269–270. [1.6]

- Auriault, J. L., Geindreau, C. and Orgeas, L. 2007 Upscaling Forchheimer law.. *Transp. Porous Media* **70**, 213–229. [1.5.2]
- Auriault, J. L., Geindreau, C. and Royer, P. 2002a Coriolis effects on filtration law in rotating porous media. *Transport in Porous Media* **48**, 315–330. [6.22]
- Auriault, J. L., Royer, P. and Geindreau, C. 2002b Filtration law for power-law fluids in anisotropic porous media. *Int. J. Engng. Sci.* **40**, 1151–1163. [1.5.4]
- Aussillou, P., Sederman, A. J., Gladden, L. F., Huppert, H. E. and Worster, M. G. 2006 Magnetic resonance imaging of structure and convection in solidifying mushy layers. *J. Fluid Mech.* **552**, 99–125. [10.2.3]
- Avila-Acevedo, J. G. and Tsotsas, E. 2008 Transient natural convection and heat transfer during the storage of granular media. *Int. J. Heat Mass Transfer* **51**, 3468–3477. [7.5]
- Avramenko, A. A. and Kuznetsov, A. V. 2004 Stability of a suspension of gyrotactic microorganisms in superposed fluid and porous layers. *Int. Comm. Heat Mass Transfer* **31**, 1057–1066. [6.25]
- Avramenko, A. A. and Kuznetsov, A.V. 2005 Linear stability analysis of a suspension of oxytactic baceria in superposed fluid and porous layers. *Transport Porous Media* **61**, 157–176. [6.25]
- Avramenko, A. A. and Kuznetsov, A. V. 2006 The onset of convection in a suspension of gyrotactic microorganisms in superimposed fluid and porous layer: effect of throughflow. *Transport Porous Media* **65**, 159–176. [6.25]
- Avroam, D. G. and Payatakes, A. C. 1995 Flow regimes and relative permeabilities during steady-state two-phase flow in porous media. *J. Fluid Mech.* **293**, 207–236. [3.5.4]
- Avtar, R. and Srivastava, R. 2006 Modelling the flow of aqueous humor in anterior chamber of the eye. *Appl. Math. Comput.* **181**, 1336–1348. [7.7]
- Awad, F. G., Sibanda, P. and Motsa, S. S. 2010 On the linear stability analysis of a Maxwell fluid with double-diffusive convection. *Appl. Math. Modell.* **34**, 3509–3517. [9.1.6.4]
- Awad, F. G., Sibanda, P., Motsa, S. S. and Makinde, O. D. 2011 Convection from an inverted cone in a porous medium with cross-diffusion effects. *Comput. Math. Appl.* **61**, 1431–1441. [9.2.1]
- Aydin, O. and Avci, M. 2011 Analytical investigation of heat transfer in Couette- Poiseuille flow through porous medium. *J Thermophys. Heat Transfer* **25**, 468–472. [4.9]
- Aydin, O. and Kaya, K. 2011 Effects of thermal radiation on steady MHD mixed convective heat transfer flow over an impermeable inclined plate embedded in a porous medium. *J. Porous Media* **14**, 617–625. [8.1.1]
- Aydin, O. and Koya, A. 2006 Mixed convection of a viscous dissipative fluid about a vertical flat plate embedded in a porous medium: constant wall temperature case. *J. Porous Media* **9**, 559–580. [8.1.1]
- Aydin, O. and Koya, A. 2008a Mixed convection of a viscous dissipative fluid about a vertical flat plate embedded in a porous medium: constant heat flux case. *J. Porous Media* **11**, 207–217. [8.1.1]
- Aydin, O. and Koya, A. 2008b Non-Darcian forced convection flow of viscous dissipating fluid over a flat plate embedded in a porous medium. *Transp. Por. Media* **73**, 173–186. [4.8]
- Aydin, O. and Koya, A. 2008c Reply to comments on “Non-Darcian forced convection flow of viscous dissipating fluid over a flat plate embedded in a porous medium.” *Transp. Por. Media* **73**, 191–193. [4.8]
- Aydin, O. and Koya, A. 2008d Reply to comments on “Non-Darcian forced convection flow of viscous dissipating fluid over a flat plate embedded in a porous medium.” *Transp. Por. Media* **75**, 271–272. [4.8]
- Aziz, A., Khan, W. A. and Pop, I. 2012 Free convection boundary layer flow past a horizontal plate embedded in porous medium filled by nanofluid containing gyrotactic microorganisms. *Int. J. Therm. Sci.* **56**, 48–57. [5.2]
- Azoumah, Y., Mazet, N. and Neveu, P. 2004 Constructal network for heat and mass transfer in a solid-gas reactive porous medium. *Int. J. Heat Mass Transfer* **47**, 2961–2970. [4.18]
- Babu, A.B., Ravi, R. and Tagare, S.C. 2012 Nonlinear rotating convection in a sparsely packed porous medium. *Comm. Nonlinear Sci. Numer. Simul.* **17**, 5042–5063. [6.22]

- Babuskin, I. A. and Demin, V. A. 2006 Experimental and theoretical investigation of transient convective regimes in a Hele-Shaw cell. *Fluid Dyn.* **41**, 323–329. [2.5]
- Bachok, N., Ishak, A. and Pop, I. 2010a Mixed convection boundary layer flow near the stagnation point on a vertical surface embedded in a porous medium with anisotropy effect. *Transp. Porous Media* **82**, 363–373. [8.1.6]
- Bachok, N., Ishak, A. and Pop, I. 2010b Mixed convection boundary layer flow over a permeable vertical flat plate embedded in an anisotropic porous medium. *Math. Prob. Engng.* #65023. [8.1.1]
- Backhaus, S., Turitsyn, K. and Ecke, R. E. 2011 Convective instability and mass transport of diffusion layers in a Hele-Shaw geometry. *Phys. Rev. Lett* **106**, #104501. [2.5]
- Badr, H. M. and Pop, I. 1992 Effect of flow direction on mixed convection from a horizontal rod embedded in a porous medium. *Trans. Can. Soc. Mech. Engng.* **16**, 267–290. [8.1.3]
- Badr, H. M. and Pop, I. 1988 Combined convection from an isothermal horizontal rod buried in a porous medium. *Int. J. Heat Mass Transfer* **31**, 2527–2541. [8.1.3]
- Badruddin, I. A., Al-Rashed, A.A.A.A., Ahmed, N.J.S., Kamangar, S. and Jeevan, K. 2012 Natural convection in a square porous annulus. *Int. J. Heat Mass Transfer* **55**, 7175–7187. [7.3.3]
- Badruddin, I. A., Zainal, Z. A., Khan, Z. A. and Mallick, Z. 2007a Effect of viscous dissipation and radiation on natural convection in a porous medium embedded within vertical annulus. *Int. J. Therm. Sci.* **46**, 221–227. [7.3.3]
- Badruddin, I. A., Zainal, Z. A., Narayana, P. A. A. and Seetharamu, K. N. 2006a Thermal non-equilibrium modeling of heat transfer through vertical annulus embedded with porous medium. *Int. J. Heat Mass Transfer* **49**, 4955–4965. [7.3.3]
- Badruddin, I. A., Zainal, Z. A., Narayana, P. A. A., and Seetharamu, K. N. 2007b Numerical analysis of convection conduction and radiation using non-equilibrium model in a square porous cavity. *Int. J. Thermal Sci.* **46**, 20–29. [7.2]
- Badruddin, I. A., Zainal, Z. A., Narayana, P. A. A., Seetharamu, K. N. and Siew, L. W. 2006b Free convection and radiation characteristics for a vertical plate embedded in a porous medium. *Int. J. Numer. Meth. Engng.* **65**, 2265–2278. [5.1.9.4]
- Badruddin, I. A., Zainal, Z. A., Narayana, P. A. A., Seetharamu, K. N. and Siew, L. W. 2006c Free convection and radiation for a vertical wall with varying temperature embedded in a porous medium. *Int. J. Therm. Sci.* **45**, 487–493. [5.1.9.4]
- Badruddin, I. A., Zainal, Z. A., Narayana, P. A. A., and Seetharamu, K. N. 2006d Heat transfer in porous cavity under the influence of radiation and viscous dissipation. *Int. Commun. Heat Mass Transfer.* **33**, 491–499. [7.2]
- Bae, J. H., Hyun, J.M. and Kim, J. W. 2004 Mixed convection in a channel with porous multiblocks under imposed thermal modulation. *Numer. Heat Transfer A* **46**, 891–908. [8.3.1]
- Báez, E. and Nicolás, N. 2006 2D Natural convection flows in tilted cavities: porous media and homogeneous fluids. *Int. J. Heat Mass Transfer* **49**, 4773–4785. [7.8]
- Báez, E. and Nicolás, N. 2007 Natural convection fluid flow and heat transfer in porous media. *J. Mech. Mater. Struct.* **2**, 1571–1584. [7.8]
- Bagai, S. 2003 Similarity solutions of free convection boundary layers over a body of arbitrary shape in a porous medium with internal heat generation. *Int. Comm. Heat Mass Transfer* **30**, 997–1003. [5.9]
- Bagai, S. 2004 Effect of variable viscosity on free convection over a non-isothermal axisymmetric body in a porous medium with internal heat generation. *Acta Mech.* **169**, 187–194. [5.9]
- Bagai, S. and Nishad, C. 2012 Effect of variable viscosity on free convective heat transfer over a non-isothermal body of arbitrary shape in a non-Newtonian fluid saturated porous medium with internal heat generation. *Transp. Porous Media* **94**, 277–288. [5.9]
- Bagchi, A. and Kulacki, F. A. 2011 Natural convection in fluid-superposed porous layers heated locally from below. *Int. J. Heat Mass Transfer* **54**, 3672–3682. [6.18]
- Bahloul, A. 2006 Boundary layer and stability analysis of natural convection in a porous cavity. *Int. J. Thermal Sci.* **45**, 635–642. [7.1.4]

- Bahloul, A., Boutana, N. and Vasseur, P. 2003 Double-diffusive and Soret-induced convection in a shallow horizontal porous layer. *J. Fluid Mech.* **491**, 325–352. [9.1.4]
- Bahloul, A., Kalla, L., Bennacer, R., Beji, H. and Vasseur, P. 2004a Natural convection in a vertical porous slot heated from below and with horizontal concentration gradients. *Int. J. Thermal Sci.* **43**, 653–663. [9.5]
- Bahloul, A., Vasseur, P. and Robillard, L. 2007 Convection of a binary fluid saturating a shallow porous cavity subjected to cross heat fluxes. *J. Fluid Mech.* **574**, 317–342. [9.5]
- Bahloul, A., Yahiaoui, M. A., Vasseur, P. and Robillard, L. 2004b Thermogravitational separation in a vertical annular porous layer. *Int. Comm. Heat Mass Transfer* **31**, 783–794. [9.4]
- Bahloul, A., Yahiaoui, M. A., Vasseur, P., Bennacer, R. and Beji, H. 2006 Natural convection of a two-component fluid in porous media bounded by tall concentric vertical cylinders. *ASME J. Appl. Mech.* **73**, 26–33. [9.2.2]
- Bahrami, M., Culham, J. R. and Yovanovich, M. M. 2006 Effective thermal conductivity of rough spherical packed beds. *Int. J. Heat Mass Transfer* **49**, 3691–3701. [2.2.1]
- Bai, H. X., Yu, P., Winoto, S. H. and Low, H. T. 2009 Lattice Boltzmann method for flows in porous and homogeneous fluid domains coupled at the interface by stress jump. *Int. J. Numer. Meth. Fluids* **60**, 691–708. [1.6]
- Bai, M. and Roegiers, J. C. 1994 Fluid flow and heat flow in deformable fractured media. *Int. J. Engng. Sci.* **32**, 1615–1663. [1.9]
- Bai, M., Ma, Q. and Roegiers, J. C. 1994a Dual porosity behaviour of naturally fractured reservoirs. *Int. J. Num. Anal. Mech. Geomech.* **18**, 359–376. [1.9]
- Bai, M., Ma, Q. and Roegiers, J. C. 1994b Nonlinear dual-porosity model. *Appl. Math. Model.* **18**, 602–610. [1.9]
- Bai, M., Roegiers, J. C. and Inyang, H. F. 1996 Contaminant transport in nonisothermal fractured porous media. *J. Env. Engng.* **122**, 416–423. [1.9]
- Bai, W. M., Xu, W. Y. and Lowell, R. P. 2003 The dynamics of submarine geothermal heat pipes. *Geophys. Res. Lett.* **30**, art. no. 1108. [11.9.2]
- Bakier, A. Y. 1997 Aiding and opposing mixed convection flow in melting from a vertical flat plate embedded in a porous medium. *Transport in Porous Media* **29**, 127–139. [10.1.7]
- Bakier, A. Y. 2001a Thermal radiation effect on mixed convection from vertical surfaces in saturated porous media. *Int. Comm. Heat Mass Transfer* **28**, 119–126. [8.1.1]
- Bakier, A. Y. 2001b Thermal radiation effect on mixed convection from vertical surfaces in saturated porous media. *Indian J. Pure Appl. Math.* **32**, 1157–1163. [8.1.1]
- Bakier, A. Y. and Gorla, R. S. R. 1996 Thermal radiation effect on mixed convection from horizontal surfaces in saturated porous media. *Transport Porous Media* **23**, 357–363. [8.1.2]
- Bakier, A. Y. and Mansour, M. A. 2007 Combined of magnetic field and thermophoresis particle deposition in free convection boundary layer from a vertical flat plate embedded in a porous medium. *Thermal Science* **11**, 65–74. [5.1.9.9]
- Bakier, A. Y., Mansour, M. A., Gorla, R. S. R. and Ebiana, A. B. 1997 Nonsimilar solutions for free convection from a vertical plate in porous media. *Heat Mass Transfer* **33**, 145–148. [5.1.9.4]
- Bakier, A. Y., Rashad, A. M. and Mansour, M. A. 2009 Group method analysis of melting effect on MHD mixed convection flow from radiate vertical plate embedded in saturated porous media. *Comm. Nonlinear Sci. Numer. Simul.* **14**, 2160–2170. [10.1.7]
- Balakotaiah, V. and Portalet, P. 1990a Natural convection effects on thermal ignition in a porous medium. I. Semenov model. *Proc. Roy. Soc. Lond. A.* **429**, 533–554. [3.4]
- Balakotaiah, V. and Portalet, P. 1990b Natural convection effects on thermal ignition in a porous medium. II. Lumped thermal model-I. *Proc. Roy. Soc. Lond. A.* **429**, 555–567. [3.4]
- Balasubramanian, R. and Thangaraj, R. P. 1998 Thermal convection in a fluid layer sandwiched between two porous layers of different permeabilities. *Acta Mech.* **130**, 81–93. [6.19.1]
- Banjer, H. and Abdullah, A. 2012 Thermal instability of superposed porous and fluid layers in the presence of a magnetic field using the Brinkman model. *J. Porous Media* **15**, 1–10. [6.19.3]
- Bankvall, C. G. 1974 Natural convection in a vertical permeable space. *Wärme-Stoffübertrag.* **7**, 22–30. [7.1.2]

- Bansod, V. J. 2003 The Darcy model for boundary layer flows in a horizontal porous medium induced by combined buoyancy forces. *J. Porous Media* **6**, 273–281. [9.2.1]
- Bansod, V. J. and Jadhav, R. K. 2009 An integral treatment for combined heat and mass transfer by natural convection along a horizontal surface in a porous medium. *Int. J. Heat Mass Transfer* **52**, 2802–2806. [9.2.1]
- Bansod, V. J., Singh, P. and Ratishkumar, B. V. 2002 Heat and mass transfer by natural convection from a vertical surface to the stratified Darcian fluid. *J. Porous Med.* **5**, 57–66. [9.2.1]
- Bansod, V. J., Singh, P. and Ratishkumar, B. V. 2005 Laminar natural convection heat and mass transfer from a horizontal in non-Darcy porous media. *J. Porous Med.* **8**, 65–72. [9.2.1]
- Banu, N. and Rees, D. A. S. 2000 The effect of inertia on vertical free convection boundary layer flow from a heated surface in porous media with suction. *Int. Comm. Heat Mass Transfer* **27**, 775–783. [5.1.7.2]
- Banu, N. and Rees, D. A. S. 2001 Effect of a traveling thermal wave on weakly nonlinear convection in a porous layer. *J. Porous Media* **4**, 225–239. [6.4]
- Banu, N. and Rees, D. A. S. 2002 Onset of Darcy-Bénard convection using a thermal non-equilibrium model. *Int. J. Heat Mass Transfer* **45**, 2221–2228. [6.5]
- Banu, N., Rees, D. A. S. and Pop, I. 1998 Steady and unsteady free convection in porous cavities with internal heat generation. *Heat Transfer 1998, Proc. 11th IHTC*, **4**, 375–380. [6.17]
- Barak, A. Z. 1987 Comments on “High velocity flow in porous media” by Hassanizadeh and Gray. *Transport in Porous Media* **2**, 533–535. [1.5.2]
- Barbosa Mota, J. P. and Saatdjian, E. 1994 Natural convection in a porous, horizontal cylindrical annulus. *ASME J. Heat Transfer* **116**, 621–626. [7.3.3]
- Barbosa Mota, J. P. and Saatdjian, E. 1995 Natural convection in porous cylindrical annuli. *Int. J. Numer. Methods Heat Fluid Flow* **5**, 3–17. [7.3.3]
- Barbosa Mota, J. P. and Saatdjian, E. 1997 Reduction of natural convection heat transfer in horizontal eccentric annuli containing saturated porous media. *Int. J. Numer. Methods Heat Fluid Flow* **7**, 401–416. [6.16.2]
- Barbosa Mota, J. P., Le Provost, J. F., Puons, E. and Saatdjian, E. 1994 Natural convection in porous, horizontal eccentric annuli. *Heat Transfer 1994, Inst. Chem. Engrs, Rugby*, Vol. 5, 435–440. [7.3.3]
- Barдан, G. and Mojtabi, A. 2000 On the Horton-Rogers-Lapwood convective instability with vertical vibration: onset of convection. *Phys. Fluids* **12**, 2723–2731. [6.24]
- Barдан, G., Pedram Razi, Y. and Mojtabi, A. 2004 Comments on the mean flow averaged model. *Phys. Fluids* **16**, 4535–4538. [6.24]
- Barдан, G., Pinaud, G. and Mojtabi, A. 2001 Onset of convection in porous cell submitted to high-frequency vibrations. *C. R. Acad. Sci. II B* **329**, 283–286. [6.24]
- Barenblatt, G. I., Entov, V. M. and Ryzhik, V. M. 1990 *Theory of Fluid Flow through Natural Rocks*, Kluwer Academic Publishers, Dordrecht. [1.9]
- Barletta, A. 2008 Comments on a paradox of viscous dissipation in relation to the Oberbeck-Boussinesq approach. *Int. J. Heat Mass Transfer* **51**, 6312–6316. [2.2.2]
- Barletta, A. 2012 Thermal instability in a horizontal porous channel with horizontal through flow and symmetric wall heat fluxes. *Transp. Porous Media* **92**, 419–437. [6.10.1]
- Barletta, A. and Celli, M. 2011 Local thermal non-equilibrium flow with viscous dissipation in a plane horizontal layer. *Int. J. Therm. Sci.* **50**, 53–60. [6.6]
- Barletta, A. and Nield, D. A. 2012a On the Hadley flow in a porous layer with vertical heterogeneity. *J. Fluid Mech.*, to appear. [7.9]
- Barletta, A. and Storesletten, L. 2010b Viscous dissipation and thermoconvective instabilities in a horizontal porous channel heated from below. *Int. J. Therm. Sci.* **49**, 621–630. [6.6]
- Barletta, A. and Storesletten, L. 2011a Onset of convective rolls in a circular porous duct with external heat transfer to a thermally stratified environment. *Int. J. Therm. Sci.* **50**, 1374–1384. [6.16.1]
- Barletta, A. and Storesletten, L. 2011b Thermoconvective instabilities in an inclined porous channel heated from below. *Int. J. Heat Mass Transfer* **54**, 2724–2733. [7.8]

- Barletta, A. and Nield, D. A. 2009a Combined forced and free convective flow in a vertical porous channel: The effects of viscous dissipation and pressure work. *Transp. Porous Media* **79**, 319–334. [8.3.2]
- Barletta, A. and Nield, D. A. 2009b Response to comment on “Combined forced and free convective flow in a vertical porous channel: The effects of viscous dissipation and pressure work” by A. Barletta and D. A. Nield. *Transp. Porous Media* **80**, 397–398. [8.3.2]
- Barletta, A. and Nield, D. A. 2010 Instability of Hadley-Prats flow with viscous heating in a horizontal porous layer. *Transp. Porous Media* **84**, 241–256. [6.10.1, 7.9]
- Barletta, A. and Nield, D. A. 2011a Linear instability of the horizontal throughflow in a plane porous layer saturated by a power-law fluid. *Phys. Fluids* **23**, #013102. [6.10.1]
- Barletta, A. and Nield, D. A. 2011b Thermosolutal convective instability and viscous dissipation effect in a fluid-saturated porous medium. *Int. J. Heat Mass Transfer* **54**, 1641–1648. [9.1.6.4]
- Barletta, A. and Nield, D. A. 2012b Variable viscosity effects on the dissipation instability in a porous layer with horizontal throughflow. *Phys. Fluids* **24**, 104102. [6.10.1]
- Barletta, A. and Rees, D. A. S. 2009 Stability analysis of dual adiabatic flows in a horizontal porous layer. *Int. J. Heat Mass Transfer* **52**, 2300–2310. [8.2.1]
- Barletta, A. and Rees, D. A. S. 2012a Local thermal non-equilibrium effects in the Darcy-Bénard instability with isoflux boundary conditions. *Int. J. Heat Mass Transfer* **55**, 384–394. [6.5]
- Barletta, A. and Rees, D. A. S. 2012b Linear instability of the Darcy-Hadley flow in an inclined porous layer. *Phys. Fluids* **24**, 07104. [7.9]
- Barletta, A. and Nield, D. A. 2012b Variable viscosity effects on the dissipation instability in a porous layer with horizontal throughflow. *Phys. Fluids* **24**, 104102. [6.10.1]
- Barletta, A. and Rossi di Schio, E. 2012 Buoyant Darcy flow driven by a horizontal temperature gradient: A linear stability analysis. *Int. J. Heat Mass Transfer* **55**, 7093–7103. [7.9]
- Barletta, A. and Storesletten, L. 2010a Stability of flow with viscous dissipation in a horizontal porous layer with an open boundary having a prescribed temperature gradient. *Transp. Porous Media* **85**, 723–741. [6.6]
- Barletta, A. and Storesletten, L. 2012 A three-dimensional study of the onset of convection in a horizontal, rectangular porous channel heated from below. *Int. J. Therm. Sci.* **55**, 1–15. [6.15.3]
- Barletta, A., Celli, M. and Kuznetsov, A. V. 2011a Transverse heterogeneity effects in dissipation induced instability of a horizontal porous layer. *ASME J. Heat Transfer* **133**, #122601. [6.6]
- Barletta, A., Celli, M. and Kuznetsov, A. V. 2012 Heterogeneity and onset of instability in Darcy’s flow with prescribed horizontal temperature gradient. *ASME J. Heat Transfer* **134**, #042602. [6.13.2]
- Barletta, A., Celli, M. and Nield, D. A. 2010a Unstably stratified Darcy flow with impressed horizontal temperature gradient, viscous dissipation and asymmetric thermal boundary conditions. *Int. J. Heat Mass Transfer* **53**, 1621–1627. [6.6]
- Barletta, A., Celli, M. and Nield, D. A. 2011a Transverse heterogeneity effects in the dissipation-induced instability of a horizontal porous layer. *ASME J. Heat Transfer* **133**, #122601. [6.6]
- Barletta, A., Celli, M. and Rees, D. A. S. 2009b The onset of convection in a porous layer induced by viscous dissipation: A linear stability analysis. *Int. J. Heat Mass Transfer* **52**, 337–344. [6.6]
- Barletta, A., Celli, M. and Rees, D. A. S. 2009a Darcy-Forchheimer flow with viscous dissipation in a horizontal porous layer: onset of convective instabilities. *ASME J. Heat Transfer* **131**, #072602. [6.6]
- Barletta, A., Lazzari, S., Magari, E. and Pop, I. 2008a Mixed convection with heating effects in a vertical porous annulus with a radially varying magnetic field. *Int. J. Heat Mass Transfer* **51**, 5777–5784. [8.4.3]
- Barletta, A., Magyari, E., Lassari, S. and Pop, I. 2009 c Closed form solutions for mixed convection with magnetohydrodynamic effect in a vertical porous annulus surrounding an electric cable. *ASME J. Heat Transfer* **131**, #064504. [8.4.3]
- Barletta, A., Magyari, E., Pop, I. and Storesletten, L. 2007 Mixed convection with viscous dissipation in a vertical channel filled with a porous medium. *Acta Mech.* **194**, 123–140. [8.3.2]

- Barletta, A., Magyari, E., Pop, I. and Storesletten, L. 2008b Buoyant flow with viscous heating in a vertical circular duct filled with a porous medium. *Transp. Porous Media* **74**, 133–151. [7.3.8]
- Barletta, A., Magyari, E., Pop, I. and Storesletten, L. 2008c Mixed convection with viscous dissipation in an inclined porous channel with isoflux impermeable walls. *Heat Mass Transfer* **44**, 979–988. [8.4.3]
- Barletta, A., Magyari, E., Pop, I. and Storesletten, L. 2008d Unified analytical approach to Darcy mixed convection with viscous dissipation in a vertical channel. *Int. J. Therm. Sci.* **47**, 408–416. [8.3.2]
- Barletta, A., Rossi di Schio, E. and Celli, M. 2011b Instability and viscous dissipation in the horizontal Brinkman flow through a porous medium. *Transp. Porous Media* **87**, 105–119. [6.6]
- Barletta, A., Rossi di Schio, E. and Storesletten, L. 2010b Convective roll instabilities of vertical throughflow with viscous dissipation in a horizontal porous layer. *Transp. Porous Media* **81**, 461–477. [6.6]
- Bars, M. L. and Worster, M. G. 2006 Interfacial conditions between a pure fluid and a porous medium: Implications for binary alloy solidification. *J. Fluid Mech.* **550**, 149–173. [1.6]
- Bartelt, P., Buser, O. and Sokratov, S. A. 2004 A nonequilibrium treatment of heat and mass transfer in alpine snowcovers. *Cold Regions Sci. Tech.* **39**, 219–242. [11.1]
- Bartlett, R. F. and Viskanta, R. 1996 Enhancement of forced convection in an asymmetrically heated duct filled with high thermal conductivity porous media. *J. Enhanced Heat Transfer* **3**, 291–299. [4.9]
- Basak, T. and Roy, S. 2008 ‘Bejan’s heatlines’ in heat flow visualization and optimal thermal mixing for differentially heated square enclosures. *Int. J. Heat Mass Transfer* **51**, 3486–3503. [4.17]
- Basak, T., Aravind, G. and Roy, S. 2009 Visualization of heat flow due to natural convection within triangular cavities using Bejan’s heatline concept. *Int. J. Heat Mass Transfer* **52**, 2824–2833. [4.17]
- Basak, T., Gunda, P. and Anandalakshmi, R. 2012 Analysis of entropy generation during natural convection in porous right-angled triangular cavities with various thermal boundary conditions. *Int. J. Heat Mass Transfer* **55**, 4521–4535. [7.3.6]
- Basak, T., Pradeep, P. V. K., Roy, S. and Pop, I. 2011 Finite element based heatline approach to study mixed convection in a porous square cavity with various wall thermal boundary conditions. *Int. J. Heat Mass Transfer* **54**, 1706–1727. [8.4.3]
- Basak, T., Roy, S. and Babu, S. K. 2008a Natural convection and flow simulation in differentially heated isosceles triangle enclosures filled with porous medium. *Chem. Engng. Sci.* **63**, 3328–3340. [7.3.6]
- Basak, T., Roy, S. and Takhar, H. S. 2007 Effects of nonuniformly heated wall(s) on a natural-convection flow in a square cavity filled with a porous medium. *Numer. Heat Transfer A* **51**, 959–978. [7.3.7]
- Basak, T., Roy, S. and Thirumalesha, C. 2008b Finite element simulations of natural convection in a right-angle triangular enclosure filled with a porous medium. *J. Porous Media* **11**, 159–178. [7.3.6]
- Basak, T., Roy, S., Babu, S. K. and Pop, I. 2008c Finite element simulations of natural convection flow in an isosceles triangular enclosure filled with a porous medium: Effects of various boundary conditions. *Int. J. Heat Mass Transfer* **51**, 2733–2741. [7.3.6]
- Basak, T., Roy, S., Matta, A. and Pop, I. 2010a Analysis of heatlines for natural convection within porous trapezoidal enclosures: Effect of uniform and non-uniform heating of bottom wall. *Int. J. Heat Mass Transfer* **53**, 5947–5961. [7.3.6]
- Basak, T., Roy, S., Paul, T. and Pop, I. 2006 Natural convection in a square cavity filled with a porous medium: Effects of various boundary conditions. *Int. J. Heat Mass Transfer* **49**, 1430–1441. [7.2]
- Basak, T., Roy, S., Ramakrishna, D. and Pandey, B. D. 2010b Analysis of heat recovery and heat transfer with entrapped porous triangular cavities via heatline approach. *Int. J. Heat Mass Transfer* **53**, 3655–3669. [7.3.6]

- Basak, T., Roy, S., Ramakrishna, D. and Pop, I. 2010b Visualization of heat transport due to natural convection for hot materials confined within two entrapped porous triangular cavities via heatline concept. *Int. J. Heat Mass Transfer* **53**, 2100–2112. [7.3.7]
- Basak, T., Roy, S., Ramakrishna, D. and Pop, I. 2010c Visualization of heat transport during natural convection within porous triangular cavities via heatline approach. *Numer. Heat Transfer A* **57**, 431–452. [7.3.6]
- Basak, T., Roy, S., Singh, A. and Balakrishnan, A. R. 2009a Natural convection flows in porous trapezoidal enclosures with various inclination angles. *Int. J. Heat Mass Transfer* **52**, 4612–4623. [7.3.7]
- Basak, T., Roy, S., Singh, A. and Pop, I. 2009b Finite element simulations of natural convection flow in a trapezoidal enclosure filled with a porous medium due to uniform and non-uniform heating. *Int. J. Heat Mass Transfer* **52**, 70–78. [7.3.7]
- Basak, T., Roy, S., Singh, S. K. and Pop, I. 2009c Finite element simulation of natural convection within porous trapezoidal enclosures for various inclination angle: Effect of various wall heating. *Int. J. Heat Mass Transfer* **52**, 4135–4150. [7.3.7]
- Bassom, A. P. and Rees, D. A. S. 1995 The linear vortex instability of flow induced by a horizontal heated surface in a porous medium. *Quart. J. Mech. Appl. Mech.* **48**, 1–19. [5.4]
- Bassom, A. P. and Rees, D. A. S. 1996 Free convection from a heated vertical cylinder embedded in a fluid-saturated porous medium. *Acta Mech.* **116**, 139–151. [5.7]
- Bassom, A. P., Rees, D. A. S. and Storesletten, L. 2001 Convective plumes in porous media: The effect of asymmetrically placed boundaries. *Int. Commun. Heat Mass Transfer* **28**, 31–38. [5.10.1.1]
- Basu, A. and Islam, M. R. 1996 Instability in a combined heat and mass transfer problem in porous media. *Chaos, Solitons, Fractals* **7**, 109–123. [9.2.4]
- Basu, A. J. and Khalili, A. 1999 Computation of flow through a fluid-sediment interface in a benthic chamber. *Phys. Fluids* **11**, 1395–1405. [6.19.3]
- Batchelor, G. K. 1967 *An Introduction to Fluid Dynamics*, Cambridge University Press. [1.5.1]
- Battiato, I. 2012 Self-similarity in coupled Brinkman/Navier-Stokes flows. *J. Fluid Mech.* **699**, 94–114. [1.6]
- Bau, H. H. 1984a Low Rayleigh number thermal convection in a saturated porous medium bounded by two horizontal, eccentric cylinders. *ASME J. Heat Transfer* **106**, 166–175. [7.3.3]
- Bau, H. H. 1984b Convective heat losses from a pipe buried in a semi-infinite porous medium. *Int. J. Heat Mass Transfer* **27**, 2047–2056. [7.11]
- Bau, H. H. 1984c Thermal convection in a horizontal, eccentric annulus containing a saturated porous medium — an extended perturbation expansion. *Int. J. Heat Mass Transfer* **27**, 2277–2287. [7.3.3]
- Bau, H. H. 1993 Controlling chaotic convection. *Theoretical and Applied Mechanics* 1992 (eds. S.R. Bodner, *et al.*), Elsevier, Amsterdam, 187–203. [6.11.3]
- Bau, H. H. and Torrance, K. E. 1981 Onset of convection in a permeable medium between vertical coaxial cylinders. *Phys. Fluids* **24**, 382–385. [6.16.1]
- Bau, H. H. and Torrance, K. E. 1982a Boiling in low permeability porous materials. *Int. J. Heat Mass Transfer* **25**, 45–55. [11.9.2]
- Bau, H. H. and Torrance, K. E. 1982b Low Rayleigh number thermal convection in a vertical cylinder filled with porous materials and heated from below. *ASME J. Heat Transfer* **104**, 166–172. [6.16.1]
- Bau, H. H. and Torrance, K. E. 1982c Thermal convection and boiling in a porous medium. *Lett. Heat Mass Transfer* **9**, 431–333. [10.3.1]
- Bau, H. H. 1986 Estimation of heat losses from flows in buried pipes. *Handbook of Heat and Mass Transfer* (ed. N.P. Cheremisinoff), Gulf Publishing Co., Houston, TX, Vol. 1, 1009–1024. [7.11]
- Bautista, O., Mendez, F. and Lizardi, J. 2008 Conjugate heat transfer analysis of the film condensation on a vertical fin immersed in a porous medium. *J. Porous Media* **11**, 145–157. [10.4]

- Baytas, A. C. 2000 Entropy generation for natural convection in an inclined porous cavity. *Int. J. Heat Mass Transfer* **43**, 2089–2099. [7.8]
- Baytas, A. C. 2003 Thermal non-equilibrium natural convection in a square enclosure filled with a heat-generating solid phase, non-Darcy porous medium. *Int. J. Energy Res.* **27**, 975–988. [6.5]
- Baytas, A. C. 2007 Entropy generation for thermal nonequilibrium natural convection with non-Darcy flow model in a porous enclosure filled with a heat-generating solid phase. *J. Porous Media* **10**, 261–275. [6.11.2]
- Baytas, A. C. and Baytas, A. F. 2005 Entropy generation in porous media. In *Transport Phenomena in Porous Media III*, (eds. D. B. Ingham and I. Pop), Elsevier, Oxford, pp. 201–224. [7.8]
- Baytas, A. C. and Pop, I. 1999 Free convection in oblique enclosures filled with a porous medium. *Int. J. Heat Mass Transfer* **42**, 1047–1057. [7.8]
- Baytas, A. C. and Pop, I. 2001 Natural convection in a trapezoidal enclosure filled with a porous medium. *Int. J. Engng. Sci.* **39**, 125–134. [7.3.7]
- Baytas, A. C. and Pop, I. 2002 Free convection in a square porous cavity using a thermal nonequilibrium model. *Int. J. Thermal Sci.* **41**, 861–870. [7.6.2]
- Baytas, A. C., Baytas, A. F. and Pop, I. 2004 Free convection in a porous cavity filled with pure or saline water. In *Applications of Porous Media (ICAPM 2004)*, (eds. A. H. Reis and A. F. Miguel), Évora, Portugal, pp. 121–125. [7.3.5]
- Baytas, A. C., Baytas, A. f., Ingham, D. B. and Pop, I. 2009 Double diffusive natural convection in an enclosure filled with a step type porous layer: Non-Darcy flow. *Int. J. Therm. Sci.* **48**, 665–673. [9.4]
- Baytas, A. C., Grosan, T. and Pop, I. 2002 Free convection in spherical annular sectors filled with a porous medium. *Transport Porous Media* **49**, 191–207. [7.3.4]
- Baytas, A. C., Liaqat, A., Grosan, T. and Pop, I. 2001 Conjugate natural convection in a square porous cavity. *Heat Mass Transfer* **37**, 467–473. [7.1.5]
- Baytas, A.C. 2004a Entropy generation for free and forced convection in a porous cavity and a porous channel. In *Emerging Technologies and Techniques in Porous Media* (D. B. Ingham, A. Bejan, E. Mamut and I. Pop, eds), Kluwer Academic, Dordrecht, pp. 259–270. [7.8]
- Baytas, A.C. 2004b Thermal non-equilibrium free convection in a cavity filled with a non-Darcy porous medium. In *Emerging Technologies and Techniques in Porous Media* (D. B. Ingham, A. Bejan, E. Mamut and I. Pop, eds), Kluwer Academic, Dordrecht, pp. 247–258. [6.5]
- Bear, J. and Bachmat, Y. 1990 *Introduction to Modeling of Transport Phenomena in Porous Media*, Kluwer Academic, Dordrecht. [1.1, 1.5.3]
- Beavers, G. S. and Joseph, D. D. 1967 Boundary conditions at a naturally permeable wall. *J. Fluid Mech.* **30**, 197–207. [1.6]
- Beavers, G. S., Sparrow, E. M. and Magnuson, R. A. 1970 Experiments on coupled parallel flows in a channel and a bounding medium. *ASME J. Basic Engng.* **92**, 843–848. [1.6]
- Beavers, G. S., Sparrow, E. M. and Masha, B. A. 1974 Boundary conditions at a porous surface which bounds a fluid flow. *AIChE J.* **20**, 596–597. [1.6]
- Beavers, G. S., Sparrow, E. M. and Rodenz, D. E. 1973 Influence of bed size on the flow characteristics and porosity of randomly packed beds of spheres. *J. Appl. Mech.* **40**, 655–660. [1.5.2]
- Beck, J. L. 1972 Convection in a box of porous material saturated with fluid. *Phys. Fluids* **15**, 1377–1383. [1.5.1, 6.15.1]
- Becker, S. M., Kuznetsov, A. V. and Avramenko, A. A. 2004 Numerical modeling of a falling bioconvection plume in a porous medium. *Fluid Dyn. Res.* **33**, 323–339. [6.25]
- Beckermann, C. and Viskanta, R. 1987 Forced convection boundary layer flow and heat transfer along a flat plate embedded in a porous medium. *Int. J. Heat Mass Transfer* **30**, 1547–1551. [4.8]
- Beckermann, C. and Viskanta, R. 1988a Natural convection solid/liquid phase change in porous media. *Int. J. Heat Mass Transfer* **31**, 35–46. [10.1.6]
- Beckermann, C. and Viskanta, R. 1988b Double-diffusive convection during dendritic solidification of a binary mixture. *PhysicoChemical Hydodyn.* **10**, 195–213. [10.2.2, 10.2.3]

- Beckermann, C. and Viskanta, R. 1993 Mathematical modeling of transport phenomena during alloy solidification. *Appl. Mech. Rev.* **46**, 1–27. [10.2.3]
- Beckermann, C. and Wang, C. Y. 1995 Multiphase/- scale modeling of alloy solidification. *Ann. Rev. Heat Transfer* **6**, 115–198. [10.2.3]
- Beckermann, C., Viskanta, R. and Ramadhyani, S. 1986 A numerical study of non-Darcian natural convection in a vertical enclosure filled with a porous medium. *Numer. Heat Transfer* **10**, 557–570. [7.6.2]
- Beckermann, C., Viskanta, R. and Ramadhyani, S. 1988 Natural convection in vertical enclosures containing simultaneously fluid and porous layers. *J. Fluid Mech.* **186**, 257–284. [7.7]
- Beg, O. A., Bakier, A. Y. and Prasad, V. R. 2009a Numerical study of magnetohydrodynamic heat and mass transfer from a stretching surface to a porous medium with Soret and Dufour effects. *Comput. Mater. Sci.* **46**, 57–65. [9.2.1]
- Beg, O. A., Takhar, H. S., Soundalgekar, V. M. and Prasad, V. 1998 Thermoconvective flow in a saturated, isotropic, homogeneous porous medium using Brinkman's model — numerical study. *Int. J. Numer. Methods Heat Fluid Flow* **8**, 559–589. [5.1.7.1]
- Beg, O. A., Yakhar, H. S., Bhargava, R., Rawal, S. and Prasad, V. R. 2008a Numerical study of heat transfer of a third grade viscoelastic fluid in non-Darcy porous media with thermophysical effects. *Physica Scripta* **77**, #065402. [7.1.6]
- Beg, O. A., Zueco, J. and Takhar, H. S. 2008b Laminar free convection from a continuously-moving vertical surface in thermally-stratified non-Darcian high-porosity medium: Network numerical study. *Int. Comm. Heat Mass Transfer* **35** 810–816. [5.1.9.9]
- Beg, O. A., Zueco, J., Beg, T. A., Takhar, H. S. and Kahya, E. 2009c NSM analysis of time-dependent nonlinear buoyancy-driven double-diffusive radiation convection flow in non-Darcy geological porous media. *Acta Mech.* **202**, 181–204. [9.2.1]
- Beg, O. A., Zueco, J., Bhargava, R. and Takhar, H. S. 2009d Magnetohydrodynamic convection flow from a sphere to a non-Darcian porous medium with heat generation or absorption effects: network simulation. *Int. J. Therm. Sci.* **48**, 913–92. [5.6.1].
- Beg, O. A., Zueco, J., Takhar, H. S., Beg, T. A. and Sajid, A. 2009e Transient nonlinear optically-thick radiative-convective double-diffusive boundary layers in a Darcian porous medium adjacent to an impulsively started surface; Network simulationsolutions. *Comm. Nonlinear Sci. Numer. Simu.* **14**, 3856–3866. [9.2.1]
- Beithou, N. 2008 Analyses of free convective flow of variable spaced plates embedded in a porous medium. *Desalination* **219**, 40–47. [7.3.1]
- Bejan, A. 2012 *Convection Heat Transfer*, 4th ed. Wiley, Hoboken. [6.26.3]
- Bejan, A. 1978 Natural convection in an infinite porous medium with a concentrated heat source. *J. Fluid Mech.* **89**, 97–107. [5.11.2]
- Bejan, A. 1979 On the boundary layer regime in a vertical enclosure filled with a porous medium. *Lett. Heat Mass Transfer* **6**, 93–102. [7.1.2, 7.2]
- Bejan, A. 1980 A synthesis of analytical results for natural convection heat transfer across rectangular enclosures. *Int. J. Heat Mass Transfer* **23**, 723–726. [7.1.3, 7.4, 7.4.2]
- Bejan, A. 1981 Lateral intrusion of natural convection into a horizontal porous structure. *ASME J. Heat Transfer* **103**, 237–241. [7.4, 7.4.1]
- Bejan, A. 1983a Natural convection heat transfer in a porous layer with internal flow obstructions. *Int. J. Heat Mass Transfer* **26**, 815–822. [7.3.1]
- Bejan, A. 1983b The boundary layer regime in a porous layer with uniform heat flux from the side. *Int. J. Heat Mass Transfer* **26**, 1339–1346. [7.2]
- Bejan, A. 1984 *Convection Heat Transfer*, Wiley, New York. [1.1, 4.1, 4.2, 4.5, 4.17, 5.1.4, 5.11.1, 6.9.2, 7.1.1, 7.1.2, 7.3.3, 7.4.2, 9.2.1, 10.1.2]
- Bejan, A. 1985 The method of scale analysis: natural convection in porous media. *Natural Convection: Fundamentals and Applications* (ed. S. Kakaç, et al.), Hemisphere, Washington, DC, 548–572. [7.1.1]

- Bejan, A. 1987 Convective heat transfer in porous media. *Handbook of Single-Phase Convective Heat Transfer* (eds. S. Kakaç, R. K. Shah, and W. Aung), Chapter 16, Wiley, New York. [6.20, 7.3.3, 7.3.4, 7.3.5]
- Bejan, A. 1989 Theory of melting with natural convection in an enclosed porous medium. *ASME J. Heat Transfer* **111**, 407–415. [10.1.3, 10.1.5]
- Bejan, A. 1990a Theory of heat transfer from a surface covered with hair. *ASME J. Heat Transfer* **112**, 662–667. [4.14]
- Bejan, A. 1990b Optimum hair strand diameter for minimum free-convection heat transfer from a surface covered with hair. *Int. J. Heat Mass Transfer* **33**, 206–209. [5.13]
- Bejan, A. 1992a Comments on “Coupled heat and mass transfer by natural convection from vertical surfaces in porous media.” *Int. J. Heat Mass Transfer* **35**, 3498. [9.2.1]
- Bejan, A. 1992b Surfaces covered with hair: optimal strand diameter and optimal porosity for minimum heat transfer. *Biomimetics* **1**, 23–38. [4.14]
- Bejan, A. 1995 The optimal spacing for cylinders in cross flow forced convection. *J. Heat Transfer* **117**, 767–770. [4.15]
- Bejan, A. 1996a *Entropy Generation Minimization*, CRC Press, Boca Raton, FL. [4.15]
- Bejan, A. 2000 *Shape and Structure, from Engineering to Nature*, Cambridge University Press, Cambridge, UK. [1.5.2, 4.18, 6.2, 6.26, 11.10]
- Bejan, A. 2004a *Convection Heat Transfer*, 3rd ed., Wiley, New York. [1.5.2, 2.1, 4.17, 4.18, 4.20]
- Bejan, A. 2004b Designed porous media: maximal heat transfer density at decreasing length scales. *Int. J. Heat Mass Transfer* **47**, 3073–3083. [4.15]
- Bejan, A. 1993 *Heat Transfer*, 2nd ed., Wiley, New York. [4.4, 4.15]
- Bejan, A. 1996b Street network theory of organization in nature. *J. Adv. Transportation* **30**, 85–107. [4.18]
- Bejan, A. 1997a Constructal-theory network of conducting paths for cooling a heat generating volume. *Int. J. Heat Mass Transfer* **40**, 799–816. [4.18]
- Bejan, A. 1997b Constructal tree network for fluid flow between a finite-size volume and one source or sink. *Rev. Gén. Thermique* **36**, 592–604. [4.18]
- Bejan, A. 1997c *Advanced Engineering Thermodynamics*, 3rd ed., Wiley, New York, [4.19, 6.26]
- Bejan, A. and Anderson, R. 1981 Heat transfer across a vertical impermeable partition imbedded in a porous medium. *Int. J. Heat Mass Transfer* **24**, 1237–1245. [5.1.5, 7.3.1]
- Bejan, A. and Anderson, R. 1983 Natural convection at the interface between a vertical porous layer and an open space. *ASME J. Heat Transfer* **105**, 124–129. [5.1.5]
- Bejan, A. and Fautrelle, Y. 2003 Constructal multi-scale structure for maximal heat transfer density. *Acta Mech.* **163**, 39–49. [4.19]
- Bejan, A. and Khair, K. R. 1985 Heat and mass transfer by natural convection in a porous medium. *Int. J. Heat Mass Transfer* **28**, 909–918. [9.2.1]
- Bejan, A. and Lage, J. L. 1991 Heat transfer from a surface covered with hair. *Convective Heat and Mass Transfer in Porous Media* (eds. S. Kakaç, et al.), Kluwer Academic, Dordrecht, 823–845. [1.2, 4.14]
- Bejan, A. and Lorente, S. 2004 The constructal law and the thermodynamics of flow systems with configuration. *Int. J. Heat Mass Transfer* **47**, 3203–3214. [4.18]
- Bejan, A. and Lorente, S. 2006 Constructal theory of generation of configuration in nature and engineering. *J. Applied Physics* **100**, #041301. [3.7]
- Bejan, A. and Lorente, S. 2008 *Design with Constructal Theory*. Wiley, Hoboken. [3.7]
- Bejan, A. and Lorente, S. 2010 The constructal law of design and evolution in nature. *Phil. Trans. Roy. Soc. B, Biological Sciences* **365**, 1335–1347. [3.7, 4.14]
- Bejan, A. and Lorente, S. 2011 The constructal law and the evolution of design in nature. *Physics of Life Reviews* **8**, 209–240. [3.7, 4.14]
- Bejan, A. and Morega, A. M. 1993 Optimal arrays of pin fins and plate fins in laminar forced convection. *J. Heat Transfer* **115**, 75–81. [4.15]
- Bejan, A. and Morega, A. M. 1993 Optimal arrays of pin fins and plate fins in laminar forced convection. *ASME J. Heat Transfer* **115**, 75–81. [4.15]

- Bejan, A. and Nield, D. A. 1991 Transient forced convection near a suddenly heated plate in a porous medium. *Int. Comm. Heat Mass Transfer* **18**, 83–91. [4.6]
- Bejan, A. and Poulikakos, D. 1984 The non-Darcy regime for vertical boundary layer natural convection in a porous medium. *Int. J. Heat Mass Transfer* **27**, 717–722. [5.1.7.2]
- Bejan, A. and Sciumba, E. 1992 The optimal spacing of parallel plates cooled by forced convection. *Int. J. Heat Mass Transfer* **35**, 3259–3264. [4.15]
- Bejan, A. and Tien, C. L. 1978 Natural convection in a horizontal porous medium subjected to an end-to-end temperature difference. *ASME J. Heat Transfer* **100**, 191–198. errata **105**, 683–684. [7.1.3, 7.3.2, 7.3.3]
- Bejan, A. and Tien, C. L. 1979 Natural convection in horizontal space bounded by two concentric cylinders with different end temperatures. *Int. J. Heat Mass Transfer* **22**, 919–927. [7.3.3]
- Bejan, A. and Zane, J. P. 2012 *Design in Nature. How the Constructal Law Governs Evolution in Biology, Physics, Technology, and Social Organization*. Doubleday, New York. [4.14, 4.18.5]
- Bejan, A., Dincer, I., Lorente, S., Miguel, A. F. and Reis, A. H. 2004 *Porous and Complex Flow Structures in Modern Technologies*. Springer, New York. [1.5.2, 2.1, 3.3, 3.7, 4.18, 4.19, 6.26, 10.1.7]
- Bejan, A., Ikegami, Y. and Ledezma, G. A. 1998 Constructal theory of natural crack pattern formation for fastest cooling. *Int. J. Heat Mass Transfer* **41**, 1945–1954. [11.10]
- Bejan, A., Lorente, S., Miguel, A. F., Pumain, D. and Reis, A. H. 2005 *Along with Constructal Theory*, Faculty of Geosciences and the Environment, University of Lausanne, Switzerland. [11.10]
- Bejan, A., Rocha, L. A. O. and Cherry, R. S. 2002 Methane hydrates in porous layers: gas formation and convection. In *Transport Phenomena in Porous Media II* (D. B. Ingham and I. Pop, eds.) Elsevier, Oxford, pp. 365–396. [10.1.7]
- Bejan, A., Zhang, Z. and Jany, P. 1990 The horizontal intrusion layer of melt in a saturated porous medium. *Int. J. Heat Fluid Flow* **11**, 284–289. [10.1.4]
- Beji, H. and Gobin, P. 1992 The effect of thermal dispersion on natural dispersion heat transfer in porous media. *Numer. Heat Transfer A* **23**, 487–500. [7.6.2]
- Beji, H., Bennacer, R. and Duval, R. 1999 Double-diffusive natural convection in a vertical porous annulus. *Numer. Heat Transfer A* **36**, 153–170. [9.4]
- Belhachmi, Z., Brighi, B. and Taous, K. 2000 Similarity solutions for a boundary layer problem in porous media. *C. R. Acad. Sci. II B* **328**, 407–410. [5.1.9.1]
- Belhachmi, Z., Brighi, B. and Taous, K. 2001 On a family of differential equations for boundary layer approximations in porous media. *Europ. J. Appl. Math.* **12**, 513–528. [5.1.9.1]
- Belhachmi, Z., Brighi, B., Sac-Eppé, J. M. and Taous, K. 2003 Numerical simulations of free convection about a vertical flat plate embedded in a porous medium. *Comp. Geosci.* **7**, 137–166. [5.1.9.1]
- Bello-Ochende, T. and Bejan, A. 2004 Maximal heat transfer density: Plates with multiple lengths in forced convection. *Int. J. Thermal Sci.* **43**, 1181–1186. [4.19]
- Bello-Ochende, T. and Bejan, A. 2005a Constructal multi-scale cylinders in cross-flow. *Int. J. Heat Mass Transfer* **48**, 1373–1383. [4.19]
- Bello-Ochende, T. and Bejan, A. 2005b Constructal multi-scale cylinders with natural convection. *Int. J. Heat Mass Transfer* **48**, 4300–4306. [4.19]
- Ben Hamed, H. and Bennacer, R. 2008 Analytical development of disturbed matrix eigenvalue problem applied to mixed convection stability analysis in Darcy media. *C. R. Mecanique* **336**, 656–663. [6.10.1]
- Ben Khelifa, N., Alloui, Z., Beji, H. and Vasseur, P. 2012 Natural convection in a vertical porous cavity filled with a non-Newtonian fluid. *AIChE J.* **58**, 1704–1716. [9.2.2]
- Ben Nasrallah, S., Mara, A. and Du Peuty, M. A. 1997 Transient free convection in a vertical cylinder filled with a granular product: Open at the extremities and heated with heat flux density : validity of the local thermal equilibrium hypothesis. *Int. J. Heat Mass Transfer* **40**, 1155–1168. [7.5]

- Ben Yedder, R. and Erchiqui, F. 2009 Convective flow and heat transfer in a tall porous cavity side-cooled with temperature profile. *Int. J. Heat Mass Transfer* **52**, 5712–5718. [7.1.2]
- Benano-Melly, L. B., Caltagirone, J.-P., Faissat, B., Montel, F. and Costeseque, P. 2001 Modelling Soret coefficient measurement experiments in porous media considering thermal and solutal convection. *Int. J. Heat Mass Transfer* **44**, 1285–1297. [9.1.4]
- Benhadji, K. and Vasseur P. 2003 Double-diffusive convection in a shallow porous cavity filled with a non-Newtonian fluid. *Int. Comm. Heat Mass Transfer* **28**, 763–772. [9.2.2]
- Benhadji, K., Robillard, L. and Vasseur P. 2003 Convection in a porous cavity saturated with water near 4 degrees C and subject to Dirichlet-Neumann thermal boundary conditions. *Int. Comm. Heat Mass Transfer* **29**, 897–906. [7.3.5]
- Bennacer, R. 2000 The Brinkman model for thermosolutal convection in a vertical annular porous layer. *Int. Comm. Heat Mass Transfer* **27**, 69–80. [9.4]
- Bennacer, R. 2004 Natural convection in anisotropic heterogeneous porous medium. In *Emerging Technologies and Techniques in Porous Media* (D. B. Ingham, A. Bejan, E. Mamut and I. Pop, eds), Kluwer Academic, Dordrecht, pp. 271–284. [9.1.6.2]
- Bennacer, R. and Lakhal, A. 2005 Numerical and analytical analysis of the thermosolutal convection in an annular field: effect of thermodiffusion. In *Transport Phenomena in Porous Media III*, (eds. D. B. Ingham and I. Pop), Elsevier, Oxford, pp. 341–365. [9.4]
- Bennacer, R., Beji, H. and Mohamad, A. A. 2003a Double diffusive convection in a vertical enclosure inserted with two saturated porous layers containing a fluid layer. *Int. J. Thermal Sci.* **42**, 141–151. [9.4]
- Bennacer, R., Beji, H., Oueslati, F. and Belgith, A. 2001a Multiple natural convection solution in porous media under cross temperature and concentration gradients. *Numer. Heat Transfer A* **39**, 553–567. [9.2.2]
- Bennacer, R., El Ganaoui, M. and Fauchais, P. 2004 On the thermal anisotropy affecting transfers in multi-layer porous medium. *Comptes Rendus Mécanique* **332**, 539–546. [9.5]
- Bennacer, R., Mahidjibo, A., Vasseur, P., Beji, H. and Duval, R. 2003b The Soret effect on convection in a horizontal porous domain under cross-temperature and concentration gradients. *Int. J. Numer. Meth. Heat Fluid Flow* **13**, 199–215. [9.2.2]
- Bennacer, R., Mohamad, A. A. and El Ganaoui, M. 2005 Analytical and numerical investigation of double diffusion in thermally anisotropic multilayer porous medium. *Heat Mass Transfer* **41**, 298–305. [9.5]
- Bennacer, R., Mohamad, A. A. and El Ganoui, M. 2009 Thermodiffusion in porous media; Multi-domain constituent separation. *Int. J. Heat Mass Transfer* **52**, 1725–1733. [9.4]
- Bennacer, R., Tobbal, A., Beji, H. and Vasseur, P. 2001b Double diffusive convection in a vertical enclosure filled with anisotropic media. *Int. J. Thermal Sci.* **40**, 30–41. [9.2.2]
- Bennamouou, L. and Belhamri, A. 2008 Mathematical description of heat and mass transfer during deep bed drying: Effect of product shrinkage on bed porosity. *Appl. Therm. Engng.* **28**, 2236–2244. [3.6]
- Bennethum, L. S. and Giorgi, T. 1997 Generalized Forchheimer equation for two-phase flow based on hybrid mixture theory. *Transport Porous Media* **26**, 261–275. [1.5.2]
- Bennisaad, S. and Ouazaa, N. 2012 Analytical and numerical study of double diffusive natural convection in a confined porous medium subjected to heat and mass fluxes. *J. Porous Media* **15**, 909–976. [9.4]
- Bennon, W. D. and Incropera, F. P. 1987 A continuum model for momentum, heat and species transport in binary-phase change systems. I. Model formulation. *Int. J. Heat Transfer* **40**, 2161–2170. [10.2.3]
- Bensouici, M. and Bessiah, R. 2010 Mixed convection in a vertical channel with discrete heat sources using a porous matrix. *Numer. Heat Transfer A* **58**, 581–604. [8.3.2]
- Benzeghiba, M., Chikh, S. and Campo, A. 2003 Thermosolutal convection in a partly porous vertical annular cavity. *ASME J. Heat Transfer* **125**, 703–715. [9.4]
- Bera, P., Kumar, P. and Khalili, A. 2011 Hot springs mediate spatial exchange of heat and mass in the enclosed sediment domain: A stability perspective. *Adv. Water Resourc.* **34**, 817–828. [9.1.6.4]

- Bera, P. and Khalili, A. 2002a Double-diffusive natural convection in an anisotropic porous cavity with opposing buoyancy forces: multi-solutions and oscillations. *Int. J. Heat Mass Transfer* **45**, 3205–3222. [9.2.2]
- Bera, P. and Khalili, A. 2002b Stability of mixed convection in an anisotropic vertical porous channel. *Phys. Fluids* **14**, 1617–1630. [8.3.1]
- Bera, P. and Khalili, A. 2006 Influence of Prandtl number on stability of mixed convective flow in a vertical channel filled with a porous medium. *Phys. Fluids* **18**, #124103. [8.3.1]
- Bera, P. and Khalili, A. 2007 Stability of buoyancy opposed mixed convection in a vertical channel and its dependence on permeability. *Adv. Water Resour.* **30**, 2296–2308. [8.3.1]
- Bera, P., Eswaran, V. and Singh, P. 1998 Numerical study of heat and mass transfer in an anisotropic porous enclosure due to constant heating and cooling. *Numer. Heat Transfer A*, **34**, 887–905. [9.2.2]
- Bera, P., Eswaran, V. and Singh, P. 2000 Double-diffusive convection in slender anisotropic porous enclosures. *J. Porous Media* **3**, 11–29. [9.2.2]
- Bera, P., Kapoor, S. and Khandelwal, M. K. 2012 Double-diffusive mixed convection in a vertical pipe: A thermal non-equilibrium approach. *Int. J. Heat Mass Transfer* **55**, 7079–7082. [9.6.2]
- Bergman, M. I. and Fearn, D. R. 1994 Chimneys on the Earth's inner-outer core boundary? *Geophys. Res. Lett.* **21**, 477–480. [6.21,11.8.2]
- Bergman, M. I., Fearn, D. R., Bloxam, J. and Shannon, M. C. 1997 Convection and channel formation in solidifying Pb-Sn alloys. *Metall. Mat. Trans. A* **28**, 859–866. [10.2.3]
- Bertola, V. and Cafaro, E. 2006 Thermal instability of viscoelastic fluids in horizontal porous layers as initial value problems. *Int. J. Heat Mass Transfer* **49**, 4003–4012. [6.23]
- Bessonov, O. A. and Brailovskaya, V. A. 2001 Three-dimensional model of thermal convection in an anisotropic porous medium bounded by two horizontal coaxial cylinders. *Fluid Dyn.* **36**, 130–138. [7.3.3]
- Betchen, L., Straatman, A. G. and Thompson, B. E. 2006 A non-equilibrium finite-volume model for conjugate fluid/porous/solid domains. *Numer. Heat Transfer A* **49**, 543–565. [2.4]
- Beukema, K. J. and Bruin, S. 1983 Three-dimensional natural convection in a confined porous medium with internal heat generation. *Int. J. Heat Mass Transfer* **26**, 451–458. [6.15.3]
- Bhadauria, B. S. 2007a Magnetoconvection in a rotating porous layer under modulated temperature on the boundaries. *ASME J. Heat Transfer* **129**, 835–843. [6.21]
- Bhadauria, B. S. 2007b Double diffusive convection in a porous medium with modulated temperature on the boundaries. *Transp. Porous Media* **70**, 191–211. [9.1.6.4]
- Bhadauria, B. S. 2007c Double diffusive convection in a rotating porous layer with temperature modulation on the boundaries. *J. Porous Media* **10**, 569–583. [9.1.6.4].
- Bhadauria, B. S. 2007d Fluid convection in a rotating porous layer under modulated temperature on the boundaries. *Transp. Porous Media* **67**, 297–315. [6.23]
- Bhadauria, B. S. 2007e Thermal modulation of Rayleigh-Bénard convection in a sparsely packed porous medium. *J. Porous Media* **10**, 175–188. [6.11.3]
- Bhadauria, B. S. 2008a Combined effect of temperature modulation and magnetic field on the onset of convection in an electrically conducting fluid-saturated porous medium. *ASME J. Heat Transfer* **130**, #052601. [6.11.3]
- Bhadauria, B. S. 2008b Effect of temperature modulation on the onset of Darcy convection in a rotating porous medium. *J. Porous Media* **11**, 361–375. [6.11.3]
- Bhadauria, B. S. 2012 Double-diffusive convection in a saturated anisotropic porous layer with internal heat source. *Transp. Porous Media* **92**, 299–310. [9.1.6.4]
- Bhadauria, B. S. and Agarwal, S. 2011a Convective transport in a nanofluid saturated porous layer with thermal non-equilibrium model. *Transp. Porous Media* **88**, 107–131. [6.23, 9.7]
- Bhadauria, B. S. and Agarwal, S. 2011b Natural convection in a nanofluid saturated rotating porous layer: A nonlinear study. *Transp. Porous Media* **87**, 585–602. [6.22, 9.7]
- Bhadauria, B. S. and Sherani, A. 2008a Onset of Darcy-convection in a magnetic fluid-saturated porous medium subject to temperature modulation of the boundaries. *Transp. Porous Media* **73**, 349–368. [6.11.3]

- Bhadauria, B. S. and Sherani, A. 2008b Onset of double diffusive convection in a thermally modulated fluid-saturated porous medium. *Z. Naturforschung A* **63**, 291–30. [6.1.6.4]
- Bhadauria, B. S. and Sherani, A. 2010 Magnetoconvection in a porous medium subject to temperature modulation of the boundaries. *Proc. Nat. Acad. Sci. India A* **80**, 47–58. [6.11.3]
- Bhadauria, B. S. and Srivastava, A. K. 2010 Magneto-double-diffusive convection in an electrically conducting-fluid-saturated porous medium with temperature modulation of the boundaries. *Int. J. Heat Mass Transfer* **53**, 2530–2538. [9.1.6.4]
- Bhadauria, B. S. and Suthar, O. P. 2009 Effect of thermal modulation on the onset of centrifugally driven convection in a rotating vertical porous layer placed far away from the axis of rotation. *J. Porous Media* **12**, 221–237. [6.22]
- Bhadauria, B. S., Siddheshwar, P. G., Kumar, J. and Suthar, O. P. 2012a Weakly nonlinear stability analysis of temperature/gravity modulated stationary Rayleigh-Bénard convection in a rotating porous medium. *Transp. Porous Media* **92**, 633–647. [6.24]
- Bhadauria, B. S., Hashim, I. and Siddheshwar, P. G. 2012b Study of heat transport in a porous medium under g-jitter and internal heating effects. *Transp. Porous Media*, to appear. [6.24]
- Bhargavi, D., and Satyamurty, V. V. 2011 Optimum porous insert configurations for enhanced heat transfer in channels. *J. Porous Media* **14**, 187–203. [4.11]
- Bhargavi, D., Satyamurthy, V. V. and Sekhar, G. P. R. 2009 Effect of porous fraction and interface stress jump on skin friction and heat transfer in flow through a channel partially filled with porous material. *J. Porous Media* **12**, 1065–1082. [4.11]
- Bhatta, D., Muddamallappa, M. S. and Riahi, D. N. 2010 On perturbation and marginal stability analysis of magneto-convection in active mushy layer. *Transp. Porous media* **82**, 385–399. [10.2.3]
- Bhatta, D., Riahi, D. N. and Muddamallappa, M. S. 2012 On nonlinear evolution of convective flow in an active mushy layer. *J. Engng. Math.* **74**, 73–89. [10.2.3]
- Bhattacharjee, S. and Grosshandler, W. L. 1988 The formation of a wall jet near a high temperature wall under a microgravity environment, *ASMR HTD* **96**, 711–716. [4.15]
- Bhattacharyya, S. and Singh, A. K. 2009 Augmentation of heat transfer from a solid cylinder wrapped with a porous layer. *Int. J. Heat Mass Transfer* **52**, 1991–2001. [5.5.1]
- Bhattacharyya, S., Pal, A. and Pop, I. 1998 Unsteady mixed convection on a wedge in a porous medium. *Int. Comm. Heat Mass Transfer* **25**, 743–752. [8.1.4]
- Bian, W. and Wang, B. X. 1993 Transient freezing and natural convection around a cylinder in saturated porous media. *Proc. 6th Int. Sympos. Transport Phenomena in Thermal Engineering*, Seoul, Korea, pp. 79–84. [10.2.1.2]
- Bian, W., Vasseur, P. and Bilgen, E. 1994a Natural convection of non-Newtonian fluids in an inclined porous layer. *Chem. Engng Commun.* **129**, 79–97. [7.8]
- Bian, W., Vasseur, P. and Bilgen, E. 1994b Boundary-layer analysis for natural convection in a vertical porous layer filled with a non-Newtonian fluid. *Int. J. Heat Fluid Flow* **15**, 384–391. [7.8]
- Bian, W., Vasseur, P. and Bilgen, E. 1996a Effect of an external magnetic field on buoyancy driven flow in a shallow porous cavity. *Numer. Heat Transfer A* **29**, 625–638. [6.21]
- Bian, W., Vasseur, P., Bilgen, E. and Meng, F. 1996b Effect of an electromagnetic field on natural convection in an inclined porous layer. *Int. J. Heat Fluid Flow* **17**, 36–44. [7.8]
- Biggs, M. J. and Humby, S. J. 1998 Lattice-gas automata methods for engineering. *Chem. Engng. Res. Design* **76**, 162–174. [2.6]
- Bilgen, E. and Mbaye, M. 2001 Bénard cells in fluid-saturated porous enclosures with lateral cooling. *Int. J. Heat Fluid Flow* **22**, 561–570. [6.8]
- Bin-Mansoor, S., Yilbas, B. S. and Al-Haddad, M. 2005 Entropy generation in the porous layer and the condensate film. *J. Enhanced Heat Transfer* **12**, 289–299. [10.4]
- Bjørlykke, K., Mo, A. and Palm, E. 1988 Modelling of thermal convection in sedimentary basins and its relevance to diagenetic reactions. *Mar. Petr. Geol.* **5**, 338–351. [11.5]
- Bjornsson, S. and Stefansson, V. 1987 Heat and mass transport in geothermal reservoirs. *Advances in Transport Phenomena in Porous Media* (eds. J. Bear and M. Y. Corapcioglu), Martinus Nijhoff, The Netherlands, 145–153. [11]

- Blake, K. R., Bejan, A. and Poulikakos, D. 1984 Natural convection near 4°C in a water saturated porous layer heated from below. *Int. J. Heat Mass Transfer* **27**, 2355–2364. [6.20]
- Blythe, P. A. and Simpkins, P. G. 1981 Convection in a porous layer for a temperature dependent viscosity. *Int. J. Heat Mass Transfer* **24**, 497–506. [6.7]
- Blythe, P. A., Daniels, P. G. and Simpkins, P. G. 1982 Thermally driven cavity flows in porous media. I. The vertical boundary layer structure near the corners. *Proc. Roy. Soc. London A* **380**, 119–136. [7.1.2]
- Blythe, P. A., Daniels, P. G. and Simpkins, P. G. 1985a Convection in a fluid saturated porous medium due to internal heat generation. *Int. Comm. Heat Mass Transfer* **12**, 493–504. [6.17]
- Blythe, P. A., Daniels, P. G. and Simpkins, P. G. 1985b Limiting behaviours in porous media cavity flows. *Natural Convection: Fundamentals and Applications* (eds. S. Kakaç, W. Aung, and R. Viskanta), Hemisphere, Washington, DC, pp. 600–611. [7.1.3]
- Blythe, P. A., Simpkins, P. G. and Daniels, P. G. 1983 Thermal convection in a cavity filled with a porous medium: a classification of limiting behaviours. *Int. J. Heat Mass Transfer* **26**, 701–708. [7.1.1]
- Bodvarsson, G. S., Pruess, K. and Lippmann, M. J. 1986 Modeling of geothermal systems. *J. Petrol. Tech.* **38**, 1007–1021. [11]
- Bogorodskii, P. V. and Nagurnyi, A. P. 2000 Under-ice meltwater puddles: a factor in the fast sea ice melting in the Arctic. *Doklady Earth Sciences* **373**, 885–887. [6.19]
- Boomsma, K. and Poulikakos, D. 2001 On the effective thermal conductivity of a three-dimensionally structured fluid-saturated metal foam. *Int. J. Heat Mass Transfer* **44**, 827–836. [2.2.1]
- Bories, S. 1970a Sur les mécanismes fondamentaux de la convection naturelle en milieu poreux. *Rev. Gén. Therm.* **9**, 1377–1401. [6.9.1]
- Bories, S. 1970b Comparaison des prévisions d'une théorie non linéaire et des résultats expérimentaux en convection naturelle dans une couche poreuse saturée horizontale. *C. R. Acad. Sci. Paris B* **271**, 269–272. [6.9.1]
- Bories, S. 1993 Convection naturelle dans une couche poroélastique inclinée. Sélection du nombre d'onde des configurations d'écoulements. *Compt. Rend. Acad. Sci., Paris, Sér. II*, **316**, 151–156. [7.8]
- Bories, S. A. 1987 Natural convection in porous media. *Advances in Transport Phenomena in Porous Media* (eds. J. Bear and M. Y. Corapcioglu), Martinus Nijhoff, The Netherlands, 77–141. [6.3, 6.5]
- Bories, S. A. 1991 Fundamentals of drying of capillary-porous bodies. *Convective Heat and Mass Transfer in Porous Media* (eds. S. Kakac, *et al.*), Kluwer Academic, Dordrecht, 391–434. [3.6]
- Bories, S. A. and Combaroum, M. A. 1973 Natural convection in a sloping porous layer. *J. Fluid Mech.* **57**, 63–79. [7.8]
- Bories, S. and Deltour, A. 1980 Influence des conditions aux limites sur la convection naturelle dans un volume poreux cylindrique. *Int. J. Heat Mass Transfer* **23**, 765–771. [6.16.1]
- Bories, S. and Thiriot, C. 1969 Échanges thermiques et tourbillons dans une couche poreuse horizontale. *La Houille Blanche* **24**, 237–245. [6.9.1]
- Borkowska-Pawlak, B. and Kordylewski, W. 1982 Stability of two-dimensional natural convection in a porous layer. *Q. J. Mech. Appl. Math.* **35**, 279–290. [6.15.1]
- Borkowska-Pawlak, B. and Kordylewski, W. 1985 Cell-pattern sensitivity to box configuration in a saturated porous medium. *J. Fluid Mech.* **150**, 169–181. [6.15.1]
- Bortolozzi, R. A. and Deibler, J. A. 2001 Comparison between two-field and one-field models for natural convection in porous media. *Chem. Engng. Sci.* **56**, 157–172. [7.3.3]
- Bouddour, A., Auriault, J. L. and Mhamdi-Alaoui, M. 1998 Heat and mass transfer in wet porous media in presence of evaporation. *Int. J. Heat Mass Transfer* **41**, 2263–2277. [3.6]
- Bourich, M., Amahmid, A. and Hasnaoui M. 2004a Double diffusive convection in a porous enclosure submitted to cross gradients of temperature and concentration. *Energy Conv. Management* **45**, 1655–1670. [9.5]

- Bourich, M., Hasnaoui, M. and Amahmid, A. 2004b Double-diffusive natural convection in a porous enclosure partially heated from below and differentially salted. *Int. J. Heat Fluid Flow* **25**, 1034–1046. [9.5]
- Bourich, M., Hasnaoui, M., Amahmid, A. 2004c A scale analysis of thermosolutal convection in a saturated porous enclosure submitted to vertical temperature and horizontal concentration gradients. *Energy Conv. Management* **45**, 2795–2811. [9.1.3]
- Bourich, M., Hasnaoui, M., Amahmid, A. and Mamou, M. 2002 Soret driven thermosolutal convection in a shallow porous enclosure. *Int. Comm. Heat Mass Transfer* **29**, 717–728. [9.1.4]
- Bourich, M., Hasnaoui, M., Amahmid, A. and Mamou, M. 2004d Soret convection in a shallow porous cavity submitted to uniform fluxes of heat and mass. *Int. Comm. Heat Mass Transfer* **31**, 773–782. [9.1.4]
- Bourich, M., Hasnaoui, M., Amahmid, A. and Mamou, M. 2005a Onset of convection and finite amplitude flow due to Soret effect within a sparsely packed porous enclosure heated from below. *Int. J. Heat Fluid Flow* **26**, 513–525. [9.1.4]
- Bourich, M., Hasnaoui, M., Mamou, M. and Amahmid, A. 2005b Hydrodynamical boundary conditions effects on Soret-driven thermosolutal convection in a shallow porous enclosure. *J. Porous Media* **8**, 455–469. [9.1.4]
- Bourich, M., Hasnaoui, M., Amahmid, A., Er-Raki, M. and Mamou, M. 2009 Analytical and numerical study of combined effects of a magnetic field and an external shear stress on convection in a horizontal porous enclosure. *Numeer. Hear Transfer A* **54**, 1042–1060. [9.1.6.4]
- Bourich, M., Hasnaoui, M., Mamou, M. and Amahmid, A. 2004e Soret effect inducing subcritical and Hopf bifurcations in a shallow enclosure filled with a clear binary fluid or a saturated porous medium: A comparative study. *Phys. Fluids* **16**, 551–568. [9.1.4]
- Bourich, M., Mamou, M., Hasnaoui, M. and Amahmid, A. 2004f On stability analysis of Soret convection within a horizontal porous layer. In *Emerging Technologies and Techniques in Porous Media* (D. B. Ingham, A. Bejan, E. Mamut and I. Pop, eds.), Kluwer Academic, Dordrecht, pp. 221–234. [9.1.4]
- Boursi, A., Bouhadef, K., Beji, H., Bennacer, R. and Nebbali, R. 2012 Heat and mass transfer in reactive porous media with local nonequilibrium. *J. Porous Media* **15**, 329–341. [9.1.6.4]
- Boussinesq, J. 1903 *Théorie Analytique de la Chaleur*, Vol. 2, Gauthier-Villars, Paris. [2.3]
- Boutana, N., Bahloul, N., Vasseur, P. and Joly, F. 2004 Soret and double diffusive convection in a porous cavity. *J. Porous Media* **7**, 41–57. [9.1.4]
- Boutin, Y. and Gosselin, L. 2009 Optimal mixed convection for maximal energy recovery with vertical porous channel (solar wall). *Renewable Energy* **34**, 2714–2721. [8.3.1]
- Boutros, Y. Z., Abd-El-Malek, M. P., Badran, N. A. and Hassan, H. S. 2006 Lie-group method of solution for steady two-dimensional boundary-layer stagnation-point flow toward a heated stretching sheet placed in a porous medium. *Meccanica* **41**, 681–691. [5.1.9.9]
- Bradean, R., Heggs, P. J., Ingham, D. B. and Pop, I. 1998a Convective heat flow from suddenly heated surfaces embedded in porous media. *Transport Phenomena in Porous Media* (eds. D. B. Ingham and I. Pop), Elsevier, Oxford, pp. 411–438. [5.5.1]
- Bradean, R., Ingham, D. B., Heggs, P. and Pop, I. 1997b Unsteady free convection adjacent to an impulsively heated horizontal circular cylinder in porous media. *Numer. Heat Transfer A* **31**, 325–346. [5.5.1]
- Bradean, R., Ingham, D. B., Heggs, P. J. and Pop, I. 1995a Buoyancy induced flow adjacent to a periodically heated and cooled horizontal surface in porous media. *Int. J. Heat Mass Transfer* **39**, 615–630. [5.2]
- Bradean, R., Ingham, D. B., Heggs, P. J. and Pop, I. 1995b Free convection fluid flow due to a periodically heated and cooled vertical plate embedded in a porous media. *Int. J. Heat Mass Transfer* **39**, 2545–2557. [5.1.9]
- Bradean, R., Ingham, D. B., Heggs, P. J. and Pop, I. 1996 Unsteady free convection from a horizontal surface embedded in a porous media. *Proc. 2nd European Thermal-Sciences and 14th UIT Nat. Heat Transfer Conference*, Edizioni ETS, Pisa Vol. 1, 329–335. [5.2]

- Braedan, R., Ingham, D. B., Heggs, P. J. and Pop, I. 1997a The unsteady penetration of free convection flows caused by heating and cooling flat surfaces in a porous media. *Int. J. Heat Mass Transfer* **40**, 665–687. [5.1.9, 5.2]
- Braedan, R., Ingham, D. B., Heggs, P. J. and Pop, I. 1998b Mixed convection adjacent to a suddenly heated horizontal circular cylinder embedded in a porous medium. *Transport Porous Media* **32**, 329–355. [8.1.3]
- Bradshaw, P. 2001 Shape and structure, from engineering to nature. *AAIA J.* **39**, 983. [4.19]
- Bradshaw, S., Glasser, D. and Brooks, K. 1991 Self-ignition and convection patterns in an infinite coal layer. *Chem. Engng Comm.* **105**, 255–278. [6.11.2]
- Braester, C. and Vadasz, P. 1993 The effect of a weak heterogeneity of a porous medium on natural convection. *J. Fluid Mech.* **254**, 345–362. [6.9.1, 6.13.4]
- Braga, E. J. and de Lemos, M. J. S. 2004 Turbulent natural convection in a porous square cavity computed with a macroscopic  $k - \epsilon$  model. *Int. J. Heat Mass Transfer* **47**, 5639–5663. [1.8]
- Braga, E. J. and de Lemos, M. J. S. 2005a Heat transfer in enclosures having a fixed amount of solid material simulated with heterogeneous and homogeneous models. *Int. J. Heat Mass Transfer* **48**, 4748–4765. [2.2.1]
- Braga, E. J. and de Lemos, M. J. S. 2005b Laminar natural convection in cavities filled with circular and square rods. *Int. Commun. Heat Mass Transfer* **32**, 1289–1297. [2.2.1]
- Braga, E. J. and de Lemos, M. J. S. 2006 Simulation of turbulent natural convection in a porous cylindrical annulus using a macroscopic two-equation model. *Int. J. Heat Mass Transfer* **49**, 4340–4351. [1.8]
- Braga, E. J. and de Lemos, M. J. S. 2008 Computation of turbulent free convection in left and right tilted porous enclosures using a macroscopic  $k$ -epsilon model. *Int. J. Heat Mass Transfer* **51**, 5279–5287. [1.8]
- Braga, E. J. and de Lemos, M. J. S. 2009 Laminar and turbulent free convection in a composite enclosure. *Int. J. Heat Mass Transfer* **52**, 588–596. [1.8]
- Brambles, O. J. and Rees, D. A. S. 2007 Curved free convection plume paths in porous media. *IDOTARAS* **111**, 109–122. [5.10.1]
- Brand, H. and Steinberg, V. 1983a Convective instabilities in binary mixtures in a porous medium. *Physica A* **119**, 327–338. [9.1.3, 9.1.4]
- Brand, H. and Steinberg, V. 1983b Nonlinear effects in the convective instability of a binary mixture in a porous medium near threshold. *Phys. Lett. A* **93**, 333–336. [9.1.3, 9.1.4]
- Brand, H. R., Hohenberg, P. C., and Steinberg, V. 1983 Amplitude equation near a polycritical point for the convective instability of a binary fluid mixture in a porous medium. *Phys. Rev. A* **27**, 591–594. [9.1.3]
- Bratsun, D. A. and Lyubimov, D. V. 1995 Co-symmetry breakdown in problems of thermal convection in porous medium. *Physica D* **82**, 398–417. [6.16.2]
- Bresch, D. and Sy, M. 2003 Convection in rotating porous media: The planetary geostrophic equations, used in geophysical fluid dynamics, revisited. *Cont. Mech. Thermodyn.* **15**, 247–263. [6.22]
- Breugem, W. P. and Rees, D. A. S. 2006 A derivation of the volume-averaged Boussinesq equations for flow in porous media with viscous dissipation. *Transport Porous Media* **63**, 1–12. [2.2.2]
- Brevdo, L. 2009 Three-dimensional absolute and convective instabilities at the onset of convection in a porous medium with inclined temperature gradient and vertical throughflow. *J. Fluid Mech.* **641**, 475–487. [7.9]
- Brevdo, L. and Cirpka, O. A. 2012 Absolute/convective instability dichotomy in a Soret-driven thermosolutal convection induced in a porous layer by inclined thermal and vertical solutal gradients. *Transp. Porous Media* **95**, 425–446. [9.5]
- Brevdo, L. and Ruderman, S. 2009a On the convection in a porous medium with inclined temperature gradient and vertical throughflow. Part I . Normal modes. *Transp. Porous Media* **80**, 137–151. [7.9]

- Brevdo, L. and Ruderman, S. 2009b On the convection in a porous medium with inclined temperature gradient and vertical throughflow. Part II . Absolute and convective instabilities, and spatially amplifying waves. *Transp. Porous Media* **80**, 153–172. [7.9]
- Brigi, B. and Hoernel, D. 2006 On the concave and convex solutions of a mixed convection boundary layer approximation in a porous medium. *Appl. Math. Lett.* **19**, 69–74. [8.1.6]
- Bringedal, C., Berra, I., Nordbotten, J. M. and Rees, D. A. S. 2011 Linear and nonlinear convection in porous media between coaxial cylinders. *Phys. Fluids* **23**, #094109. [6.16.1]
- Brinkman, H. C. 1947a A calculation of the viscous force exerted by a flowing fluid on a dense swarm of particles. *Appl. Sci. Res. A* **1**, 27–34. [1.5.3]
- Brinkman, H. C. 1947b On the permeability of media consisting of closely packed porous particles. *Appl. Sci. Res. A* **1**, 81–86. [1.5.3]
- Brinkman, H. C. 1952 The viscosity of concentrated suspensions and solutions. *J. Chem. Phys.* **20**, 571–581. [3.6]
- Budu, P. 2001 Stability results for convection in thawing subsea permafrost. *Cont. Mech. Thermodyn.* **13**, 269–285. [11.3]
- Buikis, A. and Ulanova, N. 1996 Modelling of non-isothermal gas flow through a heterogeneous medium. *Int. J. Heat Mass Transfer* **39**, 1743–1748. [2.6]
- Buonanno, G. and Carotenuto, A. 1997 The effective thermal conductivity of a porous medium with interconnected particles. *Int. J. Heat Mass Transfer* **40**, 393–405. [2.2.1]
- Buongiorno, J. 2006 Convective heat transfer in nanofluids. *ASME J. Heat Transfer* **128**, 240–250. [3.8]
- Buretta, R. J. and Berman, A. S. 1976 Convective heat transfer in a liquid saturated porous layer. *ASME J. Appl. Mech.* **43**, 249–253. [6.3, 6.9.1, 6.9.2, 6.11.2]
- Burns, A. S. and Stewart, W. E. 1992 Convection in heat generating porous media in a concentric annulus with a permeable outer boundary. *Int. Comm. Heat Mass Transfer* **19**, 127–136. [6.17]
- Burns, P. J. and Tien, C. L. 1979 Natural convection in porous media bounded by concentric spheres and horizontal cylinders. *Int. J. Heat Mass Transfer* **22**, 929–939. [7.3.3, 7.3.4]
- Burns, P. J., Chow, L. C. and Tien, C. L. 1977 Convection in a vertical slot filled with porous insulation. *Int. J. Heat Mass Transfer* **20**, 919–926. [7.1.7]
- Busse, F. H. 1985 Transition to turbulence in Rayleigh-Bénard convection. *Hydrodynamic Instabilities and the Transition to Turbulence* (eds. H. L. Swinney and J. Gollub), 2nd ed., Springer, Berlin, 97–137. [6.4]
- Busse, F. H. and Joseph, D. D. 1972 Bounds for heat transport in a porous layer. *J. Fluid Mech.* **54**, 521–543. [6.3]
- Bussiere, W., Rochette, D., Latchimy, T., Velleaud, G. and Andre, P. 2006 Measurement of Darcy and Forchheimer coefficients for silica sand beds. *High Temp. Mat. Process.* **10**, 55–78. [1.5.2]
- Butler, S. L., Huppert, H. E. and Worster, M. G. 2006 Numerical modeling of convection in a reactive porous medium with a mobile mush-liquid interface. *J. Fluid Mech.* **549**, 99–129. [10.2.3]
- Byun, S. Y., Ro, S. T., Shin, J. Y., Son, Y. S. and Lee, D. Y. 2006 Transient thermal behaviour of porous media under oscillating flow condition. *Int. J. Heat Mass Transfer* **49**, 5081–5085. [4.16.2]
- Cai, R. X., Zhang, N. and Liu, W. W. 2003 Algebraically explicit analytical solutions of two-buoyancy natural convection in porous media. *Prog. Nat. Sci.* **13**, 848–851. [9.2.2]
- Calmidi, V. V. and Mahajan, R. L. 2000 Forced convection in high porosity metal foams. *ASME J. Heat Transfer* **122**, 557–565. [4.9]
- Caltagirone, J. P. 1975 Thermoconvective instabilities in a horizontal porous layer. *J. Fluid Mech.* **72**, 269–287. [6.8]
- Caltagirone, J. P. 1976a Stabilité d'une couche poreuse horizontale soumise à des conditions aux limites périodiques. *Int. J. Heat Mass Transfer* **19**, 815–820. [6.11.3]
- Caltagirone, J. P. 1976b Thermoconvective instabilities in a porous medium bounded by two concentric horizontal cylinders. *J. Fluid Mech.* **76**, 337–362. [7.3.3]

- Caltagirone, J. P. 1980 Stability of a saturated porous layer subject to a sudden rise in surface temperature: comparison between the linear and energy methods. *Q. J. Mech. Appl. Math.* **33**, 47–58. [6.11.3]
- Caltagirone, J. P. and Bories, S. 1985 Solutions and stability criteria of natural convective flow in an inclined porous layer. *J. Fluid Mech.* **155**, 267–287. [7.8]
- Caltagirone, J. P. and Fabrie, P. 1989 Natural convection in a porous medium at high Rayleigh numbers. Part 1 – Darcy's model. *Eur. J. Mech. B* **8**, 207–227. [6.8]
- Caltagirone, J. P., Cloupeau, M. and Combarous, M. 1971 Convection naturelle fluctuante dans une couche poreuse horizontale. *C. R. Acad. Sci. Paris B* **273**, 833–836. [6.9.1]
- Caltagirone, J. P., Fabrie, P. and Combarous, M. 1987 De la convection naturelle oscillante en milieu poreux au chaos temporel? *C. R. Acad. Sci. Paris, Sér. II* **305**, 549–553. [6.8]
- Caltagirone, J. P., Meyer, G. and Mojtabi, A. 1981 Structurations thermoconvectives tridimensionnelles dans une couche poreuse horizontale. *J. Mécanique* **20**, 219–232. [6.8, 6.15.1]
- Campos, H., Morales, J. C., Lacoá, U. and Campo, A. 1990 Thermal aspects of a vertical annular enclosure divided into a fluid region and a porous region. *Int. Comm. Heat Mass Transfer* **17**, 343–354. [7.3.7]
- Cao, W. Z. and Poulikakos, D. 1991a Solidification of a binary mixture saturating a bed of glass spheres. *Convective Heat and Mass Transfer in Porous Media* (eds. S. Kakaç, et al.), Kluwer Academic, Dordrecht, 725–772. [10.2.2]
- Cao, W. Z. and Poulikakos, D. 1991b Freezing of a binary alloy saturating a packed bed of spheres. *AIAA J. Thermophys. Heat Transfer* **5**, 46–53. [10.2.3]
- Capone, F. 2001 On the onset of convection in porous media: temperature depending viscosity. *Bull. Unione Mat. Ital.* **4B**, 143–156. [6.7]
- Capone, F. and de Luca, R. 2012 Ultimately boundedness and stability of triply diffusive mixtures in rotating porous layers under the action of Brinkman law. *Int. J. Nonlinear Mech.* **47**, 799–805. [9.1.6.3]
- Capone, F. and Rionero, S. 1999 Temperature-dependent viscosity and its influence on the onset of convection in a porous medium. *Rend. Accad. Sci. Fiz. Matem. Napoli*, **66**, 159–172. [6.7]
- Capone, F. and Rionero, S. 2003 Nonlinear stability of a convective motion in a porous layer driven by a horizontally periodic temperature gradient. *Cont. Mech. Thermodyn.* **15**, 529–538. [6.14]
- Capone, F., Gentile, M. and Hill, A. A. 2009 Anisotropy and symmetry in porous media convection. *Acta Mech.* **208**, 205–214. [6.12]
- Capone, F., Gentile, M. and Hill, A. A. 2010 Penetrative convection via internal heating in anisotropic porous media. *Mec. Res. Comm.* **37**, 441–444. [6.12]
- Capone, F., Gentile, M. and Hill, A. A. 2011a Double-diffusive penetrative convection simulated via internal heating in an anisotropic porous layer with throughflow. *Int. J. Heat Mass Transfer* **54**, 1622–1626. [6.12]
- Capone, F., Gentile, M. and Hill, A. A. 2011b Penetrative convection in anisotropic porous media with variable permeability. *Acta Mech.* **216**, 49–58. [6.12]
- Carotenuto, C. and Minale, M. 2011 Shear flow over a porous layer: velocity in the real proximity of the interface via rheological tests. *Phys. Fluids* **23**, 063101. [1.6]
- Carr, M. 2003 Unconditional nonlinear stability for temperature-dependent density flow in a porous medium. *Math. Mod. Meth. Appl. Sci.* **13**, 207–220. [6.4]
- Carr, M. 2004 Penetrative convection in a superposed porous-medium – fluid layer via internal heating. *J. Fluid Mech.* **509**, 305–329. [6.19.3]
- Carr, M. and de Putter, S. 2003 Penetrative convection in a horizontally isotropic porous layer. *Cont. Mech. Thermodyn.* **15**, 33–43. [6.11.4]
- Carr, M. and Straughan, B. 2003 Penetrative convection in a fluid overlying a porous layer. *Adv. Water Res.* **26**, 263–276. [6.11.4]
- Carrillo, L. P. 2005 Convective heat transfer for viscous fluid flow through a metallic packed bed. *Interciencia* **30**, 81–8. and 109–111. [2.2.3]

- Carson, J. K., Lovatt, S. J., Tanner, D. J. and Cleland, A. C. 2005 Thermal conductivity bounds for isotropic porous materials. *Int. J. Heat Mass Transfer* **48**, 2150–2158. [2.2.1].
- Castinel, G. and Combarnous, M. 1974 Critère d'apparition de la convection naturelle dans une couch poreuse anisotrope horizontale. *C. R. Acad. Sci. Paris B* **278**, 701–704. [6.12].
- Castinel, G. and Combarnous, M. 1975 Natural convection in an anisotropic porous layer. *Rev. Gén. Therm.* **168**, 937–947. English translation, *Int. Chem. Eng.* **17**, 605–61. (1977). [6.12]
- Catton, I. 1985 Natural convection heat transfer in porous media. *Natural Convection: Fundamentals and Applications* (eds. S. Kakaç, W. Aung, and R. Viskanta), Hemisphere, Washington, DC, 514–547. [6.9.2, 6.19.2]
- Catton, I. and Chung, M. 1991 An experimental study of steam injection into a uniform water flow through porous media. *Wärme-Stoffübertrag.* **27**, 29–31. [11.9.5]
- Catton, I. and Travkin, V. S. 1996 Turbulent flow and heat transfer in high permeability porous media. *Proceedings of the International Conference on Porous Media and their Applications in Science, Engineering and Industry*, Kona, Hawaii, June 1996, (K.Vafai, editor), Engineering Foundation, New York, pp. 333–368. [1.8]
- Catton, I., Georgiadis, J. G. and Adnani, P. 1988 The impact of nonlinear convective processes in transport phenomena in porous media. *ASME HTD* **96**, Vol. 1, 767–777. [2.2.4]
- Cekmer, O., Mobedi, M., Ozerem, B. and Pop, I. 2012 Fully developed forced convection in a parallel plate channel with a centred porous layer. *Transp. Porous Media* **93**, 179–201. [4.11]
- Celli, M., Rees, D. A. S. and Barletta, A. 2010 The effect of local thermal non-equilibrium on forced convection boundary layer flow from a heated surface in porous media. *Int. J. Heat Mass Transfer* **53**, 3533–3539. [4.10]
- Cetkin, E., Lorente, S. and Bejan A. 2011a Vascularization for cooling and mechanical strength. *Int. J. Heat Mass Transfer* **54**, 2774–2781. [4.19]
- Cetkin, E., Lorente, S. and Bejan, A. 2011b Hybrid grid and tree structures for cooling and mechanical strength. *J. Appl. Phys.* **110**, #064910. [4.19]
- Cezmer, O., Mobedi, M., Ozerdem, B. and Pop, I. 2011 Fully developed forced convection heat transfer in a porous channel with asymmetric heat flux boundary conditions. *Transp. Porous Media* **90**, 791–806. [4.9]
- Chakrabarti, A. and Gupta, A. S. 1981 Nonlinear theromohaline convection in a rotating porous medium. *Mech. Res. Comm.* **8**, 9–22. [9.1.6.4]
- Chamkha, A. J. 1996 Non-Darcy hydromagnetic free convection from a cone and a wedge in porous media. *Int. Comm. Heat Mass Transfer* **23**, 875–887. [5.8]
- Chamkha, A. J. 1997a Solar radiation assisted natural convection in uniform porous medium supported by a vertical flat plate. *ASME J. Heat Transfer* **119**, 89–96. [5.1.9.4]
- Chamkha, A. J. 1997b A note on unsteady hydromagnetic free convection from a vertical fluid saturated porous medium channel. *ASME J. Heat Transfer* **119**, 638–641. [7.5]
- Chamkha, A. J. 1997c Similarity solutions for buoyancy-induced flow of a power-law fluid over a horizontal surface immersed in a porous medium. *Int. Comm. Heat Mass Transfer* **24**, 805–814. [5.2]
- Chamkha, A. J. 1997d Hydromagnetic flow and heat transfer of a heat-generating fluid over a surface in a porous medium. *Int. Comm. Heat mass Transfer* **24**, 815–825. [5.1.9.4]
- Chamkha, A. J. 1997e Hydromagnetic natural convection from an isothermal inclined surface adjacent to a thermally stratified porous medium. *Int. J. Engng. Sci.* **35**, 975–986. [5.3]
- Chamkha, A. J. 1997f Non-Darcy fully developed mixed convection in a porous medium channel with heat generation/absorption and hydromagnetic effects. *Numer. Heat Transfer A* **32**, 653–675. [8.3.1]
- Chamkha, A. J. 1997g MHD-free convection from a vertical plate embedded in a thermally stratified porous medium with Hall effects. *Appl. Math. Modelling* **21**, 603–609. [5.1.4]
- Chamkha, A. J. 1998 Mixed convection flow along a vertical permeable plate embedded in a porous medium in the presence of a transverse magnetic field. *Numer. Heat Transfer A* **34**, 93–103. [8.1.1]
- Chamkha, A. J. 1999 Magnetohydrodynamic mixed convection from a rotating cone embedded in a porous medium with heat generation. *J. Porous Media* **2**, 87–105. [8.1.4]

- Chamkha, A. J. 2000 Non-similar solutions for heat and mass transfer by hydromagnetic mixed convection flow over a plate in porous media with surface suction or injection. *Int. J. Numer. Meth. Heat Fluid Flow* **10**, 142–162. [9.6.1]
- Chamkha, A. J. 2001 Unsteady laminar hydromagnetic flow and heat transfer in porous channels with temperature-dependent properties. *Int. J. Numer. Meth. Heat Fluid Flow* **11**, 430–448. [4.16.5]
- Chamkha, A. J. 2002 Double-diffusive convection in a porous enclosure with cooperating temperature and concentration gradients and heat generation or absorption effects. *Numer. Heat Transfer A* **41**, 65–87. [9.1.6.4]
- Chamkha, A. J. 2004 Unsteady MHD convective heat mass transfer past a semi-infinite vertical permeable moving plate with heat absorption. *Int. J. Engng. Sci.* **42**, 217–230. [9.2.1]
- Chamkha, A. J. and Al-Naser, H. 2001 Double-diffusive convection in an inclined porous enclosure with opposing temperature and concentration gradients. *Int. J. Therm. Sci.* **40**, 227–244. [9.4]
- Chamkha, A. J. and Al-Naser, H. 2002 Hydromagnetic double-diffusive convection in a rectangular enclosure with opposing temperature and concentration gradients. *Int. J. Heat Mass Transfer* **45**, 2465–2483. [9.1.6.4]
- Chamkha, A. J. and Al-Humoud, J. M. 2007 Mixed convection heat and mass transfer of non-Newtonian fluids from a permeable surface embedded in a porous medium. *Int. J. Numer. Meth. Heat Fluid Flow* **17**, 195–212. [9.6.1]
- Chamkha, A. J. and Aly, A. M. 2011 Heat and mass transfer in stagnation-point flow of a polar fluid towards a stretching surface in porous media in the presence of Soret, Dufour and chemical reaction effects. *Chem. Engng. Commun.* **198**, 214–234. [9.2.1]
- Chamkha, A. J. and Ben-Nakhi, A. 2008 MHD mixed convection-radiation interaction along a permeable surface immersed in a porous medium in the presence of Soret and Dufour effects. *Heat Mass Transfer* **44**, 845–856. [9.6.1]
- Chamkha, A. J. and Khaled, A. R. A. 1999 Nonsimilar hydromagnetic simultaneous heat and mass transfer by mixed convection from a vertical plate embedded in a uniform porous medium. *Numer. Heat Transfer A* **36**, 327–344. [9.6.1]
- Chamkha, A. J. and Khaled, A. R. A. 2000a Hydromagnetic simultaneous heat and mass transfer by mixed convection from a vertical plate embedded in a stratified porous medium with thermal dispersion effects. *Heat Mass Transfer* **36**, 63–70. [9.6.1]
- Chamkha, A. J. and Khaled, A. R. A. 2000b Similarity solutions for hydromagnetic mixed convection heat and mass transfer for Hiemenz flow through porous media. *Int. J. Numer. Meth. Heat Fluid Flow* **10**, 94–115. [9.6.1]
- Chamkha, A. J. and Khaled, A. R. A. 2000c Hydromagnetic combined heat and mass transfer by natural convection from a permeable surface embedded in a fluid-saturated porous medium. *Int. J. Numer. Meth. Heat Fluid Flow* **10**, 445–476. [9.1.6.4]
- Chamkha, A. J. and Khaled, A. R. A. 2000d Hydromagnetic coupled heat and mass transfer by natural convection from a permeable constant heat flux surface in porous media. *J. Porous Media* **3**, 259–266. [9.2.1]
- Chamkha, A. J. and Khanafer, K. 1999 Nonsimilar combined convection flow over a vertical surface embedded in a variable porosity medium. *J. Porous Media* **2**, 231–249. [9.6.1]
- Chamkha, A. J. and Pop, I. 2004 Effect of thermophoresis particle deposition in free convection boundary layer from a vertical flat plate embedded in a porous medium. *Int. Comm. Heat Mass Transfer* **31**, 421–430. [9.2.1]
- Chamkha, A. J. and Quadri, M. M. A. 2001 Heat and mass transfer from a permeable cylinder in a porous medium with magnetic field and heat generation/adsorption effects. *Numer. Heat Transfer A* **40**, 387–401. [9.2.1]
- Chamkha, A. J. and Quadri, M. M. A. 2002 Combined heat and mass transfer by hydromagnetic natural convection over a cone embedded in a non-Darcian porous medium with heat generation/absorption effects. *Heat Mass Transfer* **38**, 487–495. [9.2.1]

- Chamkha, A. J. and Quadri, M. M. A. 2003 Simultaneous heat and mass transfer by natural convection from a plate embedded in a porous medium with thermal dispersion effects. *Heat Mass Transfer* **39**, 561–569. [9.2.1]
- Chamkha, A. J., Abbasbandy, S. and Rashad, A. M. 2012 Radiation effects on mixed convection over a wedge embedded in a porous medium filled with a nanofluid. *Transp. Porous Media* **91**, 261–27. [9.7.]
- Chamkha, A. J., Ahmed, S. E. and Aloraiyer, A. S. 2010a Melting and radiation effects on mixed convection from a vertical surface embedded in a non-Newtonian fluid saturated in a non-Darcy porous medium for aiding and opposing external flows. *Int. J. Phys. Sci.* **5**, 1212–1224. [10.1.7]
- Chamkha, A. J., Al-Mudhaf, A. F. and Pop, I. 2006a Effect of heat generation or absorption on thermophoretic free convection boundary layer from a vertical plate embedded in porous medium. *Int. Comm. Heat Mass Transfer* **33**, 1096–1102. [9.2.1]
- Chamkha, A. J., Aly, A. M. and Mansour, M. A. 2010b Similarity solution for unsteady heat and mass transfer from a stretching surface embedded in a porous medium with suction/injection and chemical reaction effects. *Chem. Engng. Comm.* **197**, 846–858. [9.2.1]
- Chamkha, A. J., Aly, A. M. and Rahman, M. M. 2010c Unsteady natural convective power-law fluid flow past a vertical plate embedded in a non-Darcy porous medium in the presence of a chemical reaction. *Nonlinear Anal. Modell. Control* **15**, 139–154. [5.1.9.9]
- Chamkha, A. J., and Al-Mudhaf, A. F. 2008 Double-diffusive natural convection in inclined porous cavities with various aspect ratios and temperature-dependent heat source or sink. *Heat Mass Transfer* **44**, 679–693. [9.4]
- Chamkha, A. J., Bercea, C. and Pop, I. 2006 b Free convection flow over a truncated cone embedded in a porous medium saturated with pure or saline water at low temperatures, *Mech. Res. Commun.* **33**, 433–440. [9.2.1]
- Chamkha, A. J., Issa, C. and Khanafer, K. 2001 Natural convection due to solar radiation from a vertical plate embedded in a porous medium with variable porosity. *J. Porous Media* **4**, 69–77. [5.1.9.4]
- Chamkha, A. J., Issa, C. and Khanafer, K. 2002 Natural convection from an inclined plate embedded in a variable porosity porous medium due to solar radiation. *Int. J. Therm. Sci.* **41**, 73–78. [5.3]
- Chamkha, A. J., Jaradat, M. and Pop, I. 2004 Thermophoresis free convection flow from a vertical cylinder embedded in a porous medium. *Int. J. Appl. Mech. Engng.* **9**, 471–481. [5.7]
- Chamkha, A. J., Khaled, A. R. A. and Al-Hawaj, O. 2000 Simultaneous heat and mass transfer by natural convection from a cone and a wedge in porous media. *J. Porous Media* **3**, 155–164. [9.2.1]
- Chamkha, A. J., Mansour, M. A. and Ahmed, S. E. 2010d Double-diffusive natural convection in inclined finned triangular porous enclosures in the presence of heat generation/absorption. *Heat Mass Transfer* **46**, 757–768. [9.4]
- Chamkha, A., Gorla, R. S. R. and Ghodeswar, K. 2011 Non-similar solution for natural convective boundary layer flow over a sphere embedded in a porous medium saturated with a nanofluid. *Transp. Porous Media* **86**, 13–22. [5.6.1]
- Chan, B. K. C., Ivey, C. M. and Barry, J. M. 1970 Natural convection in enclosed porous media with rectangular boundaries. *ASME J. Heat Transfer* **92**, 21–27. [7.6.2, 7.8]
- Chan, Y. T. and Banerjee, S. 1981 Analysis of transient three-dimensional natural convection in porous media. *ASME J. Heat Transfer* **103**, 242–248. [6.9.2]
- Chand, R. and Rana, G. C. 2012 On the onset of thermal convection in rotating nanofluid layer saturating a Darcy-Brinkman porous medium. *Int. J. Heat Mass Transfer* **55**, 5417–5424 [9.7]
- Chandesris, M. and Jamet, D. 2006 Boundary conditions at a planar fluid-porous interface for a Poiseille flow. *Int. J. Heat Mass Transfer* **49**, 2137–2150. [1.6]
- Chandesris, M. and Jamet, D. 2007 Boundary conditions at a fluid-porous interface: An a priori estimation of the stress jump boundary conditions. *Int. J. Heat Mass Transfer* **50**, 3422–3436. [1.6]
- Chandesris, M. and Jamet, D. 2009a Derivation of jump conditions for the turbulence  $k$ - $\varepsilon$  model at a fluid/porous interface. *Int. J. Heat Mass Transfer* **50**, 2137–2150. [1.6]

- Chandris, M. and Jamet, D. 2009b Jump conditions and surface-excess quantities at a fluid/porous interface: A multiple scale approach. *Transp. Porous Media* **78**, 419–428. [1.6]
- Chandris, M. and Jamet, D. 2009c Derivation of jump conditions for the turbulence  $k$ - $\epsilon$  model at a fluid/porous interface. *Int. J. Heat Fluid Flow* **30**, 306–318. [1.6]
- Chandris, M., Serre, G. and Sagaut, T. 2006 A macroscopic turbulence model for flow in porous media suited for channel, pipe and rod bundle flows. *Int. J. Heat Mass Transfer* **49**, 2739–2750. [1.8]
- Chandra, P. and Satyamurty, V. V. 2012 Effect of anisotropy on natural convective flow through a rectangular porous slab. *J. Porous Media* **15**, 595–605. [7.1.7]
- Chandrasekhara, B. C. 1985 Mixed convection in the presence of horizontal impermeable surfaces in saturated porous media with variable permeability. *Wärme-Stoffübertrag.* **19**, 195–201. [8.1.2]
- Chandrasekhara, B. C. and Nagaraju, P. 1988 Composite heat transfer in the case of a steady laminar flow of a gray fluid with small optical density past a horizontal plate embedded in a saturated porous medium. *Wärme-Stoffübertrag.* **23**, 343–352. [8.1.2]
- Chandrasekhara, B. C. and Nagaraju, P. 1993 Composite heat transfer in a variable porosity medium bounded by an infinite flat plate. *Wärme-Stoffübertrag.* **28**, 449–456. [5.1.9.9]
- Chandrasekhara, B. C. and Namboodiri, P. M. S. 1985 Influence of variable permeability on combined free and forced convection about inclined surfaces in porous media. *Int. J. Heat Mass Transfer* **28**, 199–206. [8.1.1]
- Chandrasekhara, B. C., Radha, N. and Kumari, M. 1992 The effect of surface mass transfer on buoyancy induced flow in a variable porosity medium adjacent to a vertical heated plate. *Wärme-Stoffübertrag.* **27**, 157–166. [5.1.9.9]
- Chang, I. D. and Cheng, P. 1983 Matched asymptotic expansions for free convection about an impermeable horizontal surface in a porous medium. *Int. J. Heat Mass Transfer* **26**, 163–173. [5.1.6]
- Chang, M. H. 2004 Stability of convection induced by selective absorption of radiation in a fluid overlying a porous layer. *Phys. Fluids* **16**, 3690–3698. [6.19.1]
- Chang, M. H. 2005 Thermal convection in superposed and porous layers subjected to a horizontal plane Couette flow. *Phys. Fluids* **17**, Art. no. 064016. [6.19.3]
- Chang, M. H. 2006 Thermal convection in superposed fluid and porous layers subjected to a plane Poiseuille flow. *Phys. Fluids* **18**, art. # 035104. [6.19.3]
- Chang, M. H., Chen, F. and Straughan, B. 2006 Instability of Poiseuille flow in a fluid overlying a porous layer. *J. Fluid Mech.* **564**, 287–303. [6.19.3]
- Chang, P. Y., Shiah, S. W. and Fu, M. N. 2004 Mixed convection in a horizontal square packed-sphere channel under uniform heating peripherally uniform wall temperature. *Numer. Heat Transfer A* **45**, 791–809. [6.19.3]
- Chang, W. J. and Chang, W. L. 1995 Mixed convection in a vertical tube partially filled with porous medium. *Numer. Heat Transfer A* **28**, 739–754. [8.3.3]
- Chang, W. J. and Chang, W. L. 1996 Mixed convection in a vertical parallel-plate channel partially filled with porous media of high permeability. *Int. J. Heat Mass Transfer* **39**, 1331–1342. [8.3.1].
- Chang, W. J. and Hsiao, C. F. 1993 Natural convection in a vertical cylinder filled with anisotropic porous media. *Int. J. Heat Mass Transfer* **36**, 3361–3367. [7.3.3]
- Chang, W. J. and Jang, J. Y. 1989a Non-Darcian effects on vortex instability of a horizontal natural convection flow in a porous medium. *Int. J. Heat Mass Transfer* **32**, 529–539. [5.4]
- Chang, W. J. and Jang, J. Y. 1989b Inertia effects on vortex instability of a horizontal natural convection flow in a saturated porous medium. *Int. J. Heat Mass Transfer* **32**, 541–550. [5.4]
- Chang, W. J. and Lin, H. C. 1994a Wall heat conduction effect on natural convection in an enclosure filled with a non-Darcian porous medium. *Numer. Heat Transfer A* **25**, 671–684. [7.1.5]
- Chang, W. J. and Lin, H. C. 1994b Natural convection in a finite wall rectangular cavity filled with an anisotropic porous medium. *Int. J. Heat Mass Transfer* **37**, 303–312. [7.3.2]
- Chang, W. J. and Wang, C. I. 2002 Heat and mass transfer in porous material. In *Transport Phenomena in Porous Media II* (D. B. Ingham and I. Pop, eds.) Elsevier, Oxford, pp. 257–275. [3.6]

- Chang, W. J. and Yang, D. F. 1995 Transient natural convection of water near its density extremum in a rectangular cavity filled with porous medium. *Numer. Heat Transfer A* **28**, 619–633. [6.20]
- Chang, W. J. and Yang, D. F. 1996 Natural convection for the melting of ice in porous media in a rectangular enclosure. *Int. J. Heat Mass Transfer* **39**, 2333–2348. [10.1.7]
- Chao, B. H., Wang, H. and Cheng, P. 1996 Stagnation point flow of a chemical reactive fluid in a catalytic porous bed. *Int. J. Heat Mass Transfer* **39**, 3003–3019. [3.4]
- Char, M. I., Lin, J. D. and Chen, H. T. 2001 Conjugate mixed convection laminar non-Darcy film condensation along a vertical plate in a porous medium. *Int. J. Engng. Sci.* **39**, 897–912. [10.4]
- Char, M. I. and Lee, G. C. 1998 Maximum density effects on natural convection in a vertical annulus filled with a non-Darcy porous medium. *Acta Mech.* **128**, 217–231. [8.3.3]
- Char, M. I. and Lin, J. D. 2001 Conjugate film condensation and natural convection between two porous media separated by a vertical plate. *Acta Mech.* **148**, 1–15. [10.4]
- Charrier-Mojtabi, M. C. 1997 Numerical simulation of two-and three-dimensional free convective flows in a horizontal porous annulus using a pressure and temperature formulation. *Int. J. Heat Mass Transfer* **40**, 1521–1533. [7.3.3]
- Charrier-Mojtabi, M. C. and Mojtabi, A. 1994 Numerical simulation of three-dimensional free convection in a horizontal porous annulus. *Heat Transfer 1994*, Inst. Chem. Engrs, Rugby, pp. 319–324. [7.3.3]
- Charrier-Mojtabi, M. C. and Mojtabi, A. K. 1998 Natural convection in a horizontal porous annulus. *Transport Phenomena in Porous Media* (eds. D. B. Ingham and I. Pop), Elsevier, Oxford, pp. 155–178. [7.3.3]
- Charrier-Mojtabi, M. C., Elhajjah, B. and Mohtabi, A. 2007 Analytical and numerical stability analysis of Soret-driven convection in a horizontal porous layer. *Phys. Fluids* **19**, #124104. [9.1.4]
- Charrier-Mojtabi, M. C., Elhajjah, B., Ouattara, B., Mojtabi, A. and Costeseque, P. 2011 Soret-driven convection and separation of binary mixtures in a porous horizontal slot submitted to a heat flux. *C. R. Mecanique* **339**, 303–309. [9.1.4].
- Charrier-Mojtabi, M. C., Karimi-Fard, M. and Mojtabi, A. 1997 Onset of thermosolutal convective regimes in rectangular porous cavity. *C. R. Acad. Sci. II B* **324**, 9–17. [9.2.2]
- Charrier-Mojtabi, M. C., Karimi-Fard, M., Azaiez, M. and Mojtabi, A. 1998 Onset of a double-diffusive convective regime in a rectangular porous cavity. *J. Porous Media* **1**, 107–121. [9.2.2]
- Charrier-Mojtabi, M. C., Maliwan, K., Pedram Razi, Y., Bardan, G. and Mojtabi, A. 2003 Contrôle des écoulements thermoconvectifs au moyen de vibration. *J. Méc. Ind.* **4**, 545–549. [6.24]
- Charrier-Mojtabi, M. C., Mojtabi, A., Azaiez, M. and Labrosse, G. 1991 Numerical and experimental study of multicellular free convection flows in an annular porous pipe. *Int. J. Heat Mass Transfer* **34**, 3061–3074. [6.16.3]
- Charrier-Mojtabi, M. C., Pedram Razi, Y. P., Maliwan, K. and Mojtabi, A. 2004 Influence of vibration on Soret-driven convection in porous media. *Numer. Heat Transfer* **46**, 981–993. [9.1.6.4]
- Charrier-Mojtabi, M. C., Pedram Razi, Y., Maliwan, K. and Mojtabi, A. 2005 Effect of vibration on the onset of double-diffusive convection in porous media. In *Transport Phenomena in Porous Media III*, (eds. D. B. Ingham and I. Pop), Elsevier, Oxford, pp. 261–286. [9.1.6.4]
- Charrier-Mojtabi, M. C., Pedram Razi, Y., Maliwan, K. and Mojtabi, A. 2006 The influence of mechanical vibration on convective motion in a confined porous cavity with emphasis on harmonic and sub-harmonic responses. Proc. 13th Int. Heat Transfer Conf., Sydney, Australia (CD Rom). [6.24].
- Chaudary, R. C. and Sharma, P. K. 2003 Three dimensional unsteady convection and mass transfer flow through porous medium. *Heat Mass Transfer* **39**, 765–770. [5.1.9.7]
- Chaudhary, M. A., Merkin, J. H. and Pop, I. 1995a Similarity solutions in free-convection boundary-layer flows adjacent to vertical permeable surfaces in porous media. 1. Prescribed surface temperature. *Europ. J. Mech. B.* **14**, 217–237. [5.1.2]

- Chaudhary, M. A., Merkin, J. H. and Pop, I. 1996 Natural convection from a horizontal permeable surface in a porous medium—numerical and asymptotic solutions. *Transport in Porous Media* **22**, 327–344. [5.2]
- Chaudhary, M. A., Merkin, J. H. and Pop, I. 1995b Similarity solutions in free convection boundary-layer flows adjacent to vertical permeable surfaces in porous media: II prescribed surface heat flux. *Heat Mass Transfer* **30**, 341–347. [5.1.2]
- Chaudhary, R. C. and Jain, A. 2007a Combined heat and mass transfer effects on MHD free convection flow past an oscillating plate embedded in a porous medium. *Roman. J. Phys.* **52**, 505–524. [9.2.1]
- Chaudhary, R. C. and Jain, P. 2007b Combined heat and mass transfer in magneto-micropolar fluid flow with radiate surface with variable permeability in slip-flow regime. *ZAMM* **87**, 549–563. [9.2.1]
- Chaudhary, R. C. and Jain, P. 2010 An exact solution of magnetohydrodynamic convection flow past an accelerated surface embedded in a porous medium. *Int. J. Heat Mass Transfer* **53**, 1609–1611. [5.1.9.9]
- Chaves, C. A., Camargo, J. R., Cardoso, S. and de Macedo, A. G. 2005 Transient natural convection heat transfer by double-diffusion from a heated cylinder buried in a saturated porous medium. *Int. J. Therm. Sci.* **44**, 720–725. [9.4]
- Chelghoum, D. E., Weidman, P. D. and Kassoy, D. R. 1987 Effect of slab width on the stability of natural convection in confined saturated porous media. *Phys. Fluids* **30**, 1941–1947. [6.15.1]
- Chellaiah, S. and Viskanta, R. 1987 Freezing of water and water-salt solutions around aluminum spheres. *Int. Comm. Heat Mass Transfer* **14**, 437–446. [10.2.1.2]
- Chellaiah, S. and Viskanta, R. 1989a On the supercooling during freezing of water saturated porous media. *Int. Comm. Heat Mass Transfer* **16**, 163–172. [10.2.1.2]
- Chellaiah, S. and Viskanta, R. 1989b Freezing of water-saturated porous media in the presence of natural convection: experiments and analysis. *ASME J. Heat Transfer* **111**, 424–432. errata 648. [10.2.1.2]
- Chellaiah, S. and Viskanta, R. 1990a Natural convection melting of a frozen porous medium. *Int. J. Heat Mass Transfer* **33**, 887–899. [10.2.1.2]
- Chellaiah, S. and Viskanta, R. 1990b Melting of ice-aluminum ball systems. *Expt. Therm. Fluid Sci.* **3**, 222–231. [10.1.7]
- Chen, B., Wang, B. and Fang, Z. 1999 Electrochemical experimental method for natural convective heat and mass transfer in porous media. *Heat Transfer Asian Res.* **28**, 266–277. [9.2.2]
- Chen, C., and Zhang, D. X. 2010 Pore-scale simulation of density-driven convection in fractured porous media during geological CO<sub>2</sub> sequestration. *WaterResources. Res.* **46**, #W11527. [11.7]
- Chen, C. F. 1995 Experimental study of convection in a mushy layer during directional solidification. *J. Fluid Mech.* **293**, 81–98. [10.2.3]
- Chen, C. H. 1996 Non-Darcy mixed convection from a horizontal surface with variable surface heat flux in a porous medium. *Num. Heat Transfer A* **30**, 859–869. [8.1.2]
- Chen, C. H. 1997a Non-Darcy mixed convection over a vertical flat plate in porous media with variable wall heat flux. *Int. Comm. Heat Mass Transfer* **24**, 427–437. [8.1.1]
- Chen, C. H. 1997b Analysis of non-Darcian mixed convection along a vertical plate embedded in a porous medium. *Int. J. Heat Mass Transfer* **40**, 2993–2997. [8.1.2]
- Chen, C. H. 1998a Mixed convection heat transfer from a horizontal plate with variable surface heat flux in a porous medium. *Heat Mass Transfer* **34**, 1–7. [8.1.2]
- Chen, C. H. 1998b Nonsimilar solutions for non-Darcy mixed convection from a non-isothermal horizontal surface in a porous medium. *Int. J. Engng. Sci.* **36**, 251–263. [8.1.2]
- Chen, C. H. and Chen, C. K. 1990a Non-Darcian mixed convection along a vertical plate embedded in a porous medium. *Appl. Math. Modelling* **14**, 482–488. [8.1.1]
- Chen, C. H. and Chiou, J. S. 1994 Conjugate free convection heat transfer analysis of a vertical plate fin embedded in non-Darcian porous media. *Int. J. Engng. Sci.* **32**, 1703–1716. [5.12.1]

- Chen, C. H. and Horng, J. H. 1999 Natural convection from a vertical cylinder in a thermally stratified porous medium. *Heat Mass Transfer* **34**, 423–428. [5.7]
- Chen, C. H., Chen, T. S. and Chen, C. K. 1996 Non-Darcy mixed convection along nonisothermal vertical surfaces in porous media. *Int. J. Heat Mass Transfer* **39**, 1157–1164. [8.1.1]
- Chen, C. K. and Chen, C. H. 1990b Nonuniform porosity and non-Darcian effects on conjugate mixed convection heat transfer from a plate fin in porous media. *Int. J. Heat Fluid Flow* **11**, 65–71. [8.1.4]
- Chen, C. K. and Chen, C. H. 1991 Non-Darcian effects on conjugate mixed convection about a vertical circular pin in a porous medium. *Comput. Struct.* **38**, 529–535. [8.1.3]
- Chen, C. K. and Lin, C. R. 1995 Natural convection from an isothermal vertical surface embedded in a thermally stratified high-porosity medium. *Int. J. Engng Sci.* **33**, 131–138. [5.1.4]
- Chen, C. K., Chen, C. H., Minkowycz, W. J. and Gill, U. S. 1992 Non-Darcian effects on mixed convection about a vertical cylinder embedded in a saturated porous medium. *Int. J. Heat Mass Transfer* **35**, 3041–3046. [8.1.3]
- Chen, C. K., Hsiao, S. W. and Cheng, P. 1990 Transient natural convection in an eccentric porous annulus between horizontal cylinders. *Numer. Heat Transfer A* **17**, 431–448. [7.3.3]
- Chen, C. K., Hung, C. I. and Horng, H. C. 1987 Transient natural convection on a vertical flat plate embedded in a high-porosity medium. *ASME J. Energy Res. Tech.* **109**, 112–118. [5.1.3]
- Chen, F. 1990 On the stability of salt-finger convection in superposed fluid and porous layers. *ASME J. Heat Transfer* **112**, 1088–1092. [9.4]
- Chen, F. 1991 Throughflow effects on convective instability in superposed fluid and porous layers. *J. Fluid Mech.* **231**, 113–133. [6.19.1.2]
- Chen, F. 1992 Salt-finger instability in an anisotropic and inhomogeneous porous substrate underlying a fluid layer. *J. Appl. Phys.* **71**, 5222–5236. [9.1.6.2]
- Chen, F. and Chen, C. F. 1988c Onset of finger convection in a horizontal porous layer underlying a fluid layer. *ASME J. Heat Transfer* **110**, 403–409. [6.19.1.1, 6.19.1.2, 9.4]
- Chen, F. and Chen, C. F. 1989 Experimental investigation of convective stability in a superposed fluid and porous layer when heated from below. *J. Fluid Mech.* **207**, 311–321. [6.19.1.1, 6.19.1.2]
- Chen, F. and Chen, C. F. 1992 Convection in superposed fluid and porous layers. *J. Fluid Mech.* **234**, 97–119. [1.6, 6.19.1.2]
- Chen, F. and Chen, C. F. 1993 Double-diffusive fingering convection in a porous medium. *Int. J. Heat Mass Transfer* **36**, 793–807. [9.1.6.3]
- Chen, F. and Chen, C. F. 1996 Analysis of heat transfer regulation and modification using intermittently emplaced porous cavities — Analysis of flow and heat transfer over an external boundary covered with a porous substrate. *ASME J. Heat Transfer* **118**, 266–267. [5.1.9.5]
- Chen, F. and Hsu, L. H. 1991 Onset of thermal convection in an anisotropic and inhomogeneous porous layer underlying a fluid layer. *J. Appl. Phys.* **69**, 6289–6301. [6.19.1.2]
- Chen, F. and Lu, J. W. 1991 Influence of viscosity variation on salt-finger instability in a fluid layer, a porous layer, and their superposition. *J. Appl. Phys.* **70**, 4121–4131. [9.4]
- Chen, F. and Lu, J. W. 1992a Variable viscosity effects on convective instability in superposed fluid and porous layers. *Phys. Fluids* **4**, 1936–1944. [6.19.1.2]
- Chen, F. and Lu, J. W. 1992b Onset of salt-finger convection in anisotropic and inhomogeneous porous media. *Int. J. Heat Mass Transfer* **35**, 3451–3464. [6.19.1.2, 9.1.6.2]
- Chen, F. and Wang, C. Y. 1993 Convective instability in a porous enclosure with a horizontal conducting baffle. *ASME J. Heat Transfer* **115**, 810–813. [7.3.7]
- Chen, F. and Wang, C. Y. 1993 Convective instability in saturated porous enclosures with a vertical insulating baffle. *Int. J. Heat Mass Transfer* **36**, 1897–1904. [7.3.7]
- Chen, F., Chen, C. F. and Pearlstein, A. J. 1991 Convective instability in superposed fluid and anisotropic porous layers. *Phys. Fluids A* **3**, 556–565. [6.19.1.2]
- Chen, F., Lu, J. W. and Yang, T. L. 1994 Convective instability in ammonium chloride solution directionally solidified from below. *J. Fluid Mech.* **276**, 163–187. [10.2.3]

- Chen, G. and Hadim, H. A. 1995 Numerical study of forced convection of a power-law fluid in a porous channel. *ASME HTD – 309*, 65–72. [4.16.3]
- Chen, G. and Hadim, H. A. 1998a Forced convection of a power-law fluid in a porous channel—numerical solutions. *Heat Mass Transfer* **34**, 221–228. [4.16.3]
- Chen, G. and Hadim, H. A. 1998b Numerical study of non-Darcy forced convection in a packed bed saturated with a power-law fluid. *J. Porous Media* **1**, 147–157. [4.16.3]
- Chen, G. and Hadim, H. A. 1999a Forced convection of a power-law fluid in a porous channel—integral solutions. *J. Porous Media* **2**, 59–69. [4.16.3]
- Chen, G. and Hadim, H. A. 1999b Numerical study of three dimensional non-Darcy forced convection in a square porous duct. *Int. J. Numer. Meth. Heat Fluid Flow* **9**, 151–169. [4.9]
- Chen, G. M. and Tsao, C. P. 2011a Effects of viscous dissipation on forced convection heat transfer in a channel embedded in a power-law fluid saturated porous medium. *Int. Comm. Heat Mass Transfer* **38**, 57–62. [4.16.3]
- Chen, G. M. and Tsao, C. P. 2011b Forced convection with viscous dissipation using a two-equation model in a channel filled with a porous medium. *Int. J. Heat Mass Transfer* **54**, 1791–1804. [4.10]
- Chen, G. M. and Tsao, C. P. 2011c A two-equation model for thermally developing forced convection in porous medium with viscous dissipation. *Int. J. Heat Mass Transfer* **54**, 5406–5414. [4.13]
- Chen, G. M. and Tsao, C. P. 2012a A thermal resistance analysis on forced convection with viscous dissipation in a porous medium using entransy dissipation concept. *Int. J. Heat Mass Transfer* **55**, 3744–3754. [4.10]
- Chen, G. M. and Tsao, C. P. 2012b Field synergy principle analysis on convective heat transfer in porous medium with uniform heat generation for thermally developing flow. *Int. J. Heat Mass Transfer* **55**, 4139–4147. [4.13]
- Chen, H. T. and Chen, C. K. 1987 Natural convection of non-Newtonian fluids about a horizontal surface in a porous medium. *ASME J. Energy Res. Tech.* **109**, 119–123. [5.2]
- Chen, H. T. and Chen, C. K. 1988a Free convection flows of non-Newtonian fluids along a vertical plate embedded in a porous medium. *ASME J. Heat Transfer* **110**, 257–259. [5.1.9.2]
- Chen, H. T. and Chen, C. K. 1988b Natural convection of a non-Newtonian fluid about a horizontal cylinder and a sphere in a porous medium. *Int. Comm. Heat Mass Transfer* **15**, 605–614. [5.5.1, 5.6.1].
- Chen, H., Besant, R. W. and Tao, Y. X. 1998a Numerical modeling of heat transfer and water vapor transfer and frosting within a fiberglass filled cavity during air infiltration. *Heat Transfer 1998, Proc. 11th IHTC*, **4**, 381–386. [3.6]
- Chen, K. S. and Ho, J. R. 1986 Effects of flow inertia on vertical natural convection in saturated porous media. *Int. J. Heat Mass Transfer* **29**, 753–759. [5.1.7.2]
- Chen, L., Li, Y. and Thorpe, G. 1998b High Rayleigh-number natural convection in an enclosure containing a porous layer. *Heat Transfer 1998, Proc. 11th IHTC*, **4**, 423–428. [1.8, 7.7]
- Chen, Q. S., Prasad, V. and Chatterjee, A. 1999b Modeling of fluid flow and heat transfer in a hydrothermal crystal growth system: use of fluid-superposed porous layer theory. *ASME J. Heat Transfer* **121**, 1049–1058. [6.19.2]
- Chen, S. C. and Vafai, K. 1996 Analysis of free surface momentum and energy transport in porous media *Numer. Heat Transfer* **29**, 281–296. [2.2.3]
- Chen, X. B., Yu, P., Winoto, S. H. and Low, H. T. 2008a A numerical method for forced convection in porous and heterogeneous fluid domains coupled at interface by stress jump. *Int. J. Numer. Meth. Fluid Flow* **18**, 635–655. [1.6]
- Chen, X. B., Yu, P., Winoto, S. H. and Low, H. T. 2008c Free convection in a porous wavy cavity based on the Darcy-Brinkman-Forchheimer extended model. *Numer. Heat Transfer A* **52**, 377–397. [7.3.7]
- Chen, X. B., Yu, P., Winoto, S. H. and Low, H. T. 2008d Numerical analysis for the flow past a porous square cylinder based on the stress-jump interfacial conditions. *Int. J. Numer. Meth. Fluids* **56**, 1705–1729. [4.11]

- Chen, X. B., Yu, P., Winoto, S. H. and Low, H. T. 2009a Natural convection in a cavity filled with porous layers on the top and bottom walls. *Transp. Porous Media* **78**, 259–276. [6.19.3]
- Chen, X. L. and Sutton, W. H. 2005 Enhancement of heat transfer: Combined convection and radiation in the entry region of circular ducts with porous inserts. *Int. J. Heat Mass Transfer* **48**, 5460–5474. [4.11]
- Chen, X., Wang, S. W., Tao, J. J. and Tan, W. C. 2011 Stability analysis of thermosolutal convection in a horizontal porous layer using a thermal non-equilibrium model. *Int. J. Heat Fluid Flow* **32**, 78–87. [9.1.6.4]
- Chen, Y. C. 2004 Non-Darcy flow stability of mixed convection in a vertical channel filled with a porous medium. *Int. J. Heat Mass Transfer* **47**, 1257–1266. [8.3.1]
- Chen, Y. C. and Chung, J. N. 1998 Stability of shear flow in a vertical heated channel filled with a porous medium. *Heat Transfer 1998, Proc. 11th IHTC*, **4**, 435–440. [8.3.1]
- Chen, Y. C., Chung, J. N., Wu, C. S. and Lue, Y. F. 2000a Non-Darcy mixed convection in a vertical channel filled with a porous medium. *Int. J. Heat Mass Transfer* **43**, 2421–2429. [8.3.1]
- Chen, Y. H. and Lin, H. T. 1997 Natural convection in an inclined enclosure with a fluid layer and a heat-generating porous bed. *Heat Mass Transfer* **33**, 247–255. [7.8]
- Chen, Z. Q., Cheng, P. and Hsu, C. T. 2000b A theoretical and experimental study on stagnant thermal conductivity of bi-dispersed porous media. *Int. Comm. Heat Mass Transfer* **27**, 601–610. [4.16.4]
- Chen, Z., Lyons, S. L. and Qin, G. 2001 Derivation of the Forchheimer equation via homogenization. *Transport Porous Media* **44**, 325–335. [1.5.2]
- Cheng, C. Y. 1999 Effect of a magnetic field on heat and mass transfer by natural convection from vertical surfaces in porous media – an integral approach. *Int. Comm. Heat Mass Transfer* **26**, 935–943. [9.2.1]
- Cheng, C. Y. 2000a An integral approach for heat and mass transfer by natural convection from truncated cones in porous media with variable wall temperature and concentration. *Int. Comm. Heat Mass Transfer* **27**, 537–548. [9.2.1]
- Cheng, C. Y. 2000b Transient heat and mass transfer by natural convection from vertical surfaces in porous media. *J. Phys. D* **33**, 1425–1430. [9.2.3]
- Cheng, C. Y. 2000c Natural convection heat and mass transfer near a wavy cone with constant wall temperature and concentration in a porous medium. *Mech. Res. Comm.* **27**, 613–620. [9.2.1]
- Cheng, C. Y. 2000d Natural convection heat and mass transfer near a vertical wavy surface with constant wall temperature and concentration in a porous medium. *Int. Comm. Heat Mass Transfer* **27**, 1143–1154. [9.2.1]
- Cheng, C. Y. 2005 An integral approach for hydromagnetic natural convection heat and mass transfer form vertical surfaces with power-law variation in wall temperature and concentration in porous media. *Int. Comm. Heat Mass Transfer* **32**, 204–213. [9.2.1]
- Cheng, C. Y. 2006a Fully developed natural convection heat and mass transfer in a vertical annular porous medium with asymmetric wall temperatures and concentrations. *Appl. Thermal Engng.* **26**, 2442–2447. [9.2.2]
- Cheng, C. Y. 2006b Natural convection heat and mass transfer from a horizontal cylinder of elliptic cross section with constant wall temperature and concentration in saturated porous media. *J. Mech.* **22**, 257–261. [5.5.1]
- Cheng, C. Y. 2006c Natural convection heat and mass transfer of non-Newtonian power law fluids with yield stress in porous media from a vertical plate with variable heat flux and mass fluxes. *Int. Comm. Heat Mass Transfer* **33**, 1156–1164. [9.2.1]
- Cheng, C. Y. 2007a Double diffusion from a vertical wavy surface in a porous medium saturated with a non-Newtonian fluid. *Int. Comm. Heat Mass Transfer* **34**, 285–294. [9.2.1]
- Cheng, C. Y. 2007b A boundary layer analysis of heat transfer by free convection from permeable horizontal cylinders of elliptic cross-section in porous media using a thermal non-equilibrium model. *Int. Comm. Heat Mass Transfer* **34**, 613–622. [5.5.1]
- Cheng, C. Y. 2007c Nonsimilar solutions for double diffusive convection near a frustum of a wavy cone in porous media. *Appl. Math. Comput.* **194**, 156–167. [9.2.1]

- Cheng, C. Y. 2008 Double-diffusive natural convection along a vertical wavy truncated cone in non-Newtonian fluid saturated porous media with thermal and mass stratification. *Int. Comm. Heat Mass Transfer* **33**, 985–990. [9.2.1]
- Cheng, C. Y. 2009a Combined heat and mass transfer in natural convection flow from a vertical wavy surface in a power-law fluid saturated porous medium with thermal and mass stratification. *Int. Comm. Heat Mass Transfer* **36**, 351–356. [9.2.1]
- Cheng, C. Y. 2009b Natural convection heat and mass transfer from a vertical truncated cone in a porous medium saturated with a non-Newtonian fluid with variable wall temperature and concentration. *Int. Comm. Heat Mass Transfer* **36**, 585–589. [9.2.1]
- Cheng, C. Y. 2009c Natural convection heat transfer of non-Newtonian fluids in porous media from a vertical cone under mixed thermal boundary conditions. *Int. Comm. Heat Mass Transfer* **36**, 693–697. [9.2.1]
- Cheng, C. Y. 2009d Soret and Dufour effects on natural convection heat and mass transfer from a vertical cone in a porous medium. *Int. Comm. Heat Mass Transfer* **36**, 1020–1024. [9.2.1]]
- Cheng, C. Y. 2009e Nonsimilar boundary layer analysis of double-diffusive convection from a vertical truncated cone in a porous medium with variable viscosity. *Appl. Math. Comput.* **212**, 185–19. [9.2.1]]
- Cheng, C. Y. 2009f Soret and Dufour effects on natural convection heat and mass transfer from a vertical cone in a porous medium. *Int. Comm. Heat Mass Transfer* **36**, 1020–1024. [9.2.1]
- Cheng, C. Y. 2010a Double diffusion from a vertical truncated cone in a non-Newtonian fluid saturated porous medium with variable heat and mass fluxes. *Int. Comm. Heat Mass Transfer* **37**, 261–265. [9.2.1]
- Cheng, C. Y. 2010b Double diffusive natural convection along an inclined wavy surface in a porous medium *Int. Comm. Heat Mass Transfer* **37**, 1471–1476. [9.2.1]]
- Cheng, C. Y. 2010c Soret and Dufour effects on free convection boundary layer over a vertical cylinder in a saturated porous medium *Int. Comm. Heat Mass Transfer* **37**, 796–800. [9.2.1]
- Cheng, C. Y. 2010d Soret and Dufour effects on heat and mass transfer by natural convection boundary layer flow over a vertical cone in a porous medium with variable wall temperature and concentration. *Int. Comm. Heat Mass Transfer* **37**, 1031–1035. [9.2.1]]
- Cheng, C. Y. 2011a Soret and Dufour effects on heat and mass transfer on natural convection boundary layer flow over a vertical cone in a porous medium with constant wall heat and mass fluxes *Int. Comm. Heat Mass Transfer* **38**, 44–48. [9.2.1]
- Cheng, C. Y. 2011b Soret and Dufour effects on free convection boundary layers of non-Newtonian power law fluids with yield stress in porous media over a vertical plate with variable wall and heat fluxes. *Int. Comm. Heat Mass Transfer* **38**, 615–619. [92.1].
- Cheng, C. Y. 2012a Soret and Dufour effects on double-diffusive free convection over a vertical truncated cone in porous media with variable wall heat flux and mass fluxes. *Transp. Porous Media* **91**, 877–888. [9.4]
- Cheng, C. Y. 2012b Soret and Dufour effects on mixed convection heat and mass transfer from a vertical wedge in a porous medium with constant wall temperature and concentration. *Transp. Porous Media* **94**, 123–132. [9.6.1]
- Cheng, C. Y. 2012c Free convection boundary layer flow over a horizontal cylinder of elliptic cross section in porous media saturated by a nanofluid. *Int. Comm. Heat Mass Transfer* **39**, 931–936. [5.5.1]
- Cheng, C. Y. 2012d Free convection of non-Newtonian nanofluids about a vertical truncated cone in a porous medium. *Int. Comm. Heat Mass Transfer* **39**, 1354–1359. [9.7]
- Cheng, G. J., Yu, A. B. and Zulli, P. 1999 Evaluation of effective thermal conductivity from the structure of a packed bed. *Chem. Eng.Sci.* **54**, 4199–4209. [2.2.1]
- Cheng, J., Liao, S. J. and Pop, I. 2005 Analytic series solution for unsteady mixed convection boundary layer flow near the stagnation point on a vertical surface in a porous medium. *Transport Porous Media* **61**, 365–379. [8.1.1]

- Cheng, L. P. and Kuznetsov, A. V. 2005 Heat transfer in a laminar flow in a helical pipe filled with a saturated porous medium. *Int. J. Thermal Sci.* **44**, 787–798. [4.5]
- Cheng, P. 1977a Constant surface heat flux solutions for porous layer flows. *Lett. Heat Mass Transfer* **4**, 119–128. [5.1.2]
- Cheng, P. 1977b The influence of lateral mass flux on free convection boundary layers in a saturated porous medium. *Int. J. Heat Mass Transfer* **20**, 201–206. [5.1.2]
- Cheng, P. 1977c Combined free and forced boundary layer flows about inclined surfaces in a porous medium. *Int. J. Heat Mass Transfer* **20**, 807–814. [4.1, 8.1.4]
- Cheng, P. 1977d Similarity solutions for mixed convection from horizontal impermeable surfaces in saturated porous media. *Int. J. Heat Mass Transfer* **20**, 893–898. [8.1.2]
- Cheng, P. 1978 Heat transfer in geothermal systems. *Adv. Heat Transfer* **14**, 1–105. [3.5, 6.9.1, 6.26, 11, 11.7]
- Cheng, P. 1981a Thermal dispersion effects in non-Darcian convective flows in a saturated porous medium. *Lett. Heat Mass Transfer* **8**, 267–270. [5.1.7.3, 5.1.8]
- Cheng, P. 1981b Film condensation along an inclined surface in a porous medium. *Int. J. Heat Mass Transfer* **24**, 983–990. [10.4]
- Cheng, P. 1982 Mixed convection about a horizontal cylinder and a sphere in a fluid saturated porous medium. *Int. J. Heat Mass Transfer* **25**, 1245–1247. [4.3, 8.1.3]
- Cheng, P. 1985a Natural convection in a porous medium: external flows. *Natural Convection: Fundamentals and Applications* (eds. S. Kakaç, W. Aung, and R. Viskanta), Hemisphere, Washington, DC, 475–513. [5, 5.1.7.3, 5.1.8, 5.3, 5.6.1, 5.10.1.2]
- Cheng, P. 1985b Geothermal heat transfer. *Handbook of Heat Transfer Applications* (eds. W. M. Rohsenow *et al.*), 2nd edition, McGraw-Hill, New York, Chapter 11. [11, 11.7]
- Cheng, P. 1987 Wall effects on fluid flow and heat transfer in porous media. *Proc. 1987 ASME JSME Thermal Engineering Joint Conf.* **2**, 297–303. [4.8]
- Cheng, P. and Ali, C. L. 1981 An experimental investigation of free convection about an inclined surface in a porous medium. *ASME 20th National Heat Transfer Conference*, Paper No. 81-HT-85. [5.3]
- Cheng, P. and Chang, I. D. 1976 On buoyancy induced flows in a saturated porous medium adjacent to impermeable horizontal surfaces. *Int. J. Heat Mass Transfer* **19**, 1267–1272. [5.2, 6.26]
- Cheng, P. and Chang, I. D. 1979 Convection in a porous medium as a singular perturbation problem. *Lett. Heat Mass Transfer* **6**, 253–258. [5.1.6]
- Cheng, P. and Chau, W. C. 1977 Similarity solutions for convection of groundwater adjacent to horizontal surface with axisymmetric temperature distribution. *Water Resour. Res.* **13**, 768–772. [5.2]
- Cheng, P. and Chui, D. K. 1984 Transient film condensation on a vertical surface in a porous medium. *Int. J. Heat Mass Transfer* **27**, 795–798. [10.4]
- Cheng, P. and Hsu, C. T. 1984 Higher-order approximations for Darcian free convective flow about a semi-infinite vertical flat plate. *ASME J. Heat Transfer* **106**, 143–151. [5.1.6]
- Cheng, P. and Hsu, C. T. 1986a Fully developed, forced convective flow through an annular packed-sphere bed with wall effects. *Int. J. Heat Mass Transfer* **29**, 1843–1853. [4.9]
- Cheng, P. and Hsu, C. T. 1986b Applications of Van Driest's mixing length theory to transverse thermal dispersion in forced convective flow through a packed bed. *Int. Comm. Heat Mass Transfer* **13**, 613–626. [4.9]
- Cheng, P. and Hsu, C. T. 1998 Heat conduction. *Transport Phenomena in Porous Media I* (eds. D. B. Ingam and I. Pop), Elsevier, Oxford, pp. 57–76. [2.2.1]
- Cheng, P. and Hsu, C. T. 1999 The effective stagnant thermal conductivity of porous media with periodic structure. *J. Porous Media*. **2**, 19–38. [2.2.1, 4.16.4]
- Cheng, P. and Minkowycz, W. J. 1977 Free convection about a vertical flat plate embedded in a porous medium with application to heat transfer from a dike. *J. Geophys. Res.* **82**, 2040–2044. [5.1.1, 10.1.5]

- Cheng, P. and Pop, I. 1984 Transient free convection about a vertical flat plate imbedded in a porous medium. *Int. J. Engng. Sci.* **22**, 253–264. [5.1.3]
- Cheng, P. and Teckchandani, L. 1977 Numerical solutions for transient heating and fluid withdrawal in a liquid-dominated geothermal reservoir. *The Earth's Crust* (ed. J. G. Heacock), Amer. Geophys. Union, Washington, DC, 705–721. [11.7]
- Cheng, P. and Verma, A. K. 1981 The effect of subcooled liquid on film boiling about a vertical heated surface in a porous medium. *Int. J. Heat Mass Transfer* **24**, 1151–1160. [10.3.2]
- Cheng, P. and Vortmeyer, D. 1988 Transverse thermal dispersion and wall channeling in a packed bed with forced convective flow. *Chem. Engng. Sci.* **43**, 2523–2532. [4.9]
- Cheng, P. and Wang, C. Y. 1996 Multiphase mixture model for multiphase, multicomponent transport in capillary porous media — II. Numerical simulation of the transport of organic compounds in the subsurface. *Int. J. Heat Mass Transfer* **39**, 3619–3632. [3.6.2]
- Cheng, P. and Zheng, T. M. 1986 Mixed convection in the thermal plume above a horizontal line source of heat in a porous medium of infinite extent. *Heat Transfer 1986*, Hemisphere, Washington, DC, **5**, 2671–2675. [8.1.4]
- Cheng, P. and Zhu, H. 1987 Effects of radial dispersion on fully-developed forced convection in cylindrical packed tubes. *Int. J. Heat Mass Transfer* **30**, 2373–2383. [4.9]
- Cheng, P., Ali, C. L. and Verma, A. K. 1981 An experimental study of non-Darcian effects in free convection in a saturated porous medium. *Lett. Heat Mass Transfer* **8**, 261–265. [5.1.8]
- Cheng, P., Chowdhury, A. and Hsu, C. T. 1991 Forced convection in packed tubes and channels with variable porosity and thermal dispersion effects. *Convective Heat and Mass Transfer in Porous Media*, (eds. S. Kakaç, et al.), Kluwer Academic, Dordrecht, 625–653. [1.7, 4.9]
- Cheng, P., Chui, D. K. and Kwok, L. P. 1982 Film boiling about two-dimensional and axisymmetric isothermal bodies of arbitrary shape in a porous medium. *Int. J. Heat Mass Transfer* **25**, 1247–1249. [10.3.2]
- Cheng, P., Hsu, C. T. and Chowdhury, A. 1988 Forced convection in the entrance region of a packed channel with asymmetric heating. *ASME J. Heat Transfer* **110**, 946–954. [4.9]
- Cheng, P., Le, T. T. and Pop, I. 1985 Natural convection of a Darcian fluid about a cone. *Int. Comm. Heat Mass Transfer* **12**, 705–717. [5.8]
- Cheng, W. T. and Lin, C. H. 2006 Transient mixed convective heat transfer with melting effect from the vertical plate in a liquid saturated porous medium. *Int. J. Engng. Sci.* **44**, 1023–1036. [10.1.7]
- Cheng, W. T. and Lin, C. H. 2007 Melting effect on mixed convective heat transfer with aiding and opposed external flows from a vertical plate in a liquid saturated porous medium. *Int. J. Heat Mass Transfer* **50**, 3026–3034. [10.1.7]
- Cheng, W. T. and Lin, C. H. 2009 Unsteady mass transfer in mixed convective flow from a vertical plate embedded in a liquid-saturated porous medium with melting effect. *Int. Comm. Heat Mass Transfer* **35**, 1350–1354. [10.1.7]
- Cheng, W. T. and Lin, H. T. 2002 Unsteady forced convection heat transfer on a flat plate embedded in the fluid-saturated porous medium with inertia effect and thermal dispersion. *Int. J. Heat Mass Transfer*, **45**, 1563–1569. [4.6.3]
- Cheng, W. T., Huang, E. N., Chuo, M. H. and Du, S. W. 2012 Transient natural convective heat transfer in porous medium with solidification of binary mixture. *Int. Comm. Heat Mass Transfer* **39**, 1132–1137. [10.2.3]
- Cherkaoui, A.S.M. and Wilcock, W.S.D. 1999 Characteristics of high Rayleigh number two-dimensional convection in an open-top porous layer heated from below. *J. Fluid Mech.* **394**, 241–260. [11.8]
- Cherkaoui, A.S.M. and Wilcock, W.S.D. 2001 Laboratory studies of high Rayleigh number circulation in an open-top Hele-Shaw cell: an analogue to mid-ocean ridge hydrothermal systems. *J. Geophys. Res.* **106**, 10983–11000. [11.8]
- Chevalier, S., Bernard, D. and Grenet, J. P. 1996 Étude expérimentale de la convection naturelle dans une couche poreuse inclinée limitée par des frontières conductrices de la chaleur. *C.R. Acad. Sci. Paris*, Sér. II, **322**, 305–311. [7.8]

- Chevalier, S., Bernard, D. and Joly, N. 1999 Natural convection in a porous layer bounded by impervious domains: from numerical approaches to experimental realization. *Int. J. Heat Mass Transfer* **42**, 581–597. [7.8]
- Chhuon, B. and Caltagirone, J. P. 1979 Stability of a horizontal porous layer with timewise periodic boundary conditions. *ASME J. Heat Transfer* **101**, 244–248. [6.11.3]
- Chiang, K. C. and Tsai, H. L. 1992 Interaction between shrinkage-induced fluid flow and natural convection during alloy solidification. *Int. J. Heat Mass Transfer*, **35**, 1771–1778. [10.2.3]
- Chiarelli, A. O. P. and Worster, M. G. 1995 Flow focusing instability in a solidifying mushy layer. *J. Fluid Mech.* **297**, 293–305. [10.2.3]
- Chiem, K. S. and Zhao, Y. 2004 Numerical study of steady/unsteady flow and heat transfer in porous media using a characteristics-based matrix-free implicit FV method on unstructured grids. *Int. J. Heat Fluid Flow* **25**, 1015–1033. [4.11]
- Chikh, S., Boumedien, A., Bouhadef, K. and Lauriat, G. 1998 Analysis of fluid flow and heat transfer in a channel with intermittent heated porous disks. *Heat Mass Transfer* **33**, 405–413. [4.11]
- Chikh, S., Boumedien, A., Bouhadef, K. and Lauriat, G. 1995a Analytical solution of non-Darcian forced convection in an annular duct partially filled with a porous medium. *Int. J. Heat Mass Transfer* **38**, 1543–1551. [4.12.1]
- Chikh, S., Boumedien, A., Bouhadef, K. and Lauriat, G. 1995b Non-Darcian forced convection analysis in an annulus partially filled with a porous material *Numer. Heat Transfer A* **28**, 707–722. [4.11]
- Chin, K. E., Nazar, R., Arifin, N. M. and Pop, I. 2007 Effect of variable viscosity on mixed convection boundary layer flow over a vertical surface embedded in a porous medium. *Int. Comm. Heat Mass Transfer* **34**, 464–473. [8.1.1]
- Cho, K. H., Lee, J., Ahn, H. S., Bejan, A. and Kim, M. H. 2010b Fluid flow and heat transfer in vascularized cooling plates. *Int. J. Heat Mass Transfer* **53**, 3607–3614. [4.19]
- Cho, K. H., Lee, J., Kim, M. H. and Bejan, A. 2010a Vascular design of constructal structures with low flow resistance and nonuniformity. *Int. J. Therm. Sci.* **49**, 2309–2318. [4.19]
- Choi, C. Y. and Kulacki, F. A. 1990 Non-Darcian effects on mixed convection in a vertical porous annulus. *Heat Transfer 1990*, Hemisphere, New York, **5**, 271–276. [8.3.4]
- Choi, C. Y. and Kulacki, F. A. 1992a Mixed convection in vertical porous channels and annuli. *Heat and Mass Transfer in Porous Media*, (ed. M. Quintard and M. Todorovic), Elsevier, Amsterdam, 61–98. [8.3]
- Choi, C. Y. and Kulacki, F. A. 1992b Mixed convection through vertical porous annuli locally heated from the inner cylinder. *ASME J. Heat Transfer* **114**, 143–151. [8.3.3]
- Choi, C. Y. and Kulacki, F. A. 1993 Non-Darcian effects on mixed convection in a vertical packed-sphere annulus. *ASME J. Heat Transfer* **115**, 506–510. [8.3.3]
- Choi, C. Y., Lai, F. C. and Kulacki, F. A. 1989 Mixed convection in vertical porous annuli. *AICHE Sympos. Ser.* **269**, 356–361. [8.3.4]
- Choi, E., Chamkha, A. and Nandakumar, K. 1998 A bifurcation study of natural convection in porous media with internal heat sources: the non-Darcy effects. *Int. J. Heat Mass Transfer* **41**, 383–392. [6.11.2]
- Choi, J. and Viskanta, R. 1992 Freezing of aqueous sodium chloride solution saturated packed bed from above. *ASME HTD* **206**, Vol. 2, 159–166. [10.2.3]
- Choi, J. and Viskanta, R. 1993 Freezing of aqueous sodium chloride solution saturated packed bed from a vertical wall of a rectangular cavity. *Int. J. Heat Mass Transfer* **36**, 2805–2813. [10.2.3]
- Chou, F. C. and Chung, P. Y. 1995 Effect of stagnant conductivity on non-Darcian mixed convection in horizontal square packed channels. *Numer. Heat Transfer A* **27**, 195–209. [8.2.1]
- Chou, F. C., Cheng, C. J. and Lien, W. Y. 1992a Analysis and experiment of non-Darcian convection in horizontal square packed-sphere channels. — 2. Mixed convection. *Int. J. Heat Mass Transfer* **35**, 1197–1207. [8.2.1]
- Chou, F. C., Chung, P. Y. and Cheng, C.J . 1992b Effects of stagnant and dispersion conductivities on non-Darcian forced convection in square packed-sphere channels. *Canad. J. Chem. Engng*, **69**, 1401–1407. [4.9]

- Chou, F. C., Lien, W. Y. and Lin, S. H. 1992c Analysis and experiment of non-Darcian convection in horizontal square packed-sphere channels —1. Forced convection. *Int. J. Heat Mass Transfer* **35**, 195–205. [4.9]
- Chou, F. C., Su, J. H. and Lien, S. S. 1994 A reevaluation of non-Darcian forced and mixed convection in cylindrical packed tubes. *ASME J. Heat Transfer*, **116**, 513–516. [4.9, 8.2.1]
- Choudhury, R. and Dey, D. 2010 Free convective visco-elastic flow with heat and mass transfer through a porous medium with periodic permeability. *Int. J. Heat Mass Transfer* **53**, 1666–1672. [9.2.1]
- Christopher, D. M. and Wang, B. X. 1993 Non-Darcy natural convection around a horizontal cylinder buried near the surface of a fluid-saturated porous medium. *Int. J. Heat Mass Transfer* **36**, 3663–3669. [7.11]
- Christopher, D. M. and Wang, B. X. 1994 Natural convection melting around a horizontal cylinder buried in frozen water-saturated porous media. *Heat Transfer 1994*, Inst. Chem. Engrs, Rugby, Vol. 4, 19–24. [10.1.7]
- Chung, C. A. and Chen, F. 2000 Convection in directionally solidifying alloys under inclined rotation. *J. Fluid Mech.* **412**, 93–123. [10.2.3]
- Chung, C. A. and Chen, F. 2000b Convection in directionally solidifying alloys under inclined rotation. *J. Fluid Mech.* **412**, 93–123. [10.2.3]
- Chung, C. A. and Chen, F. 2000 Onset of plume convection in mushy layers. *J. Fluid Mech.* **408**, 53–82. [10.2.3]
- Chung, C. A. and Chen, F. 2001 Morphological instability in a directionally solidifying binary solution with an imposed shear flow. *J. Fluid Mech.* **436**, 85–106. [10.2.3]
- Chung, C. A. and Worster, M. G. 2002 Steady-state chimneys in a mushy layer. *J. Fluid Mech.* **455**, 387–411. [10.2.3]
- Chung, J. N., Plumb, O. A. and Lee, W. C. 1992 Condensation in a porous region bounded by a cold vertical surface. *ASME J. Heat Transfer*, **114**, 1011–1018. [10.4]
- Chung, K., Lee, K. S. and Kim, W. S. 2003 Modified macroscopic turbulence modeling for the tube with channel geometry in porous media. *Numer. Heat Transfer A* **43**, 659–668. [1.8]
- Chung, T. J., Choi, C. K., Yoon, D. Y. and Kim, M. C. 2010 Onset of buoyancy-driven motion with laminar forced convection flows in a horizontal porous channel. *Int. J. Heat Mass Transfer* **53**, 5139–5146. [6.10.1]
- Chung, T. J., Park, J. H., Choi, C. K. and Yoon, D. Y. 2002 The onset of vortex instability in a laminar forced convection flow through a horizontal porous channel. *Int. J. Heat Mass Transfer* **45**, 3061–3064. [8.2.1]
- Chung, T. J., Kim, M. C. and Choi, C. K. 2009 The spatiotemporal instability of mixed convection in porous media. *Korean J. Chem. Engng.* **26**, 332–338. [8.2.1]
- Ciarletta, M., Straughan, B. and Tibullo, V. 2011 Modelling boundary and nonlinear effects in porous media flow. *Nonlinear Anal. Real World Appl.* **12**, 2839–2843. [1.6]
- Cieszko, M. and Kubik, J. 1999 Derivation of matching conditions at the contact surface between fluid-saturated porous solid and bulk fluid. *Transp. Por. Media* **34**, 319–336. [1.6]
- Cimpean, D., Pop, I., Ingham, D. B. and Merkin, J. H. 2009 Fully developed mixed convection between inclined plates filled with a porous medium. *Transp. Porous Media* **77**, 87–102. [8.4.3]
- Cimpean, D., Merkin, J. H., Pop, I. and Ingham, D. B. 2006 On a free convection problem over a vertical flat surface in a porous medium. *Transp. Porous Media* **64**, 393–411. [5.1.9.9]
- Clarksean, R., Kwendakwema, N. and Boehm, R. 1988 A study of mixed convection in a porous medium between vertical concentric cylinders. *ASME HTD* **96**, Vol. 2, 339–344. [8.3.3]
- Close, D. J. 1986 A general correlation for natural convection in liquid-saturated beds of spheres. *ASME J. Heat Transfer* **108**, 983–985. [6.9.2]
- Close, D. J., Symons, J. G. and White, R. F. 1985 Convective heat transfer in shallow gas-filled porous media: experimental investigation. *Int. J. Heat Mass Transfer* **28**, 2371–2378. [6.9.1]
- Collins, R. E. 1961 *Flow of Fluids through Porous Materials*, Reinhold, New York. [1.1]
- Combarous, M. 1970 Convection naturelle et convection mixte dans une couche poreuse horizontale. *Rev. Gén. Therm.* **9**, 1355–1375. [6.9.1]

- Combarous, M. 1972 Description du transfert de chaleur par convection naturelle dans une couche poreuse horizontale à l'aide d'un coefficient de transfert solide-fluide. *C. R. Acad. Sci. Paris A* **275**, 1375–1378. [6.5, 6.9.2]
- Combarous, M. A. and Bories, S. A. 1975 Hydrothermal convection in saturated porous media. *Adv. Hydroscience* **10**, 231–307. [6.9.1, 6.9.2]
- Combarous, M. and Bia, P. 1971 Combined free and forced convection in porous media. *Soc. Petrol. Eng. J.* **11**, 399–405. [6.9.1, 8.2.1]
- Combarous, M. and Bories, S. 1974 Modélisation de la convection naturelle au sein d'une couche poreuse horizontale à l'aide d'un coefficient de transfert solide-fluide. *Int. J. Heat Mass Transfer* **17**, 505–515. [6.9.2]
- Combarous, M. and Le Fur, B. 1969 Transfert de chaleur par convection naturelle dans une couche poreuse horizontale. *C. R. Acad. Sci. Paris B* **269**, 1009–1012. [6.3, 6.9.1]
- Combelles, L., Lorente, S. and Bejan, A. 2009 Leaf like architecture for cooling a flat body. *J. Appl. Phys.* **106**, #044906. [4.19]
- Combelles, L., Lorente, S., Anderson, R. and Bejan, A. 2012 Tree-shaped fluid flow and heat storage in a conducting solid. *J. Appl. Phys.* **111**, #014902. [4.19]
- Cooper, C. A., Glass, R. J. and Tyler, S. W. 1997 Experimental investigation of the stability boundary for double-diffusive finger convection in a Hele-Shaw cell. *Water Resources Res.* **33**, 517–526. [2.5, 9.1.1]
- Cooper, C. A., Glass, R. J. and Tyler, S. W. 2001 Effect of buoyancy ratio on the development of double-diffusive finger convection in a Hele-Shaw cell. *Water Resources Res.* **37**, 2323–2332. [9.1.1]
- Corey, A. T., Rathjens, C. H., Henderson, J. H. and Wyllie, M. R. J. 1956 Three-phase relative permeability. *Trans. Am. Inst. Min. Metall. Pet. Eng.* **207**, 349–351. [3.5.4]
- Costa, V. A. F. 2003 Unified streamline, heatline and massline methods for visualization of two-dimensional heat and mass transfer in anisotropic media. *Int. J. Heat Mass Transfer* **46**, 1309–1320. [4.17]
- Costa, V. A. F. 2004 Double-diffusive natural convection in parallelogrammic enclosures filled with fluid-saturated porous media. *Int. J. Heat Mass Transfer* **47**, 2699–2714. [9.4]
- Costa, V. A. F. 2006 Bejan's heatlines and masslines for convection visualization and analysis. *Appl. Mech. Rev.* **59**, 126–145. [4.17]
- Costa, V. A. F. 2009 Discussion: “The modeling of viscous dissipation in a saturated porous medium” (Nield, D. A., 2007, ASME J. Heat Transfer, 129, pp 1459–1463). *ASME J. Heat Transfer* **131**, #025501. [2.2.2]
- Costa, V. A. F. 2010 Comment on the paper I. A. Badruddin, Z. A., Zainal, Z. A. Khan., and Z. Mallick, Z. “Effect of viscous dissipation and radiation on natural convection in a porous medium embedded within vertical annulus.” IJTS 46(3) (2007) 221–227. *Int. J. Therm. Sci.* **49**, 1874–1875. [2.2.2]
- Costa, V. A. F. , Oliveira, L. A. and Sousa, A. C. M. 2004b Simulation of coupled flows in adjacent porous and open domains using a control volume finite-element method. *Energy Conversion and Management* **45**, 2795–2811. [1.6]
- Costa, V. A. F. , Oliveira, L. A., Baliga, B. R. and Sousa, A. C. M. 2004a Simulation of coupled flows in adjacent porous and open domains using a control volume finite-element method. *Numer. Heat Transfer A* **45**, 675–697. [1.6]
- Costa, V. A. F. , Oliveira, L. A. and Baliga, B. R. 2008 Implementation of the stress jump condition in a control-volume finite-element method for the simulation of laminar coupled flows in adjacent open and porous domains. *Numer. Heat Transfer B* **53**, 383–411. [1.6]
- Costa, V. A. F., Sousa, A. C. M. and Vasseur, P. 2012 Natural convection in square enclosures filled with fluid-saturated porous media under the influence of the magnetic field induced by two parallel vertical electric currents. *Int. J. Heat Mass Transfer* **55**, 7321–7329. [7.1.7]
- Cotta, R. M., Luz Neto, H., Alves, L. S. de B., and Quaresima, J. N. N. 2005 Integral transforms for natural convection in cavities filled with porous media. In *Transport Phenomena in Porous Media III*, (eds. D. B. Ingham and I. Pop), Elsevier, Oxford, pp. 97–119. [7.5]

- Coulaud, O., Morel, P. and Caltagirone, J. P. 1988 Numerical modelling of nonlinear effects in laminar flow through a porous medium. *J. Fluid Mech.* **190**, 393–407. [1.5.2]
- Coussot, P. 2000 Scaling approach to the convective drying of a porous medium. *European Phys. J. B* **15**, 557–566. [3.6]
- Cox, B. L. and Pruess, K. 1990 Numerical experiments on convective heat transfer in water-saturated porous media at near-critical conditions. *Transport in Porous Media* **5**, 299–323. [11.8]
- Cserepes, L. and Lenkey, L. 2004 Forms of hydrothermal and hydraulic flow in a homogeneous unconfined aquifer. *Geophys. J. Inter.* **158**, 785–797. [7.8]
- Cui, C., Huang, X. Y. and Liu, C. Y. 2000 Forced convection in a porous channel with discrete heat sources. *ASME J. Heat Transfer* **123**, 404–407. [4.16.1]
- Czechowski, L. and Kossacki, K. 2009 Thermal convection in the porous methane-soaked regolith of Titan: Investigation of stability. *Icarus* **202**, 599–606. [11.8]
- d'Hueppe, A., Chandesris, M. and Jamet, D. 2011 Boundary conditions at a fluid-porous interface for a convective heat transfer problem: Analysis of the jump relations. *flux. Int. J. Heat Mass. Transfer* **54**, 3683–3693. [2.4]
- d'Hueppe, M., Chandesris, M., Jamet, D. and Goyeau, B. 2012 Coupling a two-temperature model and a one-temperature model at a fluid-porous interface. *Int. J. Heat Mass Transfer* **55**, 2510–2523. [2.4]
- da Silva Miranda, B. M. and Anand, N. K. 2004 Convective heat transfer in a channel with porous baffles. *Numer. Heat Transfer A* **46**, 425–452. [4.11]
- da Silva, A. K. and Bejan, A. 2005 Constructal multi-scale structure for maximal heat transfer density in natural convection. *Int. J. Heat Fluid Flow* **26**, 34–44. [4.19]
- Dalal, A. and Das, M. K. 2008 Heatlines method of the visualization of natural convection in a complicated cavity. *Int. J. Heat Mass Transfer* **51**, 263–272. [4.17]
- Damronglerd, P. and Zhang Y. W. 2006 Transient fluid flow and heat transfer in a porous structure with partial heating and evaporation on the upper surface. *J. Enhanced Heat Transfer* **13**, 53–63. [10.3.1]
- Damseh, R. A. 2006 Magnetohydrodynamics-mixed convection from radiate vertical isothermal surface embedded in a saturated porous media. *ASME J. Appl. Mech.* **73**, 54–69. [8.1.6]
- Damseh, R. A. and Duwairi, H. M. 2008 Thermophoresis particle deposition: Natural convection interaction from vertical permeable surfaces embedded in a porous medium. *J. Porous Media* **12**, 79–88. [5.1.9.9]
- Damseh, R. A. and Tahat, M. S. 2009 Nonsimilar solutions of magnetohydrodynamic and thermophoretic particle deposition on mixed convection problem in porous media along a vertical surface with variable wall temperature. *Prog. Comput. Fluid Dyn.* **9**, 58–65. [8.1.6]
- Damseh, R. A., Al-Azab, T. A. and Al-Odat, M. Q. 2008 Unsteady free convection flow of viscoelastic fluid on a stretched vertical plate embedded in a non-Darcian porous medium with constant heat flux. *J. Porous Media* **11**, 117–124. [5.1.9.2]
- Daniels, P. G. 2006 Shallow cavity flow in a porous medium driven by differential heating. *J. Fluid Mech.* **565**, 441–459. [7.1.3]
- Daniels, P. G. 2007 On the boundary layer structure of differentially heated cavity flow in a stably stratified porous medium. *J. Fluid Mech.* **586**, 347–370. [7.1.3]
- Daniels, P. G. and Punpocha, M. 2004 Cavity flow in a porous medium driven by differential heating. *Int. J. Heat Mass Transfer* **47**, 3013–3030. [7.3.7]
- Daniels, P. G. and Punpocha, M. 2005 On the boundary-layer structure of cavity flow in a porous medium driven by differential heating. *J. Fluid Mech.* **532**, 321–344. [7.3.7]
- Daniels, P. G. and Simpkins, P. G. 1984 The flow induced by a heated vertical wall in a porous medium. *Q. J. Mech. Appl. Math.* **37**, 339–354. [5.12.2]
- Daniels, P. G., Blythe, P. A. and Simpkins, P. G. 1982 Thermally driven cavity flows in porous media. II. The horizontal boundary layer structure. *Proc. Roy. Soc. London Ser. A* **382**, 135–154. [7.1.1]

- Daniels, P. G., Blythe, P. A. and Simpkins, P. G. 1986 Thermally driven shallow cavity flows in porous media: the intermediate regime. *Proc. Roy. Soc. London Ser. A* **406**, 263–285. [7.1.3]
- Daniels, P. G., Simpkins, P. G. and Blythe, P. A. 1989 Thermally driven shallow cavity flows in porous media: the merged layer regime. *Proc. Roy. Soc. London Ser. A* **426**, 107–124. [7.1.3]
- Dantas, L. B., Orlandi, H. R. B. and Cotta, R. M. 2007 Improved lumped-differential formulations and hybrid solution methods for drying in porous media. *Int. J. Thermal Sci.*, **46**, 878–889. [3.6]
- Das, D. B. and Lewis, M. 2007 Dynamics of fluid circulation in coupled free and heterogeneous porous domains. *Chem. Engng. Sci.* **62**, 3549–3573. [1.6]
- Das, D. B., Hanspal, N. S. and Nassehi, V. 2005 Analysis of hydrodynamic conditions in adjacent free and heterogeneous porous flow domains. *Hydrological Processes* **19**, 2775–2799. [1.6]
- Das, S. and Morsi, Y. 2003 Natural convection in domed porous enclosures: non-Darcian flow. *J. Porous Media* **6**, 159–175. [7.3.7]
- Das, S. and Morsi, Y. S. 2005 A non-Darcian numerical modeling in domed enclosures filled with heat-generating porous media. *Numer. Heat Transfer A* **48**, 149–164. [7.3.7]
- Das, S. and Sahoo, R. K. 1999 Effect of Darcy, fluid Rayleigh and heat generation parameters on natural convection in a square enclosure: a Brinkman-extended Darcy model. *Int. Comm. Heat Mass Transfer* **26**, 569–578. [7.3.8]
- Das, S. S., Satapathy, A., Das, J. K. and Panda, J. P. 2009 Mass transfer effects on a MHD flow and heat transfer past a vertical porous plate through a porous medium under oscillatory suction and heat source. *Int. J. Heat Mass Transfer* **52**, 5962–5969. [9.2.1]
- Das, S., Sahoo, R. K. and Morsi, Y. S. 2003 Natural convection in heat generating porous enclosures: a non-Darcian model. *Canad. J. Chem. Engng.* **81**, 289–296. [6.17]
- Dash, G. C., Rath, P. K. and Mahapatra, N. 2010 Unsteady free convection MHD flow and mass transfer through porous media of a second order fluid between two heated plates with source/sink. *Proc. Nat. Acad. Sci. India A* **80**, 203–212. [9.2.2]
- Dash, S., Dash, G. C. and Misra, D. P. 2008 The MHD flow through a porous medium past a stretched vertical permeable surface in the presence of heat source/sink and a chemical reaction. *Proc. Nat. Acad. Sci. India A* **78**, 49–55. [5.1.9.9]
- Daurelle, J. V., Topin, F. and Occelli, R. 1998 Modeling of coupled heat and mass transfers with phase change in a porous medium; application to superheated steam drying. *Numer. Heat Transfer A* **33**, 39–63. [3.6]
- Davarzani, H., Marcoux, M. and Quintard, M. 2010 Theoretical predictions of the effective thermodiffusion coefficients in porous media. *Int. J. Heat Mass Transfer* **53**, 1514–1528. [9.1.4]
- David, E., Lauriat, G. and Cheng, P. 1988 Natural convection in rectangular cavities filled with variable porosity media. *ASME HTD* **96**, Vol. 1, 605–612. [7.6.2]
- David, E., Lauriat, G. and Cheng, P. 1991 A numerical solution of variable porosity effects on natural convection in a packed-sphere cavity. *ASME J. Heat Transfer* **113**, 391–399. [7.6.2]
- David, E., Lauriat, G. and Prasad, V. 1989 Non-Darcy natural convection in packed-sphere beds between concentric vertical cylinders. *AICHE Sympos. Ser.* **269**, 90–95. [7.6.2]
- Davidson, J. H., Kulacki, F. A. and Savela, D. 2009 Natural convection in water-saturated reticulated vitreous carbon foam. *Int. J. Heat Mass Transfer* **52**, 4479–4483. [6.9.3]
- Davis, A.M.J. and James, D.F. 1996 Slow flow through a model porous medium. *Int. J. Multiphase Flow* **22**, 969–989. [1.4.2]
- Davis, S. H., Rosenblat, S., Wood, J. R. and Hewitt, T. A. 1985 Convective fluid flow and diagenetic patterns in domed sheets. *Amer. J. Sci.* **285**, 207–223. [11.5]
- Dawood, A. S. and Burns, P. J. 1992 Steady three-dimensional convective heat transfer in a porous box via multigrid. *Numer. Heat Transfer A* **22**, 167–198. [7.2]
- Dayan, A., Flesh, J. and Saltiel, C. 2004 Drying of a porous spherical rock for compressed air energy storage. *Int. J. Heat Mass Transfer* **47**, 4459–4468. [3.6]
- De la Torre Juarez, M. and Busse, F. H. 1995 Stability of two-dimensional convection in a fluid-saturated porous medium. *J. Fluid Mech.* **292**, 305–323. [6.8]

- de Lemos, M. J. S. 2004 Turbulent heat and mass transfer in porous media. In *Technologies and Techniques in Porous Media* (D. B. Ingham, A. Bejan, E. Mamut and I. Pop, eds), Kluwer Academic, Dordrecht, pp. 157–168. [1.8].
- de Lemos, M. J. S. 2005a Turbulent kinetic energy distribution across the interface between a porous medium and a clear region. *Int. Comm. Heat Mass Transfer* **32**, 107–115. [1.8]
- de Lemos, M. J. S. 2005b Mathematical modeling and applications of turbulent heat and mass transfer in porous media. *Handbook of Porous Media* (ed. K. Vafai), 2nd ed., Taylor and Francis, New York, pp. 409–454. [1.8]
- de Lemos, M. J. S. 2005c The double-decomposition concept for turbulent transport in porous media. In *Transport Phenomena in Porous Media III*, (eds. D. B. Ingham and I. Pop), Elsevier, Oxford, pp. 1–33. [1.8]
- de Lemos, M. J. S. 2008 Analysis of turbulent flows in fixed and moving permeable media. *Acta Geophys.* **56**, 562–583. [1.8]
- de Lemos, M. J. S. 2009 Turbulent flow and fluid-porous interfaces computed with a diffusion-jump model for  $k$  and  $\epsilon$  transport equations. *Transp. Porous Media* **78**, 331–346. [1.8].
- de Lemos, M. J. S. 2012a Turbulent Impinging Jets into Porous Media. Springer, New York.. [1.8]
- de Lemos, M. J. S. 2012b Turbulence in Porous Media: Modeling and Applications, 2nd ed., Elsevier, Oxford. [1.8]
- de Lemos, M. J. S. and Braga, E. J. 2003 Modeling of turbulent natural convection in porous media. *Int. Comm. Heat Mass Transfer* **30**, 615–624. [1.8]
- de Lemos, M. J. S. and Dorea, F. T. 2011 Simulation of a turbulent impinging jet into a layer of porous material using a two-energy equation model. *Numer. Heat Transfer A* **59**, 769–798. [1.8]
- de Lemos, M. J. S. and Fischer, C. 2008 Thermal analysis of an impinging jet on a plate with and without a porous layer. *Numer. Heat Transfer A* **54**, 1022–1041. [1.8]
- de Lemos, M. J. S. and Mesquita, M. S. 2003 Modeling of turbulent natural convection in porous media. *Int. Comm. Heat Mass Transfer* **30**, 105–113. [1.8]
- de Lemos, M. J. S. and Pedras, M. H. J. 2000 On the definitions of turbulent kinetic energy for flow in porous media. *Int. Comm. Heat Mass Transfer* **27**, 211–220. [1.8]
- de Lemos, M. J. S. and Pedras, M. H. J. 2001 Recent mathematical models for turbulent flow in saturated rigid porous media. *ASME J. Fluids Engng.* **123**, 935–940. [1.8]
- de Lemos, M. J. S. and Rocamora, F. D. 2002 Turbulent transport modeling for heat flow in rigid porous media. *Heat Transfer 2002, Proc. 12th Int. Heat Transfer Conf.*, Elsevier, Vol. 2, pp. 791–796. [1.8]
- de Lemos, M. J. S. and Saito, M. B. 2008 Computation of turbulent heat transfer in a moving porous bed using a macroscopic two-energy equation model. *Int. Comm. Heat Mass Transfer* **35**, 1262–1266. [1.8]
- de Lemos, M. J. S. and Silva, R. A. 2006 Turbulent flow over a highly permeable medium simulated with a diffusion-jump model of the interface. *Int. J. Heat Mass Transfer* **49**, 546–556. [1.8]
- de Lemos, M. J. S. and Tofaneli, L. A. 2004 Modelling of double-diffusive turbulent natural convection in porous media. *Int. J. Heat Mass Transfer* **47**, 4233–4241. [1.8]
- de Medeiros, J. M., Gurgel, J. M. and Marcondes, F. 2006 Numerical analysis of natural convection in porous media: The influence of non-Darcy terms and thermal dispersion. *J. Porous Media* **9**, 235–250. [7.6.2]
- Debeda, V., Caltagirone, J. P. and Watremez, P. 1995 Local multigrid refinement method for natural convection in fissured porous media. *Numer. Heat Transfer* **28**, 455–467. [6.13.4]
- Degan, G. and Vasseur, P. 1995 The non-Darcy regime for boundary layer natural convection from a point source of heat in a porous medium. *Int. Comm. Heat Mass Transfer* **22**, 381–390. [5.11.1]
- Degan, G. and Vasseur, P. 1996 Natural convection in a vertical slot filled with an anisotropic porous medium with oblique principal axes. *Numer. Heat Transfer A* **30**, 397–412. [7.3.2]
- Degan, G. and Vasseur, P. 1997 Boundary-layer regime in a vertical porous layer with anisotropic permeability and boundary effects. *Int. J. Heat Fluid Flow* **18**, 334–343. [7.3.2]

- Degan, G. and Vasseur, P. 2002 Aiding mixed convection through a vertical anisotropic porous channel with oblique axes. *Int. J. Engng. Sci.* **40**, 193–209. [8.3.1]
- Degan, G. and Vasseur, P. 2003 Influence of anisotropy on convection in porous media with nonuniform thermal gradient. *Int. J. Heat Mass Transfer* **46**, 781–789. [6.12]
- Degan, G., Akowanou, C. and Awanou, N. C. 2007a Transient natural convection of non-Newtonian fluids about a vertical surface embedded in an anisotropic porous medium. *Int. J. Heat Mass Transfer* **50**, 4629–4639. [5.1.9.2]
- Degan, G., Beji, H., and Vasseur, P. 1998b Natural convection in a rectangular cavity filled with an anisotropic porous medium. *Heat Transfer 1998, Proc. 11th IHTC*, **4**, 441–446. [7.3.2]
- Degan, G., Beji, H., Vasseur, P. and Robillard, L. 1998a Effect of anisotropy on the development of convective boundary layer flow in porous media. *Int. Comm. Heat Mass Transfer* **25**, 1159–1168. [7.3.2]
- Degan, G., Gibigaye, M., Akowanou, C. and Awanou, N. C. 2007b The similarity regime for natural convection in a vertical cylindrical cell filled with an anisotropic porous medium. *J. Engng. Math.* **62**, 277–287. [7.3.3]
- Degan, G., Vasseur, P. and Bilgen, E. 1995 Convective heat transfer in a vertical anisotropic porous layer. *Int. J. Heat Mass Transfer* **38**, 1975–1987. [7.3.2]
- Degan, G., Vasseur, W. P. and Awanou, N. C. 2005 Anisotropy effects on non-Darcy natural convection from concentrated heat sources in porous media. *Acta Mech.* **179**, 111–124. [5.10.2.2]
- Degan, G., Zohoun, S. and Vasseur, P. 2002 Forced convection in horizontal porous channels with hydrodynamic anisotropy. *Int. J. Heat Mass Transfer* **45**, 3181–3188. [4.16.5]
- Degan, G., Zohoun, S. and Vasseur, P. 2003 Buoyant plume above a line source of heat in an anisotropic porous medium. *Heat Mass Transfer* **39**, 209–213. [5.10.1.1]
- Deibler, J. A. and Bortolozzi, R. A. 1998 A two-field model for natural convection in a porous annulus at high Rayleigh numbers. *Chem. Engng. Sci.* **53**, 1505–1516. [7.3.3]
- Delache, A. and Quarzazi, M. N. 2008 Weakly nonlinear interaction of mixed convection patterns in porous media heated from below. *Int. J. Therm. Sci.* **47**, 709–722. [6.10.1]
- Delache, A., Quarzazi, N. and Néel, M. C. 2002 Pattern formation of mixed convection in a porous medium confined laterally and heated from below: effect of inertia. *Comptes Rendus Mécanique* **330**, 885–891. [6.10.1]
- Delache, A., Quarzazi, M. N. and Combarous, M. 2007 Spatio-temporal stability analysis of mixed convection flows in porous media heated from below; comparison with experiments. *Int. J. Heat Mass Transfer* **50**, 1485–1499. [6.10.1]
- Delmas, A. and Arquis, E. 1995 Early initiation of natural convection in an open porous layer due to the presence of solid conductive inclusions. *ASME J. Heat Transfer* **117**, 733–739. [6.13.2]
- Demirel, Y. and Kahraman, R. 1999 Entropy generation in a rectangular packed duct with wall heat flux. *Int. J. Heat Mass Transfer* **42**, 2337–2344. [4.9]
- Demirel, Y. and Kahraman, R. 2000 Thermodynamic analysis of convective heat transfer in an annular packed bed. *Int. J. Heat Fluid Flow* **21**, 442–448. [4.16.5]
- Demirel, Y., Abu-Al-Saud, B. A., Al-Ali, H. H. and Makkawi, Y. 1999 Packing size and shape effects on forced convection in large rectangular packed ducts with asymmetrical heating. *Int. J. Heat Mass Transfer* **42**, 3267–3277. [4.16.5]
- Demirel, Y., Sharma, R. N. and Al-Ali, H. H. 2000 On the effective heat transfer parameters in a packed bed. *Int. J. Heat Mass Transfer* **43**, 327–332. [4.16.5]
- Deng, C. and Martinez, D. M. 2005 Viscous flow in a channel partially filled with a porous medium and with wall suction. *Chem. Engng. Sci.* **60**, 329–336. [1.6]
- Desaive, T., Hennenberg, M. and Dauby, P. C. 2004 Stabilite thermomagneto-convective d'un ferrofluide dans une couche poreuse en rotation. *Mecan. Industr.* **5**, 621–625. [6.21]
- Desaive, T., Hennenberg, M. and Lebon, G. 2002 Thermal instability of a rotating saturated porous medium heated from below and submitted to rotation. *Eur. Phys. J. B* **29**, 641–647. [6.22]
- Desaive, T., Lebon, G. and Hennenberg, M. 2001 Coupled capillary and gravity-driven instability in a liquid film overlying a porous layer. *Phys. Rev. E* **64**, art. no. 066304 Part 2. [6.19.3]

- Desrayaud, G. and Lauriat, G. 1991 Thermal convection around a line heat source buried in a porous medium. *ASME HTD* **172**, 17–24. [7.11]
- Dessaux, A. 1998 Analytical and numerical solutions to a problem of convection in a porous media with lateral mass flux. *Int. Comm. Heat Mass Transfer* **25**, 641–650. [5.1.9.9]
- Devi, S.N.S., Nagaraju, P. and Hanumanthappa, A. R. 2002 Effect of radiation on Rayleigh-Bénard convection in an anisotropic porous medium. *Indian J. Engng. Mater. Sci.* **9**, 163–171. [6.12]
- Dhahri, H., Boughamoura, A. and Ben Nasrallah, S. 2006 Forced pulsating flow and heat transfer in a tube partially filled with a porous medium. *J. Porous Media* **9**, 1–1. [4.16.2]
- Dhahri, H., Boughamoura, A. and Ben Nasrallah, S. 2006 Numerical study of heat transfer in a porous pipe subjected to reciprocating flow. *J. Porous Media* **9**, 289–305. [4.16.2]
- Dhanasekharan, M. R., Das, S. K. and Venkateshan, S. P. 2002 Natural convection in a cylindrical enclosure filled with heat generating anisotropic porous medium. *ASME J. Heat Transfer* **124**, 203–207. [6.16.1]
- Dharma Rao, V., Naidu, S. V. and Sarma, P. K. 1996 Non-Darcy effects in natural convection heat transfer in a vertical porous annulus. *ASME J. Heat Transfer* **118**, 502–505. [7.3.3]
- Dhifaoui, B., Ben Jabrallah, S., Belghith, A. and Corriou, J. P. 2007 Experimental study of the dynamic behaviour of a porous medium submitted to a wall heat flux in view of thermal energy storage by sensible heat. *Int. J. Therm. Sci.* **46**, 1056–1063. [7.2]
- Dhir, V. K. 1994 Boiling and two-phase flow in porous media. *Ann. Rev. Heat Transfer* **5**, 303–350. [10.3.1]
- Dhir, V. K. 1997 Heat transfer from heat-generating pools and particulate beds. *Adv. Heat Transfer* **29**, 1–57. [10.3.1]
- Diaz, E. and Brevdo, L. 2011 Absolute/convective instability dichotomy at the onset of convection in a porous layer with either horizontal or vertical solutal and inclined thermal gradients, and horizontal throughflow. *J. Fluid Mech.* **681**, 567–596. [9.1.3]
- Diaz, E. and Brevdo, L. 2012 Transition from convective to absolute instability in a porous layer with either horizontal or vertical solutal and inclined thermal gradients, and horizontal throughflow. *Transp. Porous Media* **92**, 597–617. [9.1.3]
- Dickey, J. T. and Peterson, G. P. 1997 High heat flux absorption utilizing porous material with two-phase heat transfer. *ASME J. Energy Res. Tech.* **119**, 171–179. [3.6]
- Diersch, H. J. G. 2000 Note to the opposing flow regime at mixed convection around a heated cylinder in a porous medium. *Transport in Porous Media* **38**, 345–352. [8.1.3]
- Diersch, H. J. G. and Kolditz, O. 2002 Variable-density flow and transport in porous media: approaches and challenges. *Adv. Water Res.* **25**, 899–944. [9]
- Discacciati, M., Miglio, E. and Quarteroni, A. 2002 Mathematical and numerical methods for coupling surface and groundwater flows. *Appl. Numer. Anal.* **43**, 57–74. [1.6]
- Divya, Sharma, R. C. and Sunil. 2005 Thermosolutal convection in a ferromagnetic fluid saturating a porous medium. *J. Porous Media* **8**, 393–408. [9.1.6.4]
- Dixon, A. G. and Cresswell, D. L. 1979 Theoretical predictions of effective heat transfer mechanisms in regular shaped packed beds. *AIChE Journal* **25**, 663–676. [2.2.3]
- Do, K. H., Min, J. Y. and Kim, S. J. 2007 Thermal optimization of an internally finned tube using analytical solutions based on a porous medium. *ASME J. Heat Transfer* **129**, 1408–1416. [4.11]
- Doering, C. R. and Constantin, P. 1998 Bounds for heat transport in a porous layer. *J. Fluid Mech.* **376**, 263–296. [6.3]
- Dona, C. L. G. and Stewart, W. E. 1989 Variable property effects on convection in a heat generating porous medium. *ASME J. Heat Transfer* **111**, 1100–1102. [6.17]
- Donaldson, I. G. 1962 Temperature gradients in the upper layers of the Earth's crust due to convective water flows. *J. Geophys. Res.* **67**, 3449–3459. [6.13.1]
- Donaldson, I. G. 1982 Heat and mass circulation in geothermal systems. *Ann. Rev. Earth Planet Sci.* **10**, 377–395. [11]
- Dorea, F. T. and de Lemos, M. J. S. 2010 Simulation of laminar impinging jet on a porous medium with thermal non-equilibrium model. *Int. J. Heat Mass Transfer* **53**, 5089–5101. [1.8]

- Dos Santos, G. H. and Mendes, N. 2009a Combined heat, air and moisture (HAM) transfer model for porous building materials. *J. Building Phys.* **32**, 203–220. [3.6]
- Dos Santos, G. H. and Mendes, N. 2009b Heat, air and moisture transfer through hollow porous blocks. *Int. J. Heat Mass Transfer* **52**, 2390–2398. [3.6]
- Doughty, C. and Pruess, K. 1990 A similarity solution for the two-phase fluid and heat flow near high-level nuclear waste packages emplaced in porous media. *Int. J. Heat Mass Transfer* **33**, 1205–1222. [11.9.1]
- Doughty, C. and Pruess, K. 1992 A similarity solution for two-phase water, air and heat flow near a linear heat source in a porous medium. *J. Geophys. Res.* **97**, 1821–1838. [11.9.1]
- du Plessis, J. P. 1994 Analytical quantification of coefficients in the Ergun equation for fluid friction in a packed bed. *Transport in Porous Media* **16**, 189–207. [1.5.2]
- Du, J. H. and Wang, B.X. 1999 Mixed convection in porous media between vertical concentric cylinders. *Heat Transfer Asian Res.* **28**, 95–101. [8.3.3]
- Du, Y. P., Qu, Z. G., Zhao, C. Y. and Tao, W. Q. 2010 Numerical study of conjugated heat transfer in metal foam filled double-pipe. *Int. J. Heat Mass Transfer* **53**, 4899–4907. [4.10]
- Du, Z. G. and Bilgen, E. 1990 Natural convection in vertical cavities with partially filled heat-generating porous media. *Numer. Heat Transfer A* **18**, 371–386. [7.7]
- Du, Z. G. and Bilgen, E. 1992 Natural convection in vertical cavities with internal heat generating porous medium. *Wärme-Stoffübertrag.* **27**, 149–155. [7.3.8]
- Dufour, F. and Néel, M. C. 1998 Numerical study of instability in a horizontal porous channel with bottom heating and forced horizontal flow. *Phys. Fluids* **10**, 2198–2207. [6.10.1]
- Dufour, F. and Néel, M. C. 2000 Time-periodic convection patterns in a horizontal porous layer with through-flow. *Quart. Appl. Math.* **58**, 265–281. [6.10.1]
- Dukhan, N. 2009b Developing non thermal-equilibrium convection in porous media with negligible fluid conduction. *ASME J Heat Transfer* **131**, #014501. [4.13]
- Dukhan, N. and Al-Rammahi, M. A. 2012 Analysis and experiment for Darcy flow convection in cylindrical metal foam. *AIP Conf. Proc.* **1453**, 191–196. [4.10]
- Dullien, F. A. L. 1992 *Porous Media: Fluid Transport and Pore Structure*, Academic, New York, 2nd Edit. [1.4.2]
- Duman, T. and Shavit, U. 2009 An apparent interface location as a tool to solve the porous interface problem. *Transp. Porous Media* **78**, 509–524. [1.6]
- Dunn, J. C. and Hardee, H. C. 1981 Superconvecting geothermal zones. *J. Volcanol. Geotherm. Res.* **11**, 189–201. [11.8]
- Dupuit, A. J. E. J. 1863 *Études Théoriques et Pratiques sur le Mouvement des eaux dans les Canaux Découverts et à Travers les Terrains Permeables*. Victor Dalmont, Paris. [1.5.2]
- Durlofsky, L. and Brady, J. F. 1987 Analysis of the Brinkman equation as a model for flow in porous media. *Phys. Fluids* **30**, 3329–3341. [1.5.3]
- Dutta, P. and Seetharamu, K. N. 1993 Free convection in a saturated porous medium adjacent to a vertical impermeable wall subjected to a non-uniform heat flux. *Wärme-Stoffübertrag.* **28**, 27–32. [5.1.9]
- Duval, F., Fichet, F. and Quintard, M. 2004 A local thermal non-equilibrium model for two-phase flows with phase change in porous media. *Int. J. Heat Mass Transfer* **47**, 613–639. [11.9.3]
- Duwairi, H. M. 2006 Radiation effects on mixed convection over a non isothermal cylinder and sphere in a porous media. *J. Porous Media* **9**, 251–259. [8.1.3]
- Duwairi, H. M. and Damseh, R. A. 2008a Effect of thermophoresis particle deposition on mixed convection from vertical surfaces embedded in a saturated porous medium. *Int. J. Numer. Meth. Heat Fluid Flow* **18**, 202–216. [8.1.6]
- Duwairi, H. M. and Damseh, R. A. 2008b Thermophoresis particle deposition – thermal radiation interaction on mixed convection from a vertical surface embedded in porous medium. *Canad. J. Phys.* **87**, 161–167. [9.2.1]
- Duwairi, H. M. and Damseh, R. A. 2009 Thermophoresis particle deposition – thermal radiation interaction on natural convection heat and mass transfer from vertical permeable surfaces. *Int. J. Numer. Meth. Heat Fluid Flow* **19**, 617–632. [9.2.1]

- Duwairi, H. M., Aldoss, T. K. and Jarrah, M. A. 1997 Nonsimilarity solutions for non-Darcy mixed convection from horizontal surfaces in a porous medium. *Heat Mass Transfer* **33**, 149–156. [8.1.2]
- Duwairi, H. M., Damseh, R. A. and Tashtoush, B. 2007 Transient mixed convection along a vertical plate imbedded in porous media with internal heat generation and oscillating temperature. *Chem. Engng. Comm.* **194**, 1516–1530. [8.1.6]
- Dwiek, Y. J., Rabadi, N. J. and Ghazzawi, N. A. 1994 Effect of lateral mass flux on free convection from an inclined plate embedded in a saturated porous medium. *Arab. J. Sci. Engng.* **14**, 449–460. [5.3]
- Dybbas, A. and Edwards, R. V. 1984 A new look at porous media fluid mechanics – Darcy to turbulent. *Fundamentals of Transport Phenomena in Porous Media* (eds. J. Bear and V. Carapcioglu), Martinus Nijhoff, The Netherlands, 199–256. [7.6.1]
- Dyga, R. 2010 Heat transfer during the fluid flow through a channel with wire mesh packing. *Chem. Proc. Engng.* **31**, 119–134. [4.16.5]
- Easterday, O. T., Wang, C. Y. and Cheng, P. 1995 A numerical and experimental study of two-phase flow and heat transfer in a porous formation with localized heating from below. *ASME HTD-321*, 723–732. [10.3.2]
- Ebinuma, C. D. and Nakayama, A. 1990a Non-Darcy transient and steady film condensation in a porous medium. *Int. Comm. Heat Mass Transfer* **17**, 49–58. [10.4]
- Ebinuma, C. D. and Nakayama, A. 1990b An exact solution for transient film condensation in a porous medium along a vertical surface with lateral mass flux. *Int. Comm. Heat Mass Transfer* **17**, 105–111. [4.6.2, 10.4]
- Ebinuma, C. D. and Nakayama, A. 1997 Approximate solution for non-Darcy transient film condensation in a porous medium. *J. Brazilian Soc. Mech. Sci.* **19**, 496–503. [10.4]
- Echaniz, H. L. 1984 Oscillatory convection with boiling in a water-saturated porous medium. MS thesis, Cornell University. [10.3.1]
- Egorov, S. D. and Poleshaev, V. I. 1993 Thermal convection in anisotropic porous insulation. *Heat Transfer Res.* **25**, 968–990. [7.3.2]
- Ejlali, A. and Hooman, K. 2011 Buoyancy effects on cooling a heat generating porous medium: Coal stockpile. *Transp. Porous Media* **88**, 235–248. [7.3.8]
- Ekholm, T. C. 1983 Studies of convection using a Hele-Shaw cell. Project Report, School of Engineering, University of Auckland. [6.13.2]
- Elaiw, A. M. 2008 Vortex instability of mixed convection boundary layer flow adjacent to a non-isothermal inclined surface in a porous medium with variable permeability. *ZAMM* **88**, 121–128. [5.4]
- Elaiw, A. M. and Ibrahim, E. S. 2008 Vortex instability of mixed convection boundary layer flow adjacent to a nonisothermal horizontal surface in a porous medium with variable permeability. *J. Porous Media* **11**, 305–321. [5.4]
- Elaiw, A. M., Ibrahim, F. S. and Bakr, A. A. 2007 The influence of variable permeability on vortex instability of a horizontal combined free and mixed convection flow in a saturated porous medium. *ZAMM* **87**, 528–536. [5.4]
- Elaiw, A. M., Ibrahim, F. S. and Bakr, A. A. 2009 Variable permeability and inertia effect on vortex instability of natural convection flow over horizontal plates in porous media. *Comm. Nonlinear Sci. Numer. Simul.* **14**, 2190–2201. [5.4]
- El-Amin, H. F. and Sun, S. Y. 2011 Combined effects of magnetic field and thermal dispersion on a non-Darcy mixed convection. *J. Therm. Sci.* **20**, 276–282. [8.1.6]
- El-Amin, M. F. 2003a Combined effect of magnetic field and viscous dissipation on a power-law fluid over plate with variable surface heat flux embedded in a porous medium. *J. Magn. Magn. Mater.* **261**, 228–237. [5.1.9.2]
- El-Amin, M. F. 2003b Combined effect of viscous dissipation and Joule heating on MHD forced convection over a non-isothermal horizontal cylinder embedded in a fluid saturated porous medium. *J. Magn. Magn. Mater.* **263**, 337–343. [4.3]

- El-Amin, M. F. 2004a Double dispersion effects on natural convection heat and mass transfer in non-Darcy porous medium. *Appl. Math. Comput.* **156**, 1–17. [9.2.1]
- El-Amin, M. F. 2004b Non-Darcy free convection from a vertical plate with time-periodic surface oscillations. *J. Porous Media* **7**, 331–338. [5.1.9.7]
- El-Amin, M. F. and Ebrahem, N. A. 2006 Effects of viscous dissipation on unsteady free convection in a fluid past a vertical plate immersed in a porous medium. *Transp. Porous Media* **64**, 1–14. [5.1.9.9]
- El-Amin, M. F., Aissa, W. A. and Salama, A. 2008 Effects of chemical reaction and double dispersion on non-Darcy free convection heat and mass transfer. *Transp. Porous Media* **75**, 93–109. [9.1.6.4]
- El-Amin, M. F., Ebrahem, N. A., Salama, A. and Sun, S. Y. 2011a Radiative mixed convection over an isothermal cone embedded in a porous medium with variable permeability. *J. Appl. Math.* #124590 [8.1.4]
- El-Amin, M. F., El-Hakiem, M. A. and Mansour, M. A. 2003 Effects of viscous dissipation on a power-law fluid over plate embedded in a porous medium. *Heat Mass Transfer* **39**, 807–813. [5.1.9.2]
- El-Amin, M. F., El-Hakiem, M. A. and Mansour, M. A. 2004 Combined effect of magnetic field and lateral mass transfer on non-Darcy axisymmetric free convection in a power-law fluid saturated porous medium. *J. Porous Media* **7**, 65–71. [5.2]
- El-Amin, M. F., Salama, A. and Abbas, I. 2010 Viscous dissipation effect on natural convection in a fluid saturated porous medium. *J. Porous Media* **13**, 989–997. [5.1.9.4]
- El-Amin, M. F., Salama, A., Sun, S. and Gorla, R. S. R. 2012 Development of flow and heat transfer in the vicinity of a vertical plate embedded in a porous medium with viscous dissipation effects. *Spec. Top. Rev. Porous Media* **3**, 169–175. [5.1.9.9]
- El-Amin, M. F., Sun, S., El\_Ameen, M. A., Jaha, Y. A. and Gorla, R. S. R. 2011b Non-Darcy free convection of power-law fluids over a two-dimensional body embedded in a porous medium. *Transp. Porous Media* **86**, 965–972. [5.9]
- El-Aziz, M. A. 2007 Blowing/suction effects on hydromagnetic simultaneous heat and mass transfer by natural convection from a vertical cylinder embedded in a thermally stratified porous medium. *J. Porous Media* **10**, 297–310. [9.2.1]
- Elbashbeshy, E. M. A. 2001 Laminar mixed convection over horizontal flat plate embedded in a non-Darcian porous medium with suction and injection. *Appl. Math. Comput.* **121**, 123–128. [8.1.2]
- Elbashbeshy, E. M. A. 2003 The mixed convection along a vertical plate embedded in a non-Darcian porous medium with suction and injection. *Appl. Math. Comput.* **136**, 139–149. [8.1.1]
- Elbashbeshy, E. M. A. and Bazid, M. A. 2000b The mixed convection along a vertical plate with variable heat flux embedded in porous medium. *Appl. Math. Comput.* **125**, 317–324. [8.1.1]
- Elbashbeshy, E. M. A. and Bazid, M. A. 2000a Heat transfer over a continuously moving plate embedded in a non-Darcian porous medium. *Int. J. Heat Mass Transfer* **43**, 3087–3092. [8.1.4]
- Eldabe, N. T. M. and Sallam, S. N. 2005 Non-Darcy Couette flow through a porous medium of magnetohydrodynamic viscoelastic fluid with heat and mass transfer. *Canad. J. Phys.* **83**, 1241–1263. [9.2.2]
- El-Dabe, N. T. M., Sallam, S. N., Hassan, A. A. and Hussein, M. M. 2010 The pulsatile flow of a Burger's fluid and heat transfer through a porous medium in a circular pipe. *Spec. Top. Rev. Porous Media* **1**, 243–255. [4.16.2]
- Eldabe, N. T., Ahmed, M., Fouad, A. and Sayed, A. 2008 Numerical study of flow of magnetohydrodynamic non-Newtonian fluid obeying the Eyring-Powell mode through a non-Darcy porous medium with coupled heat and mass transfer. *J. Porous Media* **11**, 691–700. [9.2.1]
- Elder, J. W. 1967a Steady free convection in a porous medium heated from below. *J. Fluid Mech.* **27**, 29–48. [2.5, 6.9.1, 6.18]
- Elder, J. W. 1967b Transient convection in a porous medium. *J. Fluid Mech.* **27**, 609–623. [6.9.1, 6.18]
- Elder, J. W. 1968 The unstable thermal interface. *J. Fluid Mech.* **32**, 69–96. {6.11.3}

- Elgazery, N. S. and Elazem, N. Y. A. 2009 Effects of variable properties on magnetohydrodynamic unsteady mixed convection in non-Newtonian fluid with variable surface temperature. *J. Porous Media* **12**, 477–488. [8.1.6]
- Elhajjar, B., Charrier-Mojtabi, M. C. and Mojtabi, A. 2008 Separation of a binary fluid mixture in a porous horizontal cavity. *Phys. Rev. E* **77**, #026310. [9.1.6.4]
- Elhajjar, B., Mojtabi, A. and Charrier-Mojtabi, M. C. 2009 Influence of vertical vibrations on the separation of a binary mixture in a horizontal porous layer heated from below. *Int. J. Heat Mass Transfer* **52**, 165–172. [9.1.4]
- Elhajjar, B., Mojtabi, A. and Charrier-Mojtabi, M. C. 2010 Separation in an inclined porous thermogravitational cell. *Int. J. Heat Mass Transfer* **53**, 4844–4851. [9.1.4]
- El-Hakiem, M. A. 2000 MHD oscillatory flow on free convection-radiation through a porous medium with constant suction velocity. *J. Magn. Magn. Mater.* **220**, 271–276. [5.1.9.4]
- El-Hakiem, M. A. 2001a Thermal dispersion effects on combined convection in non-Newtonian fluids along a non-isothermal vertical plate in a porous medium. *Transport in Porous Media* **45**, 29–40. [8.1.1]
- El-Hakiem, M. A. 2001b Combined convection in non-Newtonian fluids along a nonisothermal vertical plate in a porous medium with lateral mass flux. *Heat Mass Transfer* **37**, 379–385. [8.1.1]
- El-Hakiem, M. A. 2007 Effect of radiation on non-Darcy free convection from a vertical cylinder embedded in a fluid-saturated porous medium with a temperature-dependent viscosity. *J. Porous Media* **10**, 209–218. [5.7]
- El-Hakiem, M. A. 2009 Radiative effects on non-Darcy natural convection from a heated vertical plate in saturated porous media with mass transfer for non-Newtonian fluid. *J. Porous Media* **12**, 89–99. [9.2.1]
- El-Hakiem, M. A. and El-Amin, M. F. 2001a Thermal radiation effect on non-Darcy natural convection with lateral mass transfer. *Heat Mass Transfer* **37**, 161–165. [5.1.9.4]
- El-Hakiem, M. A. and El-Amin, M. F. 2001b Mass transfer effects on the non-Newtonian fluids past a vertical plate embedded in a porous medium with non-uniform surface heat flux. *Heat Mass Transfer* **37**, 293–297. [5.1.9.2]
- El-Kabeir, S. M. M. 2012 Soret and Dufour effects on heat and mass transfer by mixed convection over a vertical surface saturated porous medium with temperature dependent viscosity. *Int. J. Numer. Methods Fluids* **69**, 1633–1645. [9.6.1]
- El-Kabeir, S. M. M., El-Hakiem, M. A. and Rashad, A. M. 2008 Group method analysis of combined heat and mass transfer by MHD non-Darcy non-Newtonian natural convection adjacent to horizontal cylinder in a saturated porous medium. *Appl. Meth. Mod.* **32**, 2378–2395. [9.2.1]
- El-Kabeir, S. M. M., El-Hakiem, M. A. and Rashad, A. M. 2008 Lie group analysis of unsteady MHD three dimensional natural convection from an inclined stretching surface saturated porous medium. *J. Comput. Appl. Math.* **213**, 582–603. [5.3]
- El-Kabeir, S. M. M., Rashad, A. M. and Gorla, R. S. R. 2007 Unsteady MHD combined convection over a moving vertical sheet in a fluid saturated porous medium with uniform surface heat flux. *Math. Comput. Model.* **46**, 384–397. [8.1.6]
- El-Khatib, G. and Prasad, V. 1987 Effects of stratification on thermal convection in horizontal porous layers with localized heating from below. *ASME J. Heat Transfer* **109**, 683–687. [6.18]
- Ellinger, E. A. and Beckerman, C. 1991 On the effect of porous layers on melting heat transfer in an enclosure. *Exp. Therm. Fluid Sci.* **4**, 619–629. [10.1.7]
- El-Sayed, M. F. 2008 Onset of electroconvective instability of Oldroydian viscoelastic liquid layer in a Brinkman porous medium. *Arch. Appl. Mech.* **78**, 211–224. [6.23]
- El-Sayed, M. F. and Mohamed, R. A. 2010 Magnetogravitational instability of thermally conducting rotating viscoelastic fluid with Hall current in Brinkman porous medium. *J. Porous Media* **13**, 779–798. [6.21]

- El-Sayed, M. F., Eldabe, N. T. M., Ghaly, A. Y. and Sayed, H. M. 2011 Effect of chemical reaction, heat and mass transfer on non-Newtonian fluid flow through porous medium in a vertical peristaltic tube. *Transp. Porous Media* **89**, 185–212. [9.1.6.4]
- El-Shaarawi, M. A. I., Al-Nimr, M. A. and Al Yah, M. M. K. 1999 Transient conjugate heat transfer in a porous medium in concentric annuli. *Int. J. Numer. Meth. Heat Fluid Flow* **9**, 444–460. [4.6.4]
- Emami Maybodi, H. 2012 Nazar Moghaddam and Rostami's reply to my comment on their paper "Quantification of density-driven natural convection for dissolution mechanism in CO<sub>2</sub> sequestration. *Transp. Porous Media* **93**, 655–656. [11.11]
- Emmanuel, S. and Berkovitz, B. 2006a An experimental analogue for convection and phase separation in hydrothermal systems. *J. Geophys. Res.–Solid Earth* **111**, #09103. [11.8]
- Emmanuel, S. and Berkovitz, B. 2006b Suppression and stimulation of seafloor hydrothermal convection by exothermic mineral hydration. *Earth Planet. Sci. Lett.* **243**, 657–66. [11.8].
- Emmanuel, S. and Berkovitz, B. 2007a Continuous time random walks and heat transfer in porous media. *Transp. Porous Media* **67**, 413–430. [11.8]
- Emmanuel, S. and Berkovitz, B. 2007b Phase separation and convection in heterogeneous porous media: Implications for seafloor hydrothermal systems. *J. Geophys. Res.–Solid Earth* **112**, #B05210. [11.8]
- Emms, P. W. 1998 Freckle formation in a solidifying binary alloy. *J. Engng. Math.* **33**, 175–200. [10.2.3]
- Emms, P. W. and Fowler, A. C. 1994 Compositional convection in the solidification of binary alloys. *J. Fluid Mech.* **262**, 111–139. [10.2.3]
- Ene, H. I. 1991 Effects of anisotropy on the free convection from a vertical plate embedded in a porous medium. *Transport in Porous Media* **6**, 183–194. [5.1.9.5]
- Ene, H. I. 1997 Thermal flow, in *Homogenization and Porous Media* (U. Hornung, ed.) Springer, pp. 147–162. [1.4]
- Ene, H. I. 2004 Modeling the flow through porous media. In *Emerging Technologies and Techniques in Porous Media* (D. B. Ingham, A. Bejan, E. Mamut and I. Pop, eds), Kluwer Academic, Dordrecht, pp. 25–41. [1.4.3]
- Ene, H. I. and Polievski, D. 1987 *Thermal Flow in Porous Media*, Reidel, Dordrecht. [1.4.3, 5.6.2, 5.11.2]
- Ene, H. I. and Sanchez-Palencia, E. 1982 On thermal equation for flow in porous media. *Int. J. Engng. Sci.* **20**, 623–630. [2.2.3]
- Ennis-King, J. and Paterson, L. 2003 Rate of dissolution due to convective mixing in the underground storage of carbon dioxide. *Greenhouse Gas Control Tech.* 1 & 2, 507–51. and 1653–1656. [11.11]
- Ennis-King, J. and Paterson, L. 2005 Role of convective mixing in the long-term storage of carbon dioxide in deep saline formations. *SPE J.* **10**, 349–356. [6.11.3, 11.11]
- Ennis-King, J. and Paterson, L. 2007 Coupling of geochemical reactions and convective mixing in the long-term geological storage of carbon dioxide. *Int. J. Greenhouse Gas Control* **1**, 86–93. [11.11]
- Ennis-King, J., Preston, I. and Paterson, J. 2005 Onset of convection in anisotropic porous media subject to a rapid change of boundary conditions. *Phys. Fluids* **17**, art. no. 084107. [6.11.3]
- Epherre, J. F. 1975 Criterion for the appearance of natural convection in an anisotropic porous layer. *Rev. Gén. Therm.* **168**, 949–950. English translation, *Int. Chem. Engng.* **17**, 615–616. 1977. [6.12]
- Ergun, S. 1952 Fluid flow through packed columns. *Chem. Engrg. Prog.* **48**, 89–94. [1.5.2, 6.9.2]
- Er-Raki, M., Hasnaoui, M., Amahmid, A. and Bourich, M. 2005 Soret driven thermosolutal convection in a shallow porous layer with a stress-free upper surface. *Engng. Comput.* **22**, 186–205. [9.1.4]
- Er-Raki, M., Hasnaoui, M., Amahmid, A. and Bourich, M. 2011 Subcritical convection in the presence of Soret effect with a horizontal porous enclosure heated and salted from the short sides. *Int. J. Numer. Meth. Heat Fluid Flow* **21**, 150–167. [9.1.6.4]

- Er-Raki, M., Hasnaoui, M., Amahmid, A. and Mamou, M. 2006a Soret effect on the boundary layer flow regime in a vertical porous enclosure subject to horizontal heat and mass fluxes. *Int. J. Heat Mass Transfer* **49**, 3111–3120. [9.1.4]
- Er-Raki, M., Hasnaoui, M., Amahmid, A., El Ganaoui, M. 2008a Specific behaviour of thermosolutal convection induced in a vertical porous medium in the case of separation coefficient identical to the ratio of buoyancy forces. *C. R. Mecanique* **336**, 304–312. [9.1.4]
- Er-Raki, M., Hasnaoui, M., Amahmid, A., El Ganaoui, M. 2008b Thermosolutal convection within a vertical porous enclosure in the case of a buoyancy ratio balancing the separation parameter. *Int. J. Therm. Sci.* **48**, 1129–1137. [9.1.4]
- Er-Raki, M., Hasnaoui, M., Amahmid, A., Mamou, M. and Bourich, M. 2007 Soret effect on double diffusive boundary layer flows in a vertical porous cavity. *J. Porous Media* **10**, 783–795. [9.1.4]
- Errera, M. R. and Bejan, A. 1999 Tree networks for flows in composite porous media. *J. Porous Media* **2**, 1–17. [4.18]
- Erriquible, A., Bernada, P., Coutoure, F. and Roques, M. 2006b Simulation of convective drying of a porous medium with boundary conditions provided by CFD. *Chem. Engng. Res. Design* **84**, 113–123. [3.6]
- Essome, G. R. and Orozco, J. 1991 An analysis of film boiling on a binary mixture in a porous medium. *Int. J. Heat Mass Transfer* **34**, 757–766. [10.3.2]
- Estebe, J. and Schott, J. 1970 Concentration saline et cristallisation dans un milieu poreux par effet thermogravitationnel. *C. R. Acad. Sci. Paris* **271**, 805–807. [9.1.6.4]
- Eswaramurthi, M. and Kandaswamy, P. 2009 Transient double-diffusive convection of water around 4 degrees C in a porous cavity. *ASME J. Heat Transfer* **131**, #052601 [9.2.2].
- Eswaramurthi, M., Kandaswamy, P. and Lee, J. 2008 Effect of density maximum of water on natural convection in a porous cavity. *J. Porous Media* **11**, 179–19. [6.20]
- Ettefagh, J., Vafai, K. and Kim, S. J. 1991 Non-Darcian effects in open ended cavities filled with a porous medium. *ASME J. Heat Transfer* **113**, 747–756. [5.12.3]
- Evans, D. G. and Nunn, J. A. 1989 Free thermohaline convection in sediments surrounding a salt column. *J. Geophys. Res.* **94**, 12413–12422. [11.8]
- Evans, G. H. and Plumb, O. A. 1978 Natural convection from a vertical isothermal surface imbedded in a saturated porous medium. *AIAA-ASME Thermophysics and Heat Transfer Conf.*, Paper 78-HT –55, Palo Alto, California. [5.1.7.1, 5.1.8]
- Facas, G. N. 1994 Reducing the heat transfer from a hot pipe buried in a semi-infinite, saturated, porous medium. *ASME J. Heat Transfer*, **116**, 473–476. [7.11]
- Facas, G. N. 1995a Natural convection from a buried pipe with external baffles. *Numer. Heat Transfer A*, **27**, 595–609. [7.11]
- Facas, G. N. 1995b Natural convection from a buried elliptic heat source. *Int. J. Fluid Flow* **16**, 519–526. [7.11]
- Facas, G. N. and Farouk, B. 1983 Transient and steady-state natural convection in a porous medium between two concentric cylinders. *ASME J. Heat Transfer* **105**, 660–663. [7.3.3]
- Falsaperla, P., Giacobbe, A. and Mulone, G. 2012 Double diffusion in rotating porous media under general boundary conditions. *Int. J. Heat Mass Transfer* **55**, 2412–2419. [9.1.3]
- Falsaperla, P., Mulone, G. and Straughan, B. 2010 Rotating porous convection with prescribed heat flux. *Int. J. Engng. Sci.* **48**, 685–692. [6.22]
- Falsaperla, P., Mulone, G. and Straughan, B. 2011 Inertia effects on rotating porous convection. *Int. J. Heat Mass Transfe* **54**, 52–1359. [6.22]
- Fand, R. M. and Phan, R. T. 1987 Combined forced and natural convection heat transfer from a horizontal cylinder embedded in a porous medium. *Int. J. Heat Mass Transfer* **30**, 1351–1358. [8.1.3]
- Fand, R. M. and Yamamoto, L. H. 1990 Heat transfer by natural convection from a horizontal cylinder embedded in a porous medium: the wall effect. *Heat Transfer 1990*, Hemisphere, New York, **5**, 183–188. [5.5.2]

- Fand, R. M., Steinberger, T. E. and Cheng, P. 1986 Natural convection heat transfer from a horizontal cylinder embedded in a porous medium. *Int. J. Heat Mass Transfer* **29**, 119–133. [5.5.2]
- Fand, R. M., Varahasamy, M. and Greer, L. S. 1993 Empirical correlation equations for heat transfer by forced convection from cylinders embedded in porous media that account for the wall effect and dispersion. *Int. J. Heat Mass Transfer* **36**, 4407–4418. [4.8]
- Fand, R. M., Varahasamy, M. and Yamamoto, L. M. 1994 Heat transfer by natural convection from horizontal cylinders embedded in porous media whose matrices are composed of spheres: viscous dissipation. *Heat Transfer 1994, Inst. Chem. Engrs., Rugby*, vol. 5, pp. 237–242. [5.5.1]
- Fang, T., Tao, H. and Zhong, Y. 2012 Note on the unsteady mixed boundary layer in a porous medium with temperature slip: Exact solutions. *Transp. Porous Media* **94**, 189–196. [8.1.1]
- Farajzadeh, R., Ranganathan, P., Zitha, P. L. J. and Bruining, J. 2011 The effect of heterogeneity on the character of density-driven convection of CO<sub>2</sub> overlying a brine layer. *Adv. Water Res.* **34**, 327–339. [11.11]
- Farajzadeh, R., Salimi, H., Zithna, P. L. J. and Bruining, H. 2007 Numerical simulation of density-driven natural convection in porous media with application for CO<sub>2</sub> injection. *Int. J. Heat Mass Transfer* **50**, 5054–5064. [11.11]
- Farouk, B. and Shayer, H. 1988 Natural convection around a heated cylinder in a saturated porous medium. *ASME J. Heat Transfer* **110**, 642–648. [7.11]
- Farr, W. W., Gabito, J. F., Luss, D. and Balakotaiah, V. 1991 Reaction-driven convection in a porous medium: Part 1. Linear stability analysis. *AICHE J.* **37**, 963–975. [3.4]
- Faruque, D., Saghir, M. Z., Chacha, M. and Ghorayeb, K. 2004 Compositional variation considering diffusion and convection for a binary mixture in a porous medium. *J. Porous Media* **7**, 73–91. [9.1.4]
- Felicelli, S. D., Heinrich, J. C. and Poirier, D. R. 1991 Simulation of freckles during vertical solidification of binary alloys. *Metall. Trans. B* **22**, 847–859. [10.2.3]
- Feltham, D. L. and Worster, M. G. 1999 Flow-induced morphological instability of a mushy layer. *J. Fluid Mech.* **391**, 337–357. [10.2.3]
- Feltham, D. L., Untersteiner, N., Wetzlaufer, J. B. and Worster, M. G. 2006 Sea ice is a mushy layer. *Geophys. Res. Lett.* **33**, #L14501. [10.2.3]
- Feng, Z. G. and Michaelides, E. E. 1999 Unsteady mass transport from a sphere immersed in a porous medium at finite Péclet numbers. *Int. J. Heat Mass Transfer* **42**, 535–546. [8.1.3]
- Ferdows, M., Kaino, K. and Sivasankaran, S. 2009 Free convection flow in an inclined porous surface. *J. Porous Media* **12**, 997–1003. [5.3]
- Fernandez, R. T. and Schrock, V. E. 1982 Natural convection from cylinders embedded in a liquid-saturated porous medium. *Heat Transfer 1982*, Elsevier, Amsterdam, **2**, 335–340. [7.11]
- Figueiredo, J. R. and Llagostera, T. 1999 Comparative study of the unified finite approach exponential-type scheme (UNIFAES) and its application to natural convection in a porous cavity. *Numer. Heat Transfer B* **35**, 347–367. [6.8]
- Figus, C., Le Bray, Y., Bories, S. and Prat, M. 1998 Heat transfer in porous media considering phase change, capillarity and gravity. Application to capillary evaporator. *Heat Transfer 1998, Proc. 11th IHTC*, **4**, 393–398. [3.6]
- Firdaous, M., Gurmond, J. L. and Le Quéré, P. 1997 Nonlinear corrections to Darcy's law at low Reynolds Number. *J. Fluid Mech.* **343**, 331–350. [1.5.2]
- Flavin, J. N. and Rionero, S. 1999 Nonlinear stability for a thermofluid in a vertical porous slab. *Cont. Mech. Thermodyn.* **11**, 173–179. [7.1.4]
- Flick, D., Leslous, A. and Alvarez, G. 2003 Semi-empirical modeling of turbulent fluid flow and heat transfer in porous media. *Int. J. Refrig.* **26**, 349–359. [1.8]
- Fomin, S., Shimizu, A. and Hashida, T. 2002 Mathematical modeling of convection heat transfer in a geothermal reservoir of fractal geometry. *Heat Transfer 2002, Proc. 12th Int. Heat Transfer Conf.*, Elsevier, Vol. 2, pp. 809–814. [2.6]

- Fontaine, F. J., Rabinowicz, M. and Boulegue J. 2001 Permeability changes due to mineral diagenesis in fractured crust: implications for hydrothermal circulation at mid-ocean ridges. *Earth Planet. Sci. Lett.* **184**, 407–425. [11.5]
- Forchheimer, P. 1901 Wasserbewegung durch Boden. *Zeitschrift des Vereines Deutscher Ingenieure* **45**, 1736–174. and 1781–1788. [1.5.2]
- Forooghi, P., Abkar, M. and Saffar-Awal, M. 2011 Steady and unsteady heat transfer in a channel partially filled with porous media under thermal non-equilibrium conditions. *Transp. Porous Media* **86**, 207–228. [4.10]
- Foudi, W., Dhifaoui, B., Ben Jabrallah, S., Belgith, A. and Corriou, J. P. 2012 Numerical and experimental study of convective heat transfer in a vertical porous channel using a non-equilibrium approach. *J. Porous Media* **15**, 531–547. [7.1.7]
- Fourar, M., Lenormand, R., Karimi-Fard, M. and Horne, R. 2005 Inertia effects in high-rate flow through heterogeneous porous media. *Transport Porous Media* **60**, 353–370. [1.5.2]
- Fourie, J. G. and Du Plessis, J. P. 2003a A two-equation model for heat conduction in porous media. (I. Theory) *Transport Porous Media* **53**, 145–161. [2.2.3]
- Fourie, J. G. and Du Plessis, J. P. 2003b A two-equation model for heat conduction in porous media. (II. Application) *Transport Porous Media* **53**, 163–174. [2.2.3]
- Fowler, A. C. 1985 The formation of freckles in binary alloys. *IMA J. Appl. Maths.* **35**, 159–174. [10.2.3]
- Fowler, A. J. and Bejan, A. 1994 Forced convection in banks of inclined cylinders at low Reynolds numbers. *Int. J. Heat Fluid Flow* **15**, 90–99. [4.14]
- Fowler, A. J. and Bejan, A. 1995 Forced convection from a surface covered with flexible fibers. *Int. J. Heat Mass Transfer* **38**, 767–777. [1.9, 4.14]
- Francis, N. D. and Wepfer, J. W. 1996 Jet impingement drying of a moist porous solid. *Int. J. Heat Mass Transfer* **35**, 469–480. [3.6]
- Frei, K. M., Cameron, D. and Stuart, P. R. 2004 Novel drying process using forced aeration through a porous biomass matrix. *Drying Tech.* **22**, 1191–1215. [3.6]
- Friedrich, R. 1983 Einfluss der Prandtl-Zahl auf die Zellularkonvektion in einem rotierenden, mit Fluid gesättigten porösen Medium. *ZAMM* **63**, T246—T249. [6.22]
- Frizon, F., Lorente, S., Ollivier, J. P. and Thouvenot, P. 2003 Transport model for the nuclear decontamination of cementitious materials. *Comput. Materials Sci.* **27**, 507–516. [3.7]
- Fu, C. J., Zhang, Z. Y. and Tan, W. C. 2007 Numerical simulation of thermal convection of a viscoelastic fluid in a porous square box heated from below. *Phys. Fluids Art.* # 104107. [6.23]
- Fu, H. L., Leong, K. C., Huang, X. Y. and Liu, C. Y. 2001 An experimental study of heat transfer of a porous channel subjected to oscillating flow. *ASME J. Heat Transfer* **123**, 162–17. (erratum p. 1194). [4.6.4]
- Fu, W. S. and Chen, S. F. 2002 A numerical study of heat transfer of a porous block with the random porosity model in a channel flow. *Heat Mass Transfer* **38**, 695–704. [4.16.1]
- Fu, W. S. and Huang, H. C. 1999 Effects of random porosity model on heat transfer performance of porous media. *Int. J. Heat Mass Transfer* **42**, 13–25. [1.7]
- Fu, W. S. and Ke, W. W. 2000 Effects of random porosity model on double-diffusive natural convection in a porous medium enclosure. *Int. Comm. Heat Mass Transfer* **27**, 119–132. [9.2.2]
- Fu, W. S., Huang, H. C. and Liou, W. Y. 1996 Thermal enhancement in laminar channel flow with a porous block. *Int. J. Heat Mass Transfer* **39**, 2165–2175. [4.11]
- Fu, W. S., Wang, K. N. and Ke, W. W. 2001 Heat transfer of porous medium with random porosity model in a laminar channel flow. *J. Chinese Inst. Engrs.* **24**, 431–438. [4.16.5]
- Fu, X., Viskanta, R. and Gore, J. P. 1998 Prediction of effective thermal conductivity for cellular ceramics. *Int. Comm. Heat Mass Transfer* **25**, 151–161. [2.2.1]
- Fujii, Y., Ohita, K. and Hijikata, A. 1994 Unsteady heat transfer around a periodically-heated cylinder embedded in saturated porous media. *Heat Transfer 1994, Inst. Chem. Engrs, Rugby*, Vol. 5, 249–254. [4.8]
- Gabito, J. F. and Balakotaiah, V. 1991 Reaction-driven convection in a porous medium: Part 2. Numerical bifurcation analysis. *AIChE J.* **37**, 976–985. [3.4]

- Gaikwad, S. N. and Kousar, S. 2012 Analytical study of linear and nonlinear double diffusive convection in a rotating anisotropic porous layer with Soret effect. *J. Porous Media* **15**, 745–774. [9.1.4]
- Gaikwad, S. N. and Prasad, K. R. 2011 An analytical study of double diffusive convection in a porous medium saturated with couple stress fluid in the presence of Soret effect. *J. Porous Media* **14**, 1019–1031. [9.1.4]
- Gaikwad, S. N., Malashetty, M. S. and Prasad, K. R. 2009a An analytical study of linear and nonlinear double diffusive convection in a fluid saturated anisotropic porous layer with Soret effect. *Appl. Math. Modell.* **33**, 3617–3635. [9.1.4]
- Gaikwad, S. N., Malashetty, M. S. and Prasad, K. R. 2009b Linear and nonlinear double diffusive convection in a fluid-saturated anisotropic porous layer with cross-diffusion effects. *Transp. Porous Media* **80**, 537–560. [9.1.4]
- Galdi, G. P., Payne, L. E., Proctor, M. R. E. and Straughan, B. 1987 Convection in thawing subsea permafrost. *Proc. Roy. Soc. London Ser. A* **414**, 83–102. [11.3]
- Gamrat, G., Favre-Marinet, M. and Le Person, S. 2008 Numerical study of heat transfer over banks of rods in small Reynolds number cross-flow. *Int. J. Heat Mass Transfer* **51**, 853–864. [2.6]
- Ganapathy, R. 1992 Thermal convection in an infinite porous medium due to a source in a sphere. *Fluid Dyn. Res.* **9**, 223–234. [5.11.2]
- Ganapathy, R. 1994a Free convective heat and mass transfer flow induced by an instantaneous point source in an infinite porous medium. *Fluid Dyn. Res.* **14**, 313–329. [5.11.2]
- Ganapathy, R. 1994b Free convection flow induced by a line source in a sparsely packed porous medium. *Adv. Water Resources* **17**, 251–258. Corrigendum **19**, 255–257. [9.3.2]
- Ganapathy, R. 1997 Thermal convection in an infinite porous medium induced by a heated sphere. *ASME J. Heat Transfer* **119**, 647–650. [5.6.2]
- Ganapathy, R. and Purushothaman, R. 1990 Thermal convection from an instantaneous point heat source in a porous medium. *Int. J. Engng. Sci.* **28**, 907–918. [5.11.2]
- Ganapathy, R. and Purushothaman, R. 1992 Free convection in a saturated porous medium due to a traveling thermal wave. *Z. Angew. Math. Mech.* **72**, 142–145. [6.11.3]
- Ganesan, S. and Poirier, D. R. 1990 Conservation of mass and momentum for the flow of interdendritic liquid during solidification. *Mettal. Trans. B* **21**, 173–181. [10.2.3]
- Gao, D. Y. and Chen, Z. Q. 2011 Lattice Boltzmann simulation of natural convection dominated melting in a rectangular cavity filled with porous media. *Int. J. Therm. Sci.* **50**, 493–501. [10.1.7]
- Gartling, D. K. and Hickox, C. E. 1985 Numerical study of the applicability of the Boussinesq approximation for a fluid-saturated porous medium. *Int. J. Numer. Methods Fluids* **5**, 995–1013. [6.7]
- Gartling, D. K., Hickox, C. E. and Givler, R. C. 1996 Simulation of coupled viscous and porous flow problems. *Comp. Fluid Dyn.* **7**, 23–48. [1.6]
- Gasser, R. D. and Kazimi, M. S. 1976 Onset of convection in a porous medium with internal heat generation. *ASME J. Heat Transfer* **98**, 49–54. Corrections, 302–302. [6.11.2]
- Gatica, J. E., Viljoen, H. J., and Hlavacek, V. 1989 Interaction between chemical reaction and natural convection in porous media. *Chem. Eng. Sci.* **44**, 1853–1870. [3.4]
- Geiger, S., Driesner, T., Heinrich, C. A. and Matthäi, S. K. 2006a Multiphase thermohaline convection in the Earth's crust: I. A new finite element–finite volume solution technique combined with a new equation of state for NaCl-H<sub>2</sub>O. *Transport Porous Media* **63**, 399–434. [11.9.3]
- Geiger, S., Driesner, T., Heinrich, C. A. and Matthäi, S. K. 2006b Multiphase thermohaline convection in the Earth's crust: II. Benchmarking and application of a finite element—finite volume technique with a NaCl-H<sub>2</sub>O equation of state. *Transport Porous Media* **63**, 431–461. [11.9.3]
- Geiger, S., Driesner, T., Heinrich, C. A. and Matthäi, S. K. 2005 On the dynamics of NaCl-H<sub>2</sub>O fluid convection in the Earth's crust. *J. Geophys. Res.* **110**, Art. No. B07101. [11.8]

- Genc, G. and Rees, D. A. S. 2011 The onset of convection in horizontally partitioned porous layers. *Phys. Fluids* **23**, #064107. [6.10.1]
- Gentile, M. and Rionero, S. 2000 A note on the global nonlinear stability for penetrative convection in porous media with fluids of cubic density. *Rend. Accad. Sci. Fiz. Matem. Napoli*, **67**, 129–142. [6.4]
- George, J. H., Gunn, R. D., and Straughan, B. 1989 Patterned ground formation and penetrative convection in porous media. *Geophys. Astrophys. Fluid Dyn.* **46**, 135–158. [11.2]
- Georgiadis, J. G. 1991 Effect of randomness on heat and mass transfer in porous media. *Convective Heat and Mass Transfer in Porous Media* (eds. S. Kakaç, *et al.*), Kluwer Academic, Dordrecht, 499–524. [1.1]
- Georgiadis, J. G. and Catton, I. 1985 Free convective motion in an infinite vertical porous slot: the non-Darcian regime. *Int. J. Heat Mass Transfer* **28**, 2389–2392. [7.1.4]
- Georgiadis, J. G. and Catton, I. 1986 Prandtl number effect on Bénard convection in porous media. *ASME J. Heat Transfer* **108**, 284–290. [6.9.2]
- Georgiadis, J. G. and Catton, I. 1987 Stochastic modeling of unidirectional fluid transport in uniform and random packed beds. *Phys. Fluids* **30**, 1017–1022. [1.1, 1.7]
- Georgiadis, J. G. and Catton, I. 1988 Dispersion in cellular thermal convection in porous media. *Int. J. Heat Mass Transfer* **31**, 1081–1091. [1.1, 6.6]
- Gerritsen, M. G., Chen, T. and Chen, Q. 2005 Stanford University, private communication.
- Gershuni, G. Z. and Lyubimov, D. V. 1998 *Thermal Vibration Convection*. Wiley, New York. [6.24]
- Gershuni, G. Z., Zhukhovitskii, E. M. and Lyubimov, D. V. 1976 Thermo-concentration instability of a mixture in a porous medium. *Dokl. Akad. Nauk. SSSR* **229**, 575–57. (English translation *Sov. Phys. Dokl.* **21**, 375–377.) [9.2.4]
- Gershuni, G. Z., Zhukhovitskii, E. M. and Lyubimov, D. V. 1980 Stability of stationary convective flow of a mixture in a vertical porous layer. *Fluid Dynamics* **15**, 122–127. [9.2.4]
- Getachew, D., Minkowycz, W. J. and Lage, J. L. 2000 A modified form of the  $\kappa - \varepsilon$  model for turbulent flows of an incompressible fluid in porous media. *Int. J. Heat Mass Transfer* **43**, 2909–2915. [1.8]
- Getachew, D., Minkowycz, W. J. and Poulikakos, D. 1996 Natural convection in a porous cavity saturated with a non-Newtonian fluid. *J. Thermophys. Heat Transfer* **10**, 640–651. [7.1.6]
- Getachew, D., Poulikakos, D. and Minkowycz, W. J. 1998 Double diffusion in porous cavity saturated with non-Newtonian fluid. *J. Thermophys. Heat Transfer* **12**, 437–446. [9.2.2]
- Ghafir, R. and Lauriat, G. 2001 Forced convection heat transfer with evaporation in a heat generating porous medium. *J. Porous Media* **4**, 309–322. [10.4]
- Ghazanfarian, J. and Abbassi, A. 2007 Mixed convection in a square cavity filled with a porous medium and different exit port position. *J. Porous Media* **10**, 701–718. [8.4.3]
- Ghazian, O., Rezvantalab, H. and Mehdi, A. 2011 Analytical investigation of the effect of viscous dissipation on Couette flow in a channel partially filled with a porous medium *Transp. Porous Media* **89**, 1–13. [4.11]
- Ghazvini, M. , Akhavan-Behabadi, M. A. and Esmaeili, M. 2009 The effect of viscous dissipation on laminar nanofluid flow in a microchannel heat sink. *J. Mech. Engng. Sci.* **263**, 2697–2706. [4.16.5]
- Ghazvini, M. and Shokouhmand, H. 2009 Investigation of nanofluid-cooled microchannel heat sink using fin and porous media approaches. *Energy Convers. Manag.* **50**, 2373–238. [4.16.5]
- Gheorghita, St. I. 1961 The marginal stability in porous inhomogeneous media. *Proc. Camb. Phil. Soc.* **57**, 871–877. [6.13.1].
- Ghesmat, K., Hassanzadeh, H. and Abedi, J. 2011 The impact of geochemistry on convective mixing in a gravitationally unstable diffusive boundary layer in porous media: CO<sub>2</sub> storage in saline aquifers. *J. Fluid Mech.* **678**, 480–512. [11.11]
- Ghesmat, K., Hassanzadeh, H. and Abedi, J. 2011b The effect of anisotropic dispersion on the convective mixing in long term CO<sub>2</sub> storage in saline aquifers. *AIChE J.* **57**, 561–570. [11.11]

- Ghorayeb, K. and Firoozabadi, A. 2000a Numerical study of natural convection and diffusion in fractured porous media. *SPE Journal* **5**, 12–20. [1.9]
- Ghorayeb, K. and Firoozabadi, A. 2000b Modeling multicomponent diffusion and convection in porous media. *SPE Journal* **5**, 158–171. [1.9]
- Ghorayeb, K. and Firoozabadi, A. 2001 Features of convection and diffusion in porous media for binary systems. *J. Canad. Petrol. Tech.* **40**, 21–28. [1.9]
- Ghosh, P. and Ghosh, M. K. 2009 Streaming flows in differentially heated square porous cavity under sinusoidal g-jitter. *Int. J. Therm. Sci.* **48**, 514–520. [7.1.7]
- Ghosh, S., Das, T., Chakraborty, S. and Das, S. K. 2011 Predicting DNA-mediated drug delivery in interior carcinoma using electromagnetically excited nanoparticles. *Comput. Biol. Med.* **41**, 771–779. [1.9]
- Gibson, P. W. and Charmchi, M. 1997 Modeling convection/diffusion processes in porous textiles with inclusion of humidity-dependent air permeability. *Int. Comm. Heat Mass Transfer* **24**, 709–724. [3.6]
- Gill, A. E. 1969 A proof that convection in a porous vertical slab is stable. *J. Fluid Mech.* **35**, 545–547. [7.1.4]
- Gill, U. S. and Minkowycz, W. J. 1988 Boundary and inertia effects on conjugate mixed convection heat transfer from a vertical plate fin in a high-porosity porous medium. *Int. J. Heat Mass Transfer* **31**, 419–427. [5.12.1]
- Gill, U. S., Minkowycz, W. J., Chen, C. K. and Chen, C. H. 1992 Boundary and inertia effects on conjugate mixed convection-conduction heat transfer from a vertical circular fin embedded in a porous medium. *Numer. Heat Transfer A* **21**, 423–441. [8.1.4]
- Gilman, A. and Bear, J. 1996 The influence of free convection on soil salinization in arid regions. *Transport Porous Media* **23**, 275–301. [9.1.6.4, 11.8]
- Giorgi, T. 1997 Derivation of the Forchheimer law via matched asymptotic expansions. *Transport Porous Media* **29**, 191–206. [1.5.2]
- Givler, R. C. and Altobelli, S. A. 1994 A determination of the effective viscosity for the Brinkman-Forchheimer flow model. *J. Fluid Mech.* **258**, 355–370. [1.5.3]
- Gjerde, K. M. and Tyvand, P. A. 1984 Thermal convection in a porous medium with continuous periodic stratification. *Int. J. Heat Mass Transfer* **27**, 2289–2295. [6.13.2]
- Gleason, K. J., Krantz, W. B., Caine, N., George, J. H. and Gunn, R. D. 1986 Geometrical aspects of sorted patterned ground in recurrently frozen soil. *Science* **232**, 216–220. [11.2]
- Gobin, D. and Goyeau, B. 2008 Natural convection in partially porous media: a brief overview. *Int. J. Numer. Meth. Heat Fluid Flow* **18**, 465–490. [6.9]
- Gobin, D., Goyeau, B. 2012 Thermosolutal natural convection in partially porous domains. *ASME J. Heat Transfer* **134**, #031013. [1.6, 9.4]
- Gobin, D., Goyeau, B. and Neculae, A. 2005 Convective heat and solute transfer in partially porous cavities. *Int. J. Heat Mass Transfer* **48**, 1898–1908. [9.4]
- Gobin, D., Goyeau, B. and Songbe, J. P. 1998 Double diffusive natural convection in a composite porous layer. *ASME J. Heat Transfer* **120**, 234–242. [9.4]
- Goel, A. K. and Agrawal, S. C. 1998 A numerical study of the hydromagnetic thermal convection in a visco-elastic dusty fluid in a porous medium. *Indian J. Pure Appl. Math.* **29**, 929–940. [6.21]
- Goering, D. J. 2003 Passively cooled railway embankments for use in permafrost areas. *J. Cold Reg. Engng.* **17**, 119–133. [7.3.7]
- Goering, D. J. and Kumar, P. 1996 Winter-time convection in open-graded embankments. *Cold Reg. Sci. Tech.* **24**, 57–74. [7.3.7]
- Goharzadeh, A., Khalili, A. and Jørgensen, B. B. 2005 Transition layer thickness at a fluid-porous interface. *Phys. Fluids* **17**, 057102. [1.6]
- Goldobin, D. S. and Lyubimov, D. V. 2007 Soret-driven convection of binary mixture in a horizontal porous layer in the presence of a heat or concentration source. *J. Exper. Theor. Phys.* **104**, 830–836. [9.1.4]

- Goldobin, D. S. and Shklyaeva, E. V. 2008 Large-scale thermal convection in a horizontal porous layer. *Phys. Rev. E* **78**, #027301. [6.8]
- Goldstein, R. E., Pesci, A. I. and Shelley, M. J. 1998 Instabilities and singularities in Hele-Shaw flow. *Phys. Fluids* **10**, 2701–2723. [2.5]
- Golfier, F., Quintard, M. and Whitaker, S. 2002 Heat and mass transfer in tubes: an analysis using the method of volume averaging. *J. Porous Media* **5**, 169–185. [2.2.3]
- Gorin, A. V., Nakoryakov, V. E., Khoruzhenko, A. G. and Tsoi, O. N. 1988 Heat transfer during mixed convection on a vertical surface in a porous medium with deviation from Darcy's law. *J. Appl. Mech. Tech. Phys.* **29**, 133–139. [8.1.1]
- Gorin, A. V., Sikovsky, D. P., Mikhailova, T. N. and Mukhin, V. A. 1998 Forced convection heat and mass transfer from a circular cylinder in a Hele-Shaw cell. *Heat Transfer 1998, Proc. 11th IHTC*, **3**, 109–114. [2.5]
- Gorla, R. S. R. and Bakier, A. Y. 2011 Thermal analysis of natural convection and radiation in porous fins. *Int. Comm. Heat Mass Transfer* **38**, 638–645. [5.12.1]
- Gorla, R. S. R. and Chamkha, A. 2011 Natural convective boundary layer flow over a non-isothermal vertical plate embedded in a porous medium saturated with a nanofluid. *Nanoscale Microscale Thermophys. Engng.* **15**, 81–94. [5.1.9.9]
- Gorla, R. S. R. and Kumari, M. 1996 Mixed convection in non-Newtonian fluids along a vertical plate in a porous medium. *Acta Mech.* **118**, 55–64. [8.1.1]
- Gorla, R. S. R. and Kumari, M. 1998 Nonsimilar solutions for mixed convection in non-Newtonian fluids along a vertical plate in a porous medium. *Transport Porous Media* **33**, 295–307. [8.1.1]
- Gorla, R. S. R. and Kumari, M. 1999a Mixed convection in non-Newtonian fluids along a vertical plate with a variable surface heat flux in a porous medium. *Heat Mass Transfer* **35**, 221–227. [8.1.1]
- Gorla, R. S. R. and Kumari, M. 1999b Nonsimilar solutions for mixed convection in non-Newtonian fluids along a wedge with variable surface temperature in a porous medium. *Int. J. Numer. Meth. Heat Fluid Flow* **9**, 601–611. [8.1.1]
- Gorla, R. S. R. and Kumari, M. 1999c Nonsimilar solutions for free convection in non-Newtonian fluids along a vertical plate in a porous medium. *Int. J. Numer. Meth. Heat Fluid Flow* **9**, 847–859. [8.1.1]
- Gorla, R. S. R. and Kumari, M. 2000 Nonsimilar solutions for mixed convection in non-Newtonian fluids along a wedge with variable surface heat flux in a porous medium. *J. Porous Media* **3**, 181–184. [8.1.4]
- Gorla, R. S. R. and Kumari, M. 2003 Free convection in non-Newtonian fluids along a horizontal plate in a porous medium. *Heat Mass Transfer* **39**, 101–106. [5.2]
- Gorla, R. S. R. and Tornabene, R. 1988 Free convection from a vertical plate with nonuniform surface heat flux and embedded in a porous medium. *Transport in Porous Media* **3**, 95–105. [5.1.9.9]
- Gorla, R. S. R. and Zinalabedini, A. H. 1987 Free convection from a vertical plate with nonuniform surface temperature and embedded in a porous medium. *ASME J. Energy Res. Tech.* **109**, 27–30. [5.1.9.9]
- Gorla, R. S. R., Bakier, A. Y. and Byrd, L. 1996 Effects of thermal dispersion and stratification on combined convection on a vertical surface embedded in a porous medium. *Transport Porous Media* **25**, 275–282. [8.1.1]
- Gorla, R. S. R., Chamkha, A. J. and Rashad, A. M. 2011 Mixed convective boundary layer flow past a vertical cylinder in a nanofluid. *Nanoscale Res. Lett.* **6**, #207. [8.1.3]
- Gorla, R. S. R., Chamkha, A., Khan, W. A. and Murthy, P. V. S. N. 2012 Second law analysis for combined convection in non-Newtonian fluids over a vertical wedge in a porous medium. *J. Porous Media* **15**, 187–196. [8.1.4]
- Gorla, R. S. R., Mansour, M. A. and Sarhar, M. G. 1999b Natural convection from a vertical plate in a porous medium using Brinkman's model. *Transport Porous Media* **36**, 357–371. [5.1.7.1]
- Gorla, R. S. R., Mansour, M. A., Hasssanien, I. A. and Bakier, A. Y. 1999a Mixed convection effect on melting from a vertical plate in a porous medium. *Transport Porous Media* **36**, 245–254. [10.1.7]

- Gorla, R. S. R., Shammugam, K. and Kumari, M. 1998 Mixed convection in non-Newtonian fluids along nonisothermal horizontal surfaces in porous media. *Heat Mass Transfer* **33**, 281–286. [8.1.2]
- Gorla, R. S. R., Slaouti, A. and Takhar, H. S. 1997 Mixed convection in non-Newtonian fluids along a vertical plate in porous media with surface mass transfer. *Int. J. Numer. Methods Heat Fluid Flow* **7**, 598–608. [8.1.1]
- Gosink, J. P. and Baker, G. C. 1990 Salt fingering in subsea permafrost: some stability and energy considerations. *J. Geophys. Res.* **95**, 9575–9583. [11.3]
- Gounot, J. and Caltagirone, J. P. 1989 Stabilité et convection naturelle au sein d'une couche poreuse non homogène. *Int. J. Heat Mass Transfer* **32**, 1131–1140. [6.13.4]
- Gouze, P., Coudrain-Ribstein, A. and Dominique, B. 1994 Computation of porosity redistribution resulting from thermal convection in slanted porous layers. *J. Geophys. Res.* **99**, 697–706. [11.5]
- Govender, S. 2003a Oscillating convection induced by gravity and centrifugal forces in a rotating porous layer distant from the axis of rotation. *Int. J. Engng. Sci.* **41**, 539–545. [6.22]
- Govender, S. 2003b On the linear stability of large Stephan number convection in rotating mushy layers for a new Darcy equation formulation. *Transport Porous Media* **51**, 173–189. [10.2.3]
- Govender, S. 2003c Coriolis effect on the linear stability of convection in a porous layer placed far away from the axis of rotation. *Transport Porous Media* **51**, 315–326. [6.22]
- Govender, S. 2003d Finite amplitude analysis of convection in rotating mushy layers during solidification of binary alloys. *J. Porous Media* **6**, 137–147. [10.2.3]
- Govender, S. 2003e Moderate time scale finite amplitude analysis of large Stephan number convection in rotating mushy layers. *Transport Porous Media* **53**, 357–366. [10.2.3]
- Govender, S. 2004a Three-dimensional convection in an inclined porous layer heated from below and subjected to gravity and Coriolis effects. *Transport Porous Media* **55**, 103–112. [7.8]
- Govender, S. 2004b Stability of convection in a gravity modulated porous layer heated from below. *Transport Porous Media* **57**, 113–123. [6.24]
- Govender, S. 2004c Finite amplitude analysis of convection in rotating mushy layers for small variations in retardability. *J. Porous Media* **7**, 227–238. [10.2.3]
- Govender, S. 2005a Moderate Stefan number convection in rotating mushy layers: A new Darcy number formulation. *Transport Porous Media* **59**, 127–137. [10.2.3]
- Govender, S. 2005b Stefan number effect on the transition from stationary to oscillatory convection in a solidifying mushy layer subjected to rotation; Response to reviewer's comment. *Transport Porous Media* **58**, 361–369. [10.2.3]
- Govender, S. 2005c Destabilizing a fluid saturated gravity modulated porous layer heated from above. *Transport Porous Media* **59**, 215–225. [6.24]
- Govender, S. 2005d Linear stability and convection in a gravity modulated porous layer heated from below: Transition from synchronous to subharmonic oscillations. *Transport Porous Media* **59**, 227–238. [6.24]
- Govender, S. 2005e Stability analysis of a porous layer heated from below and subjected to low frequency vibration: Frozen time analysis. *Transport Porous Media*, in press . [6.24]
- Govender, S. 2005f Weak non-linear analysis of convection in a gravity modulated porous layer. *Transport Porous Media* **60**, 33–42. [6.24]
- Govender, S. 2005g Coriolis effect on flow stability in mushy layers solidifying in a microgravity environment. *J. Porous Media* **8**, 355–364. [10.2.3]
- Govender, S. 2006a Effect of anisotropy on stability of convection in a rotating porous layer distant from the centre of rotation. *J. Porous Media* **9**, 651–661. [6.22]
- Govender, S. 2006b On the effect of anisotropy on the stability of convection in rotating porous media. *Transport Porous Media* **64**, 413–422. [6.22]
- Govender, S. 2006c Stability of gravity driven convection in a cylindrical porous layer subjected to vibration. *Transp. Porous Media* **63**, 489–502. [6.24]
- Govender, S. 2007a An analogy between a gravity modulated porous layer heated from below and the inverted pendulum with an oscillating pivot point. *Transport Porous Media* **67**, 323–328. [6.24]

- Govender, S. 2007b Coriolis effect on the stability of centrifugally driven convection in a rotating anisotropic porous layer subjected to gravity. *Transport Porous Media* **67**, 219–227. [6.22]
- Govender, S. 2008a Linear stability of solutal convection in rotating mushy layers: Permeable mush-melt interface. *J. Porous Media* **11**, 683–690. [12.2.3]
- Govender, S. 2008b Natural convection in gravity-modulated porous layers. In P. Vadasz (ed.) *Emerging Topics in Heat and Mass Transfer in Porous Media*, Springer, New York, pp. 133–148. [6.24]
- Govender, S. 2011 Stability of moderate Vadasz number solutal convection in a cylindrical mushy layer subjected to vertical vibration. *Transport Porous Media* **88**, 225–234. [10.2.3]
- Govender, S. and Vadasz, P. 2007 The effect of mechanical and thermal anisotropy on the stability of gravity driven convection in rotating porous media in the presence of thermal non-equilibrium. *Transp. Porous Media* **69**, 55–66. [6.22]
- Govender, S. and Vadasz, P. 1995 Centrifugal and gravity driven convection in rotating porous media — an analogy with the inclined porous layer. *ASME HTD* **309**, 93–98. [6.22, 7.1.4]
- Govender, S. and Vadasz, P. 2002a Weak nonlinear analysis and moderate Stephan number oscillatory convection in rotating mushy layers. *Transport Porous Media* **48**, 353–372. [10.2.3]
- Govender, S. and Vadasz, P. 2002b Weak nonlinear analysis and moderate Stephan number stationary convection in rotating mushy layers. *Transport Porous Media* **49**, 247–263. [10.2.3]
- Govender, S. and Vadasz, P. 2002c Moderate time scale linear stability of moderate Stefan number convection in rotating mushy layers. *J. Porous Media* **5**, 113–121. [10.2.3]
- Goverukhin, V. N. and Shevchenko, I. V. 2006 Scenarios of the unsteady regimes in the problem of plane convective flow through a porous medium. *Fluid Dyn.* **41**, 967–975. 2006. [6.8]
- Goyeau, B. and Gobin, D. 1999 Heat transfer by thermosolutal natural convection in a vertical composite fluid-porous cavity. *Int. Comm. Heat Mass Transfer* **26**, 1115–1126. [9.4]
- Goyeau, B., Lhuillier, D. and Gobin, D. 2002 Momentum transfer at a fluid/porous interface. *Heat Transfer 2002, Proc. 12th Int. Heat Transfer Conf.*, Elsevier, Vol. 3, pp. 147–152. [1.6]
- Goyeau, B., Lhuillier, D., Gobin, D. and Velarde, M. G. 2003 Momentum transport at a fluid-porous interface. *Int. J. Heat Mass Transfer* **46**, 4071–4081. [1.6]
- Goyeau, B., Mergui, S., Songe, J. P. and Gobin, D. 1996b Convection thermosolutale en cavité partiellement occupée par une couche poreuse faiblement perméable. *C.R. Acad. Sci. Paris, Sér. II*, **323**, 447–454. [9.4]
- Goyeau, B., Songe, J. P. and Gobin, D. 1996a Numerical study of double-diffusive natural convection in a porous cavity using the Darcy-Brinkman formulation. *Int. J. Heat Mass Transfer* **39**, 1363–1378. [9.2.2]
- Graf, T. and Therrien, R. 2007a Coupled thermohaline groundwater flow and single-species reactive solute transport in fractured porous media. *Adv. Water Resour.* **30**, 742–771. [11.8]
- Graf, T. and Therrien, R. 2007b Variable-density groundwater flow and solute transport in irregular 2D fracture networks. *Adv. Water Resour.* **30**, 455–468. [11.8]
- Graf, T. and Therrien, R. 2009 Stable-unstable flow of geothermal fluids in fractured rock. *Geofluids* **9**, 138–152. [11.8]
- Graham, M. D. and Steen, P. H. 1991 Structure and mechanism of oscillatory convection in a cube of fluid-saturated porous material heated from below. *J. Fluid Mech.*, **232**, 591–609. [6.15.1]
- Graham, M. D. and Steen, P. H. 1992 Strongly interacting traveling waves and quasiperiodic dynamics in porous medium convection. *Physica D* **54**, 331–350. [6.15.1]
- Graham, M. D. and Steen, P. H. 1994 Plume formation and resonant bifurcations in porous-media convection. *J. Fluid Mech.* **272**, 67–89. [6.15.1]
- Graham, M. D., Steen, P. H. and Titi, S. 1993 Computational efficiency and approximate inertial manifolds for a Bénard convection system. *J. Nonlinear Sci.* **3**, 153–167. [6.15.1]
- Graham, M., Müller, U. and Steen, P. 1992 Time-periodic thermal convection in Hele-Shaw slots: The diagonal oscillation. *Phys. Fluids A* **4**, 2382–2393. [6.4]
- Grangeot, G., Quintard, M. and Whitaker, S. 1994 Heat transfer in packed beds: interpretation of experiments in terms of one- and two-equation models. *Heat Transfer 1994, Inst. Chem. Engrs, Rugby*, vol. 5, pp. 291–296. [2.2.3]

- Grant, M. A. 1983 Geothermal reservoir modeling. *Geothermics* **12**, 251–263. [11]
- Gratton, L. J., Travkin, V. S. and Catton, I. 1996 Influence of morphology upon two-temperature statements for convective transport in porous media. *J. Enhanced Heat Transfer* **3**, 129–145. [1.8]
- Gray, W. C. and O'Neill, K. 1976 On the general equations for flow in porous media and their reduction to Darcy's law. *Water Resources Res.* **12**, 148–154. [3.5.2]
- Green, C. P. and Ennis-King, J. 2010 Effect of vertical heterogeneity on long-term migration of CO<sub>2</sub> in saline formations. *Transp. Porous Media* **82**, 31–47. [11.11]
- Green, T. 1984 Scales for double-diffusive fingering in porous media. *Water Resources Res.* **20**, 1225–1229. [9.1.3]
- Green, T. 1990 The momentary instability of a saturated porous layer with a time-dependent temperature, and the most unstable disturbance. *Water Resources Res.* **26**, 2015–2021. [6.11.3]
- Green, T. and Freehill, R. L. 1969 Marginal stability in inhomogeneous porous media. *J. Appl. Phys.* **40**, 1759–1762. [6.13.1]
- Greenkorn, R. A. 1983 *Flow Phenomena in Porous Media*, Marcel Dekker, New York. [2.2.4]
- Griffiths, R. W. 1981 Layered double-diffusive convection in porous media. *J. Fluid Mech.* **102**, 221–248. [9.1.3]
- Grosan, T., Postelnicu, A. and Pop, I. 2010 Brinkman flow of a viscous fluid through a spherical porous medium embedded in another porous medium. *Transp. Porous Media* **81**, 89–103. [4.16.4]
- Grosan, T., Revnic, C., Pop, I. and Ingham, D. B. 2009 Magnetic field and internal heat generation effects on the free convection in a rectangular cavity filled with a porous medium. *Int. J. Heat Mass Transfer* **52**, 1525–1533. [6.17]
- Grundmann, M. and Mojtabi, A. 1995 Solution asymptotique du problème de la convection naturelle dans la cavité carrée poreuse chauffée par le bas. *C.R. Acad. Sci. Paris, Sér. II*, **321**, 401–406. [6.3]
- Grundmann, M., Mojtabi, A. and vant Hof, B. 1996 Asymptotic solution of natural convection problem in a square cavity heated from below. *Int. J. Numer. Meth. Heat Fluid Flow* **6**, 29–36. [6.3]
- Guba, P. 2001 On the finite-amplitude steady convection in rotating mushy layers. *J. Fluid Mech.* **347**, 337–365. [10.2.3]
- Guba, P. and Boda, J. 1998 The effect of uniform rotation on convective instability of a mushy layer during binary alloys solidification. *Stud. Geophys. Geodet.* **42**, 289–296. [10.2.3]
- Guba, P. and Worster, M. G. 2006a Free convection in laterally solidifying mushy regions. *J. Fluid Mech.* **558**, 69–78. [10.2.3]
- Guba, P. and Worster, M. G. 2006b Nonlinear oscillatory convection in mushy layers. *J. Fluid Mech.* **553**, 419–443. [10.2.3]
- Guedda, M. 2005a Multiple solutions of mixed convection boundary layer approximations in porous media. *Appl. Math. Lett.* **19**, 63–68. [8.1.6]
- Guedda, M., Aly Emad, H. and Ouahsine, A. 2011 Analytical and Ch PDM analysis of MHD mixed convection over a vertical flat plate embedded in a porous medium filled with water at 4 degrees C. *Appl. Math. Modell.* **35**, 5182–5197. [8.1.6]
- Guerrouddj, N. and Kahalerras, H. 2010 Mixed convection in a channel provided with heated porous blocks of various shapes. *Energy Convers. Manag.* **51**, 505–517. [8.4.1]
- Guo, J. and Kaloni, P. N. 1995a Nonlinear stability of convection induced by inclined thermal and solutal gradients. *Z. Angew. Math. Phys.* **46**, 645–654. [9.5]
- Guo, J. and Kaloni, P. N. 1995b Double-diffusive convection in a porous-medium, nonlinear stability, and the Brinkman effect. *Stud. Appl. Math.* **94**, 341–358. [9.1.6.3]
- Guo, Z. L. and Zhao, T. S. 2005a A lattice Boltzmann model for convective heat transfer in porous media. *Numer. Heat Transfer B*, **47**, 157–177. [2.6]
- Guo, Z. L. and Zhao, T. S. 2005b Lattice Boltzmann simulation of natural convection with temperature-dependent viscosity in a porous cavity. *Prog. Comput. Fluid Dyn.* **5**, 110–117. [2.6].
- Guo, Z., Kim, S. Y. and Sung, H. J. 1997a Pulsating flow and heat transfer in a pipe partially filled with a porous medium. *Int. J. Heat Mass Transfer*, **40**, 4209–4218. [4.11]

- Guo, Z., Sung, H. J. and Hyun, J. M. 1997b Pulsating flow and heat transfer in an annulus partially filled with porous media. *Numer. Heat Transfer A* **31**, 517–527. [4.11]
- Gupta, U. and Sharma, G. 2008 Thermosolutal instability of a compressible Rivlin-Ericksen fluid in the presence of rotation and Hall currents saturating a porous medium. *Appl. Math. Comput.* **196**, 158–173. [9.1.6.4]
- Gupta, V. P. and Joseph, D. D. 1973 Bounds for heat transport in a porous layer. *J. Fluid Mech.* **57**, 491–514. [6.3, 6.9.1, 6.22]
- Guria, M., Jana, R. N., Ghosh, S. K. and Pop, I. 2009 Three-dimensional free convection flow in a vertical channel filled with a porous medium. *J. Porous Media* **12**, 985–995. [7.1.7]
- Guria, M., Manna, G. and Jana, R. N. 2010 Flow and heat transfer along an infinite horizontal porous plate through a porous medium in a rotating system. *J. Porous Media* **13**, 387–393. [5.2]
- Gustafson, M. R. and Howle, L. E. 1999 Effects of anisotropy and boundary plates on the critical values of a porous medium heated from below. *Int. J. Heat Mass Transfer* **42**, 3419–3430. [6.12]
- Haajizadeh, M. and Tien, C. L. 1983 Natural convection in a rectangular porous cavity with one permeable endwall. *ASME J. Heat Transfer* **105**, 803–808. [7.3.2]
- Haajizadeh, M. and Tien, C. L. 1984 Combined natural and forced convection in a horizontal porous channel. *Int. J. Heat Mass Transfer* **27**, 799–813. [8.2.4]
- Haajizadeh, M., Ozguc, A. F. and Tien, C. L. 1984 Natural convection in a vertical porous enclosure with internal heat generation. *Int. J. Heat Mass Transfer* **27**, 1893–1902. [6.17]
- Haber, S. and Mauri, R. 1983 Boundary conditions for Darcy's flow through porous media. *Int. J. Multiphase Flow* **9**, 561–574. [1.6]
- Habibi, K., Mosahebi, A. and Shokouhmand, H. 2011 Heat transfer characteristics of reciprocating flows in channels partially filled with porous medium. *Transp. Porous Media* **89**, 139–153. [4.16.5]
- Haddad O.M., Al-Nimr, M. A. and Al-Khateeb, A. N. 2004 Validation of the local thermal equilibrium assumption in natural convection from a vertical plate embedded in porous medium. *Int. J. Heat Mass Transfer* **47**, 2037–2042. [5.1.9.3]
- Haddad O.M., Al-Nimr, M. A. and Al-Khateeb, A. N. 2005a Validity of the local thermal equilibrium assumption in natural convection from a vertical plate embedded in porous medium. *J. Porous Media* **8**, 85–95. [5.1.9.3]
- Haddad, O. M., Abuzaid, M. M. and Al-Nimr, M. A. 2005b Developing free-convection gas flow in a vertical open-ended microchannel filled with porous media. *Numer. Heat Transfer A* **48**, 693–710. [7.1.7]
- Haddad, O. M., Abuzaid, M. M. and Taamney, Y. 2006a Hydrodynamic and thermal behaviour of gas flow in microchannels filled with porous media. *J. Porous Medai* **9**, 403–414. [4.10]
- Haddad, O. M., Al-Nimr, M. A. and Abuzaid, M. M. 2006b Effect of periodically oscillating driving force on basic microflows in porous media. *J. Porous Medi* **9**, 695–707. [4.16.2]
- Haddad, O. M., Al-Nimr, M. A. and Al-Omary, J. S. 2007a Forced convection of gaseous slip-flow in porous microchannels under local thermal non-equilibrium conditions. *Transp. Porous Media* **67**, 453–471. [4.10]
- Haddad, O. M., Al-Nimr, M. A. and Sari, M. S. 2007b Forced convection gaseous slip flow in circular porous micro-channels. *Transp. Porous Media* **70**, 167–179. [4.5]
- Haddad, O. M., Al-Nimr, M. A. and Taamneh, Y. 2006c Hydrodynamic and thermal behaviour of gas flow in microchannels filled with porous media. *J. Porous Media* **9**, 403–414. [4.5]
- Haddad, O.M., Al-Nimr, M. A. and Abu-Ayyad, M. A. 2002 Numerical simulation of forced convection flow past a parabolic cylinder embedded in porous media. *Int. J. Numer. Meth. Heat Fluid Flow* **12**, 6–28. [4.3]
- Hadim, A. 1994a Forced convection in a porous channel with localized heat sources. *ASME J. Heat Transfer* **116**, 465–472. [4.11]
- Hadim, A. 1994b Numerical study of non-Darcy mixed convection in a vertical porous channel. *AIAA J. Thermophys. Heat Transfer* **8**, 371–373. [8.3.1]
- Hadim, A. and Burmeister, L. C. 1988 Onset of convection in a porous medium with internal heat generation and downward flow. *AIAA J. Thermophys. Heat Transfer* **2**, 343–351. [6.11.2]

- Hadim, A. and Burmeister, L. C. 1992 Conceptual design of a downward-convecting solar pond filled with a water-saturated, porous medium. *ASME J. Solar Energy Engng.* **114**, 240–245. [6.11.2]
- Hadim, A. and Chen, G. 1994a Non-Darcy mixed convection in a vertical porous channel with discrete heat sources at the walls. *Int. Comm. Heat Mass Transfer* **21**, 377–387. [8.3.2]
- Hadim, A. and Govindarajan, S. 1988 Development of laminar mixed convection in a vertical porous channel. *ASME HTD* **105**, 145–153. [8.3.1]
- Hadim, H. 2006 Non-Darcy natural convection of a non-Newtonian fluid in a porous cavity. *Int. Comm. Heat Mass Transfer* **33**, 1179–1189. [7.3.7]
- Hadim, H. A. and Chen, G. 1994b Non-Darcy mixed convection in a vertical porous channel with asymmetric wall heating. *AIAA J. Thermophys. Heat Transfer* **8**, 805–808. [8.3.2]
- Hadim, H. A. and Chen, G. 1995 Numerical study of non-Darcy natural convection of a power-law fluid in a porous cavity. *ASME HTD-317*, 301–307. [7.1.6]
- Hadim, H. and North, A. 2005 Forced convection in a sintered porous channel with inlet and outlet slots. *Int. J. Thermal Sci.* **44**, 33–42. [4.16.5]
- Hadim, H.A. and Bethancourt, A. 1995 Numerical study of forced convection in a partially porous channel with discrete heat sources. *ASME J. Electron. Packaging* **117**, 46–51. [4.11]
- Hady, F. M. and Ibrahim, F. S. 1997 Forced convection heat transfer on a flat plate embedded in porous media for power-law fluids. *Transport Porous Media* **28**, 125–134. [4.16.3]
- Hady, F. M., Ibrahim, F. S., Abdel-Gaied, S. M. and Eid, M. R. 2011 Influence of yield stress on free convective boundary layer flow of a non-Newtonian nanofluid past a vertical plate in a porous medium. *J. Mech. Sci. Tech.* **25**, 2043–2050. [5.1.9.2]
- Haghshenas, A., Nasr, M. R. and Rahimian, M. H. 2010 Numerical simulation of natural convection in an open-ended square cavity filled with porous medium by lattice Boltzmann method. *Int. Comm. Heat Mass Transfer* **87**, 1528–1534. [7.1.7]
- Hajipour, M. and Dehkordi, A. M. 2012 Analysis of nanofluid heat transfer in parallel-plate vertical channels partially filled with porous medium. *Int. J. Therm. Sci.* **55**, 103–113. [8.4.1]
- Haji-Sheik, A. and Vafai, K. 2004 Analysis of flow and heat transfer in porous media imbedded inside various shaped ducts. *Int. J. Heat Mass Transfer* **47**, 1889–1905. [4.13]
- Haji-Sheikh, A. 2004 Estimation of average and local heat transfer in parallel plates and circular ducts filled with porous materials. *ASME J. Heat Transfer* **126**, 400–409. [4.5]
- Haji-Sheikh, A. 2006 Fully developed heat transfer to fluid flow in rectangular passages filled with porous materials. *ASME J. Heat Transfer* **128**, 550–556. [4.5]
- Haji-Sheikh, A. and Minkowycz, W. J. 2008 Heat transfer analysis under local thermal non-equilibrium conditions. In P. Vadasz (ed.) *Emerging Topics in Heat and Mass Transfer in Porous Media*, Springer, New York, pp. 39–62. [2.2.3, 4.10]
- Haji-Sheikh, A., Minkowycz W. J. and Sparrow E. M. 2004b Green's function solution of temperature field for flow in porous passages. *Int. J. Heat Mass Transfer* **47**, 4685–4695. [4.13]
- Haji-Sheikh, A., Minkowycz W. J. and Sparrow E. M. 2005 Heat transfer to flow through porous passages using extended weighted residual method – a Green's function solution. *Int. J. Heat Mass Transfer* **48**, 1330–1349. [4.13]
- Haji-Sheikh, A., Beck, J. V. and Cole, K. D. 2010a Steady-state Green's function solution for moving media with axial conduction. *Int. J. Heat Mass Transfer* **53**, 2583–2592. [4.9]
- Haji-Sheikh, A., Minkowycz, W. J. and Manafzadeh, S. 2010b Axial conduction effect in flow through circular porous passages with prescribed wall heat flux. *Heat Mass Transfer* **46**, 727–73. [4.9]
- Haji-Sheikh, A., Minkowycz, W. J. and Manafzadeh, S. 2010c Heat transfer with upstream thermal penetration in flow through porous plate passages. *Appl. Therm. Engng.* **30**, 639–648. [4.16.5]
- Haji-Sheikh, A., Sparrow, E. M. and Minkowycz, W. J. 2004a A numerical study of heat transfer to fluid flow through circular porous passages. *Numer. Heat Transfer A* **46**, 929–955. [4.5]
- Hall, M. J. and Hiatt, J. P. 1996 Measurements of pore scale flows within and exiting ceramic foams. *Expt. Fluids* **20**, 433–440. [1.9]

- Hallworth, M. A., Huppert, H. E. and Woods, A. W. 2005 Dissolution-driven convection in a reactive porous medium. *J. Fluid Mech.* **535**, 255–285. [10.2.3]
- Hamad, M. A. A. and Pop, I. 2011 Scaling transformations for boundary layer flow near the stagnation point on a heated permeable stretching surface in a porous medium saturated with a nanofluid and heat generation/absorption effects. *Transp. Porous Media* **87**, 25–39. [5.1.9.9]
- Hamdan, M. and Al-Nimr, M. A. 2010 The use of porous fins for heat transfer augmentation in parallel-plate channels. *Transp. Porous Media* **84**, 409–420. [4.11]
- Hamdan, M. O., Al-Nimr, M. A. and Alkam, M. K. 2000 Enforcing forced convection by inserting porous substrate in the core of a parallel-plate channel. *Int. J. Numer. Meth. Heat Fluid Flow* **10**, 502–517. [4.11]
- Han, H. S. and Hyun, J. M. 2008 Buoyant convection in a parallelogrammic enclosure filled with a porous medium. General analysis and numerical simulations. *Int. J. Heat Mass Transfer* **51**, 2980–2989. [7.3.7]
- Hanamura, K. and Kaviany, M. 1995 Propagation of condensation front in steam injection into dry porous media. *Int. J. Heat Mass Transfer* **38**, 1377–1386. [3.6]
- Handley, D. and Heggs, P. J. 1968 Momentum and heat transfer mechanisms in regular shaped packings. *Trans. Inst. Chem. Engrs.* **46**, T251-T264. [2.2.3]
- Hanspal, N. S., Waghode A. N., Nashehi, V. and Wakeman, R. J. 2006 Numerical analysis of coupled Stokes/Darcy flows in industrial filtrations. *Transport Porous Media* **64**, 73–101.[1.6]
- Hao, Y. L. and Tao, Y. X. 2003a Non-equilibrium melting of granular packed bed in horizontal forced convection. Part I: Experiment. *Int. J. Heat Mass Transfer* **46**, 5017–5030. [10.1.7]
- Hao, Y. L. and Tao, Y. X. 2003b Non-equilibrium melting of granular packed bed in horizontal forced convection. Part II: Numerical simulation. *Int. J. Heat Mass Transfer* **46**, 5031–5044. [10.1.7]
- Haq, S. and Mulligan, J. C. 1990a Transient free convection about a vertical flat plate embedded in a saturated porous medium. *Numer. Heat Transfer A* **18**, 227–242. [5.1.3]
- Haq, S. and Mulligan, J. C. 1990b Transient free convection from a vertical plate to a non-Newtonian fluid in a porous medium. *J. Non-Newtonian Fluid Mech.* **36**, 395–440. [5.1.9.2]
- Hardee, H. C. and Nilson, R. H. 1977 Natural convection in porous media with heat generation. *Nucl. Sci. Engng.* **63**, 119–132. [6.11.2]
- Harris, K.T., Haji-Sheikh, A. and Nhanna, A. G. A. 2001 Phase change phenomena in porous media – a non-local thermal equilibrium model. *Int. J. Heat Mass Transfer* **44**, 1619–1625. [10.1.7]
- Harris, S. D. and Ingham, D. B. 2004 Techniques for solving the boundary-layer equations. In *Emerging Technologies and Techniques in Porous Media* (D. B. Ingham, A. Bejan, E. Mamut and I. Pop, eds), Kluwer Academic, Dordrecht, pp. 43–64. [5.1.3]
- Harris, S. D., Ingham, D. B. and Pop, I. 1996 Transient free convection from a vertical plate subjected to a change in surface heat flux in porous media. *Fluid Dyn. Res.* **18**, 313–324. [5.1.3]
- Harris, S. D., Ingham, D. B. and Pop, I. 1997a Free convection from a vertical plate in a porous media subjected to a sudden change in surface temperature. *Int. Comm. Heat Mass Transfer* **24**, 543–552. [5.1.3]
- Harris, S. D., Ingham, D. B. and Pop, I. 1997b Free convection from a vertical plate in a porous medium subjected to a sudden change in surface heat flux. *Transport in Porous Media* **26**, 205–224. [5.1.3]
- Harris, S. D., Ingham, D. B. and Pop, I. 1998 Transient mixed convection from a vertical surface in a porous medium. In *Mathematics of Heat Transfer* (G. E. Tuppenholme and A. S. Wood, eds.) Clarendon Press, Oxford, pp. 157–164. [8.1.1]
- Harris, S. D., Ingham, D. B. and Pop, I. 1999 Unsteady mixed convection boundary layer flow on a vertical surface in a porous medium. *Int. J. Heat Mass Transfer* **42**, 357–372. [8.1.1]
- Harris, S. D., Ingham, D. B. and Pop, I. 2000 Transient free convection from a horizontal surface in a porous medium subjected to a sudden change in surface heat flux. *Transport Porous Media* **39**, 97–117. [5.2]
- Harris, S. D., Ingham, D. B. and Pop, I. 2002 Thermal capacity effect on transient free convection adjacent to a fixed surface in a porous medium. *Transport Porous Media* **46**, 1–18. [8.1.1]

- Harris, S. D., Ingham, D. B. and Pop, I. 2009 Mixed convection boundary-layer flow near the stagnation point on a vertical surface in a porous medium. *Transp. Porous Media* **77**, 267–285. [8.1.6]
- Hartline, B. K. and Lister, C. R. B. 1977 Thermal convection in a Hele-Shaw cell. *J. Fluid Mech.* **79**, 379–389. [2.5]
- Hartline, B. K. and Lister, C. R. B. 1981 Topographic forcing of supercritical convection in a porous medium such as the oceanic crust. *Earth Planet. Sci. Lett.* **55**, 75–86. [11.6.2]
- Hashemi, S. M. H., Fazeli, S. A. and Shokouhmand, H. 2011 Fully developed non-Darcian forced convection slip-flow in a micro-annulus filled with a porous medium: Analytical solution. *Energy Convers. Manag.* **52**, 1054–1060. [4.16.5]
- Hasnaoui, M., Vasseur, P., Bilgen, E. and Robillard, L. 1995 Analytical and numerical study of natural convection heat transfer in a vertical porous annulus. *Chem. Engng. Comm.* **131**, 141–159. [7.3.3]
- Hassan, M. and Mujumdar, A. S. 1985 Transpiration-induced buoyancy effect around a horizontal cylinder embedded in a porous medium. *Int. J. Energy Res.* **9**, 151–163. [9.4]
- Hassanien, I. A. 2003 Variable permeability effects on mixed convection along a vertical wedge embedded in a porous medium with variable heat flux. *Appl. Math. Comp.* **138**, 41–59. [8.1.4]
- Hassanien, I. A. and Al-Arabi, T. H. 2009 Non-Darcy unsteady mixed convection flow near the stagnation point on a heated vertical surface embedded in a porous medium with thermal radiation and variable viscosity. *Comm. Nonlinear Sci. Numer. Simul.* **14**, 1366–1376. [8.1.6]
- Hassanien, I. A. and Allah, M. H. O. 2002 Oscillatory hydromagnetic flow through a porous medium with variable permeability in the presence of free convection and mass transfer flow. *Int. Comm. Heat Mass Transfer* **29**, 567–575. [9.2.1]
- Hassanien, I. A. and Eliaw, A. M. 2007 Variable permeability effect on buoyancy-induced inclined boundary layer flow in a saturated porous medium with variable wall temperature. *Heat Mass Transfer* **43**, 1241–1247. [5.3]
- Hassanien, I. A. and Omer, G.M. 2002 Nonsimilarity solutions for mixed convection flow along nonisothermal vertical plate embedded in porous media with variable permeability. *J. Porous Media* **5**, 159–167. [8.1.1]
- Hassanien, I. A. and Omer, G.M. 2005 Mixed-convection flow adjacent to a horizontal surface in a porous medium with variable permeability and surface heat flux. *J. Porous Media* **8**, 225–235. [8.1.2]
- Hassanien, I. A. and Rashed, Z. Z. 2010 Effects of variable viscosity and thermal conductivity on the Brinkman model for mixed convection flow past a horizontal circular cylinder in a porous medium. *J. Porous Media* **13**, 53–66. [8.1.3]
- Hassanien, I. A. and Rashed, Z. Z. 2011 Non-Darcy free convection flow over a horizontal cylinder in a saturated porous medium with variable viscosity, thermal conductivity and mass diffusivity. *Comm. Nonlinear Sci. Numer. Simul.* **16**, 1931–1941. [8.1.3]
- Hassanien, I. A., Bakier, A. Y. and Gorla, R. S. R. 1998 Effects of thermal dispersion and stratification on non-Darcy mixed convection from a vertical plate in a porous medium. *Heat Mass Transfer* **34**, 209–212. [8.1.1]
- Hassanien, I. A., Essawy, A. H. and Moursy, N. M. 2003a Variable viscosity and thermal conductivity effects on combined heat and mass transfer in mixed convection over a UHF/UMF wedge in porous media: the entire regime. *Appl. Math. Comput.* **145**, 667–682. [9.6.1]
- Hassanien, I. A., Essawy, A. H. and Moursy, N. M. 2003b Variable viscosity and thermal conductivity effects on heat transfer by natural convection from a cone and a wedge in porous media. *Arch. Mech.* **55**, 345–356. [5.8]
- Hassanien, I. A., Essawy, A. H. and Moursy, N. M. 2004e Natural convection flow of micropolar fluid from a permeable uniform heat flux surface in porous medium. *Appl. Math. Comput.* **152**, 3232–335. [5.1.9.2]
- Hassanien, I. A., Ibrahim, F. S. and Omer, G. M. 2006 Unsteady flow and heat transfer of a viscous fluid in the stagnation region of a three-dimensional body embedded in a porous medium. *J. Porous Media* **9**, 357–372. [5.9]

- Hassanien, I. A., Ibrahim, F. S. and Omer, G.M. 2005 The effect of variable permeability and viscous dissipation on a non-Darcy natural-convection regime with thermal dispersion. *J. Porous Media* **8**, 237–256. [5.1.9.4]
- Hassanien, I. A., Salama, A. A. and Elaiw, A. M. 2003c Variable permeability effect on vortex instability of mixed convection flow in a semi-infinite porous medium bounded by a horizontal surface. *Appl. Math. Comput.* **146**, 829–847. [8.1.2]
- Hassanien, I. A., Salama, A. A. and Elaiw, A. M. 2004a The onset of longitudinal vortices in mixed convection flow over an inclined surface in a porous medium with variable permeability. *Appl. Math. Comput.* **154**, 313–333. [8.1.2]
- Hassanien, I. A., Salama, A. A. and Elaiw, A. M. 2004b Variable permeability effect on vortex instability of a horizontal natural convection flow in a saturated porous medium with a variable wall temperature. *Zeit. Angew. Math. Mech.* **84**, 39–47. [5.4]
- Hassanien, I. A., Salama, A. A. and Moursy, N. M. 2004c Non-Darcian effects on vortex instability of mixed convection over horizontal plates porous medium with surface mass flux. *Int. Comm. Heat Mass Transfer* **31**, 231–240. [8.1.2]
- Hassanien, I. A., Salama, A. A. and Moursy, N. M. 2004d Inertia effect on vortex instability of horizontal natural convection flow in a saturated porous medium with surface mass flux. *Int. Comm. Heat Mass Transfer* **31**, 741–750. [5.4]
- Hassanizadeh, S. M. and Gray, W. G. 1988 Reply to comments by Barak on “High velocity flow in porous media” by Hassanizadeh and Gray. *Transport in Porous Media* **3**, 319–321. [1.5.2]
- Hassanizadeh, S. M. and Gray, W. G. 1993 Toward an improved description of the physics of two-phase flow. *Adv. Water Resources* **16**, 53–67. [3.5.4]
- Hassanzadeh, H., Pooladi-Darvish, M. and Keith, D. W. 2005 Modelling of convective mixing in CO<sub>2</sub> storage. *J. Cand. Petrol. Tech.* **44**, 43–51. [11.11]
- Hassanzadeh, H., Pooladi-Darvish, M. and Keith, D. W. 2006 Stability of a fluid in a horizontal porous layer: effect of nonlinear concentration profile, initial and boundary conditions. *Transport Porous Media* **65**, 193–211. [6.11.3]
- Hassanzadeh, H., Pooladi-Darvish, M. and Keith, D. W. 2007 Scaling behaviour of convective mixing with application to geological storage of CO<sub>2</sub>. *AIChE J.* **53**, 1121–1131. [11.1]
- Hassanzadeh, H., Pooladi-Darvish, M. and Keith, D. W. 2009 The effect of natural flow of aquifers and associated dispersion on the onset of buoyancy-induced convection in a saturated porous medium. *AIChE J.* **55**, 475–485. [6.6]
- Haugen, K. B. and Tyvand, P. A. 2003 Onset of thermal convection in a vertical porous cylinder with conducting wall. *Phys. Fluids* **15**, 2661–2667. [7.3.3]
- Havstad, M. A. and Burns, P. J. 1982 Convective heat transfer in vertical cylindrical annuli filled with a porous medium. *Int. J. Heat Mass Transfer* **25**, 1755–1766. [7.3.3]
- Hayat, T., Abbas, Z. and Javed, T. 2009 MHD stagnation point flow and heat transfer over a permeable surface through porous space. *J. Porous Media* **12**, 183–195. [8.1.6]
- Hayat, T., Abbas, Z. and Asghar, S. 2007a Effects of Hall current and heat transfer on the flow in a porous medium with slip condition. *J. Porous Media* **10**, 35–50. [5.1.9.9]
- Hayat, T., Abbas, Z. and Asghar, S. 2007b On heat transfer analysis for an oscillatory flow of a second-grade fluid through a porous medium. *J. Porous Media* **10**, 601–612. [4.16.2]
- Hayat, T., Abbas, Z. and Asghar, S. 2008a Effects of Hall current and heat transfer on rotating flow of a second grade fluid through a porous medium. *Commun. Nonlinear Sci. Numer. Simul.* **13**, 2177–2192. [6.23]
- Hayat, T., Abbas, Z., Pop, I. and Asghar, S. 2010a Effects of radiation and magnetic field on the mixed convection stagnation-point flow over a vertical stretching sheet in a porous medium. *Int. J. Heat Mass Transfer* **53**, 466–474. [8.1.6]
- Hayat, T., Hussain, M., Nadeem, S. and Mesioub, S. 2011a Falkner-Skan wedge flow of a power-law fluid with mixed convection and porous medium. *Compt. Fluids* **49**, 22–28. [8.4.3]
- Hayat, T., Javed, T. and Abbas, Z. 2008b Slip flow and heat transfer of a second-grade fluid past a stretching sheet through a porous space. *Int. J. Heat Mass Transfer* **51**, 4528–4534. [8.1.6]

- Hayat, T., Mustafa, M. and Pop, I. 2010b Heat and mass transfer for Soret and Dufour's effect on mixed convection boundary layer flow over a stretching vertical surface in a porous medium filled with a viscoelastic fluid. *Comm. Nonlinear Sci. Numer. Simul.* **15**, 1183–1196. [9.6.1]
- Hayat, T., Mustafa, M., Pop, I. and Obaidat, S. 2011b Flow and heat transfer due to stretching surface in an anisotropic porous medium filled with a viscoelastic fluid *J. Porous Media* **14**, 523–532. [5.1.9.9]
- Hayat, T., Qasim, M. and Abbas, S. 2010c Homotopy solution for the unsteady three-dimensional MHD flow and mass transfer in a porous space. *Comm. Nonlinear Sci. Numer. Simul.* **15**, 2375–2387. [9.2.1]
- Hayat, T., Sajjad, R., Abbas, Z., Sajid, M. and Hendi, A. A. 2011 Radiation effects on MHD flow of Maxwell fluid in a channel with porous medium. *Int. J. Heat Mass Transfer* **54**, 854–862. [7.1.6]
- Hayes, A. M., Khan, J. A., Shaaban, A. H. and Spearig, I. G. 2008 The thermal modeling of a matrix heat exchanger using a porous medium and the thermal nonequilibrium model. *Int. J. Therm. Sci.* **47**, 1306–1315. [4.10]
- Hayes, R. E. 1990 Forced convection heat transfer at the boundary layer of a packed bed. *Transport in Porous Media* **5**, 231–245. [4.8]
- Hayes, R. E., Afacan, A., Boulanger, B. and Shenoy, A. V. 1996 Modelling the flow of power law fluids in a packed bed using a volume-averaged equation of motion. *Transport in Porous Media* **23**, 175–196. [1.5.4]
- He, X. S. and Georgiadis, J. G. 1990 Natural convection in porous media: effect of weak dispersion on bifurcation. *J. Fluid Mech.* **216**, 285–298. [6.6, 6.11.2]
- He, X. S. and Georgiadis, J. G. 1992 Direct numerical solution of diffusion problems with intrinsic randomness. *Int. J. Heat Mass Flow* **35**, 3141–3151. [2.6]
- Helmy, K. A. 1998 MHD unsteady free convection flow past a vertical porous plate. *Z. Angew. Math. Mech.* **78**, 255–270. [5.1.9.9]
- Hennenberg, M., Saghir, M. Z., Rednikov, A. and Legros, J. C. 1997 Porous media and the Bénard-Marangoni problem. *Transport Porous Media* **27**, 327–355. [6.19.3]
- Herron, I. H. 2001 Onset of convection in a porous medium with heat sources and variable gravity. *Int. J. Engng. Sci.* **39**, 201–208. [6.24]
- Herwig, H. and Koch, M. 1990 An asymptotic approach to natural convection momentum and heat transfer in saturated highly porous media. *ASME J. Heat Transfer* **112**, 1085–1088. [5.1.9.9, 9.7]
- Hetsroni, G., Gurevich, M., and Rozenblit, R. 2008 Natural convection in metal foam strips with internal heat generation. *Exp. Therm. Fluid Sci.* **32**, 1740–174. [7.3.8]
- Hguyen (*sic*), T. H. and Zhang, X. 1992 Onset and evolution of penetrative convection during the melting process in a porous medium. *Heat and Mass Transfer in Porous Media* (ed. M. Quintard and M. Todorovic), Elsevier, Amsterdam, 381–392. [10.1.7]
- Hickox, C. E. 1981 Thermal convection at low Rayleigh number from concentrated sources in porous media. *ASME J. Heat Transfer* **103**, 232–236. [5.11.2]
- Hickox, C. E. and Chu, T. Y. 1990 A numerical study of convection in a layered porous medium heated from below. *ASME HTD-149*, 13–21. [6.13.2]
- Hickox, C. E. and Gartling, D. K. 1981 A numerical study of natural convection in a horizontal porous layer subjected to an end-to-end temperature difference. *ASME J. Heat Transfer* **103**, 797–802. [7.1.3]
- Hickox, C. E. and Gartling, D. K. 1985 A numerical study of natural convection in a vertical annular porous layer. *Int. J. Heat Mass Transfer* **28**, 720–723. [7.3.3]
- Hickox, C. E. and Watts, H. A. 1980 Steady thermal convection from a concentrated source in a porous medium. *ASME J. Heat Transfer* **102**, 248–253. [5.11.3]
- Hidalgo, J. J. and Carrera, J. 2009 Effect of dispersion on the onset of convection during CO<sub>2</sub> sequestration. *J. Fluid Mech.* **640**, 441–452. [11.11]
- Higuera, F. J. 1997 Conjugate natural convection heat transfer between two porous media separated by a horizontal wall. *Int. J. Heat Mass Transfer* **40**, 3157–3161. [5.1.5]

- Higuera, F. J. and Pop, I. 1997 Conjugate natural convection heat transfer between two porous media separated by a vertical wall. *Int. J. Heat Mass Transfer*, **40**, 123–129. [5.1.5]
- Higuera, F. J. and Weidman, P. D. 1995 Natural convection beneath a downward facing heated plate in a porous medium. *Eur. J. Mech. B/Fluids* **14**, 29–40. [5.2]
- Higuera, F. J. and Weidman, P. D. 1998 Natural convection far downstream of a heat source on a solid wall. *J. Fluid Mech.* **361**, 225–39. [5.11.1]
- Hill, A. A. 2003 Convection due to the selective absorption of radiation in a porous medium. *Cont. Mech. Thermodyn.* **15**, 451–462. erratum 629. [6.11.2]
- Hill, A. A. 2004a Convection induced by the selective absorption of radiation for the Brinkman model. *Cont. Mech. Thermodyn.* **16**, 43–52. [6.11.2]
- Hill, A. A. 2004b Conditional and unconditional nonlinear stability for convection induced by absorption of radiation in a non-Darcy porous medium. *Cont. Mech. Thermodyn.* **16**, 305–318. [6.11.2]
- Hill, A. A. 2005 Double-diffusive convection in a porous medium with concentration based internal heat source. *Proc. Roy. Soc. Lond. A* **461**, 561–574. [9.3.1]
- Hill, A. A. 2006 Horizontal thermal convection in a porous medium. *Cont. Mech. Thermodyn.* **18**, 253–258. [7.1.3]
- Hill, A. A. 2007 Unconditional nonlinear stability for convection in a porous medium with vertical throughflow. *Acta Mech.* **193**, 197–206. [6.10]
- Hill, A. A. 2008 Global stability for penetrative double-diffusive convection in a porous medium. *Acta Mech.* **200**, 1–10. [9.1.3]
- Hill, A. A. 2009 A differential constraint approach to obtain global stability for radiation-induced double-diffusive convection in a porous medium. *Math. Meth. Appl. Sci.* **32**, 914–921. [9.1.3]
- Hill, A. A. and Carr, M. 2010a Nonlinear stability of the one-domain approach to modeling convection in superposed fluid and porous layers. *Proc. Roy. Soc. A* **466**, 2695–2705. [6.19.2]
- Hill, A. A. and Carr, M. 2010b Sharp global nonlinear stability for a fluid overlying a highly porous material. *Proc. Roy. Soc. A* **466**, 127–140. [6.19.2]
- Hill, A. A. and Malashetty, M. S. 2012 An operative method to obtain sharp nonlinear stability for systems with spatially dependent coefficients. *Proc. Roy. Soc. Lond. A* **468**, 323–336. [9.1.3]
- Hill, A. A. and Straughan, B. 2006 A Legendre spectral element method for eigenvalues in hydrodynamic stability. *J. Comp. Appl. Math.* **193**, 363–381. [6.4]
- Hill, A. A. and Straughan, B. 2008 Poiseuille flow in a fluid overlying a porous medium. *J. Fluid Mech.* **603**, 137–149. [6.19.3]
- Hill, A. A. and Straughan, B. 2009a Global stability for thermal convection in a fluid overlying a highly porous material. *Proc. Roy. Soc. Lond. A* **465**, 207–217. [6.19.2]
- Hill, A. A. and Straughan, B. 2009b Poiseuille flow in a fluid overlying a highly porous material. *Adv. Water Resources* **32**, 1609–1614. [6.19.3]
- Hill, A. A., Rionero, S. and Straughan, B. 2007 Global stability for penetrative convection with throughflow in a porous material. *IMA J. Appl. Math.* **72**, 635–643. [6.10.2]
- Hills, R. N., Loper, D. E. and Roberts, P. H. 1983 A thermodynamically consistent model for flow through dendrites. *Quart. J. Mech. Appl. Math.* **36**, 505–539. [10.2.3]
- Himasekhar, K. and Bau, H. H. 1986 Large Rayleigh number convection in a horizontal, eccentric annulus containing saturated porous media. *Int. J. Heat Mass Transfer* **29**, 703–712. [7.3.3]
- Himasekhar, K. and Bau, H. H. 1987 Thermal convection associated with hot/cold pipes buried in a semi-infinite, saturated porous medium. *Int. J. Heat Mass Transfer* **30**, 263–273. [7.11]
- Himasekhar, K. and Bau, H. H. 1988a Thermal convection around a heat source embedded in a box containing a saturated porous medium. *ASME J. Heat Transfer* **110**, 649–654. [5.12.3, 7.11]
- Himasekhar, K. and Bau, H. H. 1988b Two-dimensional bifurcation phenomena in thermal convection in horizontal concentric annuli containing saturated porous media. *J. Fluid Mech.* **187**, 267–300. [7.3.3]
- Hirata, M. C., Hady, F. M., Abdel-Gaied, S. M. and Eid, M. R. 2010 Influence of chemical reaction on heat and mass transfer of non-Newtonian fluid with yield stress by free convection from vertical surface in porous medium considering Soret effect. *Appl. Math. Mech.-English Ed.* **31**, 675–684. [9.2.1]

- Hirata, S. C. and Ouarzazi, M. N. 2010a Influence of horizontal throughflow on the linear properties of viscoelastic fluids convection in porous media. *Compt. Rendus Mecanique* **338**, 538–544. [6.10.1]
- Hirata, S. C. and Ouarzazi, M. N. 2010b Three-dimensional absolute and convective instabilities in mixed convection of a viscoelastic fluid through a porous medium. *Phys. Lett. A.* **374**, 2661–2666. [6.10.1]
- Hirata, S. C., Goyeau, B. and Gobin, D. 2007a Stability of natural convection in superposed fluid and porous layers: Influence of the interfacial jump boundary condition. *Phys. Fluids* **19**, #058102. [6.19.3]
- Hirata, S. C., Goyeau, B. and Gobin, D. 2009a The stability of thermosolutal natural convection in superposed fluid and porous layers. *Transp. Porous Media* **78**, 525–536. [6.19.3]
- Hirata, S. C., Goyeau, B. and Gobin, D. 2012 Onset of convective instabilities in under-ice melt ponds. *Phys. Rev. E* **85**, 066306. [9.1.6.4]
- Hirata, S. C., Goyeau, B., Gobin, D., Chandresris, M. and Jamet, D. 2009b Stability of natural convection in superposed fluid and porous layers: equivalence of one- and two-domain approaches. *Int. J. Heat Mass Transfer* **52**, 533–536. [6.19.3]
- Hirata, S. C., Goyeau, B., Gobin, D. and Cotta, R. M. 2006 Stability of natural convection in superposed fluid and porous layers using integral transforms. *Numer. Heat Transfer B* **50**, 409–424. [6.19.3]
- Hirata, S. C., Goyeau, B., Gobin, D., Carr, M. and Cotta, R. M. 2007b Linear stability of natural convection in superposed fluid and porous layers: Influence of the interfacial modelling. *Int. J. Heat Mass Transfer* **50**, 1356–1367. [6.19.3]
- Hoffman, M. R. and van der Meer, F. M. 2002 A simple space-time averaged porous media model for flow in densely vegetated channels. In *Computational Methods in Water Resources* (eds. S. M. Hassanzadeh, R. J. Schotting, W. G. Gray and G. F. Pinder.) Vol. 2., Elsevier, Amsterdam. [1.8]
- Hollard, S., Layadi, M., Boisson, H. and Bories, S. 1995 Ecoulements stationnaires et instationnaires de convection naturelle en milieu poreux. *Rev. Gen. Therm.* **34**, S499-S514. [7.8]
- Holst, P. H. and Aziz, K. 1972 Transient three-dimensional natural convection in confined porous media. *Int. J. Heat Mass Transfer* **15**, 73–90. [6.8]
- Holzbecher, E. 1997 Numerical studies on thermal convection in cold groundwater. *Int. J. Heat Mass Transfer* **40**, 605–612. [6.20]
- Holzbecher, E. 2001 On the relevance of oscillatory convection regimes in porous media — review and numerical experiments. *Computers and Fluids* **30**, 189–209. [6.4]
- Holzbecher, E. 2004a The mixed convection number for porous media flow. In *Emerging Technologies and Techniques in Porous Media* (D. B. Ingham, A. Bejan, E. Mamut and I. Pop, eds), Kluwer Academic, Dordrecht, pp. 169–181. [8.1.1]
- Holzbecher, E. 2004b Free convection in open-top enclosures filled with a porous medium heated from below. *Numer. Heat Transfer A* **46**, 241–254. [6.4]
- Holzbecher, E. 2004c Free convection induced by oscillating conditions at the top. In *Applications of Porous Media* (ICAPM 2004), (eds. A. H. Reis and A. F. Miguel), Evora, pp. 147–152. [6.11.3]
- Holzbecher, E. 2005a Free and forced convection in porous media open at the top. *Heat Mass Transfer* **41**, 606–614. [6.4]
- Holzbecher, E. 2005b Groundwater flow pattern in the vicinity of a salt lake. *Hydrobiologica* **532**, 233–242. [9.1.6.4]
- Holzbecher, E. and Yusa, Y. 1995 Numerical experiments on free and forced convection in porous media. *Int. J. Heat Mass Transfer* **38**, 2109–2115. [11.8.2]
- Holzbecher, E., Kohfahi, C., Mazurowski, M., Bacik, A. and Dobies, M. 2010 The sensitivity of thermohaline groundwater circulation to flow and transport parameters: A numerical study based on double-diffusive convection above a salt dome. *Transp. Porous Media* **83**, 771–791. [9.1.6.4]
- Homsy, G. M. and Sherwood, A. E. 1976 Convective instabilities in porous media with throughflow. *AIChE J.* **22**, 168–174. [6.10.2]

- Hong, J. S. and Kim, M. C. 2007 Effect of anisotropy of porous media on the onset of buoyancy-driven convection. *Transp. Porous Media* **72**, 241–253. [6.12]
- Hong, J. S., Kim, M. C. and Choi, C. K. 2007 The onset of buoyancy-driven instability in porous media melted from below. *Transp. Porous Media* **67**, 229–241. [10.1.7]
- Hong, J. S., Kim, M. C., Yoon, D. Y., Chung, B. J. and Kim, S. 2008 Linear stability analysis of a fluid-saturated porous layer subjected to time-dependent heating. *Int. J. Heat Mass Transfer* **51**, 3044–305. [6.11.3].
- Hong, J. T. and Tien, C. L. 1987 Analysis of thermal dispersion effect on vertical-plate natural convection in porous media. *Int. J. Heat Mass Transfer* **30**, 143–150. [5.1.7.3]
- Hong, J. T., Tien, C. L. and Kaviany, M. 1985 Non-Darcian effects on vertical-plate natural convection in porous media with high porosities. *Int. J. Heat Mass Transfer* **28**, 2149–2157. [5.1.7.2]
- Hong, J. T., Yamada, Y. and Tien, C. L. 1987 Effects of non-Darcian and nonuniform porosity on vertical-plate natural convection in porous media. *ASME J. Heat Transfer* **109**, 356–362. [5.1.7.1, 5.1.7.2]
- Hooman, K. 2006 Entropy-energy analysis of forced convection in a porous-saturated circular tube considering temperature-dependent viscosity effects. *Int. J. Exergy* **3**, 436–451. [4.16.5]
- Hooman, K. 2007 Entropy generation for microscale forced convection: Effects of different thermal boundary conditions, velocity slip, temperature jump, viscous dissipation and duct geometry. *Int. Comm. Heat Mass Transfer* **34**, 945–957. [4.16.5]
- Hooman, K. 2008a A perturbation solution for forced convection in a porous-saturated duct. *J. Comput. Appl. Math.* **211**, 57–66. [4.16.5]
- Hooman, K. 2008c Heat and fluid flow in a rectangular microchannel filled with a porous medium. *Int. J. Heat Mass Transfer* **51**, 5804–5810. [4.16.5]
- Hooman, K. 2009 Slip flow forced convection in a microporous duct of rectangular cross-section. *Appl. Therm. Engng.* **29**, 1012–1019. [4.16.5]
- Hooman, K. and Ejlali, A. 2007 Entropy generation for forced convection in a porous saturated circular tube with uniform wall temperature. *Int. Comm. Heat Mass Transfer* **34**, 408–419. [4.16.5]
- Hooman, K. and Gorji-Bandpy, M. 2006 Laminar dissipative flow in a porous channel bounded by isothermal parallel plates. *Appl. Math. Mech. (English edit.)* **26**, 587–593. [4.16.5]
- Hooman, K. and Gurgenci, H. 2007a Effects of temperature-dependent viscosity variation on entropy generation, heat and fluid flow through a porous-saturated duct of rectangular cross-section. *Appl. Math. Mech. (English edit.)* **28**, 69–78. [4.16.5]
- Hooman, K. and Gurgenci, H. 2007b Effects of viscous dissipation and boundary conditions on forced convection in a channel occupied by a saturated porous medium. *Transp. Porous Media* **68**, 301–319. [4.16.5]
- Hooman, K. and Gurgenci, H. 2008a Effects of temperature-dependent viscosity on Bénard convection in a porous medium using a non-Darcy model. *Int. J. Heat Mass Transfer* **51**, 1139–1149. [6.7]
- Hooman, K. and Gurgenci, H. 2008b Effects of temperature-dependent viscosity on forced convection inside a porous medium. *Transp. Porous Media* **75**, 249–267. [4.16.1]
- Hooman, K. and Gurgenci, H. 2008c Heatline visualization of natural convection in a porous cavity occupied by a fluid with temperature-dependent viscosity. *ASME J. Heat Transfer* **130**, #012501. [6.7]
- Hooman, K. and Haji-Sheikh, A. 2007 Analysis of heat transfer and entropy generation for a thermally developing Brinkman-Brinkman forced convection problem in a rectangular duct with isoflux walls. *Int. J. Heat Mass Transfer* **50**, 4180–4194. [4.16.5]
- Hooman, K. and Merrikh, A. A. 2006 Analytical solution of forced convection in a duct of rectangular cross-section saturated by a porous medium. *ASME J. Heat Transfer* **128**, 596–600. [4.16.5]

- Hooman, K. and Mohebpour, S. R. 2007 Numerical investigation of temperature-dependent viscosity variation effects on thermally developing forced convection through a porous medium. *Heat Transfer Research* **38**, 1–8. [4.16.5]
- Hooman, K. and Ranjbar-Kani, A. A. 2003 Forced convection in a fluid-saturated porous-medium tube with iso-flux wall. *Int. Comm. Heat Mass Transfer* **30**, 1015–1026. [4.9]
- Hooman, K. and Ranjbar-Kani, A. A. 2004 A perturbation based analysis to investigate forced convection in a porous saturated tube. *J. Comp. Appl. Math.* **162**, 411–419. [4.9]
- Hooman, K., and Merrikh, A. A. 2010 Thermal analysis of natural convection in an enclosure filled with disconnected conducting square solid blocks. *Transp. Porous Media* **85**, 641–651. [4.11]
- Hooman, K., Ejlali, A. and Hooman, F. 2008a Entropy generation analysis of thermally developing forced convection in fluid-saturated porous medium. *Appl. Math. Mech. (English edit.)* **29**, 229–23. [4.13].
- Hooman, K., Gurgenci, H. and Dincer, T. 2009 Heatline and energy-flux-vector visualization of natural convection in a porous cavity occupied by a fluid with temperature-dependent viscosity. *J. Porous Media* **12**, 265–275. [4.16.5]
- Hooman, K., Gurgenci, H. and Merrikh, A. A. 2007a Heat transfer and entropy generation optimization and forced convection in porous-saturated ducts of rectangular cross-section. *Int. J. Heat Mass Transfer* **50**, 2051–2059. [4.16.5]]
- Hooman, K., Haji-Sheikh, A. and Nield, D. A. 2007b Thermally developing Brinkman-Brinkman forced convection in rectangular ducts with isothermal walls. *Int. J. Heat Mass Transfer* **50**, 3521–3533. [4.13]
- Hooman, K., Hooman, F. and Mohebpour, S. R. 2008b Entropy generation for forced convection in a porous channel with isoflux or isothermal walls. *Int. J. Exergy* **5**, 78–96. [4.16.5]
- Hooman, K., Merrikh, A. A. and Ejlali, A. 2007c Comments on “Flow, thermal and entropy generation characteristics inside a porous channel with viscous dissipation” by S. Mahmud and R. A. Frazer [Int. J. Thermal Sciences 44 (2005) 21–32.. *Int. J. Therm. Sci.* **46**, 614–616. [4.16.5]
- Hooman, K., Pourshaghaghy, A. and Ejlali, A. 2006 Effects of viscous dissipation on thermally developing forced convection in a porous saturated circular tube with an isoflux wall. *Appl. Math. Mech. (English edit.)* **27**, 683–694. [4.13]
- Hooman, K., Ranjbar-Kani, A. A. and Ejlali, A. 2003 Axial conduction effects on thermally developing forced convection in a porous medium: circular tube with uniform wall temperature. *Heat Transfer Research* **34**, 34–40. [4.13]
- Hooper, W. B., Chen, T. S. and Armaly, B. F. 1994a Mixed convection along an isothermal vertical cylinder in porous media. *AIAA J. Thermophys. Heat Transfer* **8**, 92–99. [8.1.3]
- Hooper, W. B., Chen, T. S. and Armaly, B. F. 1994b Mixed convection from a vertical plate in porous media with surface injection or suction. *Numer. Heat Transfer A* **25**, 317–329. [8.1.1]
- Horne, R. N. 1979 Three-dimensional natural convection in a confined porous medium heated from below. *J. Fluid Mech.* **92**, 751–766. [6.15.1]
- Horne, R. N. and Caltagirone, J. P. 1980 On the evaluation of thermal disturbances during natural convection in a porous medium. *J. Fluid Mech.* **100**, 385–395. [6.8, 6.15.1]
- Horne, R. N. and O'Sullivan, M. J. 1974a Oscillatory convection in a porous medium heated from below. *J. Fluid Mech.* **66**, 339–352. [6.8, 6.9.1, 6.18]
- Horne, R. N. and O'Sullivan, M. J. 1974b Oscillatory convection in a porous medium: the effect of through flow. *Proc. 5th Australasian Conf. Hydraulics Fluid Mech., Univ. Canterbury, Christchurch, New Zealand*, vol.2, pp. 234–237. [11.7]
- Horne, R. N. and O'Sullivan, M. J. 1978a Origin of oscillatory convection in a porous medium heated from below. *Phys. Fluids* **21**, 1260–1264. [6.8, 6.15.1]
- Horne, R. N. and O'Sullivan, M. J. 1978b Convection in a porous medium heated from below: the effect of temperature dependent viscosity and thermal expansion coefficient. *ASME J. Heat Transfer* **100**, 448–452. [6.18]
- Horton, C. W. and Rogers, F. T. 1945 Convection currents in a porous medium. *J. Appl. Phys.* **16**, 367–370. [6.1, 6.26]

- Hossain, M. A. and Nakayama, A. 1993 Non-Darcy free convective flow along a vertical cylinder embedded in a porous medium with surface mass flux. *Int. J. Heat Fluid Flow* **14**, 385–390. [4.3]
- Hossain, M. A. and Nakayama, A. 1994 Nonsimilar free convection boundary layer in non-Newtonian fluid saturated porous media. *AIAA J. Thermophys. Heat Transfer* **8**, 107–112. [5.1.9.2]
- Hossain, M. A. and Pop, I. 1997 Radiation effect on Darcy free convection flow along an inclined surface placed in porous media. *Heat Mass Transfer* **32**, 223–227. [5.3]
- Hossain, M. A. and Pop, I. 2001 Radiation effects on free convection over a vertical flat plate embedded in a porous medium with high porosity. *Int. J. Therm. Sci.* **40**, 289–295. [5.1.9.4]
- Hossain, M. A. and Rees, D. A. S. 1997 Non-Darcy free convection along a horizontal heated surface. *Transport Porous Media* **29**, 309–321. [5.2]
- Hossain, M. A. and Rees, D. A. S. 2003 Natural convection flow of a viscous incompressible fluid in a rectangular porous cavity heated from below with cold sidewalls. *Heat Mass Transfer* **39**, 657–663. [6.4]
- Hossain, M. A. and Wilson, M. 2002 Natural convection flow in a fluid-saturated porous medium enclosed by non-isothermal walls with heat generation. *Int. J. Therm. Sci.* **41**, 447–454. [7.3.8]
- Hossain, M. A., Banu, N. and Nakayama, A. 1994 Non-Darcy forced convection boundary layer flow over a wedge embedded in a saturated porous medium. *Numer. Heat Transfer A* **26**, 399–414. [4.16.5]
- Hossain, M. A., Banu, N., Rees, D. A. S. and Nakayama, A. 1996 Unsteady forced convection boundary layer flow through a saturated porous medium. Proceedings of the International Conference on Porous Media and their Applications in Science, Engineering and Industry, (K. Vafai and P.N. Shivakumar, eds), Engineering Foundation, New York, 85–101. [4.8]
- Hossain, M. A., Pop, I. and Rees, D. A. S. 2000 The effect of time-periodic surface oscillations on free convection from a vertical surface in a porous medium. *Transport Porous Media* **39**, 119–130. [5.1.9.7]
- Hossain, M. A., Pop, I. and Vafai, K. 1999a Combined free-convection heat and mass transfer above a near-horizontal surface in a porous medium. *Hybrid Methods Engng.* **1**, 87–102. [9.2.1]
- Hossain, M. A., Vafai, K. and Khanafer, K. M. N. 1999b Non-Darcy natural convection heat and mass transfer along a vertical permeable cylinder embedded in a porous medium. *Rev. Gén. Therm.* **38**, 854–862. [9.2.1]
- Hossain, M. A., Nakayama, A. and Pop, I. 1995 Conjugate free convection of non-Newtonian fluids about a vertical cylindrical fin in porous media. *Heat Mass Transfer* **30**, 149–153. [5.12.1]
- Howell, J. R. 2000 Radiative transfer in porous media. *Handbook of Porous Media* (K. Vafai, ed.) Marcel Dekker, New York, pp. 663–698. [2.6]
- Howells, I. D. 1998 Drag on fixed beds of fibres in slow flow. *J. Fluid Mech.* **355**, 163–192. [1.5.3]
- Howle, L. E., Behringer, R. P. and Georgiadis, J. G. 1997 Convection and flow in porous media. Part 2. Visualization by shadowgraph. *J. Fluid Mech.* **332**, 247–26. [6.9.1]
- Howle, L. and Georgiadis, J. G. 1994 Natural convection in porous media with anisotropic dispersive thermal conductivity. *Int. J. Heat Mass Transfer* **37**, 1081–1094. [6.12]
- Howle, L. E. 2002 Convection in ordered and disordered porous layers. In *Transport Phenomena in Porous Media II* (D. B. Ingham and I. Pop, eds.) Elsevier, Oxford, pp. 155–176. [6.9.1]
- Hsiao, K. T. and Advani, S. G. 1999 Modified effective thermal conductivity due to heat dispersion in fibrous porous media. *Int. J. Heat Mass Transfer* **42**, 1237–1254. [2.1.1]
- Hsiao, S. W. 1995 A numerical study of transient natural convection about a corrugated plate embedded in an enclosed porous medium. *Int. J. Num. Meth. Heat Fluid Flow* **5**, 629–646. [7.11]
- Hsiao, S. W. 1998 Natural convection in an inclined porous cavity with variable porosity and thermal dispersion effects. *Int. J. Numer. Methods Heat Fluid Flow* **8**, 97–117. [7.8]
- Hsiao, S. W. and Chen, C. K. 1994 Natural convection heat transfer from a corrugated plate in an enclosed porous medium. *Numer. Heat Transfer A* **25**, 331–345. [7.11]
- Hsiao, S. W., Chen, C. K. and Cheng, P. 1994 A numerical solution for natural convection in an inclined porous cavity with a discrete heat source on one wall. *Int. J. Heat Mass Transfer* **37**, 2193–2201. [7.8]

- Hsiao, S. W., Cheng, P. and Chen, C.K. 1992 Non-uniform porosity and thermal dispersion effects on natural convection about a heated horizontal cylinder in an enclosed porous medium. *Int. J. Heat Mass Transfer* **35**, 3407–3418. [7.11]
- Hsieh, J. C., Chen, T. S. and Armaly, B. F. 1993a Nonsimilarity solutions for mixed convection from vertical surfaces in porous media: variable surface temperature or heat flux. *Int. J. Heat Mass Transfer* **36**, 1485–1493. [8.1.1]
- Hsieh, J. C., Chen, T. S. and Armaly, B. F. 1993b Mixed convection along a non isothermal vertical flat plate embedded in a porous medium: the entire regime. *Int. J. Heat Mass Transfer* **36**, 1819–1825. [8.1.1]
- Hsieh, W. H. and Lu, S. F. 1998 Heat-transfer analysis of thermally developing region of annular porous media. *Heat Transfer* 1998, Proc. 11th IHTC 4, 447–452. [4.13]
- Hsieh, W. H. and Lu, S. F. 2000 Heat-transfer analysis and thermal dispersion in thermally-developing region of a sintered porous metal channel. *Int. J. Heat Mass Transfer* **43**, 3001–3011. [2.2.4]
- Hsieh, W. H., Wu, J. Y., Shih, W. H. and Chiu, W. C. 2004 Experimental investigation of heat-transfer characteristics of aluminum-foam heat sinks. *Int. J. Heat Mass Transfer* **47**, 5149–5157. [4.10]
- Hsu, C. T. 1999 A closure model for transient heat conduction in porous media. *ASME J. Heat Transfer* **121**, 733–739. [2.2.1]
- Hsu, C. T. 2000 Heat conduction in porous media. *Handbook of Porous Media* (K Vafai, ed.) Marcel Dekker, New York, pp. 171–200. [2.2.1]
- Hsu, C. T. 2005 Dynamic modeling of convective heat transfer in porous media. *Handbook of Porous Media* (K Vafai, ed.), 2nd ed., Taylor and Francis, New York, pp. 39–80. [2.2.1, 2.5, 2.6]
- Hsu, C. T. and Cheng, P. 1979 Vortex instability in buoyancy-induced flow over inclined heated surfaces in porous media. *ASME J. Heat Transfer* **101**, 660–665. [5.4]
- Hsu, C. T. and Cheng, P. 1980a Vortex instability of mixed convection flow in a semi-infinite porous medium bounded by a horizontal surface. *Int. J. Heat Mass Transfer* **23**, 789–798. [8.1.2]
- Hsu, C. T. and Cheng, P. 1980b The onset of longitudinal vortices in mixed convective flow over an inclined surface in a porous medium. *ASME J. Heat Transfer* **102**, 544–549. [8.1.2]
- Hsu, C. T. and Cheng, P. 1985a Effects of upstream geometry on natural convection of a Darcian fluid about a semi-infinite inclined heated surface. *ASME J. Heat Transfer* **107**, 283–292. [5.12.2]
- Hsu, C. T. and Cheng, P. 1985b The Brinkman model for natural convection about a semi-infinite vertical flat plate in a porous medium. *Int. J. Heat Mass Transfer* **28**, 683–697. [5.1.7.1]
- Hsu, C. T. and Cheng, P. 1988 Closure schemes of the macroscopic energy equation for convective heat transfer in porous media. *Int. Comm. Heat Mass Transfer* **15**, 689–703. [4.9]
- Hsu, C. T. and Cheng, P. 1990 Thermal dispersion in a porous medium. *Int. J. Heat Mass Transfer* **33**, 1587–1597. [1.5.2, 1.5.3, 2.2.4, 4.9]
- Hsu, C. T. and Fu, H. 1998 Reacting stagnation flows in catalytic porous beds. *Int. J. Heat Mass Transfer* **41**, 2335–2346. [3.4]
- Hsu, C. T., Cheng, P. and Homsy, G. M. 1978 Instability of free convective flow over a horizontal impermeable surface in a porous medium. *Int. J. Heat Mass Transfer* **21**, 1221–1228. [5.4]
- Hsu, C. T., Cheng, P. and Wong, K. W. 1994 Modified Zehner-Schundler models for stagnant thermal conductivity of porous media. *Int. J. Heat Mass Transfer* **37**, 2751–2759. [2.2.1]
- Hsu, C. T., Cheng, P. and Wong, K. W. 1995 A lumped-parameter model for stagnant thermal conductivity of spatially periodic media. *ASME J. Heat Transfer* **117**, 264–269. [2.2.1]
- Hsu, C. T., Fu, H. L. and Cheng, P. 1999 On pressure-velocity correlation of steady and oscillating flows in generators made of wire screens. *ASME J. Fluids Engng.* **121**, 52–56. [1.5.2]
- Hu, X. J., Du, J. H., Lei, S. Y. and Wang, B. X. 2001 A model for the thermal conductivity of unconsolidated porous media based on capillary pressure-saturation relation. *Int. J. Heat Mass Transfer* **44**, 247–25. (corrigendum 1267–1268). [2.2.1]
- Huang, H. and Ayoub, J. 2008 Applicability of the Forchheimer equation for non-Darcy flow in porous media. *SPE Journal* **13**, 112–122. [1.5.2]

- Huang, J. S., Tsai, R., Huang, K. H. and Huang, C. H. 2011 Thermal-diffusion and diffusion-thermo effects on natural convection along an inclined stretching surface in a porous medium with chemical reaction. *Chem. Engng. Comm.* **198**, 453–473. [9.2.1]
- Huang, M. J. and Chen, C. K. 1985 Effects of surface mass transfer on free convection flow over vertical cylinder imbedded in a saturated porous medium. *ASME J. Energy Resources Tech.* **107**, 394–396. [5.7]
- Huang, M. J., Yih, K. A., Chou, Y. L. and Chen, C. K. 1986 Mixed convection over a horizontal cylinder or a sphere embedded in a saturated porous medium. *ASME J. Heat Transfer* **108**, 469–471. [8.1.3]
- Huang, P. C. and Chen, C. C. 2012 Simulation of mixed convection in a vertical channel containing discrete porous-covering heat blocks. *Int. J. Heat Mass Transfer* **55**, 3174–3159. [8.3.1]
- Huang, P. C. and Vafai, K. 1993 Flow and heat transfer control over an external surface using a porous block array arrangement. *Int. J. Heat Mass Transfer* **36**, 4019–4032. [4.11]
- Huang, P. C. and Vafai, K. 1994a Passive alteration and control of convective heat transfer utilizing alternate porous cavity-block wafers. *Int. J. Heat Fluid Flow* **15**, 48–61. [4.11]
- Huang, P. C. and Vafai, K. 1994b Internal heat transfer augmentation in a channel using alternate set of porous cavity-block obstacles. *Numer. Heat Transfer A* **25**, 519–539. [4.11]
- Huang, P. C. and Vafai, K. 1994c Analysis of flow and heat transfer over an external boundary covered with a porous substrate. *ASME J. Heat Transfer* **116**, 768–771. [4.11]
- Huang, P. C. and Vafai, K. 1994d Analysis of forced convection enhancement in a channel using porous blocks. *AIAA J. Thermophys. Heat Transfer* **8**, 563–573. [4.11]
- Huang, P. C. and Yang, C. F. 2008 Analysis of pulsating convection from two heat sources mounted with porous blocks. *Int. J. Heat Mass Transfer* **51**, 6294–6311. [4.16.2]
- Huang, P. C., Yang, C. F. and Chang, S. Y. 2004a Mixed convection cooling of heat sources mounted with porous blocks. *J. Thermophys. Heat Transfer* **18**, 464–475. [8.3.1]
- Huang, P. C., Yang, C. F., Hwang, J. J. and Cjiu, M. T. 2004b Enhancement of forced-convection cooling of multiple heated blocks in a channel using porous covers. *Int. J. Heat Mass Transfer* **48**, 674–664. [4.11]
- Huang, Z. F., Nakayama, A., Yang, K., Yang, C. and Liu, W. 2010 Enhancing heat transfer in the core flow by using porous medium insert in a tube. *Int. J. Heat Mass Transfer* **53**, 1164–1174. [4.11]
- Huenefeld, J. S. and Plumb, O. A. 1981 A study of non-Darcy natural convection from a vertical heated surface in a saturated porous medium. ASME 20th National Heat Transfer Conf. Paper 81-HT-45. [5.1.8]
- Hung, C. I. 1991 Note on conjugate natural convection-conduction heat transfer for a vertical plate fin embedded in high-porosity medium. *Int. J. Non-linear Mech.* **26**, 135–140. [5.12.1]
- Hung, C. I. and Chen, C. B. 1997 Non-Darcy free convection in a thermally stratified porous medium along a vertical plate with variable heat flow. *Heat Mass Transfer* **33**, 101–107. [5.1.4]
- Hung, C. I., Chen, C. H. and Chen, C. B. 1999 Non-Darcy free convection along a nonisothermal vertical surface in a thermally stratified porous medium. *Int. J. Engng. Sci.* **37**, 477–495. [5.1.4]
- Hung, C. I., Chen, C. K. and Cheng, P. 1989 Transient conjugate natural convection heat transfer along a vertical plate fin in a high-porosity medium. *Numer. Heat Transfer* **15**, 133–148. [5.12.1]
- Hung, Y. M. and Tso, C. P. 2008 Temperature variations of forced convection in porous media for heating and cooling processes: internal heating effect of viscous dissipation. *Transp. Porous Media* **75**, 319–322. [4.9]
- Hung, Y. M. and Tso, C. P. 2009 Effects of viscous dissipation on fully developed forced convection in porous media *Int. Comm. Heat Mass Transfer* **36**, 597–603. [4.9]
- Hunke, E. C., Notz, D., Turner, A. K. and Vancoppenolle, M. 2011 The multiphase physics of sea ice: A review. *Cryosphere* **5**, 989–1009. [10.2.3]
- Hunt, M. L. and Tien, C. L. 1988a Effects of thermal dispersion on forced convection in fibrous media. *Int. J. Heat Mass Transfer* **31**, 301–309. [4.9]

- Hunt, M. L. and Tien, C. L. 1988b Non-Darcian convection in cylindrical packed beds. *ASME J. Heat Transfer* **110**, 378–384. [4.9]
- Hunt, M. L. and Tien, C. L. 1990 Non-Darcian flow, heat and mass transfer in catalytic packed-bed reactors. *Chem. Engng. Sci.* **45**, 55–63. [6.19.2]
- Huppert, H. E. and Worster, M. G. 2012 Flows involving phase change. In *Handbook of Environmental Fluid Mechanics* (ed. H. J. Fernando), CRC Press. [10.2.3]
- Husnain, S., Mehmood, A., Beg, O. A. and Ali, A. 2012 Suction and blowing effects on unsteady flow and heat transfer through porous media with variable viscosity. *J. Porous Media* **15**, 293–302. [5.1.9.9]
- Hutter, K. and Straughan, B. 1997 Penetrative convection in thawing subsea permafrost. *Cont. Mech. Thermodyn.* **9**, 259–272. [11.3]
- Hutter, K. and Straughan, B. 1999 Models for convection in thawing porous media in support for the subsea permafrost equations. *J. Geophys. Res.* **104**, 29249–29260. [11.3]
- Hwang, G. and Chao, C. H. 1992 Effects of wall conduction and Darcy number on laminar mixed convection in a horizontal square porous channel. *ASME J. Heat Transfer* **114**, 614–621. [8.2.5]
- Hwang, G. J. and Chao, C. H. 1994 Heat transfer measurements and analysis for sintered porous channels. *ASME J. Heat Transfer* **116**, 456–464. [4.9]
- Hwang, G. J., Cai, Y. and Cheng, P. 1992 An experimental study of forced convection in a packed channel with asymmetric heating. *Int. J. Heat Mass Transfer* **35**, 3029–3039. [4.5]
- Hwang, G. J., Wu, C. C. and Chao, C. H. 1995 Investigation on non-Darcian forced convection in an asymmetrically heated sintered porous channel. *ASME J. Heat Transfer* **117**, 725–732. [4.16.5]
- Hwang, I. G. 2001 Convective instability in porous media during solidification. *AIChE J.* **47**, 1698–1700. [10.2.3]
- Hwang, I. G. and Choi, C. K. 2008 Onset of convection in a porous mush during binary solidification. *Korean J. Chem. Engng.* **25**, 199–202. [10.2.3]
- Hwang, I. G. and Choi, C. K. 2009 Stability of buoyancy-driven convection in directional solidification of a binary melt. *Korean J. Chem. Engng.* **26**, 930–934. [10.2.3]
- Hwang, J. J., Hwang, G. J., Yeh, R. H. and Chao, C. H. 2002 Measurement of interstitial convective heat transfer and frictional drag for flow across metal foams. *ASME J. Heat Transfer* **124**, 120–124. [4.9]
- Ibrahim, F. S. and Hassanien, I. A. 2000 Influence of variable permeability on combined convection along a nonisothermal wedge in a saturated porous medium. *Transport Porous Media* **39**, 57–71. [8.1.4]
- Ibrahim, F. S., Abdel-Gaid, S. M. and Gorla, R. S. R. 2000 Non-Darcian mixed convection flow along a vertical plate embedded in a non-Newtonian fluid saturated porous medium with surface mass transfer. *Int. J. Numer. Meth. Heat Fluid Flow* **10**, 397–408. [8.1.1]
- Ibrahim, F. S., Hady, F. M., Abdel-Gaied, S. M. and Eid, M. R. 2010 Influence of chemical reaction on heat and mass transfer of Non-Newtonian fluid with yield stress by free convection from vertical surface in porous medium considering Soret effect. *Appl. Math. Mech. - English ed.* **31**, 675–684. [9.2.1]
- Ibrahim, F. S., Mansour, M. A. and Abdel-Gaid, S. M. 2005 Radiative and thermal dispersion effects on non-Darcy natural convection with lateral mass flux for non-Newtonian fluid from a vertical flat plate in a porous medium. *Transport Porous Media* **61**, 45–57. [5.1.9.2]
- Ichimiya, K., Takeda, T., Uemura, T. and Norikuni, T. 2009 Effects of a high porous material on heat transfer and flow in a circular tube. *ASME J. Heat Transfer* **131**, #024503. [4.16.5]
- Idris, R. and Hashim, I. 2010 Effects of a magnetic field on chaos for low Prandtl number convection in a porous medium *Nonlinear Dyn.* **62**, 905–917. [6.21]
- Idris, R. and Hashim, I. 2011 On the effects of a cubic temperature profile on oscillatory Rayleigh-Bénard convection in a viscoelastic fluid-filled high-porosity medium. *J. Porous Media* **14**, 437–447. [6.23]

- Imadojemu, H. and Johnson, R. 1991 Convective heat transfer from a heated vertical plate surrounded by a saturated porous medium. *Proc. ASME & JSME Thermal Engineering Joint Conference—1991*, vol.4, pp. 203–212. [5.1.8]
- Imadojemu, H. E. and Porter, L. H. 1995 Effective thermal conductivity of a saturated porous medium *AIAA J. Thermophys. Heat Transfer* **9**, 573–575. [2.2.1]
- Imani, G. R., Maerefat, M. and Hooman, K. 2012 Estimation of heat flux bifurcation at the heated boundary of a porous medium using a pore-scale numerical simulation. *Int. J. Therm. Sci.* **54**, 109–118. [4.10]
- Imhoff, P. T. and Green, T. 1988 Experimental investigation of double-diffusive groundwater fingers. *J. Fluid Mech.* **188**, 363–382. [9.1.3]
- Impey, M. D. and Riley, D. S. 1991 On exchanges between convective modes in a slightly tilted porous cavity. *Math. Proc. Camb. Phil. Soc.* **110**, 395–416. [7.8]
- Impey, M. D., Riley, D. S. and Winters, K. H. 1990 The effect of sidewall imperfections on pattern formation in Lapwood convection. *Nonlinearity* **3**, 197–230. [6.15.1]
- Inaba, H., Ozaki, K. and Nozu, S. 1993 Convective heat transfer of a horizontal-spherical particle layer heated from below and cooled from above. *Heat Transfer Japan Res.* **22**, 573–595. [4.5]
- Inaba, H., Ozaki, K. and Nozu, S. 1994 Mixed convection heat transfer in an open shallow cavity heated from below and packed with a one-step arrangement of spherical particles. *Heat Transfer Japan Res.* **23**, 66–85. [4.5, 8.2.1]
- Inaba, H., Sugawara, M. and Blumenberg, J. 1988 Natural convection heat transfer in an inclined porous layer. *Int. J. Heat Mass Transfer* **31**, 1365–1372. [7.8]
- Ingebretsen, S. E. and Hayba, D. O. 1994 Fluid-flow and heat-transport near the critical-point of  $\text{H}_2\text{O}$ . *Geophys. Res. Lett.* **21**, 2199–2202. [11.8]
- Ingebretsen, S. E., Geiger, S., Hurwitz, S. and Priesner, T. 2010 Numerical simulation of magmatic hydrothermal systems. *Rev. Geophysics* **47**, #RG1002. [11.8]
- Ingham D. B., Merkin, J. H. and Pop, I. 1985a Flow past a suddenly cooled horizontal flat surface in a saturated porous medium. *Acta Mech.* **57**, 183–202. [5.3]
- Ingham, D. B. 1986 The non-Darcy free convection boundary layer on axi-symmetric and two-dimensional bodies of arbitrary shape. *Int. J. Heat Mass Transfer* **29**, 1759–1760. [5.9]
- Ingham, D. B. 1988 An exact solution for non-Darcy free convection from a horizontal line source. *Wärme-Stoffübertrag.* **22**, 125–127. [5.10.1.1, 5.10.1.2]
- Ingham, D. B. and Brown, S. N. 1986 Flow past a suddenly heated vertical plate in a porous medium. *Proc. Roy. Soc. London Ser. A* **403**, 51–80. [5.1.3]
- Ingham, D. B. and Pop, I. 1986a Free-forced convection from a heated longitudinal horizontal cylinder embedded in a porous medium. *Wärme-Stoffübertrag.* **20**, 283–289. [8.1.3]
- Ingham, D. B. and Pop, I. 1986b A horizontal flow past a partially heated infinite vertical cylinder embedded in a porous medium. *Int. J. Engng. Sci.* **24**, 1351–1363. [8.1.3]
- Ingham, D. B. and Pop, I. 1987a Darcian free convective flow about an impermeable horizontal surface bounded by a vertical wall. *Int. J. Engng. Sci.* **25**, 373–383. [5.12.2]
- Ingham, D. B. and Pop, I. 1987b Free convection from a semi-infinite vertical surface bounded by a horizontal wall in a porous medium. *Int. J. Heat Mass Transfer* **30**, 1615–1622. [5.12.2]
- Ingham, D. B. and Pop, I. 1987c Natural convection about a heated horizontal cylinder in a porous medium. *J. Fluid Mech.* **184**, 157–181. [5.5.2]
- Ingham, D. B. and Pop, I. 1988 Higher-order effects in natural convection flow over uniform flux inclined flat plates in porous media. *Wärme-Stoffübertrag.* **22**, 239–242. [5.3]
- Ingham, D. B. and Pop, I. 1991 Mixed convection about a cylinder embedded to a wedge in porous media *AIAA J. Thermophys. Heat Transfer* **5**, 117–120. [8.1.4]
- Ingham, D. B., Al-Hadrami, A. K., Elliott, L. and Wen, X. 2006 Fluid flows through some geological discontinuities. *ASME J. Appl. Mech.* **73**, 34–40. [11.8]
- Ingham, D. B., Merkin, J. H. and Pop, I. 1982 Flow past a suddenly cooled vertical flat surface in a saturated porous medium. *Int. J. Heat Mass Transfer* **25**, 1916–1919. [5.1.3]

- Ingham, D. B., Merkin, J. H. and Pop, I. 1983 The collision of free-convection boundary layers on a horizontal cylinder embedded in a porous medium. *Quart. J. Mech. Appl. Math.* **36**, 313–335. [5.5.1]
- Ingham, D. B., Merkin, J. H. and Pop, I. 1985b Natural convection from a semi-infinite flat plate inclined at a small angle to the horizontal in a saturated porous medium. *Acta Mech.* **57**, 183–202. [5.3]
- Ingham, D. B., Pop, I. and Cheng, P. 1990 Combined free and forced convection in a porous medium between two vertical walls with viscous dissipation. *Transport in Porous Media* **5**, 381–398. [8.3.1]
- Inoue, M. and Nakayama, A. 1998 Numerical modeling of non-Newtonian fluid flow in a porous medium using a three-dimensional periodic array. *ASME J. Fluids Engng.* **120**, 131–135. [1.5.4]
- Irmay, S. 1958 On the theoretical derivation of Darcy and Forchheimer formulas. *Eos, Trans. AGU* **39**, 702–707. [1.5.2]
- Ishak, A., Nazar, R. and Pop, I. 2008a Dual solutions in mixed convection flow near a stagnation point on a vertical surface in a porous medium. *Int. J. Heat Mass Transfer* **51**, 1150–1155. [8.1.1]
- Ishak, A., Nazar, R. and Pop, I. 2008b Mixed convective boundary layer flow over a vertical surface embedded in a thermally stratified porous medium. *Phys. Lett. A* **372**, 2355–2358. [8.1.1]
- Islam, M. R. 1992 Evolution of oscillatory and chaotic flows in mixed convection in porous media in the non-Darcy regime. *Chaos, Solitons, Fractals*, **2**, 51–71. [8.2.1]
- Islam, M. R. 1993 Route to chaos in chemically enhanced thermal convection in porous media. *Chem. Engng Comm.* **124**, 77–95. [6.17]
- Islam, M. R. and Nandakumar, K. 1990 Transient convection in saturated porous layers. *Int. J. Heat Mass Transfer* **33**, 151–161. [6.17]
- Islam, R. M. and Nandakumar, K. 1986 Multiple solutions for buoyancy-induced flow in saturated porous media for large Péclet numbers. *ASME J. Heat Transfer* **108**, 866–871. [8.2.1]
- Islam, R. M. and Nandakumar, K. 1988 Mixed convection heat transfer in porous media in the non-Darcy regime. *Canad. J. Chem. Engng.* **66**, 68–74. [8.2.1]
- Israel-Cookey, C., Ogulu, A. and Omubo-Pepple, Ichimiya, K. 2003 Influence of viscous dissipation and radiation on unsteady MHD free-convection flow past an infinite heated vertical plate in a porous medium with time-dependent suction. *Int. J. Heat Mass Transfer* **46**, 2305–2311. [5.1.9.4]
- Itamura, M. T., Francis, N. D., Webb, S. W. and James, D. L. 2004 In-drift natural convection analysis of the low-temperature operating mode design. *Nuclear Tech.* **148**, 115–124. [11.8]
- Iyer, S. V. and Vafai, K. 1999 Passive heat transfer augmentation in a cylindrical annulus utilizing a porous perturbation. *Numer. Heat Transfer A* **36**, 115–128. [7.3.3]
- Izadifar, M., Biaik, O. D. and Simonson, C. J. 2006 Modeling of the packed bed drying of paddy rice using the local volume averaging (LVA) approach. *Food Research Int.* **39**, 712–720. [3.6]
- Izadpanah, M. R., Müller-Steinhagen, H. and Jamialahmadi, M. 1998 Experimental and theoretical studies of convective heat transfer in a cylindrical porous medium. *Int. J. Heat Fluid Flow* **19**, 629–635. [4.9]
- Jaballah, S., Bennacer, R., Sammouda, H. and Belghith, A. 2006 Simulation of mixed convection in a channel partially filled with porous media. *Prog. Comput. Fluid Dyn.* **6**, 335–341. [8.4.1]
- Jaballah, S., Bennacer, R., Sammouda, H. and Belghith, A. 2008 Numerical simulation of mixed convection in a channel irregularly heated and partially filled with a porous medium. *J. Porous Media* **11**, 247–257. [8.4.1]
- Jaballah, S., Sammouda, H. and Bennacer, R. 2012 Study of mixed convection in a channel with porous layers using a thermal non-equilibrium model. *J. Porous Media* **15**, 51–62. [8.4.1]
- Jaber, T. I. and Saghir, M. Z. 2011 Three-dimensional study of permeability effect on convection in heterogeneous porous medium filled with a ternary hydrocarbon mixture. *J. Porous Media* **14**, 305–315. [9.1.6.4]

- Jaber, T. J., Yan, Y. and Saghir, M. Z. 2008 Soret effect for a ternary mixture in porous cavity: Modeling with variable diffusion coefficients and viscosity. *ASME J. Fluids Engng.* **130**, #081703. [9.1.4]
- Jadhav, R. S. and Pillai, K. M. 2003 Numerical study of heat transfer during unsaturated flow in dual-scale porous media. *Numer. Heat Transfer A* **43**, 385–407. [3.6]
- Jaffrenou, J. Y., Bories, S. A. and Combarinous, M. A. 1974 Natural convective flows and mean heat transfer in a sloping porous layer. *Heat Transfer 1974*, Japan Soc. Mech. Engrs. and Soc. Chem. Engrs. Japan, Tokyo. Vol. 5, pp. 83–87. [7.8]
- Jäger, W. and Mikelić, A. 2000 On the interface boundary condition of Beavers, Joseph and Saffman. *SIAM J. Appl. Math.* **60**, 1111–1127. [1.6]
- Jäger, W. and Mikelić, A. 2009 Modeling effective interface laws for transport phenomena between an unconfined fluid and a porous medium using homogenization. *Transp. Porous Media* **78**, 489–508. [1.6]
- Jäger, W. and Mikelić, A. 2010 Letter to the Editor: Comments on “About the Beavers and Joseph boundary condition”. *Transp. Porous Media* **83**, 267–268. [1.6]
- Jäger, W., Mikelić, A. and Neuss, N. 2001 Asymptotic analysis of the laminar viscous flow over a porous bed. *SIAM J. Sci. Comp.* **22**, 2006–2028. [1.6]
- Jaiswal, B. S. and Soundalgekar, V. M. 2001 Oscillating plate temperature effects on a flow past an infinite vertical porous plate with constant suction and embedded in a porous medium. *Heat Mass Transfer* **37**, 125–131. [5.1.9.7]
- Jamalud-Din, S. D., Rees, D. A. S., Reddy, B. V. K. and Narasimhan, A. 2010 Prediction of natural convection flow using network model and numerical simulations inside enclosure with distributed solid blocks. *Heat Mass Transfer* **46**, 333–343. [7.3.9]
- James, D. F. and Davis, A. M. 2001 Flow at the interface of a model fibrous porous medium. *J. Fluid Mech.* **426**, 47–72. [1.6]
- Jamet, D. and Chandesris, M. 2009 On the intrinsic nature of jump coefficients at the interface between a porous medium and a free fluid region. *Int. J. Heat Mass Transfer* **52**, 289–300. [1.6]
- Jamet, D., Chandesris, M. and Goyeau, B. 2009 On the equivalence of the discontinuous one- and two-domain approaches for the modeling of transport phenomena at the fluid/porous interface. *Transp. Porous Media* **78**, 403–418. [1.6]
- Jamet, P., Frague, D., Costesèque, P., de Marsily, G. and Cernes, A. 1992 The thermogravitational effect in porous media: A modeling approach. *Transport Porous Media* **9**, 223–240. [9.1.4]
- Jamialahmadi, M., Muller-Steinhagen, H. and Izadpanah, M. R. 2005 Pressure drop, gas hold-up and heat transfer during single and two-phase flow through porous media. *Int. J. Heat Fluid Flow* **26**, 156–172. [3.5]
- Jamin, Y. L. and Mohamad, A. A. 2007 Enhanced heat transfer using porous carbon foam in cross flow. – Part 1 : Forced convection. *ASME J. Heat Transfer* **129**, 735–742. [4.16.5]
- Jamin, Y. L. and Mohamad, A. A. 2008 Natural convection heat transfer enhancements from a cylinder using porous carbon foam: Experimental study. *ASME J. Heat Transfer* **130**, #122502. [5.5.1]
- Jang, J. Y. and Chang, W. J. 1987 Vortex instability of inclined buoyant layer in porous media saturated with cold water. *Int. Comm. Heat Mass Transfer* **14**, 405–416. [5.4]
- Jang, J. Y. and Chang, W. J. 1988a Vortex instability of buoyancy-induced inclined boundary layer flow in a saturated porous medium. *Int. J. Heat Mass Transfer* **31**, 759–767. [5.4]
- Jang, J. Y. and Chang, W. J. 1988b The flow and vortex instability of horizontal natural convection in a porous medium resulting from combined heat and mass buoyancy effects. *Int. J. Heat Mass Transfer* **31**, 769–777. [9.2.1]
- Jang, J. Y. and Chang, W. J. 1988c Buoyancy-induced inclined boundary layer flow in a porous medium resulting from combined heat and mass buoyancy effects. *Int. Comm. Heat Mass Transfer* **15**, 17–30. [9.2.1]
- Jang, J. Y. and Chang, W. J. 1988d Buoyancy-induced inclined boundary layer flow in a saturated porous medium. *Comput. Methods Appl. Mech.* **68**, 333–344. [5.3]
- Jang, J. Y. and Chang, W. J. 1989 Maximum density effects on vortex instability of horizontal and inclined buoyancy-induced flows in porous media. *ASME J. Heat Transfer* **111**, 572–574. [5.3]

- Jang, J. Y. and Chen, C. N. 1989 Natural convection in an inclined porous enclosure with an off-centre diathermal partition. *Wärme-Stoffübertrag.* **24**, 117–123. [7.8]
- Jang, J. Y. and Chen, J. L. 1992 Forced convection in a parallel plate channel partially filled with a high porosity medium. *Int. Comm. Heat Mass Transfer* **19**, 263–273. [4.11]
- Jang, J. Y. and Chen, J. L. 1993a Thermal dispersion and inertia effects on vortex instability of a horizontal mixed convection flow in a saturated porous medium. *Int. J. Heat Mass Transfer* **36**, 383–389. [5.4]
- Jang, J. Y. and Chen, J. L. 1993b Variable porosity effect on vortex instability of a horizontal mixed convection flow in a saturated porous medium. *Int. J. Heat Mass Transfer* **36**, 1573–1583. [5.4]
- Jang, J. Y. and Chen, J. L. 1994 Variable porosity and thermal dispersion effects on vortex instability of a horizontal natural convection flow in a saturated porous medium. *Wärme-Stoffübertrag.* **29**, 153–160. [5.4]
- Jang, J. Y. and Hsu, C. T. 2007 Effects of magnetohydrodynamics on the vortex instability of natural convection flow over a horizontal plate in a saturated porous medium. *J. Chinese Soc. Mech. Engrs.* **28**, 71–80. [5.4]
- Jang, J. Y. and Hsu, C. T. 2009a Hall effect on the heat and mass transfer with MHD natural convection from a vertical plate in a porous medium. *J. Chinese Soc. Mech. Engrs.* **30**, 371–380. [9.2.1]
- Jang, J. Y. and Hsu, C. T. 2009b Vortex instability of MHD natural convection flow over a horizontal plate in a porous medium. *Comput. Fluids* **38**, 333–339. [5.4]
- Jang, J. Y. and Leu, J. S. 1992 Buoyancy-induced boundary layer flow of liquid in a porous medium with temperature-dependent viscosity. *Int. Comm. Heat Mass Transfer* **19**, 435–444. [5.1.9.9]
- Jang, J. Y. and Leu, J. S. 1993 Variable viscosity effects on the vortex instability of free convection boundary layer flow over a horizontal surface in a porous medium. *Int. J. Heat Mass Transfer* **36**, 1287–1294. [5.4]
- Jang, J. Y. and Lie, K. N. 1992 Vortex instability of mixed convection flow over horizontal and inclined surfaces in a porous medium. *Int. J. Heat Mass Transfer* **35**, 2077–2085. [5.4]
- Jang, J. Y. and Ni, J. R. 1989 Transient free convection with mass transfer from an isothermal vertical flat plate embedded in a porous medium. *Int. J. Heat Fluid Flow* **10**, 59–65. [9.2.1]
- Jang, J. Y. and Ni, J. R. 1992 Mixed convection adjacent to inclined flat surfaces embedded in a porous medium. *Wärme-Stoffübertrag.* **27**, 103–108. [8.1.1]
- Jang, J. Y. and Shiang, C. T. 1997 The mixed convection plume along a vertical adiabatic surface embedded in a non-Darcian porous medium. *Int. J. Heat Mass Transfer* **40**, 1693–1699. [8.1.4]
- Jang, J. Y., Lie, K. N. and Chen, J. L. 1995 Influence of surface mass flux on vortex instability of a horizontal mixed convection flow in a saturated porous medium. *Int. J. Heat Mass Transfer* **38**, 3305–3311. [8.1.2]
- Jang, J. Y., Tzeng, D. J. and Shaw, H. J. 1991 Transient free convection with mass transfer on a vertical plate embedded in a high porosity medium. *Numer. Heat Transfer A* **20**, 1–18. [9.2.3]
- Jang, T. M., Tzang, S. C. and Chang, C. W. 2010 Forced convection of the brass-beads packed bed situated in a vertical oncoming flow. *Int. J. Therm. Sci.* **49**, 829–837. [4.16.5]
- Jannot, M., Naudin, P. and Vianny, S. 1973 Convection mixte en milieu poreux. *Int. J. Heat Mass Transfer* **16**, 395–410. [8.1.4]
- Jany, P. and Bejan, A. 1988a Scales of melting in the presence of natural convection in a rectangular cavity filled with porous medium. *ASME J. Heat Transfer* **110**, 526–529. [10.1.1, 10.1.2]
- Jany, P. and Bejan, A. 1988b Scaling theory of melting with natural convection in an enclosure. *Int. J. Heat Mass Transfer* **31**, 1221–123. [10.1.1]
- Jasmin, S. and Prud'homme, M. 2005 Inverse determination of a heat source from a solute concentration generation model in porous medium. *Int. Comm. Heat Mass Transfer* **32**, 43–53. [9.3.1]

- Javadpour, F. and Nicot, J. P. 2011 Enhanced CO<sub>2</sub> storage and sequestration in deep saline aquifers by nanoparticles: Clogging disposal of depleted uranium and CO<sub>2</sub>. *Transp. Porous Media* **89**, 265–284. [11.11]
- Jawaheri, M., Abedi, J. and Hassanzadeh, H. 2009 Onset of convection in CO<sub>2</sub> sequestration in deep saline aquifers. *J. Canad. Petrol. Tech.* **48**, 22–47. [11.11]
- Jawaheri, M., Abedi, J. and Hassanzadeh, H. 2010 Linear stability analysis of double-diffusive convection in porous media, with application to geological storage of CO<sub>2</sub>. *Transp. Porous Medai* **84**, 441–456. [11.11]
- Jawat, J. M. and Hashim, I. 2010 Low Prandtl number chaotic convection in porous media with uniform internal heat generation. *Int. Comm. Heat Mass Transfer* **37**, 629–636. [6.11.2]
- Jayanthi, S. and Kumari, M. 2006 Effect of variable viscosity on non-Darcy free or mixed convection flow on a vertical surface in a fluid saturated porous medium. *Mech. Res. Comm.* **33**, 148–156. [8.1.6]
- Jayanthi, S. and Kumari, M. 2007 Effect of variable viscosity on non-Darcy free or mixed convection flow over a vertical surface in a non-Newtonian fluid saturated porous medium. *Appl. Math. Comput.* **186**, 1643–1659. [8.1.6]
- Jeci, R., Kramer, J. and Škerget, L. 2009 Double diffusive natural convection in a horizontal porous layer with the boundary domain integral method. *Acta Geotech. Slov.* **6**, 4–18. [9.1.6.4]
- Jecl, R. and Škerget, L. 2000 Natural convection in a vertical porous cavity. *Zeit. Angew. Math. Mech.* **80**, S691–S693. [7.1.2]
- Jecl, R. and Škerget, L. 2003 Boundary element method for natural convection in non-Newtonian fluid saturated square porous cavity. *Engng. Anal. Bound. Elem.* **27**, 963–975. [7.1.6]
- Jecl, R. and Škerget, L. 2004 Comparison between Forchheimer and the Brinkman model for natural convection in porous media by the boundary element method. In Applications of Porous Media (ICAPM 2004), (eds. A. H. Reis and A. F. Miguel), Évora, Portugal, pp. 113–120. [7.6.2]
- Jecl, R., Škerget, L. and Petresin, E. 2001 Boundary domain integral method for transport phenomena in porous media. *Int. J. Numer. Meth. Fluids* **35**, 39–54. [7.6.2]
- Jen, T. C. and Yan, T. Z. 2005 Developing flow and heat transfer in a channel partially filled with a porous medium. *Int. J. Heat Mass Transfer* **48**, 3995–4009. [4.11]
- Jeng, T. M. and Tzeng, S. C. 2007a Experimental study of forced convection in metallic porous block subject to a confined slot jet. *Int. J. Therm. Sci.* **46**, 1242–1250. [4.16.5]
- Jeng, T. M. and Tzeng, S. C. 2007b Forced convection of metallic foam heat sink under laminar slot jet confined by a parallel wall. *Heat Transfer Engng.* **28**, 484–495. [4.16.5]
- Jeng, T. M. and Tzeng, S. C. 2008 Heat transfer in a lid-driven enclosure filled with water-saturated aluminum foams. *Numer. Heat Transfer A* **54**, 178–196. [4.16.5]
- Jeng, T. M., Tzeng, S. C. and Chang, C. W. 2010 Forced convection of the brass-beads packed bed situated in a vertical oncoming flow. *Int. J. Therm. Sci.* **49**, 829–837. [4.16.5]
- Jeng, T. M., Tzeng, S. C. and Chen, Y. C. 2011 Thermal characteristics in asymmetrically heated channels fully filled with brass beads. *Int. J. Therm. Sci.* **50**, 1853–1860. [4.9]
- Jeng, T. M., Tzeng, S. C. and Hung, Y. H. 2006 An analytical study of local thermal equilibrium in porous heat sinks using fin theory. *Int. J. Heat Mass Transfer* **49**, 1907–1914. [7.3.7]
- Jha, B. K. 1997 Transient convection through vertical porous medium. *Heat Mass Transfer* **33**, 261–263. [7.5]
- Jha, B. K. 2005 Free convection flow through an annular porous medium. *Heat Mass Transfer* **41**, 675–679. [7.3.3]
- Jha, B. K., Odengle, J. O. and Kaurangini, M. L. 2011 Effect of transportation on free-convective Couette flow in a composite channel. *J. Porous Media* **14**, 627–635. [7.7]
- Jiang, C. B. J., Saghfir, M. Z. and Kawaji, M. 2006a Numerical analysis of thermal — solutal convection in heterogeneous porous media. *ASME J. Appl. Mech.* **73**, 21–25. [9.1.4]
- Jiang, C. G., Saghfir, M. Z., Kawaji, M. and Ghorayeb, K. 2004b Two-dimensional numerical simulation of thermo-gravitational convection in a vertical porous column filled with a binary mixture. *Int. J. Therm. Sci.* **43**, 1057–1065. [9.1.4]

- Jiang, C. G., Sahgir, M. Z., Kawaji, M. and Ghorayeb, K. 2004c Contribution of the thermal and molecular diffusion to convection in a vertical porous cavity. In Emerging Technologies and Techniques in Porous Media (D. B. Ingham, A. Bejan, E. Mamut and I. Pop, eds), Kluwer Academic, Dordrecht, pp. 307–320. [9.1.4]
- Jiang, C. G., Sahgir, M. Z. and Kawaji, M. 2004a Thermo-solutal convection in heterogeneous porous media. In Applications of Porous Media (ICAPM 2004), (eds. A. H. Reis and A. F. Miguel), Évora, Portugal, pp. 287–292. [9.1.4]
- Jiang, F., Liu, S., Wang, G. and Chen, H. Z. 2004d The air flow and heat transfer in gravel embankment in permafrost regions. *Science in China D* **47**, 142–151. [7.3.7]
- Jiang, P. X. and Lu, X.C. 2006 Numerical simulation of fluid flow and convection heat transfer in sintered porous plate channels. *Int. J. Heat Mass Transfer* **49**, 1685–1695. [4.16.5]
- Jiang, P. X. and Lu, X.C. 2007 Numerical simulation and theoretical analysis of thermal boundary characteristics of convection heat transfer in porous media. *Int. J. Heat Fluid Flow* **28**, 1144–1156. [4.16.5]
- Jiang, P. X. and Ren, Z. 2001 Numerical investigation of forced convection heat transfer in porous media using a thermal non-equilibrium model. *Int. J. Heat Fluid Flow* **22**, 102–110. [4.10]
- Jiang, P. X., Li, M., Ma, Y. C. and Ren, Z. P. 2004e Boundary conditions and wall effect for forced convection heat transfer in sintered porous channels. *Int. J. Heat Mass Transfer* **47**, 2073–2083. [4.9]
- Jiang, P. X., Li, M., Ma, Y. C. and Ren, Z. P. 2004f Experimental research on convection heat transfer in sintered porous channels. *Int. J. Heat Mass Transfer* **47**, 2085–2096. [4.9]
- Jiang, P. X., Li, M., Lu, T. J., Ren, Z. P. and Sun, X. J. 2002 Convection heat transfer in sintered porous plate channels. Heat Transfer 2002, Proc. 12th Int. Heat Transfer Conf., Elsevier, Vol. 2, pp. 803–808. [4.10]
- Jiang, P. X., Ren, Z. and Wang, B. X. 1999a Numerical simulation of forced convection heat transfer in porous plate channels using thermal equilibrium and non-thermal equilibrium models. *Numer. Heat Transfer A* **35**, 99–113. [4.10]
- Jiang, P. X., Shi, R. F., Xu, Y. J., He, S., and Jackson, J. D. 2006b Experimental investigation of flow resistance and convection heat transfer of CO<sub>2</sub> at supercritical pressures in a vertical porous tube. *J. Supercrit. Fluids* **38**, 339–346. [8.4.3]
- Jiang, P. X., Shi, R. F., Zhao, C. R. and Xu, Y. J. 2008 Experimental and numerical study of convection heat transfer of CO<sub>2</sub> at supercritical pressure in vertical porous tubes. *Int. J. Heat Mass Transfer* **51**, 6283–6293. [8.4.3]
- Jiang, P. X., Si, G. S., Li, M. and Ren, Z. P. 2004g Experimental and numerical investigation of forced convection heat transfer of air in non-sintered porous media. *Exp. Thermal Fluid Sci.* **28**, 545–555. [4.9]
- Jiang, P. X., Wang, B. X. and Ren, Z. P. 1994 A numerical investigation of mixed convection in a vertical porous annulus. Heat Transfer 1994, Inst. Chem. Engrs, Rugby, vol. 5, pp. 303–308. [8.3.3]
- Jiang, P. X., Wang, B. X., Juo, D. A. and Ren, Z. P. 1996 Fluid flow and convective heat transfer in a vertical annulus. *Numer. Heat Transfer A* **30**, 305–320. [8.3.3]
- Jiang, P. X., Wang, Z. and Ren, Z. 1998 Fluid flow and concentration heat transfer in a plate channel filled with solid particles. *Heat Transfer 1998, Proc. 11th IHTC* **4**, 405–410. [4.10]
- Jiang, P. X., Wang, Z., Ren, Z. and Wang, B. X. 1999b Experimental research of fluid flow and convection heat transfer in plate channels filled with glass or metallic particles. *Exp. Thermal Fluid Sci.* **20**, 45–54. [4.9]
- Jiang, P. X., Xu, Y. J. and Li, M. 2004h Experimental investigation of convection heat transfer in min-fin structures and sintered porous media. *J. Enhanced Heat Transfer* **11**, 391–405. [4.9]
- Jiang, P. X., Xu, Y. J. and Shi, R. F. 2004i Experimental investigation of convection heat transfer of CO at supercritical pressures in a porous tube. In Applications of Porous Media (ICAPM 2004), (eds. A. H. Reis and A. F. Miguel), Évora, Portugal, pp. 173–181. [4.5]

- Jiang, P. X., Xu, Y. J., Lu, J., Shi, R. F., He, S. and Jackson, J. D. 2004j Experimental investigation of convection heat transfer of CO<sub>2</sub> at supercritical pressure in vertical mini-tubes and porous media. *Appl. Thermal Engng.* **24**, 1255–1270. [4.5]
- Jiang, Y. Y. and Shoji, M. 2002 Thermal convection in a porous toroidal thermosyphon. *Int. J. Heat Mass Transfer* **45**, 3459–3470. [7.3.7]
- Jimenez-Islas, H., Calderon-Ramirez, M., Navarrete-Bolanos, J. L., Botello-Alvarez, J. E., Martinez-Gonzlaes, G. M. and Lopez-Isuna, F. 2009 Numerical study of natural convection in a 2-D square cavity with fluid-porous medium interface and heat generation. *Rev. Mex. Ing. Quim.* **8**, 169–185. [6.19.3]
- Jiménez-Islas, H., López-Isunza, F. and Ochoa-Tapia, J. A. 1999 Natural convection in a cylindrical porous cavity with internal heat source: a numerical study with Brinkman-extended Darcy model. *Int. J. Heat Mass Transfer* **42**, 4185–4195. [7.3.8]
- Jiménez-Islas, H., Navarrete-Bolanos, J. L. and Botello-Alvarez, E. 2004 Numerical study of the natural convection of heat and 2-D mass of grain stored in cylindrical silos. *Agrociencia* **38**, 325–342. [6.11.2]
- Johannsen, K. 2003 On the validation of the Boussinesq approximation for the Elder problem. *Comput. Geosci.* **7**, 169–182. [2.3]
- Johnson, C. H. and Cheng, P. 1978 Possible similarity solutions for free convection boundary layers adjacent to flat plates in porous media. *Int. J. Heat Mass Transfer* **21**, 709–718. [5.1.9.9]
- Joly, F., Vasseur, P. and Labrosse, G. 2001 Soret instability in a vertical Brinkman porous enclosure. *Numer. Heat Transfer A* **39**, 339–359. [9.1.4]
- Joly, N. and Bernard, D. 1995 Critère d'apparition de la convection naturelle dans une couche poreuse horizontale limitée par des frontières conductrices de la chaleur: effet des anisotropies. *C.R. Acad. Sci. Paris, Ser. II*, **320**, 573–579. [6.12]
- Joly, N., Bernard, D. and Menegazzi, P. 1996 ST2D3D: An FE program to compute stability criteria for natural convection in complex porous structures. *Numer. Heat Transfer B* **29**, 91–112. [1.9]
- Jones, I. P. 1973 Low Reynolds number flow past a porous spherical shell. *Proc. Camb. Phil. Soc.* **73**, 231–238. [1.6]
- Jones, M. C. and Persichetti, J. M. 1986 Convective instability in packed beds with throughflow. *AIChE J.* **32**, 1555–1557. [6.10.2]
- Jonsson, T. and Catton, I. 1987 Prandtl number dependence of natural convection in porous media. *ASME J. Heat Transfer* **109**, 371–377. [6.9.2]
- Joo, J. H., Kang, K. J., Kim, T. and Lu, T. J. 2011 Forced convective heat transfer in all metallic wire-woven bulk Kagone sandwich panels. *Int. J. Heat Mass Transfer* **54**, 5658–5662. [4.11]
- Joseph, D. D. 1976 Stability of Fluid Motions II, Springer, Berlin. [2.3, 6.3, 6.4]
- Joseph, D. D., Nield, D. A. and Papanicolaou, G. 1982 Nonlinear equation governing flow in a saturated porous medium. *Water Resources Res.* **18**, 1049–105. and 19, 591. [1.5.2]
- Joshi, V. and Gebhart, B. 1984 Vertical natural convection flows in porous media: calculations of improved accuracy. *Int. J. Heat Mass Transfer* **27**, 69–75. [5.1.6]
- Joshi, Y. and Gebhart, B. 1985 Mixed convection in porous media adjacent to a vertical uniform heat flux surface. *Int. J. Heat Mass Transfer* **28**, 1783–1786. [8.1.1]
- Jou, J. J., Kung, K. Y. and Hsu, C. H. 1996 Thermal stability of horizontally superposed porous fluid layers in a rotating system. *Int. J. Heat Mass Transfer* **39**, 1847–1857. [6.19.1.2]
- Joulin, A. and Ouarzazi, M. N. 2000 Mixed convection of a binary mixture in a porous medium. *C. R. Acad. Sci. Paris II B* **328**, 311–316. [9.1.6.4]
- Jounet, A. and Bardan, G. 2001 Onset of thermohaline convection in the presence of vertical vibration. *Phys. Fluids* **13**, 3234–3246. [9.1.6.4]
- Jue, T. C. 2000 Analysis of heat and fluid flow in partially divided fluid saturated porous cavities. *Heat Mass Transfer* **36**, 285–294. [7.3.7]
- Jue, T. C. 2001a Analysis of oscillatory flow with thermal convection in a rectangular cavity filled with a porous medium. *Int. Comm. Heat Mass Transfer* **27**, 985–994. [6.15.3]

- Jue, T. C. 2001b Analysis of Bénard convection in rectangular cavities filled with a porous medium. *Acta Mech.* **146**, 21–29. [6.8, 6.15.3]
- Jue, T. C. 2003 Analysis of thermal convection in a fluid-saturated porous cavity with internal heat generation. *Heat Mass Transfer* **40**, 83–89. [7.3.8]
- Jumar, R. J., Banat, F. A. and Abu-Al-Rub, F. 2001 Darcy-Forchheimer mixed convection heat and mass transfer in fluid saturated porous media. *Int. J. Numer. Meth. Heat Fluid Flow* **11**, 600–618. [9.2.1]
- Jumar, R. Y. and Majumdar, A. S. 2000 Free convection heat mass transfer of non-Newtonian power law fluids with yield stress from a vertical flat plate in saturated porous media. *Int. Comm. Heat Mass Transfer* **27**, 485–494. [9.2.1]
- Jumar, R. Y. and Majumdar, A. S. 2001 Natural convection heat mass transfer from a vertical flat plate with variable wall temperature and concentration to power-law fluids with yield stress in a porous medium. *Chem. Engng. Comm.* **185**, 165–182. [9.2.1]
- Jupp, T. E. and Schultz, A. 2000 A thermodynamic explanation for black smoker temperatures. *Nature* **403**, 880–883. [11.8]
- Jupp, T. E. and Schultz, A. 2004 Physical balances in subseafloor hydrothermal convection cells. *J. Geophys. Res.—Solid Earth* **109**, Art # B05101. [11.8]
- Kacur, J. and Van Keer, R. 2003 Numerical approximation of a flow and transport system in unsaturated porous media. *Chem Engng. Sci.* **58**, 4805–4813. [3.6]
- Kadir, N. F. A., Rees, D. A. S. and Pop, I. 2008 Conjugate forced convection flow past a circular cylinder with internal heat generation of the porous medium. *Int. J. Numer. Meth. Heat Fluid Flow* **18**, 730–744. [4.16.5]
- Kairi, R. R. and Murthy, P. V. S. N. 2010 Effect of double dispersion on mixed convection heat and mass transfer in a non-Newtonian fluid-saturated non-Darcy porous medium. *J. Porous Media* **13**, 749–75. [9.6.1]
- Kairi, R. R. and Murthy, P. V. S. N. 2011 Effect of viscous dissipation on natural convection heat and mass transfer from vertical cone in a non-Newtonian fluid saturate no-Darcy porous medium. *Appl. Math. Comp.* **217**, 8100–8114. [9.2.1]
- Kalita, J. C. and Dass, A. K. 2011 Higher order compact simulation of double-diffusive natural convection in a vertical porous annulus. *Engng. Appl. Comp. Fluid Mech.* **5**, 357–371. [9.4]
- Kalla, L., Mamou, M., Vasseur, P. and Robillard, L. 1999 Multiple steady states for natural convection in shallow porous cavity subject to uniform heat fluxes. *Int. Comm. Heat Mass Transfer* **26**, 761–770. [7.2]
- Kalla, L., Mamou, M., Vasseur, P. and Robillard, L. 2001a Multiple solutions for double-diffusive convection in a shallow porous cavity with vertical fluxes of heat and mass. *Int. J. Heat Mass Transfer* **44**, 4493–4504. [9.1.6.4]
- Kalla, L., Vasseur, P., Benacer, R., Beji, H and Duval, R. 2001b Double-diffusive convection within a horizontal porous layer salted from the bottom and heated horizontally. *Int. Comm. Heat Mass Transfer* **28**, 1–10. [9.5]
- Kaloni, P. N. and Qiao, Z. 1997 Non-linear stability of convection in a porous medium with inclined temperature gradient. *Int. J. Heat Mass Transfer* **40**, 1611–1615. [7.9]
- Kaloni, P. N. and Qiao, Z. 2000 Nonlinear convection induced by inclined thermal and solutal gradient with mass flow. *Cont. Mech. Thermodyn.* **12**, 185–194. [9.5]
- Kaloni, P. N. and Qiao, Z. 2001 Nonlinear convection in a porous medium with inclined temperature gradient and variable gravity effects. *Int. J. Heat Mass Transfer* **44**, 1585–1591. [7.9]
- Kaluri, R. S. and Basak, T. 2011a Role of entropy generation on thermal management during natural convection in porous square cavities with distributed heat sources. *Chem. Engng. Sci.* **66**, 2124–2140. [7.1.7]
- Kaluri, R. S. and Basak, T. 2011b Energy generation due to natural convection in discretely heated porous square cylinders. *Energy* **36**, 5065–5080. [7.3.7]
- Kaluri, R. S., and Basak, T. 2010a Efficient methodologies for processing of fluids by thermal convection within porous square. *Indus. Engng. Chem. Res.* **49**, 9771–9788. [7.1.7]

- Kaluri, R. S., and Basak, T. 2010b Heatline analysis of thermal mixing due to natural convection in discretely heated porous cavities filled with various fluids. *Chem. Engng. Sci.* **65**, 2132–2152. [7.1.7]
- Kaluri, R. S., Basak, T. and Roy, S. 2009 Bejan's heat lines and numerical visualization of heat flow and thermal mixing in various differentially heated porous space cavities. *Numer. HeatTransfer A* **55**, 487–516. [7.1.7]
- Kamath, P. M., Balaji, C. and Venkateshan, S. P. 2011 Experimental investigation of flow assisted mixed convection in high porosity foams in vertical channels. *Int. J. Heat Mass Transfer* **54**, 5231–5241. [8.3.1]
- Kamel, M. H. 2001 Unsteady MHD convection through porous medium with combined heat and mass transfer with heat source/sink. *Energy Conv. Management* **42**, 393–405. [9.2.1]
- Kamisli, F. 2009 Analysis of laminar flow and forced convection heat transfer in a porous medium. *Transp. Porous Media* **80**, 389–395. [4.16.5]
- Kamiuto, K. and Saitoh, S. 1994 Fully developed forced-convection heat transfer in cylindrical packed beds with constant wall temperatures. *JSME Int. J. Series B* **37**, 554–559. [4.5]
- Kandaswamy, P. and Eswaramurthi, M. 2008 Density maximum effect on buoyancy driven convection of water in a porous cavity with variable side wall temperatures. *Int. J. Heat Mass Transfer* **51**, 1955–1961.
- Kandaswamy, P., Eswaramurthi, M. and Lee, J. 2008a Density maximum effect on double diffusive natural convection in a porous cavity with variable wall temperature. *Transp. Por. Media* **73**, 187–189. [9.2.2]
- Kandaswamy, P., Eswaramurthi, M. and Ng, C. O. 2008b Transient buoyancy-driven convection of water around 4 degrees C in a porous cavity with internal heat generation. *Phys. Fluids* **20**, #087104. [6.17]
- Kandaswamy, P., Muthamilselvan, M. and Lee, J. 2008c Prandtl number effects on mixed convection in a lid-driven porous cavity. *J. Porous. Media* **11**, 791–801. [8.4.3]
- Kandaswamy, R. and Muhammin, I. 2010a Scaling transformation for the effect of temperature-dependent fluid viscosity with thermophoresis particle deposition on MHD-free convective heat and mass transfer over a porous stretching surface. *Transp. Porous Media* **84**, 549–568. [9.6.1]
- Kandaswamy, R. and Muhammin, I. 2010b Homotopy analysis method for thermophoretic particle deposition effect on magnetohydrodynamic mixed convective heat and mass transfer past a porous wedge in the presence of suction. *J. Appl. Mech. Tech. Phys.* **51**, 249–260. [9.6.1]
- Kandaswamy, R. and Palanima 2007 Effects of chemical reactions, heat and mass transfer on nonlinear boundary layer flow over a wedge with a porous medium in the presence of ohmic heating and viscous dissipation. *J. Porous Media* **10**, 489–501. [9.2.1]
- Kandaswamy, R., Muhammin, I. and Amin, N. S. 2010a Lie group analysis for the effect of temperature-dependent fluid viscosity with thermophoresis or magnetohydrodynamic free convective heat and mass transfer over a porous stretching surface. *Int. J. Comput. Fluid Dyn.* **24**, 1–11. [9.2.1]
- Kandaswamy, R., Muhammin, I. and Hashim, I. 2008d Thermophoresis and chemical reaction effects on non-Darcy mixed convective heat and mass transfer past a porous wedge with variable viscosity in the presence of suction or injection. *Nuclear Engng. Design* **238**, 2699–2705. [9.6.1]
- Kandaswamy, R., Muhammin, I., Ram, N. S. and Prabhu, K. K. S. 2012 Thermal stratification effects on Hiemenz flow of nanofluid over a porous wedge sheet in the presence of suction/injection due to solar energy: Lie group transformation. *Transp. Porous Media* **94**, 399–416. [9.7]
- Kandaswamy, R., Nordin, M. and Khamis, A. B. 2010b Variable viscosity and chemical reaction effects on non-Darcy magnetohydrodynamic mixed convection heat and mass transfer past a porous wedge in the presence of suction or injection. *J. Porous Media* **13**, 579–590. [9.6.1]
- Kandaswamy, R., Saravanan, R. and Prabhu, K. K. S. 2010c Chemical reaction on non-linear boundary layer flow over a porous wedge with variable stream conditions. *Chem. Engng. Comm.* **197**, 522–543. [9.2.1]

- Kaneko, T., Mohtadi, M. F., and Aziz, K. 1974 An experimental study of natural convection in inclined porous media. *Int. J. Heat Mass Transfer* **17**, 485–496. [6.9.1, 7.8]
- Kang, J. H., Fu, C. J. and Tan, W. C. 2011 Thermal convective instability of viscoelastic fluids in a rotating porous layer heated from below. *J. Non-Newtonian Fluid Dyn.* **166**, 93–101. [6.22]
- Karasozen, B. and Tsybulin, V. G. 2004 Cosymmetric families of steady states in Darcy convection and their collision. *Phys. Lett. A* **323**, 67–76. [6.4]
- Karcher, C. and Müller, U. 1995 Convection in a porous medium with solidification. *Fluid Dyn. Res.* **15**, 25–42. [10.2.2]
- Karimi-Fard, M., Charrier-Mojtabi, M. C. and Mojtabi, A. 1997 Non-Darcy effects on double-diffusive convection within a porous medium. *Numer. Heat Transfer A* **31**, 837–852. [9.2.2]
- Karimi-Fard, M., Charrier-Mojtabi, M. C. and Mojtabi, A. 1998 Analytical and numerical simulation of double-diffusive convection in a tilted cavity filled with porous medium. *Heat Transfer 1998, Proc. 11th IHTC*, **4**, 453–458. [9.4]
- Karimi-Fard, M., Charrier-Mojtabi, M. C. and Mojtabi, A. 1999 Onset of stationary and oscillatory convection in a tilted porous cavity saturated with a binary fluid: Linear stability analysis. *Phys. Fluids* **11**, 1346–1358. [9.4]
- Kassoy, D. R. and Cotte, B. 1985 The effects of sidewall heat loss on convection in a saturated porous vertical slab. *J. Fluid Mech.* **152**, 361–378. [6.15.2]
- Kassoy, D. R. and Zebib, A. 1975 Variable viscosity effects on the onset of convection in a saturated porous medium. *Phys. Fluids* **18**, 1649–1651. [6.7]
- Kassoy, D. R. and Zebib, A. 1978 Convection fluid dynamics in a model of a fault zone in the earth's crust. *J. Fluid Mech.* **88**, 769–792. [6.15.2]
- Kathare, V., Kulacki, F. A. and Davidson, J. H. 2009 Buoyant convection in superposed metal foam and water layers. *ASME J. Heat Mass Transfer* **132**, #014503. [6.19.3]
- Kathare, V., Davidson, J. H. and Kulacki, F. A. 2008 Natural convection in water-saturated metal foam. *Int. J. Heat Mass Transfer* **51**, 3794–3802. [6.16.1]
- Katto, Y. and Masuoka, T. 1967 Criterion for the onset of convective flow in a fluid in a porous medium. *Int. J. Heat Mass Transfer* **10**, 297–309. [6.9.1]
- Katz, R. F. and Worster, M. G. 2008 Simulation of directional solidification, thermochemical convection, and chimney formation in a Hele-Shaw cell. *J. Comput. Phys.* **227**, 9823–9840. [10.2.3]
- Kauffman, S. A. 1993 The Origins of Order: Self-Organization and Selection and Evolution, Oxford University Press, London. [4.18]
- Kaviany, M. 1984a Thermal convective instabilities in a porous medium. *ASME J. Heat Transfer* **106**, 137–142. [6.11.2, 6.11.3]
- Kaviany, M. 1984b Onset of thermal convection in a saturated porous medium: experiment and analysis. *Int. J. Heat Mass Transfer* **27**, 2101–2110. [6.11.3]
- Kaviany, M. 1985 Laminar flow through a porous channel bounded by isothermal parallel plates. *Int. J. Heat Mass Transfer* **28**, 851–858. [4.9]
- Kaviany, M. 1986 Non-Darcian effects on natural convection in porous media confined between horizontal cylinders. *Int. J. Heat Mass Transfer* **29**, 1513–1519. [7.6.2]
- Kaviany, M. 1987 Boundary-layer treatment of forced convection heat transfer from a semi-infinite flat plate embedded in porous media. *ASME J. Heat Transfer* **109**, 345–349. [4.8]
- Kaviany, M. 1995 Principles of Heat Transfer in Porous Media, Second Edition, Springer, New York. [1.5.2, 6.10]
- Kaviany, M. and Mittal, M. 1987 Natural convection heat transfer from a vertical plate to high permeability porous media: an experiment and an approximate solution. *Int. J. Heat Mass Transfer* **30**, 967–978. [5.1.7.2, 5.1.8]
- Kawada, Y., Yoshida, S. and Watanabe, S. 2004 Numerical simulations of mid-ocean ridge hydrothermal circulation including the phase separation of sea water. *Earth Planets Space* **56**, 193–215. [11.8]

- Kaya, A. 2011 Effects of buoyancy and conjugate heat transfer on non-Darcy mixed convection about a vertical slender hollow cylinder embedded in a porous medium with high porosity. *Int. J. Heat Mass Transfer* **54**, 818–825. [8.1.3]
- Kayhani, M. H., Khaje, E. and Sadi, M. 2011a Natural convection boundary layer along impermeable inclined surfaces embedded in porous medium. *Mechanika* **1**, 64–70. [5.3]
- Kayhani, M. H., Nazari, M. and Shakeri, E. 2011b Effects of fluid-to-solid conductivity ratio, Rayleigh number and interstitial heat transfer coefficient on TNE free convection in a porous enclosure. *Transp. Porous Media* **87**, 625–633. [7.6.2]
- Kayhani, M. H., Nazari, M. and Shakeri, E. 2012 Natural convection heat transfer in a porous cavity in the presence of a biochemical heat source which is dependent on solute concentration rate. *J. Porous Media* **15**, 383–392. [9.1.6.4]
- Kazmierczak, M. and Muley, A. 1994 Steady and transient natural convection experiments in a horizontal porous layer: The effects of a thin top fluid layer and oscillating bottom wall temperature. *Int. J. Heat Fluid Flow* **15**, 30–41. [6.9.1, 6.19.1.2]
- Kazmierczak, M. and Poulikakos, D. 1988 Melting of an ice surface in a porous medium *AIAA J. Thermophys. Heat Transfer* **2**, 352–358. [10.1.7]
- Kazmierczak, M. and Poulikakos, D. 1989 Numerical simulation of transient double diffusion in a composite porous/fluid layer heated from below. *AIChE Sympos. Ser.* **269**, 108–114. [9.4]
- Kazmierczak, M. and Poulikakos, D. 1991 Transient double diffusion in a fluid layer extending over a permeable substrate. *ASME J. Heat Transfer* **113**, 148–157. [9.4]
- Kazmierczak, M., Poulikakos, D. and Pop, I. 1986 Melting from a flat plate embedded in a porous medium in the presence of steady natural convection. *Numer. Heat Transfer* **10**, 571–582. [10.1.1, 10.1.5]
- Kazmierczak, M., Poulikakos, D. and Sadowski, D. 1987 Melting of a vertical plate in porous medium controlled by forced convection of a dissimilar fluid. *Int. Comm. Heat Mass Transfer* **14**, 507–517. [10.1.7]
- Kazmierczak, M., Sadowski, D. and Poulikakos, D. 1988 Melting of a solid in a porous medium induced by free convection of a warm dissimilar fluid. *ASME J. Heat Transfer* **110**, 520–523. [10.1.7]
- Kechil, S. A. and Hashim, I. 2008 Series solutions of boundary-layer flows in porous media with lateral mass flux. *Heat Mass Transfer* **44**, 1179–1186. [5.1.2]
- Kelliher, J. P., Teman, R. and Wang, X. M. 2011 Boundary layer associated with the Darcy–Brinkman–Boussinesq model for convection in porous media. *Physica D* **240**, 619–62. [1.6]
- Kessler, M. A. and Werner, B. T. 2003 Self-organization of sorted patterned ground. *Science* **299**, 380–383. [11.2]
- Khadiri, A., Amahmid, A. and Hasnaoui, M. 2010 Soret effect on double-diffusive convection in a square porous cavity heated and salted from below. *Numer. Heat Transfer A* **57**, 848–868. [9.1.4]
- Khadiri, A., Bennacer, R., Hasnaoui, M. and Amahmid, A. 2011 Two and three-dimensional multiple steady states in a porous cavity heated and salted from below. *Int. J. Therm. Sci.* **50**, 918–929. [9.1.6.4]
- Khadrawi, A. F. and Al-Nimr, M. A. 2003a The effect of the local inertial term on the free-convection fluid flow in vertical channels partially filled with porous media. *J. Porous Media* **6**, 59–70. [7.7]
- Khadrawi, A. F. and Al-Nimr, M. A. 2003b Examination of the thermal equilibrium assumption in transient natural convection flow in porous channel. *Transport Porous Media* **53**, 317–329. [7.5]
- Khadrawi, A. F. and Al-Nimr, M. A. 2005 The effect of the local inertial term on the transient free convection from a vertical plate inserted in a semi-infinite domain partly filled with porous material. *Transport Porous Media* **59**, 139–153. [5.1.3]
- Khadrawi, A. F., Tahat, M. S. and Al-Nimr, M. A. 2005 Validation of the thermal equilibrium assumption in periodic natural convection in porous domains. *Int. J. Thermophys.* **26**, 1633–1649. [7.10]

- Khaled, A. R. A. and Chamkha, A. J. 2001 Variable porosity and thermal dispersion effects on coupled heat and mass transfer by natural convection from a surface embedded in a non-metallic porous medium. *Int. J. Numer. Meth. Heat Fluid Flow* **11**, 413–429. [9.2.1]
- Khaled, A. R. A. and Vafai, K. 2003 The role of porous media in modeling flow and heat transfer in biological tissues. *Int. J. Heat Mass Transfer* **46**, 4989–5003. [1.9, 2.6]
- Khalili, A. and Shivakumara, I. S. 1998 Onset of convection in a porous layer with net throughflow and internal heat generation. *Phys. Fluids* **10**, 315–317. [6.10.2]
- Khalili, A. and Shivakumara, I. S. 2003 Non-Darcian effects on the onset of convection in a porous layer with throughflow. *Transport Porous Media* **53**, 245–263. [6.10.2]
- Khalili, A., Shivakumara, I. S. and Huettel, M. 2002 Effects of throughflow and internal heat generation on convective instabilities in an anisotropic porous layer. *J. Porous Media* **5**, 187–198. [6.10.2]
- Khalili, A., Shivakumara, I. S. and Suma, S. P. 2003 Convective instability in superposed fluid and porous layers with vertical throughflow. *Transport Porous Media* **51**, 1–18. [6.19.3]
- Khallouf, H., Gershuni, G. Z. and Mojtabi, A. 1996 Some properties of convective oscillations in porous medium. *Numer. Heat Transfer A* **30**, 605–618. [6.15.3]
- Khan, A. A. and Zebib, A. 1981 Double diffusive instability in a vertical layer of porous medium. *ASME J. Heat Transfer* **103**, 179–181. [9.2.4]
- Khan, I., Fakhar, K. and Shafie, S. 2011 Magnetohydrodynamic free convection flow past an oscillating plate embedded in a porous medium. *J. Phys. Soc. Japan* **80**, #104401. [5.1.9.9]
- Khan, W. A. and Aziz, A. 2011 Double-diffusive natural convective boundary layer flow in a porous medium saturated with a nanofluid over a vertical plate: Prescribed surface heat, solute and nanoparticle fluxes. *Int. J. Therm. Sci.* **50**, 2154–2160. [9.7]
- Khan, W. A. and Gorla, R. S. R. 2010a Mixed convection of water at 4 degrees C along a wedge with surface flux in a porous medium. *J. Mech. Sci. Tech.* **24**, 1919–1925. [8.1.4]
- Khan, W. A. and Gorla, R. S. R. 2010b Mixed convection of power-law fluids along a vertical wedge with convective boundary condition in a porous medium. *Transp. Porous Media* **83**, 413–424. [8.1.4]
- Khan, W. A. and Gorla, R. S. R. 2010c Nonsimilarity solutions for mixed convection of water at 4 degrees C along a wedge over a vertical surface with prescribed heat flux in a porous medium. *J. Porous Media* **13**, 1025–1032. [8.1.4]
- Khan, W. A. and Gorla, R. S. R. 2011 Entropy generation in non-Newtonian fluids along a horizontal plate in porous media. *J. Thermophys. Heat Transfer* **25**, 298–303. [8.1.2]
- Khan, W. A. and Gorla, R. S. R. 2011 Mixed convection of water at 4 degrees C along a wedge with a convective boundary condition in a porous medium. *Spec. Top. Rev. Porous Media* **2**, 227–236. [8.1.4]
- Khan, W. A. and Pop, I. 2011 Flow and heat transfer over a continuously moving flat plate in a porous medium. *ASME J. Heat Transfer* **133**, #054501. [4.16.5]
- Khanafer K. and Vafai, K. 2009 Synthesis of mathematical models representing bioheat transport. In Advances in Numerical Heat Transfer, Volume III, (ed. W. J. Minkowycz, E. M. Sparrow, J. P. Abraham), CRC Press, Boca Raton FL., pp. 1–28. [2.6]
- Khanafer, K. and Vafai, K. 2001 Isothermal surface production and regulation for high heat flux applications using porous inserts. *Int. J. Heat Mass Transfer* **44**, 2933–2947. [4.11]
- Khanafer, K. and Vafai, K. 2002 Double-diffusive mixed convection in a lid-driven enclosure filled with a fluid-saturated porous medium. *Numer. Heat Transfer A* **42**, 465–486. [9.6.2]
- Khanafer, K. and Vafai, K. 2005 Transport through porous media — a synthesis of the state of the art for the past couple of decades. *Ann. Rev. Heat Transfer* **14**, 346–383. [4.11]
- Khanafer, K. and Vafai, K. 2011 A critical analysis of thermophysical characteristics of nanofluids. *Int. J. Heat Mass Transfer* **54**, 4410–4428. [9.7]
- Khanafer, K. M. and Chamkha, A. J. 1998 Hydromagnetic natural convection from an inclined porous square enclosure with heat generation. *Numer. Heat Transfer A* **33**, 891–910. [7.8]
- Khanafer, K. M. and Chamkha, A. J. 1999 Mixed convection flow in a lid-driven enclosure filled with a fluid-saturated porous medium. *Int. J. Heat Mass Transfer* **42**, 2465–2481. [8.2.1]

- Khanafer, K. M. and Chamkha, A. J. 2003 Mixed convection with a porous bed heat generating horizontal annulus. *Int. J. Heat Mass Transfer* **46**, 1725–1735. [8.2.3]
- Khanafer, K. M., Al-Najem, N. M. and El-Refaee, M. M. 2000 Natural convection in tilted porous enclosures in the presence of a transverse magnetic field. *J. Porous Media* **3**, 79–91. [7.8]
- Khanafer, K., Al-Amin, A., Pop, I. and Bull, J. L. 2008 Flow and heat transfer in biological tissues: Applications of porous media theory. In P. Vadasz (ed.) *Emerging Topics in Heat and Mass Transfer in Porous Media*, Springer, New York, pp. 237–259. [2.6]
- Khanafer, K., Al-Amiri, A. and Pop, I. 2008 Numerical analysis of natural convection heat transfer in a horizontal annulus partially filled with a fluid-saturated porous substrate. *Int. J. Heat Mass Transfer* **51**, 1613–1627. [7.3.3]
- Khanafer, K., Al-Azmi, B., Marafie, A. and Pop, I. 2009 Non-Darcian effects of natural convection heat transfer in a wavy porous enclosure. *Int. J. Heat Mass Transfer* **52**, 1887–1896. [7.3.7]
- Khanafer, K., Bull, J. L., Pop, I. and Berquer, R. 2007 Influence of pulsatile blood flow and heating scheme on the temperature distribution during hyperthermia. *Int. J. Heat Mass Transfer* **50**, 4883–4890. [4.16.2]
- Khanafer, K., Vafai, K. and Kangarlu, A. 2003 Computational modeling of cerebral diffusion – application to stroke imaging. *Magnet. Reson. Imag.* **21**, 651–661. [2.6]
- Khandelwal, M. K. and Bera, P. 2012 A thermal non-equilibrium perspective on mixed convection in a vertical channel. *Int. J. Therm. Sci.* **56**, 23–34. [8.3]
- Khandelwal, M. K. and Bera, P. 2012 A thermal non-equilibrium perspective on mixed convection in a vertical channel. *Int. J. Therm. Sci.* **55**, 23–24. [8.3.1]
- Khandelwal, M. K., Bera, P. and Chakrabati, A. 2012 Influence of periodicity of sinusoidal bottom boundary condition on natural convection in porous enclosure. *Int. J. Heat Mass Transfer* **55**, 2889–2900. [6.15.3]
- Khani, F., Farmany, A., Raji, M. A., Aziz, A. and Samadi, F. 2009 Analytic solution for heat transfer of a third grade viscoelastic fluid in non-Darcy porous media with thermophysical effects. *Comm. Nonlinear Sci. Numer. Simul.* **14**, 3867–3878. [5.1.9.9]
- Khare, H. C. and Sahai, A. K. 1993 Thermosolutal convection in a heterogeneous fluid layer in porous medium in the presence of a magnetic field. *Int. J. Engng Sci.* **31**, 1507–1517. [9.1.6.4]
- Khashan, S. A. and Al-Nimr, M. A. 2005 Validation of the local thermal equilibrium assumption in forced convection in non-Newtonian fluids through porous channels. *Transport Porous Media* **61**, 291–305. [4.10]
- Khashan, S. A., Al-Amiri, A. M. and Al-Nimr, M. A. 2005 Assessment of the local thermal equilibrium condition in developing forced convection flows through fluid-saturated porous tubes. *Appl. Thermal Engng.* **25**, 1429–1445. [4.10]
- Khashan, S. A., Al-Amiri, A. M. and Pop, I. 2006 Numerical simulation of natural convection heat transfer in a porous cavity heated from below using a non-Darcian and thermal equilibrium model. *Int. J. Heat Mass Transfer* **49**, 1039–1049. [6.5]
- Kim, G. B. and Hyun, J. M. 2004 Buoyant convection of a power-law fluid in an enclosure filled with heat-generating porous media. *Numer. Heat Transfer A* **45**, 569–582. [6.11.2]
- Kim, G.B., Hyun, J. M. and Kwak, H. S. 2001 Buoyant convection in a square cavity partially filled with a heat-generating porous medium. *Numer. Heat Transfer A* **40**, 601–618. [6.19.3]
- Kim, K. H., Hyun, J. M. and Kim, J. W. 2005 Transient buoyant convection in a porous-medium enclosure by sudden imposition of gravity. *J. Porous Media* **8**, 311–326. [6.24]
- Kim, K. H., Kim, S. J. and Hyun, J. M. 2004a Development of boundary layers in transient convection about a vertical plate in a porous medium. *J. Porous Media* **7**, 249–259. [5.1.3]
- Kim, M. C., Kim, S., Chung, B. J. and Choi, C. K. 2003a Convective instability in a horizontal porous layer saturated with oil and a layer of gas underlying it. *Int. Comm. Heat Mass Transfer* **30**, 225–234. [6.11.2]
- Kim, M. C. 2010 Onset of buoyancy-driven convection in isotropic porous media heated from below. *Korean J. Chem. Engng.* **27**, 741–747. [6.11.3]

- Kim, M. C. and Choi, C. K. 2007 Relaxed energy stability analysis on the onset of buoyancy-driven instability in the horizontal porous layer. *Phys. Fluids* **19**, #088103. [6.11.3]
- Kim, M. C. and Choi, C. K. 2012 Linear stability analysis on the onset of buoyancy-driven convection in liquid-saturated porous medium. *Phys. Fluids* **24**, 044–102. [6.11.3, 11.11]
- Kim, M. C. and Kim, S. 2005 Onset of convective stability in a fluid-saturated porous layer subjected to time-dependent heating. *Int. Comm. Heat Mass Transfer* **32**, 416–424. [6.11.3]
- Kim, M. C., Kim, K.Y. and Kim, S. 2004b The onset of transient convection in fluid-saturated porous layer. *Int. Comm. Heat Mass Transfer* **31**, 53–62. [6.11.3]
- Kim, M. C., Kim, S. and Choi, C. K. 2002a Convective instability in fluid-saturated porous layer under uniform volumetric heat sources. *Int. Comm. Heat Mass Transfer* **29**, 919–928. [6.11.3]
- Kim, M. C., Kim, S., Chung, B. J. and Choi, C. K. 2003c Convective instability in a horizontal porous layer saturated with oil and with a layer of gas underlying it. *Int. Comm. Heat Mass Transfer* **30**, 225–234. [6.11.2, 6.11.3]
- Kim, M. C., Lee, S. B., Chung, B. J. and Kim, S. 2002b Heat transfer correlation in fluid-saturated porous layer under uniform volumetric heat sources. *Int. Comm. Heat Mass Transfer* **29**, 1089–1097. [6.11.2]
- Kim, M. C., Lee, S. B., Kim, and Chung, B. J. 2003b Thermal instability of viscoelastic fluids in porous media. *Int. J. Heat Mass Transfer* **46**, 5065–5072. [6.23]
- Kim, M. C., Song, K. H., Choi, C. K. and Yeo, J. K. 2008b Onset of buoyancy-driven convection in a liquid-saturated cylindrical porous layer supported by a gas layer. *Phys. Fluids* **20**, #054104. [6.16.1]
- Kim, M. C., Yoon, D. Y. and Choi, C. L. 2009a Onset of buoyancy-driven instability in porous medium solidified from above. *Transp. Porous Media* **78**, 295–307. [10.2.2]
- Kim, M. C., Yoon, D. Y., Moon, J. H. and Choi, C. L. 2008c Onset of buoyancy-driven convection in porous media saturated with cold water cooled from above. *Transp. Porous Media* **74**, 369–380. [6.11.4]
- Kim, S. and Kim, M. C. 2002 A scale analysis of turbulent heat transfer driven by buoyancy in a porous layer with homogeneous heat sources. *Int. Comm. Heat Mass Transfer* **29**, 127–134. [6.11.2]
- Kim, S. J., Kang, B. H. and Kim, J. H. 2001 Forced convection from aluminum foam materials in an asymmetrically heated channel. *Int. J. Heat Mass Transfer* **44**, 1451–1454. [4.9]
- Kim, S. J. and Choi, C. Y. 1996 Convective heat transfer in porous and overlying fluid layers heated from below. *Int. J. Heat Mass Transfer* **39**, 319–329. [6.19.1.2, 6.19.2]
- Kim, S. J. and Hyun, J. M. 2005 A porous medium approach for the thermal analysis of heat transfer devices. In *Transport Phenomena in Porous Media III*, (eds. D. B. Ingham and I. Pop), Elsevier, Oxford, pp. 120–146. [4.16.1]
- Kim, S. J. and Jang, S. P. 2002 Effects of the Darcy number, the Prandtl number and the Reynolds number on local thermal non-equilibrium. *Int. J. Heat Mass Transfer* **45**, 3885–3896. [4.10]
- Kim, S. J. and Kim, D. 1999 Forced convection in microstructure for electronic equipment cooling. *ASME J. Heat Transfer* **121**, 639–645. [4.9]
- Kim, S. J. and Kim, D. 2000 Discussion: “Heat transfer measurement and analysis for sintered porous channels” (Hwang, G. J. and Chao, C. H., 1994, ASME J. Heat Transfer, 116, pp. 456–469). *ASME J. Heat Transfer* **122**, 632–633. [4.9]
- Kim, S. J. and Kim, D. 2001 Thermal interaction at the interface between a porous medium and an impermeable wall. *ASME J. Heat Transfer* **123**, 527–533. [2.4]
- Kim, S. J. and Vafai, K. 1989 Analysis of natural convection about a vertical plate embedded in a porous medium. *Int. J. Heat Mass Transfer* **32**, 665–677. [5.1.7.1]
- Kim, S. J., Kim, D. and Lee, D. Y. 2000 On the local thermal equilibrium of microchannel heat sinks. *Int. J. Heat Mass Transfer* **43**, 1735–1748. [4.10]
- Kim, S. J., Yoo, J. W. and Jang, S. P. 2002 Thermal optimization of a circular-sectored finned tube using a porous medium approach. *ASME J. Heat Transfer* **124**, 1026–1033. [4.16.5]

- Kim, S. Y. and Kuznetsov, A. V. 2003 Optimization of pin-fin heat sinks using anisotropic local thermal non-equilibrium porous model in a jet impinging channel. *Numer. Heat Transfer A* **44**, 771–787. [4.16.5]
- Kim, S. Y., Kang, B. H. and Hyun, J. M. 1994 Heat transfer from pulsating flow in a channel filled with porous media. *Int. J. Heat Mass Transfer* **37**, 2025–2033. [4.12.2]
- Kim, S. Y., Koo, J. M. and Kuznetsov, A. V. 2001 Effect of anisotropy in permeability and effective thermal conductivity on thermal performance of an aluminum foam heat sink. *Numer. Heat Transfer A* **40**, 21–36. [4.16.5]
- Kim, S. Y., Paek, J. W. and Kang, B. H. 2000 Flow and heat transfer correlations for porous fin in a plate-fin heat exchanger. *ASME J. Heat Transfer* **122**, 572–578. [4.16.5]
- Kim, S., Lorente, S. and Bejan, A. 2006 Vascularized materials: tree-shaped flow and architectures matched canopy to canopy. *J. Appl. Phys.* **100**s, 063525. [4.19]
- Kim, S., Lorente, S. and Bejan, A. 2007 Vascularized materials with heating from one side and coolant forced from the other side. *Int. J. Heat Mass Transfer* **50**, 3498–3506. [4.19]
- Kim, S., Lorente, S. and Bejan, A. 2008b Dendritic vascularization for countering intense heating from the side. *Int. J. Heat Mass Transfer* **51**, 5877–5886. [4.19]
- Kim, S., Lorente, S. and Bejan, A. 2009 Transient behaviour of vascularized walls exposed to sudden heating. *Int. J. Therm. Sci.* **48**, 2046–2052. [4.19]
- Kim, S., Lorente, S., Bejan, A., Miller, W. and Morse, J. 2008a The emergence of vascular design in three dimensions. *J. Appl. Phys.* **103**, 123511. [4.19]
- Kim, W. T., Hong, K. H., Jhon, M. S., Van Osdol, J. G. and Smith, D. H. 2003d Forced convection in a circular pipe with a partially filled porous medium. *KSME Int. J.* **17**, 1583–1595. [4.11]
- Kim, Y. J. 2001a Unsteady MHD convection flow of polar fluids past a vertical moving porous plate in a porous medium. *Int. J. Heat Mass Transfer* **44**, 2791–2799. [5.1.9.2]
- Kim, Y. J. 2001b Unsteady convection flow of micropolar fluids past a vertical porous plate embedded in a porous medium. *Acta Mech.* **148**, 105–116. [5.1.9.2]
- Kim, Y. J. 2004 Heat and mass transfer in MHD micropolar flow over a vertical moving porous plate in a porous medium. *Transport Porous Media* **56**, 17–37. [9.2.1]
- Kimmich, R., Klemm, A. and Weber, M. 2001 Flow, diffusion, and thermal convection in percolation clusters: NMR experiments and numerical FEM/FVM simulations. *Magnet. Reson. Imag.* **19**, 353–361. [6.9.1]
- Kimura, S. 1988a Forced convection heat transfer about an elliptic cylinder in a saturated porous medium. *Int. J. Heat Mass Transfer* **31**, 197–199. [4.3]
- Kimura, S. 1988b Forced convection heat transfer about a cylinder placed in porous media with longitudinal flows. *Int. J. Heat Fluid Flow* **9**, 83–86. [4.3]
- Kimura, S. 1988c Transient heat transfer from a circular cylinder with constant heat flux in a saturated porous layer; application to underground water velocimetry. *Int. Symp. Geothermal Energy*, Kumamoto and Beppu, Japan, November 10–14. [4.6]
- Kimura, S. 1989a Transient forced convection heat transfer from a circular cylinder in a saturated porous medium. *Int. J. Heat Mass Transfer* **32**, 192–195. [4.6]
- Kimura, S. 1989b Transient forced and natural convection heat transfer about a vertical cylinder in a porous medium. *Int. J. Heat Mass Transfer* **32**, 617–620. [4.6.4, 5.7]
- Kimura, S. 1992 Time-dependent phenomena in porous media convection. *Heat and Mass Transfer in Porous Media* (eds. M. Quintard and M. Todorovic), Elsevier, Amsterdam, 277–292. [7.1.4]
- Kimura, S. 1998 Onset of oscillatory convection in a porous medium. *Transport Phenomena in Porous Media* (eds. D. B. Ingham and I. Pop), Elsevier, Oxford, pp. 77–102. [6.15.11]
- Kimura, S. 2003 Heat transfer through a vertical partition separating porous-porous or porous-fluid reservoirs at different temperatures. *Int. J. Energy Res.* **27**, 891–905. [7.1.5]
- Kimura, S. 2005 Dynamic solidification in a water-saturated porous medium cooled from above. In *Transport Phenomena in Porous Media III*, (eds. D. B. Ingham and I. Pop), Elsevier, Oxford, pp. 399–417. [10.2.2]

- Kimura, S. and Bejan, A. 1983 The “heatline” visualization of convective heat transfer. *J. Heat Transfer* **105**, 916–919. [4.17]
- Kimura, S. and Bejan, A. 1985 Natural convection in a stably heated corner filled with porous medium. *ASME J. Heat Transfer* **107**, 293–298. [5.12.2]
- Kimura, S. and Nigorinuma, H. 1991 Heat transfer from a cylinder in a porous medium subjected to axial flow. *Heat Transfer Jap. Res.* **20**, 368–375. [4.3]
- Kimura, S. and Okajima, A. 2000 Natural convection heat transfer in an anisotropic porous cavity heated from the side: Part 1. Theory. *Heat Transfer—Asian Research* **29**, 373–384. [7.3.2]
- Kimura, S. and Pop, I. 1991 Non-Darcian effects on conjugate natural convection between horizontal concentric cylinders filled with a porous medium. *Fluid Dyn. Res.* **7**, 241–253. [7.3.3]
- Kimura, S. and Pop, I. 1992a Conjugate natural convection between horizontal concentric cylinders filled with a porous medium. *Wärme-Stoffübertrag.* **27**, 85–91. [7.3.3]
- Kimura, S. and Pop, I. 1992b Conjugate free convection from a circular cylinder in a porous medium. *Int. J. Heat Mass Transfer* **35**, 3105–3113. [5.5.1]
- Kimura, S. and Pop, I. 1994 Conjugate free convection from a sphere in a porous medium. *Int. J. Heat Mass Transfer* **37**, 2187–2192. [5.6.1]
- Kimura, S., Bejan, A., and Pop, I. 1985 Natural convection near a cold plate facing upward in a porous medium. *ASME J. Heat Transfer* **107**, 819–825. [5.2]
- Kimura, S., Kiwata, T., Okajima, A. and Pop, I. 1997 Conjugate natural convection in porous media. *Adv. Water Resource*, **20**, 111–126. [5.12.3]
- Kimura, S., Masuda, Y. and Hayashi, K. 1993 Natural convection in an anisotropic porous medium heated from the side. *Heat Transfer Japanese Research* **22**, 139–153. [7.3.2]
- Kimura, S., Okajima, A. and Kiwata, T. 2000 Natural convection heat transfer in an anisotropic porous cavity heated from the side (2nd report, experiment by Hele-Shaw cell). *Trans. Jap. Soc. Mech. Engrs B* **66**, 2950 et seq. [7.3.2]
- Kimura, S., Schubert, G. and Straus, J. M. 1986 Route to chaos in porous-medium thermal convection. *J. Fluid Mech.* **166**, 305–324. [6.8]
- Kimura, S., Schubert, G. and Straus, J. M. 1987 Instabilities of steady, periodic and quasi-periodic modes of convection in porous media. *ASME J. Heat Transfer* **109**, 350–355. [6.8]
- Kimura, S., Schubert, G. and Straus, J. M. 1989 Time-dependent convection in a fluid-saturated porous cube heated from below. *J. Fluid Mech.* **207**, 153–189. [6.15.1]
- Kimura, S., Vynnycky, M. and Alavyoon, F. 1995 Unicellular natural circulation in a shallow horizontal porous layer heated from below by a constant flux. *J. Fluid Mech.* **294**, 231–257. [6.8]
- Kimura, S., Yoneya, M., Ikeshoji, T. and Shiraishi, M. 1994 Heat transfer to ultralarge-scale heat pipes placed in a geothermal reservoir (3rd report) — Effects of natural convection. *Geotherm. Sci. Technol.* **4**, 77–96. [8.1.4]
- Kissling, W. M. and Weir, G. J. 2005 The spatial distribution of the geothermal fields in the Taupo Volcanic Zone, New Zealand. *J. Volcan. Geotherm. Res.* **145**, 136–150. [11.8]
- Kissling, W., Ellis, S., Charpentier, F. and Bibby, H. 2009 Convective flows in a TVZ-like setting with a brittle/ductile transition. *Transp. Porous Media* **77**, 335–355. [11.8]
- Kissling, W., McGuinness, M. J., McNabb, A., Weir, G., White, S. and Young, R. 1992a Analysis of one-dimensional horizontal two-phase flow in geothermal reservoirs. *Transport in Porous Media* **7**, 223–253. [11.9.1]
- Kissling, W., McGuinness, M.J., Weir, G., White, S. and Young, R. 1992b Vertical two-phase flow in porous media. *Transport in Porous Media* **8**, 99–131. [11.9.1]
- Kiwan, S. 2007a Effect of radiative losses on the heat transfer from porous fins. *Int. J. Therm. Sci.* **46**, 1046–1055. [5.12.1]
- Kiwan, S. 2007b Thermal analysis of natural convection porous fins. *Transp. Porous Media* **67**, 17–29. [5.12.1]
- Kiwan, S. and Ali, M. E. 2008 Near-slit effects on the flow and heat transfer from a stretching plate in a porous medium. *Numer. Heat TransferA* **54**, 93–108. [5.1.9.9]

- Kiwan, S. and Alzahrany, M. S. 2008 Effect of using porous inserts on natural convection heat transfer between two concentric vertical cylinders. *Numer. Heat Transfer A* **53**, 870–889. [7.3.3]
- Kiwan, S. and Khadier, M. 2008 Natural convection heat transfer in an open-ended inclined channel partially filled with porous media. *Heat Transfer Engng.* **29**, 67–75. [7.7]
- Kiwan, S. and Zeitoun, O. 2008 Natural convection in horizontal cylindrical annulus using porous fins. *Int. J. Numer. Meth. Heat Fluid Flow* **18**, 618–634. [7.3.3]
- Kladias, N. and Prasad, V. 1989a Convective instabilities in horizontal porous layers heated from below: effects of grain size and its properties. *ASME HTD* **107**, 369–379. [6.9.2]
- Kladias, N. and Prasad, V. 1989b Natural convection in horizontal porous layers: effects of Darcy and Prandtl numbers. *ASME J. Heat Transfer* **111**, 926–935. [6.8, 6.9.2]
- Kladias, N. and Prasad, V. 1990 Flow transitions in buoyancy-induced non-Darcy convection in a porous medium heated from below. *ASME J. Heat Transfer* **112**, 675–684. [6.8, 6.9.2]
- Kladias, N. and Prasad, V. 1991 Experimental verification of Darcy–Brinkman–Forchheimer model for natural convection in porous media *AIAA J. Thermophys. Heat Transfer* **5**, 560–576. [6.9.2]
- Klarsfeld, S. 1970 Champs de température associés aux mouvements de convection naturelle dans un milieu poreux limité. *Rev. Gén. Therm.* **9**, 1403–1424. [7.1.2]
- Klinbun, W., Vafai, K. and Rattanadecho, P. 2012 Electromagnetic effects on transport through porous media. *Int. J. Heat Mass Transfer* **55**, 325–335. [4.10]
- Kneafsey, T. J. and Pruess, K. 2010 Laboratory flow experiments for visualizing carbon-dioxide-induced, density-driven brine convection. *Transp. Porous Media* **82**, 123–139. [11.11]
- Knobloch, E. 1986 Oscillatory convection in binary mixtures. *Phys. Rev. A* **34**, 1538–1549. [9.1.3]
- Knupp, P. M. and Lage, J. L. 1995 Generalization of the Forchheimer-extended Darcy flow model to the tensor permeability case via a variational principle. *J. Fluid Mech.* **299**, 97–104. [1.5.2]
- Kodah, Z. H. and Al-Gasem, A. M. 1998 Non-Darcy mixed convection from a vertical plate in saturated porous media – variable surface heat flux. *Heat Mass Transfer* **33**, 377–382. [8.1.1]
- Kodah, Z. H. and Duwairi, H. M. 1996 Inertia effects on mixed convection for vertical plates with variable wall temperature in saturated porous media. *Heat Mass Transfer* **31**, 333–338. [8.1.1]
- Koh, J. C. Y. and Colony, R. 1974 Analysis of cooling effectiveness by porous material in coolant passage. *ASME J. Heat Transfer* **96**, 324–330. [4.11]
- Koh, J. C. Y. and Stevens, R. L. 1975 Enhancement of cooling effectiveness by porous material in coolant passage, *ASME J. Heat Transfer* **97**, 309–311. [4.11]
- Kohl, M. J., Kristoffersen, M. and Kulacki, F. A. 2008 Stability and convection in impulsively heated layers. *ASME J. Heat Transfer* **130**, #112601. [6.18]
- Kokubun, M. A. E. and Fachini, F. F. 2012 Asymptotic analysis of a Hiemenz flow in a low-porosity medium with phase change. *J. Fluid Mech.* **698**, 185–210. [10.3.2]
- Kokubun, M. A. E. and Fachini, F. F. 2011 An analytical approach to Hiemenz flow in a porous medium with heat exchange. *Int. J. Heat Mass Transfer* **54**, 3613–3621. [5.1.9.3]
- Kolesnikov, A. K. 1979 Concentration-dependent convection in a horizontal porous bed containing a chemically active liquid. *J. Engng. Phys.* **36**, 97–101. [3.4]
- Koponen, E., Kandhai, D., Hellén, E., Alava, M., Hoekstra, A., Kataja, M., Niskasen, K., Sloot, P. and Timonen, J. 1998 Permeability of three-dimensional random fiber web. *Phys. Rev. lett.* **80**, 716–719. [1.5.2]
- Kordylewski, W. and Borkowska-Pawlak, B. 1983 Stability of nonlinear thermal convection in a porous medium. *Arch. Mech.* **35**, 95–106. [6.15.1]
- Kordylewski, W., Borkowska-Pawlak, B. and Slany, J. 1987 Stability of three-dimensional natural convection in a porous layer. *Arch. Mech.* **38**, 383–394. [6.15.1]
- Kou H. S. and Huang, D. K. 1996a Some transformations for natural convection on a vertical flat plate embedded in porous media with prescribed wall temperature. *Int. Comm. Heat Transfer* **23**, 273–286. [5.1.9.9]

- Kou, H. S. and Huang, D. K. 1996b Possible transformations for natural convection on a vertical flat plate embedded in porous media with prescribed wall heat flux. *Int. Comm. Heat Transfer* **23**, 1031–1042. [5.1.9.9]
- Kou, H. S. and Huang, D. K. 1997 Fully developed laminar mixed convection through a vertical annular duct filled with porous media. *Int. Comm. Heat Mass Transfer* **24**, 99–110. [8.3.3]
- Kou, H. S. and Lu, K. T. 1993a Combined boundary and inertia effects for fully developed mixed convection in a vertical channel embedded in porous media. *Int. Comm. Heat Mass Transfer* **20**, 333–345. [8.3.1]
- Kou, H. S. and Lu, K. T. 1993b The analytical solution of mixed convection in a vertical channel embedded in porous media with asymptotic wall heat fluxes. *Int. Comm. Heat Mass Transfer* **20**, 737–750. [8.3.1]
- Kowalski, S. J. and Pawlowski, A. 2008 Drying in non-stationary conditions. *Chem. Proc. Engng.* **29**, 337–344. [3.6]
- Kowalski, S. J., Musrelak, G. and Banaszak, J. 2010 Heat and mass transfer during microwave-convective drying. *AICHE J.* **56**, 24–35. [3.6]
- Kozak, R., Saghir, M. Z. and Viviani, A. 2004 Marangoni convection in a liquid layer overlying a porous layer with evaporation at the free surface. *Acta Astronautica* **55**, 189–197. [6.19.3]
- Krakov, M. S. and Nikiforov, I. V. 2008 3D thermomagnetic convection patterns in a porous cube. *Magnetohydrodynamics* **44**, 409–416. [6.21]
- Kramer, J., Jecl, R. and Skerget, L. 2007 Boundary domain integral method for the study of double diffusive natural convection in porous media. *Engng. Anal. Bound. Elem.* **31**, 897–905. [9.1.6.4]
- Krane, M. J. M. and Incropera, F. P. 1996 A scaling analysis of the unidirectional solidification of a binary alloy. *Int. J. Heat Mass Transfer* **39**, 3567–3579. [10.2.3]
- Krantz, W. B., Gleason, K. J. and Caine, N. 1988 Patterned ground. *Sci. Amer.* **159**, 44–50. [11.2]
- Krishna, C. V. S. 2001 Effects of non-inertial acceleration on the onset of convection in a second-order fluid-saturated porous medium. *Int. J. Engng. Sci* **39**, 599–609. [6.22]
- Krishna, D. J., Basak, T and Das, S. K. 2008a Natural convection in a heat generating hydrodynamically and thermally anisotropic non-Darcy porous medium. *Int. J. Heat Mass Transfer* **51**, 4691–4703. [6.12]
- Krishna, D. J., Basak, T and Das, S. K. 2008b Non-Darcy buoyancy-driven flows in a fluid saturated porous medium: the use of asymptotic computational fluid dynamics (ACFD) approach. *Heat Mass Transfer* **44**, 1117–1125. [6.12]
- Krishna, D. J., Basak, T and Das, S. K. 2009 Natural convection in a non-Darcy anisotropic porous cavity with a finite heat source at the bottom wall. *Int. J. Therm. Sci.* **48**, 1279–1293. [7.3.2]
- Krishna, D. J., Thansekhar, M. R., Venkateshan, S. P., Basak, T. and Das, S. K. 2010 Natural convection in a partially heat generating rod bundle inside an enclosure. *ASME J. Heat Transfer* **132**, #102501. [7.3.8]
- Krishnan, S., Murthy, J. Y. and Garaimella, S. V. 2004 A two-temperature model for the analysis of passive thermal control systems. *AMSE J. Heat Transfer* **126**, 628–637. [7.5]
- Krishnan, S., Murthy, J. Y. and Garimella, S. V. 2005 A two-temperature model for solid-liquid phase change in metal foams. *ASME J. Heat Transfer* **127**, 995–1004. [10.1.7]
- Krishnan, S., Murthy, J. Y. and Garimella, S. V. 2007 Analysis of solid-liquid phase change under pulsed heating. *ASME J. Heat Transfer* **129**, 395–400. [10.1.7]
- Krishnan, S., Murthy, J. Y. and Garimella, S. V. 2008 Metal foams as passive thermal control systems. In P. Vadasz (ed.) *Emerging Topics in Heat and Mass Transfer in Porous Media*, Springer, New York, pp. 261–282. [10.1.7]
- Kubik, J. and Cieszko, M. 2005 Analysis of matching conditions at the bounding surface of a fluid-saturated porous solid and a bulk fluid: the use of Lagrange multipliers. *Cont. Mech. Therm.* **17**, 351–359. [1.6]
- Kubitscheck, J. P. and Weidman, P. D. 2003 Stability of fluid-saturated porous medium heated from below by forced convection. *Int. J. Heat Mass Transfer* **46**, 3697–3705. [6.10.1].

- Kubitschek, J. P. and Weidman, P. D. 2006 Stability of a fluid-saturated porous medium contained in a vertical cylinder heated from below by forced convection. *Heat Mass Transfer* **42**, 789–794. [8.1.3]
- Kuhn, M. and Gessner, K. 2009 Coupled process models of fluid flow and heat transfer in hydrothermal systems in three dimensions. *Surv. Geophys.* **30**, 193–210. [11.8]
- Kulacki, F. A. and Freeman, R. G. 1979 A note on thermal convection in a saturated, heat generating porous layer. *ASME J. Heat Transfer* **101**, 169–171. [6.11.2]
- Kulacki, F. A. and Rajen, G. 1991 Buoyancy-induced flow and heat transfer in saturated fissured media. Convective Heat and Mass Transfer in Porous Media, (eds. S. Kakaç, B. Kilkis, F. A. Kulacki and F. Arınc), Kluwer Academic Publishers, Dordrecht, 465–498. [1.9]
- Kulacki, F. A. and Ramchandani, R. 1975 Hydrodynamic instability in porous layer saturated with heat generating fluid. *Wärme-Stoffübertrag.* **8**, 179–185. [6.11.2]
- Kumar, A. and Bera, P. 2009 Natural convection in an anisotropic porous enclosure due to nonuniform heating of the bottom wall. *ASME J. Heat Transfer* **131**, #072601. [7.3.2]
- Kumar, A. and Bhadauria, B. S. 2011a Thermal instability in a rotating anisotropic porous layer saturated by a viscoelastic fluid. *Int. J. Non-linear Mech.* **46**, 47–56. [6.22]
- Kumar, A. and Bhadauria, B. S. 2011b Double diffusive convection in a porous layer saturated with viscoelastic fluid using a thermal non-equilibrium model. *Phys. Fluids* **23**, #054101. [9.1.6.4]
- Kumar, A. and Bhadauria, B. S. 2011c Nonlinear two dimensional double-diffusive convection in a rotating porous layer saturated by a viscoelastic fluid. *Transp. Porous Media* **87**, 229–250. [9.1.6.4]
- Kumar, A., Bera, P. and Kumar, J. 2011d Non-Darcy mixed convection in a vertical pipe filled with a porous medium. *Int. J. Therm. Sci.* **50**, 725–73. [8.4.3]
- Kumar, A., Založník, M., Combeau, H., Goyeau, B. and Gobin, D. 2012 Channel segregation during columnar solidification: influence of inertia. *AIP Conf. Proc.* **1453**, 42–48. [10.2.3]
- Kumar, B. V. R., Murthy, S. V. S. S. V. G. K., Sangwan, V., Nigam, M. and Chandra, P. 2010d Non-Darcy mixed convection in a fluid-saturated square porous enclosure under suction effect. Part 1. *J. Porous Media* **13**, 537–554. [8.4.3]
- Kumar, D. S., Dass, A. K. and Dewan, A. 2009b Analysis on non-Darcy models for mixed convection in a porous cavity using a multigrid approach. *Numer. Heat Transfer A* **56**, 685–708. [8.4.3]
- Kumar, J. P., Umapathi, J. C. and Biridar, B. M. 2010a Mixed convection of a composite porous medium in a vertical channel with asymmetric wall heating conditions. *J. Porous Media* **13**, 271–285. [8.4.1]
- Kumar, J. P., Umapathi, J. C., Pop, I. and Biridar, B. M. 2009b Fully developed mixed convection flow in a vertical channel containing porous and fluid layer with isothermal or isoflux boundaries. *Transp. Porous Media* **80**, 117–135. [8.4.1]
- Kumar, J., Bera, P. and Khalili, A. 2010b Influence of inertia and drag terms on the stability of mixed convection in a vertical porous-medium channel. *Int. J. Heat Mass Transfer* **53**, 5261–5273. [8.3.1]
- Kumar, L., Bharqava, R., Bharqava, P. and Takhar, H. S. 2005 Finite element solution of mixed convection micropolar fluid flow between two vertical plates with varying temperature. *Arch. Mech.* **57**, 251–264. [8.3.2]
- Kumar, N., Gupta, S. and Jain, T. 2010c Heat and mass transfer in MHD unsteady free convective flow of a micropolar fluid over a vertical moving porous plate embedded in a porous medium in the presence of thermal radiation. *Proc. Nat. Acad. Sci. India A* **80**, 309–318. [9.2.1]
- Kumar, P. 1999 Thermal convection in Walters B' viscoelastic fluid permeated with suspended particles in porous medium. *Indian J. Pure Appl. Math.* **30**, 1117–1132. [6.23]
- Kumar, P. and Singh, M. 2006 On a viscoelastic fluid heated from below in a porous medium. *J. Non-Equil. Thermodyn.* **31**, 189–203. [6.23]
- Kumaran, V. and Pop, I. 2006 Steady free convective boundary layer over a flat plate embedded in a porous medium filled with water at 4°C. *Int. J. Heat Mass Transfer* **49**, 3240–3252. [5.1.9.9]

- Kumari, M. 2001a Effect of variable viscosity on non-Darcy free or mixed convection flow on the horizontal surface in a saturated porous medium. *Int. Comm. Heat Mass Transfer* **28**, 723–732. [5.2, 8.1.2]
- Kumari, M. 2001b Variable viscosity effects on free and mixed convection boundary layer flow from a horizontal surface in a saturated porous medium – variable heat flux. *Mech. Res. Commun.* **28**, 339–348. [5.2]
- Kumari, M. and Gorla, R. S. R. 1996 Combined convection in power-law fluids along a nonisothermal vertical plate in a porous medium. *Transport in Porous Media* **24**, 157–166. [8.1.1]
- Kumari, M. and Gorla, R. S. R. 1997 Combined convection along a non-isothermal wedge in a porous medium. *Heat Mass Transfer* **32**, 393–398. [8.1.4]
- Kumari, M. and Jayanthi, S. 2004 Non-Darcy non-Newtonian free convection flow over a horizontal cylinder in a saturated porous medium. *Int. Comm. Heat Mass Transfer* **31**, 1219–1226. [5.5.1]
- Kumari, M. and Jayanthi, S. 2005 Uniform lateral mass flux on natural-convection flow over a vertical cone embedded in a porous medium saturated with a non-Newtonian fluid. *J. Porous Media* **8**, 73–84. [5.8]
- Kumari, M. and Nath, G. 1989a Non-Darcy mixed convection boundary layer flow on a vertical cylinder in a saturated porous medium. *Int. J. Heat Mass Transfer* **32**, 183–187. [8.1.3]
- Kumari, M. and Nath, G. 1989b Unsteady mixed convection with double diffusion over a horizontal cylinder and a sphere within a porous medium. *Wärme-Stoffübertrag.* **24**, 103–109. [8.1.3]
- Kumari, M. and Nath, G. 1989c Double diffusive unsteady free convection on two-dimensional and axisymmetric bodies in a porous medium. *Int. J. Energy Res.* **13**, 379–391. [9.4]
- Kumari, M. and Nath, G. 1989d Double diffusive unsteady mixed convection flow over a vertical plate embedded in a porous medium. *Int. J. Energy Res.* **13**, 419–430. [9.4]
- Kumari, M. and Nath, G. 1990 Non-Darcy mixed convection flow over a nonisothermal cylinder and sphere embedded in a saturated porous medium. *ASME J. Heat Transfer* **112**, 518–523. [8.1.3]
- Kumari, M. and Nath, G. 1992 Simultaneous heat and mass transfer under unsteady mixed convection along a vertical slender cylinder embedded in a porous medium. *Wärme-Stoffübertrag.* **28**, 97–105. [9.6.1]
- Kumari, M. and Nath, G. 2004a Non-Darcy mixed convection in power-law fluids along a non-isothermal horizontal surface in a porous medium. *Int. J. Engng. Sci.* **42**, 353–369. [8.1.2]
- Kumari, M. and Nath, G. 2004b Radiation effect on mixed convection from a horizontal surface in a porous medium. *Mech. Res. Comm.* **31**, 483–491. [8.1.2]
- Kumari, M. and Nath, G. 2008 Unsteady natural convection from a horizontal annulus filled with a porous medium. *Int. J. Heat Mass Transfer* **51**, 5001–5007. [7.3.3]
- Kumari, M. and Nath, G. 2009a Natural convection from a vertical cone in a porous medium due to the combined effects of heat and mass diffusion with non-uniform wall temperature/concentration or heat/mass flux and suction/injection. *Int. J. Heat Mass Transfer* **52**, 3064–3069. [9.2.1]
- Kumari, M. and Nath, G. 2009b Unsteady natural convection flow in a square cavity filled with a porous medium due to impulsive change in wall temperature. *Transp. Porous Media* **77**, 463–474. [7.5]
- Kumari, M. and Nath, G. 2009c Unsteady natural convection flow over a heated cylinder buried in a fluid-saturated porous medium. *J. Porous Media* **12**, 1225–1235. [5.5.1]
- Kumari, M. and Nath, G. 2010 Natural convection on a horizontal cone in a porous medium with non-uniform wall temperature/concentration or heat/mass flux and suction/injection. *Transp. Porous Media* **84**, 275–284. [5.8]
- Kumari, M. and Nath, G. 2011 Steady mixed convection flow in a lid-driven square enclosure filled with a non-Darcy fluid-saturated porous medium with internal heat generation. *J. Porous Media* **14**, 893–905. [8.4.3]

- Kumari, M. and Pop, I. 2009 Mixed convection boundary layer flow past a horizontal circular cylinder embedded in a bidisperse porous medium. *Transp. Porous Media* **77**, 287–308. [8.1.3]
- Kumari, M., Gorla, R. S. R., and Byrd, L. 1997 Mixed convection in non-Newtonian fluids along a horizontal plate in a porous medium. *ASME J. Energy Resources Tech.* **119**, 35–37. [8.1.2]
- Kumari, M., Nath, G. and Pop, I. 1990c Non-Darcian effects on forced convection heat transfer over a flat plate in a highly porous medium. *Acta Mech.* **84**, 201–207. [4.8]
- Kumari, M., Nath, G. and Pop, I. 1993 Non-Darcy mixed convection flow with thermal dispersion on a vertical cylinder in a saturated porous medium. *Acta Mech.* **100**, 69–77. [8.1.3]
- Kumari, M., Pop, I. and Nath, G. 1985 Non-Darcy natural convection from a heated vertical plate in saturated porous media with mass transfer. *Int. Comm. Heat Mass Transfer* **12**, 337–346. [5.1.7.2]
- Kumari, M., Pop, I. and Nath, G. 1986 Non-Darcy natural convection on a vertical cylinder in a saturated porous medium. *Wärme-Stoffübertrag.* **20**, 33–37. [5.7]
- Kumari, M., Pop, I. and Nath, G. 1987 Mixed convection boundary layer over a sphere in a saturated porous medium. *Z. Ang. Math. Mech.* **67**, 569–571. [8.1.3]
- Kumari, M., Pop, I. and Nath, G. 1988c Darcian mixed convection plumes along vertical adiabatic surfaces in a saturated porous medium. *Wärme-Stoffübertrag.* **22**, 173–17. [8.1.1].
- Kumari, M., Pop, I. and Nath, G. 1990a Nonsimilar boundary layers for non-Darcy mixed convection flow about a horizontal surface in a saturated porous medium. *Int. J. Engng. Sci.* **28**, 253–263. [8.1.2]
- Kumari, M., Pop, I. and Nath, G. 1990b Natural convection in porous media above a near horizontal uniform heat flux surface. *Wärme-Stoffübertrag.*, **25**, 155–159. [5.3]
- Kumari, M., Takhar, H. S. and Nath, G. 1988a Non-Darcy double-diffusive mixed convection from heated vertical and horizontal plates in saturated porous media. *Wärme-Stoffübertrag.* **23**, 267–273. [9.4]
- Kumari, M., Takhar, H. S. and Nath, G. 1988b Double-diffusive non-Darcy free convection from two-dimensional and axisymmetric bodies of arbitrary shape in a saturated porous medium. *Indian J. Tech.* **26**, 324–328. [9.4]
- Kumari, M., Takhar, H. S. and Nath, G. 2001 Mixed convection flow over a vertical wedge embedded in a highly porous medium. *Heat Mass Transfer* **37**, 139–146. [8.1.4]
- Kurdyumov, V. N. and Liñán, A. 2001 Free and forced convection around line sources of heat and heated cylinders in porous media. *J. Fluid Mech.* **427**, 389–409. [5.5.1]
- Kuwahara, F. and Nakayama, A. 1998 Numerical modelling of non-Darcy convective flow in a porous medium. *Heat Transfer 1998, Proc. 11th IHTC*, **4**, 411–416. [1.5.2, 1.8]
- Kuwahara, F. and Nakayama, A. 1999 Numerical determination of thermal dispersion coefficients using periodic porous structure. *ASME J. Heat Transfer* **121**, 160–163. [2.2.4]
- Kuwahara, F. and Nakayama, A. 2005 Three-dimensional flow and heat transfer within highly anisotropic porous media. *Handbook of Porous Media* (K Vafai, ed.), 2nd ed., Taylor and Francis, New York, pp. 235–266. [2.2.4]
- Kuwahara, F., Yamane, I. and Nakayama, A. 2006 Large eddy simulation of turbulent flow in porous media. *Int. Comm. Heat Mass Transfer* **33**, 411–418. [1.8]
- Kuwahara, F., Kameyama, Y., Yamashita, S. and Nakayama, A. 1998 Numerical modeling of turbulent flow in porous media using a spatially periodic array. *J. Porous Media* **1**, 47–55. [1.8]
- Kuwahara, F., Nakayama, A. and Koyama, H. 1994 Numerical modelling of heat and fluid flow in a porous medium. *Heat Transfer 1994, Inst. Chem. Engrs, Rugby*, vol. 5, pp. 309–314. [2.6]
- Kuwahara, F., Nakayama, A. and Koyama, H. 1996 A numerical study of thermal dispersion in porous media. *ASME J. Heat Transfer* **118**, 756–761. [2.2.4]
- Kuwahara, F., Shiota, M. and Nakayama, A. 2001 A numerical study of interfacial convective heat transfer coefficient in two-energy model for convection in porous media. *Int. J. Heat Mass Transfer* **44**, 1153–1159. [2.2.3]
- Kuznetsov, A. 1998e Non-thermal equilibrium forced convection in porous media. *Transport Phenomena in Porous Media* (eds. D. B. Ingham and I. Pop), Elsevier, Oxford, pp.103–130. [4.6.4]

- Kuznetsov, A. V. 1994 An investigation of a wave of temperature difference between solid and fluid phases in a porous packed bed. *Int. J. Heat Mass Transfer* **37**, 3030–3033. [4.6.4]
- Kuznetsov, A. V. 1995b An analytical solution for heating a two-dimensional porous packed bed by a non-thermal equilibrium fluid flow. *Appl. Sci. Res.* **55**, 83–93. [4.6.4]
- Kuznetsov, A. V. 1996a Analytical investigation of the fluid flow in the interface region between a porous medium and a clear fluid in channels partially filled with a porous medium. *Appl. Sci. Res.* **56**, 53–67. [1.6]
- Kuznetsov, A. V. 1996b Analysis of a non-thermal equilibrium fluid flow in a concentric tube annulus filled with a porous medium. *Int. Comm. Heat Mass Transfer* **23**, 929–938. [4.6.4]
- Kuznetsov, A. V. 1996c Stochastic modeling of heating of a 1D porous slab by a flow of incompressible fluid. *Acta Mech.* **114**, 39–50. [4.6.4]
- Kuznetsov, A. V. 1996d A perturbation solution for a nonthermal equilibrium fluid flow through a three-dimensional sensible heat storage packed bed. *ASME J. Heat Transfer* **118**, 508–510. [4.6.4]
- Kuznetsov, A. V. 1996e Investigation of a non-thermal equilibrium flow of an incompressible fluid in a cylindrical tube filled with porous media. *Z. Angew. Math. Mech.* **76**, 411–418. [4.6.4]
- Kuznetsov, A. V. 1996f Analysis of heating a three-dimensional porous bed utilizing the two energy equation model. *Heat Mass Transfer* **31**, 173–177. [4.6.4]
- Kuznetsov, A. V. 1997a Determination of the optimal initial temperature distribution in a porous bed. *Acta Mech.* **120**, 61–69. [4.6.4]
- Kuznetsov, A. V. 1997b Influence of the stress jump condition at the porous-medium/clear-fluid interface on a flow at a porous wall. *Int. Comm. Heat Mass Transfer* **24**, 401–410. [1.6]
- Kuznetsov, A. V. 1997c Optimal control of the heat storage in a porous slab. *Int. J. Heat Mass Transfer* **40**, 1720–1723. [4.15]
- Kuznetsov, A. V. 1997d Thermal nonequilibrium, non-Darcian forced convection in a channel filled with a fluid saturated porous medium — a perturbation solution. *Appl. Sci. Res.* **57**, 119–131. [4.10]
- Kuznetsov, A. V. 1998a Numerical investigation of the macrosegregation during thin strip casting of carbon steel. *Numer. Heat Transfer A* **33**, 515–532. [10.2.3]
- Kuznetsov, A. V. 1998b Analytical study of fluid flow and heat transfer during forced convection in a composite channel partly filled with a Brinkman-Forchheimer porous medium. *Flow, Turbulence and Combustion* **60**, 173–192. [4.11]
- Kuznetsov, A. V. 1998c Analytical investigation of heat transfer in Couette flow through a porous medium utilizing the Brinkman-Forchheimer-extended Darcy model. *Acta Mech.* **129**, 13–24. [4.9]
- Kuznetsov, A. V. 1998d Analytical investigation of Couette flow in a composite channel partially filled with a porous medium and partially with a clear fluid. *Int. J. Heat Mass Transfer* **41**, 2556–2560. [4.16.1]
- Kuznetsov, A. V. 1999a Fluid mechanics and heat transfer in the interface region between a porous medium and a fluid layer: A boundary layer solution. *J. Porous Media* **2**, 309–321. [4.11]
- Kuznetsov, A. V. 1999b Analytical investigation of forced convection from a flat plate enhanced by a porous substrate. *Acta Mech.* **137**, 211–223. [4.11]
- Kuznetsov, A. V. 1999c Forced convection heat transfer in a parallel-plate channel with a porous core. *Appl. Mech. Engng.* **4**, 271–290. [4.11]
- Kuznetsov, A. V. 2000a Analytical studies of forced convection in partly porous configurations. Handbook of Porous Media (K. Vafai, ed.), Marcel Dekker, New York., pp. 269–312. [4.11]
- Kuznetsov, A. V. 2000b Fluid flow and heat transfer analysis of Couette flow in a composite duct. *Acta Mech.* **140**, 163–170. [4.11]
- Kuznetsov, A. V. 2000c Investigation of the effect of transverse thermal dispersion on forced convection in porous media. *Acta Mech.* **145**, 35–43. [4.9]
- Kuznetsov, A. V. 2001 Influence of thermal dispersion on forced convection in a composite parallel-plate channel. *Z. Angew. Math. Phys.* **52**, 135–150. [4.11]

- Kuznetsov, A. V. 2004a Effect of turbulence on forced convection in a composite tube partly filled with a porous medium. *J. Porous Media* **7**, 59–64. [4.11]
- Kuznetsov, A. V. 2004b Numerical modeling of turbulent flow in a composite porous/fluid duct utilizing a two-layer k-epsilon model to account for interface roughness. *Int. J. Therm. Sci.* **43**, 1047–1056. [1.8]
- Kuznetsov, A. V. 2005 Modeling bioconvection in porous media. *Handbook of Porous Media* (ed. K. Vafai), 2nd ed., Taylor and Francis, New York, pp. 645–686. [6.25]
- Kuznetsov, A. V. 2006a The onset of thermo-bioconvection in a shallow fluid saturated porous layer heated from below in the presence of oxytactic microorganisms. *Europ. J. Mech. B* **25**, 223–233. [6.23]
- Kuznetsov, A. V. 2006b Linear stability analysis of the effect of vertical vibration on bioconvection in a horizontal porous layer of finite length. *J. Porous Media* **9**, 597–608. [6.25]
- Kuznetsov, A. V. 2006c Thermo-bio-convection in porous media. *J. Porous Media* **9**, 581–589. [6.25]
- Kuznetsov, A. V. 2008 New developments in bioconvection in porous media: Bioconvection plumes, bio-thermal convection, and effects of vertical vibration. In P. Vadasz (ed.) *Emerging Topics in Heat and Mass Transfer in Porous Media*, Springer, New York, pp. 181–217. [6.25]
- Kuznetsov, A. V. 2012a Nanofluid bioconvection in a horizontal fluid saturated porous layer. *J. Porous Media* **15**, 11–27. [6.25]
- Kuznetsov, A. V. 2012b Nanofluid bioconvection in porous media: Oxytactic microorganisms. *J. Porous Media* **15**, 233–248. [6.25]
- Kuznetsov, A. V. 1995a Comparisons of the waves of temperature difference between the solid and fluid phases in a porous slab and in a semi-infinite porous body. *Int. Comm. Heat Mass Transfer* **22**, 499–506. [4.6.4]
- Kuznetsov, A. V. and Avramenko, A. A. 2002 A 2D analysis of stability of bioconvection in a fluid saturated porous medium — Estimation of the critical permeability value. *Int. Comm. Heat Mass Transfer* **29**, 175–184. [6.25]
- Kuznetsov, A. V. and Avramenko, A. A. 2003a The effect of deposition and decludging on the critical permeability in bioconvection in a porous medium. *Acta Mech.* **160**, 113–125. [6.25]
- Kuznetsov, A. V. and Avramenko, A. A. 2003b Stability analysis of bioconvection of gyrotactic motile microorganisms in a fluid saturated porous medium. *Transport Porous Media* **53**, 95–104. [6.25]
- Kuznetsov, A. V. and Avramenko, A. A. 2003c Analysis of stability of bioconvection of motile oxytactic bacteria in a horizontal fluid saturated porous layer. *Int. Comm. Heat Mass Transfer* **30**, 341–364. [6.25]
- Kuznetsov, A. V. and Avramenko, A. A. 2005 Effect of fouling on stability of bioconvection of gyrotactic micro-organisms in a porous medium. *J. Porous Media* **8**, 45–53. [6.25]
- Kuznetsov, A. V. and Becker, S. M. 2004 Effect of the interface roughness on turbulent convective heat transfer in a composite porous/fluid duct. *Int. Comm. Heat Mass Transfer* **31**, 11–20. [4.11]
- Kuznetsov, A. V. and Bubnovich, Y. 2012 Investigation of simultaneous gyrotactic and oxytactic microorganisms on nanofluid bio-thermal convection in porous media. *J. Porous Media* **15**, 617–631. [6.25, 9.7]
- Kuznetsov, A. V. and Jiang, N. 2001 Numerical investigation of bioconvection of gravitactic microorganisms in an isotropic porous medium. *Int. Comm. Heat Mass Transfer* **28**, 877–866. [6.25]
- Kuznetsov, A. V. and Jiang, N. 2003 Bioconvection of negatively geotactic microorganisms in a porous medium: The effect of cell deposition and decludging. *Int. J. Numer. Meth. Heat Fluid Flow* **13**, 341–364. [6.25]
- Kuznetsov, A. V. and Nield, D. A. 2001 Effects of heterogeneity in forced convection in a porous medium: triple layer or conjugate problem. *Numer Heat Transfer A* **40**, 363–385. [4.12]
- Kuznetsov, A. V. and Nield, D. A. 2005a Thermally developing forced convection in a channel occupied by a porous medium saturated by a non-Newtonian fluid. *International Journal of Heat and Mass Transfer* **48**, 1214–1218. [4.13]

- Kuznetsov, A. V. and Nield D. A. 2005b Thermally developing forced convection in a bi-disperse porous medium. *J. Porous Media* **9**, 393–406. [4.16.4]
- Kuznetsov, A. V. and Nield, D. A. 2006a Boundary layer treatment of forced convection over a wedge with an attached porous substrate. *J. Porous Media* **9**, 683–694. [4.11]
- Kuznetsov, A. V. and Nield, D. A. 2006b Forced convection with laminar pulsating flow in a saturated porous channel or tube. *Transp. Porous Media* **65**, 505–523. [4.61.2]
- Kuznetsov, A. V. and Nield, D. A. 2006c Thermally developing forced convection in a bidisperse porous medium. *J. Porous Media* **9**, 393–402. [4.16.4]
- Kuznetsov, A. V. and Nield, D. A. 2008a The effects of a transition layer between a fluid and a porous medium: Forced convection in a channel. *ASME J. Heat Transfer* **130**, #0945404. [4.11]
- Kuznetsov, A. V. and Nield, D. A. 2008b The effects of combined horizontal and vertical heterogeneity on the onset of convection in a porous medium: double diffusive case. *Transp. Porous Media* **72**, 157–170. [9.1.6.4]
- Kuznetsov, A. V. and Nield, D. A. 2009a Forced convection with counterflow in a circular tube occupied by a porous medium. *J. Porous Media* **12**, 657–666. [2.6, 4.16.2]
- Kuznetsov, A. V. and Nield, D. A. 2009b Forced convection with laminar pulsating counterflow in a saturated porous circular tube. *Transp. Porous Media* **77**, 447–462. [2.6, 4.16.2]
- Kuznetsov, A. V. and Nield, D. A. 2009b Thermally developing forced convection in a porous medium occupied by a rarefied gas: Parallel plate channel or circular tube with walls at constant heat flux. *Transp. Porous Media* **76**, 345–362. [4.13]
- Kuznetsov, A. V. and Nield, D. A. 2010a Forced convection in a channel partly occupied by a bidisperse porous medium: Asymmetric case. *Int. J. Heat Mass Transfer* **53**, 5167–5175. [4.16.4]
- Kuznetsov, A. V. and Nield, D. A. 2010b The Cheng-Minkowycz problem for cellular porous materials: Effect of temperature-dependent conductivity arising from radiative transfer. *Int. J. Heat Mass Transfer* **53**, 2676–2679. [2.2.5, 5.1.9.9]
- Kuznetsov, A. V. and Nield, D. A. 2010c Effect of thermal non-equilibrium on the onset of convection in a porous medium layer saturated by a nanofluid. *Transp. Porous Media* **83**, 425–436. [9.7]
- Kuznetsov, A. V. and Nield, D. A. 2010d The onset of double-diffusive nanofluid convection in a layer of a saturated porous medium. *Transp. Porous Media* **85**, 941–951. [9.7]
- Kuznetsov, A. V. and Nield, D. A. 2010e Thermal instability in a porous medium layer saturated by a nanofluid: Brinkman model. *Transp. Porous Media* **81**, 409–422. [9.7]
- Kuznetsov, A. V. and Nield, D. A. 2010f Corrigendum to “Forced convection with slip flow in a channel occupied by a hyperporous medium saturated by a rarefied gas”, TiPM 64, 161–170. 2006, and “Thermally developing forced convection in a porous medium occupied by a rarefied gas: Parallel plate channel or circular tube with walls at constant heat flux.”, TiPM 76, 345–362. 2009. *Transp. Porous Media* **85**, 657–658. [4.13]
- Kuznetsov, A. V. and Nield, D. A. 2011a The onset of convection in a tridisperse porous medium. *Int. J. Heat Mass Transfer* **54**, 3120–3127. [6.27]
- Kuznetsov, A. V. and Nield, D. A. 2011b The effect of local thermal nonequilibrium on the onset of convection in a porous medium layer saturated by a nanofluid: Brinkman model. *J. Porous Media* **14**, 285–293. [6.23]
- Kuznetsov, A. V. and Nield, D. A. 2012b The effect of strong heterogeneity and strong throughflow on the onset of convection in a porous medium: Periodic and localized variation. *Transp. Porous Media* **92**, 289–298. [6.13.6]
- Kuznetsov, A. V. and Nield, D. A. 2012c The onset of double-diffusive convection in a vertical cylinder occupied by a heterogeneous porous medium with vertical throughflow. *Transp. Porous Media* **95**, 327–336. [6.10, 6.16.1, 9.1.6.4]
- Kuznetsov, A. V. and Vafai, K. 1995b Analytical comparison and criteria for heat and mass transfer models in metal hydride packed beds. *Int. J. Heat Mass Transfer* **38**, 2873–2884. [3.4]

- Kuznetsov, A. V. and Vafai, K. 1995a Development and investigation of three-phase model of the mushy zone for analysis of porosity formation in solidifying castings. *Int. J. Heat Mass Transfer* **38**, 2557–2567. [10.2.3]
- Kuznetsov, A. V. and Xiong, M. 1999 Limitation of the single-domain approach for computation of convection in composite channels: comparisons with exact solutions. *Hybrid Methods in Engineering* **1**, 249–264. [4.11]
- Kuznetsov, A. V. and Xiong, M. 2000 Numerical simulation of the effect of thermal dispersion on forced convection in a circular duct partly filled with a Brinkman-Forchheimer porous medium. *Int. J. Numer. Meth. Heat Fluid Flow* **10**, 488–501. [4.11]
- Kuznetsov, A. V. and Xiong, M. 2003 Development of an engineering approach to computations of turbulent flows in composite porous/fluid domains. *Int. J. Therm. Sci.* **42**, 9123–919. [1.8]
- Kuznetsov, A. V., Avramenko, A. A. and Geng, P. 2003a A similarity solution for a falling plume in bioconvection of oxytactic bacteria in a porous medium. *Int. Comm. Heat Mass Transfer* **30**, 37–46. [6.25]
- Kuznetsov, A. V., Avramenko, A. A. and Geng, P. 2004 Analytical investigation a falling plume caused by bioconvection of oxytactic bacteria in a fluid saturated porous medium. *Int. J. Engng. Sci.* **42**, 557–569. [6.25]
- Kuznetsov, A. V., Cheng, L. and Xiong, M. 2002 Effects of thermal dispersion and turbulence in forced convection in a composite parallel-plate channel: Investigation of constant wall heat flux and constant wall temperature cases. *Numer. Heat Transfer A* **42**, 365–383. [4.11]
- Kuznetsov, A. V., Cheng, L. and Xiong, M. 2003b Investigation of turbulence effects on forced convection in a composite porous/fluid duct: Constant wall heat flux and constant wall temperature cases. *Heat Mass Transfer* **39**, 613–623. [4.11]
- Kuznetsov, A. V., Nield, D. A. and Simmons, C. T. 2010 The effect of strong heterogeneity on the onset of convection in a porous medium; Periodic and localized variation. *Transp. Porous Media* **81**, 123–139. [6.13.5]
- Kuznetsov, A. V., Nield, D. A. and Simmons, C. T. 2011 The onset of convection in a strongly heterogeneous porous medium with transient temperature profile. *Transp. Porous Media* **86**, 851–865. [6.13.5]
- Kuznetsov, A. V., Xiong, M. and Nield, D. A. 2003c Thermally developing forced convection in a porous medium: circular duct with walls at constant temperature, with longitudinal conduction and viscous dissipation effects. *Transport Porous Media* **53**, 331–345. [4.13]
- Kvernvold, O. 1979 On the stability of nonlinear convection in a Hele-Shaw cell. *Int. J. Heat Mass Transfer* **22**, 395–400. [2.5]
- Kvernvold, O. and Tyvand, P. A. 1979 Nonlinear thermal convection in anisotropic porous media. *J. Fluid Mech.* **90**, 609–624. [6.12]
- Kvernvold, O. and Tyvand, P. A. 1980 Dispersion effects on thermal convection in porous media. *J. Fluid Mech.* **99**, 673–686. [6.6]
- Kvernvold, O. and Tyvand, P. A. 1981 Dispersion effects on thermal convection in a Hele-Shaw cell. *Int. J. Heat Mass Transfer* **24**, 887–900. [2.5]
- Kwan, H. H. Y., Rees, D. A. S. and Pop, I. 2008 Finite Péclet number forced convection past a sphere in a porous medium using a thermal nonequilibrium model. *Heat Mass Transfer* **44**, 1391–1399. [4.10]
- Kwendakwema, N.J. and Boehm, R.F. 1991 Parametric study of mixed convection in a porous medium between vertical concentric cylinders. *ASME J. Heat Transfer* **113**, 128–134. [8.3.3]
- Kwok, L. P. and Chen, C. F. 1987 Stability of thermal convection in a vertical porous layer. *ASME J. Heat Transfer* **109**, 889–893. [7.1.4]
- Laakkonen, K. 2003 Method to model dryer fabrics in paper machine scale using small-scale simulations and porous medium model. *Int. J. Heat Fluid Flow* **24**, 114–121. [1.8]
- Lafdi, K., Mesalhy, O. and Shaikh, S. 2007 Experimental study on the influence of foam porosity and pore size on the melting of phase change materials. *J. Appl. Phys.* **102**, Art. 083549. [10.1.7]
- Lage, J. L. 1992 Effect of the convective inertia term on Bénard convection in a porous medium. *Numer. Heat Transfer A* **22**, 469–485. [1.5.2]

- Lage, J. L. 1993a Natural convection within a porous medium cavity: predicting tools for flow regime and heat transfer. *Int. Comm. Heat Mass Transfer* **20**, 501–513. [1.5.2, 6.6]
- Lage, J. L. 1993b On the theoretical prediction of transient heat transfer within a rectangular fluid-saturated porous medium enclosure. *ASME J. Heat Transfer*, **115**, 1069–1071. [7.5]
- Lage, J. L. 1996 Comments on “the effect of turbulence on solidification of a binary metal alloy with electromagnetic stirring.” *ASME J. Heat Transfer* **118**, 996–997. [10.2.3]
- Lage, J. L. 1997 Contaminant clean-up in a single rock fracture with porous obstructions. *ASME J. Fluids Engng.* **119**, 180–187. [1.4.1, 1.9]
- Lage, J. L. 1998 The fundamental theory of flow through permeable media: from Darcy to turbulence. *Transport Phenomena in Porous Media* (eds. D.B. Ingham and I. Pop), Elsevier, Oxford, pp.1–30. [1.5.2, 1.8]
- Lage, J. L. and Antohe, B. V. 2000 Darcy’s experiments and the deviation to nonlinear flow regime. *ASME J. Fluids Engng.* **122**, 619–625. [1.5.2]
- Lage, J. L. and Bejan, A. 1990 Numerical study of forced convection near a surface covered with hair. *Int. J. Heat Fluid Flow* **11**, 242–248. [5.13]
- Lage, J. L. and Bejan, A. 1991 Natural convection from a vertical surface covered with hair. *Int. J. Heat Fluid Flow* **12**, 46–53. [5.13]
- Lage, J. L. and Bejan, A. 1993 The resonance of natural convection in an enclosure heated periodically from the side. *Int. J. Heat Mass Transfer* **36**, 2027–2038. [7.10]
- Lage, J. L. and Narasimhan, A. 2000 Porous media enhanced forced convection fundamentals. *Handbook of Porous Media* (K. Vafia, ed.), Marcel Dekker, New York, pp. 357–394. [4]
- Lage, J. L. and Nield, D. A. 1997 Comments on “numerical studies of forced convection heat transfer from a cylinder from a cylinder embedded in a packed bed. *Int. J. Heat Mass Transfer* **40**, 1725–1726. [4.8]
- Lage, J. L. and Nield, D. A. 1998 Convection induced by inclined gradients in a shallow porous medium layer. *Journal of Porous Media* **1**, 57–69. [7.9]
- Lage, J. L., Antohe, B. V. and Nield, D. A. 1997 Two types of nonlinear pressure-drop versus flow rate relation observed for saturated porous media. *ASME J. Fluids Engng.* **119**, 701–706. [1.5.2]
- Lage, J. L., Bejan, A. and Georgiadis, J. G. 1992 The Prandtl number effect near the onset of Bénard convection in a porous medium. *Int. J. Heat Fluid Flow* **13**, 408–411. [6.9.2, 6.12]
- Lage, J. L., de Lemos, M. J. S. and Nield, D. A. 2002 Modeling turbulence in porous media. In *Transport Phenomena in Porous Media II* (D. B. Ingham and I. Pop, eds.) Elsevier, Oxford, pp. 198–230. [1.8]
- Lage, J. L., Krueger, P. S. and Narasimhan, A. 2005 Protocol for measuring permeability and form coefficient of porous media. *Phys. Fluids* **17**, art. no. 088101. [1.5.2]
- Lage, J. L., Merrikh, A. A. and Kulish, V.V. 2004a A porous medium model to investigate the red cell distribution effect on alveolar respiration. In *Emerging Technologies and Techniques in Porous Media* (D. B. Ingham, A. Bejan, E. Mamut and I. Pop, eds), Kluwer Academic, Dordrecht, pp. 381–407. [1.9]
- Lage, J. L., Narasimhan, A., Porneala, P.C. and Price, D. C. 2004b Experimental study of forced convection through microporous enhanced heat sinks. In *Technologies and Techniques in Porous Media* (D. B. Ingham, A. Bejan, E. Mamut and I. Pop, eds), Kluwer Academic, Dordrecht, pp. 433–452. [4.5]
- Lage, J. L., Weinert, A. K., Price, D. C. and Weber, R. M. 1996 Numerical study of a low permeability microporous heat sink for cooling phased-array radar systems. *Int. J. Heat Mass Transfer*, **39**, 3633–3647. [4.9]
- Lai, C. H., Bodvarsson, G. S. and Truesdell, A. H. 1994 Modeling studies of heat transfer and phase distribution in two-phase geothermal reservoirs. *Geothermics* **23**, 3–20. [11]
- Lai, F. C. 1990a Coupled heat and mass transfer by natural convection from a horizontal line source in saturated porous medium. *Int. Comm. Heat Mass Transfer* **17**, 489–499. [9.3.2]
- Lai, F. C. 1990b Natural convection from a concentrated heat source in a saturated porous medium. *Int. Comm. Heat Mass Transfer* **17**, 791–800. [5.11.1]

- Lai, F. C. 1991a Coupled heat and mass transfer by mixed convection from a vertical plate in a saturated porous medium. *Int. Comm. Heat Mass Transfer* **18**, 93–106. [9.6.1]
- Lai, F. C. 1991b Non-Darcy natural convection from a line source of heat in a saturated porous medium. *Int. Comm. Heat Mass Transfer* **18**, 445–457. [5.10.1.2]
- Lai, F. C. 1991c Non-Darcy mixed convection from a line source of heat in a saturated porous medium. *Int. Comm. Heat Mass Transfer* **18**, 875–887. [8.1.4]
- Lai, F. C. 1993a Improving effectiveness of pipe insulation by using radial baffles to suppress natural convection. *Int. J. Heat Mass Transfer* **36**, 899–908. [7.3.7]
- Lai, F. C. 1993b Natural convection in a horizontal porous annulus with mixed type of radial baffles. *Int. Comm. Heat Mass Transfer* **20**, 347–359. [7.3.7]
- Lai, F. C. 1994 Natural convection in horizontal porous annuli with circumferential baffles *AIAA J. Thermophys. Heat Transfer* **8**, 376–378. [7.3.7]
- Lai, F. C. 2000 Mixed convection in saturated porous media. *Handbook of Porous Media* (K. Vafia, ed.), Marcel Dekker, New York, pp. 605–661. [8]
- Lai, F. C. and Kulacki, F. A. 1987 Non-Darcy convection from horizontal impermeable surfaces in saturated porous media. *Int. J. Heat Mass Transfer* **30**, 2189–2192. [4.7, 8.1.2]
- Lai, F. C. and Kulacki, F. A. 1988a Effects of flow inertia on mixed convection along a vertical surface in a saturated porous medium. *ASME HTD* **96**, Vol. 1, 643–652. [8.1.1]
- Lai, F. C. and Kulacki, F. A. 1988b Transient mixed convection in horizontal porous layer locally heated from below. *ASME HTD* **96**, Vol. 2, 353–364. [8.2.2]
- Lai, F. C. and Kulacki, F. A. 1988c Natural convection across a vertical layered porous cavity. *Int. J. Heat Mass Transfer* **31**, 1247–1260. [7.3.2]
- Lai, F. C. and Kulacki, F. A. 1989a Thermal dispersion effects on non-Darcy convection over horizontal surfaces in saturated porous media. *Int. J. Heat Mass Transfer* **32**, 971–976. [4.7, 8.1.2]
- Lai, F. C. and Kulacki, F. A. 1989b Effects of variable fluid viscosity on film condensation along an inclined surface in saturated porous medium. *ASME HTD* **127**, 7–12. [10.4]
- Lai, F. C. and Kulacki, F. A. 1990a Coupled heat and mass transfer from a sphere buried in an infinite porous medium. *Int. J. Heat Mass Transfer* **33**, 209–215. [9.4]
- Lai, F. C. and Kulacki, F. A. 1990b The influence of surface mass flux on mixed convection over horizontal plates in saturated porous media. *Int. J. Heat Mass Transfer* **33**, 576–579. [8.1.2]
- Lai, F. C. and Kulacki, F. A. 1990c The effect of variable viscosity on convective heat transfer along a vertical surface in a saturated porous medium. *Int. J. Heat Mass Transfer* **33**, 1028–1031. [8.1.1]
- Lai, F. C. and Kulacki, F. A. 1990d The influence of lateral mass flux on mixed convection over inclined surfaces in saturated porous media. *ASME J. Heat Transfer* **112**, 515–518. [8.1.1]
- Lai, F. C. and Kulacki, F. A. 1991e Experimental study in horizontal layers with multiple heat sources *AIAA J. Thermophys. Heat Transfer* **5**, 627–630. [6.18]
- Lai, F. C. and Kulacki, F. A. 1991a Non-Darcy mixed convection along a vertical wall in a saturated porous medium. *ASME J. Heat Transfer* **113**, 252–255. [8.1.1]
- Lai, F. C. and Kulacki, F. A. 1991c Oscillatory mixed convection in horizontal porous layers locally heated from below. *Int. J. Heat Mass Transfer* **34**, 887–890. [8.2.2]
- Lai, F. C. and Kulacki, F. A. 1991d Coupled heat and mass transfer by natural convection from vertical surfaces in porous media. *Int. J. Heat Mass Transfer* **34**, 1189–1194. [9.2.1]
- Lai, F. C. and Kulacki, F. A. 1991b Experimental study of free and mixed convection in horizontal porous layers locally heated from below. *Int. J. Heat Mass Transfer* **34**, 525–541. [8.2.2]
- Lai, F. C., Choi, C. Y. and Kulacki, F. A. 1990a Free and mixed convection in horizontal porous layers with multiple heat sources *AIAA J. Thermophys. Heat Transfer* **4**, 221–227. [6.18, 8.2.2]
- Lai, F. C., Choi, C. Y. and Kulacki, F. A. 1990b Coupled heat and mass transfer by natural convection from slender bodies of revolution in porous media. *Int. Comm. Heat Mass Transfer* **17**, 609–620. [9.4]
- Lai, F. C., Kulacki, F. A. and Prasad, V. 1987a Mixed convection in horizontal porous layers: effects of thermal boundary conditions. *ASME HTD* **84**, 91–96. [8.2.2]

- Lai, F. C., Kulacki, F. A. and Prasad, V. 1991a Mixed convection in saturated porous media. Convective Heat and Mass Transfer in Porous Media (eds. S. Kakaç, et al.), Kluwer Academic, Dordrecht, 225–287. [8.1.1]
- Lai, F. C., Pop, I and Kulacki, F. A. 1991b Natural convection from isothermal plates embedded in thermally stratified porous media *AIAA J. Thermophys. Heat Transfer* **4**, 533–535. [5.1.4]
- Lai, F. C., Pop, I. and Kulacki, F. A. 1990c Free and mixed convection from slender bodies of revolution in porous media. *Int. J. Heat Mass Transfer* **33**, 1767–1769. [5.9, 8.1.4]
- Lai, F. C., Prasad, V. and Kulacki, F. A. 1987b Effects of the size of heat source on mixed convection in horizontal porous layers heated from below. Proc. ASME JSME Thermal Engineering Joint Conference vol. 2, pp. 413–419. [8.2.2]
- Lai, F. C., Prasad, V. and Kulacki, F. A. 1988 Aiding and opposing mixed convection in a vertical porous layer with a finite wall heat source. *Int. J. Heat Mass Transfer* **31**, 1049–1061. [8.3.2]
- Lai, Y. M., Li, J. J., Niu, F. J. and Yu, W. B. 2003 Nonlinear thermal analysis for Qing-Tibet railway embankments in cold regions. *Cold Regions Engng.* **17**, 171–184. [4.16.2, 7.3.7]
- Lai, Y. M., Ma, W. D., Zhang, M. Y., Yu, W. B. and Gao, Z. H. 2006a Experimental investigation on influence of boundary conditions on cooling effect and mechanism of crushed-rock layers. *Cold Regions Sci. Tech.* **45**, 114–121. [7.3.7]
- Lai, Y. M., Zhang, M. Y., Liu, Z. Q. and Yu, W. B. 2006b Numerical analysis for cooling effect of open boundary ripped-rock embankment on Qinghai-Tibetan railway. *Science in China D* **49**, 764–772. [7.3.7]
- Lai, Y. M., Zhang, S. J. and Mi, L. 2004 Effect of climatic warming on the temperature fields of embankments in cold regions and a countermeasure. *Numer. Heat Transfer* **45**, 191–210. [4.16.2, 7.3.7]
- Lai, Y. M., Zhang, S. J., Zhang, L. X. and Xiao, J. Z. 2004 Adjusting temperature distribution under the south and north slopes of embankment in permafrost regions by the ripped-rock revetment. *Cold Regions Sci. Tech.* **39**, 67–79. [4.16.2, 7.3.7]
- Lan, X. K. and Khodadadi, J. M. 1993 Fluid flow and heat transfer through a porous medium channel with permeable walls. *Int. J. Heat Mass Transfer* **36**, 2242–2245. [4.9]
- Landman, K. A., Pel, L. and Kaasschieler, E. F. 2001 Analytical modeling of drying of porous materials. *Math. Engng. Ind.* **8**, 89–122. [3.6]
- Lapwood, E. R. 1948 Convection of a fluid in a porous medium. *Proc. Camb. Phil. Soc.* **44**, 508–521. [6.1, 6.26]
- Larbi, S., Bacon, G. and Bories, S. A. 1995 Diffusion d'air humide avec condensation de vapeur d'eau en milieu poreux. *Int. J. Heat Mass Transfer* **38**, 2411–2416. [3.6]
- Larson, S. E. and Poulikakos, D. 1986 Double diffusion from a horizontal line source in an infinite porous medium. *Int. J. Heat Mass Transfer* **29**, 492–495. [9.3.2]
- Lauriat, G. and Ghafir, R. 2000 Forced convective heat transfer in porous media. Handbook of Porous Media (K. Vafia, ed.), Marcel Dekker, New York, pp. 201–267. [4]
- Lauriat, G. and Prasad, V. 1987 Natural convection in a vertical porous cavity: a numerical study for Brinkman-extended Darcy formulation. *ASME J. Heat Transfer* **109**, 688–696. [7.6.2]
- Lauriat, G. and Prasad, V. 1989 Non-Darcian effects on natural convection in a vertical porous layer. *Int. J. Heat Mass Transfer* **32**, 2135–2148. [7.6.2]
- Lauriat, G. and Prasad, V. 1991 Natural convection in a vertical porous annulus. Convective Heat and Mass Transfer in Porous Media (eds. S. Kakaç, B. Kilkis, F. A. Kulacki, and F. Arinc), Kluwer Academic, Dordrecht, pp. 143–172. [7.6.2]
- Lauriat, G. and Vafai, K. 1991 Forced convection flow and heat transfer through a porous medium exposed to a flat plate or a channel. Convective Heat and Mass Transfer in Porous Media (eds. S. Kakaç, et al.), Kluwer Academic, Dordrecht, pp. 289–327. [4.8, 4.9]
- Lawson, M. L. and Yang, W. J. 1975 Thermal instability of binary gas mixtures in a porous medium. *ASME J. Heat Transfer* **97**, 378–381. [9.1.4]
- Lawson, M. L., Yang, W. J. and Bunditkul, S. 1976 Theory of thermal stability of binary gas mixtures in porous media. *ASME J. Heat Transfer* **98**, 35–41. [9.1.4]

- Layeghi, M. and Nouri-Borujerdi, A. 2004 Fluid flow and heat transfer around circular cylinders in the presence or no-presence of porous media. *J. Porous Media* **7**, 239–247. [4.11]
- Layton, W., Schieweck, F. and Yotov, I. 2003 Coupling fluid flow with porous media flow. *SIAM J. Numer. Anal.* **40**, 2195–2218. [1.6]
- Le Bars, M. and Worster, M. G. 2006a Interfacial conditions between a pure fluid and a porous medium: implications for binary alloy solidification. *J. Fluid Mech.* **550**, 149–173. [10.2.3]
- Le Bars, M. and Worster, M. G. 2006b Solidification of a binary alloy: Finite-element single-domain simulation and new benchmark solutions. *J. Comput. Appl. Math.* **216**, 247–263. [10.2.3]
- Le Breton, P., Caltagirone, J.P. and Arquis, E. 1991 Natural convection in a square cavity with thin porous layers on its vertical walls. *ASME J. Heat Transfer* **113**, 892–898. [7.7]
- Leblond, G. and Gosselin, L. 2008 Effect of non-local equilibrium on minimal thermal resistance porous layered systems. *Int. J. Heat Fluid Flow* **29**, 281–291. [4.10]
- Lebon, G. and Cloot, A. 1986 A thermodynamical modelling of fluid flows through porous media: application to natural convection. *Int. J. Heat Mass Transfer* **29**, 381–390. [6.6]
- Ledezma, G., Morega, A. M. and Bejan, A. 1996 Optimal spacing between fins with impinging flow. *J. Heat Transfer* **118**, 570–577. [4.15]
- Lee, D. H., Yoon, D. Y. and Choi, C. K. 2000 The onset of vortex instability in laminar convection flow over an inclined plate embedded in a porous medium. *Int. J. Heat Mass Transfer* **43**, 2895–2908. [5.4]
- Lee, D. Y. and Vafai, K. 1999 Analytical characterization and conceptual assessment of solid and fluid temperature differentials in porous media. *Int. J. Heat Mass Transfer* **42**, 423–43. (erratum 4077). [4.10]
- Lee, H. M. 1983 An experimental study of natural convection about an isothermal downward-facing inclined surface in a porous medium. M.S. Thesis, University of Hawaii. [5.3]
- Lee, J. and Shivakumar, I. S. 2011 Onset of penetrative convection in a ferro-fluid saturated porous layer. *Spec. Top. Rev. Porous Media* **2**, 217–225. [6.21]
- Lee, J. S. and Ogawa, K. 1994 Pressure drop through packed bed. *J. Chem. Engng Japan* **27**, 691–693. [1.5.2]
- Lee, J., Kim, S., Lorente, S. and Bejan, A. 2008 Vascularization with trees matched canopy to canopy: diagonal channels with multiple sizes. *Int. J. Heat Mass Transfer* **51**, 2029–2040. [4.19]
- Lee, J., Lorente, S. and Bejan, A. 2009b Vascular design for thermal management of heated structures. *The Aeronautical J.* **113**, 397–407. [4.19]
- Lee, J., Lorente, S. and Bejan, A. 2009c Transient cooling of smart vascular materials for self-cooling. *J. Appl. Phys.* **105**, #064904. [4.19]
- Lee, J., Lorente, S., Bejan, A., and Kim, M. 2009a Vascular structures with flow uniformity and small resistance. *Int. J. Heat Mass Transfer* **52**, 1761–1768. [4.19]
- Lee, J., Shivakumara, I. S. and Mamatha, A. L. 2011a Effect of nonuniform temperature gradients on thermogravitational convection in a porous layer using a nonequilibrium model. *J. Porous Media* **14**, 659–669. [6.24]
- Lee, J., Shivakumara, I. S. and Ravisha, M. 2011b Effect of thermal non-equilibrium on convective instability in a ferromagnetic fluid-saturated porous medium. *Transp. Porous Media* **86**, 103–124. [6.21]
- Lee, K. B. and Howell, J. R. 1991 Theoretical and experimental heat and mass transfer in highly porous media. *Int. J. Heat Mass Transfer* **34**, 2123–2132. [1.8]
- Lee, S. L. and Yang, J. H. 1997 Modelling of Darcy-Forchheimer drag for fluid flow across a bank of circular cylinders. *Int. J. Heat Mass Transfer* **40**, 3149–3155. [1.5.2]
- Lee, S. L. and Yang, J. H. 1998 Modelling of effective thermal conductivity for a nonhomogeneous anisotropic porous medium. *Int. J. Heat Mass Transfer* **41**, 931–937. [2.2.1]
- Lehmann, P., Assouline, S. and Or, D. 2008 Characteristic length scales affecting evaporative drying of porous media. *Phys. Rev. E* **77**, 056309. [3.6]
- Lein, H. and Tankin, R. S. 1992a Natural convection in porous media — I. Nonfreezing. *Int. J. Heat Mass Transfer* **35**, 175–186. [6.9.1]

- Lein, H. and Tankin, R. S. 1992b Natural convection in porous media — II. Freezing. *Int. J. Heat Mass Transfer* **35**, 187–194. [10.2.2]
- Leong, F. C. and Lai, F. C. 2006 Natural convection in a concentric annulus with a porous sleeve. *Int. J. Heat Mass Transfer* **49**, 3016–3027. [7.7]
- Leong, J. C. and Lai, F. C. 2001 Effective permeability of a layered porous cavity. *ASME J. Heat Transfer* **123**, 512–519. [6.13.2]
- Leong, J. C. and Lai, F. C. 2004 Natural convection in rectangular layers porous cavities. *J. Thermophys. Heat Transfer* **18**, 457–463. [6.13.2]
- Leong, K. C. and Jin, L. W. 2004 Heat transfer of oscillating and steady flows in a channel filled with porous media. *Int. Comm. Heat Mass Transfer* **31**, 63–72. [4.16.5]
- Leong, K. C. and Jin, L. W. 2005 An experimental study of oscillatory flow through a channel filled with an aluminum foam. *Int. J. Heat Mass Transfer* **48**, 243–253. [4.16.5]
- Leong, K. C., Li, H. Y., Jin, L. W. and Chai, J. C. 2010 Numerical and experimental study of forced convection in graphite foams of different configurations. *Appl. Therm. Engng.* **30**, 520–532. [4.16.25]
- Leppinen, D. M. and Rees, D. A. S. 2004 Sidewall heating in shallow cavities near the density maximum. In *Emerging Technologies and Techniques in Porous Media* (D. B. Ingham, A. Bejan, E. Mamut and I. Pop, eds.), Kluwer Academic, Dordrecht, pp. 183–194. [7.1.6]
- Leppinen, D. M., Pop, I., Rees, D. A. S. and Storesletten, L. 2004 Free convection in a shallow annular cavity filled with a porous medium. *J. Porous Media* **7**, 289–302. [7.3.3]
- Lesnic, D. and Pop, I. 1998a Free convection in a porous medium adjacent to horizontal surfaces. *Zeit. Angew. Math. Mech.* **78**, 197–205. [5.2]
- Lesnic, D. and Pop, I. 1998b Mixed convection over a horizontal surface embedded in a porous medium. In *Mathematics of Heat Transfer* (G. E. Tuck and A. S. Wood, eds.) Clarendon Press, Oxford, pp. 219–224. [8.1.2]
- Lesnic, D., Ingham, D. B. and Pop, I. 1995 Conjugate free convection from a horizontal surface in a porous medium. *Z. Angew. Math. Mech.* **75**, 715–722. [5.2]
- Lesnic, D., Ingham, D. B. and Pop, I. 1999 Free convection boundary-layer flow along a vertical surface in a porous medium with Newtonian heating. *Int. J. Heat Mass Transfer* **42**, 2621–2627. [5.1.9.8]
- Lesnic, D., Ingham, D. B. and Pop, I. 2000 Free convection from a horizontal surface in a porous medium with Newtonian heating. *J. Porous Media* **3**, 227–235. [5.2]
- Lesnic, D., Ingham, D. B., Pop, I. and Storr, C. 2004 Free convection boundary-layer flow above a nearly horizontal surface in a porous medium with Newtonian heating. *Heat Mass Transfer* **40**, 665–672. [5.3]
- Leu, J. S. and Jang, J. Y. 1994 The wall and free plumes above a horizontal line source in non-Darcian porous media. *Int. J. Heat Mass Transfer* **37**, 1925–1933. [5.10.1]
- Leu, J. S. and Jang, J. Y. 1993 Variable viscosity effects on the vortex instability of the convective boundary layer flow over a horizontal uniform heat flux surface in a saturated porous medium. Proc. 6th Int. Sympos. Transport Phenomena and Thermal Engineering, Seoul, Korea. Vol.1, pp. 203–208. [5.4]
- Leu, J. S. and Jang, J. Y. 1995 The natural convection from a point heat source embedded in a non-Darcian porous medium. *Int. J. Heat Mass Transfer* **38**, 1097–1104. [5.11.1]
- Leu, J. S., Jang, J. Y. and Chou, T. 2006 Heat and mass transfer for liquid film evaporation along a vertical plate covered with a thin porous layer. *Int. J. Heat Mass Transfer* **49**, 1937–1945. [10.3.2]
- Leu, J. S., Jang, J. Y. and Chou, T. 2009 Convection heat and mass transfer along a vertical heated plate with film evaporation in a non-Darcian porous medium. *Int. J. Heat Mass Transfer* **52**, 5447–5450. [10.3.2]
- Leu, J. S., Jang, J. Y. and Chou, T. 2011 Effects of non-Darcian and inlet conditions on the forced convection along a vertical plate with film evaporation. *Heat Transfer Engng.* **32**, 981–987. [10.3.2]

- Levy, A., Levi-Hevroni, D., Sorek, S. and Ben-Dor, G. 1999 Derivation of Forchheimer terms and their verification by applications to waves propagated in porous media. *Int. J. Multiphase Flows* **25**, 683–704. [1.5.2]
- Levy, T. 1981 Loi de Darcy ou loi de Brinkman? C. R. Acad. Sci. Paris, Sér. II 292, 872–874. [1.5.3]
- Levy, T. 1990 Écoulement dans un milieu poreux avec fissures unidirectionnelles. C.R. Acad. Sci. Paris, Sér. II, 685–690. [1.9]
- Lewins, J. 2003 Bejan's constructal theory of equal potential distribution. *Int. J. Heat Mass Transfer* **46**, 1541–1543. [4.18, 4.20, 6.26, 11.10]
- Lewis, S., Bassom, A. P. and Rees, D. A. S. 1995 The stability of vertical thermal boundary-layer flow in a porous medium. *Eur. J. Mech. B/Fluids* **14**, 395–407. [5.1.9.9]
- Lewis, S., Rees, D. A. S. and Bassom, A. P. 1997 High wavenumber convection in tall porous containers heated from below. *Quart. J. Mech. Appl. Math.* **50**, 545–563. [6.15.2]
- Li, C. T. and Lai, F. C. 1998 Re-examination of double diffusive natural convection from horizontal surfaces in porous media. *J. Thermophys. Heat Transfer* **12**, 449–452. [9.2.1]
- Li, H. Y. and Leong, K. C. 2011 Experimental and numerical study of single and two-phase flow and heat transfer in aluminum foams. *Int. J. Heat Mass Transfer* **54**, 4904–4912. [10.3.1]
- Li, H. Y., Leong, K. C., Jin, L. W. and Chai, J. C. 2010a Analysis of fluid flow and heat transfer in a channel with staggered porous blocks. *Int. J. Therm. Sci.* **49**, 950–962. [4.11]
- Li, H. Y., Leong, K. C., Jin, L. W. and Chai, J. C. 2010b Three dimensional numerical simulation of fluid flow with phase change heat transfer in an asymmetrically heated porous channel. *Int. J. Therm. Sci.* **49**, 2363–2375. [10.3.1]
- Li, H. Y., Leong, K. C., Jin, L. W. and Chai, J. C. 2010c Transient behaviour of fluid flow and heat transfer with phase change in vertical porous channels. *Int. J. Heat Mass Transfer* **53**, 5209–5222. [10.3.1]
- Li, H. Y., Leong, K. C., Jin, L. W. and Chai, J. C. 2010d Transient two-phase flow and heat transfer with localized heating in porous media. *Int. J. Therm. Sci.* **49**, 1115–1127. [10.3.1]
- Li, J. M. and Wang, B. X. 1998 Investigation on wall effect of condensation in porous media. *Heat Transfer* 1998, *Proc. 11th IHTC*, **4**, 459–463. [10.4]
- Li, J. X., Lai, H. X. and Tu, S. T. 2009 Integral solution of a forced laminar boundary layer over an isothermal plate embedded in a porous medium. *Int. J. Nonlinear Sci. Numer. Simul.* **10**, 617–624. [4.1]
- Li, L. and Kimura, S. 2005 Mixed convection around a heated vertical cylinder embedded in porous medium. *Prog. Nat. Sci.* **15**, 661–664. [8.1.3]
- Li, L. and Kimura, S. 2005 Numerical simulation of mixed convection in a porous medium heated by a vertical cylinder. *Stroj. Vestik—J. Mech. Engng.* **51**, 491–494. [8.1.3]
- Li, M. C., Tian, Y. W. and Zhai, Y. C. 2006a Soret and Dufour effects in strongly endothermic chemical reaction system of porous media. *Trans. Nonferrous Met. Soc. China* **16**, 1200–1204. [9.1.4]
- Li, M., Wu, Y., Tian, Y. and Zhai, Y. 2007 Non-thermal equilibrium model of the coupled heat and mass transfer in strong endothermic chemical reaction system of porous media. *Int. J. Heat Mass Transfer* **50**, 2936–2943. [9.1.6.4]
- Li, W. Q., Qu, Z. G., He, H. L. and Tao, W. Q. 2012 Experimental and numerical studies on melting phase change heat transfer in open-cell metallic foams filled with paraffin. *Appl. Therm. Engng.* **37**, 1–9. [10.1.7]
- Li, Y. and Park, C. W. 1998 Permeability of packed beds filled with polydiverse spherical particles. *Ind. Eng. Chem Res.* **37**, 2005–2011. [1.4.2]
- Li, Z.W., Dong, M. Z. and Shirif, E. 2006b Transient natural convection induced by gas diffusion in liquid-saturated porous columns. *Industrial Engng. Chem. Research* **45**, 3311–3319. [9.2.2]
- Liao, S. J. and Magyari, E. 2006 Exponentially decaying boundary layers as limiting cases of families of algebraically decaying ones. *Z. Angew. Math. Phys.* **57**, 777–792. [5.1.9.9]
- Liao, S. J. and Pop, I. 2004 Explicit analytic solution for similarity boundary layer equations. *Int. J. Heat Mass Transfer* **47**, 75–85. [5.1.9.1]

- Libera, J. and Poulikakos, D. 1990 Parallel-flow and counter-flow conjugate convection from a vertical insulated pipe *AIAA J. Thermophys. Heat Transfer* **4**, 400–404. [5.7]
- Lie, K. N. and Jang, J. Y. 1993 Boundary and inertia effects on vortex instability of a horizontal mixed convection flow in a porous medium. *Numer. Heat Transfer A* **23**, 361–378. [5.4]
- Lienhard, J. H. 1973 On the commonality of equations for natural convection from immersed bodies. *Int. J. Heat Mass Transfer* **16**, 2121–2123. [4.3]
- Lim, J. S., Fowler, A. J. and Bejan, A., 1993, Spaces filled with fluid and fibers coated with phase-change material. *J. Heat Transfer* **115**, 1044–1050. [10.5]
- Lim, T. K., Cotton, M. A. and Axcell, B. P. 2007 Laminar forced convection and flow characteristics for the multiple plate porous insulation. *Appl. Thermal Engng.* **27**, 918–926. [4.11]
- Lin, C. H. and Payne, L. E. 2007 Structural stability for the Brinkman equations of flow in double diffusive convection. *J. Math. Anal. Appl.* **325**, 1479–1490. [9.1.6.4]
- Lin, D. K. 1992 Unsteady natural convection heat and mass transfer in a saturated porous enclosure. *Wärme-Stoffübertrag.* **28**, 49–56. [9.1.6.4]
- Lin, D. S. and Gebhart, B. 1986 Buoyancy induced flow adjacent to a horizontal surface submerged in porous medium saturated with cold water. *Int. J. Heat Mass Transfer* **29**, 611–623. [5.2]
- Lin, G., Zhao, C. B., Hobbs, B. E., Ord, A. and Muhlhaus, H. B. 2003 Theoretical and numerical analyses of convective instability in porous media with temperature-dependent viscosity. *Comm. Numer. Meth. Engng.* **19**, 787–799. [6.7]
- Lin, S., Chao, J. T., Chen, T. F. and Chen, D. K. 1998 Analytical and experimental study of drying process in a porous medium with a non-penetrating surface. *J. Porous Media* **1**, 159–166. [3.6]
- Ling, J. X. and Dybbs, A. 1992 The effect of variable viscosity on forced convection over a flat plate submersed in a porous medium. *ASME J. Heat Transfer* **114**, 1063–1065. [4.2]
- Ling, S. C., Nazar, R. and Pop, I. 2007a Steady mixed convection boundary layer flow over a vertical flat plate in a porous medium filled with water at 4 degrees C: Case of variable wall temperature. *Transport Porous Media* **69**, 359–372. [8.1.6]
- Ling, S. C., Nazar, R., Pop, I. and Merkin, J. H. 2007b Steady mixed convection boundary layer flow over a vertical flat surface in a porous medium filled with water at 4 degrees C: variable surface heat flux. *Transport Porous Media* **70**, 307–321. [8.1.6]
- Ling, S. C., Nazar, R., Pop, I. and Merkin, J. H. 2009 Mixed convection boundary layer flow in a porous medium filled with water close to its maximum density. *Transport Porous Media* **76**, 139–151. [8.1.6]
- Lipnicki, Z. and Weigand, B. 2008 Natural convection flow with solidification between two vertical plates filled with a porous medium. *Heat Mass Transfer* **44**, 1401–1407. [10.2.1.2]
- Lister, C. R. B. 1990 An explanation for the multivalued heat transport found experimentally for convection in a porous medium. *J. Fluid Mech.* **214**, 287–320. [6.4, 6.9.3]
- Liu, C. Y. and Guerra, A. C. 1985 Free convection in a porous medium near the corner of arbitrary angle formed by two vertical plates. *Int. Comm. Heat Mass Transfer* **12**, 431–440. [5.12.2]
- Liu, C. Y. and Ismail, K. A. R. 1980 Asymptotic solution of free convection near a corner of two vertical porous plates embedded in a porous medium. *Lett. Heat Mass Transfer* **7**, 457–463. [5.12.2]
- Liu, C. Y., Ismail, K. A. R. and Ibinuma, C. D. 1984 Film condensation with lateral mass flux about a body of arbitrary shape in a porous medium. *Int. Comm. Heat Mass Transfer* **11**, 377–384. [10.4]
- Liu, C. Y., Lam, C. Y. and Guerra, A. C. 1987a Free convection near a corner formed by two vertical plates embedded in a porous medium. *Int. Comm. Heat Mass Transfer* **14**, 125–136. [5.12.2]
- Liu, D., Zhao, F. Y. and Tang, G. F. 2008b Thermosolutal convection in saturated porous enclosure with concentrated energy and solute sources. *Energy Convers. Manag.* **49**, 16–31. [9.2.2]

- Liu, I. C. 2006 Flow and heat transfer of viscous fluids saturated in porous media over a permeable non-isothermal stretching sheet. *Transport Porous Media* **64**, 375–392. [5.1.9.9]
- Liu, J. Y. and Minkowycz, W. J. 1986 The effect of Prandtl number on conjugate heat transfer in porous media. *Int. Comm. Heat Mass Transfer* **13**, 439–448. [5.12.1]
- Liu, J. Y., Shih, S. D. and Minkowycz, W. J. 1987b Conjugate natural convection about a vertical cylindrical fin with lateral mass flux in a saturated porous medium. *Int. J. Heat Mass Transfer* **30**, 623–630. [5.12.1]
- Liu, P. C. 2003 Temperature distribution in a porous medium subjected to solar radiative incidence and downward flow: convective boundaries. *ASME J. Solar Energy Engng.* **125**, 190–194. [6.11.2]
- Liu, R., Liu, Q. S. and Zhao, S. C. 2008a The influence of Rayleigh effect combined with Marangoni effect on the onset of convection in a liquid layer overlying a porous layer. *Int. J. Heat Mass Transfer* **51**, 6328–6331. [6.19.3]
- Liu, S. and Masliyah, J. H. 1998 On non-Newtonian fluid flow in ducts and porous media. *Chem. Engng. Sci.* **53**, 1175–1201. [1.5.4]
- Liu, S. and Masliyah, J. H. 2005 Dispersion in porous media. *Handbook of Porous Media* (ed. K. Vafai), 2nd ed., Taylor and Francis, Boca Raton, FL, pp. 81–140. [1.5.1, 2.2.4]
- Liu, S., Afacan, A. and Masliyah, J. 1994 Steady incompressible laminar flow in porous media. *Chem. Engng Sci.* **49**, 3565–3586. [1.4.2]
- Liu, W., Shen, S. and Riffat, S. B. 2002 Heat transfer and phase change of liquid in an inclined enclosure packed with unsaturated porous media. *Int. J. Heat Mass Transfer* **45**, 5209–5219. [3.6]
- Liu, Y. 2009 Convergence and continuous dependence for the Brinkman-Forchheimer equations. *Math. Comput. Model.* **49**, 1401–1415. [1.5.3]
- Llagostera, J. and Figueiredo, J. R. 1998 Natural convection in porous cavity: application of UNIFAES discretization scheme. *Heat Transfer 1998, Proc. 11th IHTC*, **4**, 465–470. [6.8]
- Llagostera, J. and Figueiredo, J. R. 2000 Application of the UNIFAES discretization scheme to mixed convection in a porous layer with a cavity, using the Darcy model. *J. Porous Media* **3**, 139–154. [8.2.1]
- Lo Jacono, D., Burgeon, A. and Knobloch, E. 2010 Spatially localized binary fluid convection in a porous medium. *Phys. Fluids* **22**, #s073601. [9.4]
- Lombardo, S. and Mulone, G. 2002 Necessary and sufficient conditions of global nonlinear stability of rotating double-diffusive convection in a porous medium. *Cont. Mech. Thermodyn.* **14**, 527–540. [9.1.6.4]
- Lombardo, S. and Mulone, G. 2003 Nonlinear stability and convection for laminar flows in a porous medium with Brinkman law. *Math. Meth. Appl. Sci.* **26**, 453–462. [6.10.1]
- Lombardo, S., Mulone, G. and Straughan, B. 2001 Nonlinear stability in the Bénard problem for a double-diffusive mixture in a porous medium. *Math. Meth. Appl. Sci.* **24**, 1229–1246. [9.1.3]
- Loper, D. E. and Roberts, P. H. 2001 Mush-chimney convection. *Stud. Appl. Math.* **106**, 187–227. [10.2.3]
- Lopez, D. L. and Smith, L. 1995 Fluid flow at fault zones: analysis of the interplay of convective circulation and topographically driven groundwater flow. *Water Resour. Res.* **31**, 1489–1503. [11.8]
- Lorente, S. 2007 Constructal view of electrokinetic transfer through porous media. *J. Physics D: Applied Physics* **40** (9), 2941–2947. [3.7]
- Lorente, S. 2009 Vascularized materials as designed porous media. *Int. J. Energy Res.* **33**, 211–220. [4.15]
- Lorente, S. and Bejan, A. 2002 Combined “flow and strength” geometric optimization: internal structure in a vertical insulating wall with air cavities and prescribed strength. *Int. J. Heat Mass Transfer* **45**, 3313–3320. [7.7]
- Lorente, S. and Bejan, A. 2006 Heterogeneous porous media as multiscale structures for maximum flow access. *J. Appl. Phys.* **100**, #114909. [4.19]
- Lorente, S. and Bejan, A. 2009a Vascularized smart materials: Designed porous media for self-healing and self-cooling. *J. Porous Media* **12**, 1–18. [4.19]

- Lorente, S. and Bejan, A. 2009b Constructal design of vascular porous materials and electrokinetic mass transfer. *Transp. Porous Media* **77**, 305–322. [4.19]
- Lorente, S. and Ollivier, J. P. 2006 Scale analysis of electrodiffusion through porous media. *J. Porous Media* **9**, 307–320. [3.7]
- Lorente, S., Petit, M. and Javelas, R. 1996 Simplified analytical model for thermal transfer in a vertical hollow brick. *Energy Build.* **24**, 95–103. [7.7]
- Lorente, S., Petit, M. and Javelas, R. 1998 The effects of temperature conditions on the thermal resistance of walls made of different shapes vertical hollow bricks. *Energy Build.* **28**, 237–240. [7.7]
- Love, A. J., Simmons, C. T. and Nield, D. A. 2007 Double-diffusive convection in groundwater wells. *Water Resour. Res.* **43**, #W08428. [9.1.6.4]
- Lowell, R. P. 1980 Topographically driven subcritical hydrothermal convection in the oceanic crust. *Earth Planet. Sci. Lett.* **49**, 21–28. [11.4, 11.6.2]
- Lowell, R. P. 1985 Double-diffusive convection in partially molten silicate systems: its role during magma production and in magma chambers. *J. Volcanol. Geotherm. Res.* **26**, 1–24. [11.4]
- Lowell, R. P. 1991 Modeling continental and submarine hydrothermal systems. *Rev. Geophys.* **29**, 457–476. [11.8.1]
- Lowell, R. P. 2007 Numerical simulations of single-pass hydrothermal convection at mid-ocean ridges: Effects of the extrusive layer and temperature-dependent permeability. *Geochem. Geophys. Geosystems* **8**, #10. [11.8]
- Lowell, R. P. and Burnell, D. K. 1991 Mathematical modeling of conductive heat-transfer from a freezing, convecting magma chamber to a single pass hydrothermal system — Implications for sea-floor black smokers. *Earth Planet. Phys.* **104**, 59–69. [11.8]
- Lowell, R. P. and Hernandez, H. 1982 Finite amplitude convection in a porous container with fault-like geometry: effect of initial and boundary conditions. *Int. J. Heat Mass Transfer* **25**, 631–641. [6.15.2]
- Lowell, R. P. and Shyu, C. T. 1978 On the onset of convection in a water-saturated porous box: effect of conducting walls. *Lett. Heat Mass Transfer* **5**, 371–378. [6.15.2]
- Lowell, R. P., Rona, P. A. and von Herzen, R. P. 1995 Seafloor hydrothermal systems. *J. Geophys. Res.* **100**, 327–352. [11.8]
- Lu, J. W. and Chen, F. 1997 Rotation effects on the convection of binary alloys unidirectionally solidified from below. *Int. J. Heat Mass Transfer* **40**, 237–246. [10.2.3]
- Lu, N. 2001 An analytical assessment on the impact of covers on the onset of air convection in mine wastes. *Int. J. Numer. Anal. Meth. Geomech.* **25**, 347–364. [11.8]
- Lu, N. and Zhang, Y. 1997 Onset of thermally induced gas convection in mine wastes. *Int. J. Heat Mass Transfer* **40**, 2621–2636. [6.11.2]
- Lu, N., Zhang, Y. and Ross, B. 1999 Onset of gas convection in a moist porous layer with the top boundary open to the atmosphere. *Int. Comm. Heat Mass Transfer* **26**, 33–44. [6.2]
- Lu, T. and Shen, S. Q. 2007 Numerical and experimental investigation of paper drying: Heat and mass transfer with phase change in porous media. *Appl. Therm. Engng.* **27**, 1248–1258. [3.6]
- Lu, W., Zhao, C. Y. and Tassou, S. A. 2006 Thermal analysis on metal-foam filled heat exchangers. Part 1: Metal-foam filled pipes. *Int. J. Heat Mass Transfer* **49**, 2751–2761. [4.16.5]
- Ludvigsen, A., Palm, E. and McKibbin, R. 1992 Convective momentum and mass transport in sloping porous layers. *J. Geophys. Res.* **97**, 12315–12326. [7.8]
- Luna, E., Medina, A., Pérez-Rosales, C. and Treviño, C. 2004 Convection and dispersion in a naturally fractured reservoir. *J. Porous Media* **7**, 303–316. [7.8]
- Luna, N. and Mendez, F. 2005 Forced convection on a heated horizontal flat plate with finite thermal conductivity in a non-Darcian porous medium. *Int. J. Thermal Sci.* **44**, 656–664. [4.8]
- Luna, N. and Mendez, F. 2005 Forced convection on a heated horizontal flat plate with finite thermal conductivity in a non-Darcian porous medium. *Int. J. Thermal Sci.* **44**, 556–664. [4.8]
- Lundgren, T. S. 1972 Slow flow through stationary random beds and suspensions of spheres. *J. Fluid Mech.* **51**, 273–299. [1.5.3]
- Ly, H. V. and Titi, E. S. 1999 Global Gevrey regularity for the Bénard convection in a porous medium with zero Darcy-Prandtl number. *J. Nonlinear Sci.* **9**, 333–362. [6.15.1]

- Lyubimov, D. V. 1975 Convective motions in a porous medium heated from below. *J. Appl. Mech. Tech. Phys.* **16**, 257–261. [6.16.2]
- Lyubimov, D. V. 1993 Dynamical properties of thermal convection in porous medium. Instabilities in Multiphase Flows (G. Gouesbet and A. Berlement, eds.) Plenum, New York, 289–295. [7.3.3]
- Lyubimov, D. V., Lyubimova, T. P., Mojtabi, A. and Sadilov, E. S. 2008a Thermosolutal convection in a horizontal porous layer heated from below in the presence of horizontal through flow. *Phys. Fluids* **20**, #044109. [9.1.6.4]
- Lyubimov, D. V., Lyubimova, T. P., Muratov, I. D. and Shishkina, E. A. 2008b Vibration effect on convection onset in a system consisting of a horizontal pure liquid layer and a layer of liquid-saturated porous medium. *Fluid Dynamics* **43**, 789–798. [9.1.6.4]
- Lyubimov, D., Gavrilov, K. and Lyubimova, T. 2011 Soret-driven convection in a porous cavity with perfectly conducting boundaries. *C. R. Mecanique* **339**, 297–302. [9.1.4]
- Ma, H. and Ruth, D. W. 1993 The microscopic analysis of high Forchheimer number flow in porous media. *Transport Porous Media* **13**, 139–160. [1.5.2]
- Ma, W. P., Tzeng, S. C. and Jwo, W. J. 2006 Flow resistance and forced convective heat transfer effects for various flow orientations in a packed channel. *Int. Comm. Heat Mass Transfer* **33**, 319–326. [4.5]
- Ma, X. and Zabaras, N. 2008 A stabilized stochastic finite-element second-order projection method for modeling natural convection in random porous media. *J. Comput. Phys.* **227**, 8448–8471. [2.6]
- Ma, X. H. and Wang, B. X. 1998 Suction effect of a vertical coated plain porous layer on film condensation heat transfer enhancement. *Heat Transfer 1998, Proc. 11th IHTC* **5**, 387–391. [10.4]
- Macdonald, I. F., El-Sayed, M. S., Mow, K. and Dullien, F. A. L. 1979 Flow through porous media: The Ergun equation revisited. *Ind. Chem. Fundam.* **18**, 199–208. [1.5.2]
- MacDonald, M. J., Chu, C. F., Guillot, P. P. and Ng, K. M. 1991 A generalized Blake-Kozeny equation for multisized spherical particles. *AICHE J.* **37**, 1583–1588. [1.4.2]
- Macedo, H. H., Costa, U. M. S. and Almeido, M. P. 2001 Turbulent effects on fluid flow through disordered porous media. *Physica A* **299**, 371–377. [1.8]
- Mackie, C. 2000 Thermal convection in a sparsely packed porous layer saturated with suspended particles. *Int. Comm. Heat Mass Transfer* **27**, 315–324. [6.23]
- Mackie, C., Desai, P. and Myers, C. 1999 Rayleigh-Bénard stability of a solidifying porous medium. *Int. J. Heat Mass Transfer* **42**, 3337–3350. [10.2.2]
- Madani, B., Tobin, F., Rigollet, F. and Tadrist, L. 2007 Flow laws in metallic foams: Experimental determination of inertial and viscous contributions. *J. Porous Media* **10**, 51–70. [1.5.3]
- Maerefat, M., Mahmoudi, S. Y. and Mazaheri, K. 2011 Numerical simulation of forced convection enhancement in a pipe by porous inserts. *Heat Transfer Engng.* **32**, 45–56. [4.11]
- Maghrebi, M. J., Nazari, M. and Armaghans, T. 2012 Forced convection heat transfer of nanofluids in a porous channel. *Transp. Porous Media* **93**, 401–413. [4.16.5]
- Magyari, E. 2006 Paradox of the Darcy free convection over vertical plate with prescribed inverse linear surface heat flux. *J. Porous Media* **9**, 663–670. [5.1.8]
- Magyari, E. 2011b Comment on “A novel analytical solution of mixed convection about an inclined flat plate embedded in a porous medium using the DTM-Pade” by M. M. Rashidi, N. Larraqi and S. M. Sadri, Int. J. Thermal Sciences 49 (2010) 2406–2412. *Int. J. Therm. Sci.* **50**, 1339–1342. [8.1.1]
- Magyari, E. 2012 Spontaneous breakdown of the definiteness in some convective heat transfer problems. *Transp. Porous Media* **92**, 527–539. [8.1.1]
- Magyari, E. 2009a Comment on “Combined forced and free convective flow in a vertical porous channel: The effects of viscous dissipation and pressure work” by A. Barletta and D. A. Nield, Transport in Porous Media. DOI 10.1007/s11242-008-9320-y. 2009. *Transp. Porous Media* **80**, 389–395. [8.3.2]

- Magyari, E. 2009b Further comments on “Combined forced and free convective flow in a vertical porous channel: The effects of viscous dissipation and pressure work”. *Transp. Porous Media* **80**, 399–400. [8.3.2]
- Magyari, E. 2010a Consequences of the transition invariance on the Darcy free convection flow past a vertical surface. *Transp. Porous Media* **85**, 757–769. [5.1.9.9]
- Magyari, E. 2010b The “butterfly effect” in a porous slab. *Transp. Porous Media* **84**, 711–715. [6.4]
- Magyari, E. 2010c The Vadasz-Olek model regarded as a system of coupled oscillators. *Transp. Porous Media* **85**, 415–435. [6.4]
- Magyari, E. 2011a Note on the “Scaling transformations for boundary layer flow near the stagnation point on a heated permeable stretching surface in a porous medium saturated with a nanofluid and heat generation/absorption effects.” *Transp. Porous Media* **87**, 41–48. [5.1.9.9]
- Magyari, E. 2011c Reply on the reply on the Note: “Scaling transformations for boundary layer flow near the stagnation point on a heated permeable stretching surface in a porous medium saturated with a nanofluid and heat generation/absorption effects.” *Transp. Porous Media* **87**, 53–56. [5.1.9.9]
- Magyari, E. and Aly, E. H. 2006a Exact analytical solution for a thermal boundary layer in a saturated porous medium . *Appl. Math. Lett.* **19**, 1351–1355. [8.1.6]
- Magyari, E. and Aly, E. H. 2006b Mechanical and thermal characteristics of a mixed convection boundary-layer flow in a saturated porous medium. *Int. J. Heat Mass Transfer* **49**, 3855–3865. [8.1.6]
- Magyari, E. and Keller, B. 2000 Exact analytic solutions for free convection boundary layers on a heated vertical plate with lateral mass flux embedded in a saturated porous medium. *Heat Mass Transfer* **36**, 109–116. [5.1.9.1]
- Magyari, E. and Keller, B. 2002 Note on ‘A two-equation analysis of convection heat transfer in porous media’ by H. Y. Zhang and X. Y. Huang. *Transport Porous Media* **46**, 109–112. [4.10]
- Magyari, E. and Keller, B. 2003a The opposing effect of viscous dissipation allows for a parallel free convection boundary-layer flow along a cold vertical flat plate. *Transport Porous Media* **51**, 227–230. [5.1.9.4]
- Magyari, E. and Keller, B. 2003b Effect of viscous dissipation on a quasi-parallel free convection boundary-layer flow over a vertical plate in a porous medium. *Transport Porous Media* **51**, 231–236. [5.1.9.4]
- Magyari, E. and Keller, B. 2003c Buoyancy sustained by viscous dissipation. *Transport Porous Media* **53**, 105–115. [5.9.4]
- Magyari, E. and Keller, B. 2004a The free convection boundary-layer flow induced in a fluid-saturated porous medium by a non-isothermal vertical cylinder approaches the shape of Schlichting’s round jet as the porous radius tends to zero. *Transport Porous Media* **54**, 265–271. [5.7]
- Magyari, E. and Keller, B. 2004b Backward free convection boundary layers in porous media. *Transport Porous Media* **55**, 285–300. [5.1.9.1]
- Magyari, E. and Pantokratoras, A. 2011 Note on the effect of thermal radiation in the linearized Rosseland approximation on the heat transfer characteristics of various boundary layer flows. *Int. Comm. Heat Mass Transfer* **38**, 554–556. [8.1.6]
- Magyari, E. and Postelnicu, A. 2011 Double-diffusive natural convection flows with thermosolutal symmetry in porous media in the presence of the Soret-Dufour effects. *Transp. Porous Media* **88**, 147–167. [9.6]
- Magyari, E. and Rees, D. A. S. 2005 Effect of viscous dissipation on the Darcy free convection boundary-layer flow over a vertical plate with exponential temperature distribution in a porous medium. *Fluid Dyn. Res.* (submitted). [5.1.9.4]
- Magyari, E. and Rees, D. A. S. 2006 Effect of viscous dissipation on the Darcy free convection boundary-layer flow over a vertical plate with exponential distribution in a porous medium. *Fluid Dyn. Res.* **38**, 405–429. [5.1.9.4]

- Magyari, E. and Rees, D. A. S. 2008 The Entrainment Theorem for the Darcy free convection over a permeable vertical plate. *Int. J. Therm. Sci.* **47**, 1123–1130. [5.1.9.9]
- Magyari, E., Pop, I. and Keller, B. 2001b Exact dual solutions occurring in the Darcy mixed convection flow. *Int. J. Heat Mass Transfer* **44**, 4563–4566. [8.1.1]
- Magyari, E., Pop, I. and Keller, B. 2002 The “missing” self-similar free convection boundary-layer flow over a vertical permeable surface in a porous medium. *Transport Porous Media* **46**, 91–102. [8.1.1]
- Magyari, E., Pop, I. and Keller, B. 2003a New similarity solutions for boundary-layer flow on a horizontal surface in a porous medium. *Transport Porous Media* **51**, 123–140. [8.1.2]
- Magyari, E., Pop, I. and Keller, B. 2003b Effect of viscous dissipation on the Darcy forced-convection flow past a plane surface. *J. Porous Media* **6**, 111–122. [4.1]
- Magyari, E., Pop, I. and Keller, B. 2003c New analytic solutions of a well-known boundary value problem in fluid mechanics. *Fluid Dyn. Res.* **33**, 313–317. [5.1.9.1]
- Magyari, E., Pop, I. and Keller, B. 2004 Analytical solutions for unsteady free convection in porous media. *J. Engng. Math.* **48**, 93–104. [5.1.9.1]
- Magyari, E., Keller, B. and Pop, I. 2001a Exact analytic solutions of forced convection flow in a porous medium. *Int. Comm. Heat Mass Transfer* **28**, 233–241. [4.1]
- Magyari, E., Pop, I. and Keller, B. 2005a Exact solutions for a longitudinal steady mixed convection flow over a permeable vertical thin cylinder in a porous medium. *Int. J. Heat Mass Transfer* **48**, 3435–3442. [8.1.3]
- Magyari, E., Pop, I. and Keller, B. 2006 Unsteady free convection along an infinite vertical flat plate embedded in a stably stratified fluid-saturated porous medium. *Transport Porous Media* **62**, 233–249. [8.1.6]
- Magyari, E., Pop, I. and Postelnicu, A. 2007a Effect of the source term on steady free convection boundary layer flows over a vertical plate in a porous medium. Part I. *Transport Porous Media* **67**, 49–67. [5.1.9.4]
- Magyari, E., Pop, I. and Postelnicu, A. 2007b Effect of the source term on steady free convection boundary layer flows over a vertical plate in a porous medium. Part II. *Transport Porous Media* **67**, 189–201. [5.1.9.4]
- Magyari, E., Rees, D. A. S. and Keller, B. 2005b Effect of viscous dissipation on the flow in fluid saturated porous media. *Handbook of Porous Media* (ed. K. Vafai), 2nd ed., Taylor and Francis, New York, pp. 373–406. [2.2.2, 5.1.9.4, 6.6]
- Maharaj, Y. and Govender, S. 2005 Effect of the Darcy-Prandtl number on the linear stability of stationary convection in rotating mushy layers. *J. Porous Media* **8**, 271–280. [10.2.3]
- Maharaj, Y. and Govender, S. 2005 Effects of the Darcy-Prandtl number on the linear stability of stationary convection in rotating mushy layers. *J. Porous Media* **8**, 271–280. [10.2.3]
- Mahdy, A. 2009 MHD non-Darcian free convection from a vertical wavy surface embedded in porous media. *Int. Comm. Heat Mass Transfer* **36**, 1067–107. [5.1.9.9]
- Mahdy, A. 2010 Effect of chemical reaction and heat generation or absorption on double-diffusive convection from a vertical truncated cone in porous media with variable viscosity. *Int. Comm. Heat Mass Transfer* **37**, 548–554. [9.6.1]
- Mahdy, A. and Chamkha, A. J. 2010 Chemical reaction and viscous dissipation effects on Darcy-Forchheimer mixed convection in a fluid saturated porous media. *Int. J. Numer. Meth. Heat Fluid Flow* **20**, 924–940. [9.6.1]
- Mahdy, A., Mohamed, R. A. and Hady, F. M. 2008 The influence of magnetic field on natural convection flow near a wavy cone in porous media. *Latin Amer. Appl. Res.* **38**, 155–160. [5.8]
- Mahidjiba, A., Mamou, M. and Vasseur, P. 2000a Onset of double-diffusive convection in a rectangular porous cavity subject to mixed boundary conditions. *Int. J. Heat Mass Transfer* **43**, 1505–1522. [9.1.3]
- Mahidjiba, A., Robillard, L. and Vasseur, P. 2002 The horizontal anisotropic porous layer saturated with water near 4 degrees C – A peculiar stability problem. *Heat Transfer 2002*, Proc. 12th Int. Heat Transfer Conf., Elsevier, Vol. 2, pp. 797–802. [6.11.4]

- Mahidjiba, A., Robillard, L. and Vasseur, P. 2003 Linear stability of cold water layer saturating an anisotropic porous medium — effect of confinement. *Int. J. Heat Mass Transfer* **46**, 323–332. [6.11.4]
- Mahidjiba, A., Robillard, L. and Vasseur, P. 2000b Onset of convection in a horizontal porous layer saturated with water near 4 degrees C. *Int. Comm. Heat Mass Transfer* **27**, 765–774. [6.11.4]
- Mahidjiba, A., Robillard, L. and Vasseur, P. 2006 Onset of penetrative convection of cold water in a porous layer under mixed boundary conditions. *Int. J. Heat Mass Transfer* **49**, 2820–2828. [6.20]
- Mahidjiba, A., Robillard, L., Vasseur, P. and Mamou, M. 2000c Onset of convection in an anisotropic porous layer of finite lateral extent. *Int. Comm. Heat Mass Transfer* **27**, 333–342. [6.12]
- Mahjoob, S. and Vafai, K. 2009 Analytical characterization of heat transport through biological media incorporating hyperthermia treatment. *Int. J. Heat Mass Transfer* **52**, 1608–1618. [2.6]
- Mahjoob, S. and Vafai, K. 2010 Analysis of bioheat transport through a dual layer biological media. *ASME J. Heat Transfer* **132**, #031101. [2.6]
- Mahjoob, S. and Vafai, K. 2011 Analysis of heat transfer in consecutive variable cross-sectional domains: Applications in biological media and thermal management. *ASME J. Heat Transfer* **133**, #011006. [2.6]
- Mahmoud, M. A. A. 2012 Numerical solution of free-convection heat transfer over a vertical cone embedded in a non-Newtonian power-law fluid-saturated porous medium with viscous dissipation. *ASCE J. Engng. Mech.* **138**, 555–559. [5.8]
- Mahmood, T. and Merkin, J. H. 1998 The convective boundary-layer flow on a reacting surface in a porous medium. *Transport Porous Media* **32**, 285–298. [3.4, 5.12.3]
- Mahmoud, A. A. and Megahed, A. I. M. 2006 Effects of suction and injection on MHD heat transfer in an electrically conducting fluid at a stretching vertical plate embedded in a porous medium with uniform free stream. *Nuovo Cimento Soc. Ital. Fis. B* **121**, 923–935. [5.1.9.9]
- Mahmoud, M. A. A. 2011 Variable viscosity effect on free convection of a non-Newtonian power-law fluid over a vertical cone in a porous medium with variable heat flux. *European Phys. J. Plus* **126**, #5 [5.8]
- Mahmoud, M. A. A. and Megahed, A. M. 2009 Variable thermal conductivity effect on MHD free-convection flow over a vertical full cone in a non-Newtonian saturated porous medium. *Nuovo Cimento Soc. Ital. Fis. B* **124**, 731–739. [5.8]
- Mahmoudi, Y. and Maerefat, M. 2011 Analytical investigation of heat transfer enhancement in a channel partially filled with a porous material under local thermal non-equilibrium condition. *Int. J. Therm. Sci.* **50**, 2386–2401. [4.11]
- Mahmud, M. N. and Hashim, I. 2010 Small and moderate Prandtl number chaotic convection in porous media in the presence of feedback control. *Transp. Porous Media* **84**, 421–440. [6.11.3]
- Mahmud, M. N. and Hashim, I. 2011 Small and moderate Vadasz number chaotic convection in porous media in the presence of non-Boussinesq effects and feedback control . *Phys. Lett. A* **375**, 2382–2393. [6.11.3]
- Mahmud, S. and Fraser, R. A. 2004a Flow and heat transfer inside porous stack: steady state problem. *Int. Comm. Heat Mass Transfer* **31**, 951–962. [4.9]
- Mahmud, S. and Fraser, R. A. 2004b Magnetohydrodynamic free convection and entropy generation in a square porous cavity. *Int. J. Heat Mass Transfer* **47**, 3245–3256. [7.1.6]
- Mahmud, S. and Fraser, R. A. 2005a Conjugate heat transfer inside a porous channel. *Heat Mass Transfer* **41**, 568–575. [4.12]
- Mahmud, S. and Fraser, R. A. 2005b Flow, thermal, and entropy characteristics inside a porous channel with viscous dissipation. *Int. J. Thermal Sci.* **44**, 21–32. [4.9]
- Mahmud, S. and Frazer, R. A. 2006 Vibration effect of heat transfer and entropy generation in an elliptic porous cavity. *Int. J. Numer. Meth. Heat Fluid Flow* **16**, 151–171. [7.5]
- Mahmud, S. and Pop, I. 2006 Mixed convection in a square vented enclosure filled with a porous medium. *Int. J. Heat Mass Transfer* **49**, 2190–2206. [8.4.3]

- Mahmud, S., Frazer, R. A. and Pop, I. 2007 Flow, thermal, energy transfer, and entropy generation characteristics inside wavy enclosures filled with microstructures. *ASME J. Heat Transfer* **129**, 1564–1575. [4.16.5]
- Maier, R. S., Kroll, D. M., Davis, H. T. and Bernard, R. S. 1998 Simulation of flow through bead packs using the lattice Boltzmann method. *Phys. Fluids* **10**, 60–74. [1.9]
- Majumdar, A. and Tien, C. L. 1990 Effects of surface tension on film condensation in a porous medium. *ASME J. Heat Transfer* **112**, 751–757. [10.4]
- Makinde, O. D. 2009a On MHD boundary-layer flow and mass transfer past a vertical plate in a porous medium with constant heat flux. *Int. J. Heat Fluid Flow* **19**, 546–554. [9.2.1]
- Makinde, O. D. 2011a MHD mixed-convection interaction with thermal radiation and  $n^{\text{th}}$  order chemical reaction past a vertical porous plate embedded in a porous medium. *Chem. Engng. Comm.* **198**, 590–608. [9.2.1]
- Makinde, O. D. 2011b On MHD mixed convection with Soret and Dufour effects past a vertical plate embedded in a porous medium. *Latin Amer. Appl. Res.* **41**, 63–68. [9.6.1]
- Makinde, O. D. 2012 Heat and mass transfer by MHD mixed convection stagnation point flow toward a vertical plate embedded in a highly porous medium with radiation and internal heat generation. *Meccanica* **47**, 1173–1184. [9.6.1]
- Makinde, O. D. and Aziz, A. 2010 MHD mixed convection from a vertical plate embedded in a porous medium with a convective boundary condition. *Int. J. Therm. Sci.* **49**, 1813–1820. [8.1.6]
- Makinde, O. D. and Moitsheki, R. J. 2008 On nonperturbative technique for thermal radiation effect on natural convection past a vertical plate embedded in a saturated porous medium. *Math. Probl. Engng.* #689074. [5.1.9.9]
- Makinde, O. D. and Sibande, P. 2008 Magnetohydrodynamic mixed-convective flow and heat and mass transfer past a vertical plate in a porous medium with constant wall suction. *ASME J. Heat Transfer* **130**, #112602. [9.2.1]
- Makuoka, T., Tsujioka, Y., Tanigawa, H. and Izaki, H. 1994b Natural convection in porous insulation layers containing a row of heat pipes. *Heat Transfer 1994* (Proc. 10th Int. Heat Transfer Conf. Brighton, UK), Inst. Chem. Engrs, Rugby, vol. 6, pp. 385–390. [6.13.2]
- Malashetty, M. S., Swamy, M. and Heera, R. 2008 Double diffusive convection in a porous layer using a thermal non-equilibrium model. *Int. J. Therm. Sci.* **47**, 1131–1147. [9.1.6.4]
- Malashetty, M. S., Swamy, M. and Heera, R. 2009c The onset of convection in a binary viscoelastic fluid saturated porous layer. *ZAMM* **89**, 356–369. [9.1.6.4]
- Malashetty, M. S., Swamy, M. and Sidram, W. 2010b Thermal convection in a rotating viscoelastic fluid saturated porous layer. *Int. J. Heat Mass Transfer* **53**, 5747–5756. [9.1.6.4]
- Malashetty, M. S., Swamy, M. and Sidram, W. 2011 Double diffusive convection in a rotating anisotropic porous layer saturated with a viscoelastic fluid. *Int. J. Therm. Sci.* **50**, 1757–1769. [9.1.6.4]
- Malashetty, M. S., Tan, W. C. and Swamy, M. 2009e The onset of double diffusive convection in a binary viscoelastic fluid saturated anisotropic porous layer. *Phys. Fluids* **21**, #084101. [9.1.6.4]
- Malashetty, M. S. and Basavaraja, D. 2002 Rayleigh-Bénard convection subject to time dependent wall temperature/gravity in a fluid-saturated anisotropic porous medium. *Heat Mass Transfer* **38**, 551–563. [6.11.3]
- Malashetty, M. S. and Basavaraja, D. 2003 Effect of thermal/gravity modulation on the onset of convection in a horizontal anisotropic porous layer. *Int. J. Appl. Mech. Engng.* **8**, 425–439. [6.24]
- Malashetty, M. S. and Basavaraja, D. 2004 Effect of time-periodic boundary temperatures on the onset of double diffusive convection in a horizontal anisotropic porous layer. *Int. J. Heat Mass Transfer* **47**, 2317–2327. [9.1.6.4]
- Malashetty, M. S. and Begum, I. 2011a The effect of rotation on the double diffusive convection in a sparsely packed anisotropic porous layer. *Transp. Porous Media* **88**, 315–345. [9.1.6.4]

- Malashetty, M. S. and Begum, I. 2011b Effect of thermal/gravity modulation on the onset of convection in a Maxwell fluid saturated porous layer, *Transp. Porous Media* **90**, 889–909. [6.24]
- Malashetty, M. S. and Gaikwad, S. N. 2003 Onset of convective instabilities in a binary liquid mixtures with fast chemical reactions in a porous media. *Heat Mass Transfer* **39**, 415–420. [9.1.6.4]
- Malashetty, M. S. and Heera, R. 2008a Linear and nonlinear double diffusive convection in a rotating porous layer using a thermal nonequilibrium model. *Int. J. Nonlinear Mech.* **43**, 600–621. [9.1.6.4]
- Malashetty, M. S. and Heera, R. 2008b The effect of rotation on the onset of double diffusive convection in a horizontal anisotropic porous layer. *Transp. Porous Media* **74**, 105–127. [9.1.6.4]
- Malashetty, M. S. and Heera, R. 2009 The onset of double diffusive convection in a sparsely packed porous layer using a thermal non-equilibrium model. *Acta Mech.* **204**, 1–20. [9.1.6.4]
- Malashetty, M. S. and Kollur, P. 2011 The onset of double diffusive convection in a couple stress fluid saturated anisotropic porous layer. *Transp. Porous Media* **86**, 465–489. [9.1.6.4]
- Malashetty, M. S. and Kulkarni, S. 2009 The convective instability of Maxwell-fluid-saturated porous layer using a thermal non-equilibrium model. *J. Non-Newtonian Fluid Mech.* **162**, 29–37. [6.23]
- Malashetty, M. S. and Padmavathi, V. 1997 Effect of gravity modulation on onset of convection in a fluid and porous layer. *Int. J. Engng. Sci.* **35**, 829–840. [6.24]
- Malashetty, M. S. and Padmavathi, V. 1998 Effect of gravity modulation on the onset of convection in a porous layer. *J. Porous Media* **1**, 219–226. [6.24]
- Malashetty, M. S. and Swamy, M. 2007a Combined effect of thermal modulation and rotation on the onset of stationary convection in a porous layer. *Transp. Porous Media* **69**, 313–330. [6.22]
- Malashetty, M. S. and Swamy, M. 2007b Effect of temperature modulation on the onset of stationary convection in a rotating sparsely packed porous layer. *Canad. J. Phys.* **85**, 927–945. [6.22]
- Malashetty, M. S. and Swamy, M. 2007c The effect of rotation on the onset of convection in a horizontal anisotropic porous layer. *Int. J. Therm. Sci.* **46**, 1023–1032. [6.22]
- Malashetty, M. S. and Swamy, M. 2007d The onset of convection in a viscoelastic liquid saturated anisotropic porous layer. *Transp. Porous Media* **67**, 203–218. [6.23]
- Malashetty, M. S. and Swamy, M. 2010a Effect of rotation on the onset of thermal convection in a sparsely packed porous layer using a thermal non-equilibrium model. *Int. J. Heat Mass Transfer* **53**, 3088–3101. [6.22]
- Malashetty, M. S. and Swamy, M. 2010b The onset of convection in a binary fluid saturated anisotropic porous layer. *Int. J. Therm. Sci.* **49**, 867–878. [9.1.6.4]
- Malashetty, M. S. and Wadi, V. S. 1999 Rayleigh-Bénard convection subject to time-dependent wall temperature in a fluid saturated porous layer. *Fluid Dyn. Res.* **24**, 293–308. [6.11.3]
- Malashetty, M. S., Cheng, P. and Chao, B. H. 1994 Convective instability in a horizontal porous layer saturated with a chemically reacting fluid. *Int. J. Heat Mass Transfer* **37**, 2901–2908. [6.11.2]
- Malashetty, M. S., Hill, A. A. and Swamy, M. 2012 Double diffusive convection in a viscoelastic fluid-saturated porous layer using a thermal non-equilibrium model. *Acta Mech.* **223**, 967–983. [9.1.6.4]
- Malashetty, M. S., Pal, D. and Kollur, P. 2010 Double-diffusive convection in a Darcy porous medium saturated with a couple-stress fluid. *Fluid Dyn. Res.* **42**, #035502. [9.1.6.4]
- Malashetty, M. S., Pop, I. and Heera, R. 2009a Linear and nonlinear double diffusive convection in a rotating sparsely packed porous layer using a thermal non-equilibrium model. *Contin. Mech. Thermodyn.* **21**, 317–339. [9.1.6.4]
- Malashetty, M. S., Shivakumara, I. S. and Kulkarni, S. 2005a The onset of convection in an anisotropic porous layer using a thermal non-equilibrium model. *Transport Porous Media* **60**, 199–215. [6.5]

- Malashetty, M. S., Shivakumara, I. S. and Kulkarni, S. 2005b The onset of Lapwood-Brinkman convection using a non-equilibrium model. *Int. J. Heat Mass Transfer* **48**, 1155–1163. [6.5]
- Malashetty, M. S., Shivakumara, I. S. and Kulkarni, S. 2009b The onset of convection in a couple-stress fluid saturated porous layer using a thermal non-equilibrium model. *Phys. Lett. A* **373**, 781–790. [6.23]
- Malashetty, M. S., Shivakumara, I. S., Kulkarni, S. and Swamy, M. 2006a Convective instability of Oldroyd-B fluid saturated porous layer heated from below using a thermal non-equilibrium model. *Transp. Porous Media* **64**, 123–139. [6.23]
- Malashetty, M. S., Siddheshwar, P. G. and Swamy, M. 2006b The effect of thermal modulation on the onset of convection in a viscoelastic fluid saturated porous layer. *Transport Porous Media* **62**, 55–79. [6.23]
- Malashetty, M. S., Swamy, M. and Kulkarni, S. 2007 Thermal convection in a rotating porous layer using a thermal nonequilibrium model. *Phys. Fluids* **19**, #054102. [6.22]
- Malashetty, M. S., Swamy, M. S. 2011 Double-diffusive convection in a rotating anisotropic porous layer saturated with a viscoelastic fluid. *Int. J. Therm. Sci.* **50**, 1757–1769. [9.1.6.4]
- Malashetty, M. S., Umavathi, J. C. and Kumar, J. P. 2005 Flow and heat transfer in an inclined channel containing fluid layer sandwiched between two porous layers. *J. Porous Media* **8**, 443–453. [8.4.1]
- Malashetty, M. S., Umavathi, J. C. and Pratap Kumar, J. 2001 Convective flow and heat transfer in an inclined composite porous medium. *J. Porous Media* **4**, 15–22. [7.8]
- Malashetty, M. S., Umavathi, J. C. and Pratap Kumar, J. 2004 Two fluid flow and heat transfer in an inclined channel containing porous and fluid layer. *Heat Mass Transfer* **40**, 871–876. [7.8]
- Malkovski, V. I. and Pek, A. A. 1999 Onset conditions of free thermal convection of a single-phase fluid in a horizontal porous layer with depth-dependent permeability. *Fizika Zemli* (12): 27–31. [6.13.1]
- Malkovsky, V. I. and Pek, A. A. 2004 Onset of thermal convection of a single-phase fluid in an open vertical fault. *Izv. Phys. Solid Earth* **40**, 672–679. [6.2]
- Mamou, M. 2002a Stability analysis of thermosolutal convection in a vertical packed porous enclosure. *Phys. Fluids* **14**, 4302–4314. [9.1.6.4]
- Mamou, M. 2002b Stability analysis of double-diffusive convection in porous enclosures. In *Transport Phenomena in Porous Media II* (D. B. Ingham and I. Pop, eds.) Elsevier, Oxford, pp. 113–154. [9]
- Mamou, M. 2003 Stability analysis of the perturbed rest state and of the finite amplitude steady double-diffusive convection in a shallow porous enclosure. *Int. J. Heat Mass Transfer* **46**, 2263–2277. [9.1.3]
- Mamou, M. 2004 Onset of oscillatory and stationary double-diffusive convection within a tilted porous enclosure. In *Emerging Technologies and Techniques in Porous Media* (D. B. Ingham, A. Bejan, E. Mamut and I. Pop, eds), Kluwer Academic, Dordrecht, pp. 209–219. [9.4].
- Mamou, M. and Vasseur, P. 1999 Thermosolutal bifurcation phenomena in porous enclosures subject to vertical temperature and concentration gradients. *J. Fluid Mech.* **395**, 61–87. [9.1.3]
- Mamou, M., Hasnaoui, M., Amahmid, A. and Vasseur, P. 1998a Stability analysis of double diffusive convection in a vertical Brinkman porous enclosure. *Int. Comm. Heat Mass Transfer* **25**, 491–500. [9.2.2]
- Mamou, M., Mahidjiba, A., Vasseur, P. and Robillard, L. 1998b Onset of convection in an anisotropic porous medium heated from below by a constant heat flux. *Int. Comm. Heat Mass Transfer* **25**, 799–808. [6.12]
- Mamou, M., Robillard, L. and Vasseur, P. 1999 Thermoconvective instability in a horizontal porous cavity saturated with cold water. *Int. J. Heat Mass Transfer* **42**, 4487–4500. [6.11.4]
- Mamou, M., Robillard, L., Bilgen, E. and Vasseur, P. 1996 Effects of a moving thermal wave on Bénard convection in a horizontal saturated porous layer. *Int. J. Heat Mass Transfer* **39**, 347–354. [6.11.3]
- Mamou, M., Vasseur, P. and Bilgen, E. 1995a Multiple solutions for double-diffusive convection in a vertical porous enclosure. *Int. J. Heat Mass Transfer* **38**, 1787–1798. [9.2.4]

- Mamou, M., Vasseur, P. and Bilgen, E. 1998c A Galerkin finite-element study of the onset of double-diffusive convection in an inclined porous enclosure. *Int. J. Heat Mass Transfer* **41**, 1513–1529. [9.4]
- Mamou, M., Vasseur, P. and Bilgen, E. 1998d Double-diffusive convection instability in a vertical porous enclosure. *J. Fluid Mech.* **368**, 263–289. [9.2.4]
- Mamou, M., Vasseur, P., Bilgen, E. and Gobin, D. 1994 Double-diffusive convection in a shallow porous layer. *Heat Transfer* 1994, Inst. Chem. Engrs, Rugby, vol. 5, pp. 339–344. [9.1.3]
- Mamou, M., Vasseur, P., Bilgen, E. and Gobin, D. 1995b Double-diffusive convection in an inclined slot filled with porous medium. *Eur. J. Mech. B/Fluids* **14**, 629–652. [9.2.4]
- Mamun, M. A. H., Islam, M. T. and Rahman, M. M. 2010b Natural convection in a porous trapezoidal enclosure with magneto-hydrodynamic effect. *Nonlinear Anal. Control Model. Control* **15**, 159–184. [7.3.7]
- Mandy, A. 2010 Soret and Dufour effect on double diffusion mixed convection from a vertical surface in a porous medium saturated with a non-Newtonian fluid. *J. Non-newtonian Fluid Mech.* **165**, 568–575. [9.6.1]
- Mandy, A., Chamkha, A. J. and Baba, Y. 2010 Double-diffusive convection with variable viscosity from a vertical truncated cone in porous media in the presence of magnetic and radiation effects. *Comput. Math. Appl.* **59**, 3867–3878. [9.4]
- Manole, D. M. and Lage, J. L. 1993 The inertial effect on the natural convection flow within a fluid saturated porous medium. *Int. J. Heat Fluid Flow* **14**, 376–384. [1.5.2]
- Manole, D. M. and Lage, J. L. 1995 Numerical simulation of supercritical Hadley circulation, within a porous layer, induced by inclined temperature gradients. *Int. J. Heat Mass Transfer* **38**, 25–83.2593. [7.9]
- Manole, D. M., Lage, J. L. and Antohe, B. V. 1995 Supercritical Hadley circulation within a layer of fluid saturated porous medium: bifurcation to traveling wave. *ASME HTD* **309**, 23–29. [7.9]
- Manole, D. M., Lage, J. L. and Nield, D. D. 1994 Convection induced by inclined thermal and solutal gradients, with horizontal mass flow, in a shallow horizontal layer of a porous medium. *Int. J. Heat Mass Transfer* **37**, 2047–2057. [9.5]
- Mansour, A., Amahmid, A. and Hasnaoui, M. 2008 Soret effect on thermosolutal convection developed in a horizontal shallow porous layer salted from below and subject to cross fluxes of heat. *Int. J. Heat Fluid Flow* **29**, 306–314. [9.5]
- Mansour, A., Amahmid, A., Hasnaoui, M. and Bourich, M. 2004 Soret effect on double-diffusive multiple solutions in a square porous cavity subject to cross gradients of temperature and concentration. *Int. Comm. Heat Mass Transfer* **31**, 431–440. [9.5]
- Mansour, A., Amahmid, A., Hasnaoui, M. and Bourich, M. 2006 Multiplicity of solutions induced by thermosolutal convection in a square porous cavity heated from below and submitted to a horizontal concentration gradient in the presence of the Soret effect. *Numer. Heat Transfer A* **49**, 69–94. [9.5]
- Mansour, A., Amahmid, A., Hasnaoui, M. and Mamou, M. 2007 Onset of thermosolutal convection in a shallow layer heated and salted from below and subject to a horizontal heat flux balanced by a Soret mass flux. *Int. J. Heat Mass Transfer* **50**, 2148–2160. [9.5]
- Mansour, M. A. 1997 Forced convection radiation interaction heat transfer in boundary layer over a flat plate submersed in a porous medium. *Appl. Mech. Engng.* **2**, 405–413. [4.16.5]
- Mansour, M. A. and El-Shaer, N. A. 2001 Radiative effects on magnetohydrodynamic natural convection flows saturated in porous media. *J. Magn. Magn. Mater.* **237**, 327–341. [5.1.9.4]
- Mansour, M. A. and Gorla, R. S. R. 1998 Mixed convection-radiation in power-law fluids along a nonisothermal wedge embedded in a porous medium. *Transport Porous Media* **30**, 113–124. [8.1.4]
- Mansour, M. A. and Gorla, R. S. R. 2000a Thermal dispersion effects on non-Darcy natural convection with internal heat generation. *Chem. Engng. Commun.* **177**, 177–181. [5.1.9.4]
- Mansour, M. A. and Gorla, R. S. R. 2000b Combined convection in non-Newtonian fluids along a nonisothermal vertical plate in a porous medium. *Int. J. Numer. Meth. Heat Fluid Flow* **10**, 163–178. [8.1.1]

- Mansour, M. A. and Gorla, R. S. R. 2000c Radiative and thermal dispersion effects on non-Darcy natural convection. *J. Porous Media* **3**, 267–272. [5.1.9.4]
- Mansour, M. A., Abd-Elaziz, M.M. and Mohamed, R. A. 2011a Unsteady natural convection, heat and mass transfer in inclined triangular porous enclosures in the presence of heat source or sink: Effect of sinusoidal variation of boundary conditions. *Transp. Porous Media* **87**, 7–23. [9.4]
- Mansour, M. A., Chamkha, A. J., Mohamed, R. A., Abd El-Aqziz, M. M. and Ahmed, S. E. 2010a MHD natural convection in an inclined cavity filled with a fluid saturated porous medium with heat source in the solid phase. *Nonlinear Anal. Mod. Control.* **15**, 55–70. [7.8]
- Mansour, M. A., El-Anssary, N. F. and Aly, A. 2008 Effects of chemical reaction and thermal stratification on MHD free convection heat and mass transfer over a vertical stretching surface embedded in a porous media considering Soret and Dufour numbers. *Chem. Engng. J.* **145**, 340–345. [9.2.1]
- Mansour, M. A., El-Anssary, N. F., Aly, A. and Gorla, R. S. R. 2010b Chemical reaction and magnetohydrodynamic effects on free convection flow past an inclined surface in a porous medium. *J. Porous Media* **13**, 87–96. [5.3]
- Mansour, M. A., El-Aziz, M. M. A., Mohamed, R. A. and Ahmed, S. E. 2011b Numerical simulation of natural convection in wavy porous cavities under the influence of thermal radiation using a thermal non-equilibrium model. *Transp. Porous Media* **86**, 615–630. [7.3.7]
- Mansour, M. A., El-Hakiem, M. A. and El-Gaid, S. A. 1997 Mixed convection in non-Newtonian fluids along an isothermal vertical cylinder in a porous medium. *Transport Porous Media* **28**, 307–317. [8.1.3]
- Mansour, M. and El-Shaer, N. 2004 Mixed convection-radiation in power-law fluids along a non-isothermal wedge in a porous medium with variable permeability. *Transport Porous Media* **57**, 333–346. [8.1.4]
- Marafie, A. and Vafai, K. 2001 Analysis of non-Darcian effects on temperature differentials in porous media. *Int. J. Heat Mass Transfer* **44**, 4401–4411. [4.10]
- Marafie, A., Khanafer, K. and Al-Azimi, B. 2008 Non-Darcian effects on the mixed convection heat transfer for a metallic porous block with a confined slot jet. *Numer. Heat Transfer A* **54**, 665–685. [8.4.2]
- Marafie, A., Khanafer, K. and Pop, I. 2010 Non-Darcian effects on buoyancy-induced heat transfer in a partially divided square enclosure with internal heat generation. *Transp. Porous Media* **84**, 663–683. [7.3.8]
- Marcondes, F., de Medeiros, J. M., and Gurgel, J. M. 2001 Numerical analysis of natural convection in cavities with variable porosity. *Numer. Heat Transfer A* **40**, 403–420. [7.6.2]
- Marcoux, M. and Charrier-Mojtabi, M. C. 1998 Etude paramétrique de la thermogravitation en milieu poreux. *C. R. Acad. Sci., Paris* **326**, 539–546. [9.1.4]
- Marcoux, M., Charrier-Mojtabi, M. C. and Azaiez, M. 1999b Double-diffusive convection in an annular vertical porous layer. *Int. J. Heat Mass Transfer* **42**, 2313–2325. [9.4]
- Marcoux, M., Charrier-Mojtabi, M. C. and Bergeon, A. 1998 Naissance de la thermogravitation dans un mélange binaire imprégnant un milieu poreux. *Entropie* **214**, 31–36. [9.1.4]
- Marcoux, M., Karimi-Fard, M. and Charrier-Mojtabi, M. C. 1999a Onset of double-diffusive convection in a rectangular porous cavity submitted to heat and mass fluxes at the vertical walls. *Int. J. Thermal Sci.* **38**, 258–266. [9.2.4]
- Marpu, D. R. 1993 Non-Darcy flow and axial conduction effects of forced convection in porous material filled pipes. *Wärme- Stoffübertrag.* **29**, 51–58. [4.9]
- Marpu, D. R. 1995 Forchheimer and Brinkman extended Darcy flow model on natural convection in a vertical cylindrical porous annulus. *Acta Mech.* **109**, 41–48. [7.3.3]
- Marpu, D. R. and Satyamurty, V. V. 1989 Influence of variable fluid density on free convection in rectangular porous media. *ASME J. Energy Res. Tech.* **111**, 214–220. [6.15.3]
- Martínez-Suástegui, L., Trevino, C. and Méndez, F. 2003 Natural convection in a vertical strip immersed in a porous medium. *Europ. J. Mech. B/ Fluids* **22**, 5454–553. [7.1.5]

- Martins-Costa, M. L. 1996 A local model for a packed-bed heat exchanger with a multiphase matrix. *Int. Comm. Heat Mass Transfer* **23**, 1133–1142. [2.6]
- Martins-Costa, M. L. and Saldanha da Gama, R.M. 1994 Local model for the heat transfer process in two distinct flow regions. *Int. J. Heat Fluid Flow* **15**, 477–485. [2.6]
- Martins-Costa, M. L., Sampaio, R. and Saldanha da Gama, R.M. 1992 Modelling and simulation of energy transfer in a saturated flow through a porous medium. *Appl. Math. Model.* **16**, 589–597. [2.6]
- Martins-Costa, M. L., Sampaio, R. and Saldanha da Gama, R.M. 1994 Modeling and simulation of natural convection flow in a saturated porous cavity. *Meccanica* **29**, 1–13. [2.6]
- Martys, N., Bentz, D. P. and Garboczi, E. J. 1994 Computer simulation study of the effective viscosity in Brinkman equation. *Phys. Fluids* **6**, 1434–1439. [1.5.3]
- Marvel, R. L. and Lai, F. C. 2010a Homogeneous anisotropic model for natural convection in nonuniform layered porous cavities. *J. Thermophys. Heat Transfer* **24**, 331–339. [7.3.2]
- Marvel, R. L. and Lai, F. C. 2010b Natural convection from a porous cavity with sublayers of nonuniform thickness: A lumped parameter analysis. *ASME J. Heat Transfer* **132**, #032602. [7.3.2]
- Marys, N. S. 2001 Improved approximation of the Brinkman equation using a lattice Boltzmann method. *Phys. Fluids* **13**, 1807–1810. [1.5.3]
- Masoud, S. A., Al-Nimr, M. A. and Alkam, M. K. 2000 Transient film condensation on a vertical plate imbedded in porous medium. *Transport Porous Media* **40**, 345–354. [10.4]
- Massarotti, N., Nithiarasu, P. and Zienkiewicz, O. C. 2001 Natural convection in porous medium-fluid interface problems — A finite element analysis by using the CBS procedure. *Int. J. Numer. Meth. Heat Fluid Flow* **11**, 473–490. [6.19.1]
- Massmann, G., Simmons, C., Love, A., Ward, J. and James-Smith, J. 2006 On the variable density surface water-groundwater interaction: a theoretical analysis of mixed convection in a stably-stratified fresh surface water saline groundwater discharge zone. *J. Hydrol.* **329**, 390–402. [11.8]
- Masuda, Y., Yoneda, M., Ikeshoji, T., Kimura, S., Alavyoon, F., Tsukada, T. and Hozawa, M. 2002 Oscillatory double-diffusive convection in a porous enclosure due to opposing heat and mass fluxes on the vertical walls. *Int. J. Heat Mass Transfer* **45**, 1365–1369. [9.1.6.4]
- Masuda, Y., Yoneda, M., Sumi, S., Kimura, S. and Alavyoon, F. 1999 Double-diffusive natural convection in a porous medium under constant heat and mass fluxes. *Heat Transfer Asian Res.* **28**, 255–265. [9.1.6.4]
- Masuda, Y., Yoneya, M., Suzuki, A. and Alavyoon, F. 2008 Numerical analysis of double-diffusive convection in a porous enclosure due to opposing heat and mass fluxes on the vertical walls. Why does peculiar oscillation occur? *Int. J. Heat Mass Transfer* **51**, 383–388. [9.2.2]
- Masuda, Y., Yoneya, M., Suzuki, A., Kimura, S. and Alavyoon, F. 2010 Numerical analysis of re-oscillation and non-centrosymmetric convection in a porous enclosure due to opposing heat and mass fluxes on the vertical walls. *Int. Comm. Heat Mass Transfer* **37**, 250–255. [9.2.2]
- Masuoka, T. 1986 Natural convection in stratified porous media heated from the side.(In Japanese) *Trans. ASME B* **52**, 866–869. [7.3.2]
- Masuoka, T. and Takatsu, Y. 1996 Turbulence model for flow through porous media. *Int. J. Heat Mass Transfer* **39**, 2803–2809. [1.8]
- Masuoka, T. and Takatsu, Y. 2002 Turbulence characteristics in porous media. In *Transport Phenomena in Porous Media II* (D. B. Ingham and I. Pop, eds.) Elsevier, Oxford, pp. 231–256. [1.8]
- Masuoka, T., Kakimoto, Y., Nomura, A. and Ooba, M. 2004 Fluid flow through a permeable porous obstacle. In *Applications of Porous Media (ICAPM 2004)*, (eds. A. H. Reis and A. F. Miguel), Évora, Portugal, pp. 107–112. [4.11]
- Masuoka, T., Nishimura, T., Kawamoto, S. and Tsuruta, T. 1991 Effects of mid-height cooling on natural convection in a porous layer heated from below. Proc. ASME, JSME Thermal Engineering Joint Conference — 1991, vol. 4, pp. 325–330. [6.13.2]

- Masuoka, T., Shibata, K., Nakumura, H., Tanaka, T. and Tsuruta, T. 1988 Natural convection in porous insulation layers with peripheral gaps. Proc. 2nd Symposium on Heat Transfer, Tsinghua Univ. Beijing, China. [6.13.2]
- Masuoka, T., Takatsu, Y., Kawamoto, S., Koshino, H. and Tsuruta, T. 1995b Buoyant plume through a permeable porous layer located above a line heat source in an infinite fluid space. *JSME Int. J., Series B* **38**, 79–85. [5.10.1.2]
- Masuoka, T., Takatsu, Y., Tsuruta, T. and Nakamura, H. 1994 Buoyancy-driven channeling flow in vertical porous layer. *JSME Int. J., Series B* **37**, 915–923. [7.7]
- Masuoka, T., Tanigawa, H., Tsuruta, T. and Izaki, H. 1995a Studies on the improvement of the performances of insulation layers with isothermal screens. Proc. 3rd. ASME/JSME Thermal Engineering Joint Conference, vol.3, pp. 333–338. [6.13.2]
- Masuoka, T., Tohda, Y., Tsurota, Y. and Yasuda, Y. 1986 Buoyant plume above a concentrated heat source in stratified porous media (in Japanese). *Trans JSME Ser. B* , 2656–2662. [5.10.2]
- Masuoka, T., Yokote, Y. and Katsuhara, T. 1981 Heat transfer by natural convection in a vertical porous layer. *Bull. JSME* **24**, 995–1001. [7.1.2]
- Mat, M. D. and Illegbusi, O. J. 2002 Application of a hybrid model of mushy zone to macrosegregation in alloy solidification. *Int. J. Heat Mass Transfer* **45**, 279–289. [10.2.3]
- Matsumoto, K., Okada, M., Murakami, M. and Yabushita, Y. 1993 Solidification of porous medium saturated with aqueous solution in a rectangular cell. *Int. J. Heat Mass Transfer* **36**, 2869–2880. [10.2.3]
- Matsumoto, K., Okada, M., Murakami, M. and Yabushita, Y. 1995 Solidification of porous medium saturated with aqueous solution in a rectangular cell — II. *Int. J. Heat Mass Transfer* **38**, 2935–2943. [10.2.3]
- Mauran, S., Riguad, L. and Coudeville, O. 2001 Application of the Carman-Kozeny correlation to a high porosity and anisotropic consolidated medium: The compressed expanded natural graphite. *Transport Porous Media* **43**, 355–376. [1.4.2]
- Maxwell, J. C. 2004 *A Treatise on Electricity and Magnetism*, 2<sup>nd</sup> ed., Oxford University Press, Cambridge. [3.8]
- Mbaye, M. and Bilgen, E. 1992 Natural convection and conduction in porous wall, solar collector systems with porous absorber. *ASME J. Solar Engng.*, **114**, 41–46. [7.3.1]
- Mbaye, M. and Bilgen, E. 1993 Conduction and convection heat transfer in composite solar collector systems with porous absorber. *Wärme-Stoffübertrag.* **28**, 267–274. [7.3.1]
- Mbaye, M. and Bilgen, E. 2001 Subcritical oscillatory instability in porous beds. *Int. J. Thermal Sci.* **40**, 595–602. [9.1.3]
- Mbaye, M. and Bilgen, E. 2006 Natural convection in composite systems with phase change materials. *Heat Mass Transfer* **42**, 636–644. [10.5]
- Mbaye, M., Bilgen, E. and Vasseur, P. 1993 Natural-convection heat transfer in an inclined porous layer boarded by a finite-thickness wall. *Int. J. Heat Fluid Flow* **14**, 284–291. [7.8]
- McCarthy, J. F. 1994 Flow through arrays of cylinders: lattice gas cellular automata simulations. *Phys. Fluids* **6**, 435–437. [2.6]
- McGuinness, M. J. 1996 Steady solution selection and existence in geothermal heat pipes — I. The convective case. *Int. J. Heat Mass Transfer* **39**, 259–274. [11.9.2]
- McGuinness, M. J., Blakely, M., Pruess, K. and O'Sullivan, M. J. 1993 Geothermal heat pipe stability: solution selection by upstreaming and boundary conditions. *Transport in Porous Media* **11**, 71–100. [11.9.2]
- Mchirgui, A., Hidouri, N., Magherbi, M. and Ben Brahim, A. 2012 Entropy generation in double diffusive convection in a square porous cavity using Darcy-Brinkman formulation. *Transp. Porous Media* **93**, 223–240. [9.2.2]
- McKay, G. 1992 Patterned ground formation and solar radiation ground heating. *Proc. Roy. Soc. Lond. A* **438**, 249–263. [11.2]
- McKay, G. 1996 Patterned ground formation and convection in porous media with phase change. *Contin. Mech. Thermodyn.* **8**, 189–199. [11.2]

- McKay, G. 1998a Onset of buoyancy-driven convection in superposed reacting fluid and porous layers. *J. Engng. Math.* **33**, 31–46. [6.19.1]
- McKay, G. 1998b Onset of double-diffusive convection in a saturated porous layer with time-periodic surface heating. *Cont. Mech. Thermodyn.* **10**, 241–251. [9.1.6.4]
- McKay, G. 2000 Double-diffusive convective motions for a saturated porous layer subject to a modulated surface heating. *Cont. Mech. Thermodyn.* **12**, 69–78. [9.1.6.4]
- McKay, G. and Straughan, B. 1991 The influence of a cubic density law on patterned ground formation. *Math. Models Meth. Appl. Sci.* **1**, 27–39. [11.2]
- McKay, G. and Straughan, B. 1993 Patterned ground formation under water. *Continuum Mech. Thermodyn.* **5**, 145–162. [11.2]
- McKibbin, R. 1983 Convection in an aquifer above a layer of heated impermeable rock. *N. Z. J. Sci.* **26**, 49–64. [6.13.1]
- McKibbin, R. 1985 Thermal convection in layered and anisotropic porous media: a review. *Convective Flows in Porous Media* (eds. R. A. Wooding and I. White), Dept. Sci. Indust. Res., Wellington, New Zealand, pp. 113–127. [6.12]
- McKibbin, R. 1986a Thermal convection in a porous layer: effects of anisotropy and surface boundary conditions. *Transport in Porous Media* **1**, 271–292. [6.12]
- McKibbin, R. 1986b Heat transfer in a vertically-layered porous medium heated from below. *Transport in Porous Media* **1**, 361–370. [6.13.4]
- McKibbin, R. 1998 Mathematical models for heat and mass transport in geothermal systems. *Transport Phenomena in Porous Media* (eds. D. B. Ingham and I. Pop), Elsevier, Oxford, pp. 131–154. [11]
- McKibbin, R. 2005 Modeling heat and mass transport processes in geothermal systems. *Handbook of Porous Media* (ed. K. Vafai), 2nd ed., Taylor and Francis, New York, pp. 545–571. [11]
- McKibbin, R. 2009 Weak 2D convective plumes in a sloping porous layer. *Transp. Porous Media* **77**, 229–242. [7.8]
- McKibbin, R. 2012 Instability in sloping layered warm-water aquifers. *AIP Conf. Proc.* **1453**, 257–26. [7.8]
- McKibbin, R. and O'Sullivan, M. J. 1980 Onset of convection in a layered porous medium heated from below. *J. Fluid Mech.* **96**, 375–393. [6.13.2]
- McKibbin, R. and O'Sullivan, M. J. 1981 Heat transfer in a layered porous medium heated from below. *J. Fluid Mech.* **111**, 141–173. [6.13.2]
- McKibbin, R. and Tyvand, P. A. 1982 Anisotropic modelling of thermal convection in multilayered porous media. *J. Fluid Mech.* **118**, 315–319. [6.13.3]
- McKibbin, R. and Tyvand, P. A. 1983 Thermal convection in a porous medium composed of alternating thick and thin layers. *Int. J. Heat Mass Transfer* **26**, 761–780. [6.13.3]
- McKibbin, R. and Tyvand, P. A. 1984 Thermal convection in a porous medium with horizontal cracks. *Int. J. Heat Mass Transfer* **27**, 1007–1023. [6.13.3, 6.13.4]
- McKibbin, R., Hale, N., Style, R. W. and Walters, N. 2011 Convection and heat transfer in layered sloping, warm-water aquifers. *J. Porous Media* **14**, 329–343. [7.8]
- McKibbin, R., Tyvand, P. A. and Palm, E. 1984 On the recirculation of fluid in a porous layer heated from below. *N. Z. J. Sci.* **27**, 1–13. [6.12]
- McLellan, J. G., Oliver, N. H. S., Hobbs, B. E. and Rowland, J. V. 2010 Modelling fluid convection stability in continental faulted rifts with applications to the Taupo Volcanic Zone, New Zealand. *J. Vulcan. Geotherm. Res.* , 109–122. [11.8]
- McNabb, A. 1965 On convection in a porous medium. Proc. 2nd Australasian Conf. Hydraulics and Fluid Mech., University of Auckland, pp. C161–171. [5.12.3]
- Mealey, L. and Merkin, J. H. 2008 Free convection boundary layers on a vertical surface in a heat-generating porous medium. *IMA J. Appl. Math.* **73**, 231–253. [5.1.9.4]
- Mealey, L.R. and Merkin, J. H. 2009 Steady finite Rayleigh number convective flows in a porous medium with internal heat generation. *Int. J. Therm. Sci.* **48**, 1068–1080. [6.11.2]
- Medina, A., Luna, E., Perez-Rosales, C. and Higuera, F. J. 2002 Thermal convection in tilted porous fractures. *J. Phys. Condensed Matter* **14**, 2467–2474. [7.8]

- Mehmood, A. 2008 Analytical solution of three-dimensional viscous flow and heat transfer over a stretching flat surface by homotopy analysis method. *ASME J. Heat Transfer* **130**, #121701. [5.2]
- Mehmood, A., Ali, A. and Mahmood, T. 2010 Unsteady magnetohydrodynamic oscillatory flow and heat transfer analysis of a viscous fluid in a porous channel filled with a saturated porous medium. *J. Porous Media* **13**, 573–577. [4.16.2]
- Mehravian, R., Keane, M. and Flemings, M. C. 1970 Interdendritic fluid flow and macrosegregation: influence of gravity. *Metall. Trans. B* **1**, 1209–1220. [10.2.3]
- Mehta, K. N. and Nandakumar, K. 1987 Natural convection with combined heat and mass transfer buoyancy effects in non-homogeneous porous medium. *Int. J. Heat Mass Transfer* **30**, 2651–2656. [9.2.2]
- Mehta, K. N. and Rao, K. N. 1994 Buoyancy induced flow of non-Newtonian fluids over a non-isothermal horizontal plate embedded in a porous medium. *Int. J. Engng Sci.* **32**, 521–525. [5.2]
- Mehta, K. N. and Sood, S. 1992a Transient free convective flow about a non-isothermal vertical flat plate immersed in a saturated inhomogeneous porous medium. *Int. Comm. Heat Mass Transfer* **19**, 687–699. [5.1.3]
- Mehta, K. N. and Sood, S. 1992b Transient free convective flow with temperature dependent viscosity in a fluid saturated porous medium. *Int. J. Engng Sci.* **30**, 1083–1087. [5.1.9.9]
- Mehta, K. N. and Sood, S. 1994 Free convection about axisymmetric bodies immersed in inhomogeneous porous medium. *Int. J. Engng Sci.* **32**, 945–953. [5.9]
- Mei, C. C., Auriault, J. L. and Ng, C. O. 1996 Some applications of the homogenization theory. *Adv. Appl. Mech.* **32**, 278–348. [1.4.4]
- Mejni, F. and Ouarzazi, M. N. 2009 Global instabilities in inhomogeneous mixed convection flows in semi-infinite porous media. *Mech. Res. Comm.* **76**, 260–264. [6.10.1]
- Melnikov, D. E. and Shevtsova, V. M. 2011 Separation of a binary liquid mixture in compound system: *Fluid-porous-fluid*. *Acta Astronaut.* **69**, 381–386. [9.4]
- Memari, M., Golmakan, A. and Dehkordi, A. M. 2011 Mixed convection flow of nanofluids and regular fluids in vertical porous media with viscous heating. *Industr. Engng. Chem. Res.* **50**, 9403–9414. [9.7]
- Méndez, F., Luna, E., Treviño, C. and Pop, I. 2004 Asymptotic and numerical transient analysis of the free convection cooling of a vertical plate embedded in a porous medium. *Heat Mass Transfer* **40**, 593–602. [5.1.5]
- Méndez, F., Treviño, C., Pop, I. and Liñán, A. 2002 Conjugate free convection along a thin vertical plate with internal heat generation in a porous medium. *Heat Mass Transfer* **38**, 631–638. [7.1.5]
- Mercier, J. F., Weisman, C., Firdaouss, M. and le Quéré, P. 2002 Heat transfer associated to natural convection flow in a partly porous cavity. *ASME J. Heat Transfer* **124**, 130–143. [7.7]
- Merkin, J. H. 1978 Free convection boundary layers in a saturated porous medium with lateral mass flux. *Int. J. Heat Mass Transfer* **21**, 1499–1504. [5.1.2, 5.5.1]
- Merkin, J. H. 1979 Free convection boundary layers on axisymmetric and two-dimensional bodies of arbitrary shape in a saturated porous medium. *Int. J. Heat Mass Transfer* **22**, 1461–1462. [5.5.1, 5.6.1, 5.9]
- Merkin, J. H. 1980 Mixed convection boundary layer flow on a vertical surface in a saturated porous medium. *J. Engng. Math.* **14**, 301–313. [8.1.1]
- Merkin, J. H. 1985 On dual solutions occurring in mixed convection in a porous medium. *J. Engng. Math.* **20**, 171–179. [8.1]
- Merkin, J. H. 1986 Free convection from a vertical cylinder embedded in a saturated porous medium. *J. Acta Mech.* **62**, 19–28. [5.7]
- Merkin, J. H. 2008 Free convective boundary-layer flow in a heat-generating porous medium: Similarity solutions. *Q. J. Mech. Appl. Math.* **61**, 205–218. [5.1.9.4]
- Merkin, J. H. 2009 Natural convective boundary-layer flow in a heat generating porous medium with prescribed wall heat flux. *ZAMP* **60**, 543–564. [5.1.9.4]
- Merkin, J. H. 2012 Natural convective boundary layer flow in a heat generating porous medium with a constant surface heat flux. *European J. Mech. B* **36**, 75–81. [5.1.4]

- Merkin, J. H. and Kumaran, V. 2011 Free convection stagnation-point boundary-layer flow in a porous medium with a density maximum. *Int. J. Therm. Sci.* **50**, 2176–2183. [5.1.9.9]
- Merkin, J. H. and Mahmood, T. 1998 Convective flows on reactive surfaces in porous media. *Transport Porous Media* **33**, 279–293. [3.4, 5.12.3]
- Merkin, J. H. and Needham, D. J. 1987 The natural convection flow above a heated wall in a saturated porous medium. *Q. J. Mech. Appl. Math.* **40**, 559–574. [5.1.9.9]
- Merkin, J. H. and Pop, I. 1987 Mixed convection boundary layer on a vertical cylinder embedded in a porous medium. *Acta Mech.* **66**, 251–262. [8.1.3]
- Merkin, J. H. and Pop, I. 1989 Free convection above a horizontal circular disk in a saturated porous medium. *Wärme-Stoffübertrag.* **24**, 53–60. [5.12.3]
- Merkin, J. H. and Pop, I. 1997 Mixed convection on a horizontal surface embedded in a porous medium: the structure of a singularity. *Transport Porous Media* **29**, 355–364. [8.1.2]
- Merkin, J. H. and Pop, I. 2000 Free convection near a stagnation point in a porous medium resulting from an oscillatory wall temperature. *Int. J. Heat Mass Transfer* **43**, 611–621. [5.5.1]
- Merkin, J. H. and Pop, I. 2010 Natural convection boundary-layer flow in a porous medium with temperature-dependent boundary conditions. *Transp. Porous Media* **85**, 397–414. [5.1.9.9]
- Merkin, J. H. and Zhang, G. 1990a On the similarity solutions for free convection in a saturated porous medium adjacent to impermeable horizontal boundaries. *Wärme-Stoffübertrag.* **25**, 179–184. [5.2]
- Merkin, J. H. and Zhang, G. 1990b Free convection in a horizontal porous layer with a partly heated wall. *J. Engng Math.* **24**, 125–149. [6.18]
- Merkin, J. H. and Zhang, G. 1992 Boundary-layer flow past a suddenly heated vertical surface in a saturated porous medium. *Wärme-Stoffübertrag.* **27**, 299–304. [5.1.3]
- Merkin, J. H., Pop, I., Rohni, A. M. and Ahmad, S. 2012 A further note on the unsteady mixed convection boundary layer in a porous medium with temperature slip: An exact solution. *Transp. Porous Media* **95**, to appear. [8.1.1]
- Merkin, J. H., Rohni, A. M., Amad, S. and Pop, I. 2012 On the temperature slip boundary condition in a mixed convection boundary-layer flow in a porous medium. *Transp. Porous Media* **94**, 133–147. [8.1.6]
- Merrikh, A. A. and Lage, J. L. 2005 From continuum to porous continuum: The visual resolution impact on modeling natural convection in heterogeneous media. In *Transport Phenomena in Porous Media III*, (eds. D. B. Ingham and I. Pop), Elsevier, Oxford, pp. 60–96. [2.2.1]
- Merrikh, A. A. and Mohamad, A. A. 2000 Transient natural convection in differentially heated porous enclosures. *J. Porous Media* **3**, 165–17. (erratum 4, 195). [7.5]
- Merrikh, A. A. and Mohamad, A. A. 2002 Non-Darcy effects in buoyancy driven flows in an enclosure filled with vertically layered porous media. *Int. J. Heat Mass Transfer* **45**, 4305–4313. [7.3.2]
- Merrikh, A. A., Lage, J. L. and Mohamad, A. A. 2002 Comparison between pore-level and porous medium models for natural convection in a nonhomogeneous enclosure. *AMS Contemp. Math.* **295**, 387–396. [2.2.1]
- Merrikh, A. A., Lage, J. L. and Mohamad, A. A. 2005a Natural convection in an enclosure with disconnected and conducting solid blocks. *Int. J. Heat Mass Transfer* **46**, 1361–1372. [2.2.1]
- Merrikh, A. A., Lage, J. L. and Mohamad, A. A. 2005b Natural convection in non-homogeneous heat generating media: Comparison of continuum and porous-continuum models. *J. Porous Media* **8**, 149–163. [2.2.3]
- Mharzi, M., Daguenet, M. and Daoudi, S. 2000 Thermosolutal natural convection in a vertically layered fluid-porous medium heated from the side. *Energy Conv. Management* **41**, 1065–1090. [9.2.2]
- Mhimid, A., Ben Nasrallah, S. and Fohr, J. P. 2000 Heat and mass transfer during drying of granular products — simulation with convective and conductive boundary conditions. *Int. J. Heat Mass Transfer* **43**, 2779–2791. [3.6]
- Mhimid, A., Fohr, J. P. and Ben Nasrallah, S. 1999 Heat and mass transfer during drying of granular products by combined convection and conduction. *Drying Tech.* **17**, 1043–1063. [3.6]

- Michael, K., Arnot, M., Cook, P., Ennis-King, J., Funnell, R., Kaldi, J., Kirtse, D., Paterson, L., Gale, J., Herzog, H., and Braithwaite, J. 2009 CO<sub>2</sub> storage in saline aquifers I — current state of scientific knowledge. *Greenhouse Gas Control Tech.* **9**, 3197–3204. [11.11]
- Miglio, E., Quarteroni, A. and Saleri, F. 2003 Coupling of free surface and groundwater flows. *Compt. Fluids* **32**, 73–83. [1.6]
- Mihoubli, D. and Bellagi, A. 2009 Drying induced stresses using convective and combined microwave and convective drying of saturated porous media. *Drying Tech.* **27**, 851–856. [3.6]
- Milne, J. E. and Butler, S. L. 2007 A numerical investigation of the effects of compositional and thermal buoyancy on transient plumes in a porous layer. *J. Porous Media* **10**, 151–173. [9.2.3]
- Min, J. Y. and Kim, S. J. 2005 A novel methodology for thermal analysis of a composite system consisting of a porous medium and an adjacent fluid layer. *ASME J. Heat Transfer* **127**, 648–656. [1.6, 2.4]
- Minkowycz, W. J. and Cheng, P. 1976 Free convection about a vertical cylinder embedded in a porous medium. *Int. J. Heat Mass Transfer* **19**, 805–813. [5.7]
- Minkowycz, W. J. and Cheng, P. 1982 Local non-similar solutions for free convective flow with uniform lateral mass flux in a porous medium. *Lett. Heat Mass Transfer* **9**, 159–168. [5.1.2]
- Minkowycz, W. J. and Haji-Sheikh, A. 2006 Heat transfer in parallel plates and circular porous passages with axial conduction. *Int. J. Heat Mass Transfer* **49**, 2381–239. [4.9]
- Minkowycz, W. J. and Haji-Sheikh, A. 2009 Asymptotic behaviour of heat transfer in porous passages with axial conduction. *Int. J. Heat Mass Transfer* **52**, 3101–3108. [4.9]
- Minkowycz, W. J., Cheng, P. and Chang, C. H. 1985a Mixed convection about non-isothermal cylinders and spheres in a porous medium. *Numer. Heat Transfer* **8**, 349–359. [8.1.3]
- Minkowycz, W. J., Cheng, P. and Hirschberg, R. N. 1984 Non-similar boundary layer analysis of mixed convection about a horizontal heated surface in a fluid-saturated porous medium. *Int. Comm. Heat Mass Transfer* **11**, 127–141. [8.1.2]
- Minkowycz, W. J., Cheng, P. and Moalem, F. 1985b Effect of surface mass transfer on buoyancy-induced Darcian flow adjacent to a horizontal heated surface. *Int. Comm. Heat Mass Transfer* **12**, 55–65. [5.2]
- Minkowycz, W. J., Haji-Sheikh, A. and Vafai, K. 1999 On departure from local thermal equilibrium in porous media due to rapidly changing heat source: the Sparrow number. *Int. J. Heat Mass Transfer* **42**, 3373–3385. [4.10]
- Minto, B. J., Ingham, D. B. and Pop, I. 1998 Free convection driven by an exothermic reaction on vertical surface embedded in porous media. *Int. J. Heat Mass Transfer* **41**, 11–23. [5.1.9.9]
- Miranda, B. M. D. and Anand, N. K. 2004 Convective heat transfer in a channel with porous baffles. *Numer. Heat Transfer A* **46**, 425–452. [4.11]
- Mishra, A. K., Paul, T. and Singh, A. K. 2002 Mixed convection flow in a porous medium bounded by two vertical walls. *Forch. Ingen.* **67**, 198–205. [8.3.1]
- Misirlioglu, A. 2006 The effect of rotating cylinder on the heat transfer in a square cavity filled with porous medium. *Int. J. Engng. Sci.* **44**, 1173–1187. [8.4.3]
- Misirlioglu, A. 2007 Thermally developing forced convection inside a parallel-plate channel filled with a non-Darcy porous medium. *J. Porous Media* **10**, 311–317. [4.13]
- Misirlioglu, A., Baytas, A. C. and Pop, I. 2005 Free convection in a wavy cavity filled with a porous medium. *Int. J. Heat Mass Transfer* **48**, 1840–1850. [7.3.7]
- Misirlioglu, A., Baytas, A. C. and Pop, I. 2006a Free convection in a wavy cavity filled with heat-generating porous media. *J. Porous Media* **9**, 207–222. [7.3.7]
- Misirlioglu, A., Baytas, A. C. and Pop, I. 2006b Natural convection inside an inclined wavy enclosure filled with a porous medium. *Transp. Porous Media* **64**, 229–246. [7.3.7]
- Misra, D. and Sarkar, A. 1995 A comparative study of porous media models in a differentially heated square cavity using a finite element method. *Int. J. Numer. Meth. Heat Fluid Flow* **5**, 735–752. [7.6.2]
- Mitrovic, J. and Maletić, R. 2006 b Heat transfer with laminar forced convection in a porous channel exposed to a thermal asymmetry. *Int. J. Heat Mass Transfer* **50**, 1106–1121. [4.9]

- Mitrovic, J. and Maletic, R. 2006a Effect of thermal asymmetry on laminar forced convection heat transfer in a porous annular channel. *Chem. Engng. Tech.* **29**, 750–760. [4.9]
- Mittal, R. and Rana, U. S. 2009 Effect of dust particles on a layer of micropolar ferromagnetic fluid heated from below saturating a porous medium. *Appl. Math. Comput.* **215**, 2591–2607. [6.21]
- Miyauchi, H., Kataoka, H. and Kikuchi, T. 1976 Gas film coefficients of mass transfer in low Péclet number region for sphere packed beds. *Chem. Engng. Sci.* **31**, 9–13. [2.2.3]
- Mobedi, M., Cekmer, O. and Pop, I. 2010 Forced convection heat transfer inside an anisotropic porous channel with oblique principal axes: Effect of viscous dissipation. *Int. J. Therm. Sci.* **49**, 1984–1993. [4.16.5]
- Modather, M., Abdou, M. and El-Kabeir, S. M. M. 2007 Magnetohydrodynamics and radiative effects on free convection flow of fluid with variable viscosity from a vertical plate through a porous medium. *J. Porous Media* **10**, 503–514.
- Moghaddam, R. N., Rostami, B., Pourafshary, P. and Fallahzadeh, Y. 2012 Quantification of density-driven natural convection for dissolution mechanism in CO<sub>2</sub> sequestration. *Transp. Porous Media* **92**, 439–456. [11.11]
- Moghari, M. 2008 A numerical study of non-equilibrium convective heat transfer in porous media. *J. Enhanced Heat Transfer* **18**, 81–99. [4.10]
- Moghimi, M. A., Talbizadeh, P. and Mehrabian, M. A. 2011 Heat generation/absorption effects on magneto-hydrodynamic natural convection flow over a sphere in a non-Darcian porous medium. *Proc. Inst. Mech. Engrs. E* **225**, 29–39. [5.6.1]
- Mohais, R. and Bhatt, B. 2009 Heat transfer of coupled fluid flow within a channel with a permeable base. *ASME J. Heat Transfer* **131**, #112601. [4.11]
- Mohamad, A. A. and Sezai, I. 2002 Effect of lateral aspect ratio on three-dimensional double diffusive convection in porous enclosures with opposing temperature and concentration gradients. *Heat Transfer Research* **33**, 318–325. [9.2.2]
- Mohamad, A. A. 2000 Nonequilibrium natural convection in a differentially heated cavity filled with a saturated porous matrix. *ASME J. Heat Transfer* **122**, 380–384. [7.6.2]
- Mohamad, A. A. 2001 Natural convection from a vertical plate in a saturated porous medium: nonequilibrium theory. *J. Porous Media* **4**, 181–186. [5.1.9.3]
- Mohamad, A. A. and Bennacer, R. 2001 Natural convection in a confined saturated porous medium with horizontal temperature and vertical solutal gradients. *Int. J. Thermal Sci.* **40**, 82–93. [9.5]
- Mohamad, A. A. and Bennacer, R. 2002 Double diffusion, natural convection in an enclosure filled with saturated porous medium subjected to cross-gradients: stably stratified fluid. *Int. J. Heat Mass Transfer* **45**, 3725–3740. [9.5]
- Mohamad, A. A. and Karim, G. A. 2001 Flow and heat transfer with segregated beds of solid particles. *J. Porous Media* **4**, 215–224. [4.6.4]
- Mohamad, A. A. and Rees, D. A. S. 2004 Conjugate free convection in a porous medium attached to a wall held at a constant temperature. In Applications of Porous Media (ICAPM 2004), (eds. A. H. Reis and A. F. Miguel), Évora, Portugal, pp. 93–97. [7.1.5]
- Mohamad, A. A., Bennacer, R. and Azaiez, J. 2004 Double-diffusion natural convection in a rectangular enclosure filled with binary fluid saturated porous media: the effect of lateral aspect ratio. *Phys. Fluids* **16**, 184–199. [9.1.3]
- Mohamed, R. A. and Abo-Dahab, S. M. 2009 The influence of chemical reaction and thermal radiation in the heat and mass transfer in MHD microplar flow over a vertical moving porous plate in a porous medium with heat generation. *Int. J. Therm. Sci.* **48**, 1800–1813. [5.1.9.4s]
- Mohamed, R. A., Abo-Dahab, S. M. and Nafal, T. A. 2010 Thermal radiation and MHD effects on free convective flow in a polar fluid through a porous medium in the presence of internal heat generation and chemical reaction. *Math. Prob. Engng.* #804719. [5.1.9.4]
- Mohammedain, A. A. and Al Shear, N. A. 2011 Heat transfer in boundary layer flow past a curved surface in a saturated porous medium with variable permeability. *J. Porous Media* **14**, 265–271. [9.2.1]

- Mohammadien, A. A., Mansour, M. A., Abd el Gaied, S. M. and Gorla, R. S. R. 1998 Radiative effect on natural convection flows in porous media. *Transport Porous Media* **32**, 263–283. [5.1.9.4]
- Mohammadien, A. A. and El-Amin, M. F. 2000 Thermal dispersion-radiation effects on non-Darcy natural convection in a fluid saturated porous medium. *Transport Porous Media* **40**, 153–163. [5.1.9.4]
- Mohammadien, A. A. and El-Amin, M. F. 2001 Thermal radiation effects on power-law fluids over a horizontal plate embedded in a porous medium. *Int. Comm. Heat Mass Transfer* **27**, 1025–1035. [5.2]
- Mohammadien, A. A. and El-Shaer, N. A. 2004 Influence of variable permeability on combined free and forced convection past a semi-infinite vertical plate in a saturated porous medium. *Heat Mass Transfer* **40**, 341–346. [8.1.1]
- Mojtabi, A. 2002 Influence of vibrations on the onset of thermo-convection in porous medium. Proc. 1st Int. Conf. Applications of Porous Media, 704–721. [6.24]
- Mojtabi, A. and Charrier-Mojtabi, M. C. 1992 Analytic solution of steady natural convection in an annular porous medium evaluated with a symbolic algebra code. *ASME J. Heat Transfer* **114**, 1065–1068. [7.3.3]
- Mojtabi, A. and Charrier-Mojtabi, M. C. 2000 Double-diffusive convection in porous media. Handbook of Porous Media (K. Vafai, ed.), Marcel Dekker, New York., pp. 559–603. [3.3, 9]
- Mojtabi, A. and Charrier-Mojtabi, M. C. 2005 Double-diffusive convection in porous media. Handbook of Porous Media (K. Vafai, ed.), 2nd ed., Taylor and Francis, New York., pp. 269–320. [3.3, 9]
- Mojtabi, A. and Rees, D. A. S. 2011 The effect of conducting bounding plates on the onset of Horton-Rogers-Lapwood convection. *Int. J. Heat Mass Transfer* **54**, 293–305. [6.2]
- Mojtabi, A., Charrier-Mojtabi, M. C., Maliwan, K. and Pedramrazi, Y. 2004 Active control of the onset of convection in a porous medium. In Emerging Technologies and Techniques in Porous Media (D. B. Ingham, A. Bejan, E. Mamut and I. Pop, eds), Kluwer Academic, Dordrecht, pp. 195–207. [6.24]
- Montillet, A. 2004 Flow through a finite packed bed of spheres: A note on the limit of applicability of the Forchheimer-type equation. *ASME J. Fluids Engng.* **126**, 139–143. [1.5.2]
- Moraga, N. O., Sanchez, G. C. and Riquelme, J. A. 2010 Unsteady mixed convection in a vented enclosure partially filled with two non-Darcian porous layers. *Numer. Heat Transfer A* **57**, 473–495. [8.4.1]
- Morega, A. M. and Bejan, A. 1994 Heatline visualization of convection in porous media. *Int. J. Heat Fluid Flow* **15**, 42–47. [4.17]
- Morega, A. M., Bejan, A. and Lee, S. W. 1995 Free stream cooling of a stack of parallel plates. *Int. J. Heat Mass Transfer* **38**, 519–531. [4.15]
- Moreno, R. M. and Tao, Y. X. 2006 Thermal and flow performance of a microconvective heat sink with three-dimensional constructal channel configuration. *J. Heat Transfer* **128**, 740–751. [4.19]
- Morland, L. W., Zebib, A. and Kassoy, D. R. 1977 Variable property effects on the onset of convection in an elastic porous matrix. *Phys. Fluids* **20**, 1255–1259. [6.7]
- Mosaad, M. 1999 Natural convection in a porous medium coupled across an impermeable vertical wall with film condensation. *Heat Mass Transfer* **35**, 177–183. [10.4]
- Mosaad, M. 2012 Conjugate heat transfer between free convection in porous medium and forced convection. *J. Porous Media* **15**, 477–484. [7.7]
- Mota, J. P. B., Esteves, A. A. C., Portugal, C. A. M., Esperança, J. M. S. S. and Saatdjain, E. 2000 Natural convection heat transfer in horizontal eccentric elliptic annuli containing saturated porous media. *Int. J. Heat Mass Transfer* **43**, 4367–4379. [7.3.3]
- Moukalled, F. and Darwiche, M. 2010 Natural convection heat transfer in a porous rhombic annulus. *Numer. Heat Transfer A* **58**, 101–124. [7.3.7]
- Moutsopoulos, K. N. and Koch, D. L. 1999 Hydrodynamic and boundary-layer dispersion in bidisperse porous media. *J. Fluid Mech.* **385**, 359–379. [4.16.4]

- Moya, R. E. S., Prata, A. T. and Cunha Neto, J. A. B. 1999 Experimental analysis of unsteady heat and moisture transfer around a heated cylinder buried in a porous medium. *Int. J. Heat Mass Transfer* **42**, 2187–2198. [3.6]
- Moya, S. L., Ramos, E. and Sen, M. 1987 Numerical study of natural convection in a tilted rectangular porous material. *Int. J. Heat Mass Transfer* **30**, 741–756. [7.8]
- Muasovi, S. M. and Shahnazari, M. R. 2008 Investigation of natural convection in a vertical cavity filled with anisotropic porous layer. *Iranian J. Chem. Chem. Engng.* **27**, 39–45. [9.2.2]
- Muhaimin, I., Kandaswamy, R. and Hashim, I. 2009a Thermophoresis and chemical reaction effects on non-Darcy MHD mixed convective heat and mass transfer past a porous wedge in presence of variable stream condition. *Chem. Engng. Res. Design* **87**, 1527–1535. [9.2.1]
- Muhaimin, I., Kandaswamy, R. and Khamis, A. B. 2009b Numerical investigation of variable viscosities and thermal stratification effects on MHD mixed convective heat and mass transfer past a porous wedge in the presence of a chemical reaction. *Appl. Math. Mech.- English Ed.* **30**, 1353–1364. [9.6.1]
- Muhaimin, I., Kandaswamy, R. and Khamis, A. B. 2010a Thermophoresis and chemical reaction effects on MHD mixed convective heat and mass transfer past a porous wedge in presence of suction. *Latin Amer. Appl. Res.* **40**, 153–159. [9.6.1]
- Muhaimin, I., Kandaswamy, R., Hashim, I. and Khamis, A. B. 2010b Local nonsimilarity solution on MHD convective heat transfer flow past a porous wedge in the presence of suction/injection. *J. Porous Media* **13**, 487–495. [5.3]
- Mukhopadhyay, S. 2008 Natural convection flow on a sphere through porous medium in presence of heat source/sink near a stagnation point. *Math. Model. Anal.* **13**, 513–520. [5.6.1]
- Mukhopadhyay, S. 2009 Effect of thermal radiation on unsteady mixed convection flow and heat transfer over a porous stretching surface in porous medium. *Int. J. Heat Mass Transfer* **52**, 3261–3265. [8.1.6]
- Mukhopadhyay, S. and Layek, C. C. 2009 Radiation effect on forced convective flow and heat transfer over a porous plate in a porous medium. *Mecanica* **44**, 587–597. [4.7]
- Mullis, A. M. 1995 Natural convection in porous, permeable media & sheets, wedges and lenses. *Marine Petrol. Geol.* , 17–25. [11.8.2]
- Mulone, G. and Straughan, B. 2006 An operative method to obtain necessary and sufficient stability conditions for double diffusive convection in porous media. *ZAMM* **86**, 507–520. [9.1.3]
- Muralidhar, K. 1989 Mixed convection flow in a saturated porous annulus. *Int. J. Heat Mass Transfer* **32**, 881–888. [8.2.3, 8.3.3]
- Muralidhar, K. 1992 Study of heat transfer from buried nuclear waste canisters. *Int. J. Heat Mass Transfer* **35**, 3493–3495. [7.11]
- Muralidhar, K. 1993 Near-field solution for heat and mass transfer from buried nuclear waste canisters. *Int. J. Heat Mass Transfer* **36**, 2665–2674. [7.11]
- Muralidhar, K. and Misra, D. 1997 Determination of dispersion coefficients in a porous medium using the frequency response method. *Expt. Heat Transfer* **10**, 109–118. [2.2.4]
- Muralidhar, K. and Suzuki, K. 2001 Analysis of flow and heat transfer in a regenerator mesh using a non-Darcy thermally non-equilibrium model. *Int. J. Heat Mass Transfer* **44**, 2493–2504. [4.10]
- Muralidhar, K., Bauchalk, R.A. and Kulacki, F.A. 1986 Natural convection in a horizontal porous annulus with a step distribution in permeability. *ASME J. Heat Transfer* **108**, 889–893. [7.3.3]
- Murata, K. 1995 Heat and mass transfer with condensation in a fibrous insulation slab bounded on one side by a cold surface. *Int. J. Heat Mass Transfer* **38**, 3253–3262. [10.4]
- Murdoch, A. and Soliman, A. 1999 On the slip-boundary condition for liquid flow over planar boundaries. *Proc. Roy. Soc. Lond. A.* **455**, 1315–1340. [1.6]
- Murphy, H. D. 1979 Convective instabilities in vertical fractures and faults. *J. Geophys. Res.* **84**, 6121–6130. [6.15.2]
- Murray, B. T. and Chen, C. F. 1989 Double-diffusive convection in a porous medium. *J. Fluid Mech.* **201**, 147–166. [9.1.3]
- Murthy, P. V. S. N. 1998 Thermal dispersion and viscous dissipation effects on a non-Darcy mixed convection in a saturated porous medium. *Heat Mass Transfer* **33**, 295–300. [8.1.1]

- Murthy, P. V. S. N. 2000 Effect of double dispersion on mixed convection heat and mass transfer in non-Darcy porous medium. *ASME J. Heat Transfer* **122**, 476–484. [9.2.1]
- Murthy, P. V. S. N. 2001 Effect of viscous dissipation on mixed convection in a non-Darcy porous medium. *J. Porous Media* **4**, 23–32. [8.1.1]
- Murthy, P. V. S. N. and Singh, P. 1997a Effects of viscous dissipation on a non-Darcy natural convection regime. *Int. J. Heat Mass Transfer* **40**, 1251–1260. [5.1.9.4]
- Murthy, P. V. S. N. and Singh, P. 1997b Thermal dispersion effects on non-Darcy natural convection with lateral mass flux. *Heat Mass Transfer* **33**, 1–5. [8.1.1]
- Murthy, P. V. S. N. and Singh, P. 1997c Thermal dispersion effects on non-Darcy natural convection over horizontal plate with surface mass flux. *Arch. Appl. Mech.* **67**, 487–495. [8.1.2]
- Murthy, P. V. S. N. and Singh, P. 1999 Heat and mass transfer by natural convection in a non-Darcy porous medium. *Acta Mech.* **138**, 243–254. [9.2.1]
- Murthy, P. V. S. N. and Singh, P. 2000 Thermal dispersion effects on non-Darcy convection over a cone. *Comp. Math. Appl.* **40**, 1433–1444. [8.1.4]
- Murthy, P. V. S. N., Mukherjee, S., Srinivasacharya, D. and Krishna, P. V. S. S. R. 2004a Combined radiation and mixed convection from a vertical wall with suction/injection in a non-Darcy porous medium. *Acta Mech.* **168**, 145–156. [8.1.1]
- Murthy, P. V. S. N., Partha, M. K. and Sekhar, G. P. R. 2005 Mixed convection heat and mass transfer with thermal radiation in a non-Darcy porous medium. *J. Porous Media* **8**, 541–549. [9.6.1]
- Murthy, P. V. S. N., Ratish Kumar, B. V. and Singh, P. 1997 Natural convection from a horizontal wavy surface in a porous enclosure. *Numer. Heat Transfer* **31**, 207–221. [6.15.3]
- Murthy, P. V. S. N., Srinivasacharya, D. and Krishna, P. V. S. S. R. 2004b Effect of double stratification on free convection in a Darcian porous medium. *ASME J. Heat Transfer* **126**, 297–300. [9.2.1]
- Murthy, S. V. S. S. N. V. G. K., Ratish Kumar, B. V. , Sangwan, V., Nigam, M. and Chandara, P. P. 2010a Non-Darcy mixed convection in a porous square enclosure under suction/injection effects with non-isothermal wall. *Numer. Heat Transfer A* **57**, 580–602. [8.4.3]
- Murthy, S. V. S. S. N. V. G. K., Ratish Kumar, B. V. , Sangwan, V., Nigam, M. and Chandara, P. P. 2010b Non-Darcy mixed convection in a fluid saturated square enclosure under suction effect: Part II. *J. Porous Media* **13**, 799–805. [8.4.3]
- Murty, V. D., Camden, M. P., Clay, C. L. and Paul, D. B. 1989 Natural convection in porous media between concentric and eccentric cylinders. *AIChE Sympos. Ser.* **269**, 96–101. [7.6.2]
- Murty, V. D., Camden, M. P., Clay, C. L. and Paul, D. B. 1990 A study of non-Darcian effects on forced convection heat transfer over a cylinder embedded in a porous medium. *Heat Transfer* 1990, Hemisphere, Washington, DC, vol. 5, pp. 201–206. [4.3]
- Murty, V. D., Clay, C. L., Camden, M. P. and Paul, D. B. 1994 Natural convection around a cylinder buried in a porous medium — non-Darcian effects. *Appl. Math. Modell.* **18**, 134–141. [7.11]
- Murugesan, K., Lo, D. C., Young, D. L., Chen, C. W. and Fan, C. M. 2008 Convective drying analysis of three-dimensional porous solid by mass lumping finite element technique. *Heat Mass Transfer* **44**, 401–412. [3.6]
- Muthamilselvan, M. and Das, M. K. 2012 Double diffusion in a porous cavity near its density maximum. *J. Porous Media* **15**, 765–774. [9.1.6.4]
- Muthamilselvan, M., Das, M. K. and Kandaswamy, P. 2010 Convection in a lid-driven heat generating porous cavity with alternative thermal boundary conditions. *Transp. Porous Media* **82**, 337–346. [6.17]
- Muthuraj, R. and Srinivas, S. 2010 Mixed convective heat and mass transfer in a vertical wavy channel with traveling thermal waves and porous medium. *Comput. Math. Appl.* **59**, 3516–3528. [9.6.2]
- Na, T. Y. and Pop, I. 1996 A note to the solution of Cheng-Minkowycz equation arising in free convection in porous media. *Int. Comm. Heat Mass Transfer* **23**, 697–703. [5.1.9.9]
- Na, T. Y. and Pop, I. 1999 A note to the solution of Cheng-Chang equation arising in free convection in porous media. *Int. Comm. Heat Transfer* **26**, 145–151. [5.2]

- Naakteboren, C., Krueger, P. S. and Lage, J. L. 2012 Inlet and outlet pressure-drop effects on the determination of permeability and form coefficient of a porous medium. *ASME J. Fluids Engng.* **134**, 051209. [1.5.2]
- Nabovati, A. and Amon, C. H. 2012 Hydrodynamic boundary conditions at open-porous interface: A pore-level lattice Boltzmann study. *Transp. Porous Media*, to appear. [1.6]
- Naidu, S. V., Dharma Rao, V., Sarma, P. K. and Subrahmanyam, T. 2004a Performance of a circular fin in a cylindrical enclosure. *Int. Comm. Heat Transfer* **31**, 1209–1218. [7.3.7]
- Naidu, S. V., Rao, V. D., Sarma, P. K. and Subrahmanyam, Y. 2004b Performance of a circular fin in a cylindrical porous enclosure. *Int. Comm. Heat Mass Transfer* **31**, 1209–1218. [7.3.3]
- Najjari, M. and Ben Nasrallah, S. 2002 Numerical study of boiling with mixed convection in a vertical porous layer. *Int. J. Therm. Sci.* **41**, 936–948. [10.3]
- Najjari, M. and Ben Nasrallah, S. 2005 Numerical study of the effects of geometric dimensions on a liquid-vapor phase change and free convection in a rectangular porous cavity. *J. Porous Media* **8**, 1–12. [10.3]
- Najjari, M. and Ben Nasrallah, S. 2006 Liquid-vapor phase-change and mixed convection in a porous layer discretely heated. *J. Porous Media* **9**, 671–681. [10.3.1]
- Najjari, M. and Ben Nasrallah, S. 2008 Effects of latent heat storage on heat transfer in a forced flow in a porous layer. *Int. J. Therm. Sci.* **47**, 825–833. [10.3.1]
- Najjari, M. and Ben Nasrallah, S. 2009 Heat transfer between a porous layer and a forced flow: Influence of layer thickness. *Drying Technology* **27**, 336–343. [3.6]
- Nakagano, K., Mochida, T. and Ochiai, K. 2002 Influence of natural convection on forced horizontal flow in saturated porous media for aquifer thermal energy storage. *Appl. Therm. Engng.* **22**, 1299–1311. [6.10.1]
- Nakayama, A. 1991 A general treatment for non-Darcy film condensation within a porous medium in the presence of gravity and forced flow. *Wärme-Stoffübertrag.* **27**, 119–124. [10.4]
- Nakayama, A. 1993a A similarity solution for free convection from a point heat source embedded in a non-Newtonian fluid-saturated porous medium. *ASME J. Heat Transfer* **115**, 510–513. [5.11.1]
- Nakayama, A. 1993b Free convection from a horizontal line heat source in a power-law fluid-saturated porous medium. *Int. J. Heat Fluid Flow* **14**, 279–283. [5.10.1.2, 8.1.5]
- Nakayama, A. 1994 A unified theory for non-Darcy free, forced and mixed convection problems associated with a horizontal line heat source in a porous medium. *ASME J. Heat Transfer* **116**, 508–513. [5.10.1, 8.1.5]
- Nakayama, A. 1995 PC-Aided Numerical Heat Transfer and Convective Flow. CRC Press, Tokyo. [8.1.5]
- Nakayama, A. 1998 Unified treatment of Darcy-Forchheimer boundary-layer flows. *Transport Phenomena in Porous Media* (eds. D. B. Ingham and I. Pop), Elsevier, Oxford, pp. 179–204. [8.1.5]
- Nakayama, A. and Ashizawa, T. 1996 A boundary layer analysis of combined heat and mass transfer by natural convection from a concentrated source in a saturated porous medium. *Appl. Sci. Res.* **56**, 1–11. [9.3.1, 9.3.2]
- Nakayama, A. and Ebinuma, C. D. 1990 Transient non-Darcy forced convective heat transfer from a flat plate embedded in a fluid-saturated porous medium. *Int. J. Heat Fluid Flow* **11**, 249–263. [4.6, 4.7]
- Nakayama, A. and Hossain, M. A. 1994 Free convection in a saturated porous medium beyond the similarity solution. *Appl. Sci. Res.* **52**, 133–145. [5.1.9.9]
- Nakayama, A. and Hossain, M. A. 1995 An integrated treatment for combined heat and mass transfer by natural convection in a porous medium. *Int. J. Heat Mass Transfer* **38**, 761–765. [9.2.1]
- Nakayama, A. and Koyama, H. 1987a Free convective heat transfer over a nonisothermal body of arbitrary shape embedded in a fluid-saturated porous medium. *ASME J. Heat Transfer* **109**, 125–130. [5.9]

- Nakayama, A. and Koyama, H. 1987b A general similarity transformation for combined free and forced-convection flows within a fluid-saturated porous medium. *ASME J. Heat Transfer* **109**, 1041–1045. [8.1.4]
- Nakayama, A. and Koyama, H. 1987c Effect of thermal stratification on free convection within a porous medium. *AAIA J. Thermophys. Heat Transfer* **1**, 282–285. [5.1.4]
- Nakayama, A. and Koyama, H. 1988a A similarity transformation for subcooled mixed convection film boiling in a porous medium. *Appl. Sci. Res.* **45**, 129–143. [10.3.2]
- Nakayama, A. and Koyama, H. 1988b Subcooled forced convection film boiling over a vertical flat plate embedded in a fluid-saturated porous medium. *Wärme-Stoffübertrag.* **22**, 269–273. [10.3.2]
- Nakayama, A. and Koyama, H. 1989 Similarity solutions for buoyancy induced flows over a non-isothermal curved surface in a thermally stratified porous medium. *Appl. Sci. Res.* **46**, 309–323. [5.9]
- Nakayama, A. and Koyama, H. 1991 Buoyancy-induced flow of non-Newtonian fluids over a non-isothermal body of arbitrary shape in a fluid-saturated porous medium. *Appl. Sci. Res.* **48**, 55–70. [5.9]
- Nakayama, A. and Kuwahara, F. 1999 A macroscopic turbulence model for flow in a porous medium. *ASME J. Fluids Engng.* **121**, 427–433. [1.8]
- Nakayama, A. and Kuwahara, F. 2000 Numerical modeling of convective heat transfer in porous media using microscopic structures. *Handbook of Porous Media* (K. Vafai, ed.), Marcel Dekker, New York., pp. 441–488. [1.8]
- Nakayama, A. and Kuwahara, F. 2004 Closure to discussion [by B. Yu]. *ASME Heat Transfer* **126**, 1062. [2.2.4]
- Nakayama, A. and Kuwahara, F. 2005 Three-dimensional numerical models for periodically-developed heat and fluid flows within porous media. In *Transport Phenomena in Porous Media III*, (eds. D. B. Ingham and I. Pop), Elsevier, Oxford, pp. 174–200. [1.8]
- Nakayama, A. and Kuwahara, F. 2008 A general bioheat transfer model based on the theory of porous media. *Int. J. Heat Mass Transfer* **51**, 3190–3199. [2.6]
- Nakayama, A. and Kuwahara, F. 2008 A general macroscopic turbulence model for flows in packed beds, channels, pipes and rod bundles. *ASME J. Fluids Engng.* **130**, #101205. [1.8]
- Nakayama, A. and Pop, I. 1991 A unified similarity transformation for free, forced and mixed convection in Darcy and non-Darcy porous media. *Int. J. Heat Mass Transfer* **34**, 357–367. [8.1.5]
- Nakayama, A. and Pop, I. 1989 Free convection over a non-isothermal body in a porous medium with viscous dissipation. *Int. Comm. Heat Mass Transfer* **16**, 173–180. [5.9]
- Nakayama, A. and Pop, I. 1993 Momentum and heat transfer over a continuously moving surface in a non-Darcian fluid. *Wärme-Stoffübertrag.* **28**, 177–184. [4.16.5]
- Nakayama, A. and Shenoy, A. V. 1992 A unified similarity transformation for Darcy and non-Darcy forced-, free- and mixed-convection heat transfer in non-Newtonian inelastic fluid-saturated porous media. *Chem. Engng J./ Biochems. Engng J.* **50**, 33–45. [8.1.1]
- Nakayama, A. and Shenoy, A. V. 1993a Combined forced and free convection heat transfer in power-law fluid-saturated porous media. *Appl. Sci. Res.* **50**, 83–95. [8.1.1]
- Nakayama, A. and Shenoy, A. V. 1993b Non-Darcy forced convective heat transfer in a channel embedded in a non-Newtonian inelastic fluid-saturated porous medium. *Canad. Chem. Engng.* **71**, 168–173. [4.16.3]
- Nakayama, A., Kokudai, T. and Koyama, H. 1988 Integral method for non-Darcy free convection over a vertical flat plate and cone embedded in a fluid-saturated porous medium. *Wärme-Stoffübertrag.* **23**, 337–341. [5.8]
- Nakayama, A., Kokudai, T. and Koyama, H. 1990a Non-Darcian boundary layer flow and forced convective heat transfer over a flat plate in a fluid-saturated porous medium. *ASME J. Heat Transfer* **112**, 157–162. [4.8, 8.1.5]

- Nakayama, A., Kokudai, T. and Koyama, H. 1990b Forchheimer free convection over a nonisothermal body of arbitrary shape in a saturated porous medium. *ASME J. Heat Transfer* **112**, 511–515. [5.9]
- Nakayama, A., Koyama, H. and Kuwahara, F. 1987 Two-phase boundary layer treatment for subcooled free-convection film boiling around a body of arbitrary shape in a porous medium. *ASME J. Heat Transfer* **109**, 997–1002. [10.3.2]
- Nakayama, A., Koyama, H. and Kuwahara, F. 1988 An analysis on forced convection in a channel filled with a porous medium: Exact and approximate solutions. *Wärme-Stoffübertrag.* **23**, 291–296. [4.9]
- Nakayama, A., Koyama, H. and Kuwahara, F. 1989 Similarity solution for non-Darcy free convection from a non-isothermal curved surface in a fluid-saturated porous medium. *ASME J. Heat Transfer* **111**, 807–811. [5.9]
- Nakayama, A., Koyama, H. and Kuwahara, F. 1991 A general transformation for transient non-Darcy free and forced convection within a fluid-saturated porous medium. Proc. ASME/JSME Thermal Engineering Joint Conference —1991, vol. 4, pp. 287–293. [5.9]
- Nakayama, A., Kuwahara, F. and Hayashi, T. 2004 Numerical modeling for three-dimensional heat and fluid flow through a bank of cylinders with yaw. *J. Fluid Mech.* **498**, 139–159. [1.8]
- Nakayama, A., Kuwahara, F. and Kodama, Y. 2006 An equation for thermal dispersion-flux transport and its mathematical modeling for heat and fluid flow in a porous medium. *J. Fluid Mech.* **563**, 81–96. [2.2.4]
- Nakayama, A., Kuwahara, F. and Koyama, H. 1993 Transient non-Darcy free convection between parallel vertical plates in a fluid-saturated porous medium. *Appl. Sci. Res.* **50**, 29–43. [7.5]
- Nakayama, A., Kuwahara, F. and Liu, W. 2011 A general set of bioheat transfer equations based on volume averaging theory. In K. Vafai (ed.), *Porous Media: Applications in Biological Systems and Biotechnology*, CRC Press, Baton Roca, FL, pp. 535–567. [2.2.4]
- Nakayama, A., Kuwahara, F., Kawamura, Y. and Koyama, H. 1995 Three-dimensional numerical simulation of flow through microscopic porous structure. Proc. ASME/JSME Thermal Engineering Conf., vol. 3, pp. 313–318. [1.5.2]
- Nakayama, A., Kuwahara, F., Sugiyama, M. and Xu, G. 2001 A two-energy model for conduction and convection in porous media. *Int. J. Heat Mass Transfer* **44**, 4375–4379. [4.10]
- Nakayama, A., Kuwahara, F., Unemoto, T. and Hatashi, T. 2002 Heat and fluid flow within an anisotropic porous medium. *ASME J. Heat Transfer* **124**, 746–753. [4.16.5]
- Nandakumar, K. and Weinitzschke, H.J. 1992 A bifurcation of chemically driven convection in a porous medium. *Chem. Engng Sci.* **47**, 4107–4120. [3.4]
- Nandakumar, K., Weinitzschke, H. J. and Sankar, S. R. 1987 The calculation of singularities in steady mixed convection flow in porous media. *ASME HTD* **84**, 67–73. [8.2.1]
- Nandapurkar, P., Poirier, D. R., Heinrich, J. C. and Felicelli, S. 1989 Thermosolutal convection during dendritic solidification of alloys: Part 1. Linear stability analysis. *Metall. Trans. B* **20**, 711–721. [10.2.3]
- Nanjundappa, C. E., Ravisha, M., Lee, J. and Shivakumara, I. S. 2011a Penetrative ferroconvection in a porous layer. *Acta Mech.* **216**, 243–257. [6.21]
- Nanjundappa, C. E., Shivakumara, I. S., Lee, J. and Ravisha, M. 2011b The onset of ferroconvection in an anisotropic porous medium. *Int. J. Engng. Sci.* **49**, 497–508. [6.21]
- Nanjundappa, C. E., Shivakumara, I. S. and Prakash, H. N. 2012 Penetrative ferroconvection via internal heating in a saturated porous layer with constant heat flux at the lower boundary. *J. Magnet. Magnet. Mater.* **324**, 1670–1678. [6.21]
- Nanjundappa, C. E., Shivakumara, I. S. and Ravisha, M. 2010 The onset of buoyancy-driven convection in a ferromagnetic fluid saturated porous medium. *Meccanica* **45**, 213–226. [6.21]
- Nanjundappa, C. E., Shivakumara, I. S., Lee, J. and Ravisha, M. 2011c Effect of internal heat generation on the onset of Brinkman-Bénard convection in a ferrofluid saturated porous layer. *Int. J. Therm. Sci.* **50**, 160–168. [6.21]
- Narasimhan, A. and Lage, J. L. 2001a Modified Hazen-Dupuit-Darcy model for forced convection of a fluid with temperature-dependent viscosity. *ASME J. Heat Transfer* **123**, 31–38. [4.16.1]

- Narasimhan, A. and Lage, J. L. 2001b Forced convection of a fluid with temperature-dependent viscosity through a porous medium channel. *Numer. Heat Transfer A* **40**, 801–820. [4.16.1]
- Narasimhan, A. and Lage, J. L. 2002 Inlet temperature influence on the departure from Darcy flow of a fluid with variable viscosity. *Int. J. Heat Mass Transfer* **45**, 2419–2422. [4.16.1]
- Narasimhan, A. and Lage, J. L. 2003 Temperature-dependent viscosity effects on the thermo-hydraulics of heated porous-medium channel flows. *J. Porous Media* **6**, 149–158. [4.16.1]
- Narasimhan, A. and Lage, J. L. 2004a Predicting inlet temperature effects on the pressure-drop of heated porous medium channel flows using the M-HDD model. *ASME J. Heat Transfer* **126**, 301–303. [4.16.1]
- Narasimhan, A. and Lage, J. L. 2004b Pump power gain for heated porous medium channel flows. *ASME J. Fluids Engng.* **126**, 494–497. [4.16.1]
- Narasimhan, A. and Lage, J. L. 2005 Variable viscosity forced convection in porous medium channels. *Handbook of Porous Media* (ed. K. Vafai), 2nd ed., Taylor and Francis, New York, pp. 195–234. [4.16.1]
- Narasimhan, A. and Raju, K. S. 2007 Effect of variable permeability porous medium interconnector on the thermo-hydraulics of heat exchanger modelled as porous media. *Int. J. Heat Mass Transfer* **50**, 4052–4062. [2.6]
- Narasimhan, A. and Reddy, B. V. K. 2010 Natural convection inside a bidisperse porous medium enclosure. *ASME J. Heat Transfer* **132**, #012502. [7.3.9]
- Narasimhan, A. and Reddy, B. V. K. 2011a Laminar forced convection in a heat generating bi-disperse porous medium channel. *Int. J. Heat Mass Transfer* **54**, 636–644. [7.3.9]
- Narasimhan, A. and Reddy, B. V. K. 2011b Resonance of natural convection inside a bidisperse porous medium enclosure. *ASME J. Heat Transfer* **133**, #042601. [7.3.9]
- Narasimhan, A., Lage, J. L. and Nield, D. A. 2001b New theory for forced convection through porous media by fluids with temperature-dependent viscosity. *ASME J. Heat Transfer* **123**, 1045–1051. [4.16.1]
- Narasimhan, A., Lage, J. L., Nield, D. A. and Porneala, D. C. 2001a Experimental verification of two new theories predicting temperature-dependent viscosity effects on the forced convection in a porous channel. *ASME J. Fluids Engng.* **123**, 948–951. [4.16.1]
- Narasimhan, A., Reddy, B. V. K. and Dutta, P. 2012 Thermal management using the bi-disperse porous medium approach. *Int. J. Heat Mass Transfer* **55**, 538–546. [4.16.4]
- Narayana, M. and Sibanda, P. 2012 Double diffusive convection due to a horizontal wavy surface in a porous medium. *AIP Conf. Proc.* **1453**, 42–48. [9.1.6.4]
- Narayana, M., Sibanda, P., Motsa, S. S. and Lakshmi-Narayana, P. A. 2012 Linear and nonlinear stability analysis of binary Maxwell fluid convection in a porous medium. *Heat Mass Transfer* **48**, 863–874. [9.1.6.4]
- Narayana, P. A. L., Murthy, P. V. S. N. and Postelnicu, A. 2009 Soret and Dufour effects on free convection of non-Newtonian power law fluids with yield stress from a vertical flat plate in saturated porous media. *J. Porous Media* **12**, 967–981. [9.2.1]
- Narayana, P. A. L. and Murthy, P. V. S. N. 2006 Free convective heat and mass transfer in a doubly stratified non-Darcy porous medium. *ASME J. Heat Transfer* **128**, 1204–1212. [9.2.1]
- Narayana, P. A. L. and Murthy, P. V. S. N. 2007 Soret and Dufour effects on free convection heat and mass transfer in a doubly-stratified porous medium. *J. Porous Media* **10**, 613–623. [9.1.4]
- Narayana, P. A. L. and Murthy, P. V. S. N. 2008 Soret and Dufour effects on free convection heat and mass transfer from a horizontal flatplate in a Darcy porous medium. *ASME J. Heat Transfer* **130**, #104504. [9.2.1]
- Narayana, P. A. L. and Sibanda, P. 2010 Soret and Dufour effects on free convection along a vertical wavy surface in a fluid saturated porous medium. *Int. J. Heat Mass Transfer* **53**, 3030–3034. [9.2.1]
- Narayana, P. A. L., Murthy, P. V. S. N. and Gorla, R. S. R. 2008 Soret-driven thermosolutal convection induced by inclined thermal and solutal gradients in a shallow horizontal layer of a porous medium. *J. Fluid Mech.* **612**, 1–9. [9.5]

- Nasr, K., Ramadhyani, S. and Viskanta, R. 1994 An experimental investigation on forced convection heat transfer from a cylinder embedded in a packed bed. *ASME J. Heat Transfer* **116**, 73–78. [4.3]
- Nasr, K., Ramadhyani, S. and Viskanta, R. 1995 Numerical studies of forced convection heat transfer from a cylinder embedded in a packed bed. *Int. J. Heat Mass Transfer* **38**, 2353–2366. [4.8]
- Nasrabadi, H., Ghorayeb, K. and Firoozabadi, A. 2006 Two-phase multicomponent diffusion and convection for reservoir initialization. *SPE Reservoir Eval. Engng.* **9**, 530–542. [11.9.3]
- Nassehi, V. 1998 Modelling of combined Navier-Stokes and Darcy flows in crossflow membrane filtration. *Chem. Engng. Sci.* **53**, 1253–1265. [1.6]
- Natale, M. F. and Santillan Marcus, E. A. 2003 The effect of heat convection on drying of porous semi-infinite space with a heat flux condition on the fixed face  $x = 0$ . *Appl. Math. Comp.* **137**, 109–129. [3.6]
- Nath, P. R., Prasad, P. M. V. and Rao, D. R. V. P. 2010 Computational hydrodynamic mixed convective heat and mass transfer through a porous medium in a non-uniformly heated vertical channel with heat sources and dissipation. *Comput. Math. Appl.* **59**, 803–811. [9.6.2]
- Nayak, K. C., Saha, S. K., Srinivasan, K. and Dutta, P. 2006 A numerical model for heat sinks with phase change materials and thermal conductivity enhancers. *Int. J. Heat Mass Transfer* **49**, 1833–1844. [10.5]
- Naylor, D. and Oosthuizen, P. H. 1995 Free convection in a horizontal enclosure partly filled with a porous medium *AIAA J. Thermophys. Heat Transfer* **9**, 797–800. [7.7]
- Nazar, R. and Pop, I. 2004 Unsteady mixed convection boundary layer flow near the stagnation point on a horizontal surface in a porous medium. In Applications of Porous Media (ICAPM 2004), (eds. A. H. Reis and A. F. Miguel), Évora, Portugal, pp. 215–221. [8.1.2]
- Nazar, R., Amin, N. and Pop, I. 2004 Unsteady mixed convection boundary layer flow near a stagnation point on a vertical surface in a porous medium. *Int. J. Heat Mass Transfer* **47**, 2681–2688. [8.1.1]
- Nazar, R., Amin, N., Filip, D. and Pop, I. 2003b The Brinkman model for mixed convection boundary layer flow past a horizontal circular cylinder in a porous medium. *Int. J. Heat Mass Transfer* **46**, 3167–3178. [8.1.3]
- Nazar, R., Arafat, N. M. and Pop, I. 2006 Free convection boundary layer flow over vertical and horizontal flat surfaces embedded in a porous medium under mixed thermal boundary conditions. *Int. Comm. Heat Mass Transfer* **33**, 87–93. [5.1.9.8]
- Nazar, R., Tham, L., Pop, I. and Ingham, D. B. 2011 Mixed convection boundary layer flow over a horizontal circular cylinder embedded in a porous medium filled with a nanofluid. *Transp. Porous Media* **86**, 547–566. [9.7]
- Neagu, M. 2011 Free convective heat and mass transfer induced by a constant heat and mass fluxes vertical wavy wall in a non-Darcy double stratified porous medium. *Int. J. Heat Mass Transfer* **54**, 2310–2318. [9.2.1]
- Neale, G. and Nader, W. 1974 Practical significance of Brinkman's extension of Darcy's law: coupled parallel flows within a channel and a bounding porous medium. *Canad. J. Chem. Engng.* **52**, 475–478. [1.6]
- Nebbali, R. and Bouhadef, K. 2006 Numerical study of forced convection in a 3D flow of a non-Newtonian fluid through a porous duct. *Int. J. Numer. Meth. Heat Fluid Flow* **16**, 870–889. [4.16.3]
- Nebbali, R. and Bouhadef, K. 2011 Non-Newtonian fluid flow in plane channels: Heat transfer enhancement using porous blocks. *Int. J. Therm. Sci.* **50**, 1984–1995. [4.11]
- Néel, M. C. 1990a Convection in a horizontal porous layer of infinite extent. *Eur. J. Mech. B* **9**, 155–176. [6.15.1]
- Néel, M. C. 1990b Convection naturelle dans une couche poreuse horizontale d'extension infinie: chauffage inhomogène. *C. R. Acad. Sci. Paris, Sér. II* **309**, 1863–1868. [6.15.1]
- Néel, M. C. 1992 Inhomogeneous boundary conditions and the choice of convective patterns in a porous layer. *Int. J. Engng Sci.* **30**, 507–521. [6.14]

- Néel, M. C. 1998 Driven convection in porous media: deviations from Darcy's law. *C. R. Acad. Sci. Paris II B* **326**, 615–620. [6.10.1]
- Néel, M. C. and Nemrouch, F. 2001 Instabilities in an open top horizontal porous layer subjected to pulsating thermal boundary conditions. *Cont. Mech. Thermodyn.* **13**, 41–58. [6.11.3]
- Neichloss, H. and Dagan, G. 1975 Convection currents in a porous layer heated from below: the influence of hydrodynamic dispersion. *Phys. Fluids*, **18** 757–761. [6.6]
- Neilson, D. G. and Incropera, F. P. 1993 Effect of rotation on fluid motion and channel formation during unidirectional solidification of a binary alloy. *Int. J. Heat Mass Transfer* **36**, 489–505. [10.2.3]
- Nejad, M., Saghar, M. Z. and Islam, M. R. 2001 Role of thermal diffusion on heat and mass transfer in porous media. *Int. J. Comput. Fluid Dyn.* **15**, 157–168. [9.1.4]
- Nelson, R. A., Jr, and Bejan, A. 1998 Constructal optimization of internal flow geometry in convection. *ASME J. Heat Transfer* **120**, 357–364. [6.2, 6.26]
- Nepf, H. M. 1999 Drag, turbulence, and diffusion in flow through emergent vegetation. *Water Resources Res.* **35**, 479–489. [1.8]
- Neto, H. L., Quaresima, J. N. N. and Cotta, R. M. 2004 Transient natural convection in three-dimensional cavities: Reference results via integral transforms. In *Applications of Porous Media* (ICAPM 2004), (eds. A. H. Reis and A. F. Miguel), Évora, Portugal, pp. 165–172. [7.5]
- Neto, H. L., Quaresma, J. N. N. and Cotta, R. M. 2002 Natural convection in three-dimensional porous cavities. *Int. J. Heat Mass Transfer* **45**, 3013–3032. [7.5]
- Neufeld, J. A. and Wettlaufer, J. S. 2008 Shear-enhanced convection in a mushy layer. *J. Fluid Mech.* **612**, 339–361. [10.2.3]
- Neufeld, J. A. and Wettlaufer, J. S. 2011 Shear flow, phase change and matched asymptotic expansions: Pattern formation in mushy layers. *Physica D* **240**, 140–149. [10.2.3]
- Nganhou, J. 2004 Heat and mass transfer through a thick bed of cocoa beans during drying. *Heat Mass Transfer* **40**, 727–735. [3.6]
- Ngo, C. C. and Lai, F. C. 2000 Effective permeability for natural convection in a layered porous annulus. *J. Thermophys. Heat Transfer* **14**, 363–367. [6.13.2]
- Ngo, C. C. and Lai, F. C. 2005 Effects of backfill on heat transfer from a buried pipe. *ASME J. Heat Transfer* **127**, 780–784. [7.11]
- Ngo, C. C. and Lai, F. C. 2009 Heat transfer analysis of soil heating systems. *Int. J. Heat Mass Transfer* **52**, 6021–6027. [5.5.1]
- Nguyen, D. and Balakotaiah, V. 1995 Reaction-driven instabilities in down-flow packed beds. *Proc. Roy. Soc. Lond. A* **450**, 1–21. [3.4]
- Nguyen, H. D. and Paik, S. 1994 Unsteady mixed convection from a sphere in water-saturated porous media with variable surface temperature - heat flux. *Int. J. Heat Mass Transfer* **37**, 1783–1793. [8.1.3]
- Nguyen, H. D., Paik, S. and Douglass, R. W. 1997a Double-diffusive convection in a porous trapezoidal enclosure with oblique principal axes. *AAIA J. Thermophysics Heat Transfer* **11**, 309–312. [9.4]
- Nguyen, H. D., Paik, S. and Douglass, R. W. 1994 Study of double-diffusive convection in layered anisotropic porous media. *Numer. Heat Transfer B* **26**, 489–505. [9.1.6.2]
- Nguyen, H. D., Paik, S. and Pop, I. 1997b Transient thermal convection in a spherical enclosure containing a fluid core and a porous shell. *Int. J. Heat Mass Transfer*, **40**, 379–392. [7.5]
- Nguyen, H. D., Paik, S., Douglass, R. W. and Pop, I. 1996 Unsteady non-Darcy reaction-driven flow from an anisotropic cylinder in porous media. *Chem. Engng. Sci.* **51**, 4963–4977. [5.5.1]
- Nguyen, T. H., Lepalec, G., Nguyen-Quang, T. and Bahloul, A. 2004 Bioconvection: spontaneous pattern formation of micro-organisms. In *Applications of Porous Media* (ICAPM 2004), (eds. A. H. Reis and A. F. Miguel), Évora, Portugal, pp. 521–526. [6.25]
- Nguyen-Quang, T. 2008 Onset of gravitactic bioconvection in a square anisotropic porous medium with arbitrary orientation of the principal axes. *Int. J. Heat Mass Transfer* **51**, 1497–1504. [6.25]

- Nguyen-Quang, T., Bahloul, A. and Nguyen, T. H. 2005 Stability of gravitactic microorganisms in a fluid-saturated porous medium. *Int. Comm. Heat Mass Transfer* **32**, 54–63. [6.25]
- Nguyen-Quang, T., Guichard, F. and Nguyen, T. H. 2011 Spatial pattern formation of motile microorganisms: From gravitactic bioconvection to protozoan culture dynamics. In K. Vafai (ed.), *Porous Media: Applications in Biological Systems and Biotechnology*, CRC Press, Baton Roca, FL, pp. 535–56. [6.25]
- Nguyen-Quang, T., Nguyen, H., Guichard, F., Nicolau, A., Szatmari, G., LePalec, G., Dusser, M., Lafossee, J., Bonnet, J. L. and Bohatier, J. 2009 Two-dimensional gravitactic bioconvection in a protozoan (*Tetrahymena pyriformis*) culture. *Zoological Science* **26**, 54–65. [6.25]
- Nguyen-Quang, T., Nguyen, H. and Lepalec, G. 2008 Gravitactic bioconvection in a fluid saturated porous medium with double diffusion. *J. Porous Media* **11**, 751–764. [6.25]
- Ni, J. and Beckermann, C. 1991a Natural convection in a vertical enclosure filled with anisotropic porous media. *ASME J. Heat Transfer* **113**, 1033–1037. [7.3.2]
- Ni, J. and Beckermann, C. 1991b A volume-averaged two-phase model for transport phenomena during solidification. *Metall. Trans. B* **22**, 349–361. [10.2.3]
- Ni, J. and Incropera, F. P. 1995a Extension of the continuum model for transport phenomena occurring during metal alloy solidification—I. The conservation equations. *Int. J. Heat Mass Transfer* **38**, 1271–1284. [10.2.3]
- Ni, J. and Incropera, F. P. 1995b Extension of the continuum model for transport phenomena occurring during metal alloy solidification—II. Microscopic considerations. *Int. J. Heat Mass Transfer* **38**, 1285–1296. [10.2.3]
- Nield, D. A. 1968 Onset of thermohaline convection in a porous medium. *Water Resources Res.* **11**, 553–560. [6.2, 9.1.1, 11.4]
- Nield, D. A. 1975 The onset of transient convective instability. *J. Fluid Mech.* **71**, 441–454. [6.11.1]
- Nield, D. A. 1977 Onset of convection in a fluid layer overlying a layer of a porous medium. *J. Fluid Mech.* **81**, 513–522. [6.19.1.2]
- Nield, D. A. 1982 Onset of convection in a porous layer saturated by an ideal gas. *Int. J. Heat Mass Transfer* **25**, 1605–1606. [6.7]
- Nield, D. A. 1983 The boundary correction for the Rayleigh-Darcy problem: limitations of the Brinkman equation. *J. Fluid Mech.* **128**, 37–46. Corrigendum 150, 503. [1.6, 6.19.1.2]
- Nield, D. A. 1987a Convective instability in porous media with throughflow. *AIChE J.* **33**, 1222–1224. [6.10.2]
- Nield, D. A. 1987b Convective heat transfer in porous media with columnar structure. *Transport in Porous Media* **2**, 177–185. [6.3, 6.13.4]
- Nield, D. A. 1990 Convection in a porous medium with inclined temperature gradient and horizontal mass flow. *Heat Transfer 1990, Hemisphere, New York*, vol. **5**, pp. 153–158. [7.9]
- Nield, D. A. 1991a Convection in a porous medium with inclined temperature gradient. *Int. J. Heat Mass Transfer* **34**, 87–92. [7.9]
- Nield, D. A. 1991b Estimation of the stagnant thermal conductivity of saturated porous media. *Int. J. Heat Mass Transfer* **34**, 1575–1576. [2.2.1]
- Nield, D. A. 1993 Correlation formulas for mixed convection heat transfer in a saturated porous medium. *Int. J. Heat Fluid Flow* **14**, 206. [8.3.4]
- Nield, D. A. 1994a The effect of channeling on heat transfer across a horizontal layer of a porous medium. *Int. J. Heat Fluid Flow* **15**, 247–248. [6.9.1, 6.19.1.2]
- Nield, D. A. 1994b Modelling high speed flow of a compressible fluid in a saturated porous medium. *Transport in Porous Media* **14**, 85–88. [1.5.1]
- Nield, D. A. 1994c Estimation of an effective Rayleigh number for convection in a vertically inhomogeneous porous medium or clear fluid. *Int. J. Heat Fluid Flow* **15**, 337–340. [5.4, 6.7, 6.13.2]
- Nield, D. A. 1994d Convection in a porous medium with inclined temperature gradient: additional results. *Int. J. Heat Mass Transfer* **37**, 3021–3025. [7.9]

- Nield, D. A. 1995 Onset of convection in a porous medium with nonuniform time-dependent volumetric heating. *Int. J. Heat Fluid Flow* **16**, 217–222. [6.11.3]
- Nield, D. A. 1996 The effect of temperature-dependent viscosity on the onset of convection in a saturated porous medium. *ASME J. Heat Transfer* **118**, 803–805. [6.7]
- Nield, D. A. 1997a Discussion of a discussion by F. Chen and C.F. Chen. *ASME J. Heat Transfer* **119**, 193–194. [1.6]
- Nield, D. A. 1997b Notes on convection in a porous medium: (i) an effective Rayleigh number for an anisotropic layer, (ii) the Malkus hypothesis and wavenumber selection. *Transport in Porous Media* **27**, 135–142. [6.4, 6.9.1, 6.12]
- Nield, D. A. 1997c Comments on “Turbulence model for flow through porous media”. *Int. J. Heat Mass Transfer* **40**, 2499. [1.8]
- Nield, D. A. 1998a Effects of local thermal nonequilibrium in steady convective processes in a saturated porous medium: forced convection in a channel. *J. Porous Media* **1**, 181–186. [2.2.3, 4.10]
- Nield, D. A. 1998b Convection in a porous medium with inclined temperature gradient and vertical throughflow. *Int. J. Heat Mass Transfer* **41**, 241–243. [7.9]
- Nield, D. A. 1998c Modeling the effect of surface tension on the onset of natural convection in a saturated porous medium. *Transport Porous Media* **31**, 365–368. [6.19.3]
- Nield, D. A. 1999 Modeling the effects of a magnetic field or rotation on flow in a porous medium: momentum equation and anisotropic permeability analogy. *Int. J. Heat Mass Transfer* **42**, 3715–3718. [6.22]
- Nield, D. A. 2000 Resolution of a paradox involving viscous dissipation and nonlinear drag in a porous medium. *Transport Porous Media* **41**, 349–357. [2.2.2]
- Nield, D. A. 2001a Comments on ‘Fully developed free convection in open-ended vertical channels partially filled with porous material’ by M. A. Al-Nimr and O. M. Hadad. *J. Porous Media* **4**, 97–99. [7.7]
- Nield, D. A. 2001b Alternative models of turbulence in a porous medium, and related matters. *ASME J. Fluids Engng.* **123**, 928–931. [1.8]
- Nield, D. A. 2001c Some pitfalls in the modeling of convective flows in porous media. *Transport Porous Media* **43**, 597–601. [6.7]
- Nield, D. A. 2002 A note on the modeling of local thermal non-equilibrium in a structured porous medium. *Int. J. Heat Mass Transfer* **45**, 4367–4368. [4.10]
- Nield, D. A. 2003 The stability of flow in a channel or duct occupied by a porous medium. *Int. J. Heat Mass Transfer* **46**, 4351–4354. [1.8]
- Nield, D. A. 2004a Comments on ‘The onset of transient convection in bottom heated porous media’ by K. K. Tan, T. Sam and H. Jamaludin: Rayleigh and Biot numbers. *Int. J. Heat Mass Transfer* **47**, 641–643. [6.11.3]
- Nield, D. A. 2004b Comments on ‘A new model for viscous dissipation in porous media across a range of permeability values’. *Transport in Porous Media* **55**, 253–254. [2.2.2]
- Nield, D. A. 2004c Forced convection in a plane plate channel with asymmetric heating. *Int. J. Heat Mass Transfer* **47**, 5609–5612. (Erratum 51 (2008), 2108–2108.) [4.9]
- Nield, D. A. 2006 A note on a Brinkman-Brinkman forced convection problem. *Transp. Porous Media* **64**, 185–188. [4.9, 4.16.5]
- Nield, D. A. 2007b The modeling of viscous dissipation in a saturated porous medium. *ASME J. Heat Transfer* **129**, 1459–1463. [2.2.2]
- Nield, D. A. 2007a Comment on the effect of anisotropy on the onset of convection in a porous medium. *Adv. Water Resources* **30**, 696–697. [6.12]
- Nield, D. A. 2008a Comments on Reply to Comments on “Non-Darcian forced convection flow of viscous dissipating fluid over a flat plate embedded in a porous medium.” *Transp. Porous Media* **75**, 269–270. [4.8, 8.1.1]
- Nield, D. A. 2008c General heterogeneity effects on the onset of convection in a porous medium. In P. Vadasz, (ed.), *Emerging Topics in Heat and Mass Transfer in Porous Media*, Springer, New York, pp. 63–84. [6.13.5]

- Nield, D. A. 2009a Closure to “Discussion of ‘The modeling of viscous dissipation in a saturated porous medium.’” (2009, ASME J. Heat Transfer, 131, p. 025501), *ASME J. Heat Transfer* **131**, #025502. [2.2.2]
- Nield, D. A. 2009b The modeling of form drag in a porous medium saturated by a power-law fluid. *ASME Journal of Heat Transfer* **131**, #104501. [1.5.2]
- Nield, D. A. 2009c The Beavers-Joseph boundary condition and related matters: A historical and critical note. *Transp. Porous Media* **78**, 537–540. [1.6]
- Nield, D. A. 2011a A note on convection patterns in an inclined porous layer. *Transp. Porous Media* **86**, 23–25. [7.8]
- Nield, D. A. 2011b A note on the onset of convection in a layer of a porous medium saturated by a non-Newtonian nanofluid of power-law type. *Transp. Porous Media* **87**, 121–123. [6.23]
- Nield, D. A. 2011c A further note on the onset of convection in a layer of a porous medium saturated by a non-Newtonian nanofluid of power-law type. *Transp. Porous Media* **88**, 187–191. [6.23]
- Nield, D. A. 2012 A note on local thermal non-equilibrium in porous media near boundaries and interfaces. *Transp. Porous Media*, **95**, 581–584. [2.2.3]
- Nield, D. A. and Barletta, A. 2009 The Horton-Rogers-Lapwood problem revisited: The effect of pressure work, *Transp. Porous Media* **77**, 143–156. [6.1]
- Nield, D. A. and Barletta, A. 2010a Comment on the comment by V. A. F. Costa, IJTS 49(9) (2010) 1874–1875. on the paper by I. A. Badruddin, Z.A. Zainal, Z. A. Khan, Z. Mallick “Effect of viscous dissipation and radiation on natural convection in a porous medium embedded within vertical annulus” IJST 46(3)(2007) 221–227. *Int. J. Therm. Sci.* **49**, 2491–2492. [2.2.2]
- Nield, D. A. and Barletta, A. 2010b Extended Oberbeck-Boussinesq approximation study of convective instabilities in a porous layer with horizontal flow and bottom heating. *Int. J. Heat Mass Transfer* **53**, 577–585. [6.10.1]
- Nield, D. A. and Hooman, K. 2006 Heat transfer in the thermal entrance region for flow through rectangular porous passages. *Int. J. Heat Mass Transfer* **49**, 3004–3015. [4.16.5]
- Nield, D. A. and Joseph, D. D. 1985 Effects of quadratic drag on convection in a saturated porous medium. *Phys. Fluids* **28**, 995–997. [6.6]
- Nield, D. A. and Kuznetsov, A. V. 1999 Local thermal nonequilibrium effects in forced convection in a porous medium channel: a conjugate problem. *Int. J. Heat Mass Transfer* **42**, 3245–3252. [4.10]
- Nield, D. A. and Kuznetsov, A. V. 2000 Effects of heterogeneity in forced convection in a porous medium: parallel plate channel or circular duct. *Int. J. Heat Mass Transfer* **43**, 4119–4134. [4.12]
- Nield, D. A. and Kuznetsov, A. V. 2001a Effects of heterogeneity in forced convection in a porous medium: parallel plate channel, asymmetric property variation, and asymmetric heating. *J. Porous Media* **4**, 137–148. [4.12]
- Nield, D. A. and Kuznetsov, A. V. 2001b The interaction of thermal nonequilibrium and heterogeneous conductivity effects in forced convection in layered porous channels. *Int. J. Heat Mass Transfer* **44**, 4369–4373. [4.12]
- Nield, D. A. and Kuznetsov, A. V. 2003a Effects of gross heterogeneity and anisotropy in forced convection in a porous medium: layered medium analysis. *J. Porous Media* **6**, 51–57. [4.12]
- Nield, D. A. and Kuznetsov, A. V. 2003b Effects of temperature-dependent viscosity in forced convection in a porous medium: layered medium analysis. *J. Porous Media* **6**, 213–222. [4.16.6]
- Nield, D. A. and Kuznetsov, A. V. 2003c Effects of heterogeneity in forced convection in a porous medium: parallel-plate channel, Brinkman model. *J. Porous Media* **6**, 257–266. [4.12]
- Nield, D. A. and Kuznetsov, A. V. 2003d Boundary-layer analysis of forced convection with a plate and a porous substrate. *Acta Mech.* **166**, 141–148. [4.11]

- Nield, D. A. and Kuznetsov, A. V. 2004a Interaction of transverse heterogeneity and thermal development of forced convection in a porous medium. *Transport Porous Media* **57**, 103–111. [4.13]
- Nield, D. A. and Kuznetsov, A. V. 2004b Forced convection in a helical pipe filled with a saturated porous medium. *Int. J. Heat Mass Transfer* **47**, 5175–5180. [4.5]
- Nield, D. A. and Kuznetsov, A. V. 2004c Forced convection in a bi-disperse porous medium channel: a conjugate problem. *Int. J. Heat Mass Transfer* **47**, 5375–5380. [4.16.4]
- Nield, D. A. and Kuznetsov, A. V. 2005a Thermally developing forced convection in a channel occupied by a porous medium saturated by a non-Newtonian fluid. *Int. J. Heat Mass Transfer* **48**, 1214–1218. [4.13]
- Nield, D. A. and Kuznetsov, A. V. 2005b A two-velocity two-temperature model for a bi-dispersed porous medium: forced convection in a channel. *Transport in Porous Media*, **59**, 325–339. [4.16.4]
- Nield, D. A. and Kuznetsov, A. V. 2005c Heat transfer in bidisperse porous media. In *Transport Phenomena in Porous Media III*, (eds. D. B. Ingham and I. Pop), Elsevier, Oxford, pp. 34–59. [4.16.4]
- Nield, D. A. and Kuznetsov, A. V. 2005d Thermal development of forced convection in a channel or duct partly occupied by a porous medium. *J. Porous Media* **8**, 627–638. [4.11]
- Nield, D. A. and Kuznetsov, A. V. 2006 Forced convection with slip-flow in a channel or duct occupied by a hyper-porous medium saturated by a rarefied gas. *Transport Porous Media* **64**, 161–170. [4.9]
- Nield, D. A. and Kuznetsov, A. V. 2006a Forced convection with slip-flow in a channel or duct occupied by a hyper-porous medium saturated by a rarefied gas. *Transp. Porous Media* **64**, 161–170. [4.9]
- Nield, D. A. and Kuznetsov, A. V. 2006b The onset of convection in a bidisperse porous medium. *Int. J. Heat Mass Transfer* **49**, 3068–3074. [6.27]
- Nield, D. A. and Kuznetsov, A. V. 2007a Reply to comments on ‘Forced convection with slip-flow in a channel or duct occupied by a hyper-porous medium saturated by a rarefied gas. *Transp. Porous Media* **67**, 169–170. [4.9]
- Nield, D. A. and Kuznetsov, A. V. 2007b The effects of combined horizontal and vertical heterogeneity on the onset of convection in a porous medium. *Int. J. Heat Mass Transfer* **50**, 1909–1915. [6.13.5]
- Nield, D. A. and Kuznetsov, A. V. 2007c The effects of combined horizontal and vertical heterogeneity on the onset of convection in a bidisperse porous medium. *Int. J. Heat Mass Transfer* **50**, 3329–3339. [6.13.5]
- Nield, D. A. and Kuznetsov, A. V. 2007d The effects of combined horizontal and vertical heterogeneity and anisotropy on the onset of convection in a porous medium. *Int. J. Therm. Sci.* **46**, 1211–1218. [6.13.5]
- Nield, D. A. and Kuznetsov, A. V. 2007e The onset of convection in a shallow box occupied by a heterogeneous porous medium with constant flux boundaries. *Transp. Porous Media* **67**, 441–451. [6.13.5]
- Nield, D. A. and Kuznetsov, A. V. 2007f The onset of convection in a porous medium occupying an enclosure of variable width or height. *ASME J. Heat Transfer* **129**, 1714–1718. [6.1.3.5]
- Nield, D. A. and Kuznetsov, A. V. 2008a A bioheat transfer model: forced convection in a channel occupied by a porous medium with counterflow. *Int. J. Heat Mass Transfer* **51**, 5534–5541. [2.6. 4.16.2]
- Nield, D. A. and Kuznetsov, A. V. 2008b Natural convection about a vertical plate embedded in a bidisperse porous medium. *Int. J. Heat Mass Transfer* **51**, 1658–1664. [5.1.9.9]
- Nield, D. A. and Kuznetsov, A. V. 2008c The effects of combined horizontal and vertical heterogeneity on the onset of convection in a porous medium: Moderate heterogeneity. *Int. J. Heat Mass Transfer* **51**, 2361–2367. [6.13.5.]
- Nield, D. A. and Kuznetsov, A. V. 2008d The effects of combined horizontal and vertical heterogeneity on the onset of transient convection in a porous medium: *J. Porous Media* **11**, 377–387. [6.13.5]

- Nield, D. A. and Kuznetsov, A. V. 2009a Forced convection with laminar pulsating counterflow in a saturated porous channel. *ASME J. Heat Transfer* **131**, #101005. [2.6, 4.16.2]
- Nield, D. A. and Kuznetsov, A. V. 2009b The Cheng-Minkowycz problem for natural convective boundary layer flow in a porous medium saturated by a nanofluid. *Int. J. Heat Mass Transfer* **52**, 5792–5795. [9.7]
- Nield, D. A. and Kuznetsov, A. V. 2009c The effect of a transition layer between a fluid and a porous medium: shear flow in a channel. *Transp. Porous Media* **78**, 477–487. [1.6]
- Nield, D. A. and Kuznetsov, A. V. 2009d Thermal instability in a porous medium layer saturated by a nanofluid. *Int. J. Heat Mass Transfer* **52**, 5796–5801. [3.8, 9.7]
- Nield, D. A. and Kuznetsov, A. V. 2010a The onset of convection in a layer of cellular porous material : Effect of temperature dependent conductivity arising from radiative transfer. *ASME J. Heat Transfer* **132**, #074503. [2.2.5, 6.27]
- Nield, D. A. and Kuznetsov, A. V. 2010b Forced convection with phase-lagged oscillatory counterflow in a saturated porous channel. *J. Porous Media* **13**, 601–611. [2.6, 4.16.2]
- Nield, D. A. and Kuznetsov, A. V. 2010c Forced convection in cellular porous materials: Effect of temperature-dependent conductivity arising from radiative transfer. *Int. J. Heat Mass Transfer* **53**, 2680–2684. [2.2.5]
- Nield, D. A. and Kuznetsov, A. V. 2010d The onset of convection in a heterogeneous porous medium with transient temperature profile. *Transp. Porous Media* **85**, 691–702. [6.18]
- Nield, D. A. and Kuznetsov, A. V. 2011a The Cheng-Minkowycz problem for the double-diffusive natural convection boundary layer flow in a porous medium saturated by a nanofluid. *Int. J. Heat Mass Transfer* **54**, 374–378. [9.7]
- Nield, D. A. and Kuznetsov, A. V. 2011b A three-velocity three-temperature model for a tridisperse porous medium. Forced convection in a channel. *Int. J. Heat Mass Transfer* **54**, 2490–2498. [4.16.4]
- Nield, D. A. and Kuznetsov, A. V. 2011c The Cheng-Minkowycz problem for natural convection about a vertical plate embedded in a tri-disperse porous medium. *Int. J. Heat Mass Transfer* **54**, 3505–3513. [5.1.9.4]
- Nield, D. A. and Kuznetsov, A. V. 2011d Effect of vertical throughflow on thermal instability in a porous medium layer saturated by a nanofluid. *Transp. Porous Media* **87**, 765–775. [9.7]
- Nield, D. A. and Kuznetsov, A. V. 2011e The onset of convection in a heterogeneous porous medium with vertical throughflow. *Transp. Porous Media* **88**, 347–355. [6.13.5]
- Nield, D. A. and Kuznetsov, A. V. 2011f Onset of convection in a porous medium with strong vertical throughflow. *Transp. Porous Media* **90**, 883–888. [6.10.2]
- Nield, D. A. and Kuznetsov, A. V. 2011g Effect of vertical throughflow on the onset of convection in a porous medium in a rectangular box. *Transp. Porous Media* **90**, 993–1000. [6.10.2]
- Nield, D. A. and Kuznetsov, A. V. 2012a The onset of convection in a layer of a porous medium saturated by a nanofluid: Effects of conductivity and viscosity variation and cross-diffusion. *Transp. Porous Media* **92**, 837–846. [9.7]
- Nield, D. A. and Kuznetsov, A. V. 2012b The onset of strong heterogeneity and strong throughflow on the onset of convection in a porous medium: Non-periodic global variation. *Transp. Porous Media* **91**, 927–938. [6.13.6]
- Nield, D. A. and Kuznetsov, A. V. 2012c Forced convection in a channel partly occupied by a bidisperse porous medium: Symmetric case. *ASME J. Heat Transfer* **134**, to appear. [2.2.3]
- Nield, D. A. and Kuznetsov, A. V. 2011f The effects of combined horizontal and vertical heterogeneity on the onset of convection in a porous medium with horizontal throughflow. *Int. J. Heat Mass Transfer* **54**, 5595–5601. [6.10.1]
- Nield, D. A. and Lage, J. L. 1997 Discussion of a Discussion by K. Vafai and S.J. Kim. *ASME J. Heat Transfer* **119**, 195–197. [1.5.3]
- Nield, D. A. and Lage, J. L. 1998 The role of longitudinal diffusion in a fully developed forced convective slug flow in a channel. *Int. J. Heat Mass Transfer* **41**, 4375–4377. [4.5]
- Nield, D. A. and Simmons, C. T. 2007 A discussion on the effect of heterogeneity on the onset of convection in a porous medium. *Transp. Porous Media* **68**, 413–421. [6.13.6]

- Nield, D. A. and White, S. P. 1982 Natural convection in an infinite porous medium produced by a line heat source. *Mathematics and Models in Engineering Science* (ed. A. McNabb et al.) Dept. Sci. Indust. Res., Wellington, New Zealand, pp. 121–128. [5.10.2]
- Nield, D. A., Barletta, A. and Celli, M. 2011a The effect of viscous dissipation on the onset of convection in an inclined porous layer. *J. Fluid Mech.* **679**, 544–558. [7.8]
- Nield, D. A., Junqueira, S. L. M. and Lage, J. L. 1996 Forced convection in a fluid saturated porous medium with isothermal and isoflux boundaries. *J. Fluid Mech.* **322**, 201–214. [4.5]
- Nield, D. A., Kuznetsov, A. V. and Avramenko, A. A. 2004c The onset of bioconvection in a horizontal porous medium layer. *Transport in Porous Media* **54**, 335–344. [6.25]
- Nield, D. A., Kuznetsov, A. V. and Simmons, C. T. 2010b The effect of strong heterogeneity on the onset of convection in a porous medium: 2D/3D localization and spatially correlated random permeability fields. *Transp. Porous Media* **83**, 465–477. [6.13.6]
- Nield, D. A., Kuznetsov, A. V. and Xiong, M. 2002 Effect of local thermal non-equilibrium on thermally developing forced convection in a porous medium. *Int. J. Heat Mass Transfer* **45**, 4949–4955. [4.13]
- Nield, D. A., Kuznetsov, A. V. and Xiong, M. 2003a Thermally developing forced convection in a porous medium: parallel plate channel with walls at uniform temperature, with axial conduction and viscous dissipation effects. *Int. J. Heat Mass Transfer* **46**, 643–651. [4.13]
- Nield, D. A., Kuznetsov, A. V. and Xiong, M. 2003b Thermally developing forced convection in a porous medium: parallel-plate channel or circular tube with walls at constant heat flux. *J. Porous Media* **6**, 203–212. [4.13]
- Nield, D. A., Kuznetsov, A. V. and Xiong, M. 2004a Thermally developing forced convection in a porous medium: parallel-plate channel or circular tube with isothermal walls. *J. Porous Media* **7**, 19–27. [4.13]
- Nield, D. A., Kuznetsov, A. V. and Xiong, M. 2004b Effects of viscous dissipation and flow work on forced convection in a channel filled by a saturated porous medium. *Transport Porous Media* **56**, 351–367. [4.9]
- Nield, D. A., Manole, D. M. and Lage, J. L. 1993 Convection induced by inclined thermal and solutal gradients in a shallow layer of a porous medium. *J. Fluid Mech.* **257**, 559–574. [9.5]
- Nield, D. A., Porneala, D. C. and Lage, J. L. 1999 A theoretical study, with experimental verification, of the temperature-dependent viscosity effect on the forced convection through a porous medium channel. *ASME J. Heat Transfer* **121**, 500–503. [4.16.1]
- Nield, D. A., Simmons, C. T., Kuznetsov, A. V. and Ward, J. D. 2008c On the evolution of salt lakes: Episodic convection beneath an evaporating salt lake. *Water Resor. Res.* **44**, #W02439. [11.8]
- Nilsen, T. and Storesletten, L. 1990 An analytical study on natural convection in isotropic and anisotropic porous channels. *ASME J. Heat Transfer* **112**, 396–401. [6.15.3]
- Nilson, R. H. 1981 Natural convective boundary layer on two-dimensional and axisymmetric surfaces in high-Pr fluids or in fluid saturated porous media. *ASME J. Heat Transfer* **103**, 803–807. [5.6.1]
- Nimvari, M. E., Maerefat, M. and El-Hossaini, M. K. 2012 Numerical simulation of turbulent flow and heat transfer in a channel partially filled with a porous media. *Int. J. Therm. Sci.* **60**, 131–141. [4.11]
- Nishimura, T. and Wakamatsu, M. 2000 Natural convection suppression and crystal growth during unidirectional solidification of a binary system. *Heat Transfer Asian Res.* **29**, 120–131. [10.2.3]
- Nishimura, T., Kunitsugu, K. and Itoh, T. 1996 Natural convection suppression by azimuthal partitions in a horizontal porous annulus. *Numer. Heat Transfer A* **29**, 65–81. [7.3.3]
- Nishimura, T., Takumi, T., Shiraishi, M., Kawamura, Y. and Ozoe, H. 1986 Numerical analysis of natural convection in a rectangular enclosure horizontally divided into fluid and porous regions. *Int. J. Heat Mass Transfer* **29**, 889–898. [7.7]
- Nisse, L. and Neél, M. C. 2005 Spectral stability of convective rolls in porous media. *ZAMM* **85**, 366–383. [6.4]

- Nithiarasu, P. 1999 Finite element modeling of a leaky third component migration from a heat source buried into a fluid saturated porous medium. *Math. Comput. Model.* **29**, 27–39. [9.3.1]
- Nithiarasu, P., Seetharamu, K. N. and Sundararajan, T. 1999a Numerical investigations of buoyancy driven flow in a fluid saturated non-Darcian porous medium. *Int. J. Heat Mass Transfer* **42**, 1205–1215. [7.1.6]
- Nithiarasu, P., Seetharamu, K. N. and Sundararajan, T. 1997b Non-Darcy double-diffusive natural convection in axisymmetric fluid saturated porous cavities. *Heat Mass Transfer* **32**, 427–433. [9.4]
- Nithiarasu, P., Seetharamu, K. N. and Sundararajan, T. 1998 Effect of porosity on natural convective heat transfer in a fluid saturated porous medium. *Int. J. Heat Fluid Flow* **19**, 56–58. [7.6.2]
- Nithiarasu, P., Seetharamu, K. N. and Sundararajan, T. 2002 Finite element modeling of flow, heat and mass transfer in fluid saturated porous media. *Arch. Comp. Meth. Engng.* **9**, 3–42. [7.1.6]
- Nithiarasu, P., Seetharamu, K. N. and Sundararajan, T. 1997a Natural convective heat transfer in a fluid saturated variable porosity medium. *Int. J. Heat Mass Transfer* **40**, 3955–3957. [7.6.2]
- Nithiarasu, P., Seetharamu, K.N. and Sundararajan, T. 1996 Double-diffusive natural convection in an enclosure filled with a fluid-saturated porous medium: a generalized non-Darcy approach. *Numer. Heat Transfer A* **30**, 413–426. [6.6]
- Nithiarasu, P., Sujatha, K. S., Sundararajan, T. and Seetharamu, K. N. 1999b Buoyancy driven flow in a non-Darcian, fluid saturated porous enclosure subjected to uniform heat flux — A numerical study. *Comm. Numer. Meth. Engng.* **15**, 765–776. [7.1.6]
- Niu, J., Fu, C. and Tan, W. C. 2010a Thermal convection of a viscoelastic fluid in an open-top porous layer heated from below. *J. Non-Newtonian Fluid Mech.* **165**, 203–211. [6.23]
- Niu, J., Fu, C. J. and Tan, W. C. 2010b Stability of thermal convection of an Oldroyd-B fluid in a porous medium with Newtonian heating. *Phys. Lett. A* **374**, 4607–4613. [6.23]
- Niu, Y., Simon, T. and Ibrahim, M. 2006 Direct measurements of eddy transport and thermal dispersion in high-porosity matrix. *J. Thermophys. Heat Transfer* **20**, 101–106. [2.2.4]
- Nnanna, A. G. A., Haji-Sheikh, A. and Harris, K. T. 2004 Experimental study of local thermal equilibrium phenomena during phase change in porous media. *Int. J. Heat Mass Transfer* **47**, 4365–4375. [2.2.3]
- Nnanna, A. G. A., Harris, K. T. and Haji-Sheikh, A. 2005 An experimental study of non-Fourier thermal response in porous media. *J. Porous Media* **8**, 31–44. [2.2.3]
- Noh, J. S., Lee, K. B. and Lee, C. G. 2006 Pressure loss and forced convective heat transfer in an annulus filled with aluminum foam. *Int. Comm. Heat Mass Transfer* **33**, 434–444. [4.16.5]
- Noor, N. F. M. and Hashim, I. 2010 MHD viscous flow over a linearly stretching sheet embedded in a non-Darcian porous medium. *J. Porous Media* **13**, 349–355. [5.1.9.9]
- Notz, D. and Worster, M. G. 2009 Desalination processes in sea ice revisited. *J. Geophys. Res.* **114**, (C5). [10.2.3]
- Nouri-Borjerdi, A., Noghrehabadi, A. R. and Rees, D. A. S. 2007a The linear stability of a developing thermal front in a porous medium: The effect of local thermal non-equilibrium. *Int. J. Heat Mass Transfer* **50**, 3090–3099. [6.11.3]
- Nouri-Borjerdi, A., Noghrehabadi, A. R. and Rees, D. A. S. 2007b The effect of local thermal non-equilibrium on conduction in porous channels with a uniform heat source. *Transport Porous Media* **69**, 281–288. [2.2.3]
- Nouri-Borjerdi, A., Noghrehabadi, A. R. and Rees, D. A. S. 2007c Onset of convection in a horizontal porous channel with uniform heat generation using a thermal nonequilibrium model. *Transport Porous Media* **69**, 343–357. [6.11.2]
- Nouri-Borjerdi, A., Noghrehabadi, A. R. and Rees, D. A. S. 2008 Influence of the Darcy number on the onset of convection in a porous layer with a uniform heat source. *Int. J. Therm. Sci.* **47**, 1020–1025. [6.11.2]
- Nsofor, E. C. and Adebiyi, G. A. 2003 Forced-convection gas-to-wall heat transfer in a packed bed for high-temperature storage. *Exper. Heat Transfer* **16**, 81–95. [4.9]

- Nygard, H. S. and Tyvand, P. A. 2010 Onset of convection in a porous box with partly conducting and partly penetrative sidewalls. *Transp. Porous Media* **84**, 55–73. [6.15.3]
- Nygard, H. S. and Tyvand, P. A. 2011a Onset of convection in a vertical porous cylinder with partly conducting and partly penetrative cylindrical wall. *Transp. Porous Media* **86**, 259–271. [6.15.3]
- Nygard, H. S. and Tyvand, P. A. 2011b Onset of convection in a porous rectangle with buoyancy along an open sidewall. *Transp. Porous Media* **90**, 403–420. [6.15.1]
- O'Sullivan, M. J., Pruess, K. and Lippman, M. J. 2000 Geothermal reservoir simulation: the state-of-practice and emerging trends. Proc. World Geothermal Congr. 2000, Kyushu-Tohoku, Japan, pp. 4065–4070. [11]
- O'Sullivan, M. J., Pruess, K. and Lippman, M. J. 2001 State of the art of geothermal reservoir simulation. *Geothermics* **30**, 395–429. [11]
- Oberbeck, A. 1879 Ueber die Wärmeleitung der Flüssigkeiten bei Berücksichtigung der Strömungen infolge von Temperaturdifferenzen. *Ann. Phys. Chem.* **7**, 271–292. [2.3]
- Ochoa-Tapia, J. A. and Whitaker, S. 1995a Momentum transfer at the boundary between a porous medium and a homogeneous fluid — I. Theoretical development. *Int. J. Heat Mass Transfer* **38**, 2635–2646. [1.5.3, 1.6]
- Ochoa-Tapia, J. A. and Whitaker, S. 1995b Momentum transfer at the boundary between a porous medium and a homogeneous fluid—II. Comparison with experiment. *Int. J. Heat Mass Transfer* **38**, 2647–2655. [1.6]
- Ochoa-Tapia, J. A. and Whitaker, S. 1997 Heat transfer at the boundary between a porous medium and a heterogeneous fluid. *Int. J. Heat Mass Transfer* **40**, 2691–2707. [2.4]
- Ochoa-Tapia, J. A. and Whitaker, S. 1998 Momentum jump condition at the boundary between a porous medium and a homogeneous fluid: Inertia effects. *J. Porous Media* **1**, 201–207. [1.6]
- Ochoa-Tapia, J. A., Valdes-Parada, F. J. and Alvarez-Ramirez, J. 2007 A fractional-order Darcy's law. *Physica A* **374**, 1–14. [1.4.3]
- Okada, M., Matsumoto, K. and Yabushita, Y. 1994 Solidification around horizontal cylinder in porous medium saturated with aqueous solution. *Heat Transfer 1994, Inst. Chem. Engrs, Rugby*, vol. **4**, pp. 109–114. [10.2.3]
- OkhuySEN, B. S. and Riahi, D. N. 2008 Flow instabilities of liquid and mushy regions during alloy solidification and under high gravity environment induced by rotation. *Int. J. Engng. Sci.* **46**, 189–201. [10.2.3]
- Oldenburg, C. M. and Pruess, K. 1998 Layered thermohaline convection in hypersaline geothermal systems. *Transport Porous Media* **33**, 29–63. [11.8]
- Oldenburg, C. M. and Pruess, K. 1999 Plume separation by transient thermohaline convection in porous media. *Geophys. Res. Lett.* **26**, 2997–3000. [11.8]
- Olek, S. 1998 Heat transfer regimes for free convection in rotating porous media. *Heat Transfer 1998, Proc. 11th IHTC*, **4**, 423–428. [7.12]
- Oliveira, L. S. and Haghghi, K. 1998 Conjugate heat and mass transfer in convective drying of porous media. *Numer. Heat Transfer A* **34**, 105–117. [3.6]
- Oliver, M. and Titi, E. S. 2000 Gevrey regularity for the attractor of a partially dissipative model of Bénard convection in a porous medium. *J. Differ. Equations* **163**, 292–311. [6.15.1]
- Oliveski, R. D. C. and Macrczak, L. D. F. 2008 Natural convection in a cavity filled with a porous medium with variable porosity and Darcy number. *J. Porous Media* **11**, 655–667. [7.3.7]
- Oliveski, R. D. C. and Macrczak, L. D. F. 2008 Natural convection in a cavity filled with a porous medium with variable porosity and Darcy number. *J. Porous Media* **11**, 655–667. [7.3.7]
- Omsuthar, R., Bhaduria, B. S. and Khan, A. 2009 Modulated centrifugal convection in a vertical rotating porous layer distant from the axis of rotation. *Transp. Porous Media* **79**, 255–264. [6.22]
- Omsuthar, R., Bhaduria, B. S. and Khan, A. 2011 Rotating Brinkman-Lapwood convection with modulation. *Transp. Porous Media* **88**, 369–383. [6.22]
- Oosthuizen, P. H. 1987 Mixed convection heat transfer from a cylinder in a porous medium near an impermeable surface. *ASME HTD* **84**, 75–82. [8.1.3]

- Oosthuizen, P. H. 1988a The effects of free convection on steady-state freezing in a porous medium-filled cavity. *ASME HTD* **96**, Vol. 1, 321–327. [10.2.1]
- Oosthuizen, P. H. 1988b Mixed convective heat transfer from a heated horizontal plate in a porous medium near an impermeable surface. *ASME J. Heat Transfer* **110**, 390–394. [8.1.4]
- Oosthuizen, P. H. 1995 Heat transfer from a cylinder with a specified surface heat flux buried in a frozen porous medium in an enclosure with a cooled top surface. *Proc. ASME/JSME Thermal Engineering Joint Conf.* vol. 3, pp. 379–386. [7.11]
- Oosthuizen, P. H. 2000 Natural convective heat transfer in porous-media-filled enclosures. *Handbook of Porous Media* (K. Vafai, ed.), Marcel Dekker, New York, pp. 489–520. [7]
- Oosthuizen, P. H. and Naylor, D. 1996a Natural convective heat transfer from a cylinder in an enclosure partly filled with a porous medium. *Int. J. Numer. Meth. Heat Fluid Flow* **6**, 51–63. [7.11]
- Oosthuizen, P. H. and Naylor, D. 1996b Heat transfer from a heated cylinder with a specified surface heat flux buried in a frozen porous medium in an enclosure with non-uniform wall temperatures. *ASME HTD* **331**, 43–52. [7.11]
- Oosthuizen, P. H. and Paul, J. T. 1992 Heat transfer from a heated cylinder buried in a frozen porous medium in an enclosure. *Heat and Mass Transfer in Porous Media* (ed. M. Quintard and M. Toderovic), Elsevier, Amsterdam, pp. 315–326. [7.11]
- Or, A. C. 1989 The effects of temperature-dependent viscosity and the instabilities in convection rolls of a layer of fluid-saturated porous medium. *J. Fluid Mech.* **206**, 497–515. [6.8]
- Ordonez, J. C., Bejan, A. and Cherry, R. S. 2003 Designed porous media: Optimally nonuniform flow structures connecting one point with more points. *Int. J. Therm. Sci.* **42**, 857–870. [4.19]
- Ormond, A. and Genton, P. 1993 3-D thermoconvection in an anisotropic inclined sedimentary layer. *Geophys. J. Int.* **112**, 257–263. [11.8]
- Ormond, A. and Ortoleva, P. 2000 Numerical modeling of reaction-induced cavities in a porous rock. *J. Geophys. Res.—Solid Earth* **105**, 16737–16747. [11.8]
- Orozco, J. 1992 Condensation of a downward flowing vapor on a horizontal cylinder embedded in a porous medium. *ASME J. Energy Resour. Tech.* **113**, 300–304. [10.4]
- Orozco, J. and Zhu, K. H. 1993 Mixed convection film boiling of a binary mixture on a horizontal cylinder embedded in a porous medium. *Chem., Engng Comm.* **135**, 91–104. [10.3.2]
- Orozco, J., Stellman, R. and Gutjahr, M. 1988 Film boiling heat transfer from a sphere and a horizontal cylinder embedded in a liquid-saturated porous medium. *ASME J. Heat Transfer* **110**, 961–967. [10.3.2]
- O'Sullivan, M. J. 1985a Geothermal reservoir simulation. *Int. J. Energy Res.* **9**, 319–332. An edited version was reprinted in *Applied Geothermics* (eds. M. Economides and P. Ungemach), Wiley, New York, 1987. [11]
- O'Sullivan, M. J. 1985b Convection with boiling in a porous layer. *Convective Flows in Porous Media* (eds. R. A. Wooding and I. White), Dept. Sci. Indust. Res., Wellington, N.Z., pp. 141–155. [10.3.1]
- O'Sullivan, M. J. and McKibbin, R. 1986 Heat transfer in an unevenly heated porous layer. *Transport in Porous Media* **1**, 293–312. [6.14]
- Otero, J., Dontcheva, L. A., Johnston, H., Worthing, R. A., Kurganov, A., Petrova, G. and Doering, C. R. 2004 High-Rayleigh number convection in a fluid saturated porous layer. *J. Fluid Mech.* **500**, 263–282. [6.8]
- Ouarzazi, M. N. and Bois, P. A. 1994 Convective instability of a fluid mixture in a porous medium with time-dependent temperature gradient. *Eur. J. Mech. B/Fluids* **13**, 275–295. [9.1.6.4]
- Ouarzazi, M. N., Bois, P. A. and Taki, M. 1994 Nonlinear interaction of convective instabilities and temporal chaos of a fluid mixture in a porous medium. *Eur. J. Mech. B/Fluids* **13**, 423–438. [9.1.6.4]
- Ouarzazi, M. N., Mejni, F., Delache, A. and Labrosse, G. 2008a Nonlinear global modes in inhomogeneous mixed convection flows in porous media. *J. Fluid Mech.* **595**, 367–377. [6.10.1]

- Oueslati, F., Bennacer, R., Sammouda, H. and Belghith, A. 2008b Thermosolutal convection during melting in a porous medium saturated with aqueous solution. *Numer. Heat Transfer* **54**, 315–330. [10.1.7]
- Oueslati, F., Sammouda, H., Bennacer, R. and Belghith, A. 2006 Numerical study of thermosolutal convection in anisotropic porous media subject to cross-fluxes of heat and mass. *J. Porous Med.* **9**, 69–81. [9.5]
- Ouid-Amer, Y. and Bennacer, R. 2012 Free convection across a bilayered and inclined porous cavity submitted to nonsymmetrical heating. *J. Porous Media* **15**, 403–414. [7.8]
- Ould-Amer, Y., Chikh, S., Bouhadef, K. and Lauriat, G. 1998 Forced convection cooling enhancement by use of porous materials. *Int. J. Heat Fluid Flow* **19**, 251–258. [4.11]
- Ouattara, B., Khouzam, A., Mojtabi, A. and Charrier-Mojtabi, M. C. 2012 Analytical and numerical stability analysis of Soret-driven convection in a horizontal porous layer: the effect of conducting boundary plates. *Fluid Dyn. Res.* **44**, 031415. [9.1]
- Ozaki, K. and Inaba, H. 1997 Convective heat transfer of horizontal spherical particle layer heated from below and cooled above—Part II. Effect of thickness of the layer. *Heat Transfer Japan Res.* **26**, 176–192. [6.9.2]
- Ozdemir, M. and Ozguc, F. 1997 Forced convection heat transfer in porous medium of wire screen meshes. *Heat Mass Transfer* **33**, 129–136. [4.16.5]
- Oztop, H. F. 2006 Combined convection heat transfer in a porous lid-driven enclosure due to heater with finite length. *Int. Comm. Heat Mass Transfer* **33**, 772–779. [8.4.3]
- Oztop, H. F. 2007 Natural convection in partially cooled and inclined porous rectangular enclosures. *Int. J. Therm. Sci.* **46**, 149–156. [7.8]
- Oztop, H. F. and Varol, A.. 2009 Combined convection in inclined porous lid-driven enclosures with sinusoidal thermal boundary conditions. *Prog. Comput. Fluid Dyn.* **9**, 127–131. [8.1.1, 8.4.3]
- Oztop, H. F., Al-Salem, M. F. and Sun, S. Y. 2011a Combined effect of magnetic field and thermal dispersion on a non-Darcy mixed convection. *J. Them. Sci.* **20**, 276–282. [8.4.3]
- Oztop, H. F., Al-Salem, M. F., Varol, Y. and Pop, I. 2011b Natural convection heat transfer in a partially opened cavity filled with porous media. *Int. J. Heat Mass Transfer* **54**, 2253–2261. [7.1.7]
- Oztop, H. F., Varol, Y. and Pop, I. 2008 Effects of wall conduction on natural convection in a porous triangular enclosure. *Acta Mech.* **200**, 155–165. [7.3.6]
- Oztop, H. F., Varol, Y. and Pop, I. 2009 Investigation of natural convection in triangular enclosure filled with porous media saturated with water near 4 degrees C. *Energy Conv. Manag.* **50**, 1473–1480. [7.3.6]
- Paek, J. W., Kang, B. H. and Hyun, J. M. 1999a Transient cool-down of a porous medium in pulsating flow. *Int. J. Heat Mass Transfer* **42**, 3523–3527. [4.16.5]
- Paek, J. W., Kang, B. H., Kim, S. Y. and Hyun, J. M. 2000 Effective thermal conductivity and permeability of aluminum foam materials. *Int. J. Thermophys.* **21**, 435–464. [2.2.1]
- Paek, J. W., Kim, S. Y., Kang, B. H. and Hyun, J. M. 1999b Forced convective heat transfer from anisotropic aluminum foam in a channel flow. *Proc. 33rd Nat. Heat Transfer Conf., NHTC* 99–158. 1–8. [4.12]
- Paik, S., Nguyen, H. D. and Pop, I. 1998 Transient conjugate mixed convection from a sphere in a porous medium saturated with cold pure or saline water. *Heat Mass Transfer* **34**, 237–245. [8.1.3]
- Pak, J. and Plumb, O. A. 1997 Melting in a two-component packed bed. *ASME J. Heat Transfer* **119**, 553–559. [10.1.7]
- Pakdee, W. and Rattanadecho, P. 2006 Unsteady effects on natural convective heat transfer through porous media in cavity due to top surface partial convection. *Appl. Thermal Engng.* **26**, 2316–2326. [6.18]
- Pakdee, W. and Rattanadecho, P. 2009 Numerical analysis of natural convection in porous cavities with partial convective cooling conditions. *J. Porous Media* **12**, 1083–1100. [6.18]

- Pakdee, W. and Rattanadecho, P. 2011 Natural convection in a saturated variable porosity medium due to microwave heating. *ASME J. Heat Transfer* **133**, #062502. [6.11.2]
- Pal, D. 2010 Magnetohydrodynamic non-Darcy mixed convection heat transfer from a vertical heated plate embedded in a porous medium with variable porosity. *Comm. Nonlinear Sci. Numer. Simul.* **15**, 3974–3987. [8.1.6]
- Pal, D. and Chatterjee, S. 2010 Heat and mass transfer in MHD non-Darcian flow of a micropolar fluid over a stretching sheet embedded in a porous media with non-uniform heat source and thermal radiation. *Comm. Nonlinear Sci. Numer. Simul.* **15**, 1843–1857. [9.2.1]
- Pal, D. and Chatterjee, S. 2011 Mixed convection magnetohydrodynamic heat and mass transfer past a stretching surface in a micropolar fluid-saturated porous medium under the influence of Ohmic heating, Soret and Dufour effects. *Comm. Nonlinear Sci. Numer. Simul.* **16**, 1329–1346. [9.6.1]
- Pal, D. and Hiremath, P. S. 2010 Computational modeling of heat transfer over an unsteady stretching surface embedded in a porous medium. *Meccanica* **45**, 415–424. [5.1.9.9]
- Pal, D. and Mondal, H. 2009 Radiation effects on combined convection over a vertical flat plate embedded in a porous medium of variable porosity. *Meccanica* **44**, 133–144. [8.1.1]
- Pal, D. and Mondal, H. 2010a Effect of variable viscosity on MHD non-Darcy mixed convection heat transfer over a stretching sheet embedded in a porous medium with non-uniform heat source/sink. *Comm. Nonlinear Sci. Numer. Simul.* **15**, 1553–1564. [8.1.1]
- Pal, D. and Mondal, H. 2010b Hydromagnetic non-Darcy flow and heat transfer over a stretching sheet in the presence of thermal radiation and ohmic dissipation. *Comm. Nonlinear Sci. Numer. Simul.* **15**, 1197–1209. [9.2.1]
- Pal, D. and Mondal, H. 2011a Effects of Soret, Dufour, chemical reaction and thermal radiation on MHD non-Darcy unsteady mixed convective heat and mass transfer over a stretching sheet. *Comm. Nonlinear Sci. Numer. Simul.* **16**, 1942–1958. [9.6.1]
- Pal, D. and Mondal, H. 2011b MHD non-Darcian mixed convection heat and mass transfer over a non-linear stretching sheet with Soret-Dufour effects and chemical reaction. *Int. Comm. Heat Mass Transfer* **38**, 463–467. [9.6.1]
- Pal, D. and Mondal, H. 2011c Influence of thermal radiation on hydrodynamic Darcy-Forchheimer mixed convection flow past a stretching sheet embedded in a porous medium. *Meccanica* **46**, 739–753. [8.1.6]
- Pal, D. and Mondal, H. 2012a MHD non-Darcy mixed convective diffusion of species over a stretching sheet embedded in a porous medium with non-uniform heat source/sink, variable viscosity and Soret effect. *Comm. Nonlinear Sci. Numer. Simul.* **17**, 672–684.
- Pal, D. and Mondal, M. 2012b Hydromagnetic convective diffusion of species in Darcy-Forchheimer porous medium with non-uniform heat source/sink and variable viscosity. *Int. Comm. Heat Mass Transfer* **39**, 913–917. [9.2.1]
- Pal, D. and Talukdar, B. 2010 Buoyancy and chemical reaction effects on MHD mixed convection heat and mass transfer in a porous medium with thermal radiation and Ohmic heating. *Comm. Nonlinear Sci. Numer. Simul.* **15**, 2878–2893. [9.6.1]
- Pal, D. and Talukdar, B. 2011 Combined effects of Joule heating and chemical reaction on unsteady magnetohydrodynamic mixed convection of a viscous dissipating fluid over a vertical plate in porous media with thermal radiation. *Math. Comput. Mod.* **54**, 3016–3036. [9.6.1]
- Pal, D. and Talukdar, B. 2012 Influence of fluctuating thermal and mass diffusion on unsteady MHD buoyancy driven convection past a vertical surface with chemical reaction and Soret effects. *Comm. Nonlinear Sci. Numer. Simul.* **17**, 1597–1614. [9.2.3]
- Pallares, J. and Grau, F. X. 2010 A modification of a Nusselt number correlation for forced convection in porous media. *Int. Comm. Heat Mass Transfer* **37**, 1187–1190. [2.2.3]
- Palm, E. 1990 Rayleigh convection, mass transport, and change in porosity in layers of sandstone. *J. Geophys. Res.* **95**, 8675–8679. [11.5]
- Palm, E. and Tveitereid, M. 1979 On heat and mass flux through dry snow. *J. Geophys. Res.* **84**, 745–749. [11.1, 11.5]

- Palm, E. and Tyvand, P. 1984 Thermal convection in a rotating porous layer. *J. Appl. Math. Phys. (ZAMP)* **35**, 122–123. [6.22]
- Palm, E., Weber, J. E. and Kvernvold, O. 1972 On steady convection in a porous medium. *J. Fluid Mech.* **54**, 153–161. [6.3, 6.6]
- Pan, C. P. and Lai, F. C. 1995 Natural convection in horizontal-layered porous annuli *AIAA J. Thermophys. Heat Transfer* **9**, 792–795. [7.3.3]
- Pan, C. P. and Lai, F. C. 1996 Re-examination of natural convection in a horizontal layered porous annulus. *ASME J. Heat Transfer* **118**, 990–992. [7.3.3]
- Panilov, M. and Fourar, M. 2006 Physical splitting of nonlinear effects in high-velocity stable flow through porous media. *Adv. Water Resources* **29**, 30–41. [1.5.2]
- Pantokratoras, A. 2006 Natural convection of air and water with variable thermophysical properties about a vertical isothermal flat plate embedded in a Darcy porous medium. *Prog. Comput. Fluid Dyn.* **6**, 498–510. [5.1.9.9]
- Pantokratoras, A. 2007a Fully developed Couette flow of three fluids with variable thermophysical properties flowing through a porous medium channel heated asymmetrically with large temperature difference. *ASME J. Heat Transfer* **129**, 1742–1747. [4.16.1]
- Pantokratoras, A. 2007b Fully developed forced convection of three fluids with variable thermophysical properties flowing through a porous medium channel heated asymmetrically with large temperature differences. *J. Porous Media* **10**, 409–419. [4.16.1]
- Pantokratoras, A. 2007c Non-Darcian forced convection heat transfer over a flat plate in a porous medium with variable viscosity and variable Prandtl number. *J. Porous Media* **10**, 201–208. [4.8]
- Pantokratoras, A. 2008b Comment on “Unsteady MHD combined convection over a moving vertical sheet in a fluid saturated porous medium with uniform surface heat flux”, S.S.M. El-Kabeir, A. M. Rashad, Rama Subba Gorla, Mathematical and Computer Modelling 46 (2007) 384–397. *Math. Comput. Modelling* **48**, 662–663. [8.1.6]
- Pantokratoras, A. 2008a Comment on “Radiative effect of natural convection flows in porous media”, A. A. Mohammadein, M. A. Mansour, Sahar M. Abd el Gaiel and Rama Subba Gorla [Transport in Porous Media 32: 263–283. 1998. *Transp. Porous Media* **75**, 273–274. [5.1.9.4]
- Pantokratoras, A. 2008c Mixed convection in a vertical porous channel (vol. 61, pg 315, 2005). *Transp. Porous Media* **74**, 347–348. [8.3.1]
- Pantokratoras, A. 2009a Comments on “Perturbation analysis of radiative effect on free convection flows in porous medium in presence of pressure work and dissipation, by A. M. Rashad [Commun. Nonlinear Sci. Numer. Simul. 2009: 14: 140–153. *Commun. Nonlinear Sci. Numer. Simul.* **14**, 345–346. [5.1.9.4]
- Pantokratoras, A. 2009b Mixed convection in water near the density extremum along a vertical plate with a sinusoidal surface temperature variation embedded in a porous medium. *Transp. Porous Media* **76**, 309–325. [8.1.6]
- Pantokratoras, A. and Magyari, E. 2010 Forced convection flow of power-law fluids over a flat plate embedded in a Darcy-Brinkman porous medium. *Transp. Porous Media* **85**, 143–155. [4.16.3]
- Papathanasiou, T. D., Markicevic, B. and Dendy, E. D. 2001 A computational evaluation of the Ergun and Forchheimer equations for fibrous porous media. *Phys. Fluids* **13**, 2795–2804. [1.5.2]
- Parang, M. and Keyhani, M. 1987 Boundary effects in laminar mixed convection flow through an annular porous medium. *ASME J. Heat Transfer* **109**, 1039–1041. [8.3.3]
- Park, H. M., Lee, H. S. and Cho, D. H. 1996 Thermal convective instability in translucent porous media with radiative heat transfer. *Chem. Engng. Comm.* **145**, 155–171. [6.11.2]
- Park, J. H., Chung, T. J., Choi, C. K. and Kim, M. C. 2006 The onset of mixed convection in a porous layer heated with a constant heat flux. *AIChE J.* **52**, 2677–2683. [6.10.1]
- Parmentier, E. M. 1979 Two-phase natural convection adjacent to a vertical heated surface in a permeable medium. *Int. J. Heat Mass Transfer* **22**, 849–855. [10.3.2]

- Partha, M. K. 2008 Thermophoresis particle deposition in a non-Darcy porous medium under the influence of Soret, Dufour effects. *Heat Mass Transfer* **44**, 969–977. [9.2.1]
- Partha, M. K. 2009 Suction/injection effects on thermophoresis particle deposition in a non-Darcy porous medium under the influence of Soret, Dufour effects. *Int. J. Heat Mass Transfer* **52**, 1971–1979. [9.2.1]
- Partha, M. K. 2010 Nonlinear convection in a non-Darcy porous medium. *Appl. Math. Mech. English Edition* **31**, 565–574. [9.1.4]
- Partha, M. K., Murthy, P. V. S. N. and Raja Sekhar, G. P. 2006 Soret and Dufour effects in a non-Darcy porous medium. *ASME J. Heat Transfer* **128**, 605–610. [9.2.1]
- Parthiban, C. and Patil, P. R. 1993 Effect of inclined temperature gradient on thermal instability in an anisotropic porous medium. *Wärme-Stoffübertrag.* **29**, 63–69. [7.9]
- Parthiban, C. and Patil, P. R. 1994 Effect of inclined gradients on thermohaline convection in porous medium. *Wärme-Stoffübertrag.* **29**, 291–297. [9.5]
- Parthiban, C. and Patil, P. R. 1995 Effect of non-uniform boundary temperatures on thermal instability in a porous medium with internal heat source. *Int. Comm. Heat Mass Transfer* **22**, 683–692. [6.11.2, 7.9]
- Parthiban, C. and Patil, P. R. 1996 Convection in a porous medium with velocity slip and temperature jump boundary conditions. *Heat Mass Transfer* **32**, 7–31. [6.7]
- Parthiban, C. and Patil, P. R. 1997 Thermal instability in an anisotropic porous medium with internal heat source and inclined temperature. *Int. Comm. Heat Mass Transfer* **24**, 1049–1058. [7.9]
- Parvathy, C. P. and Patil, P. R. 1989 Effect of thermal diffusion on thermohaline interleaving in a porous medium due to horizontal gradients. *Indian J. Pure Appl. Math.* **20**, 716–727. [9.5]
- Pascal, H. 1990 Rheological effects of non-Newtonian fluids on natural convection in a porous medium. [5.1.9.2]
- Pascal, J. P. and Pascal, H. 1997 Free convection in a non-Newtonian fluid saturated porous medium with lateral mass flux. *Int. J. Non-Linear Mech.* **32**, 471–482. [5.7]
- Paterson, I. and Schlanger, H. P. 1992 Convection in a porous thermosyphon imbedded in a conducting medium. *Int. J. Heat Mass Transfer* **35**, 877–886. [11.8]
- Patil, P. M. 2008 Effects of free convection on the oscillatory flow of a polar fluid through a porous medium in presence of variable heat flux. *J. Engng. Phys. Thermophys.* **81**, 905–922. [5.1.9.2]
- Patil, P. M. and Kulkarni, P. S. 2008 Effects of chemical reaction on free convective flow of a polar fluid through a porous medium in the presence of internal heat generation. *Int. J. Therm. Sci.* **47**, 1043–1054. [9.2.1]
- Patil, P. M., Chamkha, A. J. and Roy, S. 2012 Effects of chemical reaction on mixed convection flow of a polar fluid through a porous medium in the presence of internal heat generation. *Mecanica* **47**, 483–499. [9.6]
- Patil, P. R. 1982 Soret driven instability of a reacting fluid in a porous medium. *Israel J. Tech.* **19**, 193–196. [9.1.6.4]
- Patil, P. R. and Rudraiah, N. 1973 Stability of hydromagnetic thermoconvective flow through porous medium. *Trans. ASME, J. Appl. Mech. E* **40**, 879–884. [6.21]
- Patil, P. R. and Rudraiah, N. 1980 Linear convective stability and thermal diffusion of a horizontal quiescent layer of a two-component fluid in a porous medium. *Int. J. Engng. Sci.* **18**, 1055–1059. [9.1.4]
- Patil, P. R. and Subramanian, L. 1992 Soret instability in anisotropic porous medium with temperature dependent viscosity. *Fluid Dyn. Res.* **10**, 159–168. [9.1.6.2]
- Patil, P. R. and Vaidyanathan, G. 1981 Effect of variable viscosity on the setting up of convection currents in a porous medium. *Int. J. Engng. Sci.* **19**, 421–426. [6.7]
- Patil, P. R. and Vaidyanathan, G. 1982 Effect of variable viscosity on thermohaline convection in a porous medium. *J. Hydrol.* **57**, 147–161. [9.1.6.2]
- Patil, P. R. and Vaidyanathan, G. 1983 On setting up of convective currents in a rotating porous medium under the influence of variable viscosity. *Int. J. Engng Sci.* **21**, 123–130. [6.22]

- Patil, P. R., Parvathy, C. P. and Venkatakrishnan, K. S. 1990 Effect of rotation on the stability of a doubly diffusive layer in a porous medium. *Int. J. Heat Mass Transfer* **33**, 1073–1080. [9.1.6.4]
- Patil, P. R., Parvathy, C.P. and Venkatakrishnan, K. S. 1989 Thermohaline instability in a rotating anisotropic porous medium. *Appl. Sci. Res.* **46**, 73–88. [9.1.6.4]
- Pau, G. S. H., Bell, J. B., Pruess, K., Almgren, A. S., Lijewski, M. J. and Zhang, K. N. 2010 High-resolution simulation and characterization of density-driven flow in CO<sub>2</sub> storage in saline aquifers. *Adv. Water Res.* **33**, 443–455. [11.11]
- Paul, T. and Singh, A. K. 1998 Natural convection between co-axial vertical cylinders partially filled with a porous material. *Forschung Ingen.* **64**, 157–162. [7.7]
- Paul, T., Jha, B. K. and Singh, A. K. 1998 Free-convection between vertical walls partially filled with porous medium. *Heat Mass Transfer* **33**, 515–519. [7.7]
- Paul, T., Singh, A. K. and Misra, A. K. 2001 Transient natural convection between two vertical walls filled with a porous material having variable porosity. *Math. Engng. Ind.* **8**, 177–185. [7.5]
- Paul, T., Singh, A. K., and Thorpe, G. R. 1999 Transient natural convection in a vertical channel partially filled with a porous medium. *Math. Engng. Ind.* **7**, 441–455. [7.7]
- Pavel, B. I. and Mohamad, A. A. 2004a An experimental and numerical study on heat transfer enhancement for gas heat exchangers fitted with porous media. *Int. J. Heat Mass Transfer* **47**, 4939–4952. [4.11]
- Pavel, B. I. and Mohamad, A. A. 2004b Experimental and numerical investigation of heat transfer enhancement using porous material. In Applications of Porous Media (ICAPM 2004), (eds. A. H. Reis and A. F. Miguel), Évora, Portugal, pp. 331–338. [4.11]
- Pavel, B. I. and Mohamad, A. A. 2004c Experimental investigation of the potential of metallic porous inserts in enhancing forced convection heat transfer. *ASME J. Heat Transfer* **126**, 540–545. [4.11]
- Payne, L. E. and Song, J. C. 1997 Spatial decay estimates for the Brinkman and Darcy flows in a semi-infinite cylinder. *Cont. Mech. Thermodyn.* **9**, 175–190. [1.5.3]
- Payne, L. E. and Song, J. C. 2000 Spatial decay for a model of double diffusive convection in Darcy and Brinkman flow. *Z. Angew. Math. Phys.* **51**, 867–889. [1.5.3]
- Payne, L. E. and Song, J. C. 2002 Spatial decay bounds for the Forchheimer equation. *Int. J. Engng. Sci.* **40**, 943–956. [1.5.3]
- Payne, L. E. and Straughan, B. 1998a Analysis of the boundary condition at the interface between a viscous fluid and a porous medium and related modelling questions. *J. Math. Pures Appl.* **77**, 317–354. [1.6]
- Payne, L. E. and Straughan, B. 1998b Structure stability for the darcy equations of flow in porous media. *Proc. Roy. Soc. Lond. A.* **454**, 1691–1698. [1.5.3]
- Payne, L. E. and Straughan, B. 1999 Convergence and continuous dependence for the Brinkman–Forchheimer equations. *Stud. Appl. Math.* **102**, 419–439. [1.5.3]
- Payne, L. E. and Straughan, B. 2000a A naturally efficient numerical technique for porous convection stability with non-trivial boundary conditions. *Int. J. Numer. Anal. Meth. Geomech.* **24**, 815–836. [11.8]
- Payne, L. E. and Straughan, B. 2000b Unconditional nonlinear stability in temperature-dependent viscosity flow in a porous medium. *Stud. Appl. Math.* **105**, 59–81. [6.7]
- Payne, L. E., Rodrigues, J. F. and Straughan, B. 2001 Effect of anisotropic permeability on Darcy's law. *Math. Meth. Appl. Sci.* **24**, 427–438. [1.5.3]
- Payne, L. E., Song, J. C. and Straughan, B. 1988 Double-diffusive porous penetrative convection — thawing subsea permafrost. *Int. J. Engng. Sci.* **26**, 797–809. [11.3]
- Payne, L., Song, J. and Straughan, B. 1999 Continuous dependence and convergence results for Brinkman and Forchheimer models with variable viscosity. *Proc. Roy. Soc. Londaon A* **455**, 2173–2190. [1.5.3]
- Pedram Razi, Y., Charrier-Mojtabi, M. C. and Mojtabi, A. 2008 Thermal vibration convection in a porous medium saturated by a pure or binary fluid. In P. Vadasz (ed.) Emerging Topics in Heat and Mass Transfer in Porous Media, Springer, New York, pp. 149–17. [6.24]

- Pedram Razi, Y., Maliwan, K. and Mojtabi, A. 2002 Two different approaches for studying the Horton-Rogers-Lapwood problem under the effect of vertical vibration. *Proc. 1st Int. Conf. Applications of Porous Media*. pp. 479–488. [6.24]
- Pedram Razi, Y., Maliwan, K., Charrier-Mojtabi, M. C. and Mojtabi, A. 2005 Influence of vibrations on buoyancy induced convection in porous media. *Handbook of Porous Media* (ed. K. Vafai), 2nd ed., Taylor and Francis, New York, pp. 321–370. [6.24]
- Pedram Razi, Y., Mojtabi, I. and Charrier-Mojtabi, M.C. 2009 A summary of new predictive high frequency thermo-vibrational modes in porous media. *Transp. Porous Media* **77**, 207–208. [6.24]
- Pedras, M. H. J. and de Lemos, M. J. S. 2000 On the definition of turbulent kinetic energy for flow in porous media. *Int. Comm. Heat Mass Transfer* **27**, 211–220. [1.8]
- Pedras, M. H. J. and de Lemos, M. J. S. 2001a Macroscopic turbulence modeling for incompressible flow through undeformable porous media. *Int. J. Heat Mass Transfer* **44**, 1081–1093. [1.8]
- Pedras, M. H. J. and de Lemos, M. J. S. 2001b Simulation of turbulent flow in porous media using a spatially periodic array and low Re two-equation closure. *Numer. Heat Transfer A* **39**, 35–59. [1.8]
- Pedras, M. H. J. and de Lemos, M. J. S. 2001c On the mathematical description and simulation of turbulent flow in a porous medium formed by an array of elliptical rods. *ASME J. Fluids Engng.* **123**, 941–947. [1.8]
- Pedras, M. H. J. and de Lemos, M. J. S. 2003 Computation of turbulent flow in porous media using a low Reynolds number  $k - \epsilon$  model and an infinite array of transversely displaced elliptic rods. *Numer. Heat Transfer A* **43**, 585–602. [1.8]
- Peirotti, M. B., Giavedoni, M. D. and Deiber, J. A. 1987 Natural convective heat transfer in a rectangular porous cavity with variable fluid properties – validity of the Boussinesq approximation. *Int. J. Heat Mass Transfer* **30**, 2571–2581. [7.3.2]
- Peng, C., Zeng, T. and Cheng, G. 1992 Free convection about vertical needles embedded in a saturated porous medium *AIAA J. Thermophys. Heat Transfer* **6**, 558–561. [5.12.1]
- Peng, S. W., Besant, R. W. and Strathdee, G. 2000 Heat and mass transfer in granular potash fertilizer with a surface dissolution reaction. *Cand. J. Chem. Engng.* **78**, 1076–1086. [3.6]
- Peppin, S. S. L., Aussillous, P., Huppert, H. E. and Worster, M.G. 2007 Steady-state mushy layers: experiments and theory. *J. Fluid Mech.* **570**, 69–77. [10.2.3]
- Peppin, S. S. L., Huppert, H. E. and Worster, M. G. 2008 Steady-state solidification of aqueous ammonium chloride. *J. Fluid Mech.* **599**, 465–476. [10.2.3]
- Perng, S. W., Wu, H. W., Wang, R. H. and Jue, T. C. 2011 Unsteady convection heat transfer for a porous square cylinder varying cylinder-to-channel height ratio. *Int. J. Therm. Sci.* **50**, 2006–2015. [4.9]
- Pestov, I. 1997 Structured geothermal systems: application of dimensional methods. *Mathl. Comput. Modelling* **25**, 43–63. [11.9.1]
- Pestov, I. 1998 Stability of vapour-liquid counterflow in porous media. *J. Fluid Mech.* **364**, 273–295. [11.9.1]
- Peterson, G. P. and Chang, C. S. 1997 Heat transfer analysis and evaluation for two-phase flow in porous-channel heat sinks. *Numer. Heat Transfer A* **31**, 113–130. [11.9.3]
- Peterson, G. P. and Chang, C. S. 1998 Two-phase heat dissipation utilizing porous-channels of high-conductivity material. *ASME J. Heat Transfer* **120**, 243–252. [11.9.3]
- Peterson, J. W., Murray, B. T. and Carey, G. F. 2010 Multi-resolution simulation of double-diffusive convection in porous media. *Int. J. Numer. Meth. Heat Fluid Flow* **20**, 37–65. [9.1.3]
- Petit, F., Fichot, F. and Quintard, M. 1999 Two-phase flow in porous media: local non-equilibrium model. *Rev Gén. Therm.* **38**, 250–257. [2.2.3]
- Petrusch, J., Meier, F., Friess, H. and Steinfeld, A. 2008 Tomography based determination of permeability, Dupuit-Forchheimer coefficient, and interfacial heat transfer coefficient in reticulate porous ceramics. *Int. J. Heat Fluid Flow* **29**, 315–326. [2.6]
- Petrescu, S. 1994 Comments on the optimal spacing of parallel plates cooled by forced convection. *Int. J. Heat Mass Transfer* **37**, 1283. [4.15, 4.19, 4.20]
- Phanikumar, M. S. and Mahajan, R. L. 2002 Non-Darcy natural convection in high porosity metal foams. *Int. J. Heat Mass Transfer* **45**, 3781–3793. [7.3.7]

- Philip, J. R. 1982a Free convection at small Rayleigh number in porous cavities of rectangular, elliptical, triangular and other cross sections. *Int. J. Heat Mass Transfer* **25**, 1503–1510. [7.3.7]
- Philip, J. R. 1982b Axisymmetric free convection at small Rayleigh number in porous cavities. *Int. J. Heat Mass Transfer* **25**, 1689–1699. [7.3.7]
- Philip, J. R. 1988 Free convection in porous cavities near the temperature of maximum density. *Phys. Chem. Hydron.* **10**, 283–294. [7.3.7]
- Phillips, O. M. 1991 Flow and Reactions in Permeable Rocks, Cambridge Univ. Press, New York. [11.5]
- Phillips, O. M. 2009 Geological Fluid Dynamics: Subsurface Flow and Reactions, Cambridge University Press, Cambridge, UK. [11], [11.12]
- Pien, S. J. and Sen, M. 1989 Hysteresis effects in three-dimensional natural convection in a porous medium. ASME HTD 107, 343–348. [7.8]
- Pieters, G. J. M. and Schuttlelaars, H. M. 2008 On the nonlinear dynamics of a saline boundary layer formed by throughflow near the surface of a porous medium. *Physica D* **237**, 3075–3088. [9.1.6.4]
- Pieters, G. J. M. and van Duijn, C. J. 2006 Transient growth in linearly stable gravity-driven flow in porous media. *European J. Mech.* **25**, 83–94. [6.10.2]
- Pillatsis, G., Taslim, M. E. and Narusawa, U. 1987 Thermal instability of a fluid-saturated porous medium bounded by thin fluid layers. *ASME J. Heat Transfer* **109**, 677–682. [6.19.1.2]
- Pillay, S. K and Govender, S. 2005 Stability of convection in a gravity modulated mushy layer during solidification of binary alloys. *Transp. Porous Media* **60**, 183–197. [6. 24, 10.2.3]
- Pillay, S. K and Govender, S. 2007 Moderate time scale finite amplitude analysis of large Stefan number convection in a gravity modulated mushy layer during the solidification of binary alloys. *Transp. Porous Media* **69**, 331–341. [10.2.3]
- Piller, M. and Stalio, E. 2012 Numerical investigation of natural convection in inclined parallel-plate channels partly filled with metal foams. *Int. J. Heat Mass Transfer* **55**, 6506–6513. [7.7]
- Pinson, F., Gregoire, O. and Simonin, O. 2006 Kappa-epsilon macroscale modeling of turbulence based on a two-scale analysis in porous media. *Int. J. Heat Fluid Flow* **27**, 955–966. [1.8]
- Pinson, F., Gregoire, O. and Simonin, O. 2007 Macroscale turbulence modeling for flows in media laden with solid structures. *Comptes Rendus Mecanique* **335**, 13–19. [1.8]
- Platten, J. K. and Costeseque, P. 2004 The Soret coefficient in porous media. *J. Porous Media* **7**, 317–329. [3.3]
- Platten, J. K. and Legros, J. C. 1984 Convection in Liquids, Springer, New York. [3.3]
- Ploude, F. and Prat, M. 2003 Pore network simulations of drying of capillary porous media. Influence of thermal gradient. *Int. J. Heat Mass Transfer* **46**, 1293–1307. [3.6]
- Plumb, O. A. 1998 The effect of thermal dispersion on heat transfer in packed bed boundary layers. Proc. ASME JSME Thermal Engineering Joint Conference **2**, 17–22. [5.1.7.3]
- Plumb, O. A. 1991a Heat transfer during unsaturated flow in porous media. Convective Heat and Mass Transfer in Porous Media (eds S. Kakaç, B. Kilkis, F. A. Kulacki and F. Arinç), Kluwer Academic, Dordrecht, 435–464. [3.6]
- Plumb, O. A. 1991b Drying complex porous materials – modelling and experiments. Convective Heat and Mass Transfer in Porous Media (eds. S. Kakaç, B. Kilkis, F. A. Kulacki and F. Arinç), Kluwer Academic, Dordrecht, 963–984. [3.6]
- Plumb, O. A. 1994a Convective melting of packed beds. *Int. J. Heat Mass Transfer* **37**, 829–836. [10.1.7]
- Plumb, O. A. 1994b Analysis of near wall heat transfer in porous media. Heat Transfer 1994, *Inst. Chem. Engrs, Rugby*, vol. **5**, pp. 363–368. [4.8]
- Plumb, O. A. 2000 Transport phenomena in porous media: modeling the drying process. Handbook of Porous Media (K. Vafai, ed.), Marcel Dekker, New York., pp. 755–785. [3.6]
- Plumb, O. A. and Huenefeld, J. C. 1981 Non-Darcy natural convection from heated surfaces in saturated porous media. *Int. J. Heat Mass Transfer* **24**, 765–768. [5.1.7.2, 5.1.8]
- Poirier, D. R., Nandapurkar, P.J . and Ganesan, S. 1991 The energy and solute conservation equations for dendritic solidification. *Metall. Trans. B* **22**, 889–900. [10.2.3]

- Poirier, H. 2003 Une théorie explique l'intelligence de la nature. *Science & Vie* **1034**, 44–63. [4.18]
- Polyaev, V. M., Mozhaev, A. P., Galitseysky, B. A. and Lozhkin, A. L. 1996 A study of internal heat transfer in nonuniform porous structures. *Expt. Therm. Fluid Sci.* **12**, 426–432. [2.2.3]
- Pop, I. 2004 Some boundary-layer problems in convective flows. In *Emerging Technologies and Techniques in Porous Media* (D. B. Ingham, A. Bejan, E. Mamut and I. Pop, eds), Kluwer Academic, Dordrecht, pp. 65–91. [5]
- Pop, I. 2011 Reply to the Paper TIPM1512: Note on the “Scaling transformations for boundary layer flow near the stagnation point on a heated permeable stretching surface in a porous medium saturated with a nanofluid and heat generation/absorption effects.” by E. Magyari . *Transp. Porous Media* **87**, 49–51.[5.1.9.9]
- Pop, I. and Cheng, P. 1986 An integral solution for free convection of a Darcian fluid about a cone with curvature effects. *Int. Comm. Heat Mass Transfer* **13**, 433–438. [5.8]
- Pop, I. and Gorla, R. S. R. 1991 Horizontal boundary-layer natural convection in a porous medium saturated with a gas. *Transport in Porous Media* **6**, 159–171. [5.2]
- Pop, I. and Herwig, H. 1990 Transient mass transfer from an isothermal vertical flat plate embedded in a porous medium. *Int. Comm. Heat Mass Transfer* **17**, 813–821. [9.5]
- Pop, I. and Herwig, H. 1992 Free convection from a vertical surface in a porous medium saturated with fluids of variable properties: an asymptotic approach. *Heat and Mass Transfer in Porous Media* (ed. M. Quintard and M. Todorovic), Elsevier, Amsterdam, 337–348. [5.1.9.9]
- Pop, I. and Ingham, D. B. 1990 Natural convection about a heated sphere in a porous medium. *Heat Transfer 1990, Hemisphere*, New York, vol. 2, pp. 567–572. [5.6.2, 5.6.3]
- Pop, I. and Ingham, D. B. 2000 Convective boundary layers in porous media: external flows. *Handbook of Porous Media* (K. Vafai, ed.), Marcel Dekker, New York., pp. 313–356. [5]
- Pop, I. and Ingham, D. B. 2001 Convection Heat Transfer: Mathematical and Computational Modelling of Viscous Fluids and Porous Media, Elsevier, Oxford. [5]
- Pop, I. and Merkin, J. H. 1995 Conjugate free convection on a vertical surface in a saturated porous medium. *Fluid Dyn. Res.* **16**, 71–86. [5.1.5]
- Pop, I. and Na, N. Y. 1994 Natural convection of a Darcian fluid about a wavy cone. *Int. Comm. Heat Mass Transfer* **21**, 891–899. [5.8]
- Pop, I. and Na, T. Y. 1995 Natural convection over a frustum of a wavy cone in a porous medium. *Mech. Res. Comm.* **22**, 181–190. [5.8]
- Pop, I. and Na, T. Y. 1997 Free convection from an arbitrarily inclined plate in a porous medium. *Heat Mass Transfer* **32**, 55–59. [5.3]
- Pop, I. and Na, T. Y. 1998 Darcian mixed convection along slender vertical cylinders with variable surface heat flux embedded in a porous medium. *Int. Comm. Heat Mass Transfer* **25**, 251–260. [8.1.3]
- Pop, I. and Na, T. Y. 2000 Conjugate free convection over a vertical slender hollow cylinder embedded in a porous medium. *Heat Mass Transfer* **36**, 375–379. [5.7]
- Pop, I. and Nakayama, A. 1994 Conjugate free convection from long vertical plate fins in a non-Newtonian fluid-saturated porous medium. *Int. Comm. Heat Mass Transfer* **21**, 297–305. [5.12.1]
- Pop, I. and Nakayama, A. 1999 Conjugate free and mixed convection heat transfer from vertical fins embedded in porous media. In *Recent advances in Analysis of Heat Transfer for Fin Type Surfaces* (B. Sundén and P. J. Heggs, eds.), Computational Mechanics Publications, Southampton, pp. 67–96. [5.12.1]
- Pop, I. and Yan, B. 1998 Forced convection flow past a circular cylinder and a sphere in a Darcian fluid at large Péclet numbers. *Int. Comm. Heat Mass Transfer* **25**, 261–267. [4.3]
- Pop, I., Angirasa, D. and Peterson, G. P., 1997 Natural convection in porous media near L-shaped corners. *Int. J. Heat Mass Transfer* **40**, 485–490. [5.12.2]
- Pop, I., Cheng, P. and Le, T. 1989 Leading edge effects on free convection of a Darcian fluid about a semi-infinite vertical plate with uniform heat flux. *Int. J. Heat Mass Transfer* **32**, 493–501. [5.1.6]

- Pop, I., Harris, S. D., Ingham, D. B. and Rhea, S. 2003 Three-dimensional stagnation point free convection on a reactive surface in a porous medium. *Int. J. Energy Res.* **27**, 919–939. [5.12.3]
- Pop, I., Ingham, D. B. and Bradean, R. 1996 Transient free convection about a horizontal circular cylinder in a porous medium with constant surface flux heating, *Acta Mech.* **119**, 79–91. [5.5.1]
- Pop, I., Ingham, D. B. and Cheng, P. 1992a Transient natural convection in a horizontal concentric annulus filled with a porous medium. *ASME J. Heat Transfer* **114**, 990–997. [7.3.3]
- Pop, I., Ingham, D. B. and Cheng, P. 1992a Transient free convection about a horizontal circular cylinder in a porous medium. *Fluid Dyn. Res.*, **12**, 295–305. [5.5.1]
- Pop, I., Ingham, D. B. and Cheng, P. 1993b Transient free convection between two concentric spheres filled with a porous medium *AIAA J. Thermophys. Heat Transfer* **7**, 724–727. [7.5]
- Pop, I., Ingham, D. B. and Merkin, J. H. 1998a Transient convection heat transfer in a porous medium: External flows. *Transport Phenomena in Porous Media* (eds. D.B. Ingham and I. Pop), Elsevier, Oxford, pp. 205–232. [5.1.3]
- Pop, I., Ingham, D. B. and Miskin, I. 1995a Mixed convection in a porous medium produced by a line heat source. *Transport in Porous Media* **18**, 1–13. [8.1.4]
- Pop, I., Ingham, D. B., Heggs, P. J. and Gardner, D. 1986 Conjugate heat transfer from a downward projecting fin immersed in a porous medium. *Heat Transfer 1986, Hemisphere, Washington, DC*, **5**, 2635–2640. [5.12.1]
- Pop, I., Kumari, M. and Nath, G. 1992b Free convection about cylinders of elliptic cross section embedded in a porous medium. *Int. J. Engng Sci.* **30**, 35–45. [5.5.1]
- Pop, I., Lesnic, D. and Ingham, D. B. 1995b Conjugate mixed convection on a vertical surface in a porous medium. *Int. J. Heat Mass Transfer* **38**, 1517–1525. [8.1.1]
- Pop, I., Lesnic, D. and Ingham, D. B. 2000 Asymptotic solutions for the free convection boundary layer flow along a vertical surface in a porous medium with Newtonian heating. *Hybrid Methods in Engineering* **2**, 31–40. [5.1.9.8]
- Pop, I., Merkin, J. H. and Ingham, D. B. 2002 Chemically driven convection in porous media. In *Transport Phenomena in Porous Media II* (D. B. Ingham and I. Pop, eds.) Elsevier, Oxford, pp. 341–364. [5.12.3]
- Pop, I., Rees, D. A. S. and Egbers, C. 2004 Mixed convection flow in a narrow vertical duct filled with a porous medium. *Int. J. Therm. Sci.* **43**, 489–498. [8.3.2]
- Pop, I., Rees, D. A. S. and Storesletten, L. 1998 Free convection in a shallow annular cavity filled with a porous medium. *Journal of Porous Media* **1**, 227–241. [7.3.3]
- Pop, I., Sunada, J. K., Cheng, P. and Minkowycz, W. J. 1985 Conjugate free convection from long vertical plate fins embedded in a porous medium at high Rayleigh numbers. *Int. J. Heat Mass Transfer* **28**, 1629–1636. [5.12.1]
- Pop, S. R., Grosan, T. and Pop, I. 2008 Effect of variable viscosity on free convection flow in a horizontal porous channel with a partially heated or cooled wall. *Revista Chim.* **59**, 1210–1212. [6.18]
- Popov, V. N., Tsivinskaya, Y. S., Bekker, T. B., Kokh, K. A. and Kokh, A. E. 2006 Numerical investigation of heat-mass transfer processes in hydrothermal growth system *J. Crystal Growth* **289**, 652–658. [6.19.3]
- Postelnicu, A. 2004 Influence of a magnetic field on heat and mass transfer by natural convection from vertical surfaces in porous media considering Soret and Dufour effects. *Int. J. Heat Mass Transfer* **47**, 1467–1472. [9.2.1]
- Postelnicu, A. 2007a Effect of inertia on the onset of mixed convection in a porous layer using a thermal nonequilibrium model. *J. Porous Media* **10**, 515–524. [6.10.1]
- Postelnicu, A. 2007b Effects of thermophoresis particle deposition in free convection boundary layer from a horizontal flat plate embedded in a porous medium. *Int. J. Heat Mass Transfer* **50**, 2981–2985. [5.2]
- Postelnicu, A. 2007c Influence of chemical reaction on heat and mass transfer by natural convection from vertical surfaces in porous media considering Soret and Dufour effects. *Heat Mass Transfer* **43**, 595–602. [9.2.1]

- Postelnicu, A. 2008 The onset of convection using a thermal nonequilibrium model. Part II. *Int. J. Therm. Sci.* **47**, 1587–1594. [6.5]
- Postelnicu, A. 2009 Onset of convection in a horizontal porous layer driven by catalytic surface reaction on the lower wall. *Int. J. Heat Mass Transfer* **52**, 2466–2470. [9.1.6.4]
- Postelnicu, A. 2010a Heat and mass transfer by natural convection at a stagnation point in a porous medium considering Soret and Dufour effects. *Heat Mass Transfer* **46**, 831–840. [9.2.1]
- Postelnicu, A. 2010b The effect of a horizontal pressure gradient on the onset of a Darcy-Bénard convection in thermal non-equilibrium conditions. *Int. J. Heat Mass Transfer* **53**, 68–75. [6.10.1]
- Postelnicu, A. and Pop, I. 1999 Similarity solutions of free convection boundary layers over vertical and horizontal surfaces in porous media with internal heat generation. *Int. Comm. Heat Mass Transfer* **26**, 1183–1191. [5.1.9.4]
- Postelnicu, A. and Rees, D. A. S. 2001 The onset of convection in an anisotropic porous layer inclined at a small angle from the horizontal. *Int. Comm. Heat Mass Transfer* **28**, 641–650. [7.8]
- Postelnicu, A. and Rees, D. A. S. 2003 The onset of Darcy-Brinkman convection in a porous layer using a thermal nonequilibrium model – Part I: Stress free boundaries. *Int. J. Energy Res.* **27**, 961–973. [6.5]
- Postelnicu, A., Grosan, T. and Pop, I. 2000 Free convection boundary-layer over a vertical permeable flat plate in a porous medium with internal heat generation. *Int. Comm. Heat Mass Transfer* **27**, 729–738. [5.1.9.4]
- Postelnicu, A., Grosan, T. and Pop, I. 2001 The effect of variable viscosity on forced convection flow past a horizontal flat plate in a porous medium with internal heat generation. *Mech. Res. Comm.* **28**, 331–337. [5.2]
- Postelnicu, A., Magyari, E. and Pop, I. 2009 The effect of uniform horizontal throughflow on the Darcy free convection over a permeable vertical plate with volumetric heat generation. *Transp. Porous Media* **80**, 101–115. [5.1.9.4]
- Poulikakos, D. 1984 Maximum density effects on natural convection in a porous layer differentially heated in the horizontal direction. *Int. J. Heat Mass Transfer* **27**, 2067–2075. [7.3.5]
- Poulikakos, D. 1985a On buoyancy induced heat and mass transfer from a concentrated source in an infinite porous medium. *Int. J. Heat Mass Transfer* **28**, 621–629. [9.3.1]
- Poulikakos, D. 1985b Onset of convection in a horizontal porous layer saturated with cold water. *Int. J. Heat Mass Transfer* **28**, 1899–1905. [6.20]
- Poulikakos, D. 1985c The effect of a third diffusing component on the onset of convection in a horizontal porous layer. *Phys. Fluids* **28**, 3172–3174. [9.1.6.4]
- Poulikakos, D. 1986 Double diffusive convection in a horizontally sparsely packed porous layer. *Int. Comm. Heat Mass Transfer* **13**, 587–598. [9.1.6.3]
- Poulikakos, D. 1987a Buoyancy driven convection in a horizontal fluid layer extending over a porous substrate. *Phys. Fluids* **29**, 3949–3957. [6.19.2]
- Poulikakos, D. 1987b Thermal instability in a horizontal fluid layer superposed on a heat-generating porous bed. *Numer. Heat Transfer* **12**, 83–100. [6.19.2]
- Poulikakos, D. and Bejan, A. 1983a Natural convection in vertically and horizontally layered porous media heated from the side. *Int. J. Heat Mass Transfer* **26**, 1805–1814. [7.3.2]
- Poulikakos, D. and Bejan, A. 1983b Numerical study of transient high Rayleigh number convection in an attic-shaped porous layer. *ASME J. Heat Transfer* **105**, 476–484. [7.3.6]
- Poulikakos, D. and Bejan, A. 1983c Unsteady natural convection in a porous layer. *Phys. Fluids* **26**, 1183–1191. [7.5]
- Poulikakos, D. and Bejan, A. 1984a Natural convection in a porous layer heated and cooled along one vertical side. *Int. J. Heat Mass Transfer* **27**, 1879–1891. [7.4.3]
- Poulikakos, D. and Bejan, A. 1984b Penetrative convection in porous medium bounded by a horizontal wall with hot and cold spots. *Int. J. Heat Mass Transfer* **27**, 1749–1757. [7.4.3]
- Poulikakos, D. and Bejan, A. 1985 The departure from Darcy flow in natural convection in a vertical porous layer. *Phys. Fluids* **28**, 3477–3484. [7.6.1]

- Poulikakos, D. and Kazmierczak, M. 1987 Forced convection in a duct partially filled with a porous material. *ASME J. Heat Transfer* **109**, 653–662. [4.9]
- Poulikakos, D. and Renken, K. 1987 Forced convection in a channel filled with porous medium, including the effects of flow inertia, variable porosity, and Brinkman friction. *ASME J. Heat Transfer* **109**, 880–888. [4.9]
- Poulakos, D., Bejan, A., Selimos, B. and Blake, K. R. 1986 High Rayleigh number convection in a fluid overlying a porous bed. *Int. J. Heat Fluid Flow* **7**, 109–116. [6.19.2]
- Pourshaghagh, A., Hakkaki-Fard, A. and Mahdavi-Nejad, A. 2007 Direct simulation of natural convection in a square porous enclosure. *Energy Conv. Manag.* **48**, 1579–1589. [2.6]
- Powers, D., O'Neill, K. and Colbeck, S. C. 1985 Theory of natural convection in snow. *J. Geophys. Res.* **90**, 10641–10649. [11.1]
- Prakash, D., Muthtamilselvan, M. and Don, D. H. 2012 Effect of heat generation on forced convection through a porous saturated duct. *Transp. Porous Media* **95**, to appear. [4.16.5]
- Prakash, J., Sekhar, G. P. R., De, S. and Bohm, M. 2010 Convection, diffusion and reaction inside a spherical porous pellet in the presence of oscillatory flow. *European J. Mech. B* **29**, 483–493. [7.3.4]
- Prakash, K. and Kumar, N. 1999a Effects of suspended particles, rotation and variable gravity field on the thermal instability of Rivlin-Ericksen visco-elastic fluid in porous medium. *Indian J. Pure Appl. Math.* **30**, 1157–1166. [6.2.3]
- Prakash, K. and Kumar, N. 1999b Thermal instability in Rivlin-Ericksen elastico-viscous fluid in the presence of finite Larmor radius and variable gravity in porous medium. *J. Phys. Soc. Japan* **68**, 1168–1172. [6.23]
- Prasad, A. and Simmons, C. T. 2003 Unstable density-driven flow in heterogeneous porous media: A stochastic study of the Elder [1967b] “short heater” problem. *Water Resour. Res.* **39**, Art. No. 1007. [11.8]
- Prasad, K. V., Abel, M. S., Khan, S. K. and Datti, P. S. 2002 Non-Darcy forced convective heat transfer in a viscoelastic fluid flow over a non-isothermal sheet. *J. Porous Media* **5**, 41–47. [4.16.3]
- Prasad, K. V., Vajravelu, K. and van Gorder, R. A. 2011 Non-Darcian flow and heat transfer along a permeable vertical surface with nonlinear density temperature variation. *Acta Mech.* **220**, 139–154. [5.1.9.9]
- Prasad, V. 1986 Numerical study of natural convection in a vertical porous annulus with constant heat flux on the inner wall. *Int. J. Heat Mass Transfer* **29**, 841–853. [7.2]
- Prasad, V. 1987 Thermal convection in a rectangular cavity filled with a heat-generating, Darcy porous medium. *ASME J. Heat Transfer* **109**, 697–703. [6.17]
- Prasad, V. 1991 Convective flow interaction and heat transfer between fluid and porous layers. *Convective Heat and Mass Transfer in Porous Media* (eds. S. Kakaç, B. Kilkis, F. A. Kulacki and F. Arinç), Kluwer Academic, Dordrecht, pp. 563–615. [6.19.2]
- Prasad, V. 1993 Flow instabilities and heat transfer in fluid overlying horizontal porous layers. *Exp. Therm. Fluid Sci.*, **6**, 135–146. [6.19.2]
- Prasad, V. and Chui, A. 1989 Natural convection in a cylindrical porous enclosure with internal heat generation. *ASME J. Heat Transfer* **111**, 916–925. [6.17]
- Prasad, V. and Kladias, N. 1991 Non-Darcy natural convection in saturated porous media. *Convective Heat and Mass Transfer in Porous Media* (eds. S. Kakaç, B. Kilkis, F. A. Kulacki and F. Arinç), Kluwer Academic, Dordrecht, pp. 173–224. [7.6.2]
- Prasad, V. and Kulacki, F. A. 1984a Natural convection in a rectangular porous cavity with constant heat flux on one vertical wall. *ASME J. Heat Transfer* **106**, 152–157. [7.2]
- Prasad, V. and Kulacki, F. A. 1984b Convective heat transfer in a rectangular porous cavity. Effect of aspect ratio on flow structure and heat transfer. *ASME J. Heat Transfer* **106**, 158–165. [7.1.3]
- Prasad, V. and Kulacki, F. A. 1984c Natural convection in a vertical porous annulus. *Int. J. Heat Mass Transfer* **27**, 207–219. [7.3.3]
- Prasad, V. and Kulacki, F. A. 1985 Natural convection in porous media bounded by short concentric vertical cylinders. *ASME J. Heat Transfer* **107**, 147–154. [7.3.3]

- Prasad, V. and Kulacki, F. A. 1986 Effects of size of heat source on natural convection in horizontal porous layers heated from below. *Heat Transfer 1986, Hemisphere, Washington, DC, vol. 5*, pp. 2677–2682. [6.18]
- Prasad, V. and Kulacki, F. A. 1987 Natural convection in horizontal fluid layers with localized heating from below. *ASME J. Heat Transfer* **109**, 795–796. [6.18]
- Prasad, V. and Tian, Q. 1990 An experimental study of thermal convection in fluid-superposed porous layers heated from below. *Heat Transfer 1990, Hemisphere, Washington, DC, vol. 5*, pp. 207–212. [6.19.2]
- Prasad, V. and Tuntomo, A. 1987 Inertial effects on natural convection in a vertical porous cavity. *Numer. Heat Transfer* **11**, 295–320. [7.6.1]
- Prasad, V. R. and Reddy, N. B. 2008 Radiation and mass transfer effects on an unsteady MHD convection flow past a semi-infinite vertical permeable plate embedded in a porous medium with viscous dissipation. *Indian J. Pure Appl. Phys* **46**, 81–92. [9.2.1]
- Prasad, V. R., Vasu, B., Beg, O. A. and Parshad, R. D. 2012 Thermal radiation effects on magnetohydrodynamic free convection heat and mass transfer from a sphere in a variable porosity regime. *Comm. Nonlinear Sci. Numer. Simul.* **17**, 654–671. [9.4]
- Prasad, V., Brown, K. and Tian, G. 1989a Flow visualization and heat transfer experiments in fluid-superposed porous layers heated from below. *ASME HTD* **117**, 75–83. [6.19.2]
- Prasad, V., Brown, K. and Tian, Q. 1991 Flow visualization and heat transfer experiments in fluid-superposed packed beds heated from below. *Exp. Therm. Fluid Sci.* **4**, 12–24. [6.19.2]
- Prasad, V., Kladias, N., Bandyopadhyaya, A. and Tian, Q. 1989b Evaluation of correlations for stagnant thermal conductivity of liquid-saturated porous beds of spheres. *Int. J. Heat Mass Transfer* **32**, 1793–1796. [2.2.1]
- Prasad, V., Kulacki, F. A. and Keyhani, M. 1985 Natural convection in porous media. *J. Fluid Mech.* **150**, 89–119. [6.9.2, 7.3.3, 7.6.2]
- Prasad, V., Kulacki, F. A. and Kulkarni, A. V. 1986 Free convection in a vertical, porous annulus with constant heat flux on the inner wall — experimental results. *Int. J. Heat Mass Transfer* **29**, 713–723. [7.2]
- Prasad, V., Lai, F. C. and Kulacki, F. A. 1988 Mixed convection in horizontal porous layers heated from below. *ASME J. Heat Transfer* **110**, 395–402. [8.2.2]
- Prasad, V., Lauriat, G. and Kladias, N. 1992 Non-Darcy natural convection in a vertical porous cavity. *Heat and Mass Transfer in Porous Media* (eds. M. Quintard and M. Todorovic), Elsevier, Amsterdam, pp. 293–314. [7.6.2]
- Prat, M. 2007 On the influence of pore shape, contact angle and film flows on drying of capillary porous media. *Int. J. Heat Mass Transfer* **50**, 1455–1468. [3.6]
- Prats, M. 1966 The effects of horizontal fluid flow on thermally induced convection currents in porous mediums. *J. Geophys. Res.* **71**, 4835–4837. [6.10.1]
- Prax, C., Sadat, H and Slagnac, P. 1996 Diffuse approximation method for solving natural convection in porous media. *Transport in Porous Media* **22**, 215–223. [2.6]
- Prescott, P. J. and Incropera, F. P. 1995 The effect of turbulence on solidification of binary metal alloy with electromagnetic stirring. *ASME J. Heat Transfer* **117**, 716–724. [1.8, 10.2.3]
- Prescott, P. J. and Incropera, F. P. 1996 Convection heat and mass transfer in alloy solidification. *Advances in Heat Transfer* **28**, 231–329. [10.2.3]
- Prichard, D. and Richardson, C. N. 2007 The effect of temperature-dependent solubility on the onset of thermosolutal convection in a horizontal porous layer. *J. Fluid Mech.* **571**, 59–95. [9.1.6.4]
- Pringle, S. E. and Glass, R. J. 2002 Double-diffusive finger convection: influence of concentration at fixed buoyancy ratio. *J. Fluid Mech.* **462**, 161–183. [9.1.3]
- Pringle, S. E., Glass, R. J. and Cooper, C. A. 2002 Double-diffusive finger convection in a Hele-Shaw cell: An experiment exploring the evolution of concentration fields, length scales and mass transfer. *Transport Porous Media* **47**, 195–214. [9.1.6.4]

- Prommas, R. 2011 Theoretical and experimental study of heat and mass transfer mechanisms during convective drying of a multi-layered porous packed bed. *Int. Comm. Heat Mass Transfer* **38**, 900–905. [3.6]
- Prommas, R., Keangin, P. and Rattanadecho, P. 2010 Energy and exergy analyses in convective drying process of a multi-layered porous packed bed. *Int. Comm. Heat Mass Transfer* **37**, 1106–1114. [3.6]
- Prud'homme, M. and Bougerara, H. 2001 Linear stability of free convection in a vertical cavity heated by uniform heat fluxes. *Int. Comm. Heat Mass Transfer* **28**, 783–750. [7.2]
- Prud'homme, M. and Jasmin, S. 2001 Component analysis of a steady inverse convection solution in a porous medium. *Int. Comm. Heat Mass Transfer* **28**, 911–921. [7.2]
- Prud'homme, M. and Jasmin, S. 2003 Determination of a heat source in porous medium with convective mass diffusion by an inverse method. *Int. J. Heat Mass Transfer* **46**, 2065–2075. [9.3.1]
- Prud'homme, M. and Jiang, H. 2003 Inverse determination of concentration in porous medium with thermosolutal convection. *Int. Comm. Heat Mass Transfer* **30**, 303–312. [9.2.3]
- Prud'homme, M. and Nguyen, T. H. 2001 Solution of the inverse steady state convection problem in a porous medium by adjoint equations. *Int. Comm. Heat Mass Transfer* **28**, 11–21. [7.2]
- Prud'homme, M., Nguyen, T. H. and Bougerara, H. 2003 Stability of convection flow in a horizontal fluid layer heated by uniform heat fluxes. *Int. Comm. Heat Mass Transfer* **30**, 163–172. [7.2]
- Pruess, K. and Zhang, K. 2008 Numerical modeling studies of the dissolution-diffusion-convective process during storage in saline aquifers. Lawrence Berkeley National Laboratory, <http://escholarship.org/uc/item/2fc5v69p>. [11.11]
- Pu, W. L., Cheng, P. and Zhao, T. S. 1999 Mixed-convection heat transfer in vertical packed channels. *J. Thermophys. Heat Transfer* **13**, 517–521. [8.3.1]
- Purushothaman, R., Ganapathy, R. and Hiremath, P. S. 1990 Free convection in an infinite porous medium due to a pulsating point heat source. *Z. Angew. Math. Mech.* **70**, 41–47. [5.11.2]
- Qiao, Z. and Kaloni, P. N. 1997 Convection induced by inclined temperature gradient with mass flow in a porous medium. *ASME J. Heat Transfer* **119**, 366–370. [7.9]
- Qiao, Z. and Kaloni, P. N. 1998 Non-linear convection in a porous medium with inclined temperature. *Int. J. Heat Mass Transfer* **41**, 2549–2552. [7.9]
- Qin, Y. and Chadam, J. 1995 A nonlinear stability problem for ferromagnetic fluids in a porous medium. *Appl. Math. Lett.* **8**, 25–29. [6.21]
- Qin, Y. and Chadam, J. 1996 Nonlinear convective stability in a porous medium with temperature-dependent viscosity and inertial drag. *Stud. Appl. Math.* **96**, 273–288. [6.7]
- Qin, Y. and Kaloni, P. N. 1994 Convective instabilities in anisotropic porous media. *Stud. Appl. Math.* **91**, 189–204. [6.12]
- Qin, Y. and Kaloni, P. N. 1993 A nonlinear stability problem of convection in a porous vertical slab. *Phys. Fluids A* **5**, 2067–2069. [7.1.4]
- Qin, Y. and Kaloni, P. N. 1995 Nonlinear stability problem of a rotating porous layer. *Quart. Appl. Math.* **53**, 129–142. [6.22]
- Qin, Y., Guo, J. L. and Kaloni, P.N. 1995 Double diffusive penetrative convection in porous media. *Int. J. Engrg Sci.* **33**, 303–312. [9.1.6.4]
- Qu, Z. G., Wang, T. S., Tan, W. G. and Lu, T. J. 2012a A theoretical octet-truss lattice unit cell model for effective thermal conductivity of consolidated porous materials saturated with fluid. *Heat Mass Transfer* **48**, 1385–1395. [2.2.1]
- Qu, Z. G., Xu, H. J. and Tao, W. G. 2012b Fully developed forced convection in an annulus partly filled with metallic foams: An analytical solution. *Int. J. Heat Mass Transfer* **55**, to appear. [4.11]
- Quintard, M. and Prouvost, L. 1982 Instabilités de zones de diffusion thermique instationnaires en milieu poreux. *Int. J. Heat Mass Transfer* **25**, 37–44. [6.10.2]
- Quintard, M. and Whitaker, S. 2000 Theoretical modeling of transport in porous media. Handbook of Porous Media (K. Vafai, ed.), Marcel Dekker, New York., pp. 1–52. [2.2.3]

- Quintard, M. and Whitaker, S. 2005 Coupled, nonlinear mass transfer and heterogeneous reaction in porous media. *Handbook of Porous Media* (K. Vafai, ed.), 2nd ed., Taylor and Francis, New York., pp. 3–38. [3.4]
- Quintard, M., Kaviany, M. and Whitaker, S. 1997 Two-medium treatment of heat results in porous media: Numerical results for effective properties. *Adv. Water Resources* **20**, 77–94. [2.4]
- Rabadi, N. J. and Hamdan, E. M. 2000 Free convection from inclined permeable walls embedded in variable permeability porous media with lateral mass flux. *J. Petrol. Sci. Engng.* **26**, 241–251. [5.3]
- Rabinowicz, M., Sempéré, J. C. and Genthon, P. 1999 Thermal convection in a vertical permeable slot: implications for hydrothermal circulation along mid-ocean ridges. *J. Geophys. Res.* **104**, 29275–29292. [6.15.2]
- Rachedi, R. and Chikh, S. 2001 Enhancement of electronic cooling by insertion of foam materials. *Heat Mass Transfer* **37**, 371–378. [4.11]
- Raffensperger, J. P. and Vlassopoulos, D. 1999 The potential for free and mixed convection in sedimentary basins. *Hydrol. J.* **7**, 505–520. [6.10.1]
- Rahimian, M. H. and Poushaghay, A. 2002 Direct simulation of forced convection in a parallel plate channel filled with porous media. *Int. Comm. Heat Mass Transfer* **29**, 867–878. [2.6]
- Rahli, O., Tadrist, L., Miscevic, M. and Santini, R. 1997 Fluid flow through randomly packed monodisperse fibers: the Kozeny-Carman parameter analysis. *ASME J. Fluids Engng.* **119**, 188–192. [1.4.2]
- Rahman, M. M. and Al-Lawatia, M. 2010 Effects of higher order chemical reaction on micropolar fluid flow on a power law, permeable stretched sheet with variable concentration in a porous medium. *Canad. J. Chem. Engng.* **88**, 23–32. [9.2.1]
- Rahman, M. M. and Sattar, M. A. 2006 Magnetohydrodynamic convective flow of a micropolar fluid past a continuously moving porous plate in the presence of heat generation/absorption. *ASME J. Heat Transfer* **128**, 142–152. [5.1.9.9]
- Rahman, S. U. 1999 An experimental study on buoyancy-driven convective mass transfer from spheres embedded in saturated porous media. *Heat Mass Transfer* **35**, 487–491. [5.6.1]
- Rahman, S. U. and Badr, H. M. 2002 Natural convection from a vertical wavy surface embedded in saturated porous media. *Ind. Engng. Chem. Res.* **41**, 4422–4429. [5.1.8]
- Rahman, S. U., Al-Saleh, M. A. and Sharma, R. N. 2000 An experimental study on natural convection from heated surfaces embedded in porous media. *Indust. Engng. Chem. Res.* **39**, 214–218. [5.1.8]
- Rajamani, R., Srinivas, C., Nithiarasu, P. and Seetharamu, K. N. 1995 Convective heat transfer in axisymmetric porous bodies. *Int. J. Numer. Meth. Heat Fluid Flow* **5**, 829–837. [7.3.3]
- Rajen, G. and Kulacki, F. A. 1987 Natural convection in a porous layer locally heated from below — a regional laboratory model for a nuclear waste repository. *ASME HTD* **67**, 19–26. [6.18]
- Ramakrishna, D., Basak, T., Roy, S. and Pop, I. 2012 Numerical study of mixed convection within porous square cavities using Bejan's heatlines: Effects of thermal aspect ratio and thermal boundary conditions. *Int. J. Heat Mass Transfer* **55**, 5436–544. [8.4.3]
- Ramanathan, A. and Surendra, P. 2003 Effect of magnetic field on viscosity of ferroconvection in an anisotropic sparsely distributed porous medium. *Indian J. Pure Appl. Phys.* **41**, 522–526. [6.21]
- Ramanathan, A. and Suresh, G. 2004 Effect of magnetic field dependent viscosity and anisotropy of porous medium on ferroconvection. *Int. J. Engng. Sci.* **42**, 411–425. [6.21]
- Ramanbason D. S. R. and Vasseur, P. 2007 Influence of a magnetic field on natural convection in a shallow porous enclosure saturated with a binary fluid. *Acta Mech.* **191**, 21–35. [9.1.6.4]
- Ramaniah, G. and Malarvizhi G. 1991 Note on exact solutions of certain non-linear boundary value problems governing convection in porous media. *Int. J. Non-linear Mech.* **26**, 345–347. [5.1.9.9, 5.2]
- Ramaniah, G. and Malarvizhi G. 1994 Note on the boundary value problem arising in free convection in porous media. *Int. J. Engng Sci.* **32**, 2011–2013. [5.1.9.9]

- Ramaniah, G. and Malarvizhi, G. 1990 Non-Darcy regime mixed convection on vertical plates in saturated porous media with lateral mass flux. *Acta Mech.* **81**, 191–200. [8.1.1]
- Ramaniah, G., Malarvizhi, G. and Merkin, J. H. 1991 A unified treatment of mixed convection on a permeable horizontal plate. *Wärme-Stoffübertrag.* **26**, 187–192. [8.1.2]
- Ramazanov, M. M. 2000 Convection in a obliquely heated thin porous elliptic ring. *Fluid Dyn.* **35**, 910–917. [7.3.7]
- Ramazanov, M. M. 2001 Convection in a obliquely heated thin porous elliptic ring. *Fluid Dyn.* **36**, 279–284. [9.1.6.4]
- Ramazanov, M. M. 2010 Perfect gas convection in a porous medium between two co-axial horizontal cylinders of large length. *Fluid Dynamics* **45**, 241–253. [7.3.3]
- Ramesh, P. S. and Torrance, K. E. 1990 Stability of boiling in porous media. *Int. J. Heat Mass Transfer* **33**, 1895–1908. [10.3.1]
- Ramesh, P. S. and Torrance, K. E. 1993 Boiling in a porous layer heated from below: effects of natural convection and a moving liquid/two-phase surface. *J. Fluid Mech.* **257**, 289–309. [10.3.1]
- Ramirez, N. E. and Saez, A. E. 1990 The effect of variable viscosity on boundary-layer heat transfer in a porous medium. *Int. Comm. Heat Mass Transfer* **17**, 477–485. [4.2]
- Rana, R., Horne, R. N. and Cheng, P. 1979 Natural-convection in a multi-layered geothermal reservoir. *ASME Heat Transfer* **101**, 411–416. [6.13.2]
- Ranganathan, P., Farzadeh, R., Bruining, H. and Zitha, P. L. J. 2012 Numerical simulation of natural convection in heterogeneous porous media for CO<sub>2</sub> geological storage. *Transp. Porous Media* **95**, 25–54. [11.11]
- Ranganathan, R. and Viskanta, R. 1984 Mixed convection boundary-layer flow along a vertical surface in a porous medium. *Numer. Heat Transfer* **7**, 305–317. [8.1.1]
- Ranjbar-Kani, A. A. and Hooman, K. 2004 Viscous dissipation effects on thermally developing forced convection in a porous medium: circular duct with isothermal wall. *Int. Comm. Heat Mass Transfer* **31**, 897–907. [4.13]
- Rao, B. K. 2001 Heat transfer to power-law fluid flows through porous media. *J. Porous Media* **4**, 339–347. [4.16.3]
- Rao, B. K. 2002 Internal heat transfer to power-law fluid flows through porous media. *Exper. Heat Transfer* **15**, 73–88. [4.16.3]
- Rao, K.N. and Pop, I. 1994 Transient free convection in a fluid saturated porous medium with temperature dependent viscosity. *Int. Comm. Heat Mass Transfer* **21**, 573–591. [5.1.9.9]
- Rao, Y. F. and Glakpe, E. K. 1992 Natural convection in a vertical slot filled with porous medium. *Int. J. Heat Fluid Flow* **31**, 97–99. [7.1.2]
- Rao, Y. F. and Wang, B. X. 1991 Natural convection in vertical porous enclosures with internal heat generation. *Int. J. Heat Mass Transfer* **34**, 247–252. [7.3.3]
- Rao, Y. F., Fukuda, K. and Hasegawa, S. 1987 Steady and transient analyses of natural convection in a horizontal porous annulus with the Galerkin method. *ASME J. Heat Transfer* **109**, 919–927. [7.3.3]
- Rao, Y. F., Fukuda, K. and Hasegawa, S. 1988 Numerical study of three dimensional natural convection in a horizontal porous annulus with Galerkin method. *Int. J. Heat Mass Transfer* **31**, 698–707. [7.3.3]
- Rapaka, S., Chen, S. Y., Pawar, R. J., Stauffer, P. H. and Zhang, D. X. 2008 Non-modal growth of perturbations in density-driven convection in porous media. *J. Fluid Mech.* **609**, 227–244. [6.18]
- Rapaka, S., Pawar, R. J., Stauffer, P. H., Zhang, D. X. and Chen, S. Y. 2009 Onset of convection over a transient base-state in anisotropic and layered porous media. *J. Fluid Mech.* **641**, 285–303. [6.18]
- Rappoldt, C., Pieters, G. J. J. M., Adema, E. B., Baaijens, G. J., Grootjans, A. P. and van Duijn, C. J. 2003 Buoyancy-driven flow in a peat moss layer as a mechanism for solute transport. *Proc. Nat. Acad. Sci.* **100**, 14937–14942. [6.11.3, 11.8]

- Raptis, A. 1998 Radiation and free convection flow through a porous medium. *Int. Comm. Heat Mass Transfer* **25**, 289–295. [5.1.9.4]
- Raptis, A. and Tzivanidis, G. 1984 Unsteady flow through a porous medium with the presence of mass transfer. *Int. Comm. Heat Mass Transfer* **11**, 97–102. [9.2.1]
- Raptis, A., Tzivanidis, G. and Kafousias, N. 1981 Free convection and mass transfer flow through a porous medium bounded by an infinite vertical limiting surface with constant suction. *Lett. Heat Mass Transfer* **8**, 417–424. [9.2.1]
- Raptis, A. and Perdikis, C. 2004 Unsteady flow through a highly porous medium in the presence of radiation. *Transport Porous Media* **57**, 171–17. [5.1.9.4]
- Rashad, A. M. 2008 Influence of radiation on MHD free convection from a vertical flat plate embedded in porous media with thermophoretic deposition of particles. *Commun. Nonlinear Sci. Numer. Simul.* **13**, 2213–2222. [5.1.9.9]
- Rashad, A. M. 2009a Perturbation analysis of radiative effect on free convection flows in porous medium in presence of pressure work and dissipation. *Commun. Nonlinear Sci. Numer. Simul.* **14**, 140–153. [5.1.9.4]
- Rashad, A. M. 2009b Response to the comments of Asterios Pantokratoras on “Perturbation analysis of radiative effect on free convection flows in porous medium in presence of pressure work and dissipation.” *Commun. Nonlinear Sci. Numer. Simul.* **14**, 347–349. [5.1.9.4]
- Rashad, A. M. and El-Khabeir, S. M. M. 2010 Heat and mass transfer in transient flow by mixed convection boundary layer over a stretching sheet embedded in a porous medium with chemically reactive species. *J. Porous Media* **13**, 75–85. [9.6.1]
- Rashad, A. M., Bakier, A. Y. and Gorla, R. S. R. 2010 Viscous dissipation and ohmic heating effects on magnetohydrodynamic mixed convection along a vertical moving surface embedded in a fluid-saturated porous medium. *J. Porous Media* **13**, 159–170. [8.1.6]
- Rashidi, F., Bahrami, A. and Soroush, H. 2000 Prediction of time required for onset of convection in a porous medium saturated with oil and a layer of gas underlying the oil. *J. Petrol. Sci. Engng.* **26**, 311–317. [6.11.3]
- Rashidi, M. M., Laraqi, N. and Sadri, S. M. 2010 A novel analytical solution of mixed convection about an inclined flat plate embedded in a porous medium using the DTM-Pade. *Int. J. Therm. Sci.* **49**, 2405–2412. [8.1.1]
- Rastogi, S. K. and Poulikakos, D. 1993 Double diffusion in a liquid layer under a permeable solid region saturated with a non-Newtonian fluid. *Numer. Heat Transfer A* **24**, 427–449. [9.4]
- Rastogi, S. K. and Poulikakos, D. 1995 Double diffusion from a vertical surface in a porous region saturated with a non-Newtonian fluid. *Int. J. Heat Mass Transfer* **38**, 935–946. [9.2.1]
- Rastogi, S. K. and Poulikakos, D. 1997 Experiments on double-diffusion in a composite system comprised of a packed layer of spheres and an underlying layer. *Heat Mass Transfer* **32**, 181–191. [9.4]
- Ratish Kumar, B. V. 2000 A study of free convection induced by a vertical wavy surface with heat flux in a porous enclosure. *Numer. Heat Transfer A* **37**, 493–510. [6.14]
- Ratish Kumar, B. V. and Murthy, S. V. S. S. N. V. G. K. 2010a Mixed convection in a non-Darcian fluid-saturated square porous enclosure under multiple suction effect. *Int. J. Heat Mass Transfer* **53**, 5764–5773. [8.4.3]
- Ratish Kumar, B. V. and Murthy, S. V. S. S. N. V. G. K. 2010b Soret and Dufour effects on double-diffusive free convection from a corrugated surface in a non-Darcy porous medium. *Transp. Porous Media* **85**, 117–130. [9.2.1]
- Ratish Kumar, B. V. and Murthy, S. V. S. S. N. V. G. 2012 Double diffusive free convection induced by vertical wavy surface in a doubly stratified Darcy porous medium under the influence of Soret and Dufour effect. *J. Porous Media* **15**, 877–890. [9.1.6.4]
- Ratish Kumar, B. V. and Singh, P. 1998 Effect of thermal stratification on free convection in a fluid-saturated porous enclosure. *Numer. Heat Transfer A* **34**, 343–356. [5.1.4]
- Ratish Kumar, B. V. and Shalini 2003a Free convection in a non-Darcian wavy porous enclosure. *Int. J. Engng. Sci.* **41**, 1827–1848. [7.3.7]

- Ratish Kumar, B. V. and Shalini 2003b Natural convection in a thermally stratified wavy vertical porous enclosure. *Numer. Heat Transfer A* **43**, 753–776. [6.14]
- Ratish Kumar, B. V. and Shalini 2004a Free convection in a thermally stratified non-Darcian porous enclosure. *J. Porous Media* **7**, 261–277. [7.3.7]
- Ratish Kumar, B. V. and Shalini 2004b Double-diffusive natural convection in a stratified porous medium. *J. Porous Media* **7**, 279–288. [9.2.1]
- Ratish Kumar, B. V. and Shalini 2004c Non-Darcy free convection induced by a vertical wavy surface in a thermally stratified porous medium. *Int. J. Heat Mass Transfer* **47**, 2353–2363. [6.14]
- Ratish Kumar, B. V. and Shalini 2005 Combined influence of mass and thermal stratification on double-diffusion on non-Darcian natural convection from a wavy vertical wall to porous media. *ASME J. Heat Transfer* **127**, 637–674. [9.4]
- Ratish Kumar, B. V. and Shalini 2005 Double diffusive natural convection in a doubly stratified wavy porous enclosure. *Appl. Math. Comput.* **171**, 180–202. [9.2.1]
- Ratish Kumar, B. V., Singh, P. and Bansod, V. J. 2002 Effect of thermal stratification on free convection in a fluid-saturated porous enclosure. *Numer. Heat Transfer A* **41**, 421–447. [9.2.2]
- Ratish Kumar, B. V., Murthy, P. V. S. N. and Singh, P. 1998 Free convection heat-transfer from an isothermal wavy surface in a porous enclosure. *Int. J. Numer. Meth. Fluids* **28**, 633–661. [6.14]
- Ratish Kumar, B. V., Singh, P. and Murthy, P. V. S. N. 1997 Effect of surface undulations on natural convection in a porous square cavity. *ASME J. Heat Transfer* **119**, 848–851. [6.14]
- Rawat, S., Bhargava, R., Bhargava, R. and Beg, O.A. 2009 Transient magneto-micropolar free convection heat and mass transfer through a non-Darcy porous medium channel with variable thermal conductivity and heat source effects. *IME J. Mech. Engrg Sci.* **223**, 2341–2355. [9.2.2]
- Ray, R. J., Krantz, W. B., Caine, T. N. and Gunn, R. D. 1983 A model for sorted ground regularity. *J. Glaciology* **29**, 317–337. [11.2]
- Reda, D. C. 1983 Natural convection experiments in a liquid-saturated porous medium bounded by vertical coaxial cylinders. *ASME J. Heat Transfer* **105**, 795–802. [6.16.1]
- Reda, D. C. 1986 Natural convection experiments in a stratified liquid-saturated porous medium. *ASME J. Heat Transfer* **108**, 660–666. [7.3.3]
- Reda, D. C. 1988 Mixed convection in a liquid-saturated porous medium. *ASME J. Heat Transfer* **110**, 147–154. [8.1.3, 8.3.4]
- Reddy, B. V. K. and Narasimhan, A. 2010 Heat generation in natural convection inside a porous annulus. *Int. Comm. Heat Mass Transfer* **37**, 607–610. [7.3.3]
- Reddy, K. S. and Karthikeyan, P. 2009 Estimation of effective thermal conductivity of two-phase materials using collocated parameter model. *Heat Transfer Engng.* **30**, 998–1011. [2.2.1]
- Rees, D. A. S. 1988 The stability of Prandtl-Darcy convection in a vertical porous layer. *Int. J. Heat Mass Transfer* **31**, 1529–1534. [7.1.4]
- Rees, D. A. S. 1990 The effect of long-wavelength thermal modulations on the onset of convection in an infinite porous layer heated from below. *Q. J. Mech. Appl. Math.* **43**, 189–214. [6.14]
- Rees, D. A. S. 1993 Numerical investigation of the nonlinear wave stability of vertical thermal boundary layer flow in a porous medium. *Z. Angew. Math. Phys.* **44**, 306–313. [5.1.9.9]
- Rees, D. A. S. 1996a The effect of inertia on free convection from a horizontal surface embedded in a porous medium. *Int. J. Heat Mass Transfer* **39**, 3425–3430. [5.2]
- Rees, D. A. S. 1996b The effect of inertia on the stability of convection in a porous layer heated from below. *J. Theor. Appl. Fluid Dyn.* **1**, 154–171. [6.4]
- Rees, D. A. S. 1997a The effect of inertia on the onset of mixed convection in a porous layer heated from below. *Int. Comm. Heat Mass Transfer* **24**, 277–283. [6.9.3]
- Rees, D. A. S. 1997b Three-dimensional free convective boundary layers in porous media induced by a heated surface with spanwise temperature gradient. *ASME J. Heat Transfer* **119**, 792–798. [5.2] [5.1.9.9]
- Rees, D. A. S. 1998 Thermal boundary layer instabilities in porous media: a critical review. *Transport Phenomena in Porous Media* (eds. D.B. Ingham and I. Pop), Elsevier, Oxford, pp. 233–259. [5.4]

- Rees, D. A. S. 1999 Free convective boundary-layer flow from a heated surface in a layered porous medium *J. Porous Media* **2**, 39–58. [5.1.9.5]
- Rees, D. A. S. 2000 The stability of Darcy-Bénard convection. *Handbook of Porous Media* (K. Vafai, ed.), Marcel Dekker, New York., pp. 521–588. [6.4]
- Rees, D. A. S. 2001 Vortex instability from a near-vertical heated surface in a porous medium. I. Linear instability. *Proc. Roy. Soc. Lond. A* **457**, 1721–1734. [5.4]
- Rees, D. A. S. 2002a Vortex instability from a near-vertical heated surface in a porous medium. II. Nonlinear evolution. *Proc. Roy. Soc. Lond. A* **458**, 1773–1782. [5.4]
- Rees, D. A. S. 2002b The onset of Darcy-Brinkman convection in a porous layer: an asymptotic analysis. *Int. J. Heat Mass Transfer* **45**, 2213–2220. [6.6]
- Rees, D. A. S. 2002c Recent advances in the instability of free convective boundary layers in porous media. In *Transport Phenomena in Porous Media II* (D. B. Ingham and I. Pop, eds.), Elsevier, Oxford, pp. 54–81. [5.4]
- Rees, D. A. S. 2003 Vertical free convective boundary-layer flow in a porous medium using a thermal nonequilibrium model: elliptical effects. *Z. Angew. Math. Phys.* **54**, 437–448. [5.1.9.3]
- Rees, D. A. S. 2004a Convection in a sidewall-heated porous cavity in the presence of viscous dissipation. In *Applications of Porous Media (ICAPM 2004)*, (eds. A. H. Reis and A. F. Miguel), Évora, Portugal, pp. 231–236. [7.6.2]
- Rees, D. A. S. 2004b Nonlinear vortex instabilities in free convective boundary layers in porous media. In *Emerging Technologies and Techniques in Porous Media* (D. B. Ingham, A. Bejan, E. Mamut and I. Pop, eds), Kluwer Academic, Dordrecht, pp. 235–245. [5.4]
- Rees, D. A. S. 2009a Comment on “Effects of chemical reaction on free convective flow of a polar fluid through a porous medium in the presence of internal heat generation” by Patil and Kulkarni, *Int. J. Therm. Sci.* **47** (2008)1043–1054. *Int. J. Therm. Sci.* **48**, 847–848. [9.2.1]
- Rees, D. A. S. 2009b The onset and nonlinear development of vortex instabilities in a horizontal forced convection boundary layer with uniform surface suction. *Transp. Porous Media* **77**, 243–265. [5.4]
- Rees, D. A. S. 2010 Microscopic modeling of the two-temperature model for conduction in heterogeneous media *J. Porous Media* **13**, 125–143. [2.2.3]
- Rees, D. A. S. 2011 The effect of local thermal nonequilibrium on the stability of convection in a vertical porous channel. *Transp. Porous Media* **87**, 459–464. [7.1.4]
- Rees, D. A. S. and Barletta, A. 2011 Linear instability of the isoflux Darcy-Bénard problem in an inclined porous layer. *Transp. Porous Media* **87**, 665–678. [7.8]
- Rees, D. A. S. and Bassom, A. P. 1991 Some exact solutions for free convective flows over heated semi-infinite surfaces in porous media. *Int. J. Heat Mass Transfer* **34**, 1564–1567. [5.8]
- Rees, D. A. S. and Bassom, A. P. 1993 The nonlinear non-parallel wave instability of boundary-layer flow induced by a horizontal heated surface in porous media. *J. Fluid Mech.* **253**, 267–295. [5.2]
- Rees, D. A. S. and Bassom, A. P. 1994 The linear wave instability of boundary layer flow induced by a horizontal heated surface in porous media. *Int. Comm. Heat Mass Transfer* **21**, 143–150. [5.2]
- Rees, D. A. S. and Bassom, A. P. 1998 The onset of convection in an inclined porous layer heated from below. *Heat Transfer 1998, Proc. 11th IHTC*, **4**, 497–502. [7.8]
- Rees, D. A. S. and Bassom, A. P. 2000 Onset of Darcy-Bénard convection in an inclined layer heated from below. *Acta Mech.* **144**, 103–118. [7.8]
- Rees, D. A. S. and Genc, G. 2011 The onset of convection in porous layers with multiple horizontal partitions. *Int. J. Heat Mass Transfer* **54**, 3081–3089. [6.13.2]
- Rees, D. A. S. and Hossain, M. A. 1999 Combined effect of inertia and a spanwise pressure gradient on free convection from a vertical surface in porous media. *Numer. Heat Transfer A* **36**, 725–736. [5.1.7.2]
- Rees, D. A. S. and Hossain, M. A. 2001 The effect of inertia on free convective plumes in porous media. *Int. Comm. Heat Mass Transfer* **28**, 1137–1142. [5.10.1.2]

- Rees, D. A. S. and Lage, J. L. 1996 The effect of thermal stratification on natural convection in a vertical porous medium layer. *Int. J. Heat Mass Transfer* **40**, 111–121. [6.15.2, 7.1.4]
- Rees, D. A. S. and Magyari, E. 2008 Comments on the paper “Non-Darcian forced convection flow of viscous dissipating fluid over a flat plate embedded in a porous medium,” by O. Aydin and A. Kaya. *Transp. Por. Media* **73**, 187–189. [4.8, 8.1.1]
- Rees, D. A. S. and Mojtabi, A. 2011 The effect of conducting boundaries on weakly nonlinear Darcy–Bénard convection. *Transp. Porous Media* **88**, 45–63. [6.4]
- Rees, D. A. S. and Pop, I. 1994a A note on free convection along a vertical wavy surface in a porous medium. *ASME J. Heat Transfer* **116**, 505–508. [5.1.9.6]
- Rees, D. A. S. and Pop, I. 1994b Free convection induced by a horizontal wavy surface in a porous medium. *Fluid Dyn. Res.* **14**, 151–166. [5.2]
- Rees, D. A. S. and Pop, I. 1995a Free convection induced by a vertical wavy surface with uniform heat flux in a porous medium. *ASME J. Heat Transfer* **117**, 547–550. [5.1.9.6]
- Rees, D. A. S. and Pop, I. 1995b Non-Darcy natural convection from a vertical wavy surface in a porous medium. *Transport in Porous Media* **20**, 223–234. [5.1.9.6]
- Rees, D. A. S. and Pop, I. 1997 The effect of longitudinal surface waves on free convection from vertical surfaces in porous media. *Int. Comm. Heat Mass Transfer* **24**, 419–425. [5.1.9.6]
- Rees, D. A. S. and Pop, I. 1999 Free convective stagnation-point flow in a porous medium using a thermal nonequilibrium model. *Int. Comm. Heat Mass Transfer* **26**, 945–954. [5.1.9.3, 5.12.3]
- Rees, D. A. S. and Pop, I. 2000a Vertical free convection in a porous medium with variable permeability effects. *Int. J. Heat Mass Transfer* **43**, 2565–2571. [5.1.9.5]
- Rees, D. A. S. and Pop, I. 2000b The effect of g-jitter on vertical free convection boundary-layer flow in porous media. *Int. Comm. Heat Mass Transfer* **27**, 415–424. [5.1.9.7]
- Rees, D. A. S. and Pop, I. 2000c Vertical free convective boundary-layer flow in a porous medium using a thermal nonequilibrium model. *J. Porous Media* **3**, 31–44. [5.1.9.3]
- Rees, D. A. S. and Pop, I. 2001 The effect of g-jitter on free convection near a stagnation point in a porous medium. *Int. J. Heat Mass Transfer* **44**, 877–883. [5.12.3]
- Rees, D. A. S. and Pop, I. 2002 Comments on ‘Natural convection from a vertical plate in a saturated porous medium : nonequilibrium theory’ by A. A. Mohamad. *J. Porous Media* **5**, 225–227. [5.1.9.3]
- Rees, D. A. S. and Pop, I. 2003 The effect of large-amplitude g-jitter vertical free convection boundary-layer flow in porous media. *Int. J. Heat Mass Transfer* **46**, 1097–1102. [5.1.9.7]
- Rees, D. A. S. and Pop, I. 2005 Local thermal non-equilibrium in porous media convection. In Transport Phenomena in Porous Media III, (eds. D. B. Ingham and I. Pop), Elsevier, Oxford, pp. 147–173. [5.1.9.3]
- Rees, D. A. S. and Pop, I. 2010 Discussion on the paper : Vortex instability of mixed convection boundary layer flow adjacent to a non-isothermal horizontal surface in a porous medium with variable permeability. *J. Porous Media* **13**, 945–949. [5.4]
- Rees, D. A. S. and Postelnicu, A. 2001 The onset of convection in an inclined anisotropic porous layer. *Int. J. Heat Mass Transfer* **44**, 4127–4138. [7.8]
- Rees, D. A. S. and Riley, D. S. 1985 Free convection above a near horizontal semi-infinite heated surface embedded in a saturated porous medium. *Int. J. Heat Mass Transfer* **28**, 183–190. [5.3]
- Rees, D. A. S. and Riley, D. S. 1986 Free convection in an undulating saturated porous layer. *J. Fluid Mech.* **166**, 503–530. [6.14]
- Rees, D. A. S. and Riley, D. S. 1989a The effects of boundary imperfections on convection in a saturated porous layer: near-resonant wavelength excitation. *J. Fluid Mech.* **199**, 133–154. [6.14]
- Rees, D. A. S. and Riley, D. S. 1989b The effects of boundary imperfections on convection in a saturated porous layer: non-resonant wavelength excitation. *Proc. Roy. Soc. London Ser. A* **421**, 303–339. [6.14]
- Rees, D. A. S. and Riley, D. S. 1990 The three-dimensionality of finite-amplitude convection in a layered porous medium heated from below. *J. Fluid Mech.* **211**, 437–461. [6.13.2]

- Rees, D. A. S. and Storesletten, L. 1995 The effect of anisotropic permeability on free convective boundary layer flow in porous media. *Transport in Porous Media* **19**, 79–92. [5.1.9.5]
- Rees, D. A. S. and Storesletten, L. 2002 The linear stability of a thermal boundary layer with suction in an anisotropic porous medium. *Fluid Dyn. Res.* **30**, 155–168. [5.3]
- Rees, D. A. S. and Tyvand, P. A. 2004a The Helmholtz equation for convection in two-dimensional porous cavities with conducting boundaries. *J. Engrg. Math.* **49**, 181–193. [6.15.1]
- Rees, D. A. S. and Tyvand, P. A. 2004b Degeneracy and the time-dependent onset of convection in porous cavities with conducting boundaries. Emerging Technologies and Techniques in Porous Media (D. B. Ingham et al., eds.), Kluwer Academic, Dordrecht, 459–467. [6.15.1]
- Rees, D. A. S. and Tyvand, P. A. 2004c Oscillatory convection in a two-dimensional porous box with asymmetric lateral boundary conditions. *Phys. Fluids* **16**, 3706–3714. [6.15.1]
- Rees, D. A. S. and Tyvand, P. A. 2009 Onset of convection in a porous layer with continuous periodic horizontal stratification. Part 1. Two-dimensional convection. *Transp. Porous Media* **77**, 187–20. [6.13.2]
- Rees, D. A. S. and Vafai, K. 1999 Darcy-Brinkman free convection from a heated horizontal surface. *Numer. Heat Transfer A* **35**, 191–204. [5.2]
- Rees, D. A. S., Bassom, A. P. and Pop, I. 2003a Forced convection past a heated cylinder in a porous medium using a thermal non-equilibrium model: boundary layer analysis. *European J. Mech. B* **22**, 473–476. [5.1.9.3, 5.7]
- Rees, D. A. S., Bassom, A. P. and Siddheshwar, P. G. 2008a Local thermal non-equilibrium effects arising from the injection of a hot fluid into a porous medium. *J. Fluid Mech.* **594**, 379–398. [7.1.7]
- Rees, D. A. S., Magyari, E. and Keller, B. 2003b The development of the asymptotic viscous dissipation profile in a vertical free convective boundary layer flow in a porous medium. *Transport Porous Media* **53**, 347–355. [5.1.9.4]
- Rees, D. A. S., Magyari, E., Keller, B. 2005a Vortex instability of the asymptotic dissipation profile in porous media. *Transport Porous Media* **61**, 1–14. [5.1.9.4, 6.6]
- Rees, D. A. S., Nield, D. A. and Kuznetsov, A. V. 2008b Vertical free convective boundary-layer flow in a bidisperse porous medium. *ASME J. Heat Transfer* **130**, #092601. [5.1.9.9]
- Rees, D. A. S., Postelnicu, A. and Bassom, A. P. 2008c The linear vortex instability of the near-vertical line source plume in porous media. *Transp. Porous Media* **74**, 221–238. [5.10.1.1]
- Rees, D. A. S., Postelnicu, A. and Storesletten, L. 2006a The onset of Darcy-Forchheimer convection in inclined porous layers heated from below. *Transport Porous Media* **64**, 15–25. [7.8]
- Rees, D. A. S., Selim, A. and Ennis-King, J. P. 2008d The instability of unsteady boundary layers in porous media. In P. Vadasz (ed.) *Emerging Topics in Heat and Mass Transfer in Porous Media*, Springer, New York, pp. 85–110. [6.11.3]
- Rees, D. A. S., Storesletten, L. and Bassom, A. P. 2002 Convective plume paths in anisotropic porous media. *Transport Porous Media* **49**, 9–25. [5.10.1.1]
- Rees, D. A. S., Storesletten, L. and Postelnicu, A. 2006b The onset of convection in an inclined anisotropic porous layer with oblique principal axes. *Transport Porous Media* **62**, 139–156. [7.8]
- Rehberg, I. and Ahlers, G. 1985 Experimental observation of a codimension-two bifurcation in a binary fluid mixture. *Phys. Rev. Lett.* **55**, 500–503. [9.1.3]
- Reis, A. H. 2006 Constructal theory: From engineering to physics, and how flow systems develop shape and structure. *Appl. Mech. Rev.* **59**, 1–6. [4.18.5]
- Reis, A. H. and Gama, C. 2010 Sand size versus beachface slope — An explanation based on the constructal law. *Geomorphology* **114**, 276–283. [4.18.5]
- Reis, A. H., Miguel, A. F. and Bejan, A. 2006 Constructal theory of particle agglomeration and design of air-cleaning devices. *J. Appl. Phys. D* **39**, 2311–231. [4.18.5]
- Renken, K. J. and Raich, M. R. 1996 Forced convection steam condensation experiments within thin porous coatings. *Int. J. Heat Mass Transfer* **39**, 2937–2945. [10.4]
- Renken, K. J. and Aboye, M. 1993a Analysis of film condensation promotion within thin inclined porous coatings. *Int. J. Heat Fluid Flow* **14**, 48–53. [10.4]

- Renken, K. J. and Aboye, M. 1993b Experiments on film condensation promotion within thin porous coatings. *Int. J. Heat Mass Transfer* **36**, 1347–1355. [10.4]
- Renken, K. J. and Poulikakos, D. 1988 Experiment and analysis of forced convective heat transport in a packed bed of spheres. *Int. J. Heat Mass Transfer* **31**, 1399–1408. [4.9]
- Renken, K. J. and Poulikakos, D. 1989 Experiments on forced convection from a horizontal heated plate in a packed bed of glass spheres. *ASME J. Heat Transfer* **111**, 59–65. [4.8]
- Renken, K. J. and Poulikakos, D. 1990 Mixed convection experiments about a horizontal isothermal surface embedded in a water-saturated packed bed of spheres. *Int. J. Heat Mass Transfer* **33**, 1370–1373. [8.1.2]
- Renken, K. J., and Meechan, K. 1995 Impact of thermal dispersion during forced convection condensation in a thin porous/fluid composite system. *Chem. Engr. Comm.* **131**, 189–205. [10.4]
- Renken, K. J., Carneiro, M. J. and Meechan, K. 1994 Analysis of laminar forced convection condensation within porous coatings *AIAA J. Thermophys. Heat Transfer* **8**, 303–308. [10.4]
- Renken, K. J., Soltykiewicz, D. J. and Poulikakos, D. 1989 A study of laminar film condensation on a vertical surface with a porous coating. *Int. Comm. Heat Mass Transfer* **16**, 181–192. [10.4]
- Revellin, R., Thome, J. R., Bejan, A. and Bonjour, J. 2009 Constructal tree-shaped microchannel networks for maximizing the saturated critical heat flux. *Int. J. Thermal Sci.* **48**, 342–352. [4.19]
- Revinic, C., Grosan, T., Pop, I. and Ingham, D. B. 2011 Magnetic field effect on the unsteady free convection flow in a square cavity filled with a porous medium with constant heat generation. *Int. J. Heat Mass Transfer* **54**, 1734–1742. [7.8]
- Revinic, C., Grosan, Y., Pop, I. and Ingham, D. B. 2009 Free convection in a square cavity filled with a bidisperse porous medium. *Int. J. Therm. Sci.* **48**, 1876–1883. [7.3.9]
- Rhee, S. J., Dhir, V. K. and Catton, I. 1978 Natural convection heat transfer in beds of inductively heated particles. *ASME J. Heat Transfer* **100**, 78–85. [6.11.2]
- Riahi, D. N. 1983 Nonlinear convection in a porous layer with finite conducting boundaries. *J. Fluid Mech.* **129**, 153–171. [6.4]
- Riahi, D. N. 1989 Nonlinear convection in a porous layer with permeable boundaries. *Int. J. Non-Linear Mech.* **24**, 459–463. [6.10.2]
- Riahi, D. N. 1993a Preferred pattern of convection in a porous layer with a spatially non-uniform boundary temperature. *J. Fluid Mech.* **246**, 529–543. [6.14]
- Riahi, D. N. 1993b Effect of rotation on the stability of the melt during the solidification of a binary alloy. *Acta Mech.* **99**, 95–101. [10.2.3]
- Riahi, D. N. 1994 The effect of Coriolis force on nonlinear convection in a porous medium. *Int. J. Math. Math. Sci.* **17**, 515–536. [6.22]
- Riahi, D. N. 1996 Modal package convection in a porous layer with boundary imperfections. *J. Fluid Mech.* **318**, 107–128. [6.14]
- Riahi, D. N. 1997 Effects of centrifugal and Coriolis forces on chimney convection during alloy solidification. *J. Crystal Growth* **179**, 287–296. [10.2.3]
- Riahi, D. N. 1998a On the structure of an unsteady convecting mushy layer. *Acta Mech.* **127**, 83–96. [10.2.3]
- Riahi, D. N. 1998b High gravity convection in a mushy layer during alloy solidification. In Nonlinear Instability, Chaos and Turbulence, Vol. 1 (L. Debnath and D. N. Riahi, eds.) WIT Press, Boston, pp. 301–336. [10.2.3]
- Riahi, D. N. 1999 Effect of surface corrugation on convection in a 3D finite box of fluid saturated porous material. *Theor. Comput. Fluid Dyn.* **13**, 189–208. [6.14]
- Riahi, D. N. 2002a Effects of rotation on convection in a porous layer during alloy solidification. In Transport Phenomena in Porous Media II (D. B. Ingham and I. Pop, eds.) Elsevier, Oxford, pp. 316–340. [10.2.3]
- Riahi, D. N. 2002b On nonlinear convection in mushy layers. Part 1. Oscillatory modes of convection. *J. Fluid Mech.* **467**, 331–359. [10.2.3]
- Riahi, D. N. 2003a Nonlinear steady convection in rotating mushy layers. *J. Fluid Mech.* **485**, 279–306. [10.2.3]

- Riahi, D. N. 2003b On stationary and oscillatory modes of flow instability during alloy solidification. *J. Porous Media* **6**, 177–188. [10.2.3]
- Riahi, D. N. 2004 On nonlinear convection in mushy layers. Part 2. Mixed oscillatory and stationary modes of convection. *J. Fluid Mech.* **517**, 71–101. [10.2.3]
- Riahi, D. N. 2005 Flow instabilities in a horizontal dendrite layer roatating about an inclined axis. *J. Porous Media* **8**, 327–342. [10.2.3]
- Riahi, D. N. 2006a Effect of permeability on steady flow in a dendrite layer. *J. Porous Media* **9**, 135–153. [10.2.3]
- Riahi, D. N. 2006b Nonlinear oscillatory convection in rotating mushy layers. *J. Fluid Mech.* **553**, 389–400. [10.2.3]
- Riahi, D. N. 2007a Inertial and coriolis effects on oscillatory flow in a horizontal dendrite layer. *Transp. Porous Media* **69**, 301–312. [10.2.3]
- Riahi, D. N. 2007b Inertial effects on rotating flow in a porous layer. *J. Porous Media* **10**, 343–356. [10.2.3]
- Riahi, D. N. 2010 On nonlinear evolution approach for convective flow during alloy solidification. *Transp. Porous Media* **84**, 655–662. [10.2.3]
- Riahi, D. N. 2012 Effect of a vertical magnetic field on nonlinear convection in a mushy layer. *J. Porous Media* **15**, 805–821. [10.2.3]
- Riahi, D. N. and Sayre, T. L. 1996 Effect of rotation on the structure of a convecting mushy layer. *Acta Mech.* **118**, 109–119. [10.2.3]
- Riaz, A., Hesse, M., Tchelepi, H. A. and Orr, F. M. 2006 Onset of convection in a gravitationally unstable diffusive boundary layer in porous media. *J. Fluid Mech.* **548**, 87–111. [6.11.3, 11.11]
- Ribando, R. J. and Torrance, K. E. 1976 Natural convection in a porous medium: effects of confinement, variable permeability, and thermal boundary conditions. *ASME J. Heat Transfer* **98**, 42–48. [6.13.1]
- Ribando, R. J., Torrance, K. E. and Turcotte, D. L. 1976 Numerical models for hydrothermal circulation in the oceanic crust. *J. Geophys. Res.* **81**, 3007–3012. [11.6.1]
- Richardson, L. and Straughan, B. 1993 Convection with temperature dependent viscosity in a porous medium; nonlinear stability and the Brinkman effect. *Atti Accad. Naz. Lincei* **4**, 223–230. [6.7]
- Richardson, S. 1971 A model for the boundary condition of a porous material. Part 2. *J. Fluid Mech.* **49**, 327–336. [1.6]
- Riley, D. S. 1988 Steady two-dimensional thermal convection in a vertical porous slot with spatially periodic boundary imperfections. *Int. J. Heat Mass Transfer* **31**, 2365–2380. [7.1.4]
- Riley, D. S. and Rees, D. A. S. 1985 Non-Darcy natural convection from arbitrarily inclined heated surfaces in saturated porous media. *Q. J. Mech. Appl. Math.* **38**, 277–295. [5.12.2]
- Riley, D. S. and Winters, K. H. 1989 Modal exchange mechanisms in Lapwood convection. *J. Fluid Mech.* **204**, 325–358. [6.15.1]
- Riley, D. S. and Winters, K. H. 1990 A numerical bifurcation study of natural convection in a tilted two-dimensional porous cavity. *J. Fluid Mech.* **215**, 309–329. [7.8]
- Riley, D. S. and Winters, K. H. 1991 Time-periodic convection in porous media: the evolution of Hopf bifurcations with aspect ratio. *J. Fluid Mech.* **223**, 457–474. [6.15.1]
- Rionero, S. and Straughan, B. 1990 Convection in a porous medium with internal heat source and variable gravity effects. *Int. J. Engng. Sci.* **28**, 497–503. [6.11.2]
- Rionero, S. 2007 A new approach to nonlinear L-2-stability of double diffusive convection in porous media: Necessary and sufficient conditions for global stability via a linearization principle. *J. Math. Ana. Appl.* **333**, 1036–1057. [9.1.6.4]
- Rionero, S. 2010 Long-time behaviour of multicomponent fluid mixtures in porous media. *Int. J. Engng. Sci.* **48**, 1519–1533. [9.1.6.4]
- Rionero, S. 2011 Onset of convection in porous materials with vertically stratified porosity. *Acta Mech.* **222**, 261–272. [6.13.2]
- Rionero, S. 2012 Global non-linear stability in double-diffusive convection via hidden symmetries. *Int. J. Nonlinear Mech.* **47**, 61–66. [9.1.3]

- Ritchie, L. T. and Prichard, D. 2011 Natural convection and the evolution of a reactive porous medium. *J. Fluid Mech.* **673**, 286–317. [11.8]
- Roberts, P. H. and Loper, D. E. 1983 Towards a theory of the structure and evolution of a dendrite layer. *Stellar and Planetary Magnetism* (ed. A. M. Soward), Gordon and Braech, New York, 329–349. [10.2.3]
- Roberts, P. H., Loper, D. E. and Roberts, M. F. 2003 Convective instability of a mushy layer: I. Uniform permeability. *Geophys. Astrophys. Fluid Dyn.* **97**, 97–134. [10.2.3]
- Robillard, L. and Torrance, K. E. 1990 Convective heat transfer inhibition in an annular porous layer rotating at weak angular velocity. *Int. J. Heat Mass Transfer* **33**, 953–963. [7.3.3]
- Robillard, L. and Vasseur, P. 1992 Quasi-steady state natural convection in a tilted porous layer. *Canad. J. Chem. Engng.* **70**, 1094–1100. [7.8]
- Robillard, L., Bahloul, A. and Vasseur, P. 2006 Hydromagnetic natural convection of a binary fluid in a vertical porous enclosure. *Chem. Engng. Comm.* **193**, 1431–1444. [9.2.2]
- Robillard, L., Wang, C. H. and Vasseur, P. 1988 Multiple steady states in a confined porous medium with localized heating from below. *Numer. Heat Transfer* **13**, 91–110. [6.18]
- Robillard, L., Zhang, X. and Zhao, M. 1993 On the stability of a fluid-saturated porous medium contained in a horizontal circular cylinder. *ASME HTD* **264**, 49–55. [6.16.2]
- Rocamora, F. D. and de Lemos, M. J. S. 2000 Analysis of convective heat transfer for turbulent flow in saturated porous media. *Int. Comm. Heat Mass Transfer* **27**, 825–834. [1.8]
- Rocha, L. A. O., Lorente, S. and Bejan A. 2009 Tree-shaped vascular wall designs for localized intense cooling. *Int. J. Heat Mass Transfer* **52**, 4535–4544. [4.19]
- Rocha, L. A. O., Neagu, M., Bejan, A. and Cherry, R. S. 2001 Convection with phase change during gas formation from methane hydrates via depressurization of porous layers. *J. Porous Media* **4**, 283–295. [10.1.7]
- Rodrigues, J. F. and Urbano, J. M. 1999 Darcy-Stefan problem arising in freezing and thawing of saturated porous media. *Cont. Mech. Thermodyn.* **11**, 181–191. [10.2.1.2]
- Rogers, J. A. 1992 Funicular and evaporation front regimes in convective drying of granular beds. *Int. J. Heat Mass Transfer* **35**, 469–480. [3.6]
- Rohni, A. M., Amad, S., Pop, I. and Merkin, J. H. 2012 Unsteady mixed convection boundary-layer flow with suction and temperature slip effects near the stagnation point on a vertical permeable surface embedded in a porous medium. *Transp. Porous Media* **92**, 1–14. [8.1.1]
- Rohni, A. M., Amad, S., Merkin, J. H. and Pop, I. and Merkin, J. H. 2012b Mixed convection boundary-layer flow along a vertical permeable cylinder embedded in a porous medium filled by a nanofluid. *Transp. Porous Media*, to appear. [8.1.3]
- Rohsenow, W. M. and Choi, H. Y. 1961 Heat, Mass and Momentum Transfer. Prentice-Hall, Englewood Cliffs, NJ. [4.5]
- Rohsenow, W. M. and Hartnett, J. P. 1973 Handbook of Heat Transfer. McGraw-Hill, New York. [4.5]
- Romero, L. A. 1994 Low or high Péclet number flow past a sphere in a saturated porous medium. *SIAM J. Appl. Math.* **54**, 42–71. [4.3]
- Romero, L. A. 1995a Low or high Péclet number flow past a prolate spheroid in a saturated porous medium. *SIAM J. Appl. Math.* **55**, 952–974. [4.3]
- Romero, L. A. 1995b Forced convection past a slender body in a saturated porous medium. *SIAM J. Appl. Math.* **55**, 975–985. [4.16.5]
- Rong, F. M., Guo, Z. L., Chai, Z. H. and Shi, B. C. 2010a A lattice Boltzmann method for axisymmetric thermal flows through porous media. *Int. J. Heat Mass Transfer* **53**, 5519–5527. [2.6]
- Rong, F. M., Guo, Z. L., Zhang, T. and Shi, B. C. 2010b Numerical study of Bénard convection with temperature-dependent viscosity in a porous cavity via lattice Boltzmann method. *Int. J. Modern Phys. C* **21**, 1407–1419. [6.7]
- Roper, S. M., Davis, S. H. and Voorhees, P. W. 2007 Convection in a mushy zone forced by sidewall heat losses. *Metall. Mater. Trans. A* **38**, 1069–1079. [10.2.3]
- Roper, S. M., Davis, S. H. and Voorhees, P. W. 2011 Localization of convection in mushy layers by weak background flow. *J. Fluid Mech.* **675**, 518–528. [10.2.3]

- Rosa, R. N., Reis, A. H. and Miguel, A. F. 2004 Bejan's Structural Theory of Shape and Structure, Évora Geophysical Center, University of Évora, Portugal. [4.18]
- Rosali, H., Ishak, A. and Pop, I. 2011 Mixed convection stagnation-point flow past a vertical plate with prescribed heat flux embedded in a porous medium: Brinkman-extended Darcy formulation. *Transp. Porous Media* **90**, 709–719. [8.4.2]
- Rosali, H., Ishak, A. and Pop, I. 2012 Micropolar fluid flow towards a stretching/shrinking sheet in a porous medium with suction. *Int. Comm. Heat Mass Transfer* **39**, 826–829. [5.1.9.2]
- Rosca, A. V., Rosca, N. C., Grosan, T. and Pop, I. 2012 Non-Darcy mixed convection from a horizontal plate embedded in a nanofluid saturated porous medium. . *Int. Comm. Heat Mass Transfer* **39**, 1080–1085. [8.1.2, 9.7]
- Rosenberg, N. D. and Spera, F. J. 1990 Role of anisotropic and/or layered permeability in hydrothermal convection. *Geophys. Res. Lett.* **17**, 235–238. [6.13.2]
- Rosenberg, N. D. and Spera, F. J. 1992 Thermohaline convection in a porous medium heated from below. *Int. J. Heat Mass Transfer* **35**, 1261–1273. [9.1.5]
- Rosenberg, N. D., Spera, F. J. and Haymon, R. M. 1993 The relationship between flow and permeability field in seafloor hydrothermal systems. *Earth Planet. Sci. Lett.* **116**, 135–153. [6.12]
- Roslan, R., Mahmud, M. N. and Hashim, I. 2011 Effects of feedback control on chaotic convection in fluid-saturated porous media. *Int. J. Heat Mass Transfer* **54**, 404–412. [6.11.3]
- Rossi di Schio, E., Celli, M. and Pop, I. 2011 Buoyant flow in a vertical fluid saturated porous annulus: The Brinkman model. *Int. J. Heat Mass Transfer* **54**, 1665–1670. [7.3.3]
- Roussellet, V., Niu, X. D., Yamaguchi, H. and Magoules, F. 2011 Natural convection of temperature-sensitive magnetic fluids in porous media. *Adv. Appl. Math. Mech.* **3**, 121–130. [2.6]
- Royer, J. J. and Flores, L. 1994 Two-dimensional natural convection in an anisotropic and heterogeneous porous medium with internal heat generation. *Int. J. Heat Mass Transfer* **37**, 1387–1399. [6.11.2]
- Royer, P., Auriault, J. L. and Boutin, C. 1995 Contribution de l'homogénéisation à l'étude de la filtration d'un fluide en milieux poreux fracturé. *Rev. Inst. Franc. Petr.* **50**, 337–352. [1.9]
- Rubin, H. 1974 Heat dispersion effect on thermal convection in a porous medium layer. *J. Hydrol.* **21**, 173–184. [2.2.4]
- Rubin, H. 1975 Effect of solute dispersion on thermal convection in a porous medium layer. 2. *Water Resources Res.* **11**, 154–158. [9.1.6.1]
- Rubin, H. 1976 Onset of thermohaline convection in a cavernous aquifer. *Water Resources Res.* **12**, 141–147. [9.1.6.1]
- Rubin, H. 1981 Onset of thermohaline convection in heterogeneous porous media. *Israel J. Tech.* **19**, 110–117. [6.13.1, 9.1.6.2]
- Rubin, H. 1982a Thermohaline convection in a nonhomogeneous aquifer. *J. Hydrol.* **57**, 307–320. [9.1.6.2]
- Rubin, H. 1982b Application of the aquifer's average characteristics for determining the onset of thermohaline convection in a heterogeneous aquifer. *J. Hydrol.* **57**, 321–336. [9.1.6.2]
- Rubin, H. and Roth, C. 1978 Instability of horizontal thermohaline flow in a porous medium layer. *Israel J. Tech.* **16**, 216–223. [9.1.6.1]
- Rubin, H. and Roth, C. 1983 Thermohaline convection in flowing groundwater. *Adv. Water Resources* **6**, 146–156. [9.1.6.1]
- Rubinstein, J. 1986 Effective equations for flow in random porous media with a large number of scales. *J. Fluid Mech.* **170**, 379–383. [1.5.3]
- Rudraiah, N. 1984 Linear and non-linear magnetoconvection in a porous medium. *Proc. Indian Acad. Sci. (Math. Sci.)* **93**, 117–135. [6.21]
- Rudraiah, N. 1985 Coupled parallel flows in a channel and a bounding porous medium of finite thickness. *ASME J. Fluids Engng.* **107**, 322–329. [1.6]
- Rudraiah, N. 1988 Turbulent convection in porous media with non-Darcy effects. *ASME HTD* **96**, vol. **1**, 747–754. [1.8]

- Rudraiah, N. and Gyathri, M. S. 2009 Effect of thermal modulation on the onset of electroconvection in a dielectric fluid saturated porous medium. *ASME J. Heat Transfer* **131**, #101009. [6.21]
- Rudraiah, N. and Malashetty, M. S. 1990 Effect of modulation on the onset of convection in a sparsely packed porous layer. *ASME J. Heat Transfer* **112**, 685–689. [6.11.3]
- Rudraiah, N. and Ng, C. O. 2007 Dispersion in porous media with and without reaction – a review. *J. Porous Media* **10**, 219–248. [2.2.4]
- Rudraiah, N. and Prasad, V. 1998 Effect of Brinkman boundary layer on the onset of Marangoni convection in a fluid-saturated porous layer. *Acta Mech.* **127**, 235–246. [6.19.3]
- Rudraiah, N. and Siddheshwar, P. G. 1998 A weak nonlinear stability analysis of double-diffusive convection with cross-diffusion in a fluid-saturated porous medium. *Heat Mass Transfer* **33**, 287–293. [9.1.4]
- Rudraiah, N. and Srimani, P. K. 1980 Finite-amplitude cellular convection in a fluid-saturated porous layer. *Proc. Roy. Soc. London Ser. A* **373**, 199–222. [6.3]
- Rudraiah, N. and Vortmeyer, D. 1978 Stability of finite-amplitude and overstable convection of a conducting fluid through fixed porous bed. *Wärme Stoffübertrag.* **11**, 241–254. [6.21]
- Rudraiah, N. and Vortmeyer, D. 1982 The influence of permeability and of a third diffusing component upon the onset of convection in a porous medium. *Int. J. Heat Mass Transfer* **25**, 457–464. [9.1.6.4]
- Rudraiah, N., Kaloni, P. N. and Radhadevi, P. V. 1989 Oscillatory convection in a viscoelastic fluid through a porous layer heated from below. *Rheol. Acta* **28**, 48–53. [6.23]
- Rudraiah, N., Masuoka, T. and Nair, P. 2007 Effect of combined Brinkman-electric boundary layer on the onset of Marangoni electroconvection in a poorly conducting fluid-saturated porous layer cooled from below in the presence of an electric field. *J. Porous Media* **10**, 421–433. [6.21]
- Rudraiah, N., Sheela, R. and Srimani, P. K. 1987 Mixed thermohaline convection in an inclined porous layer. *ASME HTD* **84**, 97–101. [9.6.1]
- Rudraiah, N., Shivakumara, I. S. and Friedrich, R. 1986 The effect of rotation on linear and nonlinear double-diffusive convection in a sparsely packed, porous medium. *Int. J. Heat Mass Transfer* **29**, 1301–1317. [9.1.6.4]
- Rudraiah, N., Siddheshwar, P. G. and Masuoka, T. 2003 Nonlinear convection in porous media: A review. *J. Porous Media* **6**, 1–32. [6.4]
- Rudraiah, N., Srimani, P. K. and Friedrich, R. 1982a Finite amplitude convection in a two-component fluid saturated porous layer. *Int. J. Heat Mass Transfer* **25**, 715–722. [9.1.3]
- Rudraiah, N., Veerappa, B. and Balachandra Rao, S. 1980 Effects of nonuniform thermal gradient and adiabatic boundaries on convection in porous media. *ASME J. Heat Transfer* **102**, 254–260. [6.11.2]
- Rudraiah, N., Veerappa, B. and Balachandra Rao, S. 1982b Convection in a fluid-saturated porous layer with non-uniform temperature gradient. *Int. J. Heat Mass Transfer* **25**, 1147–1156. [6.11.2]
- Ruth, D. and Ma, H. 1992 On the derivation of the Forchheimer equation by means of the averaging theorem. *Transport in Porous Media* **7**, 255–264. [1.5.2]
- Ryland, D. K. and Nandakumar, K. 1992 Bifurcation study of convective heat transfer in porous media. Part II. Effect of tilt on stationary and nonstationary solutions. *Phys. Fluids A* **4**, 1945–1958. [6.17]
- Saada, M. A., Chikh, S. and Campo, A. 2007 Natural convection around a horizontal solid cylinder wrapped with a layer of fibrous or porous material. *Int. J. Heat Fluid Flow* **28**, 483–495. [7.7]
- Saada, M. A., Chikh, S. and Campo, A. 2009 Natural convection reduction in a composite air/porous annular region with horizontal orientation. *ASME J. Heat Transfer* **131**, #022601. [7.3.3]
- Saada, M. A., Chikh, S. and Campo, A. 2010 Augmentation or suppression of natural convective heat transfer in horizontal annuli with air and partially filled with a porous layer. *Heat Transfer Research* **41**, 573–597. [7.3.3]
- Saatdjian, E., Lam, R. and Mota, J. P. B. 1999 Natural convection heat transfer in the annular region between porous confocal ellipses. *Int. J. Numer. Meth. Fluids* **31**, 513–522. [7.3.3]

- Saati, A. A. and Mohamad, A. A. 2007 Heat transfer enhancement in a composite parallel plate channel: Utilizing the low-Reynolds-number k-epsilon model. *J. Porous Media* **10**, 249–259. [4.11]
- Saeid, N. F. and Mohamad, A. A. 2005a Periodic free convection from a vertical plate in a saturated porous medium, non-equilibrium model. *Int. J. Heat Mass Transfer* **48**, 3855–3863. [5.1.9.7]
- Saeid, N. F. and Mohamad, A. A. 2005b Natural convection in a porous cavity with spatial sidewall temperature variation. *Int. J. Numer. Meth. Heat Fluid Flow* **15**, 555–566. [7.2]
- Saeid, N. H. 2005 Natural convection in porous cavity with sinusoidal bottom wall temperature variation. *Int. Comm. Heat Mass Transfer* **32**, 454–463. [6.18]
- Saeid, N. H. 2006c Natural convection in a square porous cavity with an oscillating wall temperature. *Arab. J. Sci. Engng.* **31**, 35–46. [7.5]
- Saeid, N. H. 2006a Analysis of free convection about a horizontal cylinder in a porous media using a thermal non-equilibrium model. *Int. Comm. Heat Mass Transfer* **33**, 158–165. [5.5.1]
- Saeid, N. H. 2006b Natural convection from two thermal sources in a vertical porous layer. *ASME J. Heat Transfer* **128**, 104–109. [7.3.7]
- Saeid, N. H. 2007a Conjugate natural convection in a vertical porous layer sandwiched by finite thickness walls. *Int. Comm. Heat Mass Transfer* **34**, 210–216. [7.1.5]
- Saeid, N. H. 2007b Jet impingement interaction with cross flow in horizontal porous layer under thermal non-equilibrium conditions. *Int. J. Heat Mass Transfer* **50**, 4265–4274. [6.14, 8.4.2]
- Saeid, N. H. 2007c Maximum density effects on natural convection in a porous cavity under thermal non-equilibrium conditions. *Acta Mech.* **188**, 55–68. [7.3.5]
- Saeid, N. H. 2007d Conjugate natural convection in a porous enclosure; effect of conduction in one of the vertical walls. *Int. J. Therm. Sci.* **46**, 531–539. [7.1.5]
- Saeid, N. H. 2008 Conjugate natural convection in a porous enclosure sandwiched by finite walls under thermal non-equilibrium conditions. *J. Porous Media* **11**, 259–275. [7.1.5]
- Saeid, N. H. 2004 Analysis of mixed convection in a vertical porous layer using non-equilibrium model. *Int. J. Heat Mass Transfer* **47**, 5619–5627. [8.3.1]
- Saeid, N. H. and Mohamad, A. A. 2006 Jet impingement cooling of a horizontal surface in a confined porous medium: Mixed convection regime. *Int. J. Heat Mass Transfer* **49**, 3906–3913. [8.4.2]
- Saeid, N. H. and Pop, I. 2004a Transient free convection in a square cavity filled with a porous medium. *Int. J. Heat Mass Transfer* **47**, 1917–1924. [7.5]
- Saeid, N. H. and Pop, I. 2004b Viscous dissipation effects on free convection in a porous cavity. *Int. Comm. Heat Mass Transfer* **31**, 723–732. [7.5]
- Saeid, N. H. and Pop, I. 2004c Maximum density effects on natural convection from a discrete heater in a cavity filled with a porous medium. *Acta Mech.* **171**, 203–212. [7.3.5]
- Saeid, N. H. and Pop, I. 2005a Non-Darcy natural convection in a square cavity filled with a porous medium. *Fluid Dyn. Res.* **36**, 35–43. [7.6.1]
- Saeid, N. H. and Pop, I. 2005b Natural convection from a discrete heater in a square cavity filled with a porous medium. *J. Porous Media* **8**, 55–63. [7.3.7]
- Saeid, N. H. and Pop, I. 2005c Mixed convection from two thermal sources in vertical porous layer. *Int. J. Heat Mass Transfer* **48**, 4150–4160. [8.1.1]
- Saeid, N. H. and Pop, I. 2006 Periodic mixed convection in horizontal porous layer heated from below by isoflux heater. *Arab. J. Sci. Engng.* **31**, 153–164. [8.4.2]
- Saez, A. E., Perfetti, J. C. and Rusinek, I. 1991 Prediction of effective diffusivities in porous media using spatially periodic models. *Transport Porous Media* **11**, 187–199. [1.5.2]
- Saffman, P. 1971 On the boundary condition at the surface of a porous medium. *Stud. Appl. Math.* **50**, 93–101. [1.6]
- Saghir, M. Z. 1998 Heat and mass transfer in a multiporous cavity. *Int. Comm. Heat Mass Transfer* **25**, 1019–1030. [9.4]
- Saghir, M. Z. and Islam, M. R. 1999 Double diffusive convection in dual-permeability dual-porosity porous media. *Int. J. Heat Mass Transfer* **42**, 437–454. [9.4]

- Saghir, M. Z., Comi, P. and Mehrvar, M. 2002 Effects of interaction between Rayleigh and Marangoni convection in superposed fluid and porous layers. *Int. J. Thermal Sci.* **41**, 207–215. [6.19.3]
- Saghir, M. Z., Jiang, C. G., Chacha, M., Khawaja, M. and Pan, S. 2005a Thermodiffusion in porous media. In *Transport Phenomena in Porous Media III*, (eds. D. B. Ingham and I. Pop), Elsevier, Oxford, pp. 227–260. [9.1.4]
- Saghir, M. Z., Mahendran, P. and Hennenberg, M. 2005b Marangoni and gravity driven convection in a liquid layer overlying a porous layer: lateral and bottom heating conditions. *Energy Sources* **27**, 151–171. [6.19.2, 6.19.3]
- Saghir, M. Z., Nejad, M., Vaziri, H. H. and Islam, M. R. 2001 Modeling of heat and mass transfer in a fractured porous medium. *Int. J. Comput. Fluid Dyn.* **15**, 279–292. [1.9]
- Sahimi, M. 1993 Flow phenomena in rocks: from continuum models to fractals, percolation, cellular automata, and simulated annealing. *Rev. Mod. Phys.* **65**, 1393–1534. [1.9]
- Sahraoui, M. and Kaviany, M. 1992 Slip and no-slip velocity boundary conditions at the interface of porous, plain media. *Int. J. Heat Mass Transfer* **35**, 927–943. [1.6]
- Sahraoui, M. and Kaviany, M. 1993 Slip and no-slip temperature boundary conditions at the interface of porous, plain media: conduction. *Int. J. Heat Mass Transfer* **36**, 1019–1033. [2.4]
- Sahraoui, M. and Kaviany, M. 1994 Slip and no-slip temperature boundary conditions at the interface of porous, plain media: convection. *Int. J. Heat Mass Transfer* **37**, 1029–1044. [2.4]
- Saidi, M. H. and Khiaabani, R. H. 2007 Forced convective heat transfer in parallel flow multilayer microchannels. *ASME J. Heat Transfere* **129**, 1230–1236. [4.16.5]
- Saied, N. H. 2007 Conjugate natural convection in a porous enclosure: effect of conduction in one of the vertical walls. *Int. J. Thermal Sci.* **46**, 531–539. [7.1.5]
- Saija, U. K., Udaya, K. and Felicelli, S. D. 2011 Modeling freckle segregation with mesh adaptation. *Metal. Mat. Trans. B* **42**, 1118–1129. [10.2.3]
- Saito, M. B. and de Lemos, J. S. 2006 A correlation for interfacial heat transfer coefficient for turbulent flow over an array of square rods. *ASME J. Heat Transfer* **128**, 444–452. [1.8]
- Saito, M. B. and de Lemos, M. J. S. 2005 Interfacial heat transfer coefficient in non-equilibrium convective transport in porous media. *Int. Comm. Heat Mass Transfer* **32**, 666–676. [2.2.3]
- Saito, M. B. and de Lemos, M. J. S. 2009 Laminar heat transfer in a porous channel simulated with a two-energy equation model. *Int. Comm. Heat Mass Transfer* **36**, 1002–1007. [1.8]
- Saito, M. B. and de Lemos, M. J. S. 2010 A macroscopic two-energy equation model for turbulent flow and heat transfer in highly porous media. *Int. J. Heat Mass Transfer* **53**, 2424–2433. [1.8]
- Sajid, M., Ahmad, I. and Hayat, T. 2009 Unsteady boundary layer flow due to a stretching sheet in a porous medium with partial slip. *J. Porous Media* **12**, 911–917. [5.1.9.9]
- Sakamoto, H. and Kulacki, F. A. 2007 Buoyancy driven flow in saturated porous media. *ASME J. Heat Transfer* **129**, 727–734. [7.2]
- Sakamoto, H. and Kulacki, F. A. 2008 Effective thermal diffusivity of porous media in the wall vicinity. *ASME J. Heat Transfer* **130**, #022601. [1.7]
- Salagnac, P., Dutournie, P. and Glouannec, P. 2008 Optimal operating conditions of microwave-convective drying of a porous medium. *Indust. Engng. Chem. Res.* **47**, 133–144. [3.6]
- Salagnac, P., Glouannec, P. and Lecharpentier, D. 2004 Numerical modeling of heat and mass transfer in porous medium during combined hot air, infrared and microwaves drying. *Int. J. Heat Mass Transfer* **44**, 4479–4489. [3.6]
- Salama, A. 2011a On the Brinkman equation and the concept of viscous dissipation in porous media. *Spec. Top. Rev. Porous Media* **2**, 83–89. [2.2.2]
- Salama, A., El-Amin, M. F., Abbas, I. and Sun, S. Y. 2011 On the viscous dissipation modeling of thermal fluid flow in a porous medium *Arkiv. Appl. Mech.* **81**, 1865–1878. [2.2.2, 5.1.9.9]
- Salama, F. A. 2011b Lie group analysis for thermophoretic and radiative augmentation of heat and mass transfer in a Brinkman-Darcy flow over a flat surface with heat generation. *Acta Mech. Sinica* **27**, 531–540. [9.4]

- Saleh, H., Hashim, I. and Saeid, N. 2010 Effect of time-periodic boundary conditions on convective flows in a porous square enclosure with non-uniform internal heating. *Transp. Porous Media* **85**, 885–903. [6.11.2]
- Saleh, H., Roslan, R. and Hashim, I. 2011a Natural convection in a porous trapezoidal enclosure with an inclined magnetic field. *Comput. Fluids* **47**, 155–169. [7.3.7]
- Saleh, H., Saeid, N. and Hashim, I. 2011b Effect of conduction in bottom wall on Darcy-Bénard convection in a porous medium. *Transp. Porous Media* **88**, 357–368. [6.2]
- Saleh, H., Mustafa, Z., Hashim, I. and Roslan, R. 2012 Feedback control of flows in a porous square enclosure having nonuniform internal heating. *J. Porous Media* **15**, 785–792. [7.1.7]
- Salem, A. M. 2006a Coupled heat and mass transfer in Darcy-Forchheimer mixed convection from a vertical flat plate embedded in a fluid-saturated porous medium under the effects of radiation and viscous dissipation. *J. Korean Phys. Soc.* **48**, 409–413. [9.6.1]
- Salem, A. M. 2006b Thermal-diffusion and diffusion-thermal effects on convection heat transfer in a visco-elastic fluid flow through a porous medium over a stretching sheet. *Commun. Numer. Meth. Engng.* **22**, 955–966. [9.2.1]
- Salem, A. M. 2009 Temperature-dependent viscosity effects on non-Darcy hydromagnetic free-convection heat transfer from a vertical wedge in porous media. *Nouvo Cim. Soc. Ital. Fis. B* **124**, 959–974. [5.3]
- Salem, A. M. 2010 Temperature-dependent viscosity effects on non-Darcy hydrodynamic free convection heat transfer from a vertical wedge in porous media. *Chinese Phys. Lett.* **27**, #064401. [5.3]
- Salinger, A. G., Aris, R. and Derby, J. J. 1994a Finite element formulations for large-scale, coupled flows in adjacent porous and open fluid domains. *Int. J. Numer. Meth. Fluids* **18**, 1185–1209. [1.6]
- Salinger, A. G., Aris, R. and Derby, J. J. 1994b Modeling the spontaneous ignition of coal stockpiles. *AIChE J.* **40**, 991–1004. [3.4]
- Sallam, S. N. 2010 Thermal diffusion and diffusion-thermo effects on mixed convection heat and mass transfer in a porous medium. *J. Porous Media* **13**, 331–345. [9.6.1]
- Salt, H. 1988 Heat transfer across a convecting porous layer with flux boundaries. *Transport in Porous Media* **3**, 325–341. [6.3]
- Samantray, P. K., Karthikeyan, P. and Reddy, K. S. 2006 Estimating effective thermal conductivity of two-phase materials. *Int. J. Heat Mass Transfer* **49**, 4209–4219. [2.2.1]
- Sanchez, F. A. and Medina, A. 2006 Passive dispersion in symmetrically interconnected layers under natural convection. *J. Fluid Mech.* **567**, 235–259. [7.8]
- Sanchez, F., Higuera, F. J. and Medina, A. 2005a Natural convection in tilted cylindrical cavities embedded in rocks. *Phys. Rev. E* **71**, art. # 066308. [7.8]
- Sanchez, F., Perez-Rosales, C. and Medina, A. 2005b Natural convection in symmetrically interconnected tilted layers. *J. Phys. Soc. Japan* **74**, 1170–1180. [7.7]
- Sander, A. 2007 Thin-layer drying of porous materials: Selection of the appropriate mathematical model and relationships between thin-layer models parameters. *Chem. Engng. Process.* **46**, 1324–1331. [3.6]
- Sandner, H. 1986 Double diffusion effects in a cylindrical porous bed filled with salt water. *Heat Transfer* 1986, Hemisphere, Washington, DC, vol. 5, pp. 2623–2627. [9.4]
- Sankar, M., Buvaneshwari, M., Sivasankaran, S. and Do, Y. 2011a Buoyancy induced convection in a porous cavity with partially thermally active sidewalls. *Int. J. Heat Mass Transfer* **54**, 5173–518. [7.11]
- Sankar, M., Kim, B., Lopez, J. M. and Do, Y. 2012b Thermosolutal convection from a discrete heat and solute source in a vertical porous annulus. *Int. J. Heat Mass Transfer* **55**, 4116–4128. [9.4]
- Sankar, M., Park, Y., Lopez, J. M. and Do, Y. 2011b Numerical study of natural convection in a vertical porous annulus with discrete heating. *Int. J. Heat Mass Transfer* **54**, 1483–1505. [7.3.7]
- Sankar, M., Park, Y., Lopez, J. M. and Do, Y. 2012a Double diffusive convection from a discrete heat and solute source in a vertical porous annulus. *Transp. Porous Media* **91**, 753–775. [9.2.2]

- Sano, T. 1996 Unsteady forced and natural convection around a sphere immersed in a porous medium. *J. Engng Math.* **30**, 515–525. [5.6.2]
- Sano, T. and Makizono, K. 1998 Unsteady mixed convection around a sphere in a porous medium at low Péclet numbers. *Fluid Dyn. Res.* **23**, 45–61. [8.1.3]
- Sano, T. and Okihara, R. 1994 Natural convection around a sphere immersed in a porous medium at small Rayleigh numbers. *Fluid Dyn. Res.* **13**, 39–44. [5.6.2]
- Santos, N. B. and de Lemos, M. J. S. 2006 Flow and heat transfer in a parallel-plate channel with porous and solid baffles. *Numer. Heat Transfer A* **49**, 471–494. [4.11]
- Saravanan, S. 2009a Centrifugal acceleration induced convection in a magnetic fluid saturated anisotropic rotating porous medium. *Transp. Porous Media* **77**, 79–86. [6.22]
- Saravanan, S. 2009b Thermal non-equilibrium porous convection with heat generation and density maximum. *Transp. Porous Media* **76**, 35–43. [6.11.2]
- Saravanan, S. and Jegajoth, R. 2010 Stationary fingering instability in a non-equilibrium porous medium with coupled molecular diffusion. *Transp. Porous Media* **84**, 755–771. [9.1.4]
- Saravanan, S. and Arunkumar, A. 2010 Convective instability in a gravity modulated anisotropic thermally stable porous medium. *Int. J. Engng. Sci.* **48**, 742–750. [6.24]
- Saravanan, S. and Kandaswamy, P. 2003a Non-Darcian thermal stability of a heat generating fluid in a porous annulus. *Int. J. Heat Mass Transfer* **46**, 4863–4875. [6.17]
- Saravanan, S. and Kandaswamy, P. 2003b Convection currents in a porous layer with a gravity gradient. *Heat Mass Transfer* **39**, 693–699. [7.9]
- Saravanan, S. and Keerthana, S. 2012 Effect of double diffusion on centrifugal filtration convection. *J. Porous Media* **15**, 495–500. [9.1.6.4]
- Saravanan, S. and Premalatha, D. 2012 Effect of couple stress on the onset of thermovibrational convection in a porous medium. *Int. J. Therm. Sci.* **57**, 71–77. [6.24]
- Saravanan, S. and Purusothaman, A. 2009 Floquet instability of a gravity modulated Rayleigh–Bénard problem in an anisotropic porous medium. *Int. J. Therm. Sci.* **48**, 2085–2091. [6.24]
- Saravanan, S. and Sivakumar, T. 2010 Onset of convection in a vibrating medium: The Brinkman model. *Phys. Fluids* **22**, #034104. [6.24]
- Saravanan, S. and Sivakumar, T. 2011a Thermovibrational instability in a fluid saturated anisotropic porous medium. *ASME J. Heat Transfer* **133**, #051601. [6.24]
- Saravanan, S. and Sivakumar, T. 2011b Onset of thermovibrational filtration convection: Departure from thermal equilibrium. *Phys. Rev. E* **84**, #026307. [6.24]
- Saravanan, S. W. and Brindha, D. 2010 Global stability of centrifugal filtration convection. *J. Math. Anal. Appl.* **367**, 116–128. [6.22]
- Saravanan, S. W. and Brindha, D. 2011 Linear and non-linear stability limits for centrifugal convection in an anisotropic layer. *Int. J. Nonlinear Mech.* **46**, 65–72. [6.22]
- Sarkar, A. and Phillips, O. M. 1992a Effects of horizontal gradients on thermohaline instabilities in infinite porous media. *J. Fluid Mech.* **242**, 79–98. [9.5]
- Sarkar, A. and Phillips, O. M. 1992b Effects of horizontal gradients on thermohaline instabilities in a thick porous layer. *Phys. Fluids A* **4**, 1165–1175. [9.5]
- Sarler, B. 2000 DRBEM solution of porous media natural convection problems with internal heat generation. *Z. Angew. Math. Mech.* **80**, S703–S704, Supp. 3. [2.9, 7.3.8]
- Sarler, B., Gobin, D., Goyeau, B., Perko, J. and Power, H. 2000a Natural convection in porous media – dual reciprocity boundary element method solution of the Darcy model. *Int. J. Numer. Meth. Fluids* **33**, 279–312. [7.3.8]
- Sarler, B., Perko, J. and Chen, C. S. 2004a Radial basis function collocation method of solution of natural convection in porous media. *Int. J. Numer. Meth. Heat Fluid Flow* **14**, 187–212. [2.9, 7.3.8]
- Sarler, B., Perko, J., Gobin, D., Goyeau, B. and Power, H. 2000b Dual reciprocity boundary element method of natural convection in Darcy–Brinkman porous media. *Engng. Anal. Boundary Elements* **28**, 23–41. [2.9, 7.3.8]

- Sarler, B., Perko, J., Gobin, D., Goyeau, B. and Power, H. 2004b Dual reciprocity boundary element method of natural convection in Darcy-Brinkman porous media. *Engng. Anal. Boundary Elem.* **28**, 23–41. [2.9, 7.3.8]
- Sasaguchi, K. 1995 Effect of density inversion of water on the melting process of frozen porous media. Proc. ASME/JSME Thermal Engineering Joint Conf. vol. 3, pp. 371–378. [10.1.7]
- Sasaki, A., Aiba, S. and Fukusako, S. 1990 Numerical study on freezing heat transfer in water-saturated porous media. *Numer. Heat Transfer A* **18**, 17–32. [10.2.1.2]
- Sasaki, A., and Aiba, S. 1992 Freezing heat transfer in water-saturated porous media in a vertical rectangular vessel. *Wärme-Stoffübertrag.*, **27**, 289–298. [10.2.1.2]
- Sathe, S. B. and Tong, T. W. 1988 Measurements of natural convection in partially porous rectangular enclosures of aspect ratio 5. *Int. Comm. Heat Mass Transfer* **15**, 203–212. [7.7]
- Sathe, S. B. and Tong, T. W. 1989 Comparison of four insulation schemes for reduction of natural convective heat transfer in rectangular enclosures. *Int. Comm. Heat Mass Transfer* **16**, 795–802. [7.7]
- Sathe, S. B., Lin, W. Q. and Tong, T. W. 1988 Natural convection in enclosures containing an insulation with a permeable-fluid-porous interface. *Int. J. Heat Fluid Flow* **9**, 389–395. [7.7]
- Sathe, S. B., Tong, T. W. and Faruque, M. A. 1987 Experimental study of natural convection in a partially porous enclosure. *AIAA J. Thermophys. Heat Transfer* **1**, 260–267. [7.7]
- Sathiyamoorthy, M. 2011 Analysis of convective heat transfer in a square cavity filled with a porous medium under a magnetic field. *Spec. Top. Rev. Porous Media* **2**, 171–180. [7.6.2]
- Sathiyamoorthy, M., and Narasimman , S. 2011 Effect of thin film on non-Darcy buoyancy flow in a square cavity filled with porous medium. *J. Porous Media* **14**, 975–988. [7.6.2]
- Sathiyamoorthy, M., Basak, T. and Roy, S. 2011 Non-Darcy buoyancy flow in a square cavity filled with porous medium for various temperature difference aspect ratios. *J. Porous Media* **14**, 649–657. [7.6.2]
- Sathiyamoorthy, M., Basak, T., Roy, S. and Pop, I. 2007 Steady natural convection in a square cavity filled with a porous medium for linearly heated side wall(s). *Int. J. Heat Mass Transfer* **50**, 1892–1901. [7.6.2]
- Satik, C., Parlar, M. and Yortsos, Y. C. 1991 A study of steady-state, steam-water counterflow in porous media. *Int. J. Heat Mass Transfer*, **34**, 1755–1771. [11.9.1,11.9.2]
- Sattar, M. D. A. 1993 Free and forced convection boundary flow through a porous medium with large suction. *Int. J. Energy Res.* **17**, 1–7. [4.16.2]
- Satya Sai, B. V. K., Seetharamu, K. N. and Aswathanarayana, P. A. 1997a Finite element analysis of heat transfer by natural convection in porous media in vertical enclosures: Investigations in Darcy and non-Darcy regimes. *Int. J. Numer. Methods Heat Fluid Flow* **7**, 367–400. [7.3.3]
- Satya Sai, B. V. K., Seetharamu, K. N. and Aswathanarayana, P. A. 1997b *Int. J. Numer. Meth. Heat Fluid Flow* **7**, 367–400. [7.6.2]
- Satyamurty, W. and Bhargavi, D. 2010 Forced convection in thermally developing region of a channel partially filled with a porous material and optimal porous fraction. *Int. J. Therm. Sci.* **49**, 319–322. [4.11]
- Sayre, T. L. and Riahi, D. N. 1996 Effect of rotation on flow instabilities during solidification of a binary alloy. *Int. J. Engng Sci.* **34**, 1631–1645. [10.2.3]
- Sayre, T. L. and Riahi, D. N. 1997 Oscillatory instabilities of the liquid and mushy layers during solidification of alloys under rotational constraint. *Acta Mech.* **121**, 143–152. [10.2.3]
- Scheidegger, A. E. 1974 The Physics of Flow through Porous Media, University of Toronto Press, Toronto. [1.2]
- Schincariol, R. A., Schwartz, F. W. and Mendoza, C. A. 1997 Instabilities in variable density flows: stability analyses for homogeneous and heterogeneous media. *Water Resour. Res.* **33**, 31–41. [11.8]
- Schneider, K. J. 1963 Investigation on the influence of free thermal convection on heat transfer through granular material. Proc. 11th Int. Cong. of Refrigeration, Pergamon Press, Oxford, Paper 11–4. 247–253. [6.9.1, 6.9.2, 7.1.2]

- Schneider, M. C. and Beckermann, C. 1995 A numerical study of the combined effects of microsegregation, mushy zone permeability and flow, caused by volume contraction and thermosolutal convection, on macrosegregation and eutectic formation in binary alloy solidification. *Int. J. Heat Mass Transfer* **38**, 3455–3473. [10.2.3]
- Schoofs, S. and Hansen, U. 2000 Depletion of a brine layer at the base of ridge-crest hydrothermal systems. *Earth Planet. Sci. Lett.* **180**, 341–353. [11.8]
- Schoofs, S. and Spera, F. J. 2003 Transition to chaos and flow dynamics of thermochemical porous medium convection. *Transport Porous Media* **50**, 179–195. [9.1.3]
- Schoofs, S., Spera, F. J. and Hansen, U. 1999 Chaotic thermohaline convection in low-porosity hydrothermal systems. *Earth Planet. Sci. Lett.* **174**, 213–229. [9.1.3]
- Schoofs, S., Trompert, R. A. and Hansen, U. 1998 The formation and evolution of layered structures in porous media. *J. Geophys. Res.* **103**, 20843–20858. [11.8]
- Schoofs, S., Trompert, R. A. and Hansen, U. 2000a The formation and evolution of layered structures in porous media: effects of porosity and mechanical dispersion. *Phys. Earth Planet. Inter.* **118**, 205–225. [11.8]
- Schoofs, S., Trompert, R. A. and Hansen, U. 2000b Thermochemical convection in and between intracratonic basins: Onset and effects. *J. Geophys. Res.* **105**, 25567–25585. [11.8]
- Schöpf, W. 1992 Convection onset for a binary mixture in a porous medium and in a narrow cell: a comparison. *J. Fluid Mech.* **245**, 263–278. [2.5]
- Schubert, G. and Straus, J. M. 1977 Two-phase convection in a porous medium. *J. Geophys. Res.* **82**, 3411–3421. [10.3.1]
- Schubert, G. and Straus, J. M. 1979 Three-dimensional and multicellular steady and unsteady convection in fluid-saturated porous media at high Rayleigh numbers. *J. Fluid Mech.* **94**, 25–38. [6.8, 6.15.1]
- Schubert, G. and Straus, J. M. 1980 Gravitational stability of water over steam in vapor-dominated geothermal systems. *J. Geophys. Res.* **85**, 6505–6512. [10.3.1]
- Schubert, G. and Straus, J. M. 1982 Transitions in time-dependent thermal convection in fluid-saturated porous media. *J. Fluid Mech.* **121**, 301–303. [6.15.1]
- Schulenberg, T. and Müller, U. 1984 Natural convection in saturated porous layers with internal heat sources. *Int. J. Heat Mass Transfer* **27**, 677–685. [6.19.2]
- Schulze, T. P. and Worster, M. G. 1998 A numerical investigation of steady convection in mushy layers during the directional solidification of binary alloys. *J. Fluid Mech.* **356**, 199–220. [10.2.3]
- Schulze, T. P. and Worster, M. G. 1999 Weak convection, liquid inclusions and the formation of chimneys in mushy layers. *J. Fluid Mech.* **388**, 197–215. [10.2.3]
- Scott, N. L. 2012a Convection in a horizontal layer of high porosity with a exothermic surface reaction on the lower boundary. *Int. J. Therm. Sci.* **56**, 70–76. [9.1.6.4]
- Scott, N. L. 2012b Convection in saturated porous medium with an exothermic chemical surface reaction and Soret effect. *Int. Comm. Heat Mass Transfer*, 1331–1335. [9.1.6.4]
- Scott, N. L. and Straughan, B. 2011 Convection in a porous layer with a surface reaction. *Int. J. Heat Mass Transfer* **54**, 5653–5657. [9.1.6.4]
- Scurtu, N. D., Postelnicu, A. and Pop, I. 2001 Free convection between two horizontal cylinders filled with a porous medium – a perturbation solution. *Acta Mech.* **151**, 115–125. [7.3.3]
- Seddeek, M. A. 2002 Effects of magnetic field and variable viscosity on forced non-Darcy flow about a flat plate with variable wall temperature in porous media in the presence of suction and blowing. *J. Appl. Mech. Tech. Phys.* **43**, 13–17. [4.16.1]
- Seddeek, M. A. 2005 Effects of non-Darcian on forced convection heat transfer over a flat plate in a porous medium with temperature dependent viscosity. *Int. Comm. Heat Mass Transfer* **32**, 258–265. [4.16.1]
- Seddeek, M. A. 2006 Influence of viscous dissipation and thermophoresis on Darcy-Forchheimer mixed convection in a fluid-saturated porous media. *J. Colloid Interface Sci.* **293**, 137–142. [8.1.6]

- Seddeek, M. A. 2007 Chebyshev finite differences method for hydromagnetic free convection from a cone and a wedge through porous media with radiation. *J. Porous Media* **10**, 99–108. erratum p. 420. [5.8]
- Seetharamu, K. N. and Dutta, P. 1990 Free convection in a saturated porous medium adjacent to a non-isothermal vertical impermeable wall. *Wärme-Stoffübertrag.* **25**, 9–15. [5.1.9.9]
- Seguin, D., Montillet, A., Comiti, J. and Huet, F. 1998 Experimental characterization of flow regimes in various porous media — II: Transition to turbulent regime. *Chem. Engng. Sci.* **53**, 3897–3909. [1.8]
- Sekar, R. and Vaidyanathan, G. 1993 Convective instability of a magnetized ferrofluid in a rotating porous medium. *Int. J. Engng. Sci.* **31**, 1139–1150. [6.21]
- Sekar, R., Ramanathan, A. and Vaidyanathan, G. 1998 Effect of rotation on ferrothermohaline convection saturating a porous medium. *Indian J. Eng. Mater. Sci.* **5**, 445–452. [9.1.6.4]
- Selim, A. and Rees, D. A. S. 2007a The stability of a developing thermal front in a porous medium. I – Linear theory. *J. Porous Media* **10**, 1–15. [6.11.3]
- Selim, A. and Rees, D. A. S. 2007b The stability of a developing thermal front in a porous medium. II – Nonlinear evolution. *J. Porous Media* **10**, 17–33. [6.11.3]
- Selim, A. and Rees, D. A. S. 2010 The instability of a developing thermal front in a porous medium. III – Subharmonic instabilities. *J. Porous Media* **13**, 1039–1058. [6.11.3]
- Selimos, B. and Poulikakos, D. 1985 On double diffusion in a Brinkman heat generating porous layer. *Int. Comm. Heat Mass Transfer* **12**, 149–158. [9.1.6.4]
- Sen, A. K. 1987 Natural convection in a shallow porous cavity – the Brinkman model. *Int. J. Heat Mass Transfer* **30**, 855–868. [7.6.2]
- Sen, M., Vasseur, P. and Robillard, L. 1987 Multiple steady states for unicellular natural convection in an inclined porous layer. *Int. J. Heat Mass Transfer* **30**, 2097–2113. [7.8]
- Sen, M., Vasseur, P. and Robillard, L. 1988 Parallel flow convection in a tilted two-dimensional porous layer heated from all sides. *Phys. Fluids* **31**, 3480–3487. [7.8]
- Senapati, N. and Dhal, R. K. 2011 MHD free convective flow past an exponentially accelerated vertical plate through porous medium with diffusion of chemically reactive species. *Proc. Nat. Acad. Sci. Indai A* **81**, 39–48. [5.1.9.9]
- Serkitjjs, M. 1995 Natural convection heat transfer in a horizontal thermal insulation layer underlying an air layer. PhD thesis, Chalmers University of Technology, Göteborg. [6.19.2]
- Seta, T., Takegoshi, E. and Okui, K. 2006 Lattice Boltzmann simulation of natural convection in porous media. *Math. Comput. Simult.* **72**, 195–200. [2.6]
- Seyf, H. R. and Layeghi, M. 2010 Numerical analysis of convective heat transfer from an elliptical pin fin heat sink with and without metal foam insert. *ASME J. Heat Transfer* **132**, #071401. [5.12.1]
- Sezai, I. and Mohamad, A. A. 1999 Three-dimensional double-diffusive convection in a porous cubic enclosure due to opposing gradients of temperature and concentration. *J. Fluid Mech.* **400**, 333–353. [9.2.2]
- Sezai, I. 2005 Flow patterns in a fluid-saturated porous cube. *J. Fluid Mech.* **523**, 393–410. [6.15.1]
- Sghaier, J., Jomaa, W. and Belgith, A. 2008 Superheated steam drying of a spherical porous particle. *J. Porous Media* **11**, 633–646. [3.6]
- Shah, C. B. and Yortsos, Y. C. 1995 Aspects of flow of power-law fluids in porous media. *AIChE J.* **41**, 1099–1112. [1.5.4]
- Shakeri, E., Nazari, M. and Kayhani, M. H. 2012 Free convection heat transfer over a vertical cylinder in a saturated porous medium using a local thermal non-equilibrium model. *Transp. Porous Media* **93**, 453–460. [5.7]
- Shankar, V. and Hagentoft, C. E. 2000 Numerical investigations of natural convection in horizontal porous media heated from below: comparison with experiments. *J. Thermal Envel. Build. Sci.* **23**, 318–338. [7.3.7]
- Shantha, G. and Shanker, B. 2010 Free convective flow of a conducting couple stress fluid in a porous medium: A state space approach. *Int. J. Numer. Meth. Heat Fluid Flow* **20**, 250–264. [5.1.9.2]

- Sharma, B. K., Jha, A. K. and Chaudhary, R. C. 2007 Hall effect on MHD mixed convective flow of a viscous incompressible fluid past a vertical porous plate immersed in porous medium with heat sources/sink. *Roman. J. Phys.* **52**, 487–503. [8.1.6]
- Sharma, P. K. 2005 Simultaneous thermal and mass diffusion on a three-dimensional mixed convection flow through a porous medium. *J. Porous Media* **8**, 409–417. [9.6.1]
- Sharma, R. C. and Gupta, U. 1995 Thermal convection in micropolar fluids in porous medium. *Int. J. Engng Sci.* **33**, 1887–1892. [6.23]
- Sharma, R. C. and Kango, S. K. 1999 Thermal convection in Rivlin-Ericksen elastico-viscous fluid in porous medium in hydromagnetics. *Czech. J. Phys.* **49**, 197–203. [6.23]
- Sharma, R. C. and Kumar, P. 1996 Hall effect on thermosolutal instability in a Maxwellian viscoelastic fluid in porous medium. *Arch. Mech.* **48**, 199–209. [9.1.6.4]
- Sharma, R. C. and Kumar, P. 1997 On micropolar fluids heated from below in hydromagnetics in porous medium. *Czech. J. Phys.* **47**, 637–647. [6.23]
- Sharma, R. C. and Kumar, P. 1998 Effect of rotation on thermal convection in micropolar fluids in porous medium. *Indian J. Pure Appl. Math.* **29**, 95–104. [6.22]
- Sharma, R. C. and Sharma, M. 2004 On couple-stress fluid permeated with suspended particles heated and soluted from below in porous medium. *Indian J. Phys. B* **78**, 189–194. [9.1.6.4]
- Sharma, R. C. and Thakur, K. D. 2000 On couple-stress fluid heated from below in porous medium in hydromagnetics. *Czech. J. Phys.* **50**, 753–758. [9.1.6.4]
- Sharma, R. C., Sunil and Chand, S. 1998 Thermosolutal instability of Rivlin-Ericksen rotating fluid in porous medium. *Indian J. Pure Appl. Math.* **29**, 433–440. [9.1.6.4]
- Sharma, R. C., Sunil and Chand, S. 1999a Thermosolutal instability of Walters rotating fluid (model B') in porous medium. *Arch. Mech.* **51**, 181–191. [9.1.6.4]
- Sharma, R. C., Sunil and Chandel, R. S. 1999b Thermal convection in Walters viscoelastic fluid B' permeated with suspended particles through porous medium. *Stud. Geotech. Mech.* **21**, 3–14. [9.1.6.4]
- Sharma, R. C., Sunil and Pal, M. 2001 Thermosolutal convection in Rivlin-Erickson rotating fluid in porous medium in hydromagnetics. *Indian J. Pure Appl. Math.* **32**, 143–156. [9.1.6.4]
- Sharma, R., Bhargava, R. and Bhargava, P. 2010 A numerical solution of unsteady MHD convection heat and mass transfer past a semi-infinite vertical porous plate using element free Galerkin method. *Comput. Mater. Sci.* **48**, 537–543. [9.2.1]
- Sharma, V. and Kishor, K. 2001 Hall effect on thermosolutal instability of Rivlin-Erikson fluid with varying gravity field in porous medium. *Indian J. Pure Appl. Math.* **32**, 1643–1657. [9.1.6.4]
- Sharma, V. and Rana, G. C. 2001 Thermal instability of a Walters (model B') elastico-viscous fluid in the presence of a variable gravity field and rotation in porous medium. *J. Non-Equil. Thermodyn.* **26**, 31–40. [9.1.6.4]
- Sharma, V. and Rana, G. C. 2002 Thermosolutal instability of Walters (model B') visco-elastic rotating fluid permeated with suspended particles and variable gravity field in porous medium. *Indian J. Pure Appl. Math.* **33**, 97–109. [9.1.6.4]
- Sharma, V. and Sharma, S. 2000 Thermosolutal convection of micropolar fluids in hydromagnetics in porous medium. *Indian J. Pure Appl. Math.* **31**, 1353–1367. [9.1.6.4]
- Sharp, J. M. and Shi, M. 2009 Heterogeneity effects on a possible salinity-driven free convection in low-permeability strata. *Geofluids* **9**, 263–274. [11.8]
- Shateyi, S. and Motsa, S. S. 2011 Hydromagnetic non-Darcy flow, heat and mass transfer over a stretching sheet in the presence of thermal radiation and ohmic dissipation. *Canad. J. Chem. Engng.* **89**, 1388–1400. [9.6.1]
- Shateyi, S., Motsa, S. S. and Sibanda, P. 2010 The effects of thermal radiation, Hall currents, Soret and Dufour on MHD flow by mixed convection over a vertical surface in porous media. *Math. Prob. Engng.* #627475. [9.6.1]
- Shattuck, M. D., Behringer, R. P., Johnson, G. A. and Georgiadis, J. G. 1997 Convection and flow in porous media. Part 1. Visualization by magnetic resonance imaging. *J. Fluid Mech.* **332**, 215–245. [6.9.1]

- Shavit, U., Bar-Yosef, G., Rosenzweig, R. and Assouline, S. 2002 Modified Brinkman equation for a free flow problem at the interface of porous surfaces: The Cantor-Taylor brush configuration case. *Water Resour. Res.* **38**, 1320–1334. [1.6]
- Shavit, U., Rosenzweig, R. and Assouline, S. 2004 Free flow at the interface of porous surfaces: A generalization of the Taylor brush configuration. *Transport Porous Media*. **54**, 345–360. [1.6]
- Shehadeh, F. G. and Duwairi, H. M. 2009 MHD natural convection in porous media-filled enclosures. *Appl. Math. Mech- English ed.* **30**, 1113–1120. [7.8]
- Shen, S., Liu, W. and Tao, W. Q. 2003 Analysis of field synergy on natural convective heat transfer in porous media. *Int. Comm. Heat Mass Transfer* **30**, 1081–1090. [3.6]
- Shenoy, A. V. 1992 Darcy natural, forced and mixed convection heat transfer from an isothermal vertical flat plate in a porous medium saturated with an elastic fluid of constant viscosity. *Int. J. Engng Sci.* **30**, 455–467. [4.12.3, 5.1.9.2, 8.1.1]
- Shenoy, A. V. 1993a Darcy-Forchheimer natural, forced and mixed convection heat transfer in non-Newtonian power-law fluid-saturated porous media. *Transport in Porous Media* **11**, 219–241. [4.16.3, 5.1.9.2, 8.1.1]
- Shenoy, A. V. 1993b Forced convection heat transfer to an elastic fluid of constant viscosity flowing through a channel filled with a Brinkman-Darcy medium. *Wärme-Stoffübertrag.* **28**, 295–297. [4.16.3]
- Shenoy, A. V. 1994 Non-Newtonian fluid heat transfer in porous media. *Adv. Heat Transfer* **24**, 101–190. [1.5.4]
- Sheridan, J., Williams, A. and Close, D. J. 1992 Experimental study of natural convection with coupled heat and mass transfer in porous media. *Int. J. Heat Mass Transfer* **35**, 2131–2143. [9.1.5]
- Sheu, L. J. 2006 An autonomous system for chaotic convection in a porous medium using a thermal non-equilibrium model. *Chaos Solitons Fractals* **30**, 672–689. [6.5]
- Sheu, L. J. 2011 Thermal instability in a porous medium layer saturated with a viscoelastic nanofluid. *Transp. Porous Media* **88**, 461–477. [6.23]
- Sheu, L. J., Tam, L. M., Chen, J. H., Chen, H. K., Lin, K. T. and Kang, Y. 2008 Chaotic convection of viscoelastic fluids in porous media. *Chaos Solitons Fractals* **37**, 113–124. [6.23]
- Shi, W. L. and Vafai, K. 2010 Mixed convection in obstructed open-ended cavity. *Numer. Heat Transfer A* **57**, 709–729. [8.4.3]
- Shih, M. H. and Huang, M. J. 2002 A study of liquid evaporation on forced convection in porous media with non-Darcy effects. *Acta Mech.* **154**, 215–231. [4.16.5]
- Shih, M. H., Huang, M. J. and Chen, C. K. 2005 A study of the liquid evaporation with darcian resistance effect on mixed convection in porous media. *Nt. Comm. Heat Mass Transfer* **32**, 685–694. [10.3.2]
- Shih, M. H., Luo, W. J. and Yu, K. C. 2008 Evaporation of non-Newtonian fluid in porous medium under mixed convection. *J. Mech.* **24**, 153–162. [10.3.2]
- Shiina, Y. and Hishida, M. 2010 Critical Rayleigh number of natural convection in high porosity anisotropic horizontal porous layers. *Int. J. Heat Mass Transfer* **53**, 1507–1513. [6.12]
- Shim, K. I., Yoo, J. W. and Kim, S. J. 2002 Thermal analysis of an internally finned tube using a porous medium approach. *Heat Transfer 2002*, Proc. 12th Int. Heat Transfer Conf., Elsevier, Vol. 2, pp. 785–790. [4.16.5]
- Shin, U. C., Khedari, J., Mbow, C. and Daguenet, M. 1994 Convection naturelle thermique à l'intérieur d'une calotte cylindrique poreuse d'axe horizontal: Etude théorique. *Rev. Gen. Therm.* **33**, 30–37. [7.3.7]
- Shiralkar, G. S., Haadzizadeh, M. and Tien, C. L. 1983 Numerical study of high Rayleigh number convection in a vertical porous enclosure. *Numer. Heat Transfer A* **6**, 223–234. [7.1.2]
- Shivakumara, I. S. 1999 Boundary and inertia effects on convection in porous media with throughflow. *Acta Mech.* **137**, 151–165. [6.10.2]
- Shivakumara, I. S. 2010 Onset of convection in a couple-stress fluid-saturated porous medium: Effects of non-uniform temperature gradients. *Arch. Appl. Mech.* **80**, 949–957. [6.23]
- Shivakumara, I. S. and Khalili, A. 2001 On the stability of double diffusive convection in a porous layer with throughflow. *Acta Mech.* **152**, 1–8. [9.1.6.4]

- Shivakumara, I. S. and Nanjundappa, C. E. 2006 Effects of quadratic drag and throughflow on double diffusive convection in a porous layer. *Int. Comm. Heat Mass Transfer* **33**, 357–363. [9.1.6.4]
- Shivakumara, I. S. and Sumithra, R. 1999 Non-Darcian effects of double diffusive convection in a sparsely packed porous medium. *Acta Mech.* **132**, 113–127. [9.1.6.3]
- Shivakumara, I. S. and Sureshkumar, S. 2007 Convective instabilities in a viscoelastic-fluid-saturated porous medium with throughflow. *J. Geophys. Engng* **4**, 104–115. [6.23]
- Shivakumara, I. S. and Sureshkumar, S. 2008 Effects of throughflow and quadratic drag on the stability of a doubly diffusive Oldroyd-B fluid-saturated porous layer. *J. Geophys. Engng.* **5**, 268–280. [9.1.6.4]
- Shivakumara, I. S., Lee, J. and Devaraju, N. 2011b Throughflow and quadratic drag effects on thermal convection in a rotating porous layer. *Transp. Porous Meda* **87**, 485–501. [6.22]
- Shivakumara, I. S., Lee, J. and Chavaraddi, K. B. 2011a Onset of surface tension driven convection in a fluid layer overlying a layer of an anisotropic porous medium. *Int. J. Heat Mass Transfer* **54**, 994–1001. [6.19.3]
- Shivakumara, I. S., Lee, J. and Kumar, S. S. 2011j Linear and nonlinear stability of double diffusive convection in a couple stress fluid-saturated porous layer. *Arch. Appl. Mech.* **81**, 1697–1715. [9.1.6.4]
- Shivakumara, I. S., Lee, J. Nanjundappa, C. E and Ravisha, M. 2011d Ferromagnetic convection in a rotating ferrofluid saturated porous layer. *Transp. Porous Medai* **87**, 251–273. [6.22]
- Shivakumara, I. S., Lee, J. Nanjundappa, C. E. and Ravisha, M. 2010a Brinkman-Bénard-Marangoni convection in a magnetized ferrofluid saturated porous layer. *Int. J. Heat Mass Transfer* **53**, 5835–5846. [6.19.3]
- Shivakumara, I. S., Lee, J., Malashetty, M. S. and Sureshkumar, S. 2011e Effect of thermal modulation on the onset of convection in Walters B viscoelastic fluid-saturated porous medium. *Transp. Porous Media* **87**, 291–307. [6.23]
- Shivakumara, I. S., Lee, J., Mamatha, A. L. and Ravisha, M. 2011c Boundary and thermal non-equilibrium effects on convective instability in an anisotropic porous layer. *J. Mech. Sci. Technol.* **25**, 911–921. [6.12]
- Shivakumara, I. S., Lee, J., Ravisha, M. and Reddy, R. G. 2011f Effects of MFD viscosity and LTNE on the onset of convection in a porous medium. *Int. J. Heat Mass Transfer* **54**, 2630–2641. [6.21]
- Shivakumara, I. S., Lee, J., Ravisha, M. and Reddy, R. G. 2012a The effects of thermal nonequilibrium and MFD viscosity on the onset of Brinkman ferroconvection. *Meccanica* **47**, 1359–1378. [6.21]
- Shivakumara, I. S., Lee, J., Vajravelu, K. and Mamatha, A. L. 2011i Effects of nonequilibrium and non-uniform temperature gradients on the onset of convection in a heterogeneous porous medium. *Int. Comm. Heat Mass Transfer* **38**, 906–910. [6.13.2]
- Shivakumara, I. S., Malshetty, M. S. and Chavaraddi, K. B. 2006a Onset of convection in a viscoelastic-fluid saturated sparsely packed porous layer using a thermal nonequilibrium model. *Cand. J. Phys.* **84**, 973–990. [6.23]
- Shivakumara, I. S., Mamatha, A. L. and Ravisha, M. 2010b Boundary and thermal non-equilibrium effects on the onset of Darcy-Brinkman convection in a porous layer. *J. Engng. Math.* **67**, 317–328. [6.5]
- Shivakumara, I. S., Mamatha, A. L. and Ravisha, M. 2010c Effects of variable viscosity and density maximum on the onset of Darcy-Bénard convection using a thermal nonequilibrium model. *J. Porous Media* **13**, 613–622. [6.5]
- Shivakumara, I. S., Nanjundappa, C. E and Chavaraddi, K. B. 2009a Darcy-Bénard-Marangoni convection in porous media. *Int. J. Heat Mass Transfer* **52**, 2815–2823. [6.19.3]
- Shivakumara, I. S., Nanjundappa, C. E and Ravisha, M. 2009b Effect of boundary conditions on the onset of thermomagnetic convection in a ferrofluid saturated porous medium. *ASME J. Heat Transfer* **131**, #101003. [6.21]

- Shivakumara, I. S., Nanjundappa, C. E and Ravisha, M. 2010d Thermomagnetic convection in a magnetic nanofluid saturated porous medium. *Int. J. Appl. Math. Engng. Sci.* **2**, 157–170. [6.32]
- Shivakumara, I. S., Ng, C. O. and Nagashree, M. S. 2011g The onset of electroconvection in a rotating Brinkman porous layer. *Int. J. Engng. Sci.* **49**, 646–663. [6.21]
- Shivakumara, I. S., Prasana, B. M. R., Rudraiah, N. and Venkatachalappa, M. 2002 Numerical study of natural convection in a vertical cylindrical annulus using a non-Darcy equation. *J. Porous Media*, **5**, 87–102. [7.3.3]
- Shivakumara, I. S., Savitha, M. N., Chavaraddi, K. B. and Devaraju, N. 2009c Bifurcation analysis for thermal convection in a rotating porous layer. *Meccanica* **44**, 225–238. [6.22]
- Shivakumara, I. S., Suma, S. P., Chavaraddi, K. B. and Devaraju, N. 2006b Onset of surface driven convection in superposed layers of fluid and saturated porous medium. *Arch. Mech.* **58**, 71–92. [6.19.3]
- Shivakumara, I. S., Suma, S. P., Indira, R. and Gangadharaiah, Y. H. 2012b Effect of internal heat generation on the onset of Marangoni convection in a fluid layer overlying a layer of an anisotropic porous medium. *Transp. Porous Media* **92**, 727–743. [6.19.3]
- Shivakumara, I. S., Sureshkumar, S. and Devaraju, N. 2011h Coriolis effect on thermal convection in a couple-stress fluid-saturated rotating rigid porous layer. *Arch. Appl. Mech.* **81**, 513–530. [6.22]
- Shokouhmand, H. and Sayehvand, H. 2010 Study of forced convection in a pipe partially filled with a porous medium. *J. Enhanced Heat Transfer* **17**, 205–221. [4.11]
- Shokouhmand, H., Isfahani, A. H. M. and Shirani, E. 2010 Friction and heat transfer coefficient in micro and nano channels filled with porous media for wide range of Knudsen number. *Int. Comm. Heat Mass Transfer* **37**, 890–894. [4.9]
- Shokouhmand, H., Jam, F. and Slimpour, M. R. 2009 Simulation of laminar flow and convective heat transfer in conduits filled with porous medium using Lattice Boltzmann method. *Int. Comm. Heat Mass Transfer* **36**, 378–384. [2.6]
- Shu, J. J. and Pop, I. 1997 Inclined wall plumes in porous media. *Fluid Dyn. Res.* **21**, 303–317. [5.3]
- Shu, J. J. and Pop, I. 1998 Transient conjugate free convection from a vertical flat plate in a porous medium subjected to a sudden change in surface heat flux. *Int. J. Engng. Sci.* **36**, 207–214. [5.1.5]
- Shu, J. J. and Pop, I. 1999 Thermal interaction between free convection and forced convection along a conducting plate embedded in a porous medium. *Hybrid Meth. Engng.* **1**, 55–66. [8.1.1]
- Shuja, S. Z. ,Yilbas, B. S. and Kassas, M. 2009a Flow over porous blocks in a square cavity: influence of heat flux and porosity on heat transfer rates. *Int. J. Therm. Sci.* **48**, 1564–1573. [4.11]
- Shuja, S. Z. ,Yilbas, B. S. and Kassas, M. 2009b Flow over porous blocks in an open cavity: Effect of block aspect ratio and porosity on heat transfer characteristics. *Int. J. Therm. Sci.* **48**, 1564–1573. [4.11]
- Siddheshwar, P. G. and Krisna, C. V. S. 2003 Linear and non-linear analyses of convection in a micropolar fluid occupying a porous medium. *Int J. Nonlinear Mech.* **38**, 1561–1579. [6.23]
- Siddheshwar, P. G., Vanishree, R. K. and Melson, A. C. 2012 Study of heat transport in Bénard-Darcy convection with g-jitter and thermomechanical anisotropy in variable viscosity liquids. *Transp. Porous Media* **92**, 277–288. [6.24]
- Silva, R. A. and de Lemos, M. J. S. 2003a Numerical analysis of the stress jump interface condition for laminar flow over a porous layer. *Numer. Heat Transfer A* **43**, 603–617. [1.6]
- Silva, R. A. and de Lemos, M. J. S. 2003b Turbulent flow in a channel occupied by a porous layer considering the stress jump at the interface. *Int. J. Heat Mass Transfer* **46**, 5113–5136. [1.8]
- Simmons, C. T. and Narayan, K. A. 1997 Mixed convection processes below a saline disposal basin. *J. Hydrol.* **194**, 263–285. [11.8]
- Simmons, C. T., Fenstemaker, T. R. and Sharp, J. M. 2001 Variable-density groundwater flow and solute transport in heterogeneous porous media: approaches, resolutions and future challenges. *J. Contam. Hydrol.* **52**, 245–275. [11.8]

- Simmons, C. T., Kuznetsov, A. V. and Nield, D. A. 2010 Effect of strong heterogeneity on the onset of convection in a porous medium: Importance of spatial dimensionality and geologic controls. *Water Resour. Res.* **46**, #W09539. [6.13.6]
- Simmons, C. T., Narayan, K. A. and Wooding, R. A. 1999 On a test case for density-dependent groundwater flow and solute transport models: The salt lake problem. *Water Resources Res.* **35**, 3607–3620. [9.1.6.4]
- Simmons, C. T., Sharp, J. M. and Nield, D. A. 2008 Modes of free convection in fractured porous media. *Water Resour. Res.* **44**, #W03431. [11.8]
- Simms, M. A. and Garven, G. 2004 Thermal convection in faulted extensional sedimentary basins: Theoretical results from finite-element modeling. *Geofluids* **4**, 109–130. [11.8]
- Simpkins, P. G. and Blythe, P. A. 1980 Convection in a porous layer. *Int. J. Heat Mass Transfer* **23**, 881–887. [7.1.2]
- Singh, A. K. 2005 Three-dimensional flow of a viscous fluid with heat and mass transfer. *Int. Comm. Heat Mass Transfer* **32**, 1420–1429. [9.2.1]
- Singh, A. K. 2008 Three-dimensional free convection flow of a viscous fluid through a nonhomogeneous porous medium. *J. Porous Media* **11**, 603–615. [5.1.9.9]
- Singh, A. K. and Gorla, R. S. R. 2008 Heat transfer between two vertical parallel walls partially filled with a porous medium: Use of the Brinkman-extended Darcy model. *J. Porous Media* **11**, 457–466. [7.7]
- Singh, A. K. and Thorpe, G. R. 1995 Natural convection in a confined fluid overlying a porous layer — a study of different models. *Indian J. Pure Appl. Math.* **26**, 81–95. [7.7]
- Singh, A. K., , Singh, P. P. and Singh, N. P. 2011c Effects of periodic permeability and suction velocity on three-dimensional free convection flow past a vertical porous plate embedded in a highly porous medium. *J. Porous Media* **14**, 451–460. [5.1.9.9]
- Singh, A. K., Agnihotri, P., Singh, N. P. and Singh, A. K. 2011a Transient and non-Darcian effects on natural convection flow in a vertical channel partially filled with porous medium: Analysis with Forchheimer-Brinkman extended Darcy model. *Int. J. Heat Mass Transfer* **54**, 1111–1120. [7.7]
- Singh, A. K., Leonardi, E. and Thorpe, G. R. 1993 Three-dimensional natural convection in a confined fluid overlying a porous layer. *ASME J. Heat Transfer* **115**, 631–638. [7.7]
- Singh, A. K., Paul, T. and Thorpe, G. R. 1999 Natural convection due to heat and mass transfer in a composite system. *Heat Mass Transfer* **35**, 39–48. [9.4]
- Singh, A. K., Paul, T. and Thorpe, G. R. 2000 Natural convection in a non-rectangular porous enclosure. *Fortsch. Ingenieurwesen* **65**, 301–308. [7.3.7]
- Singh, A. K., Roy, S. and Basak, K. 2012 Analysis of Bejan's heatlines on visualization of heat flow and thermal mixing in titled square cavities. *Int. J. Heat Mass Transfer* **55**, 2965–2983. [4.17]
- Singh, A. K., Singh, H., Singh, U. and Singh, N. P. 2011b Hydromagnetic convection boundary layer flow caused by stretching a porous wall embedded within porous medium. *Proc. Nat. Acad. Sci. Indai A* **81**, 59–64. [5.1.9.9]
- Singh, A. K., Kumar, R., Singh, U., Singh, N. P. and Singh, A. K. 2011d Unsteady hydromagnetic convective flow in a vertical channel using Darcy-Brinkman-Forchheimer extended mode with heat generation/absorption: Analysis with asymmetric heating/cooling of the channel walls. *Int. J. Heat Mass Transfer* **54**, 5633–5642. [7.2]
- Singh, B. B. and Chandarki, I. M. 2009 Integral treatment of coupled heat and mass transfer by natural convection from a cylinder in porous media. *Int. Comm. Heat Mass Transfer* **36**, 269–273. [9.2.1]
- Singh, K. D. and Kumar, R. 2009 Combined effects of Hall current and rotation on free convection MHD flow in a porous channel. *Indian J. Pure Appl. Phys.* **47**, 617–623. [7.12]
- Singh, K. D. and Kumar, R. 2010 Effects of chemical reactions on unsteady MHD free convection and mass transfer for flow past a hot vertical porous plate with heat generation/absorption through porous medium. *Indian J Phys.* **84**, 93–106. [9.2.1]
- Singh, M. and Kumar, P. 2011 Magneto and rotatory thermosolutal convection in couple-stress fluid in porous medium. *J. Porous Media* **14**, 637–648. [9.1.6.4]

- Singh, N. P., Singh, A. K. and Singh, H. 2010 Mixed convection flow past a porous vertical plate bounded by a porous medium in a rotating system in the presence of a magnetic field. *J. Porous Media* **13**, 623–633. [8.1.6]
- Singh, P. and Tewari, K. 1993 Non-Darcy free convection from vertical surfaces in thermally stratified porous media. *Int. J. Engng Sci.* **31**, 1233–1242. [5.1.4]
- Singh, P., Misra, J. K. and Narayan, K. A. 1988 Three-dimensional convective flow and heat transfer in a porous medium. *Indian J. Pure Appl. Math.* **19**, 1130–1135. [5.1.9.9]
- Singh, P., Queeny and Sharma, R. N. 2002 Influence of lateral mass flux on mixed convection heat and mass transfer over inclined surfaces in porous media. *Heat Mass Transfer* **38**, 233–242. [9.6.1]
- Singh, R. 2011 Predictions of thermal conductivity of complex materials. In Heat Transfer in Multiphase Materials (eds. A. Oechsner, G. E. Murch), Springer, pp. 235–274. [2.2.1]
- Singh, T. and Gorla, M. G. 2010 Three-dimensional MHD flow and heat transfer through porous medium bounded by a porous vertical surface with heat source and variable permeability. *Proc. Nat. Acad. Sci. India A* **80**, 369–375. [5.1.9.9]
- Sinha, R., Nayak, A. K. and Sehgal, B. R. 2008 Modeling the natural convection heat transfer and dryout heat flux in a porous debris bed. *ASME J. HeatTransfer* **130**, #104503. [3.6]
- Sinha, S. K., Sundararajan, T. and Garg, V. K. 1992 A variable property analysis of alloy solidification using the anisotropic porous medium approach. *Int. J. Heat Mass Transfer* **35**, 2865–2877. [10.2.3]
- Sinha, S. K., Sundararajan, T. and Garg, V. K. 1993 A study of the effects of macrosegregation and buoyancy-driven flow in binary mixture solidification. *Int. J. Heat Mass Transfer* **36**, 2349–2358. [10.2.3]
- Siraev, R. R. and Yakushin, V. I. 2008 Investigation of convection in a horizontal cylindrical layer of a saturated porous medium. *Fluid Dyn.* **43**, 240–247. [7.3.3]
- Sivasamy, A., Sellurai, V. and Kanna, P. R. 2010a Mixed convection on jet impingement cooling of a constant flux horizontal porous layer. *Int. J. Therm. Sci.* **49**, 1238–1246. [8.4.2]
- Sivasamy, A., Kanna, P. R. and Sellurai, V. 2011 Jet impingement cooling of a horizontal surface in an unconfined porous medium: Mixed convection regime. *Int. J. Heat Mass Transfer* **54**, 4127–4134. [8.4.2]
- Sivasamy, A., Selladurai, V. and Kanna, P. R. 2010b Jet impingement cooling of a constant heat flux horizontal surface in a confined porous medium: Mixed convection regime. *Int. J. Heat Mass Transfer* **53**, 5847–5855. [8.4.2]
- Sivasankaran, S., Do, Y. and Sankar, M. 2011 Effect of discrete heating on natural convection in a rectangular porous enclosure. *Transp. Porous Media* **86**, 291–311. [7.2]
- Sivasankaran, S., Kandaswamy, P. and Ng, C. O. 2008 Double-diffusive convection of anomalous density fluids in a porous cavity. *Transp. Porous Media* **71**, 133–145. [9.2.2]
- Siyyam, H., Merabet, N. and Hamdan, M. H. 2007 Standard numerical schemes for coupled parallel flow over porous layers. *Appl. Math. Comput.* **194**, 38–45. [1.6]
- Skikiatden, J. and Roberts, J. S. 2007 Predicting moisture profiles in potato and carrot during convective hot air drying using isothermally measured effective diffusivity. *J. Food Engng.* **84**, 516–525. [3.6]
- Skjetne, E. and Auriault, J. L. 1999a New insights on steady, nonlinear flow in porous media. *Europ. J. Mech. B – Fluids* **18**, 131–145. [1.5.2]
- Skjetne, E. and Auriault, J. L. 1999b Homogenization of wall-slip gas flow through porous media. *Transport Porous Media* **36**, 293–306. [1.6]
- Skudarnov, P. V., Lin, C. X., Wang, M. H., Pradeep, N. and Ebadian, M. A. 2002 Evolution of convection pattern during the solidification process of a binary mixture: effect of initial solutal concentration. *Int. J. Heat Mass Transfer* **45**, 5191–5200. [10.2.3]
- Slim, A. C. and Ramakrishnan, T. S. 2010 Onset and cessation of time-dependent dissolution-driven convection in porous media. *Phys. Fluids* **22**, #124103. [11.11]
- Slimi, K. 2009 A two-temperature model for predicting heat and fluid flow by natural convection and radiation within a saturated porous vertical channel. *J. Porous Media* **12**, 43–63. [7.1.7]

- Slimi, K. 2006 Entropy generation for unsteady natural convection and radiation within a tilted saturated porous channel. *Int. J. Exergy* **3**, 174–190. [7.8]
- Slimi, K., Ben Nasrallah, S. and Fohr, J. P. 1998 Transient natural convection in a vertical cylinder opened at the extremities and filled with a fluid saturated porous medium: validity of Darcy flow model and thermal boundary layer approximations. *Int. J. Heat Mass Transfer* **41**, 1113–1125. [7.3.3]
- Slimi, K., Mhimid, A., Ben Salah, M., Ben Nasrallah, S., Mohamad, A. A. and Storesletten, L. 2005 Anisotropy effects on heat and fluid flow by unsteady natural convection and radiation in saturated porous media. *Numer. Heat Transfer A* **48**, 763–790. [6.11.2]
- Slimi, K., Zili-Ghedira, L., Ben Nasrallah, S. and Mohamad, A. A. 2004 A transient study of coupled natural convection and radiation in a porous vertical channel using the finite-volume method. *Numer. Heat Transfer A* **45**, 451–478. [7.3.3]
- Smith, C. 2006 Influence of density inversion on thawing round a cylinder in a frozen saturated porous medium. *Transport Porous Media* **63**, 223–237. [10.1.7]
- Sobera, M. P., Klein, C. R., van den Akker, H. A. and Brasser, P. 2003 Convective heat and mass transfer to a cylinder sheathed by a porous layer. *AICHE J.* **49**, 3018–3028. [4.11]
- Sobha, V. V., Vasudava, R. Y., Ramakrishnan, K. and Latha, K. H. 2010 Non-Darcy mixed convection with thermal dispersion in a saturated porous medium. *ASME J. Heat Transfer* **132**, #014501. [8.1.6]
- Soboleva, E. B. 2008 Effects of strong compressibility in natural convective flows through porous media with a near-critical fluid. *Fluid Dyn.* **43**, 217–228. [7.5]
- Sohouli, A. R., Domairry, D., Famouri, M. and Mohsenzadeh, A. 2008 Analytical solution of natural convection of Darcian fluid about a vertical full cone embedded in porous media prescribed wall temperature by means of HAM. *Int. Comm. Heat Mass Transfer* **35**, 1380–1384. [5.8]
- Sohouli, A. R., Famouri, M., Kimiaeifar, A. and Domairry, D. 2010 Application of homotopy analysis method for natural convection of Darcian fluid about a vertical full cone embedded in porous media prescribed heat flux. *Comm. Nonlinear Sci. Numer. Simul.* **15**, 1691–1699. [5.8]
- Sokolov, V. E. 1982 Mammal Skin, University of California Press, Berkeley, CA. [4.14]
- Solmus, I., Rees, D. A. S., Yamili, C., Baker, D. and Kaftanoglu, B. 2012 Numerical investigation of coupled heat and mass transfer inside the absorbent bed of an adsorption cooling unit. *Int. J. Refrig.* **35**, 652–662. [999]
- Solomon, T. H. and Hartley, R. R. 1998 Measurements of the temperature field of mushy and liquid regions during solidification of aqueous ammonium chloride. *J. Fluid Mech.* **358**, 87–106. [10.2.3]
- Somerton, C. W. 1983 The Prandtl number effect in porous layer convection. *Appl. Sci. Res.* **40**, 333–344. [6.9.2]
- Somerton, C. W. and Catton, I. 1982 On the thermal instability of superimposed porous and fluid layers. *ASME J. Heat Transfer* **104**, 160–165. [1.6, 6.19.1.2, 6.19.2]
- Somerton, C. W., McDonough, J. M. and Catton, I. 1984 Natural convection in a volumetrically heated porous layer. *ASME J. Heat Transfer* **106**, 241–244. [6.11.2]
- Sommerfeld, R. A. and Rocchio, J. E. 1993 A study of the effects of macrosegregation and buoyancy-driven flow in binary mixture solidification. *Water Resour. Res.* **29**, 2485–2490. [11.1]
- Sondergeld, C. H. and Turcotte, D. L. 1977 An experimental study of two-phase convection in a porous medium with applications to geological problems. *J. Geophys. Res.* **82**, 2045–2053. [10.3.1]
- Sondergeld, C. H. and Turcotte, D. L. 1978 Flow visualization studies of two-phase thermal convection in a porous layer. *Pure Appl. Geophys.* **117**, 321–330. [10.3.1]
- Song, J. 2002 Spatial decay estimate in time-dependent double-diffusive Darcy plane flow. *J. Math. Anal. Appl.* **267**, 76–88. [1.5.3]
- Song, M. and Viskanta, R. 1994 Natural convection flow and heat transfer within a rectangular enclosure containing a vertical porous layer. *Int. J. Heat Mass Transfer* **37**, 2425–2438. [7.7]

- Song, M. and Viskanta, R. 2001 Lateral freezing of an anisotropic porous medium saturated with an aqueous salt solution. *Int. J. Heat Mass Transfer* **44**, 733–751. [10.2.1.2]
- Song, M., Choi, J. and Viskanta, R. 1993 Upward solidification of a binary solution saturated porous medium. *Int. J. Heat Mass Transfer* **36**, 3687–3695. [10.2.3]
- Souhar, K., Aniss, S. and Ouazzani, M. T. 2011 Effect of temperature modulation on the onset of convection in a Hele-Shaw cell. *J. Porous Media* **14**, 533–539. [6.11.3]
- Soundalgekar, V. M., Lahuriher, R. M. and Pohanerkar, S. G. 1991 Heat transfer in unsteady flow through a porous medium between two infinite parallel plates in relative motion. *Forschung. Ing.* **57**, 28–31. [4.12.2]
- Sousa, A. C. M. 2005 Heat transfer distribution for a free/porous system with forced convection and heat generation — a numerical study. *Strojnicki Vestnik: J. Mech. Engng.* **51**, 519–526. [4.11]
- Souto, H. P. A. and Moyne, C. 1997a Dispersion in two-dimensional periodic porous media. 1. Hydrodynamics. *Phys. Fluids* **9**, 2243–2252. [2.2.4]
- Souto, H. P. A. and Moyne, C. 1997b Dispersion in two-dimensional periodic porous media. 2. Dispersion tensor. *Phys. Fluids* **9**, 2253–2263. [2.2.4]
- Sovran, O., Bardan, G., Mojtabi, A. and Charrier-Mojtabi, M. C. 2000 Finite frequency external modulation in doubly diffusive convection. *Numer. Heat Transfer A* **37**, 877–896. [9.1.6.4]
- Sovran, O., Charrier-Mojtabi, M. C. and Mojtabi, A. 2001 Onset of Soret-driven convection in an infinite porous layer. *C. R. Acad. Sci. IIB* **329**, 287–293. [9.1.4]
- Sovran, O., Charrier-Mojtabi, M. C., Azaiez, M. and Mojtabi, A. 2002 Onset of Soret-driven convection in porous medium under vibration. *Heat Transfer 2002*, Proc. 12th Int. Heat Transfer Conf., Elsevier, Vol. 2, pp. 839–844. [9.1.6.4]
- Sözen, M. and Kuzay, T. M. 1996 Enhanced heat transfer in round tubes with porous inserts. *Int. J. Heat Fluid Flow* **17**, 124–129. [4.12.1]
- Sözen, M. and Vafai, K. 1990 Analysis of the non-thermal equilibrium condensing flow of a gas through a packed bed. *Int. J. Heat Mass Transfer* **33**, 1247–1261. [4.6.5, 10.4]
- Sözen, M. and Vafai, K. 1991 Analysis of oscillating compressible flow through a packed bed. *Int. J. Heat Fluid Flow* **12**, 130–136. [4.9]
- Sözen, M. and Vafai, K. 1993 Longitudinal heat dispersion in porous beds with real-gas flow. *AIAA J. Thermophys. Heat Transfer* **7**, 153–157. [4.6.5]
- Spaid, M. A. A. and Phelan, F. R. 1997 Lattice Boltzmann methods for modeling microscale flow in fibrous porous media. *Phys. Fluids* **9**, 2468–2474. [2.6]
- Spanos, T. J. T. 2012 Relative permeability. *Mathematical and Numerical Modeling in Porous Media : Applications in Geoscience* (ed. M. A. Diaz Vierra, P. N. Sahay, M. Coronado and A. Ortiz Tapia), CRC Press, pp. 1012. [3.5.4]
- Spiga, M. and Morini, G. L. 1999 Transient response of nonthermal equilibrium packed beds. *Int. J. Engng. Sci.* **37**, 179–186. [4.10]
- Sri Krishna, C. V. 2002 Effects of non-inertial acceleration on the onset of convection in a second-order fluid-saturated porous medium. *Int. J. Engng. Sci.* **39**, 599–609. [6.23]
- Srinivas, S. and Muthuraj, R. 2010a Effects of thermal radiation and space porosity on MHD mixed convection flow in a vertical channel using homotopy analysis method. *Comm. Nonlinear Sci. Numer. Simul.* **15**, 2098–2108. [8.1.6]
- Srinivas, S. and Muthuraj, R. 2010b MHD flow with slip effects and temperature-dependent heat source in a vertical wavy porous space. *Chem. Engng. Comm.* **197**, 1387–1403. [7.3.7]
- Srinivas, S. and Muthuraj, R. 2011 Effects of chemical reaction and space porosity on MHD mixed convective flow in a vertical asymmetric channel with peristalsis. *Math. Comp. Mod.* **54**, 1213–1227. [9.6.2]
- Srinivasacharya, D. and RamReddy C. 2010 Heat and mass transfer by natural convection in a doubly-stratified non-Darcy micropolar fluid. *Int. Comm. Heat Mass Transfer* **37**, 873–880. [9.2.1]
- Srinivasacharya, D. and RamReddy C. 2011b Soret and Dufour effects on mixed convection in a non-Darcy porous medium saturated with a micropolar fluid. *Nonlinear Anal. Model. Control* **16**, 100–115. [9.6.1]

- Srinivasacharya, D. and RamReddy, C. 2011a Free convective heat and mass transfer in a doubly stratified non-Darcy micropolar fluid. *Korean J. Chem. Engng.* **28**, 1824–1832. [9.4]
- Srinivasacharya, D., Pranitha, J. and RamReddy C. 2011 Magnetic effect on free convection in a non-Darcy porous medium saturated with doubly stratified power law fluid. *J. Brazil Soc. Mech. Sci. Engng.* **33**, 8–14. [9.2.1]
- Srinivasan, V., Vafai, K. and Christenson, R. N. 1994 Analysis pf heat transfer and fluid flow through a spirally fluted tube using a porous substrate approach. *ASME J. Heat Transfer* **116**, 543–551. [4.11]
- Srivastava, A. K. and Bhaduria, B. S. 2011 Linear stability of solutal convection in a mushy layer subjected to gravity modulation. *Comm. Nonlinear Sci. Numer. Simul.* **16**, 3548–3558. [10.2.3]
- Srivastava, A. K., Bhaduria, B. S. and Gupta, V. K. 2012 Magneto-convection in an anisotropic porous layer with Soret effect. *Int. J. Nonlinear Mech.* **47**, 426–438. [9.1.6.4]
- Srivastava, A. K., Bhaduria, B. S. and Kumar, J. 2011 Magnetoconvection in an anisotropic porous layer using thermal non-equilibrium model. *Spec. Top. Rev. Porous Media* **2**, 1–10. [6.21]
- Stalio, E., Breugem, W. P. and Boersma, B. J. 2004 Numerical study of turbulent heat transfer above a porous wall. In Applications of Porous Media (ICAPM 2004), (eds. A. H. Reis and A. F. Miguel), Évora, Portugal, pp. 191–198. [4.11]
- Stamps, D. W., Arpacı, V. S. and Clark, J. A. 1990 Unsteady three-dimensional natural convection in a fluid-saturated porous medium. *J. Fluid Mech.* **213**, 377–396. [6.15.1]
- Stanescu, G., Fowler, A. J. and Bejan, A. 1996 The optimal spacing of cylinders in free-stream cross-flow forced convection. *Int. J. Heat Mass Transfer* **39**, 311–317. [4.15]
- Staufer, P.H., Auer, L.H. and Rosenberg, N.D. 1997 Compressible gas in porous media: a finite amplitude analysis of natural convection. *Int. J. Heat Mass Transfer* **40**, 1585–1589. [6.7]
- Steen, P. H. 1983 Pattern selection for finite-amplitude convection states in boxes of porous media. *J. Fluid Mech.* **136**, 219–241. [6.15.1]
- Steen, P. H. 1986 Container geometry and the transition to unsteady Bénard convection in porous media. *Phys. Fluids* **29**, 925–933. [6.15.1]
- Steen, P. H. and Aidun, C. K. 1988 Time-periodic convection in porous media: transition mechanism. *J. Fluid Mech.* **196**, 263–290. [6.8]
- Steinbeck, M. J. 1999 Convective drying of porous material containing a partially miscible mixture. *Chem. Engng. Process.* **38**, 487–502. [3.6]
- Steinberg, V. and Brand, H. 1983 Convective instabilities of binary mixtures with fast chemical reaction in a porous medium. *J. Chem. Phys.* **78**, 2655–2660. [9.1.6.4]
- Stemmelin, D., Moyne, C. and Degiovanni, A. 1992 Thermoconvective instability of a boiling liquid in porous medium. *C.R. Acad. Sci. Paris, Sér. II*, **314**, 769–775. [10.3.1]
- Stevens, J. D., Sharp, J. M., Simmons, C. T. and Fenstemaker, J. R. 2009 Evidence of free convection in groundwater: Field-based experiments near wind-tidal flats. *J. Hydrol.* **375**, 394–409. [11.8]
- Stewart, W. E. and Burns, A. S. 1992 Convection in a concentric annulus with heat generating porous media and a permeable inner boundary. *Int. Comm. Heat Mass Transfer* **19**, 859–868. [6.17]
- Stewart, W. E. and Dona, C. L. G. 1988 Free convection in a heat-generating porous medium in a finite vertical cylinder. *ASME J. Heat Transfer* **110**, 517–520. [6.17]
- Stewart, W. E., Cai, L. and Stickler, L. A. 1994 Convection in heat-generating porous media with permeable boundaries — natural ventilation of grain storage bins. *ASME J. Heat Transfer* **116**, 1044–1046. [6.17]
- Stewart, W. E., Greer, L. A. and Stickler, L. A. 1990 Heat transfer in a partially insulated enclosure of heat generating porous media. *Int. Comm. Heat Mass Transfer* **17**, 597–607. [6.15.3]
- Storesletten, L. 1993 Natural convection in a porous layer with anisotropic thermal diffusivity. *Transport in Porous Media* **12**, 19–29. [6.12]
- Storesletten, L. 1998 Effects of anisotropy on convective flow through porous media. *Transport Phenomena in Porous Media* (eds. D. B. Ingham and I. Pop), Elsevier, Oxford, pp. 261–184. [6.12]

- Storesletten, L. 2004 Effects of anisotropy on convection in horizontal and inclined porous layers. In Emerging Technologies and Techniques in Porous Media (D. B. Ingham, A. Bejan, E. Mamut and I. Pop, eds), Kluwer Academic, Dordrecht, pp. 285–306. [6.12]
- Storesletten, L. and Barletta, A. 2009 Linear instability of mixed convection of cold water in a porous layer induced by viscous dissipation. *Int. J. Therm. Sci.* **48**, 655–664. [6.10.1]
- Storesletten, L. and Pop, I. 1996 Free convection in a vertical porous layer with walls of non-uniform temperature. *Fluid Dyn. Res.* **17**, 107–119. [6.15.2]
- Storesletten, L. and Rees, D. A. S. 1998 The influence of higher-order effects on the linear instability of thermal boundary layer flow in porous media. *Int. J. Heat Mass Transfer* **41**, 1833–1843. [5.1.9.9]
- Storesletten, L. and Rees, D. A. S. 2004 Onset of convection in an inclined porous layer with internal heat generation. In Applications of Porous Media (ICAPM 2004), (eds. A. H. Reis and A. F. Miguel), Évora, Portugal, pp. 139–145. [7.8]
- Storesletten, L. and Rees, D. A. S. 1997 An analytical study of free convective boundary layer flow in porous media: the effect of anisotropic diffusivity. *Transport in Porous Media* **27**, 289–304. [5.1.9.9]
- Storesletten, L. and Tveitereid, M. 1987 Thermal convection in a porous medium confined by a horizontal cylinder. *ASME HTD* **92**, 223–230. [6.16.2]
- Storesletten, L. and Tveitereid, M. 1991 Natural convection in a horizontal porous cylinder. *Int. J. Heat Mass Transfer* **34**, 1959–1968. [6.16.2]
- Storesletten, L. and Tveitereid, M. 1999 Onset of convection in an inclined porous layer with anisotropic permeability. *Appl. Mech. Engng.* **4**, 575–587. [7.8]
- Strange, R. and Rees, D. A. S. 1996 The effect of fluid inertia on the stability of free convection in a saturated porous medium heated from below. Proceedings of the International Conference on Porous Media and their Applications in Science, Engineering and Industry, (eds. K. Vafai and P.N. Shivakumar), Engineering Foundation, New York. [6.6]
- Straughan, B. 1988 A nonlinear analysis of convection in a porous vertical slab. *Geophys. pp. 71–84.* [6.6] *Astrophys. Fluid Dyn.* **42**, 269–276. [7.1.4]
- Straughan, B. 2001b Surface-tension driven convection in a fluid overlying a porous layer. *J. Comput. Phys.* **170**, 320–337. [6.19.3]
- Straughan, B. 2001c A sharp nonlinear stability threshold in rotation porous convection. *Proc. Roy. Soc. Lond. A* **457**, 87–93. [6.22]
- Straughan, B. 2002 Effect of property variation and modeling on convection in a fluid overlying a porous layer. *Int. J. Numer. Anal. Meth. Geomech.* **26**, 75–97. [6.19.1]
- Straughan, B. 2004a Resonant porous penetrative convection. *Proc. Roy. Soc. Lond. A* **460**, 2913–2927. [6.11.4]
- Straughan, B. 2004b The Energy Method, Stability, and Nonlinear Convection, 2nd ed., Springer, New York. [1.6, 6.4, 6.19.3, 11.2, 11.3]
- Straughan, B. 2006 Global nonlinear stability in porous convection with a thermal non-equilibrium model. *Proc. Roy. Soc. Lond. A* **462**, 409–418. [6.5]
- Straughan, B. 2009 On the Nield-Kuznetsov theory for convection in bidisperse porous media. *Transp. Porous Media* **77**, 159–168. [6.27]
- Straughan, B. 2010a Green-Naghdi fluid with non-thermal equilibrium effects. *Proc Roy. Soc. Lond. A* **466**, 2021–2032. [6.23]
- Straughan, B. 2010b Porous convection with Cattaneo heat flux. *Int. J. Heat Mass Transfer* **53**, 2808–2812. [6.24]
- Straughan, B. 2010c Structure of the dependence of Darcy and Forchheimer coefficients on porosity. *Int. J. Engng. Sci.* **48**, 1610–1621. [1.5.2]
- Straughan, B. 2011a Continuous dependence on the heat source in resonant porous penetrative convection. *Stud. Appl. Math.* **127**, 30–31. [6.11.4].
- Straughan, B. 2011b Tipping points in Cattaneo-Christov thermohaline convection. *Proc Roy. Soc. Lond. A* **467**, 7–18. [9.1.6.4]

- Straughan, B. and Hutter, K. 1999 A priori bounds and structural stability for double-diffusive convection incorporating the Soret effect. *Proc. Roy. Soc. Lond. A* **445**, 767–777. [9.1.4]
- Straughan, B. and Walker, D. W. 1996a Anisotropic porous penetrative convection. *Proc. Roy. Soc. Lond. A* **452**, 97–115. [6.12]
- Straughan, B. and Walker, D. W. 1996b Two very accurate and efficient methods for computing eigenvalues and eigenfunctions in porous convection problems. *J. Comput. Phys.* **127**, 128–141. [7.9]
- Straus, J. M. 1974 Large amplitude convection in porous media. *J. Fluid Mech.* **64**, 51–63. [6.4, 6.6, 6.8, 6.9.1]
- Straus, J. M. and Schubert, G. 1977 Thermal convection of water in a porous medium: effects of temperature- and pressure-dependent thermodynamic and transport processes. *J. Geophys. Res.* **82**, 325–333. [6.7]
- Straus, J. M. and Schubert, G. 1979 Three-dimensional convection in a cubic box of fluid-saturated porous material. *J. Fluid Mech.* **91**, 155–165. [6.15.1]
- Straus, J. M. and Schubert, G. 1981 Modes of finite-amplitude three-dimensional convection in rectangular boxes of fluid-saturated porous material. *J. Fluid Mech.* **103**, 23–32. [6.15.1]
- Stroh, F. and Balakotaiah, V. 1991 Modeling of reaction-induced flow maldistributions in packed beds. *AICHE J.* **37**, 1035–1052. [3.4]
- Stroh, F. and Balakotaiah, V. 1992 Stability of uniform flow in packed-bed reactors. *Chem. Engng Sci.* **47**, 593–604. [3.4]
- Stroh, F. and Balakotaiah, V. 1993 Flow maldistributions in packed beds: effect of reactant consumption. *Chem. Engng Sci.* **48**, 1629–1640. [3.4]
- Strong, N. 2008a Double-diffusive convection in a porous layer in the presence of vibration. *SIAM J. Appl. Math.* **69**, 1263–1276. [6.24]
- Strong, N. 2008b Effect of vertical modulation on the onset of filtration convection. *J. Math. Fluid Mech.* **10**, 488–502. [6.24]
- Stubos, A. K. and Buchlin, J. M. 1993 Analysis and numerical simulation of the thermodynamic behaviour of a heat dissipating debris bed during power transients. *Int. J. Heat Mass Transfer* **36**, 1391–1401. [6.11.2]
- Stubos, A. K., Kanellopoulos, V. and Tassopoulos, M. 1994 Aspects of transient modelling of a volumetrically heated porous bed: a combination of microscopic and macroscopic approach. *Heat Transfer 1994*, Inst. Chem. Engrs, Rugby, vol. 5, pp. 387–392. [11.9.1]
- Stubos, A. K., Pérez Caseiras, C., Buchlin, J. M. and Kanellopoulos, N. K. 1997 Numerical investigation of vapor-liquid flow and heat transfer in capillary porous media. *Numer. Heat Transfer A* **31**, 143–166. [11.9.1]
- Stubos, A. K., Satik, C. and Yortsos, Y. C. 1993a Critical heat flux hysteresis in vapor-liquid counterflow in porous media. *Int. J. Heat Mass Transfer* **36**, 227–231. [11.9.2]
- Stubos, A. K., Satik, C. and Yortsos, Y. C. 1993b Effects of capillary heterogeneity on vapo-liquid counterflow in porous media. *Int. J. Heat Mass Transfer* **36**, 967–976. [11.9.1]
- Sturm, M. and Johnson, J. B. 1991 Natural convection in the subarctic snow cover. *J. Geophys. Res.* **96**, 11657–11671. [11.1]
- Subagyo, Standish, N. and Brooks, G. A. 1998 A new model of velocity distribution of a single-phase fluid flowing in packed beds. *Chem. Engng. Sci.* **53**, 1375–1385. [2.6]
- Subramanian, L. and Patil, P. R. 1991 Thermohaline convection with coupled molecular diffusion in an anisotropic porous medium. *Indian J. Pure Appl. Math.* **22**, 169–193. [9.1.6.4]
- Subramanian, S. 1994 Convective instabilities induced by exothermic reactions occurring in a porous medium. *Phys. Fluids* **6**, 2907–2922. [9.1.6.4]
- Subramanian, S. and Balakotaiah, V. 1995 Mode interactions in reaction-driven convection in a porous medium. *Chem. Engrg Sci.* **50**, 1851–1868. [3.4]
- Subramanian, S. and Balakotaiah, V. 1997 Analysis and classification of reaction-driven stationary convective patterns in a porous medium. *Phys. Fluids* **9**, 1674–1695. [3.5]
- Suekane, T., Kitani, T., Kusano, K. and Deguchi, Y. 2012 Natural convection of miscible two phases due to density difference in saturated porous media. *AIP Conf. Proc.* **1453**, 173–178. [11.11]

- Sugawara, M., Inaba, H. and Seki, N. 1988 Effect of maximum density of water on freezing of a water-saturated horizontal porous layer. *ASME J. Heat Transfer* **110**, 155–159. [10.2.2]
- Sultana, Z. and Hyder, M. N. 2007 Non-Darcy free convection inside a wavy enclosure. *Int. Comm. Heat Mass Transfer* **34**, 136–146. [7.3.7]
- Suma, S. P., Ganagadharaiyah, Y. H., Indira, R. and Shivakumara, I. S. 2012 Throughflow effects on penetrative convection in superposed fluid and porous layers. *Transp. Porous Media* **95**, 91–110. [6.19.3]
- Sun, B. X., Xu, X. Z., Lai, Y. M., and Fang, M. X. 2005a Evaluation of fractured rock layer heights in ballast railway embankment based on cooling effect of natural convection in cold regions. *Cold Regions Sci. Tech.* **42**, 120–144. [7.3.7]
- Sun, B. X., Xu, X. Z., Lai, Y. M., Wang, S. J. and Zhang, J. Z. 2005b Mechanism of evolution on winter-time natural convection cooling effect of fractured-rock embankment in permafrost regions. *Chinese Sci. Bull.* **50**, 2744–2754. [7.3.7]
- Sun, B. X., Yang, L. J. and Xu, X. Z. 2007 Onset and evaluation of winter-time natural convection cooling effectiveness of crushed rock highway embankment. *Cold Regions Sci. Tech.* **48**, 218–231. [7.3.7]
- Sun, B. X., Yang, L. J., Liu, Q., Wang, W. and Xu, X. Z. 2009 Numerical analysis for critical thickness of crushed rock revetment layer on Qinghai-Tibet railway. *Cold Regions Sci. Tech.* **57**, 131–138. [7.3.7]
- Sun, Q. and Pop, I. 2011 Free convection in a triangle cavity filled with a porous medium saturated with nanofluids with flush mounted heater on wall. *Int. J. Therm. Sci.* **50**, 2141–2153. [5.12.3]
- Sun, Z. S., Tien, C. and Yen, Y. C. 1970 Onset of convection in a porous medium containing liquid with a density maximum. *Heat Transfer* 1970, Elsevier, Amsterdam, vol. 4, paper NC 2.11. [6.20]
- Sundaravadivelu, K. and Tso, C. P. 2003 Influence of viscosity variations on the forced convection flow through two types of heterogeneous porous media with isoflux boundary condition. *Int. J. Heat Mass Transfer* **46**, 2329–2339. [4.12]
- Sundfor, H. O. and Tyvand, P. A. 1996 Transient free convection in a horizontal porous cylinder with a sudden change in wall temperature. *Waves and Nonlinear Processes In Hydrodynamics* (eds. J. Grue, B. Gjevik and J. E. Weber), Kluwer, Dordrecht, pp. 291–302. [7.5]
- Sung, H. J., Kim, S. Y. and Hyun, J. M. 1995 Forced convection from an isolated heat source in a channel with porous medium. *Int. J. Heat Fluid Flow* **16**, 527–535. [4.16.5]
- Sunil 1994 Thermosolutal hydromagnetic instability of a compressible and partially ionized plasma in a porous medium. *Arch. Mech.* **46**, 819–828. [9.1.6.4]
- Sunil 1999 Finite Larmor radius effect on thermosolutal instability of a Hall plasma in a porous medium. *Phys. Plasmas* **6**, 50–56. [9.1.6.4]
- Sunil 2001 Thermosolutal instability of a compressible finite Larmor radius, Hall plasma in a porous medium. *J. Porous Media* **4**, 55–67. [9.1.6.4]
- Sunil and Mahajan, A. 2008a A nonlinear stability analysis in a double-diffusive magnetized ferrofluid layer saturating a porous medium. *J. Geophys. Engng.* **5**, 311–322. [9.1.6.4]
- Sunil and Mahajan, A. 2008b Thermoconvective magnetized ferrofluid with internal angular momentum saturating a porous medium: A nonlinear stability analysis. *Appl. Math. Comp.* **205**, 403–416. [6.21]
- Sunil and Mahajan, A. 2009a A nonlinear stability analysis for rotating magnetized ferrofluid heated from below saturating a porous medium. *ZAMP* **60**, 344–362. [6.21]
- Sunil and Mahajan, A. 2009b A nonlinear stability analysis for thermoconvective magnetized ferrofluid saturating a porous medium. *Transp. Porous Media* **76**, 327–343. [6.21]
- Sunil and Mahajan, A. 2009c A nonlinear stability analysis in a double-diffusive magnetized ferrofluid with magnetic-field-dependent viscosity saturating a porous medium. *Canad. J. Phys.* **87**, 659–673. [9.1.6.4]
- Sunil and Sharma, A. 2005 Effect of dust particles on a layer of rotating ferromagnetic fluid heated and soluted from below saturating a porous medium. *Indian J. Phys.* **79**, 1285–1292. [9.7]

- Sunil and Singh, P. 2000 Thermal instability of a porous medium with relaxation and inertia in the presence of Hall effects. *Arch. Appl. Mech.* **70**, 649–658. [6.21]
- Sunil, Bharti, P. K. and Sharma, R. C. 2003a On Bénard convection in a porous medium in the presence of throughflow and rotation in magnetics. *Arch. Mech.* **55**, 257–274. [6.21]
- Sunil, Bharti, P. K., Sharma, D. and Sharma, R. C. 2004a The effect of magnetic field dependent viscosity on the thermal convection in a ferromagnetic fluid in a porous medium. *Z. Naturfor. A* **59**, 397–406. [6.21]
- Sunil, Chand, P. and Mahajan, A. 2010c Marginal stability of dusty magnetized ferrofluid with internal angular momentum saturating a porous medium. *Proc. Nat. Acad. Sci. India A* **80**, 261–268. [6.21]
- Sunil, Divya and Sharma, R. C. 2005a Effect of dust particles on a ferromagnetic fluid heated and soluted from below saturating a porous medium. *Appl. Math. Comput.* **169**, 832–853. [9.1.6.4]
- Sunil, Divya and Sharma, R. C. 2005b Effect of magnetic-field dependent viscosity on a rotating ferromagnetic fluid heated and soluted from below, saturating a porous medium. *J. Porous Media* **8**, 569–588. [9.1.6.4]
- Sunil, Divya and Sharma, R. C. 2005b The effect of rotation on ferromagnetic fluid heated and salted from below saturating a porous medium. *J. Geophys. Engng.* **1**, 116–127. [9.1.6.4]
- Sunil, Divya and Sharma, R. C. 2005c The effect of magnetic-field-dependent viscosity on ferromagnetic convection in a porous medium in the presence of dust particles. *J. Geophys. Engng.* **1**, 277–286. [6.21]
- Sunil, Divya and Sharma, R. C. 2005d Thermosolutal convection in a ferromagnetic fluid saturating a porous medium. *J. Porous Media* **8**, 393–408. [9.1.6.4]
- Sunil, Divya and Sharma, V. 2005c Effect of dust particles on a rotating ferromagnetic fluid heated from below saturating a porous medium. *J. Colloid Interface Sci.* **291**, 152–161. [6.21]
- Sunil, Divya, and Sharma, R. C. 2005a The effect of magnetic-field-dependent viscosity on thermo-solutal convection in a ferromagnetic fluid saturating a porous medium. *Transport Porous Media* **60**, 251–274. [9.1.6.4]
- Sunil, Divya, Sharma, R. C. and Sharma, V. 2003b Compressible couple-stress fluid permeated with suspended particles heated and soluted from below in porous medium. *Indian J. Pure Appl. Phys.* **41**, 602–611. [9.1.6.4]
- Sunil, Sharma P. and Mahajan, A. 2009b A nonlinear stability analysis for thermoconvective magnetized ferrofluid with magnetic-field-dependent viscosity saturating a porous medium. *J. Porous Media* **12**, 667–682. [6.21]
- Sunil, Sharma P. and Mahajan, A. 2010a Nonlinear ferroconvection in a porous layer using a thermal nonequilibrium model. *Spec. Top. Rev. Porous Media* **1**, 105–121. [6.21]
- Sunil, Sharma P. and Mahajan, A. 2010b Onset of Darcy-Brinkman double-diffusive convection in a magnetized ferrofluid layer using a non-equilibrium model: a nonlinear stability analysis. *J. Geophys. Engng.* **7**, 417–430. [9.1.6.4]
- Sunil, Sharma P. and Mahajan, A. 2011 Onset of Darcy-Brinkman ferroconvection in a rotating porous layer using a thermal non-equilibrium model: A nonlinear stability analysis. *Transp. Porous Media* **88**, 421–439. [6.21]
- Sunil, Sharma, A. and Kumar, P. 2006a Effect of magnetic field dependent viscosity and rotation on ferroconvection in the presence of dust particles. *Appl. Math. Comput.* **182**, 82–88. [6.21]
- Sunil, Sharma, A., Bharti, P. K. and Shandil, R. G. 2006b Effect of rotation on a layer of micropolar ferromagnetic fluid heated from below saturating a porous medium. *Int. J. Engng. Sci.* **44**, 683–698. [6.21]
- Sunil, Sharma, A., Bharti, P. K. and Shandil, R. G. 2007 Linear stability of double-diffusive convection in a micropolar ferromagnetic fluid saturating a porous medium. *Int. J. Mech. Sci.* **49**, 1047–1059. [9.1.6.4]
- Sunil, Sharma, A., Kumar, P. and Gupta, U. 2005c The effect of magnetic-field-dependent viscosity and rotation on ferromagnetic convection saturating a porous medium in the presence of dust particles. *J. Geophys. Engng.* **2**, 238–251. [9.1.6.4]

- Sunil, Sharma, A., Shandil, R. G. and Gupta, U. 2005d Effect of magnetic-field dependent viscosity and rotation on ferroconvection saturating a porous medium in the presence of dust particles. *Int. Comm. Heat Mass Transfer* **32**, 1387–1399. [6.21]
- Sunil, Sharma, D. and Sharma, R. C. 2005b Effect of dust particles on thermal convection in ferromagnetic fluid saturating a porous medium. *J. Magnet. Magnet. Mater.* **288**, 183–195. [6.21]
- Sunil, Sharma, P. and Mahajan, A. 2009a A nonlinear stability analysis of a rotating double-diffusive magnetized ferrofluid saturating a porous medium. *Heat Transfer Res.* **40**, 351–378. [9.1.6.4]
- Sunil, Sharma, R. C. and Chandel, R. S. 2004d Effect of suspended particles on couple-stress fluid heated and soluted from below in porous medium. *J. Porous Media* **7**, 9–18. [9.1.6.4]
- Sunil, Sharma, R. C. and Pal, M. 2001 Hall effect on thermosolutal instability of a Rivlin-Ericksen fluid in a porous medium. *Non-Equil. Thermodyn.* **26**, 373–386. [9.1.6.4]
- Sunil, Sharma, R. C. and Pal, M. 2002 On a couple-stress fluid heated from below in a porous medium in the presence of a magnetic field and rotation. *J. Porous Media* **5**, 149–158. [6.22]
- Surasani, V. K., Metzger, T. and Tsotsas, E. 2008a Consideration of heat transfer in pore network modelling of convective drying. *Int. J. Heat Mass Transfer* **51**, 2506–2518. [3.6]
- Surasani, V. K., Metzger, T. and Tsotsas, E. 2008b The influence of heating mode on drying behaviour of capillary porous media. *Chem. Engng. Sci.* **63**, 5218–5228. [3.6]
- Suresh, C. S. Y., Krishna, Y. V., Sundararajan, T. and Das, S. K. 2005 Numerical simulation of three-dimensional natural convection inside a heat generating anisotropic porous medium. *Heat Mass Transfer* **41**, 799–809. [7.3.8]
- Suthar, O. P., Bhaduria, B. S. and Khan, A. 2009 Modulated centrifugal convection in a vertical rotating porous layer distant from the axis of rotation. *Transp. Porous Media* **79**, 255–264. [6.22]
- Suthar, O. P., Bhaduria, B. S. and Khan, A. 2011 Rotating Brinkman-Lapwood convection with modulation. *Transp. Porous Media* **88**, 369–383. [6.22]
- Suthar, O. P., Bhaduria, B. S. and Khan, A. 2012 Effect of g-jitter on the onset of thermosolutal viscoelastic convection in the absence of local thermal equilibrium. *Spec. Top. Rev. Porous Media* **3**, 239–246. [9.1.6.4]
- Sutton, F. M. 1970 Onset of convection in a porous channel with net through flow. *Phys. Fluids* **13**, 1931–1934. [6.10.2]
- Swamy, M. S. , Naduvinamani, N. B. and Sidram, W. 2012 The onset of Darcy-Brinkman convection in a binary viscoelastic fluid saturated porous layer. *Transp. Porous Media* **94**, 399–416. [9.1.6.4]
- Swift, D. W. and Harrison, W. D. 1984 Convective transport of brine and thaw of subsea permafrost: result of numerical simulations. *J. Geophys. Res.* **89**, 2080–2086. [11.3]
- Tada, S. and Ichimiya, K. 2007a Analysis of laminar dissipative flow and heat transfer in a porous saturated circular tube with constant wall heat flux. *Int. J. Heat Mass Transfer* **50**, 2406–2413. [7.3.6]
- Tada, S. and Ichimiya, K. 2007b Numerical simulation of forced convection in a porous circular tube with constant wall heat flux: An extended Graetz problem with viscous dissipation. *Chem. Engng. Tech.* **30**, 1362–1368. [4.13]
- Tagare, S. G. and Babu, A. B. 2007 Nonlinear convection due to compositional and thermal buoyancy. *J. Porous Media* **10**, 823–839. [9.1.4]
- Tai, B. C. and Char, M. I. 2010 Soret and Dufour effects on free convection flow of non-Newtonian fluids along a vertical plate embedded in a porous medium with thermal radiation. *Int. Comm. Heat Mass Transfer* **37**, 480–483. [9.2.1]
- Tait, S. and Jauport, C. 1992 Compositional convection in a reactive crystalline mush and melt differentiation. *J. Geophys. Res.* **97**, 6735–6756. [10.2.3]
- Tait, S., Jahrling, K. and Jaupart, C. 1992 The planform of compositional convection and chimney formation in a mushy layer. *Nature* **359**, 406–408. [10.2.3]
- Tak, S. S. , Mathur, R., Gehlot, R. K. and Khan, A. 2010 MHD free convection-radiation interaction along a vertical surface embedded in Darcian porous medium in presence of Soret and Dufour's effects. *Thermal Science* **14**, 137–145. [9.2.1]

- Takata, Y., Fukuda, K., Hasegawa, S., Iwashige, K., Shimomura, H. and Sanokawa, K. 1982 Three-dimensional natural convection in a porous medium enclosed with concentric inclined cylinders. *Heat Transfer 1982*, Hemisphere, Washington, DC, vol. 2, pp. 351–356. [7.8]
- Takatsu, Y. and Masuoka, T. 1998 Turbulent phenomena in flow through porous media. *J. Porous Media* **1**, 243–251. [1.8]
- Takatsu, Y., Masuoka, T., Hashimoto, Y. and Yokota, K. 1997 Natural convection along a vertical porous surface. *Heat Transfer Japan. Res.* **26**, 385–397. [5.1.9.9]
- Takhar, H. S. and Beg, O. A. 1997 Non-Darcy effects on convective boundary-layer flow past a semi-infinite vertical plate in saturated porous media. *Heat Mass Transfer* **32**, 33–34. [8.1.1]
- Takhar, H. S. and Ram, P. C. 1994 Magnetohydrodynamic free convection flow of water at 4°C through a porous medium. *Int. Comm. Heat Mass Transfer* **21**, 371–376. [8.2.1]
- Takhar, H. S., Chamkha, A. J. and Nath G. 2002 Natural convection on a vertical cylinder embedded in a thermally stratified high-porosity medium. *Int. J. Thermal Sci.* **41**, 83–93. [5.7]
- Takhar, H. S., Chamkha, A. J. and Nath G. 2003 Effects of non-uniform temperature or mass transfer in finite sections of an inclined plate on the MHD natural convection flow in a temperature stratified high-porosity porous medium. *Int. J. Thermal Sci.* **42**, 829–836. [5.3]
- Takhar, H. S., Kumari, M. and Bèg, O. A. 1998 Computational analysis of coupled radiation-convection dissipative non-gray gas flow in a non-Darcy gas flow in a non-Darcy porous medium using the Keller box implicit difference scheme. *Int. J. Energy Res.* **22**, 141–159. [5.1.9.4]
- Takhar, H. S., Roy, S. and Nath, G. 2003 Unsteady free convection flow over an infinite vertical porous plate due to the combined effects of thermal and mass diffusion, magnetic field and Hall currents. *Heat Mass Transfer* **39**, 825–834. [9.2.1]
- Takhar, H. S., Soundalgekar, V. M. and Gupta, A. S. 1990 Mixed convection of an incompressible viscous fluid in a porous medium past a hot vertical plate. *Int. J. Non-Linear Mech.* **25**, 723–728. [8.1.1]
- Tam, C. K. W. 1969 The drag on a cloud of spherical particles in low Reynolds number flow. *J. Fluid Mech.* **38**, 537–546. [1.5.3]
- Tamayol, A., Hooman, K. and Bahrami, M. 2010 Thermal analysis of flow in a porous medium over a permeable stretching wall. *Transp. Porous Media* **85**, 661–676. [5.1.9.9]
- Tan, K. K., Sam, T. and Jamaludin, H. 2003 The onset of transient convection in bottom heated porous media. *Int. J. Heat Mass Transfer* **46**, 2857–2873. [6.11.3]
- Tan, K. K., Tan, Y. W. and Choong, T. S. Y. 2009 Onset of convection induced by bottom-up transient mass diffusion in porous media. *Powder Tech.* **191**, 55–60. [6.11.3]
- Tan, W. C. and Masuoka, T. 2007 Stability analysis of a Maxwell fluid in a porous medium heated from below. *Phys. Lett. A* **360**, 454–460. [6.23]
- Tang, J. and Bau, H. H. 1993 Feedback control stabilization of the no-motion state of a fluid confined in a horizontal porous layer heated from below. *J. Fluid Mech.* **257**, 485–505. [6.11.3]
- Tao, Z., Wu, H., Chen, G. and Deng, H. 2005 Numerical simulation of conjugate heat and mass transfer process within cylindrical porous media with cylindrical dielectric cores in microwave freeze-drying. *Int. J. Heat Mass Transfer* **48**, 561–572. [3.6]
- Tashtoush, B. 2000 Analytic solution for the effect of viscous dissipation on mixed convection in saturated porous media. *Transport in Porous Media* **41**, 197–209. [8.1.1]
- Tashtoush, B. 2005 Magnetic and buoyancy effects on melting from a vertical plate embedded in saturated porous media. *Energy Conv. Manag.* **46**, 2566–2577. [10.1.7]
- Tashtoush, B. and Kodah, Z. 1998 Non slip boundary effects in non-Darcian mixed convection from a vertical wall in saturated porous media. *Heat Mass Transfer* **34**, 35–39. [8.1.1]
- Taslim, M. E. and Narusawa, U. 1986 Binary fluid convection and double-diffusive convection. *ASME J. Heat Transfer* **108**, 221–224. [9.1.4]
- Taslim, M. E. and Narusawa, U. 1989 Thermal instability of horizontally superposed porous and fluid layers. *ASME J. Heat Transfer* **111**, 357–362. [6.19.1.2]
- Taunton, J. W., Lightfoot, E. N. and Green, T. 1972 Thermohaline instability and salt fingers in a porous medium. *Phys. Fluids* **15**, 748–753. [9.1.3]

- Tavman, I. H. 1996 Effective thermal conductivity of granular porous materials. *Int. Comm. Heat Mass Transfer* **23**, 169–176. [2.2.1]
- Taylor, G. I. 1971 A model for the boundary condition of a porous material, Part 1. *J. Fluid Mech.* **49**, 319–326. [1.6]
- Teamah, M. A., El-Maghiany, W. M. and Dawood, M. M. K. 2011 Numerical simulation of laminar forced convection in horizontal pipe partially or completely filled with porous material. *Int. J. Therm. Sci.* **50**, 1512–1522. [4.11]
- Telles, R. S. and Trevisan, O.V. 1993 Dispersion in heat and mass transfer natural convection along vertical boundaries in porous media. *Int. J. Heat Mass Transfer* **36**, 1357–1365. [9.2.1]
- Teng, H. and Zhao, H. 2000 An extension of Darcy's law to non-Stokes flow in porous media. *Chem. Eng. Sci.* **55**, 2727–2735. [1.5.2]
- Tewari, K. and Singh, P. 1992 Natural convection in a thermally stratified fluid-saturated porous medium. *Int. J. Engng Sci.* **30**, 1003–1008. [5.1.4]
- Tewari, P. K. 1982 A study of boiling and convection in fluid-saturated porous media. MS thesis, Cornell University. [10.3.1]
- Tewari, P. K. and Torrance, K. E. 1981 Onset of convection in a box of fluid-saturated porous material with a permeable top. *Phys. Fluids* **24**, 981–983. [6.15.1]
- Thangaraj, R. P. 2000 Effect of a nonuniform basic temperature gradient on the convective instability of a fluid-saturated porous layer with general velocity and thermal conditions. *Acta Mech.* **141**, 85–97. [6.11.1]
- Thansekhar, M. R., Babu, I. M. and Sekhar, A. C. 2009 Free convection in a vertical cylindrical annulus filled with anisotropic porous medium. *Thermal Science* **13**, 37–45. [7.3.3]
- Thevenin, J. 1995 Transient forced convection heat transfer from a circular cylinder embedded in a porous medium. *Int. Comm. Heat Mass Transfer* **22**, 507–516. [4.6.5]
- Thevenin, J. and Sadaoui, D. 1995 About enhancement of heat transfer over a circular cylinder embedded in a porous medium. *Int. J. Heat Mass Transfer* **22**, 295–304. [4.3]
- Thiele, M. 1997 Heat dispersion in stationary mixed convection flow about horizontal surfaces in porous media. *Heat Mass Transfer* **33**, 7–16. [8.1.2]
- Thompson, A. F., Huppert, H. E., Worster, G. M. and Aitta, A. 2003 Solidification and compositional convection of a ternary alloy. *J. Fluid Mech.* **497**, 167–199. [10.2.3]
- Tian, Y. and Zhao, C. Y. 2011 A numerical investigation of heat transfer in phase change materials (PCMs) embedded in porous metals. *Energy* **36**, 5539–5546. [10.1.7]
- Tien, C. L. and Hunt, M. L. 1987 Boundary layer flow and heat transfer in porous beds. *Chem. Engng. Proc.* **21**, 53–63. [4.9]
- Tien, C. L. and Vafai, K. 1990a Convective and radiative heat transfer in porous media. *Adv. Appl. Mech.* **27**, 225–281. [3.6]
- Tien, H. C. and Vafai, K. 1990b Pressure stratification effects on multiphase transport across a vertical slot porous insulation. *ASME J. Heat Transfer* **112**, 1023–1031. [7.1.7]
- Tiwari, A. K. and Singh, A. K. 2010 Natural convection in a porous medium bounded by a long vertical wavy wall and a parallel flat wall. *Z. Naturforsch. A* **65**, 800–810. [7.3.9]
- Tiwari, R. K. and Das, M. K. 2007 Heat transfer augmentation in a two-sided lid-driven differentially heated square cavity utilizing nanofluids. *Int. J. Heat Mass Transfer* **50**, 2002–2018. [3.8]
- Tobbal, T. and Bennacer, R. 1998 Heat and mass transfer in anisotropic porous layer. *Trends in Heat, Mass and Momentum Transfer* **3**, 129–137. [9.2.2]
- Toda, S., Hsu, W. S., Hashizume, H. and Kawaguchi, T. 1998 Unsteady heat transfer of steam flow with condensation in porous media. *Heat Transfer 1998, Proc. 11<sup>th</sup> IHTC*, **6**, 463–468. [10.4]
- Tofanelli, L. A. and de Lemos, M. J. S. 2009 Double-diffusive turbulent natural convection in a porous square cavity with opposing temperature and concentration gradients. *Int. Comm. Heat Mass Transfer* **36**, 991–995. [9.1.6.4]
- Tong, T. W. and Orangi, S. 1986 A numerical analysis for high modified Rayleigh number natural convection in enclosures containing a porous medium. *Heat Transfer 1986*, Hemisphere, Washington, DC, vol. 5, pp. 2647–2652. [7.6.2]

- Tong, T. W. and Subramanian, E. 1985 A boundary-layer analysis for natural convection in vertical porous enclosures – use of the Brinkman-extended Darcy model. *Int. J. Heat Mass Transfer* **28**, 563–571. [7.6.2]
- Tong, T. W. and Subramanian, E. 1986 Natural convection in rectangular enclosures partially filled with a porous medium. *Int. J. Heat Fluid Flow* **7**, 3–10. [7.7]
- Tong, T. W., Sharatchandra, M. C. and Gdoura, Z. 1993 Using porous inserts to enhance heat transfer in laminar fully-developed flows. *Int. Comm. Heat Mass Transfer* **20**, 761–770. [4.11]
- Tong, X., Khan, J. A. and Amin, M. R. 1996 Enhancement of heat transfer by inserting a metal matrix into a phase change material. *Numer. Heat Transfer* **30**, 125–141. [10.1.7]
- Tosco, T., Marchisio, D. L., Lince, F. and Sethi, R. 2012 Extension of the Darcy-Forchheimer law for shear-thinning fluids and validation in pore-scale simulations. *Transp. Porous Media*, to appear. [1.5.2]
- Tournier, C., Genton, P. and Rabinowicz, M. 2000 The onset of convection in vertical fault planes: consequences for the thermal regime in crystalline basements and for heat recovery experiments. *Geophys. J. Int.* **110**, 500–508. [6.15.2]
- Toutant, A., Chandesris, M. and Jamet, D. 2009 Jump conditions for filtered quantities at an under-resolved discontinuous interface. Part I; Theoretical development. *Int. J. Multiphase Flow* **35**, 1100–1118. [1.6]
- Tracey, J. 1996 Multi-component convection-diffusion in a porous medium. *Cont. Mech. Thermodyn.* **8**, 361–381. [9.1.3]
- Tracey, J. 1998 Penetrative convection and multi-component diffusion in a porous medium. *Adv. Water Res.* **22**, 399–412. [9.1.6.4]
- Travis, B. J. and Schubert, G. 2005 Hydrothermal convection in carbonaceous chondrite parent bodies. *Earth Planet. Sci. Lett.* **240**, 234–250. [11.8]
- Travkin, V. and Catton, I. 1995 A two-temperature model for turbulent flow and heat transfer in a porous layer. *ASME J. Fluids Engng.* **117**, 181–188. [1.8]
- Travkin, V. S. and Catton, I. 1994 Turbulent transport of momentum, heat and mass in a two-level highly porous medium. *Heat Transfer* 1994, Inst. Chem. Engrs, Rugby, vol. 6, pp. 399–404. [1.8]
- Travkin, V. S. and Catton, I. 1998 Porous media transport descriptions – non-local, linear and nonlinear against effective thermal/fluid properties. *Adv. Colloid Interface Sci.* **77**, 389–443. [1.8]
- Travkin, V. S. and Catton, I. 1999 Nonlinear effects in multiple regime transport of momentum in longitudinal capillary porous medium morphology. *J. Porous Media* **2**, 277–294. [1.8]
- Trevisan, O. V. and Bejan, A. 1985 Natural convection with combined heat and mass transfer buoyancy effects in a porous medium. *Int. J. Heat Mass Transfer* **28**, 1597–1611. [9.2.2]
- Trevisan, O. V. and Bejan, A. 1986 Mass and heat transfer by natural convection in a vertical slot filled with porous medium. *Int. J. Heat Mass Transfer* **29**, 403–415. [9.2.2]
- Trevisan, O. V. and Bejan, A. 1987a Combined heat and mass transfer by natural convection in a vertical enclosure. *J. Heat Transfer* **109**, 104–109. [9.2.2]
- Trevisan, O. V. and Bejan, A. 1987b Mass and heat transfer by high Rayleigh number convection in a porous medium heated from below. *Int. J. Heat Mass Transfer* **30**, 2341–2356. [9.1.5]
- Trevisan, O. V. and Bejan, A. 1989 Mass and heat transfer by natural convection above a concentrated source buried at the base of a shallow porous layer. *ASME HTD* **127**, 47–54. [9.4]
- Trevisan, O. V. and Bejan, A. 1990 Combined heat and mass transfer by natural convection in a porous medium. *Adv. Heat Transfer* **20**, 315–352. [9]
- Trew, M. and McKibbin, R. 1994 Convection in anisotropic inclined porous layers. *Transport in Porous Media* **17**, 271–283. [7.8]
- Tsai, R. and Huang, J. S. 2009a Numerical study of Soret and Dufour effects on heat and mass transfer from natural convection flow over a vertical porous medium with variable wall heat fluxes. *Comput. Mater. Sci.* **47**, 23–30. [9.2.1]
- Tsai, R. and Huang, J. S. 2009b Heat and mass transfer for Soret and Dufour effects on Hiemenz flow through a porous medium onto a stretching surface. *Int. J. Heat Mass Transfer* **52**, 2399–2406. [9.6.1]

- Tsai, R. and Huang, J. S. 2010 Combined effects of thermophoresis and electrophoresis on particle deposition onto a vertical plate from mixed convection flow through a porous medium. *Chem. Engrg. J.* **157**, 52–59. [8.1.6]
- Tsybulin, V. G. and Karasozan, B. 2008 Destruction of the family of steady states in the planar problem of Darcy convection. *Phys. Lett. A* **372**, 5639–5643. [6.4]
- Tsybulin, V. G., Karasozan, B. and Ergenc, I. 2006 Selection of steady states in planar Darcy convection. *Phys. Lett. A* **356**, 189–194. [6.4]
- Tung, V. X. and Dhir, V. K. 1993 Convective heat transfer from a sphere embedded in unheated porous media. *ASME J. Heat Transfer* **115**, 503–506. [4.3, 8.1.3]
- Turcotte, D. L., Ribando, R. J. and Torrance, K. E. 1977 Numerical calculation of two-temperature thermal convection in a permeable layer with application to the Steamboat Springs thermal system, Nevada. *The Earth's Crust* (ed. J. G. Heacock), Amer. Geophys. Union, Washington, DC, pp. 722–736. [11.7]
- Tveitereid, M. 1977 Thermal convection in a horizontal porous layer with internal heat sources. *Int. J. Heat Mass Transfer* **20**, 1045–1050. [6.11.2]
- Tyvand, P. A. 1977 Heat dispersion effect on thermal convection in anisotropic porous media. *J. Hydrol.* **34**, 335–342. [2.2.4, 6.12]
- Tyvand, P. A. 1980 Thermohaline instability in anisotropic porous media. *Water Resources Res.* **16**, 325–330. [9.1.6.2]
- Tyvand, P. A. 1981 Influence of heat dispersion on steady convection in anisotropic porous media. *J. Hydrol.* **52**, 13–23. [2.2.4, 6.12]
- Tyvand, P. A. 1995 First-order transient free convection about a horizontal cylinder embedded in a porous medium. *Fluid Dyn. Res.* **15**, 277–290. [5.5.1]
- Tyvand, P. A. and Storesletten, L. 1991 Onset of convection in an anisotropic porous medium with oblique principal axes. *J. Fluid Mech.* **226**, 371–382. [6.12]
- Tzeng, S. C. 2006 Convective heat transfer in a rectangular channel filled with sintered bronze beads and periodically spaced heated blocks. *ASME J. Heat Transfer* **128**, 453–464. [4.11]
- Tzeng, S. C. 2007 Spatial thermal regulation of aluminum foam heat sink using a sintered porous conductive pipe. *Int. J. Heat Mass Transfer* **50**, 117–126. [4.16.5]
- Tzeng, S. C. and Jeng, T. M. 2006 Convective heat transfer in porous channels with a 90 degree turned flow. *Int. J. Heat Mass Transfer* **49**, 1452–1461. [4.16.5]
- Tzeng, S. C. and Ma, W. P. 2004 Experimental investigation of heat transfer in sintered porous heat sink. *Int. Comm. Heat Mass Transfer* **31**, 827–836. [4.16.5]
- Tzeng, S. C., Jeng, T. M. and Wang, Y. C. 2006 Experimental study of forced convection in asymmetrically heated sintered porous channels with/without periodic baffles. *Int. J. Heat Mass Transfer* **49**, 78–88. [4.16.5]
- Tzeng, S. C., Ma, W. P. and Wang, Y. C. 2007 Friction and forced convective heat transfer in a sintered porous channel with obstacle blocks. *Heat Mass Transfer* **43**, 687–697. [4.11]
- Tzeng, S. C., Soong, C. Y. and Wong, S. C. 2004 Heat transfer in rotating channel with open cell porous aluminum foam. *Int. Comm. Heat Mass Transfer* **31**, 261–272. [4.16.5]
- Uddin, M. J., Khan, W. A. and Ishmail, A. I. M. 2012 Free convection boundary layer flow from a heated upward facing horizontal flat plate embedded in a porous medium filled by a nanofluid with convective boundary condition. *Transp. Porous Media* **92**, 867–881. [9.7]
- Umauthi, J. C. and Malashetty, M. S. 1999 Oberbeck convection flow of couple stress fluid through a vertical porous stratum. *Int. J. Nonlinear Mech.* **34**, 1037–1045. [7.1.6]
- Umauthi, J. C. and Veereshetty, S. 2012 Non-Darcy mixed convection in a vertical porous channel with boundary conditions of the third kind. *Transp. Porous Media* **95**, 111–131. [8.3.1]
- Umauthi, J. C., Chamkha, A. J. and Sridhar, K. S. R. 2010 Generalised plane Couette flow and heat transfer in a composite channel. *Transp. Porous Media* **85**, 157–169. [4.11S]
- Umauthi, J. C., Kumar, J. P., Chamkha, A. J. and Pop, I. 2005 Mixed convection in a vertical porous channel. *Transport Porous Media* **61**, 315–335. Erratum 75 (2008) 129–132. [8.3.1]
- Umauthi, J. C., Prathap Kumar, J. and Shekar, M. 2012 Convective flow between a corrugated and a smooth wall. *J. Porous Media* **15**, 975–988. [8.3.1]

- Umla, R. Augustin, M., Huke, B. and Lücke, M. 2010 Roll convection of binary fluid mixtures in porous media. *J. Fluid Mech.* **649**, 165–186. [9.1.3]
- Vadasz, J. J. , Roy-Aikins, J. E. A. and Vadasz, P. 2005 Sudden or smooth transitions in porous media natural convection. *Int. J. Heat Mass Transfer* **48**, 1096–1106. [6.4]
- Vadasz, P. 1990 Bifurcation phenomena in natural convection in porous media. *Heat Transfer 1990*, Hemisphere, Washington, DC, vol. 5, pp. 147–152. [6.13.4]
- Vadasz, P. 1992 Natural convection in porous media induced by the centrifugal body force: the solution for small aspect ratio. *ASME J. Energy Res. Tech.* **114**, 250–254. [6.22]
- Vadasz, P. 1993 Three-dimensional free convection in a long rotating porous box: analytical solution. *ASME J. Heat Transfer* **115**, 639–644. [7.12]
- Vadasz, P. 1994a Stability of free convection in a narrow porous layer subject to rotation. *Int. Comm. Heat Mass Transfer* **21**, 881–890. [7.12]
- Vadasz, P. 1994b Centrifugally generated free convection in a rotating porous box. *Int. J. Heat Mass Transfer* **37**, 2399–2404. [6.22]
- Vadasz, P. 1995 Coriolis effect on free convection in a long rotating box subject to uniform heat generation. *Int. J. Heat Mass Transfer* **38**, 2011–2018. [7.12]
- Vadasz, P. 1996a Stability of free convection in a rotating porous layer distant from the axis of rotation. *Transport in Porous Media* **23**, 153–173. [7.12]
- Vadasz, P. 1996b Convection and stability in a rotating porous layer with alternating direction of the cylindrical body force. *Int. J. Heat Mass Transfer* **39**, 1639–1647. [7.12]
- Vadasz, P. 1997a Flow in rotating porous media. In *Fluid Transport in Porous Media* (P. Du Plessis, ed.), Computational Mechanics Publications, Southampton, Chapter 4. [6.22]
- Vadasz, P. 1998a Coriolis effect on gravity-driven convection in a rotating porous layer heated from below. *J. Fluid Mech.* **376**, 351–375. [6.22]
- Vadasz, P. 1998b Free convection in rotating porous media. *Transport Phenomena in Porous Media* (eds. D. B. Ingham and I. Pop), Elsevier, Oxford, pp. 285–312. [6.22]
- Vadasz, P. 1999a Local and global transitions to chaos and hysteresis in a porous layer heated from below. *Transport Porous Media* **37**, 213–245. [6.4]
- Vadasz, P. 1999b A note and discussion on J.-L. Auriault's letter "Comments on the paper 'Local and global transitions to chaos and hysteresis in a porous layer heated from below' by P. Vadasz." *Transport Porous Media* **37**, 251–254. [6.4]
- Vadasz, P. 2000a Flow and thermal convection in rotating porous media. *Handbook of Porous Media* (K. Vafai, ed.), Marcel Dekker, New York., pp. 395–439. [6.22]
- Vadasz, P. 2000b Weak turbulence and transitions to chaos in porous media. *Handbook of Porous Media* (K. Vafai, ed.), Marcel Dekker, New York., pp. 699–754. [6.4]
- Vadasz, P. 2001a Heat transfer regimes and hysteresis in porous media convection. *ASME J. Heat Transfer* **123**, 145–156. [6.4]
- Vadasz, P. 2001b Equivalent initial conditions for compatibility between analytical and computational solutions of convection in porous media. *Int. J. Nonlinear Mech.* **36**, 197–208. [6.4]
- Vadasz, P. 2001c The effect of thermal expansion on porous media convection. Part 1: Thermal expansion solution. *Transport Porous Media* **44**, 421–443. [6.7]
- Vadasz, P. 2001d The effect of thermal expansion on porous media convection. Part 2: Thermal convection solution. *Transport Porous Media* **44**, 445–463. [6.7].
- Vadasz, P. 2002 Fundamentals of thermal convection in rotating porous media. *Heat Transfer 2002*, Proc. 12th Int. Heat Transfer Conf., Elsevier, Vol.1, pp. 117–128. [6.22]
- Vadasz, P. 2003 Small and moderate Prandtl number convection in a porous layer heated from below. *Int. J. Energy Res.* **27**, 941–960. [6.4]
- Vadasz, P. 2005a Explicit conditions for local thermal equilibrium in porous media heat conduction. *Transport Porous Media* **59**, 341–355. [2.2.3]
- Vadasz, P. 2005b Lack of oscillations in dual-phase-lagging heat conduction for a porous slab subject to imposed heat flux and temperature. *Int. J. Heat Mass Transfer* **48**, 2822–2828. [2.2.3]

- Vadasz, P. 2006a Chaotic dynamics and hysteresis in thermal convection. *IME J. Mech. Engng. Sci.* **220**, 309–323. [6.4]
- Vadasz, P. 2006b Exclusion of oscillations in heterogeneous and bi-composite media thermal conduction. *Int. J. Heat Mass Transfer* **49**, 4886–4892. [2.2.3]
- Vadasz, P. 2007 On the paradox of heat conduction in porous media subject to lack of local thermal equilibrium. *Int. J. Heat Mass Transfer* **50**, 4131–4140. [2.1.3]
- Vadasz, P. 2008a Analytical transition to weak turbulence and chaotic natural convection in porous media. In P. Vadasz (ed.) *Emerging Topics in Heat and Mass Transfer in Porous Media*, Springer, New York, pp. 111–132. [6.4]
- Vadasz, P. 2008b Nanofluids suspensions and bi-composite media as derivatives of interface heat transfer modeling in porous media. In P. Vadasz (ed.) *Emerging Topics in Heat and Mass Transfer in Porous Media*, Springer, New York, pp. 283–326. [2.2.3]
- Vadasz, P. 2010a Controlling chaos in porous media convection by using feedback control. *Transp. Porous Media* **85**, 287–298. [6.11.3]
- Vadasz, P. 2010b Heat flux dispersion in natural convection in porous media. *Int. J. Heat Mass Transfer* **53**, 3394–3404. [6.9.2]
- Vadasz, P. 2011a Heat transfer augmentation in nanofluids via nanofins. *Nanoscale Research Letters* **6**, #154. [9.7]
- Vadasz, P. 2011b Nanofins as a means of enhancing heat transfer; leading order results. *Transp. Porous Media* **89**, 165–183. [9.7]
- Vadasz, P. 2011c Basic natural convection in a vertical porous layer differentially heated from its sidewalls subject to lack of local thermal equilibrium. *Int. J. Heat Mass Transfer* **54**, 2387–2396. [7.1.7]
- Vadasz, P. 2012 Small Nield number convection in a porous layer heated from below via a constant heat flux and subject to lack of local equilibrium. *J. Porous Media* **15**, 249–258. [6.5]
- Vadasz, P. and Braester, C. 1992 The effect of imperfectly insulated sidewalls on natural convection in porous media. *Acta Mech.* **91**, 215–233. [6.15.3]
- Vadasz, P. and Govender, G. 1998 Two-dimensional convection induced by gravity and centrifugal forces in a rotating porous layer far away from the axis of rotation. *Int. J. Rotating Machinery* **4**, 73–90. [7.12]
- Vadasz, P. and Govender, S. 2001 Stability and stationary convection induced by gravity and centrifugal forces in a rotation porous layer distant from the axis of rotation. *Int. J. Engng. Sci.* **39**, 715–732. [6.22]
- Vadasz, P. and Heerah, A. 1998 Experimental confirmation and analytical results of centrifugally driven free convection in porous media. *J. Porous Media* **1**, 261–272. [7.1.4]
- Vadasz, P. and Olek, S. 1998 Transitions and chaos for free convection in a rotating porous layer. *Int. J. Heat Mass Transfer* **41**, 1417–1435. [6.8]
- Vadasz, P. and Olek, S. 1999a Weak turbulence and chaos for low Prandtl number gravity driven convection in porous media. *Transport Porous Media* **37**, 69–91. [6.4]
- Vadasz, P. and Olek, S. 1999b Computational recovery of the homoclinic orbit in porous media convection. *Int. J. Nonlinear Mech.* **34**, 1071–1075. [6.4]
- Vadasz, P. and Olek, S. 2000a Route to chaos for moderate Prandtl number convection in a porous layer heated from below. *Transport Porous Media* **41**, 211–239. [6.4]
- Vadasz, P. and Olek, S. 2000b Convergence and accuracy of Adomian's decomposition method for the solution of Lorenz equations. *Int. J. Heat Mass Transfer* **43**, 1715–1734. [6.4]
- Vadasz, P., Braester, C. and Bear, J. 1993 The effect of perfectly conducting side walls on natural convection in porous media. *Int. J. Heat Mass Transfer* **36**, 1159–1170. [6.15.3]
- Vafai, K. 1984 Convective flow and heat transfer in variable-porosity media. *J. Fluid Mech.* **147**, 233–259. [4.8]
- Vafai, K. 1986 Analysis of the channeling effect in variable-porosity media. *ASME J. Energy Res. Tech.* **108**, 131–139. [4.8]

- Vafai, K. and Amiri, A. 1998 Non-Darcian effects in confined forced convection flows. In *Transport Phenomena in Porous Media* (D. B. Ingham and I. Pop, eds.) Elsevier, Oxford, pp. 313–329. [4.9]
- Vafai, K. and Huang, P. C. 1994 Analysis of heat transfer regulation and modification employing intermittently emplaced porous cavities. *ASME J. Heat Transfer* **116**, 604–613. [4.11]
- Vafai, K. and Kim, S. J. 1989 Forced convection in a channel filled with a porous medium: an exact solution. *ASME J. Heat Transfer* **111**, 1103–1106. [4.9]
- Vafai, K. and Kim, S. J. 1990 Analysis of surface enhancement by a porous substrate. *ASME J. Heat Transfer* **112**, 700–706. [4.8, 4.14]
- Vafai, K. and Kim, S. J. 1997 Closure. *ASME J. Heat Transfer* **119**, 197–198. [1.5.3]
- Vafai, K. and Sarkar, S. 1986 Condensation effects in a fibrous insulation slab. *ASME J. Heat Transfer* **108**, 667–675. [10.4]
- Vafai, K. and Sarkar, S. 1987 Heat and mass transfer in partial enclosures. *AIAA J. Thermophys. Heat Transfer* **1**, 253–259. [10.4]
- Vafai, K. and Sözen, M. 1990a Analysis of energy and momentum transport for fluid flow through a porous bed. *ASME J. Heat Transfer* **112**, 690–699. [4.6.5]
- Vafai, K. and Sözen, M. 1990b An investigation of a latent heat storage porous bed and condensing flow through it. *ASME J. Heat Transfer* **112**, 1014–1022. [4.6.5]
- Vafai, K. and Thiagarajah, R. 1987 Analysis of flow and heat transfer at the interface region of a porous medium. *Int. J. Heat Mass Transfer* **30**, 1391–1405. [4.8]
- Vafai, K. and Tien, C. L. 1982 Boundary and inertial effects on convective mass transfer in porous media. *Int. J. Heat Mass Transfer* **25**, 1183–1190. [1.5.3]
- Vafai, K. and Tien, C. L. 1989 A numerical investigation of phase change effects in porous materials. *Int. J. Heat Mass Transfer* **32**, 1261–1277. [4.10]
- Vafai, K. and Tien, C. L. 1981 Boundary and inertia effects on flow and heat transfer in porous media. *Int. J. Heat Transfer* **24**, 195–203. [1.5.3, 4.9]
- Vafai, K. and Whitaker, S. 1986 Simultaneous heat and mass transfer accompanied by phase change in porous insulation. *ASME J. Heat Transfer* **108**, 132–140. [10.4]
- Vafai, K. and Yang, K. 2012 A note on local thermal non-equilibrium in porous media and bifurcation phenomenon in porous media. *Transp. Porous Media*, to appear. [2.2.3]
- Vafai, K., Alkire, R. L. and Tien, C. L. 1985 An experimental investigation of heat transfer in variable porosity media. *ASME J. Heat Transfer* **107**, 642–647. [4.8]
- Vafai, K., Bejan, A., Minkowycz, W. J. and Khanfer, K. 2006 A critical synthesis of pertinent models for turbulent transport through porous media. In *Handbook of Numerical Heat Transfer* (W. J. Minkowycz, E. M. Sparrow, J. Y. Murthy, eds.), 2nd ed., Wiley, New York, pp. 389–416. [1.8]
- Vafai, K., Desai, C.P. and Chen, S.C. 1993 An investigation of heat transfer process in a chemically reacting packed bed. *Numer. Heat Transfer A* **24**, 127–142. [3.4]
- Vafai, K., Minkowycz, W. J., Bejan, A. and Khanfer, K. 2006 Synthesis of models for turbulent transport through porous media. *Handbook of Numerical Heat Transfer* (eds. W. J. Minkowycz and E. M. Sparrow), Wiley, New York, ch. 12. [1.8]
- Vaidyanathan, G., Ramanathan, A. and Maruthamanikandan, S. 2002a Effect of magnetic field dependent viscosity on ferroconvection in a sparsely distributed porous medium. *Indian J. Pure Appl. Phys.* **40**, 166–171. [6.21]
- Vaidyanathan, G., Sekar, R. and Balasubramanian, R. 1991 Ferroconvective instability of fluids saturating a porous medium. *Int. J. Engng Sci.* **29**, 1259–1267. [6.23]
- Vaidyanathan, G., Sekar, R. and Ramanathan, A. 2002b Ferroconvection in an anisotropic densely packed porous medium. *Indian J. Chem. Tech.* **9**, 446–449. [6.21]
- Vaidyanathan, G., Sekar, R., Vasanthakumari, R. and Ramanathan, A. 2002c Effect of magnetic field dependent viscosity on ferroconvection in a rotating sparsely distributed porous medium. *J. Magn. Magn. Mater.* **250**, 65–76. [6.21]

- Vajravelu, K., Prasad, K. V., van Gorder, R. A. and Lee, J. 2011 Free convection boundary layer flow past a vertical surface in a porous medium with temperature-dependent properties. *Transp. Porous Media* **90**, 977–992. [5.1.9.9]
- Valdes-Parada, F. J., Alvarez-Ramirez, J., Goyeau, B. and Ochoa-Tapia, J. A. 2009a Computation of jump coefficients for momentum transfer between a porous medium and a fluid using a closed generalized transfer equation. *Transp. Porous Media* **78**, 439–457. [1.6]
- Valdes-Parada, F. J., Alvarez-Ramirez, J., Goyeau, B. and Ochoa-Tapia, J. A. 2009b Jump condition for diffusive and convective mass transfer between a porous medium and a fluid involving adsorption and chemical reaction. *Transp. Porous Media* **78**, 459–476. [2.4]
- Valdes-Parada, F. J., Goyeau, B. and Ochoa-Tapia, J. A. 2007a Jump momentum boundary condition at a fluid-porous dividing surface: Derivation of the closure problem. *Chem. Engng. Sci.* **62**, 4025–4039. [1.6]
- Valdés-Parada, F. J., Ochoa-Tapia, J. A. and Alvarez-Ramirez, J. 2007b Diffusive mass transport in the fluid-porous inter-region: Closure problem solution for the one-domain approach. *Chem. Engng. Sci.* **62**, 6054–6068. [1.6]
- Valdes-Parada, F. J., Ochoa-Tapia, J. A. and Alvarez-Ramirez, J. 2007c On the effective viscosity for the Darcy-Brinkman equation. *Physica A* **385**, 69–79. [1.5.3]
- Valencia-Lopez, J. J. and Ochoa-Tapia, J. A. 2001 A study of buoyancy-driven flow in a confined fluid overlying a porous layer. *Int. J. Heat Mass Transfer* **44**, 4725–4736. [6.19.2]
- Valencia-Lopez, J. J., Espinosa-Paredes, G. and Ochoa-Tapia, J. A. 2003 Mass transfer jump condition at the boundary between a porous medium and a homogeneous fluid. *J. Porous Media* **6**, 33–49. [2.4]
- Valipour, M. S. and Ghadi, A. Z. 2012 Numerical investigation of forced convective heat transfer around and through a porous circular cylinder with internal heat generation. *ASME J. Heat Transfer* **134**, 062601. [4.11]
- Van Dam, R. L., Simmons, C. T., Hyndman, D. W. and Wood, W. W. 2009 Natural free convection in porous media: First field documentation in groundwater. *Geophys. Res. Lett.* **36**, L 11403. [11.8]
- van Duijn, C. J., Pieters, G. J. M., Wooding, R. A. and van der Ploeg, A. 2002 Stability criteria for the vertical boundary layer formed by throughflow near the surface of a porous medium. Environmental Mechanics — Water, Mass and Energy Transfer in the Biosphere (eds. P. A. C. Raats, D. Smiles and A. W. Warrick), American Geophysical Union, pp. 155–169. [6.10.2]
- Van Dyne, D. G. and Stewart, W. E. 1994 Natural convection heat and mass transfer in a semi-cylindrical enclosure filled with a heat generating porous medium. *Int. Comm. Heat Mass Transfer* **21**, 271–281. [6.17]
- Vanishree, R. K. and Siddheshwar, P. G. 2010 The effect of rotation on thermal convection in an anisotropic porous medium with temperature-dependent viscosity. *Transp. Porous Media* **81**, 73–87. [6.22]
- Vanover, D. E. and Kulacki, F. A. 1987 Experimental study of mixed convection in a horizontal porous annulus. *ASME HTD* **84**, 61–66. [8.2.3]
- Varahasamy, M. and Fand, R. M. 1996 Heat transfer by forced convection in pipes packed with porous media whose matrices are composed of spheres. *Int. J. Heat Mass Transfer* **39**, 3931–3947. [4.9]
- Vargas, J. V. C., Laursen, T. A. and Bejan, A. 1995 Nonsimilar solutions for mixed convection on a wedge embedded in a porous medium. *Int. J. Heat Fluid Flow* **16**, 211–216. [8.1.4]
- Varol, Y. 2010 Natural convection in divided trapezoidal cavities filled with fluid saturated porous media. *Int. Comm. Heat Mass Transfer* **37**, 1350–1358. [7.3.7]
- Varol, Y. 2011 Natural convection in porous triangular enclosure with centered conducting body. *Int. Comm. Heat Mass Transfer* **38**, 368–376. [7.3.6]
- Varol, Y. and Oztop, H. F. 2008 A comparative numerical study on natural convection in inclined wavy and flat-plate solar collectors. *Building and Environment* **43**, 1535–1548. [7.3.7]

- Varol, Y. and Oztop, H. F. 2009 Control of buoyancy-induced temperature and flow fields with an embedded adiabatic thin plate in porous triangular cavities. *Appl. Therm. Engng* **29**, 558–566. [7.3.6]
- Varol, Y., Oztop, H. F. and Avci, E. 2008a Estimation of thermal and flow fields due to natural convection using support vector mechanics (SVM) in a porous cavity with discrete heat sources. *Int. Comm. Heat Mass Transfer* **35**, 928–936. [7.3.7]
- Varol, Y., Oztop, H. F. and Pop, I. 2008b Influence of inclination angle on buoyancy driven convection in triangular enclosure filled with a fluid-saturated porous medium. *Heat Mass Transfer* **44**, 617–624. [7.3.6]
- Varol, Y., Oztop, H. F. and Pop, I. 2008c Natural convection flow in porous enclosures with heating and cooling on adjacent walls and divided by a triangular massive partition. *Int. Comm. Heat Mass Transfer* **35**, 476–491. [7.3.6]
- Varol, Y., Oztop, H. F. and Pop, I. 2008d Natural convection in porous media-filled triangular enclosure with a conducting thin film on the hot vertical wall. *Proc. Inst. Mech. Engrs. C: J. Mech. Engng. Sci.* **222**, 1735–1743. [7.3.6]
- Varol, Y., Oztop, H. F. and Pop, I. 2008e Numerical analysis of natural convection for a porous rectangular enclosure with sinusoidally varying temperature profile on the bottom wall. *Int. Comm. Heat Mass Transfer* **35**, 56–64. [6.14]
- Varol, Y., Oztop, H. F. and Pop, I. 2008f Numerical analysis of natural convection in an inclined trapezoidal enclosure filled with a porous medium. *Int. J. Therm. Sci.* **47**, 1316–1331. [7.3.7]
- Varol, Y., Oztop, H. F. and Pop, I. 2009a Conduction-natural convection in a partitioned triangular enclosure filled with fluid saturated porous media. *J. Porous Media* **12**, 593–611. [7.3.6]
- Varol, Y., Oztop, H. F. and Pop, I. 2009b Conjugate heat transfer in porous triangular enclosure with thick bottom wall. *Int. J. Numer. Meth. Heat Fluid Flow* **19**, 650–664. [7.3.6]
- Varol, Y., Oztop, H. F. and Pop, I. 2009c Entropy analysis due to conjugate-buoyant flow in a right-angle trapezoidal enclosure filled with a porous medium bounded by a solid vertical wall. *Int. J. Therm. Sci.* **48**, 1161–1175. [7.3.6]
- Varol, Y., Oztop, H. F. and Pop, I. 2009d Entropy generation due to natural convection in non-uniformly heated porous isosceles triangular enclosure at different positions. *Int. J. Heat Mass Transfer* **52**, 1193–1205. [7.3.6]
- Varol, Y., Oztop, H. F. and Pop, I. 2009e Natural convection in right-angle porous trapezoidal enclosure partially cooled from inclined wall. *Int. Comm. Heat Mass Transfer* **36**, 6–15. [7.3.6]
- Varol, Y., Oztop, H. F. and Pop, I. 2009f Natural convection in a diagonally divided square cavity filled with a porous medium. *Int. J. Therm. Sci.* **48**, 1405–1415. [7.3.6]
- Varol, Y., Oztop, H. F. and Pop, I. 2010a Maximum density effects on buoyancy-driven convection in a porous trapezoidal cavity. *Int. Comm. Heat Mass Transfer* **37**, 401–409. [7.3.7]
- Varol, Y., Oztop, H. F. and Varol, A. 2006 Free convection in porous media filled right-angle triangular enclosures. *Int. Comm. Heat Mass Transfer* **33**, 1190–1197. [7.3.6]
- Varol, Y., Oztop, H. F. and Varol, A. 2007a Effects of thin fin on natural convection in porous triangular enclosures. *Int. J. Therm. Sci.* **46**, 1033–1045. [7.3.6]
- Varol, Y., Oztop, H. F. and Varol, A. 2007b Natural convection in porous triangular enclosures with a solid adiabatic fin attached to the horizontal wall. *Int. Comm. Heat Mass Transfer* **34**, 19–27. [7.3.6]
- Varol, Y., Oztop, H. F. and Varol, A. 2008g Free convection heat transfer and flow field in rectangular enclosures filled with porous media. *J. Porous Media* **11**, 103–115. [7.3.7]
- Varol, Y., Oztop, H. F. and Yilmaz, T. 2007c Two-dimensional natural convection in a porous rectangular enclosure with a square body. *Int. Comm. Heat Mass Transfer* **34**, 238–247. [7.3.7]
- Varol, Y., Oztop, H. F., Mobedi, M. and Pop, I. 2008h Visualization of natural convection heat transport using heatline method in porous non-isothermally heated triangular cavity. *Int. J. Heat Mass Transfer* **51**, 5040–5051. [7.3.6]
- Varol, Y., Oztop, H. F., Mobedi, M. and Pop, I. 2010b Visualization of heat flow using Bejan's heatline due to natural convection of water near 4 degrees C in thick walled porous cavity. *Int. J. Heat Mass Transfer* **53**, 1691–1698. [7.1.7]

- Vasantha, R., Pop, I. and Nath, G. 1986 Non-Darcy natural convection over a slender vertical frustum of a cone in a saturated porous medium. *Int. J. Heat Mass Transfer* **29**, 153–156. [5.8]
- Vasile, C., Lorente, S. and Perrin, B. 1998 Study of convective phenomena inside cavities coupled with heat and mass transfers through porous media – Application to vertical hollow bricks — a first approach. *Energy Build.* **28**, 229–235. [7.7]
- Vasseur, P. and Degan, G. 1998 Free convection along a vertical heated plate in a porous medium with anisotropic permeability. *Int. J. Numer. Methods Heat Fluid Flow* **8**, 43–63. [5.1.9.5]
- Vasseur, P. and Robillard, L. 1987 The Brinkman model for boundary layer regime in a rectangular cavity with uniform heat flux from the side. *Int. J. Heat Mass Transfer* **30**, 717–728. [7.6.2]
- Vasseur, P. and Robillard, L. 1993 The Brinkman model for natural convection in a porous layer: effects of non-uniform thermal gradient. *Int. J. Heat Mass Transfer* **36**, 4199–4206. [6.11.1]
- Vasseur, P. and Robillard, L. 1998 Natural convection in enclosures filled with anisotropic porous media. *Transport Phenomena in Porous Media* (eds. D. B. Ingham and I. Pop), Elsevier, Oxford, pp. 331–356. [7.3.2]
- Vasseur, P. and Wang, C. H. 1992 Natural convection heat transfer in a porous layer with multiple partitions. *Chem. Engng Comm.* **114**, 145–167. [6.13.2]
- Vasseur, P., Nguyen, T. H., Robillard, L. and Thi, V. K. T. 1984 Natural convection between horizontal concentric cylinders filled with a porous layer with internal heat generation. *Int. J. Heat Mass Transfer* **27**, 337–349. [6.17]
- Vasseur, P., Robillard, L. and Anochiravani, I. 1988 Natural convection in an inclined rectangular porous cavity with uniform heat flux from the side. *Wärme-Stoffübertrag.* **22**, 69–77. [7.8]
- Vasseur, P., Satish, M. G. and Robillard, L. 1987 Natural convection in a thin, inclined, porous layer exposed to a constant heat flux. *Int. J. Heat Mass Transfer* **30**, 537–550. [7.8]
- Vasseur, P., Wang, C. H. and Sen, M. 1989 The Brinkman model for natural convection in a shallow porous cavity with uniform heat flux. *Numer. Heat Transfer* **15**, 221–242. [6.19.1.2, 7.6.2]
- Vasseur, P., Wang, C. H. and Sen, M. 1990 Natural convection in an inclined rectangular porous slot: the Brinkman-extended Darcy model. *ASME J. Heat Transfer* **112**, 507–511. [7.8]
- Vaszi, A. Z., Elliot, L., and Ingham, D. B. 2003 Conjugate free convection from vertical fins embedded in a porous medium. *Numer. Heat Transfer A* **44**, 743–770. [5.1.5]
- Vaszi, A. Z., Elliot, L., Ingham, D. B. and Pop, I. 2001a Conjugate free convection above a cooled finite horizontal flat plate embedded in a porous medium. *Int. Comm. Heat Mass Transfer* **28**, 703–712. [5.2]
- Vaszi, A. Z., Elliot, L., Ingham, D. B. and Pop, I. 2002a Conjugate free convection above a heated finite horizontal flat plate embedded in a porous medium. *Int. J. Heat Mass Transfer* **45**, 2777–2795. [5.2]
- Vaszi, A. Z., Elliot, L., Ingham, D. B. and Pop, I. 2002b Conjugate free convection from a vertical plate fin embedded in a porous medium. *Heat Transfer 2002*, Proc. 12th Int. Heat Transfer Conf., Elsevier, Vol. 2, pp. 827–832. [5.12.1]
- Vaszi, A. Z., Elliot, L., Ingham, D. B. and Pop, I. 2004 Conjugate free convection from a vertical plate fin with a rounded tip embedded in a porous medium. *Int. J. Heat Mass Transfer* **47**, 2785–2794. [5.12.1]
- Vaszi, A. Z., Ingham, D. B., Lesnic, D., Munslow, D. and Pop, I. 2001b Conjugate free convection from a slightly inclined plate embedded in a porous medium. *Zeit. Angew. Math. Mech.* **81**, 465–479. [5.3]
- Vaszi, A., Elliot, L. and Ingham, D. B. 2004 A study of conjugate natural convection from vertical fins at various shapes embedded in a porous medium. In *Applications of Porous Media* (ICAPM 2004), (eds. A. H. Reis and A. F. Miguel), Évora, Portugal, pp. 96–106. [5.1.5]
- Vedha-Nayagam, M., Jain, P. and Fairweather, G. 1987 The effect of surface mass transfer on buoyancy induced flow in a variable-porosity medium adjacent to a horizontal heated plate. *Int. Comm. Heat Mass Transfer* **14**, 495–506. [5.2]
- Weinberg, A. K. 1967 Permeability, electrical conductivity, dielectric constant and thermal conductivity of a medium with spherical and ellipsoidal inclusions. *Soviet Phys. Dokl.* **11**, 593–595. [10.1.6]

- Venkataraman, P. and Rao, P. R. M. 2000 Validation of Forchheimer's law for flow through porous media with converging boundaries. *J. Hydr. Engng.* **126**, 63–71. [1.5.2]
- Venugopal, G., Balaji, C. and Venkateshan, S. P. 2010a Application of transient experimental techniques for developing a heat transfer correlation for mixed convection in porous medium. *Inverse Prob. Sci. Engng.* **18**, 1129–1150. [8.4.3]
- Venugopal, G., Balaji, C. and Venkateshan, S. P. 2010b Experimental study of mixed convection heat transfer in a vertical duct filled with metallic porous structures. *Int. J. Therm. Sci.* **49**, 340–348. [8.4.3]
- Vigneswaran, N. V., Ray, S. N. and Soundalgekar, M. V. 2001 Oscillating plate temperature effects on mixed convection flow past a semi-infinite vertical porous plate. *Defence Sci. J.* **51**, 415–418. [8.1.1]
- Vigo, T. L. and Bruno, J. S., 1987 Temperature-adaptable textiles containing durably bound polyethylene glycols. *Textile Res. J.* **57**, 427–429. [10.5]
- Viljoen, H. J., Gatica, J. E. and Hlavacek, V. 1990 Bifurcation analysis of chemically driven convection. *Chem. Engng. Sci.* **45**, 503–517. [6.19.2]
- Villemure, C., Gosselin, L. and Gendion, G. 2008 Minimizing hot spot temperature of porous stackings in natural convection. *Int. J. Heat Mass Transfer* **51**, 4025–4037. [7.3.7]
- Vincourt, M. C. 1989a Competition between two directions of convective rolls in a horizontal porous layer, non-uniformly heated. *Mechanics* **16**, 19–24. [6.15.1]
- Vincourt, M. C. 1989b Influence of a heterogeneity on the selection of convective patterns in a porous layer. *Int. J. Engng. Sci.* **27**, 377–392. [6.15.1]
- Virtol, L., Carbonell, M., Castilla, R. and Gamez-Montero, P. J. 2009 Heating of saturated porous media in practice: Several causes of local thermal non-equilibrium. *Int. J. Heat Mass Transfer* **52**, 5412–5422. [2.2.3]
- Vishnampet Ramanathan, Narasimhan, A. and Babu, V. 2011 High Rayleigh number natural convection inside 2D porous enclosures using the lattice Boltzmann method. *ASME J. Heat Transfer* **133**, #062501. [2.6]
- Vishnuvardhanarao, E. and Das, M. K. 2008 Laminar mixed convection in a parallel two-sided lid-driven differentially heated square cavity filled with a fluid-saturated porous medium. *Numer. Heat Transfer A* **53**, 88–110. [8.4.3]
- Vishnuvardhanarao, E. and Das, M. K. 2009 Mixed convection in a buoyancy-assisted two-sided lid-driven cavity filled with a porous medium. *Int. J. Numer. Meth. Heat Fluid Flow* **19**, 329–351. [8.4.3]
- Vishnuvardhanarao, E. and Das, M. K. 2010 Buoyancy opposed mixed convection in a two-sided lid-driven differentially heated square cavity filled with a porous medium. *J. Porous Media* **13**, 1059–1072. [8.4.3]
- Viskanta, R. 2005 Combustion and heat transfer in inert porous media. *Handbook of Porous Media* (ed. K. Vafai), 2nd ed., Taylor and Francis, New York, pp. 607–644. [3.3]
- Viskanta, R. 2009 Overview of radiative transfer in cellular porous materials. HT2009: Proc ASME Summer Heat Transfer Conf. 2009, Vol. 1. pp.457–565. [2.2.5,6.27]
- Visser, C. J., Malan, A. G. and Meyer, J. P. 2008a An artificial compressibility algorithm for modelling natural convection in saturated packed pebble beds. *Int. J. Numer. Meth. Engng.* **75**, 1214–123. [2.6]
- Visser, C. J., Malan, A. G. and Meyer, J. P. 2008b An artificial compressibility method for buoyancy-driven flow in heterogeneous saturated packed beds: A homogeneous approach. *Int. J. Numer. Meth. Heat Fluid Flow* **18**, 900–918. [2.6]
- Vitanov, N. K. 2000 Upper bounds on the heat transport in a porous layer. *Physica D* **136**, 322–339. [6.3]
- Voon, M. J. , Ngo, C. C. and Lai, F. C. 2006 Application of lumped-system analysis to layered porous cavities heated from below. *J. Thermophys. Heat Transfer* **20**, 925–930. [6.13.2]
- Vorontsov, S.S., Gorin, A. V., Nakoyakov, V. Ye., Khoruzhenko, A.G. and Chupin, V.M. 1991 Natural convection in a Hele-Shaw cell. *Int. J. Heat Mass Transfer* **34**, 703–709. [2.5]

- Voss, C. I., Simmons, C. T. and Robinson, N. I. 2010 Three-dimensional benchmark for variable-density flow and transport simulation: matching semi-analytic stability modes for steady unstable convection in an inclined porous box. *Hydrogeology J.* **18**, 5–23. [11.8]
- Vynnycky, M. and Kimura, S. 1994 Conjugate free convection due to a vertical plate in a porous medium. *Int. J. Heat Mass Transfer* **37**, 229–236. [5.1.5]
- Vynnycky, M. and Kimura, S. 1995 Transient conjugate free convection due to a vertical plate in a porous medium. *Int. J. Heat Mass Transfer* **38**, 219–231. [5.1.5]
- Vynnycky, M. and Pop, I. 1997 Mixed convection due to a finite horizontal flat plate embedded in a porous medium. *Journal Fluid Mech.* **351**, 359–378. [8.1.2]
- Waheed, M. 2009 Heatfunction formulation of thermal convection in rectangular enclosures filled with porous media. *Numer. Heat Transfer A* **55**, 185–204. [7.1.7]
- Wahlgren, P. 2007 Overview and literature survey of natural and forced convection in attic insulation. *J. Building Phys.* **30**, 351–370. [7.3.6]
- Waite, M. W. and Amin, M. R. 1999 Numerical investigation of two-phase fluid flow and heat transfer in porous media heated from the side. *Numer. Heat Transfer A* **35**, 271–290. [11.9.3]
- Wakao, N. and Kaguei, S. 1982 Heat and Mass Transfer in Packed Beds, Gordon and Breach, New York. [2.2.3, 4]
- Wakao, N., Kaguei, S. and Funazkri, T. 1979 Effect of fluid dispersion coefficients on particle-to-fluid heat transfer coefficients in packed beds. *Chem. Engng. Sci.* **34**, 325–336. [2.2.3]
- Wakao, N., Tanaka, K. and Nagai, H. 1976 Measurement of particle-to-gas mass transfer coefficients from chromatographic adsorption experiments. *Chem. Engng. Sci.* **31**, 1109–1113. [2.2.3]
- Walker, K. L. and Homsy, G. M. 1977 A note on convective instabilities in Boussinesq fluids and porous media. *ASME J. Heat Transfer* **99**, 338–339. [6.6]
- Walker, K. L. and Homsy, G. M. 1978 Convection in a porous cavity. *J. Fluid Mech.* **87**, 449–474. [7.1.3]
- Wang, B. X. and Du, J. H. 1993 Forced convection heat transfer in a vertical annulus filled with porous media. *Int. J. Heat Mass Transfer* **36**, 4207–4213. [4.9]
- Wang, B. X. and Zhang, X. 1990 Natural convection in liquid-saturated porous media between concentric inclined cylinders. *Int. J. Heat Mass Transfer* **33**, 827–833. [7.8]
- Wang, C. and Tu, C. 1989 Boundary-layer flow and heat transfer of non-Newtonian fluids in porous media. *Int. J. Heat Fluid Flow* **10**, 160–165. [4.16.3]
- Wang, C. Y. 1994 Thermal convective instability of a horizontal saturated porous layer with a segment of inhomogeneity. *Appl. Sci. Res.* **52**, 147–160. [6.13.4]
- Wang, C. Y. 1997 Onset of natural convection in a sector-shaped box containing a fluid-saturated porous medium. *Physics Fluids* **9**, 3570–3571. [6.15.1]
- Wang, C. Y. 1998a Modeling multiphase flow and transport in porous media. *Transport Phenomena in Porous Media* (eds. D. B. Ingham and I. Pop). Elsevier, Oxford, pp. 383–410. [10.3.1]
- Wang, C. Y. 1998b Onset of natural convection in a fluid-saturated porous medium inside a cylindrical enclosure bottom heated by constant flux. *Int. Comm. Heat Mass Transfer* **25**, 593–598. [6.16.1]
- Wang, C. Y. 1999a Onset of convection in a fluid saturated porous layer overlying a solid layer which is heated by a constant flux. *ASME J. Heat Transfer* **121**, 1094–1097. [6.19.1]
- Wang, C. Y. 1999b Onset of convection in a fluid-saturated rectangular box, bottom heated by constant flux. *Phys. Fluids* **11**, 1673–1675. [6.15.1]
- Wang, C. Y. 1999c Thermo-convective stability of a fluid-saturated porous medium inside a cylindrical enclosure: Permeable top constant flux heating. *Mech. Res. Commun.* **26**, 603–608. [6.16.1]
- Wang, C. Y. 2002 Convective stability in a rectangular box of fluid-saturated porous medium with constant pressure top and constant flux bottom heating. *Transport Porous Media* **46**, 37–42. [6.15.1]
- Wang, C. Y. 2008 Analytical solution for forced convection in a semi-circular channel filled with a porous medium. *Transp. Porous Media* **73**, 369–378. [4.16.5]

- Wang, C. Y. 2009 Analytical solution for free convection in an open vertical rectangular duct filled with a porous medium. *J. Porous Media* **12**, 1113–1120. [7.3.7]
- Wang, C. Y. 2010a Analytical solution for forced convection in a sector duct filled with a porous medium. *ASME J. Heat Transfer* **132**, #084502. [4.16.5]
- Wang, C. Y. 2010b Flow through super-elliptic ducts filled with a Darcy-Brinkman medium. *Transp. Porous Media* **81**, 207–217. [4.16.5]
- Wang, C. Y. 2011 Forced convection in a lens-shaped duct filled with a porous medium. *J. Porous Media* **14**, 743–749. [4.5]
- Wang, C. Y. 2012 Optimum natural convection in a porous medium between a vertical polygonal duct and a heated core. *ASME J. Heat Transfer* **134**, 084501. [7.3.7]
- Wang, C. Y. and Beckermann, C. 1993 A two-phase model of liquid-gas flow and heat transfer in capillary porous media.— II. Application to pressure-driven boiling flow adjacent to a vertical heated plate. *Int. J. Heat Mass Transfer* **36**, 2759–2768. [10.3.1]
- Wang, C. Y. and Beckermann, C. 1995 Boundary layer analysis of buoyancy driven two-phase flow in capillary porous media. *ASME J. Heat Transfer* **117**, 1082–1087. [10.3.1, 10.4]
- Wang, C. Y. and Cheng, P. 1996 A multiphase mixture model for multiphase, multicomponent transport in capillary porous media.— I. Model development. *Int. J. Heat Mass Transfer* **39**, 3607–3618. [3.5.5]
- Wang, C. Y. and Cheng, P. 1997 Multiphase flow and heat transfer in porous media. *Adv. Heat Transfer* **30**, 93–196. [3.6]
- Wang, C. Y. and Cheng, P. 1998 Multidimensional modeling of steam injection into porous media. *ASME J. Heat Transfer* **120**, 286–290. [3.6]
- Wang, C. Y., Beckermann, C. and Fan, C. 1994a Transient natural convection and boiling in a porous layer heated from below. *Heat Transfer 1994, Inst. Chem. Engrs, Rugby*, vol 5, pp. 411–416. [10.3.1]
- Wang, C. Y., Beckermann, C. and Fan, C. 1994b Numerical study of boiling and natural convection in capillary porous media using the two-phase mixture model. *Numer. Heat Transfer A* **26**, 375–398. [10.3.1]
- Wang, C. Y., Wu, C. Z., Tu, C. J. and Fukusako, S. 1990a Freezing around a vertical cylinder immersed in porous media incorporating the natural convection effect. *Wärme-Stoffübertrag.* **26**, 7–15. [10.2.1.2]
- Wang, C., Liao, S. J. and Zhu, J. M. 2003a An explicit solution for the combined heat and mass transfer by natural convection from a vertical wall in a non-Darcy porous medium. *Int. J. Heat Mass Transfer* **46**, 4813–4822. [9.2.1]
- Wang, C., Liao, S. J. and Zhu, J. M. 2003b An explicit analytic solution for non-Darcy natural convection over horizontal plate with surface mass and thermal dispersion effects. *Acta Mech.* **165**, 139–150. [9.2.1]
- Wang, C., Tu, C. and Zhang, X. 1990b Mixed convection of non-newtonian fluids from a vertical plate embedded in a porous medium. *Acta Mech. Sinica* **6**, 214–220. [8.1.1]
- Wang, C., Zhu, J. M., Liao, S. J. and Pop, I. 2003c On the explicit analytic solution of Cheng-Chang equation. *Int. J. Heat Mass Transfer* **46**, 1855–1860. [5.2]
- Wang, G., Wang, Q. W., Zeng, M. and Ozoe, H. 2008a Natural convection heat transfer in an inclined porous cavity under time-periodic boundary conditions with positive/negative inclined angles. *J. Porous Media* **11**, 541–555. [7.8]
- Wang, G., Wang, Q. W., Zeng, M. and Ozoe, H. 2008b Numerical study of natural convection heat transfer in an inclined porous cavity with time-periodic boundary conditions. *Transp. Porous Media* **74**, 293–309. [7.8]
- Wang, H. and Takle, E. 1995 Boundary-layer flow and turbulence near porous obstacles. *Boundary-Layer Meteorol.* **74**, 73–88. [1.8]
- Wang, K. M., Lorente, S. and Bejan, A. 2006 Vascularized networks with two optimized channel sizes. *J. Phys. D: Appl. Phys.* **39**, 3086–3096. [4.19]
- Wang, K. M., Lorente, S. and Bejan A. 2009b Vascular materials cooled with grids and radial channels. *Int. J. Heat Mass Transfer* **52**, 1230–1239. [4.19]

- Wang, K. M., Lorente, S. and Bejan, A. 2007 Vascularization with grids of channels: multiple scales, loops and body shapes. *J. Phys. D: Appl. Phys.* **40**, 4740–4749. [4.19]
- Wang, K. M., Lorente, S. and Bejan, A. 2009a The transient response of vascular composites cooled with grids and radial channels. *Int. J. Heat Mass Transfer* **52**, 4175–4183. [4.19]
- Wang, K. M., Lorente, S. and Bejan, A. 2010 Vascular structures for volumetric cooling and mechanical strength. *J. Applied Phys.* **107**, # 044901. [4.19]
- Wang, L. Q. and Fan, J. 2011 Modeling bioheat transfer at macroscale. *ASME J. Heat Transfer* **133**, #011010. [2.6]
- Wang, L., Xu, M. and Wei, X. 2008d Dual-phase-lagging and porous-medium heat conduction processes. In P. Vadasz (ed.) *Emerging Topics in Heat and Mass Transfer in Porous Media*, Springer, New York, pp.1–37. [2.2.1]
- Wang, M. and Bejan, A. 1987 Heat transfer correlation for Bénard convection in a fluid saturated porous layer. *Int. Comm. Heat Mass Transfer* **14**, 617–626. [6.9.2]
- Wang, M. and Georgiadis, J. G. 1996 Conjugate forced convection in crossflow over a cylinder array with volumetric heating. *Int. J. Heat Mass Transfer* **39**, 1351–1361. [4.16.5]
- Wang, M., He, J., Yu, J. and Pan, N. 2007a Lattice Boltzmann modeling of the effective thermal conductivity for fibrous materials. *Int. J. Therm. Sci.* **46**, 848–855. [2.6]
- Wang, M., Kassoy, D. R. and Weidman, P. D. 1987 Onset of convection in a vertical slab of saturated porous media between two impermeable conducting blocks. *Int. J. Heat Mass Transfer* **30**, 1331–1341. [6.15.2]
- Wang, Q. W., Yang, J., Zeng, M., and Wang, G. 2010 Three-dimensional numerical study of natural convection in an inclined porous cavity with time sinusoidal oscillating boundary conditions. *Int. J. Heat Fluid Flow* **31**, 70–82. [7.8]
- Wang, Q. W., Zeng, M., Huang, Z. P., Wang, G. and Ozoe, H. 2007b Numerical investigation of natural convection in an inclined enclosure filled with a porous medium under a magnetic field. *Int. J. Heat Mass Transfer* **50**, 3684–3689. [7.8]
- Wang, S. C., Chen, C. K., Yang, Y. T. and Yang, Y. T. 2002 Natural convection of non-Newtonian fluids through permeable axisymmetric and two-dimensional bodies in a porous medium. *Int. J. Heat Mass Transfer* **45**, 393–408. [5.9]
- Wang, S. C., Yang, Y. T. and Chen, C. K. 2003d Effect of uniform suction on laminar filmwise condensation on a finite-size horizontal flat surface in a porous medium. *Int. J. Heat Mass Transfer* **46**, 4003–4011. [10.4]
- Wang, S. W. and Tan, W. C. 2008c Stability analysis of double-diffusive convection of Maxwell fluid in a porous medium heated from below. *Phys. Lett. A* **372**, 3046–3050. [9.1.6.4]
- Wang, S. W. and Tan, W. C. 2009 The onset of Darcy-Brinkman thermosolutal convection in a horizontal porous layer. *Phys. Lett. A* **373**, 776–780. [9.1.6.4]
- Wang, S. W. and Tan, W. C. 2011 Stability analysis of Soret-driven double-diffusive convection of Maxwell fluid in a porous medium. *Int. J. Heat Fluid Flow* **32**, 88–94. [9.1.6.4]
- Wang, W. and Sangani, A. S. 1997 Nusselt number for flow perpendicular to arrays of cylinders in the limit of small Reynolds and large Pécelt numbers. *Phys. Fluids* **9**, 1529–1539. [4.16.5]
- Wang, X., Thauvin, F. and Mohanty, K. K. 1999 Non-Darcy flow through anisotropic porous media. *Chem. Engng. Sci.* **54**, 1859–1869. [1.5.2]
- Ward, J. C. 1964 Turbulent flow in porous media. *ASCE J. Hydraul. Div.* **90** (HY5), 1–12. [1.5.2, 10.1.6]
- Ward, J. D., Simmons, C. T. and Dillon, P. J. 2008 Variable-density modelling of multiple-cycle aquifer storage and recovery (ASR): Importance of anisotropy and layered heterogeneity in brackish aquifers. *J. Hydrology* **356**, 93–105. [11.8]
- Weaver, J. A. and Viskanta, R. 1986 Freezing of liquid saturated porous media. *ASME J. Heat Transfer* **108**, 654–659. [10.2.2]
- Webb, S. W., Francis, N. D., Dunn, S. D., Itamura, M. T. and James, D. L. 2003 Thermally induced natural convection effects in Yucca mountain drifts. *J. Contam. Hydrol.* **62**, 713–730. [11.8]
- Weber, J. E. 1974 Convection in a porous medium with horizontal and vertical temperature gradients. *Int. J. Heat Mass Transfer* **17**, 241–248. [7.9]

- Weber, J. E. 1975a Thermal convection in a tilted porous layer. *Int. J. Heat Mass Transfer* **18**, 474–475. [7.8]
- Weber, J. E. 1975b The boundary-layer regime for convection in a vertical porous layer. *Int. J. Heat Mass Transfer* **18**, 569–573. [7.1.2, 7.1.3, 7.2, 7.6.1, 10.1.2]
- Weber, M. and Kimmich, R. 2002 Rayleigh–Bénard percolation transition of thermal convection in porous media: Computational fluid dynamics, NMR velocity mapping, NMR temperature mapping. *Phys. Rev. E* **66**, article no. 056301. [6.9.1]
- Weber, M., Klemm, A. and Kimmich, R. 2001 Rayleigh–Bénard percolation transition study of thermal convection in porous media: Numerical simulation and NMR experiments. *Phys. Rev. Lett.* **86**, 4302–4305. [6.9.1]
- Wei, Q. 2004 Bounds on convective heat transfer in a rotating porous layer. *Mech. Res. Commun.* **31**, 269–276. [6.22]
- Wei, Q. 2007 Bounds on natural convective heat transfer in a porous layer with fixed heat flux. *Int. Comm. Heat Mass Transfer* **34**, 456–463. [6.3]
- Weidman, P. D. and Amberg, M. F. 1996 Similarity solutions for steady laminar convection along heated plates with variable oblique suction: Newtonian and Darcian fluid flow. *Quart. J. Mech. Appl. Math.* **49**, 373–403. [8.1.1]
- Weidman, P. D. and Kassoy, D. R. 1986 Influence of side wall heat transfer on convection in a confined saturated porous medium. *Phys. Fluids* **29**, 349–355. [6.15.2]
- Weidman, P. D. and Medina, A. 2008 Porous media convection between vertical walls: Continuum of solutions from capped to open ends. *Acta mech.* **199**, 206–216. [7.3.7]
- Weinert, A. and Lage, J. L. 1994 Porous aluminum-alloy based cooling devices for electronics. SMU-MED-CPMA Inter. Rep. 1.01/94, Southern Methodist University, Dallas, TX. [1.5.3]
- Weinitschke, H. J., Nandakumar, K. and Sankar, S. R. 1990 A bifurcation study of convective heat transfer in porous media. *Phys. Fluids A* **2**, 912–921. [6.17]
- Weir, G. J. 1991 Geometric properties of two phase flow in geothermal reservoirs. *Transport in Porous Media* **6**, 501–517. [11.9.1]
- Weir, G. J. 1994a The relative importance of convective and conductive effects in two-phase geothermal fields. *Transport in Porous Media* **16**, 289–295. [11.9.1]
- Weir, G. J. 1994b Nonreacting chemical transport in two-phase reservoirs — factoring diffusive and wave properties. *Transport in Porous Media* **17**, 201–220. [11.9.1]
- Weisman, C., Le Quéré, P. and Firdauss, M. 1999 On the closed form solution of natural convection in a cavity partially filled with a porous medium. *C. R. Acad. Sci. Paris, IIB*, **327**, 235–240. [7.7]
- Weiss, D. W., Stickler, L. A. and Stewart, W. E. 1991 The effect of water density extremum on heat transfer within a cylinder containing a heat-generating porous medium. *Int. Comm. Heat Mass Transfer*, **18**, 259–271. [6.17]
- Wells, A. J., Wettlaufer, J. S. and Orszag, S. A. 2010 Maximal potential energy transport: A variational principle for solidification problems. *Phys. Rev. Lett.* **105**, #254502. [10.2.3]
- Wen, B. L., Dianati, N., Lunasin, E., Chini, G. P. and Doering, C. R. 2012 New upper bounds and reduced dynamical modeling for Rayleigh–Benard convection in a fluid saturated porous layer. *Comm. Nonlinear Sci. Numer. Simul.* **17**, 2191–2199. [6.8]
- Wessel-Berg, D. 2009 On a linear stability problem related to underground CO<sub>2</sub> storage. *SIAM J. Appl. Math.* **70**, 1219–1238. [11.11]
- Wettlaufer, J. S., Worster, M. G. and Huppert, H. E. 1997 Natural convection during solidification of an alloy from above with application to the evolution of sea ice. *J. Fluid Mech.* **344**, 291–316. [10.2.3]
- Whitaker, S. 1986 Flow in porous media I: A theoretical derivation of Darcy's law. *Transport in Porous Media* **1**, 3–25. [1.4.3]
- Whitaker, S. 1996 The Forchheimer equation: a theoretical development. *Transport in Porous Media* **25**, 27–61. [1.5.2]
- Whitaker, S. 1999 The Method of Volume Averaging. Springer, New York. [1.1, 3.5]

- White, S. M. and Tien, C. L. 1987 Analysis of laminar film condensation in a porous medium. *Proceedings 1987 ASME JSME Thermal Engineering Joint Conference*, ASME, New York, vol. 2, pp. 401–406. [10.4]
- Wilcock, W. S. D. 1998 Cellular convection models of mid-ocean ridge hydrothermal circulation and the temperatures of black smoker fluids. *J. Geophys. Res.* **103**, 2585–2596. [11.8]
- Wilkes, K. F. 1995 Onset of natural convection in a horizontal porous medium with mixed thermal boundary conditions. *ASME J. Heat Transfer* **117**, 543–547. [6.2]
- Wilson, A. and Ruppel, C. 2007 Salt tectonics and shallow subseafloor fluid convection: models of coupled fluid-heat-salt transport. *Geofluids* **7**, 377–386. [11.8]
- Wong, J. C. and Xie, J. L. 2011 Inverse determination of a heat source from natural convection in a porous cavity. *Comput. Fluids* **52**, 1–14. [7.11]
- Wong, K. C. and Saeid, N. H. 2009a Jet impingement cooling of a finite thickness solid layer conjugated with porous medium. Numerical study of mixed convection on jet impingement cooling in a horizontal porous layer using Brinkman-extended Darcy model. *Int. Comm. Heat Mass Transfer* **36**, 45–50. [8.4.2]
- Wong, K. C. and Saeid, N. H. 2009b Numerical study of mixed convection on jet impingement cooling in an open cavity filled with a porous medium. *Int. Comm. Heat Mass Transfer* **36**, 155–160. [8.4.2]
- Wong, K. C. and Saeid, N. H. 2009c Numerical study of mixed convection on jet impingement cooling in a horizontal porous layer using Brinkman-extended Darcy model. *Int. J. Therm. Sci.* **48**, 96–104. [8.4.2]
- Wong, K. C. and Saeid, N. H. 2009d Numerical study of mixed convection on jet impingement cooling in a horizontal porous layer under local thermal non-equilibrium conditions. *Int. J. Therm. Sci.* **48**, 860–870. [8.4.2]
- Wong, K. C. and Saeid, N. H. 2009e Numerical study of non-Darcian effects on jet impingement cooling in a horizontal porous layer in the mixed convection regime. *Int. Comm. Heat Mass Transfer* **36**, 45–50. [8.4.2]
- Wong, K. C. and Saeid, N. H. 2009f Unsteady mixed convection of a confined jet in a fluid-superposed high porosity medium. *Numer. Heat Transfer A* **56**, 827–845. [8.4.2]
- Wong, K. C., Saeid, N. H. and Tan, C. S. 2009 Visualization of mixed convective rolls of a slot jet in a fluid-superposed metallic porous foam heated from below. *Numer. Heat Transfer A* **56**, 20–41. [8.4.2]
- Wong, W. S., Rees, D. A. S. and Pop, I. 2004 Forced convection past a heated cylinder in a porous medium using a nonequilibrium model; finite Péclet number effects. *Int. J. Thermal Sci.* **43**, 213–220. [4.10]
- Wood, B. D., Radakovich, K. and Golfier, F. 2007 Effective reaction at a fluid-solid interface: Applications to biotransformations in porous media. *Adv. Water Resor.* **30**, 1630–1647. [2.6]
- Wood, J. R. and Hewett, T. A. 1982 Fluid convection and mass transfer in porous limestone: a theoretical model. *Geochim. Cosmochim. Acta* **46**, 1707–1713. [11.12.2]
- Wooding, R. A. 1957 Steady state free thermal convection of liquid in a saturated permeable medium. *J. Fluid Mech.* **2**, 273–285. [1.5.1]
- Wooding, R. A. 1959 The stability of a viscous liquid in a vertical tube containing porous material. *Proc. Roy. Soc. London Ser. A* **252**, 120–134. [6.16.1, 11.3].
- Wooding, R. A. 1960 Rayleigh instability of a thermal boundary layer in flow through a porous medium. *J. Fluid Mech.* **9**, 183–19. [8.1.1]
- Wooding, R. A. 1963 Convection in a saturated porous medium at large Reynolds number or Péclet number. *J. Fluid Mech.* **15**, 527–544. [5.10.1.1, 5.11.1]
- Wooding, R. A. 1978 Large-scale geothermal field parameters and convection theory. *N. Z. J. Sci.* **27**, 219–228. [6.12, 6.13.3]
- Wooding, R. A. 1985 Convective plumes in saturated porous media. *Convective Flows in Porous Media* (eds. R. A. Wooding and I. White) Dept. Sci. Indust. Res., Wellington, N. Z., pp. 167–178. [5.11.1]

- Wooding, R. A. 2007 Variable-density saturated flow with modified Darcy's law: The salt lake problem and circulation. *Water Resources Res.* **43**, W02429. [1.3, 9.1.6.4]
- Wooding, R. A., Tyler, S. W. and White, I. 1997a Convection in groundwater below an evaporating salt lake: 1. Onset of instability. *Water Resources Res.* **33**, 11999–1217. [6.10, 9.1.6.4]
- Wooding, R. A., Tyler, S. W., White, I. and Anderson, P. A. 1997b Convection in groundwater below an evaporating salt lake: 2. Evolution of fingers or plumes. *Water Resources Res.* **33**, 1219–1228. [6.10, 9.1.6.4]
- Woods, A. W. 1999 Liquid and vapor flow in superheated rock. *Ann. Rev. Fluid Mech.* **31**, 171–199. [11.9.3]
- Worster, M. G. 1991 Natural convection in a mushy layer. *J. Fluid Mech.* **224**, 335–359. [10.2.3]
- Worster, M. G. 1992 Instabilities of the liquid and mushy regions during solidification of alloys. *J. Fluid Mech.* **237**, 649–669. [10.2.3]
- Worster, M. G. 1997 Convection in mushy layers. *Annu. Rev. Fluid Mech.* **29**, 91–122. [10.2.3]
- Worster, M. G. 2000 Solidification of fluids. Perspectives in Fluid Dynamics (eds. G. K. Batchelor, H. K. Moffat and M. G. Worster), Cambridge University press, Cambridge, UK, pp. 393–446. [10.2.3]
- Worster, M. G. and Kerr, R. C. 1994 The transient behavior of alloys solidified from below prior to the formation of chimneys. *J. Fluid Mech.* **269**, 23–44. [10.2.3]
- Wright, S. D., Ingham, D. B. and Pop, I. 1996 On natural convection from a vertical plate with a prescribed surface heat flux in porous media. *Transport in Porous Media* **22**, 181–193. [5.1.1]
- Wu J. and Yu, B. 2007 A fractal resistance model for flow through porous media. *Int. J. Heat Mass Transfer* **50**, 3925–3932. [1.4.3]
- Wu, C. C. and Hwang, G. J. 1998 Flow and heat transfer characteristics inside packed and fluidized beds. *ASME J. Heat Transfer* **120**, 667–673. [4.6.5]
- Wu, R. S., Cheng, K. C. and Craggs, A. 1979 Convective instabilities in porous media with maximum density and throughflow effects by finite-difference and finite-element methods. *Numer. Heat Transfer* **2**, 303–318. [6.10.2]
- Xie, Y. Q., Simmons, C. T., Werner, A. D. and Diersch, H. J. G. 2012 Prediction and uncertainty of free convection phenomena in porous media. *Water Resour. Res.* **48**, W02535. [9.1.3]
- Xiong, M. and Kuznetsov, A. V. 2000 Forced convection in a Couette flow in a composite duct: An analysis of thermal dispersion and non-Darcian effects. *J. Porous Media* **3**, 245–255. [4.11]
- Xu, H. 2004 An explicit analytic solution for free convection about a vertical plate embedded in a porous medium by means of homotopy analysis method. *Appl. Math. Comput.* **158**, 433–443. [5.1.1]
- Xu, H. J., Qu, Z. G. and Tao, W. Q. 2011a Analytical solution of forced convective heat transfer in tubes partially filled with metallic foam using the two-equation model. *Int. J. Heat Mass Transfer* **54**, 3846–3855. [4.11]
- Xu, H. J., Qu, Z. G. and Tao, W. Q. 2011b Thermal transport analysis in parallel-plate channel filled with open-celled metallic foams. *Int. Comm. Heat Mass Transfer* **38**, 868–873. [4.11]
- Xu, W. and Lowell, R. P. 1998 Oscillatory instability of one-dimensional two-phase hydrothermal flow in heterogeneous porous media. *J. Geophys. Res.* **103**, 20859–20868. [11.9.1]
- Xu, X. F., Chen, S. Y. and Zhang, D. X. 2006 Convective stability analysis of the long-term storage of carbon dioxide in deep saline aquifers. *Adv. Water Resources* **29**, 397–407. [11.11]
- Xu, X. F., Chen, S. Y. and Zhang, D. X. 2007b Comment on the effect of anisotropy on the onset of convection in a porous medium – Reply. *Adv. Water Resources* **30**, 698–699. [6.12]
- Xu, Y. S., Liu, Y. and Huang, G. 2005 Lattice-Boltzmann simulation of momentum and energy transfer in a porous medium. *Mod. Phys Lett. B* **19**, 1531–1534. [2.6]
- Xu, Y. S., Liu, Y., Yang, X. F. and Wu, F. M. 2008 Lattice Boltzmann simulation of convection in a porous medium with temperature jump and velocity boundary conditions. *Commun. Theor. Phys.* **49**, 1319–1322. [2.6]

- Yadav, D., Bhargava, R. and Agrawal, G. S. 2012 Boundary and internal source effects on the onset of Darcy-Brinkman convection in a porous layer saturated by nanofluid. *Int. J. Therm. Sci.* **60**, 244–254. [9.7]
- Yamaguchi, Y., Asako, Y. and Nakamura, H. 1993 Three-dimensional natural convection in a vertical porous layer with a hexagonal core of negligible thickness. *Int. J. Heat Mass Transfer* **36**, 3403–3406. [7.3.7]
- Yamamoto, K. 1974 Natural convection about a heated sphere in a porous medium. *J. Phys. Soc. Japan* **37**, 1164–1166. [5.6.2]
- Yan, B. and Pop, I. 1998 Unsteady forced convection heat transfer about a sphere in a porous medium. In Mathematics of Heat Transfer (G. E. Tupholme and A. S. Wood, eds.) Clarendon Press, Oxford, pp. 337–344. [4.6.4]
- Yan, B., Pop, I. and Ingham, D. B. 1997 A numerical study of unsteady free convection from a sphere in a porous medium. *Int. J. Heat Mass Transfer* **40**, 893–903. [5.6.1]
- Yan, W. W., Liu, Y., Guo, Z. L. and Xu, Y. S. 2006 Lattice Boltzmann simulation on natural convection heat transfer in a two-dimensional cavity filled with heterogeneous porous medium. *Int. J. Modern Phys. C* **17**, 771–783. [2.6]
- Yan, Y. H., Ochterbeck, J. M. and Peng, X. F. 1998 Numerical study of capillary rewetting in porous media. *Heat Transfer 1998, Proc. 11th IHTC*, **4**, 509–514. [3.6]
- Yang, C. H., Rastogi, S. K. and Poulikakos, D. 1993a Freezing of a water-saturated inclined packed bed of beads. *Int. J. Heat Mass Transfer* **36**, 3583–3592. [10.2.1.2]
- Yang, C. H., Rastogi, S. K. and Poulikakos, D. 1993b Solidification of a binary mixture saturating an inclined bed of packed spheres. *Int. J. Heat Fluid Flow* **14**, 268–278. [10.2.3]
- Yang, C., Ando, K. and Nakayama, A. 2011 A local thermal non-equilibrium analysis of fully developed forced convection flow in a tube filled with a porous medium. *Transp. Porous Media* **89**, 237–249. [4.10]
- Yang, C., Nakayama, A. and Liu, W. 2012a Heat transfer performance assessment for forced convection in a tube partially filled with a porous medium. *Int. J. Therm. Sci.* **54**, 98–108. [4.11]
- Yang, D., Zeng, R. and Zhang, D. 2011 Numerical simulation of convective stability of short-term storage of CO<sub>2</sub> in saline aquifers. *Int. J. Greenhouse Gas Control* **5**, 986–994. [11.11]
- Yang, J. H. and Lee, S. L. 1999 Effect of anisotropy on transport phenomena in anisotropic porous media. *Int. J. Heat Mass Transfer* **42**, 2673–2681. [4.16.5]
- Yang, J. W. and Edwards, R. N. 2000 Predicted groundwater circulation in fractured and unfractured anisotropic porous media driven by nuclear fuel waste heat generation. *Canad. J. Earth Sci.* **37**, 1301–1308. [2.6]
- Yang, J., Wang, J., Bu, S. S., Zeng, H., Wang, Q. W. and Nakayama, A. 2012b Experimental analysis of forced convective heat transfer in novel structured packed beds of particles. *Chem. Engng. Sci.* **71**, 126–137. [2.2.3, 4.16.5]
- Yang, J., Wang, Q. W., Zeng, M. and Nakayama, A. 2010a Computational study of forced convection heat transfer in structured packed beds with spherical or ellipsoidal particles. *Chem. Engng. Sci.* **65**, 726–738. [4.16.5]
- Yang, J., Zeng, M., Wang, Q. W., and Nakayama, A. 2010b Forced convection heat transfer enhancement by porous pin fins in rectangular channels. *ASME J. Heat Transfer* **132**, 051702. [4.11]
- Yang, K. and Vafai, K. 2010 Analysis of temperature gradient bifurcation in porous media: An exact solution. *Int. J. Heat and Mass Transfer* **53**, 4316–4325. [2.2.3, 4.10]
- Yang, K. and Vafai, K. 2011a Transient aspects of heat flux bifurcation in porous media; A exact solution. *ASME J. Heat Transfer* **133**, #052602. [2.2.3, 4.10]
- Yang, K. and Vafai, K. 2011b Analysis of heat flux bifurcation inside porous media incorporating inertial and dispersion effects: An exact solution. *Int. J. Heat and Mass Transfer* **54**, 5286–5297. [2.2.3, 4.10]
- Yang, K. and Vafai, K. 2011c Restrictions on the validity of the thermal conditions at the porous-fluid interface — An exact solution. *ASME J. Heat Transfer* **133**, #112601. [2.2.3, 4.10]

- Yang, X. and Liu, X. M. 2006 Temperature profiles of local thermal nonequilibrium for thermally developing forced convection in porous medium parallel plate channel. *Appl. Math. Mech. (English ed.)* **27**, 1123–1131. [4.13]
- Yang, Y. T. and Hwang, C. Z. 2003 Calculation of turbulent flow and heat transfer in a porous-baffled channel. *Int. J. Heat Mass Transfer* **46**, 771–780. [1.8]
- Yang, Y. T. and Hwang, M. L. 2008 Numerical simulation of turbulent fluid flow and heat transfer characteristics in a rectangular porous channel with periodically spaced heated blocks. *Numer. Heat Transfer A* **54**, 819–836. [4.11]
- Yang, Y. T. and Wang, S. J. 1996 Free convection heat transfer of non-Newtonian fluids over axisymmetric and two-dimensional bodies of arbitrary shape embedded in a fluid-saturated porous medium. *Int. J. Heat Mass Transfer* **39**, 203–210. [5.9]
- Yang, Z. and Garimella, S. V. 2010 Melting of phase change materials with volume change in metal foams, *ASME J. Heat Transfer* **132**, #062301. [10.1.7]
- Yao, H. and Gu, W. Y. 2007 Convection and diffusion in charged hydrated soft tissues: a mixture theory approach. *Biomech. Model. Mechanobiol.* **6**, 63–72. [2.6]
- Yee, C. K. and Lai, F. C. 2001 Effects of a porous manifold on thermal stratification in a liquid storage tank. *Solar Energy* **71**, 241–254. [8.3.1]
- Yee, S. S. and Kamiuto, K. 2002 Effect of viscous dissipation on forced-convection heat transfer in cylindrical packed beds. *Int. J. Heat Mass Transfer* **45**, 461–464. [4.9]
- Yee, S. S. and Kamiuto, K. 2005 Combined forced-convective and radiative heat transfer in cylindrical packed beds with constant wall temperatures. *J. Porous Media* **8**, 481–492. [4.16.5]
- Yen, Y. C. 1974 Effects of density inversion on free convective heat transfer in porous layer heated from below. *Int. J. Heat Mass Transfer* **17**, 1349–1356. [6.9.1, 6.9.2]
- Yih, K. A. 1997 The effect of transpiration on coupled heat and mass transfer in mixed convection over a vertical plate embedded in a saturated porous medium. *Int. Comm. Heat Mass Transfer* **24**, 265–275. [9.6.1]
- Yih, K. A. 1997 The effect of uniform lateral mass flux on free convection about a vertical cone embedded in a saturated porous medium. *Int. Comm. Heat Mass Transfer* **24**, 1195–1205. [5.8]
- Yih, K. A. 1998a Heat source/sink effect on MHD mixed convection in stagnation flow on a vertical permeable plate in porous media. *Int. Comm. Heat Mass Transfer* **25**, 427–442. [8.1.4]
- Yih, K. A. 1998b Uniform lateral mass flux effect on natural convection on non-Newtonian fluids over a cone in porous media. *Int. Comm. Heat Mass Transfer* **25**, 959–968. [5.8]
- Yih, K. A. 1998c Coupled heat and mass transfer in mixed convection over a wedge with variable wall temperature and convection in porous media: The entire regime. *Int. Comm. Heat Mass Transfer* **25**, 1145–1158. [9.6.1]
- Yih, K. A. 1998d The effect of uniform suction/blowing on heat transfer of magnetohydrodynamic Hiemenz flow through porous media. *Acta Mech.* **130**, 147–158. [4.16.5]
- Yih, K. A. 1998e Blowing/suction effect on non-Darcy forced convection flow about a flat plate with variable wall temperature in porous media. *Acta Mech.* **131**, 255–265. [4.16.5]
- Yih, K. A. 1998f Coupled heat and mass transfer in mixed convection over a vertical flat plate embedded in saturated porous media: PST/PSC or PHF/PMF. *Heat Mass Transfer* **34**, 55–61. [9.6.1]
- Yih, K. A. 1998g Coupled heat and mass transfer in mixed convection about a vertical cylinder in a porous medium: the entire regime. *Mech. Res. Commun.* **25**, 623–630. [9.6.1]
- Yih, K. A. 1999a Uniform transpiration effect on combined heat and mass transfer by natural convection over a cone in saturated porous media: uniform wall temperature, concentration or heat flux. *Int. J. Heat Mass Transfer* **42**, 3533–3537. [19.2.1]
- Yih, K. A. 1999b Uniform transpiration effect of coupled heat and mass transfer, in mixed convection about inclined surfaces in porous media: the entire regime. *Acta Mech.* **132**, 229–240. [9.6.1]
- Yih, K. A. 1999c Coupled heat and mass transfer in mixed convection over a VHF/VMF wedge in porous media – the entire regime. *Acta Mech.* **137**, 1–12. [9.6.1]
- Yih, K. A. 1999d Coupled heat and mass transfer by free convection over a truncated cone in porous media: VWT-VWC or VHF-VMF. *Acta Mech.* **137**, 83–97. [9.2.1]

- Yih, K. A. 1999e Coupled heat and mass transfer in mixed convection over a wedge with variable wall temperature and convection in porous media: The entire regime. *Int. Comm. Heat Mass Transfer* **26**, 259–267. [5.7]
- Yih, K. A. 1999f Coupled heat and mass transfer by natural convection adjacent to a permeable horizontal cylinder in a saturated porous medium. *Int. Comm. Heat Mass Transfer* **26**, 431–440. [9.2.1]
- Yih, K. A. 1999g Mixed convection about a cone in a porous medium — the entire regime. *Int. Comm. Heat Mass Transfer* **26**, 1041–1050. [8.1.4]
- Yih, K. A. 1999h Uniform transpiration effect on coupled heat and mass transfer in mixed convection about a vertical cylinder in porous media: the entire regime. *J. Chinese Soc. Mech. Engrs.* **20**, 81–86. [9.6.1]
- Yih, K. A. 1999i Blowing/suction effect on combined convection in stagnation flow over a vertical plate embedded in a porous medium. *Chinese J. Mech. A.* **15**, 41–45. [8.1.1]
- Yih, K. A. 2000a Viscous and Joule heating effects on non-Darcy MHD natural convection flow over a permeable sphere in porous media with internal heat generation. *Int. Comm. Heat Mass Transfer* **27**, 591–600. [5.6.1]
- Yih, K. A. 2000b Combined heat and mass transfer in mixed convection adjacent to a VWT/VWC or VHF/VMF cone in a porous medium: The entire regime. *J. Porous Media* **3**, 185–191. [9.6.1]
- Yih, K. A. 2001a Radiation effect on mixed convection over an isothermal wedge in porous media: The entire regime. *Heat Transfer Engng.* **22**, 26–32. [8.1.4]
- Yih, K. A. 2001b Radiation effect on mixed convection over an isothermal cone in porous media. *Heat Mass Transfer* **37**, 53–57. [8.1.4]
- Yin, C., Fu, C. and Tan, W. 2012 Onset of thermal convection in a Maxwell fluid-saturated porous medium: The effects of hydrodynamic boundary and constant flux heating conditions. *Transp. Porous Media* **91**, 777–790. [6.23]
- Yiotis, A. G., Tsipanogiannis, I. N., Stubos, A. K. and Yortsos, Y. C. 2007 Coupling between external and internal mass transfer during drying of a porous medium. *Water Resour. Res.* **43**, #W06403. [3.6]
- Yokoyama, Y. and Kulacki, F. A. 1996 Mixed convection in a horizontal duct with a sudden expansion and local duct heating. *ASME HTD.* **331**, 33–41. [8.2.2]
- Yokoyama, Y., Kulacki, F. A. and Mahajan, R. L. 1999 Mixed convection in a horizontal porous duct with a sudden expansion and local heating from below. *ASME J. Heat Transfer* **121**, 653–661. [8.2.1]
- Yoo, H and Viskanta, R. 1992 Effect of anisotropic permeability in the transport process during solidification of a binary mixture. *Int. J. Heat Mass Transfer* **35**, 2335–2346. [10.2.3]
- Yoo, J. S. 2003 Thermal convection in a vertical porous slot with spatially periodic boundary conditions: low Ra flow. *Int. J. Heat Mass Transfer* **46**, 381–384. [7.1.6]
- Yoo, J. S. and Schultz, W. W. 2003 Thermal convection in a horizontal porous layer with spatially periodic boundary temperature temperatures: small Ra flow. *Int. J. Heat Mass Transfer* **46**, 4747–4750. [6.14]
- Yoon, D. Y. and Choi, C. K. 1989 Thermal convection in a saturated porous medium subjected to isothermal heating. *Korean J. Chem. Engng.* **6**, 144–149. [6.11.3]
- Yoon, D. Y., Choi, C. K. and Yoo, J. S. 1992 Analysis of thermal instability in a horizontal, porous layer heated from below. *Int. Chem. Engng.* **32**, 181–191. [6.11.3]
- Yoon, D. Y., Kim, D. S. and Chang, K. C. 2004 The onset of oscillatory convection in a horizontal porous layer saturated with viscoelastic liquid. *Transport Porous Media* **55**, 275–284. [6.23]
- Yoon, D. Y., Kim, D. S. and Choi, C. K. 1998 Convective instability in packed beds with internal heat sources and throughflow. *Korean J. Chem. Engng.* **15**, 341–344. [6.11.2]
- Yoon, D. Y., Kim, M. C. and Choi, C. K. 2003 Oscillatory convection in a horizontal porous layer saturated with a viscoelastic fluid. *Korean J. Chem. Engng.* **20**, 27–31. [6.23]
- Yoshino, M. and Inamura, T. 2003 Lattice Boltzmann simulations for flow and heat/mass transfer problems in a three-dimensional porous structure. *Int. J. Numer. Meth. Fluids* **43**, 183–198. [2.6]

- You, H. I. and Song, J. S. 1999 Heat transfer analysis of non-Darcian flow in local thermal non-equilibrium. *J. Chinese Soc. Mech. Engrs.* **20**, 75–80. [4.10]
- Young, R. 1993a Two-phase brine mixtures in the geothermal context and the polymer flood model. *Transport in Porous Media* **11**, 179–185. [11.9.1]
- Young, R. 1993b Two-phase geothermal flows with conduction and the connection with Buckley-Leverett theory. *Transport in Porous Media* **12**, 261–278. [11.9.1]
- Young, R. and Weir, G. 1994 Constant rate production of geothermal fluid from a two-phase vertical column. I: Theory. *Transport in Porous Media* **14**, 265–286. [11.9.1]
- Young, R. M. 1996a Phase transitions in one-dimensional steady state hydrothermal flows. *J. Geophys. Res.* **101**, 18011–18022. [11.9.2]
- Young, R. M. 1996b A basic model for vapour-dominated geothermal reservoirs. Proceedings of the 18th NZ Geothermal Workshop, University of Auckland, Auckland, New Zealand, 301–304. [11.9.2]
- Young, R. M. 1998a Classification of one-dimensional steady-state two-phase geothermal flows including permeability variations: Part 1. Theory and special cases. *Int. J. Heat Mass Transfer* **41**, 3919–3935. [11.9.2]
- Young, R. M. 1998b Classification of one-dimensional steady-state two-phase geothermal flows including permeability variations: Part 2. The general case. *Int. J. Heat Mass Transfer* **41**, 3937–3948. [11.9.2]
- Young, T. J. and Vafai, K. 1998 Convective flow and heat transfer in a channel containing multiple heated obstacles. *Int. J. Heat Mass Transfer* **41**, 3279–3298. [4.11]
- Young, T. J. and Vafai, K. 1999 Experimental and numerical investigation of forced convective characteristics of arrays of channel mounted obstacles. *ASME J. Heat Transfer* **121**, 34–42. [4.11]
- Younsi, R. 2009 Computational analysis of MHD flow, heat and mass transfer in trapezoidal porous cavity. *Thermal Science* **13**, 13–22. [9.4]
- Younsi, R., Harkati, A. and Kalache, D. 2001 Heat and mass transfer in composite fluid-porous layer: effect of permeability. *Arab J. Sci. Engng.* **26**, 145–155. [9.4]
- Younsi, R., Harkati, A. and Kalache, D. 2002a Numerical simulation of double-diffusive natural convection in a porous cavity: opposing flow. *Arab J. Sci. Engng.* **27**, 181–194. [9.6.2]
- Younsi, R., Harkati, A. and Kalache, D. 2002b Numerical simulation of thermal and concentration natural convection in a porous cavity in the presence of an opposing flow. *Fluid Dyn.* **37**, 854–864. [9.6.2]
- Yu, B. 2004 Discussion: “A numerical study of thermal dispersion in porous media” and “Numerical determination of thermal dispersion coefficients using a periodic porous structure.” *ASME J. Heat Transfer* **126**, 1060–1061. [2.2.4]
- Yu, B. M. and Cheng P. 2002a Fractal models for the effective thermal conductivity of bidispersed porous media. *J. Thermophys. Heat Transfer* **16**, 22–29. [4.16.4]
- Yu, B. M. and Cheng P. 2002b A fractal permeability model for bi-dispersed porous media. *Int. J. Heat Mass Transfer* **45**, 2983–2993. [4.16.4]
- Yu, F., Wei, G. S., Zhang, X. X. and Chen, K. 2006a Two effective thermal conductivity models with porous media with hollow spherical agglomerates. *Int. J. Thermophys.* **27**, 293–303. [2.2.1]
- Yu, P., Lee, T. S., Zeng, Y. and Low, H. T. 2007 A numerical method for flows in porous and homogeneous fluid domains coupled at the interface by a stress jump. *Int. J. Numer. Meth. Fluids* **53**, 1755–1775. [1.6]
- Yu, Q. J., Thompson, B. E. and Straatman, A. G. 2006b A unit cube-based model for heat transfer and fluid flow in porous carbon foam. *ASME J. Heat Transfer* **128**, 352–360. [2.6]
- Yu, W. B., Ya, Y. M., Zhang, X. F., Zhang, S.J. and Xiao, J. Z. 2004 Laboratory investigation on coding effect of coarse rock layer and fine rock layer in permafrost regions. *Cold Regions Sci. Tech.* **38**, 31–42. [4.16.5]
- Yu, W. P., Wang, B. X. and Shi, M. H. 1993 Modelling of heat and mass transfer in unsaturated wet porous medal with consideration of capillary hysteresis. *Int. J. Heat Mass Transfer* **36**, 3671–3676. [3.6]

- Yu, W. S., Lin, H. T. and Lu, C. S. 1991 Universal formulations and comprehensive correlations for non-Darcy natural convection and mixed convection in porous media. *Int. J. Heat Mass Transfer* **34**, 2859–2868. [8.1.1, 8.1.2]
- Yuan, K., Ji, Y. and Chung, J. N. 2008 Feasibility study of cooling enhancement with porous metal inserts. *J. Thermophys. Heat Transfer* **22**, 493–500. [4.11]
- Yücel, A. 1990 Natural convection heat and mass transfer along a vertical cylinder in a porous medium. *Int. J. Heat Mass Transfer* **33**, 2265–2274. [9.4]
- Yücel, A. 1993 Mixed convective heat and mass transfer along a vertical surface in a porous medium. *ASME HTD* **240**, 49–57. [9.6.1]
- Yucel, N. and Guven, R. T. 2007 Forced-convection cooling enhancement of heating elements in a parallel-plates channel using porous inserts. *Numer. Heat Transfer A* **51**, 293–312. [4.11]
- Yucel, N. and Guven, R. T. 2008 Numerical study of heat transfer in a rectangular channel with porous covering obstacles. *Transp. Porous Media* **77**, 41–58. [4.11]
- Zahi, N., Boughamoura, A., Dhahr, H. and Ben Nasrallah, S. 2008 Flow and heat transfer in a cylinder with a porous medium insert along the compression stroke. *J. Porous Media* **11**, 525–540. [4.11]
- Zahmatkesh, I. 2008 On the importance of thermal boundary conditions in heat transfer and entropy generation for natural convection inside a porous enclosure. *Int. J. Therm. Sci.* **47**, 339–346. [7.2]
- Zahrani, M. S. and Kiwan, S. 2009 Mixed convection heat transfer in the annulus between two concentric vertical cylinders using porous layers. *Transp. Porous Media* **76**, 391–40. [8.4.1]
- Zaturska, M. B. and Banks, W. H. H. 1987 On the spatial stability of free-convection flows in a saturated porous medium. *J. Engng. Math.* **21**, 41–46. [5.1.9.9]
- Zebib, A. 1978 Onset of natural convection in a cylinder of water saturated porous media. *Phys. Fluids* **21**, 699–700. [6.16.1]
- Zebib, A. and Kassoy, D. R. 1977 Onset of natural convection in a box of water-saturated porous media with large temperature variation. *Phys. Fluids* **20**, 4–9. [6.7]
- Zebib, A. and Kassoy, D. R. 1978 Three dimensional natural convection motion in a confined porous medium. *Phys. Fluids* **21**, 1–3. [6.15.1]
- Zehforoosh, A. and Hossainpour, S. 2010 Numerical investigation of pressure drop reduction without surrendering heat transfer enhancement in partially porous channel. *Int. J. Therm. Sci.* **49**, 1649–1662. [4.11]
- Zeng, X., Dai, W. and Bejan, A. 2010 Vascular countercurrent network for 3D triple-layered skin structure with radiation heating. *Numer. Heat Transfer A* **75**, 369–391. [4.19]
- Zenkowskaya, S. M. 1992 Action of high-frequency vibration on filtration convection. *J. Appl. Mech. Tech. Phys.* **32**, 83–86. [6.24].
- Zenkowskaya, S. M. and Rogovenko, T. N. 1999 Filtration convection in a high-frequency vibration field. *J. Appl. Mech. Tech. Phys.* **40**, 379–385. [6.24].
- Zhang, B. L. and Zhao, Y. 2000 A numerical method for simulation of forced convection in a composite porous/fluid system. *Int. J. Heat Fluid Flow* **21**, 432–441. [4.11]
- Zhang, H. Y. and Huang, X. Y. 2001 A two-equation analysis of convection in porous media. *Transport Porous Media* **44**, 305–324. [Correction in 46 (2002), 113–115.] [4.10]
- Zhang, H., Lorente, S. and Bejan, A. 2007a Vascularization with trees that alternate with upside-down trees. *J. Appl. Phys.* **101**, #094904. [4.19]
- Zhang, H., Lorente, S. and Bejan, A. 2009a Vascularization with line-to-line trees in counterflow heat exchange. *Int. J. Heat Mass Transfer* **52**, 4327–4342. [4.19]
- Zhang, J., Subotic, M. and Lai, F. C. 2010 Transient and steady natural convection from a heat source embedded in thermally stratified porous layer. *Int. J. Them. Sci.* **49**, 1527–1535. [5.11.1]
- Zhang, K., Liao, X. H. and Schubert, G. 2005a Pore water convection within carbonaceous chondrite parent bodies: Temperature-dependent viscosity and flow structure. *Phys. Fluids* **17**, art. no. 086602. [6.17]

- Zhang, M. Y., Cheng, G. D. and Li, S. Y. 2009b Numerical study of the influence of geometrical parameters on natural convection cooling of the crushed rock revetment. *Sci. China E* **52**, 539–545. [7.3.7]
- Zhang, M. Y., Lai, Y. M., Gao, Z. H. and Yu, W. B. 2006a Influence of boundary conditions on the cooling effect of crushed-rock embankment in permafrost regions of the Qinhai-Tibetan plateau. *Cold Regions Sci. Tech.* **44**, 225–239. [7.3.7]
- Zhang, M. Y., Lai, Y. M., Lin, Z. Q. and Gao, Z. H. 2005b Nonlinear analysis for the cooling effect of Qinhai-Tibetan railway embankment with different structures in permafrost regions. *Cold Regions Sci. Tech.* **42**, 237–249. [7.3.7]
- Zhang, M. Y., Lai, Y. M., Yu, W. B. and Huang, Z. J. 2007b Experimental study of influence of particle size on cooling effect of crushed rock layer under closed and open tops. *Cold Regions Sci. Tech.* **48**, 232–238. [7.3.7]
- Zhang, M. Y., Lai, Y. M., Yu, W. B. and Qi, J. L. 2006b Laboratory investigation of the heat transfer characteristics of a trapezoidal crushed-rock layer under impermeable and permeable boundaries. *Exper. Heat Transfer* **19**, 251–254. [7.3.7]
- Zhang, X. 1993 Natural convection and heat transfer in a vertical cavity filled with an ice-water saturated porous medium. *Int. J. Heat Mass Transfer* **36**, 2881–2890. [10.1.7]
- Zhang, X. and Nguyen, T. H. 1990 Development of convective flow during the melting of ice in a porous medium heated from above. *ASME HTD* **156**, 1–6. [10.1.7]
- Zhang, X. L. and Kawawita, R. 1994 Ice water convection in an inclined rectangular cavity filled with a porous medium. *Wärme-Stoffübertrag.* **30**, 9–16. [7.8]
- Zhang, X. L. and Nguyen, T. H. 1994 Numerical study of convection heat transfer during the melting of ice in a porous layer. *Numer. Heat Transfer A* **25**, 559–574. [10.1.7]
- Zhang, X. L. and Nguyen, T. H. 1999 Solidification of a superheated fluid in a porous medium: effects of convection. *Int. J. Numer. Meth. Heat Fluid Flow* **9**, 72–91. [10.2.2]
- Zhang, X. L., Nguyen, T. H. and Kawawita, R. 1997 Effects of anisotropy in permeability on two-phase flow and heat transfer in porous cavity. *Heat Mass Transfer* **32**, 167–174. [10.1.7]
- Zhang, X. W. and Liu, W. 2008 New criterion for local thermal equilibrium in porous media. *J. Thermophys. Heat Transfer* **22**, 649–653. [4.10]
- Zhang, X. W., Liu, W. and Liu, Z. C. 2009c Criterion for local thermal equilibrium in forced convection flow through porous media. *J. Porous Media* **12**, 1103–1111. [4.10]
- Zhang, X. Y. and Nepf, H. M. 2011 Exchange flow between open water and floating vegetation. *Exp. Fluid Mech.* **11**, 531–546. [1.6]
- Zhang, X., Hung, N. T. and Kawawita, R. 1993 Convective flow and heat transfer in an anisotropic porous layer with principal axes non-coincident with the gravity vector. *ASME HTD* **264**, 79–86. [6.12]
- Zhang, X., Nguyen, T. H. and Kawawita, R. 1991a Melting of ice in a porous medium heated from below. *Int. J. Heat Mass Transfer* **34**, 389–405. [10.1.7]
- Zhang, Y., Khodadadi, J. M. and Shen, F. 1999 Pseudosteady-state natural convection inside spherical containers partially filled with a porous medium. *Int. J. Heat Mass Transfer* **42**, 2327–2336. [7.7]
- Zhang, Y., Lu, N. and Ross, B. 1994 Convective instability of moist gas in a porous medium. *Int. J. Heat Mass Transfer* **37**, 129–138. [6.7]
- Zhang, Z. and Bejan, A. 1987 The horizontal spreading of thermal and chemical deposits in a porous medium. *Int. J. Heat Mass Transfer* **30**, 2289–2303. [9.2.3]
- Zhang, Z. J., Du, J. H. and Wang, B. X. 1999 Effect of viscous dissipation on forced-convection heat transfer in porous media. *J. Shanghai Jiaotong Univ.* **33**, 979–982. [4.9]
- Zhang, Z. Y., Fu, C. J. and Tan, W. C. 2008 Linear and nonlinear stability analysis of thermal convection for Oldroyd-B fluids in porous media heated from below. *Phys. Fluids* **20**, art. # 084103. [6.23]
- Zhang, Z. Y., Fu, C. J., Tan, W. C. and Wang, C. Y. 2007c Onset of oscillatory convection in a porous cylinder saturated with a viscoelastic fluid. *Phys. Fluids* **19**, art. # 098104. [6.23]

- Zhang, Z., Bejan, A. and Lage, J. L. 1991b Natural convection in a vertical enclosure with internal permeable screen. *ASME J. Heat Transfer* **113**, 377–383. [7.7]
- Zhao, C. B., Hobbs, B. E. and Mühlhaus, H. B. 1998a Finite element modeling of temperature gradient driven rock alteration and mineralization in porous rock masses. *Comput. Meth. Appl. Math.* **165**, 175–187. [11.8]
- Zhao, C. B., Hobbs, B. E. and Mühlhaus, H. B. 1999a Effects of medium thermoelasticity on high Rayleigh number steady-state heat transfer and mineralization in deformable fluid-saturated porous media heated from below. *Comput. Meth. Appl. Mech. Engng.* **173**, 41–54. [11.8]
- Zhao, C. B., Hobbs, B. E. and Mühlhaus, H. B. 1999b Theoretical and numerical analyses of convective instability in porous media with upward throughflow. *Int. J. Numer. Anal. Methods Geomech.* **23**, 629–646. [6.10.2]
- Zhao, C. B., Hobbs, B. E. and Ord, A. 2008a Convective and Advective Heat Transfer in Geological Systems, Springer, Berlin. [11.8]
- Zhao, C. B., Hobbs, B. E., Ord, A., Mühlhaus, H. B. and Lin, G. 2003a Effect of material anisotropy on the onset of convective flow in three-dimensional fluid-saturated faults. *Math. Geology* **35**, 141–154. [11.8]
- Zhao, C. B., Hobbs, B. E., Baxter, K., Mühlhaus, H. B. and Ord, A. 1999c A numerical study of pore-fluid, thermal and mass flow in fluid-saturated porous rock basins. *Engng. Comput.* **16**, 202–214. [11.8]
- Zhao, C. B., Hobbs, B. E., Hornby, P., Ord, A. and Peng, S. L., 2006a Numerical modeling of fluids mixing, heat transfer and non-equilibrium redox chemical reactions in fluid-saturated rocks. *Int. J. Numer. Meth. Engng.* **66**, 1061–1078. [11.8]
- Zhao, C. B., Hobbs, B. E., Mühlhaus, H. B. and Ord, A. 1999d Finite-element analysis of flow problems near geological lenses in hydrodynamic and hydrothermal systems. *Geophys. J. Inter.* **138**, 146–158. [11.8]
- Zhao, C. B., Hobbs, B. E., Mühlhaus, H. B., Ord, A. and Lin, G. 2002 Analysis of steady-state heat transfer through mid-crustal vertical cracks with upward throughflow in hydrothermal systems. *Int. J. Numer. Anal. Meth. Geomech.* **26**, 1477–1491. [11.8]
- Zhao, C. B., Hobbs, B. E., Mühlhaus, H. B., Ord, A. and Lin, G. 2000a Numerical modeling of double diffusion driven reactive flow transport in deformable fluid-saturated porous media with particular consideration of temperature-dependent chemical reaction rates. *Engng. Comput.* **17**, 367–385. [11.8]
- Zhao, C. B., Hobbs, B. E., Mühlhaus, H. B., Ord, A. and Lin, G. 2001a Finite element modeling of three-dimensional convection problems in fluid-saturated porous media heated from below. *Comm. Numer. Methods Engng.* **17**, 101–114. [11.8]
- Zhao, C. B., Hobbs, B. E., Mühlhaus, H. B., Ord, A. and Lin, G. 2003b Convective instability of 3-D fluid-saturated geological fault zones heated from below. *Geophys. J. Int.* **155**, 213–220. [11.8]
- Zhao, C. B., Hobbs, B. E., Ord, A., Kuhn, M., Mulhaus, H. B. and Peng, S. I. 2006b Numerical simulation of double-diffusion driven convective flow and rock alteration in three-dimensional fluid-saturated geological fault zones. *Comput. Meth. Appl. Mech. Engng.* **195**, 2816–2840. [11.8]
- Zhao, C. B., Hobbs, B. E., Ord, A., Lin, G. and Mühlhaus, H. B. 2003c An equivalent algorithm for simulating thermal effects of magma intrusion problems in porous rocks. *Comput. Meth. Appl. Mech. Engng.* **192**, 3397–3408. [11.8]
- Zhao, C. B., Hobbs, B. E., Ord, A., Peng, S. L., Mühlhaus, H. B. and Liu, L. M. 2004a Theoretical investigation of convective instability in inclined and fluid-saturated three-dimensional fault zones. *Tectonophysics* **387**, 47–64. [11.8]
- Zhao, C. B., Hobbs, B. E., Ord, A., Peng, S. L., Mühlhaus, H. B. and Liu, L. M. 2005 Double diffusion-driven convective instability of three-dimensional fluid-saturated geological fault zones heated from below. *Math. Geology* **37**, 373–391. [11.8]
- Zhao, C. B., Hobbs, B. E., Walshe, J. L., Mühlhaus, H. B., and Ord, A. 2001b Finite element modeling of fluid-rock interaction problems in pore-fluid saturated hydrothermal/sedimentary basins. *Comput. Meth. Appl. Mech. Engng.* **190**, 2277–2293. [11.8]

- Zhao, C. B., Mühlhaus, H. B. and Hobbs, B. F. 1997 Finite element analysis of steady state natural convection problems in fluid-saturated porous media heated from below. *Int. J. Numer. Anal. Methods Geomech.* **21**, 863–881. [11.8]
- Zhao, C. B., Peng, S. L., Liu, L. M., Hobbs, B. E. and Ord, A. 2011a Computational simulation of convective flow in the Earth crust under consideration of dynamic crust-mantle interactions. *J. Central South Univ. Tech.* **18**, 2080–2084. [11.8]
- Zhao, C. Y. and Lu, T. J. 2002 Analysis of microchannel heat sinks for electronic cooling. *Int. J. Heat Mass Transfer* **45**, 4857–4869. [4.10]
- Zhao, C. Y., Dai, L. N., Tang, G. H., Qu, Z. G. and Li, Z. Y. 2010a Numerical study of natural convection in porous media (metals) using lattice Boltzmann method. *Int. J. Heat Fluid Flow* **31**, 925–934. [2.6]
- Zhao, C. Y., Kim, T., Lu, T. J. and Hodson, H. P. 2004b Thermal transport in high porosity cellular metal foams. *J. Thermophys. Heat Transfer* **18**, 309–317. [4.9]
- Zhao, C., Mühlhaus, H. B. and Hobbs, B. F. 1998b Effects of geological inhomogeneity on high Rayleigh number steady state heat and mass transfer in fluid-saturated porous media heated from below. *Numer. Heat Transfer A* **33**, 415–431. [11.8]
- Zhao, F. Y., Liu, D. and Tang, G. F. 2007b Free convection from one thermal and solute source in a confined porous medium. *Transp. Porous Media* **70**, 407–452. [9.2.2]
- Zhao, F. Y., Liu, D. and Tang, G. F. 2007a Application issues of the streamline, heatline and massline for conjugate heat and mass transfer. *Int. J. Heat Mass Transfer* **50**, 320–334. [4.17]
- Zhao, F. Y., Liu, D. and Tang, G. F. 2008b Natural convection in a porous enclosure with a partial heating and salting element. *Int. J. Therm. Sci.* **47**, 569–583. [9.1.6.4]
- Zhao, F. Y., Liu, D. and Tang, G. F. 2008c Natural convection in an enclosure with localized heating and salting from below. *Int. J. Heat Mass Transfer* **51**, 2889–2904. [9.1.6.4]
- Zhao, H. and Bau, H. H. 2006 Limitations of linear control of thermal convection in a porous medium. *Phys. Fluids* **18**, #074109. [6.11.3]
- Zhao, J. Z. and Chen, T. S. 2002 Inertia effects on non-parallel thermal instability of natural convection flow over horizontal and inclined plates in porous media. *Int. J. Heat Mass Transfer* **45**, 2265–2276. [5.4]
- Zhao, J. Z. and Chen, T. S. 2003 Non-Darcy effects on non-parallel thermal instability of horizontal natural convection flow. *J. Thermophys. Heat Transfer* **17**, 150–158. [5.4]
- Zhao, K., Xuan, Y. M. and Li, Q. A. 2010b Investigation on the mechanism of convective heat and mass transfer with double diffusive effect inside a complex porous medium using lattice Boltzmann method. *Chinese Sci. Bull.* **55**, 3051–3059. [2.6]
- Zhao, M., Robillard, L. and Prud'homme, M. 1996 Effect of weak rotation on natural convection in a horizontal porous cylinder. *Heat Mass Transfer* **31**, 403–409. [6.17]
- Zhao, P. and Chen, C. F. 2001 Stability analysis of double-diffusive convection in superposed fluid and porous layers using a one-equation model. *Int. J. Heat Mass Transfer* **44**, 4625–4633. [9.4]
- Zhao, S. C., Liu, Q. S., Liu, R., Nguyen-Thi, H. and Billia, B. 2010c Thermal effects on Rayleigh-Marangoni-Bénard instability in a system of superposed fluid and porous layers. *Int. J. Heat Mass Transfer* **53**, 2951–2954. [6.19.3]
- Zhao, S. C., Liu, Q. S., Nguyen-Thi, H. and Billia, B. 2011 Gravity-driven instability in a liquid film overlying an inhomogeneous porous layer. *Chinese Phys. Lett.* **28**, #024702. [6.19.3]
- Zhao, S. C., Liu, R. and Liu, Q. S. 2008e Thermocapillary convection in a homogeneous porous layer. *Chinese Phys. Lett.* **25**, 620–623. [6.19.3]
- Zhao, T. S. 1999 Coupled heat and mass transfer of a stagnation point flow in a heated porous bed with liquid film evaporation. *Int. J. Heat Mass Transfer* **42**, 861–872. [10.3.2]
- Zhao, T. S. and Liao, Q. 2000 On capillary-driven flow and phase-change heat transfer in a porous structure heated by a finned surface: measurements and modeling. *Int. J. Heat Mass Transfer* **43**, 1141–1155. [3.6]
- Zhao, T. S. and Song, Y. J. 2001 Forced convection in a porous medium heated by a permeable wall perpendicular to the flow direction: analyses and measurements. *Int. J. Heat Mass Transfer* **44**, 1031–1037. [4.16.5]

- Zhao, T. S., Cheng, P. and Wang, C. Y. 2000b Buoyancy-induced flows and phase-change heat transfer in a vertical capillary structure with symmetric heating. *Chem. Engng. Sci.* **55**, 2653–2661. [11.9.3]
- Zhao, T. S., Liao, Q. and Cheng, P. 1999e Variations of buoyancy-induced mass flux from single-phase to two-phase flow in a vertical porous tube with constant heat flux. *ASME J. Heat Transfer* **121**, 646–652. [11.9.3]
- Zhekamukhov, M. K. and Zhekamukhova, I. M. 2002 On convective instability of air in the snow cover. *J. Engng. Phys. Thermophys.* **75**, 849–858. [11.1]
- Zheng, W., Robillard, L. and Vasseur, P. 2001 Convection in a square cavity filled with an anisotropic porous medium saturated with water near 4 degrees C. *Int. J. Heat Mass Transfer* **44**, 3463–3470. [7.3.2]
- Zhong, J. Q., Fregaso, A. T., Wells, A. J. and Wettlaufer, J. S. 2012 Finite-sample-size effects on convection in mushy layers. *J. Fluid Mech.* **704**, 89–108. [10.2.3]
- Zhou, M. J. and Lai, F. C. 2002 Aiding and opposing mixed convection from a cylinder in a saturated porous medium. *J. Porous Media* **5**, 103–111. [8.1.3]
- Zhou, S. B., Chen, L. G. and Sun, F. R. 2008 Constructal optimization for a solid-gas reactor based on triangular element. *Science in China E* **51**, 1554–1562. [4.18.5]
- Zhu, J. and Kuznetsov, A. V. 2005 Forced convection in a composite parallel plate channel: modeling the effect of interface roughness and turbulence using a  $k-\epsilon$  model. *Int. Comm. Heat Mass Transfer* **32**, 10–18. [1.8]
- Zhu, N. and Vafai, K. 1996 The effects of liquid-vapor coupling and non-Darcian transport on asymmetrical disk-shaped heat pipes. *Int. J. Heat Mass Transfer* **39**, 2095–2113. [3.6]
- Zhu, N. and Vafai, K. 1999 Analysis of cylindrical heat pipes incorporating the effects of liquid-vapor coupling and non-Darcian transport – a closed form solution. *Int. J. Heat Mass Transfer* **42**, 3405–3418. [11.9.2]
- Zili, L. and Ben Nasrallah, S. 1999 Heat and mass transfer during drying in cylindrical packed beds. *Numer. Heat Transfer A* **36**, 210–228. [3.6]
- Zili-Ghedira, L., Slimi, K. and Ben Nasrallah, S. 2003 Double diffusive natural convection in a cylinder filled with moist porous grains and exposed to a constant wall heat flux. *J. Porous Media* **6**, 123–136. [3.6]
- Zimmerman, W., Painter, B. and Behringer, R. 1998 Pattern formation in an inhomogeneous environment. *Europ. Phys. J. B* **5**, 757–770. [11.2]
- Zimmermann, W., Seeßelberg, M. and Petruccione, F. 1993 Effects of disorder in pattern formation. *Phys. Rev. E* **48**, 2699–2703. [6.9.1]
- Zueco, J. 2008 Unsteady free-convection-radiation flow over a vertical wall embedded in a porous medium. *Comm. Numer. Meth. Engng.* **24**, 1093–1105. [5.1.9.4]
- Zueco, J., Beg, O. A. and Takhar, H. S. 2011a Unsteady buoyancy-driven thermal convection in a non-Darcian porous medium vertical channel with asymmetric boundary conditions. *J. Porous Media* **14**, 73–79. [7.2]
- Zueco, J., Beg, O. A., Beg, T. A. and Takhar, H. S. 2009a Numerical study of chemically reactive buoyancy-driven heat and mass transfer across a horizontal cylinder in a high-porosity non-Darcian regime. *J. Porous Media* **12**, 519–535. [9.2.1]
- Zueco, J., Beg, O. A.,.. and Takhar, H. S. 2009b Network numerical analysis of magneto-micropolar convection through a vertical circular non-Darcy porous medium conduit. *Comput. Mater. Sci.* **46**, 1028–1037. [7.3.7]
- Zueco, J., Beg, O. A.,.. and Takhar, H. S. 2011b Unsteady buoyancy-driven thermal convection in a non-Darcian porous medium vertical channel with asymmetric boundary conditions. *J. Porous Media* **14**, 73–79. [7.2]
- Zukauskas, A. 1987 Convective heat transfer in cross flow. *Handbook of Single-Phase Convective Heat Transfer* (eds. S. Kakac, R. K. Shah and W. Aung), Wiley, New York, Chapter 6. [4.15]

# Index

## A

Acceleration, 8–10, 95, 140, 224, 294, 300, 319, 320, 346, 396, 407, 420, 432  
Allometry,  
Analogies  
layering and anisotropy, 278–279  
rotation and inclination,  
Anisotropy, 108, 122, 171, 202, 208, 260, 265, 270, 272–275, 278–279, 283, 292, 310, 315–318, 321, 348, 352–356, 359, 388, 389, 391, 436, 438–439, 441, 442, 464, 468, 498, 500, 538  
Annulus, 108, 122, 171, 202, 208, 260, 265, 270, 272–275, 278–280, 283, 292, 310, 315–318, 321, 348, 352–356, 359, 388, 389, 391, 436, 438–439, 441, 442, 464, 468, 498, 500, 538  
Area-to-point flow, 298  
Asymmetric heating, 99, 101, 108, 121, 355, 362, 419  
Attic-shaped enclosure, 363  
Averaging, 1–4, 6, 9, 13–16, 18, 22, 23, 25, 26, 33, 38, 41, 45, 54–56, 58, 75, 228, 319, 327, 390, 499, 538  
Axisymmetric cavities, 362  
Axisymmetric surface, 198–200

## B

Beavers–Joseph condition, 20, 21, 307, 309  
Bejan number, 116, 142, 143  
porous medium, 116, 142  
Bidisperse porous media (BDPM), 119–121, 329, 366

Bifurcation, 39, 128, 134, 242, 246, 247, 251, 256, 264, 265, 274, 283, 286–291, 293, 297, 298, 317, 320, 356–358, 387, 431, 432, 434, 440, 454, 463, 501

Binary alloys, 499–506  
Bioconvection, 29, 177, 319–320  
Bioheat transfer, 29, 45–46  
Boiling, 64, 135, 506–518, 520  
Boundary conditions  
hydrodynamic, 18–25  
Newtonian, 177, 195  
thermal, 43–44  
Boundary friction, 90–103, 159–161, 217, 242, 346, 378–380, 387, 402, 408, 422, 489, 518  
Boundary imperfections, 346  
Boundary layer, 9, 35, 70, 145, 240, 332, 397, 437, 472, 527  
Brinkman model, 16, 17, 23, 26, 94, 97, 100, 106–109, 120, 152, 159, 160, 168, 170, 178, 258, 265, 267, 271, 275, 299, 312, 315, 316, 321, 346, 355, 360, 364, 375, 378, 381, 387, 403, 407, 430–441, 454, 461, 462, 467, 520  
Bulk temperature, 79  
Buoyancy ratio, 427, 431, 437, 440, 446, 450, 451, 456, 459–462, 465, 501, 502, 536  
Buried heat sources, 79

## C

Carbon dioxide sequestration, 549–550  
Carman–Kozeny formula, 9  
Cellular porous material, 329  
Centrifugally driven convection, 247  
Channel flow, 37, 117, 126

- Channeling, 21, 25, 34, 41, 100, 101, 182, 247, 250, 309, 355, 382, 402, 535
- Chemical reaction, 44, 47, 53–54, 169, 181, 265, 299, 312, 436, 440–442, 447–449, 455, 458, 466, 467, 523, 550
- Coarse porous media, 1
- Coated fibers, 521
- Complex porous structures, 28–29
- Compressibility effect, 8, 46, 243, 244, 265, 375, 441
- Condensation, 64, 83, 469, 518–520, 544
- Cone, 181, 194–199, 204, 249, 408, 409, 448, 464, 466, 468, 516–518
- Conjugate convection, 157, 181, 217, 227, 347, 358, 360, 364, 383, 402, 407, 408, 495
- Constructal law, 67, 113, 134–137, 323, 546
- Constructal theory, 12, 117, 127, 133, 135–138, 225, 320, 322–329, 546, 549
- of Bénard convection, 135, 322–329
  - of crack formation, 544
  - of laminar-turbulent transition, 12
- Continuity of mass. *See* Mass conservation
- Convection with change of phase, 469–522
- Crack formation, 546
- Cracks in shrinking solid, 546–549
- Crossed gradients, 465–466
- Cylinder, 11, 45, 73, 157, 257, 355, 404, 443, 494, 528 *See also* Horizontal cylinder; Vertical cylinder
- Cylindrical enclosures, 296, 299, 356, 360, 364
- D**
- Darcy number, 12, 17, 22, 35, 88, 95, 96, 98, 100, 103, 104, 109, 117, 159, 160, 224, 240, 241, 255, 271, 308–311, 314, 316, 317, 354, 378, 380, 419, 440
- Darcy's law, 5–19, 23, 27, 35, 54, 74, 76, 117, 141, 146, 159, 160, 167, 221, 282, 375, 394, 395, 430, 499, 503, 512
- Deformable media, 28–29, 537
- Designed porous media, 1, 2, 114–117, 137, 141, 143
- Diagenetic processes, 530–532
- Dispersion, 9, 15, 27, 28, 33, 39–42, 44, 60, 87–90, 94–105, 154, 159–166, 168, 170, 182, 204, 210, 217, 240–243, 248, 256, 257, 264, 274, 275, 378–380, 383, 388, 389, 394, 400–404, 407–409, 414, 415, 421, 424, 431, 438, 442, 447, 448, 466, 468, 491, 520, 550
- Double diffusion, 46, 180, 322, 434, 468
- Drying, 64, 65, 130, 541, 546
- Dufour effect, 52, 434, 447, 448, 464, 466
- Dupuit–Forchheimer relationship, 5, 8, 32, 51
- E**
- Earth's core, 535, 537, 546
- Elastic matrix, 243
- Electrodiffusion, 65–67
- Elemental volume, 31, 32, 128–131
- Energy equation, 27, 31–42, 44, 50, 54, 59, 60, 62, 63, 71, 82, 92, 110, 124, 153, 175, 196, 208, 238, 252, 336, 373, 375, 411, 413, 500, 525, 533
- Entropy generation, 101, 102, 109, 118, 123, 136, 363, 365, 375, 388, 404, 520
- Ergun's equation, 13
- Evaporating salt lake, 443, 537
- Evaporation, 119, 122, 312, 438, 443, 455, 469, 506–517, 544
- Experimental investigations, 166–168
- F**
- Fibers, 7, 11, 12, 17, 18, 29, 113, 241, 520–522
- Fick's law, 50
- Finite-amplitude convection, 245–247, 271, 276, 291
- Fins, 104–107, 114–116, 122, 157, 216–218, 259, 464
- First construct, 131–132
- Fissures, 29, 141, 438
- Fluid and porous regions, 380–383
- Fluid flow, 1–29, 45, 54, 69, 88, 106, 113, 115, 119, 127, 169, 200, 364, 512, 530, 537, 546
- Forced convection, 35, 37–39, 41, 42, 45, 69–143, 170, 186, 237, 258, 315, 363, 383, 393, 394, 397, 399, 411, 414, 416–421, 424, 493, 517, 519, 520, 534, 547, 548
- Forchheimer model, 104, 154, 172, 186, 188, 200, 202–205, 210, 217, 245, 257, 267, 291, 348, 358, 360, 374, 378, 380, 381, 383, 394, 403, 404, 407, 409, 414, 415, 419, 421, 447, 456, 493, 494, 519, 520
- Fourier number, 471
- Fractured media, 28–29
- Freezing, 395, 495–506, 521, 525, 528
- G**
- Geometry generation in nature.
- See* Constructal theory

- Geophysical aspects, 523–553  
Geothermal reservoirs, 534–535, 543  
Gradient reaction, 552–553
- H**  
Hair, 3, 110–113, 218–220  
Heat and mass transfer, 33, 38, 51–53, 126, 299, 394, 425–429, 440, 442–451, 453, 454, 456, 462, 466, 506, 517, 520, 525, 537  
Heatlines, 123–126, 348  
Heat pipe, 119, 277, 409, 544–546  
Heat transfer, 1, 31, 47, 69, 149, 222, 331, 400, 432, 471, 525  
Hele-Shaw analogy, 44–45  
Heterogeneity, 14, 108, 109, 171, 243, 258, 275–284, 352–355, 392, 439, 454, 527, 538, 539, 544, 550  
Higher-order transitions, 242, 245–247  
Horizontal cylinder, 184–190, 218, 220, 296–297, 355–356, 375, 383, 404–407, 448, 462, 468, 494, 498, 499, 516, 517, 520  
Horizontal line heat source, 200–208, 395, 408  
Horizontal plate, 72, 173, 175–179, 182, 404, 409, 410, 448, 468  
Horton-Rogers-Lapwood problem, 221–222, 384, 389, 425–429, 467, 525  
Hyperporous medium, 17, 103
- I**  
Icy water, 174, 258, 271–272, 299, 348, 355, 362, 363, 409, 414, 421, 448, 455  
Ideal gas, 48, 66, 244  
Inclined gradients, 265  
Inclined layer or enclosure, 275, 346, 387, 389, 391, 463, 466, 565  
Inclined plate, 177, 179–183, 402, 403, 424  
Inclined temperature gradient, 389–392  
Inertia, 8–10, 13–15, 17, 22, 34, 58, 59, 82, 83, 87–90, 92, 94–103, 152, 159–166, 168, 178, 181, 182, 195, 197, 200, 204, 210, 242, 243, 245, 247, 251, 252, 258, 260, 290, 318, 346, 348, 373–378, 400–403, 407, 410, 431, 438, 456, 489, 491, 495, 505  
Integral method, 91, 150–152, 173, 177, 311, 326, 341, 441  
Internal heating, 33, 37, 177, 200, 262–265, 268, 297–299, 312, 315, 321, 348, 365–366, 415
- Internal partitions, 350–352  
Intersection of asymptotes method, 141, 143, 325, 329, 547  
Iontophoresis, 65
- J**  
Jet. *See* Line source; Point source; Wake
- L**  
Layered porous media, 276–278  
Line source, 77–79, 160, 181, 186, 200–204, 208, 213, 462  
Localized heating, 299–303, 382, 416–417, 419–423, 442  
Local Reynolds number, 12
- M**  
Magma, 504, 529–530, 535–537  
Magnetic field, 10, 104, 118, 169, 174, 177, 181, 183, 187, 299, 313–315, 366, 388, 389, 403, 423, 424, 441, 449, 455, 464, 466, 493, 500, 505, 536  
Mass conservation, 49–51, 68, 129, 153, 205, 211, 373  
Mass transfer, 33, 38, 44, 47–68, 126, 168, 173, 177, 190, 195, 299, 394, 409, 425–459, 468, 506, 517, 520, 525, 531, 537, 546  
Melting, 313, 469–522, 526, 530  
Micropolar fluid, 169, 315, 317, 318, 356, 420, 441, 448, 449, 455, 465, 467  
Mixed convection  
double-diffusive, 407, 447, 466–467  
external, 466–467  
internal, 467  
Mixing zone, 553  
Mixtures, 14, 44, 45, 47–54, 64, 67, 425, 426, 432–435, 440, 463, 494, 499, 500, 504–506, 511–512, 517, 520, 530, 543, 553  
Momentum equation, 5–8, 10, 14, 15, 18, 43, 57, 59, 90, 208, 214, 221, 255, 274, 316, 320, 346, 375–377, 425, 499  
Multicomponent and multiphase flows, 47–68  
Multiscale flow structures, 137–141  
Mushy zone, 24, 314, 439, 499, 500, 503, 504, 536

**N**

Nanofluid, 38, 67–68, 122, 169, 174, 179, 187, 190, 219, 315, 318, 322, 408, 423, 467–468

**Natural convection**

- external, 42, 145–220, 443–449
- internal, heating from below, 221–329
- internal, heating from the side, 331–396

Nernst-Planck equation, 65

Net mass flow, 257–260

Non-Boussinesq effects, 36, 243–245

Nonequilibrium, thermal, 36, 76, 88, 94, 103–104, 108, 109, 169–170, 187, 195, 219, 239, 240, 243, 258, 265, 270, 278, 315, 317, 318, 321, 347, 348, 350, 360, 362, 365, 375, 378–380, 393, 419, 421, 423, 436, 441–443, 467–468, 494, 517, 546

Nonlinear basic temperature profile, 249, 261–272

Non-Newtonian fluid, 18, 104, 106, 119, 169, 195, 198, 200, 217, 317, 318, 347–348, 404, 407–409, 414, 441, 447, 448, 455, 467, 468, 494, 517

Nonuniform heating, 284–286, 355

Nusselt number, 23, 26, 37, 38, 71, 73–75, 79, 80, 92–94, 96–101, 104, 108, 109, 117–119, 121, 124, 149, 152, 154, 155, 157–168, 175, 176, 180, 184, 188, 192, 196–197, 199, 217, 229, 230, 233, 235, 238, 239, 241, 242, 247, 249, 250, 255, 257, 273, 275, 276, 281, 283, 289, 291, 300–303, 311, 316, 317, 334, 338, 340, 343, 349, 350, 352, 357, 359, 360, 362, 376, 378, 379, 381, 383, 385, 387, 399–402, 406, 411, 413, 416–418, 420, 421, 431–432, 437, 440, 453, 472–474, 476, 477, 479, 481–486, 489, 493, 494, 496, 516

**O**

Oberbeck-Boussinesq approximation, 42–43, 146, 221, 470, 512

Oceanic crust, 532–534

Optimal enclosure shape,

Optimization. *See* Constructal theory;

Designed porous media

Oscillatory flows, 118, 169, 247, 300, 361, 394, 407, 417, 429, 432

**P**

Parabolic density model, 362

Paraboloid, 199, 408

Partitions. *See* Internal partitions

Patterned ground, 272, 525–527

Péclet number,

Penetrative convection, 245, 260, 271–272, 312, 315, 366–371, 433, 493

Periodic heating, 392–393

Permafrost, 122, 364, 526–529

Permeability, 1, 44, 59, 101, 152, 222, 332, 400, 435, 491, 525

Phase change, 469–471, 477, 485, 490–492, 494–495, 497, 498, 505, 506, 512, 520–522, 524, 527, 544, 546

Point source, 77–79, 127, 208, 213–216, 459–461

Porosity, 3, 4, 6–8, 14–16, 21, 22, 24–26, 28, 31, 33, 35, 37, 41, 42, 50–51, 54, 55, 90–103, 110, 113, 120, 122, 154, 164, 173, 177, 181, 182, 188, 217, 219, 220, 247, 250, 255, 256, 278, 316, 341, 346, 354, 374, 378–380, 382, 388, 394, 401, 402, 404, 407, 408, 414, 415, 419, 429, 435, 454, 455, 463, 467, 494, 500, 518, 521, 530–532, 552

Porosity variation, 16, 25–26, 33, 41, 90–103, 188, 247, 255, 346, 379, 382, 401, 402, 404, 407, 454, 463

Porous materials, 2–4, 6, 33, 79, 80, 87, 104, 105, 152, 329, 360, 370, 380, 381, 383, 410, 542

Porous medium, 1, 31, 47, 69, 145, 221, 331, 397, 430, 469, 530

Pressure changes, 31, 34–36, 243

Properties, 3, 4, 24, 29, 43, 44, 60, 88, 114, 115, 118, 127, 141, 173, 174, 245, 252, 283, 322, 332, 352, 353, 421, 435, 470, 472, 491, 508, 520–521, 538

**R**

Radiation, 42, 46, 59, 76, 106, 107, 113, 122, 123, 165, 169–171, 173, 177, 181, 195, 198, 265, 312, 329, 348, 350, 356, 360, 389, 400, 402, 403, 408–409, 414, 433, 447–449, 463–468, 494, 527

Rayleigh number, 116, 145, 224, 334, 415, 432, 471, 525

Reaction front, 321, 551–552

Rectangular box or channel, 286–294

Representative elementary volume, 2–4, 54, 59, 68, 348  
 Resonance, 29, 235–236, 250, 289, 392, 393, 504  
 Reynolds number  
   local, 12  
 pore, 37, 41, 42, 91, 115, 377, 378  
 Rotation, 8, 10, 297, 310, 315–318, 358, 392, 395–396, 436, 441, 443, 455, 468, 502–500

**S**  
 Scale analysis, 16, 35, 41, 65, 67, 70, 71, 82–83, 213, 252, 253, 255, 278, 320, 323, 357, 360, 361, 374, 376, 385, 392, 393, 433, 436, 444, 445, 447, 450, 456, 475–477, 480  
 Seepage velocity, 5, 10, 12, 13, 18, 20, 23, 32, 41, 62, 146, 148, 151, 205, 208, 222, 524  
 Similarity solution, 72, 89, 94, 147–150, 152, 154, 161, 164, 167, 169, 172, 175, 177, 179, 193, 196–198, 200, 204, 209, 210, 216, 217, 326, 327, 368, 398, 401–403, 408, 413, 445, 453, 462, 466, 486, 487, 517, 544  
 Single-phase flow, 1, 6, 535–539  
 Sintered materials, 102  
 Slenderness, 485  
 Snow, 523–525, 531  
 Solidification, 24, 439, 495–506, 521, 522, 537  
 Soret diffusion, 52  
 Sources in confined regions, 393–395  
 Spacings, 79, 115, 116, 136, 138, 140–142, 345, 371, 381, 546, 547  
 Sphere, 73–77, 87, 104, 157, 184, 189–193, 203, 214, 215, 220, 404–408, 416, 462, 463, 498, 517  
 Spherical annulus, 357, 360, 361  
 Spherical enclosures, 360–361  
 Stability, 17, 34, 52, 173, 222, 346, 415, 427, 499, 526  
 Stefan number, 478–480, 482, 484, 488, 502–504  
 Stratification, 152–154, 181, 195, 297, 298, 303, 343, 347, 348, 402, 419, 447–449, 453, 455, 468  
 Superconvection, 535  
 Superheating, 477–485, 488, 489, 515  
 Surface per unit volume, 3, 36

Surfaces covered with porous layers, 110–114  
 Surface tension, 24, 64, 312, 518, 519

**T**  
 Temperature-dependent viscosity, 117–118, 160, 173, 177, 181, 195, 245, 300, 404, 432, 448, 449, 518  
 Thermal conductivity, 31–34, 38–40, 42, 43, 50, 59–61, 67, 80, 90, 94, 100–102, 107, 108, 111, 120, 139, 141, 155, 177, 198, 222, 236, 272, 274, 276, 277, 279, 281–283, 292, 310, 311, 320, 347, 354, 355, 375, 380, 388, 395, 397, 402, 406, 415, 417, 455, 466, 491, 494, 497, 514, 518, 528, 531, 536, 548  
 Thermal development, 106, 107, 109  
 Thermodynamics, 31, 36, 43, 52, 96, 102, 136, 418, 435  
 Thoughtflow. *See* Net mass flow  
 Time-dependent gravity and heating, 172  
 Tortuosity, 15, 33, 45, 51  
 Transient effects, 81–88, 265, 275, 371–375, 383, 456–458  
 Trapezoidal enclosure, 363, 364, 464  
 Tree networks, 126–137  
 Turbulence, 10, 12, 24, 26–28, 37, 105, 107, 135, 237, 382, 438, 500  
 Two-phase flow, 1, 14, 38, 61, 63, 64, 512, 520, 539–546

**U**  
 Unsaturated porous media, 64–65

**V**  
 Variable gravity, 318–321, 391  
 Variable porosity, 22, 94, 100, 101, 154, 173, 181, 182, 354, 374, 378–380, 388, 402, 408, 414, 415, 518  
 Vertical annulus. *See* Annulus  
 Vertical channel or slot, 347, 348, 355, 356, 383, 418–423, 467  
 Vertical cylinder, 87, 193–195, 260, 294–296, 298, 356, 365, 407, 408, 422, 443, 448, 462, 466, 498, 528  
 Vertical plate, 145–175, 177, 180, 191, 216–218, 374, 400–402, 406, 408, 414, 423, 446–448, 456–458, 466–468, 493, 494, 498, 517, 520

- Vibration, 319–322, 375, 442, 505  
Viscoelastic fluid, 119, 169, 258, 317, 318, 348, 441, 443, 447, 449, 467  
Viscous dissipation, 31, 34–36, 59, 72, 76, 95, 102–104, 106, 107, 109, 119, 123, 170–171, 174, 187, 198, 200, 221, 228, 240–243, 348, 350, 360, 374, 378–380, 387, 389, 392, 402, 403, 409, 414, 415, 418–420, 429, 442, 447, 466  
Visualization, 126, 248, 256, 296, 311, 382, 431, 498, 506
- Volume-to-point flow, 126–137  
Volumetric heating. *See* Internal heating  
Vortex instability, 170, 180–184, 202, 404, 415
- W**  
Wake, 77–79, 172, 173, 407  
Water near 4°C. *See* Icy water  
Wavy surface, 168, 171–172, 178, 198, 286, 447  
Weakly nonlinear theory, 283, 284, 415